

## **Co-creation of Affordable and Clean Pumped Irrigation for Smallholders Lessons from Nepal and Malawi**

Intriago Zambrano, Juan Carlo; van Dijk, Ruben W.; Michavila, Jaime; Arenas, Eva; Diehl, Jan-Carel; Ertsen, Maurits

### **Publication date**

2019

### **Document Version**

Final published version

### **Published in**

Conference Proceedings

### **Citation (APA)**

Intriago Zambrano, J. C., van Dijk, R. W., Michavila, J., Arenas, E., Diehl, J.-C., & Ertsen, M. (2019). Co-creation of Affordable and Clean Pumped Irrigation for Smallholders: Lessons from Nepal and Malawi. In *Conference Proceedings: Water for All - Water for Nature, Reliable Water Supply, Wastewater Treatment and Reuse* (First ed., pp. 466-473). University of Chemistry and Technology, Prague.

### **Important note**

To cite this publication, please use the final published version (if applicable).  
Please check the document version above.

### **Copyright**

Other than for strictly personal use, it is not permitted to download, forward or distribute the text or part of it, without the consent of the author(s) and/or copyright holder(s), unless the work is under an open content license such as Creative Commons.

### **Takedown policy**

Please contact us and provide details if you believe this document breaches copyrights.  
We will remove access to the work immediately and investigate your claim.

# 11<sup>th</sup> Eastern European Young Water Professionals Conference



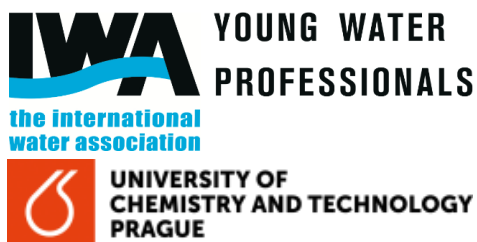
## Conference Proceedings

Water for All - Water for Nature,  
Reliable Water Supply, Wastewater Treatment  
and Reuse

1-5 October 2019, Prague, Czech Republic  
<http://iwa-ywp.eu/>



Organised by:



More information:



Organised under the auspices of:



Czech Water Association



The Faculty of Civil Engineering of the Czech Technical University in Prague



The Faculty of Agrobiolgy, Food and Natural Resources of the Czech University of Life Sciences Prague



The Water Supply and Sewerage Association of the Czech Republic

Co-organised by:



YWP CZ



Budapest University of Technology and Economics



Wrocław University of Science and Technology



The Faculty of Chemical and Food Technology of the Slovak University of Technology

**11<sup>th</sup> Eastern European Young  
Water Professionals  
Conference**



**CONFERENCE PROCEEDINGS**

**Water for All – Water for Nature, Reliable Water Supply, Wastewater  
Treatment and Reuse**

1-5 October 2019, Prague, Czech Republic

**Editors:**

Maryna Feierabend

Jiří Wanner

Petra Vachová

**Typesetting:**

Eva Sebestyén

Liudmyla Odud

Maja Djogo

Maria Danilycheva

Olha Novytska

**Cover Design:**

Maryna Feierabend

**Prague 2019**



## SPONSORS

Gold Sponsor - WTE (Germany)



Gold Sponsor - Endress+Hauser (Germany)



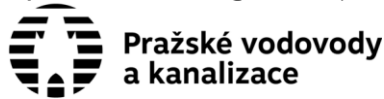
Sponsor - Energie AG (Czech Republic)



Sponsor - SUEZ (Czech Republic)



Sponsor - Energie AG (Czech Republic)



## ORGANISING COMMITTEE

Chair: Dr. Feierabend M. (IWA YWP, Germany)

Co-Chair: Vachová P. (Co-Chair IWA YWP of Czech Republic, VWS Memsep, Czech Republic)

### Committee members:

Dr. Lavrnić S. (University of Bologna, Italy/Serbia)

Ibrahimllari A. (IWA YWP Program, Albania)

Dr. Schilling K. (IAWD – Danube Water Program, Austria)

Sebestyén É. (UTB Envirotec Ltd., Hungary)

Dr. Djogo M. (University of Novi Sad, Serbia)

Dejus S. (Riga Technical University, Latvia)

Danilycheva M. (Moscow State University of Civil Engineering, Russia)

Ciepliński J. (Cracow University of Technology, Poland)

Proft R. (WTE, Germany)

Dr. Nuić I. (University of Split, Faculty of Chemistry and Technology, Croatia)

Odud L. (Rivne regional water supply company, Ukraine)

Mohseni E. (Technical University of Dresden, Germany)

Filipic A. (National Institute of Biology, Slovenia)

Ikizoglu Z. R. (Tübitak Marmara Research Center, Turkey)

Čiháková P. (University of Chemistry and Technology, Czech Republic)

Harciník F. (Chair IWA YWP of Czech Republic, Severočeské vo-dovody a kanalizace, a.s., Czech Republic)

Kelbich P. (Pražské vodovody a kanalizace, a.s., Czech Republic)

Sochor J. (Gymnázium Blovice, Czech Republic)

Soukupová K. (Czech Technical University in Prague, Czech Republic)



## **PROGRAMME COMMITTEE**

Chair: Prof. Wanner J. (University of Chemistry and Technology, Czech Republic)

Co-Chair: Prof. Jobbágy A. (Budapest University of Technology & Economic, Hungary)

### Committee members:

Mr. Förster G. (BESINO Environment Ltd., China)

Prof. Krampe J. (TU Vienna, Austria)

Dr. Hübner U. (TU Munich, Germany)

Dr. Vasyukova E. (WTE, Germany)

Prof. Makinia J. (Gdansk University of Technology, Poland)

Dr. Wójtowicz P. (Wrocław University of Science and Technology, Poland)

Dr. Vouk D. (University of Zagreb, Croatia)

Dr. Szlachta M. (Wrocław University of Science and Technology, Poland)

Dr. Bakos V. (Budapest University of Technology and Economics, Hungary)

Prof. Juhna T. (Riga Technical University, Latvia)

Dr. Novytska O. (National University of Water and Environmental Engineering, Ukraine)

Dr. Rudic Z. (Institute for the Development of Water Resources "Jaroslav Cerni", Serbia)

Dr. Çelebi A. (Sakarya University, Turkey)

Dr. Drewnowski J. (Gdansk University of Technology, Poland)

Dr. Langone M. (University of Trento, Italy)

Dr. Srb M. (Pražské vodovody a kanalizace, a.s., Czech Republic)

# CONTENTS

## WATER MANAGEMENT

<b>Andjelic L., Andjelic N., Jacimovic N., Petkovic S., Pavlovic M., Vlajic D.</b> Urban Rainwater Harvesting System: Possible Application for Car Washing	10
<b>Andjelic N., Andjelic L., Ivanovic S., Erić R.</b> Application of SWMM Software Package for Management of Rainwater Drainage Systems of Urban Basins – Example of Drainage for Combined Cycle Power Plant	16
<b>Asatryan V. L., Dallakyan M. R.</b> The Rapid Biological Assessment of Ecological Status of Arpa River (Armenia)	23
<b>Celik A., Hasar H.</b> Fabrication and Characterization of Bipolar Membranes for Acid and Base Recovery	31
<b>Costa B. F., Brito L. K. S., Costa M. E. L., Koide S., Roig H. L.</b> Evaluation of the Impact of Residential Urban Patterns on Water Ecosystem Services in Federal District, Brazil	37
<b>Danylenko Iu., Bohaienko V.</b> Patterns of Changes in Soil Moisture Content Depending on Agrolandscapes Structure in Southern Ukraine	44
<b>Dezhina I. S., Orlov V. A.</b> Influence of the Internal Protective Coatings Surface Texture to the Transport Capacity of the Pipelines	51
<b>Diaz-Sosa V., Tapia-Salazar M., Wanner J., Cardenas-Chavez D.</b> Toxicology Assessment of Emerging Contaminants Found in Secondary Effluent of Prague's WWTP on Aquatic Species with Ecological and Economical Relevance	58
<b>Gevorkov L., Mikhelashvili I.</b> Simulation of Sensorless Flow Measurement System for Centrifugal Pump System	64
<b>Kudlek E.</b> Chlorine Presence Influence on Transformation of Contaminants of Emerging Concern (Cecs) During UV-Based Processes	71
<b>Kupczyk A., Kolecka K.</b> Beach Wrack Management as Example of Circular Economy	79
<b>Nováková J., Ručka J., Fučík D.</b> Statistical Description of Time Series of Water Consumption in the Consumption Area	85
<b>Sezen C., Partal T.</b> Daily Rainfall-runoff Modelling by Support Vector Regression, Symbolic Regression and GR4J Models	93
<b>Stroganova M. S., Kushnerov A. I., Shishkin A. I.</b> Integrated Assessment of Technogenic Load on Water Ecosystems Based on Biodiversity and Hydrochemical Indexes	101

**Unlu D.**

Synthesis and Performance Evaluation of Chitosan Membrane Filled with UiO-66 Nanoparticles for Dewatering of Biobutanol by Pervaporation 109

**Yalçın İ., Kazezyılmaz-Alhan C. M., Javanshour K., Aytakin M., Gülbaz S.**

A Hydrological Model for Ayamama Watershed in Istanbul, Turkey Using HEC-HMS 116

**DRINKING WATER****Amvrosieva T. V., Paklonskaya N. V., Belskaya I. V., Laziuk S. K., Kazinets O. N., Shilova Yu. A.**

Possible Indicator Role of Adenoviruses for Assessing Viral Contamination of Water 123

**Bibok A.**

Hydraulic Model Calibration and Performance Assessment of Pressure Managed Areas with Multiple Inlets 129

**Fakioglu M., Gulhan H., Ozgun H., Ersahin E., Ozturk I.**

Determination of Optimum Operational Conditions for the Removal of 2-MIB from Drinking Water by Peroxone Process: A Pilot Scale Study 137

**Ferreira M. A., Brandão C. C. S., Simões C. P. P., Braga F. M. G.**

A Pilot-Scale Experimental Study on the Adequacy of Filtration Mode of Operation and Filter Media in the Brasília Water Treatment Plant - Federal District - Brazil 145

**Fonseca I. R., Cárdenas D. V., Prauchner M. J., Ginoris Y. P.**

Removal of Cylindrospermopsis by Adsorption onto Activated Carbon Synthesized from Coconut Shell 153

**Gönczi G., Kreka R.**

Energy Consumption Reduction and Utilization of Renewable Energy in Pump Stations 161

**Govedarica O. R., Rajaković-Ognjanović V. N., Đukić A. R., Lekić B.M., Babić B. B.**

Improving Quality of Drinking Water in the Water Treatment Plant by Decrease of Hardness with Respect to Sodium Concentration Control 168

**Huzsvár T., Wéber R., Hós C.**

Fire and Drinking Water Capacity Enhancement in Water Distribution Networks 175

**Mandić M., Štrbački J.**

Comparative Analyzes of Hydro-chemical Properties of Bottled Waters in Serbia 182

**Sam S., Yukselen M. A., Can Z. S.**

Investigation of the Effect of Pre-ozonation on Organic Matter Removal via Flocculation 188

**Saprykina M. N., Bolgova E. V., Melnyk L. O., Goncharuk V. V.**

Water Disinfection from Microorganisms Using Chitosan 196

**Šíblová D., Biela R.**

Experimental Determination of Efficiency Adsorbent Bayoxide E33 of Removal Micropollutants from Water 204



<b>Tonev R., Dimova G.</b>	
Investigation of Chlorine Wall Decay in Decommissioned Metallic Pipe Using Pipe Section Reactor	211
<b>Trusz A., Wolf-Baca M., Leluk K.</b>	
Search for Materials Used for Tap Water Transmission Reducing the Capacity for Development of Biofilm – Preliminary Research	219
<b>Vojdani Z., Gorczyca B.</b>	
Natural Organic Matter Biodegradability and THMFP in High DOC Waters	227
<b>Wolf-Baca M., Siedlecka A.</b>	
Prevalence of <i>Legionella spp.</i> and <i>Escherichia coli</i> in the Drinking Water Distribution System of Wrocław (Poland)	234
<b>Yermakovych I., Vystavna Y.</b>	
Pollution of Urban Groundwater by Emerging Contaminants in Kharkiv Region, Ukraine	242
<b>Zakhar R., Zembjaková I., Villaverde I. C., Čacho F., Derco J., Hudec P.</b>	
Comparison of Different Adsorption Materials for Pentavalent Arsenic Removal from Drinking Water	249

#### WASTEWATER

<b>Aghajani Shahrivar A., Hagare D., Maheshwari B., Muhitur Rahman M.</b>	
The Effect of Irrigation Using Secondary and Advance Treated Wastewaters on Soil Properties under Kikuyu Grass Production	257
<b>Antić K., Petrović M., Adamović D., Turk-Sekulić M., Sakulski D., Radonić J.</b>	
Characterization of Leachate from Non-sanitary Municipal Solid Waste Landfill in Novi Sad	265
<b>Bawiec A., Pawęska K.</b>	
Changes of the Granulometric Composition of Particles in Wastewater Flowing through the Hydroponic Lagoon in III <sup>o</sup> Wastewater Treatment Plant	273
<b>Bolgár A., Boldizsár G., Miskei S. M., Blanc R.</b>	
Evaluation of Sentry Sensor for Real-time Biochemical Oxygen Demand Measurement Capabilities	281
<b>Caglak A., Sari Erkan H., Onkal Engin G.</b>	
Micropollutants Removal in Submerged Membrane Bioreactors at Different SRT Values and Variations of Extracellular Polymeric Substances	287
<b>Dalgıç Bozyiğit G., Fırat M., Chormey D. S., Onkal Engin G., Bakırdere S.</b>	
Enhancing the Accuracy and Precision in Quantifying the Pesticides Present in Complex Environmental and Food Samples by GC-MS Using Matrix Matching Calibration and Isotopically Labelled Internal Standard	294
<b>Essert S. M., Zacharias N., Brunsch A. F., Christoffels E., Kistemann T., Schreiber C.</b>	
Performance of Retention soil Filters for the Reduction of Antibiotic-resistant Bacteria and Other Pathogenic Microorganisms in Raw and Treated Wastewater before Being Discharged into Surface Waters	302

<b>Guerra A. A. A. M., Damasceno F. L., Barreto C. C. K., Campos A. F., Amorim A. K. B.</b>	
Application of Core-shell Bimagnetic Nanoparticles for Removal of Phosphorus from Aqueous Solution	310
<b>Harciník F., Pečenka M., Vrábel M.</b>	
Limits of Increased Simultaneous Phosphorus Precipitation in WWTP Bílina	317
<b>Klimonda A., Kowalska I.</b>	
Separation and Concentration of Cationic Surfactant Solutions with the Use of Ceramic Modules	324
<b>Kolomazníková M., Havlíček K., Lederer T.</b>	
The Dependency and Behaviour of Suspended and Immobilized Biomass in Activated Sludge	332
<b>Kumi A.G., Ibrahim M. G., Nasr M., Manabu F.</b>	
Synthesis, Characterisation and Adsorption Properties of a Sewage Sludge Derived Biochar Modified With Eggshell	339
<b>Miłobędzka A., Vejmelková D., Bartáček J.</b>	
Antibiotic Resistance Genes in Different DNA Fractions Sampled at Wastewater Treatment Plant	347
<b>Nardi A., Mannucci A., Polizzi C., Spennati F., Munz G.</b>	
On-Line Titrimeter: Full Scale Biosensor for Control in Wastewater Treatment	355
<b>Nigiz F. U., Yucak A. I., Hilmioglu N. D.</b>	
Purification of Emulsified Oil by Polyvinylidene Fluoride/Polyvinylpyrrolidone Membrane	362
<b>Pawęska K., Bawiec A., Baran J.</b>	
Wastewater Flow Conditions in a Hydroponic Lagoon in Terms of Quality of Treated Sewage	370
<b>Peterková E., Pečenka M., Wanner J., Nováková Z., Srb M.</b>	
Wastewater Recycling for Use in Water Management in the Cities of Future	377
<b>Reinhardt T., Gómez Elordi M., Minke R., Schönberger H., Rott E.</b>	
Batch Studies of Phosphonate Adsorption on Granular Ferric Hydroxides	384
<b>Spennati F., Mora M., Bardi A., Becarelli S., Siracusa G., Di Gregorio S., Gabriel D., Mori G., Munz G.</b>	
Characterization and Modelling of Fungal and Bacterial Tannin-degrading Biofilms with Respirometric Techniques	393
<b>Szombathy P., Jobbágy A.</b>	
Cost Effective Improvement of the Performance of an SBR System Using a Floating Seal	401
<b>Tomaszewski M., Gamoń F., Łukowiec D., Zgórska A., Ziemińska-Buczyńska A.</b>	
Ecotoxicity Effects of Carbon Nanomaterials on the Activated Sludge Microorganisms	408
<b>Toth A. J.</b>	
Investigation of Tetrahydrofuran Removal Technology from Process Wastewater	416

<b>Toth A. J., Ladanyi R., Szilagyi B., Haaz E.</b>	
Isopropanol Removal from Pharmaceutical Process Wastewater with Combination of Distillation and Pervaporation	422
<b>Unlu D.</b>	
Recovery of Cutting Oil from Wastewater by Pervaporation Process Using Natural Clay Modified PVA Membrane	429
<b>Unugul T., Nigiz F. U.</b>	
Purification of Copper Metal Using Carbonized Mandarin Peel	436
<b>Veréb G., Engin Gayır V., Nascimben Santos E., Fazekas Á., Kertész Sz., Hodúr C., László Zs.</b>	
Purification of Real Car Wash Wastewater with Complex Coagulation/Flocculation Methods Using Polyaluminum Chloride, Polyelectrolyte, Clay Mineral and Cationic Surfactant	444
<b>Zakar M., Beszédes S., Hanczné Lakatos E., Keszthelyi-Szabó G., László Zs.</b>	
Purification and Improved Biogas Production from Real Dairy Wastewaters by Combining Membrane Separation with Fenton-reaction and Ozone as Pre-treatments	452
<b>OTHER</b>	
<b>Diniz A. B. N. , Fernandes Junior J., Soares A. K.</b>	
Numerical Modelling of Hydraulic Transients Considering Dynamics Effects in a Water Pumping System	458
<b>Intriago Zambrano J. C., van Dijk R., Michavila J., Arenas Pinilla E., Diehl J.-C., Ertsen M. W.</b>	
Co-creation of Affordable and Clean Pumped Irrigation for Smallholders: Lessons from Nepal and Malawi	466
<b>Kancheva V. G., Gadjalska N. I.</b>	
Assessment of the Reliability of a Hydraulic Model of the Topolnitza River with a Limited Number of Data	474
<b>Laskawiec E.</b>	
Evaluation of Migration Potential of Water-Based Paints Used in Flexographic Printing into the Aqueous Environment from Selected Plastics	482
<b>Lempart A., Kudlek E., Dudziak M.</b>	
Concentrations of Emerging Organic Contaminants in Swimming Pools	489
<b>Maamoun I., Eljamal O., Falyouna O. A., Eljamal R., Sugihara Y.</b>	
Stimulating Effect of Magnesium Hydroxide on Aqueous Characteristics of Iron Nanocomposites	497
<b>Mentes A., Stournara P., Spyrou D., Samaras A., Galiatsatou P.</b>	
The Smart-Water Project: Smart Metering in the City of Thessaloniki	505
<b>Mentes A., Stournara P., Spyrou D.</b>	
Towards Smart Infrastructure: A Case Study in the Water Supply System of Thessaloniki	513



**Nigiz F. U., Kibar M. E.**

UV-Assisted Desalination of Seawater Using Titanium Dioxide Nanotube Doped Polyether Block Amide Membrane **520**

**Rybalova O., Artemiev S., Yermakovich I., Korobkova H., Kyrpychova I.**

Determination of the Ecological Risk of Deterioration in the Water Flow of the Udy River Basin of Kharkiv Region, Ukraine **528**

**Wencki K.**

Linkages Between Energy Management and Management Accounting: An Empirical Study with Special Focus on German Water Supplying Companies **536**

# Urban Rainwater Harvesting System: Possible Application for Car Washing

L. Andjelic\*, N. Andjelic\*\*, N. Jacimovic\*\*\*, S. Petkovic\*, M. Pavlovic\* and D. Vlajic\*

\* Mining Institute I.t.d., Batajnicket put 2, 11080 Belgrade, Serbia (E-mails: *lazar.andjelic@ribeograd.ac.rs*; *lazar.andjelic84@gmail.com*)

\*\* Energoprojekt - ENTEL, Boulevard Mihaila Pupina 12, 11080 Belgrade, Serbia

\*\*\* Faculty of Civil Engineering, University of Belgrade, Boulevard Kralja Aleksandra 73, 11000 Belgrade, Serbia

## Abstract

Rainwater harvesting (RWH) is the collection of rainwater runoff for use. Runoff can be collected from roofs, streets, parking lots and all other impermeable areas. That kind of collected runoff is stored, and then it can be used for a range of non-potable purposes, for example, flushing toilets, washing machines, irrigation etc. In this paper is examined possibility to use rainwater harvesting system for washing cars. The examination was done for a period of five years, between 2013 and 2017, for two different impermeable areas: building rooftop, and parking lot. In both areas, different size of storage tank was set. In results are shown graphic view of water level in tanks. In conclusion is explained for what this kind of examination can be used, and what are the possibilities for using rainwater runoff.

## Keywords

Rainwater harvesting; RWH; runoff; precipitation; car washing; rooftop; parking lot

## INTRODUCTION

Rainwater harvesting (RWH) is the collection of rainwater runoff for use. Runoff can be collected from roofs and other impermeable areas, stored, treated (where required) and then used as a supply of water for domestic, commercial, industrial and/or institutional properties. The collected water can generally be used for a range of non-potable purposes, such as flushing toilets, washing machines (which may require adaptation) and for external uses such as car washing and irrigation (Woods Ballard et. al., 2015).

### Rainwater harvesting (RWH) system

Rainwater Harvesting (RWH) is probably the most ancient practice in use in the world to cope with water supply needs. In recent decades, as a result of new technological possibilities, many countries are supporting updated implementation of such practice to address the increase in water demand pressures associated with climatic, environmental and societal changes (Amos et al., 2016).

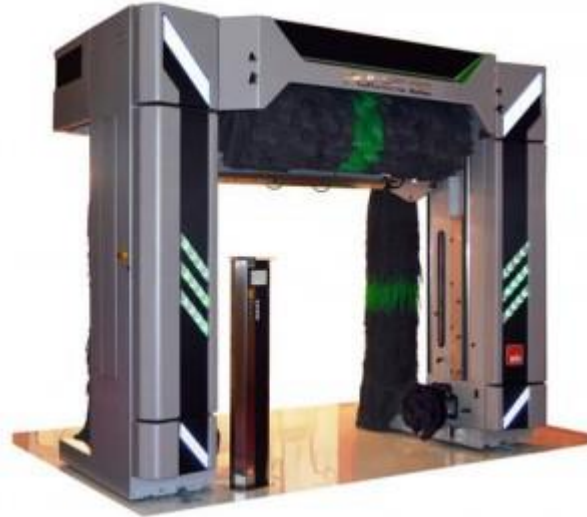
In urban areas, RWH consists of the concentration, collection, storage and treatment of rainwater from rooftops, terraces, courtyards, and other impervious building surfaces for on-site use. Civil uses of collected rainwater are disparate, but all aim to reduce consumption of drinking water from centrally supplied sources (Campisano et al., 2017).

GhaffarianHoseini et al. (2016) suggest these uses can globally account for 80-90 % of overall household water consumption, and highlight the significant water conservation benefits associated with RWH implementation. Consequently, installation of RWH systems increases water self-sufficiency of cities and can help delay the need to construct new centralized water infrastructures (Steffen et al., 2012).

## TESTING POSSIBLE APPLICATION OF RWH SYSTEM FOR CAR WASH

### Input data

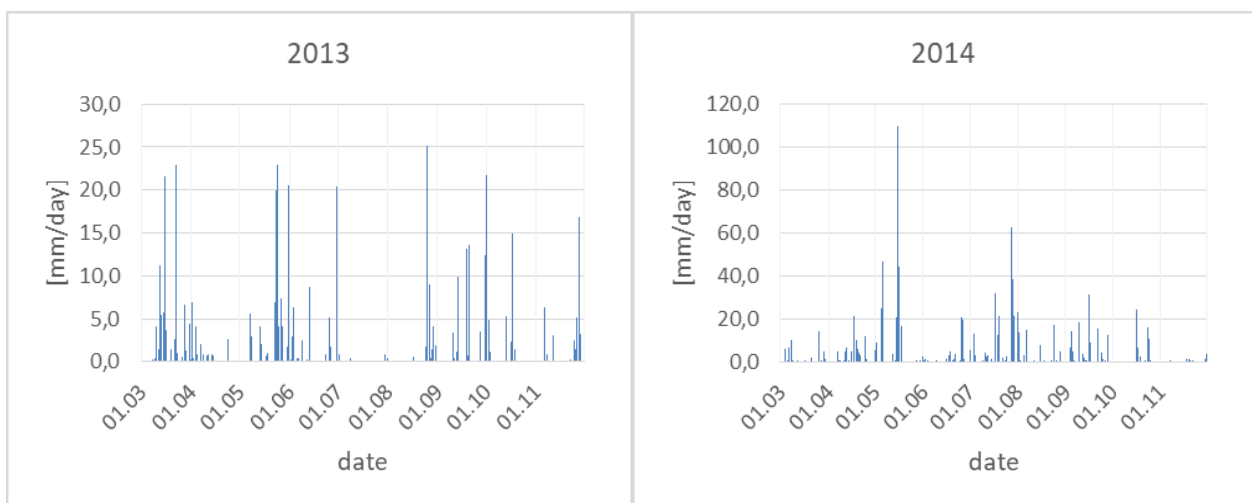
In this paper the application of RWH systems for car wash was examined for 2 different impermeable areas: rooftop of building with 20 apartments (cars) and parking lot for 100 cars. Based on research and experience, the assumption is that the required amount of water for washing one car is 200 l (0.2 m<sup>3</sup>). In this calculations, the system for automatic car washing is provided. The example of that kind of system for washing cars is shown in the Figure 1.



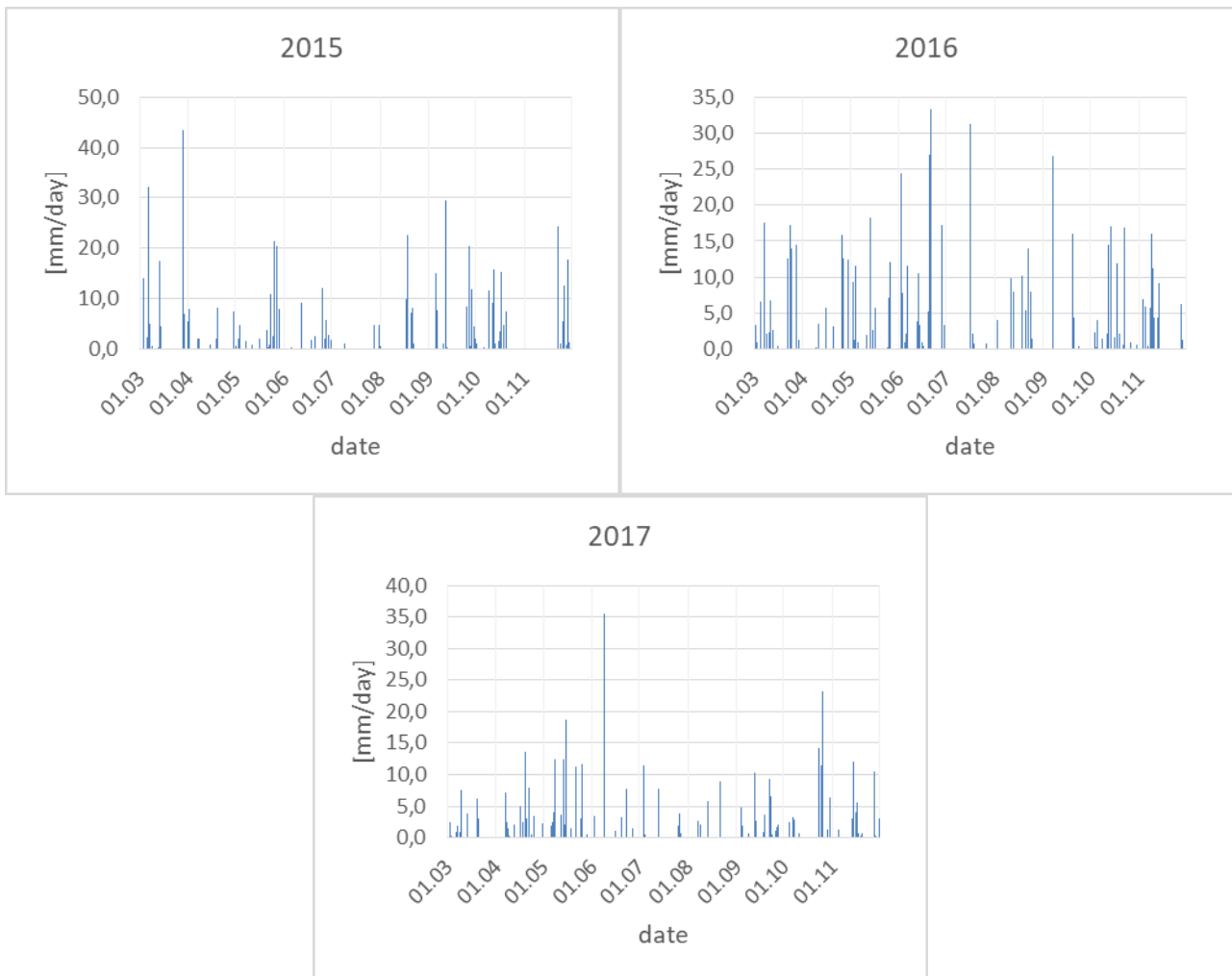
**Figure 1.** System for automatic car washing

The examination for this paper was done for a period of five years, between 2013 – 2017 year, for “non-winter season” (march – november), with real recorded precipitation in the urban area of Belgrade, Serbia. In Figure 2 are shown the graphic views of precipitation in period march-november, 2013 – 2017.

For this work, different volume of water tank was tested, and in this paper is presented the results for the tank that will not be empty for more than 10 consecutive days, during the examination period, for the adopted conditions.







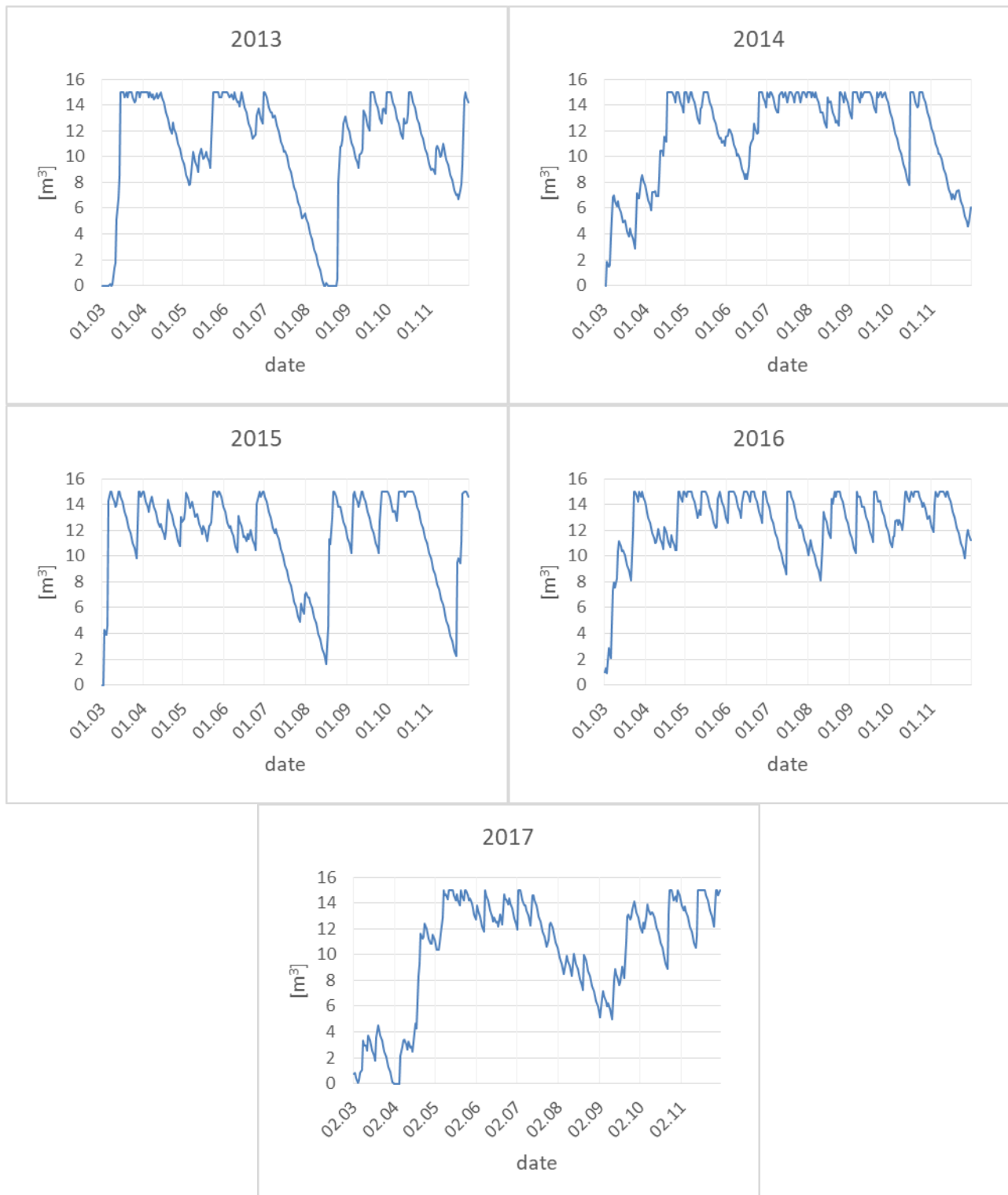
**Figure 2.** Daily recorded precipitation in the urban area of Belgrade, Serbia, for 2013 – 2017 year

Also, the assumption is that after the rain, more people will wash their cars, but the longer the drought period (period without rain), the smaller that number will be, so it was adopted for this paper that 10 % of all users wash their car every “dry” day (day without precipitation). It cannot be precisely predicted, but for this level of examination, it is good enough.

## Results

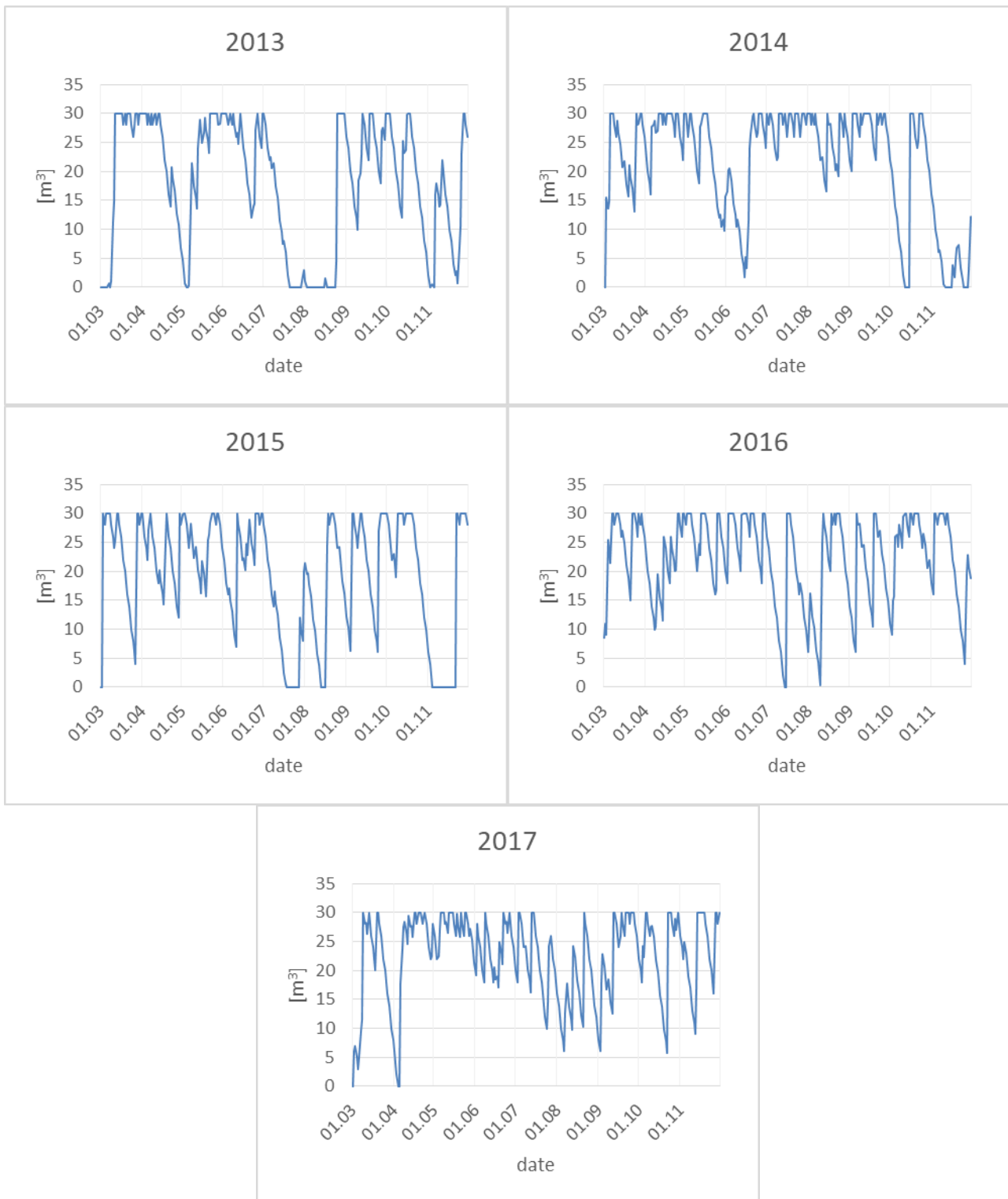
In this paper is shown that urban rainwater harvesting system can find good application for car washing. It is important to note, that in combination with other possibilities for using rainwater (irrigation, for example), the results could be much better, and the need for drinking water could be significantly reduced. As results, in this paper, is shown graphic view of water tank volume changing, for both cases of impermeable areas, during all five years. According the results, in the paper is given the recommendation for tank size for both cases.

For the first case, the rooftop of the building is 300 m<sup>2</sup>, and the volume of the tank is 15 m<sup>3</sup>. Number of the apartments in that kind of building is 20, so it was predicted that there is 20 cars. The volume of water for washing one car is 200l (0.2 m<sup>3</sup>), and according to an earlier assumption, it will be 2 cars washed every day without precipitation (0.4 m<sup>3</sup>). In Figure 3 is shown graphic preview of water level in tank for first case, for period 2013 – 2017 year.



**Figure 3.** Water level in tank – volume 15m<sup>3</sup> for building rooftop area for period 2013 – 2017 year

In second case, the parking lot is on the area of 2500 m<sup>2</sup>, and it is set for 100 cars. The volume of water for washing one car is 200l (0.2 m<sup>3</sup>), and according to an earlier assumption, it will be 10 cars washed every day without precipitation (2 m<sup>3</sup>). In Figure 4 is shown graphic preview of water level in tank for second case, parking lot for 100 cars, for period 2013 – 2017 year.



**Figure 4.** Water level in tank – volume 30m<sup>3</sup> for parking lot area (2500m<sup>2</sup>) for period 2013 – 2017 year

## CONCLUSION

Rainwater harvesting (RWH) is the collection of rainwater runoff for use. The collected water can generally be used for a range of non-potable purposes, such as flushing toilets, washing machines (which may require adaptation) and for external uses such as car washing and irrigation. In this paper the application of RWH systems for car wash was examined for 2 different impermeable

areas: rooftop of building with 20 apartments (cars) and parking lot for 100 cars.

As it is shown in graphic previews in results, predicted tanks are big enough for water storage and usage for car washing. It is important to note, that storage tanks are not too big, considering surface of area of rooftop and parking lot. Also, for using rainwater runoff in this purposes it is necessary to made some kind of water treatment, to remove all large and coarse particles.

This kind of examination, made for longer period, and for some specific location, can be used to predict volume and manage use of rainwater runoff in different purposes. Also, can be used to plan different kind of combinations for using the water from tank, not only for car washing.

Maybe one of the biggest advantages of setting this kind of system is that can be used for flood protection and also for protection from storm (big volume of rainwater in small period of time). Before predicted storm, or big rain, the tank can be emptied, by discharging water into the atmospheric sewer. Also, the tank can be made with permeable bottom, or sides, to slowly discharge water in the ground.

All of this mentioned are just some of the possible ways to use rainwater. The theme of this paper is possibility to use rainwater for car washing, and conclusion is that this is possible, this can reduce usage of clean, drinking water, it doesn't take up too much space, does not require too much construction work, and it is applicable in a large number of urban locations.

## REFERENCES

- Amos, C. C, Rahman, A, Gathanya, J. M. (2016) Economic analysis and feasibility of rainwater harvesting systems in urban and peri-urban environments: a review of the global situation with a special focus on Australia and Kenya, *Water*, **8**(4), 149.
- Campisano, A, Butler, D, Ward, S, Burns, J. M, Friedler, E., DeBusk, K., Fisher-Jeffes, N. L, Ghisi, E., Rahman, A., Furumai, H., Han, M. (2017) Urban rainwater harvesting systems: Research, implementation and future perspectives. *Water Research*, **115**, 195-209.
- GhaffarianHoseini, A., Tookey, J., GhaffarianHoseini, A., Yusoff, S. M., Hassan, N. B. (2016) State of the art of ranwater harvesting systems towards promoting green built environments: a review. *Desalinat. Water Treat.*, **57**(1), 95-104.
- Woods Ballard, B., Wilson, S., Udale-Clarke, H., Illman, S., Scott, T., Ashley, R., Kellagher, R. (2015) The SuDS Manual, CIRIA. ISBN: 978-0-86017-760-9.

## Application of SWMM Software Package for Management of Rainwater Drainage Systems of Urban Basins – Example of Drainage for Combined Cycle Power Plant

N. Andjelic\*, L. Andjelic\*\*, S. Ivanovic\* and R. Erić\*\*\*

\*"Energoprojekt – Entel", Boulevard Mihaila Pupina 12, 11070 Beolrade, Serbia ([nandjelic@ep-entel.com](mailto:nandjelic@ep-entel.com); [andjelic669@gmail.com](mailto:andjelic669@gmail.com))

\*\* Mining Institute I.t.d., Batajnicket put 2, 11080 Belgrade, Serbia

\*\*\* Faculty of Forestry, University of Belgrade, Knez Visoslav 1, 11030 Belgrade, Serbia

### Abstract

Nowadays, knowledge and using of software packages during the production and monitoring of condition of rainwater sewage at urban basins became very important and even necessary. EPA Storm Water Management Model (SWMM) is dynamic, physically based and conceptual model which serves for simulation of processes transformation of precipitation to flow, and which is based on the basic hydrodynamic laws. It can be used to simulate one happening or for continual simulation of flow quantity and quality, primary from urban basins. In this paper are shown possibility of application of this software package in domain of flow and rainwater sewage from urban basins with the example drainage at Combined Cycle Power Plant.

### Keywords

EPA Storm Water Management Model; SWMM; sewage model; atmospheric sewage; model

### INTRODUCTION (ABOUT SWMM)

The Storm Water Management Model (EPA SWMM) is a hydrologic and hydraulic model use to simulate flows in both storm water runoff and sanitary sewage (Martinez-Solano et al., 2016). It was developed by the United States Environmental Protection Agency, and it is a program that is able to solve the hydraulic equations of a network by using three different algorithms: steady flow, kinematic wave and dynamic wave (James et al., 2011). EPA Storm Water Management Model (SWMM) is dynamic, physically based model which simulate transformation process of precipitation to run off (Lewis and Rossman, 2010). This is conceptual model based on basic hydrodynamic laws (the law of energy conservation and the law of mass conservation). It can be used for simulation of one development or for continuous simulation run off quantity and quality.

It is primarily used for runoff simulations from urban catchments. Network design (Mays and Yen, 1975; Elimam et al., 1990), real time control (Van Nooijen and Kolechkina, 2013) are some examples of applications that require a hydraulic simulation of the sewerage network.

This model calculates the flow through collectors, nodes and objects network, for flow distribution to the system output nodes. The following objects are simulated in this way: collectors, overflows, openings and outflow objects. The system is idealized system as a set of links or pipes that are connected by nodes. Nodes are elements of a water retention system that, in a real physical system, correspond to manholes or pipe connections. Variables related to nodes are volume and piezometer levels. The primary dependent variable is the piezometer level. Inflows or input hydrographs, as well as output hydrographs, in the idealized network, are in nodes. The change in the nodes volume during the time step is the basis for calculations of piezometer levels and flows. Collectors are pipes or channels that transport water from upstream to downstream node of the system. The choice cross section is done by selection one of the program defined shapes.

SWMM program offers the choice of the calculation model. The choice is possible between steady-state, kinematic or dynamic wave models. It use Manning equation to define the relationship between flow ( $Q$ ), cross section area ( $A$ ), hydraulic radius ( $R$ ) and slope of opened and partially filled closed collectors.

## DESCRIPTION OF THE STORM WATER SEEAGE NETWORK CALCULATION

Pollution of atmospheric water depends on the pollution of surfaces through which they are drawn. Storm waters from the new roadways, roofs and plateaus shall be collected by a special network of closed collectors installed beneath the road which gravitate towards the cadastral parcel boundary line, and then towards the recipient.

Calculation of discharge of the atmospheric water is done for rain return period 5 years, duration of 20 min and, according to the data issued by the Republic Hydro-Meteorological Institute in Belgrade, amount of water is 145.70 l/s/ha.

Figure 1 shown layout and area organization within plant, which is base for calculation of discharge water amount. For every area, runoff coefficient is defining which is taken into account for calculations.



**Figure 1.** Area catchment within Power Plant

The amount of water is calculated as follows equation 1:

$$Q=A*I*\Psi/10000, \quad (1)$$

where Q - total outflow [l/s];  $\Psi$  - outflow coefficient (adopted outflow coefficient for asphalt surfaces is 0.85, for gravel 0.5 and 0.2 for grass); I - rain intensity [l/s/ha] for rainfall duration corresponding to the time of the concentration of the system for selected return period (145.7 l/s/ha); A - catchment area [m<sup>2</sup>].

Total amount of water collected by atmospheric sewage system within the Plant from different type of catchment areas is shown in the Table 1.

**Table 1.** Amount of water in depending of catchment type

Catchment type	Area [m <sup>2</sup> ]	Return Period [years]	Rain intensity [l/s/ha]	Runoff coefficient [-]	Flow [l/s]
Grass	2579.04	5	145.70	0.20	7.52
Gravel	789.94	5	145.70	0.50	5.75
Plain concrete	1089.48	5	145.70	0.85	13.49
Concrete tile	284.88	5	145.70	0.85	3.53
Roofs	6523.99	5	145.70	1.00	95.05
Roads	6284.86	5	145.70	0.85	77.83
<b>Total:</b>					<b>203.18 l/s</b>

Total amount of clean atmospheric water discharging in recipient is approximately 203 l/s. Atmospheric water collected by collector diameter of DN 200 mm to DN 500 mm with slope between 0.5 % and 1.5 %. The main collector, diameter DN 500 mm and slope of 0.5 %, discharge collected water out of CCPP boundary and towards to recipient.

### ATMOSPHERIC SEWAGE MODEL IN SWMM

The SWMM program provides a hydraulic calculation of atmospheric wastewater flow through a sewer system. A network of collectors and manholes has been entered.

The equations which are necessary for calculation are choose in the program. Velocity and pipe fill are calculated for every section using the Darcy - Weisbach/ Colebrook-White equation for the gravity flow of partially filled pipes (no flow under pressure), all based on the recommendations of the applicable. The equation 2 is:

$$V=(-2*\log(k/3.7/4/R+2.51*v/4/R/\sqrt{(2*g*4*R*Id)})*\sqrt{(2*g*4*R*I)}), \quad (2)$$

where V - flow rate for partially filled pipes [m / s]; g - gravitational acceleration [m/s<sup>2</sup>], g = 9.81 m/s<sup>2</sup>; R - hydraulic radius [m], R = A / O; A - area of broken cross section [m<sup>2</sup>], and O; O - bevelled volume [m]; I - pipe slope [m/m]; k - absolute pipe shortness, for PP and PVC pipes is k = 0.01mm; n - kinematic viscosity of water at a temperature of 10 ° C in m<sup>2</sup> / s.

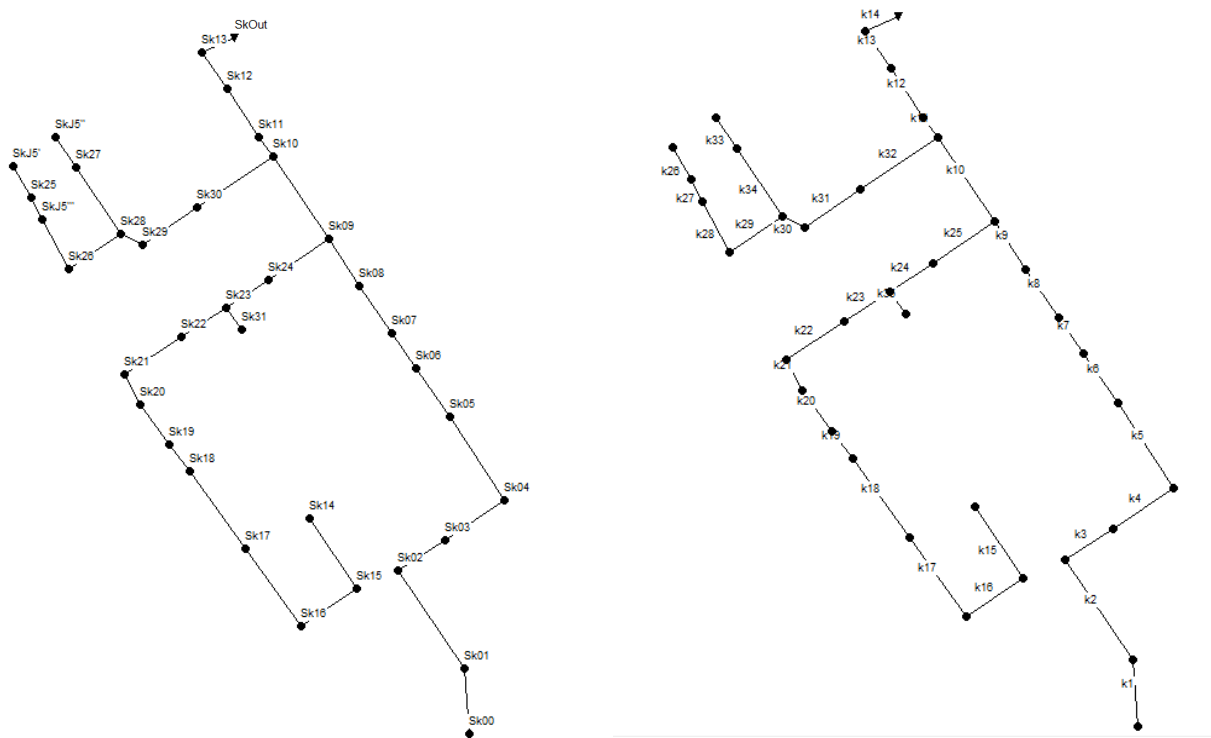
Hydraulic calculation is done using the Manning's equation 3:

$$Q=1/n*A*R^{2/3}*\sqrt{I}, \quad (3)$$

where Q - channel flow [m<sup>3</sup>/s]; n - Manning friction coefficient [sm<sup>-1/3</sup>].



The Figure 2 shows the model in the program. The picture on the left shows the nodes on the model (manholes), while the figure on the right shows the name of the sewer system collectors. This model consist 34 pipes and 35 nodes. The most downstream node (SkOut) represent outfall for discharge water to recipient.



**Figure 2.** Model in the program SWMM

When creating a model, the program requires defining the diameter, and the slope of the pipe. In addition to this information, each node introduces its inflow, which is calculated through the rational method, which is explained in the *DESCRIPTION OF THE STORM WATER SEWAGE NETWORK CALCULATION*. The surface runoff from the catchment areas, as well as the runoff from the roof surfaces of the facilities, was taken into account.

## RESULTS

After a successful calculation, the result can be presented as a diagram or as a table. Depending on the interest, the need for further analysis and the transparency of the results, the following are presented:

- For collectors – flow, velocity, depth (filling), capacity, beveled volume,
- For nodes – volume, depth, lateral or total inflow,
- For catchments – precipitation, evaporation, infiltration, discharge or
- Longitudinal section with filling of the collector network in every time.

After successes the calculation for the model of power plant is completed, the results are summarized within the tables, showing the flow, velocity and filling of each collector. The Table 2 shows the data on the collectors given in the model (diameter and length of the pipe), with the aforementioned data representing the result of the calculation (flow through the pipe, the velocity of the water in the pipe and the filling of the collector).



**Table 2.** Data on the collectors given in the model and results of calculation

Pipe number	Length	Diameter	Flow	Velocity	Depth
	[m]	[m]	[l/s]	[m/s]	[m]
k1	20	0.2	9.58	0.85	0.39
k2	36.85	0.2	9.57	0.84	0.39
k3	17.7	0.2	9.57	0.86	0.39
k4	21.8	0.2	17.89	1	0.55
k6	18.15	0.3	21.59	1.03	0.34
k7	12.95	0.3	30.19	1.13	0.4
k11	6.5	0.5	34.16	1.14	0.44
k12	17.45	0.5	42.73	1.22	0.5
k13	13.6	0.5	55.11	1.34	0.56
k14	2.32	0.5	151.71	1.73	0.46
k15	26.5	0.2	185.98	1.74	0.53
k16	20.5	0.2	193.59	1.83	0.52
k17	29.55	0.3	197.11	1.84	0.53
k18	29.8	0.3	202.68	1.73	0.57
k19	9.65	0.3	6.81	0.77	0.32
k20	14.85	0.3	59.56	1.76	0.48
k21	10	0.3	63.21	1.78	0.5
k22	21	0.3	66.29	1.8	0.52
k23	33.5	0.3	70.58	1.44	0.65
k24	15.5	0.3	87.35	1.95	0.61
k25	21.7	0.3	90.2	2.28	0.55
k26	10.3	0.2	1.68	0.45	0.13
k36	15.1	0.3	3.29	0.59	0.18
k37	21.7	0.3	6.26	0.73	0.28
k27	9.1	0.2	14.13	0.92	0.46
k28	17.6	0.2	23.62	1.38	0.5
k29	20.2	0.2	28.45	1.42	0.56
k30	6.78	0.2	31.64	1.45	0.6
k31	20.2	0.2	1.63	0.46	0.13
k32	28.3	0.2	3.19	0.56	0.18
k33	11.5	0.2	15.8	1.04	0.49
k34	25.3	0.2	59.56	1.76	0.48

In addition to the table view, SWMM provides the ability to view longitudinal profiles of atmospheric sewage model. By looking at the longitudinal profile at the critical moment of the calculation (when all the pipes are maximally filled), it can be concluded whether the network is satisfactory, ie whether the diameters and slopes of the collector adopted are sufficient to carry the required amount of water to the discharge. The Figures 3, 4 and 5 show the three most critical profiles in a given network, namely the pipelines between the collectors: Sk00- SkOut, Sk14- SkOut and SkJ5'- SkOut.

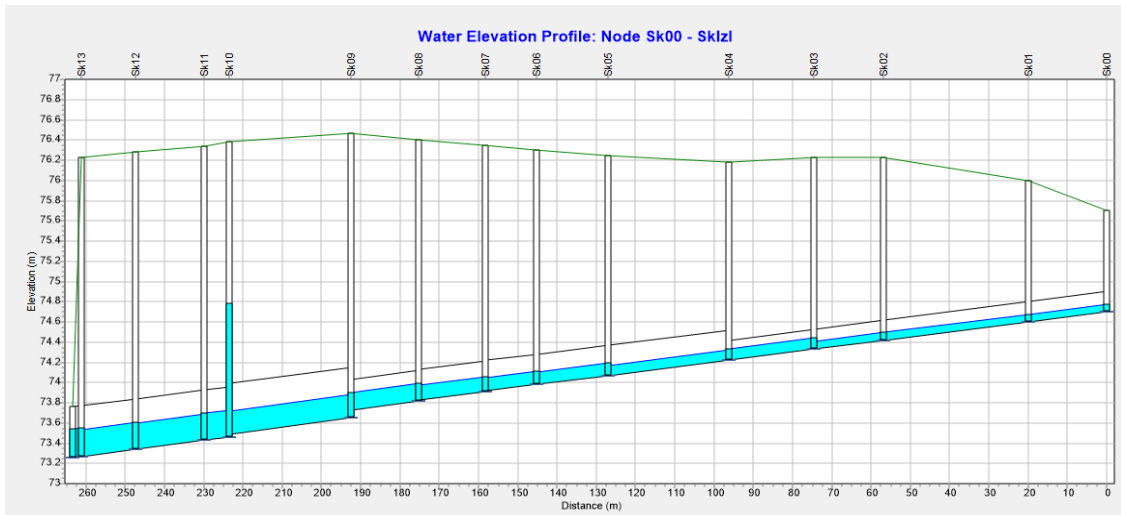


Figure 3. Longitudinal section from Sk00 to outfall SkOut

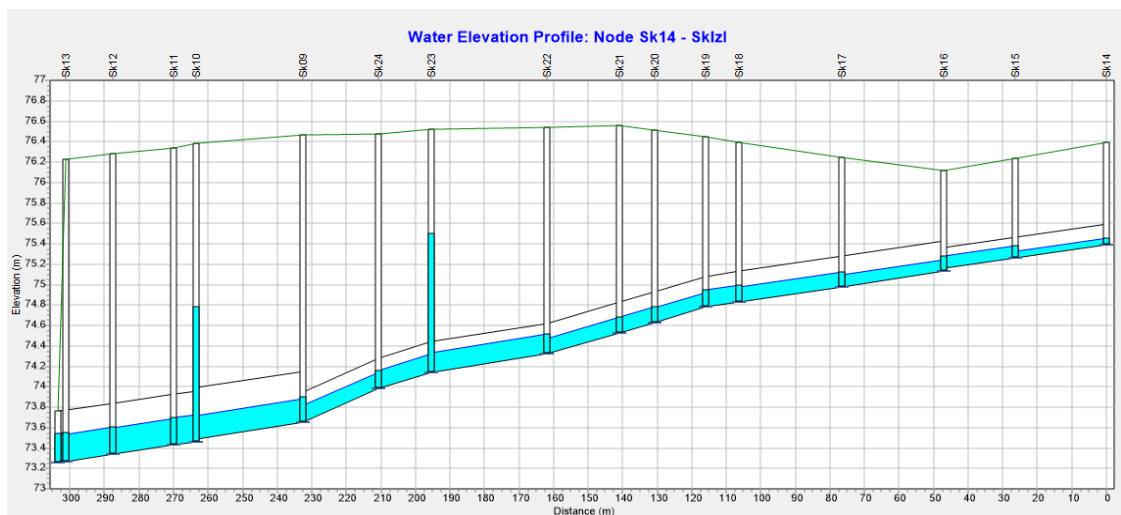


Figure 4. Longitudinal section from Sk14 to outfall SkOut

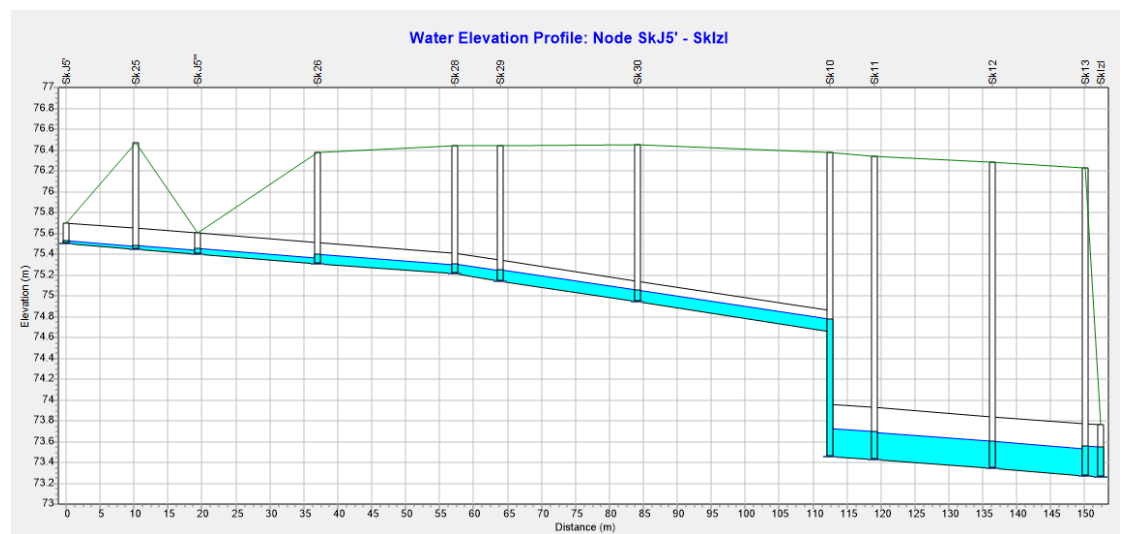


Figure 5. Longitudinal section from SkJ5' to outfall SkOut

The longitudinal sections show that there are no manholes with overflow, there is no pressure flow in the pipes and the network is dimensioned that all the water collected from the plant is drained and

discharged into the recipient.

## CONCLUSION

The Storm Water Management Model (EPA SWMM) is a hydrologic and hydraulic model use to simulate flows in both storm water runoff and sanitary sewage. This program can be used to calculate runoff mainly from urban areas, as well as to simulate flow through closed collectors and hydraulic flow calculation.

SWMM program offers the choice of the calculation model. The choice is possible between steady-state, kinematic or dynamic wave models. It use Manning equation to define the relationship between flows, cross section area, hydraulic radius and slope of opened and partially filled closed collectors. In this regard, in the program it is necessary to choose equations first and the model of the flow calculation through the collector network. After the calculation method is selected, the network geometry is set. For each pipe, a length, a cross-sectional view, and a slope (given through the start and end levels of the pipe) are specified.

The network modelled and presented in this paper consists 34 pipes, 35 nodes and outfall.

The results can be presented in the form of tables, graphs or with longitudinal sections at the most critical moment, when the pipes are most filled.

For the pipes, a table with all the data and calculation results is presented, as well as the three most critical action profiles. The calculation is stable and the results show that there are no manholes with overflow, there is no pressure flow in the pipes and the network is dimensioned that all the water collected from the plant is drained and discharged into the recipient.

## REFERENCES

- Elimam, A. A, Charalambous, C, Ghobrial, F. H. (1990) Optimum design of large sewer networks. *J. Environ. Eng.*, **115**, 1171-1190.
- James, W, Huber, W. C, Dickinson, R. E, Pitt, R. E, James, W. R. C, Roesner, L. A, Aldrich, J. A. (2011) User's guide to SWMM5-CHI Publications, 13<sup>th</sup> ed, CHI Water: Guelph, ON, Canada.
- Martinez-Solano, F. J, Iglesias-Rey, P. L, Saldarriaga, J. G, Vallejo, D. (2016) Creation of an SWMM toolkit for its application in urban drainage networks optimization. *Water*, **8**, 259.
- Mays, L. W, Yen, B. C. (1975) Optimal cost design of branched sewer systems. *Water Resour. Res.*, **11**, 37-47.
- Mijić, A. (2006) Implementation of SWMM software package for urban runoff modelling.
- Van Nooijen, R. R, Kolechkina, A. (2013) Speed of discrete optimization solvers for real time sewer control. *Urban Water J.*, **10**, 354-363.

# The Rapid Biological Assessment of Ecological Status of Arpa River (Armenia)

V. L. Asatryan\* and M. R. Dallakyan\*

\* Institute of Hydroecology and Ichthyology of SCZHE of NAS of RA, 7 P. Sevak str., 0014, Yerevan, Armenia (E-mails: [vardanasatryan@yahoo.com](mailto:vardanasatryan@yahoo.com); [dallakyan.marine@gmail.com](mailto:dallakyan.marine@gmail.com))

## Abstract

In accordance with the principles of EU Water Framework Directive (EU WFD), the decision 927-N of the Government of the Republic of Armenia (RA) has highlighted the necessity to ensure the ecologically balanced status, as well as the proper management and conservation of RA water resources. Baseline hydro-biological studies in the areas of 6 basin management areas (BMA) established in RA have been initiated since 2012. Current work completes the results of hydro-biologic baseline studies of ecological status conducted in the territory of Arpa River drainage basin which covers the biggest part of “Ararat BMA”. Rapid Biological Assessment methodology, developed for Armenia and 5 other Eastern European countries in accordance with the EU requirements was used and the results of assessments were mapped. Baseline study showed that only river mouth parts of Darb and Yeghegis tributaries as well as of Arpa River were not in compliance with the minimum requirement of EU WFD towards surface water bodies – to achieve “good” ecological status. Even though there were no parts where Rapid Biological Assessment score were the highest, but the ecological status of upper course parts of Yeghegis and Darb tributaries were corresponded to “high” quality. Also, it’s been shown that although the ecological status of river mouth part of Darb tributary was assessed as moderate, but it’s hardly affected the ecological status of Arpa River as even during the minimum flow period the ecological status of Arpa River was good after confluence with Darb tributary.

## Keywords

Arpa River; ecological status; rapid biological assessment; EU WFD; benthic macroinvertebrates

## INTRODUCTION

Following the principles of EU Water Framework Directive (EU WFD 2000/60/EC, 2000) the decision 927-N of the Government of the Republic of Armenia (RA) (Decision, 2011) has highlighted the necessity to ensure the ecologically balanced status, as well as the proper management and conservation of RA water resources. For that, 6 basin management areas (BMA) have been established in RA and baseline hydro-biological studies according to requirements of EU WFD have initiated since 2012. Biological assessments of ecological status are mainly addressing the cumulative impacts of all stressors, especially habitat degradation, and chemical contamination, which result in a loss of biological diversity. In order to make biological assessments more cost and time effective, various Rapid Biological Assessment (RBA) methods were developed (Barbour et al., 1999; Wright et al., 1993). But the most popular among that methods are the RBA’s based upon the benthic macroinvertebrate assemblages (Southerland and Stribling, 1995). The approach of assessing rivers’ ecological state based on its ecological components - specifically macroinvertebrates – is being testing in different river basins in Armenia (Fokkens et al., 2013), and Arpa River is one of the first studied areas.

Thus, the aim of this study was the baseline assessment of the ecological status of Arpa River using RBA method/index established for the needs of Armenia, Georgia, Azerbaijan, Belarus, Moldova and Ukraine according to EU WFD (Cheshmedjiev, 2013; Rapid, 2013). The advantages of chosen technique are as following:

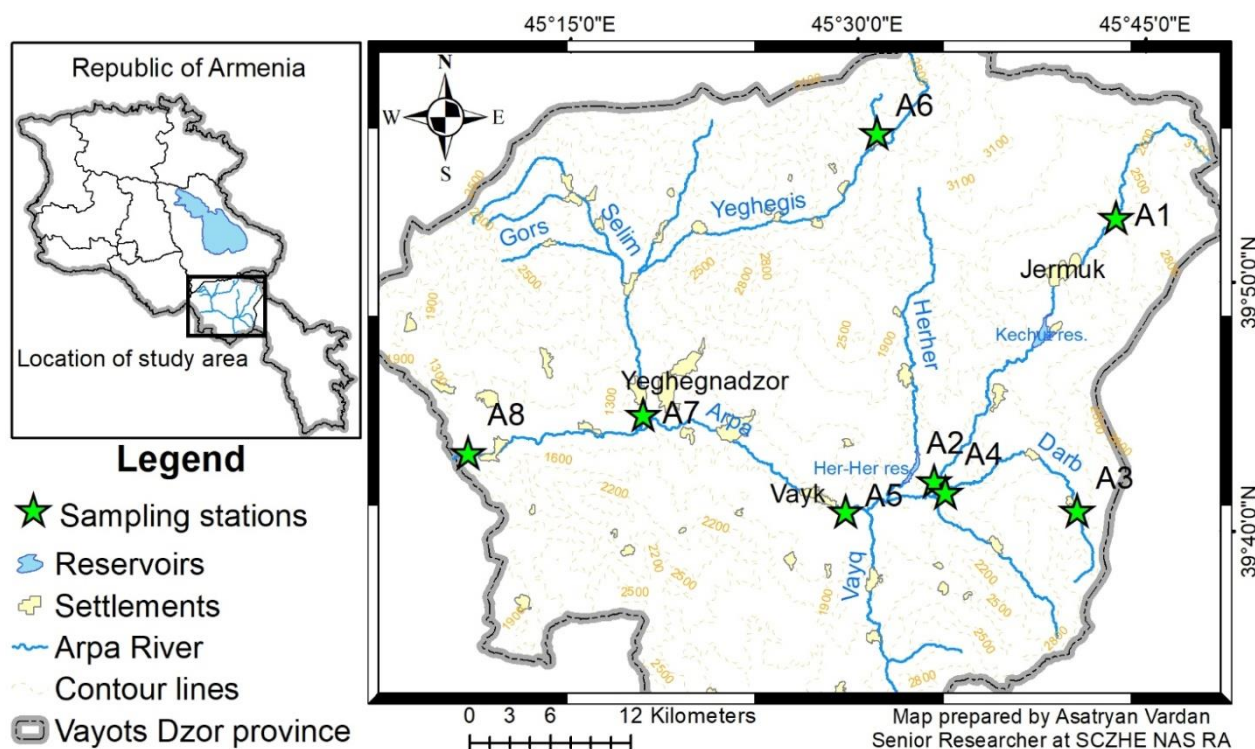
- cost-effective, scientifically valid procedures for biological surveys, risk assessment and integrated monitoring and assessment in compliance with WFD principles.
- Provisions for multiple site investigations in a field season
- Quick turn-around of results for management decisions.
- Monitoring and survey report easily translated to decision-makers/water managers and the public.

Arpa River is the largest river in Ararat BMA and the main water vein of Vayots Dzor region. Being transboundary river between RA and Azerbaijan it's intensively used for irrigation and production of electricity in the territory of RA. The study also shows that more than 80% of used in domestic and agricultural fields water is returning to the river (Sargsyan and Abrahamyan, 2007). The baseline study is of high importance because since 2016 the works on exploitation of gold ore mining site Amulsar has begun in the upper course part of the river and at the end of 2018 new government of Armenia has frozen the project to carry independent research of ecological status of the river and assess potential risks of further exploitation. Thus, the role of current study as a baseline assessment of ecological status of the river before Amulsar mining exploitation is of paramount importance. Also, since the end of the current study, 22 small hydropower plants (SHPP's) were established or planned to operate on the tributaries (National Statistical, 2018) and could seriously alter the structure of macrozoobenthos of the basin. Thus, the manuscript could also serve as a platform for assessments of changes in the structure of macrozoobenthos and ecological status of the river under the impact of SHPP operation. After the establishment of pilot BMO's in Armenia few studies related to biology and ecology of Arpa River were conducted based on phytoplankton, zooplankton and microbial communities (Hambaryan and Gevorgyan, 2019; Gevorgyan, 2017; Hayrapetyan et al., 2016) as well as hydro-chemical status (Gevorgyan et al., 2017; Pirumyan and Simonyan, 2016). Thus, the studies of the benthic-macroinvertebrates and the Rapid Biological Assessment of ecological status of Arpa River in the current period were carried out by us for the first time.

## **MATERIAL AND METHODS**

### **Study area and sampling sites**

Arpa River originates in North-West of Syunig plateau and southern slopes of Vardenis range, at an altitude of about 3050 m, then flows 92 km in the territory of Armenia and 36km in the territory of Azerbaijan (Nakhichevan Autonomus Republic) where confluence with Araks River on the border with Turkey. The drainage basin area is 2630 km<sup>2</sup> (Hydrology, 1981). Two relatively big water reservoirs are built in Arpa River – Kechut in the upper course part and Her-Her on the tributary. River flows through the gorge in the upper course part then through the wide valley in the middle course, and Araks plain in lower course parts. Major tributaries are Yeghegis, Darb and Her-Her. GIS analyses of its watershed show that the drop of elevations in the territory of Armenia is about 2100 m, thus, the average stream gradient is 22,8 ‰, which seriously contribute in self-purification potential of Arpa River in the upper and middle course parts. It feeds mainly by meltwater (57 %), which means that variations in extreme flows are huge – from 4 m<sup>3</sup>/sec to 136 m<sup>3</sup>/sec (Vardanian and Muradyan, 2014). Part of annual flow every year is being transported into Lake Sevan from Kechut reservoir by Arpa-Sevan hydro-technical tunnel. About 56000 people living in the drainage basin (National, 2018) and leaving their ecological footprint by consuming river ecosystem services like water for irrigation and electricity generation, fish farming, waste dumping and sewage discharge (Support, 2016). Sampling sites network (Figure 1) was included all parts of Arpa River and main tributaries which allows also to estimate their effects on the main river water quality.



**Figure 1.** The sampling sites of Arpi river basin

### Sampling procedure and ecological status assessment

Studies were conducted during summer seasons in 2012 and 2013 which coincides with minimum flow. This let us to carry sampling at all parts of river transect. Sampling was carried out using Surber sampler with the frame of 0.09m<sup>2</sup> and mesh size of 500µm in accordance with the EU standards (EN ISO 10870:2012; EN 16150:2012; AQEM Manual, 2002; Rosenberg et al., 1998). Samples were fixed in 96 % solution of ethanol and placed into a collection jar clearly marked with the sample geographical coordinates recorded by Garmin eTrex 20 GPS receiver and sampling date and time. Further processing of samples and determination was realized in the laboratory using the keys (Bestimmungshilfen-macrozoobenthos, 2010; Waringer and Graf, 2011; Taxonomie für die Praxis, 2010).

Relative abundance of benthic macroinvertebrates was assessed according to Cheshmedjiev (2013) (Table 1).

**Table 1.** Relative abundance of benthic macroinvertebrates (individual/m<sup>2</sup>)

Individual/m <sup>2</sup>	Relative Abundance
1-5	Few
6-20	Present
21-50	Common
51-100	Plantiful
100+	Dominant

Following RBA requirements, Hirudinea, Mollusca, Megaloptera, Ephemeroptera and Turbellaria taxa were identified to genera level and Oligochaeta, Crustacea, Plecoptera, Trichoptera, Odonata, Heteroptera, Coleoptera, Diptera taxa - to family level. Also, the tolerance groups (from the sensitive taxa (A group) to the most tolerant taxa (E group)) were considered according to Cheshmedjiev (2013). RBA was conducted by the following form (Table 2).

**Table 2.** Scheme of RBA of ecological status for Armenian BMAs

Indicator groups	N of taxa in the indicator group	Total number of taxa				
		0-1	2-5	6-10	11-15	≥16
		Ecological Status				
		Bad	Poor	Moderate	Good	High
		Value of RBA index (%)				
A (sensitive)	≥3	N/A	75	80	90	100
	2	N/A	60	75	80	95
	1	5	40	60	75	85
B (less sensitive)	≥4	N/A	40	60	75	80
	1-3	5	25	50	65	70
C (tolerant)	All above indicator groups absent	5	25	35	45	55
D (very tolerant)	All above indicator groups absent*	5	20	25	30	N/A
E (most tolerant)	All above indicator groups absent*	0	10	15	N/A	N/A

Note: \* few specimen of above indicator groups could present in the sample

Spatial interpolation of ecological status assessment by RBA method and mapping of the results was realized by ArcMap10.6 software.

In order to reveal quantitative changes in assemblage of benthic macro-invertebrates among different parts of the river Sorensen-Dice index (Concise, 2014) was used equation 1:

$$K = \frac{2J}{A+B}, \quad (1)$$

where J is the number of species common for both sites, A and B are the total number of species at each site.

## RESULTS AND DISCUSSION

The results of RBA showed that in general there are three parts which are not in compliance with the minimum requirements of EU WFD towards ecological status of surface water bodies: river mouth parts of the left left-hand tributary Darb (A4 station) and the right-hand tributary Yeghegis (A7 station) as well as the lower course part of Arpa River (A8 station). Spatial generalization of the results showed, that the main course of Arpa River was mainly corresponded to “good” ecological status. Both the parameters of total number of taxa and RBA was corresponded to high ecological status only in the upper course parts of Darb and Yeghegis tributaries, which were initially chosen as reference areas for the basin along with A1 station (Table 3). However, it was revealed that there was no part in the basin with the highest score of RBA, thus, A1 station initially chosen as reference site was not corresponding to that role in the scale of all basin.

Although, ecological status recorded at the lower course part of Darb (station A3) tributary was “moderate”, but the ecological status of Arpa river downstream from conjunction with Darb was “good”. This means that the negative effect of Darb on Arpa River is weak. The main reason for such “worsening of ecological status” of the tributary in the river mouth part could be the alteration of river regime through the operation of SHPP nearby as representatives of 3 “less sensitive” taxa were registered there, which prove the absence of strong pollution.

Stronger effect on Arpa River was revealed in case of Yeghegis tributary. The main economic activities in the basin of Yeghegis are hydroelectricity production, cattle farming and breeding, livestock grazing as well as crop harvesting and wine making. As there is no any water treatment plant in Yeghegis tributary basin, besides strong and regular alterations of hydrological parameters



of the river, all the wastewater and sewage discharges into the river, making water quality worse at lower course part (A6 station). Because Yeghegis has higher discharge than Darb, it's also contributed more in worsening of Arpa River ecological status after conjunction. The situation with Yeghegis tributary is the most worrying now, as many new SHPP's are being built on the tributary since the end of the studies and ecological transformations are already obvious (Gevorgyan, 2017).

**Table 3.** The structure of benthic community of the Arpa River basin and Indicator Groups (IG)

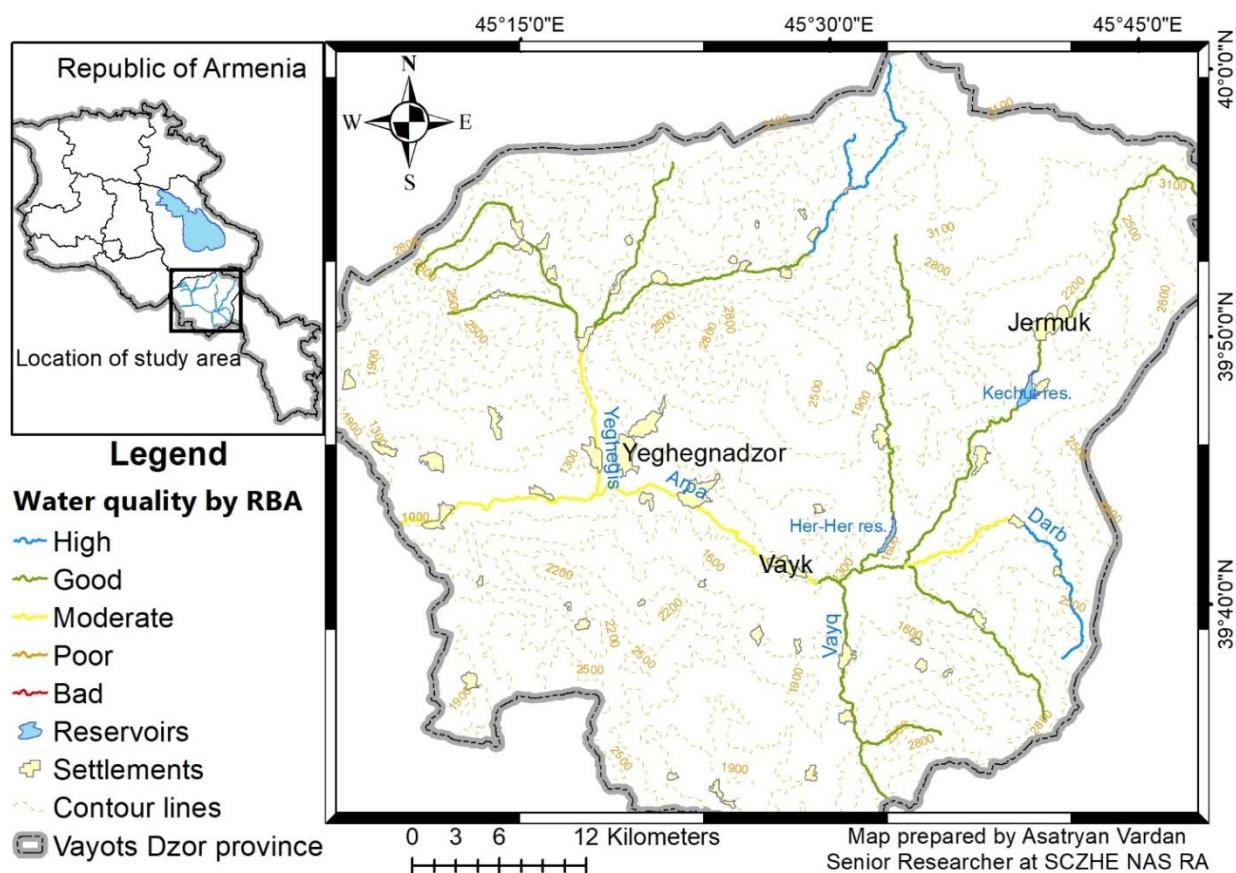
Order	Family	Genus	IG	A1	A2	A3	A4	A5	A6	A7	A8
Trichoptera	Lymnephilidae	Lymnephilus	B	53 <sup>+</sup>	6	7	8	2	2	2	0
Trichoptera	Rhyacophilidae	Rhyacophila	B	9	7	1	0	0	1	0	0
Trichoptera	Hydropsychidae	Hydropsyche	C	27	81 <sup>+</sup>	70 <sup>+</sup>	68 <sup>+</sup>	38	34	225 <sup>*</sup>	14
Ephemeroptera	Heptageniidae	Ecdyonurus	B	4	53 <sup>+</sup>	20	60 <sup>+</sup>	51 <sup>+</sup>	61 <sup>+</sup>	9	1
Ephemeroptera	Ephemerellidae	Ephemerella	B	2	9	43	6	33	0	16	5
Ephemeroptera	Caenidae	Caenis	C	0	1	0	5	0	0	4	12
Ephemeroptera	Baetidae	Baetis	C	344 <sup>*</sup>	122 <sup>*</sup>	63 <sup>+</sup>	28	23	28	6	1
Diptera	Chironomidae	-	D	651 <sup>*</sup>	102 <sup>*</sup>	4	7	115 <sup>*</sup>	1	415 <sup>*</sup>	73 <sup>+</sup>
Coleoptera	Helmidae	Helmis	C	14	6	209 <sup>*</sup>	7	3	40	1	0
Diptera	Athericidae	Atherix	B	0	0	0	0	0	9	0	0
Diptera	Simuliidae	-	C	5	30	57 <sup>+</sup>	13	0	0	2	1
Diptera	Tabanidae	Tabanus	C	1	0	1	0	0	1	0	0
Tricladida	Dugesidae	Dugesia	B	1	0	14	0	0	0	0	0
Plecoptera	Perlodea	Perloides	A	2	0	7	0	0	1	0	0
Diptera	Blephariceridae	Blepharocera	A	0	6	1	0	1	1	0	0
Gastropoda	Lymnaeidae	Lymnaea	D	0	0	0	0	14	0	0	0
Hygrophila	Planorbidae	Ancylus	C	0	0	1	0	1	0	0	0
Amphipoda	Gammaridae	Gammarus	C	0	0	7	0	0	0	0	0
Odonata	Aeshnidae	Aeshna	B	0	0	0	0	1	0	0	0
Total number of taxa				12	11	15	9	11	11	9	8
RBA				75	75	80	50	60	80	50	50

Note: \* - Dominant taxa, +-Plentiful taxa;

Not less important factor is uneven distribution of settlement system in the basin of Arpa River due to terrain. Particularly, the biggest part of population of the region live close to the lower course part of Arpa River and Yeghegis tributary in relatively lower altitudes. The intensity of agriculture in these parts are consequently higher.

The analysis of dominant groups of benthic macroinvertebrates at all stations on Arpa mother bad showed that there were no A (sensitive) or B (less sensitive) group representatives in the studied parts. The dominant taxa at all stations was represented by C (tolerant) or lesser groups. This means that pollution to some extent is present at all parts of the river.





**Figure 2.** Spatial interpolation of the results of ecological status assessment by RBA index

Sorensen-Dice index calculation has shown that the composition of benthic macroinvertebrates has not been dramatically changed along the river course and even between the parts where water quality has worsened by two categories (Tab. 4). However, the analysis of changes has revealed the main pattern of structural changes in the community of macrozoobenthos - sensitive and less sensitive taxa representatives have disappeared in lower course parts of both the river and its tributaries and only tolerant species have been registered. The most significant changes in the structure (by 58 %) was registered among A6 and A8 sites, where the difference in ecological status was also the highest. This also means, that the use of RBA method for the assessment of ecological status and its changes for Arpa River is efficient enough.

**Table 4.** Coincidence of species composition between sampling sites by Sorensen-Dice index (%)

Sampling site	A2	A3	A4	A5	A6	A7	A8
A1	78	88	76	60	78	76	60
A2		76	80	72	72	90	73
A3			66	69	76	66	52
A4				70	60	100	82
A5					63	70	52
A6						60	42
A7							82

In general, the comparisons of the results of baseline assessment of ecological status of Arpa River based on RBA method with the current works carried by different specialists has shown the worsening of both hydro-biological and hydro-chemical conditions nowadays, thus it could be valuable to start a new stage of studies in the basin based on RBA approaches.

## CONCLUSION

The baseline study of ecological status of Arpa River has shown, that before the exploitation of Amulsar mining site as well as the system of newly established SHPP's, there were no serious signs of pollution in the upper course parts of the river and its tributaries. The main sources of pollution – agriculture and domestic wastewater mainly threat the lower course parts of the river which at that period of time was not corresponded to “good” ecological status desirable for the Government of Armenia. As the main direction of economic development were changed in the region and newly established industries was spatially allocated mainly close to the upper course parts of the river, it can be expected to have the changes in ecological status of all the system of the river in a short time perspective and current work could strongly contribute in revealing of those changes. The issue is of high importance nowadays as the last studies based on different components of ecological state has already fixed the increased level of pollution in the basin (Hambaryan and Gevorgyan, 2019; Gevorgyan, 2017; Gevorgyan et al., 2017; Pirumyan and Simonyan, 2016). Also, it can be concluded that because of differences in discharge between Arpa River and its tributaries, as well as gradient of the river in the upper and middle course parts the negative effects of Darb tributary on water quality of Arpa River were weaker than its self-purification potential.

## REFERENCES

- AQEM Manual (2002) Manual for the application of the AQEM system. A comprehensive method to assess European streams using benthic macro invertebrates, developed for the purpose of the water framework directive, 202.
- Barbour, M. T., Gerritsen, J., Snyder, B. D., Stribling, J. B. (1999) Rapid Bioassessment Protocols for Use in Streams and Wadeable Rivers: Periphyton, Benthic Macroinvertebrates and Fish, Second Edition. EPA 841-B-99-002. U.S. Environmental Protection Agency; Office of Water; Washington, D.C
- Bestimmungshilfen-makrozoobenthos (1) (2010) LANUVArbeitsblatt 14, Landesamt für Natur, Umwelt und Verbraucherschutz Nordrhein-Westfalen (Auxiliary aid macrozoobenthos (1) LANUV Worksheet 14, State Agency for Nature, Collections and Protection of Consumer Rights of North Rhine-Westphalia, Germany.
- Cheshmedjiev, S. (2013). Rapid biological assessment (RBA) based on analysis of benthic macroinvertebrate communities. Environmental Protection of International River Basins Project, Hulla & Co. Human Dynamics KG, 22.
- Concise Encyclopedia of Bioinformatics & Computational Biology (2014) Attwood, T., Hancock, J.(ed.), Zvelebil, M.(ed.), 2nd Edition, John Wiley & Sons Ltd.
- Decision 927-N (2011) The Government of the Republic of Armenia from June 30, 2011.
- EN 16150:2012 (2012) Water quality– Guidance on pro-rata multi-habitat sampling of benthic macro-invertebrates from wadeable rivers. European Standard, Brussels, 16.
- EN ISO 10870:2012 (2012) Water quality — Guidelines for the selection of sampling methods and devices for benthic macroinvertebrates in fresh waters. European Standard, Brussels, 36.
- European Commission Directive 2000/60/EC (2000) The European Parliament and of the Council of 23 October 2000 establishing a framework for community action in the field of water policy. *Off. J. Eur. Communities*.
- Fokkens, B., Janes, M., Leummens, H., Rodriguez, I., Terrier, B. (2013) Towards river restoration in Armenia. Expert mission to the Arpa river basin, 24.
- Gevorgyan, G. A. (2017) Assessment of the sanitary-bacteriological state of the Arpa and Yeghegis rivers, Armenia. *Biol. Journal of Armenia*, 3(69), 47-51.
- Gevorgyan, G., Hayrapetyan, A., Mamyán, A., Gabrielyan, B. (2017) Hydroecological risk assessment of small hydropower plants operation in Armenia (Based on example of Vardenis,

- Karchaghbyur and Arpa rivers). *Eurasian-American journal of sustainable agriculture*, **11**(5), 59-67.
- Hambaryan, L. R., Gevorgyan, G. A. (2019) Investigations of formation phytoplankton community in the Arpa river (Armenia) and its main tributaries. *Proceedings of YSU, Chemistry and biology*, **53**(1), 46-52.
- Hayrapetyan, A. H., Bolotov, S. E., Gevorgyan, G. A., Gabrielyan, B. K. (2016) Investigation of different environmental factors role in the formation of zooplankton community in the Arpa river (Armenia) and its main tributaries. *Proceedings of the Yerevan State University*, **241**(3), 53-59.
- Hydrology of Armenian SSR, Ed. Baghdasaryan A. Arm SSR Academy of Sciences (1981) Yerevan, 175.
- National Statistical Service of Armenia (2018) Vayots Dzor Province.
- Pirumyan, G. P., Simonyan, A. G. (2016) Analysis of the ecological state of the river Arpa. *Science bulletin*, **2**(8), 44-49.
- Rapid Biological Assessment Protocols: An Introduction (2013) [online] <http://www.epa.gov/watertrain>.
- Rosenberg, M. D., Davies, J. ., Donald, C., Wiens P. A. (1998) Protocols for measuring biodiversity: Benthic Macroinvertebrates in Fresh Waters by. Canada: Report for the Ecological Monitoring and Assessment Network (EMAN) Biodiversity Science Board (BSB).
- Sargsyan, V. H., Abrahamyan, H. A. (2007) Assessment of economic activity on the minimal flow of Armenian rivers. *Proceedings of the NAS RA: Technical sciences*, **60**(3), 464-468.
- Support to SHPP-relating Reforms through the Dialogue of Public and RA Nature Protection Ministry for Sustainable Use of River Ecosystems (2016). Handbook, UNDP/GEF SGP, 39.
- Southerland, M. T, Stribling, J. B. (1995) Status of biological criteria development and implementation. Pages 81-96 in W.S. Davis and T.P. Simon (editors). *Biological assessment and criteria: Tools for water resource planning and decision making*. Lewis Publishers, Boca Raton, Florida.
- Taxonomie fur die Praxis (2010) Bestimmungshilfen-macrozoobenthos (1), Recklinghausen, 189.
- Vardanian, T. G., Muradyan, Z. Z. (2014) Peculiarities of extreme runoffs formation and changes dynamics in Arpa River basin. *Proceedings of Yerevan State University*, **1**, 32-37.
- Waringer, J., Graf, W. (2011) *Atlas of Central European Trichoptera Larvae*, 469.
- Wright, J. F., Furse, M. T., Armitage, P. D., (1993) RIVPACS - a technique for evaluating the biological quality of rivers in the UK. *European Water Pollution Control.*, **3**(4), 15-25.

# Fabrication and Characterization of Bipolar Membranes for Acid and Base Recovery

A. Celik\* and H. Hasar\*\*

\* Department of Environmental Engineering, Faculty of Engineering, Firat University, 23119-Elazığ, Turkey (E-mail: [aytekincelik23@gmail.com](mailto:aytekincelik23@gmail.com))

\*\* Department of Environmental Engineering, Faculty of Engineering, Firat University, 23119-Elazığ, Turkey (E-mail: [hhasar@firat.edu.tr](mailto:hhasar@firat.edu.tr))

## Abstract

In this study, characterizations of some bipolar membranes have been compared by considering different amine groups and membrane thickness. In total, 4 types of membranes produced which their electrical resistances were 6.45, 290, 8.7 and 25.65 ohm respectively. The initial water separation potentials of these membranes were 8.4, 31, 2.9 and 9.6V, respectively. Moreover, the thickness of these membranes were determined as 130, 290, 120 and 220 $\mu\text{m}$ , respectively. The result of the study showed that the single kind of amine group was more effective on the electrical resistance on the membrane compared to the mixed amine groups. Another result showed that membrane thickness was an important parameter in bipolar membranes.

## Keywords

Ionic membranes; membrane resistance; amine groups

## INTRODUCTION

Bipolar membrane (BM) consisting of cation and anion exchange layer can split water into  $\text{OH}^-$  and  $\text{H}^+$  ions at the intermediate layer under reverse bias conditions and directly convert organic salts into organic acids (Liu., 2014.; Hwang., 2016). When a direct electrical potential is applied, water molecules present in hydrophilic part between cation and anion exchange layers of bipolar membranes are split into  $\text{H}^+$  and  $\text{OH}^-$  ions. Anions and cations of salt solution passing through anion and cation exchange membranes combine with  $\text{H}^+$  and  $\text{OH}^-$  ions to produce a separate mixture of corresponding acid and base, respectively (Badruzzaman., 2009).

The basic working principle of bipolar membrane is the separation of water molecules under electrical field (Shee, vd. 2007). Separation of membrane water into hydrogen and hydroxyl ions by means of electrolyte solution due to electrical field effect (Amokrane vd. 1997). It is possible to produce acid and base salt from the salt without secondary salt pollution with bipolar membranes. It is therefore a technology that provides economic and environmental benefits.

Due to its benefits, electro dialysis bipolar membrane systems (EDBM) are used in the chemical, food, biochemical and environmental protection sectors. Bipolar membrane electro dialysis (BMED) is a method which has high efficiency to produce acid and base from the salt solution (Li et al. 2016). This process includes three types of membranes which are cation exchange, anion exchange and bipolar membranes. The BMED technique is an integration of bipolar membrane (BM) with conventional electro dialysis. Meanwhile, the BM comprises an anion-exchange layer, an intermediate catalytic layer, and a cation-exchange layer.

The aim of this study manufacture bipolar membranes and determine their electrical resistance and some properties

## **MATERIAL AND METHODS**

The polymers used in the study were polystyrene and Polychloromethylstyrene for anion exchange layer and the polybutadiene-co-styrene for cation exchange layer. The functional group bound to the cation exchange polymer of bipolar was the sulfone, while the functional group bound to the anion exchange polymer was triethylene amin and diamine propane. H<sub>2</sub>SO<sub>4</sub> was used as the sulfone source. And chloroform was used as the polymer solvent. While the bipolar membrane was formed, the cation exchange polymer layer was first cast and then the anion exchange polymer was poured onto it. It is then left in the oven at a certain temperature and left to the coagulation bath consisting of 0.1M NaCl solution.

### **Bipolar membrane pouring/casting system**

Flat sheet membrane casting system consist of micrometer adjustable film applicator and stand in the operation. Micrometer adjustable film applicator, sheen instruments which adjust the thickness and casting of the polymer, code 096114/25, 1117 / 200 mm blade was used. The stand which was made of glass placed on a 3cm thick Zehnter Zaa 2300 pulling mechanism. A magnetic stirrer, shaker, coagulation bath made of 30 L plastic in which the solvent was separated from the polymer and an oven were also used to provide operation at a certain temperature in this system.

### **Chemicals**

The chemical agents used during the study were N, N, N', N'-tetramethyl-1,3-propanediamine (Cas-no: 110-95-2), triethyl amine (Cas-no: 121-44-8) as the amine group and % 96 of 306657-encoded sulfuric acid as sulfone group. The polymers were polystyrene (Cas- no: 9003-50-4) for the anion-exchange membrane and poly (butadiene- co-styrene) (Cas-no: 9003-55-8) for the cation exchange membrane. In addition, solvents were chloroform (Cas- no 67-66-3), n, n-dimethyl form amide (Cas- no 68-12-2). Formaldehyde (Product No: F 3402), hydrochloric acid (Cas- No: 7647-01-0) zinc sulfate (Cas- no: 7546-85-7) were also used for the chloromethylation process. Methanol and distilled water were also used as washing solution.

### **Chloromethylation of Polymers**

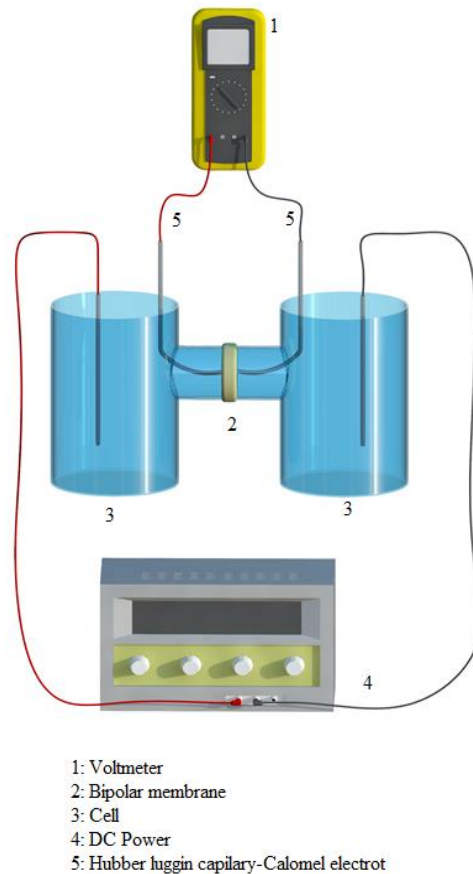
The polymer was first chloromethylated to fix a neutral polymeric anion exchanger group. In this study, chloromethylation was applied to polystyrene and polysulfone polymers were prepared as follows: 20 gr of polystyrene was first dissolved in chloroform, then 50 ml of formaldehyde + 50 ml of HCl and 5 gr of zinc sulfate were added as catalyst and the reaction was allowed at 60 °C for 3 hours. The mixture was then poured into methanol to precipitate the chloromethylated polymer and then the polymer was further purified by reprecipitation in chloroform. Finally, it was washed with pure water and left to dry at 80 °C

### **Sulfonation of Polymers**

Firstly, sulfone group was fixed to polymer which was prepared as follows: 10 g of poly (butadiene-co-styrene) and 50 ml of sulfuric acid were added to the glass bottle and the mixture was stirred at 60 ° C for 1 hour. Then this sulfonated polymer was washed with methanol and the excess sulfuric acid on the polymer was removed roughly to used in the preparation of the cation exchange membrane. The polymer was dried at 70 °C after washed several times with dimethyl form amide and finally washed with methanol and distilled water. Thus the sulfonated poly (butadiene-co-styrene) was prepared for dissolving in chloroform.

### Electrical resistance

The apparatus for calculating the electrical resistances of bipolar membranes was shown in Figure 1. The surface area of each membrane was  $12.56 \text{ cm}^2$ . The active surface area of each membrane used in the electro dialysis cell was  $64 \text{ cm}^2$ . In addition, two-part electro dialysis cell, two platinum-plated titanium electrodes, a calomel electrode, two Huber-luggin capillary, a voltmeter and a power supplier were used to read potential and to determine resistance between the membranes.



**Figure 1.** Electrical resistance determination system

### RESULTS

In this study, four types of bipolar membranes were produced. The membrane cation side 1 was composed of a 20 % polybutadiene-co-styrene anion side of 17 % polystyrene and polychloromethylstyrene mixture with NNNN diamine propane + trimethylamine. The difference of membrane 2 from membrane 1 was only thickness. The difference of membrane 3 from membrane 1 was the amine group, whereas the difference of membrane 4 from membrane 3 was only thickness. As the amine groups of membrane 1 and 2 were the same but the thicknesses were different, the electrical resistance of the membrane 1 was 6.45 ohm and the number 2 membrane was 290 ohms in Figure 2. Although the thickness of the membranes 1 and 3 were close electrical resistance of the membrane 1 was lower than 3 because of different amin groups.

**Table 1.** Characterization of bipolar membranes

Membran No	Anion groups	Thickness (mm)	Initial water separation potential (V)	Swelling (%)	Membran stress Mpa	Contact Angle
1	2ml NNNN diamin propan + 2ml trietilamin	0.13	8,4	18,4	786.52	68.93±0.29
2	2ml NNNN diamin propan + 2ml trietilamin	0.29	31	24,4	1271.34	64.69±0.93
3	4ml NNNN diamin propan	0.12	2,9	17,5	1076.46	67.61±0.23
4	4ml NNNN diamin propan	0.22	9.1	27	581.07	66.68±0.1

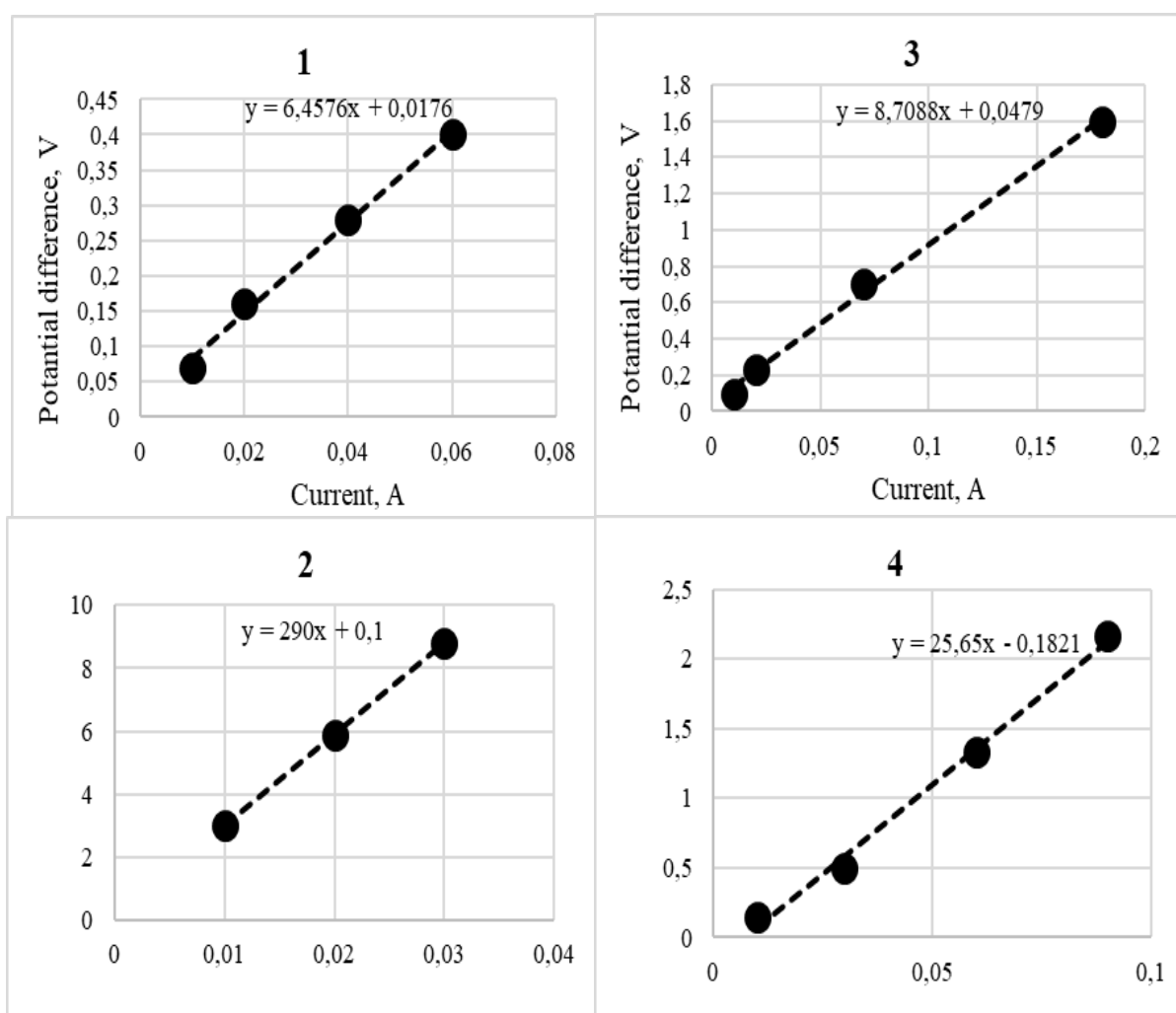
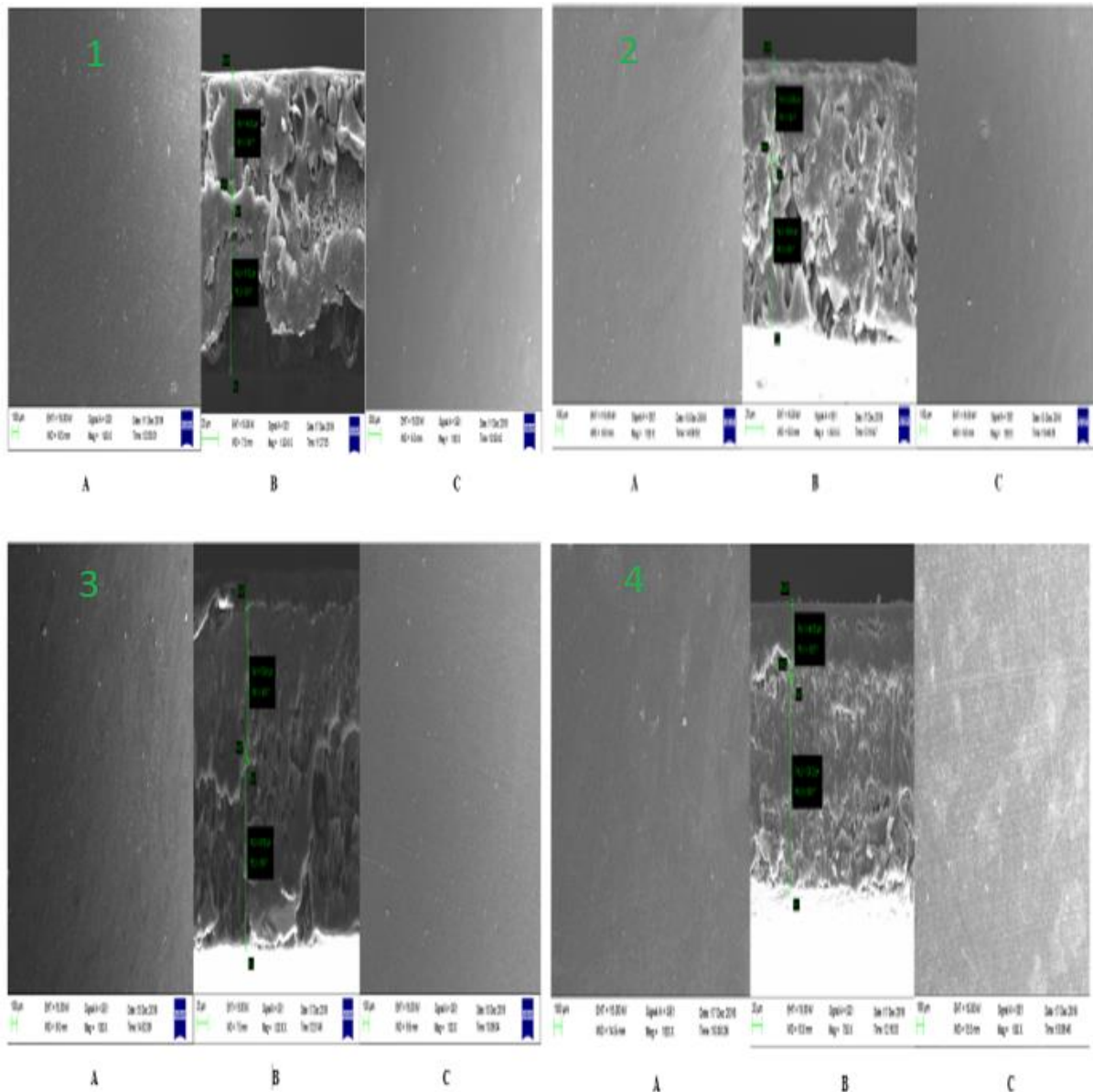
**Figure 2.** Electrical resistance of different bipolar membrane



Figure 3 showed SEM images of bipolar membranes. A showed the SEM images of the anion layer, B, the intermediate layer and C, the cation layer of the bipolar membrane in figure 3. When SEM images of membranes 1, 2, 3 and 4 were examined, it was understood that micro-nano level polymers did not dissolve in the membrane as general. In addition, these images showed that the membranes produced were not porous.



**Figure 3.** SEM images of Bipolar membranes

## REFERENCES

- Amokrane, A., Comel, C. ve Veron, J. (1997) Landfill Leachates Pretreatment by Coagulation-Flocculation. *Water Research*, **31**(11), 2775-2782.
- Badruzzaman, M., Oppenheimer, J., Adham, S., Kumar, M. (2009) Innovative beneficial reuse of reverse osmosis concentrate using bipolar membrane electrodialysis and electrochlorination processes. *J. Membr. Sci.*, **326**, 392-399.
- Hwang, U.-S., Choi, J.-H. (2009) Changes in the electrochemical characteristics of a bipolar membrane immersed in high concentration of alkaline solutions. *Sep. Purif. Technol.*, **48**, 16-23.



- Li, Y., Shi, S., Cao, H., Wu, X., Zhao, Z., Wang, L. (2016) Bipolar membrane electro dialysis for generation of hydrochloric acid and ammonia from simulated ammonium chloride wastewater. *Water Res.*, **89**, 201-209.
- Liu, G., Luo, H., Wang, H., Wang, B., Zhang, R., Chen, S. (2014) Malic acid production using a biological electro dialysis with bipolar membrane. *J. Membr. Sci.*, **471**, 179-184.
- Shee, F. L. T., Arul, J., Brunet, S. ve Bazinet, L., (2007) Chitosan solubilization by bipolar membrane electro acidification: Reduction of membrane fouling. *Journal of Membrane Science*, **290**, 29-35.

# Evaluation of the Impact of Residential Urban Patterns on Water Ecosystem Services in Federal District, Brazil

B. F. Costa\*, L. K. S. Brito\*\*, M. E. L. Costa\*\*, S. Koide\*\* and H. L. Roig\*

\* Geosciences Institute, University of Brasília, Darcy Ribeiro Campus, Asa Norte, Brasília, Federal District, Brazil (E-mails: [bferrazcosta@gmail.com](mailto:bferrazcosta@gmail.com); [roig@unb.br](mailto:roig@unb.br))

\*\* Department of Civil and Environmental Engineering University of Brasília, Darcy Ribeiro Campus, Asa Norte, Brasília, Federal District, Brazil (E-mails: [sanchesbrito.leticia@gmail.com](mailto:sanchesbrito.leticia@gmail.com); [mariaelisa@unb.br](mailto:mariaelisa@unb.br); [skoide@unb.br](mailto:skoide@unb.br))

## INTRODUCTION

The accelerated and large-scale urban growth leads to land use conversion and impacts on ecosystem services, which relationship between them depend on study area characteristics (Wang et al., 2019). Ecosystem services are the benefits obtained by people that are related to human well-being, whether directly or indirectly (MEA, 2005). By applying the concept of ecosystem services to the urban sphere, this paper analyzes how the Water Ecosystem Services (WES) is affected by the urbanization in residential areas. Including, stormwater runoff provides ecosystem services, as soil moisture, interflow, baseflow, groundwater recharge, and filtration of water through the environment (Roy et al., 2008; Burns et al., 2012; Barbosa et al., 2012; Walsh et al., 2016; Prudencio and Null, 2018).

Water management is one of the challenges of urbanization and land use policies have to defined in order to achieve sustainable urban development. Drainage is an interface between the occupation of urban space and stormwater runoff. Therefore, land use planning laws should be applied to guide urban development and this demand detailed data about the built environment (Lam and Conway, 2018). Mapping using urban morphology examines the urban fabric details, observing the layout of buildings, infrastructure, and green spaces. Then, Urban Structure Types (UST) are defined as areas with homogenous characteristics, which are distinguished in the built environment by a specific form of buildings and open spaces (Wickop, 1998). The USTs also are characterized by urban density, buildings structure and constructive materials, amount of green areas, and surface imperviousness and it is a good classification to evaluate the ecosystem in an urban environment.

The Federal District (FD) – Brazil characterized by intense and uncontrolled urban expansion and growing economic inequality, that is strongly reflected in absence of appropriated land use planning. Castro et al. (2019) developed tools to support decision-making in managing the land use and sustainable development of urban areas, considering 25 types of urban structure in FD, where the most extensive areas were Remaining Spaces (29 %), Green Spaces (10 %), Agricultural Spaces (9 %), Consolidation Areas of type SH1 (7.6 %), Community Equipment (6.7 %) and Residential Areas of type RH1 (5.9 %).

The purpose of this paper is to analyze the impact of urban residential patterns on water ecosystem services by using the Storm Water Management Model (SWMM) and the Urban Structures Types (UST) method, applied by GIS software. Thus, this study identified and systematized the interfaces between land use occupation at Riacho Fundo watershed in Brazil with 3 main groups of UST to provide for decision-makers with the scientific and technical knowledge required to develop an integrated urban water management strategy.

## MATERIAL AND METHODS

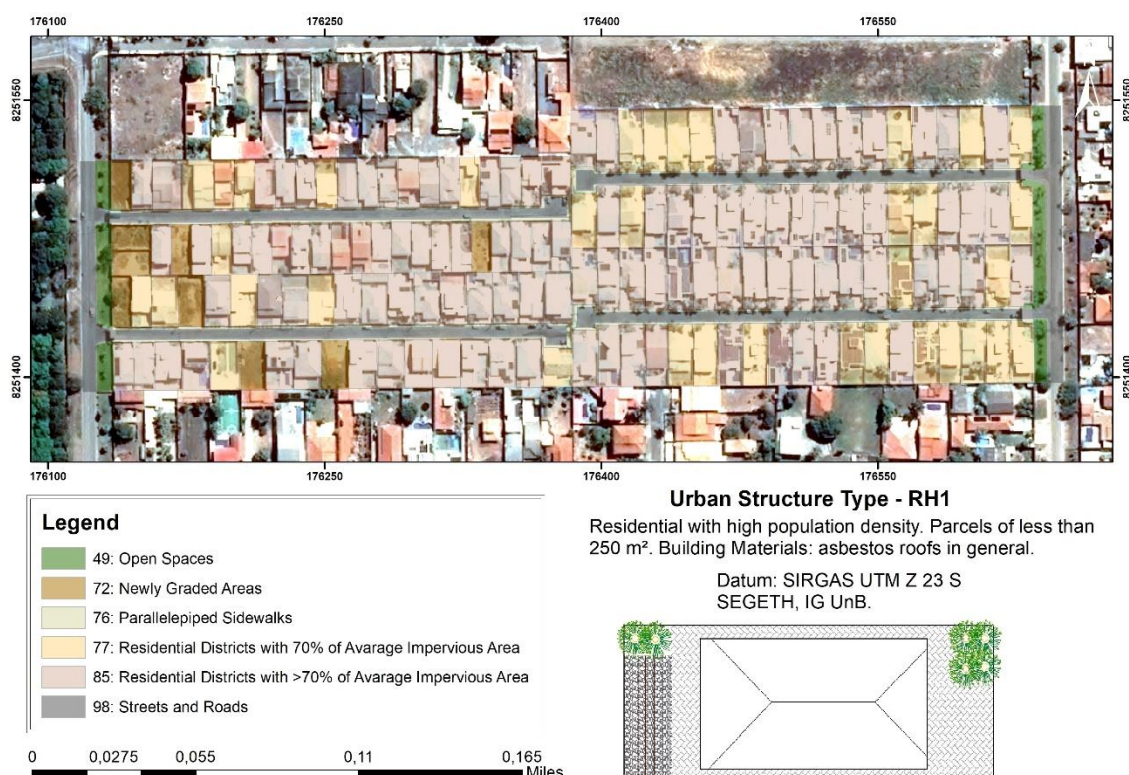
The study area is the Riacho Fundo watershed, situated in Paranoá river's basin, in the Federal District, Brazil. The watershed has 225.5 km<sup>2</sup> and is the most urbanized of the Lake Paranoá watershed (Mitsuko et al., 2019). In recent years, water resources availability is becoming critical, and thus preservation of water resources has extreme importance, therefore the evaluation of the impacts of urban morphology in ecosystem services such as groundwater recharge and infiltration is very relevant.

The climate of the study area is tropical, with two very defined seasons: very dry from May to September with low precipitation rates and high evaporation rates, and a rainy season between October and April, with storms with and very high rainfall intensity. The average annual precipitation varies in the range of 1,200 to 1,700 mm in a territory of about 6,000 km<sup>2</sup> (Fonseca et al., 2001).

The Riacho Fundo watershed major type of soil is Latossol, very permeable, with low silt content and high clay percentage. Even though the high clay percentage, Latossol has a different hydraulic behavior, due to its structure, it can be classified as a soil of group A, in USGS hidrological classification (Reatto et al., 2004; Carvalho et al., 2012).

For this article, some residential structure types are defined for this analysis and its characteristics are:

- RH1: high population density, units with residential parcels of less than 250 m<sup>2</sup> (Figure 1).
- RH5: low/medium population density, units with residential parcels with area between 1,000 and 2,000 m<sup>2</sup> (Figure 2).
- GS: green areas between urbanized areas. May have infrastructure like buildings and parking lots.



**Figure 1.** Schematic RH1 occupations and Curve Numbers

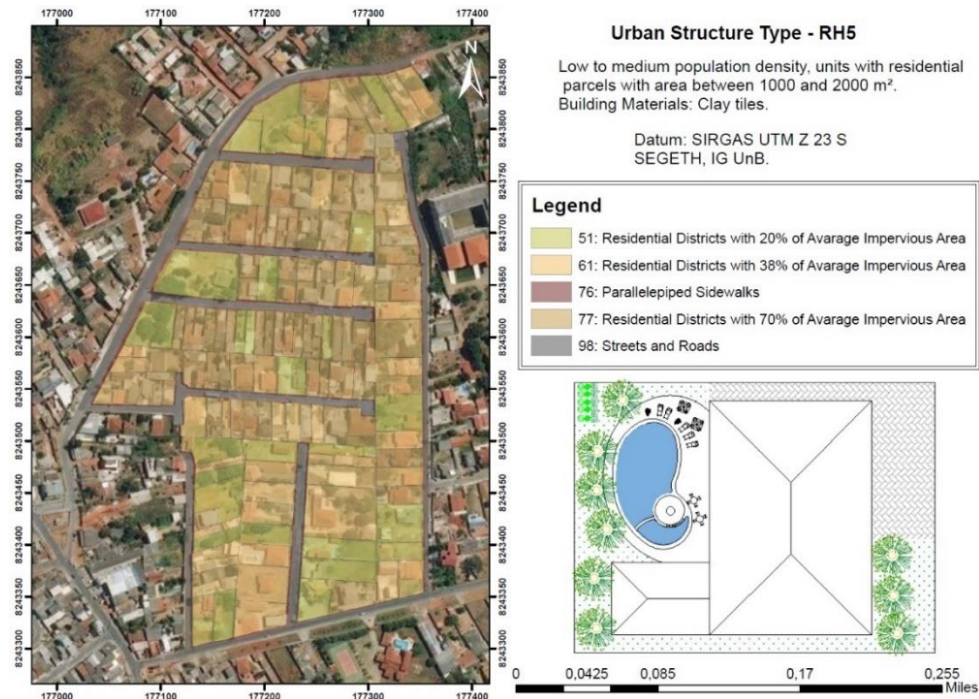


Figure 2. Schematic RH5 occupations and Curve Numbers

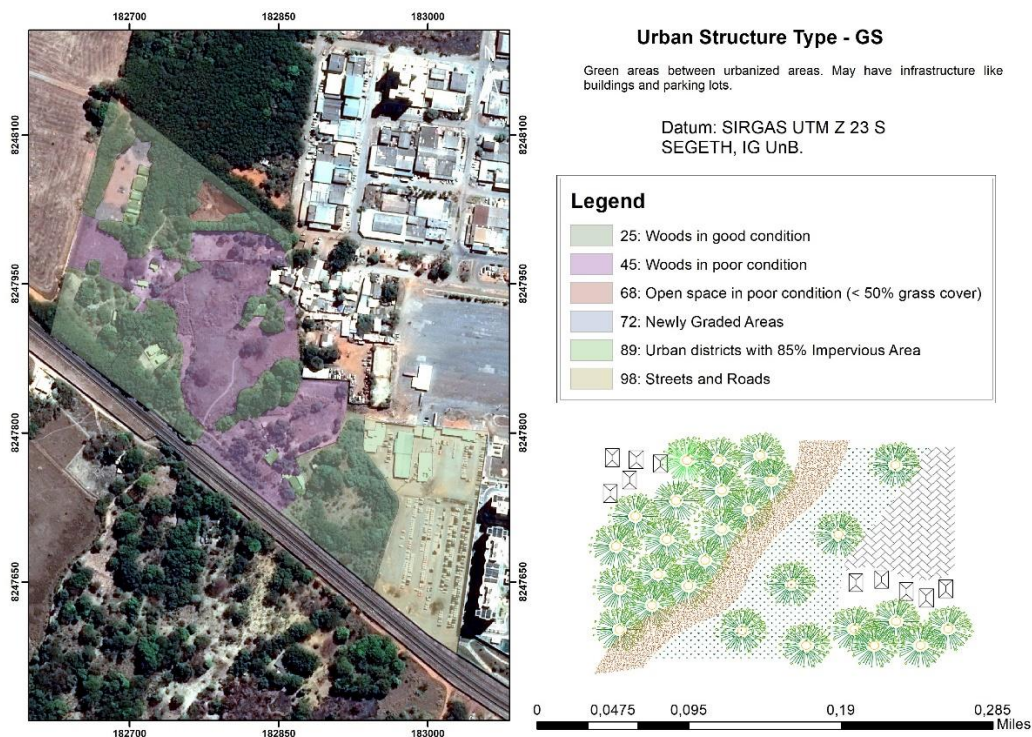


Figure 3. Schematic GS occupations and Curve Numbers

For the simulation on SWMM it was adopted a rectangular flat slope, similar to the original geomorphology of the study area. It was assumed a unitary rainfall with 24 hours of duration to simulate the infiltration and runoff index, calculated using the hydric balance. The infiltration was modeled with the SCS Curve Number method, and the CN adopted to each UST was 88.73 to RH1, 56.12 to RH5 and 41.73 to GS.

The runoff results obtained in this study allow the Aquifer Recharge Potential to be calculated



through two indicators: Maximum Soil Water Retention Capacity (S) and Potential Water Availability, using the methodology of Gonçalves et al., (2009).

The maximum soil water retention capacity (S), also expressed as soil saturation capacity, is influenced by the infiltration/runoff ratio. It is expressed in millimeters and can be obtained by the Equation 1:

$$S = 25400/X - 254, \quad (1)$$

where X is the runoff obtained in the SWMM method.

Potential water availability is given as a percentage, referring to the percentage of water that may be available for the recharge, and is calculated as the ratio between the value of S and the amount of millimeters of rainfall. Aquifer recharge potential is given as a percentage of the amount of available water that can be used for aquifer recharge, calculated by the multiplication between the potential water availability value and infiltration index, for each UST.

## RESULTS AND DISCUSSION

Based on the UST classification, three structural parameters can be determined: the amount of green and paved spaces, soil retention based on geomorphology and land use. These parameters were used to quantify the infiltration ecosystem service in each UST, to make a qualitative analysis.

Applying a unitary rainfall, with 1 cm per hour of intensity, for 24 hours (240 mm of rainfall), the results showed that RH5 has more infiltration potential than RH1. The hydric balance is showed in Table 1. Evapotranspiration was disregarded in this analysis.

**Table 1.** Hydric Balance and Infiltration Index for the studied USTs

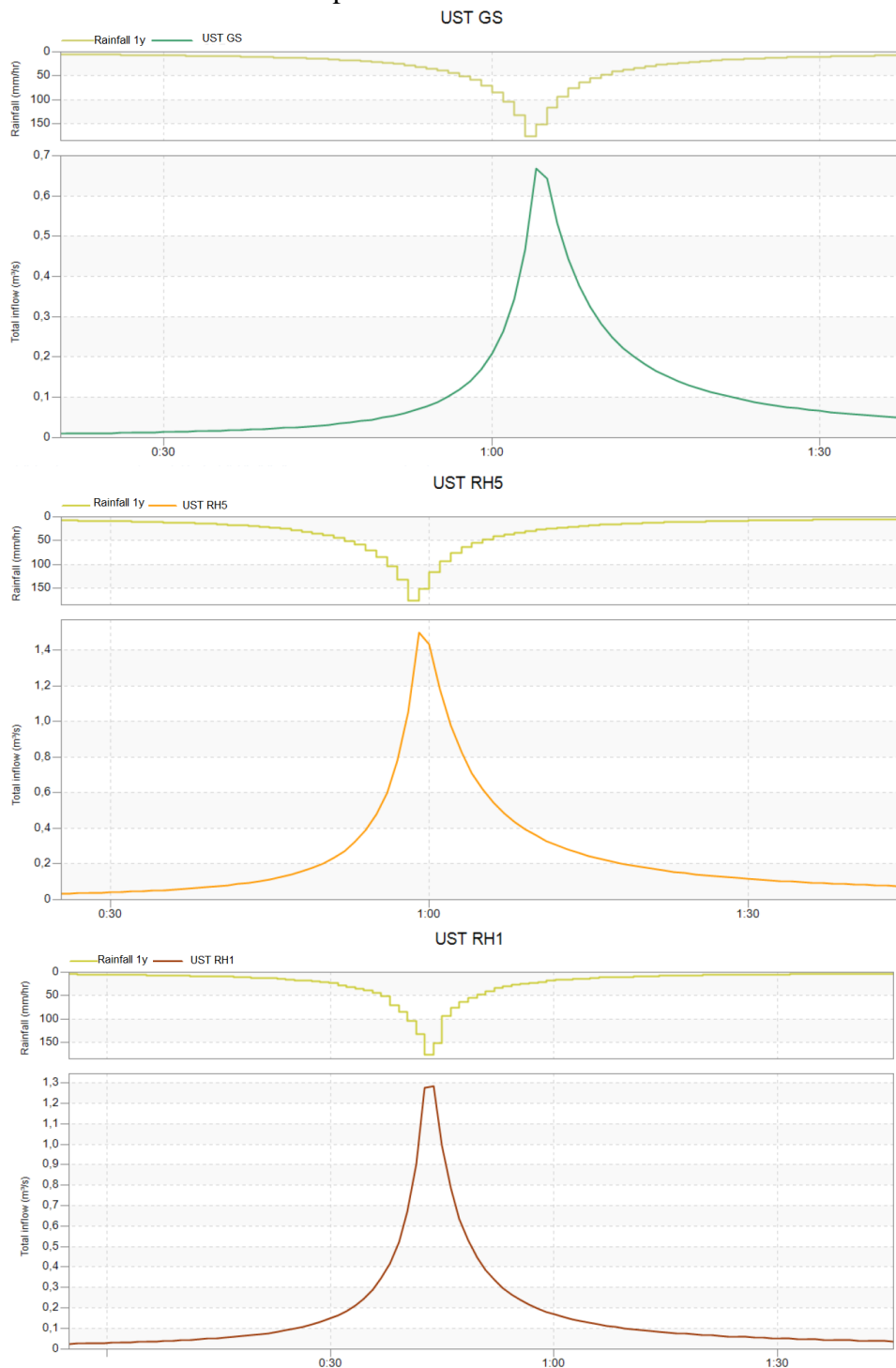
	Total Rainfall (mm)	Infiltration Loss (mm)	Runoff (mm)	Infiltration Index
UST Green Spaces (GS)	60.603	51.759	8.844	85.41 %
UST Residential Low Density (RH5)	60.603	46.434	14.169	76.62 %
UST Residential High Density (RH1)	60.603	21.054	39.549	34.74 %

The behavior of aquifer recharge potential, potential water availability and maximum soil water retention capacity followed the same logic: the higher the urban density, the lower the ecosystem service provided. Table 2 shows the results obtained for PWA and its indicators, calculated for each UST, using the runoff value from Table 1.

**Table 2.** Results for aquifer recharge potential, potential water availability and maximum soil water retention for each UST

	Aquifer Recharge Potential (%)	Potential Water Availability (%)	Maximum Soil Water Retention (mm)
UST Green Spaces (GS)	36.90	43.20	2618.00
UST Residential Low Density (RH5)	19.45	25.39	1538.65
UST Residential High Density (RH1)	2.23	6.40	388.24

The hydrographs presented in Figure 3, shows the magnitude difference of the runoff flow in each UST, with the same rainfall volume. The runoff rate of RH1 is almost the double of the rate in GS, due its high tax of imperviousness. The runoff rate of RH5, on the other hand is closer to GS, due its parcel size and minor allotment occupation tax.



**Figure 3.** Rainfall/Runoff response of the USTs

Regarding the allotment occupation in each UST, an analysis in a parcel scale can accurately more the functionality of the ecosystem services. The RH1 pattern is characterized by a smaller allotment area and higher building density. In the other side, RH5 has a bigger allotment area and a low-density occupation. This can be observed by the building characteristics material, allotments arrangement and the presence of improvements such as swimming pools and private gardens. The

presence of this improvements can also tell us about the socioeconomic characteristics of the UST formation.

Clearly building density affects directly the infiltration capacity. In regions that the urbanistic index (allotment permeability, front and side setbacks, building pattern) is more permissive, it is possible to have a situation which the allotment occupation is 100 %, and it doesn't have any permeable area. Here in Brazil, we have a lot of cases like that in many cities around the country. Rethink the allotment occupation and implementing green infrastructure in parcel or regional scale is a good instrument to re-establish the ecosystem services nearly urban development, and improve water quality and quantity. Besides that, the idea of Low Impact Development – LID applied a drainage system help to controls stormwater volume and timing, however they also promote ecosystem services, which are the benefits that ecosystems provide to humans (Prudencio and Null, 2018).

The UST RH5 allows water to infiltrate more easily than RH1, so in regions with a A or B hydrological soil group, and more sensitive to urban deployment, the UST RH5 is more indicated than RH1. The urban planners must predict before the installation of new building parcels, the best urban morphology that takes advantage of the basin natural conditions, such as geomorphology, soil, hillslope features and vegetation cover.

Conventional stormwater management directly routes runoff to nearby bodies of water through storm drains, gutters, and underground systems, reducing ecosystems services from stormwater (Roy et al., 2008) by reducing infiltration and groundwater recharge, and contaminating stormwater as runoff over impervious surfaces picks up pollutants such as heavy metals, suspended solids, nutrients, salts, oil and hydrocarbons (Tsihrintzis and Hamid, 1997).

Papers discussed ecosystem services, but less than 40 % quantified ecosystem services.

## CONCLUSIONS

We recommend that future research provide metrics and quantify ecosystem services, integrate disciplines to measure ecosystem services from green stormwater infrastructure, and better incorporate stormwater management into environmental policy. Our conclusions outline promising future research directions at the intersection of stormwater management and ecosystem services

## REFERENCES

- Barbosa, A. E., Fernandes, J. N., David, L. M. (2012) Key issues for sustainable urban stormwater management. *Water Res.*, **46**, 6787-98.
- Burns, M. J., Fletcher, T. D., Walsh, C. J., Hatt, B., Lason, T. (2012) Hydrologic shortcomings of conventional urban stormwater management and opportunities for reform. *Landscape Urban Plan.*, **105**, 230-40.
- Carvalho, J. C., Gitirana Jr, G. F. N., Carvalho, E. (2012) Infiltration Topics: Theory and practice applied to tropical soils. Technology College, University of Brasilia (UnB), Brazil.
- Castro, K. B., Roig, H., Rolim, M., Rossi, M., Paula, A., Réquia, W., Barbosa, A. B. C., Höfer, R. (2019) New perspectives in land use mapping based on urban morphology: A case study of the Federal District, Brazil. *Land Use Policy*, **87**. DOI: 10.1016/j.landusepol.2019.104032.
- Dobbs, C., Kendal, D., Nitschke, C. R. (2014) Multiple ecosystem services and disservices of the urban forest establishing their connections with landscape structure and sociodemographics.

*Ecological Indicators*, **43**, 44-55.

- Lam, S. T., Conway, T. M. (2018) Ecosystem services in urban land use planning policies: A case study of Ontario municipalities. *Land use policy*, **77**, 641-651.
- MEA, Millennium Ecosystem Assessment. (2005) Ecosystems and human well-being: current state and trends. Island Press, Washington, DC.
- Niazi, M., Nietch, C., Maghrebi, M., Jackson, N., Bennett, B., Tryby, M., Massoudieh, A. (2017) Storm Water Management Model: Performance Review and Gap Analysis. *J. Sustainable Water Built Environ.*, **3**(2):04017002, 1-32. DOI: 10.1061/JSWBAY.0000817.
- Prudencio, L., Null, S. E. (2018) Stormwater management and ecosystem services: a review. *Environ. Res. Lett.*, **13**, 033002.
- Reatto, A., Martins, E. D. S., Farias, M. F. R., da Silva, A. V., de Carvalho Júnior, O. A. (2004) Pedological digital map: Federal District scale 1: 100,000 and a explanatory text. Embrapa Cerrados-Documentos.
- Roy, A. H., Wenger, S. J., Fletcher, T. D., Walsh, C. J., Ladson, A. R., Shuster, W. D., Thurston, H. W., Brown, R. R. (2008) Impediments and solutions to sustainable, watershed-scale urban stormwater management: lessons from Australia and the United States. *Environ. Manage.*, **32**, 344-59.
- Tsuji, T. M., Costa, M. E. L., Koide, S. (2019) Diffuse pollution monitoring and modelling of small urban watershed in Brazil Cerrado. *Water Sci. Technol.*
- Walsh C. J. et al (2016) Principles for urban stormwater management to protect stream ecosystems. *Urban Streams Perspect.*, **35**, 398-411.
- Wang, J., Zhou, W., Pickett, S. T., Yu, W., Li, W. (2019) A multiscale analysis of urbanization effects on ecosystem services supply in an urban megaregion. *Science of The Total Environment*, **662**, 824-833.
- Wickop, E. (1998) Environmental Quality Targets for Urban Structural Units in Leipzig with a View to Sustainable Urban Development. In: J. Breuste, H. Feldmann, & O. Uhlmann (Eds.). *Urban Ecology* (Chap. 01, pp. 49-55). Springer-Verlag Berlin Heidelberg, New York.



# Patterns of Changes in Soil Moisture Content Depending on Agrolandscapes Structure in Southern Ukraine

Iu. Danylenko\* and V. Bohaienko\*\*

\* Institute of Water Problems and Land Reclamation of NAAS of Ukraine, Kyiv, Ukraine  
(E-mail: [iuliia.danylenko@gmail.com](mailto:iuliia.danylenko@gmail.com))

\*\* VM Glushkov Institute of Cybernetics of NAS of Ukraine, Kyiv, Ukraine  
(E-mail: [sevab@ukr.net](mailto:sevab@ukr.net))

## Abstract

In the paper, we study the impact of agrolandscapes components, particularly, shelterbelts on biomass response to soil moisture content for the arid conditions of southern Ukraine. Biomass and soil moisture content are determined by NDVI (Normalized Difference Vegetation Index) and VTCI (Vegetation Temperature Condition Index) spectral indices, correspondingly. Dependencies between soil moisture content and the values of VTCI index were obtained along with the dependencies between VTCI and NDVI. It is shown that, such relationships differ in time and with the change of biomass. The presented analysis shows NDVI and VTCI indices allow estimating the level of shelterbelts influence both in field and in regional scales.

## Keywords

Water management; soil moisture; remote sensing; agrolandscapes

## INTRODUCTION

Anthropogenic changes within catchment areas performed without considering the structure of landscapes have a negative impact on the restorative and self-regulating capacity of ecosystems, transformed agricultural and urban landscapes. Together with climate change, this causes a deterioration of the state of territories and increases aridization. Thus, it is highly important to study the principles of how agrolandscapes should be spatially organized and how their components influence the formation and distribution of water resources. Such principles can be considered in regional scale planning of agrolandscapes' development to minimize climatic and weather risks for local population and agricultural producers.

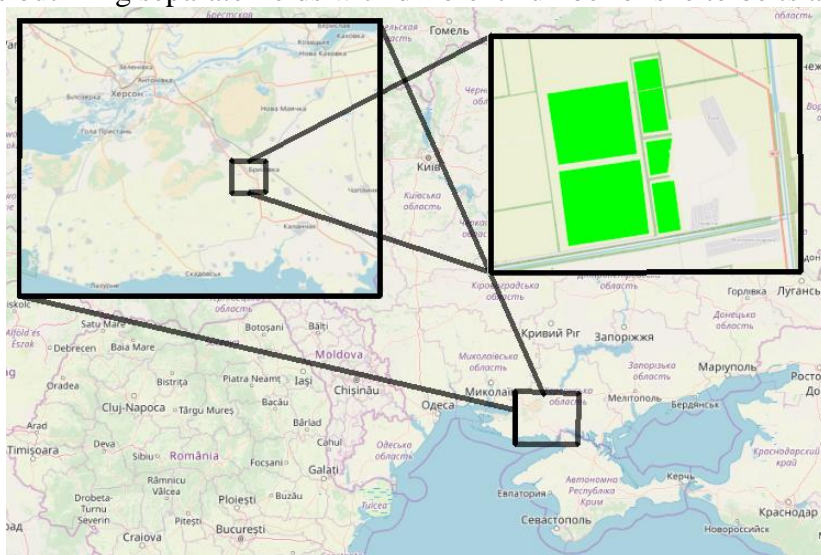
For the arid conditions of the south of Ukraine, irrigation and shelterbelts should be emphasized as the most influential components of agrolandscapes. Shelterbelts positively influence soil state and the formation of microclimate (Siryk, 1991). They help fighting against droughts and wind erosion of soils (Vysotsky, 1983), absorbs the surface water runoff protecting soil from water erosion, hinders the formation and growth of ravines and hollows (Zonn, 1959), improves the distribution of snow on fields (Logginov, 1949). Due to political and economic reasons, the development and study of protective forestry in the South of Ukraine was almost completely stopped within the last 25 years. Most of the published papers focus either on engineering effects in the small scale specific situations (e.g. Maliuga, 2012) or on theoretical aspects in the country scale (e.g. Stadnyk, 2004). The issue of medium scale agrolandscapes' influence on such an important for the South of Ukraine economic factor as soil moisture distribution remains poorly studied. Since the determination of statistical descriptions of shelterbelts' and irrigation's impacts requires a large amount of ground

measurements, the use of selectively verified remote sensing data is relevant. Indirect estimation of moisture content in the root layer of soil can be carried out using the data of passive remote sensing based on the hypothesis that the volume of moisture available to plants correlates with their biomass in the dry Steppe zone of Southern Ukraine. Currently, studies on establishing such correlations between moisture content and vegetation indices (Lui and Kogan, 1996; Farrar et al., 1994), in particular NDVI (Normalized Difference Vegetation Index) and EVI (Enhanced Vegetation Index), are fairly widespread (Wang et al., 2007). The means of active remote sensing also permit estimating soil moisture content due to its influence on soil dielectric properties (Jackson et al., 1995; Sahebi et al., 2004; Yu and Zhao, 2011). Another type of methods, the so-called drought indices, are aimed at the determining the state of drought (Zargar et al., 2011) and, thus, indirectly, soil moisture content. Among the indices that combine information of different physical meaning there are temperature vegetation index (Deering et al., 1975), temperature vegetation dryness index (Sandholt et al., 2002), and vegetation temperature condition index (Wang et al., 2001).

Within the above-mentioned broader context, we study the impact of shelterbelts and irrigation on soil moisture distribution. The main goal of the presented study is to analyze differences between how moisture content and biomass are spatially interconnected on agricultural lands in Southern Ukraine depending on the saturation by shelterbelts and irrigation; and to obtain the corresponding relationships that can be further used to optimize the structure of forest plantings in regional scale. We use remote sensing to assess biomass by NDVI index and to assess soil moisture content by VTCI index.

## AREA OF STUDY

Field studies were conducted in 2018 on the fields of the State Enterprise “DG Brylivske” located in the Kherson region of Ukraine (Figure 1). Annual precipitation in the area of study is equal to 300 - 450 mm. The vegetation season accounts for 2/3 of annual rainfall that often occurs in the form of showers accompanied by hails and storms. The hydrothermal coefficient of the territory is about 0.7. Almost annually, there are significant periods without precipitation. In average, once per two years, such periods last more than 40 days leading to soil droughts. Soil moisture measurements were carried out using a portable MG-44 device on irrigated and non-irrigated fields in points organized as a grid. Irrigation in the area of study is performed using center pivot irrigation machines. Further, we made a survey of the structural components of agrolandscapes for the fields of the farm and neighboring fields outlining separate fields with different number of shelterbelts around it.



**Figure 1.** Area of study

## SOIL MOISTURE CONTENT ASSESSMENT USING REMOTE SENSING

To assess soil moisture content we use Vegetation Temperature Condition Index (VTCI) (Wang et.al, 2001) which can be considered as a generalization of the Temperature Vegetation Dryness Index (TVDI) (Sandholt et al., 2002) and combines the assessments of surface temperature and biomass state. We calculate the values of VTCI index using the images acquired by the Landsat-8 satellite.

VTCI index (Wang et.al, 2001) values are calculated upon the following formula:

$$VTCI=(a+bNDVI- T_s)/(a+bNDVI- a'-b'NDVI), \quad (1)$$

where  $T_s$  is the temperature of surface,  $a+bNDVI$  is the linear dependency of the maximal surface temperature for a fixed value of NDVI from NDVI,  $a'+b'NDVI$  is the linear dependency of the minimal surface temperature for a fixed value of NDVI from NDVI; NDVI is a value of the Normalized Difference Vegetation Index.

The linear dependencies present in formula (1) are calculated manually based on the distribution graph of the NDVI values and the surface temperature within the studied area. The quality of computation of their coefficients significantly influence absolute values of the VTCI index while maintaining the following general tendency: at a fixed level of biomass, considering that the evaporation is directly proportional to soil moisture content and is the main factor of the surface temperature changes, the higher surface temperature means less evaporation and, accordingly, lesser moisture content and lesser VTCI values. The values of the VTCI index was calculated using the Landsat-8 satellite images with a spatial resolution of 30 m for the bands needed to calculate the NDVI index and 60 m for the bands needed to calculate surface temperature. Such a resolution allows evaluating moisture content within a specific field and, to a certain extent, to capture the influence of agrolandscape components on it.

We calculate NDVI as  $NDVI=(b5-b4)/(b5+b4)$  where  $b5$  and  $b4$  are digital numbers from 5-th and 4-th bands of Landsat-8 image. Land surface temperature was calculated according to the algorithm used in Anandababu et al., 2018.

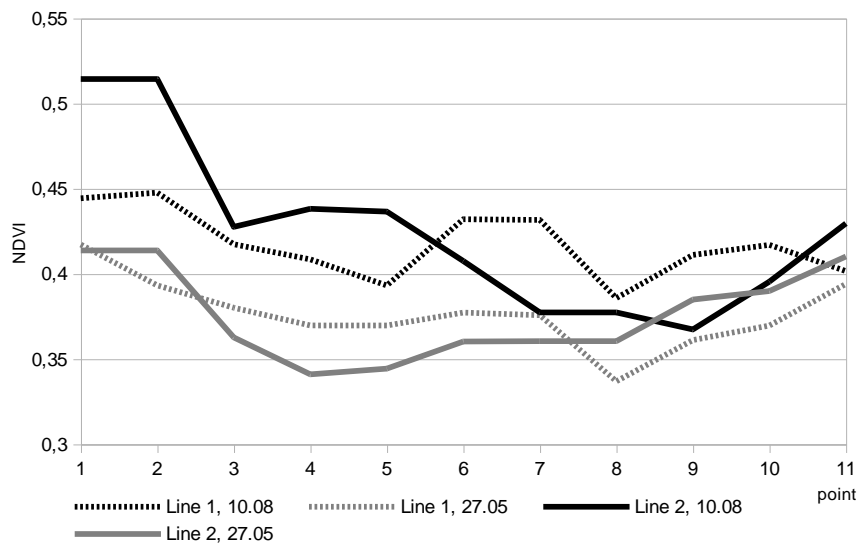
## VERIFICATION OF VTCI USAGE FOR SOIL MOISTURE CONTENT ASSESSMENT

To verify the reliability of VTCI usage for evaluating soil moisture content in the considered conditions, we obtained the correlations between its values and the average moisture content in the layer of soil with the depth up to 50 cm measured on August 8, 2018 by a portable moisture content sensor MG-44 on the experimental field of the State Enterprise "DG Brylivske". 36 values of moisture content in the grid of points were obtained averaging the results of 3 measurements in each point. A linear correlation with  $R^2=0.48$  was observed between the values of VTCI and NDVI indices. The similar correlation between VTCI and moisture content has  $R^2=0.65$ . The satellite images were acquired on August 10, 2018.

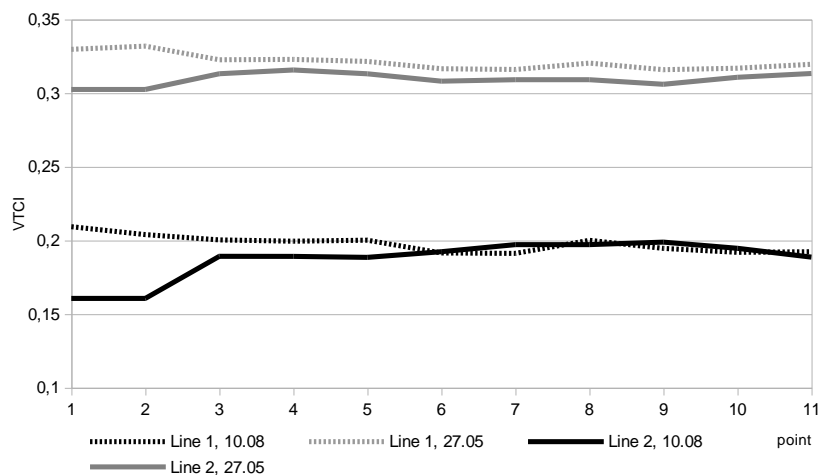
The determination coefficient  $R^2=0.65$  of linear dependency between VTCI values and the measured soil moisture values is significant but, unlike theoretical expectations, had an inverse character. At the same time, there is also a weaker ( $R^2=0.48$ ) negative correlation between the values of the VTCI and the NDVI indices. The dependency between the NDVI and soil moisture content is significantly weaker. The reason for the differences between the theoretical expectations and the resulting dependencies may be due to the passage of some time between the measurements and the reception of satellite images. Cumulative evaporation during this time significantly influenced the moisture content while much less influencing the surface temperature. On the other hand, the absorption of moisture by plants increases the values of the NDVI biomass index.

Regardless the above mentioned, the high correlation between the measured soil moisture content and the values of the VTCI index allows it to be used as an indirect indicator for the evaluation of moisture content. Additionally, within the experimental fields, the possibility of remote sensing identification of the influence of agrolandscapes' components on soil moisture content was studied. Changes in the values of the NDVI and VTCI indices were analyzed for two lines within a field where sunflower was grown without irrigation. The first one (line 1) on the one side borders with the adjacent irrigated field, and on the other side - with a medium density shelterbelt. The second one (line 2) borders with two shelterbelts of high and medium density. Changes in the NDVI are shown in Figure 2 for 10.08.2018 and 27.05.2018. Changes in the VTCI for the same dates are shown in Figure 3.

As can be seen from Figures 2,3, remote sensing data captures the influence of shelterbelts on soil moisture and biomass. The value of the VTCI index, and therefore soil moisture, decreases in the zone of influence of the dense shelterbelt (Figure 3, line 2, points 1 and 2, distance from 30 m to 60 m from the shelterbelt) and increases in the zone of influence of the adjacent field where irrigation was carried out (Figure 3, line 1, points 1 and 2). Biomass in both cases increased (Figure 2). The average shelterbelt's density (lines 1 and 2, points 10, 11) significantly reduced the moisture content while positively influencing the growth of biomass.



**Figure 2.** Changes in the NDVI values

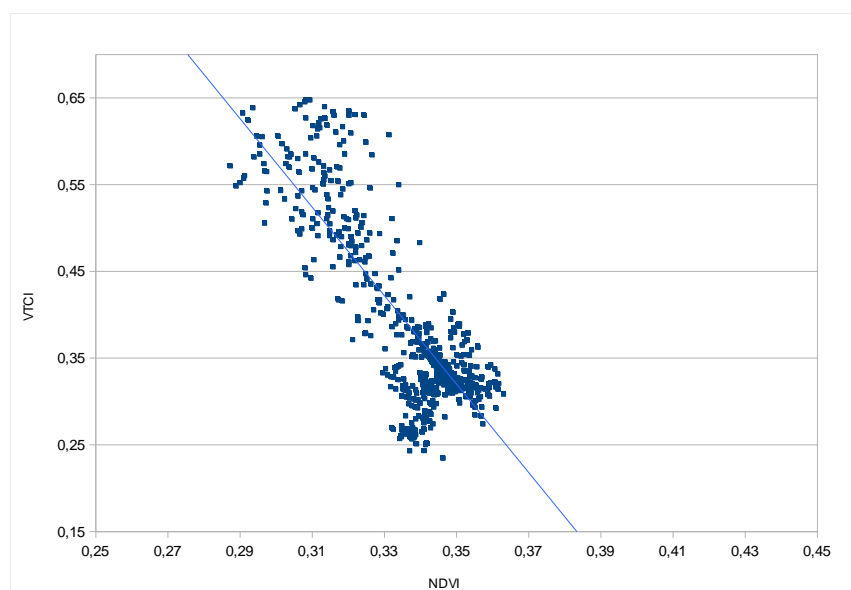


**Figure 3.** Changes in the VTCI values

## BIOMASS RESPONSE TO MOISTURE CONTENT CHANGE FOR THE DIFFERENT STRUCTURES OF AGROLANDSCAPES

To study the changes in the correlations between biomass and moisture content for the different structures of agrolandscapes, on the studied territory we selected areas that have up to four shelterbelts around the fields. Then, for satellite images acquired on May 27, 2018, July 11, 2018, and August 10, 2018 the correlations between the values of NDVI and VTCI indices were obtained.

For an image with low average biomass ( $NDVI < 0.4$ ) acquired in May, there were inverse linear correlations between NDVI and soil moisture content indirectly estimated using VTCI index. With an increase in the number of shelterbelts up to two, slope of the correlation increased (Figure 4). This fact can be explained by the extraction of soil moisture by shelterbelts and, thus, a decrease in moisture with an increase of biomass. In the case of three and four shelterbelts, the slope of the correlation decreased comparing with the case of two shelterbelts. This may be due to the reduction of evaporation from the fields surrounded by shelterbelts caused by the lowering of wind velocity and their other reclamation effects.



**Figure 4.** Scatterplot of NDVI and VTCI values on the fields with two shelterbelts for the image acquired May 27, 2018

For the image taken in July, trends were similar to those observed in May. However, the inverse correlation here persists only when no shelterbelts are present. When irrigation was used and in the presence of shelterbelts, the greater biomass corresponded to higher moisture content. The distributions of NDVI and VTCI values for the image taken in August behave the same way. Moreover, primarily due to intensive irrigation, the correlations had a weak exponential form.

The distribution of index values in July and August can be divided into three groups in which the nature of the correlations between them varies. These groups include areas of weak or absent vegetation ( $NDVI < 0.3$ ), areas of rainfed crop cultivation ( $0.3 \leq NDVI < 0.6$ ) and irrigated areas. We assume that area was irrigated in the case of  $NDVI \geq 0.6$  since, as it was previously established, in the conditions of arid climate of the Kherson region of Ukraine and in the absence of regular precipitations, the achievement of such level of biomass is possible only when irrigation is applied. The linear correlations between VTCI and NDVI values for the three NDVI ranges computed based on the image acquired on August 10, 2018 are shown in Table 1.

**Table 1.**  $VTCI=a+b*NDVI$  correlations for different number of shelterbelts and different NDVI ranges for the image acquired on August 10, 2018

Number of shelterbelts	NDVI<0.3		0.3<=NDVI<0.6		NDVI>=0.6		
	a	b	A	b	A	b	
0		-0.23	1.59	0.91	-1.65	-1.54	2.67
1		-0.09	1.12	2.73	-7.07	-0.62	1.35
2		-0.12	1.22	-1.58	4.90	-0.32	0.96
>=3		-0.22	1.53	-0.58	2.18	-0.74	1.47

The correlations in the case of absent or weak vegetation are close. In the case of rainfed crop cultivation, the number of shelterbelts substantially affects the slope of correlation: it is negative when number of shelterbelts is less than two and positive when there is a complete or almost complete contour of shelterbelts. This can be explained by the retention of moisture by shelterbelts which leads to an increase of moisture content with the increase of biomass when two or more shelterbelts are present in the structure of the plot.

The correlations for the irrigated fields are close in all cases of shelterbelts presence. These areas are irrigated by center pivot machines, and this behavior of dependencies shows the impact of irrigation as a key factor for the development of biomass and maintaining a level of soil moisture content, leveling other factors (e.g. the positive or negative effects of shelterbelts), the impact of which is not so great comparing with the effect of irrigation, especially for the conditions of the Steppe. The greater slope of the correlation between moisture content and biomass for the areas with no shelterbelts is because these areas are small private fields where excessive watering is usually applied.

## CONCLUSIONS

The conducted analysis of field and remote sensing data shows that the usage of NDVI and VTCI indices allows estimating the level of shelterbelts influence on biomass response to soil moisture content. Linear dependencies between soil moisture content and the values of VTCI index were obtained along with the dependencies between VTCI and NDVI. In the conditions of southern Ukraine, such influence differs in time and with the change of biomass.

The obtained dependencies allow determining the conditions when such aspects of shelterbelts influence as the extraction or retention of soil moisture, or the reduction of evaporation are manifested. Further studies can use the results of the paper to produce recommendations on planning the creation or reconstruction of shelterbelts in the South of Ukraine.

## REFERENCES

- Anandababu, D., Purushothaman, B. M., Suresh, B. S. (2018) Estimation of Land Surface Temperature using LANDSAT 8 Data. *International Journal of Advance Research, Ideas and Innovations in Technology*, **4**(2), 177-186.
- Deering, D. W., Rouse, J. W., Haas, R. H., Schell, J. A. (1975) Measuring Forage Production of Grazing Units from Landsat MSS Data. *Proceedings of the 10th International Symposium on Remote Sensing of Environment*, **2**, 1169-1178.
- Farrar, T. J., Nicholson, S. E., Lare, A. R. (1994) The influence of soil type on the relationships between NDVI, rainfall and soil moisture in semiarid Botswana. II. NDVI response to soil moisture. *Remote Sensing of Environment*, **50**, 121-133. DOI: 10.1016/0034-4257(94)90039-6.
- Jackson, T. J., Le Vine, D. M., Swift, C. T., Schmugge, T. J., Schiebe, F. R. (1995) Large area

- mapping of soil moisture using the ESTAR passive microwave radiometer in Washita'92. *Remote Sensing of Environment*, **53**, 27-37. DOI: 10.1016/0034-4257(95)00084-E.
- Liu, W. T., Kogan, F. N. (1996) Monitoring regional drought using the vegetation condition index. *International Journal of Remote Sensing*, **17**, 2761-2782. DOI: 10.1080/01431169608949106.
- Logginov, B. I. (1949) Field-protective forest plantings in the Steppes of Ukrainian SSR, Academy of sciences of Ukrainian SSR, Kyiv, USSR, (in Ukrainian).
- Maliuga, V. V. (2012) Influence of shelterbelts on the development of flooding processes. *Visnyk agrarnoji nauky*, **11**, 70-72.
- Sahebi, M. R., Bonn, F., Béné, G. B. (2004) Neural networks for the inversion of soil surface parameters from synthetic aperture radar satellite data. *Can. J. Civ. Eng.*, **31**, 95-108. DOI: 10.1139/103-079.
- Sandholt, I., Rasmussen, K., Andersen, J. (2002) A simple interpretation of the surface temperature/vegetation index space for assessment of surface moisture status. *Remote Sens. Environ.*, **79**(2-3), 213-224.
- Siryk, A. A. (1991) The climate-forming role of artificial forests in the steppe of Ukraine (in Ukrainian). *Lisivnytstvo i agrolisomelioratsija*, **83**, 7-12.
- Stadnyk, A. P. (2004) Agroforestry zoning of Ukraine as the landscape and ecological basis of the creation of countrywide optimized system of protective forest plantings. *Lisivnytstvo i agrolisomelioratsija*, **106**, 137-149, (in Ukrainian).
- Vysotsky, G. N. (1983) Protective forestry, Naukova Dumka, Kyiv, Ukraine, (in Russian).
- Wang, P., Li, X., Gong, J., Song, C. (2001) Vegetation temperature condition index and its application for drought monitoring. *Geoscience and Remote Sensing Symposium IGARSS'01*, 141-143.
- Wang, X., Xie, H., Guan, H., Xiaobing, Z. (2007) Different responses of MODIS-derived NDVI to root-zone soil moisture in semi-arid and humid regions. *Journal of Hydrology*, **340**, 12-4. DOI: 10.1016/j.jhydrol.2007.03.022.
- Yu, F., Zhao, Y. (2011) A new semi-empirical model for soil moisture content retrieval by ASAR and TM data in vegetation-covered areas. *Sci. Chin. Earth Sci.*, **54**, 1955-1964. DOI: 10.1007/s11430-011-4204-3.
- Zargar, A., Sadiq, R., Naser, D., Khan F. I. (2011) A review of drought indices. *Environ. Rev.*, **19**, 333-349. DOI: 10.1139/a11-013.
- Zonn, S. V. (1959) Soil moisture and forest plantings (in Russian), Academy of Sciences of USSR, Moscow, USSR.



# Influence of the Internal Protective Coatings Surface Texture to the Transport Capacity of the Pipelines

I. S. Dezhina\* and V. A. Orlov\*

\* Moscow State University of Civil Engineering (National Research University), 129337, Yaroslavskoe shosse 26, Moscow, Russia (E-mails: [dejina07@mail.ru](mailto:dejina07@mail.ru); [orlov950@yandex.ru](mailto:orlov950@yandex.ru))

## Abstract

Increase of the flow transporting capacity in the non-pressure sewage pipelines at low water flow rates is one of the ways to ensure the operating efficiency of the pipelines. This aim is highly relevant for the narrower diameters of the pipeline network, where it is necessary to prevent sedimentation of suspended substance (sand) from falling in the tray sections of the pipeline networks. Prevention of suspended substance sedimentation in the pipelines tray is theoretically possible by using textured surfaces, for example during trenchless repair-works by pulling special flexible polymer sleeves with a corrugated surface into the pipeline. The main aim of this research was to study the fluid flow behaviour around artificially- created obstacles and identify opportunities to utilise vortex flow to increase the transport capacity of pipelines.

## Keywords

Microturbulence; suspended substance; artificially-created obstacles; turbulence; sewage pipelines

## INTRODUCTION

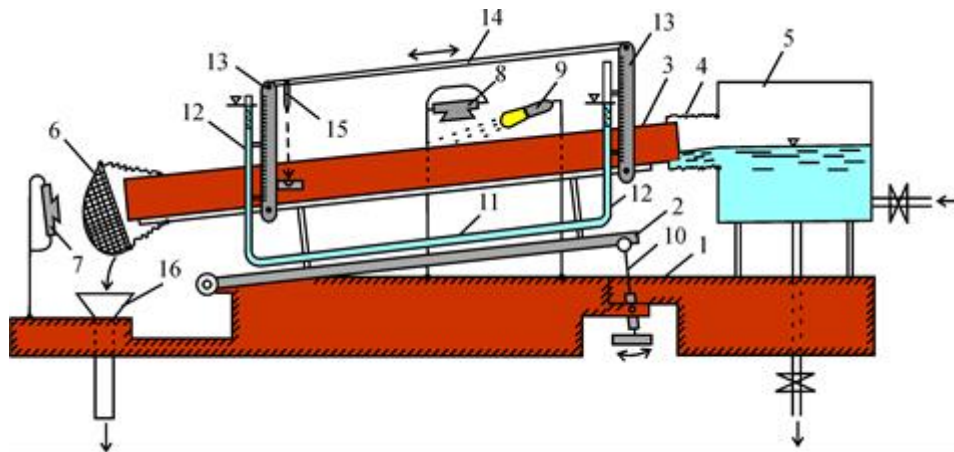
The problem of sediment deposition in pipelines can lead to multiple problems; many being environmental. Formation of a dense layer of sediment in the tray part of the pipeline can lead to certain problems, besides the high increase in friction losses. One example would be the potential microbiological corrosion under the deposit layer, as well as needed of more frequent cleaning of the pipeline, which in turn increases the cost of sewage networks operation.

The main idea of design is to create a microturbulence effect in pipelines with low speed flows. This can be achieved by placing obstacles on the inner surface of the pipeline tray. This will create microturbulence in the flow, forcing suspension of sediment up into the flow instead of enabling deposition (Ebtehaj, 2014; Grossmann, 2017). Thus, experimental research of improving the transporting ability of non-pressure sewage pipelines at low water flow can be considered as an actual direction of scientific research and an extremely important aspect for development of pipelines reconstruction projects (Santiago, 2013).

The research and its results were aimed to study the behavior of fluid flow around various artificially-created obstacles with the identify of the optimal patterned structures as to ensure microturbulence due to the geometric shape and location of the obstacles and the increase of the flow transferring ability. In parallel, the aim was to investigate the influence of fine and coarse sediments (loose and cohesive sand) to the vortex formation in the transition from laminar to turbulent flow (Loisel, 2013; Kleinstreuer, 2017).

## MATERIALS AND METHODS

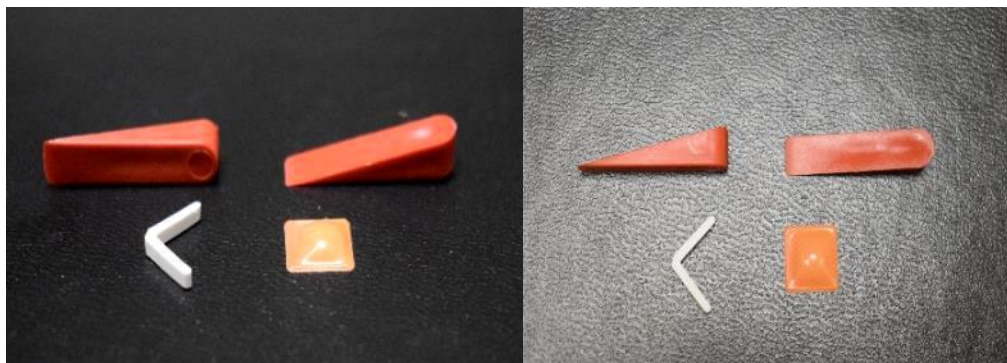
*The first stage of experimental research* of turbulence on corrugated surface has been studied on a specially designed and patented “Testing stand for the study of turbulence and carrying capacity of the fluid flow by optical means”. The experiments were carried out based on the light-shadow effect with relevant cameras.



**Figure 1.** Schematic depiction of the testing stand: 1 - fixed frame; 2 - movable platform; 3 - open tray; 4 - rubber corrugated pipe; 5 - holding tank for liquid; 6 - removable mesh trap of foreign particulate inclusions; 7, 8 – cameras, respectively, of frontal and coaxial shooting; 9 - source of light; 10 - mechanical jack; 11 - waterway; 12 - flexible transparent connecting pipes; 13 - movable measuring lines; 14 - plate; 15 - laser plummet; 16 - receiving measuring tank

The corrugated surfaces in the tray sections of the pipeline were created by sets of different obstacles (wedges, corners, etc). Obstacles were located in the middle of the flow or with some relative displacement (small and large) from the tray axis. It was critical to detect the sizes (nature, length and width of turbulence zone) of vortices (per object) and overpressure, in the form of ripples, in front of the obstacle.

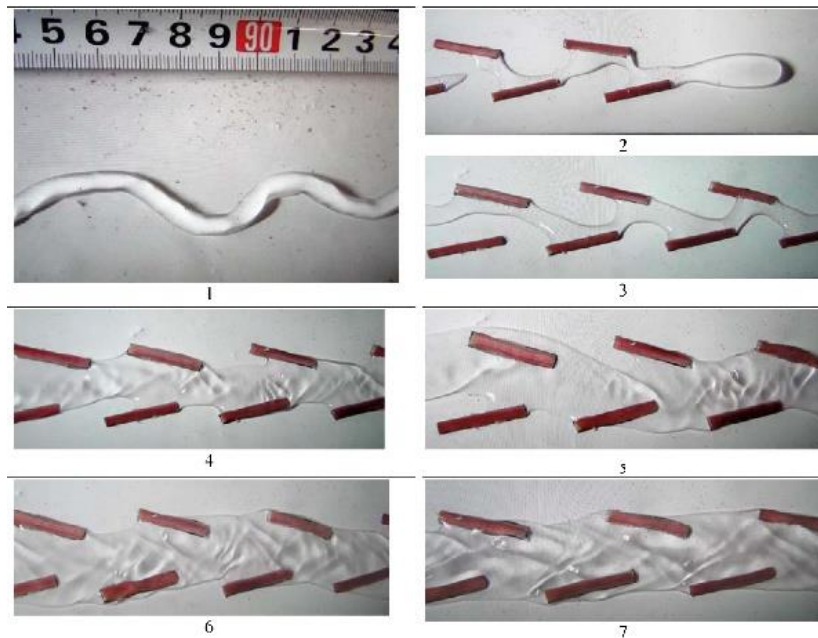
The shape, size, quantity, and locations of the obstacles will differ depending on the type of pipe, sediment, and typical rates of water flow within the pipeline. It is not a “one size fits all” solution – the obstacles will be customised in order to create maximum efficiency for the specific system. It is this personalization that especially makes the product stand out. A “saltation” (leap-frog) movement of the sediments in the flow was considered as an effective model of the motion. In this case, the amount of sediment remains minimal regardless of the speed and water level in the pipeline.



**Figure 2.** General view of the obstacles: on the left and right photos from different angles: wedges, corner, and pyramid

11 types of obstacles were investigated (rectangular bars (also on a hydrophobic surface), cylinders, an extended hexagonal prism, an inverted spherical segment, a hexagon in the form of a nut, etc.).







Specific nature of the flow is observed on a hydrophobic surface with the group of obstacles.



**Figure 3.** Dynamic of the flow pattern change on a hydrophobic surface with obstacles with a gradual increase of the flow speed from 0.08 to 0.35 m/s

The results of experiments are described and interpreted in the form of the formation of vortices (coherent flow or vortex flow), considering the sizes of the vortices and geometric characteristics of the turbulence zones (both lengths and areas, before and after obstacles).

Below, as an example, are presented some of the most characteristic results of the experiments carried out with the group obstacles in the speed range of 0.2-0.6 m/s.

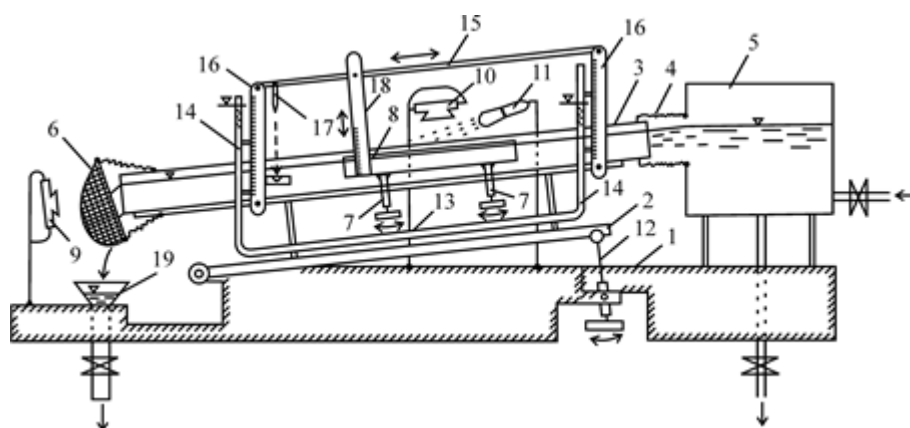
Frontal view	Coaxial view	Speed, m/s
		< 0,2
		0,2
		0,4
		0,6
		> 0,7

**Figure 4.** The obstacles in the form of narrow rectangular cross section, arranged crosswise

The main conclusion is that the active turbulization of the flow can be observed at speeds of 0.4 m/s, i.e. below the self-cleaning speed, which was used for subsequent experiments. Based on the

obtained results, it is shown that practically any obstacle can in some way influence the turbulence effect of the flow at less than its rate of self-cleaning.

The second stage of experimental research were carried out on an updated testing bench.



**Figure 5.** Testing stand for the research of the transportation ability of the open trays with different relief of their inner surface: 1 - fixed frame; 2 - movable platform; 3 - open tray; 4 - rubber corrugated pipe; 5 - holding tank for liquid; 6 - removable mesh trap of foreign particulate inclusions; 7 – small mechanical jacks; 8 – pipeline section in form of open tray with the different relief of the inner surface; 9, 10 – cameras, respectively, of frontal and coaxial shooting; 11 - source of light; 12 - big mechanical jack; 13 - waterway; 14 - flexible transparent connecting pipes; 15 - plate; 16 - movable measuring lines; 17 - laser plummet; 18 - retractable measuring line, connected with plate; 19 - receiving measuring tank

Vortex flow has been investigated behind obstacles in the form of refraction (deformation) of the reflected light from a special lamp with two parallel installed spotlights.

Results of one experiment (the one with the “pyramid” obstacles) are presented on the figure 6 below. The photograph clearly shows the contour of the light-shadow path, which is refracted with increasing flow velocity. The last line (number of experiment 4) already shows signs of coherence, i.e. separation of the vortices.

*The third stage of experimental research.* The experiments were carried out on the same stand, which was mentioned earlier. The subject of the study was two-phase flow “water + sand”, where sand of various fractions dimensions was used (0.01-0.3 mm) together with the presence of the different types of obstacles with a different location order (direct and reverse herringbone, etc.) and a certain area (length) of the sand belt with the similar mass of sand.

The final stage of the experiments was the calculation of the relative transport capacity of the stream with the different locations and types of obstacles, specifically:

- per cm<sup>2</sup> of the area of the sand dune (ridge): mg/s per cm<sup>2</sup>;
- per cm of the length of the sand dune: mg/s per cm;
- per second.

In parallel, experiments were conducted on the open pipeline tray without obstacles, which made it possible to determine the delta between the flow rates of water along a tray with sand without obstacles and with obstacles, at which the effect of transporting the sandy mass is observed. Example of the observed results is presented below on the figure 7.



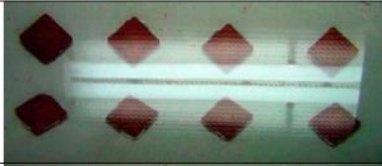
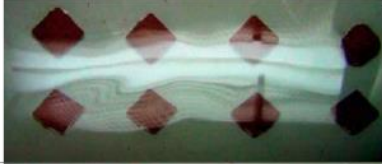


№ of exp.	Indicators of time, flow rate, height of the water layer and water level					Deformation (reflection) of light-shadow path
	Time $T_{md}$ , s (per 1m)	Speed $V_{md}$ , m/s	Height $h_{md}$ , mm	Water level $h/d_{md}$		
1	15	0,066	20	0,154		
2	6	0,167	35	0,269		
3	4,5	0,222	40	0,308		
4	3,3	0,303	50	0,385		

Figure 6. Flow visualization and its characteristics

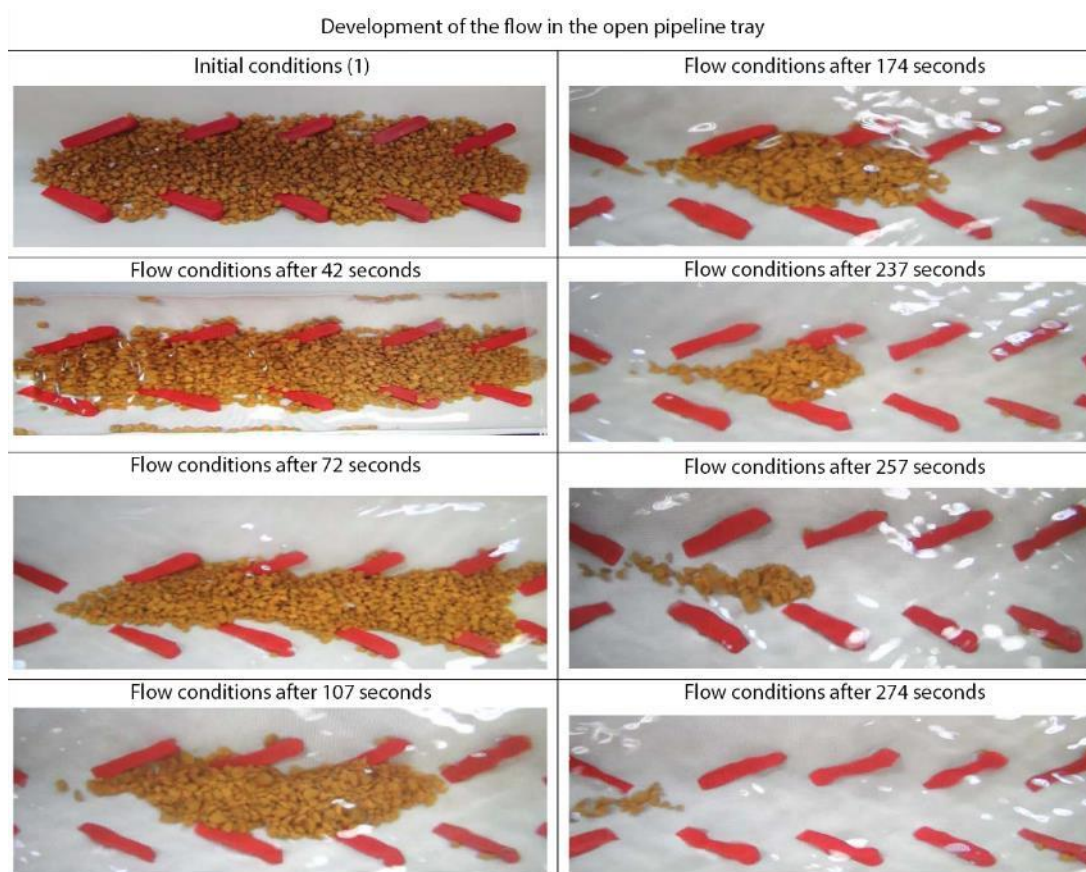


Figure 7. Illustration of the sand dune development in the open tray in time

The dynamic of sand mass removal in time is traced here with a gradual increasing of speed and its stabilization by the time of intensive sand removal (after 174 seconds), which is indicated in table in the form of constant speeds and water levels.

**Table 1.** Dynamic of the sand mass removal from the tray

No of experiment	Time $T_{md}$ (per 1 m) (s)	Speed $V_{md}$ (m/s)	Height $h_{md}$ (mm)	Water level $h/d_{md}$ -
1	2	3	4	5
1	Initial condition of the sand dune			
2	7.6	0.131	25	0.192
3	6.5	0.154	35	0.269
4	4.9	0.204	45	0.364
5	2.9	0.345	58	0.426
6	2.9	0.345	58	0.446
7	2.9	0.345	58	0.446
8	2.9	0.345	58	0.446

## CONCLUSION

1. Experiments were carried out to study the hydraulic parameters of single-phase and two-phase flows in the open trays without a textured surface and with different relief of their inner surface in a wide range of water level in the pipeline (0.05-0.6) and velocities (0.1-0.6 m/s) of fluid flow, as well as transportation of various sand fractions (0.1-3.0 mm).
2. It has been established that the obstacles in form of the wedge or semicircular, located with a sharp end to the flow, are the most effective solutions for transportation of sand fractions along tray. Ranges of their transporting abilities are in the speed range (0.345-0.5 m/s) and water levels (0.377-0.446) for sand with a fraction size of 2.5-3 mm were their transporting abilities, respectively, per the dune areas 1,336-1.482 mg/s per  $cm^2$  and per dune lengths 6.01-6.67 mg/s per cm.
3. It has been established that in a tray without obstacles and with the obstacles in the form of wedges, under identical conditions, speed range more than 0.588 m/s and water level not less than 0.446 are necessary for complete removal of sand fractions. At the same time, the transporting capacity is, respectively, per unit area of the dune, 1.155 mg/s per  $cm^2$  and per unit length of the dune, 5,2 mg/s per cm, which is 18 % less than in the pipeline trays with modified surface.
4. It was found out that depends on the type and location of obstacles, the transporting ability of sand removal significantly differs for a fraction size of 0.1-0.3 mm and for a fraction size of 2.5-3.0 mm. The difference per unit area is about 53.1 %, and per unit length of the dune is 46.6%. Thus, the smaller the size of the sand fraction is, the more efficient is the transporting.
5. Experiments have shown that the obstacles in the form of pyramids and the corners are ineffective because they do not provide complete removal of sand fractions from the surface of the tray.

## REFERENCES

- Arolla, S. K., Desjardins, O. (2015) Transport modeling of sedimenting particles in a turbulent pipe flow using Euler–Lagrange large eddy simulation. *International Journal of Multiphase Flow*–

*Elsevier*, **75**. 1-11.

- Bailey, S. C. C., Vallikivi, M., Hultmark, M., Smits, A. J. (2014) Estimating the value of von Kármán's constant in turbulent pipe flow. *Fluid Mech. Cambridge University Press*, **749**, 79-98.
- Ebtehaj, I., Bonakdari, H. (2014) Comparison of genetic algorithm and imperialist competitive algorithms in predicting bed load transport in clean pipe. *Water Sci Technol.*, **70**(10), 695-701.
- Grossmann, S., Lohse, D. (2017) Curvature effects on the velocity profile in turbulent pipe flow *Eur. Phys. J. E.*, **40**.
- Houghtalen, R., Osman, A., Akan, A., Hwang, N. (2016) *Fundamentals of Hydraulic Engineering Systems*, 5th edition, Pearson, 528.
- Kleinstreuer, C. (2017) *Two-phase flow: theory and applications*, Routledge.
- Lee, C.-H., Low, Y. M., Chiew, Y.-M. (2016) Multi-dimensional rheology-based two-phase model for sediment transport and applications to sheet flow and pipeline scour. *Physics of Fluids.*, **28**, 053305.
- Loisel, V., Abbas, M., Masbernat, O., Climent, E. (2013) The effect of neutrally buoyant finite-size particles on channel flows in the laminar-turbulent transition regime. *Physics of Fluids*, **25**(12), 123304.
- Santiago, A., Durango, M. (2012) Most advanced technology for pipeline inspection in the world: see, measure and navigate in 3D through pipes and manholes. Proceedings of the International Conference and Exhibition NO-DIG 2012, Sao Paulo, Brasil.



# Toxicology Assessment of Emerging Contaminants found in secondary effluent of Prague's WWTP on Aquatic Species with Ecological and Economical Relevance

V. Diaz-Sosa\*\*\*, M. Tapia-Salazar\*\*\*, J. Wanner\*\* and D. Cardenas-Chavez\*

\* Tecnologico de Monterrey, School of Engineering and Science, Atlixcáyotl 5718, Reserva Territorial Atlixcáyotl, Puebla, Pue. Mexico, 72453 (E-mail: [diana.cardenas@tec.mx](mailto:diana.cardenas@tec.mx))

\*\* University of Chemistry and Technology Prague, Department of Water Technology and Environmental Engineering, Technická 5, 166 28 Praha 6, Czechia (E-mail: [diazsosv@vscht.cz](mailto:diazsosv@vscht.cz))

\*\*\* Universidad Autónoma de Nuevo León, Facultad de Ciencias Biológicas, Pedro de Alba, Niños Héroes, Ciudad Universitaria, San Nicolás de los Garza, N.L. Mexico (E-mail: [mireya.tapiasl@uanl.edu.mx](mailto:mireya.tapiasl@uanl.edu.mx))

## Abstract

Emerging Contaminants (ECs) are substances that are not monitored nor regulated in a consistent matter, however they pose negative effects on human health and ecosystem balance. Common products, such as pharmaceuticals and personal care products (PPCPs) are one of the main sources of these contaminants. The problem starts when they are disposed into the environment, because the current wastewater treatment plants (WWTPs) do not have the capacity to retain, treat or eliminate the great majority of them. In this study we identified some ECs in the secondary effluent of the WWTP of the City of Prague and selected three of them that, to the best of our knowledge, did not have toxicology information based on *Artemia Salina* as study model. *A. salina* is an important organism for ecological balance and also of great economic relevance in aquaculture. We performed toxicity test to determine the LC50 at 24 and 48 hours at room temperature and 28 °C for Furosemide, Hydrochlorothiazide and Tramadol. The lethal doses for half the population ranged from 225,01 mg/L for furosemide up to above 14000 mg/L for tramadol. We also determined the changes in enzymatic activity of glutathione-S-transferase (GST), glutathione peroxidase (GPx), and lactate dehydrogenase (LDH) when the organism was exposed to the LC25 identified for each contaminant. Toxicity in associated changes in these biochemical markers was evident. Our findings demonstrate the toxicity of these commonly used pharmaceuticals in a aquatic specie as *Artemia salina*, and proves the need of further research on the implications of their bioaccumulation, and on the toxicity of other emerging contaminants.

## Keywords

Emerging contaminants; eco-toxicity; *Artemia salina*; LC50; oxidative stress; enzymes

## INTRODUCTION

Most research about water quality and its impact in human health is focused mainly in physico-chemical and microbiological parameters, heavy metals, pesticides and petroleum hydrocarbons. However, the increase in the global population and the need to cover more food and services requirements, have redirected our attention to a new and growing environmental threat known as Emerging Contaminants (ECs). These new pollutants are defined as natural or synthetic substances that are not monitored nor regulated in a consistent matter, however they pose negative effects on human health and ecosystem balance (Geissen et al., 20015). The main concern about this group of pollutants is that their effects can start manifesting from concentrations as low as µg/L (Jurado et al., 2012). Common products, such as pharmaceuticals and personal care products (PPCPs) are one of the main sources of these contaminants. The problematic of these compounds starts when they are disposed into the environment, because the current wastewater treatment plants (WWTPs) do not have the capacity to retain, treat or eliminate the great majority of the ECs reported (Tong et al., 2011). This has caused the occurrence of these contaminants in water bodies and even in drinking water sources around the world (Rosi-Marshall and Royer, 2012).

However, there is not much information available about this kind of pollutants, so *in vivo* studies are needed to establish possible effects along with determining the concentration in which the repercussions are relevant in an ecological and economical level. In a previous study we analysed the secondary effluent of the WWTP of the City of Prague for a spectrum of 47 emerging contaminants, where only 9 of them were not present in the water samples. It is important to mention that this effluent is usually discharged into natural water bodies. Many of the ECs detected in such effluent had already some degree of toxicity information available, but from the ones that –to the best of our knowledge– did not have reports of toxicity on *Artemia salina* are: furosemide, hydrochlorothiazide and tramadol. Furosemide and hydrochlorothiazide are known diuretic pharmaceuticals used to treat high blood pressure and swelling due to fluid build-up; whereas tramadol is a very common analgesic known for its strong effect due to the fact that it is a derivate from opium.

*Artemia* was chosen as study model because its great economic relevance in aquaculture, constituting the principal component of the diet of fish and shrimp and its important role in marine ecological balance. Therefore, this project aims to evaluate the effect of the three ECs above mentioned and characterize their toxicity using an important indicator organism such as *Artemia salina*, and also to set a precedent on the monitoring and regulation of ECs for the treated wastewater disposal and/or the different processes for water consumption. In addition, being a reference for the study of other pollutants in Czechia and all over the world.

## MATERIALS AND METHODS

*Artemia Salina* was purchased as canned cysts (Biogrow, Proaqua® - Mexico). A pre-treatment for decapsulation was firstly applied to the cysts: 7.6ml of commercial chorine (bleach) combined with 7.6ml of distilled water and 150mg of NaOH. One gram of cysts were mixed in this solution and stirred continuously for 7 to 10 minutes. Later the mix was diluted with tap water and filtrated. Filtered cysts were then placed in a glass container with marine water (Instant Ocean® 29.9mg/L and distilled water) under constant aeration for 24 hours. Since nauplii are attracted to light, a lamp was placed on one side of the container to concentrate them.

### LC50 determination

Chemical contaminants (analytical grade) were supplied by Sigma-Aldrich® (MO, USA). These were dissolved in milli-Q water (tramadol) or methanol (furosemide and hydrochlorothiazide). The different concentrations of each compound were prepared using marine water in order to maintain same salinity concentration among treatments. Toxicity tests were performed in *Artemia* nauplii at 2 temperatures: room temperature (ranging from 20.5 to 23.5 °C) and at 28 °C, and 2 exposition times: 24 and 48 hours. All individuals were kept fasting during the total length of the bio-assays. Experiments were performed in 96-micro well cell culture plates: first adding 20µl of marine water containing 10 nauplii and then adding 230µl of each contaminant dilution to the well (250µl total working volume). Negative and positive controls containing marine water or potassium dichromate, respectively, were included in all the experiments. Each compound was evaluated by triplicate for each condition and after 24 or 48 hours the survival was recorded. Lethal concentration for half the population (LC50) was determined by linear regression for each bio-assay and then compared to calculate an average. These regressions were obtained using Microsoft Excel® software.

### Enzymatic activity

To test the effect of each emerging contaminant on oxidative stress enzymes of *Artemia Salina*, it was exposed to the LC25 of each one, at 24 and 48 hours, and at room temperature and 28 °C; this concentrations were calculated using the same equations obtained for LC50. 100mg of *Artemia* biomass from each assay were resuspended into phosphate buffer, sonicated and centrifuged at 4°C

and 3500 RPM during 10 minutes. The supernatant was recovered and used to perform the enzymatic analysis. Glutathione peroxidase (GPx) and Lactate dehydrogenase (LDH) were assayed using kits and protocols provided by Cayman chemical® (MI, USA) and reactions were measured quantifying the absorbance at the wavelengths of 340 and 490nm, respectively. For glutathione-S-transferase (GST), we used a continuous spectrophotometric rate determination method described by Habig et al. (1978), employing 1-chloro-2, 4-dinitrobenzene as substrate and measuring the absorbance at a wavelength of 340nm.

## RESULTS AND DISCUSSION

The LC50 values calculated from the three assays performed for each emerging contaminant at different experimental conditions are showed in Table 1. Furosemide was the most toxic compound as the median lethal concentrations were the lowest of the three contaminants tested. This effect remained quite stable for all conditions, with concentrations ranging between 225 and 274 mg/L. Tramadol followed the expectation that LC50 would be lower at 28 °C (1748,57 mg/L) than at room temperature (>14000 mg/L), as even the positive control tends to have lower survival at this temperature; however, furosemide and hydrochlorothiazide had an inverse behaviour. The lethal concentrations 50 for these two compounds was always higher at 28 °C, and the LC50 for hydrochlorothiazide at this temperature and 24 hours exposition was not possible to obtain in an accurate matter as it exceeded 3000 mg/L, concentration where the compound tended to precipitate in the dilution, interfering with the results analysis. Tramadol showed the least toxic effects in terms of killing half of the population, although the concentrations reached were very high (e.g. 14,000 mg/L at room temperature for 24 h). However, the effects of the compound could be seen almost immediately as *Artemia salina* started swimming very slowly, almost like trembling and not displacing from one side to another, as it commonly moved (data not shown). Survival for negative control (containing only marine water) was over 95 %, and the LC50 for the positive control K<sub>2</sub>Cr<sub>2</sub>O<sub>7</sub> ranged 4,36 to 37,07 mg/L depending of temperature and time of exposition.

**Table 1.** Mean values of three or more bio-assays to calculate the LC50 for each of the three ECs evaluated, at two different temperatures and during 24 and 48 hours. The LC50 of potassium dichromate used as positive control is also shown along with the survival on the negative control where only marine water was used as medium

Emerging Contaminant	Temperature	LC50	LC50	LC50	LC50	Control	Control
		(mg/L)	(mg/L)	K <sub>2</sub> Cr <sub>2</sub> O <sub>7</sub>	K <sub>2</sub> Cr <sub>2</sub> O <sub>7</sub>	Survival	Survival
		24 h	48 h	(µg/L)	(µg/L)	(%)	(%)
FUROSEMIDE	28°C	273.95	242.27	22.73	5.92	98±4	96±7
	Room Temperature	256.63	225.01	37.07	8.62	96±5	90±8
HYDROCHLORO-THIAZIDE	28°C	>3000	957.99	22.49	5.40	97±7	96±6
	Room Temperature	1564.13	918.42	35.78	5.29	98±5	90±9
TRAMADOL	28°C	4419.41	838.46	26.73	4.36	99±3	97±6
	Room Temperature	>14000	1748.57	36.42	9.28	98±4	98±4

As for the enzymatic activity, it is possible to see on Table 2 that only applying the concentrations corresponding to the LC25 of these compounds had impact in a cellular level for these organisms. The role of Glutathione-S-transferase (GST) is to detoxify and defend the cell against oxidative stress. GST detoxifies cellular endogenous compounds that are helpful in breaking down harmful xenobiotic compounds. It is remarkable how the enzymatic activity of GST is significantly bigger

for the samples exposed to the three compounds tested. Furosemide had been the most toxic of the three according to the LC50, and this can be confirmed by having very high enzymatic activity at 24 hours, especially at room temperature where it reported the highest activity of the three compounds. However, at 48 hours the enzymatic activity reported is much smaller but still reaching increases of three times the control GST activity.

Similar to GST, Glutathione peroxidase (GPx) is another enzyme with peroxidase activity, whose primal role is to protect the organism from oxidative damage (Muthukumar and Nachiappan, 2010). Nevertheless, we can see in the results that the control activities of GPx at room temperature were even higher than the ones observed for the assays employing the emerging contaminants at same temperature. At 28 °C the effect was different, all compounds presented a higher GPx activity, especially tramadol at 24 hours of exposition, where the activity went above the double of the control, and furosemide at 48 hours that increased almost 50 % the control activity. This means that somehow the higher temperature, the higher the oxidative stress of *Artemia*, and at lower temperatures the oxidative stress caused by the pharmaceuticals was reduced.

**Table 2.** Mean values and standard deviation of the enzymatic activity (mU/ml) measured for glutathione-S-transferase (GST), glutathione peroxidase (GPx), and lactate dehydrogenase (LDH) from three assays of each compound and experimental condition (two different temperatures during 24 and 48 hours). The control is also reported, where no contaminant was added and the medium consisted of plain marine water

Emerging Contaminant	Temperature	GST activity (mU/ml)		GPx activity (mU/ml)		LDH activity (mU/ml)	
		24 h	48 h	24 h	48 h	24 h	48 h
FUROSEMIDE	28°C	296.56 ± 41.44	83.12 ± 3.87	15.89 ± 7.29	29.57 ± 4.87	2.4 ± 0.2	1.5 ± 0.2
	Room Temperature	242.44 ± 32.07	161.38 ± 26.17	34.32 ± 4.91	20.59 ± 1.44	2.3 ± 0.2	2.6 ± 0.2
HYDROCHLORO-THIAZIDE	28°C	109.79 ± 20.24	218.87 ± 21.0	16.67 ± 1.61	19.28 ± 3.18	1.1 ± 0.1	1.9 ± 0.1
	Room Temperature	182.91 ± 18.52	16.79 ± 1.89	22.74 ± 0.67	19.29 ± 0.94	6.9 ± 0.5	0.8 ± 0.1
TRAMADOL	28°C	335.41 ± 15.05	160.36 ± 21.85	32.77 ± 2.10	20.93 ± 2.17	2.1 ± 0.2	1.6 ± 0.1
	Room Temperature	156.79 ± 13.39	174.19 ± 12.84	22.92 ± 2.93	22.59 ± 3.18	6.4 ± 0.6	2.1 ± 1.1
CONTROL (not contaminated)	28°C	69.72 ± 1.42	26.76 ± 3.19	15.87 ± 2.49	20.68 ± 1.63	1.5 ± 0.2	1.19 ± 0.2
	Room Temperature	114.56 ± 5.39	83.26 ± 8.88	36.6 ± 4.09	22.33 ± 2.39	1.3 ± 0.1	1.39 ± 0.2

Lactate dehydrogenase (LDH) is an enzyme in nearly all-living cells. It is released during tissue damage, and is a marker of common injuries and disease; in these cases the LDH activity level tends to be very high. In the present study, the three compounds reported an increased activity compared to the uncontaminated control assay. For 24 hours exposure, room temperature tended to increase the activity of this enzyme in *A. salina* above 5 times for Hydrochlorothiazide and Tramadol and almost double for Furosemide. At 28 °C the increased activity was much lower, except for furosemide, which had already shown the tendency to behave in an inverse manner in respect to temperature. For 48 hours exposure the enzymatic activity increase is higher at room temperature than at 28 °C for furosemide and tramadol, which is easier to explain in tramadol as room temperatures had higher doses, but for furosemide this principle does not apply. However, for Hydrochlorothiazide it caused a decrease of LDH activity at room temperature and around the same activity as the control for 28 °C, following its LC50 where smaller concentrations were needed at room temperature.

There is no proof in this study that the tested compounds were up-taken and that bioaccumulation through the trophic chain can be possible, however, other studies in *Artemia salina* have proved the bioaccumulation of other kind of contaminants (nanoparticles particularly) and the possible biomagnification of these when *Artemia salina* fed from algae that had up-taken the particles (Madhav et al., 2017; Bhuvaneshwarriet al., 2018).

## CONCLUSION

We might conclude from these results that the three pharmaceutical compounds tested, and included in the Emerging Contaminants classification, are indeed toxic for *Artemia Salina* in a higher or lower degree depending on the environmental conditions and the compound itself. The concentrations found for LC50 range from 225,01 mg/L for furosemide up to above 14,000 mg/L for tramadol; these concentrations are quite high compared to the ones found in the secondary effluent of the City of Prague in our previous study, which range from 810 to 2700 ng/L. However, it is important to emphasize that the three pharmaceutical compounds tested are very commonly used and have been found in water bodies around the world, therefore the accumulative effect of them must not be ignored, requiring further and intensive studies. *Artemia salina* is the base of marine trophic chain, meaning that whatever it can uptake and bioaccumulate can be passed through all of the species involved in that chain. Aside of that, it is the main food source of food for the aquaculture industry, that is why it is a very important indicator organism for toxicology. If our results indicate that being in contact with a small dose, such as the calculated LC25 for a period of 24 and 48 hours disrupts the cellular balance and triggers enzymatic activity to protect the cells, being exposed to lower concentrations for longer period could have the same effect, possibly even worse. Attention must be paid to these and many other emerging contaminants to set proper water treatment to remove these concentrations and to start regulating the disposal and concentration limits for water supply around the world.

## ACKNOWLEDGEMENT

The research described in this paper was financially supported by Consejo Nacional de Ciencia y Tecnologia of Mexico (Scholarship no. 543296), Tecnologico de Monterrey and the Technological Agency of the Czech Republic. Project No. TH03030080 “Wastewater reuse in water management of the cities of the future”.

## REFERENCES

- Bhuvaneshwari, M., Thiagarajan, V., Nemade, P., Chandrasekaran, N., Mukherjee, A. (2018) Toxicity and trophic transfer of P25 TiO<sub>2</sub> NPs from *Dunaliella salina* to *Artemia salina*: Effect of dietary and waterborne exposure. *Environmental research*, **160**, 39-46.
- Geissen, V., Mol, H., Klumpp, E., Umlauf, G., Nadal, M., van der Ploeg, M., van de Zee, S. E., Risema, C. J. (2015) Emerging Pollutants in Water – Review 2015. *International Soil and Water Conservation Research*, **3**, 57-65.
- Habig, W. H., Pabst, M. J., Jakoby, W. B. (1974) Glutathione S-transferases the first enzymatic step in mercapturic acid formation. *Journal of biological Chemistry*, **249**(22), 7130-7139.
- Jurado, A., Vázquez-Suñé, E., Carrera, J., López de Alda, M., Pujades, E., Barceló, D. (2012) Emerging organic contaminants in groundwater in Spain: A review of sources, recent occurrence and fate in a European context. *Science of the Total Environment*, **440**, 82-94.
- Madhav, M. R., David, S. E. M., Kumar, R. S., Swathy, J. S., Bhuvaneshwari, M., Mukherjee, A., Chandrasekaran, N. (2017) Toxicity and accumulation of Copper oxide (CuO) nanoparticles in different life stages of *Artemia salina*. *Environmental toxicology and pharmacology*, **52**, 227-

238.

Muthukumar, K., Nachiappan, V. (2010) Cadmium-induced oxidative stress in *Saccharomyces cerevisiae*.

Rosi-Marshall, E. J., Royer, T. V. (2012) Pharmaceutical Compounds and Ecosystem Function: An Emerging Research Challenge for Aquatic Ecologists. *Ecosystems*, **15**, 867-880.

Tong, A. Y. C., Peake, B. M., Braund, R. (2011) Disposal Practices for Unused Medications around the World. *Environment International*, **37**, 292-298.

# Simulation of Sensorless Flow Measurement System for Centrifugal Pump System

L. Gevorkov\* and I. Mikhelashvili\*\*

\* Faculty of Electrical Engineering, University of West Bohemia, Univerzitni 8, 30100, Pilsen, Czech Republic (E-mail: [levon.gevorkov@ttu.ee](mailto:levon.gevorkov@ttu.ee))

\*\* Analysis and Consulting Team, Shalikashvili Str.8 Tbilisi, Georgia (E-mail: [imikhelashvili@gmail.com](mailto:imikhelashvili@gmail.com))

## Abstract

Centrifugal pumping equipment is widely applied in modern industrial activities, like water production and distribution, sewerage systems, oil industries, and many others. These centrifugal pumping plants are one of the major electrical power consumers nowadays. It is estimated that pumps consume from 10% to 40% of total produced electricity. The automation of the processes that take place in the centrifugal pumping plants will certainly help to improve their performance. It makes the centrifugal pump system a subject of intensive study for efficiency improvement. One of the most important parameters of the pumping systems is flowrate. It is necessary to find ways for affordable and at the same time effective flow estimation possibilities.

## Keywords

Centrifugal pumps; flow measurement; simulation; modelling

## INTRODUCTION

The main goal of this paper is to represent the model of the centrifugal pump system that is designed to calculate the flowrate of the pumping unit. The calculated data can be used later for the stabilization and maintenance of flow at a determined level or regulation in accordance to needs of specific industrial conditions (A. T. De Almeida, 2011). The main advantage of designed model is that it contains standard functional blocks and, therefore, is easy to readjust for various pumping systems with different parameters. The developed algorithm for a programmable logic controller allows implementing the real flow calculation based on the model parameters (Ferreira, 2011). Thus helping to tune real pumping control system respectively.

The structure of the paper is following. At the beginning, a functional circuit of developed Simulink model is described. Next, the developed method of sensorless flow calculation system is presented with the received simulation data. At the end, the experimental outcomes of developed model are discussed and the conclusions drawn.

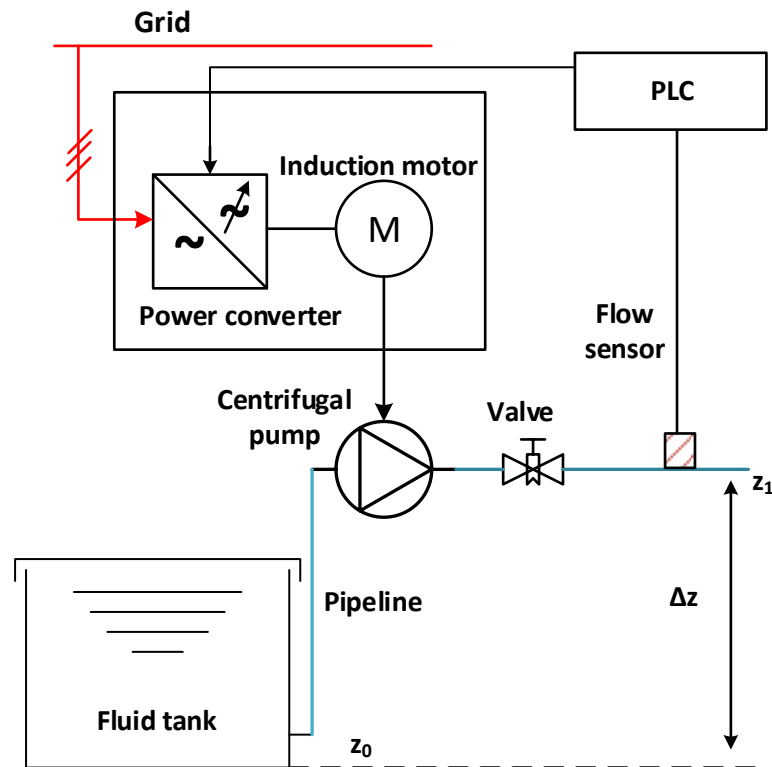
## STRUCTURE OF CENTRIFUGAL PUMP SYSTEM

A conventional topology of centrifugal pumping system consists of several main components:

- Pipeline for fluid transportation.
- Centrifugal pump.
- Variable speed drive (VSD).
- Feedback with a flow sensor.
- Regulation valve.
- Fluid tank.

Figure 1 represents the structure of a centrifugal pump system.





**Figure 1.** Structure of pumping system

The system consists of the centrifugal pump directly connected to induction motor that is fed by the power converter. The supply grid is connected to the power converter. A power converter, induction motor and the programmable logical controller (PLC) represent main parts of VSD. The liquid enters the centrifugal pump along the rotating axis. This side is called suction side of the pump and after acceleration by the impeller, it flows outward into a diffuser from which it exits the pump.

Every centrifugal pump can be described with the help of its main parameters, capacity  $Q$  ( $\text{m}^3/\text{s}$ ), energy head  $H$  (m) and pressure  $p$  (bar) at a certain rotational speed  $n$  (rpm). Every manufacturer usually supplies pumps with manuals that include working characteristics. These characteristics consist of nonlinear dependences between  $Q$  and  $H$ ,  $Q$  and  $P$  - power for the nominal rotational speed  $n_{nom}$ . Particularly working characteristics for Ebara CDX 120/12 centrifugal pumps from ABB company that have been used in experiments are given in (Centrifugal Pumps CDX).

Dependences between main characteristics of hydraulic system can be expressed in the form of affinity laws (Krivchenko, 1994):

$$\frac{Q_1}{Q_2} = \frac{n_1}{n_2} \quad (1)$$

$$\frac{p_1}{p_2} = \left( \frac{n_1}{n_2} \right)^2 \quad (2)$$

where index 1 is related the initial state and index 2 – is related to the final state of the process variables

**SIMULINK MODEL OF A CENTRIFUGAL PUMP**

Centrifugal pump model consists of several blocks. The structure of developed Simulink model is shown in Figure 2. Main block consists of two sub-blocks Figure 3, Figure 4.

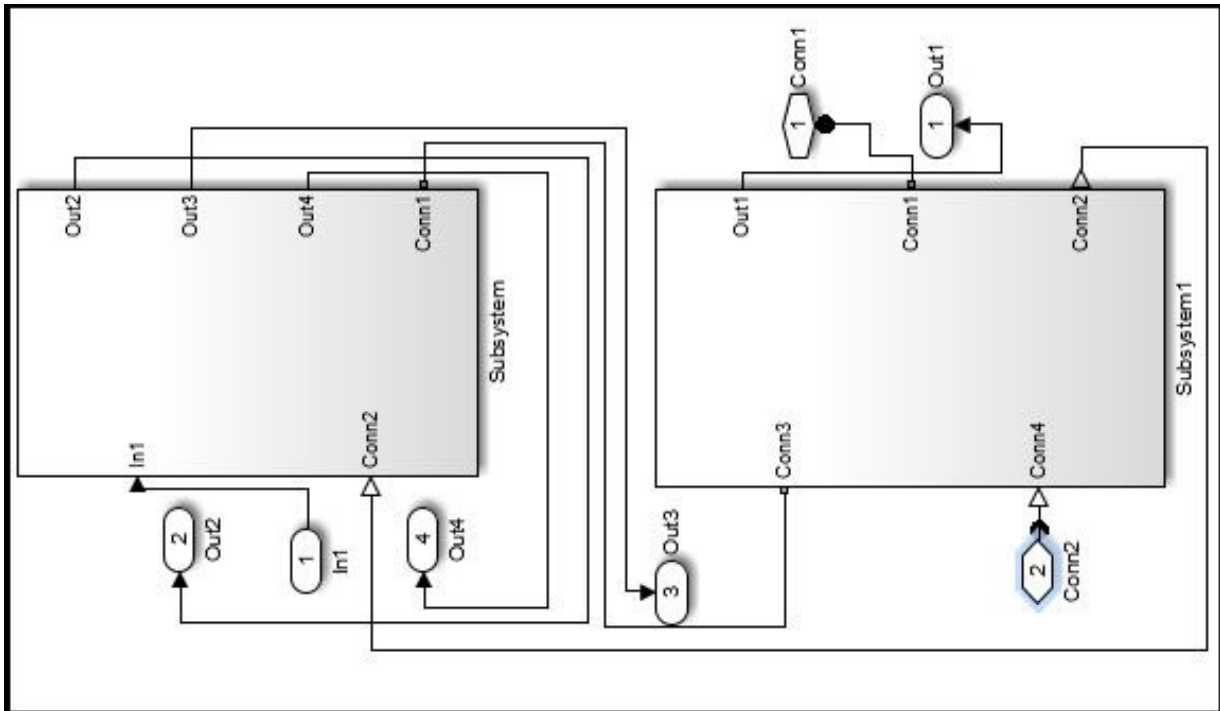


Figure 2. Sub blocks of a model

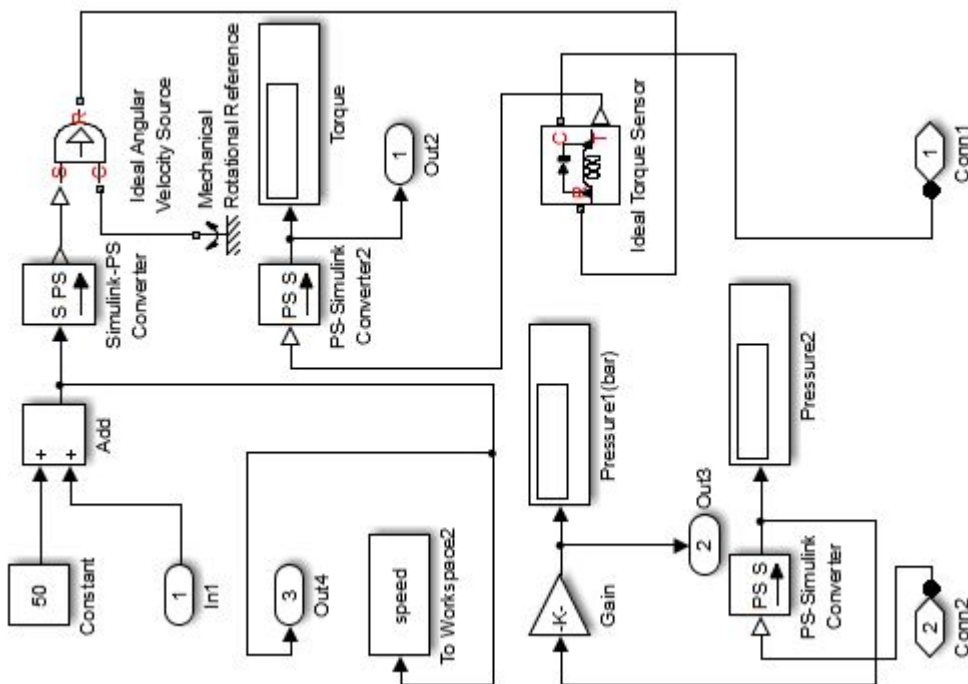


Figure 3. First sub block of a model

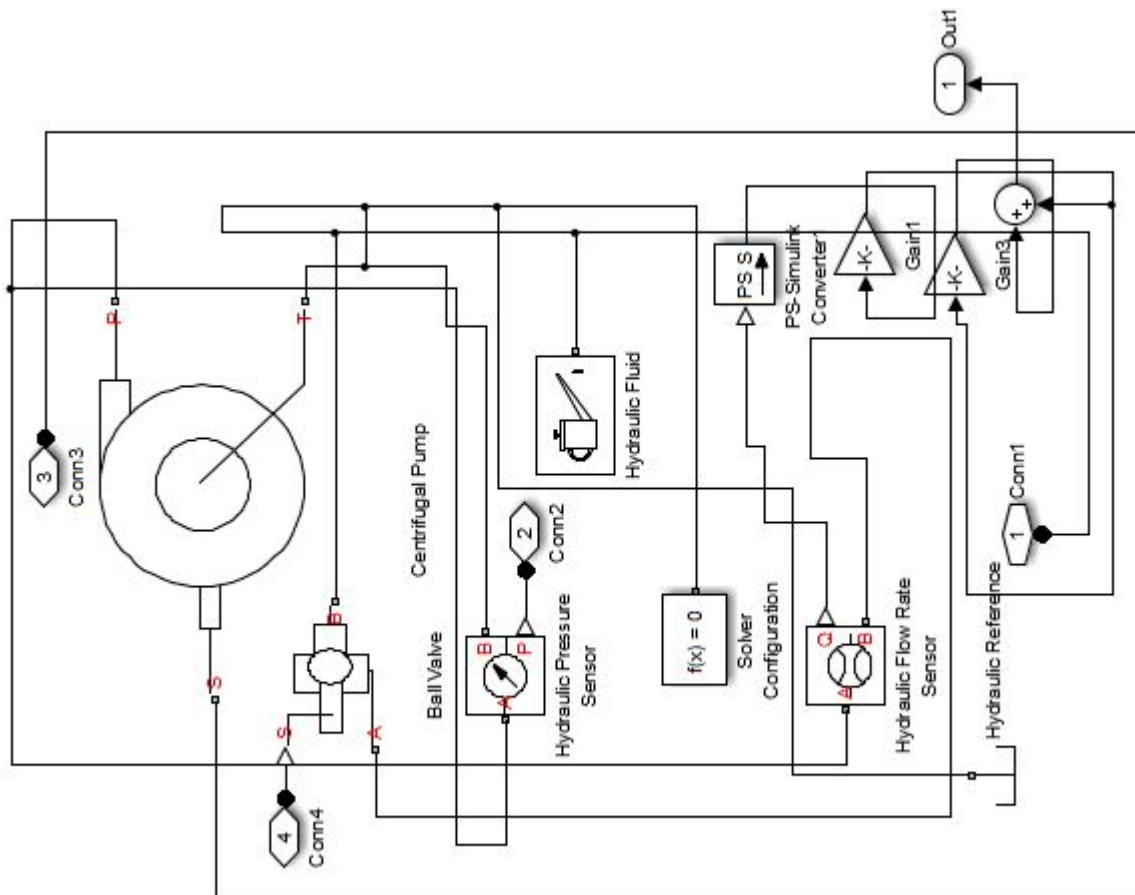


Figure 4. Second sub block of a model

Figure 2 represents two main sub-blocks of developed model. The first block contains ideal angular velocity source that allows setting desired speed of the pump. This function block generates speed proportional to input signal. In addition, sub-block contains speed, pressure-measuring tools, Figure 3. Measuring blocks contain special converter block that transfers measured numerical values into physical values (Qiu, 2010). These values later are stored in the memory and can be used for graphical plotting. Description of the nodes and functional blocks are following:

- In1 – speed input.
- Conn2 – connection of hydraulic pressure to measuring device (in Pa).
- Conn4 – input of regulation valve.
- Out1 – flow measurement output (in m<sup>3</sup>/h).
- Out2 – torque measurement output.
- Out3 – pressure measurement output (in bar).
- Out4 – speed measurement output.

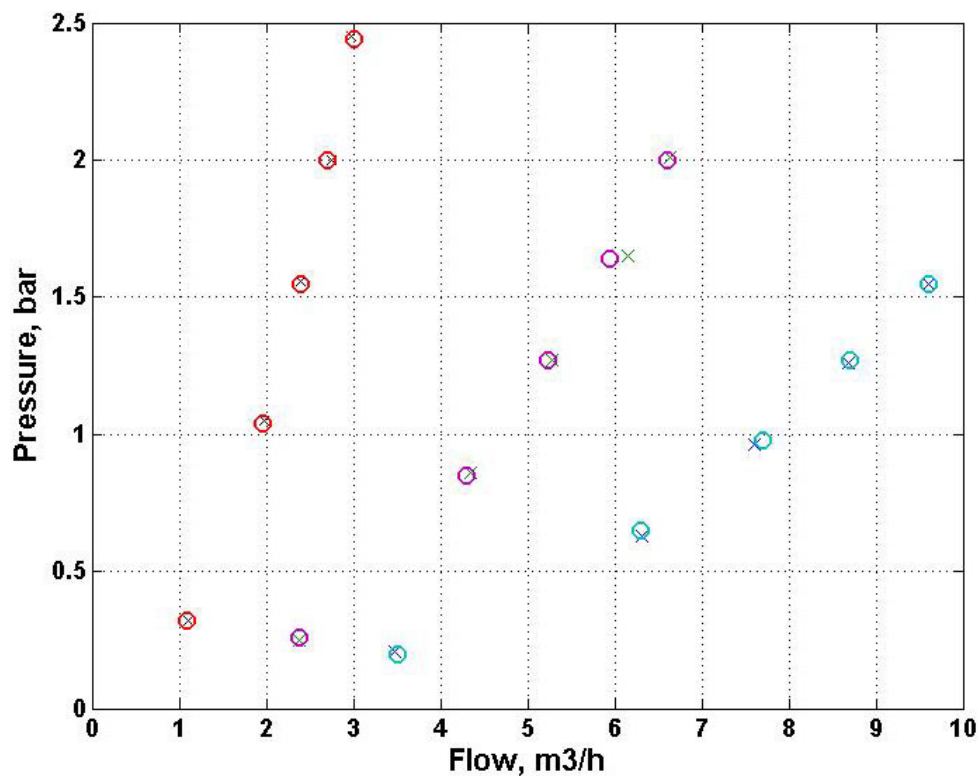
First sub block plays the role of control system. The control signal from PI regulator is connected to In1. The output signal of ideal angular velocity source is connected to centrifugal pump that is located in second sub block. Thus this block helps to operate the pumping system and regulate the flow in accordance to reference signal. Second block contains centrifugal pump, reservoir, regulation valve, pressure and flow sensors, and plays the role of main part of pumping system, Figure 4.

The reservoir is represented as a hydraulic reference block. Pipeline is a connection between suction side of a centrifugal pump – T and discharge side – P, Figure 4. To measure the pressure, hydraulic pressure sensor is used (Ghafouri, 2012). The outputs are denoted on Figure 4. The parameters of

centrifugal pump were taken from manufacturer's documentation. To create a correct model of a centrifugal pump, parameterization by pressure differential  $p - Q$  and brake power versus capacity  $P - Q$  was used. For estimation liquid volume in the reservoir and other hydraulic parameters, some additional measurements have been conducted:

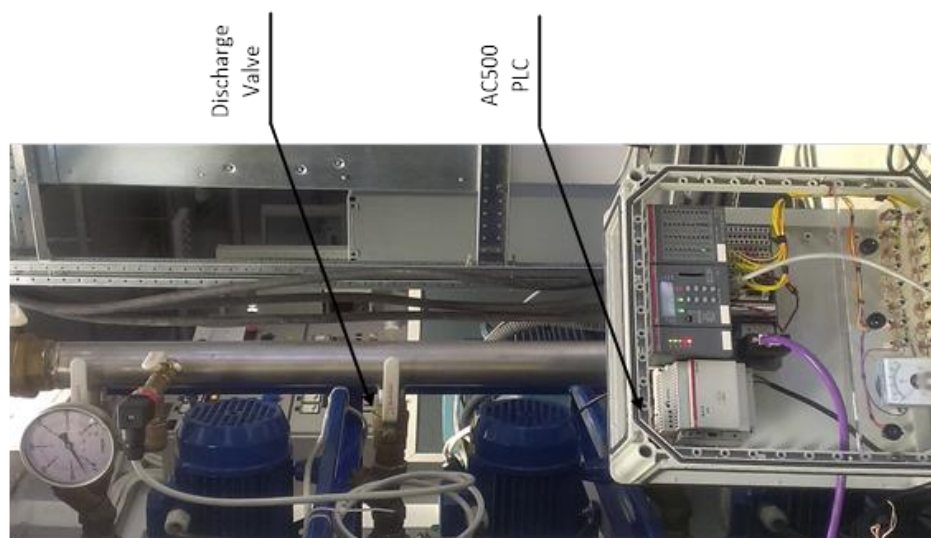
- tank total volume – 0.12264(m<sup>3</sup>),
- fluid volume – 0.09417(m<sup>3</sup>),
- pipeline length – 3.7(m),
- pipe inner diameter – 58(mm),
- wall thickness – 1.5(mm),
- pipe material – stainless steel,
- pipe roughness – 0.15(mm),
- type of valves – ball valve,
- angle of pipeline bends - 90°.
- $\Delta z$  – pipeline elevation, 1.1 (m).

To evaluate the model some tests were conducted. At first so-called system curves were estimated for different rotational speeds: 2760, 2500, 2200, 1800, 1000, Figure 5. The accuracy of designed model varies from 0.6 % to 3.1 %. That shows high precision of the model.



**Figure 5.** Family of system curves at – n=2760, 2500, 2200, 1800, 1000 rpm for pump model - ‘o’, and ‘x’ for real test bench

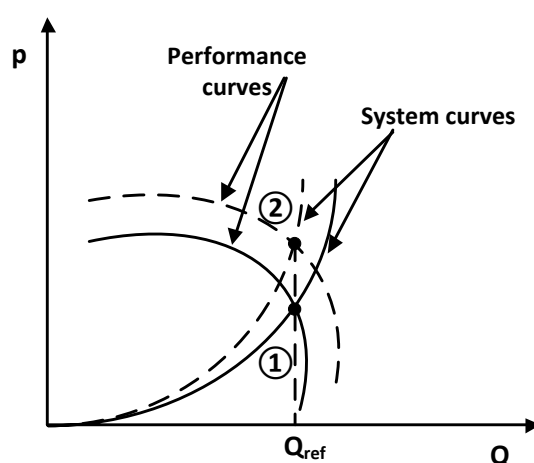
The developed flow rate control system is based on the ABB AC500 PLC chosen because of a powerful processor and large memory. To establish communication with other devices, this PLC uses such possibilities like Ethernet, Profibus DP, Modbus TCP, and Modbus serial. PLC is connected with the frequency converter. CM572 DP is used as an interface between CPU and profibus adapter module. The system topology is shown in Figure 6, it represents how the system looks in reality.



**Figure 6.** Experimental pumping station

To design the system, the ABB Control Builder was chosen. This software possesses all the necessary tools needed for programming, simulation and maintenance of the projects related to automation field. For this particular application of AC500 PLC, the control panel with switches, resistive potentiometers, and a voltage measuring device has been designed (Centrifugal Pumps CDX).

The algorithm of the designed PLC program is based on the performance curves (p-Q) of a centrifugal pump shown in Figure 7. When the flow changes because of the system curve transition from the solid line to the dashed one, the algorithm searches a new performance curve (dashed line) to keep the previously assigned flow rate  $Q_{ref}$ . As a result, in the previous working point (1) and in the new one (2) the flow is the same though the pressure is different. Thus, the constant flow on the outcome of a pump is maintained.

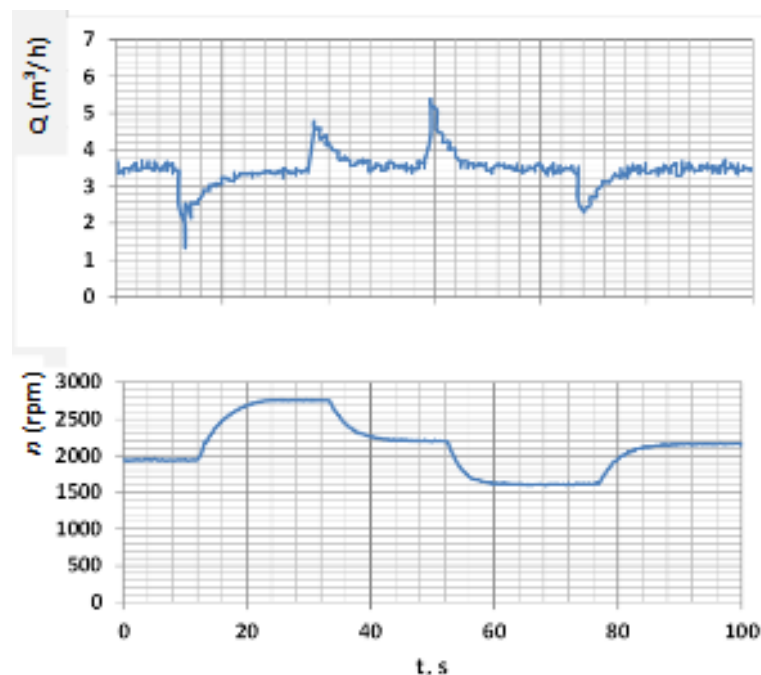


**Figure 7.** Performance and system curves

## EXPERIMENTAL RESULTS

To validate the model, a series of experiments has been conducted based on the experimental pump test bench accomplished with the developed flow rate control system. AC500 PLC has been connected to the frequency converter ACQ810 and the flow rate was regulated and maintained from

the user interface. During these experiments, the flow has been stabilizing at the rate of 3.5 m<sup>3</sup>/h. To change the system curve, a discharge valve has been installed in the pipeline (Figure 6). The discretely changed valve angles and the appropriate speed- flow responses are shown in Figure 8.



**Figure 8.** Speed–flow transients

## CONCLUSION

The developed model of centrifugal pump and related simulation approach are proposed in the paper. Simulations show that designed model is quite flexible and easy to tune. High accuracy of the model during dynamic and static modes, allows using this model for sensorless flow-measurement system for centrifugal pumps.

## REFERENCES

- De Almeida, A. T., Ferreira, F. J. T. E., Fong, J. A. C. (2011) Standards for Efficiency of Electric Motors. *Industry Applications Magazine, IEEE*, **17**(1), 12-19.
- Ferreira, F. J. T. E., Fong, J. A. C., De Almeida A. T. (2011) Ecoanalysis of Variable-Speed Drives for Flow Regulation in Pumping Systems. *Proceedings of the IEEE Transactions on Industrial Electronics*, **58**(6), 2117-2125.
- Krivchenko, G. I. (1994) *Hydraulic machines: Turbines and Pumps*, Lewis Publishers, 414.
- Qiu, X., Chen, L., Jiang, W. (2010) Simulation of the Flow Control of Radial Piston Pump Based on Simulink. *Proceedings of the 2nd International Conference on Information Engineering and Computer Science (ICIECS)*, 1-3, Dec., 2010.
- Ghafouri, J., Khayatzadeh, H. (2012) Dynamic Modeling of Variable Speed Centrifugal Pump Utilizing MATLAB/SIMULINK. *International Journal of Science and Engineering Investigation*, **1**(5), 1-7.
- Centrifugal Pumps CDX. [online] <http://www.ebara-pumps-online.com/acatalog/CDX-CDXM.html>.

# Chlorine Presence Influence on Transformation of Contaminants of Emerging Concern (Cecs) During UV-Based Processes

E. Kudlek\*

\* Silesian University Technology, Institute of Water and Wastewater Engineering, ul. Konarskiego 18, 44-100 Gliwice, Poland (E-mail: [edyta.kudlek@polsl.pl](mailto:edyta.kudlek@polsl.pl))

## Abstract

A significant amount of compounds occurring in the water environment undergo different transformations. These transformations lead to the formation of a large number of intermediates, which are considered to be toxic against living organisms even in trace concentrations. The paper presents an attempt of the identification of by-products generated during the decomposition of selected contaminants of emerging concern subjected to single chlorination and UV-based processes supported by the action of chlorine and hydrogen peroxide or ozone. The chromatographic analysis of post-processing water samples containing benzocaine, acridine and  $\beta$ -estradiol indicated the formation of 7, 5 and 3 compound intermediates respectively. The number and the concentration of the by-products decreased with the time of UV irradiation. The UV-based processes had also a beneficial influence on the decrease of the toxicity of post-processed water solutions.

## Keywords

Organic micropollutants; advanced oxidation processes; chlorination; by-products

## INTRODUCTION

The chlorination process is still one of the most common used and effective methods for water disinfection during the treatment of drinking water in Water Treatment Plants. This disinfection method is mainly performed using  $\text{Cl}_2$ ,  $\text{ClO}_2$  or  $\text{NaOCl}$  reagents. The main reactive agent, which is responsible for the oxidizing effect is hypochlorous acid ( $\text{HOCl}$ ). This reactant is formed by the aqueous transformation of chlorine ( $\text{Cl}_2$ ) according Equation (1) (Rott et al., 2018).  $\text{HOCl}$  can dissociate to hypochlorite anions ( $\text{ClO}^-$ ), which are considered to be a less effective oxidant in samples of a neutral pH (Deborde et al., 2008).



The addition of another reactive agent to the reaction medium, like  $\text{H}_2\text{O}_2$  or  $\text{O}_3$ , can improve the decomposition of compounds by the direct action with the contaminant molecule or by the generation of other high reactive species (Kudlek and Dudziak, 2018). Also the implementation of the chlorination process in assistance with UV irradiation can lead to the improvement of the contaminant decomposition. This is related to the generation of several radicals, like:  $\text{HO}^\bullet$ ,  $\text{Cl}^\bullet$  and  $\text{O}^\bullet$  (Yang et al., 2016; Li et al., 2016). Oxidizing agents and formed radicals not only lead to the removal or deactivation of pathogenic microorganisms but also reaction with compounds present in the disinfected water matrix.

The most known chlorination by-products are trihalomethanes (THMs) and haloacetic acids (HAAs) (Legay et al., 2019; Villanueva et al., 2015). However these intermediates are not the only that are present in water after disinfection. Also chlorination by-products of several organic micropollutants, belonging to the group of contaminants of emerging concern (CECs), are identified



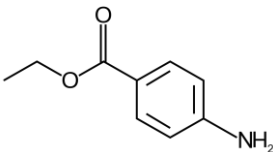
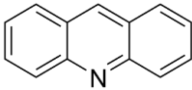
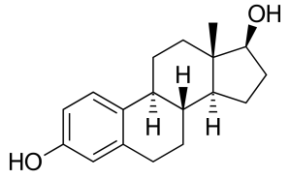
in chlorinated water. The occurrence of these compounds especial in drinking water can have a harmful impact on human health (Bolong et al., 2009).

The paper presents the identification of decomposition by-products of selected CECs, which belong to the group of pharmaceutical compounds, dye additives and synthetic hormones formed during UV-based oxidation processes performed in the presence of chlorine hydrogen peroxide and ozone. The tests were carried out on both deionized and surface water micropollutant solutions. The generated compound intermediates were identified based on their mass spectra compared to the National Institute of Standards and Technology NIST v17 database. Additionally a toxicological evaluation of the post-process water samples was performed.

## MATERIAL AND METHODS

The research subject constituted water solutions prepared on deionized water and surface water matrices spiked with CECs: benzocaine (BE), acridine (ACR) and  $\beta$ -estradiol (E2). The concentration of the contaminants was set on 500  $\mu\text{g/L}$ . Standards of the tested compounds with a purity of over 99 %, 97 % and 98 % were purchased from Sigma-Aldrich (Poznań, Poland). The characteristic of the compound is presented in Table 1.

**Table 1.** Physicochemical characteristic of studied contaminants of emerging concern

Compound group	pharmaceutical compound	dye and pharmaceutical additive	hormone
Name	benzocaine (BE)	acridine (ACR)	$\beta$ -estradiol (E2)
Structural formula			
Molecular formula	$\text{C}_9\text{H}_{11}\text{NO}_2$	$\text{C}_{13}\text{H}_9\text{N}$	$\text{C}_{18}\text{H}_{24}\text{O}_2$
CAS-RN	94-09-7	260-94-6	50-28-2
Molecular weight, g/mol	165.19	179.22	272.38
Solubility in water, mg/L	1310	5.6	3.6

All water matrices were subjected to the chlorination process, which was carried out by the use of sodium hypochlorite ( $\text{NaClO}$ ) with a nominal free chlorine content of 6 % (w/v) purchased from Chemoform (Sosnowiec, Poland). The chlorine dose, measured as a total chlorine concentration, used in the experiment was equal to 0.5, 1.0, 2.0 and 3.0 mg/L. The single chlorination process was carried out in a dark chamber to omit the influence of any light source on the decomposition of tested micropollutants. Chlorinated water samples were also exposed to UV irradiation supported by the presence of hydrogen peroxide ( $\text{H}_2\text{O}_2$ ) or ozone ( $\text{O}_3$ ). The  $\text{H}_2\text{O}_2$  and  $\text{O}_3$  dose was estimated in preliminary studies and set on 3.0 mg/L. The single chlorination process was carried out 10, 20 and 30 min and stopped by sodium thiosulphate ( $\text{Na}_2\text{S}_2\text{O}_3$ ) at a dose of 100 mg/L, which act as an excess chlorine removing agent.  $\text{Na}_2\text{S}_2\text{O}_3$  with a purity of 98 % was purchased from Merck KGaA (Darmstadt, Germany).  $\text{O}_3$  was generated by Ozoner FM500 WRC Multiozon (Sopot, Poland) and introduced in the tested CECs water samples by the use of a ceramic diffuser. The  $\text{O}_3$  was measured by the use of a photometric method  $\text{O}_3$  Spectroquant<sup>®</sup> by Merc Sp. z o.o. (Warszawa, Poland). The reaction was topped after the end of the UV irradiation time by sodium sulphite  $\text{Na}_2\text{SO}_3$  at a

concentration of 24 mmol/L. Furthermore the UV irradiation was carried out by the use of a 150 Watt mercury lamp placed in a glass cooling sleeve by Heraeus (Hanau, Germany) with a radiation flux summarized in Table 2. The time of irradiation was set on 2, 5, 10, and 20 min.

The experiments were performed for all CECs separately in neutral conditions, therefore the pH of each tested matrix was adjusted to 7.0 using 0.1 mol/L NaOH.

**Table 2.** Physicochemical characteristic of studied contaminants of emerging concern (Data achieved from the supplier of Heraeus UV lamp reactors KENDROLAB Sp. z o.o.)

	Radiation flux $\Phi$ , W															
Wavelength $\lambda$ , nm	238/40	254	265	280	297	302	313	334	366	390	405/08	436	492	546	578	
Direct lamp radiation	1.0	4.0	1.4	0.7	1.0	1.8	4.3	0.5	6.4	0.1	3.2	4.2	0.1	5.1	4.7	
Radiation passing through the sleeve	-	-	-	-	0.1	0.5	2.5	0.4	5.8	0.1	2.9	3.6	0.1	4.6	4.2	

The analytical procedure of investigated compounds was performed by solid phase extraction of the analytes and their chromatographic analysis according to guidelines presented in (Kudlek, 2018). The chromatographic measurement was carried out by the use of the 7890B GC-MS(EI) chromatograph by Perlan Technologies (Warszawa, Poland). The column oven temperature program was set on: 80 °C (6 min), 5 °C/min up to 260 °C, 20 °C/min up to 300 °C (2 min). Helium was used as the carrier gas. The temperature of the ion trap, ion source and injector were equal to 150 °C, 230 °C and 250 °C respectively. The mass detector operated in the total ion current (TIC) mode in the range of 50 to 400 m/z.

Toxicological evaluation of the post-processed samples was carried out by the use of bioluminescent *Aliivibrio fischeri* bacteria indicator organisms in the Microtox<sup>®</sup> test by Modern Water (Warsaw, Poland). To exclude the impact of the possible chlorine which left in the post-processed water solutions, the collected samples were subjected to toxicological test after 24 h incubation in a cooled dark chamber.

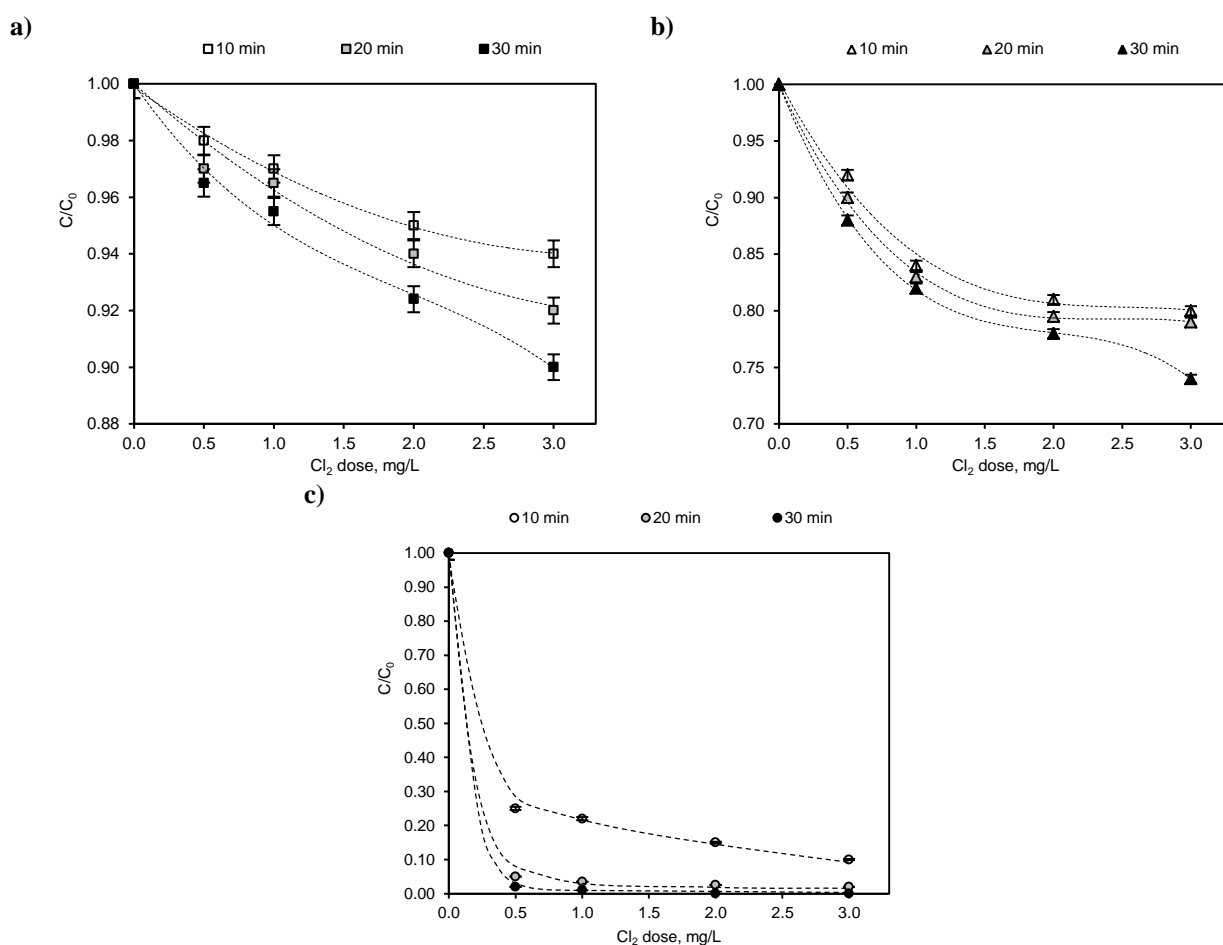
Assignment errors marked on figures, were estimated on the basis of the standard deviation for three repetitions of each test. The errors values for all tested samples did not exceed 2.0 %.

## RESULTS AND DISCUSSION

Figure 1 shows the influence of chlorine dose on the decomposition of tested CECs in deionized water solutions. It was noted, that the removal degree of all compounds increases with the increase of the chlorine concentration. BE was characterized by the least susceptibility to decompose under the influence of chlorine. The removal of BE noted after a 10 min reaction time for the chlorine dose equal to 0.5, 1.0, 2.0 and 3.0 mg/L was only 2, 3, 5 and 6 % respectively. An extension of the reaction time to 30 min allow for a 3.5 % removal of this compound noted for 0.5 mg/L of chlorine and a 10 % removal for the chlorine content equal to 3.0 mg/L. Higher removal degrees were noted for ACR. This contaminant decomposed in the presence of 3.0 mg/L of chlorine by over 20 % after 10 min and over 26 % after 30 min of process duration. It can be concluded that single chlorination by the use of NaClO is not sufficient for the decomposition of BE and ACR. A reverse observation was noted in the case of E2 chlorination. The addition of 0.5 mg/L of chlorine to the compound solution leads to his over 75 and 98 % decomposition after 10 and 30 min respectively. A complete removal of E2 was observed after 30 min of reaction with the chlorine dose equal to 2 mg/L. Li et

al. (2017) also noted a complete removal of E2 during the chlorination process carried out in neutral conditions.

The results obtained for test carried out on surface water were similar to those obtained for deionized water (Figure 1S). Only in the case of the decomposition of ACR a 5 % increase of the compound removal was noted.

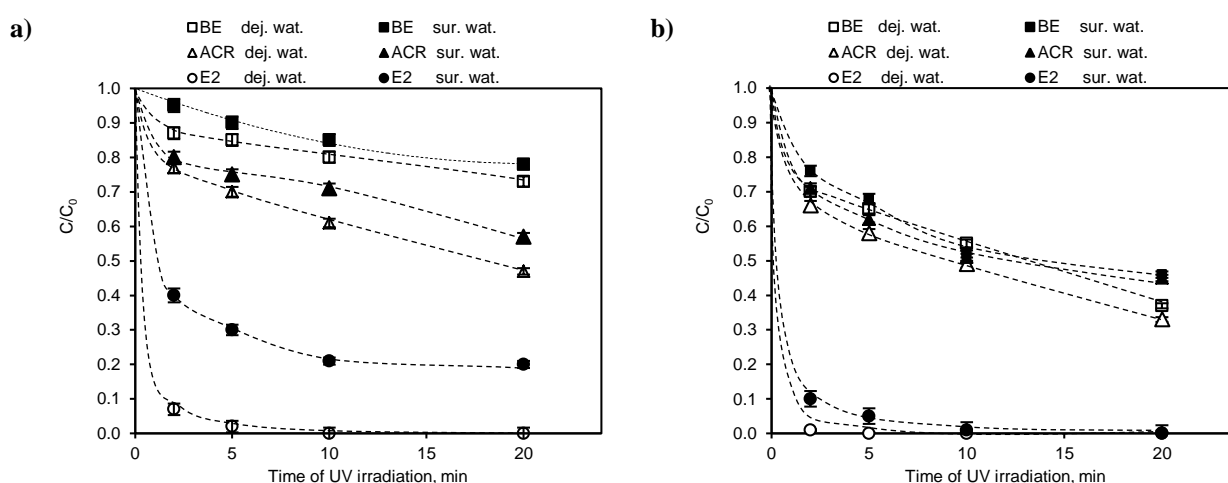


**Figure 1.** Change of a) BE, b) ACR and c) E2 concentration during chlorination of deionized water solutions

The low removal degrees of BE and ACR observed during single chlorination forces the use of another treatment process. Therefore UV-based processes supported by the presence of  $H_2O_2$  and  $O_3$  were implemented. Figure 2 compares the decrease of CECs concentration observed in deionized and surface water solution subjected to UV irradiation in the presence of chlorine and  $H_2O_2$  (UV/ $Cl_2$ / $H_2O_2$  process) or  $O_3$  (UV/ $Cl_2$ / $O_3$ ). In both processes preferable removal degrees were observed for micropollutants occurring in deionized water matrixes. This difference in process effectiveness was especially notable during the UV/ $Cl_2$ / $H_2O_2$  process. For example, 2 min of process implementation lead to the 60 % removal of E2 in the surface water solution, while the removal of this compound noted in the deionized water matrix exceeded 93 %. After 20 min of process duration a complete removal of E2 in deionized water was noted. The concentration of this contaminant occurring in surface water was reduced by 80 % (20 min of process duration). The final removal of BE and ACR noted in deionized water samples was equal to 27 and 53 %, whereas the removal of this compounds observed in surface water reached only 22 and 43 % respectively. Higher removal degrees were noted during the UV/ $Cl_2$ / $O_3$  process. E2 occurring in deionized was completely removed after 5 min of UV irradiation, and after 20 min of process implementation a

completely removal of this compound was also noted in the surface water matrix. The concentration of BE and ACR was decreased in deionized water by over 63 % and in the surface water only by 45 %. It can be concluded that the higher effectiveness of the UV/Cl<sub>2</sub>/O<sub>3</sub> against the UV/Cl<sub>2</sub>/H<sub>2</sub>O<sub>2</sub> process was the result of the formation of a larger number of radicals during the O<sub>3</sub> self-decomposition in water. Among these radicals HO<sup>•</sup>, HO<sub>2</sub><sup>•</sup>, HO<sub>3</sub><sup>•</sup>, HO<sub>4</sub><sup>•</sup>, O<sub>2</sub><sup>•-</sup> and O<sub>3</sub><sup>•-</sup> can be mentioned (da Silva and Wilson, 2006). Whereas the irradiation of H<sub>2</sub>O<sub>2</sub> with UV light leads to the formation of OH<sup>•</sup> radicals. (Mierzwa et al., 2018). However OH<sup>•</sup> radicals are endowed with the strongest oxidation potential and they are able to abate compounds which are resistant for O<sub>3</sub> or H<sub>2</sub>O<sub>2</sub> decomposition (Bourgin et al., 2017).

The implementation of the tested CECs decomposition processes not only allows for a decrease of the contaminant concentration but also leads to the generation of several by-products. These intermediates were formed during reactions occurring between the parent compounds and chlorine and/or other reactive species.



**Figure 2.** Change of compound concentration during the a) UV/Cl<sub>2</sub>/H<sub>2</sub>O<sub>2</sub> and b) UV/Cl<sub>2</sub>/O<sub>3</sub> (dej. wat. – deionized water solutions, sur. wat. – surface water solutions)

By-products were identified based on their mass spectra by the use of the NIST v17 database (Table 1). The identified intermediates decompose more slowly than the parent micropollutants and were detected even after 20 of UV-based process implementation. The single chlorination process lead to the formation of four BE intermediates: Ethyl 4-chlorobenzoate, 4-Chloroaniline, Chlorohydroquinone and 2,5-Dichlorohydroquinone, while the chlorination of ACR solutions resulted in the formation of 9-Chloroacridine and Salicylic acid. During the implementation of both UV-based processes, the occurrence of all CECs intermediates listed in table 3 was noted. Intermediates detected in each individual process were summarized in Table S1.

Ethyl 4-hydroxybenzoate and Ethyl 4-chlorobenzoate were formed by the denitration of the BE molecule and the substitution of the nitric group by the hydroxyl group and chlorine respectively. Other BE intermediates were possibly generated by the attack of OH<sup>•</sup> and chlorine on the phenolic ring of the compound. The ACR decomposition by-products Acridone, Acridine-10-oxide and 2-Hydroxyacridine were mainly formed by the attack of oxygen reactive species of the compound molecule, while 9-Chloroacridine is the result of the substitution of chlorine to the phenolic ring.

The applied analytical method based on gas chromatography allow only for the detection of three E2 intermediates, which are results of oxygen reactive species action. Li et al. (2017) pointed that the decomposition of E2 take place by the halogenation of the aromatic ring followed by the

cleavage of the benzene moiety and chlorine substitution formation, and generation of THMs and HAAs from phenolic intermediates.

**Table 3.** Identified CECs by-products during the performed experiments

Parent compound	Identified compound	Structural formula	CAS-RN	Similarity,%	Molecular weight
BE	Ethyl 4-hydroxybenzoate	C <sub>9</sub> H <sub>10</sub> O <sub>3</sub>	120-47-8	74	166.17
	Ethyl 4-chlorobenzoate	C <sub>9</sub> H <sub>9</sub> ClO <sub>2</sub>	7335-27-5	84	184.62
	4-Chloroaniline	C <sub>6</sub> H <sub>6</sub> ClN	106-47-8	86	127.57
	4-Chlorophenol	C <sub>6</sub> H <sub>5</sub> ClO	106-48-9	99	128.55
	3,4-Dichlorophenol	C <sub>6</sub> H <sub>4</sub> Cl <sub>2</sub> O	95-77-2	98	163.00
	Chlorohydroquinone	C <sub>6</sub> H <sub>5</sub> ClO <sub>2</sub>	615-67-8	75	144.55
	2,5-Dichlorohydroquinone	C <sub>6</sub> H <sub>4</sub> Cl <sub>2</sub> O <sub>2</sub>	824-69-1	80	179.00
ACR	Acridone	C <sub>13</sub> H <sub>9</sub> NO	578-95-0	70	195.22
	Acridine-10-oxide	C <sub>13</sub> H <sub>9</sub> NO	10399-73-2	75	195.22
	2-Hydroxyacridine	C <sub>13</sub> H <sub>9</sub> NO	22817-17-0	90	195.22
	9-Chloroacridine	C <sub>13</sub> H <sub>8</sub> ClN	1207-69-8	72	213.66
	Salicylic acid	C <sub>7</sub> H <sub>6</sub> O <sub>3</sub>	69-72-7	80	138.12
E2	2-Hydroxyestradiol	C <sub>18</sub> H <sub>24</sub> O <sub>3</sub>	362-05-0	92	288.40
	Estradiol-3,4-quinone	C <sub>18</sub> H <sub>22</sub> O <sub>3</sub>	144082-88-2	78	286.40
	4-(1-Hydroxyethyl)phenol	C <sub>8</sub> H <sub>10</sub> O <sub>2</sub>	2380-91-8	80	138.16

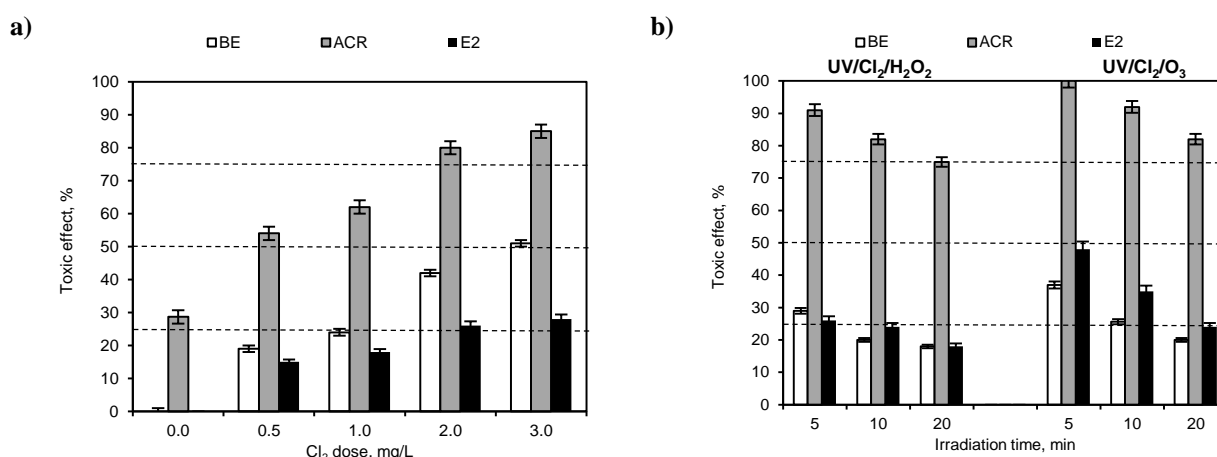
It should be noted that chlorine is used in water treatment processes to protect water before secondary contamination (Du et al., 2017). Therefore it should be toxic to pathogens and so also to small test organisms. The adopted sample preparation methodology before the proper toxicological test allowed for the exclusion of chlorine influence on test bacteria. Chlorinated water samples without the addition of tested CECs were characterized by a toxicological effect lower than 9 % (Figure S2), which classified them, according to the guidelines given by Mahugo Santana et al. (2009), as non-toxic. The results shown in Figure 3 present the toxicological effect resulted from the generated parent compound intermediates.

ACR surface water samples before the addition of NaClO were low toxic (25.0 % < toxic effect ≤ 50.0 %) against the test bacteria. Whereas BE and E2 were non-toxic (toxic effect ≤ 25.0 %). The presence of chlorine initiated the decomposition of the compounds, and therefore also leads to an increase of the toxicity. It was noted that the toxic effect increases with the increase of the chlorine dose (Figure 3a). For example BE and E2 solutions treated by 1.0 mg/L of chlorine were still non-toxic, while the dose of 3.0 mg/L resulted in the increase of the BE solution toxicity to a toxic level (50.0 % < toxic effect ≤ 75.0 %) and the E2 solution toxicity to a low toxic level. The highest toxicity was observed for ACR post-processed solution. The addition of 0.5 or 1.0 mg/L of chlorine to the ACR water solution led to the formation of several toxic intermediates, which increased the toxicity to a toxic level, and the addition of 2.0 and 3.0 mg/L of chlorine resulted in the generation of high toxic solutions (toxic effect > 75.0 %). The results obtained for deionized water solutions were characterized by the same tendency (Figure S3). The toxicity noted for BE, ACR and E2

deionized water solutions was 5 %, 8 % and 2 % respectively higher than those noted for surface water solutions.

The post-processed samples obtained during the UV-based treatment methods were also subjected to toxicological tests (Figure 3b). It was noted that the implementation of UV irradiation supported by the action of 1.0 mg/L chlorine and H<sub>2</sub>O<sub>2</sub> or O<sub>3</sub> resulted by an increase of the toxicity of all tested compound solutions in the first 5 min of the treatment process compared to the single chlorination process. This phenomenon confirm the generation of toxic by-products identified during the chromatographic analysis. In general, the toxicity of samples collected after the process carried out with the presence of H<sub>2</sub>O<sub>2</sub> was higher than the toxicity of samples subjected to the simultaneously action of UV light, chlorine and O<sub>3</sub>. For example, E2 solutions irradiated for 10 and 20 min in the presence of H<sub>2</sub>O<sub>2</sub> were characterized by non-toxicity, while samples of the same contaminant subjected to O<sub>3</sub> supported irradiation were classified after 10 min as low toxic but after 20 min as non-toxic. The chromatographic analysis indicted that signals caused by the formed intermediates after 10 min of UV irradiation become weaker. This means that after this time of the process, the concentration of by-products decreases. This was also reflected in the toxicity results. The toxicity decreased after 10 and 20 min of process implementation. For example the toxicity of the ACR solution treated by UV light supported by NaClO and H<sub>2</sub>O<sub>2</sub> decreased form a high toxic level to a toxic level and the BE and E2 solutions decreased during both treatment processes from a low toxic to a non-toxic level.

Donner at al. (2013) noted an increase of the toxicity during the irradiation of carbamazepine solutions with UV light in the first 30 min. ACR is a toxic decomposition by-product of carbamazepine. The occurrence of this compound and other carbamazepine intermediates increased the toxicity. A future irradiation of the pharmaceutical solution leads to the decomposition of acridine and a decrease of the solution toxicity.



**Figure 3.** Change in the toxicity of the CECs surface water solution after a) single chlorination (30 min of process duration) and b) selected UV-based processes (5, 10 and 20 min of UV irradiation)

## CONCLUSIONS

The chlorination process of organic contaminants occurring in deionized and surface water lead to their decomposition and the formation of several intermediates. With the increase of the chlorine concentration a decrease of compound concentration and an increase of the forming by-products were observed. The implementation of the UV radiation in the presence of oxidants results in the decrease of the number and concertation of forming by-products. The UV-based processed had also a beneficial influence on the toxicity of the post-processed solutions.

## ACKNOWLEDGMENTS

This work was supported by Ministry of Science and Higher Education Republic of Poland within statutory funds.

## REFERENCES

- Bolong, N., Ismail, A. F., Salim, M. R., Matsuura, T. (2009) A review of the effects of emerging contaminants in wastewater and options for their removal. *Desalination*, **239**, 229-246.
- Bourgin, M., Borowska, E., Helbing, J., Hollender, J., Kaiser, H.-P., Kienle, C., McArdell, C. S., Simon, E., von Gunten, U. (2017) Effect of operational and water quality parameters on conventional ozonation and the advanced oxidation process O<sub>3</sub>/H<sub>2</sub>O<sub>2</sub>: Kinetics of micropollutant abatement, transformation product and bromate formation in a surface water. *Water Res.*, **122**, 234-245.
- da Silva, L. M., Wilson, J. F. (2006) Trends and strategies of ozone application in environmental problems. *Química Nova*, **29**, 310-317.
- Deborde, M., von Gunten, U. (2008) Reactions of chlorine with inorganic and organic compounds during water treatment—Kinetics and mechanisms: A critical review. *Water Res.*, **42**, 13-51.
- Donner, E., Kosjek, T., Qualmann, S., Kusk, K. O., Heath, E., Revitt, D. M., Ledin, A., Andersen, H. R. (2013) Ecotoxicity of carbamazepine and its UV photolysis transformation products. *Sci Total Environ*, **443**, 870-876.
- Du, Y., Lv, X.-T., Wu, Q.-Y., Zhang, D.-Y., Zhou, Y.-T., Peng, L., Hu, H.-Y. (2017) Formation and control of disinfection byproducts and toxicity during reclaimed water chlorination: A review. *J. Environ. Sci.*, **58**, 51-63.
- Kudlek, E. (2018) Decomposition of contaminants of emerging concern in advanced oxidation processes. *Water*, **10**(7), 955.
- Kudlek, E., Dudziak, M. (2018) Toxicity and degradation pathways of selected micropollutants in water solutions during the O<sub>3</sub> and O<sub>3</sub>/H<sub>2</sub>O<sub>2</sub> process. *Desalin. Water Treat.*, **117**, 88-100.
- Legay, C., Leduc, S., Dubé, J., Levallois, P., Rodriguez, M. J. (2019) Chlorination by-product levels in hot tap water: Significance and variability. *Sci Total Environ*, **651**(2), 1735-1741.
- Li, C., Dong, F., Crittenden, J. C., Luo, F., Chen, X., Zhao, T. (2017) Kinetics and mechanism of 17β-estradiol chlorination in a pilot-scale water distribution systems. *Chemosphere*, **178**, 73-79.
- Li, M., Xu, B., Liungai, Z., Hu, H.-Y., Chen, C., Qiao, J., Lu, Y. (2016) The removal of estrogenic activity with UV/chlorine technology and identification of novel estrogenic disinfection by-products. *J. Hazard. Mater.*, **307**, 119-126.
- Mahugo Santana, C., Sosa Ferrera, Z., Torres Padron, M. E., Santana Rodríguez, J. J. (2009) Methodologies for the extraction of phenolic compounds from environmental samples: New Approaches. *Molecules*, **14**, 298-320.
- Mierzwa, J. C., Rodrigues, R., Teixeira, A. C. S. C. (2018) UV-Hydrogen Peroxide Processes. *Advanced Oxidation Processes for Wastewater Treatment: Emerging Green Chemical Technology*, 13-48.
- Rott, E., Kuch, B., Lange, C., Richter, P., Kugele, A., Minke, R. (2018) Removal of Emerging Contaminants and Estrogenic Activity from Wastewater Treatment Plant Effluent with UV/Chlorine and UV/H<sub>2</sub>O<sub>2</sub> Advanced Oxidation Treatment at Pilot Scale. *Int. J. Environ. Res. Public Health.*, **15**(5), 935.
- Villanueva, C. M., Cordier, S., Font-Ribera, L., Salas, L. A., Levallois, P. (2015) Overview of disinfection by-products and associated health effects. *Curr. Environ. Health Rep.*, **2**(1), 107-115.
- Yang, X., Sun, J., Fu, W., Shang, C., Li, Y., Chen, Y., Gan, W., Fang, J. (2016) PPCP degradation by UV/chlorine treatment and its impact on DBP formation potential in real waters. *Water Res.*, **98**, 309-318.



# Beach Wrack Management as Example of Circular Economy

A. Kupczyk\* and K. Kolečka\*

\* Department Water and Waste-Water Technology, Faculty of Civil And Environmental Engineering, Gdańsk University of Technology, Gabriela Narutowicza 11/12, 80-233 Gdańsk, Poland  
(E-mails: [alikuscz@pg.edu.pl](mailto:alikuscz@pg.edu.pl); [katkolec@pg.edu.pl](mailto:katkolec@pg.edu.pl))

## Abstract

The phenomenon of beach wrack, occurring all over the world, has not been given too much attention so far. It is a material with a specific composition, whose precise qualitative description is difficult. Material washed out by the sea during the year changes quantity and quality. Establishing a precise definition and the amount accumulated on beaches is a task that causes problems. The law clearly does not specify what is included in it and how it should be dealt with, which is a challenge for institutions managing beaches. In addition in the Baltic Sea region, beach wrack is a factor that enhances the problem of eutrophication, through the high content of nutrients released during the decomposition of accumulated material on the coasts of beaches. As part of the CONTRA project, various options for beach wrack management in the region of the Baltic Sea will be explored. An interesting solution seems to be the use of reed bed system technology, which has been used in the case of sewage sludge, as a beach wrack processing method. This solution seems to be a good idea due to similar material of beach wrack and sewage sludge. In addition, this solution fits in with the circular economy that is being introduced now, departing from a linear approach.

## Keywords

Beach wrack; eutrophication; utilization; reed bed system; fertilizer; compost

## BEACH WRACK PROBLEM

Beach wrack is a natural occur phenomenon, which is observed on the beaches around the world. The sea thrown out organic material by waves, tides and wind. These factors are also responsible for recycling it back to the sea (Macredie et al., 2017). Determining what is actually beach wrack is not as easy as according to Macredie et al. 2017. The material washed out to coast does not consist only of organic ingredients, but also can be find plastics, glass, metals (mainly wastes made by human beings).

In Poland term beach wrack was not found. In Polish literature, can be found the term "kidzina" which means a beach roller created by organic debris thrown by waves to the seashore., and it is a natural habitat protected in the Natura 2000 network. It is understood as principally organic vegetable matter; snail and mussel shells; small organisms and eggs of marine animals; all material thrown by wave and currents on the sea shore. The material thrown out to the beaches changes in terms of quality throughout the year. On the Polish side of the Baltic Sea coast you can find: summer- mainly scums of cyanobacteria; autumn- seagrass and shells, which are thrown by storms; winter and early spring- bridge remains of sticks and leaves; may- filamentous algae. (Szymelfenig et al., 2005). Kidzina includes both items of natural and antropogenic origin. The plant material contained mainly vascular plants (*Potamogeton* spp.) and macroalgae, with a small proportion of seagrass (*Zostera marina*) and unicellular algae. Identified – green algae (*Cladophra* spp., *Enteromorpha* spp.) brown (*Pilayella littoralis*, *Ectocarpus* spp.) and red algae (*Furcellaria fastigata*, *Ceramium* spp), with the dominant species being *Cladophora* spp., *Enteromorpha* spp., *Pilayella littoralis* and *Ceramium* spp. (Filipowska et al., 2008). Manmade waste include: miscellaneous plastic, glass, rubber, paper and textile impurities, mainly from households.

Another term used in Poland in reference to beach wrack is seagrass. It's mainly about organic material. Characteristic long sea grass leaves, in various degradation states, fresh green leaves on the water line, close to dunes, the material is completely dried out. Typically seagrass (*Zostera marina*) without the addition of other organic components. A small part is anthropogenic waste (plastic, glass, metal, etc.).

This raises a discussion about what should be call the term "beach wrack". The basic question that comes to mind in this case is whether it is only organic material or also that which contains inorganic ingredients and whether the term beach wrack can be combined only with natural ingredients or also those of human origin. Based on current research and discussions with countries struggling with the beach wrack problem, it can be described as a mixture of marine vegetation, animal waste, and natural and ananthropogenic land wastes. In order to take effective actions to management the beach wrack, it is necessary to establish a clear definition of what exactly it is.

### **Impact of beach wrack on environmental and social**

Beach wrack material has many benefits for the marine ecosystem, which is not covered by the problem of eutrophication. It is a habitat for various animals, including birds. In addition, the beach wrack affects the protection of the coastline by establishing a physical barrier that disperses the impact force of waves. The fibrous structure perfectly binds the sand, affecting the reduction of the erosion process of the dunes. The beach wrack phenomenon supports the marine food chain by providing nutrients from the decomposing material (Government of south Australia).

Beach wrack thrown out the shore is rich in nutrients, which released to the sea cause the eutrophication process, which is disadvantageous for high-trophic reservoirs like Baltic Sea. According to the research conducted for the benefit of: the Assessment of the state of the environment of Polish sea areas of the Baltic Sea on the basis of monitoring data from 2017 against the background of the decade 2007-2016, the state of none of the basins (The Bornholm Basin, The Eastern Gotland Basin and The Gdańsk Basin) has not been assessed as good, which indicates that the Baltic Sea is struggling with the problem of eutrophication. The direct cause is mainly the high content of total and mineral nitrogen and phosphorus, which caused increased blooms of phytoplankton, which contributed to a higher concentration of chlorophyll-a and increased turbidity of Baltic waters as well as poor oxygenation of the deep-water zone (Krzyimiński, 2018). Certainly, supplying an additional dose of nutrients from decomposing beach wrack material will not contribute to the improvement of the quality of the Baltic Sea.

Furthermore organic material quick decompose on the shore, giving off unpleasant smell, which deter tourists (Szymelfenig et al., 2005). The material washed out by the sea, reduces the attractiveness of seaside resorts, whose economy is based mainly on local activities directly related to tourism.

Beach wrack is not only environmental problem for eutrophicated water reservoir but also a specific social problem for local authorities, which in accordance with the European Union Directive on bathing water quality (2006/7 /EC), are obligated to remove of macroalgae laying on the coast. Pursuant to Directive 2006/31 / EC of the European Parliament and of the Council (EU) 2018/850, material of beach wrack must be utilize, because the collection of biodegradable waste on landfills is prohibited. Proper management of beach waste material is therefore a challenge, the solution of which will not only benefit the environment, but also for society.

Possibilities of Beach Wrack management tested in CONTRA.

Gdańsk University of Technology (Poland) is involved in the project CONTRA- "Baltic Beach Wrack- Conversion of Nuisance To a Resource and Asset", which raise the problem of beach wrack, as part of the Interreg Baltic Sea Region program. The project assumes a thorough examination of the problem of the beach wrack phenomenon. The main goal is to change the approach to the material thrown out by the Baltic Sea. Project is to contribute to finding positive aspects of this material, which has been recognized as a nuisance, and to show how it can be a source of benefits for institutions dealing with beach management. The result of the work under the project is to be a toolkit that propose specific beach wrack processing technologies and the positive effects that flow from them. The project will conduct research on six case studies.



**Figure 1.** The distribution of planned research in the Baltic Sea countries participating in the CONTRA project (based on google maps)

**Table 1.** Main assumptions of CONTRA case studies

Case Study	Name	Place	Main aim
1	Wreck4soil	Bad-Doberan Macklenburg Western Pomerania, Germany	Fertilizer and soil improvement products recycled from beach wrack
2	BWC- Beach Wrack Conversion	Island Rügen, Germany	Pre-feasibility assessment of development of special technologies of bio-char production and its further possible applications
3	Wrackover- beach wrack for bio-cover	Køge Municipality, Denmark	Using beach wrack as compost material in a methane inhibiting biocover
4	Wrack4coast- beach wrack for costal protection installations	Curonian Spits, Russia	Assessment of beach wrack applicability for dune restoration measures
5	ALERA- AlgeaReactor	Kalmar, Sweden	Gasification, experimental setup and testing of innovation feasibility
6a	WAIT- WATERimprovement	Puck Bay, Poland	Beach wrack removal for water quality improvement
6b	FERTIWRACK	Swarzewo, Puck Bay, Poland	Use beach wrack for fertilizers

### **Occurrence and quantity of beach wrack**

The lack of monitoring in the area of Polish shore of the Baltic Sea as like seasonal changes in occurrence of beach wrack contribute to difficulties in accurately estimating the quantity of it. According to Maritime Institute in Gdańsk, the amount of biomass of algae lying on the beach in Sopot (North Part of Poland, famous place for holidays) ranges from 160-800 tons dry weight per year (Schultz-Zehden and Matczak 2013). According to MOSiR Sopot (Municipal Sports and Recreation Center) it is possible to collect from 180 to 796 tons of wet weight from beaches for the season. IO PAN (Institute of Oceanology, Polish Academy of Sciences) estimated this amount at 220 - 440 tons per season (Hansson et al., 2013).

### **FERTIWRACK- CASE STUDY**

One of the ideas of beach wrack utilization is using a reed bed system to obtain final product - more likely as fertilizer or as an addition / enrichment to compost.

The reed system is related to the simulation of processes occurring in natural wetland ecosystems. Until now, this technology has been used to dewater and stabilize sewage sludge. The use of this system in relation to beach wrack is an innovative solution.

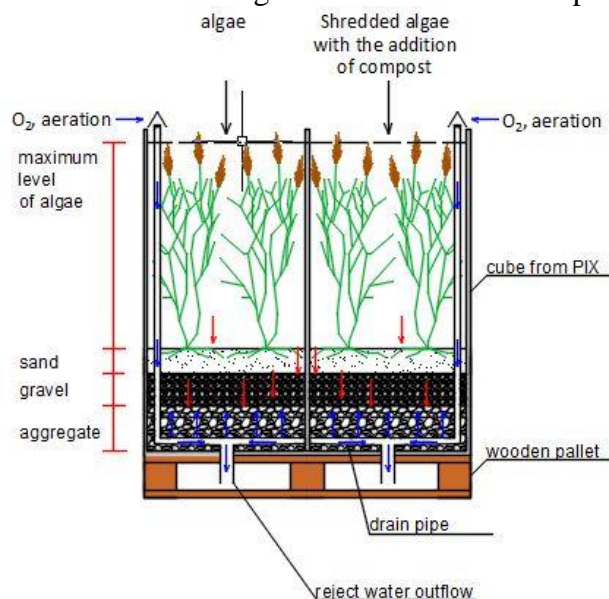
The dewatering process takes place in a similar way as naturally occurring in wetlands, mainly the water infiltration through the bed and outflow in the form of reject water and the evapotranspiration of water from above-ground parts of reeds (Nielsen and Cooper 2011). This process leads to a reduction in both the volume and mass of the raw material as well as the increase in the content of dry matter.

Stabilization occurs through differences in oxidation-reducing potentials, resulting in mineralization of organic matter as well as nitrogen transformations. The effect of stabilization is to lower the content of organic compounds, which reduces the combustibility and elimination of unpleasant odors. To the array of this method's advantages could be included:

- simple construction of reed system (Kołecka and Rohde, 2018) - simple technical solutions influence to easier availability for layman, easier understanding of technology and also lower risk of expensive repairs during exploitation time;
- low investment and exploitation costs (Kołecka and Rohde, 2018) – finance is a very important issue for local authorities responsible for beach wrack management, low costs related to the construction and maintenance of reed bed systems are a factor favoring the choice of this method, additionally, it is intended to produce a fertilizer that can be an extra influence to the budget of the institution which will decide on such a solution;
- natural look, which enables easy fit in existing landscape (Sobczyk and Sypuła, 2011)- natural and easily fitting appearance of reed bed systems in the case of application beach wrack is a factor increasing its potential, the profitability of this type of method depends on the distance of the raw material collecting site to the processing site, due to the eye-pleasing appearance, the object can be built in close distance to the beach because it will be a great complement to the seaside landscape ;
- lack of necessity use of chemicals; low emission and energy consumption (Obarska-Pempkowiak et al., 2015)- the processes occurring in the reed bed are based on natural mechanisms, do not need, as in the case of mechanical dewatering, the addition of polyelectrolytes to improve the efficiency of the process, lack of additional foreign substances introduced into the environment provides an ecologically friendly solution, this method also consumes energy only for the supply of the sewage sludge by pump to beds, low emissivity is associated with lower production of carbon dioxide than in the case of traditional methods and reduction of methane by plants in a well-functioning system.

### Technological aspects

Planned pilot reed system will use cubes, situated on the wooden pallets. As a filling will be used some aggregate, gravel and sand. On the layer of sand will be situated reed. Each cube will be divided into four parts. From the bottom of each part of cube will be lead out drain pipe, which will drain away reject water and will introduce air to the reed system. In different parts of cube will be put different form of algae structure or mix algae with addition of compost in the different ratio.



**Figure 1.** Scheme of pilot reed system based on cube's modules (own study)

During the CONTRA project duration, tests will be carried out on the quality of the stabilized and dewatered beach wrack material and beach wrack mixed with compost (to improve fertilizer values) as well as reject water from individual parts. An effect similar to that obtained for the use of sewage sludge on reed bed system is expected- the volume is reduced and the dry matter content is increased by dewatering, as well as elimination of odors and lowering the content of organic compounds occurred by stabilization.

### Management aspects

Different amounts and seasonally occur of beach wrack are not problems for the reed system, because it works in an alternating cycle (irrigation and rest phase). The reed bed system, will use beach wrack to produce some kind of fertilizer, which means change nuisance to resource. Moreover use of this end product can allow to reuse biogenic compounds, which means reintroduction them to the matter cycle. The reed bed systems fits in circular economy methods, because they use processes which natural occur in wetlands, they do not need additional chemicals so they haven't got negative influence to the environmental. This solution is also low-energy consumption and low-emission. Such a solution would cause the reuse of biogenic compounds, thus entering the circular economy, which is in accordance with European Union recommendations.

What's more, the reed system can be built close to the beach, which reduces the distance needed to transport the beach wrack. The system can be used to build and reconstruct the dunes. Reed system produced fertilize, which could be income and additional advantage for potential users. The reed system will be profitable, if it will be situated in neighborhood of place where beach wrack is collected. High water content makes transport for a long distance too expensive. For the reed system necessary is adequate surface. It could be a problem for potential interested invest. In addition different amendments like mature compost or biopreparates to enhance the decay are to be tested.

## SUMMARY

Beach wrack is a specific problem. It is necessary to do research to management material from beaches located at highly eutrophicated water reservoirs such as the Baltic Sea. Collecting beach material and using it on a reed system, seems to be good idea.

## ACKNOWLEDGMENTS

Thanks for the European Regional Development Fund (ERDF), the main institution financing the CONTRA project "Baltic Beach Wrack - Conversion of Nuisance To a Resource and Asset" (Project Number: # R090) in the Interreg Baltic Sea Region program. Authors would like also to thank the management staff of the Gdańsk University of Technology for consent to conduct research and their assistance during the research. The authors are also grateful to the Wastewater Treatment Plant in Swarzewo for sharing space for the construction for pilot plant of reed bed system for beach wrack.



## REFERENCES

- Filipkowska, A., Lubecki, L., Szymczak-Żyła, M., Kowalewska, G., Żbikowski, R., Szefer, P. (2008) Utilisation of macroalgae from the Sopot Beach (Baltic Sea). *Oceanologia*, **50**(2), 255-273.
- Government of South Australia, Coast Protection Board (2017) What is beach wrack? Coastline Factsheet, 38.
- Hansson, A., Tjernström, E., Gradin, M., Finnis, P. (2012) Wetlands Algae Biogas - A Southern Baltic Sea Eutrophication Counteract Project. Municipality of Trelleborg Editors. ISBN 978-91-87407-00-0.
- Kołecka, K., Rohde, D. (2018) Zalety i problemy związane z zagospodarowaniem osadów ściekowych metodą trzcinową. *Rynek Instalacyjny*, **5**, 20-25.
- Krzywiński, W., Inspekcja Ochrony Środowiska (2018) Ocena Stanu Środowiskapolskich Obszarów Morskich Bałtyku Na Podstawiedanych Monitoringowych Z Roku 2017 Na Tle Dziesięciolecia 2007-2016 (The assessment of the state of the environment of Polish sea areas of the Baltic Sea on the basis of monitoring data from 2017 against the background of the decade 2007-2016).
- Macreadie, P. I., Trevathan-Tackett, S. M., Baldock, J. A., Kelleway, J. J. (2017) Converting beach-cast seagrass wrack into biochar: A climate-friendly solution to a coastal problem. *Science of the Total Environment*, **574**, 90-94.
- Nielsen, S., Cooper, D. J. (2011) Dewatering sludge originating in water treatment works in reed bed systems. *Water Science & Technology*, **64**(2), 362.
- Obarska-Pempkowiak, H., Kołecka, K., Buchholtz, K., Gajewska, M. (2015) Ekoinżynieria w zintegrowanym odwadnianiu i stabilizacji osadów ściekowych w systemach trzcinowych. *Przemysł Chemiczny*, **94**(12), 2299-2303.
- Schultz-Zehden, A., Matczak, M. (2013) Kompendium Submariner: Ocena Innowacyjnych i Zrównoważonych Sposobów Wykorzystania Zasobów Morza Bałtyckiego, Instytut Morski w Gdańsku. ISBN 978-83-62438-14-3.
- Sobczyk, R., Sypuła, M. (2011) Wykorzystanie makrofitów do przetwarzania osadów ściekowych na mursz. *Forum Instalatora*, **4**, 46-48.
- Szymelfenig, M., Urbański, J., Węśławski, J. M. (2005) Plaża przewodnik użytkowania, Center of Excellence for Shelf Seas Science, Sopot. ISBN 83-911901-9-6.



# Statistical Description of Time Series of Water Consumption in the Consumption Area

J. Novakova\*, J. Rucka\* and D. Fucik\*

\* Institute of Municipal Water Management, Faculty of Civil Engineering, Brno University of Technology, Zizkova 17, 602 00 Brno, Czech Republic (E-mails: [novakova.j1@fce.vutbr.cz](mailto:novakova.j1@fce.vutbr.cz); [Jan.Rucka@vut.cz](mailto:Jan.Rucka@vut.cz); [fucik.d@fce.vutbr.cz](mailto:fucik.d@fce.vutbr.cz))

## Abstract

This paper is focused on the description of time series of water consumption in the non-transit consumption area. The described minimum night flow and maximum water consumption per hour characteristics are one of the important quantities of water consumption. The aim of the paper is to find the most reliable method for determining these characteristics. The presented statistical method of percentile is compared with other statistical methods and adjusted on the basis of their results. This article describes how to determine the basic characteristics of water consumption using statistical methods, thereby speeding up and simplifying the entire process of water consumption analysis.

## Keywords

Water demand; water consumption; district metered area; minimum night flow; maximum water consumption per hour

## INTRODUCTION

For the efficient operation and management of the drinking water distribution systems (DWDSs) it is necessary to have a detailed overview of the technical and hydraulic parameters of the network (dimensions, material, pressure conditions, etc.). One of the basic entry data is the water consumption in a consumption area. The analysis of water consumption determines the basic DWDS data, thanks to which we may consider other technical interventions (e.g. reduction or increase of pipeline capacity). Such data include determination of average and maximum consumption per day, maximum consumption per hour, minimum night flow, minimum water consumption per hour respectively. The determination of the minimum night flow, which is used to evaluate the water losses from the DWDSs, is essential. For DWDSs, the design or redesign is usually based on mathematical modelling and simulation methods (Kovar et al., 2014).

Act No. 274/2001 Coll., on public water mains and sewerage for public use, stipulates by Decree No. 428/2001 Coll. an obligation for water infrastructure owners to record technical and operational information about the distribution network. Operational data include, for example, the total amount of water entering the system and the volume of water loss related to the length of the DWDS. This information is forwarded to the competent water authority. The water authority processes this information and submits it to the Ministry of Agriculture of the Czech Republic, which, in cooperation with the Czech Statistical Office, publishes this data in Annual Report.

Water supply systems in the Czech Republic are provided with relatively detailed monitoring. Operators and owners of water infrastructure have a relatively good overview of the amount of water flowing in the DWDS. The flow is monitored on many parts of the distribution system: on the water inflow pipe from the water source, on the water outflow pipe from the tanks and water treatment plants, on the main trunks connection (if there is only one water source for more than one consumption areas). Measurement is also performed on the entrance pipe each district metered area (DMA) into which the large DWDS is divided. Each connection is also equipped with a water



meter, which is the second method of measuring household water consumption in addition to group measurement (Maksimovic et al., 2003). The accuracy of measuring devices plays an important role in monitoring. Accuracy of flow meters and water meters is ensured by proper design (correct nominal flow rate, maximum and minimum flow rate etc.), correct installation and regular calibration of measuring devices (Holyszewski, 2017). Incorrectly measuring devices can cause significant financial losses to the operator, among other things, because each cubic meter of raw water taken from source is charged, even though it was not actually consumed in consumption area. Accurate and detailed monitoring of the water supply system (house connections as well as partial measurement on the network within self-contained measuring districts) is also a tool for loss reduction, as it enables faster and more accurate identification of pipeline failures and thus their faster correction (Klucka, 2019; Jeremiah, 2018).

Reducing water losses has been one of the priorities of water utilities for a long time. And this goal is the same regardless of whether the DWDS is operated and managed by professional water utility or by the municipalities, which are also owners of distribution systems. With the reduction of water losses, the optimization of pressure conditions in the DWDS is very closely related (Tuhovcak et al., 2018). Water losses are unavoidable part of the MNF. The lowest technically achievable annual volume of Real Losses, at the current operating pressure, is the Unavoidable Annual Real Losses (Lambert and Fantozzi, 2005). In connection with the drought and the related decrease in the capacity of some water sources in the Czech Republic, the issue of reduction of water losses has become a populist slogan used for political purposes, which creates even greater pressure on water utilities. The reduced capacity of water resources due to drought also presents other related problems, for example, reduced water consumption and associated increased water residence time in the pipeline and increased water age. In combination with other factors (such as increased outdoor temperature that heats the flowing drinking water through the soil in which the pipeline is stored; deteriorative raw water quality due to climatic conditions supporting the development of an organic water component and, for example, or inappropriate dose of water disinfectant), certain parts of the DWDS are at risk of deteriorating drinking water quality. The deterioration of water quality may cause loss of hygiene safety. To avoid this, various operational measures must be taken. One of them is regular flushing of the pipeline. So called dead ends and part of DWDS with low consumption are most vulnerable to this problem (Rajnochova et al., 2019).

### **Water losses in the Czech Republic**

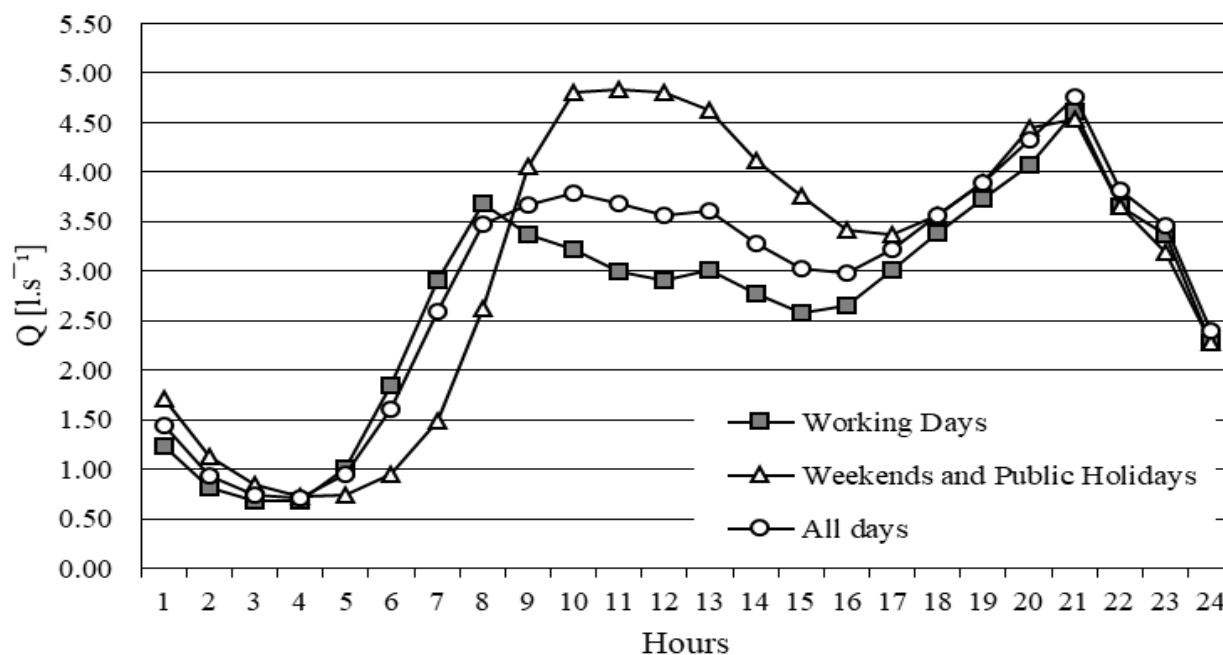
The level of water losses in the Czech Republic is generally very good even in comparison with economically more advanced countries. Water losses have been systematically reduced since 1994. One of the most used characteristic of water losses is % NRW (non-revenue water). The average value of % NFW (a ratio of total volume water incoming to DWDS and total volume of water which has not been bill to consumers) was 16.4 % in the Czech Republic in 2017.

### **Water demand in the Czech Republic**

Another characteristic of Czech water management is specific water demand ( $q_{\text{spec}}$ ). Its level has been rapidly decreased during the past 30 years. In 1989, specific water demand of households was 171 liters per person per day, in 2017 it was only 88.7 liters per person per day. With actual level of  $q_{\text{spec}}$  per households, the Czech Republic is categorized to the group of countries with lower water demand. Water demand is influenced by several factors (Nguyen and Teller, 2018).

Difference between water consumption during working days and water consumption during weekends and public holidays is typical for the Czech Republic and is shown on the Figure 1. This difference is due to other habits and daily routine of consumers during these days. One curve shows the course of water consumption during working days in 2016 (total 252 days) and the second one

shows the course of water consumption during all weekends and public holidays in 2017 (total 114 days), third curve shows the course of consumption irrespective of the type of day. Morning peak usually occurs between 06:00 – 09:00 a.m. during working day. During non-working days, the morning peak starts at 08:00 a.m. and slowly decreases until afternoon. Evening peaks occur at the same time (between 07:00 – 10:00 p.m.).



**Figure 1.** Courses of water consumptions in the DMA 7 in 2016

## METHODOLOGY

The statistical description of the time series of water consumption was performed using statistical functions of MS Office Excel software. Maximum water consumption per hour ( $Q_h$ ) and minimum night flow (MNF) were described by quantiles (also called percentiles), which are defined as statistical characteristics of the statistical file level indicating the magnitude of the phenomenon in a given set of data. Percentiles were determined from raw input data of average hourly flows by the MS Office Excel statistical function. It was not differentiated whether it was a working day or a non-working day.

The percentiles from  $x_{0.02}$  to  $x_{0.08}$  were determined to define MNF. This means that 2 – 8 % of the total input data set (depending on the selected percentile) is less than or equal to the values corresponding to the percentiles  $x_{0.02}$  -  $x_{0.08}$ . The rate of MNF determined in this way includes the actual amount of water consumption and the losses that are greatest in this period. Values lower than the set percentiles are, for example, measurement failures, instrument error, or sudden and exceptional consumer consumption.

The percentiles  $x_{0.80}$ ,  $x_{0.82}$ ,  $x_{0.84}$ ,  $x_{0.86}$ ,  $x_{0.88}$  and  $x_{0.90}$  were determined to define  $Q_h$ . Flow rates higher than those corresponding to the specified percentiles include error flows, consumption for firefighting purposes, water used for pipe flushing and other unexpected and non-regular consumptions.

### Verification of specified percentile levels

To determination the specific percentile value representing MNF and  $Q_h$  a comparison was made.

Accordance with the most frequent flow rate interval was decisive for determining the correct percentile value. This interval was determined by frequency analysis.

In the first step of the frequency analysis step, a suitable range of values was chosen, the size of this interval depended on the rounding rate of the input data and the total range of values. In the first step of the frequency analysis step, a suitable range of values was chosen, the size of this interval depended on the rounding rate of the input data and the total range of values

In the second step the frequencies of occurrence of flow rates at these intervals were determined. The comparison interval was based on the assumption that MNF occurs between 02:00 and 04:00 and  $Q_h$  occurs at evening peak hours between 19:00 and 22:00.

In addition, the raw input data determined the mode with which the percentiles and frequency analysis intervals were compared. The mode determination was only applicable to those input data files that were rounded by average hourly flow rates (to tenths, quarters, or half integers).

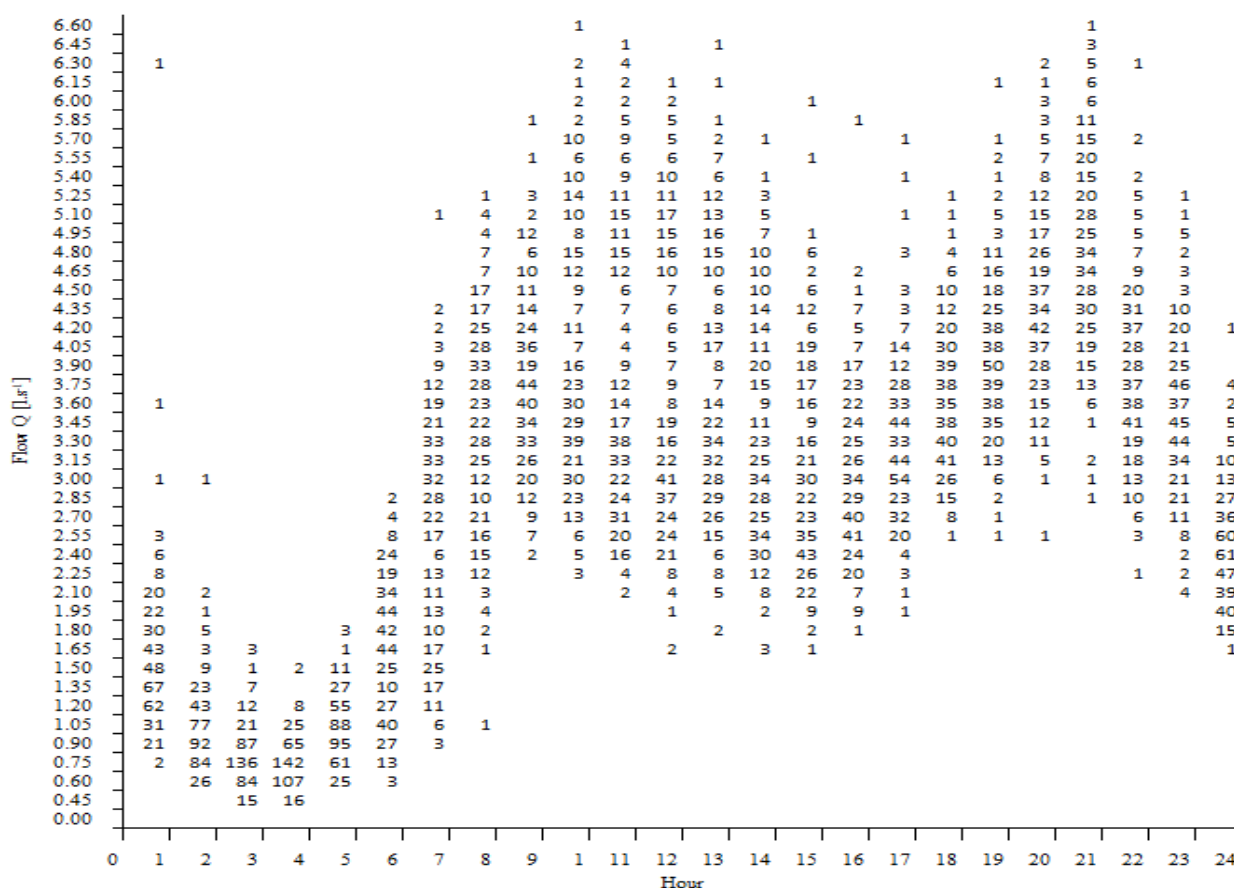


Figure 2. Flow rate frequency analysis in DMA 7

### CASE STUDIES

The minimum and maximum hourly flow rates were determined on 9 DMA real distribution networks. For all DMA, these flow characteristics were determined by the indicated methods and confirmed by the indicated statistical quantities. The measuring areas are summarized in the following table.

All DMAs are non-transit, that is, the water flowing through the input node into the DMA is consumed in this zone and is not transferred to the next pressure zone. Average hourly flows were

available over a period ranging from 2 months (DMA 1) to 1 year (DMA 2 – DMA 9).

**Table 1.** Selected technical and operational indicators characterizing DMAs

	Length of DWDS (km)	Pipe material	Household connections (pcs)	Population supplied (persons)	Average pressure (MPa)	Type of development
DMA 1	20.20	Plastic, steel, cast iron	448	1400	48.37	Rural
DMA 2	5.22	Plastic, steel	248	1296	2.96	Rural
DMA 3	2.83	Plastic, steel, cast iron	41	741*	43.46	Housing estate
DMA 4	7.12	Plastic, steel, cast iron	267	1867*	48.69	Urban
DMA 5	10.85	Plastic, steel, cast iron	242	2846*	44.64	Individual
DMA 6	4.43	Plastic, steel, cast iron	128	1163*	52.24	Rural
DMA 7	9.79	Plastic, steel, cast iron	361	2568*	43.42	Individual
DMA 8	8.92	Plastic, steel, cast iron	230	524*	43.19	Rural
DMA 9	11.93	Plastic, cast iron	367	886*	43.67	Rural

\*) estimate based on the number of water connections and the type of development (real values are not known)

## RESULTS

The minimum night flow rates determined by these methods are shown in the following table. Conformity of the established percentile with frequency and modus analysis results are highlighted.

**Table 2.** Determination of minimum night flow

	Percentile							Frequency analysis			Mode of the ToO
	X <sub>0.02</sub>	X <sub>0.03</sub>	X <sub>0.04</sub>	X <sub>0.05</sub>	X <sub>0.06</sub>	X <sub>0.07</sub>	X <sub>0.08</sub>	MNF interval	Frequency of MNF	Time of Occurrence	
DMA 1	1.91	2.00	2.07	2.12	2.18	2.22	2.27	2.25 - 2.50	22	2:00 - 3:00	NA
DMA 2	0.17	<b>0.18</b>	0.19	0.20	0.21	0.21	0.22	0.15 - 0.20	135	2:00 - 3:00	0.18
DMA 3	0.05	0.05	0.05	0.10	0.10	0.15	0.15	0.10 - 0.20	159	3:00 - 4:00	0.05
DMA 4	0.75	0.75	<b>1.00</b>	<b>1.00</b>	<b>1.00</b>	<b>1.00</b>	1.25	0.75 - 1.00	100	3:00 - 4:00	1.00
DMA 5	0.50	0.50	<b>0.60</b>	<b>0.60</b>	<b>0.60</b>	0.70	0.70	0.45 - 0.60	115	3:00 - 4:00	0.60
DMA 6	0.20	0.30	0.30	0.30	0.30	<b>0.40</b>	<b>0.40</b>	0.30 - 0.40	124	2:00 - 3:00	0.40
DMA 7	0.60	0.60	0.65	<b>0.70</b>	<b>0.70</b>	0.75	0.75	0.60 - 0.75	142	3:00 - 4:00	0.70
DMA 8	0.20	<b>0.21</b>	0.24	0.25	0.28	0.31	0.34	0.20 - 0.30	106	3:00 - 4:00	0.21
DMA 9	0.20	0.20	0.20	0.20	<b>0.40</b>	<b>0.40</b>	<b>0.40</b>	0.30 - 0.40	144	2:00 - 4:00	0.40

The most common agreement of all variables was observed at the percentile  $x_{0.06}$ .

The maximum hourly flow rates determined by these methods are shown in the following table. Conformity of the established percentile with frequency and modus analysis results are highlighted.

**Table 3.** Determination of maximum hourly flow

	Percentile						Frequency analysis			Mode of the ToO
	$x_{0.80}$	$x_{0.82}$	$x_{0.84}$	$x_{0.86}$	$x_{0.88}$	$x_{0.90}$	$Q_h$ interval	Frequency of $Q_h$	Time of Occurrence	
DMA 1	10.20	10.29	10.42	10.51	10.60	10.73	10.75 - 11.00	11	20:00-21:00	NA
DMA 2	1.37	1.40	1.44	1.48	1.52	1.57	1.55 - 1.60	38	19:00-20:00	1.60
DMA 3	2.10	2.20	2.25	2.35	2.40	2.50	2.60 - 2.70	28	20:00-21:00	2.65
DMA 4	5.50	5.50	5.75	5.75	6.00	6.00	6.00 - 6.25	41	20:00-21:00	6.50
DMA 5	5.10	5.30	5.40	5.60	5.90	6.10	4.65 - 4.80	25	20:00-21:00	4.70
DMA 6	2.20	2.30	2.30	<b>2.40</b>	2.50	2.60	2.30 - 2.40	31	20:00-21:00	2.40
DMA 7	4.05	4.10	4.20	4.30	4.45	<b>4.60</b>	4.50 - 4.80	34	20:00-21:00	4.70
DMA 8	1.70	1.74	1.79	1.84	1.89	1.96	1.70 - 1.80	46	19:00-20:00	1.59
DMA 9	2.60	<b>2.80</b>	<b>2.80</b>	3.00	3.00	3.20	2.70 - 2.80	43	20:00-21:00	2.80

Multiple recurrences of all occurring quantities were not proved. If the rounding level of these values were changed and if only two (and not all three) values had to be matched, the maximum hourly flow would be closest to the percentile  $x_{0.90}$ .

The following table shows the values of MNF and  $Q_h$ , which correspond to the minimum and maximum flow values contained in the input data which were not adjusted or cleaned in any way. In the next columns there are input data, which were sorted and cleaned under  $3\sigma$ -rule. This statistical methodology is based on the precondition that the relevant statistical set values are at a maximum distance of 3 times the standard deviation from the mean value. This means that all values that do not accomplish the  $\mu \pm 3\sigma$  condition are excluded from the data set.

**Table 4.** MNF and  $Q_h$  values determined from input data and adjusted according to the  $3\sigma$ - rule

	MNF input data ( $l.s^{-1}$ )	MNF $3\sigma$ -rule ( $l.s^{-1}$ )	$Q_h$ input data ( $l.s^{-1}$ )	$Q_h$ $3\sigma$ -rule ( $l.s^{-1}$ )	Compliance with percentile, frequency analysis or mode
DMA 1	1.71	1.71	12.90	12.90	No match
DMA 2	0.02	0.02	4.58	2.55	No match
DMA 3	0.00	0.05	4.30	4.30	No match
DMA 4	0.00	0.25	9.50	9.00	No match
DMA 5	0.00	0.20	12.00	10.30	No match
DMA 6	0.00	0.10	10.70	4.50	No match
DMA 7	0.40	0.40	13.10	6.55	No match
DMA 8	0.00	0.10	6.29	3.55	No match
DMA 9	0.00	0.20	10.60	5.20	No match

The values of MNF and  $Q_h$  in the raw input data represent random extremes in the outflow of water to the DMA, which may have occurred in real terms (unless it was a measurement error) but do not characterize the consumption from a long-term point of view. According to the original assumptions of the authors, by applying the  $3\sigma$ -rule, the flows should have cleared of these random extremes or zero flows. In relation to the size of the DWDSs, complexity, material variability, pressure conditions and age of the DWDSs, the occurrence of zero flow rates in these consumption areas is unlikely. These DMAs are prerequisites for water leakage.

Zero values of MNF are also refuted by the theories of theoretically unavoidable water losses (UARL). UARL are water losses that can never be completely avoided on the DWDS, their value depends on household connection density and average operating pressure (Lambert, 2002). However, as can be seen, the application of the  $3\sigma$ -rule was not reflected in some DMAs. In other cases,  $Q_h$  was decreased by  $3\sigma$ -rule. However, when these results are compared with the  $Q_h$  established percentiles, verified by frequency analysis or modus, they are still very high and do not correspond to the statistically most frequent flow rates in DMA.

## CONCLUSION

The basic characteristics of water consumption can be determined in several ways. The advantage of the presented methodology based on the determination of the percentile is speed and simplicity. This methodology for the determination of MNF and  $Q_h$  does not need to sort the input data into 24-hour sub sets. At the same time, it is not necessary to create hourly averages if we have available flow rates in a shorter time step. The determined percentile values correspond to the minimum and maximum hourly consumption in selected consumption areas in the Czech Republic.

The paper had fulfilled its aims. Percentiles to describe the minimum night flow and maximum hourly water consumption have been defined. When defining the percentile describing the minimum night flow, compliance with the most commonly occurring MNF value has been demonstrated. Frequency analysis also confirmed that MNF occurs between 02:00 and 04:00 a.m. In the case of the  $Q_h$  definition, the percentile method was not as accurate. Only the approximate agreement of the percentile value with the flow intervals during the evening peak period was demonstrated.

In the future, the issue of describing the characteristics of the time series of water consumption offers the opportunity to focus on the definition of maximum hourly consumption, respectively to finding a suitable statistical quantity that would more accurately describe this flow characteristic.

## ACKNOWLEDGEMENT

This paper was financially supported by the research project of the BUT reg. no: FAST-S-18-5526.

## REFERENCES

- Holyszewski, A. (2017) Water meter: Basic Installation Requirements, Aid For Projection Documents. [on-line] [https://www.enbra.cz/data/file/7/6237-vodomery-pomucka-k-projekcnim-podkladum\\_12\\_199.pdf](https://www.enbra.cz/data/file/7/6237-vodomery-pomucka-k-projekcnim-podkladum_12_199.pdf), (In Czech).
- Jeremiah (2018) Advantages and Disadvantages of Smart Meters. [online] <http://sparkonline.com.ng/2018/06/advantages-disadvantages-smart-meters.html>.
- Klucka, T. (2019) Implementation of Smart Water Measurement Technology into Small Municipal Waterworks Environment. Faculty of Civil Engineering, Brno University of Technology, Brno,

- Czech Republic, (In Czech).
- Kovar, J., Rucka, J., Andrs, O. (2014) Simulation Modelling of Water-supply Network as Mechatronic System. Proceedings of the 16th International Conference on Mechatronics – Mechatronika, Brno, Czech Republic, 697-700.
- Lambert, A. (2002) International Report on Water Losses Management and Techniques: Report to IWA Berlin Congress. *Water Science and Technology: Water Supply*, 2(4).
- Lambert, A., Fantozzi, M. (2005) Recent advances in calculating economic intervention frequency for active leakage control, and implications for calculation of economic leakage levels. *Water Science and Technology: Water Supply*, 5. DOI: 10.2166/ws.2005.0072.
- Maksimovic, C., Butler D., Memon, F. A. (2003) Advances in water supply management. Proceedings of the International Conference on Computing and Control for the Water Industry, 15-17 September 2003, London, UK. ISBN 9789058096081.
- Nguyen, B-N., Teller, J. (2018) A Review of Residential Water Consumption Determinants. DOI: 10.1007/978-3-319-95174-4\_52.
- Rajnochova, M., Rucka, J., Suchacek, T., Dufkova, Z. (2019) Influence of Controlled Flushing of Water Network on Quality of Transported Drinking Water. In *Vodárenská biologie*. Chrudim: Vodní zdroje EKOMONITOR spol. s r.o., 14-19, (In Czech). ISBN: 978-80-88238-12-6.
- Tuhovcak, L., Suchacek, T., Rucka, J. (2018) The Dependence of Water Consumption on the Pressure Conditions and Sensitivity Analysis of the Input Parameters. Proceedings.



# Daily Rainfall-runoff Modelling by Support Vector Regression, Symbolic Regression and GR4J Models

C. Sezen\* and T. Partal\*

\* Department of Civil Engineering, Faculty of Engineering, University of Ondokuz Mayıs, 55139, Atakum, Samsun, Turkey (E-mails: [cenk.sezen@omu.edu.tr](mailto:cenk.sezen@omu.edu.tr); [turgay.partal@omu.edu.tr](mailto:turgay.partal@omu.edu.tr))

## Abstract

Rainfall-runoff modelling is important for the improvement of water resources management and planning. Forecasting of runoff can take a significant role for the prevention of natural disasters such as droughts and floods in the future. In this study, performance of Support Vector Regression (SVR), Symbolic Regression based Genetic Programming (SR-GP) and Ge'nie Rural a` 4 parametres Journalier (GR4J) models were compared for daily rainfall-runoff modelling in two rivers, USA. As evaluation criteria, Nash Sutcliffe efficiency (NSE), root mean square error (RMSE) and Kling-Gupta efficiency (KGE) were used. Accordingly, it was obtained that GR4J lumped conceptual model yields better than SVR and SR-GP models in case only precipitation (P (t)) and evapotranspiration data (PE (t)) are used as input. On the other hand, it was observed that selection of input variables affect the performance of SVR and SR-GP models, considerably.

## Keywords

Modelling; rainfall; runoff; USA

## INTRODUCTION

Hydrological modelling has become more important for the future projections with regard to the better planning and management of water resources as well as taking precautions against the natural disasters which occur more frequent especially due to the climate change in recent years. In this regard, there have been a lot of studies that focus on the determination of relationship between hydrological variables and prediction of them (Ancil et al., 2004; Goyal et al., 2017; Sezen et al., 2019). Aqil et al. (2007) implemented two types of the artificial neural network (ANN) structures (i.e. recurrent and feed forward neural networks) by using different training algorithms for river flow forecasting. They indicated that feed forward neural network which is trained with Levenberg-Marquardt algorithm yields better performance for the river flow prediction. Komasi and Sharghi (2016) investigated the performance of wavelet based Support Vector Machine (SVM) for the rainfall-runoff modelling in Aghchai and Eel Rivers. They stated that wavelet based SVM is more convenient than the ANN and SVM models because of the multi scale analysis of rainfall and runoff data. Kurtulus and Razack (2010) used the ANN and Adaptive Neuro-Fuzzy Interference System (ANFIS) for the daily discharge forecasting of karstic aquifers in south-western France. They referred that ANFIS exhibits a better performance than the ANN model especially with regard to the forecasting of high flow. Furthermore, they also pointed out that usage of different input data affects the performance of both models. Hadi and Tombul (2018) used the Discrete Wavelet Transformation (DWT), Continuous Wavelet Transformation (CWT) and hybrid Discrete Continuous Wavelet Transformation (DCWT) with the data-driven models such as ANN, SVM, and ANFIS models for streamflow forecasting. They stated that the new approach (i.e. DCWT) developed particularly the performance of ANN as compared with the SVM and ANFIS models. Tian et al. (2013) implemented the Ge'nie Rural a` 4 parametres Journalier (GR4J), Hydrologiska Byråns Vattenbalansavdelning (HBV) and Xinanjiang models for the high flow simulation for the period of 2011-2040 in Jinhua River basin. They maintained that risk of flood could be higher in the future according to the GR4J and HBV model predictions, whereas it can be lower estimated by Xinanjiang model under the scenario A1B. Zhu et al. (2016) researched the performance of SVM

by combining it with the different decomposition methods such as DWT and Empirical Mode Decomposition (EMD) for the streamflow forecasting in Jinsha River. All these studies aimed to improve the performance of hydrological models.

In this study, the performance of GR4J, SVM and Symbolic Regression based Genetic Programming (SR-GP) is investigated for the daily rainfall-runoff modelling in two rivers in USA. The model results are compared by using the Nash Sutcliffe efficiency (NSE), root mean square error (RMSE) and Kling-Gupta efficiency (KGE).

## DATA AND METHODOLOGY

### Data

To compare the performance of GR4J, SVM and SR-GP models for rainfall-runoff modelling, daily temperature (T) (used for the evapotranspiration calculation), precipitation (P) and streamflow (Q) data of Blanco River and Chunky River in USA were used. Data cover the period of 01.01.1982-30.09.2002 for both rivers. %75 of dataset was used for the training, whereas rest of dataset was used for testing. Statistical information regarding the precipitation, temperature and streamflow data was given in Table 1. Used data is part of the MOPEX dataset (URL 1, 2019). Evapotranspiration (PE) was calculated by using the formula which was given by Oudin et al. (2005). One can refer Oudin et al (2005) for the calculation of evapotranspiration.

**Table 1.** Daily data statistics in used rivers

Rivers	Period	P		T		Q	
		Mean	Std.	Mean	Std.	Mean	Std.
		(mm)		(°C)		(mm/d)	
Blanco River	01.01.1982-30.09.2002	2.4	7.8	19	7.9	0.5	2
Chunky River	01.01.1982-30.09.2002	3.9	9.4	17.5	8	1.3	2.7

### Methods

#### Support Vector Machine

The Support Vector Machine, which was improved by Vapnik (1995), is a learning algorithm that is used for the classification and regression analysis of data. Support Vector Regression (SVR) is a methodology which is based on a regression problem by using SVM (Zhu et al., 2016). Details regarding the formulations for the SVR can be found in the literature (Lin et al., 2009; Zhu et al., 2016; Goyal et al., 2017). In this study, different kernel types such as linear and radial were chosen and cross-validation was performed to find the most convenient model. For the SVR model, different input combinations which include P, PE, Q were used for the daily rainfall-runoff modelling.

#### Symbolic Regression based Genetic Programming

Symbolic regression includes certain techniques that target producing equations which determine the relationship between variables from a dataset (Confroth and Lipson, 2015; Koza and Koza, 1992; Schmidt and Lipson, 2009; Klotz et al., 2017). In this study, genetic programming was used for producing the symbolic regression models in order for the daily rainfall-runoff model. For the SR-GP model, different input combinations which contain precipitation, evapotranspiration and streamflow data were used as input data in similar with the SVR model. Regarding the symbolic regression models one can refer (Koza and Koza, 1992; Augusto and Barbosa, 2000).

### GR4J Model

GR4J model is a daily lumped conceptual model which was developed by Perrin et al. (2003). Daily precipitation and evapotranspiration data are used as input data for runoff modelling in GR4J model which has four free parameters,  $x_1$  (Maximum capacity of the production store),  $x_2$  (Groundwater exchange coefficient),  $x_3$  (One day ahead maximum capacity of the routing store) and  $x_4$  (Time base of unit hydrograph). GR4J model was used via airGR package (Coron et al., 2017; Coron et al., 2019) that is part of R software. One can refer the study of Perrin et al. (2003) for the elaborate description of GR4J model.

### Evaluation Criteria for Model Performance

To assess the performance of SVM, SR-GP and GR4J models, Nash Sutcliffe efficiency (NSE), root mean square error (RMSE) and Kling-Gupta efficiency (KGE) are used. The equations belong to each criteria can be seen as follow, respectively.

$$NSE = 1 - \frac{\sum_{i=1}^N (Q_{obs,i} - Q_{sim,i})^2}{\sum_{i=1}^N (Q_{obs,i} - \overline{Q_{obs}})^2}, \quad (1)$$

$$RMSE = \sqrt{\frac{1}{N} \sum_{i=1}^N (Q_{sim,i} - Q_{obs,i})^2}, \quad (2)$$

$$KGE = 1 - \sqrt{(r-1)^2 + (\alpha-1)^2 + (\beta-1)^2}. \quad (3)$$

$N$ ,  $Q_{obs,i}$  and  $Q_{sim,i}$  represent the length of data, observed flow and simulated flow for  $i^{\text{th}}$  time, respectively in equation (1) and equation (2).  $\overline{Q_{obs}}$  is the mean of the observed values in equation (1). Furthermore,  $r$  is the correlation coefficient between observed and simulated flow,  $\alpha$  is the proportion of mean simulated flow to mean observed flow and  $\beta$  is the proportion of standard deviation of the simulated flow to the standard deviation of the observed flow in equation (3).

## RESULTS

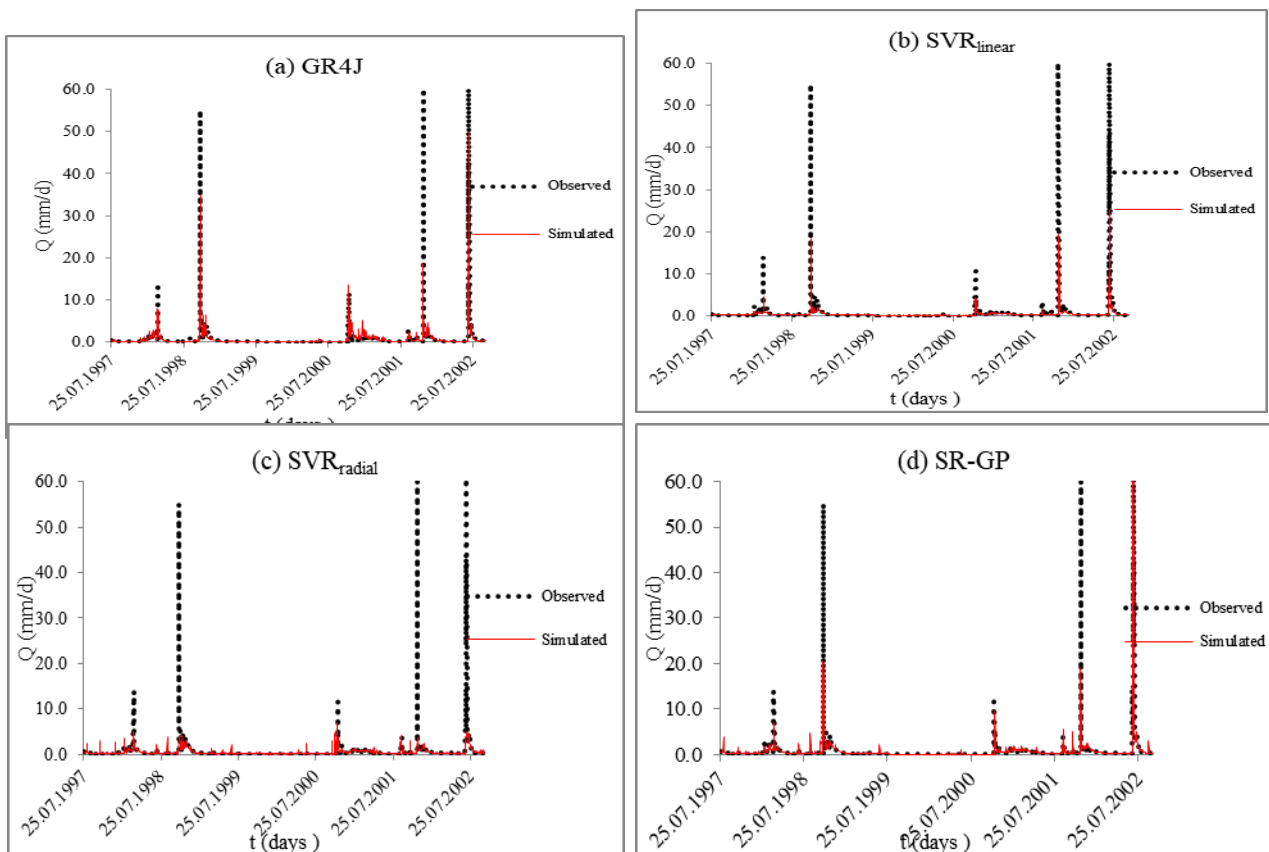
First, the P (t) and PE (t) (input combination 1) were used as input in each model to evaluate their performance in case the same input data are utilized. It is seen that GR4J model outperforms SVR<sub>linear</sub> (SVR for linear kernel type) and SVR<sub>radial</sub> (SVR for radial kernel type) and SR-GP models according to Table 2 when all evaluation criteria are taken into consideration in both rivers. As for the SVR and SR-GP, performance of SR-GP model yields better than SVR models (both SVR<sub>linear</sub> and SVR<sub>radial</sub>) especially in Blanco River. SVR models seem to be worst among all models for daily rainfall-runoff modelling in both rivers. Then, different input combinations which include precipitation data the preceding days such as P (t-1) and P (t-2) and stream flow data the preceding days such as Q (t-1) and Q (t-2) were also tried for SVR and SR-GP models. The results for the input combination (input combination 2) that contains the P (t-2), P (t-1), P (t), PE (t) and Q (t-2), Q(t-1) were presented in Table 3, Fig. 1 and Fig. 2 for Blanco River and Table 3, Fig. 3 and Fig. 4 for Chunky River.

**Table 2.** Performance of models for input combination 1

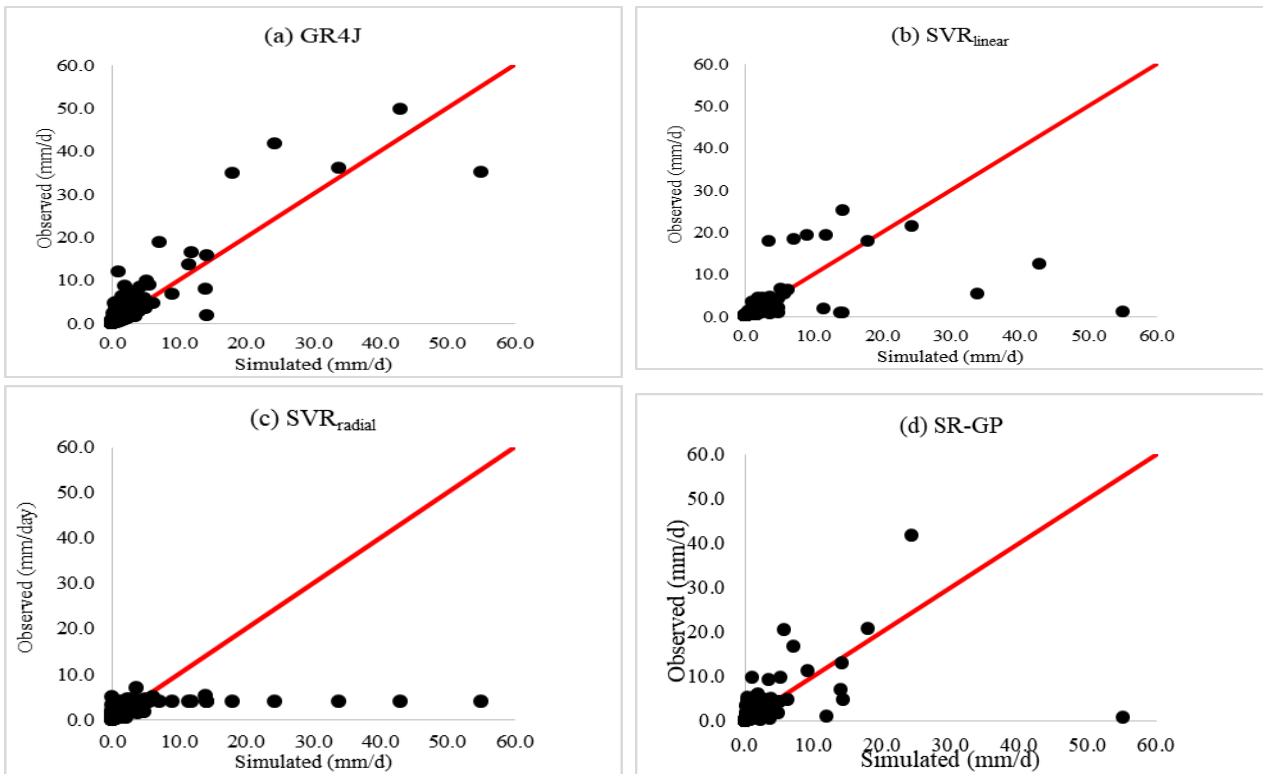
Performance of the Models for Validation Period				
Stations	Models	NSE	RMSE (mm/d)	KGE
Blanco River	GR4J	0.71	1.6	0.75
	SVR <sub>linear</sub>	0.02	2.9	-0.19
	SVR <sub>radial</sub>	0.13	2.7	-0.06
	SR-GP	0.37	2.3	0.59
Chunky River	GR4J	0.84	0.9	0.81
	SVR <sub>linear</sub>	0.04	2.1	-0.15
	SVR <sub>radial</sub>	0.04	2.1	-0.14
	SR-GP	0.03	2.1	-0.08

**Table 3.** Performance of SVR<sub>linear</sub>, SVR<sub>radial</sub> and SR-GP models for the input combination 2

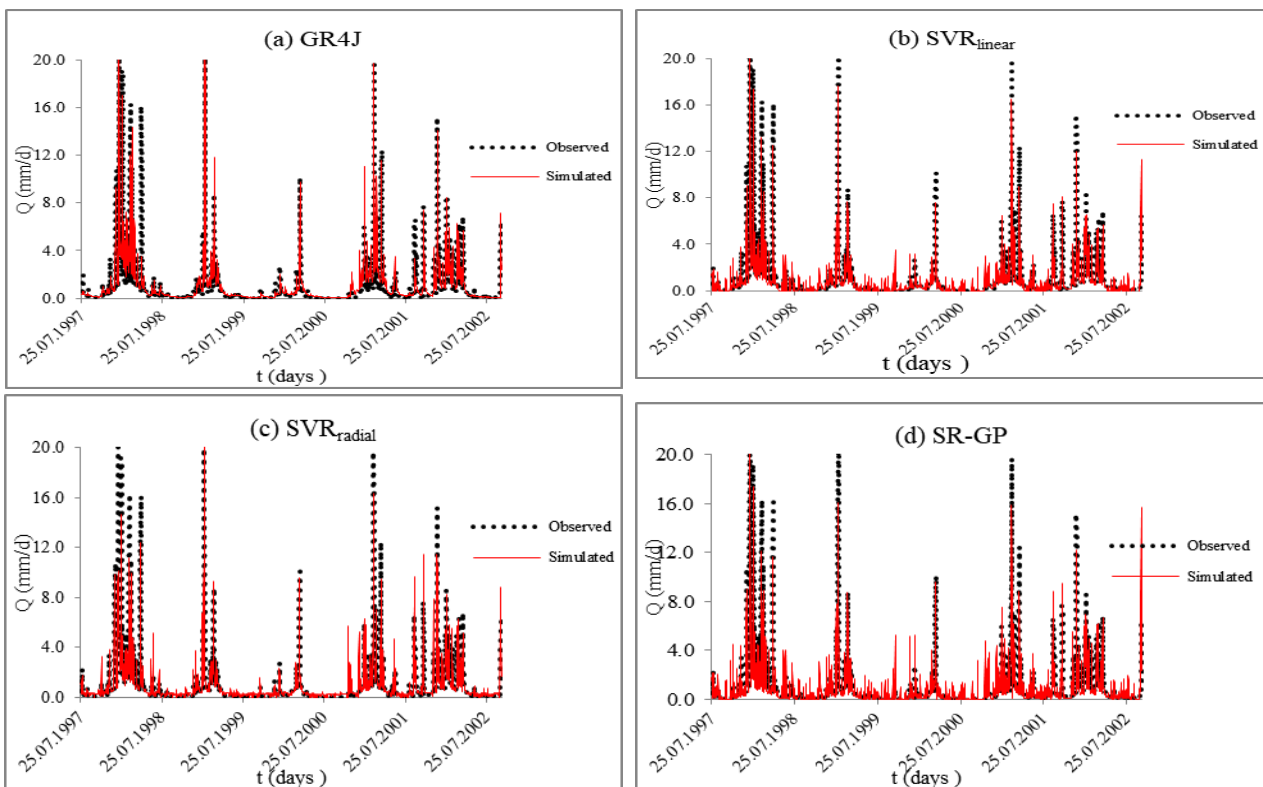
Performance of the Models for Validation Period				
Stations	Models	NSE	RMSE (mm/d)	KGE
Blanco River	SVR <sub>linear</sub>	0.27	2.5	0.27
	SVR <sub>radial</sub>	0.18	2.6	0.08
	SR-GP	0.41	2.2	0.69
Chunky River	SVR <sub>linear</sub>	0.85	0.8	0.87
	SVR <sub>radial</sub>	0.83	0.9	0.82
	SR-GP	0.83	0.9	0.85



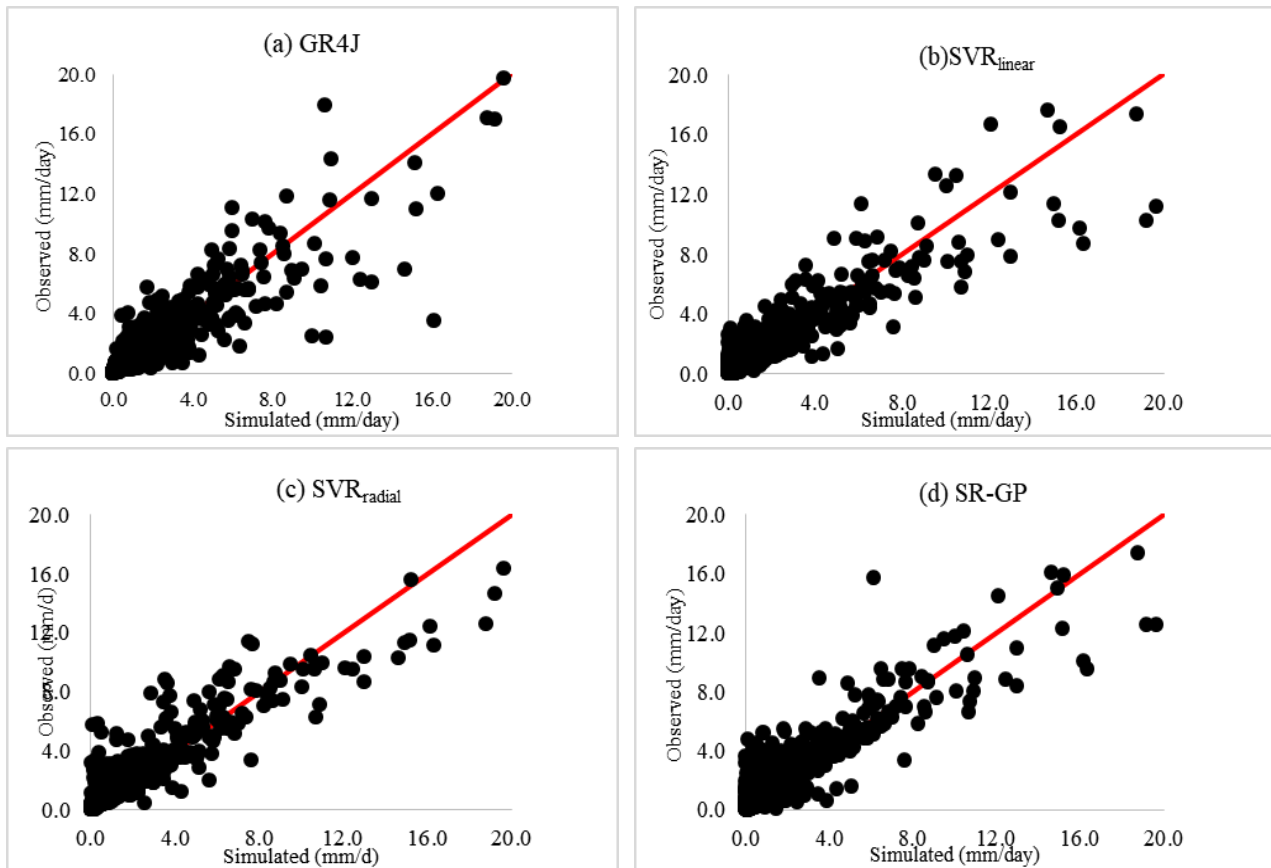
**Figure 1.** Relationship between observed and simulated flow for (a) GR4J, (b) SVR<sub>linear</sub>, (c) SVR<sub>radial</sub> and (d) SR-GP model in Blanco River (input combination 1 for GR4J; input combination 2 for SVR<sub>linear</sub>, SVR<sub>radial</sub> and SR-GP models)



**Figure 2.** Scatter diagrams for (a) GR4J, (b) SVR<sub>linear</sub>, (c) SVR<sub>radial</sub> and (d) SR-GP model in Blanco River (input combination 1 for GR4J; input combination 2 for SVR<sub>linear</sub>, SVR<sub>radial</sub> and SR-GP models)



**Figure 3.** Relationship between observed and simulated flow for (a) GR4J, (b) SVR<sub>linear</sub>, (c) SVR<sub>radial</sub> and (d) SR-GP model in Chunky River (input combination 1 for GR4J; input combination 2 for SVR<sub>linear</sub>, SVR<sub>radial</sub> and SR-GP models)



**Figure 4.** Scatter diagrams for (a) GR4J, (b)  $SVR_{linear}$ , (c)  $SVR_{radial}$  and (d) SR-GP model in Chunky River (input combination 1 for GR4J; input combination 2 for  $SVR_{linear}$ ,  $SVR_{radial}$  and SR-GP models)

Accordingly, it is seen from Table 3 that performance of SVR and SR-GP models remarkably developed by the addition of precipitation and streamflow preceding day data to the input combination in both rivers. Even though performance of GR4J is still higher than the other models in Blanco River, performance of  $SVR_{linear}$ ,  $SVR_{radial}$  and SR-GP models is very similar to the GR4J model in Chunky River. In Figure 1 and Figure 2, it can be observed that GR4J model is better than the other models for the daily flow forecasting especially with regard to the high flow estimation for Blanco River. On the other hand,  $SVR_{linear}$ ,  $SVR_{radial}$  and SR-GP exhibit also a good performance for the daily rainfall-runoff modelling in Chunky River as seen in Figure 3 and Figure 4. When scattering diagrams are taken into consideration in Figure 4, scattering is a little bit more for the GR4J model as compared with the data-mining models. In this regard, it is seen that utilization of different input combinations affect the performance of data-mining models. In other words, the relationship between input variables and target variable could be significant in terms of the forecasting performance of data-mining models.

## CONCLUSION

Hydrological modelling becomes more important not only for water resource management but also prevention of natural disasters such as drought and floods. In this study, daily rainfall-runoff modelling was carried out by using GR4J conceptual model and  $SVR_{linear}$ ,  $SVR_{radial}$ , SR-GP data mining models in Blanco and Chunky Rivers, USA as a case study. It is found out that in case only precipitation ( $P(t)$ ) and evapotranspiration ( $PE(t)$ ) data are used as input in data mining models, GR4J outperforms the  $SVR_{linear}$ ,  $SVR_{radial}$  and SR-GP models in both rivers. On the other hand,

usage of additional input variables such as precipitation the preceding days ( $P(t-2)$ ,  $P(t-1)$ ) and stream flow the preceding days ( $Q(t-2)$ ,  $Q(t-1)$ ), the performance of data mining models significantly improved especially for Chunky River. As a result, it was observed that performance of conceptual and data mining models can change from catchment to catchment and the selection of input variables is important for the performance of data mining models. In future studies, performance of conceptual and data mining models in different catchments and possible drivers, which affect the model performance, will be investigated.

## REFERENCES

- Anctil, F., Michel, C., Perrin, C., Andréassian, V. (2004) A soil moisture index as an auxiliary ANN input for stream flow forecasting. *Journal of Hydrology*, **286**(1-4), 155-167.
- Aqil, M., Kita, I., Yano, A., Nishiyama, S. (2007) Neural networks for real time catchment flow modeling and prediction. *Water Resources Management*, **21**(10), 1781-1796.
- Augusto, D. A., Barbosa, H. J. (2000) Symbolic regression via genetic programming. Proceedings of Sixth Brazilian Symposium on Neural Networks, **1**, 173-178.
- Confroth, W. T., Lipson, H. (2015) A hybrid evolutionary algorithm for the symbolic modeling of multiple-time-scale dynamical systems. *Evolutionary Intelligence*, **8**, 149-164.
- Coron, L., Thirel, G., Delaigue, O., Perrin, C., Andréassian, V. (2017) The Suite of Lumped GR Hydrological Models in an R package. *Environmental Modelling and Software*, **94**, 432-440.
- Coron, L., Delaigue, O., Thirel, G., Perrin, C., Michel, C. (2019) airGR: Suite of GR Hydrological Models for Precipitation-Runoff Modelling. R package version 1.3.2.23. [online] <https://CRAN.R-project.org/package=airGR>.
- Goyal, M. K., Sharma, A., Katsifarakis, K. L. (2017) Prediction of flow rate of karstic springs using support vector machines. *Hydrological Sciences Journal*, **62**(13), 2175-2186.
- Hadi, S. J., Tombul, M. (2018) Streamflow Forecasting Using Four Wavelet Transformation Combinations Approaches with Data-Driven Models: A Comparative Study. *Water Resources Management*, **32**(14), 4661-4679.
- Klotz, D., Herrnegger, M., Schulz, K. (2017) Symbolic regression for the estimation of transfer functions of hydrological models. *Water Resources Research*, **53**(11), 9402-9423.
- Komasi, M., Sharghi, S. (2016) Hybrid wavelet-support vector machine approach for modelling rainfall-runoff process. *Water Science and Technology*, **73**(8), 1937-1953.
- Koza, J. R., Koza, J. R. (1992) Genetic programming: on the programming of computers by means of natural selection. *MIT press*, 1.
- Kurtulus, B., Razack, M. (2010) Modeling daily discharge responses of a large karstic aquifer using soft computing methods: artificial neural network and neuro-fuzzy. *Journal of Hydrology*, **381**(1-2), 101-111.
- Lin, G. F., Chen, G. R., Huang, P. Y., Chou, Y. C. (2009) Support vector machine-based models for hourly reservoir inflow forecasting during typhoon-warning periods. *Journal of Hydrology*, **372**(1-4), 17-29.
- Oudin, L., Hervieu, F., Michel, C., Perrin, C., Andréassian, V., Anctil, F., Loumagne, C. (2005) Which potential evapotranspiration input for a lumped rainfall-runoff model?: Part 2—Towards a simple and efficient potential evapotranspiration model for rainfall-runoff modelling. *Journal of Hydrology*, **303**(1-4), 290-306.
- Perrin, C., Michel, C., Andréassian, V. (2003) Improvement of a parsimonious model for streamflow simulation. *Journal of Hydrology*, **279**(1-4), 275-289.
- Schmidt, M., Lipson, H. (2009) Distilling free-form natural laws from experimental data. *Science*, **324**(5923), 81-85.
- Sezen, C., Bezak, N., Bai, Y., Šraj, M. (2019) Hydrological modelling of karst catchment using lumped conceptual and data mining models. *Journal of Hydrology*. **576**, 98-110.



- Tian, Y., Xu, Y. P., Zhang, X. J. (2013) Assessment of climate change impacts on river high flows through comparative use of GR4J, HBV and Xinanjiang models. *Water Resources Management*, **27**(8), 2871-2888.
- URL 1, National Weather Service, NOAA (2018). [online] [http://www.nws.noaa.gov/ohd/mopex/mo\\_datasets.htm](http://www.nws.noaa.gov/ohd/mopex/mo_datasets.htm).
- Vapnik, V.N. (1995) *The nature of statistical learning theory*. Springer, New York.
- Zhu, S., Zhou, J., Ye, L., Meng, C. (2016) Streamflow estimation by support vector machine coupled with different methods of time series decomposition in the upper reaches of Yangtze River, China. *Environmental Earth Sciences*, **75**(6), 531.

# Integrated Assessment of Technogenic Load on Water Ecosystems Based on Biodiversity and Hydrochemical Indexes

M. S. Stroganova\*, A. I. Kushnerov\* and A.I. Shishkin\*

\*Higher School of Technology and Energy of Saint Petersburg State University of Industrial Technologies and Design, Ivana Chernykh 4, 198095 Saint Petersburg, Russia  
(E-mails: *masha199407@list.ru*; *kushnerov.a.i@yandex.ru*)

## Abstract

Approaches for integrated assessment of the aquatic ecosystems ecological state and the level of anthropogenic impact with the determination of changes in abiotic and biotic components are considered. Seasonal researches data are generalized and analyzed and indexes and complex indexes of water bodies of various types for the long-term period are calculated. The method of integrated assessment of technogenic load on water bodies is developed.

## Keywords

Integrated assessment; integrated approach; technogenic load; aquatic ecosystems; species diversity; hydrochemical indexes

## INTRODUCTION

Assessment and regulation of technogenic load on aquatic ecosystems, due to the interaction of heterogeneous factors, is determined by a set of biotic and abiotic parameters and characteristics. Only a comprehensive assessment of these indicators allows us to assess the level of a man-made impact, positive or negative, with the specification of the list of impact indicators and methods for determining its absolute and relative values, conclusions about the likely values of impact indicators and impact in general (Stroganova, 2017; Shishkin et al., 2018). For each of the considered systems "technogenic influence – water object" the most significant factors of influence and their indicator indicators are defined.

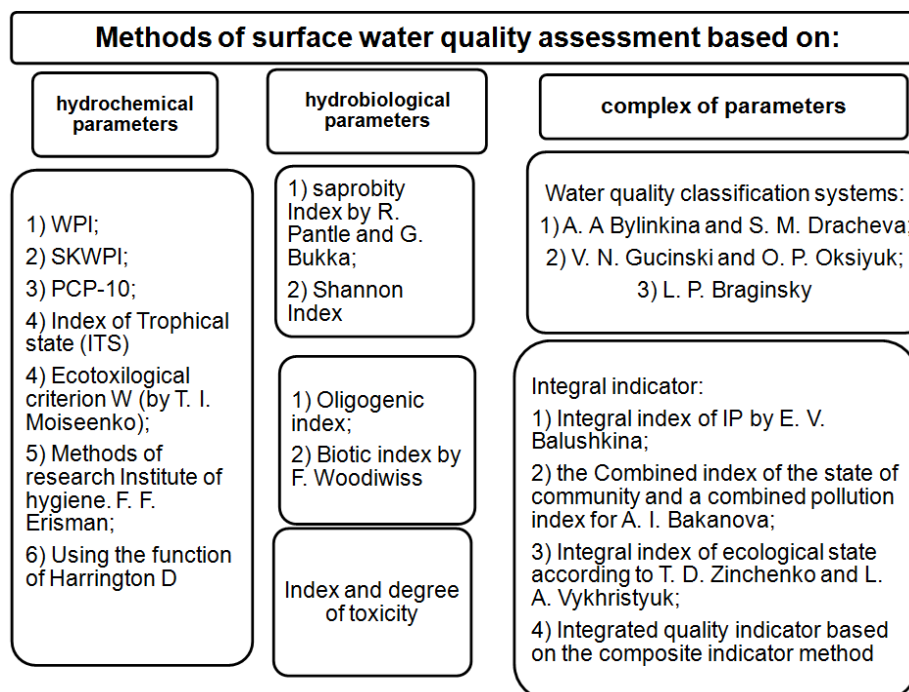
## METHODS AND MATERIALS

The integrated assessment of the ecological state of the aquatic ecosystem is based on the principle of establishing the boundaries of quantitative changes in ecosystem parameters, provided that its structure and functions are preserved, as well as all environmental components necessary for accounting in household activities (Khaustov and Redina, 2008).

The process of assessing the anthropogenic impact begins with the analysis of the impact of various factors, both natural and anthropogenic, on the ecosystem. This approach is implemented in three stages: impact assessment, ecosystem sustainability assessment and impact assessment, i.e. changes in ecosystem functions. Impact assessment is understood as a quantitative (integral) assessment of the response of the ecosystem as a whole to anthropogenic load (Galtsova and Dmitriev, 2007). An integrated ecosystem approach to assessing the quality of the aquatic ecosystem requires taking into account the natural relationships between them, for example, migration routes of chemical elements, and thresholds of impact on biota.

In reference (Shitikov et al., 2003) presents a review of integrated assessments that include an integrated hydrochemical and hydrobiological indicators. Identification of zones of an emergency ecological situation taking into account change of natural environment of surface reservoirs is

carried out separately on chemical and biological indicators (Shitikov et al., 2003). In their work, the criteria for the assessment and degree of chemical pollution of surface waters are hydrochemical and hydrobiological indicators of natural water quality and indices by which the level of water pollution is judged. In addition, it was noted that the parameters of the indicators proposed for the allocation of environmental safety zones should be considered taking into account the regional characteristics, category and trophic status of the reservoir. In the analysis of the literature, a classification of existing methods for assessing the quality of water bodies was developed (Figure 1).



**Figure 2.** Classification of existing methods of water quality assessment

In the course of research work, a generalized assessment of the trophic state index, Shannon index and ecological state is given in Table 1.

**Table 1.** Generalized assessment of indices and water quality indicators (Stroganova, 2017)

Shannon Index	ITS	Environmental assessment of trophicity	Saprobity index	WPI	Pollution rate	Water quality class
>4.00	< 5.7 ±0,3	Ultraoligotrophic	≤0.50	<0,2	Very clean	I
2.51-4.00	6.3 ±0,3	Oligotrophic	0.51-1.50	0.2–1.0	Clean	II
2.01-2.5	7.0 ±0.3	Mesotrophic	1.51-2.50	1.0–2.0	Moderately polluted	III
1.01-2	7.7 ±0.3	Eutrophic	2.51-3.50	2.0–4.0	Polluted	IV
<1.00	> 8.3 ±0.3	Hyper-eutrophic	3.51-4.00	4.0–6.0	Dirty	V

The developed indicator of trophic state (Index of tropical state) for rapid assessment of the state of aquatic ecosystems is based on the theoretical position that the violation of the production-destructive balance leads primarily in any ecosystem to a change in the ratio of the concentrations of oxygen O<sub>2</sub> and carbon dioxide CO<sub>2</sub> (Tsvetkova et al., 2007). When the rate of decomposition is ahead of the rate of formation of organic substances, the concentration of CO<sub>2</sub> in the environment increases, and the concentration of O<sub>2</sub> falls, and vice versa.

The state of the biotic balance of the water body, expressed in terms of "trophic state", is a function of  $f(pH, O_2, \%)$  and can be characterized by a relationship between the pH and oxygen saturation of the water. The following formula 1 is used to calculate ITS (Tsvetkova et al., 2007):

$$ITS = \frac{\sum_{i=1}^n pH_i}{n} + a \left( 100 - \frac{\sum_{i=1}^n [O_2]_i}{n} \right), \quad (1)$$

where  $pH_i$ - the pH as measured for a certain period,  $[O_2]$  - the concentration of dissolved oxygen in percent saturation, %;  $n$  – number of measurements,  $a$  - the constant.

The index of tropical state (ITS) is calculated on the basis of pH values and the level of water body saturation with dissolved oxygen. The Shannon index determines the species diversity of zooplankton and the trophic status of the water body.

The interrelation between WPI and the saprobity index is determined (Table 1). The water pollution index is calculated using 6 hydrochemical indicators – ammonium, iron, phosphates, nitrites and limiting indicators -  $BOD_5$  and dissolved oxygen:

$$WPI = \frac{1}{n} \sum_{i=1}^n \frac{c_i}{TLV_i}, \quad (2)$$

where  $C_i$  is concentration of the  $i^{th}$  component;  $n$  is the number of indicators used for calculating the index ( $n = 6$ );  $TLV_i$  is the established threshold limit value for the  $i^{th}$  component for the appropriate water body type (Shitikov et al., 2003).

The approach of integrated assessment of natural water quality is also considered. Determination of water quality by individual indicators (concentration of pollutants, dissolved oxygen, BOD, hydrogen index, the number of zoobenthos and zooplankton organisms, etc.), and on their basis the calculation of integrated indicators (WPI, ITS, Shannon index, saprobity index, etc.) is a comprehensive assessment, which is widely used at the present stage. But with this approach, each indicator or index gives its own qualitative characteristic, that is, the assessment is ambivalent.

A great contribution to the solution of this issue was made by Dmitriev V. V., who was able to give an objective integral assessment, including various hydrobiological and hydrochemical parameters. This approach for integrated assessment is called the "composite indicator method" CIM (Dmitriev and Frumin, 2004) and is used in many scientific fields. CIM is used to collate information and allows for the integration of various indicators, ranging from "simple" to complex, which has different ranges and dimensions. For the tasks of assessing the quality of watercourses and reservoirs as criteria is individual, complex and integrated assessment. After selecting the criteria in the second stage combine their classification into a single system.

The third step refers to the translation of all the scales (dimensions) criteria to a single scale in the following way (Kushnerov, 2012):

1. Defining the type of criteria:

- "direct" criterion – the greater their value, the better;
- "reverse" criterion – the smaller their value, the better.

2. Recalculate the criteria scales from 0 to 1 (0 is the best value, 1 is the worst value) using the following formulas:

- for the "direct" criterion:

$$q_i = q_i(x_i) = \begin{cases} 1, & \text{if } x_i \leq \min_i, \\ \left( \frac{\max_i - x_i}{\max_i - \min_i} \right), & \text{if } (\min_i < x_i \leq \max_i), \\ 0, & \text{if } x_i > \max_i, \end{cases} \quad (3)$$

where  $q_i$  - is the converted criterion value;  $x_i$  is the current criterion value;  $\min_i$  - is the minimum criterion value;  $\max_i$  - is the maximum criterion value.

- for the "reverse" criterion:

$$q_i = q_i(x_i) = \begin{cases} 0, & \text{if } x_i \leq \min_i, \\ \left( \frac{x_i - \min_i}{\max_i - \min_i} \right), & \text{if } (\min_i < x_i \leq \max_i), \\ 1, & \text{if } x_i > \max_i. \end{cases} \quad (4)$$

At the fourth stage, the type of integral indicator  $Q(q, p)$  is chosen. The integral index is constructed in such a way that it depends not only on the  $q_i$  indicators, but also on their significance determined by the weight coefficients  $p_i$ , the sum of which should be equal to 1. As an expression for an integral indicator, we can offer a linear convolution of indicators of the form:

$$Q_i = \sum_{i=1}^n q_i \cdot p_i, \quad (5)$$

where  $n$  - is the number of evaluation criteria.

At the fifth stage, the values of the weight coefficients  $p_i$  are determined using different methods (Fedorov, 2007):

1. Ranking method:

Consider the problem when there are three criteria. Originally carried out the ranking of criteria by experts. Suppose the following ratio of criteria and, accordingly, their weight coefficients:  $p_1 > p_2 > p_3$ . To determine the values of the importance coefficients, use the following formula depending on the ordinal number of the criterion:

$$p_i = \frac{1}{i \cdot \sum_{i=1}^n \left( \frac{1}{i} \right)}. \quad (6)$$

Then  $p_1=0.55$ ;  $p_2=0.27$ ;  $p_3=0.18$ .

2. The method of paired comparisons:

Consider the same case  $p_1 > p_2 > p_3$ . Make a Table to compare the importance of criteria ( $K_i$ ).

**Table 2.** Comparison of importance criteria

$K_i$	$K_1$	$K_2$	$K_3$	$v_i$	$p_i$
$K_1$	X	1	1	2	0.67
$K_2$	0	x	1	1	0.33
$K_3$	0	0	x	0	0

When comparing, the following conditions are used: it makes no sense to compare the same criterion (x), if the criterion located vertically is more important than the criterion located horizontally, then assign 1 point; if the criterion located vertically is not more important than the criterion located horizontally, then assign 0 points.

Next, for each criterion, the points are summed and the importance coefficients are calculated by the formula (7):

$$p_i = \frac{v_i}{\sum v_i}, \quad (7)$$

where  $v_i$  – is the total number of points for each criterion.

The disadvantage of this approach is that the numerical value of the importance coefficient for the third criterion  $p_3=0$ . In order to avoid this, a conditional criterion with a coefficient of importance  $p_4^*$  is introduced. Wherein  $p_1 > p_2 > p_3 > p_4^*$ . A new Table 3 is drawn up taking into account the fourth criterion, the importance of which will eventually be zero.

**Table 3.** Comparison of criteria importance given, the conditional criterion

$K_i$	$K_1$	$K_2$	$K_3$	$K_4^*$	$v_i$	$p_i$
$K_1$	X	1	1	1	3	0.50
$K_2$	0	X	1	1	2	0.33
$K_3$	0	0	x	1	1	0.17
$K_4^*$	0	0	0	X	0	0

If the criteria are equal or it is impossible to determine their weights, the following formula is used to calculate the importance factor:

$$p_i = \frac{1}{n}, \quad (8)$$

where  $n$  – is the number of evaluation criteria.

On the sixth the final stage displays the formula of the integral index using equation 3-5, and then calculated the boundary values for the development of a new classification. Based on this method, a comprehensive assessment was carried out taking into account the abiotic and biotic components of the quality of water bodies. In the framework of composite indicators, there are the following indexes - saprobity index by R. Pantle and G. Bukka, F. Woodiwiss index, specific combinatorial water pollution index (SCWPI). Next step - enter the General quality classes for the three indexes and adjust the index values (Table 4).

**Table 4.** The original classification to assess the quality

Class/ indication	Relatively clean Oligosaprobity zone I	Slightly contaminated $\beta$ -meso- saprobity zone II	Contaminated $\alpha$ - meso- saprobity zone III	Dirty polysaprobity zone IV	Very dirty hypersaprobity zone V
SCWPI	[0; 1]	(1; 2]	(2; 4]	(4; 8]	(8; 11]
Saprobity index by R. Pantle and G. Bukka;	[0; 1.5]	(1.5; 2.5]	(2.5; 3.5]	(3.5; 4]	(4; 4.5]
Biotic Index of F. Woodiwiss	[10;7]	[6; 5]	[4; 3]	[3; 2]	[1; 0]

The next step is to translate all the scales to a single, that is, get rid of the dimension. The best value was 0 and the worst value was 1 (Table 5).

**Table 5.** Rationed values of initial parameters

Class/ indication	Relatively clean Oligosaprobity zone I	Slightly contaminated $\beta$ -meso- saprobity zone II	Contaminated $\alpha$ - meso- saprobity zone III	Dirty polysaprobity zone IV	Very dirty hypersaprobity zone V
SCWPI	[0; 0.09]	(0.09; 0.18]	(0.18; 0.36]	(0.36; 0.73]	(0.73; 1]
Saprobity index by R. Pantle and G. Bukka;	[0; 0.33]	(0.33; 0.56]	(0.56; 0.78]	(0.78; 0.89]	(0.89; 1]
Biotic Index of F. Woodiwiss	[0; 0.3]	[0.4; 0.5]	[0.6; 0.7]	[0.7; 0.8]	[0.9; 1]

After transferring to a single dimensionless scale, over the values of the criteria, it is possible to perform mathematical operations in order to obtain an integral indicator.

Next, choose the type of integral indicator  $Q(q, p)$ . The complex index is constructed in such a way that depends not only on  $q_i$  indicators, but also on their significance, determined by weight coefficients  $p_i$ , the sum of which should be 1. As an expression for the integral indicator, we can offer a linear convolution of type indicators (formula 5). The estimated weighting coefficients  $p_i$  are determined. In the simplest case, with equal weights of the initial parameters, the weight is determined by a simple formula:

$$p_i = \frac{1}{n}. \quad (9)$$

In that case:  $p_i = 1/3 = 0,333$ .

For the left and right borders of each cash desk, the value of  $Q_i$  is calculated. The results are presented in Table 6.

**Table 6.** Estimated values of water quality indexes

Class/ indication	Relatively clean Oligosaprobity zone I	Slightly contaminated $\beta$ -meso- saprobity zone II	Contaminated $\alpha$ - meso- saprobity zone III	Dirty polysaprobity zone IV	Very dirty hypersaprobity zone V
SCWPI	[0; 0.09]	(0.09; 0.18]	(0.18; 0.36]	(0.36; 0.73]	(0.73; 1]
Saprobity index by R. Pantle and G. Bukka;	[0; 0.33]	(0.33; 0.56]	(0.56; 0.78]	(0.78; 0.89]	(0.89; 1]
Biotic Index of F. Woodiwiss	[0; 0.3]	[0.4; 0.5]	[0.6; 0.7]	[0.7; 0.8]	[0.9; 1]
Integral quality parameter $Q_i$	[0; 0.26]	[0.26; 0.43]	[0.43; 0.61]	[0.61; 0.82]	[0.82; 1]

As a result of mathematical calculations using the method of summary indicators was derived formula multi-criteria index  $Q$ :

$$Q = \frac{1}{3} \cdot \left( 1 + \frac{q_1}{11} + \frac{q_2}{4,5} - \frac{q_3}{10} \right), \quad (10)$$

where  $q_1$  - is the specific combinatorial index of pollution (SCWPI);  $q_2$  - saprobity index according to R. Pantle and G. Bucca;  $q_3$  - biotic index according to F. Woodwyss.

Further, a new classification of water quality by the multi-criteria index  $Q$  was formed, which allows determining the class and characteristics of water quality (Table 6). Using the method of summary indicators, many researchers have already developed various integrated assessments, but the inclusion of the SCWPI index was first implemented in this work. An integrated approach using a multi-criteria index based on monitoring of water bodies is one of the mechanisms for managing the quality of water bodies, which allows for the allocation of more and less polluted water bodies.

The integral index Q can be used for determine the qualitative characteristics of water bodies, comparing the results over time, comparing of water sites, water bodies and the basin as a whole in terms of power of impact, determine the load on the water body, identify sources of pollution.

## RESULTS AND DISCUSSIONS

The objects of research in the period from 2015 to spring 2019 were 20 objects of the Kurortny district of St. Petersburg and the Vyborg district of the Leningrad region.

Based on the method of complex of parameters, a comprehensive assessment was carried out taking into account the abiotic and biotic components of the quality of water bodies using the example of the basin of the north-eastern part of the Gulf of Finland. With the help of the IndQ program, the water quality index was tested according to the environmental monitoring data of the northeast part of the Gulf of Finland basin. Calculated complex indicators and indices for Malaya Sestra river, Suzdalski Lakes, Sestroretsk reservoir, Blue Lakes.

Baseline data for 2010 on water bodies of the Leningrad Region as well as the results of calculations of a multi-criteria index are shown in Table 7.

**Table 7.** Estimated table of multi-criteria index of water quality

Name of water body	Water quality indexes			
	SCWPI	Saprobity index by R. Pantle and G. Bukka;	Biotic Index of F. Woodiwiss	Integral quality parameter $Q_i$
Blue lakes	2.37(III)	1.56 (II)	3.37 (III)	0.41(II)
Gladyshevskoe lake	2.43 (III)	1.45 (I)	2.5 (IV)	0.43 (III)
River Black	3.39 (III)	1.74 (II)	1.94 (IV)	0.50 (III)
Smolyachkov stream	6.45 (IV)	1.86 (II)	2.82 (IV)	0.57 (III)
Sestroretsk reservoir	3.32 (III)	1.6 (II)	2.27 (IV)	0.48 (III)
River Malaya Sestra	4.23 (IV)	1.59 (II)	2.44 (IV)	0.50 (III)

It should be immediately noted that with insufficient data, we get a very rough estimate. There is a need to increase the number of water quality classes. The result of the analysis was that, in addition to hydrochemical parameters, it is also necessary to use hydrobiological to determine the quality of water bodies. The integrated assessment of water quality by species diversity and hydrochemical indices of the water bodies studied is presented in the diagram (Figure 2).

For the entire period of research on Shannon, species diversity is less in spring than in summer. The smallest variety of zooplankton was recorded in March 2017 (0.56), and the maximum in August 2015.

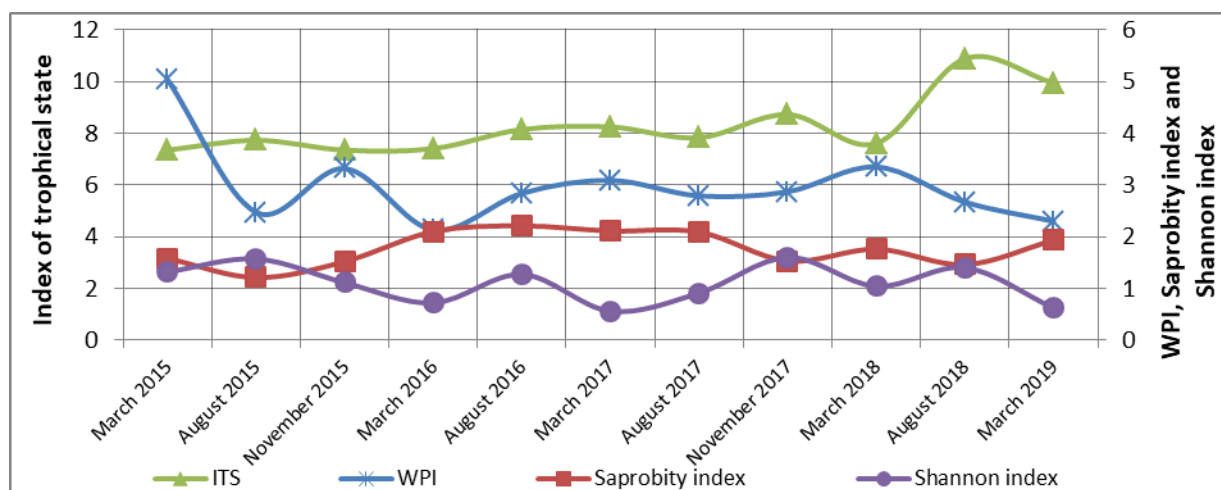
The general trend for the study period is decreasing diversity. The trophic index gradually increased from 7 to 10 in the direction of the eutrophication of water bodies. An increase in pollution by the saprobity index is also observed, but at the same time, the values of the hydrochemical index of water pollution decrease.

Thus, based on the method of complex of parameters, a comprehensive assessment was carried out taking into account the abiotic and biotic components of the quality of water bodies using the example of the basin of the north-eastern part of the Gulf of Finland. Calculated complex indicators and indexes for Malaya Sestra River, Suzdalski Lake, Sestroretsk reservoir, Blue Lakes. The result



of the analysis was that, in addition to hydrochemical parameters, it is also necessary to use hydrobiological to determine the quality of water bodies.

The combined use of hydrobiological and hydrochemical indicators allows you to perform a comprehensive assessment of water quality and apply it to standardize and distribute the load among water user groups. It is supposed to take into account territorial inter-branch norms and standards of environmental safety.



**Figure 2.** Seasonal changes in water quality indices of the studied aquatic ecosystems

## REFERENCES

- Dmitriev, V. V., Frumin, G. T. (2004) Ecological regulation and sustainability of natural systems, Science, Saint Petersburg, 294.
- Fedorov, M. P. (2007) Ecological bases of management of natural-technical systems, SPbSPU, Saint Petersburg, 506.
- Galtsova, V. V., Dmitriev, V. V. (2007) Workshop on aquatic ecology and monitoring of the status of aquatic ecosystems: study guide, St. Petersburg State University, Saint Petersburg, 364.
- Khaustov, A. P., Redina, M. M. (2008) Rationing of anthropogenic impacts and assessments of the environmental intensity of territories, RUDN, Moscow, 282.
- Kushnerov, A. I. (2012) Development of a multi-criteria assessment of surface water quality. Proceedings of the international and interregional Bios Forum and the XVII Youth Bios Olympiad, **1**, 98-104.
- Shishkin, I. A., Shishkin, A. I., Zhilnikova, N. A. (2018) The modern concept and methods of regulation of technogenic load on water bodies and prevent flooding. Biosphere, **2**(10), 143-175.
- Shitikov, V. K., Rosenberg, G. S., Zinchenko, T. D. (2003) Quantitative hydroecology: methods of system identification, IESB RAS, Tolyatti, 463.
- Stroganova, M. S. (2017) Development of methodology for assessment of limiting factors of anthropogenic and natural interaction for quotas of the load of water users of the basin district, Master's thesis, Higher School of Technology and Energy of Saint Petersburg State University of Industrial Technologies and Design, Saint Petersburg.
- Tsvetkova, L. I., Alekseev, M. I., Podporin, A. V. (2007) Development of methodology for the integrated assessment of the status of aquatic ecosystems, Report on research work, Saint Petersburg, 74.

# Synthesis and Performance Evaluation of Chitosan Membrane Filled with UiO-66 Nanoparticles for Dewatering of Biobutanol by Pervaporation

D. Unlu\*

\* Chemical Engineering Department, Faculty of Engineering and Natural Sciences, Bursa Technical University, 16310, Yildirim, Bursa, Turkey (E-mail: [derya.unlu@btu.edu.tr](mailto:derya.unlu@btu.edu.tr))

## Abstract

Biobutanol is an important alternative to fossil fuel. It has superior properties compared to the some of known biofuels. Aim of this study is to dewatering of biobutanol for the using as fuel in the engine. Hydrophilic chitosan membrane was synthesized for that purpose and it was used in pervaporation system. In order to improve the separation performance of chitosan membrane, UiO-66 nanoparticles were synthesized and added to the membrane. The separation performances of membranes were investigated at different UiO-66 ratios and different feed concentration. Swelling behaviours of membranes were compared by using pristine chitosan membrane and UiO-66 loaded chitosan membrane. Membrane structure was characterized by FTIR and SEM. Separation success of membranes was calculated by using flux and separation factor values. The highest separation value was obtained at UiO-66 loaded chitosan membrane. The highest separation factor of 249 and flux of 1.28 kg/m<sup>2</sup>h were obtained at 4 wt.% feed water concentration when the UiO-66 loaded chitosan membrane was used.

## Keywords

Biobutanol; chitosan; dewatering; UiO-66; pervaporation

## INTRODUCTION

Pervaporation is a membrane-based separation process for the liquid-liquid mixtures. Pervaporation has three successive steps: (i) adsorption from the liquid phase on the membrane surface, (ii) diffusion through the membrane; (iii) desorption into the vapor phase. The membrane allows the target component in the mixture to transport through it (Smitha et al., 2004; Wijmans et al., 1995; Huang et al., 1991). Pervaporation is generally use for the removal of minor component in feed mixture, thus rather low amount liquid is evaporated, and less energy is consumed in the separation process. In recent years, the alcohol dewatering gain interest owing to the application of alcohols as biofuels. Alcohol-water mixtures are mostly azeotropic mixtures. Azeotropic mixtures can be separated by traditional methods such as distillation, but these processes are high energy consuming. The dewatering of alcohols is the high cost step in the production of biofuels (Huang et al., 2014 ). Pervaporation is a good alternative to conventional separation processes because of their unique properties such as low energy consumption, easy operation, low cost and high selectivity.

Butanol is an important biofuel of the future. It has superior fuel properties compared with ethanol. Butanol is mainly obtained from biomass by the fermentation technique. After the fermentation, the butanol is obtained as less than 3 % concentration. Therefore, the purification of butanol comprises of two stages: (i) the recovery of butanol from dilute aqueous solutions by distillation in order to obtain a high butanol-enriched mixture, and (ii) the dewatering of butanol in order to obtain a greater than 99.5 % concentration of butanol (Liu et al., 2013; Niemisto et al., 2013; Dong et al., 2014). In literature, enrichment of butanol had been studied greatly, but application of dewatering of butanol are limited. Mostly, hydrophobic membranes were used (Guo et al., 2004; Lin et al., 2018; Lizon et al., 2002; Tsou et al., 2015). In this study, pervaporation was used for dewatering of

biobutanol in order to fill the knowledge gaps in literature and hydrophilic membrane had been used. Polymeric hydrophilic membranes are widely used in pervaporation applications due to the advantages such as easy production, scale-up, and low cost. High permeability and high selectivity are the main criteria in evaluating a membrane. However, the simultaneous obtainment of them is difficult. Therefore, researchers are developed mixed matrix membranes.

Mixed matrix membranes occur with combination of polymeric matrix and inorganic fillers. Zeolites, carbon molecular sieves, silicas, metal oxides, carbon nanotubes and graphene oxides have been widely used inorganic filler material in pervaporation applications. In addition to all these, metal organic frameworks (MOFs) are promising materials. They have large surface area, tuneable chemical properties and high adsorption capacity. Metal organic frameworks have been received significant attention due to the these unique characteristic properties.

Among various metal organic frameworks, UiO-66 has an important place in the membrane application. UiO-66 based membranes show great potential in water reuse (Xu and Chung, 2017). Therefore, in this study, UiO-66 was chosen as inorganic filler for dewatering of biobutanol. Chitosan was used as polymeric matrix. Although UiO-66 based mixed matrix membrane have a wide range of applications as aforementioned, to my best knowledge, there is no study of UiO-66 based chitosan membranes for pervaporation. This study may provide useful insights to develop high performance UiO-66 based mixed matrix membranes for alcohol dewatering via pervaporation.

## **EXPERIMENTAL METHODS**

### **UiO-66 nanoparticle synthesis**

Zirconium (IV) chloride ( $ZrCl_4$ ), terephthalic acid and acetic acid were mixed into dimethylformamide. The solution was stirred at 100 °C for 24 h. The solution is allowed to cool at room temperature. The UiO-66 nanoparticles were obtained by centrifugation and further purified by washing with fresh DMF for several times (Naixin et al., 2017).

### **Membrane preparation**

1.1 wt.% of chitosan solution was prepared in aqueous acetic acid solution under stirring at 25 °C for 24 h. Chitosan membrane filled with UiO-66 nanoparticles were manufactured by certain amount UiO-66 addition. Priming method was applied to the mixed matrix membranes. Priming is a method to avoid a non-adhesive contact between the polymer and nanoparticle. Firstly, UiO-66–water was mixed for 3 h, then it was dispersed in sonicator during 3 h. A little amount of chitosan membrane solution was added to the UiO-66 solution and UiO-66 particles were coated by the chitosan membrane solution. The mixed matrix membrane was poured on a clean plate and dried at room temperature. The obtained mixed matrix membrane was crosslinked with  $H_2SO_4$  in 50% v/v aqueous acetone solution for 5 min. The prepared membranes were characterized by FTIR and SEM.

### **Pervaporative dewatering**

Pervaporative dewatering experiments were carried out in a laboratory scale pervaporation system. It consisted of a membrane cell, agitator, thermocouple, Dewar flasks and a vacuum pump. The effective membrane surface area is 9.61 cm<sup>2</sup>. Feed solution was pump to a membrane cell. The concentration of water was changed from 5 wt. % to 35 wt. %. Pervaporation tests were also conducted at different UiO-66 nanoparticle loading ratio as 0.5 wt.%, 1 wt.% and 2 wt.%. UiO-66 ratio was calculated base of PVA amount in the membrane solution. The volume of the feed solution was 100 ml. Performance of pervaporation process was determined by calculation of flux

and separation factor. The flux and separation factor values were determined as follows equations:

$$J = \frac{m}{A.t} \quad (1)$$

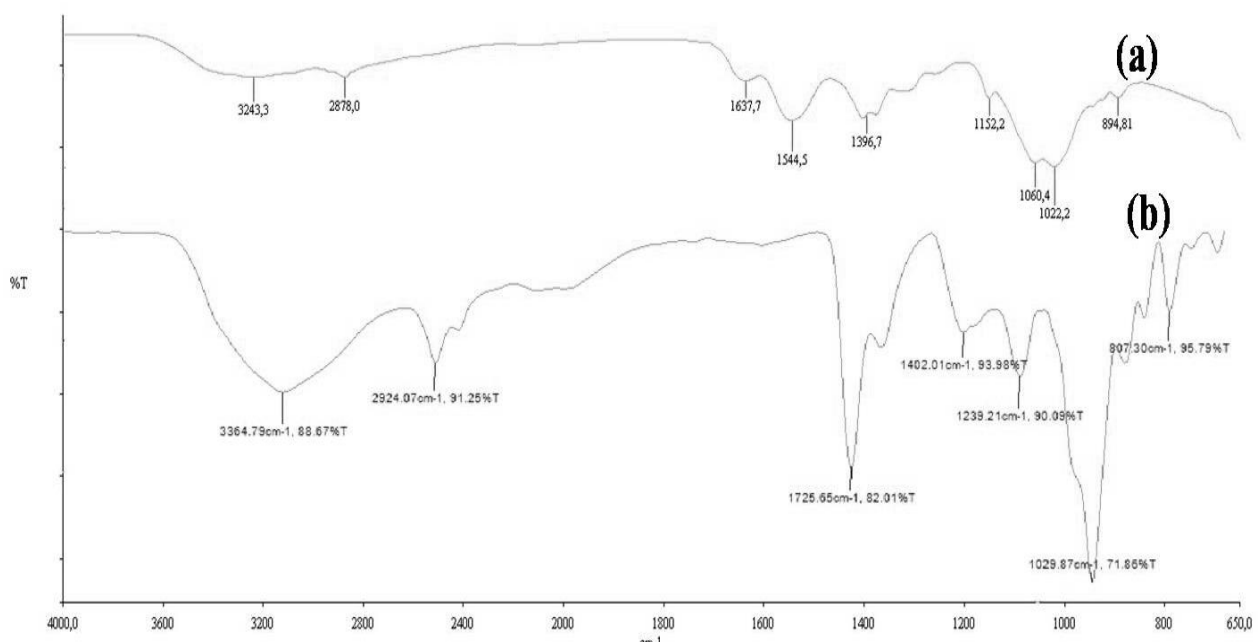
$$\alpha = \frac{(y_a / y_b)_{\text{permeate}}}{(x_a / x_b)_{\text{feed}}} \quad (2)$$

where  $J$  is the flux,  $m$  is the permeation mass,  $t$  is the time in Equation 1,  $y_a$  and  $x_a$  is the weight fraction of phenol in the permeate and feed streams, and  $y_b$  and  $x_b$  is the weight fraction of water in the permeate and feed streams in Equation 2.

## RESULTS AND DISCUSSION

### Characterization of membranes

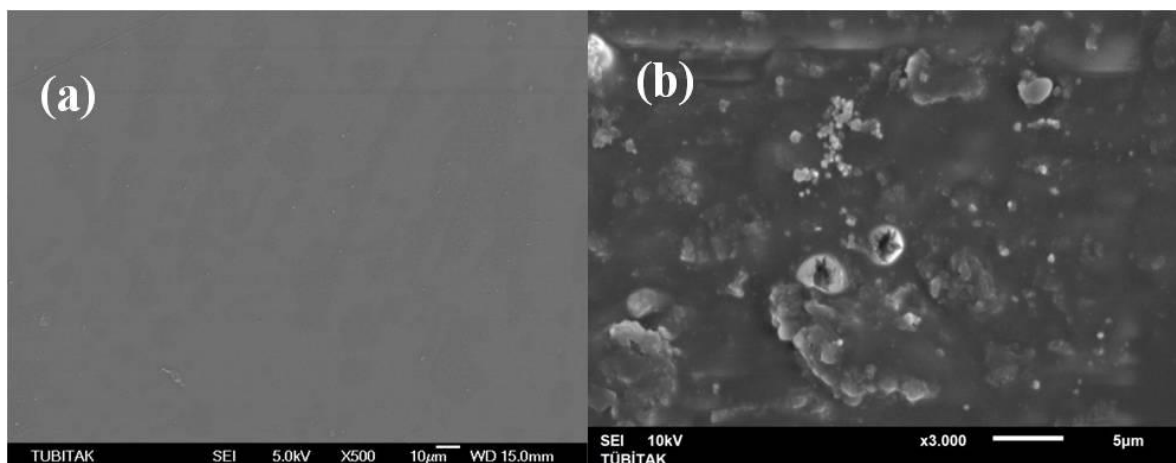
Structural change of chemical bonds in membranes were analysed by FTIR. Figure 1 shows the FT-IR spectra of membranes.



**Figure 1.** FTIR spectrum of pristine (a) and mixed matrix membrane (b)

For the pristine chitosan membrane, the adsorption bands at 3243, 2878, 1637 and 1544  $\text{cm}^{-1}$  represent the stretching vibration of -OH, C-H, C=O and N-H, respectively. For UiO-66/chitosan, (2 wt% loading), the -OH peak shifts to 3364, 2924, 1725, and 1402  $\text{cm}^{-1}$  respectively due to the hydrogen-bonds formation between chitosan and UiO-66 (Fig.1 (b)). The peaks at 1725, 1402, 1239, 1029, and 807  $\text{cm}^{-1}$  are attributed to the presence of UiO-66 in the membrane (Premakshi et al., 2015).

Morphologic analysis of membranes was carried out by a scanning electron microscopy (SEM). The SEM images of membranes are shown in Figure 2. Surface images of membranes show that while the pristine chitosan membrane has smooth surface, the surface of UiO-66 loaded chitosan membrane has UiO-66 nanoparticles. Mixed matrix structure of UiO-66 loaded chitosan membrane can be seen in cross section images. Pristine chitosan membrane has only chitosan polymer matrix.



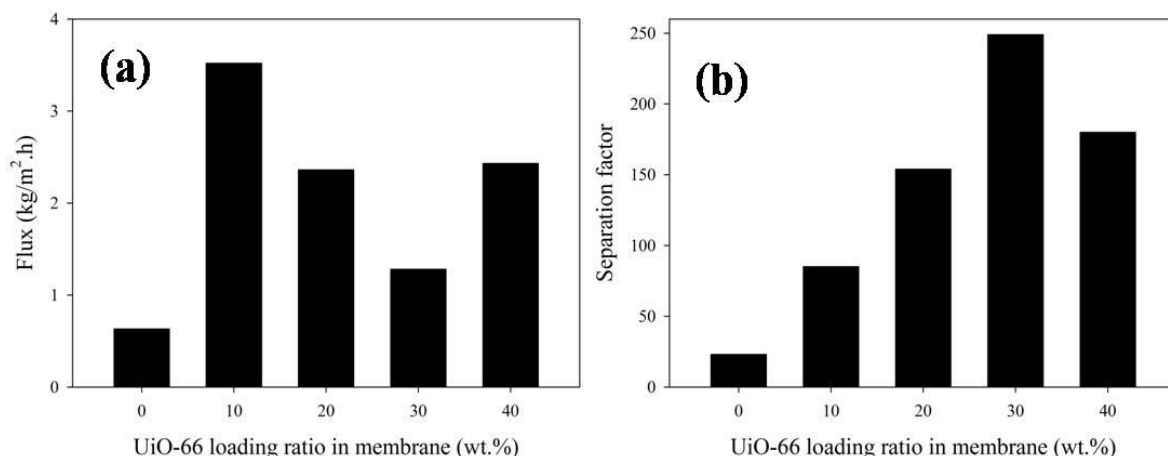
**Figure 2.** SEM images of the (a) pristine membrane surface (b) mixed matrix membrane surface

### **Pervaporation performance of UiO-66/Chitosan mixed matrix membranes for biobutanol dewatering**

Dewatering performance of biobutanol by pervaporation was determined by flux and separation factor. UiO-66 nanoparticle amount is an important factor for the separation performance of mixed matrix chitosan membranes. Therefore, UiO-66 loaded chitosan membranes were prepared with different UiO-66 loading ratios. Figure 3 presents the biobutanol dewatering performance of the pristine chitosan membrane and mixed matrix membrane as a function of UiO-66 loading at 45 °C. The highest flux for biobutanol dewatering is 1.28 kg/m<sup>2</sup>h when the chitosan membrane contains 30 wt. % UiO-66. This obtained flux value is more than two times higher than that of the pristine chitosan membrane. The increments of flux are attributed to two factors: higher solubility and diffusivity. UiO-66 is a hydrophilic structure and the hydrophilic groups in UiO-66 has more water sorption sites and act as water selective fillers. Therefore, the UiO-66 loaded membrane has higher flux values than pristine membrane. UiO-66 helps diffusion of water through the membrane easily. As a consequence, the all UiO-66 loaded chitosan membranes present a higher flux according to pristine chitosan membrane.

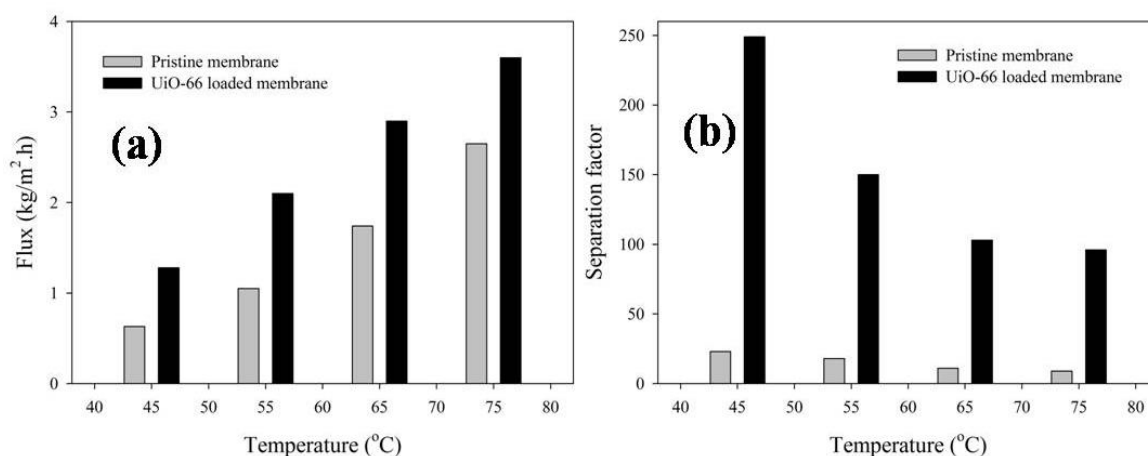
The effect of UiO-66 amount on separation efficiency could be explained as two manner. Firstly, high UiO-66 loading ratio would increase the free volume in the membrane matrix and this increment is resulted in decrease of diffusivity selectivity. Second effect, as can be seen in the figure of sorption degree above, a higher UiO-66 loading may result in membrane that possess higher solubility selectivity. High solubility selectivity has a positive effect of the separation efficiency and water separation factor increases. These two effects cause to occur different results for different binary mixtures (Xu and Chung, 2017). For butanol dewatering, as the loading of UiO-66 particles increased, the separation factor of the mixed matrix membrane had increased, the permeate flux had decreased.

As shown in Figure 3, UiO-66 loading ratio is increased from 10 wt.% to 30 wt.%, the separation factor of the mixed matrix membrane increased while the permeate flux decreased. However, when the amount of UiO-66 particles further increased to 40 wt.%, the separation factor of the mixed matrix chitosan membranes decreased while the permeate flux increased. It showed that the excessive loading had a negative effect on the separation performance of the mixed matrix chitosan membranes. This can be explained that the excess usage of UiO-66 is leading to agglomeration of nanoparticles, the distribution of them in chitosan matrix is not homogeneous. This situation causes the decrease of separation performance. Taking into account all of the flux and separation factor values, the optimal loading of UiO-66 particles was determined as 30 wt.% (Wang et al., 2017; Xu et al., 2018).



**Figure 3.** Effect of UiO-66 amount on flux (a) and separation factor (b)

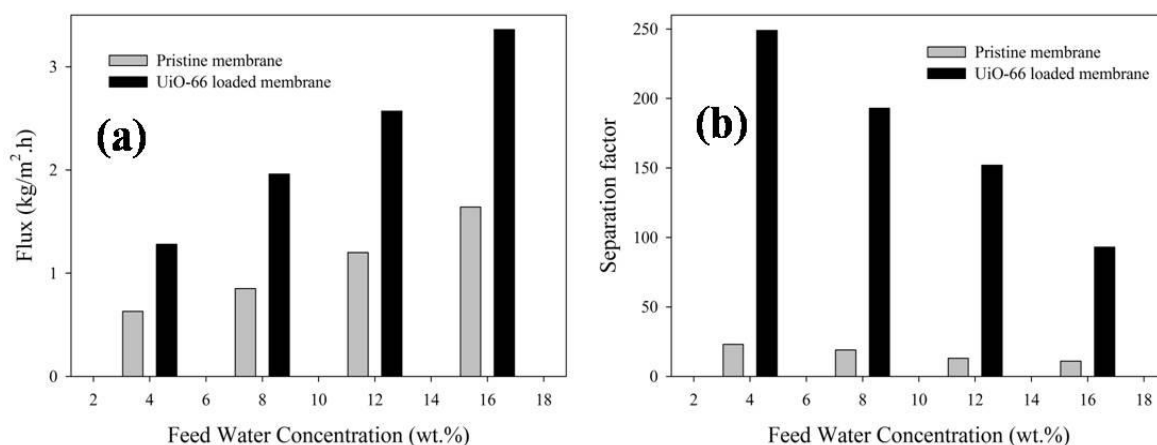
A mixed matrix membrane containing 30 wt.% UiO-66 was chosen to study the effect of temperature. Dewatering of biobutanol by pervaporation was investigated in 45, 55, 65 and 75 °C of temperatures. The effect of temperature on flux and separation factor is shown in Figure 4. The flux increases with an increase in operating temperature from 45 to 75 °C. The operation temperature affects the driving force and the membrane permeability. The saturated vapour pressures of both water and butanol increases with increase in the operation temperature, these differences of temperature created driving force for the diffusion. An increase in the operation temperature facilitates the diffusion of the feed components and flux increases. The increase in flux is also related to the flexibility of polymer chains at higher temperature, flexibility causes larger free volumes in the chitosan membrane and diffusion of butanol and water increases. Separation factor decreases with temperature for this reason. The flux rises from 1.28 to 3.60 kg/m<sup>2</sup>h as the temperature increases from 45 to 75 °C, while the separation factor decreases from 249 to 96. The highest separation factor value of 249 is observed working a temperature of 45 °C. As a result, the feed temperature of 45 °C is optimal for the separation of water from butanol based on this work.



**Figure 4.** Effect of operation temperature on flux (a) and separation factor (b)

Feed concentration also play an important role in the PV performances of the mixed matrix membranes. To study the effect of feed concentration, pervaporation performance of a MMM with 30 wt% UiO-66 loading was tested under three different feed concentrations: 4 wt.%, 8 wt.% 12

wt.% and 16 wt.% water. As the feed water concentration increases, the flux shows an increasing trend. The increase in flux may be due to the swelling of the mixed matrix membrane at the high feed concentration. The swollen membrane causes a decline in membrane separation factor, because the swollen and plasticized membrane would allow the diffusion of butanol molecules through the membrane along with water molecules (Devi et al., 2007; Wei et al., 2018). The results show that as the feed water increased from 4 wt% to 16 wt%, the flux increased from 1.28 to 3.36 kg/m<sup>2</sup>h whereas the separation factor dropped from 249 to 93 (Figure 5).



**Figure 5.** Effect of feed concentration on flux (a) and separation factor (b)

## CONCLUSIONS

In conclusion, membrane filled with UiO-66 nanoparticles were prepared for dewatering of biobutanol by pervaporation. Metal organic framework UiO-66 particles were fabricated and added to membrane solution, mixed matrix membrane was synthesized. UiO-66 particles have hydrophilic groups for the responsible in water permeation. The morphologies and structures of the pristine and UiO-66 loaded chitosan membrane were characterized by SEM and FTIR. The effect of UiO-66 amount, operation temperature and feed concentration on separation performance was investigated. Higher feed composition and operation temperature had resulted in higher membrane swelling and driving force. Therefore, an increase of temperature and feed concentration had caused in the increase of flux and the decrease of separation factor value. The UiO-66 loaded mixed matrix membrane has shown excellent separation performance for the butanol dewatering. When the feed solution was 4 wt% water/butanol mixtures at 45°C, the separation factor and permeate flux of the mixed matrix membrane was 249 and 1.28 kg/m<sup>2</sup>h. Therefore, these results indicated that UiO-66 particles can be used as a new membrane filler material for dewatering process. In conclusion, UiO-66 nanoparticles were fabricated as porous fillers incorporated into chitosan because of their high thermal, water and acid stability. The morphologies and structures of the UiO-66 loaded chitosan mixed matrix membranes were characterized. The mixed matrix membranes used for dewatering butanol/water mixtures. The obtained results showed comparable separation performance with the membranes reported in the reference. Therefore, these results indicated that UiO-66 nanoparticles can be used as a new membrane material for biobutanol dewatering.

## ACKNOWLEDGEMENTS

The author gratefully acknowledge the financial supports from Bursa Technical University Scientific Research Projects Unit (Project No. 182N04).

## REFERENCES

- Brüschke, H. E. A., Wynn, N. P. (2000) Membrane separations/pervaporation, in: I.D. Wilson, E.D. Adlard, M. Cooke, C.F. Poole (Eds.), *Encyclopedia of Separation Science*, Academic Press, Germany, 1776-1778.
- Devi, D. A., Smitha, B., Sridhar, S., Jawalkar, S. S., Aminabhavi, T. M. (2007) Novel sodium alginate/polyethyleneimine polyion complex membranes for pervaporation dehydration at the azeotropic composition of various alcohols. *Journal of Chemical Technology & Biotechnology*, **82**(11), 993-1003.
- Dong, Z., Liu, G., Liu, S., Liu, Z., Jin, W. (2014) High performance ceramic hollow fiber supported PDMS composite pervaporation membrane for bio-butanol recovery. *Journal of Membrane Science*, **450**, 38-47.
- Gallego-Lizon, T., Edwards, E., Lobiundo, G., Freitas dos Santos, L. (2002) Dehydration of water/t-butanol mixtures by pervaporation: comparative study of commercially available polymeric, microporous silica and zeolite membranes. *Journal of Membrane Science*, **197**(1-2), 309-319.
- Guo, W. F., Chung, T.-S., Matsuura, T. (2004) Pervaporation study on the dehydration of aqueous butanol solutions: a comparison of flux vs. permeance, separation factor vs. selectivity. *Journal of Membrane Science*, **245**(1-2), 199-210.
- Huang, R. Y. M. (1991) *Pervaporation Membrane Separation Processes*, 1st ed., Elsevier, Science Publishers BV, Amsterdam, 1991.
- Huang, B., Liu, Q., Caro, J., Huang, A. (2014) Iso-butanol dehydration by pervaporation using zeolite LTA membranes prepared on 3-aminopropyltriethoxysilane-modified alumina tubes. *Journal of Membrane Science*, **455**, 200-206.
- Jie, L., Jiding, L., Quan, C., Xiaoduan, L. (2018) Performance of a pervaporation system for the separation of an ethanol-water mixture using fractional condensation. *Water Science and Technology*, **77**(7), 1861-1869.
- Lin, Y.-F., Wu, C.-Y., Liu, T.-Y., Lin, K.-Y. A., Tung, K.-L., Chung, T.-W. (2018) Synthesis of mesoporous SiO<sub>2</sub> xerogel/chitosan mixed-matrix membranes for butanol dehydration. *Journal of Industrial and Engineering Chemistry*, **57**, 297-303.
- Liu, S., Liu, G., Zhao, X., Jin, W. (2013) Hydrophobic-ZIF-71 filled PEBA mixed matrix membranes for recovery of biobutanol via pervaporation. *Journal of Membrane Science*, **446**, 181-188.
- Naixin, W., Guojun, Z., Lin, W., Jie, L., Quanfu, A., Shulan, J. (2017) Pervaporation dehydration of acetic acid using NH<sub>2</sub>-UiO-66/PEI mixed matrix membranes. *Separation and Purification Technology*, **186**, 20-27.
- Niemistö, J., Kujawski, W., Keiski, R. L. (2013) Pervaporation performance of composite poly(dimethyl siloxane) membrane for butanol recovery from model solutions. *Journal of Membrane Science*, **434**, 55-64.
- Premakshi, H. G., Sajjan, A. M., Kariduraganavar, M. Y. (2015) Development of pervaporation membranes using chitosan and titanium glycine-N,N-dimethylphosphonate for dehydration of isopropanol. *Journal of Materials Chemistry A*, **3**(7), 3952-3961.
- Smitha, B., Suhanya, D., Sridhar, S., Ramakrishna, M. (2004) Separation of organic-organic mixtures by pervaporation—a review. *Journal of Membrane Science*, **241**(1), 1-21.
- Tsou, C.-H., An, Q.-F., Lo, S.-C., De Guzman, M., Hung, W.-S., Hu, C.-C., Lai, J.-Y. (2015) Effect of microstructure of graphene oxide fabricated through different self-assembly techniques on 1-butanol dehydration. *Journal of Membrane Science*, **477**, 93-100.
- Wang, N., Zhang, G., Wang, L., Li, J., An, Q., Ji, S. (2017) Pervaporation dehydration of acetic acid using NH<sub>2</sub>-UiO-66/PEI mixed matrix membranes. *Separation and Purification Technology*, **186**, 20-27.



# A Hydrological Model for Ayamama Watershed in Istanbul, Turkey using HEC-HMS

İ. Yalçın\*, C. M. Kazezyılmaz-Alhan\*, K. Javanshour\*, M. Aytekin\*\* and S. Gülbaz\*

\* Department of Civil Engineering, Istanbul University-Cerrahpasa Avcılar Campus, 34320 Avcılar, Istanbul, Turkey (E-mails: [inciyalcin@ogr.iu.edu.tr](mailto:inciyalcin@ogr.iu.edu.tr); [meleka@istanbul.edu.tr](mailto:meleka@istanbul.edu.tr); [keivanjavanshour@ogr.iu.edu.tr](mailto:keivanjavanshour@ogr.iu.edu.tr); [sezarg@istanbul.edu.tr](mailto:sezarg@istanbul.edu.tr))

\*\* Department of Forest Engineering, Istanbul University-Cerrahpasa 34473 Sarıyer, Istanbul, Turkey (E-mail: [aytekinm.mustafa@gmail.com](mailto:aytekinm.mustafa@gmail.com))

## Abstract

Floods are among the most common natural disasters which result in both big economic loss and human life. Especially, in urbanized regions with high population density, the effect of floods become more pronounced. One of the fatal events occurred in Ayamama River in Istanbul on September 9, 2009. The overall flooding was the result of successive and persistent storm with high intensity over a 3-day period which generated more than 250-mm rainfall over the region. The flood resulted in fatality of 32 people and caused extensive environmental and infrastructural damage in the region. In this study, a hydrological model for the Ayamama Watershed is generated by using Hydrologic Engineering Center Hydrologic Modeling System (HEC-HMS). The basin area is divided into the subbasins; the sections and parameters of the natural water channel are defined; infiltration is taken into account with Green-Ampt method and Clark Unit Hydrograph method is used for calculation of the hydrograph over the watershed. The rainfall data measured during the aforementioned flood event is used in simulation and the results are evaluated in light of observations after the flood event. Peak flow of the hydrographs for the subbasins, of which are heavily affected by the flood event, are obtained and compared with the results of the hydrological model generated by Rational Method in WMS in a former study (Gülbaz et al, 2019). The results obtained by HEC-HMS model are in good agreement with the results obtained by Rational Method in WMS. Moreover, the subbasins located downstream of the Ayamama River are determined as the most critical region.

## Keywords

Ayamama watershed; flooding; hydrologic model; HEC-HMS

## INTRODUCTION

The intensity and frequency of floods have increased due to several reasons in recent years (Xiao et al., 2019). Climate change is undoubtedly one of the most important reason. According to the Intergovernmental Panel on Climate Change evaluation report (IPCC, 2014), concerns about climate change are generally seen as an increase in temperature, an increase in heavy rainfall events on land, and coastal floods. Another main reason of floods is the increase in impervious surfaces due to urbanization (Vaillancourt et al., 2019). The decrease of vegetation and the disappearance of the natural reservoir result in malfunction of stream flow regime that influences the balance of hydrology (Legowo et al. 2019). Floods occur after extreme regional rains in many countries (Wurjanto et al. 2019) and it is the biggest economic natural disasters after earthquakes (Uşkay and Aksu, 2002). For example in United States, floods cause an annual damage over USD 4 billion and the deaths of almost 200 people (Pielke et al., 2002). In recent years, as a result of the increase in population, settlements in urbanized regions have increased and spread towards river beds in Turkey. As a result, the number of flood damages has increased (Bayazıt, 2002). Between 1955 and 1995, more than 1000 people lost their lives due to the floods in Turkey. The economic loss of these floods was more than USD 650 million (Ceylan et al., 2007).

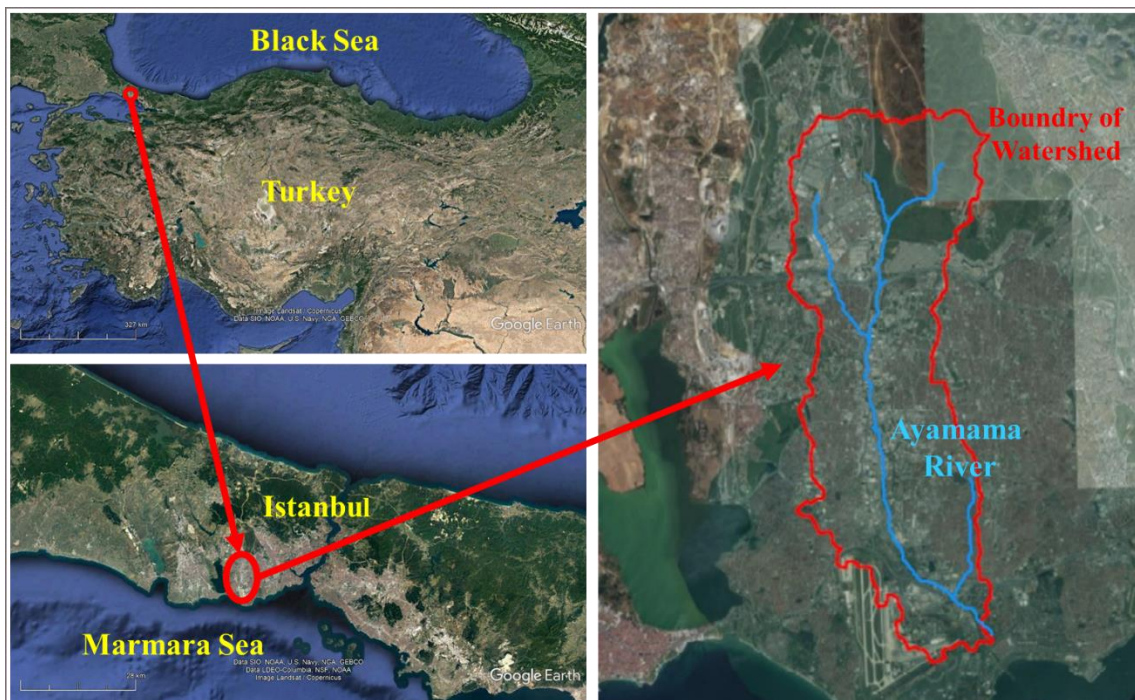
In the Marmara region, the most severe floods occurred in the last years; particularly, the one that occurred during the period of 7 and 10 September 2009, was one of the severe floods. Istanbul and Tekirdağ provinces were the most affected provinces of the Marmara region. The said flood event was the third greatest disaster among the flood events in Turkey after the floods occurred in Izmir and in the Western Black Sea (Kömüşçü and Çelik, 2013). The flooding event occurred in Ayamama River in Istanbul was the result of successive and persistent storm with high intensity over a 3-day period which generated more than 250-mm rainfall over the region. The flood resulted in fatality of 32 people and caused extensive environmental and infrastructural damage in the region (Gülbaz et al., 2019).

In order to investigate the physical mechanisms of floods and take precautions, flood simulations of the specific regions are necessary. Therefore, generation of hydrological models for different watersheds has gained importance (Sikder, 2019). The aim of this study is to generate a hydrological model for the Ayamama Watershed and compare its results with the results of a calibrated model generated in a former study by Gülbaz et al., 2019. HEC-HMS is employed for simulation of the flood event. Peaks of the hydrographs for the subbasins, which are heavily affected by the flood event, are compared with the results of the hydrological model generated by Rational Method in WMS in the former study.

## MATERIAL AND METHODS

### Study Site

Ayamama watershed is located on the European Continental side of Istanbul in Turkey. The main stream length is 21 km with many tributaries feeding the river. The surface area of the watershed is 74 km<sup>2</sup>. TEM highway, International Atatürk Airport and Ikitelli Organized Industrial Zone are located in this region and the basin is exposed to rapid urbanization (Gülbaz et al., 2019). Figure 1 shows the location of Ayamama Watershed and Ayamama Stream and the region affected by the flood event.



**Figure 1.** Location and boundary of Ayamama River watershed ( Google Earth, Data SIO, NOAA, U.S. Navy, NGA, GEBCO, Image Landsat/Copernicus © 2018 Basarsoft, © 2018 Google)

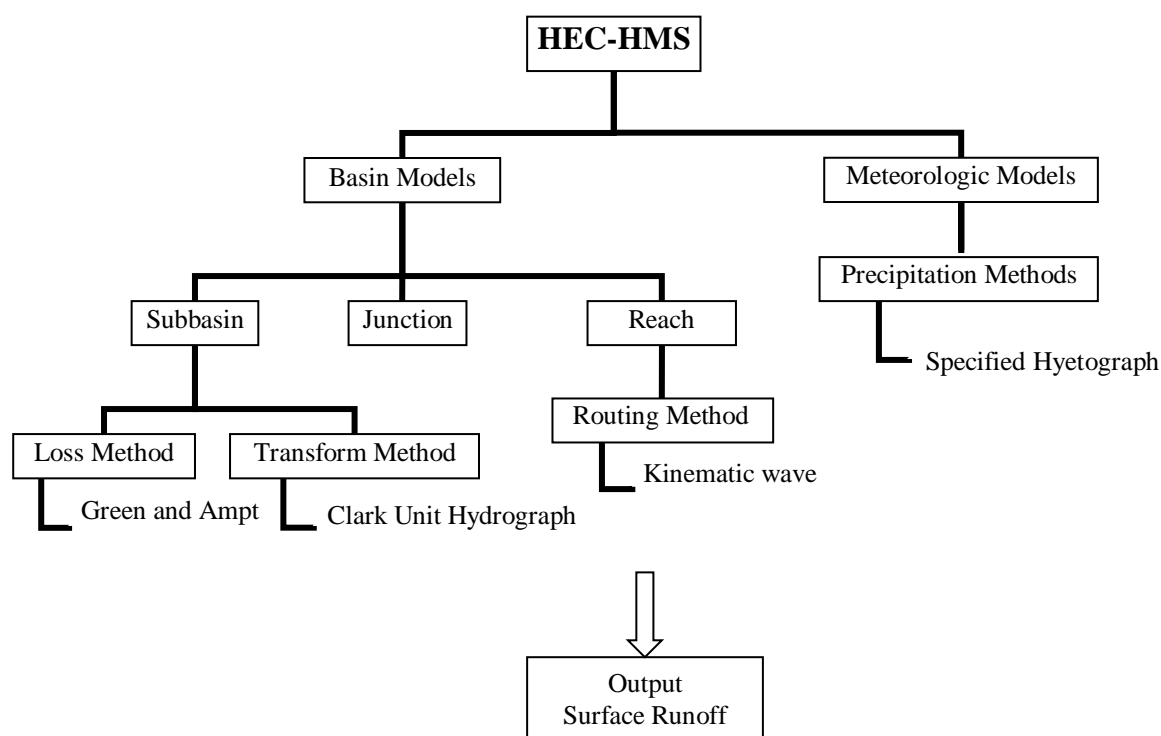
**Hydrologic Engineering Center-Hydrologic Modeling System (HEC-HMS)**

Hydrologic Modeling System has developed by the U.S. Army Corps of Engineers (Fieldman, 2000). HEC-HMS models precipitation-runoff processes of dendritic watershed systems. It has the capability of simulating the floods and natural watershed runoff as well as meteorological phenomena such as evapotranspiration, snow melting and precipitation. The software is able to report a database, data entry tools, calculation engine and results. The modeling results are employed in evaluating current water budget and flow estimations. The primary model components are basin models, meteorologic models and control specifications. A simulation calculates the precipitation-runoff response in the basin model given input from the meteorologic model. The control specifications define the time period and time step of the simulation run (Fleming and Brauer, 2016). All hydrological elements are connected to a network in order to model the relationship between precipitation and flow. Basin-subbasin, reaches and junctions are main hydrological elements (Scharffenberg, 2016).

*Basin Models.* The system provides a variety of methods for calculating loss in subbasin and transforming of precipitation to flow. Green and Ampt, Deficit and Constant, SCS Curve Number are the main methods to estimate loss in basin. Green and Ampt method is chosen in this study to calculate infiltration. The parameters of Green and Ampt method are initial moisture content, saturated moisture content, wetting front soil suction head, and hydraulic conductivity (Rossman, 2015).

It is provided Clark Unit Hydrograph, ModClark, and User specified Unit Hydrograph are the available methods in HEC-HMS to calculate precipitation-flow transformation. Clark Unit Hydrograph method chosen in this study is a synthetic hydrograph method that utilizes an instantaneous unit hydrograph (Clark, 1945). Obtaining a unit hydrograph through the analysis of past observed hydrographs is not requisite (Scharffenberg, 2016). The technique called as the time-area method (Kull and Fieldman, 1998) assumes that the discharge at any point in time is a function of translation and storage properties of the basin. The translation is obtained by calculating the surface and channel travel time of runoff. Delay caused by the storage effects of a watershed is also taken into account (Viessman and Lewis, 2012). The translation of the hydrograph is satisfied by routing through a linear reservoir to account for storage attenuation effects in the basin (Scharffenberg, 2016). The components of method are time of concentration and storage coefficient. Kinematic wave, Modified Puls and Muskingum translation are available routing options in pipes or open channels. The current study is performed with kinematic wave. In kinematic wave routing method, the acceleration and pressure terms in the momentum equation are negligible. The wave motion is described by the equation of continuity (Chow et al., 1988). The energy slope is equal to the bed slope according to this method. As the method allows flow and area to vary both spatially and temporally within a conduit, it can result in attenuated and delayed outflow hydrographs (Rossman, 2015). The parameters of the method are length, slope, Manning's coefficient and cross section.

*Meteorologic Model.* Meteorologic model purposes are to prepare meteorologic boundary conditions for subbasins. A common meteorologic model can be used with many different basin models. The method of precipitation is selected as specified hyetograph for meteorologic model of this study. The Specified Hyetograph method allows for definition of a specific time-series rainfall data at subbasins (Scharffenberg, 2016).



**Figure 2.** Chart for the HEC-HMS and the selected methods of this study

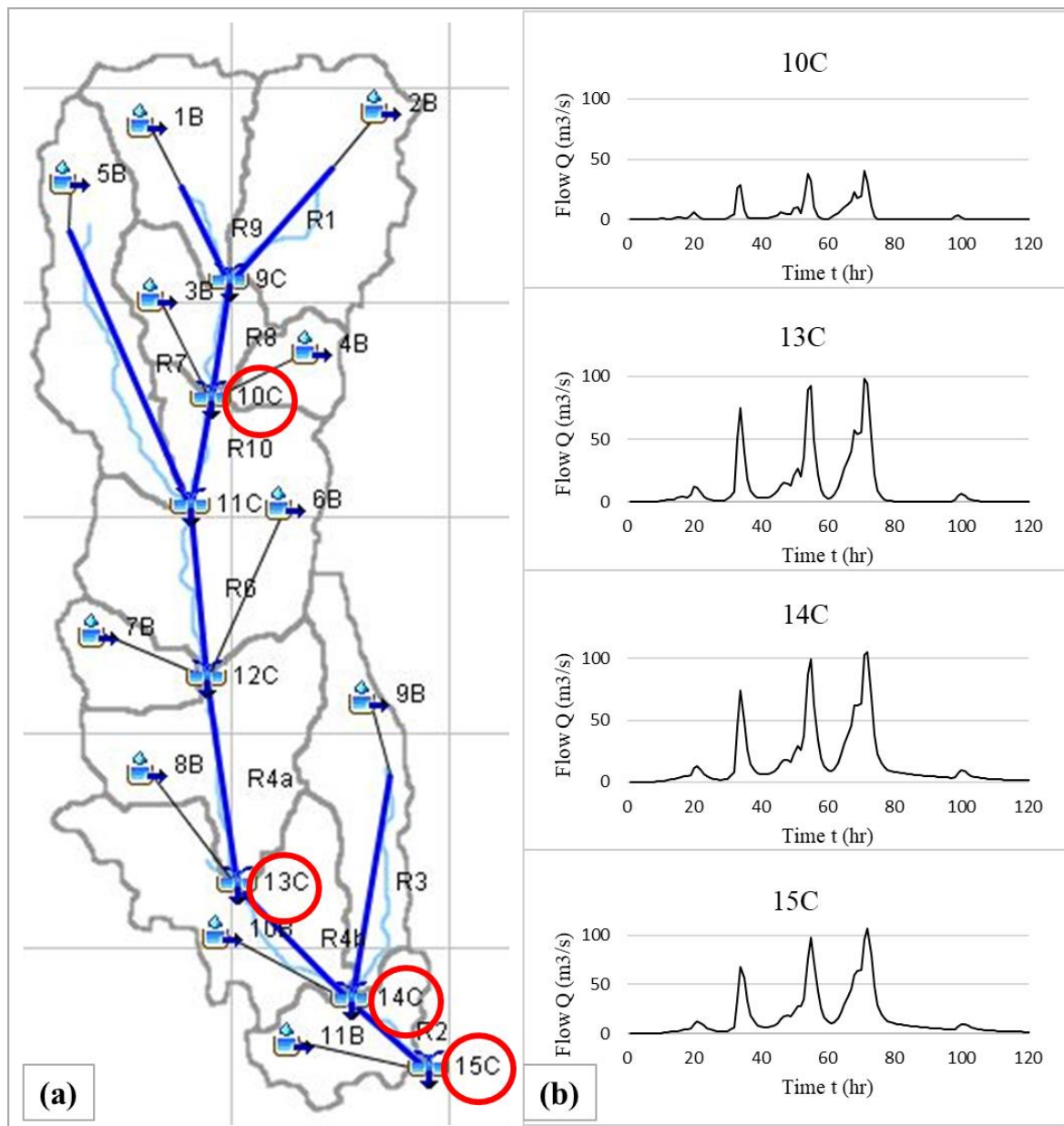
### Modeling

For modeling of the Ayamama Watershed with HEC-HMS, a topographical map, cross-sectional area of the main river, soil properties of the study area and precipitation data for the flood event are used. Area informations and Ayamama river length of the watershed are determined based on ArcGIS. Cross-sectional area informations of the river are obtained from the former study on the region. Soil type is determined as loamy sand and required characteristics are obtained from EPA SWMM User's Manual. The precipitation data for the flood event was provided by the Turkish State Meteorological Service (MGM).

Control of a large basin is more difficult than a small basin. Basins can be separated into sub-basins and more precise control can be provided. For this reason, sub-basins were formed by specifying the relevant exit points in the Ayamama Basin. The basin area is divided into 11 subbasins and area information is defined. Infiltration is taken into account with Green-Ampt method. In order to find the amount of loss, the values of the initial moisture content, saturated moisture content, suction head, and hydraulic conductivity parameters are defined. These values vary according to the soil type. Due to the high urbanization in the watershed, 95 % imperviousness is defined. Clark Unit Hydrograph method is used for calculation of the hydrograph over the watershed. Within the scope of the method, time of concentration of subbasins and storage coefficient parameters of the soil are defined in the system. Junctions are added to each sub-basin outlet to collect the incoming water. The reaches representing the Ayamama river are defined in the model. Total length of all reaches are approximately 20 km. As a routing method for each reach, the kinematic wave method is used which asks for the roughness and the channel cross section shape. Their length, slopes, manning's roughness coefficient ( $n$ ) and cross sections are defined into the model.

Figure 3 presents the hydrological model of the Ayamama watershed generated in HEC-HMS. Here, blue squares represent the subbasins, dark blue lines represent the reaches and blue rectangles represent junctions. After the model is launched, the Meteorologic model is selected as a Specified

Hyetograph. The rainfall data, which belongs to September 7–11, 2009, is provided by the Turkish State Meteorological Service (MGM) and is used in the watershed model to simulate the hydrological response of the region. Precipitation is defined in all subbasins. System control is provided for the related days via Control specifications.



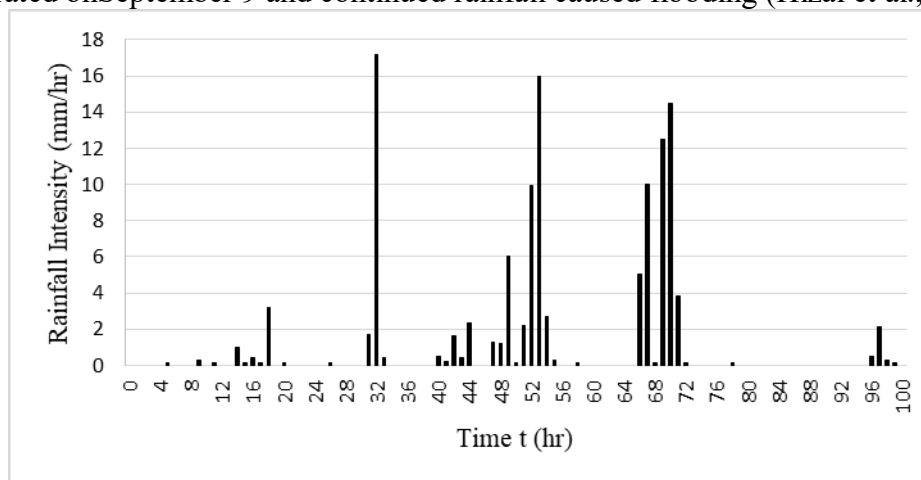
**Figure 3.** (a) Hydrological model of the Ayamama Watershed with HEC-HMS (b) Outlets of subbasins, Hydrographs for subbasins

## RESULTS

The flood event occurred on September 9, 2009 is simulated by using HEC-HMS. The watershed is divided to 11 subbasins and they are called as 1B-11B, respectively. The junctions are defined for collection of water to outlets of subbasins and are called as 9C-15C. The flood hydrograph is obtained at different locations along the Ayamama River. Atatürk, Evren, İnönü, and Çobançeşme districts's outlets are represented with 10C, 13C, 14C, and 15C, respectively which were heavily influenced by the flood. Location of these outlets is seen in Figure 4. Flood peaks of the

hydrographs are obtained as 40.3 m<sup>3</sup>/s, 98.5 m<sup>3</sup>/s, 105.2 m<sup>3</sup>/s and 107.4 m<sup>3</sup>/s in these locations. Flow reaches these values at 74<sup>th</sup> hours.

Rainfall intensity of the flood is shown on Figure 4. Total amount of precipitation was more than 250-mm rainfall over the region. As a result of the studies in the region, it was determined that the soil was saturated on September 9 and continued rainfall caused flooding (Hızal et al., 2009).



**Figure 4.** Rainfall intensity of flood (September 7–11, 2009)

Results for critical points in HEC-HMS modeling are compared with the results of the calibrated hydrological model generated by Rational Method in WMS in a former study (Gülbaş et al., 2019). Gülbaş et al., 2019 used Rational Method which is used for hydrological modeling in WMS. WMS includes an interface to the rational method which can be used for computing peak flows on small urban and rural watersheds. In this study, the HEC-HMS model was calibrated in order to adapt to the same rate in the regions towards the basin exit. Table 1 presents the calibrated HEC-HMS results and WMS peak flow values and the difference between the two hydrological models.

**Table 1.** Peak flowrate of the hydrographs and the difference between rational method used for hydrological modeling in WMS (Gülbaş et al., 2019) and HEC-HMS

Location	Peak Flow (m <sup>3</sup> /s)		
	HEC-HMS	Rational Method (Gülbaş et al., 2019)	% Difference
10 C	40.3	53.6	33.0
13 C	98.5	103	4.6
14 C	105.2	104	1.1
15 C	107.4	105	2.3

## CONCLUSIONS

In this study, a hydrological model is generated for Ayamama River Watershed in Istanbul using HEC-HMS. Hydrographs for the subbasins are obtained and compared with the results of the calibrated hydrological model generated by Rational Method in WMS in a former study (Gülbaş et al., 2019). The results obtained by HEC-HMS model are in good agreement with the results obtained by WMS. Moreover, the subbasins located downstream of the Ayamama River are determined as the most critical regions. The model produced in this study can be used to develop flood management studies for this region.



**REFERENCES**

- Bayazıt, M. (2002) Türkiye'de Taşkınlar ve Taşkın Kontrolü Yönetimi. Türkiye Mühendislik Haberleri, **47**(2), 27-29, (in Turkish).
- Ceylan, A., Alan, İ., Uğurlu, A. (2007) Causes and Effects of Flood Hazards in Turkey. Proceedings of the International Congress on River Basin Management, 22-24 March, 2007, Antalya, Turkey, 415-423.
- Chow, V. T., Maidment, D. R., Mays, L. W. (1988) Applied Hydrology, McGraw-Hill, Inc., 283
- Clark, C.O. (1945) Storage and the Unit Hydrograph. *ASCE Trans.*, **110**, 1419-1146.
- Fieldman, A. D. (2000) Hydrologic Modeling System HEC-HMS, Technical Reference Manuel, U.S. Army Corps of Engineers, Institute for Water Resources, Hydrologic Engineering Center (CEIWR-HEC).
- Fleming, M., Brauer, T. (2006) Hydrologic Modeling System HEC-HMS Quick Start Guide, U.S. Army Corps of Engineers, Institute for Water Resources, Hydrologic Engineering Center (CEIWR-HEC).
- Gülbaz, S., Kazezyılmaz-Alhan, C. M., Bahçeçi, A., Boyraz, U. (2019) Flood Modeling of Ayamama River Watershed in Istanbul, Turkey. *Journal of Hydrologic Engineering*, **24**(1).
- Hızal, A., Şengönül, K., Çelik, H. E., Aşk, K., Küçükkaya, İ. (2009) İstanbul İlinde 8-9 Eylül 2009 Tarihlerinde Meydana Gelen Sellere İlişkin Orman Mühendisleri Odası Komisyonu Raporu. Orman Mühendisleri Odası Yayın Kurulu, (in Turkish).
- IPCC (2014) Climate Change 2014: Synthesis Report. Contribution of Working Groups I, II and III to the Fifth Assessment Report of the Intergovernmental Panel on Climate Change [Core Writing Team, R.K. Pachauri and L.A. Meyer (eds.)]. IPCC, Geneva, Switzerland, 151.
- Kömüşçü, A. Ü., Çelik, S. (2013) Analysis of the Marmara Flood in Turkey, 7-10 September 2009: An assesment from hydrometeorological perspective. *Natural Hazards*, **66**(2), 781-808.
- Kull, D. and Feldman, A. (1998) Evolution of Clark's Unit Graph Method to Spatially Distributed Runoff. *Journal of Hydrologic Engineering*, **3**(1).
- Legowo, S., Hadihardaja, I. K., Haji, T. S., Enung, A. (2019) Application of Digital Elevation Method (DEM) For Flood Estimation on Upstream Ciliwung River, West Java, Indonesia. *International Journal of Geomate*, **17**(59), 154-165.
- Rossmann, L. A. (2015) Storm Water Management Model, User's Manual Version 5.1. EPA- 600/R-14/413b. Cincinnati: Water Supply and Water Resources Division, National Risk Management Research Laboratory, USEPA.
- Scharffenberg, W. (2016) Hydrologic Modeling System HEC-HMS User's Manual, U.S. Army Corps of Engineers, Institute for Water Resources, Hydrol. Engineering Center (CEIWR-HEC).
- Sikder, M. S., Ahmad, S., Hossain, F., Gebregiorgis, A. S., Lee, H. (2019) Case Study: Rapid Urban Inundation Forecasting Technique Based on Quantitative Precipitation Forecast for Houston and Harris County Flood Control District. *Journal of Hydrologic Engineering*, **24**(8).
- Pielke, Jr., Downton, M. W., Barnard Miller, J. Z. (2002) Flood Damage in the United States, 1926–2000: A Reanalysis of National Weather Service Estimates, UCA,. Boulder, CO.
- Uşkay, S., Aksu, S. (2002) Ülkemizde Taşkınlar, Nedenleri, Zararları ve Alınması Gereken Önlemler. Türkiye Mühendislik Haberleri, **47**(4-6), 133-13, (in Turkish).
- Vaillancourt, C., Duchesne, S., Pelletier, G. (2019) Hydrologic Performance of Permeable Pavement as an Adaptive Measure in Urban Areas: Case Studies near Montreal, Canada. *Journal of Hydrologic Engineering*, **24**(8).
- Viessman, W., Lewis, G.L. (2012) Introduction to Hydrology Fifth Edition, Pearson Education, Inc., 294.
- Wurjanto, A., Tarigan, A. T., Mukhti, J. A. (2019) Flood Routing Analysis of the Way Seputih River, Central Lampung, Indonesia. *International Journal of Geomate*, **17**(63), 307-314.
- Xiao, Z., Liang, Z., Li, B., Hou, B. (2019) New Flood Early Warning and Forecasting Method Based on Similarity Theory. *Journal of Hydrologic Engineering*, **24**(8).

## Possible Indicator Role of Adenoviruses for Assessing Viral Contamination of Water

T. V. Amvrosieva\*, N. V. Paklonskaya\*, I. V. Belskaya\*, S. K. Laziuk\*, O. N. Kazinets\* and Yu. A. Shilova\*

\* Laboratory of natural reservoir infections, The Republican Research and Practical Centre for Epidemiology & Microbiology, 23 Filimonova str., Minsk 220114, Belarus (E-mail: [labsanvir@gmail.com](mailto:labsanvir@gmail.com))

### Abstract

The article presents the results of comparative studies of drinking water in order to detect enteroviruses (EVs), which are controlled pathogens in the Republic of Belarus when assessing water safety by virological indicators, and adenoviruses (HAdVs) as supposed indicative agents of viral contamination of drinking water. In this study, (n= 173) water samples (water sources, tap and bottled water) were collected and concentrated during 2016-2019. Occurrences of contaminant viruses in these samples were determined using real-time PCR assays, their concentration in the samples were also established.

According to the results of the molecular genetic analysis of water, the HAdV's DNA was found in 5.78 % of the analyzed samples, whereas no RNA of EVs was detected in them. HAdV genotype 2 and HAdV genotype 5 presented the typical composition of detected waterborne pathogens. Obtained data on the presence of adenoviruses in water samples in which enteroviruses were absent suggest the use of HAdV as a relevant candidate indicator organism of drinking water contamination to be more appropriate.

### Keywords

Human adenovirus; contamination; drinking water; virological control; polymerase chain reaction

## INTRODUCTION

Control of the epidemiological safety of drinking water supply, aimed at ensuring the access of the population to consistently high-quality water, is important as a matter of health and development at the national, regional and local levels. Thus, according to the World Health Organization, at least 2 billion people use a source of drinking water contaminated by feces. Experts estimate that poor-quality water annually causes 502.000 deaths from intestinal infections (WHO, 2019). This problem necessitates, on the one hand, the improvement of existing water purification and treatment systems for water sources, and on the other, the rational choice of representative indicator microorganisms of drinking water contaminated assessing its quality against infectious pathogens.

Microbiological water quality is usually assessed by determining the presence of bacterial indicators of fecal contamination such as *E.coli*. However, nowadays it is common knowledge that pathogenic intestinal human viruses can be detected in water with its normative quality according to bacteriological indicators, which often leads to waterborne outbreaks of various sizes (Bofill-Mas, 2013). The reason of viral occurrence is connected with their high resistance to disinfecting procedures, as well as their lower infectious dose compared to bacterial and protozoal pathogens. On this basis, there is flagrant necessity of using direct virological indicators in the study of water quality and the assessment of its epidemic safety.

In the Republic of Belarus, the monitoring of viral contamination of water is based on indication of EVs. EVs have a high epidemic significance due to their ability to cause waterborne outbreaks. From these positions, detection of these pathogens in water is extremely important during periods of epidemic rise of enterovirus morbidity (USEPA, 2016). At the same time, EVs like most other



intestinal viruses with water pathway of transmission (rota-, norovirus) demonstrate seasonality in their spread with marked ups and downs. During periods of reduced incidence of enteroviral agents they cannot reliably reflect the level of viral contamination of drinking water, since the intensity of their circulation at this time is rather low among the people. Given this circumstance, HAdVs can be considered as indicator objects of water analysis to detect its viral contamination as a result of fecal pollution (Bofill-Mas, 2013).

There are several advantages of using HAdV for this purpose over other intestinal viruses. They are extremely widespread in waterbodies (drinking, river and wastewater) are able to persist there for a long time, also they are highly resistant to chemical and physical factors, including prolonged UV water treatment (Jiang, 2006). HAdVs are characterized by a pronounced virus infection carrier state, which causes their widespread and ubiquitous distribution both at the level of the human population and in the external environment. Of particular interest is the fact that the circulation of adenoviral agents among the population has no pronounced seasonality. These advantages of HAdVs over EVs and other intestinal viruses suggest that the levels of waterbodies contamination are not associated with seasonal increases in the incidence of adenoviral infections, but represent fecal contamination of waterbodies and violations of water treatment and water use technology. Also due to the double-strained DNA quantitative determination of HAdVs is simpler to carry out since their detection does not require a reverse transcription stage (Ogorzaly, 2013).

Currently, 90 HAdV genotypes have been identified (HAWG, 2019). HAdVs have a tropism for the mucous epithelium of various organs and organ systems, which determines a wide range of clinical forms of infection, including gastroenteritis, acute respiratory diseases, conjunctivitis, hemorrhagic cystitis, myocarditis, damage to the nervous system, etc. (De Grazia, 2019). They are released into the environment with feces, urine and respiratory secretions with great intensity and the timing of their release from the respiratory apparatus and urinary tract is 25-50 days, with faeces is more than 50 days. It is estimated that more than 90 % of the human population are seropositive to one or more HAdV serotypes, which are released in high concentrations from infected patients (about 1000 viral particles per gram of feces) (Ogorzaly, 2013). All this makes it possible to attribute HAdV to reliable indicators of fecal contamination of various waterbodies (found in rivers, coastal waters of seas, swimming pool waters, water sources, etc.) (Jiang, 2006; Fong, 2010).

Detection of AdV is carried out using both cultural (Kamen and Henry, 2004) and molecular genetic methods (Ogorzaly, 2013). However, intestinal HAdVs species F (40, 41 genotypes), which cause infections of the gastrointestinal tract and most often excreted in faeces, are poorly cultured and rarely isolated in cell cultures (Kim et al., 2010). Therefore, the detection of non-cultivated HAdVs is performed using polymerase chain reaction in real-time (PCR-RT). In quantitative modification, it allows to assess the viral load in the sample not only qualitatively but also quantitatively while maintaining high sensitivity in a short time (several hours) (Ogorzaly, 2013).

The aim of this study was to conduct comparative studies on the detection and molecular identification of HAdVs and EVs in drinking water and water sources as part of the study based on the possibility of using these pathogens as indicators of viral contamination of waterbodies.

## **MATERIALS AND METHODS**

Samples of underground and surface water sources, drinking water (bottled and tap), n=173 were collected during 2016-2019. Concentration of viruses was conducted by using Kit for adsorption and concentration of viruses from drinking water using trap device (RRPCEM, Belarus). Viral nucleic acids extraction was carried out with RIBO-prep (AmpliSens, Russia). Detection of EV's

RNA was performed by using EV-PCR Kit (RRPCEM, Belarus). Detection of HAdV's DNA and quantity estimate were performed by using quantitative real-time polymerase chain reaction (PCR) with designed and evaluated set of primer and probe sequences for a conserved region of the hexon. Adjusted concentration dilutions of plasmid vector containing the target sequence for the primers were used as calibrators. Identification of HAdV species F among the number of positive samples was performed with All screen-FRT (AmpliSens, Russia).

Samples from water sources and drinking water (bottled and tap, n = 173) of one of the largest cities of the Republic of Belarus were collected and investigated during 2016-2019. The capture of viruses and their concentration were performed from 1000 liters of water using Kit for adsorption and concentration of viruses from drinking water using trap device (RRPCEM, Belarus) in accordance with the instructions for use. Viral nucleic acids extraction was carried out with RIBO-prep (AmpliSens, Russia).

Detection of EV's RNA was performed by using EV-PCR (RRPCEM, Belarus) with reverse transcription stage conducted with REVERT-L Kit (AmpliSense, Russia). Identification of HAdV species F among the number of positive samples was realized with All screen-FRT (AmpliSens, Russia).

The design of oligonucleotide primers and probes for identification HAdV's DNA in PCR-RT was carried out based on the analysis of the conserved region of hexon gene using the software Primer3 (v. 0. 4. 0) (Primer3, 2012), considering such parameters as degeneracy, T<sub>m</sub>, GC%, ΔG, GC clamp, the formation of dimers and hairpins. PCR-RT mixture contained the developed primers (Primetech, Republic of Belarus), deoxyribonucleoside triphosphates (dNTP), 200 μmol each, 3.5mM MgCl<sub>2</sub>, 1 unit of thermostable DNA polymerase (ArtBioTech, Republic of Belarus). Fluorescence levels were analyzed using the Rotor-Gene Q amplifier software (Qiagen, Germany). Adjusted concentration dilutions of the developed plasmid vector pJET1.2-adefib containing the target sequence for the primers were used as calibrators and positive control of the PCR-RT stage.

Amplification of a hexon gene fragment that contains hypervariable regions was performed in a reaction mixture containing 1 unit of Flash DNA polymerase (ArtBioTech), 200 μM solution of four dNTPs mixture, 20 pmol forward and reverse primers (IDT, USA). In the second stage, the reaction product of the first round of amplification was used as a template for the second round with primers for nested PCR. The results of PCR stage were monitored with agarose gel electrophoresis. Necessary fragments were cut out and purified from the gel using the kit for isolating DNA fragments from the agarose gel ArtDNA MiniSpin Gel (ArtBioTech).

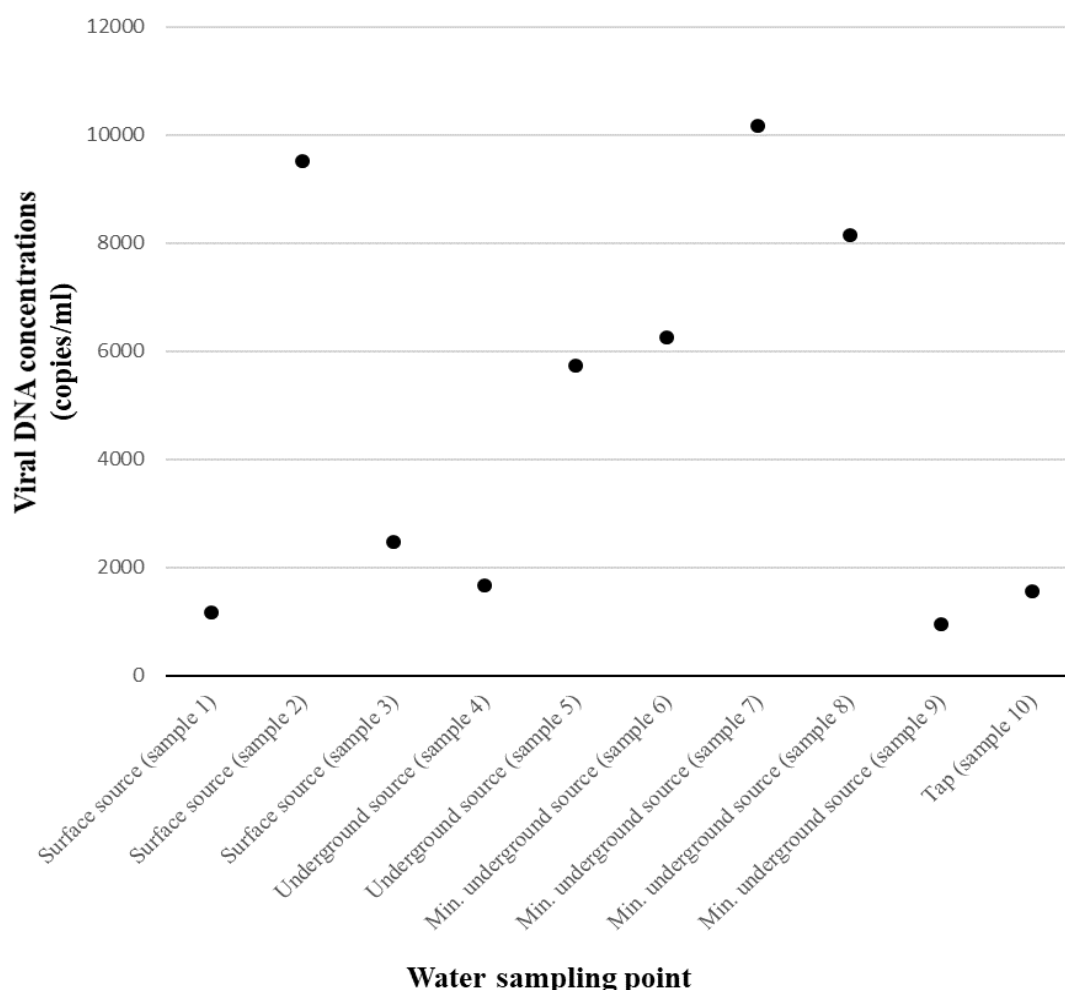
Cyclic sequencing reaction products obtained using the GenomeLab DTCS kit QuickStartKit (Beckman Coulter, USA) were analyzed using CEQ8000 (Beckman Coulter). The deduced nucleotide sequences were processed using MEGA7.0 software (Kumar et al., 2016).

## RESULTS

The algorithm of studies used to identify viral pathogens in drinking water and water sources included sampling and sample processing (preparation of eluates), indication of contaminant viruses and their molecular typing. As detected viruses in the analyzed water samples were HAdVs and EVs, the detection of which was carried out by PCR-RT.

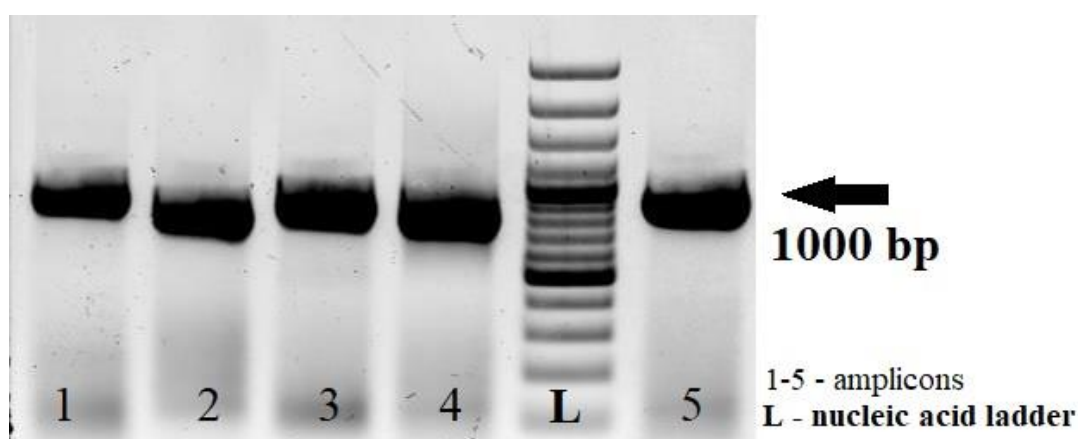
According to the results of the studies, HAdVs were detected in 10 (5.78 %) of the 173 water samples, while EVs were not identified in any of them. The analysis was done in two takes in three

independent assays accompanied by the presence of negative controls to be confident the false-positive results are absent. The concentration of viruses was established using the developed calibrators in known concentrations.



**Figure 1.** Average HAdV’s DNA concentrations in analysed samples of water

Genotype of five HAdV isolates detected in water samples were established. Fragments of the hexone gene containing hypervariable regions (880-910 bp) were accumulated using primers for nested PCR.



**Figure 1.** Products of hexon gene fragment amplification

At the next stage, sequencing of the amplified fragments was carried out in order to identify the HAdV's genotype.

**Table 1.** Results of presence and molecular typing of HAdV in source (n = 9) and tap (n=1) water samples

Water sampling point	Sampling date	HAdV's genotype
Surface source (before cleaning)	October 25, 2017	HAdV 2
Surface source (before cleaning)	January 29, 2018	not established*
Surface source (before cleaning)	April 15, 2019	not established*
Source underground	November 11, 2016	not established*
Source underground	November 11, 2016	HAdV 2
Mineral source underground	November 11, 2016	HAdV 2
Mineral source underground	November 11, 2016	HAdV 2
Mineral source underground	July 20, 2017	HAdV 5
Mineral source underground	July 20, 2017	not established*
Tap	April 19, 2017	not established*

\* - the genotype of the virus could not be established due to the low concentration of its genetic material in the sample and the inability to accumulate the necessary amount for performing a sequencing reaction

## CONCLUSIONS

The presented results indicate the frequency of drinking water and water sources contamination with HAdVs was 5.78 % while RNA of enteroviruses was not detected in water samples. The data obtained on the detection of HAdV in samples, in which EVs were absent, indicate the need for further, more extensive research in this field to substantiate the use of HAdVs as the supposed indicative agents of viral contamination of water. The indicator role of adenoviral pathogens is caused not only by their significantly increased frequency of detection in the water in comparison with EVs, but also by resistance to environmental factors, as well as the lack of seasonality in their prevalence among the human population. In addition, viral load quantitative estimation may allow calculating the health risks associated with water use.

## REFERENCES

- Bofill-Mas, S. (2013) Quantification of human and animal viruses to differentiate the origin of the fecal contamination present in environmental samples. *Biomed. Res. Int.*, **2013**, 9-11.
- De Grazia, S. (2019) Performance evaluation of gastrointestinal viral ELite panel multiplex RT-PCR assay for the diagnosis of rotavirus, adenovirus and astrovirus infection. *J. Virol. Methods*, **268**, 48-52.
- Fong, T. T. (2010) Quantitative detection of human adenoviruses in wastewater and combined sewer overflows influencing a Michigan river, *Appl. Environ. Microbiol.*, **76**(3), 715-723.
- HAWG (2019) Adenovirus research community. [online] <http://hadvwg.gmu.edu>.
- Jiang, S. C. (2006) Human adenoviruses in water: occurrence and health implications: a critical review. *Environ Sci Technol*, **40**(23), 7132-40.
- Kamen, A., Henry, O. (2004) Development and optimization of an adenovirus production process. *Appl. Environ. Microbiol.*, **6**(1), 184-192.

- Kim, M., Lim, M. Y., Ko, G. (2010) Enhancement of enteric adenovirus cultivation by viral transactivator proteins, *Appl. Environ. Microbiol.*, **76**(8), 2509-2516.
- Kumar, S., Stecher, G., Tamura, K. (2016) MEGA7: Molecular Evolutionary Genetics Analysis Version 7.0 for Bigger Datasets. *Mol. Biol. Evol.*, **33**(7), 1870-1874.
- Ogorzaly, L. (2013) Development of a quantitative immunocapture real-time PCR assay for detecting structurally intact adenoviral particles in water, *J. Virol. Methods*, **194**(1), 235-241.
- Primer3 (2012) [online] <http://bioinfo.ut.ee/primer3-0.4.0/>.
- USEPA (2016) Contaminant Candidate List (CCL) and Regulatory Determination. [online] <https://www.epa.gov/ccl/microbial-contaminants-ccl-4>.
- WHO (2019) Drinking water. [online] <https://www.who.int/ru/news-room/fact-sheets/detail/drinking-water>.

# Hydraulic Model Calibration and Performance Assessment of Pressure Managed Areas with Multiple Inlets

A. Bibok\*

\* Budapest Waterworks, 182 Váci Road, Budapest, Hungary (E-mails: [Attila.bibok@vizmuvek.hu](mailto:Attila.bibok@vizmuvek.hu); [Bibok.attila@epito.bme.hu](mailto:Bibok.attila@epito.bme.hu))

## Abstract

Pressure management is a widely adopted technique in the toolset of drinking water distribution system operators. It has multiple benefits, like reducing physical losses in pipe networks with excessive leakage, prolong the expected lifetime of the pipes and protecting home appliances from unacceptably high pressure. In some case, even legislation compliance can be the motivation behind pressure management: It is mandatory to supply water at the customer's connection between 1.5 and 6.0 bar in Hungary since 2011. Diaphragm pressure reducing valves are widespread in the drinking water distribution networks. Although, their sensitivity for gas pocket accumulation in the valve house makes hydraulic calibration of these pressure managed areas a challenging task for hydraulic modelers and network operators. This is especially true when more than one inlet is used to supply the same area in order to increase resilience and flow capacity. This paper investigates the hydraulic properties of pressure reduced areas with multiple inlet points. Model calibration using a single valve and minor loss was found insufficient, because the additional pressure loss referenced to the pressure setting has a non-quadratic relationship with flow-rate on the discharge side under real-life circumstances. This phenomenon can be handled by using a PRV (pressure reducing valve) + GPV (general purpose valve) in series.

## Keywords

Calibration; hydraulic modelling; pressure management; EPANET

## INTRODUCTION

There are 46 pressure reduced areas in the drinking water distribution system of Budapest Waterworks, which are supplied by 101 pressure reducing valves. Most of the pressure reduced areas have at least two inlets to keep the resilience of the system high and to provide continuous water supply even during maintenance and repair tasks.

Even with these measures, some zones had an increased number of consumer complaints about low service pressure. A well-metered pressure reduced area was investigated in order to find the cause of the increase in complaints.

There are six unknown variables in the aforementioned network layout. Three pressure setting values and three minor headloss coefficients, which assumes a quadratic relationship between headloss and flow-rate. The calibration runs using this conventional setup showed a trade-off between the downstream pressures (Bibok and Fülöp, 2018).

This paper investigates a different approach to accurately model the steady-state hydraulics of a multi-inlet pressure reduced zone. The evaluation and performance assessment of these diaphragm pressure reducing valves is essential to.

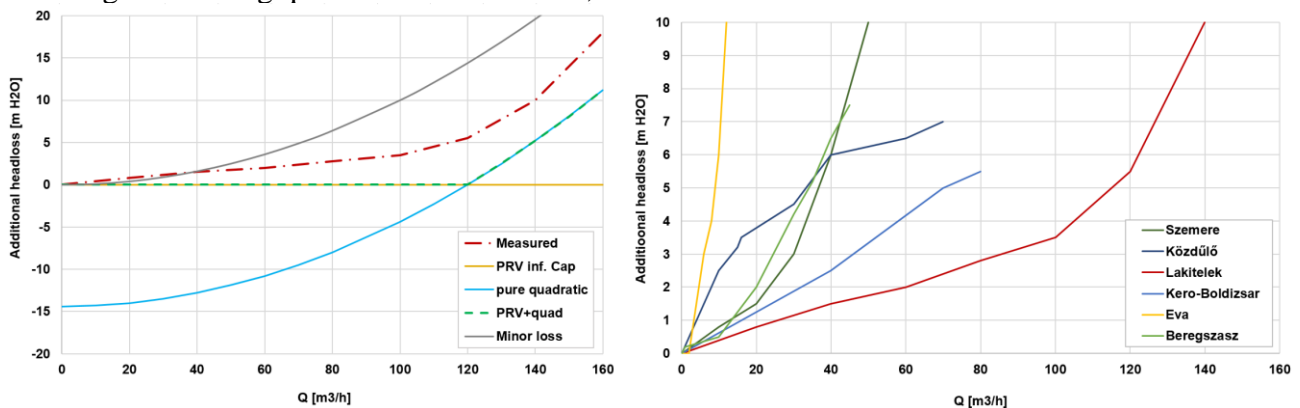


**Figure 1.** Network layout of the modelled multi-inlet pressure reduced zone

**MODEL SETUP**

A new model setup was proposed in which the minor loss coefficient was substituted by a GPV (general purpose valve). The advantage of this layout is that custom, non-quadratic headloss-flow-rate relationships can be introduced into the model. It is important to note that the GPV is not representing a real valve, but is used to introduce the PRV’s custom headloss-flow relationship into the model. This approach increases the dimensionality of the problem by the additional unknown variables. The more detailed the GPV curves, the more complex the model gets as the number of unknown variables increases.

As Figure 2 shows that it is not suitable to model the hydraulic behaviour of a diaphragm pressure reducing valve using quadratic loss functions, also known as minor losses.

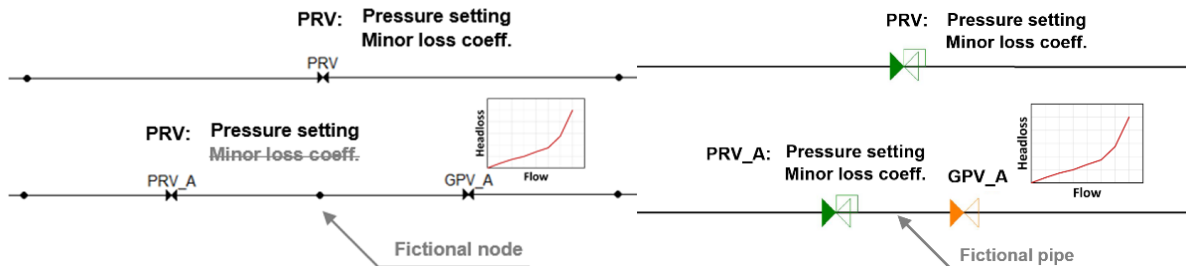


**Figure 2.** Different headloss curves against flow-rate (right) and the approximation methods (left)

**PRVs using EPANET**

The proposed model setup is not specific to a proprietary modeling software or framework. All the widespread commercial and open-source distribution network modeling tools are capable of

implementing the proposed PRV scheme. The main reason behind it is the EPANET compatibility because most of the commercial software was forked from EPANET at some point. Figure 3 indicates the difference between the original modeling approach (above) and the proposed setup (below).



**Figure 3.** Implementation of PRV+GPV layout in EPANET (left) and WaterGEMS (right)

### PRVs using Bentley’s WaterGEMS

Bentley Systems’ WaterGEMS (Bentley Systems, 2019) is a commercial, closed-source hydraulic modeling software, which is highly popular among drinking water hydraulics professionals. It is compatible with EPANET input files, but it handles nodes and link slightly differently on a topological level. Valves are considered as nodal objects in WaterGEMS, in contrary to EPANET in which they are links (Figure 3). Otherwise, their hydraulic behaviour is the same, so the proposed calibration methodology is also valid in the WaterGEMS environment.

## METHODOLOGY

### Calibration

During the hydraulic model calibration the following assumptions were made:

- All the demands are met, hence DDA(demand driven analysis) is valid
- Constant nodal demand weights are used based on the billed consumption
- Physical losses are distributed in the network proportional to the billed consumption since the minimum night flow is considered low

The following measurements were available for the pressure reducing valves:

- Flow rate before the pressure reducing valve
- Pressure on the PRV’s downstream pipe
- Pressure on the PRV’s upstream pipe

The timeframe of the available time-series started at 2017.06.01 and it was 10 days long. The resolution of the regular time-series was 30 minutes. The flow-rate and pressure values were time-weighted averages calculated from irregular samplings. The time-series was divided into calibration and validation parts. The first 5 days out of 10 were used to calibrate the models. The last day was utilized to validate the calibrated model. These days were sequential, hence the day of the week was not stationary. The water demand patterns might change due to this aforementioned condition, but the headloss curves of the PRV’s do not depend on the actual water demand. It was assumed, that the demand weights used to distribute the zonal demand was constant during the simulating, because the demand weights calculated from the annual or monthly billed consumption were considered stationary in time.

The number of free variables can be calculated from the number of inlet valves and the resolution of the GPV headloss-curves:

$$D = n_{PRV} + \sum_{i=1}^{n_{PRV}} n_{segment,i} \tag{1}$$



where:  $D$ : number of variables in the optimization problem,  $nPRV$ : number of PRV's to calibrate,  $nsegment,i$ : the number of curve segments of the  $i$ 'th PRV.

A custom performance function was written in python utilizing scikit-learn package (Pedregosa et al., 2011) and epanettools. Epanettools is based on EPANET version 2.0, which lacks functions to alter curves in memory – version 2.2 is going to include these functions, which is not yet finalized and released. A custom .INP altering method was implemented in python to overcome this limitation, although it requires the reloading of the .INP file before every iteration.

The three different unconstrained optimization methods were chosen to solve this multidimensional optimization problem. Constrained optimization methods were excluded from the research to have a more general result on optimization performance, not limited by the constraints.

*Powell*: Powell's method (Powell, 1964; Teukolsky, 1986) doesn't require the loss function to be differentiable nor any derivatives are taken. It generates a sequence of points along each base vectors. It is a robust, but generally inefficient due to the geometry of multivariate functions (Mathews and Fink, 2004).

*Nelder-Mead simplex method*: The Nelder-Mead is a simplex method (Nelder and Mead, 1965), (Gao and Han, 2012) also known as downhill simplex method. A simplex consists of  $N+1$  vertices in an  $N$  dimensional search space. The hyperparameters can be adjusted in order to provide better performance in case of high-dimensional problems (Gao and Han, 2012). It is a widely-adopted optimization method, also present in MatLab.

*BFGS*: BFGS is an implementation of the quasi-Newton method by Broyden, Fletcher, Goldfarb, and Shanno (Nocedal and Wright, 2006). Quasi-Newton-type methods might not converge in case of non-smooth optimization, although BFGS was found to have acceptable performance even in these cases (Bonnans et al., 2006). BFGS is also widely-adopted in cases of unconstrained optimization and cases of nonlinear systems of equations.

### **Operational performance assessment of a pressure-reduced zone**

Hydraulic modeling usually assumes ideal conditions, although these conditions are rarely met in real-life operation. There are several measures to analyze in order to get more detailed insight into the operation of a pressure reduced area:

- Pressure management index (Trow, 2009)
- Infrastructure Leakage Index (ILI)
- Inlet supply ratio – in case of multiple inlets
- Inlet valve performance

PMI is more useful during the design and commissioning phase of a pressure management task, but the latter two are more suitable to assess actual operational performance and detect anomalies in operation. The maintenance requirements of mechanically operated pressure reducing valves vary by manufacturer and model.

*Pressure management index (PMI)*: The Pressure Management Index (PMI) is a performance indicator introduced by Trow (Trow, 2009). It is usually used along with the Infrastructure Leakage Index (ILI). Both of these indicators' optimal value is 1.0, which makes visualization and evaluation easier in a multi-objective optimization. Furthermore, their product is considered the Global Leakage Index (GLI) proposed by E. Renaud (Renaud, 2010). It gives a general overview on the performance of pressure management. Although, it gives no information about the remaining pressure reduction headroom in the system.

*Inlet Supply Ratio:* The operation of the pressure reduced zones with multiple inlets can be characterized by the ratio of inlet flow-rates. The actual ratio depends on multiple factors, like:

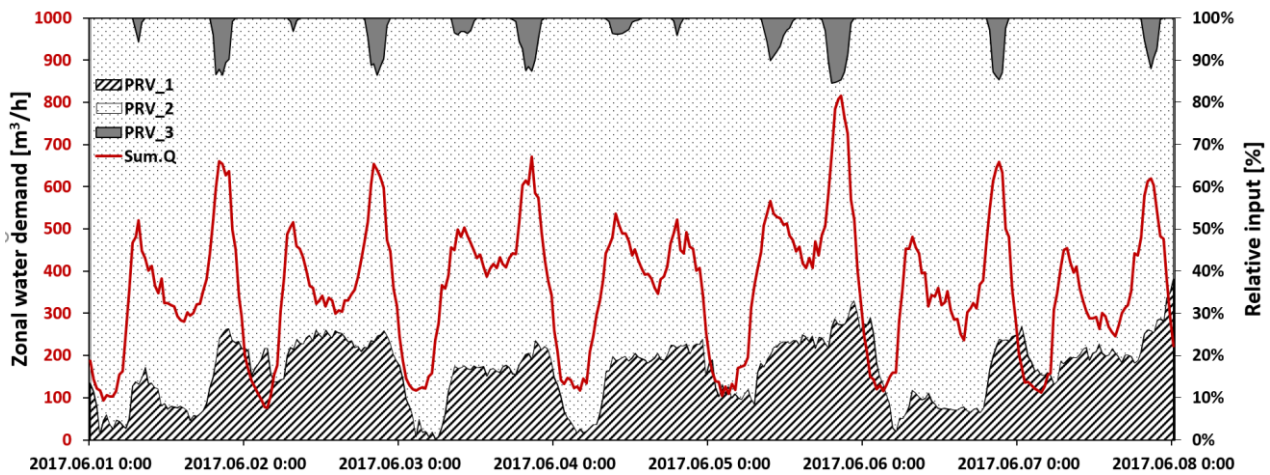
- Headloss curves of the valves
- Pressure setting of the valves
- Demand distribution in time
- Demand distribution along the network
- Total water demand of the area

The ratio of flow-rates can be calculated by the following equation for each time-step:

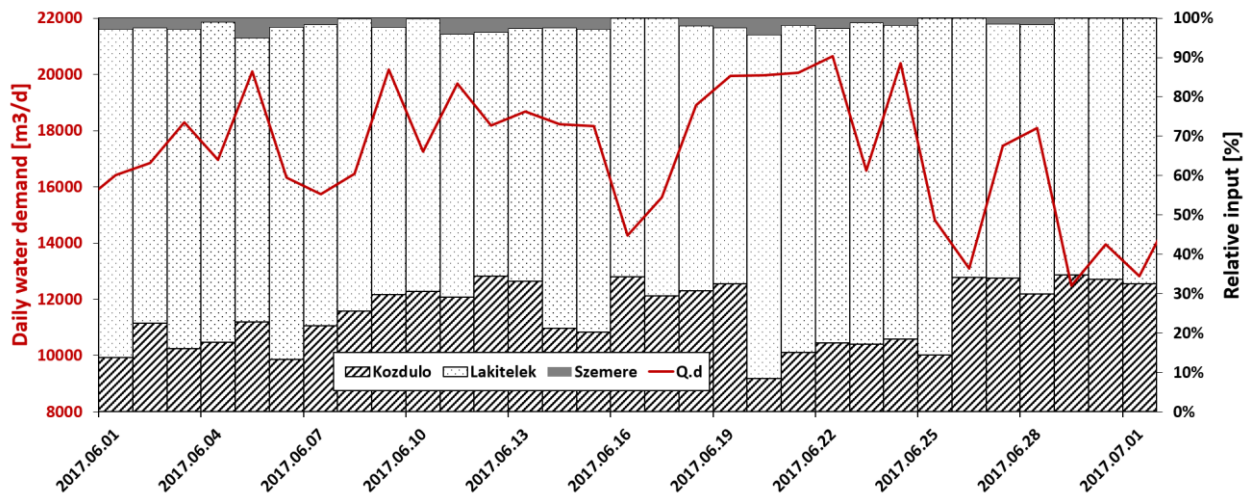
$$Q_{rel,i,j} = \frac{Q_{i,j}}{\sum_i Q_{i,j}}, \quad (2)$$

where:  $Q_{rel,i,j}$  is the unitless supply ratio of valve 'I' in timestep 'j'  $Q_{i,j}$ : actual flow-rate at valve 'I' in time 'j'.

As Figure 4 indicates, the ratio of inlet flow-rates varies by time during the day as water demand changes. The resolution of the graph was the same as the default time-step of the simulation: 30 minutes.



**Figure 4.** Inlet Supply Ratio with a resolution of 30min. The ISR change during the day as a function of water demand



**Figure 5.** Inlet Supply Ratio daily time-series against the daily water demand. Changes in daily Inlet Supply Ratio indicates events, which alter the spatial or temporal distribution of demand in the zone

The change in the daily supply ratio can indicate various events in the network:

- Movement of the demand's point of gravity due to:
  - Burst
  - Seasonal trends
- Change in the performance of a valve due to:
  - Air accumulation
  - Malfunction

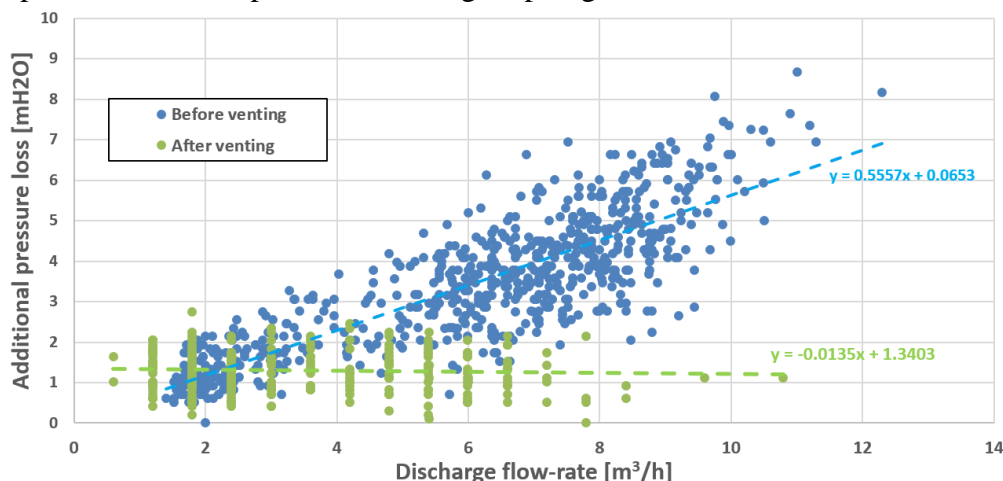
These events can be detected by time-series analysis. ARMA models are suitable to detect level-shift anomalies in time series like the aforementioned

### Valve performance evaluation

The operation performance of pressure reducing valves can be described by the flow rate at which the downstream pressure head starts to drop below the pressure setting. This flow rate would be equal to the theoretical capacity of the valve in an ideal situation. The theoretical capacity is usually characterized by the Kv (or Kc in imperial units) value of the fully open valve. It is possible to calculate the relative opening of the valve if the valve closure curve is available. Valves have different closing characteristics depending on the shape of the orifice. If the operating points of the valve is plotted against the theoretical headloss curve, the difference between the actual and the theoretical operation can be visualized. The evaluation of the operating points can be enumerated by fitting a linear function on them. The first-order coefficient is a good indicator of operational performance. If the coefficient is near 0, that means the valve performance is good on the observed flow-rate domain. If the coefficient's value is positive, that indicates additional pressure loss compared to the pressure setting.

*Effect of gas accumulation:* Water distribution networks are generally treated as a one-phase, fully pressurized system. Although, air can get into the distribution network at specific events, like main burst, repairs or at negative pressures. Furthermore, soluted gases can dissolve if pressure drops at higher elevation.

These small air pockets usually exit the distribution network through the consumers' taps, hydrants or ventilation air valves at high points. The PRV's characteristic headloss curve can change, if these traveling air pockets reach the pressure reducing diaphragm valve.



**Figure 6.** Effect of gas accumulation in a pressure reducing valve on its capacity

As Figure 1 indicates, releasing accumulated gas pockets from the pressure reducing diaphragm valve is essential for a stable and reliable operation. Releasing trapped air is possible manually by opening a valve, or by automatic air-valve. If the change in headloss curve is detected, a maintenance checkup can be assigned to the valve preventing the valve's subpar performance at peak demands.

## RESULTS AND DISCUSSION

### Calibration results

According to Table 1 it is clear that using a simple quadratic headloss, there is trade-off between the downstream pressure heads. The use of segmented quadratic headlosses provided better results, but it is still far from the target calibration accuracy. It is possible to achieve good fit on the measured values using the combined PRV+GPV approach. Unitless error measures were used to evaluate the calibration performance because both pressure and flow-rate measurements were utilized during the calibration and validation as the average of Normalized Root Mean Squared Error (NRMSE) of measurements. The average NRMSE was 13 to 18 % regardless of the chosen optimization method. Although, just like every machine learning method, it tends to overfit if the iteration numbers are excessive. This phenomenon should be handled in future simulation runs. The GPV headloss curves can be directly calculated from the measured discharge pressures by fitting a multi-point curve on it. If all the necessary measurements are available, the utilization of meta-heuristic optimization methods can be omitted. If one of the downstream pressure measurements is missing, the unknown headloss curve can be calibrated using the aforementioned optimization methods.

### Valve performance results

Real-world operational data at Budapest Waterworks showed that pressure drop usually occurred even at 10 % of the theoretical flow rate capacity – regardless of the manufacturer of the valve. This value is considered extremely low indicating that the manufacturer provided Kv coefficients are assuming ideal conditions, which are clearly not met in practice. Pressure managed areas with multiple inlets requires special care during design, commissioning and operation. Commissioning is possible with temporary pressure and flow-rate measurements, but the support of operation and maintenance can only be achieved by installed meters integrated into the SCADA system. The lack of instrumentation makes harder to set the valves to their target pressure settings, which was determined during the design phase. If additional pressure loss occurs during normal operation and water demand, the synchronization of the valves is exceptionally challenging, especially if the valves lack pressure or flow measurements.

If the inlet valve lacks pressure measurement upstream it prohibits the calculation of  $dP$ , hence there the risk of cavitation cannot be assessed. The Table 1 summarizes, which tasks can be achieved at certain instrumentation levels.

**Table 1.** The instrumentation needs of different tasks related to pressure reducing valves and multi-inlet pressure reduced zones

Available measurements	Alternating	Cavitation	Performance	Offset detection	Capacity assessment
Q	X				
P1+Q	X				
P1+P2		X			
Q+P2	X		X	X	
Q+P1+P2	X	X	X	X	X
Q+P1+P2+h	X	X	X	X	X

The headloss-curve of the PRVs is an important indicator of valve operational performance and actual capacity. Sub-par performance can be detected by evaluating these curves, hence it is

possible to correct it by maintenance, even before customer complaints would directly indicate the need of maintenance. The curve evaluation was performed manually, but automated anomaly detection performed on these measured headloss curves holds great potential. It has to be noted that the hydraulic simulations were conducted assuming steady-state conditions. This boundary condition prevents us from implementing hysteresis curves during steady-state hydraulics simulations, which affects the operating point of the valve (Talamini et al., 2018).

## CONCLUSIONS

Hydraulic model calibration of multi-inlet pressure reduced zones can be performed accurately by using a PRV+GPV combination of objects using EPANET-related software. The GPV object is used to simulate the non-linear and non-quadratic relationship between flow-rate and additional headloss compared to the pressure setting of the PRV. The daily Inlet Supply Ratio of a pressure reduced zone with multiple inlets is a good indicator of stationarity regarding the spatial and temporal distribution of water demand in the distribution network. Any disturbance in this ratio indicates an event, which alters these distributions and should be investigated. The actual flow-rate capacity of the valves seems one order lower than what the technical specifications indicated regardless of manufacturer. The gas accumulation and the lack of automated air valves can decrease the flow-rate capacity and stability of these pressure reducing valves in real-life conditions.

## REFERENCES

- Bentley Systems (2019) "WaterGEMS User's Guide", Bentley Systems, Inc., Exton, PA.
- Bibok, A., Fülöp, R. (2018) Hydraulic Model Calibration of Pressure Reduced Zones with Multiple Input Valves, HIC 2018. Proceedings of the 13th International Conference on Hydroinformatics, **3**, 274-281.
- Bonnans, J. F., Gilbert, J. C., Lemaréchal, C., Sagastizábal, C. A. (2006) "Newtonian Methods". *Numerical Optimization: Theoretical and Practical Aspects* (Second ed.), Berlin: Springer, 51-66. ISBN 3-540-35445-X.
- Gao, F., Han, L. (2012) Implementing the Nelder-Mead simplex algorithm with adaptive parameters. *Computational Optimization and Applications*, **51**(1), 259-277.
- Mathews, J. H., Fink, K. K. (2004) Numerical Methods Using Matlab, 4th Edition. ISBN: 0-13-065248-2.
- Nelder, J A, Mead, R. (1965) A Simplex Method for Function Minimization. *The Computer Journal*, **7**, 308-13.
- Nocedal, J., Wright, S. J. (2006) Numerical Optimization, Springer, New York.
- Pedregosa et al. (2011) Scikit-learn: Machine Learning in Python. *JMLR*, **12**, 2825-2830.
- Powell, M J D. (1964) An efficient method for finding the minimum of a function of several variables without calculating derivatives. *The Computer Journal*, **7**, 155-162.
- Renaud, E. (2010) Towards a global performance indicator for losses from water supply systems. Proceedings of Water Loss 2010 Conference, Jun 2010, Sao Paulo, Brazil, 11.
- Talamini Junior, M. V., de Araujo, A. C. S., de Camargo, A. P., Saretta, E., Frizzone, J. A. (2018) Operational Characterization of Pressure Regulating Valves. *The Scientific World Journal*, Article ID 1213638, 9 pages. DOI: <https://doi.org/10.1155/2018/1213638>.
- Teukolsky, S. A., Press, W., Vetterling, W. T., Flannery, B. P. (1986) Numerical Recipes (any edition), Cambridge University Press.
- Trow, S. W. (2009) Development of a Pressure Management Index. Proceedings of IWA Water Loss 2009 Conference.
- Wright, M. H. (1996) Direct search methods: Once scorned, now respectable, in Numerical Analysis 1995. Proceedings of the 1995 Dundee Biennial Conference in Numerical Analysis (Eds. D F Griffiths and G A Watson), Addison Wesley Longman, Harlow, UK, 191-208.

## Determination of Optimum Operational Conditions for the Removal of 2-MIB from Drinking Water by Peroxone Process: A Pilot Scale Study

M. Fakioglu\*, H. Gulhan\*, H. Ozgun\*, M. E. Ersahin\* and I. Ozturk\*

\* Department of Environmental Engineering, Istanbul Technical University, Maslak, 34469, Istanbul, Turkey  
(E-mails: [fakioglu@itu.edu.tr](mailto:fakioglu@itu.edu.tr); [gulhan@itu.edu.tr](mailto:gulhan@itu.edu.tr); [ozgunha@itu.edu.tr](mailto:ozgunha@itu.edu.tr); [ersahin@itu.edu.tr](mailto:ersahin@itu.edu.tr); [ozturkiz@itu.edu.tr](mailto:ozturkiz@itu.edu.tr))

### Abstract

Taste and odor in drinking water are one of the main problems of water supply and treatment sector. Peroxone is an effective advanced oxidation process, which combines ozone with hydrogen peroxide to create hydroxyl radicals that decompose organic compounds. 2-methylisoborneol (2-MIB) is one of the significant taste and odor causing compounds, which can be removed with peroxone process. In this study, removal of 2-MIB compound by peroxone process was investigated in a pilot scale treatment plant and optimum operational conditions were determined. For safety reasons, it is important that residual  $O_3$  and  $H_2O_2$  concentrations in the water leaving the reactor should not exceed to 0.1 and 0.5 mg/L, respectively. Results indicate that while dissolved ozone concentration was below the indicated limit for all experiments, concentrations over 0.5 mg/L residual  $H_2O_2$  was observed during the experiments with a  $H_2O_2:O_3$  ratio of 0.5. This limit exceedance affected the decision of the ideal peroxone ratio along with the 2-MIB removal results. Therefore; optimum  $H_2O_2:O_3$  ratio was determined as 0.3. 2-MIB removal efficiency of 81 % was achieved at the optimum  $H_2O_2:O_3$  ratio with a contact time of 15 min. According to the results, 2-MIB removal rate had a linear correlation with the contact time.

### Keywords

Drinking water treatment; taste and odor; 2-MIB; geosmin; pilot plant

## INTRODUCTION

Taste and odor in drinking water affect the perception of customers. Two of the most common taste and odor compounds, 2-methylisoborneol (2-MIB) and geosmin, are detectable even at concentrations below 10 ng/L (Fakioglu, 2017). Water authorities do not only search for the cause of taste and odor problem, but also try to find an effective process that can be integrated to existing water treatment plants.

Previous studies have shown that conventional water treatment processes such as coagulation, flocculation, sedimentation and chlorination were ineffective for the removal of taste and odor compounds. However; processes including powdered activated carbon, ozonation, and biofiltration have been found successful for the removal of these compounds (Cook, 2001; Hsieh, 2010; Wang, 2014; Ho, 2009; Srinivasan, 2010).

Removal of taste and odor compounds by peroxone process, that is a combination of ozone ( $O_3$ ) and hydrogen peroxide ( $H_2O_2$ ) was proven to be effective by several studies (Fakioglu, 2017; Srinivasan, 2010). These studies have shown that removal of 2-MIB and geosmin compounds were quite higher with peroxone process in comparison to sole  $O_3$  application at the same  $O_3$  dosage. Determining an ideal peroxone ratio ( $H_2O_2:O_3$  by mole) was the main objective of these studies.

In this study, optimum operational conditions such as peroxone ratio and contact time were determined for removal of 2-MIB at a pilot-scale peroxone system. Water samples used in all experiments were taken from one of the main drinking water sources of a mega city. Other important parameters such as geosmin, total organic carbon and bromate were also determined along with the 2-MIB. During the experimental study, residual (dissolved) O<sub>3</sub> and residual H<sub>2</sub>O<sub>2</sub> were monitored in order to investigate whether the applied chemical dosages were reasonable or not.

## MATERIAL&METHODS

### Characteristics of raw water and reagents

Raw water was obtained from the outlet of an aeration unit in a full-scale drinking water treatment plant. Characterization of the raw water is provided in Table 1. 2-MIB and geosmin concentrations were lower than 10 ng/L during the sampling period, which is known as the limit concentrations to be perceived. Therefore, 2-MIB was spiked into the water samples to obtain a concentration of 90 ng/L. Chromatographic grade 2-MIB standard (Supelco, USA) (10 mg/ml) was used for maintaining the required concentration of 2-MIB in the water samples. Since 2-MIB is more difficult to be removed with O<sub>3</sub> in comparison to geosmin, operational conditions for 2-MIB removal were investigated to set the process design requirements. All reagents and solvents for H<sub>2</sub>O<sub>2</sub> analysis were at least of analytical grade. All solutions were prepared with deionized water.

**Table 1.** Raw water quality

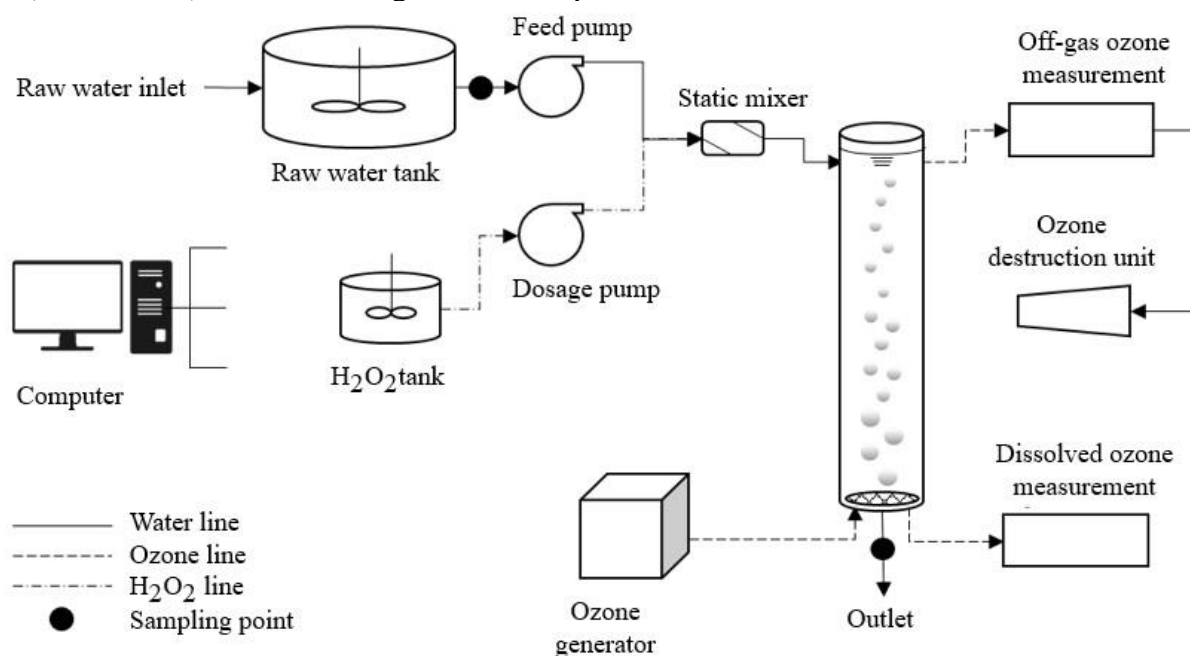
Parameter	Unit	Value
Chlorine	(mg/L)	20.4
Color	(Pt-Co)	8.0
Conductivity (25 °C)	(µS/cm)	320
pH	-	7.71
Iron	(mg/L)	0.213
Manganese	(mg/L)	0.058
Sulfate	(mg/L)	19.9
Sodium	(mg/L)	16.87
Potassium	(mg/L)	3.11
Total Organic Carbon (TOC)	(mg/L)	2.7
Turbidity	(NTU)	3.6
UV <sub>254</sub>	(cm <sup>1</sup> )	0.07
2-MIB	(ng/L)	<0.5
Geosmin	(ng/L)	0.28
Bromide	(mg/L)	0.01
Total Dissolved Solids (TDS)	(mg/L)	192
Total Hardness	(mg CaCO <sub>3</sub> /L)	144
Total Alkalinity	(mg CaCO <sub>3</sub> /L)	116.4

### Pilot plant set-up

Pilot plant consisted of a raw water storage tank, reactor column (ozone contact column, with 2.4 m diameter and 5 m height), hydrogen peroxide (H<sub>2</sub>O<sub>2</sub>) dosing system and ozone generator along with the required pipes and measuring equipments (Figure 1). Raw water storage tank, which was fed with water from the aeration unit outlet of a full-scale water treatment plant, was made of polyethylene (PE) (with 2.8 m diameter, 2.4 m height and 15 m<sup>3</sup> total volume) and contained low speed mixer (1.5 kW, 6-8 rev/min) along with an ultrasonic water level sensor (Sick AG, Germany). Ozone contact reactor was made of plexiglass (with 0.24 m diameter, 5 m height and 0.226 m<sup>3</sup>

volume). Raw water was fed with a centrifuge feed pump (Ebara, Japan) to the reactor. The ozonation reactor contained an ultrasonic water level measuring device (Keller, Switzerland), a gas phase ozone measuring device (2B Technologies Model 106-M, USA), a dissolved ozone measuring device (Chemitec 42 Series, China), a thermometer (Chemitec 42 Series, China) and a pH meter (Chemitec 42 Series, China). Ozone was produced by the ozone generator (BNP, China) which was fed with an air compressor. Ozone was then transferred to the reactor by a ceramic diffuser (with 0.185 m diameter). H<sub>2</sub>O<sub>2</sub> solution was dosed by a solenoid dosage pump (Sisdoz, Turkey) to a pipe equipped with a static mixer (Polyvinylchloride, PVC), which delivered water to the reactor.

Gas phase ozone at the inlet and at the outlet of the reactor was measured with ozone measurement devices (2B Technologies, USA). Surplus (off-gas) ozone was destroyed by an ozone destruction unit (BNP, China) before reaching to the atmosphere.



**Figure 1.** Layout of the pilot-scale set-up

### Experimental plan

*Relation between ozone consumption and reactor height.* Before starting the experiments to determine the ideal peroxone ratio and contact time experiments, ozone consumption versus reactor height was investigated through running the system in batch mode. Experiments were performed with different reactor heights (1 m, 2 m, 3 m, 4 m and 4.5 m) while initial ozone concentration and contact time were set to 4 mg O<sub>3</sub>/L and 10 minutes, respectively. Ozone consumption was calculated by using the inlet and the off-gas ozone concentrations. All experiments were conducted in duplicate and average values were used when presenting the results.

*Determination of ideal peroxone ratio and contact time.* Different H<sub>2</sub>O<sub>2</sub>:O<sub>3</sub> ratios were tested in order to find the ideal ratio for the removal of 2-MIB (Table 2). Inlet O<sub>3</sub> dose was set to 4 mg/L and the reactor was continuously fed with 2-MIB spiked water. Average water temperature in the pilot plant was recorded as around 16 °C. After the determination of the optimum H<sub>2</sub>O<sub>2</sub>:O<sub>3</sub> ratio, reactor was operated at different contact times including 5, 10 and 15 min (Table 2). TOC and geosmin removal efficiencies were also determined throughout the experimental study. Additionally, variations in residual H<sub>2</sub>O<sub>2</sub> concentration were measured during each experiment.



**Table 2.** Experimental plan applied to determine the optimum H<sub>2</sub>O<sub>2</sub>:O<sub>3</sub> ratio and contact time

(a) Determination of optimum H <sub>2</sub> O <sub>2</sub> :O <sub>3</sub> ratio			(b) Determination of optimum contact time		
H <sub>2</sub> O <sub>2</sub> :O <sub>3</sub>	Inlet O <sub>3</sub> concentration	Contact time	Contact time	Inlet O <sub>3</sub> concentration	H <sub>2</sub> O <sub>2</sub> :O <sub>3</sub>
0					
0.1			5 min		
0.3	4 mg/L	10 min	10 min	4 mg/L	Selected H <sub>2</sub> O <sub>2</sub> :O <sub>3</sub> ratio
0.5			15 min		

### Analytical and instrumental procedures

Residual H<sub>2</sub>O<sub>2</sub> concentration in the liquid phase was analysed following the iodide/molybdate method (HP-02) (Klassen, 1994). Concentrations of 2-MIB and geosmin were measured by a gas chromatograph (Agilent Technologies 7890B, USA) using Method 8270D (USEPA, 1998). TOC analysis was conducted by a TOC analyzer (Shimadzu TOC-L Series, Japan). Bromate analysis was conducted by following the Method 300.1 (USEPA, 1999).

## RESULTS AND DISCUSSIONS

### Relation between ozone consumption and reactor height

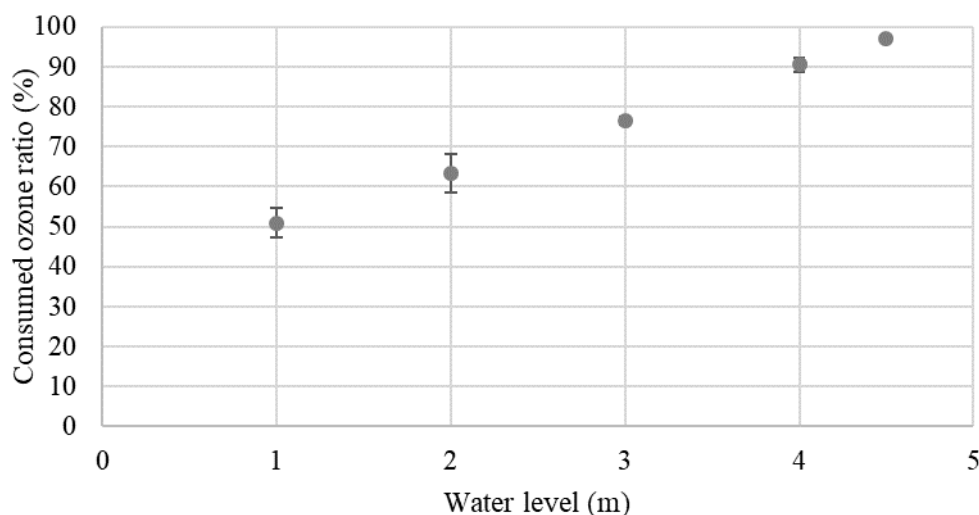
Results obtained from the experiments conducted in pilot treatment plant are given in Table 3 and Figure 1. Ozone consumption ratio was found as 51 % at 1 m reactor height and 97 % at 4.5 m reactor height by applying 4 mg/L inlet ozone concentration. In order to reach ozone consumption ratio above 75 %, at least 3 m reactor height was required.

Along with the ozone consumption ratio, TOC removal was investigated during study. As seen in Table 3, TOC removal was lower than 6% for all operating conditions. Based on the results obtained from this study, ozone cannot remove TOC effectively alone. However, ozone is proven to increase the colloidal destabilization which dramatically increases the removal efficiencies of organic compounds by coagulation, flocculation and filtration units in water treatment plants (Yuksel, 2002).

Results indicated that consumed ozone increased with increasing reactor height. With increasing heights, ozone contact time can be extended since water will stay longer in the reactor. Therefore, ozone fed at the bottom of the reactor could have more time to react with the compounds in the water and could be consumed in higher ratios.

**Table 3.** Ozone consumption and TOC removal at different reactor heights

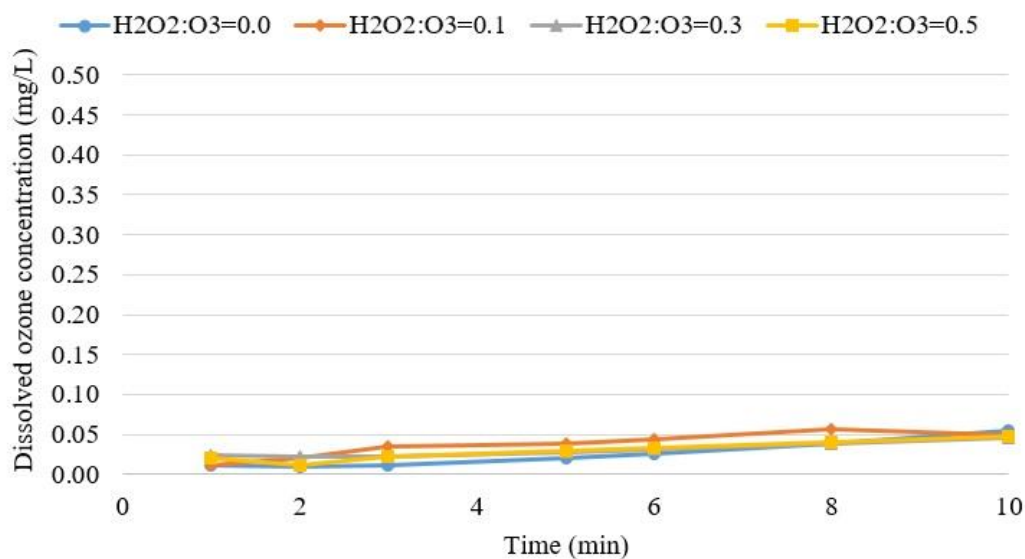
Inlet ozone concentration (mg/m <sup>3</sup> )	4000				
Reactor height (m)	1	2	3	4	4.5
Inlet ozone concentration (mg/m <sup>3</sup> )	4031	4072	4057	3968	3984
Off-gas ozone concentration (mg/m <sup>3</sup> )	1976	1492	953	378	114
Ozone consumption (mg/m <sup>3</sup> )	2055	2580	3104	3590	3870
Ozone consumption ratio (%)	51	63	77	90	97
TOC removal (%)	0	4	5	2	2



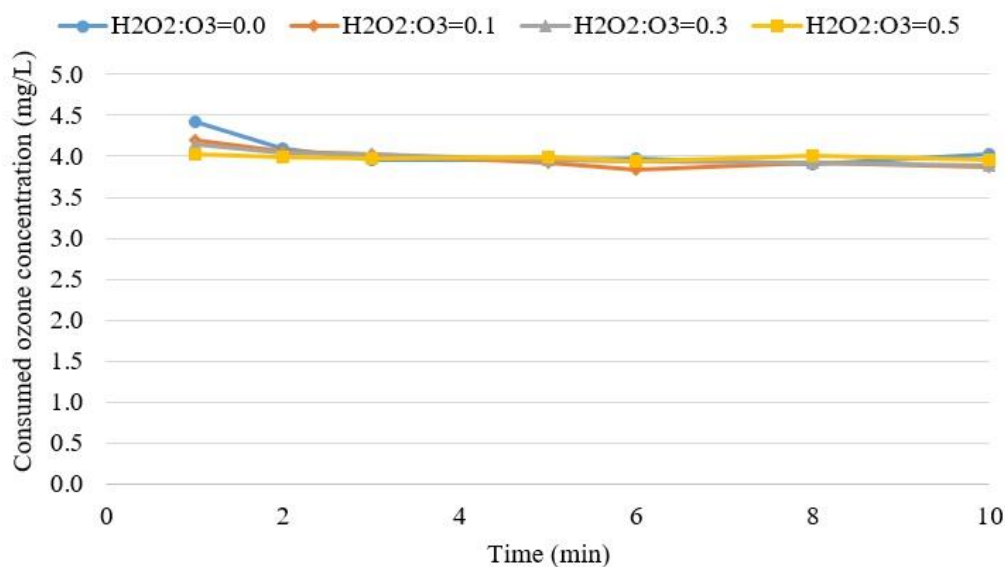
**Figure 1.** Consumed ozone ratio depending on reactor height

### Determination of ideal peroxone ratio and contact time

*Variations in dissolved  $O_3$  and residual  $H_2O_2$  concentrations.* Dissolved and consumed  $O_3$  concentrations were measured for each  $H_2O_2:O_3$  ratio at a contact time of 10 minutes (Figure 3 and Figure 4). It is essential that the residual  $O_3$  concentration in the water leaving the reactor should not exceed 0.1 mg/L for safety reasons (WQTS, 2009). Considering Figure 3, dissolved (residual)  $O_3$  concentration was around 0.05 mg/L, below 0.1 mg/L for each  $H_2O_2:O_3$  ratio while consumed  $O_3$  concentration was around 4 mg/L.

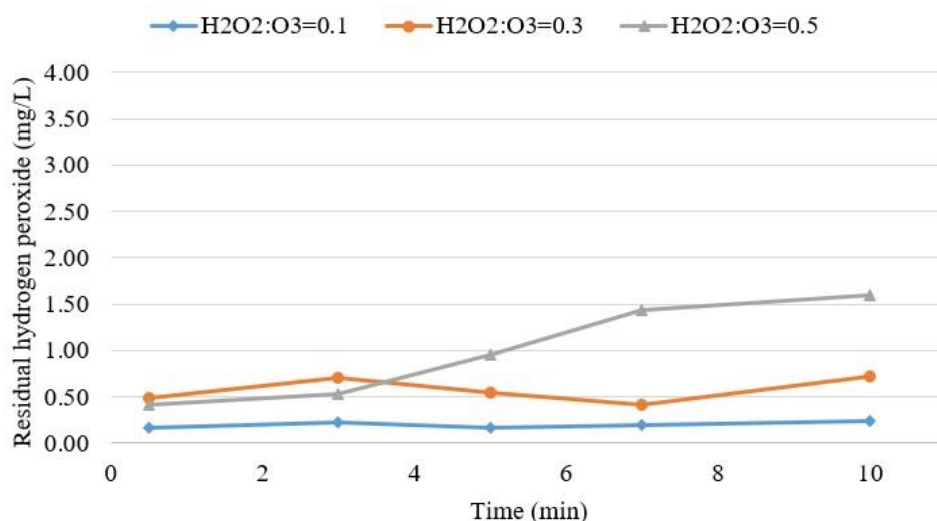


**Figure 3.** Dissolved  $O_3$  concentrations for various peroxone ratios



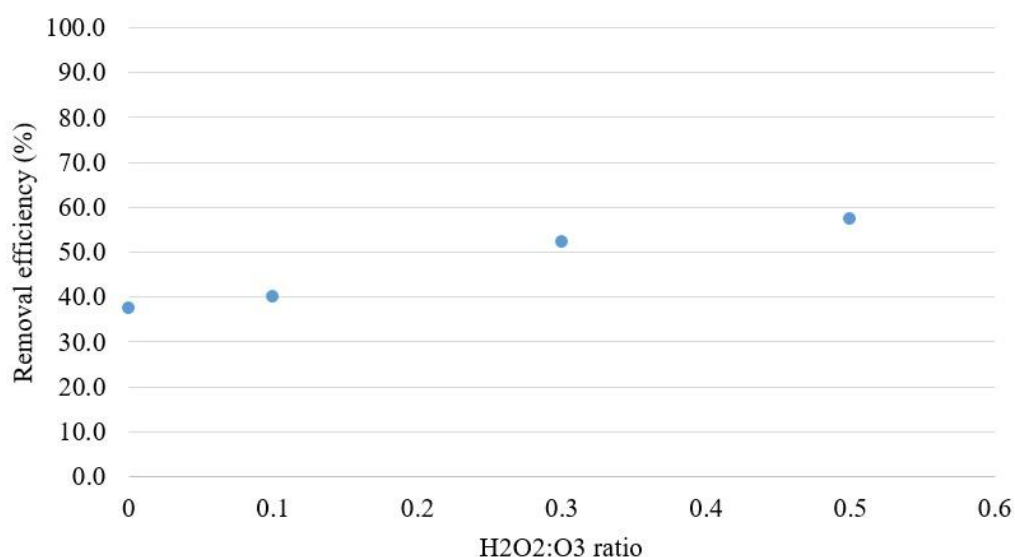
**Figure 4.** Consumed O<sub>3</sub> concentrations at various peroxone ratios

Residual H<sub>2</sub>O<sub>2</sub> concentration in the peroxone process was recommended not to exceed 0.5 mg/L (Oturán, 2014) since higher concentrations might cause operational problems such as residual chlorine consumption in the water treatment plants. Figure 5 shows that limit residual H<sub>2</sub>O<sub>2</sub> was not exceeded during the experiments at a contact time of 10 min and H<sub>2</sub>O<sub>2</sub>:O<sub>3</sub> ratios of 0.1 and 0.3. However, residual H<sub>2</sub>O<sub>2</sub> concentration of over 0.5 mg/L was observed even at the 4<sup>th</sup> min at a H<sub>2</sub>O<sub>2</sub>:O<sub>3</sub> ratio of 0.5.



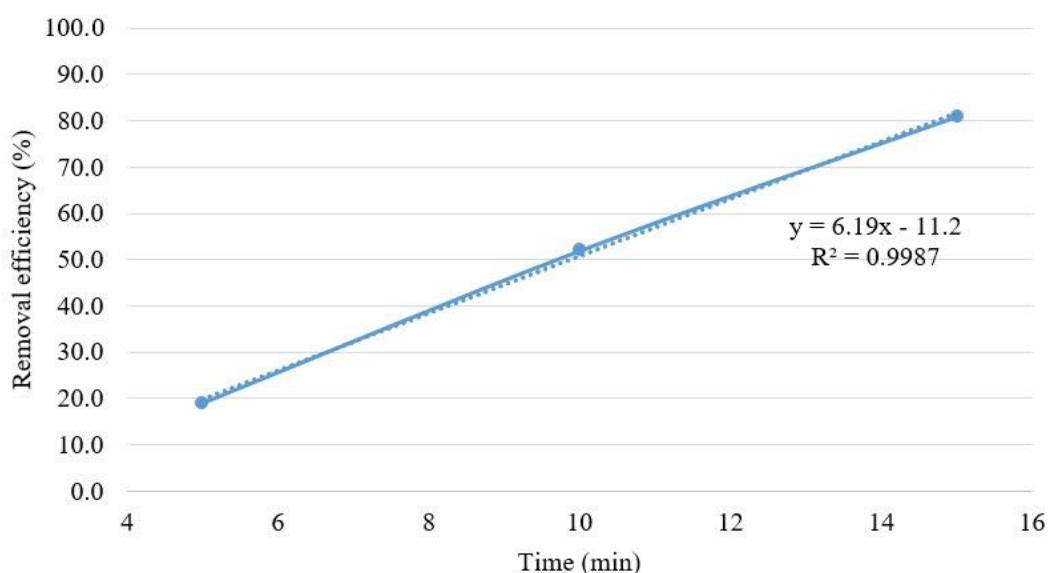
**Figure 5.** Residual H<sub>2</sub>O<sub>2</sub> concentrations along experiments for different peroxone ratios

*Impact of H<sub>2</sub>O<sub>2</sub>:O<sub>3</sub> ratio on treatment performance.* TOC removal efficiencies were below 10 % during the experiments at each peroxone ratio. Geosmin removal efficiencies could not be evaluated depending on the quite low initial geosmin concentrations, which were close to detection limit. Bromate concentrations were below detection limits for all the experiments (< 2 µg/L). 2-MIB removal efficiency was found to be between 37.5-57.3 % (Figure 6). High residual H<sub>2</sub>O<sub>2</sub> concentration was observed in the reactor effluent during the experiments with H<sub>2</sub>O<sub>2</sub>:O<sub>3</sub> ratio of 0.5. According to the results obtained from the pilot plant study, ideal H<sub>2</sub>O<sub>2</sub>:O<sub>3</sub> ratio was determined as 0.3.



**Figure 6.** 2-MIB removal efficiency at different peroxone ratios

*Impact of contact time on treatment performance.* Optimum contact time at the ideal H<sub>2</sub>O<sub>2</sub>:O<sub>3</sub> ratio was determined regarding 2-MIB removal efficiency (Figure 7). TOC removal efficiencies were below 9% during the experiments conducted at different peroxone ratios. According to the results, 2-MIB removal efficiency had a linear correlation with the contact time. Thus, the best removal efficiency (81 %) was obtained at a contact time of 15 min by applying an O<sub>3</sub> dose of 4 mg/L. Overall results confirmed the significance of contact time on the 2-MIB removal efficiency.



**Figure 7.** 2-MIB removal efficiency at different contact times (H<sub>2</sub>O<sub>2</sub>:O<sub>3</sub> ratio: 0.3).

## CONCLUSIONS

Relation between the ozone consumption and reactor height was determined in this study. Results indicated that consumed ozone increased with increasing reactor height. In order to reach ozone consumption ratio above 75 %, at least 3 m reactor height was needed. TOC could not be removed by only ozone application.

Optimum operational conditions were investigated for the removal of 2-MIB by peroxone process. It is recommended that the residual O<sub>3</sub> concentration in the outlet of the reactor should not exceed

0.1 mg/L for safety reasons. Dissolved (residual) ozone concentration was below the limit residual O<sub>3</sub> concentration at all H<sub>2</sub>O<sub>2</sub>:O<sub>3</sub> ratios. Besides, it is important not to exceed 0.5 mg/L of residual H<sub>2</sub>O<sub>2</sub> concentration in peroxone process. However, residual H<sub>2</sub>O<sub>2</sub> concentrations of over 0.5 mg/L was measured at a H<sub>2</sub>O<sub>2</sub>:O<sub>3</sub> ratio of 0.5. Therefore; optimum H<sub>2</sub>O<sub>2</sub>:O<sub>3</sub> ratio was determined as 0.3 for the peroxone process in tested conditions. 2-MIB removal efficiency of 81% was achieved at the optimum H<sub>2</sub>O<sub>2</sub>:O<sub>3</sub> ratio with a contact time of 15 min. According to the results, 2-MIB removal rate had a linear correlation with the contact time.

Authors suggest that further studies should be conducted for both ozone and peroxone processes regarding the formation of disinfection by-products. In addition to this, if the water treatment plant has a disinfection concern other than the taste and odor problem, virus and bacteria inactivation rates should be investigated with peroxone process. Last but not least, effect of temperature for the removal of taste and odor compounds in a full scale water treatment should be taken into consideration.

### ACKNOWLEDGEMENTS

This research was funded by Istanbul Water and Sewerage Administration (ISKI). The authors express their gratitude to Fatih Turan, General Director of ISKI. The authors would like to thank the Head and all staff of the Water Treatment Department of ISKI for their support.

### REFERENCES

- Cook, D., Newcombe, G., Sztajn bok, P. (2001) The application of powdered activated carbon for mib and geosmin removal: predicting PAC doses in four raw waters. *Water Research*, **35**(5) 1325-33.
- Fakioglu, M. (2017) Removal of taste and odor causing compounds in drinking water by peroxone process, Master's Thesis, Istanbul Technical University.
- Hsieh, S. T., Lin, T. F., Wang, G. S. (2010) Biodegradation of MIB and geosmin with slow sand filters. *Journal of Environmental Science and Health*, **45**(8), 951-57.
- Ho, L. (2009) Optimising water treatment practices for the removal of *Anabaena circinalis* and its associated metabolites, geosmin and saxitoxins. *Journal of Water and Health*, **7**(4), 544-56.
- Klassen, N. V., Marchington, D., McGowan, C. E. (1994) Method HP-02 Analysis of hydrogen peroxide. *Analytical Chemistry*, **66**, 2921-25.
- Oturan, M. A., Aaron, J. J. (2014) Advanced oxidation processes in water/wastewater treatment: principles and applications. A review. *Critical Reviews in Environmental Science and Technology*, **44**(23), 2577-2641.
- Srinivasan, R. Sorial, G. A. (2010) Treatment of taste and odor causing compounds 2-methyl isoborneol and geosmin in drinking water: A critical review. *Journal of Environmental Sciences*, **23**(1), 1-13.
- USEPA (1998) EPA Method 8270D, U.S. Environmental Protection Agency.
- USEPA (1999) Determination of inorganic anions in drinking water by ion chromatography, EPA Method 300.1, U.S. Environmental Protection Agency.
- WQTS (2009) Evaluation of ozone and peroxone for water quality enhancement at the del valle and patterson pass water treatment plants, Water Quality and Solutions Inc. Project Report.
- Wang, Y. (2014) Addition of hydrogen peroxide for the simultaneous control of bromate and odor during advanced drinking water treatment using ozone. *Journal of Environmental Sciences*, **26**(3), 550-54.
- Yuksel, E., Akgiray, O., Saatci, A. M., Sarikaya, H. Z., Koyuncu, I. (2002) Effect of ozone injection location on filter performance in direct filtration. *Water Science and Technology*, **46**(9), 171-77.

# A Pilot-Scale Experimental Study on the Adequacy of Filtration Mode of Operation and Filter Media in the Brasília Water Treatment Plant - Federal District - Brazil

M. A. Ferreira\*, C. C. S. Brandão\*, C. P. P. Simões\*\* and F. M. G. Braga\*\*

\* Department of Civil and Environmental Engineering, University of Brasília, Brasília 70 910-900, Brazil  
(E-mails: [almeida-matheus.ma@aluno.unb.br](mailto:almeida-matheus.ma@aluno.unb.br); [cbrandao@unb.br](mailto:cbrandao@unb.br))

\*\* Company of Environmental Sanitation of the Federal District, Brasília 71 928-720, Brazil  
(E-mails: [claudiasimoes@caesb.df.gov.br](mailto:claudiasimoes@caesb.df.gov.br); [fuadbraga@caesb.df.gov.br](mailto:fuadbraga@caesb.df.gov.br))

## Abstract

Filtration plays an important role in ensuring safe drinking water and protecting public health. The filtration performance is influenced by filtration rate, filter media characteristics and rate control system. In the Brasília Water Treatment Plant (Brasília WTP), problems related to available head and rate control system resulted in negative pressures in the filter media, decreasing the filter run length and the effluent quality. In this scenario the aim of this study was, using a pilot-scale filtration system, to compare the performance of a single (sand) and a dual-media (anthracite-sand) filter, operated under variable declining-rate filtration mode, in order to evaluate the feasibility of changing the filter media and the rate control system at Brasília WTP. The coagulation pH, coagulant dosage, influent and effluent turbidity, filtration rate and head losses in the filters were monitored. For the sand filter, average turbidity removal efficiencies were, 86 % and 80 % at, respectively, 15 m<sup>3</sup>/m<sup>2</sup>.h and 19 m<sup>3</sup>/m<sup>2</sup>.h filtration rates, with residual turbidity 83 % of the samples below 0.5 NTU. For the anthracite-sand filter, turbidity removal was around 92 %, with residual turbidity 100 % of the samples below 0.5 NTU, independently of the rate. The filter runs were about 28 to 39 h for the sand filter and around 21 h for the anthracite-sand filter operating under variable declining-rate filtration mode. Comparing the actual duration of the filtration runs at Brasília WTP, 16-20 h, whose sand filter are operated under constant-rate filtration mode, with the results obtained in the pilot plant operating under variable declining-rate filtration mode, it is suggested that rate control system of Brasília WTP should be changed. In addition, despite the shorter filter run lengths, independently of the filtration rate and mode of operation, the anthracite-sand filter produces higher effluent quality and should be adopted in the Brasília WTP.

## Keywords

Rapid filtration; declining rate filtration; water treatment

## INTRODUCTION

High levels of turbidity may protect microorganisms from the effects of disinfection, and it requires a multiple barriers system for ensuring safe drinking water (WHO, 2017). All too often, filtration is the last, and sometimes the only, physical particulate barrier for removal of turbidity (pathogens and impurities) not removed during the preceding water treatment processes. The Ordinance No. 5/2017 of the Brazilian Ministry of Health establishes that filtered water turbidity, in rapid filtration, should be maintained below 0.5 NTU (nephelometric turbidity unit) in at least 95 percent of samples (BRASIL, 2017). However, in several Brazilian Water Treatment Plants keeping filtered water turbidity consistently below 0.5 NTU requires significant improvements in filtration performance.

It is well known that the filtration rate, filter media characteristics and rate control play an important role in maintaining optimal filter efficiency. In the Brasília Water Treatment Plant (Brasília WTP), the constant-rate rapid downflow filters has experienced problems with negative pressures, probably due the lack of proper rate control system and low head available for operation, resulting in the decreasing of filter run length and of effluent quality.

In gravity constant head filters, especially constant-rate filters, when the head loss at any point in the filter media exceeds the static head to that point, the absolute pressure drops below atmospheric pressure, causing air binding and reduction in the effective filter surface area (Di Bernardo e Sabogal Paz, 2008). Negative pressure tends to happen as the filter run progresses since the build-up of head loss is not compensated for by increasing the water level above the filter. According to Cleasby (1990) gravity filters operated under variable declining-rate filtration (VDRF) mode demand less total head, avoiding negative pressures, and have less tendency for terminal breakthrough than constant-rate filters. In addition, VDRF systems operate without effluent rate control devices on each filter, which make it easy to operate.

In South America, declining-rate filtration systems have been widely used as a result of Di Bernardo and co-workers research over 1980 e 1990 decades. The development and improvement of mathematical models to predict the behaviour of variable declining-rate filtration system has increased over the years (Arboleda et al., 1985; Di Bernardo, 1986; Akgiray and Saatçi, 1988; Machado and Di Bernardo, 1995), allowing the dissemination and utilisation of this system. According Dąbrowski (2011), several water treatment plants using declining-rate filters in the U.S.A. and in the European Community operate successfully.

Pilot-scale comparative studies on constant-rate *versus* declining-rate filtration system have been conducted (Costa, 2001; Santos, 2004) focusing on turbidity removal and filter run length in order to evaluated the feasibility of applying the variable declining-rate filtration system in existing water treatment plants. These studies concluded that filters operated under VDRF mode generally present higher effluent quality and longest filter runs.

Therefore, using a pilot-scale filtration system, the aim of this study was to compare the performance of two different filter media (sand and anthracite-sand), regarding turbidity removal and filter run length, operated under variable declining-rate filtration mode, in order to evaluate the feasibility of changing the filter media and the rate control system at Brasília WTP.

## **MATERIALS AND METHODS**

### **Brasília Water Treatment Plant**

The Brasília WTP is a conventional surface water treatment plant (coagulation, flocculation, dissolved air flotation, rapid filtration and disinfection) located in Brasília, Federal District, Brazil. The raw water is taken from Santa Maria Dam, Torto and Bananal Rivers, depending on seasonal variation and water demands. The plant, with a nominal capacity of 10.080 m<sup>3</sup>/h, is managed and operated by Company of Environmental Sanitation of the Federal District (Caesb).

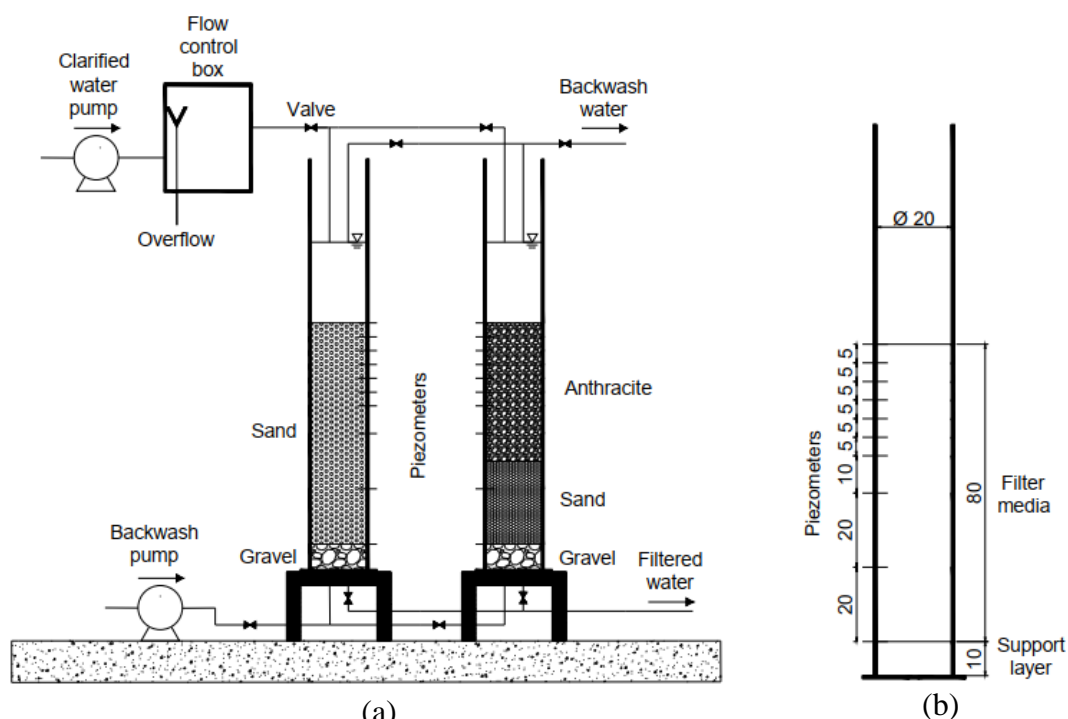
This plant has two banks of twelve filters. Each filter has a surface area of 35.75 m<sup>2</sup> and 3 m depth, 0.8 m being the thickness of the filter media. The filters were originally designed for use with a dual-media configuration of anthracite over sand but this has been changed to a single-media configuration of sand (80 cm depth, effective size of 2.17±0.06 mm and uniformity coefficient of 1.5). The filters are operated under constant head and constant-rate filtration mode, but with inadequate devices for this purpose. Currently in Brasília WTP, typical filter run is about 16-20 h.

### **Experimental set-up**

A pilot-scale filtration system (Figure 1a) was located at the Brasília WTP. The pilot system consisted of two filter columns with an internal diameter of 200 mm and 3 m height. Each pilot filter was filled with a different filter media. The first pilot filter was filled with a sand filter bed (80 cm depth, effective size of 1.25±0.05 mm and uniformity coefficient of 1.2). The second pilot

filter was filled with a dual-media filter bed, consisting of anthracite (50 cm depth, effective size of  $1.00 \pm 0.05$  mm and uniformity coefficient of 1.4) over sand (30 cm depth, effective size of  $0.53 \pm 0.20$  mm and uniformity coefficient of 1.5).

A constant influent flow rate was maintained by using a flow control box. Sampling points were properly installed and piezometers for measuring head loss were distributed along the height of the filter media bed, designed with 5, 10 and 20 cm intervals (Figure 1b). The filtered water from the Brasília WTP was used for backwashing and to achieve a bed expansion of 20 % a backwash rate was  $82.8 \text{ m}^3/\text{m}^2\cdot\text{h}$  for the sand filter and  $43.2 \text{ m}^3/\text{m}^2\cdot\text{h}$  for the anthracite-sand filter.



**Figure 1.** (a) schematic diagram of the filtration pilot plant. (b) pilot filter column design (all dimensions are in cm)

**Teixeira’s method of pilot plant operation**

Teixeira (1991) proposed a method for estimating the filter run length under variable declining-rate filtration mode, based on a single pilot filter operated under a constant-rate and variable head mode. The pilot filter operating parameters are obtained by using a mathematical model of VDRF developed by Di Bernardo (1986). A recent study, commissioned by Caesb, applied the Di Bernardo's model considering two banks of twelve filter with maximum allowed head loss (H) of 1.52 m, operating at average filtration rate (R) of  $11.67 \text{ m}^3/\text{m}^2\cdot\text{h}$ . Two situations were simulated by changing the percent opening of the effluent flow control valve, resulting in different ratios of the maximum to the mean flow rate (Table 1).

**Table 1.** Summary of the Di Bernardo’s model results

Valve opening	Total head loss equation	Output parameters
77.7 %	$H = 4.103 \cdot 10^{-6} \cdot R^2 + 6.9 \cdot 10^{-6} \cdot R^{1.85} + 3.29 \cdot 10^{-3} \cdot R^{0.667} + 0.8 \cdot 10^{-3} \cdot R^1 + 3.10^{-5} \cdot R^{1.268}$	+Maximum filtration rate: $15 \text{ m}^3/\text{m}^2\cdot\text{h}$ ; +Difference between maximum and minimum head loss: 0.076 m.
100 %	$H = 7.03 \cdot 10^{-7} \cdot R^2 + 6.9 \cdot 10^{-6} \cdot R^{1.85} + 3.29 \cdot 10^{-3} \cdot R^{0.667} + 0.8 \cdot 10^{-3} \cdot R^1 + 3.10^{-5} \cdot R^{1.268}$	+Maximum filtration rate: $19 \text{ m}^3/\text{m}^2\cdot\text{h}$ ; +Difference between maximum and minimum head loss: 0.149 m.



The pilot filter should be operated at the maximum filtration rate and the filter run should be terminated when the maximum allowed head loss has been reached. After obtaining the pilot filter run length, the filter run under VDRF mode is estimated by multiplying the pilot filter run length by the number of filters in a bank.

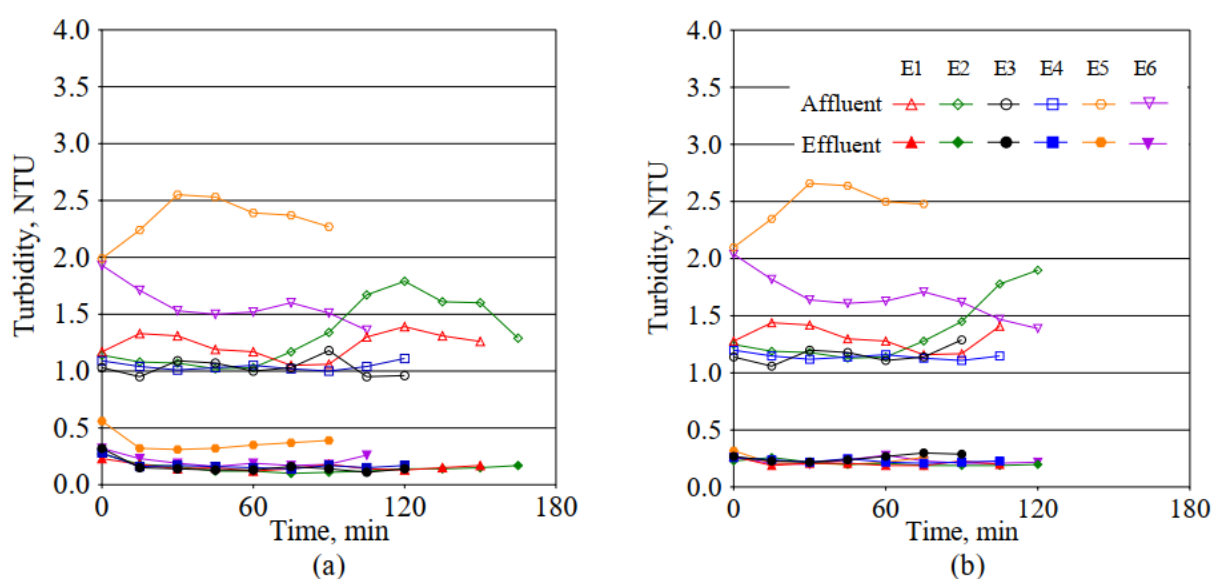
### Experimental procedure

The rapid gravity pilot filters were supplied with dissolved air flotation (DAF) clarified water from Brasília WTP and operated in parallel at filtration rates of 15 m<sup>3</sup>/m<sup>2</sup>.h and 19 m<sup>3</sup>/m<sup>2</sup>.h, with maximum allowed head loss of 0.076 m and 0.149 m, respectively. The filtration performance was evaluated at coagulation pH values in a range of 6.4 to 7.1 and coagulant dosage of polyaluminum chloride (PAC) in a range of 4.0 to 7.5 mg/L.

In order to evaluate the filtration efficiency, grab samples of DAF clarified and filtered water, taken every 15 minutes, were analysed regarding turbidity and pH. The effluent flow rate (determined volumetrically) and the head loss were monitored every 15 minutes to allow the estimation of the filter run length, under VDRF mode, as described in Teixeira's method.

## RESULTS AND DISCUSSIONS

During the pilot study, the raw water was composed of about 70 % from Torto River and 30 % from Bananal River. Six experiments were carried out with filtration rate of 15 m<sup>3</sup>/m<sup>2</sup>.h and other 6 experiments with filtration rate of 19 m<sup>3</sup>/m<sup>2</sup>.h. The highest values of filtered water turbidity were observed during the ripening period and also when a filter has reached the end of its run. The pilot filter runs were terminated when the maximum allowed head loss, obtained when using Di Bernardo's model, has been reached. The average turbidity of DAF clarified water (filter feeding water) was 1.37 ± 0.44 NTU for filters operated at filtration rate of 15 m<sup>3</sup>/m<sup>2</sup>.h. After the ripening period both filters were able to maintain filtered water turbidity below 0.5 NTU, as observed in Figure 2.



**Figure 2.** Turbidity of DAF clarified (affluent) and filtered (effluent) water during filtration runs at filtration rate of 15 m<sup>3</sup>/m<sup>2</sup>.h. (a) sand filter. (b) anthracite-sand filter

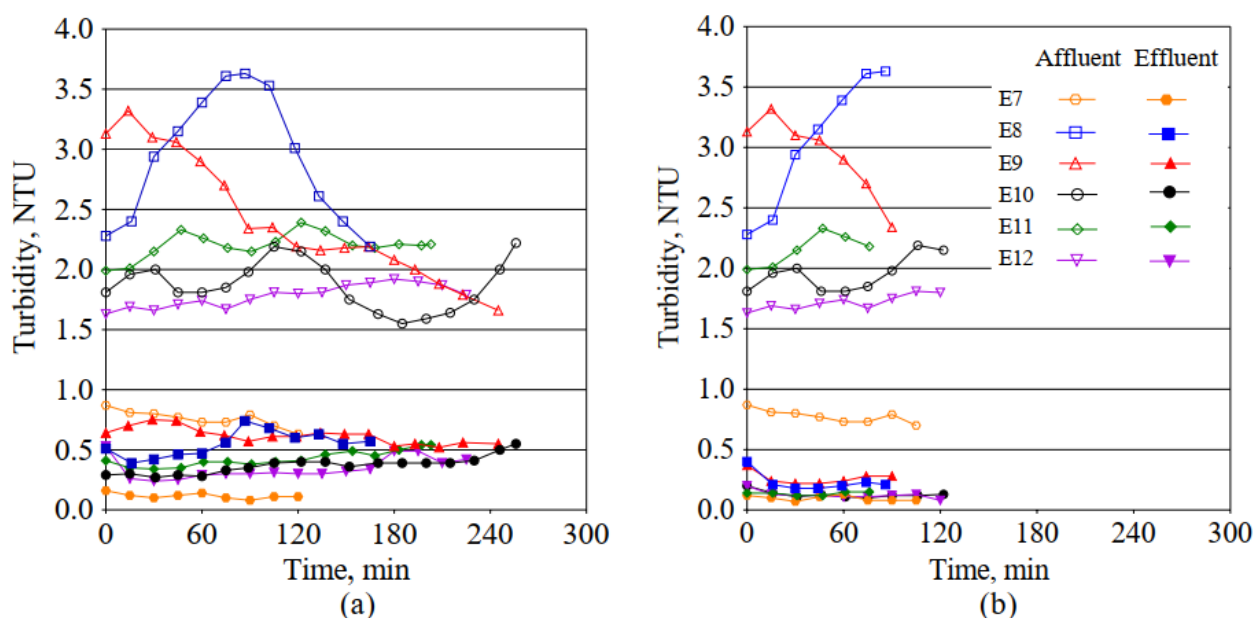
As shown in Table 2, higher filtered water quality and shorter filter runs were observed in the anthracite-sand filter, caused by the filter media clogging due to particulates retention, achieving more quickly the maximum allowed head loss, in comparison with the sand filter. Generally, with

both filters operating at the filtration rate of  $15 \text{ m}^3/\text{m}^2\cdot\text{h}$ , increasing in the PAC dosage resulted in shorter filter runs and inferior effluent quality, despite variations in the DAF clarified water turbidity. This occurs because higher coagulant dosages result in higher clogging head losses in the filter media bed (Eyvaz et al., 2015).

**Table 2.** Summary of filter runs parameter at filtration rate of  $15 \text{ m}^3/\text{m}^2\cdot\text{h}$  in the pilot plant

PAC, mg/L	Coagulation pH	Sand Filter			Anthracite-sand Filter			
		Initial Turbidity, NTU	Residual Turbidity, NTU	Filter Run, min	Initial Turbidity, NTU	Residual Turbidity, NTU	Filter Run, min	
E1	4.0	$6.9 \pm 0.2$	$1.23 \pm 0.11$	$0.16 \pm 0.03$	149	$1.20 \pm 0.11$	$0.10 \pm 0.03$	101
E2	4.0	$7.1 \pm 0.0$	$1.32 \pm 0.28$	$0.15 \pm 0.05$	173	$1.26 \pm 0.29$	$0.10 \pm 0.02$	122
E3	4.5	$7.0 \pm 0.1$	$1.03 \pm 0.08$	$0.16 \pm 0.06$	126	$1.05 \pm 0.07$	$0.15 \pm 0.03$	91
E4	4.5	$6.9 \pm 0.0$	$1.04 \pm 0.04$	$0.17 \pm 0.04$	142	$1.04 \pm 0.03$	$0.12 \pm 0.02$	102
E5	7.0	$6.9 \pm 0.1$	$2.33 \pm 0.19$	$0.37 \pm 0.09$	104	$2.35 \pm 0.21$	$0.13 \pm 0.05$	80
E6	7.0	$6.9 \pm 0.1$	$1.58 \pm 0.17$	$0.21 \pm 0.05$	133	$1.55 \pm 0.19$	$0.12 \pm 0.03$	118

Contrary to expectations, in both filter the increase in filtration rate, from  $15 \text{ m}^3/\text{m}^2\cdot\text{h}$  to  $19 \text{ m}^3/\text{m}^2\cdot\text{h}$ , and average DAF clarified water turbidity, from  $1.37 \pm 0.44 \text{ NTU}$  to  $2.05 \pm 0.71 \text{ NTU}$ , resulted in longest filter runs. However, the effluent quality degraded, especially in the sand filter (Figure 3a). In this filter, the Brazilian Maximum Contaminant Level (MCL) of filtered water turbidity ( $0.5 \text{ NTU}$ ) has been exceeded in 33 % of samples. The anthracite-sand filter was able to produce effluent turbidity below  $0.5 \text{ NTU}$  in all experiments (Figure 3b).



**Figure 3.** Turbidity of DAF clarified (affluent) and filtered (effluent) water during filtration runs at filtration rate of  $19 \text{ m}^3/\text{m}^2\cdot\text{h}$ . (a) sand filter. (b) anthracite-sand filter

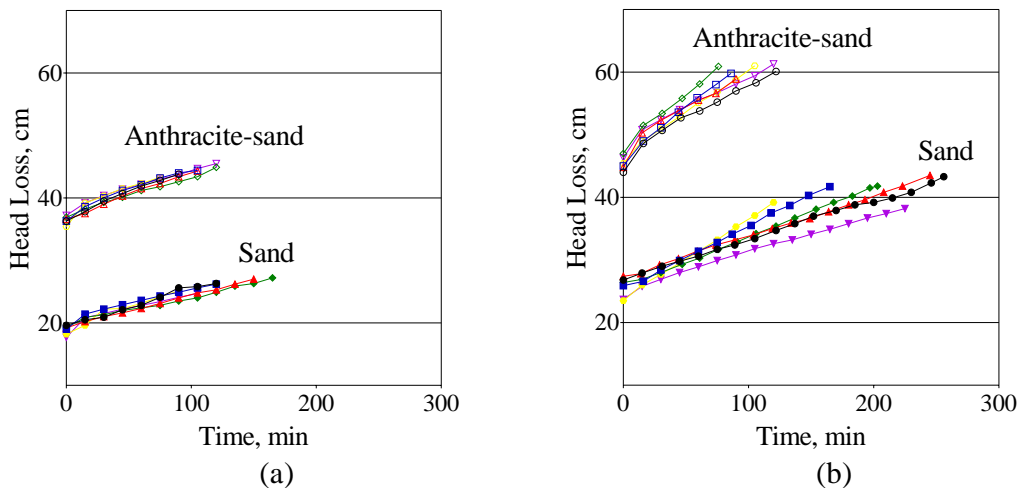
Averages of turbidity removal efficiencies at filtration rates of  $15 \text{ m}^3/\text{m}^2\cdot\text{h}$  and  $19 \text{ m}^3/\text{m}^2\cdot\text{h}$  were, respectively, 86 % and 80 % for the sand filter and around 92 % for the anthracite-sand filter, independently of the filtration rate. The experiments, especially those operating at filtration rate of  $19 \text{ m}^3/\text{m}^2\cdot\text{h}$ , showed that that the filter run length was more affected by variation in coagulation conditions (pH and PAC dosage) than DAF clarified water turbidity, indicating that the filters were able to produce stable effluent quality by dampening fluctuations in DAF clarified water turbidity,

as shown in Table 3. The dampening effect is important, since the Brasília WTP has been facing operational difficulties in maintaining filtered water quality when the DAF clarified water turbidity changes.

**Table 3.** Summary of filter runs parameter at filtration rate of 19 m<sup>3</sup>/m<sup>2</sup>.h in the pilot plant

	PAC, mg/L	Coagulation pH	Sand Filter		Anthracite-sand Filter			
			Initial Turbidity, NTU	Residual Turbidity, NTU	Filter Run, min	Initial Turbidity, NTU	Residual Turbidity, NTU	Filter Run, min
<b>E7</b>	4.0	6.5 ± 0.0	0.76 ± 0.07	0.12 ± 0.02	117	0.78 ± 0.05	0.10 ± 0.02	105
<b>E8</b>	5.0	6.7 ± 0.1	2.93 ± 0.54	0.55 ± 0.10	150	3.06 ± 0.55	0.23 ± 0.08	89
<b>E9</b>	5.0 - 7.0	6.6 ± 0.1	2.41 ± 0.52	0.62 ± 0.07	230	2.94 ± 0.33	0.26 ± 0.05	107
<b>E10</b>	7.0 - 5.0	6.6 ± 0.1	1.87 ± 0.20	0.37 ± 0.07	239	1.95 ± 0.15	0.13 ± 0.03	124
<b>E11</b>	7.0 - 6.0	6.5 ± 0.1	2.20 ± 0.11	0.43 ± 0.07	188	2.15 ± 0.13	0.14 ± 0.01	86
<b>E12</b>	7.5	7.0 ± 0.1	1.78 ± 0.09	0.35 ± 0.09	246	1.72 ± 0.06	0.12 ± 0.03	134

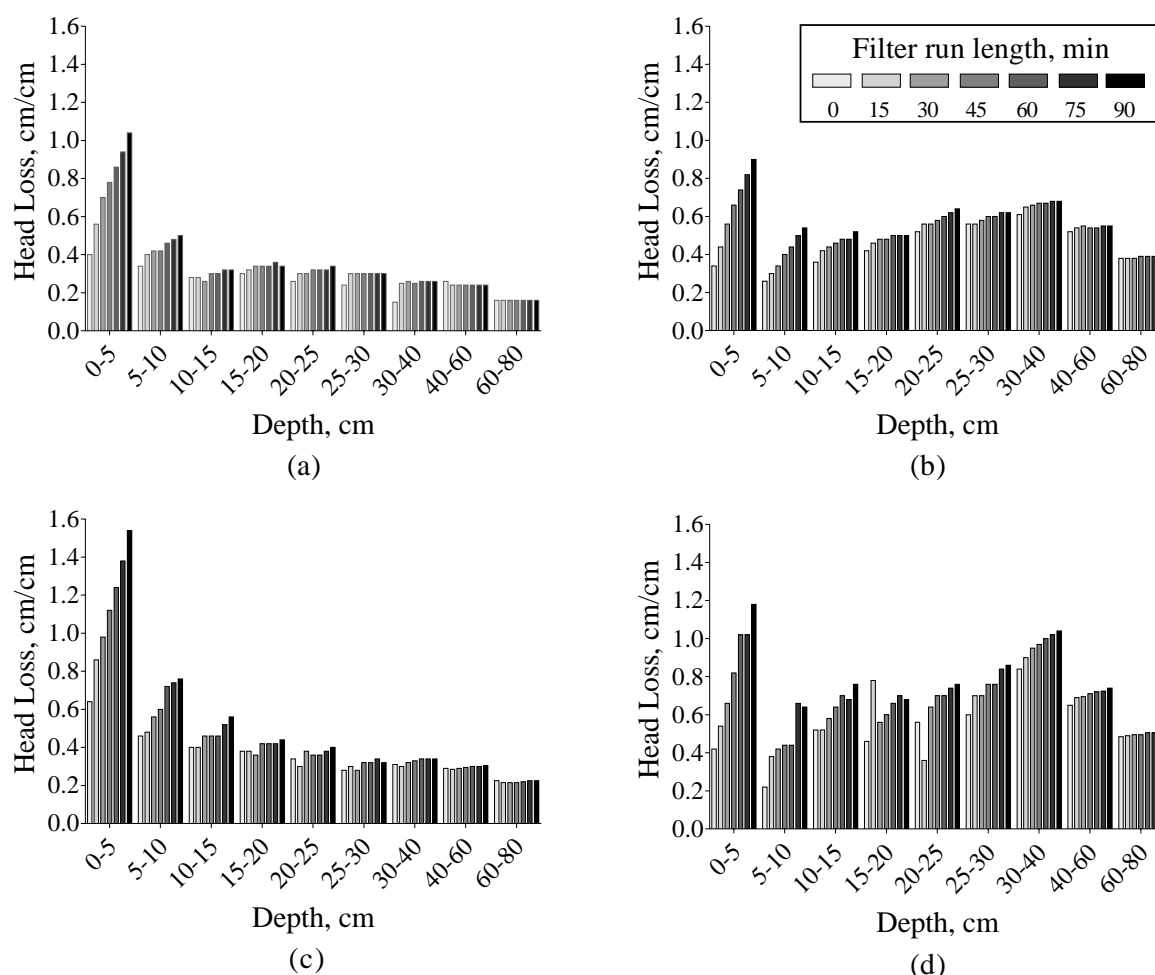
Changes in PAC doses during the filter runs operating at filtration rate of 19 m<sup>3</sup>/m<sup>2</sup>.h disturbed significantly the build-up of the head losses, as a result of altering the rate of head loss, compromising the filtration performance. Those experiments in which the PAC dosage was maintained constant during the filter run presented a similar build-up head loss behavior with similar values of rate of head loss (Figure 4a). As can be observed in Figure 4b, the similarity of build-up head loss behavior was not observed when the PAC dosage was changed during the filter run length.



**Figure 4.** Build-up of total head loss during filtration runs at rate of: (a) 15 m<sup>3</sup>/m<sup>2</sup>.h; (b) 19 m<sup>3</sup>/m<sup>2</sup>.h

The longest filter runs were obtained at higher filtration rate of 19 m<sup>3</sup>/m<sup>2</sup>.h (Table 3). It was notably observed in the experiments in which the PAC dosage was changed during the filter run, probably by changing the surface charge of the particles and reducing the adhesive forces between the particles and the collector surfaces.

The decreasing in adhesive forces may cause premature turbidity breakthrough by decreasing solids retention. In addition, the reduction of solids retention decreases the rate of head loss, as the head loss builds up as a result of filter clogging, and promotes longest filter runs. Despite PAC dose changes, the increase in filter runs length caused by increasing the shear stress and favouring depth filtration over surface filtration was also observed (Figure 5).



**Figure 5.** Increase of head loss due to solids retention in experiments conducted under similar coagulation conditions. (a) sand filter and (b) anthracite-sand filter operated at rate of 15 m<sup>3</sup>/m<sup>3</sup>.h. (c) sand filter and (d) anthracite-sand filter operated at rate of 19 m<sup>3</sup>/m<sup>3</sup>.h

As shown in Figure 6, surface filtration was predominant in the sand filter, differently from the anthracite-sand filter, in which there was a predominance of depth filtration, independently of the filtration rate. Despite the surface filtration, longest filter runs were obtained in sand filter due to lowest turbidity removal and the media characteristics, in comparison with the anthracite-sand filter.

The averages of filtration runs estimated by using the method proposed by Teixeira (1991) were 27.6-39.0 h for the sand filter and 20.5-21.5 h for the anthracite-sand filter operating under variable declining-rate filtration mode. These values are higher than the averages of filtration runs observed in the actual filters at Brasília WTP, 16.0-20.0 h, which are operated under constant-rate filtration mode. Even though the effective size of the actual sand filters of Brasília WTP is significantly greater than the effective size of both filter media experimentally tested in this study, the sand and anthracite-sand filter tested were able to provided longest filter runs, probably caused by changing the mode of operation. Based on the comparison between the filter runs, declining-rate filtration mode showed a better performance than constant-rate filtration mode.

## CONCLUSIONS

The performance of a single-media filter consisting of sand was compared with a dual-media filter consisting of anthracite over sand, in order to evaluate the feasibility of changing the rate control system at Brasília WTP.

At filtration rate of 15 m<sup>3</sup>/m<sup>2</sup>.h there were no significant differences in filtered water turbidity between the single and dual media filter. However, the filter runs were shorter in the anthracite-sand filter. When the filtration rate was 19 m<sup>3</sup>/m<sup>2</sup>.h, the sand filter was not able to maintain filtered water turbidity below 0.5 NTU differently from the anthracite-sand filter. Both filters can produce satable effluent quality by dampening fluctuation in affluent water turbidity. The increasing coagulant dose favored reduction of filter run length. In addition, changes in the coagulant dose during filter cycle may promote premature turbidity breakthrough.

Averages duration of filter runs at filtration rate of 15 m<sup>3</sup>/m<sup>2</sup>.h were 28±5 h for the sand filter and 20±3 h for the anthracite-sand filter. At filtration rate of 19 m<sup>3</sup>/m<sup>2</sup>.h the averages duration of filter runs were 39±11 h for the sand filter and 22±4 h for the anthracite-sand filter. In both pilot filters, the filter runs obtained under VDRF mode exceed the actual filter runs, under constant-rate mode, suggesting that rate control system of Brasília WTP should be changed. Also, despite the shorter filter run lengths, independently of the filtration rate and mode of operation, the anthracite-sand filter produces higher effluent quality and should be adopted in the Brasília WTP.

## REFERENCES

- Akgiray, Ö., Saatçi, A. M. (1998) An algorithm for bank operation of declining rate filters. *Water Res*, **32**(7), 2095-2105.
- Arboleda, J., Giraldo, R., Snel, H. (1985) Hydraulic behaviour of declining rate filtration. *J. Am. Water Works Assoc.*, **77**(12), 67-74.
- Brasil (2017) Ministério da Saúde. Portaria de consolidação N° 5. Diário Oficial da União, Brasília, 5 set. 2017, (in Portuguese).
- Cleasby, J. L. (1990) Filtration. In *Water Quality and Treatment - A Handbook of community Water Supplies (AWWA)*, 4th Edition, MacGraw Hill, Inc.
- Costa, E. R. H. (2001) Avaliação do funcionamento de uma instalação de filtração direta descendente com taxa declinante variável em escala real e piloto. Tese de Doutorado em Hidráulica e Saneamento, Escola de Engenharia de São Carlos, Universidade de São Paulo, São Carlos, Brasil, 285, (in Portuguese).
- Dąbrowski, W. (2011) Rational operation of variable declining rate filters. *Environ. Prot. Eng.*, **37**(4), 35-53.
- Di Bernardo, L., Sabogal Paz, L. P. (2008). Seleção de Tecnologias de Tratamento de Água. Editora LdiBe, São Carlos, Brasil, 1560, (in Portuguese).
- Di Bernardo, L. (1986). Hidráulica da filtração com taxa declinante. *Revista DAE*, **46**(146), 259-267, (in Portuguese).
- Eyvaz, M., Akgiray, Ö., Yuksel, E. (2015) An experimental investigation on the hydraulic behavior of declining rate filtration. *Desalination and Water Treatment*, **51**(31), 6137-6147.
- Machado, R., e Di Bernardo, L. (1995) Proposição de modelação matemática para sistemas de filtração com taxa declinante variável incluindo armazenamento de água a montante dos filtros. Universidade de São Paulo, São Carlos, (in Portuguese).
- Santos, E. P. C. C. (2004) Coagulação da água da represa Vargem das Flores visando tratamento por filtração direta. Dissertação de Mestrado, Programa de Pós-graduação em Saneamento, Meio Ambiente e Recursos Hídricos, Universidade Federal de Minas Gerais, Belo Horizonte, Minas Gerais, 167, (in Portuguese).
- Teixeira, B. A. N. (1991) Proposição de um método para obtenção e operação de sistemas de filtração com taxa declinante. Tese de Doutorado - Escola de Engenharia de São Carlos, Universidade de São Paulo. São Carlos, Brasil, 208, (in Portuguese).
- World Health Organization. (2017) Guidelines for drinking-water quality - fourth edition incorporating first addendum, 4th Edition, World Health Organization.

## Removal of Cylindrospermopsin by Adsorption onto Activated Carbon Synthesized from Coconut Shell

I. R. Fonseca\*, D. Valencia-Cárdenas\*, M. J. Prauchner\*\* and Y. P. Ginoris\*

\* Department of Civil and Environmental Engineering, University of Brasília, Brasília 70 910-900, Brazil (E-mails: [iararesendedafonseca@gmail.com](mailto:iararesendedafonseca@gmail.com); [dvalenciacar@gmail.com](mailto:dvalenciacar@gmail.com); [yovanka.perez@gmail.com](mailto:yovanka.perez@gmail.com))

\*\* Chemistry Institute, University of Brasília, Brasília 70 910-900, Brazil (E-mail: [marcosjp@unb.br](mailto:marcosjp@unb.br))

### Abstract

Cylindrospermopsin occurrence has been documented in different regions all over the globe, especially in water supply reservoirs, which are favourable environments for cylindrospermopsin producers' blooms. Due to its high toxicological potential, it may warn to human health and safety. Different water treatment techniques can be applied to cylindrospermopsin removal, amongst them adsorption onto activated carbon in granular or powdered forms. Activated carbons can be produced by different activation methods and from different starting materials, in present study it was used coconut shell as raw material and chemical activation using phosphoric acid. Two acid rates were used during activation process, then both combinations led to types of activated carbons with high surface area and pores volume. Cylindrospermopsin adsorption experiments were conducted in ultrapure water and Paranoa lake water for both activated carbons. Results showed a slightly difference between their adsorption performances in ultrapure water. Also, it was verified a high impact of organic matter on adsorption efficacy in lake water experiments.

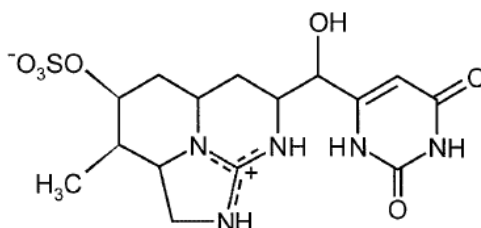
### Keywords

Water treatment; adsorption; activated carbon; cylindrospermopsin; activated carbon synthesis

## INTRODUCTION

Cyanobacterial blooms producing toxins have been reported all over the world. Favourable geographic spreading of toxic blooms and adequate environmental conditions emphasizes the need for increasing monitoring of cyanotoxins in drinking supply reservoirs in Brazil (Bittencourt-Oliveira et al., 2014). In Brazil, major occurrence of these organisms has been reported on the subtropical region due to more concentration of studies in this area. Although, studies in tropical area has increased after a tragic event in Caruaru, state of Pernambuco, where water contaminated with cyanotoxins was used for a haemodialysis treatment, in 1996.

According to Bittencourt-Oliveira et al. (2014), most recurrent toxins in Brazilian water bodies are microcystin, however cylindrospermopsin (CYN) has been reported in different reservoirs which may warn for the danger of their spread. CYN is classified as an hepatotoxin, which may cause diseases in humans related to liver disfunction. Humpage and Falconer (2003) performed experiments using different doses of CYN in several mices and according to their body weight changes, they proposed a guideline value of 1 µg/L for CYN in drinking water.



**Figure 2.** Chemical structure of CYN (Ohtani et al., 1992)

The removal of large concentrations of CYN by conventional treatments is hampered by its hydrophilic property, especially when it is found in extracellular form. Faced with the challenge of removing these toxins, there is a need for the use of advanced water treatment techniques. As a method of advanced water treatment, the use of activated carbon (AC) in powdered and granular forms stands out. These activated carbons can be synthesized from different raw materials, which will develop different physical and chemical characteristics in their structure. Studies have been done evaluating the removal of CYN in commercial activated carbon made by vegetal and mineral raw materials, including coconut shell, an abundant raw material in Brazilian coast.

Ho et al. (2008) evaluated two types of commercially available activated carbon at CYN adsorption on a reservoir water, CYN concentrations ranged from 2.7 to 37.4  $\mu\text{g/L}$ . One was coal based, with higher micropores volume and BET surface, and the other one was wood based. The first one presented a better adsorption performance, reaching up to 70 % of CYN removal at 20 mg/L of CAP.

Valencia-Cárdenas (2016) also appraised two types of commercial powdered activated carbon (PAC) at CYN adsorption, PAC 2 was mineral based and physically activated, PAC 1 was wood based and chemically activated. BET surface area in PAC 2 represented more than twice of the area in PAC 1 and a higher micropore and mesopore volumes, which led to a better performance of PAC 1 in adsorption process. Both studies indicated better removals of CYN are obtained in activated carbons with a higher superficial area and mesopores volume, independently of AC starting material.

Furthermore, additional studies must be developed to define which characteristics an activated carbon must have to ensure high CYN removals. The aim of this study was evaluating CYN removal onto two activated carbons synthesised from coconut shell under different conditions.

## EXPERIMENT PROCEDURES

Carbon synthesis started using dried endocarp of coconut origin from Brazil as precursor, which particles were sieved in the range of 0.177 to 0.105 mm. Two sorts of carbon were produced following Prauchner and Rodríguez-Reinoso (2012) study. Both were activated by chemical activation using phosphoric acid, the difference consisted on acid ratio utilized where AC 1 used 0.54 g of precursor per g  $\text{H}_3\text{PO}_4$  and AC 2 0.27 g/g. First the precursor was impregnated with the acid under the temperature of 85°C for 2 hours and then the temperature was increased to boiling point to force the incorporation of the acid. Second, the mixture was carbonized in a tubular horizontal furnace up to 450 °C and stayed at this degree for 2 hours.

After completing the synthesis, both carbons were submitted to characterization analysis in Quantachrome NovaWin gas sorption equipment. Adsorption-desorption isotherms of  $\text{N}_2$  were used to evaluate superficial area and pores volume. Chemical characterization consisted on determining the potential of zero charge ( $\text{pH}_{\text{zcp}}$ ) based on Moreno-Castilla et al. (2000) study.

Once synthesised both AC adsorption experiments were conducted using two study waters: ultrapure water and Paranoá lake water, both spiked with an extract obtained from freeze dried cells of a strain (CYP011K) CYN producer in order to reach an initial concentration of approximately 60  $\mu\text{g/L}$  of CYN dissolved, during preparation both waters were adjusted to pH 6.5. All samples were analysed using ELISA method produced by ABRAXIS.

First experiments were done in order to obtain kinetic adsorption model and contact time to be used



on the following adsorption capacity experiments. Experimental part was conducted using carbon dose fixed at 6 mg/L and contact times of 0, 60, 90, 120, 180 and 240 minutes. After experiments, modeling part consisted on applying kinetic models to evaluate the interaction mechanism between adsorbate-adsorbent, thus, following models were used: pseudo-first-order (Lagergren, 1898), pseudo-second-order (Ho and McKay, 1999), intraparticle diffusion (Weber and Morris, 1963) and Elovich (Roginsky and Zeldovich, 1934).

Finally, experiments determining the adsorption capacity of both activated carbons were conducted, following the requirements of ASTM (2014). Adsorption experiments were done using AC doses of 0, 3, 6, 9 and 12 mg/L. The isotherm models used in this study were Langmuir, Freundlich, Redlich-Peterson and Sips (Langmuir-Freundlich), with their expressions are presented in the equations (1), (2), (3) and (4), respectively (Foo and Hameed, 2010).

$$q_e = \frac{Q_0 b C_e}{1 + b C_e} \quad (1) \quad q_e = K_F C_e^{1/n} \quad (2)$$

$$q_e = \frac{K_R C_e}{1 + a_R C_e^g} \quad (3) \quad q_e = \frac{K_S C_e^{\beta_S}}{1 + a_S C_e^{\beta_S}} \quad (4)$$

Where  $q_e$  is solid phase sorbate concentration at equilibrium ( $\mu\text{g}/\text{mg}$ ),  $C_e$  is aqueous phase sorbate concentration at equilibrium ( $\mu\text{g}/\text{L}$ ),  $Q_0$  is maximum monolayer coverage capacities ( $\mu\text{g}/\text{mg}$ ),  $b$  is Langmuir isotherm constant ( $\text{L}/\mu\text{g}$ ),  $K_F$  is Freundlich isotherm constant ( $\text{L}/\text{mg}$ ) related to adsorption capacity,  $n$  is adsorption intensity,  $1/n$  is the heterogeneity factor,  $K_R$  is Redlich-Peterson isotherm constant ( $\text{L}/\text{mg}$ ),  $a_R$  is Redlich-Peterson isotherm constant ( $\text{L}/\mu\text{g}$ ),  $g$  is Redlich-Peterson isotherm exponent,  $K_S$  is Sips isotherm model constant ( $\text{L}/\text{mg}$ ),  $a_S$  is Sips isotherm model constant ( $\text{L}/\mu\text{g}$ ) and  $\beta_S$  is Sips isotherm model exponent.

The parameters of the Langmuir and Freundlich adsorption models were determined using the linear forms of the equations (1) and (2), presented in the equations (5) and (6), respectively.

$$\frac{C_e}{q_e} = \frac{1}{b Q_0} + \frac{C_e}{Q_0} \quad (5) \quad \log_{10} q_e = \log_{10} K_F + \frac{1}{n} \log_{10} C_e \quad (6)$$

The parameters of the Redlich-Peterson and Sips adsorption models were determined using nonlinear regression of the experimental data,  $q_e$  and  $C_e$ , using *LAB Fit*, a free curve fitting software (<http://zeus.df.ufcg.edu.br/labfit/index.htm>), with a maximum number of iterations of 10000 and a tolerance of  $10^{-6}$ .

## RESULTS AND DISCUSSION

### Activated carbons characterization

The results showed that AC 1, obtained using the higher fraction of the  $\text{H}_3\text{PO}_4$  presented a lower BET surface area but the highest volume of mesopores in its structure, representing 35 % of total pores volume, as expected, due to high acid rate comparing to AC 2. Furthermore, AC 2, which received a lower fraction of  $\text{H}_3\text{PO}_4$ , presented a greater BET surface area with a predominance of micropores in its structure, as shown in Table 1.



**Table 1.** Physical characteristics of synthesised activated carbons

	AC 1	AC 2
<b>BET surface area (m<sup>2</sup>/g)</b>	1408	1735
<b>Micropores volume (cm<sup>3</sup>/g)</b>	0.613	0.826
<b>Mesopores volume (cm<sup>3</sup>/g)</b>	0.331	0.038
<b>Potential of zero charge</b>	2.10	2.28

**Kinetic of adsorption**

According to Ho and McKay (1999), pseudo-second-order model has been successfully used to describe adsorption onto granular activated carbon. This model describes the rate constant of sorption of some amount of sorbate on the surface sorbent at any time until its reach the equilibrium, correlating the number of available active sites.

For CYN adsorption onto both activated carbons, pseudo-second-order kinetic was the model that better described kinetic adsorption. The model parameters are shown on Table 2.

**Table 2.** Kinetic parameters for AC 1 and AC 2

	AC 1	AC 2
<b>K<sub>2</sub> (µg.mg<sup>-1</sup>.min<sup>-1</sup>)</b>	0.0253	0.0155
<b>q<sub>e</sub> (µg.mg<sup>-1</sup>)</b>	4.029	2.797
<b>R<sup>2</sup></b>	0.969	0.932

According to model parameters, prediction of AC doses required to remove CYN in ultrapure water was done in order to estimate doses to be applied in two different scenarios, as can be seen in Table 3. Contact times were chosen based on a hypothetical emergency situation in which the activated carbon could be applied in rapid mixing unit of a water treatment plant. Also, CYN concentration was chosen based on Falconer (2005) and Ho et al. (2008) studies.

**Table 3.** AC 1 and AC 2 doses and contact times required to remove CYN to 1 µg/L in ultrapure water

Contact time (min)	Initial CYN concentration (µg/L)									
	15		10		5		3		2	
	AC dose requirement (mg/L)									
	AC 1	AC 2	AC 1	AC 2	AC 1	AC 2	AC 1	AC 2	AC 1	AC 2
15	5.74	12.69	3.69	7.66	0.89	3.62	0.35	1.81	0.41	0.91
30	4.61	8.84	2.96	5.69	0.49	2.53	0.66	1.26	0.33	0.63
60	4.04	6.92	2.60	4.45	0.24	1.98	0.58	0.99	0.29	0.49

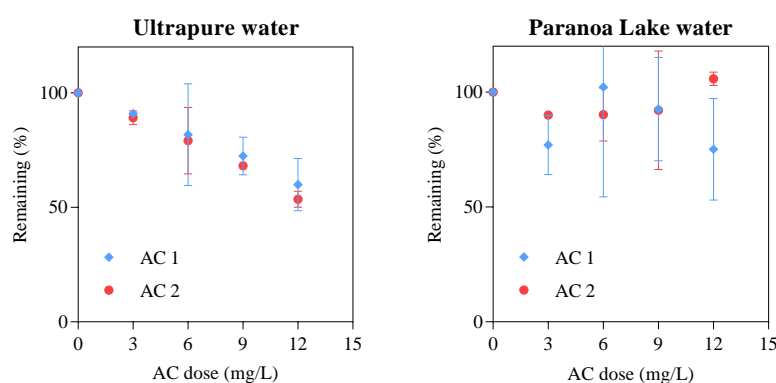
The difference between the quantities of both carbons needed to reduce CYN concentration to 1 µg/L can be attributed to the higher number of mesopores presented on AC 1. It has been noticed on previous studies the trend of activated carbons with high volume of mesopores to present greater CYN adsorption capacity (Costa et al., 2012; Valencia-Cárdenas, 2016). As well, comparing with quantities of commercially activated carbon for the same contact time required to obtain 1 µg/L of CYN found by Ho et al. (2008), the doses of AC 1 and 2 required to reach the same CYN concentration are much lower. For example, in Ho et al. (2008) study for 30 min of contact time and 5 µg/L of CYN it was necessary 33 mg/L of PAC. In the present study requirements were

0.49 mg/L for AC 1 and 2.53 mg/L for AC 2. It is important to mention that in the present study the experiments were conducted using ultrapure water spiked with an extract of CYN (only containing cytoplasmic organic dissolved matter), while the Ho et al. (2008) study was carried out using a reservoir water as matrix containing organic dissolved matter.

Based on kinetic experiments, 4 hours was chosen as contact time for further experiments.

### Adsorption capacity

Adsorption capacity results showed a similar removal of CYN for both carbons in ultrapure water (Figure 2). Although pores distribution was different, AC 1 and AC 2 remaining values for 12 mg/L dose were alike, correspondingly to averages of 59.90 % and 53.53 % for ultrapure water. On Paranoá lake water experiment, the organic matter presented a high influence on adsorption of CYN.



**Figure 2.** Remaining values of adsorption capacity of CYN for the study waters. Initial CYN concentration in ultrapure water for AC 1 and AC 2 was  $57.85 \pm 3.31 \mu\text{g/L}$  and  $59.32 \pm 0.89 \mu\text{g/L}$ , respectively. For Paranoá lake water initial concentrations were  $67.25 \pm 8.31 \mu\text{g/L}$  for AC 1 and  $62.27 \pm 0.51 \mu\text{g/L}$  for AC 2

### Equilibrium isotherms

The equilibrium isotherms describe the adsorption process and lead to optimize water treatment processes that include adsorption steps. The optimization of adsorption processes, based on the isotherms, depends on the experimental data fit to the either theoretical or empirical equations. Therefore, it is important to establish the best correlation for the equilibrium data of CYN adsorption onto the 2 carbons tested in ultrapure water and Paranoá lake water. The fitted parameter values, for the adsorption data of this study are shown in the Table 4.

*Langmuir isotherm.* The results for the AC 1 indicate that the data do not follow the Langmuir adsorption model, possibly because there is not monolayer adsorption onto the AC 1. Despite the correlation coefficients for the AC 2 close to 0.9, the adsorption data neither follow the Langmuir model. The maximum monolayer coverage capacity,  $Q_0$ , and the Langmuir isotherm constant,  $b$ , presented negative values, indicating the insufficiency of this model for explaining this adsorption process (Alshabanat et al., 2013).

*Freundlich isotherm.* Considering the correlation coefficients, the experimental data does not match with the Freundlich model in none of the performed tests.

The Freundlich adsorption isotherm (Freundlich, 1907) assumes that adsorption occurs in

multilayers on a heterogeneous surface, increasing the amount of adsorbate on the surface as the concentration in the liquid phase increases, according to the equation (2). The heterogeneity factor,  $1/n$ , is also related to the bonding energy. Negative values for this parameter could indicate a null binding force between the AC surface and the CYN. Therefore, there is no correlation between the data and the model.

In addition,  $K_F$  values were up to  $2.474 \times 10^{15}$  times higher than others CYN adsorption studies with good approximations to the Freundlich model (Ho et al., 2008), showing parameter values without physical meaning.

*Redlich-Peterson isotherm.* The determined parameters for this isotherm were all positives and the AC 2 showed a better fit than the AC 1. However, the Redlich-Peterson isotherm exponent,  $g$ , in all cases, were higher than 1. According to Wu et al. (2010), the values for this parameter are usually less than 1; consequently, none of the approaches to the Redlich-Peterson isotherm meets this requirement.

**Table 4.** Isotherm constants for the adsorption of CYN onto each AC and matrix water

	AC 1		AC 2	
	Ultrapure water	Paranoá lake water	Ultrapure water	Paranoá lake water
<b>Langmuir</b>				
$Q_0$ ( $\mu\text{g}/\text{mg}$ )	2.862	0.067	1.941	-0.035
$b$ ( $\text{L}/\mu\text{g}$ )	0.032	-0.020	-0.248	-0.017
$R^2$	0.3881	0.7778	0.9839	0.8722
$\chi^2$	2	2	2	2
<b>Freundlich</b>				
$K_F$ ( $\text{L}/\text{mg}$ )	0.329	$4.205 \times 10^{14}$	3.733	0.824
$1/n$	0.430	-8.338	-0.147	$4.543 \times 10^{13}$
$R^2$	0.2311	0.7471	0.5076	0.0000
$\chi^2$	2	2	2	2
<b>Redlich-Peterson</b>				
$K_R$ ( $\text{L}/\text{mg}$ )	0.045	17871.070	2071.514	$9.592 \times 10^9$
$a_R$ ( $\text{L}/\mu\text{g}$ )	$4.904 \times 10^{-8}$	$2.996 \times 10^{-5}$	542.238	$5.000 \times 10^8$
$G$	3.966	5.875	1.153	10.819
$R^2$	0.3579	0.3656	0.5281	0.7578
$\chi^2$	1	1	1	1
<b>Sips</b>				
$K_S$ ( $\text{L}/\text{mg}$ )	$8.693 \times 10^{-8}$	$6.368 \times 10^{18}$	2.263	0.164
$a_S$ ( $\text{L}/\mu\text{g}$ )	$4.586 \times 10^{-8}$	$1.489 \times 10^{18}$	1.051	-35.443
$\beta_S$	5.026	-10.405	26.906	-0.887
$R^2$	0.3165	0.4514	0.0000	0.9187
$\chi^2$	1	1	1	1

The Redlich-Peterson parameters were also determined using the linear approach proposed por Wu et al. (2010) (data not shown); however, most of the constant values were negative. The range of the Redlich-Peterson constant varies from 0.01 to several hundred (Wu et al., 2010). Thus, none of the calculated parameters fit the ranges indicated in the literature

*Sips isotherm.* The Sips isotherms fits also do not follow this adsorption model. The value of  $R^2$  for the adsorption data of the AC 2 in the Paranoá lake water were 0.9187. This does not mean that the fit was correct, since the values of the constants were negative, which as previously commented,

lacks physical significance. The fits for the isotherm adjustments for AC 1 data presented values outside those usually found in the literature (Debrassi et al., 2011; Nethaji et al., 2012).

To date, only a few studies related to the CYN adsorption under water treatment plant conditions, have been done (Ho et al., 2008; Ho et al., 2011). Any of the consulted literature involving adsorption of CYN onto AC presented attempts to fit the data to the Redlich-Peterson or Sips models. It should be mentioned that in the present study an extract obtained from lyophilized cells of *C. raciborskii* was used to spike ultrapure water and Paranoá Lake water. Thus, the cytoplasmic organic dissolved matter from cells could influence the adsorption of CYN in both matrixes. Nevertheless, dissolved organic matter analyses were not performed.

## CONCLUSIONS

In summary, synthesised carbons presented physics characteristics favourable to CYN adsorption. Based on kinetic experiments, a higher predominance of mesopores on AC 1 led to a greater CYN adsorption rate.

None of the isotherm models fit to the experimental data. One of the possible explanations is the interference of the organic matter and its competition for the adsorption surface. New studies and isotherm models adjustments can be performed in order to include the influence of the organic matter on the adsorption of CYN.

In pursuance for knowing exactly the influence of organic matter in Paranoa Lake water, analyses of dissolved organic matter of the water matrix should be performed.

Furthermore, the present study points out to a necessity of producing others activated carbons under different conditions such as different acid ratio or incorporation of functional groups on carbon surface that could improve the affinity with CYN molecules.

## REFERENCES

- Alshabanat, M., Alsenani, G., Almufarij, R. (2013) Removal of crystal violet dye from aqueous solutions onto date palm fiber by adsorption technique. *Journal of Chemistry*, **2013**, 1-6.
- ASTM (2014) Practice for Determination of Adsorptive Capacity of Activated Carbon by Aqueous Phase Isotherm Technique. In, ASTM Standards, 1-4.
- Bittencourt-Oliveira, M. d. C., Piccin-Santos, V., Moura, A. d. N., Aragão-Tavares, N. K. C., Cordeiro-Araújo, M. K. (2014) Cyanobacteria, microcystins and cylindrospermopsin in public drinking supply reservoirs of Brazil. *Anais da Academia Brasileira de Ciências*, **86**(1), 297-310.
- Costa, D. S., Vizzotto, C. S., Primo, M. d. C., Brandão, C. C. S., (2012) Remoção de Cylindrospermopsina por meio de Adsorção em Carvões Ativados Produzidos no Brasil. In: *Congresso da AIDIS – Associação Interamericana de Engenharia Sanitária e Ambiental*, ABES – Associação Brasileira de Engenharia Sanitária e Ambiental, Salvador/BA, Brasil, 8.
- Debrassi, A., Largura, M. C. T., Rodrigues, C. A. (2011) Adsorção do corante vermelho congo por derivados da o-carboximetilquitosana hidrofobicamente modificados. *Química nova*, **34**(5), 764-770.
- Falconer, I. R. (2005) Cyanobacterial toxins of drinking water supplies: cylindrospermopsins and microcystins, CRC Press, Boca Ratón.
- Foo, K. Y., Hameed B. H. (2010) Insights into the modeling of adsorption isotherm systems. *Chemical Engineering Journal*, **156**(1), 2-10.
- Freundlich, H. (1907) Über die adsorption in lösungen. *Zeitschrift für physikalische Chemie*, **57**(1),

385-470.

- Ho, L., Lambling, P., Bustamante, H., Duker, P., Newcombe, G. (2011) Application of powdered activated carbon for the adsorption of cylindrospermopsin and microcystin toxins from drinking water supplies. *Water Res*, **45**(9), 2954-2964.
- Ho, L., Slyman, N., Kaeding, U., Newcombe G. (2008) Optimizing PAC and chlorination practices for cylindrospermopsin removal. *Journal AWWA*, **100**(11), 88-96.
- Ho, Y. S., McKay, G. (1999) Pseudo-second order model for sorption processes. *Process Biochemistry*, **34**(5), 451-465.
- Humpage, A. R., Falconer, I. R. (2003) Oral toxicity of the cyanobacterial toxin cylindrospermopsin in male Swiss albino mice: determination of no observed adverse effect level for deriving a drinking water guideline value. *Environ Toxicol*, **18**(2), 94-103.
- Lagergren, S. (1898) Zur theorie der sogenannten adsorption geloster stoffe. *Kungliga svenska vetenskapsakademiens. Handlingar*, **24**, 1-39.
- Moreno-Castilla, C., López-Ramón, M. V., Carrasco-Marín, F. (2000) Changes in surface chemistry of activated carbons by wet oxidation. *Carbon*, **38**(14), 1995-2001.
- Nethaji, S., Sivasamy, A., Mandal, A. B. (2012) Adsorption isotherms, kinetics and mechanism for the adsorption of cationic and anionic dyes onto carbonaceous particles prepared from *Juglans regia* shell biomass. *International Journal of Environmental Science and Technology*, **10**(2), 231-242.
- Ohtani, I., Moore, R. E., Runnegar, M. T. C. (1992) Cylindrospermopsin: A Potent Hepatotoxin from the Blue-Green Alga *Cylindrospermopsis raciborskii*. *Journal of the American Chemical Society*, **114**(20), 7941-7942.
- Prauchner, M. J., Rodríguez-Reinoso, F. (2012) Chemical versus physical activation of coconut shell: a comparative study. *Microporous and Mesoporous Materials*, **152**, 163-171.
- Roginsky, S., Zeldovich, J. (1934) The catalytic oxidation of carbon monoxide on manganese dioxide. *Acta Physicochimica U.R.S.S.*, **1**, 554.
- Valencia-Cárdenas, D. (2016) Avaliação em escala de bancada da remoção de *Cylindrospermopsis raciborskii* e cilindrospermopsinas pelo processo combinado de flotação e adsorção em carvão ativado utilizando quitosana e sulfato de alumínio como coagulantes. Mestrado Dissertação, Tecnologia Ambiental e Recursos Hídricos, Departamento de Engenharia Civil e Ambiental, Universidade de Brasília, Brasília.
- Weber, W. J., Morris, J. C. (1963) Kinetics of adsorption on carbon from solution. *Journal of the Sanitary Engineering Division*, **89**(2), 31-60.
- Wu, F.-C., Liu, B.-L., Wu, K.-T., Tseng R.-L. (2010) A new linear form analysis of Redlich-Peterson isotherm equation for the adsorptions of dyes. *Chemical Engineering Journal*, **162**(1), 21-27.

# Energy Consumption Reduction and Utilization of Renewable Energy in Pump Stations

G. Gönczi\* and R. Kreka\*

\* Budapest Waterworks Co. Ltd., H-Budapest XIII., Váci út 23-27. (E-mails: [gabor.gonczi@vizmuvek.hu](mailto:gabor.gonczi@vizmuvek.hu); [ramon.kreka@vizmuvek.hu](mailto:ramon.kreka@vizmuvek.hu))

## Abstract

A theoretical research was conducted from 2016 to 2018 which aimed to reduce the head loss of pipe networks in the pump stations. The results were promising and predicted an average of head loss reduction by 30 %. Afterwards physical experiments were carried out to test the effectiveness of the new pipe designs. Two new prototype pipe sections were installed into one of our pump stations, during a R&D project. The experiment was successful as two unique pipe section installed in the discharge section reduced the head loss of the pump station by 25-26 %. According to these results we can set a target value of 30 % head loss reduction at full pump station pipe reconstruction, this makes the technology financially recoverable. The electrical costs of the pump station operation can be reduced by 1 % with the reduction of pressure loss.

The utilisation of the excess heat capacity of drinking water in pump stations is not a new concept. The role of the heat exchanger in the system is crucial as it “takes out” the excess heat capacity from water so it has to meet multiple operational and water-safety criteria. Currently there are no serial production heat exchangers on the market that meet all the criteria and can be installed in pump stations without any modification. Our newly developed heat exchanger for discharge pipe installation meets all the criteria and works without drinking water extraction, it can be attached to heat pump systems available on the market. The utilisation of the excess heat capacity of the drinking water was highly effective as the coefficient of performance (COP) value of the test system was 4.6, which is above the average COP value of the corresponding heat pump systems. With this technology the efficient heating of the pump houses and surrounding offices is achievable.

## Keywords

Energy consumption reduction; pressure loss; turbulent flow; excess heat capacity; drinking water heat exchanger

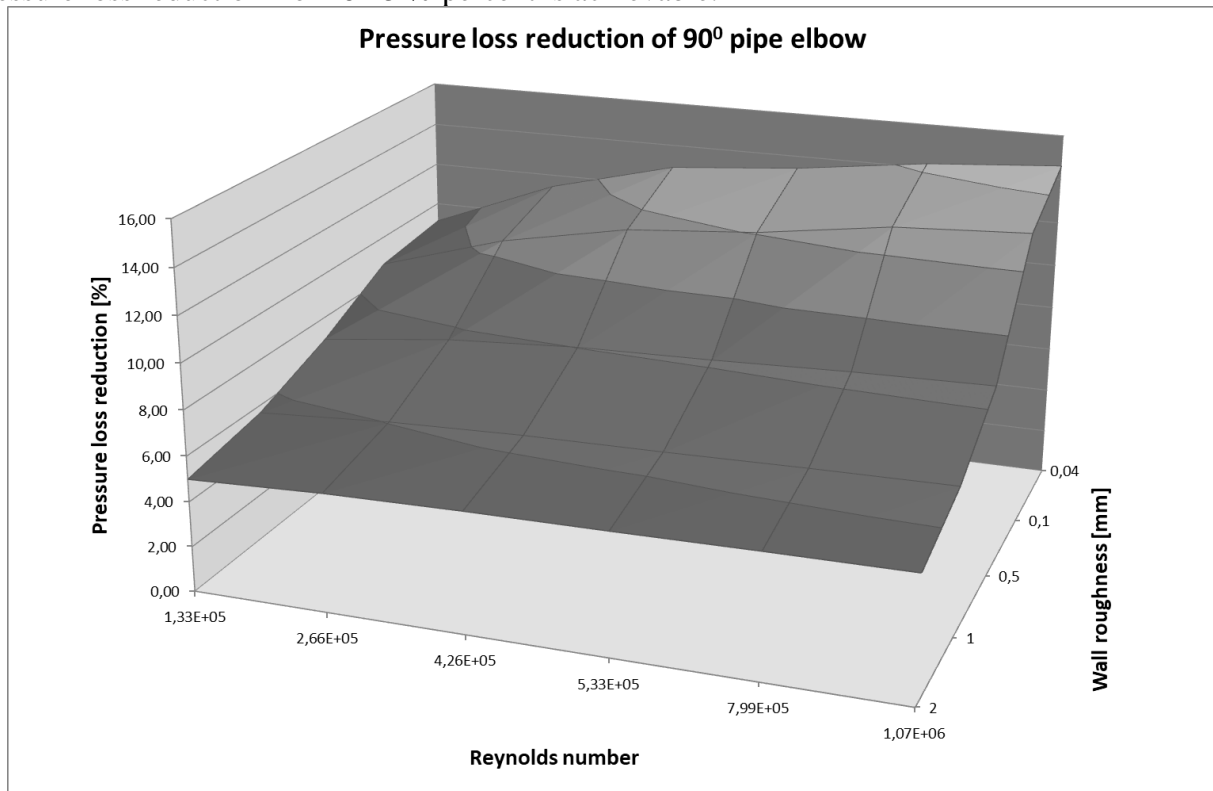
## INTRODUCTION

One of the main focuses of water utility companies is the energy efficient supply of drinking water. Pump stations are key locations in energy efficiency. They have the highest velocity values of the water network system and the highest pressure loss values are also present here. Reduction of pressure loss at these facilities is the most feasible and most advantageous solution. Pump houses also provide an accessible location for the utilisation of the drinking water's excess heat capacity which can be used for the heating of the surrounding facilities.

## ENERGY CONSUMPTION REDUCTION

A theoretical research was conducted from 2016 to 2018 which aimed to reduce the head loss of pipe networks in the pump stations. The analysis used a new method to reduce pressure loss. Numerical calculations were carried out on the original standard pipe elements to determine the problematic fluid dynamic zones where pressure loss occurs. The two indicator quantities of these zones are turbulence kinetic energy and streamlines of the section. The problematic zones have a high turbulence kinetic energy value and the streamlines in and near these zones are not parallel to each other. After the problematic zones are identified geometry changes aiming to reduce these can be made and tested numerically.

The first pipe element that was analysed was a standard 90° degree pipe elbow with R1,5 radius. With modifying the internal geometry depending on the flow velocity and surface roughness a pressure loss reduction from 6-15 % percent is achievable.



**Figure 1.** Pressure loss reduction of 90° degree pipe elbow

The theoretical research continued on pump house pipe systems, in this approach the whole pump house pipe system was analysed and geometrical changes were carried out on the whole length of the pipe system taking into account how the flow of the individual element effect each other. The results were promising and predicted an average of head loss reduction by 30 %.

### Physical experiment on new prototype pipe elements

Afterwards physical experiments were carried out to test the effectiveness of the new pipe design methodology. Two new prototype pipe elements were installed into one of our pump stations, during a R&D project. A conventional T pipe junction was replaced by a modified pipe junction geometry and a pipe elbow was also replaced with modified geometry just after the pump.



**Figure 2.** New pipe elements in the discharge pip of the pump house

The experiment was successful as two unique pipe elements installed in the discharge pipe section reduced the head loss of the pump station by 25-26 %.

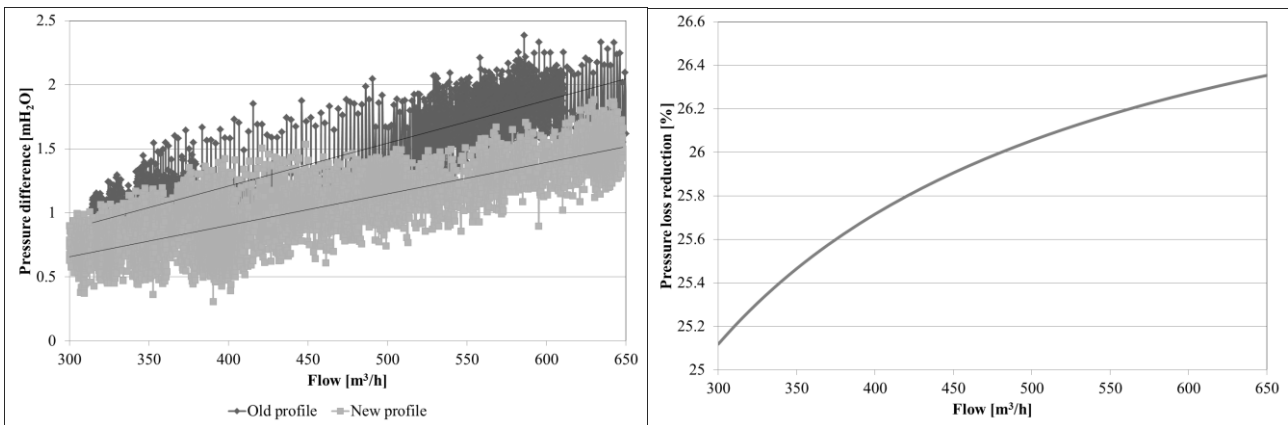


Figure 2. Result of the two prototype pipe sections

**Integrating new pipe design methodology in to pump house reconstruction**

The developed pipe design technology can be applied at pump house reconstruction where old pipes need to be changed. To prove that this methodology of pipe design is better than a conventional method we compared an existing reconstruction pipe geometry plan with a geometry designed by the new methodology.

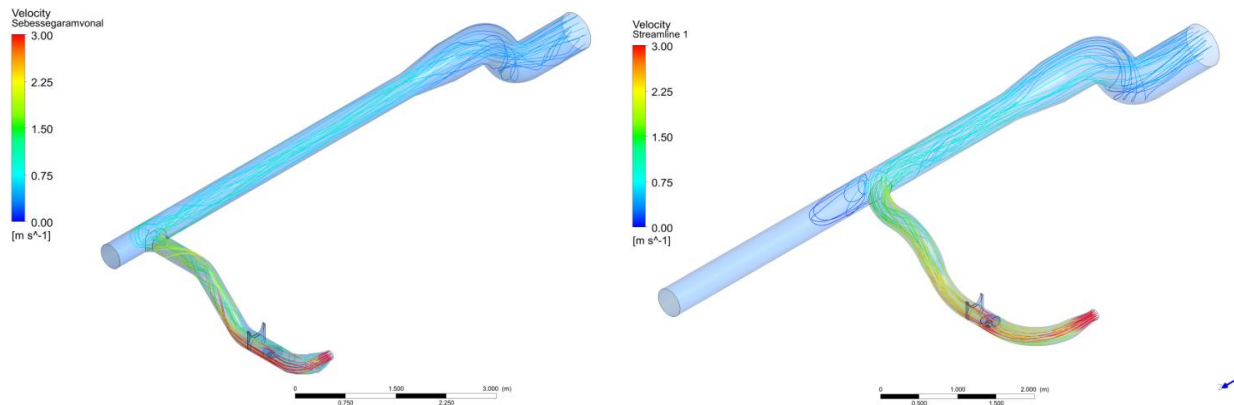


Figure 3. Left Pipe geometry with conventional design method. Right: Pipe geometry with new design methodology

Table 1. Comparing the pressure loss of the two pipe designs

	[Pa]	[mH <sub>2</sub> O]	Pressure loss reduction [%]
Pressure loss in the original pipe design	5663.4	0.58	
Pressure loss reduction in the new design	3611.5	0.37	<b>36.21</b>



According to these results we can set a target value of 30 % head loss reduction at full pump station pipe reconstruction, this makes the technology financially recoverable. The electrical costs of the pump station operation can be reduced by 1 % with the reduction of pressure loss. Furthermore the new pipe elements reduce the chance of impeller damage caused by instable flow and it also reduces the damage caused by highly turbulent flow on valves and check valves.

### **UTILIZATION OF RENEWABLE ENERGY IN PUMP STATIONS**

The utilisation of the excess heat capacity of drinking water in pump stations is not a new concept. The first device at our company was installed to a gravitational channel where the 7-13 °C drinking water was directly diverted to a heat exchanger and via a heat pump the heating of the nearby service building was achievable. Multiple studies were made in this topic throughout the years regarding how to utilise the excess heat capacity of drinking water. All of them highlighted the heat exchanger as the primary problem of the system as currently there is no such heat exchanger on the market that is suitable for utilisation in drinking water. Utilisation of a heat exchanger in drinking water environment poses a huge water quality risk as the hydrochlorofluorocarbon (HFC) working fluid in the heat pump can mix with drinking water in case of failure. Other water quality issues with standard heat exchangers are the risk of formation of low velocity/ stagnant zones in the small diameter tubular system of the exchanger and in case of cooling operation of the heat pump the drinking water in the heat exchanger can warm up to biologically critical values. This is why we decided to design a new heat exchanger which can be utilised in drinking water environment.

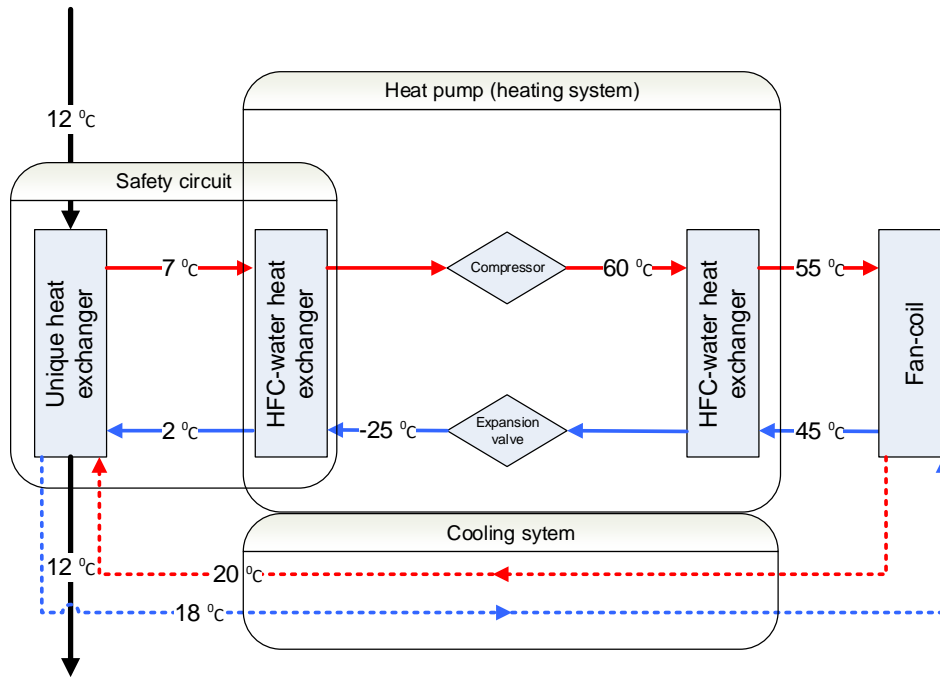
#### **Objectives of the new heat exchanger design**

The role of the heat exchanger in the system is crucial as it “takes out” the excess heat capacity from the drinking water so it has to meet multiple strict operational and water-safety criteria which are the following:

- The material of the heat exchanger must be stainless steel.
- The device must withstand 150 % of the operational pressure. The pressure must be different in the primer and secondary circuit of the heat exchanger.
- The pressure of the secondary circuit pump cannot exceed the operational pressure of drinking water pipe system even at valve closing peak pressures.
- The operation of the circulatory pumps must be immediately stopped and the safety valves should be closed when pressure fluctuates over 0.5 [bar] from the pre-set values.

#### **Concept of the heat exchanger**

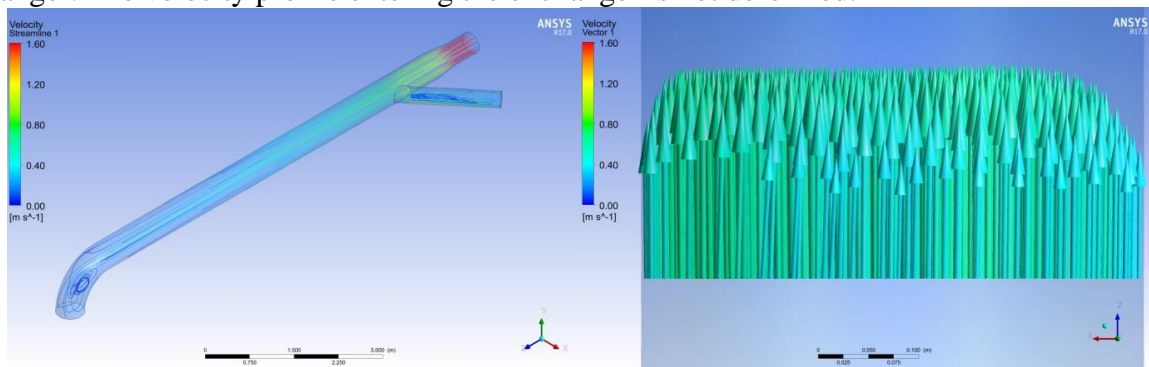
Currently there are no serial production heat exchangers on the market that meet all the criteria and can be installed in pump stations without any modification. Our newly developed heat exchanger for discharge pipe installation meets all the criteria and works without drinking water extraction, it can be attached to heat pump systems available on the market. The heat exchanger is connected to the heat pump via a safety circuit (filled with water), this eliminates the possibility of HFC contamination in case of failure. During heating operation the heat pump extracts the excess heat from the drinking water pipe by adding mechanical work and elevating the temperature of the working substance. During cooling operation the heat pump can be bypassed as the drinking water temperature is 12 °C on average in summer period.



**Figure 4.** Schematics of the system

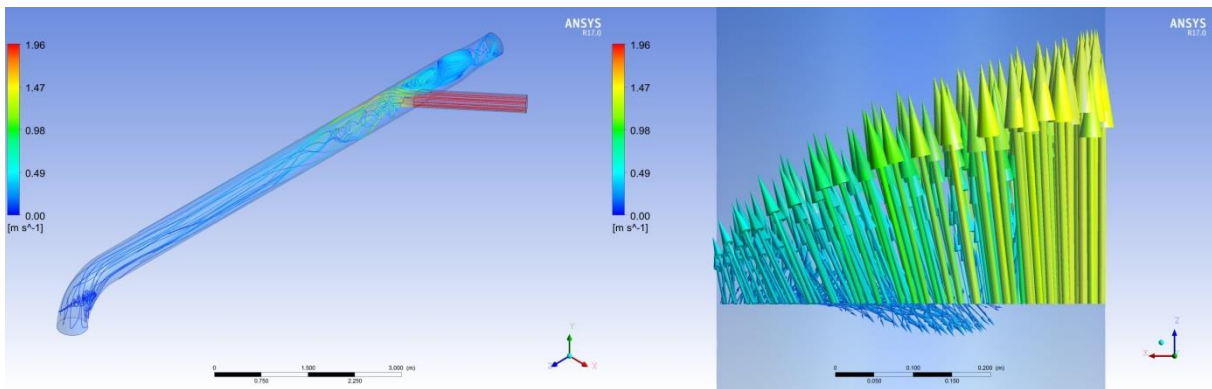
**Placement of the prototype heat exchanger**

Selecting the correct drinking water pipe is crucial for the efficient operation of the heat pump. The pipe must have at least DN 300 diameter and a minimum continuous flow of 0.5 m/s to have enough excess heat capacity for utilisation. The only place that fulfils these criteria are the pump houses, but there are some limitations here also. Multiple pump hoses have a periodic operation for example pump houses that are filling a reservoir periodically. These pump houses stop at night so during this period no heat extraction is possible thus hindering the possibility of heating or cooling. The location of the pipe within the pump house is also crucial due to the pressure criteria (pressure must be lower in the secondary circuit). The heat exchanger can only be installed at the collector discharge pipe where the pressure is high and there is continuous flow dependent of witch pump is operating. We selected Budafoki pump house as the site to test the prototype heat exchanger and the heat pump system because the pump house is being renovating and new offices and working quarters are being created and the new system can provide heating and cooling for these premises. The pump house has four pumps which are connected by a 4.892 m long collector pipe, this is an ideal place to install the heat exchanger. The pump house has a continuous operation also, with a flow ranging from 400 to 800 m<sup>3</sup>/h. The operation of the first, second, and third pump has no effect on the heat exchanger. The velocity profile entering the exchanger is not deformed.



**Figure 5.** Inlet velocity profile of the heat exchanger at the operation of the second pump at a flow rate of 700 m<sup>3</sup>/h

The connection of the fourth pump is the closest to the heat exchanger section. The operation of this pump alters the velocity profile entering to the exchanger.

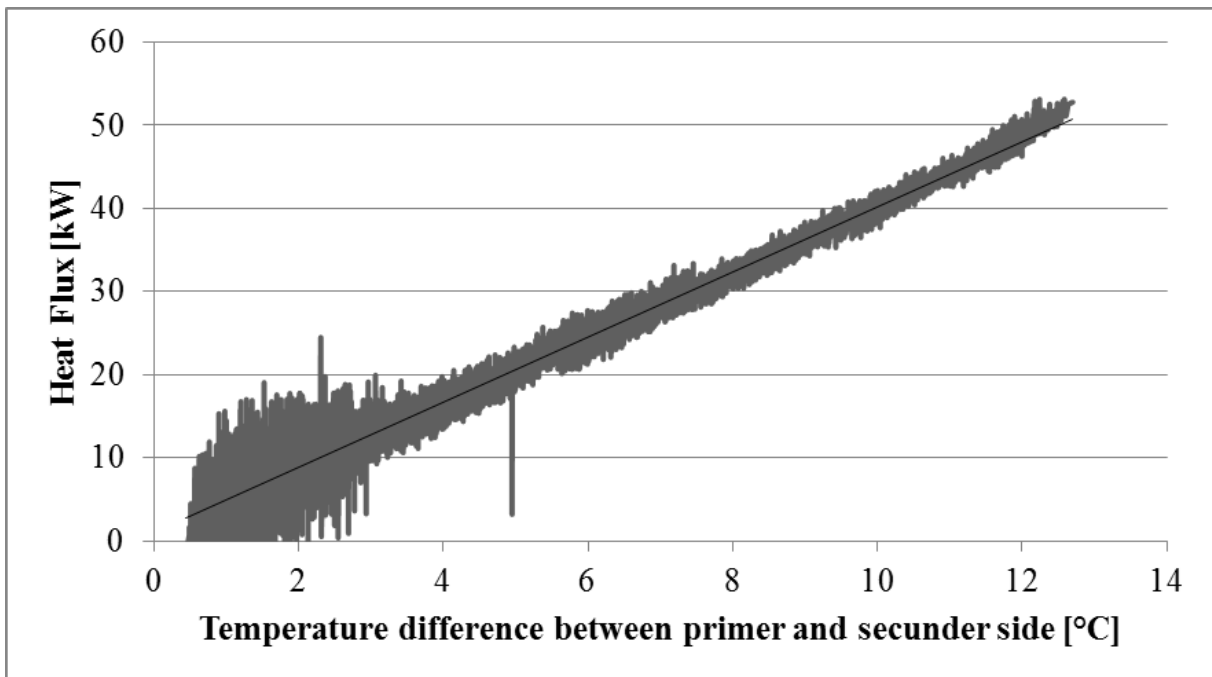


**Figure 6.** Inlet velocity profile of the heat exchanger at the operation of the fourth pump at a flow rate of 480 m<sup>3</sup>/h

Typically the first and second pump operate, which have rev. control so the new heat exchanger was designed for the undisturbed velocity profile. A 10 % of efficiency decrease is present in case the fourth pump is operating due to the disturbed velocity profile.

**Testing the prototype heat exchanger**

We tested the unique heat exchanger before coupling it to the heat pump system. The useful output of the heat exchanger is between 8 and 20 kW when the flow rate of the secondary circuit is 1.47 l/s and the temperature difference between the two circuits is 2-5 °C.



**Figure 7.** Left: performance of prototype heat exchanger

After the successful test of the heat exchanger we connected it to the heat pump system and the test operation started from 2019 January. During the heating test operation the system operated flawlessly providing efficiency values as expected, coefficient of performance (COP) value of 4.6

was achieved which is above the average value of ground water heat pump systems.

**Table 2.** Test operation during 6 °C outside temperature

<i>COP</i>	4,6
Heating demand	14,6 [kW]
Heat gained from drinking water	11,4 [kW]
Electrical power usage	3,2 [kW]

## CONCLUISON

Energy consumption reduction in pump houses is possible via the new methodology of pipe design. According to the results 30 % of head loss reduction is possible. The electrical costs of the pump station operation can be reduced by 1 %, this means savings in the magnitude of multiple thousands Euros. Furthermore the new pipe elements reduce the chance of impeller damage caused by instable flow and it also reduces the damage caused by highly turbulent flow on valves and check valves.

The utilisation of the excess heat capacity of drinking water is possible with our new heat exchanger design, without any water quality risk or induced pressure loss. The exchanger coupled to a standard heat pump can provide heating and cooling to the pump house and premises, with above average COP values.

## REFERENCES

- György, J. (1995) Csővezetékek és csővezeték elemek, (in Hungarian).
- Hiliding Beij, K. (1938) Pressure losses for fluid flow in 900 pipe bends. Part of Journal of Research of the National Bureau of Standards, Volume 21.
- Tu, J., Yeoh, G. H., Liu, C. (2008) Computational Fluid Dynamics a Practical Approach.
- János, B. (2000) Műszaki hőtán mérnököknek
- Yener, Y., Kakac, S. (1979) Heat Conduction.

# Improving Quality of Drinking Water in the Water Treatment Plant by Decrease of Hardness with Respect to Sodium Concentration Control

O. R. Govedarica\*, V. N. Rajaković-Ognjanović, A. R. Đukić, B. M. Lekić and B. B. Babić

\* Institute for Hydraulic and Environmental Engineering Faculty of Civil Engineering, University of Belgrade, Bulevar kralja Aleksandra 73, Belgrade, Serbia (E-mail: [ogovedarica@grf.bg.ac.rs](mailto:ogovedarica@grf.bg.ac.rs))

## Abstract

In this research the object of the analysis was the groundwater used for drinking which needs certain improvements. Improvements involve removal of magnesium and manganese. Improvements also mean the choice of proper water treatment technology which could meet the standards for drinking water quality. Technologies that are suitable for removal of these ions vary from classical to modern. Lime was not considered, ion exchange was an option, but membrane technologies were the ones that meet all the criteria. Since reverse osmosis (RO) is very expensive, and nanofiltration (NF) meets the required removal demands, meaning removal of divalent ions, it has been selected as the right choice for this case.

## Keywords

Drinking water; hardness; membrane technologies; ion exchange

## INTRODUCTION

Raw groundwater usually doesn't meet the standards expected from drinking water quality with respect to water hardness, sodium, nitrate and heavy metal ions (iron and manganese) concentrations (Azimi et al., 2019). Water hardness is one of the issues that has been in focus from different aspects, which cover maintenance of the equipment and reliability of water supply network. With increased consumption and demand for better drinking water quality, softening has become even more important (Boyd et al., 2016; Sanjuan et al., 2019). The choice and the application of technologies for softening differ according to quality of raw water and specific demands (available space, cost, trained operators, etc.).

Lime has been traditionally used for removal of ions of calcium, magnesium. Cold lime softening has disadvantages (the consumption of the chemicals and disposal of sludge) that decrease the usage of this technology in comparison to other known technologies (Van der Bruggen and Vandecasteele, 2003). Ion exchange has been successfully used for removal of ions of calcium, magnesium, and softening of groundwater, together with removal of organic substances (Levchuk et al., 2018). In the field of ion exchange sorbents are still improved and thoroughly studied. Different types of sorbents, such as zeolites, carbon nanotubes, activated carbon, graphenes, antibacterial hydrogel beads have been tested for softening of water (Fernandez et al., 2016; Shahmirzadi et al., 2018; Mohammadian et al., 2019). Ion exchange with natural zeolite as sorbent has many benefits, specially from financial and environmental aspect (Hailu et al., 2019). Membrane technologies used for separation and removal of different ions from water have also been applied for water softening. When considering membrane technologies, both reverse osmosis and nanofiltration can be applied. Considering specific task, the removal of divalent ions such as magnesium and calcium, the best option is nanofiltration (Hamayoo et al., 2010; Nanda et al., 2010; Rahimpour et al., 2010). In Figure 1 the effectiveness of different membrane technologies is presented.

In this research the object of the analysis was the groundwater used for drinking in the existing

water treatment plant in Serbia. Analysis showed that the concentration of magnesium and manganese exceed the limited values. The goal was to choose the proper water treatment technology which could meet the standards for drinking water quality.

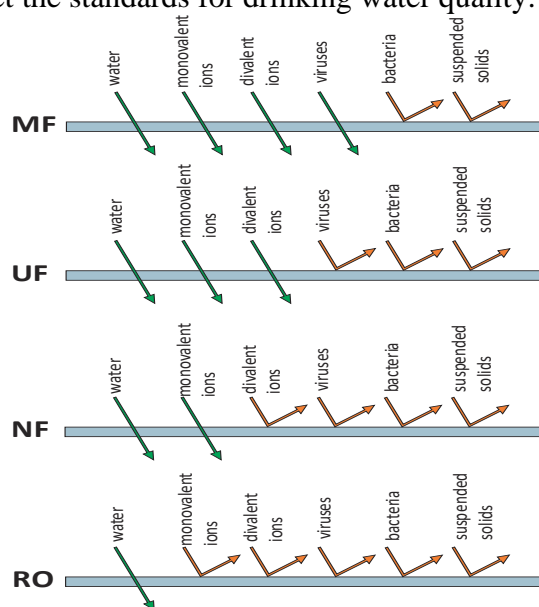


Figure 1. Comparison of effective removal of membrane technologies

**EXPERIMENTAL PART**

As mentioned, the object of the research was the analysis of drinking water that is produces in the existing water treatment plant in Serbia.

Table 1. The applied analytical methods

Parameter	Applied analytical methods and standards	Instrumental technique
<b>Physical-Chemical parameters</b>		
pH value	Electrometric method, 4500-H <sup>+</sup> B *	WTW pHmeter 340i
Conductivity	EPA 120.1:1982	Conductivity meter
UV	UV-Vis spectrometry	UV-Vis Sp.photometer
p-alkalinity	SMEW 22ND:2320B	Volummetric
m- alkalinity	SMEW 22ND:2320B	Volummetric
HCO <sub>3</sub> <sup>-</sup>	SMEW 22ND:2320B	Volummetric
Total hardness	SMEW 22ND:2320B	Volummetric
TOC		
Consumption of KMnO <sub>4</sub>	SRPS EN ISO 8467:2007	Volummetric
<b>Cations</b>		
(Na <sup>+</sup> , K <sup>+</sup> , Mg <sup>2+</sup> , Ca <sup>2+</sup> )	ISO 14911:1998	Ion Chromatography
<b>Anions</b>		
(Cl <sup>-</sup> , SO <sub>4</sub> <sup>2-</sup> )	ISO 10304-1:2007	Ion Chromatography
Ba <sup>2+</sup> , Be <sup>2+</sup> , B <sup>3+</sup> , Cu <sup>2+</sup> , Zn <sup>2+</sup> , Si <sup>4+</sup> , Se <sup>4+</sup> , Sr <sup>2+</sup> , Hg <sup>2+</sup> , As <sup>3,5+</sup> , Al <sup>3+</sup>	Atomic absorption spectroscopy (AAS), SM 3111b:1999;	AAS, Perkin Elmer 4100ZL Agilent 7500ce ICP-MS system

\* APHA, AWWA, WEF 2012 Standard methods for the examination of water and wastewater, 22nd edition

Currently water doesn't meet the standards for drinking water quality. The standard that is considered is National regulation on hygienic quality of drinking water, published in Official gazette of Republic of Serbia 42/98 and 44/99, published in Official gazette of Republic of Serbia 28/2019. List of measured parameters, instrumental techniques and analytical methods are presented in Table 1.

## RESULTS AND DISCUSSION

Within this part the results of the analysis of the quality of drinking water are presented. Besides, the technological scheme and current treatment are described and illustrated in Figure 2. In Table 2 the measured values of water quality parameters are presented. The values which exceed maximal allowed values are presented in bold.

### Water quality in existing water treatment plant: current status

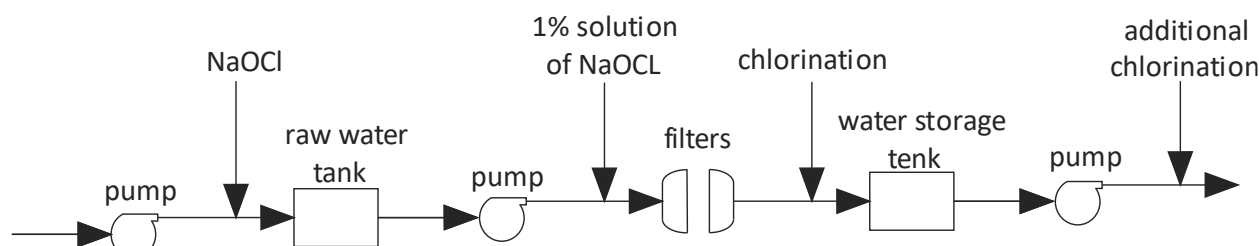
**Table 2** Water quality analysis

Analysed parameters	Unit	Proscribed values	Inlet water	Outlet water
pH	-	6.8-8.5	7.25	7.66
Conductivity	μS/cm	<2500	1297	1387
UV	l/cm	/	0.048	0.062
p-alkalinity	mg CaCO <sub>3</sub> /L	/	0	0
m- alkalinity	mg CaCO <sub>3</sub> /L	/	555.5	580.0
HCO <sub>3</sub> <sup>-</sup>	mg/L	/	677.7	680.8
Total hardness	mg CaCO <sub>3</sub> /L	/	524.5	542.5
TOC	mgC/L	/	2.82	3.22
Consumption of KMnO <sub>4</sub>		<8	3.77	1.26
Cl <sup>-</sup>		250.0	69.58	96.34
SO <sub>4</sub> <sup>2-</sup>		250.0	53.54	65.54
Ca <sup>2+</sup>		200.0	131.14	133.15
Mg <sup>2+</sup>	mg/L	50.0	47.85	<b>51.01</b>
Na <sup>+</sup>		200.0	/	111.0
K <sup>+</sup>		12.0	3.99	4.16
Fe <sup>2,3+</sup>		0.3	0.07	<0.005
Mn <sup>2,4+</sup>		0.05	<b>0.11</b>	<b>0.09</b>
Ba <sup>2+</sup>		700.0	256.9	256.9
Be <sup>2+</sup>		/	<5	<5
B <sup>3+</sup>		1000.0	<20	<20
Cu <sup>2+</sup>		2000.0	<2	4.6
Zn <sup>2+</sup>		3000.0	11.6	19.6
Si <sup>4+</sup>	μg/L	/	29.6	29.3
Se <sup>4+</sup>		10.0	<20	<20
Sr <sup>2+</sup>		/	690.1	720.1
Hg <sup>2+</sup>		1.0	<1	<1
As <sup>3,5+</sup>		10.0	<20	<20
Al <sup>3+</sup>		200.0	<40	<40

The existing drinking water treatment plant is designed for capacity of 70 L/s, with two parallel lines, each with capacity of 35 L/s. The technological scheme and operations are described in the following paragraph. The feed water is groundwater which is being pumped and stored in the tank for raw water. Before entering the tank sodium-hypochlorite is added to water due to the oxidation of iron and manganese. Water from the tank is pumped further to the filters. Before filtration, a 1 %

solution of sodium-hypochlorite and flocculant (if necessary) is added. Filtration consists of two pairs of filters: sand filters which have layers of quartz as catalyst and anthracite and active carbon filters. After filtration, the water is stored in water storage tank. Additional chlorination and control of residual chlorine are also part of technological operational line.

As presented in Table 2 the parameters that are above the maximal proscribed values are:  $Mn^{2+}$  content,  $Mg^{2+}$  content and even though the water hardness is not limited it needs to be taken into account as it will affect the reliability of water supply networks and cause precipitation of  $CaCO_3$ . Also, it can be noticed that  $Na^+$  concentration is very high. Special task is to maintain sodium concentration after the treatment below the limited values.



**Figure 2.** Existing drinking water plant technological scheme

### Technologies for improvement of water quality: removal of water hardness and sodium

For improvement of existing water quality, or even more precisely, for meeting the standards for drinking water quality and for reaching adequate water quality in distribution network and for drinking water supply several technologies have been considered.

Since manganese concentration and magnesium concentration are above the maximum permissible value and sodium concentration and water hardness are very high (it gets higher than 500 mg  $CaCO_3/L$ ), one of the options for improved water treatment is ion exchange technology. As mentioned before, water hardness is not a parameter that has defined maximum value, but what is important is that for high value of water hardness there are lots of negative effects (Van der Bruggen et al., 2009). The most pronounced are negative effects on:

- the functionality of process equipment (it is rapidly destroyed)
- the distribution network that manifest through precipitation of carbonates on the surface of pipes, and
- the quality of drinking water, which can be observed by the complains of the consumers.

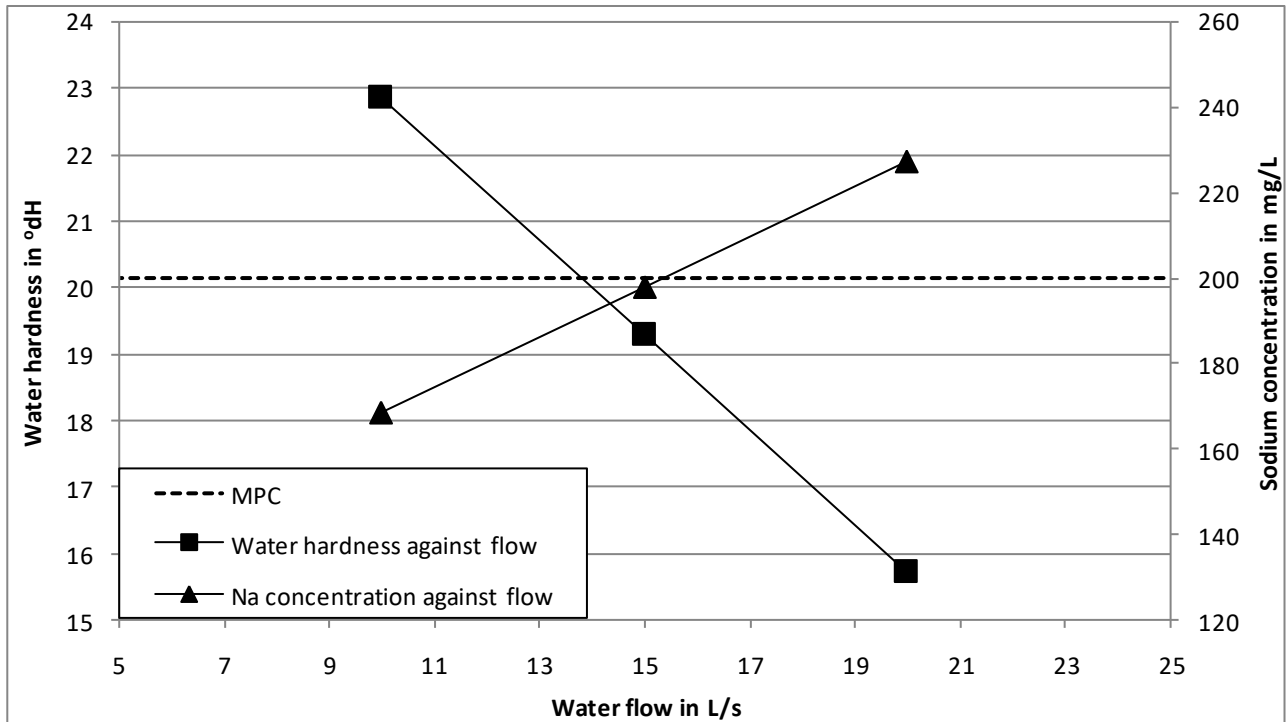
One of the technologies that are often used are ion exchange processes. In the ion-exchange processes  $Mg^{2+}$  and  $Ca^{2+}$  ions are substituted by  $Na^+$ -ions, as presented in equation (1):



When calculations based on the effect of added NaCl are done, it can be concluded that for removal of one German degree of hardness ( $^{\circ}dH$ ) or 17.9 mg/L of  $CaCO_3$ , the concentration of  $Na^+$  increases for 8.2 mg/L. When these calculations are adopted and applied for this case the effectiveness of softening can be illustrated as presented in Figure 2.

From looking at Figure 3 it can be seen that for water hardness of 19.2  $^{\circ}dH$ , concentration of  $Na^+$  is 200 mg/L, and water flow through ion exchange resin is 15.37 L/s. Since the optimal value of hardness from the operational perspective and recommended values according to experienced utilities is around 10  $^{\circ}dH$ , value of  $Na^+$  would be far above the regulated value.

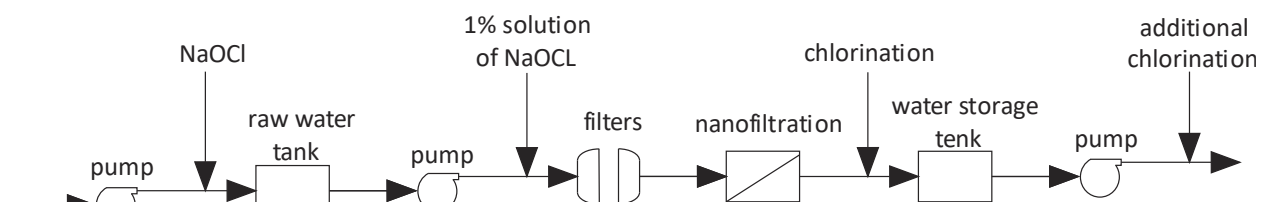




**Figure 3.** Calculations based on the effect of added NaCl for existing water quality on water hardness and sodium concentration depending on the water flow

For this reason the option of using ion-exchange technology for removal of water hardness is not the best option. In analysed water concentration of Na<sup>+</sup>-ions is already relatively high. When additional Na<sup>+</sup>-ions are released in water it is more than probable that the maximal concentration for Na<sup>+</sup>-ions in drinking water will be exceeded.

As mentioned in the introduction, membrane filtration processes can be applied for water softening. Reverse osmosis (RO), was one of the options that was considered. RO is a technology used in the desalination process of sea water, as well as in water treatment in pharmaceutical and electronics industry (Magara et al., 2000; Le and Nunes, 2016; Tang et al., 2017). The reverse osmosis process allows the removal of, practically, all ions from the water. Separation takes place not only on the basis of pore size, but also due to the interaction between charged particles and membrane material. Reverse osmosis requires high pressure. The use of RO in the water treatment is very expensive, therefore nanofiltration (NF) was also taken into consideration. NF is a membrane filtration process widely used for separating multivalent solutes from univalent salts, as presented in Figure 3. And NF, unlike RO, requires low pressure (Labban et al, 2017). It is a potential and pressure-driven membrane separation process that is finding widespread use in the treatment of water, wastewater and seawater, particularly for water-softening applications (Mohammad et al., 2015; Su et al., 2015). The technological scheme with recommended treatment is illustrated in Figure 4.



**Figure 4.** Recommended drinking water plant technological scheme

## CONCLUDING REMARKS: RECOMMENDED TECHNOLOGY

Since water quality of the existing water treatment plants can change over time there is a need for improvement or reconstruction of the existing plants. That was the case in this research. The improvements in this case had to involve removal of magnesium and manganese. Both of these ions are divalent ions. Technologies that are suitable for removal of these ions vary from classical to modern. As shown ion exchange was an option, but since there is expected increase of sodium concentration after ion exchange treatment it had to be rejected. Membrane technologies were fulfilling all the expectations. Since reverse osmosis (RO) is very expensive, nanofiltration (NF) meets the required removal demands it has been selected as the right choice for this case.

## REFERENCES

- Azimi, S., Azhdary Moghaddam, M., Hashemi Monfared S. A. (2019) Prediction of annual drinking water quality reduction based on Groundwater Resource Index using the artificial neural network and fuzzy clustering. *Journal of Contaminant Hydrology*, **220**, 6-17.
- Boyd, C. E., Tucker, C. S., Somridhvej, B. (2016) Alkalinity and hardness: critical but elusive concepts in aquaculture. *Journal of the World Aquaculture Society*, **47**(1), 6-41.
- Fernandez, E., Vidal, L., Canals, A. (2016) Zeolite/iron oxide composite as sorbent for magnetic solid-phase extraction of benzene, toluene, ethylbenzene and xylenes from water samples prior to gas chromatography-mass spectrometry. *Journal of Chromatography A*, **1458**, 18-24.
- Hailu, Y., Tilahun, E., Brhane, A., Resky, H., Sahu, O. (2019) Ion exchanges for calcium magnesium and total hardness from ground water with natural zeolite. *Groundwater for Sustainable Development*, **8**, 457-467.
- Homayoonfal, M., Akbari, A., Reza Mehrnia, M. (2010) Preparation of polysulfone nanofiltration membranes by UV-assisted grafting polymerization for water softening. *Desalination*, **263**, 217-225.
- Levchuk, I., Marquez, J. J. R., Sillanpaa, M. (2018) Removal of natural organic matter (NOM) from water by ion exchange – A review. *Chemosphere*, **192**, 90-104.
- Le, N. L., Nunes, S. P. (2016) Materials and membrane technologies for water and energy sustainability. *Sustainable Materials and Technologies*, **7**, 1-28.
- Lobban, O., Liu, C., Chong, T. H., Lienhard V, J. H. (2017) Fundamentals of low-pressure nanofiltration: Membrane characterization, modelling, and understanding the multi-ionic interactions in water softening. *Journal of Membrane Science*, **521**, 18-32.
- Magara, Y., Kawasaki, M., Sekino, M. (2000) Development of reverse osmosis membrane seawater desalination in Japan. *Water Science and Technology*, **41**(10-11), 1-8.
- Mogammad, A. W., Teow, Y. H., Amg, W. L., Chung, Y. T., Oatley-Radcliff, D. L., Hilal, N. (2015) Nanofiltration membranes review: Recent advances and future prospects. *Desalination*, **356**, 226-254.
- Mohammadian, M., Sahraei, R., Ghaemy, M. (2019) Synthesis and fabrication of antibacterial hydrogel beads based on modified-gum tragacanth/poly(vinyl alcohol)/Ag<sup>0</sup> highly efficient sorbent for hard water softening. *Chemosphere*, **225**, 259-269.
- Nanda, D., Tung, K. L., Li, Y. L., Lin, N. J., Chuang, C. J. (2010) Effect of pH on membrane morphology, fouling potential, and filtration performance of nanofiltration membrane for water softening. *Journal of Membrane Science*, **349**, 411-420.
- National regulation on hygienic quality of drinking water, Official gazette of Republic of Serbia 42/98 and 44/99.
- National regulation on hygienic quality of drinking water, Official gazette of Republic of Serbia 28/2019.
- Rahimpourt, A., Jahanshahi, M., Mortazavian, N., Madaeni, S. S., Mansourpanah, Y. (2010)

- Preparation and characterization of asymmetric polyethersulfone and thin-film composite polyamide nanofiltration membranes for water softening. *Applied Surface Science*, **256**, 1657-1663.
- Sanjuan, I., Benavente, D., Exposito, E., Montiel, V. (2019) Electrochemical water softening: Influence of water composition on the precipitation behavior. *Separation and Purification Technology*, **211**, 857-865.
- Shahmirzadi, M. A. A., Hosseini, S. S., Luo, J., Ortiz, I. (2018) Significance, evolution and recent advances in adsorption technology, materials and processes for desalination, water softening and salt removal. *Journal of Environmental Management*, **215**, 324-344.
- Su, B., Wu, T., Zhechao, L., Cong, X., Gao, X., Gao, C. (2015) Pilot study of seawater nanofiltration softening technology based on integrated membrane system. *Desalination*, **368**, 193-201.
- Tang, S. C. N., Birnhack, L., Nativ, P., Lahav, O. (2017) Highly-selective separation of divalent ions from seawater and seawater RO retentate. *Separation and Purification Technology*, **175**, 460-468.
- Van der Bruggen, B., Vandecasteele, C., (2003) Removal of pollutants from surface water and groundwater by nanofiltration: overview of possible application in the drinking water industry. *Environmental Pollution*, **122**, 435-445.
- Van der Bruggen, B., Goossens, H., Everard, P.A., Stemgee, K., Rogge, W. (2009) Cost-benefit analysis of central softening for production of drinking water. *Journal of Environmental Management*, **91**, 541-549.

# Fire and Drinking Water Capacity Enhancement in Water Distribution Networks

T. Huzsvár\*, R. Weber\* and C. J. Hos\*

\* Department of Hydrodynamic Systems, Budapest University of Technology and Economics, Muegyetem rkp. 3, Budapest 1111, Hungary (E-mails: [thuzsvar@hds.bme.hu](mailto:thuzsvar@hds.bme.hu); [rweber@hds.bme.hu](mailto:rweber@hds.bme.hu); [cshos@hds.bme.hu](mailto:cshos@hds.bme.hu))

## Abstract

The purpose of the present study is to introduce a newly developed capacity increment (also pressure sensitivity reduction) technique in the case of drinking water distribution systems (WDS). The main novelty of this method is based on a correlation between two parameters of the water distribution network – one characterises its robustness on a topology specific way, the other can be calculated with only one hydraulic simulation. With the help of connection the topology optimisation – the identification of the optimal place for installing a new pipe – can be determined within short processing time, and without the implementation of a stochastic optimiser algorithm. The first part of the paper presents high pressure sensitivity caused problems and introduce the mathematical background of the method, besides that it discusses the details of the algorithm. After that, the second part presents the results gained by the implementation of the method in two case studies: real-life water distribution systems of a small and a medium-sized town. For the small town, a verification is possible by comparing the result of our method with the total hydraulical evaluation of the WDS. The results indicate that the water capacity of these water distribution networks' critically sensitive area can be increased by ~20 % with connecting a new nearly hundred-meter-long pipe to sufficient locations of each networks. At last, the results of the case studies were analysed from viewpoint of the operating cost, and the results suggest that the operating point of the system after the topology modification remain the same as in their pre-modification states, thus the operating cost of the WDSs do not change.

## Keywords

Pressure sensitivity; topology optimisation; capacity increment; water distribution systems

## INTRODUCTION

The water distribution systems (WDSs) are crucially important infrastructural elements of every settlement (from small villages to large cities). Therefore, pressure fluctuations originating mostly from the unpredictable consumption variation inflict significant financial loss to the provider and discomfort to the inhabitants. As Ghorbani et al. (Ghorbani, 2016) found, this problem has two main aspects. On the first hand, if the pressure of the water distribution system decreases below a critical level, the consumers experience demand fulfilment injury as a consequence of the low outflow. Due to this phenomenon the providers in this area experience growth in the number of retail compliments and financial decrement. On the other hand, the water distribution systems supply water for the fire hydrants. If the system pressure falls below the minimal pressure requirement of the hydrants, the discharge rate of the hydrant is not adequate, thus it raises disaster management concerns and can cause a significant fine for the provider, as it is mentioned by Snyder et al. (Snyder, 2002). These pressure and demand uncertainties, as House-Peters and Chang (House-Peters, 2011) reviews, are originated from the nearly unpredictably complex human and natural processes, uncertainty and resilience across spatial and temporal scales. As a result, many researchers focus their effort on the pressure robustness increment of the WDSs. As Mala-Jetmarova et al. (Mala-Jetmarova, 2018) summarizes this, the commonly used method for WDS topology optimisation is the implementation of a stochastic global optimiser algorithm (e.g. genetic algorithm as Saldarriaga et al. (Saldarriaga, 2015) or self adaptive differential evolution as Zheng et al. (Zheng, 2013)) and forming one (or many different) objective function(s) (e.g. as Babayan et al. (Babayan, 1998)). In contrast, Pudar and Liggett (Pudar, 1992) were the first to use a fully analytical

optimisation technique where they used the nodal pressure sensitivity as a robustness property of a WDS for the identification of the unreported pipe bursts. Based on this work Izquierdo et al. (Izquierdo, 2008) used this method for the recognition of sundry and relative importance of different pipes in a water distribution network, and to help in assessing their impact on the hydraulic performance of the network. While the global stochastic optimiser algorithms need a lot of calculation time to find the optimal topological modification, the analytical methods find the solution instantly, but the implementation for larger networks can be problematic due to the exponential increment of linear algebraic equations. Addressing these issues, our goal is to identify the minimal topological modification (adding a single pipeline to the system) which leads to the largest increment in the pressure robustness of the network, with a combination of the above described two approaches.

## APPROACH

To determine the location where the installation of a new pipeline eventuate the largest pressure sensitivity decrement, and through that the largest capacity increment in the water distribution network, a new method was defined based on the sensitivity matrix defined by Pudar and Ligget (Pudar, 1992). The implementation of this method is done using Staci one dimensional hydraulic modelling software developed by Hos et al. (Hos, 2012).

### The objective function of the sensitivity analysis

As it is suggested by Pudar and Ligget (Pudar, 1992) we take the linear equation system describing a WDS in the following form

$$\underline{F}(p(d), d) = \underline{0}, \quad (1)$$

where  $p$  is the vector of the nodal pressures, and  $d$  is the nodal demands. The calculation of the derivate of this equation with the respect of the demands results

$$\frac{\partial \underline{F}}{\partial \underline{x}} \frac{\partial \underline{x}}{\partial d} + \frac{\partial \underline{F}}{\partial d} = \underline{0}, \quad (2)$$

where the  $\frac{\partial \underline{F}}{\partial \underline{x}}$  is the Jacobian matrix, and  $\frac{\partial \underline{x}}{\partial d}$  is the sensitivity matrix. The sensitivity matrix beholds the derivatives of the nodal pressures with respect to the demands, in the following form

$$S_d^p = \left[ \frac{\partial p_i}{\partial d_j} \right] = \begin{pmatrix} \frac{\partial p_1}{\partial d_1} & \dots & \frac{\partial p_1}{\partial d_n} \\ \vdots & \ddots & \vdots \\ \frac{\partial p_n}{\partial d_1} & \dots & \frac{\partial p_n}{\partial d_n} \end{pmatrix}, \quad (3)$$

where  $n$  is the number of nodes in the WDS. Based on the sensitivity matrix, three new parameters namely local, average and peak sensitivity are introduced. If the demand increases in a node, the pressure of the system changes. To characterise the pressure robustness of a node, the local pressure sensitivity ( $S_{local}^i$ ) is introduced, which is the row wide summation of the elements of the pressure sensitivity matrix. The peak sensitivity ( $S_{peak}$ ) is the pressure sensitivity of the node which has the highest local sensitivity, while the average sensitivity ( $\bar{S}$ ) describes the whole system through the average value of the local sensitivities.

We can extend these parameters between two topological state of the WDS as the following

$$\Delta S_{peak} = \left( 1 - \frac{S_{peak}^{new}}{S_{peak}^{old}} \right) \cdot 100 [\%], \quad (4)$$

where “new” superscript means the topology after, and “old” superscript means the topology before

connecting a new pipeline in the system. We can define a new parameter which characterises the effect of a topological modification, the peak sensitivity difference. If we do the same with average sensitivity value, we get the average sensitivity difference

$$\Delta\bar{S} = \left(1 - \frac{S^{new}}{S^{old}}\right) \cdot 100 [\%] \quad (5)$$

We found that  $\Delta\bar{S}$  and  $\Delta S_{peak}$  parameters are topology specific values, as the calculation of these parameters before and after the virtual installation of a new pipeline describe its effect on the pressure robustness of the system.

### The implementation of the method

With the help of the  $\Delta\bar{S}$  and  $\Delta S_{peak}$  parameters, we define the following fitness function

$$f(ID_1, ID_2) = \max(\Delta\bar{S}) \quad (6)$$

where  $(ID_1)$  and  $(ID_2)$  means the identification number of the connected nodes. If we are not limited by the calculation time – because the exponential growth of the possibilities as a function of the system's size – we could use trial and error method for all of the possibilities, but for the industrial use and real-life water distribution analysis a faster technique is needed. At the beginning, we used the genetic algorithm toolbox published and developed by (Wall, 1996). Later the differential evolution algorithm was implemented following the work of (Storn, 1995). But in all cases, we experienced convergence problems with these fitness functions, that was originated from the randomness of the identification numbers, and through that the non-smooth of the fitness function.

To solve this problem, we searched for new variables that can be used for the refinement of the fitness function. First, fully synthetic networks are created where the optimal pipeline connection is known. As we analysed the parameters of these synthetic networks we found that the local pressure sensitivity difference described as

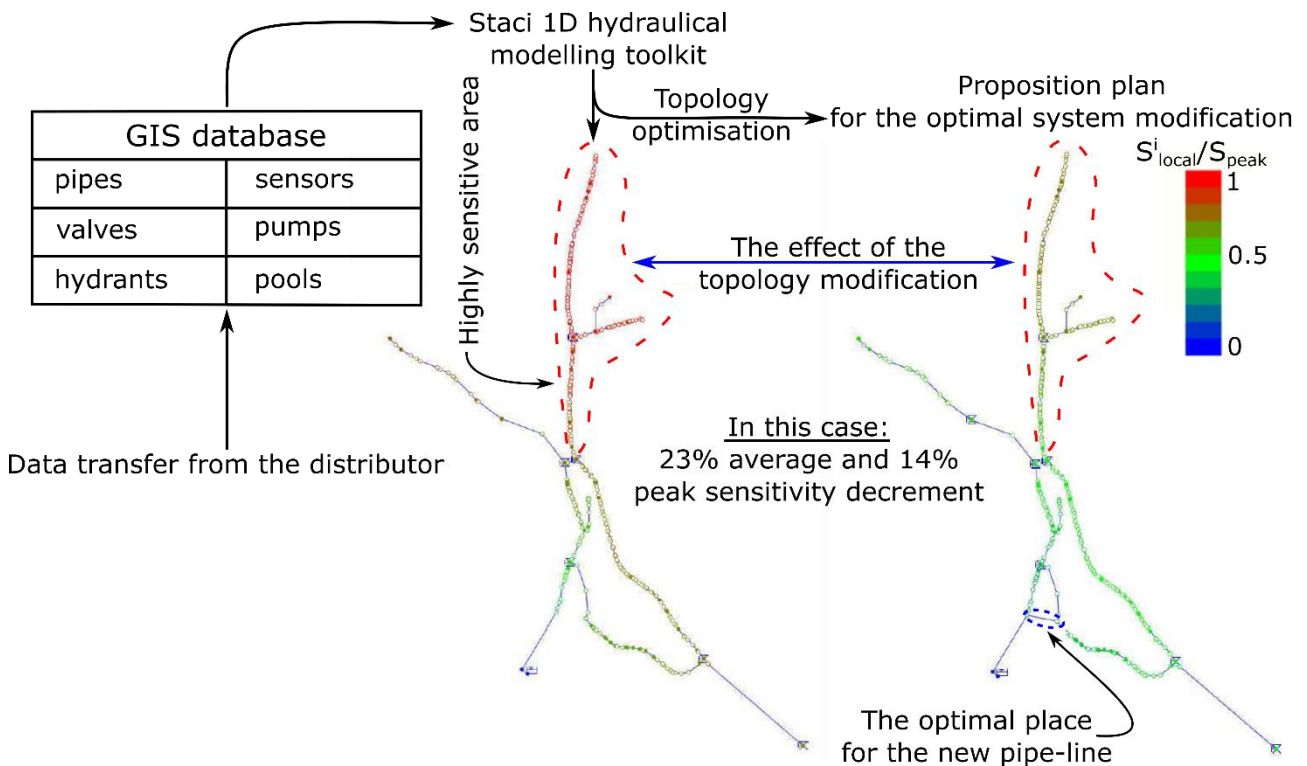
$$\Delta S_{local} = \left( \frac{|S_{local}^i - S_{local}^j|}{\max(\Delta S_{local})} \right) \quad (7)$$

shows strong correlation with the optimal pipeline connection. Namely, where the local pressure sensitivity difference is maximal – where we connect a very robust node to a very poorly conditioned – the optimal pipeline connection is found. The main novelty in our method is finding that the local pressure sensitivity difference between two nodes (without pipe connection between them) predicts the possible achievable average and peak robustness growth, resulted by the pipeline connection. With the help of this connection, the identification of the pipeline which maximizes the pressure robustness of the system can be determined with only one hydraulic simulation. In the case of a real WDS, the steps of the method are the following:

- First, based on the GIS (Geographic Information System) database of the distributor a one-dimensional hydraulic simulation model is built in Staci modelling toolbox.
- After that, a hydraulic and sensitivity calculation is performed and all of the possible node connections – within an economic limit (maximalized pipeline-length) – are organized as pairs.
- At the end, for all of the node pairs the local pressure sensitivity difference is determined and the pairs with the ten highest value are chosen, and hydraulically simulated for the evaluation of the peak and average sensitivity difference between the topologically extended and original state of the WDS.
- In order to reach a common optimum between the investment cost and robustness growth, out of the ten solutions the cheapest build-highest robustness gain construction can be chosen by the provider.

**DISCUSSION**

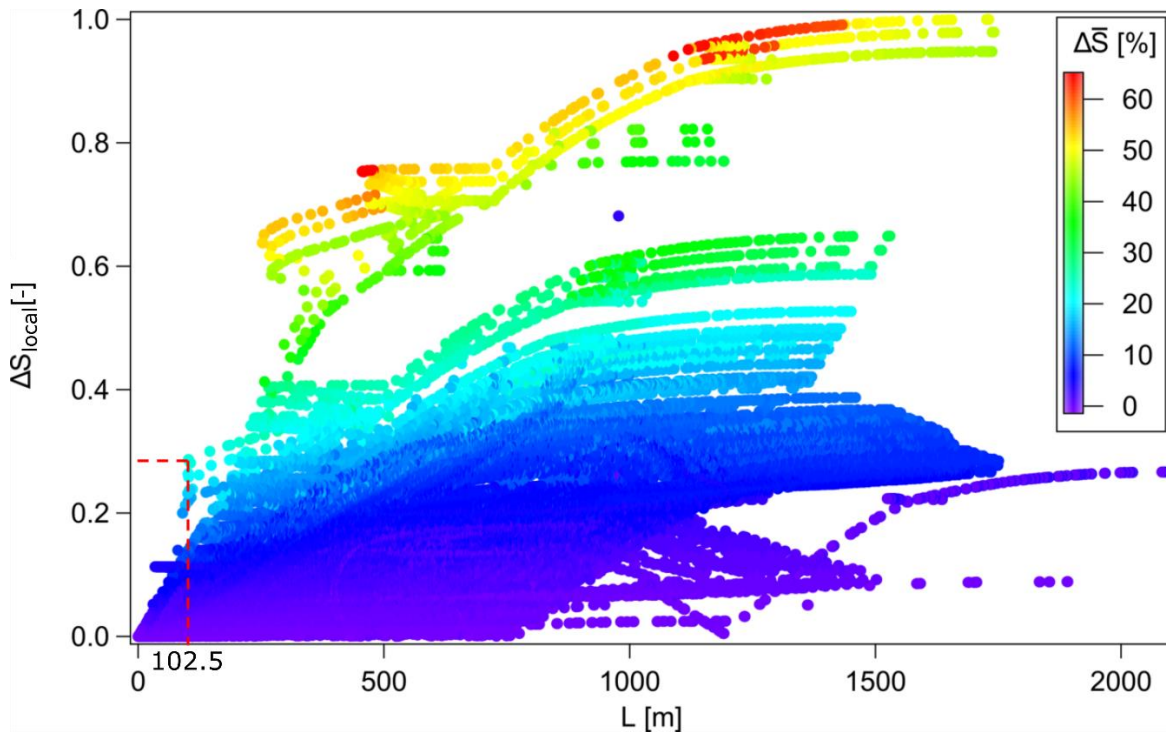
The described method was tested on the simulation model of real-life water distribution networks, which was built using the provider’s geographical information system (GIS) data. We found that the method only needs a few seconds runtime even in the case of a large network (more than 6000 nodes). The first analysed real-life network was the WDS of a small western Hungarian town, which has 400 nodes and distributes water for 1000 inhabitants. As the results show, this small town has a large, highly sensitive area near its upper end. With the help of the described method, we found a solution – within the economic limit of 120 m maximal pipe length – which reduces the average sensitivity by 23 % and the peak sensitivity by 14 %, while a 102.5-meter-long pipeline is connected (see the pipe marked by the blue dashed line in figure below).



**Figure 1.** The effect of the determined pipe connection. The two sensitivity maps have the same colour scale

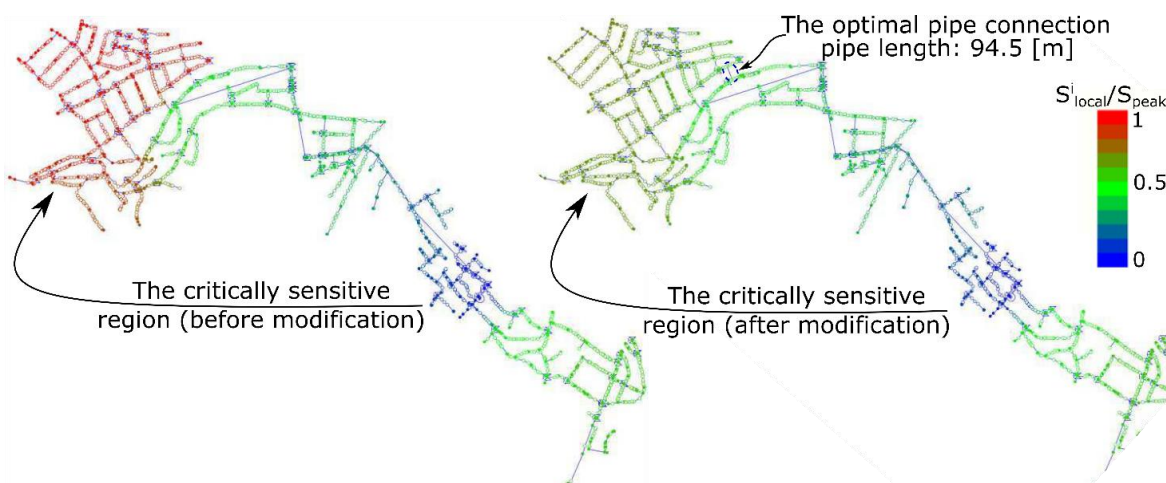
The smallness of this network makes it possible to verify the results of our method with the complete evaluation of the possible pipe connections. With the help of 79800 hydraulical simulations, the robustness map of the network is calculated, as it can be seen in the following figure. As it is clearly seen, the result of the complete evaluation and the result of our method give exactly the same result (102.5 m long pipe, 23 % average sensitivity decrement). Since the hydraulical simulation cost of the total evaluation scales exponentially with the size of the network, until our method, need just a few simulations even in the case of the largest networks, to reach the same result.





**Figure 2.** The complete sensitivity map of the smallest analysed WDS, the red dashed line indicates the optimal solution within the 120 m pipeline-length economical limit

After the verification of the method, a larger network was analysed. The network presented below is also located in Western Hungary, and provides water for 3500 people and has 2700 nodes. The figure below shows its pressure sensitivity map, on left without, and on the right with the proposed new pipe connection. The possible pipe length was maximized in 120 meter again. As a result, the algorithm found a pipeline which causes 25 % decrement in average and 28 % decrement in peak sensitivity, with only a 94.5-meter-long pipe connection.

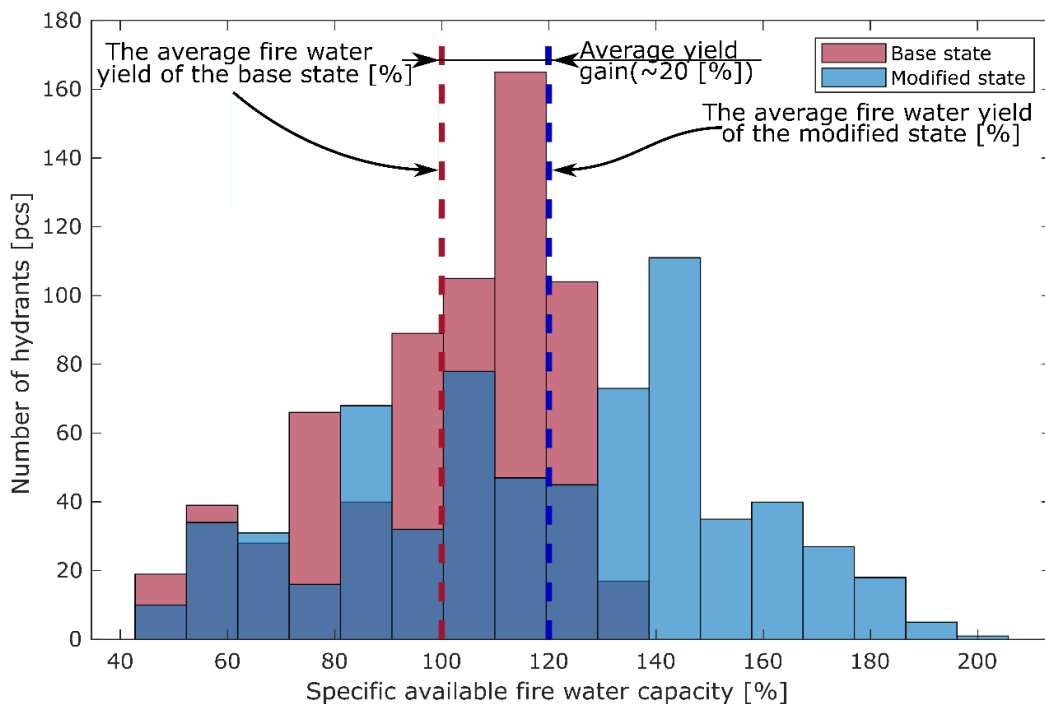


**Figure 3.** The effect of the determined pipe connection. The two sensitivity maps were created with the same colour scale

At last, the extended system was analysed from a new aspect. The consultation with the operating company of the WDS revealed capacity problems in the critically sensitive region of the second network (see the red coloured region in left panel of the figure above). To analyse the results from the aspect of the maximal reachable demand, a hydrant model was created. Most of the hydrants are passive hose connections for the fire service, as a result, the fire extinguisher capacity is deeply



based on the pressure stability of the system and it is a good indicator for the local outflow capacity of a network segment. Thus, if a hydrant is opened, a new large demand is applied for one specific node of the WDS. In the case of such largely sensitive area, this size of demand increment decreases the pressure and through that the hydrant outflow capacity. The hydrant model was a simple choked outflow for the atmosphere. The choked opening for the atmosphere – the hydrant model – was connected only for one node at a time, and for every case a new simulation was calculated to gain the output volume of the system before and after the optimised pipe connection. To obtain detailed information about the firewater capacity of the system, 672 different nodes from the highly sensitive area were used for the histogram creation. As the last diagram clearly indicates this, the average firewater capacity of the critical area is increased with 20 percent. Besides that, some of the hydrants gained extremely high capacity. While the hydrants in the unmodified case have maximally 140 percent of the average firewater flowrate, in the modified case, a few hydrants can produce 200 percent of the original average flowrate. The impact of the modification was analysed from the aspect of the pump operation point and the results of the simulations verified its equality with the pre-modification state. As a result, it can be said that this method is able to solve the WDSs pressure fluctuation and firewater capacity problems with the lowest possible investment cost and without increasing the operating cost of the system.



**Figure 4.** The capacity histogram of the critically sensitive area. The original state is marked with red, the results of the modification is marked with blue colour

## SUMMARY

In this paper, we introduced a highly computational time-efficient method for the identification of the optimal location for a new pipeline in the viewpoint of the pressure robustness and capacity increment of the network. The mathematical and physical background of this method, and the algorithm itself was presented in the first part, while the second part introduce two case studies where the method was implemented on two real-life WDSs. The validity of the method was verified through the compartment with the results of the evaluation of the all possible pipe connections, in the case of the smallest test network. After the verification of the method, the second case study present the effect of the topology optimisation in the viewpoint of the firewater capacity increment. As a result, we found, that the reachable firewater capacity in the highly pressure sensitivity city

district shows large increment. At last, the effect of the topology is considered in the aspect of the operating cost, and the simulation results suggest that the operating point of the system does not change due to the modification of the topology, thus it can be said that the operating cost remain on the original level.

In this paper, we worked out and verified a new method, which can be utilized to increase sustainability and cost-efficiency of WDSs. The method relies on increasing the pressure robustness of the system through the optimisation of the network topology. A new connection was found between the local pressure sensitivity difference and the topology-dependent average pressure sensitivity. Thus, it takes only a few simulations to reach the same result as the evaluation of all possible connections.

## REFERENCES

- Ghorbanian, V., Karney, B., Guo, Y. (2016) Pressure Standards in Water Distribution Systems: Reflection on Current Practice with Consideration of Some Unresolved Issues. *Journal of Water Resources Planning and Management*, **142**(8), 04016023.
- Snyder, K., Deb, J. K., Grablutz, A. M., McCammon, F. B., Grayman, S., Clark, W., Okun, R. A., Daniel, M., Tyler, S., Dragan, S. (2002) Impacts of fire flow on distribution system water quality, design and operation.
- House-Peters, L. A., Chang, H. (2011) Urban water demand modeling: Review of concepts, methods, and organizing principles. *Water Resources Research*, **47**(5).
- Mala-Jetmarova, H., Savic, D., Sultanova, N. (2018) Lost in optimisation of water distribution systems? A literature review of system design. *Water*, 10(3).
- Saldarriaga, J., Páez, D., León, N., López, L., Cuero, P. (2015) Power use methods for optimal design of WDS: history and their use as post-optimization warm starts. *Journal of Hydroinformatics*, **17**(3), 404-421.
- Feifei, Z., Aaron, Z., Angus, S. (2013) A self-adaptive differential evolution algorithm applied to water distribution system optimization. *Journal of Computing in Civil Engineering*.
- Babayan, A. V., Liong, S.-Y., Walters, G. A., Babovic, V., Savic, D. A., Phoon, K.-K. (2010) Multiobjective Optimization of Water Distribution System Design Under Uncertain Demands. *Hydroinformatics*, 906-913.
- Ranko, S. P., James, A. L. (1992) Leaks in Pipe Networks. *ASCE Journal of Hydraulic Engineering*, **118**. 1031-1046. 10.1061/(ASCE)0733-9429(1992)118:7(1031).
- Izquierdo, J., Montalvo, I., Pérez, R., Herrera, M. (2008). Sensitivity analysis to assess the relative importance of pipes in water distribution networks. *Mathematical and Computer Modelling*, **48**, 268-278. 10.1016/j.mcm.2007.10.010.
- Wall, M. (1996) GALib: A C++ library of genetic algorithm components. Mechanical Engineering Department, Massachusetts Institute of Technology, 87(August), 54. 1996.
- Storn, R., Price, K. (1995) Differential Evolution- A Simple and Efficient Adaptive Scheme for Global Optimization over Continuous Spaces. Technical Report TR-95-012, 1-12.
- Diao, K. et al. (2016) Global resilience analysis of water distribution systems. *Water Research*, **106**, 383-393.
- Fiorini Morosini, A., Costanzo, F., Veltri, P., Savic, D. (2014) Identification of measurement points for calibration of water distribution network models, In 16th Water Distribution System Analysis Conference, WDSA2014 – Urban Water Hydroinformatics and Strategic Planning, **89**, 693-701.
- Selek, I., Gergely Bene, J., Hős, C. (2012) Optimal (short-term) pump schedule detection for water distribution systems by neutral evolutionary search. *Applied Soft Computing*, **12**, 2336-2351.
- Wood, D. J., Charles, C. O. A. (1972) Hydraulic network analysis using linear theory, *Journal of the Hydraulics Division*, **98**(7), 1157-1170.

## Comparative Analysis of Hydro-chemical Properties of Bottled Waters in Serbia

M. Mandić\* and J. Štrbački\*

\* Department of Hydrogeology, University of Belgrade, Faculty of Mining and Geology, Đušina 7, Belgrade, Serbia (E-mails: [marijana.mandic@rgf.rs](mailto:marijana.mandic@rgf.rs); [jana.stojkovic@rgf.bg.ac.rs](mailto:jana.stojkovic@rgf.bg.ac.rs))

### Abstract

Bottled water production is a multidisciplinary enterprise which requires the involvement of hydrogeologists as well as other experts (physicians, marketing specialists, etc.). Being at the forefront of this procedure implies that the hydrogeologist should be aware of the entire bottling process. The main goal of this research was to obtain all bottled waters available on the Serbian market and make a comparative analysis of their chemical content. The total of 74 samples was collected, carbonated and non-carbonated, domestic as well as imported brands. The medicinal properties of the examined waters were also evaluated and the effects these waters have on the consumer's health were explained. Finally, an inquiry was conducted to assess the user's opinion on bottled waters and the influence marketing has on their choice of brand, as well as to determine their preferred drinking water source. This research showed that bottled waters available on the Serbian market have diverse chemical composition, a wide range of mineralization, as well as different dissolved gas contents. It was concluded that in spite of the bottled waters' quality, availability and overall appeal, the majority of respondents prefer water from a public supply.

### Keywords

Groundwater, bottled water, hydro-chemical characteristics, health, marketing

## INTRODUCTION

A long time ago in amphorae - today in glass or plastic bottles - back then as a medicine, and today - for daily usage. Regardless of the age in history, commercially bottled groundwater always differed from the "plain" groundwater intended for public water supply. With the evolution of the market economy, changing and adapting to customer demand, the term "bottled water" changed as well. Today, consumers of bottled water expect as low mineralization as possible and consume this product daily. Bottled water often completely replaces the tap water even though it has a much higher price. The question is: how did we get here? Is it necessary and justified for the bottled water to replace entirely the public water supply?

The process of water production starts with the hydrogeologist canvassing the general area in search of groundwater which might fit the legal requirements for bottled water. This is a multidisciplinary process, that also involves experts from the fields of medicine and marketing. This paper examines the total of 74 bottled water brands available in Serbia: their chemical characteristics, the effect they have on the consumer's health as well as the role of the advertisement on the consumer's choice.

### The term bottled water and usage

The term bottled water specifies any kind of groundwater determined for human use that reaches the surface naturally, through a well or springs, packed in bottles or any other sanitary packages (Krunić, 2012; The Official Gazette RS, 2013; Mandić, 2018). The modern term "packaged water" is more precise. Packaged water represents a unique product, protected by its name and its hydrogeological origin. (Krunić, 2012; Mandić, 2018). However, when referring to water packaged in bottles the most widespread term is still "bottled water". The legal framework has been put in place to prevent just any water from reaching the market. In the Republic of Serbia, two directives

are in place: Directive regarding the sanitary quality of drinking water (The Official Gazette SRJ 42/98 and 44/99) and Directive regarding the quality of natural mineral water, natural spring water and table water (The Official Gazette RS 43/13).

Bottled water is divided into the water of natural origin and those that have received treatment. There are two types of natural water: naturally mineral and natural spring water. Both types can only be bottled if they satisfy the mandated requirements on quality and exploitation regulated by guidelines. Difference between the types lies in the fact that the natural spring water is bottled at the source or in its vicinity, and its composition is not necessarily stable and characteristic as in the case of natural mineral water. In the case of treated or table water, it is permitted to alter its composition as to bring it closer to the specified directive requirements, but what is not permitted is using tap water in said process. The other important classification of bottled water, disregarding its origin, is carbonated (with CO<sub>2</sub>), and non-carbonated (without CO<sub>2</sub>) (The Official Gazette RS 43/13).

Looking back into the history of bottled water usage, it was determined that, in most cases, non-mineral “plain” groundwater wasn’t used. Those kinds of waters were regarded for their mineral properties, traces of carbon-dioxide and medicinal properties. They were used sporadically and did not replace common drinking sources (Reimann and Birke, 2010; Mandić, 2018). With the development of the market, the term bottled water was adjusted and brought closer to consumers. Consumers nowadays expect lower mineralization from bottled water and use it every day as a substitute for tap water. The reasons for that are in dissatisfaction with the quality of tap water, higher living standards in some countries, and to some degrees marketing.

### **Plastic and glass packaging**

One of the main characteristics of packaged (bottled) water is its packaging. Forty years back plastic packaging overwhelmed glass bottles which opened the water market to a new opportunity. For production and transportation resilience to breaking on top of its smaller weight has shown to be its substantial benefit over glass bottles. In the last years, there have been many stories regarding the impact of packaging on water. Research has shown that every type of packaging can affect the water and its composition. What’s interesting is that glass packaging contaminates water with many more elements than plastic ones. Also, color packaging (regardless of material) seeps more elements than transparent ones (Reimann and Birke, 2010; Mandić 2018). Scientists have found traces of plastic in bottled water of some brands. There is also the problem of plastic bottle disposal. Most of the bottle can be recycled easily, but problems arise with the extensive usage and it becomes more difficult to collect them before they reach the ocean. For said reasons, the European Union requires its members to reduce bottled water consumption, by providing quality tap water to its citizens.

### **METHODS USED**

During the summer of 2018, 74 different bottled water samples were acquired, mostly from Belgrade’s supermarkets. A small number of bottled waters were imported from other countries (Croatia, Bosnia and Hercegovina, Slovenia, Italy, France, and Austria). The analysis was done based on the data from the labels since all the info consumers get is the info provided on the product itself. Chemical properties of each sample were analyzed first, followed by the determination of the water type: concentrations in mg/l were converted to %eq and only ions with the content > 20%eq were considered. Data were plotted using AquaChem software (Schlumberger Water Services). Regarding medical information, the author has consulted a nutritionist from the Clinical Center of Serbia, Ljiljana Putniković. The aspects of bottled water advertising were analyzed using commercials and internet pages of different brands. Finally, a survey was taken to determine consumer’s preferred sources of drinking water.

## RESULTS AND DISCUSSION

The results of the hydro-chemical analysis of the acquired bottled waters are shown for every water type (natural mineral water, natural spring water, and table water), so that the types can be compared. The impact of bottled water on human health, as well as the impact of marketing on consumer's choice, is shown regardless of the water type.

### Natural mineral water

Out of 74 analyzed samples, 54 were natural mineral waters. Most of the natural mineral water (34) belonged to water with low mineralization (50-500 mg/l of dry residue). Only in this type of bottled water two more groups can be found, 15 belongs to natural mineral waters (500-1500 mg/l of dry residue), and 10 belongs to water with high mineralization (over 1500 mg/l of dry residue). When it comes to the types, most belong to the HCO<sub>3</sub>-Ca type. A significant number of natural mineral waters are carbonated, 30 in total. This number is not surprising, having in mind the long history of carbonating waters and the human need for non-alcoholic refreshment. Note that, when it comes to purchasing water, consumers expect it to differ from their regular tap water, and the existence of CO<sub>2</sub> is one of the most obvious differences (Mandić, 2018). Because of a vast number of naturally carbonated mineral waters, its significance and characteristics, non-carbonated and carbonated waters are separated within this group.

*Non-carbonated natural mineral waters.* Most of the non-carbonated natural mineral waters are of HCO<sub>3</sub>-Ca-Mg type, where a significant portion is in the 500 mg/l mineralization range. Only in the case of Mg Mivela do we see mineralization of 1522 mg/l. The results were shown on the Piper diagram (Figure 1). In the diamond part of the diagram, the size of the circle was proportional to the mineralization of the sample, applies for every diagram henceforth.

*Carbonated mineral waters.* In its base carbonated, bottled waters are separated into naturally carbonated and those carbonated with the addition of CO<sub>2</sub>. Naturally carbonated waters are far more interesting. When they come in contact with rocks, because of its acidic nature, their dissolving properties are enhanced, which in turn explains why such waters have an elevated amount of non-organic components (base cations and silicates) and different microelements (Reimann and Birke, 2010; Stojković, 2013; Mandić, 2018). On the other hand, the addition of CO<sub>2</sub> into natural mineral waters will not have an impact on most of the soluble components in them. This will result in a greater acidity due to carbonic acid, which will disrupt the existing chemical equilibrium, and create partial pressure in CO<sub>2</sub> (Reimann and Birke, 2010; Mandić, 2018).

When comparing Piper diagrams for non-carbonated and carbonated natural mineral waters (Figure 2.), carbonated have greater mineralization and possess more types. Most are in the HCO<sub>3</sub>-Na type. Donat Mg water has the highest mineralization (8000 mg/l).

### Natural spring waters

In the directive regarding bottled waters ((The Official Gazette RS nm. 43/13), not enough emphasis is placed on the difference between natural and spring mineral waters, which is probably why the characteristics of natural mineral waters are lacking. Clear is the difference in the place of bottling, what isn't clear is whether natural spring waters must contain mineralization greater than 1 g/l, elevated temperature, or specific components (Mandić, 2018). For this paper, 14 natural mineral water brands were collected (Figure 3.) Two were carbonated with added CO<sub>2</sub> (Jazak and Vila waters). Most belong to the HCO<sub>3</sub>-Ca-Mg type. What is interesting is that 2 water brands from this group have the lowest mineralization of all the collected samples, Vlasina (27 mg/l) and Rosa (54 mg/l).

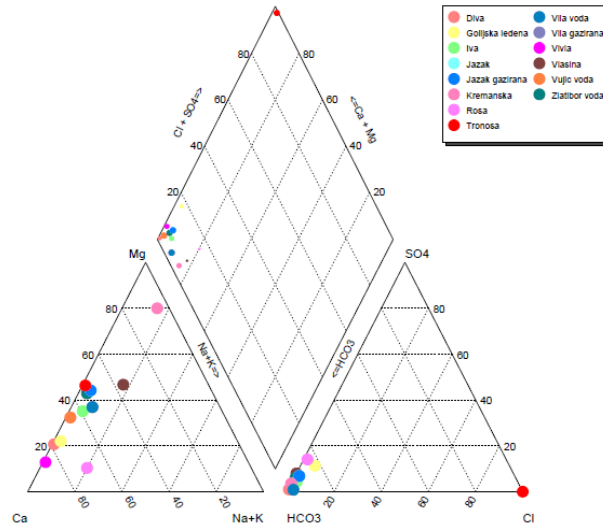


Figure 1. Piper diagram for non-carbonated natural mineral waters (Mandić, 2018)

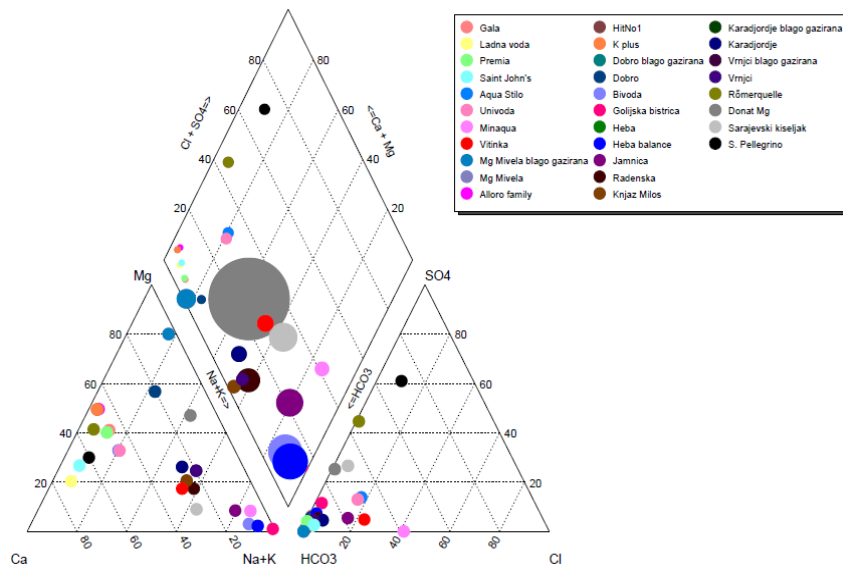


Figure 2. Piper diagram for carbonated natural mineral waters (Mandić, 2018)

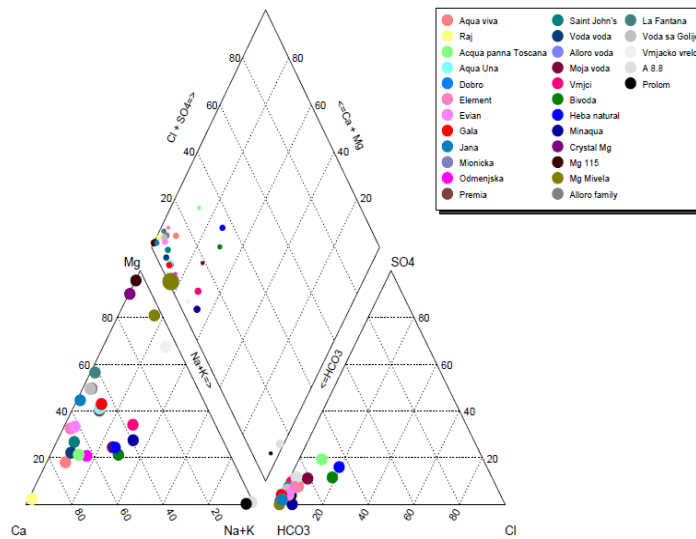


Figure 3. Piper diagram for natural spring waters (Mandić, 2018)

### **Table waters**

The only table water found on the market was Smart water. Its label described the procedure used in making of this water. Water was heated until it becomes vapor, then when it came to the point of condensation minerals were added (calcium, magnesium, and potassium). This procedure could be used in making waters with different composition, adding for example microelements.

### **Impact of bottled waters on human health**

When it comes to questions regarding the impact of bottled water on human health verbal consultations were made with a nutritionist from Clinical center of Serbia, Ljiljana Putniković (9 August 2018), who stated that: *"Prerequisites for bottled water recommendation are that the consumer is in good health and has a balanced diet. Having that in mind, the best course is to recommend non-carbonated water with dry residue under 500 mg/l. Even if the user decides on the water with very low mineralization, it will have no side-effects, because minerals are replenishable through food. If the user suffers from any health problems, which might cause him to alter his diet, specifically the amount of mineral content, this person must be careful when reading the label, especially with carbonated waters. The mineral content of public water supply, if it fulfills all the established quality criteria, suits everyone. Moderation is one of the basic principles of a healthy diet, therefore bottled water should also be consumed in moderation."*

### **Marketing of bottled water**

The modern marketing concepts were described in Arsić's (2012) paper: "According to the modern marketing concepts, the consumer is defined as the key to a company's success on the market. Knowing his needs, wishes, expectations, and values teach us ways in which he forms beliefs and judgments regarding consumer product, and about his purchasing decisions. That's the bases for forming an effective marketing and communication strategy. In modern markets higher emphasis is placed on emotionally branding products, that's based on emotional ties between consumer and brand.

The concept of "wellness" is one of the greatest trends in the 21st century. It has influenced all the aspects of modern ways of living. One of its aspects is the concept of "healthy diet", and together with it the idea of "healthy water" which is referring to pure, drinkable water with characteristics beneficial to human health. None of the brands has missed the opportunity to market their product in such away. By becoming a part of the mentioned concept, bottled water brands have taken a prominent place in consumer consciousness (Mandić, 2018).

### **Survey on the choice of drinking water**

For determining which drinking water is used daily in Serbia and why a survey was conducted. 77 people were surveyed, out of which the oldest was born in 1968., while the youngest was born in 2001. The highest percentage, 71.4% had a higher degree.

On the question which specific water their everyday choice is, **57.1%** of the surveyed decided on publicly supplied water. The most common reasons are, they considered that tap water has a good quality, price, availability, and some even have built-in filtering systems. Of the rest, **42.9%**, answered that the bottled water is their everyday choice. The reason was the unsatisfactory condition of the public water. Most of the bottled water consumers marked Rosa or Prolom as their water of choice. Rosa because of availability, taste, and price. Prolom because of its influence on health. Furthermore, **64.5%** answered that they pay no attention to water labels.



## CONCLUSION

One of the most important duties hydrogeologist has is discovering groundwater, which can later be used for drinking purposes - water for public supply systems. For human's water is a necessity, and one of the major conditions for a healthy life is having available quality water. Research and discovering of groundwater, used for bottling, is also part of hydrogeologist's job, but even with the efforts of companies for bottling water and marketing, such water isn't meant for everyone. One of the common reasons is the price, but not the only one. Even though packaging and transportation have improved significantly to the point where it's possible to distribute bottled water to everyone, there are still some issues. Research has shown that all forms of packaging contaminate bottled water, with that none are a truly safe choice. Aside from that, there is a problem with a huge amount of plastic waste as a by-product of usage. Recycling isn't effective enough in dealing with this issue. Vehicles used in transportation are a huge contaminator of the environment. There also exist problems with transporting water via public water systems, but those are by-products of lack of maintenance. If there exists a system of tracking, controlling, and maintaining, this system is safe.

Bottled waters available on the Serbian market are characterized by diverse chemical composition, a wide range of mineralization, as well as different dissolved gas contents. Regardless of their quality, availability and overall appeal, we should always keep in mind that bottled water is a commercial product whose primary purpose is to make profits. Public water systems, on the other hand, have a goal of providing drinking water for the population in whole. Therefore, it is unacceptable for bottled water to become the primary source of drinkable water. One of the most important issues every country should address is providing quality drinking water for its citizens. Hydrogeologists play an important and irreplaceable role in water supply projects.

## REFERENCES

- Arsić, S. (2012) Pozicioniranje brenda u svesti potrošača. (Master rad u rukopisu), Univerzitet Singidunum, Beograd, (in Serbian).
- Krunić, O. (2012) Mineralne vode. Univerzitetski udžbenik, Rudarsko-geološki fakultet, Beograd, (in Serbian).
- Mandić, M. (2018) Komparativna analiza hidrohemijskih karakteristika flaširanih voda na domaćem tržištu. (Diplomski rad u rukopisu), Rudarsko-geološki fakultet, Beograd, (in Serbian).
- Pravilnik o higijenskoj ispravnosti vode za piće. (1999). Službeni list Savezne Republike Jugoslavije, br. 42/98 i 44/99, (in Serbian).
- Pravilnik o kvalitetu i drugim zahtevima za prirodnu mineralnu vodu, prirodnu izvorsku vodu i stonu vodu. (2013). Službeni list Republike Srbije, br. 43/13, (in Serbian).
- Reimann, C., Birke, M. (2010) Geochemistry of European Bottled Water, Borntraeger Science Publishers, Stuttgart.
- Stojković, J. (2013) Hidrogeohemijska valorizacija esencijalnih mikroelemenata mineralnih voda Srbije. (Doktorska disertacija u rukopisu), Rudarsko-geološki fakultet, Beograd, (in Serbian).



## Investigation of the Effect of Pre-ozonation on Organic Matter Removal via Flocculation

S. Sam\*, M. A. Yukselen\*\* and Z. S. Can\*

\* Department of Environmental Engineering, Faculty of Engineering, Marmara University, Goztepe Campus, 34722 Kadikoy, Istanbul, Turkey (E-mail: [serdar.sam@marmara.edu.tr](mailto:serdar.sam@marmara.edu.tr))

\*\* Faculty of Engineering, European University of Lefke, Lefke, Northern Cyprus (E-mail: [serdar.sam@marmara.edu.tr](mailto:serdar.sam@marmara.edu.tr))

### Abstract

Using a range of different humic acid and ozone concentrations, the effect of pre-ozonation on humic acid removal with aluminium sulphate and polyaluminium chloride coagulants was investigated. By optically monitoring floc formation dynamically in conventional jar test procedure, it was found that increasing ozone dose led to decreased floc size. Once ruptured, only limited regrowth of flocs occurred, indicating irreversible floc breakage. Larger flocs were formed with polyaluminium chloride compared to aluminium sulphate, thus lower residual organic carbon concentrations were measured. The findings showed that the use of pre-ozonation provided beneficial results to improve organic carbon removal at lower humic acid concentrations. However, organic carbon removal was hindered at the highest humic acid concentration studied.

### Keywords

Natural organic matter; humic acid; ozonation; flocculation

## INTRODUCTION

Ozone has been used in water and wastewater treatment since 1970s in the control of disinfection, and disinfection by-products (DBPs), for the oxidation of iron and manganese, and for the reduction of taste, colour and odour. Ozonation of natural organic matter (NOM) yields major changes in its structure. Despite the fact that there are many studies in literature reporting the effects of pre-ozonation on organic matter flocculation and removal, many of them contradicts one another. Some researchers indicated that pre-ozonation diminished the organic matter removal (Schneider and Tobiasson, 2000; Hailong et al., 2007; Bose and Reckhow, 2007), while others claimed the opposite (Marhaba and Pipada, 2000; Singer et al., 2003; Pei et al., 2007; Jasim et al., 2008). And some informed that effect of ozonation depended on the concentration of organic matter (O'Melia et al., 1999) and ozone dose (Singer, 1990; Edwards et al., 1993). It is thought that the nature of water samples is the main reason why so many different results are involved in literature. The studies revised were carried out with natural waters. However, the structure and characteristics of NOM may exhibit significant regional and seasonal variations. Hence, a study in which all conditions are controlled, as in this study, is essential to investigate the effect of ozonation on the removal of organic matter.

Contradicting results in literature necessitate a study in which experiments are conducted with synthetic model suspensions under controlled operating conditions so as to better understand the effect of ozone on organic matter flocculation and removal. In this study, humic acid was chosen as the model NOM because humic acid part of NOM is more aromatic and has a larger molecular size, therefore it is hydrophobic, highly reactive and relatively easily removable by coagulation (Randtke, 1988; Owen et al., 1995). Humic substances constitute the major part of NOM and are more determinative in NOM's behaviour (Sharp et al., 2006; Bose and Reckhow, 2007).

## MATERIALS AND METHODS

Contradicting results in literature necessitate a study in which experiments are conducted with synthetic model suspensions under controlled operating conditions so as to better understand the effect of ozone on organic matter flocculation and removal. In this study, humic acid was chosen as the model NOM because humic acid part of NOM is more aromatic and has a larger molecular size, therefore it is hydrophobic, highly reactive and relatively easily removable by coagulation (Randtke, 1988; Owen et al., 1995). Humic substances constitute the major part of NOM and are more determinative in NOM's behaviour (Sharp et al., 2006; Bose and Reckhow, 2007).

Pre-ozonated (no ozone and three different ozone doses) raw waters containing humic acid (three different concentrations) were flocculated through batch jar test procedure using an on-line optical monitoring technique for evaluating the effect of ozonation on floc formation.

### Model Waters

Model waters with a series of humic acid concentration (5, 10 and 20 mg/L) were prepared dissolving commercial Aldrich humic acid (sodium salt) in deionised water. Hardness was adjusted to 100 mg/L as CaCO<sub>3</sub> with addition from 0.1 M CaCO<sub>3</sub> stock solution, alkalinity to 100 mg/L as CaCO<sub>3</sub> with addition from 0.1 M NaHCO<sub>3</sub> stock solution and pH to around 7.0 with addition from 0.1 N H<sub>2</sub>SO<sub>4</sub> stock solution.

Afterwards, those synthetic waters were ozonated to give ozone concentrations of 2.5, 5 and 10 mg/L. The ozone was generated from oxygen by an ozone generator (PCI GL-1) and was diffused into the suspension via a ceramic diffuser. The ozone concentrations were applied ozone doses, device output supplied by the manufacturer.

### Coagulants

Aluminium sulphate octadeca hydrate (Al<sub>2</sub>(SO<sub>4</sub>)<sub>3</sub> · 18H<sub>2</sub>O, Merck, >96 %) 'alum', was dissolved in deionised water at a concentration of 0.1 M. A commercial polyaluminium chloride (PACl) product (PAX XL-9, Kemira Kemi AB, Helsingborg, Sweden) was used. XL-9 had a degree of neutralisation,  $r (=OH/Al)$ , of 2.1, supplied as a 4.6 % Al solution.

### Apparatus

Aggregation was monitored continuously by an optical flocculation monitor (PDA 2000, Rank Brothers Ltd., Cambridge, UK) in a modified batch jar test procedure. The 800-mL test sample was contained in 1-L beakers equipped with stirrer units from a Flocculator 2000 (Kemira), semi-automatic jar test device. This enables the rapid and slow stirring speeds and times to be pre-set. For dynamic monitoring, the sample from one beaker was circulated through transparent plastic tubing (3 mm i.d.) by means of a peristaltic the pump. The pump was located after the PDA instrument to avoid effects of possible floc breakage in the pinch portion of pump. The tubing was clamped in the PDA instrument so that the flowing sample was illuminated by a narrow light beam (850 nm wavelength). The PDA 2000 measures the average transmitted light intensity (dc value) and the rms value of the fluctuating component. The PDA 2000 does not measure actual floc size, however, the ratio (rms/dc) provides a sensitive measure of particle aggregation (Flocculation Index - FI) (Gregory and Nelson, 1986).

### Procedure

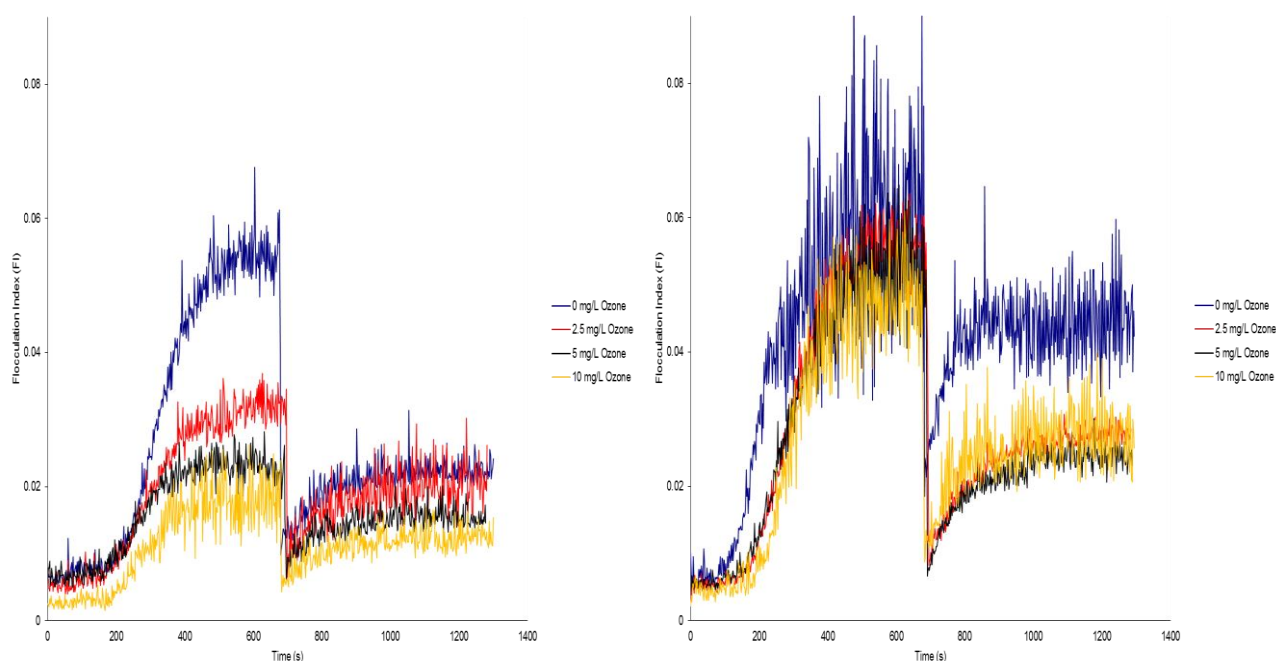
Unozonated synthetic model waters containing 5 mg/L humic acid were flocculated with different alum doses to determine the optimum dose. The optimum alum dose giving the highest FI value and lowest residual colour and total organic carbon concentration after settling for 20 minutes was

determined to be 3.4 mg/L as Al. An equivalent (in terms of mg/l as Al) dose of PACl was used for comparison purposes. This optimum coagulant dose was used in jar tests performed with 800 mL of test waters (containing 5, 10 and 20 mg/L humic acid) treated with four different doses of pre-ozone (0, 2.5, 5 and 10 mg/L).

The details of dynamic monitoring of floc growth and regrowth can be found in Sam et al. (2010). After each jar test the flocculated suspension was left to settle for 20 minutes. At the end of settling a 50 mL-sample was drawn for TOC (Tekmar Dohrmann Apollo 9000) measurement. All experiments were carried out at least 3 times for reproducibility of data at 20 °C.

## RESULTS

A series of jar tests employing aluminium sulphate and polyaluminium chloride (PACl) were performed using synthetic raw waters with a range of humic acid concentration (5, 10 and 20 mg/L) pre-ozonated with different ozone doses (0, 2.5, 5 and 10 mg/L). Online monitoring of floc formation (Figure 1) showed that increasing pre-ozone dose led to gradual reduction in floc size. The onset of flocculation was delayed and the time required to reach a steady-state fully grown floc size distribution was longer with increasing ozone dose. With PACl relatively larger flocs were formed. PACl also exhibited faster floc formation and earlier reach to steady-state fully grown floc size distribution, both make its performance superior to alum.



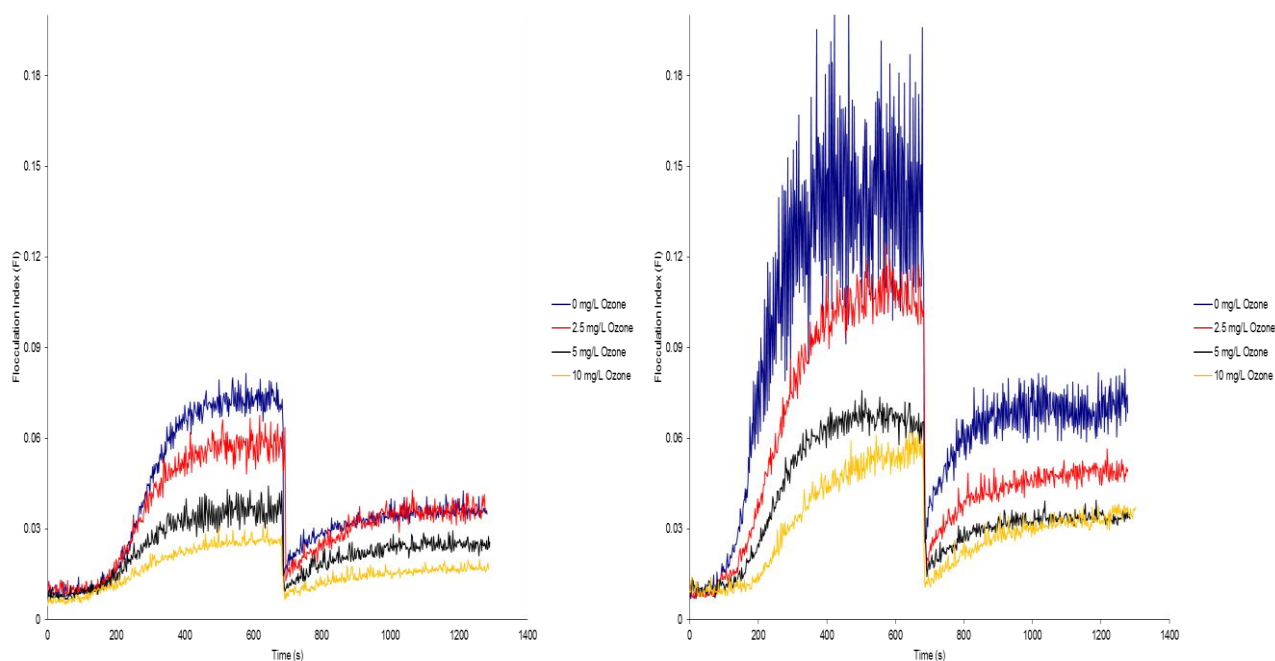
**Figure 1.** Floc growth and regrowth with alum (left) and PACl (right) in flocculation of pre-ozonated synthetic waters containing 5 mg/L humic acid

When no ozone (0 mg/L) was applied alum and PACl formed similar sized fully grown flocs at the humic acid concentration of 5 mg/L whilst the relative size difference between the flocs formed with alum was higher when pre-ozonation was applied. It shows that flocculation with alum is affected more by ozonation compared to PACl, which can be attributed to pre-hydrolysed Al species content of PACl. Also, irreversible floc breakage was observed with both coagulants, i. e. when fully grown flocs are exposed to higher shear rate they break up and can only grow to some

extent, which is natural with sweep flocculation because the nature of aggregation is entrapment of organic molecules in growing amorphous metal hydroxide precipitate rather than electrostatic attraction.

Jar test experiments were carried out in exactly the same way, but this time using 10 mg/L of humic acid (Figure 2). Floc growth curves of similar form to those in Figure 1 were obtained but the initial plateau value of the Flocculation Index (fully grown flocs) was higher, indicating that larger flocs were formed when the humic acid concentration is increased to 10 mg/L. This could be attributed to higher collision efficiency when the concentration of organic matter to be flocculated was increased. The floc breakage and regrowth behaviour was similar to that with 5 mg/L humic acid; once ruptured, flocs could not grow to their size before breakage. Again, remarkably larger flocs were formed with PACl owing to its highly charged cationic species content.

Similar to the findings presented in Figure 1, increasing pre-ozonation dose was observed to have a negative effect on flocculation, i.e., caused formation of smaller flocs, a delay on the onset of aggregation and longer time to reach a steady-state fully grown floc size distribution (Figure 2).

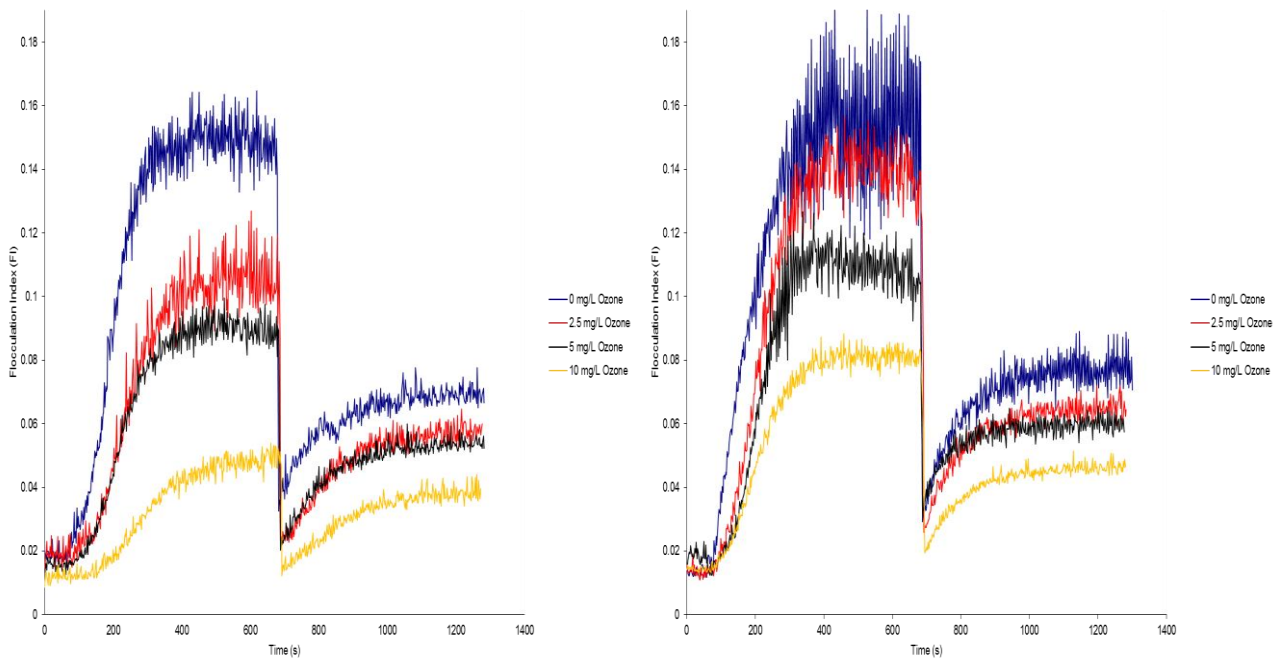


**Figure 2.** Floc growth and regrowth with alum (left) and PACl (right) in flocculation of pre-ozonated synthetic waters containing 10 mg/L humic acid

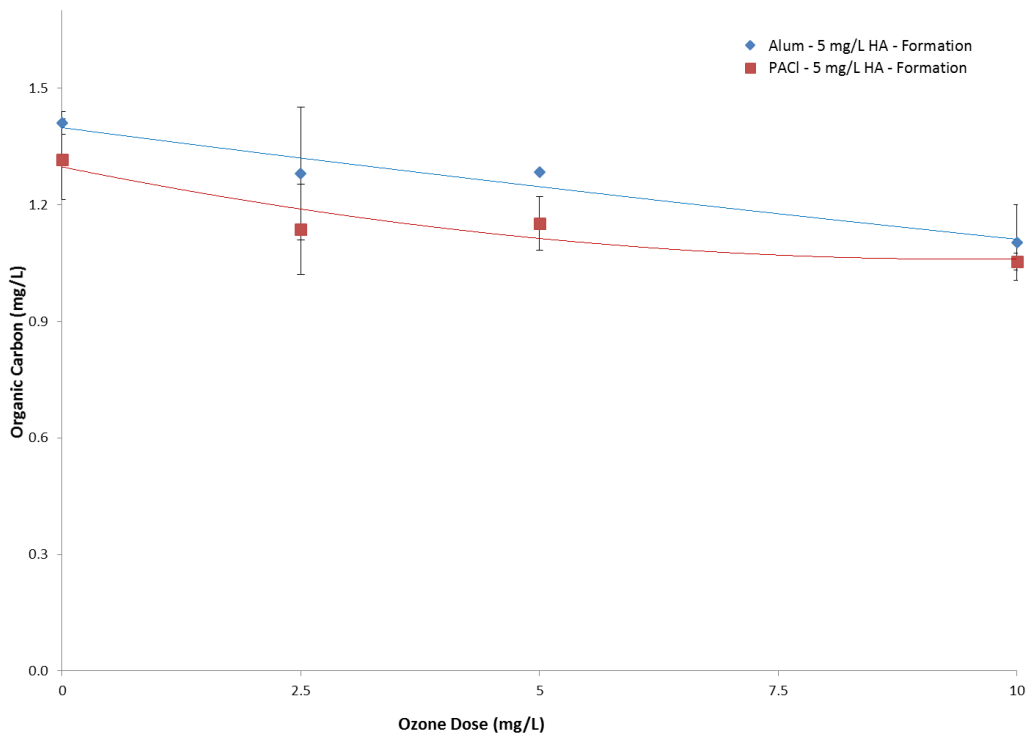
When the humic acid concentration was further increased to 20 mg/L (Figure 3) larger flocs were formed with both coagulants. An increasing trend in floc size with increasing humic acid concentration was observed when Figure 1 to 3 is examined. This could be due to increasing collision efficiency.

Similar floc growth and regrowth curves were recorded with both of the coagulants, showing irreversible floc break-up. Again, at each pre-ozonation dose larger flocs were obtained with PACl. Examining the three figures exhibits that the size difference between alum flocs with increasing pre-ozonation dose was higher than that between PACl flocs, which can be interpreted that PACl is less

affected by pre-ozonation compared to alum. Both features are likely because of PACl's pre-hydrolysed Al hydroxide content.



**Figure 3.** Floc growth and regrowth with alum (left) and PACl (right) in flocculation of pre-ozonated synthetic waters containing 20 mg/L humic acid



**Figure 4.** Change in residual total organic carbon concentration with ozone dose at 5 mg/L humic acid concentration

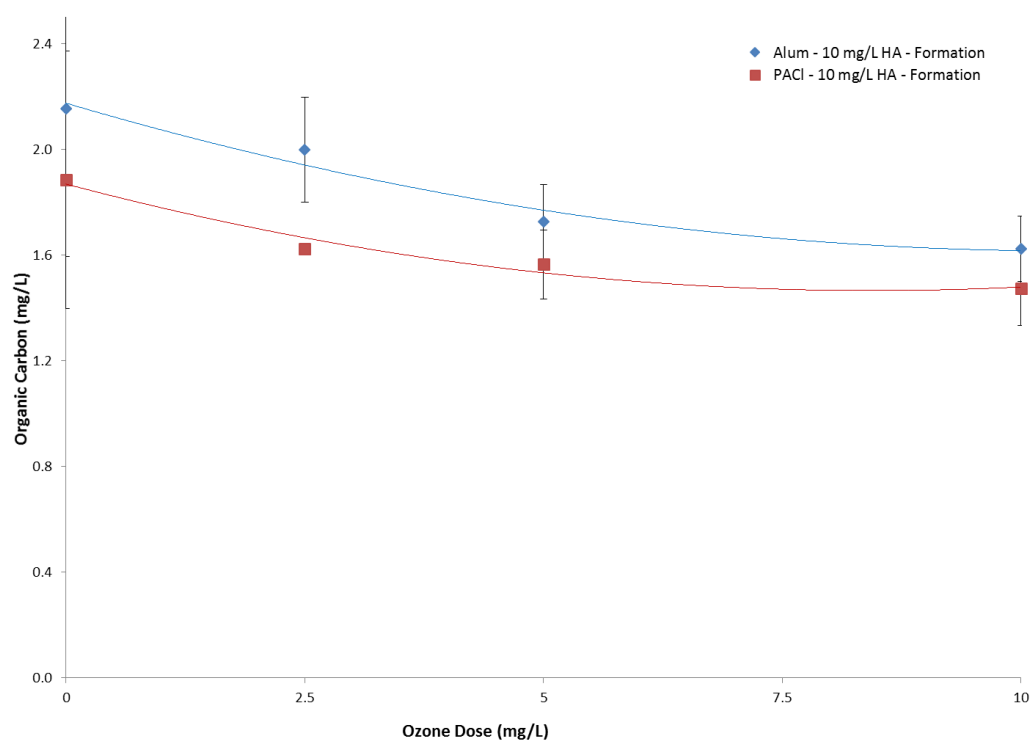
It is clearly seen that pre-ozonation hindered floc formation at 20 mg/L humic acid concentration, similar to that observed at 5 mg/L and 10 mg/L humic acid concentrations. With increasing pre-

ozonation dose floc size gradually decreased, the onset of flocculation was delayed and time to reach steady-state floc size distribution got longer.

Figure 4 presents how residual total organic carbon concentration after alum and PACl flocculation changes when unozonated synthetic raw waters containing 5 mg/L humic acid are pre-ozonated with 2.5, 5 and 10 mg/L ozone. That is, data plotted in Figure 4 are the supernatant total organic carbon content measurements of the flocculation experiment exhibited in Figure 1.

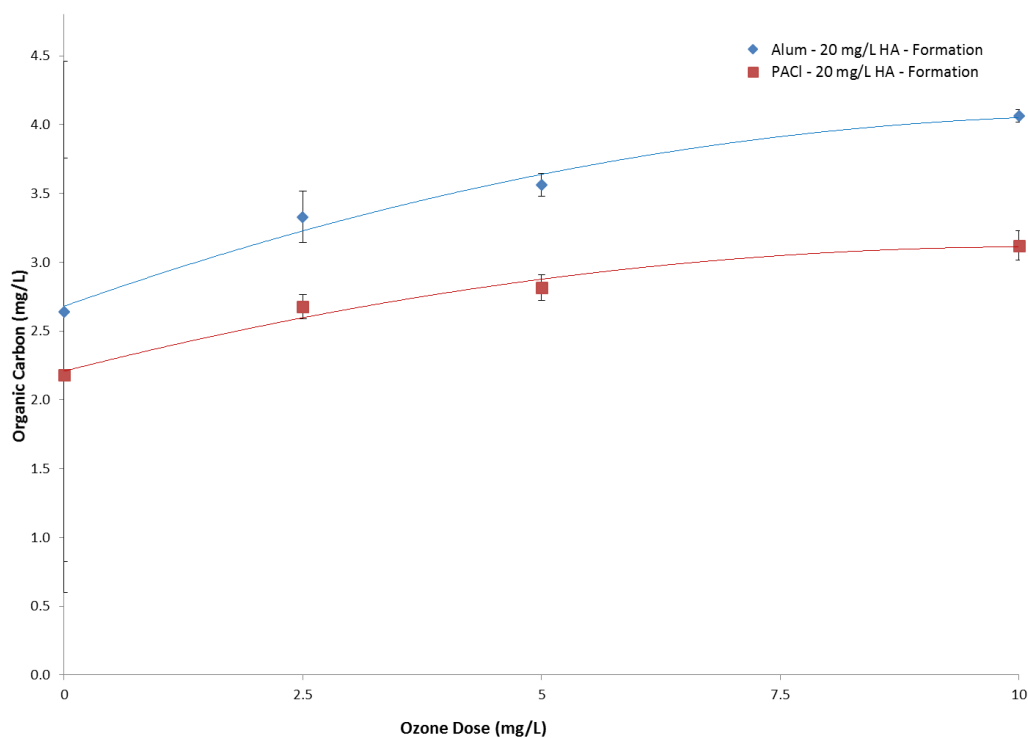
Consistent with floc size data, lower residual total organic carbon values were measured with PACl (Figure 4). PACl's better removal performance over alum is because it contains pre-hydrolysed Al species. However, residual total organic carbon concentration decreased as the pre-ozonation dose was increased, which is inconsistent with floc size data.

It can be expected that since relative floc sizes (FI) decreased as the pre-ozonation dose was increased then the organic matter removal should be hindered; nonetheless the results of total organic carbon measurements do not agree with that argument.



**Figure 5.** Change in residual total organic carbon concentration with ozone dose at 10 mg/L humic acid concentration

Similar to the results of experiments performed with synthetic waters containing 5 mg/L humic acid concentration PACl showed better performance in removing organic matter at 10 mg/L humic acid concentration compared to alum (Figure 5). It can be said that PACl was less affected by increasing pre-ozonation dose than alum. As the pre-ozonation dose was increased both coagulants exhibited gradually increasing total organic carbon removal in the ozone dose range studied. By examining the dynamic floc formation data (Figure 2) it might be expected the opposite though this finding is consistent with the previous one in Figure 4 when the humic acid concentration was 5 mg/L. These results (at 5 and 10 mg/L humic acid concentrations) show similarity to those in Sam et al. (2010).



**Figure 6.** Change in residual total organic carbon concentration with ozone dose at 20 mg/L humic acid concentration

When the humic acid concentration was increased to 20 mg/L, the total organic carbon removals with both of the coagulants (Figure 6) showed correlation with the relative floc size data in Figure 3; i.e. when the 20 mg/L humic acid containing synthetic raw water was pre-ozonated with increasing ozone dose floc sizes decreased with both coagulants and as one might expect that total organic carbon removals diminished. Nevertheless, this result contradicts with the findings when the concentration of humic acid was 5 and 10 mg/L.

Among others who claimed that pre-ozonation hindered the removal of organic matter (Schneider and Tobiasson, 2000; Hailong et al., 2007; Bose and Reckhow, 2007), and those who reported that pre-ozonation enhanced the removal of organic matter (Marhaba and Pipada, 2000; Singer et al., 2003; Pei et al., 2007; Jasim et al., 2008) these results seem rather similar to those of O'Melia et al. (1999) who informed that the effect of ozonation depended on the concentration of organic matter and of Singer (1990) and Edwards et al. (1993) who found that the effect of ozonation depended on the ozone dose.

## CONCLUSION

All the humic acid concentrations studied sizes of flocs formed with both aluminium sulphate and polyaluminium chloride were found to be decreased as the pre-ozonation dose was increased. However, residual total organic carbon measurements showed that organic matter removal was enhanced at lower humic acid concentrations (5 and 10 mg/L) whereas it was hindered at the highest humic acid concentration (20 mg/L) investigated. Ozone is a powerful oxidant, when humic waters are ozonated it converts long chain organic molecules to oxidised shorter chain ones, which are mainly negatively charged. When 5 and 10 mg/L humic acid containing raw waters were ozonated prior to flocculation, alum and polyaluminium chloride coagulants seemed to cope with



those negatively charged oxidised shorter chain organics, although sizes of flocs gradually decreased with increased pre-ozonation dose aggregation was probably sufficient to put them on the settleable side. However, when the humic acid concentration was as high as 20 mg/L it is likely that ozonation produced considerably high amount of negatively charged oxidised organic molecules, which resulted in hindrance of their removal.

## REFERENCES

- Bose, P., Reckhow, D. A. (2007) The effect of ozonation on natural organic matter removal by alum coagulation. *Water Research*, **41**, 1516-1524.
- Edwards, M., Boller, M., Benjamin, M. M. (1993) Effect of pre-ozonation on removal of organic-matter during water-treatment plant-operations. *Water Science and Technology*, **27**(11), 37-45.
- Gregory, J., Nelson, D. W. (1986) Monitoring of aggregates in flowing suspensions. *Colloids and Surfaces*, **18**, 175-188.
- Hailong, L., Dongsheng, W., Min, W., Hongxiao, T., Min, Y. (2007) Effect of pre-ozonation on coagulation with IPF-PACls: Role of coagulant speciation. *Colloids and Surfaces A: Physicochemical Engineering Aspects*, **294**, 111-116.
- Jasim, S. Y., Ndiongue, S., Johnson, B., Schweitzer, L., Borikar, D. (2008) The effect of ozone on cold water coagulation. *Ozone: Science & Engineering*, **30**(1), 27-33.
- Marhaba, T. F., Pipada, N. S. (2000) Coagulation: effectiveness in removing natural organic matter fractions. *Environmental Engineering Science*, **17**(2), 107-115.
- O'Melia, C. R., Becker, W. C., Au, K.-K. (1999) Removal of humic substances by coagulation. *Water Science and Technology*, **40**(9), 47-54.
- Owen, D. M., Amy, G. L., Chowdhury, Z. K., Paode, R., McCoy, G., Viscosil, K. (1995) NOM - Characterization and treatability. *Journal of AWWA*, **87**(1), 46-63.
- Pei, Y. S., Yu, J. W., Guo, Z. H., Zhang, Y., Yang, M., Zhang, J. S., Junji, H. (2007) Pilot study on pre-ozonation enhanced drinking water treatment process. *Ozone: Science & Engineering*, **29**(5), 317-323.
- Randtke, S. J. (1988) Organic contaminant removal by coagulation and related process combinations. *Journal of AWWA*, **80**(5), 40-56.
- Sam, S., Yukselen, M. A., Zorba, M., Gregory, J. (2010) The Effect of Ozone on the Reversibility of Flocculation Breakage: Suspensions with High Humic Acid Content. *Ozone: Science & Engineering*, **32**(6), 435-443.
- Schneider, O. D., Tobiasson, J. E. (2000) Pre-ozonation effects on coagulation. *Journal of AWWA*, **92**(10), 74-87.
- Sharp, E. L., Jarvis, P., Parsons, S. A., Jefferson, B. (2006) Impact of fractional character on the coagulation of NOM. *Colloids and Surfaces A: Physicochemical and Engineering Aspects*, **286**, 104-111.
- Singer, P. C. (1990) Assessing ozonation research needs in water-treatment. *Journal of AWWA*, **82**(10), 78-88.
- Singer, P. C., Arlotta, C., Snider-Sajdak, N., Miltner, R. (2003) Effectiveness of pre- and intermediate ozonation on the enhanced coagulation of disinfection by-product precursors in drinking water. *Ozone: Science & Engineering*, **25**(6), 453-471.



## Water Disinfection from Microorganisms Using Chitosan

M. N. Saprykina\*, E. V. Bolgova\*, L. O. Melnyk\* and V. V. Goncharuk\*

\*A. V. Dumansky Institute of Colloid and Water Chemistry, 42, Vernadsky Blvd, Kyiv, Ukraine, 03680  
(E-mail: *saprykina\_m@ukr.net*)

### Abstract

It is established that the effectiveness of the process of water disinfection depends on both the molecular weight of chitosan, the degree of its deacetylation, and the type of microorganism. The optimal pH value of the medium for inactivating the culture of *C.albicans* was determined. For the first time, a significant contribution of the flocculation of microorganisms with chitosan to the total effect of water disinfection is shown. It is also shown that the presence of organic and inorganic impurities in water reduces both the disinfecting and flocculating effects of the polysaccharide on the microbiological object. The impact of temperature on the antimicrobial effect of chitosan was revealed.

### Keywords

Water disinfection; chitosan; bactericidal effect; flocculating effect

## INTRODUCTION

Nowadays, the studies on the disinfection and purification of water using chitosan (CTN) and materials made on its base are being intensively carried out in the world, which is associated with the need to improve the environmental friendliness of water treatment processes, as well as make the requirements for drinking water quality stricter (Qin et al., 2006; Unuabonah et al., 2017; Li et al., 2008; Fabris et al., 2010; Yang et al., 2016; Abebe et al., 2016; Kangama et al., 2018; Zeng et al., 2008).

Chitosan obtained from chitin (a natural polymer) by deacetylation in an alkaline medium due to the variety of physicochemical and biological characteristics is widely used in the food industry, cosmetology, biomedical engineering, and agriculture (Kong et al., 2010; Frederick, 2016).

The papers (Tymchuk and Grubnyak, 2017; Kong et al., 2008) note the important advantages of chitosan, such as biodegradability and high disinfecting ability against gram-positive and gram-negative bacteria, while there is no toxicity towards mammalian cells. This creates prospects for the use of chitosan as an antibacterial agent alone or in a mixture with other natural polymers.

As it was shown in (Goy et al., 2009; Raafat et al., 2008; Chung and Chen, 2008; Eaton et al., 2008; Helander et al., 2001; Liu et al., 2004), one of the most likely mechanisms of chitosan antibacterial effect is the electrostatic interaction of protonated amino groups of its molecules with a negatively charged microbial cell membrane, mainly due to competition with  $\text{Ca}^{2+}$  ions for electronegative sites on the cell membrane surface. This leads to a double effect. Firstly, the permeability of the membrane wall changes, which causes an internal osmotic imbalance and, therefore, inhibits the growth of microorganisms. Secondly, due to the hydrolysis of peptidoglycans in the wall of microorganisms, intracellular electrolyte (i.e., potassium ions, low molecular weight protein components: proteins, nucleic acids, glucose and the lactate dehydrogenase enzyme) leaks.

Chitosan and its various derivatives are also considered as potential environmentally safe coagulants and flocculants for water treatment, given their environmental safety and high efficiency

*11<sup>th</sup> Eastern European Young Water Professionals Conference IWA YWP,  
1-5 October 2019, Prague, Czech Republic*

at relatively low doses (Li et al., 2013). Thus, according to (Frederick, 2016), the optimal doses of aluminum sulfate, ferric chloride and chitosan in the process of coagulation of lake water, determined by the turbidity of the settled water, are 30, 30 and 8 mg/dm<sup>3</sup>, respectively. However, in work (Frederick, 2016) it is noted that chitosan has not been studied enough as a coagulant for drinking water.

The purpose of this work was to study the disinfecting effect of high molecular weight and low molecular weight CTN with different degrees of deacetylation on *E.coli* and *C.albicans* microorganisms depending on the physicochemical parameters of the water and determine the contribution of flocculation of microorganisms with chitosan to the total effect of water disinfection in order to meet the drinking water quality requirements.

## METHODS

Water disinfection was carried out using a 0.1 % chitosan working solution in a 0.1 mol/dm<sup>3</sup> solution of acetic acid. High molecular weight CTN<sub>1</sub> (with the molecular weight (Mw) constituting 100–300 kDa) and low molecular weight CTN<sub>2</sub> (with a Mw constituting 50-60 kDa) with a degree of deacetylation of 95 and 75-85 %, respectively, were investigated.

The culture of sanitary indicative test microorganism *Escherichia coli* 1257 was obtained from the collection of Tarasevich State Institute of Standardization and Control of Biomedical Preparations (Moscow). Suspension of *Escherichia coli* 1257 bacteria (10<sup>7</sup> CFU/cm<sup>3</sup>) was prepared according to (Goncharuk et al., 2001). Yeast-like fungus *Candida albicans* 10231 was received from L.V. Gromashevsky Institute of Epidemiology and Infectious Diseases of the NAMS of Ukraine. Cultivation of yeast-like fungi was carried out in a liquid nutrient medium Saburo, which was prepared according to (Grigorieva, 1981). The preparation of a suspension of yeast-like fungi was carried out similarly to (Goncharuk et al., 2008).

Conducting the study of the disinfecting effect of CTN, the cups of 100 cm<sup>3</sup> were filled with water contaminated with microorganisms, the necessary amount of CTN was added, so that the concentration of the latter was 0.1, 0.5, 1.0, 5.0 or 8.0 mg/dm<sup>3</sup>. After a certain period of time, an aliquot of the treated water was taken and sown on a nutrient medium with further counting of the colonies.

Studying the joint bactericidal and flocculating effect of CTN on the process of water disinfection, the 100-cm<sup>3</sup>-volume cups were filled with water contaminated with microorganisms and the necessary amount of CTN, so that the concentration of the latter was 0.1, 0.5, 1.0, 5.0 or 8.0 mg/dm<sup>3</sup>. At certain intervals the treated water was passed through paper filters (i.e., a white tape – Whatman Grade 40 filter paper 8 µm, which simulates filtration through a sand filter (Kong et al., 2010)), an aliquot of the filtrate was collected and sown on a nutrient medium with further counting of the colonies.

The survival of microorganisms was determined by the presence of CFU when sowing water samples taken on Saburo agar medium for *Candida albicans* and Endo agar medium for *Escherichia coli*. Microorganisms were cultured for 14-18 hours at 37 °C. The result was expressed as the logarithm of the ratio of the test microorganism concentration in the solution after treatment with CTN (N<sub>t</sub>) to the concentration of the microorganism in the initial solution (N<sub>0</sub>).

Conducting the research, distilled water (DW), tap water (TW), and water after ultrafiltration treatment with an UPM-20 membrane (UFW) were used. The physico-chemical characteristics of the types of water in question are presented in Table 1.

**Table 1.** Physico-chemical composition of the investigated waters

Type of water	Name of indicators					
	Conductivity at 18 °C, $\mu\text{S}/\text{cm}$	Color, degrees	Turbidity, $\text{mg}/\text{dm}^3$	pH	Sulfates, $\text{mg}/\text{dm}^3$	Chlorides, $\text{mg}/\text{dm}^3$
DW	2	< 2	< 0.3	5.3	0.5	0.02
TW	382	18	0.9	7.2	57.6	26.0
UFW	298	8	0.1	7.3	14.6	16.0

Studying the effect of water pH on the efficiency of the disinfection process, a 0.1% NaOH solution or a 0.1% HCl solution was used to adjust the pH value. The pH value was determined using an I-160M ionomer.

Studying the effect of temperature on the disinfection of water with CTN, the investigated water samples were thermostated at 42, 37, 27, 17 and 7 °C.

## RESULTS AND DISCUSSION

Table 2 shows that the efficiency of distilled water disinfection from gram-negative bacteria *Escherichia coli* with two types of chitosan (concentration 0.1  $\text{mg}/\text{dm}^3$ ) practically does not depend on the molecular weight of the polymer and the degree of its deacetylation. Already after one hour of contact of *Escherichia coli* (initial concentration 500000  $\text{CFU}/\text{cm}^3$ ) with CTN, the degree of culture inactivation constitutes two orders of magnitude, and CTN has a pronounced bactericidal effect, since there is no growth of culture over time.

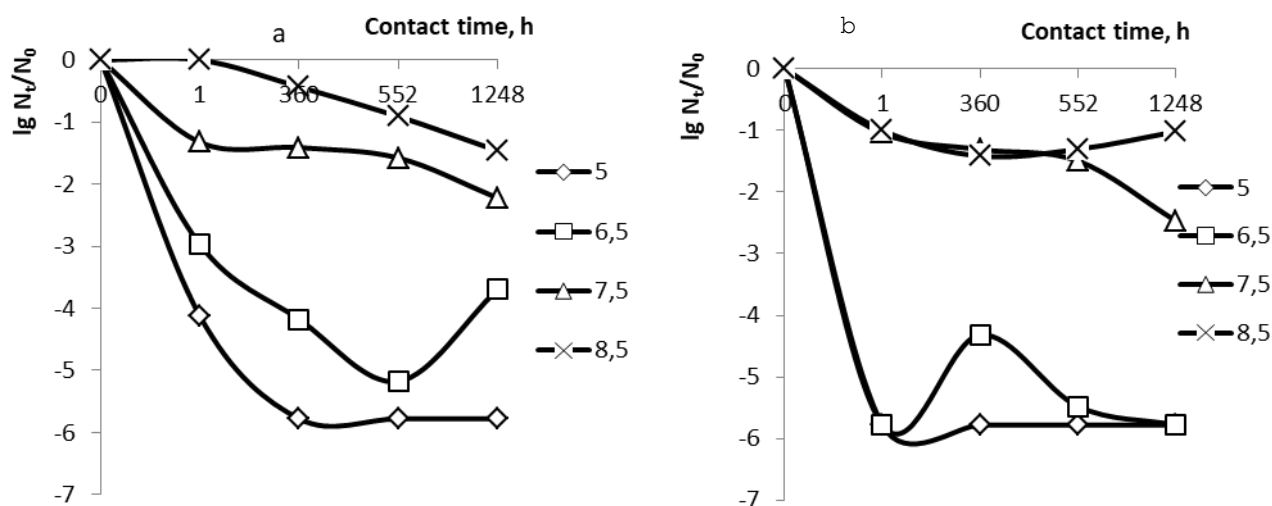
**Table 2.** Disinfection of distilled water from *E.coli* and *C.albicans* with chitosan (0.1  $\text{mg}/\text{dm}^3$ ) with different molecular weights (pH – 6.6; t – 13 °C)

t, h	$\text{CFU}/\text{cm}^3$			
	<i>E.coli</i>		<i>C. albicans</i>	
	CTN <sub>1</sub> (300000)	CTN <sub>2</sub> (60000)	CTN <sub>1</sub> (300000)	CTN <sub>2</sub> (60000)
0	500000	500000	2400000	2400000
1	5000	2900	13000	60000
168	0	0	20000	10000
504	0	0	130	18000

In the case of disinfection of the yeast-like fungus *C.albicans* at its initial concentration of 2400000  $\text{CFU}/\text{cm}^3$  under similar conditions, it was found (see Table 2) that the degree of inactivation of micromycete by chitosan depends on the molecular weight and degree of deacetylation of the latter. A low molecular weight CTN with a degree of deacetylation amounting to 75-85 % inactivates only slightly more than one culture order after an one hour of contact, while high molecular weight CTN with a deacetylation degree constituting 90 % inactivates over a similar period of more than two and a half culture order. It has been established that *C.albicans* is more stable in comparison with *E.coli* to the effect of the disinfecting agent, which is especially noticeable with an increase in the time of

contact of the culture with CTN. Obviously, this effect is associated with a different cell structure. The yeast cell is surrounded by a rather thick cell wall (Cell wall of fungi).

The results obtained confirm our conclusion in previous studies (Bolgova et al., 2016) that *C.albicans* is a more suitable test object for evaluating the effectiveness of disinfection processes compared to *E.coli*. Based on the obtained results, CTN<sub>1</sub> was selected for further research in this work. The results of the study of the influence of pH on the efficiency of disinfection of water from *C.albicans* with CTN<sub>1</sub> are presented in Figure 1.



**Figure 1.** The kinetics of disinfection of distilled water with CTN<sub>1</sub> (0.1 mg/dm<sup>3</sup>) from *C.albicans* at different pH values: a) the bactericidal effect of CTN<sub>1</sub>; b) joint bactericidal and flocculating effect of CTN<sub>1</sub>

Figure 1 shows that the highest degree of inactivation of the culture is achieved in a weakly acidic medium (pH 5.0), whereas at pH 8.5 the disinfecting effect is insignificant. Comparison of Figure 1a and Figure 1b indicates a significant contribution of flocculation of microorganisms with chitosan to the total effect of water disinfection, which is especially noticeable at relatively short periods of contact of culture with chitosan. Thus, the concentration of *C.albicans* with a contact duration of an one hour decreases by about 4 and 6 orders of magnitude, respectively, with the bactericidal (see Fig. 1a) and the joint bactericidal and flocculating action (see Fig. 1b) of chitosan.

It is important to note that the degree of retention of *E.coli* and *C.albicans* when filtered through paper in the absence of chitosan did not exceed 0.1-0.3 order of the initial concentration.

The higher efficiency of the disinfecting and flocculating effect of chitosan in a weakly acidic environment is associated with a high degree of protonation of the polymer amino groups under these conditions, which contributes to the electrostatic interaction between negatively charged microorganisms and positively charged molecules of chitosan, causing, on the one hand, changes in the permeability of the cell membrane and its violation functioning, and, on the other hand, cell aggregation and flocculating effect (Yang et al., 2016; Goy et al., 2009; Raafat et al., 2008).

As the further studies have shown, the presence of various impurities in water significantly impairs the efficiency of its disinfection with chitosan (see Table 3 and 4). Figures 3 and 4 show that the bactericidal effect of chitosan as well as its joint bactericidal and flocculating effect on *C.albicans* micromycetes is most pronounced in distilled water – in the experimental conditions the decrease in

the concentration of the microorganism constitutes 4-5 orders of magnitude (The initial amount of culture varies from  $8,5 \cdot 10^4$  to  $6 \cdot 10^5$ ). At the same time, in tap water and tap water after ultrafiltration treatment, the degree of disinfection of *C.albicans* under similar conditions does not exceed 1-2 orders of magnitude, being higher in water that underwent additional membrane cleaning.

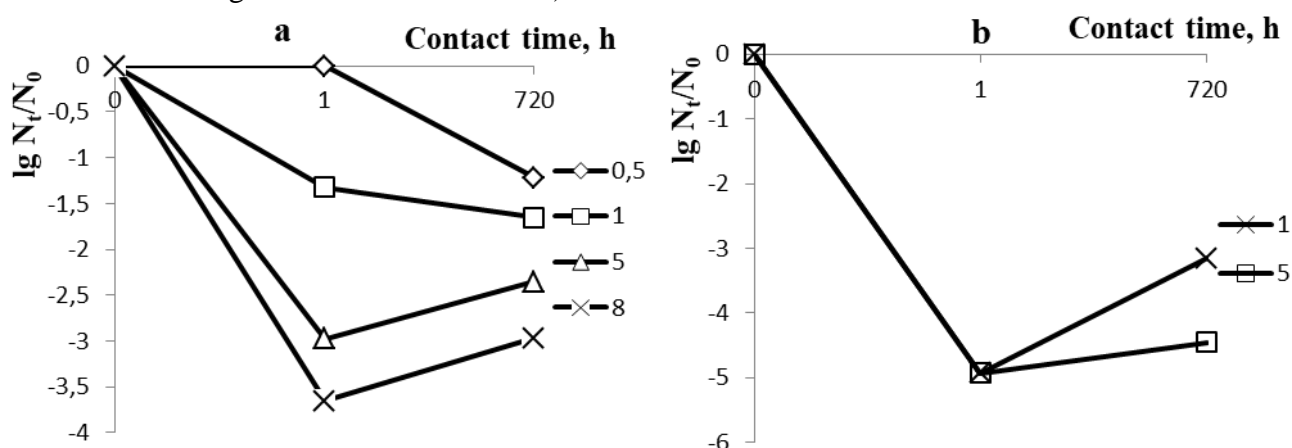
**Table 3.** The kinetics of disinfection of various types of water from *C.albicans* with CTN<sub>1</sub> (0.1 mg/dm<sup>3</sup>) at pH 5.0

τ, h	Type of water		
	TW	UFW	DW
	CFU/cm <sup>3</sup>		
1	$1.2 \cdot 10^5$	$2.0 \cdot 10^4$	$4,5 \cdot 10^1$
360	$4.3 \cdot 10^4$	$3.9 \cdot 10^3$	1
720	$1.2 \cdot 10^4$	$2.3 \cdot 10^3$	1

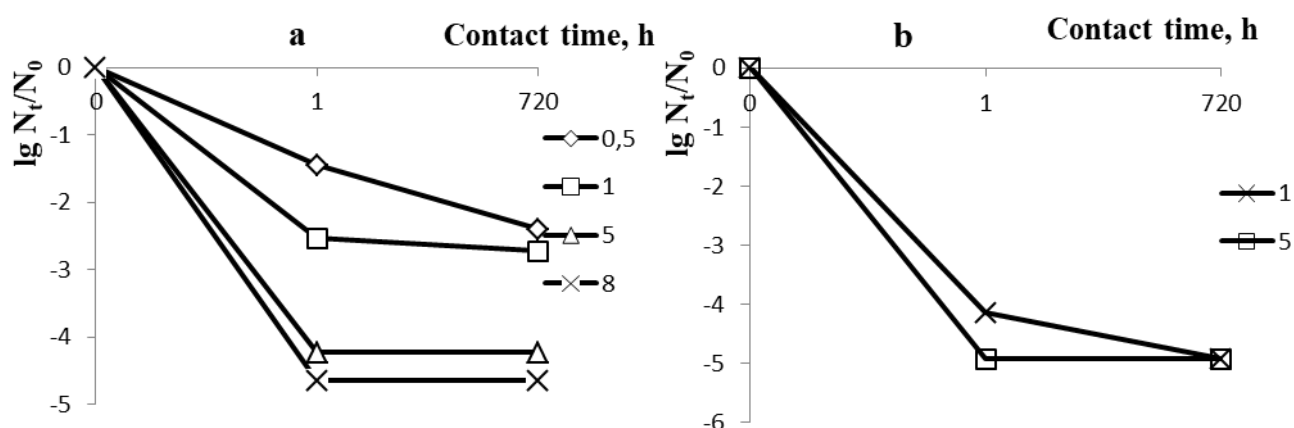
**Table 4.** The kinetics of joint bactericidal and flocculating effect of CTN<sub>1</sub> (0.1 mg/dm<sup>3</sup>) on various types of water disinfected from *C.albicans* at pH 5.0

τ, h	Type of water		
	TW	UFW	DW
	CFU/cm <sup>3</sup>		
1	$7.8 \cdot 10^4$	$1.2 \cdot 10^3$	1
360	$4.3 \cdot 10^4$	$3.2 \cdot 10^2$	1
720	$2.0 \cdot 10^4$	$7.5 \cdot 10^1$	1

The results obtained can be explained by the presence in the TW and UFW of a whole range of organic and inorganic impurities that compete with microorganisms for interaction with CTN molecules, reducing both the disinfecting and flocculating effect of the polysaccharide on the microbial object. Thus, as arises from the results presented above, the use of chitosan at a concentration of 0.1 mg/dm<sup>3</sup> for disinfection of tap water as well as ultrafiltration-treated tap water is ineffective. To obtain the desired result, it is obviously necessary to increase the dose of chitosan during water treatment. Figures 2 and 3 show the results of disinfection of tap water as well as tap water treated using ultrafiltration method from *C.albicans* (with the concentration in the source water constituting  $1 \cdot 10^4 - 1 \cdot 10^5$  CFU/cm<sup>3</sup>) at various concentrations of chitosan in the solution.



**Figure 2.** The kinetics of disinfection of water from *C.albicans* at various concentrations of CTN<sub>1</sub> (figures indicated on the curves, mg/dm<sup>3</sup>): a) tap water (pH = 7.1); b) tap water after ultrafiltration (pH = 7.1)



**Figure 3.** The kinetics of water disinfection from *C.albicans* with the joint bactericidal and flocculating effect of different concentrations of CTN<sub>1</sub> (figures indicated on curves, mg/dm<sup>3</sup>): a) tap water (pH = 7.1); b) tap water after ultrafiltration (pH = 7.1)

As can be seen from Figure 2a and Figure 3a, an increase in the concentration of chitosan in tap water from 0.5 to 8.0 mg/dm<sup>3</sup> significantly increases the degree of its disinfection from *C.albicans*, moreover, as in the patterns shown in Figure 1, a significant contribution of the flocculating effect of chitosan to this process is found. Almost complete disinfection of tap water from *C.albicans* is observed after an one hour of contact of the culture with chitosan at a concentration of the latter constituting 8.0 mg/dm<sup>3</sup> and additional filtration of the chitosan treated water through a paper filter. Effective disinfection of water that has passed the preliminary ultrafiltration treatment is observed at a lower concentration of chitosan (5.0 mg/dm<sup>3</sup>), which was obvious considering the results presented above.

It is established that the antimicrobial effect of chitosan in relation to the selected microorganisms significantly increases with increasing temperature from 7 to 42 °C (data not shown). A decrease in the degree of inactivation of the culture with a decrease in temperature may be associated with a decrease in the number of reactive groups on the cell surface for binding to chitosan. Such changes in the cell arise because of the stress factor acting thereon, namely, a low temperature.

## CONCLUSIONS

Experimental studies conducted lead to the following conclusions.

The degree of inactivation of the *E.coli* culture does not depend on the type of chitosan studied in the work (a high molecular weight CTN<sub>1</sub> (with molecular weight (Mw) constituting 100-300 kDa) and low molecular weight CTN<sub>2</sub> (with Mw constituting 50-60 kDa) with a degree of deacetylation constituting, 95 and 75-85 %, respectively), whereas, in the case of *C.albicans*, a high molecular weight CTN with a degree of deacetylation amounting to 95 % is a more effective disinfecting agent.

The highest degree of inactivation of the culture of *C.albicans* with CTN<sub>1</sub> is achieved in a weakly acidic medium (pH 5.0), whereas at pH 8.5 the disinfecting effect is insignificant.

For the first time a significant contribution of the flocculation of microorganisms with chitosan to the total effect of water disinfection is shown. This factor is essential when choosing a rational scheme of disinfection of water with chitosan, because it indicates the possibility of reducing the

dose of chitosan required for disinfection in the case of applying the water filtration after treatment with chitosan.

It is shown that the presence of organic and inorganic impurities in water reduces both the disinfecting and flocculating effect of the polysaccharide on the microbiological object, which is obviously connected with the competing influence of these impurities on the interaction of CTN molecules with microorganisms.

It is shown that the antimicrobial effect of chitosan increases with increasing temperature from 7 to 42 °C. Achieving a high degree of disinfection of water at low temperatures requires increasing the dose of chitosan.

## REFERENCES

- Abebe, L., Chen, X., Sobsey, M. (2016) Chitosan Coagulation to Improve Microbial and Turbidity Removal by Ceramic Water Filtration for Household Drinking Water Treatment. *International Journal of Environmental Research and Public Health*, **13**(3), 269.
- Bolgova, E. S., Saprykina, M. N., Goncharuk, V. V. (2016) New test object for assessing the quality of disinfected water. *Water and water puring technologies. Scientific and technical portal*, **3**(20), 3-7, (in Ukrainian).
- Cell wall of fungi. Kletochnaia stenka gribov, (in Russian). [online] <http://ru.wikipedia.org>.
- Chung, Y.-C., Chen, C.-Y. (2008) Antibacterial characteristics and activity of acid-soluble chitosan. *Bioresource Technology*, **99**(8), 2806-2814.
- Eaton, P., Fernandes, J. C., Pereira, E., Pintado, M. E., Xavier Malcata, F. (2008) Atomic force microscopy study of the antibacterial effects of chitosans on *Escherichia coli* and *Staphylococcus aureus*. *Ultramicroscopy*, **108**(10), 1128-1134.
- Fabris, R., Chow, C. W. K., Drikas, M. (2010) Evaluation of chitosan as a natural coagulant for drinking water treatment. *Water Science and Technology*, **61**(8), 2119-2128.
- Frederick, W. (2016) Pontius Chitosan as a Drinking Water Treatment Coagulant. *American Journal of Civil Engineering*, **4**(5), 205-215.
- Goncharuk, V. V., Potapchenko, N. G., Kosinova, V. N., Sova, A. N. (2001) Water chemistry and technology, **23**(4), 427-438, (in Russian).
- Goncharuk, V. V., Potapchenko, N. G., Vakulenko, V. F., Savluk, O. S., Kosinova, V. N., Sova, A. N. (2008) Disinfection of water with ozone and UV-irradiation simultaneously in flow mode. *Water chemistry and technology*, **30**(1), 91-105, (in Russian).
- Goy, R. C., de Britto, D., Assis, O. B. G. (2009) A review of the antimicrobial activity of chitosan. *Polímeros*, **19**(3), 241-247.
- Grigorieva, L.V. (1986) Handbook on sanitary microbiology, Cartea Moldoveneasca, Chisinau, 206, (in Russian).
- Helander, I., Nurmiäho-Lassila, E.-L., Ahvenainen, R., Rhoades, J., Roller, S. (2001) Chitosan disrupts the barrier properties of the outer membrane of Gram-negative bacteria. *International Journal of Food Microbiology*, **71**(2-3), 235-244.
- Kangama, A., Zeng, D., Tian, X., Fang, J. (2018) Application of Chitosan Composite Flocculant in Tap Water Treatment. *Journal of Chemistry*, 1-9.
- Kong, M., Chen, X. G., Xing, K., Park, H. J. (2010) Antimicrobial properties of chitosan and mode of action: A state of the art review. *International Journal of Food Microbiology*, **144**(1), 51-63.
- Kong, M., Chen, X. G., Liu, C. S., Liu, C. G., Meng, X. H., Yu, L. J. (2008) Antibacterial mechanism of chitosan microspheres in a solid dispersing system against *E. coli*. *Colloids and Surfaces B: Biointerfaces*, **65**(2), 197-202.

- Li, Q., Mahendra, S., Lyon, D. Y., Brunet, L., Liga, M. V., Li, D., Alvarez, P. J. J. (2008) Antimicrobial nanomaterials for water disinfection and microbial control: Potential applications and implications. *Water Research*, **42**(18), 4591-4602.
- Li, J., Jiao, S., Zhong, L., Pan, J., Ma, Q. (2013) Optimizing coagulation and flocculation process for kaolinite suspension with chitosan. *Colloids and Surfaces A: Physicochemical and Engineering Aspects*, **428**, 100-110.
- Liu, H., Du, Y., Wang, X., Sun, L. (2004) Chitosan kills bacteria through cell membrane damage. *International Journal of Food Microbiology*, **95**(2), 147-155.
- Qin, C., Li, H., Xiao, Q., Liu, Yi., Zhu, J., Du, Yu. (2006) Water solubility of chitosan and its antimicrobial activity. *Carbohydrate Polimers*, **63**, 367-373.
- Raafat, D., von Barga, K., Haas, A., Sahl, H.-G. (2008) Insights into the Mode of Action of Chitosan as an Antibacterial Compound. *Applied and Environmental Microbiology*, **74**(12), 3764-3773.
- Tymchuk, A. F., Grubnyak, A. E. (2017) Effect of natural and synthetic flocculants on the sedimentation stability of suspensions. *ONU Bulletin. Chemistry*, **22**(2(62)), 71-81, (in Russian).
- Unuabonah, E. I., Adewuyi, A., Kolawole, M. O., Omorogie, M. O., Olatunde, O. C., Fayemi, S. O., Taubert, A. (2017) Disinfection of water with new chitosan-modified hybrid clay composite adsorbent. *Heliyon*, **3**(8), 1-29.
- Yang, R., Li, H., Huang, M., Yang, H., Li, A. (2016) A review on chitosan-based flocculants and their applications in water treatment. *Water Research*, **95**, 59-89.
- Zeng, D., Wu, J., Kennedy, J. F. (2008) Application of a chitosan flocculant to water treatment. *Carbohydrate Polymers*, **71**(1), 135-139.



# Experimental Determination of Efficiency Adsorbent Bayoxide E33 of Removal Micropollutants from Water

D. Šiblová\* and R. Biela\*

\* Institute of Municipal Water Management, Faculty of Civil Engineering, Brno University of Technology, Žižkova 17, 602 00, Brno, Czech Republic (E-mails: [siblova.d@fce.vutbr.cz](mailto:siblova.d@fce.vutbr.cz); [biela.r@fce.vutbr.cz](mailto:biela.r@fce.vutbr.cz))

## Abstract

Micropollutants are current topic in the water management field. In the world new technologies are tested to elimination micropollutants from water, because they are harmful not only for the environment, but also for people. Standard water treatment processes for removing micropollutants from water are: adsorption, advanced oxidation process and membrane process. For experimental determination of efficiency adsorbent Bayoxide E33 selected adsorbents were removed using adsorption. The efficiency of removing microfouling was determined compared by removing three micropollutants namely removing a metal, a pharmaceutical and a pesticide. Bayoxide E33 removed metal successfully, but pharmaceutical and pesticide was not removed, because desorption occurred during removal.

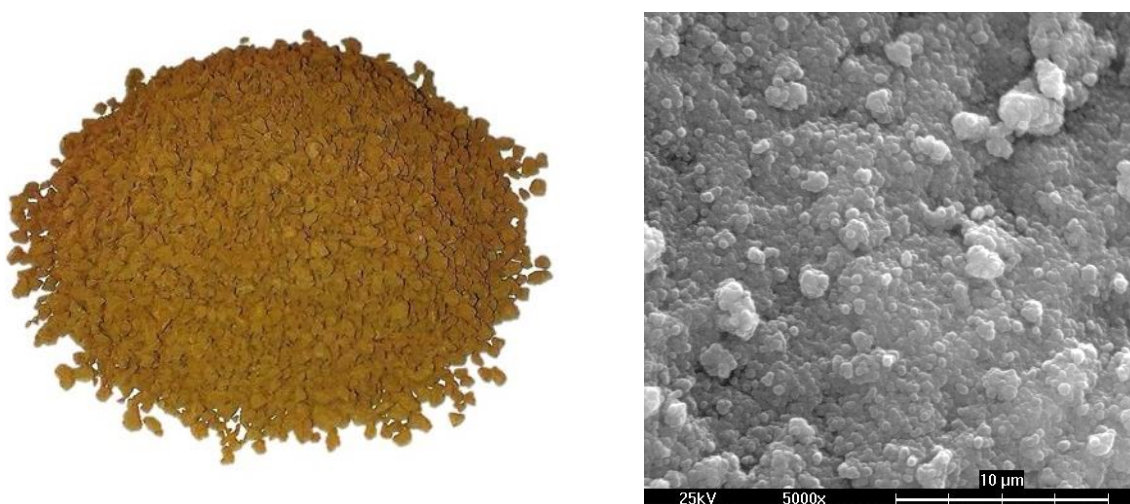
## Keywords

Water treatment; adsorption; micropollutants; sorption materials

## MATERIALS AND METHODS

### Sorption material

Bayoxide E33 is a dry crystalline medium developed by Severn Trent and designed for removal of arsenic, antimony and other metals, such as iron and manganese from water. The advantages of the material are long life continuous water treatment, low investment costs and long life dry medium (Ilavský and Barloková, 2008). The sorption material is marketed in two forms, Bayoxide E33 granules and Bayoxide E33P in tablet form (Severn Trent Services, 2005). Figure 1 shows the original material Bayoxide E33 and material at 5000 times magnification.



**Figure 1.** Original sorption material Bayoxide E33 and material at 5000 times magnification

### **Selected micropollutants**

The presence of micropollutants in drinking water sources may be of natural origin, but also of anthropogenic origin. Three different types of micropollutants were selected for the experiment. Arsenic, which is one of the common metals occurring in the environment, was chosen as the metal to be removed. The pesticide chosen was Metazachlor ESA, mainly used for crop protection. The pharmaceutical removed was salicylic acid, which is contained in frequently used cosmetic products.

*Arsenic* occurs mainly in the form of sulphides in nature, it accompanies most sulphide ores and is part of various rocks and soil. It can get into groundwater and surface waters by weathering. The concentration of arsenic in groundwater and surface water is up to 10 µg/l. About 20 % of groundwater sources contain arsenic at concentrations of 100 µg/l to 250 µg/l. Arsenic adsorbs strongly on suspended solids and sediments containing hydrated iron and hydrated alumina and clay particles. With these particles it is then remotely transported by surface water. Anthropogenic sources of arsenic are combustion fossil fuels, metallurgical and ore industry, tanneries and also application of some pesticides. A significant amount of arsenic is contained in extracts from power fly ash. Arsenic is highly toxic and long-term ingestion of water with low concentrations of arsenic causes chronic diseases. In some countries, arsenic is the most important toxic metal found in groundwater and drinking water. Cases of chronic arsenic poisoning have been observed such as India, Taiwan, and Bangladesh. In the Czech Republic, the highest limit value for arsenic in drinking water is 10 µg/l (Pitter, 2015).

*Metazachlor ESA* is a metabolite of the pesticide Metazachlor, which belongs to the group of herbicides. This pesticide is used to eliminate a wide range of unwanted weeds in crop cultivation, ornamental trees and shrubs. Through application of pesticide to crop it can reach to groundwater. To the surface water is Metazachlor get by flushing farmland which the pesticide has been applied can reach. Metazachlor is approved for use in all European Union countries (FOOTPRINT, 2007). The metabolite is significant or relevant whether its natural properties are comparable to those of the parent substances. It is also relevant if to the effect on the biological target, or poses a higher risk to organisms than the parent or comparable risk, or that it has certain toxicological properties which are considered unacceptable. The methodology of the European Commission is used to assess the relevance of metabolites of pesticides ;Guidance document on the assessment of the relevance of metabolites in groundwater of substances regulated under Council directive 91/414/EEC. According to the methodology, the recommended limit value of the metabolite in drinking water is 0.05 mg/l, provided that the parent substance Metazachlor is less than 0.01 µg/l (NIPH, 2014).

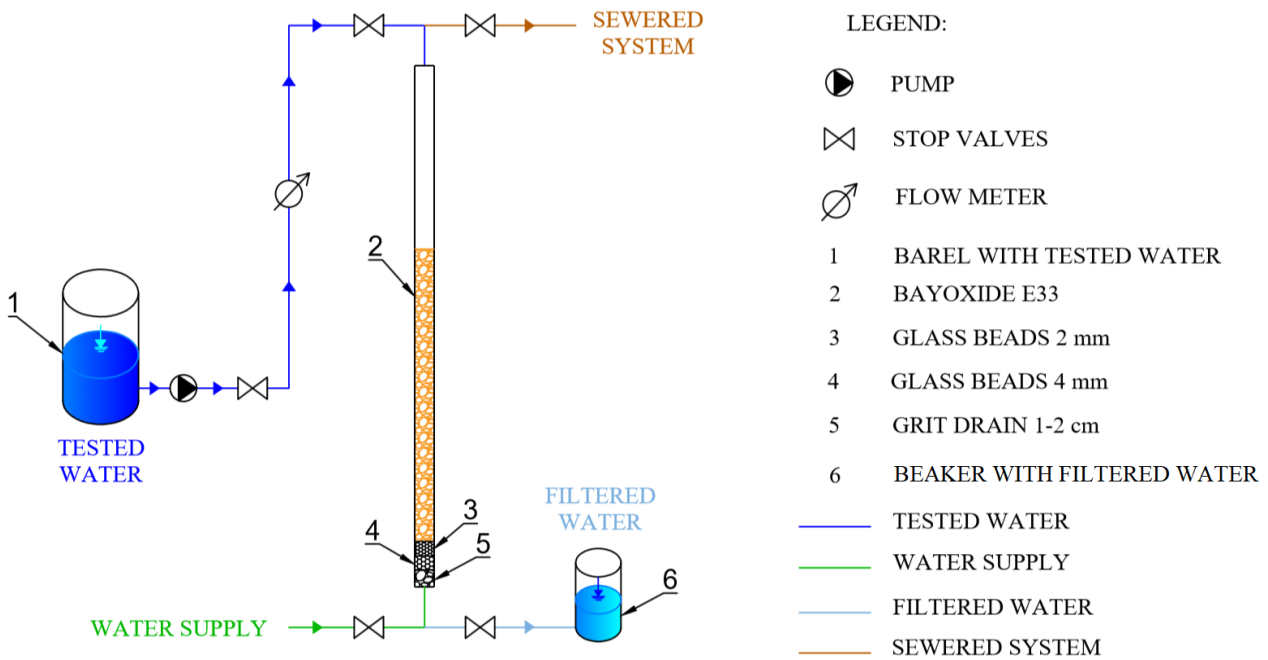
*Salicylic acid* is colorless organic acid often used in dermatological medicine. Salicylic acid is obtained from the bark of white willow. It has anti-inflammatory effects and is therefore classified as non-steroidal anti-inflammatory drugs. Anti-inflammatory drugs alone do not cure anything but only suppress the unpleasant manifestations of various diseases (Šíbllová, 2017). Already in the 18th century it was known that the extract of the bark of white willow reduces fever and in 1870 it managed to find a substance we call salicylic acid. Previously, salicylic acid was not an ideal drug because it was administered in the form of a bitter solution that induced vomiting and irritated the stomach walls. Therefore, in 1899 acetylsalicylic acid was produced by synthesis of an acetylated derivative. This acid has good analgesic and anti-inflammatory effects such as salicylic acid, but its use is safer and more pleasant. Acetylsalicylic acid has become a major component of Aspirin (Iversen, 2006). Because pharmaceuticals are present in very low concentrations in water, there are no limit values specified in legislation.

**Adsorption and desorption**

Adsorption is a phase transfer process that is widely used in practice to remove substances from fluid phases (gases or liquids). It can also be observed as natural process in different environmental compartments. The most general definition describes adsorption as an enrichment of chemical species from a fluid phase on the surface of a liquid or a solid. Since adsorption is a surface process, surface area is a key quality parameter for adsorbents. The proposed adsorbents are typically highly porous materials with surface areas ranging between  $10^2$  and  $10^3$  m<sup>2</sup>/g. The substance which is adsorbed is called adsorbate and the material on which adsorption takes place is called an adsorbent. The desorption may be caused by the exhausted capacity of the sorbent and also by the different properties of the sorbed pollutants. Because desorption is the opposite process of adsorption, all conditions that lead to a decrease in adsorption increase the amount of adsorbate that can be desorbed. The adsorbate that is desorbed is an aqueous solution, which may be affected by properties such as concentration, temperature and pH as compared to the original adsorbate. So in the case of an experiment desorbate is model water (Worch, 2012). The specific surface area of Bayoxide E33 ranges from 100 to 200 m<sup>2</sup>/g (Severn Trent Services, 2005).

**The proces of removing micropollutants from water**

Raw water for the removing of metal and drugs was prepared in a laboratory at the Institute of Municipal of Water Management at the Faculty of Civil Engineering in Brno by adding a micropollutant to the drinking water. Raw water for pesticide removal was taken from the river Svratka in Brno. The filtration of the model water through the Bayoxide E33 sorption material was the same for all three micropolutans. A column with sorption material Bayoxide E33 was used for filtration. Before commencement of the adsorption process the sorption material was prepared according to the manufacturer’s instruction. The sorption fill was wetted and washed in the direction opposite to the filtration direction until clear water was flowing from the column. The washing water was drained to sewerage during the material preparation. The minimum height of the filter bed was 0.6 m according to the manufacturer's recommendations.



**Figure 2.** The diagram of the filter device with adsorbent Bayoxide E33

A sample of model water was taken before filtration began. During filtration, raw water was passed through a flow meter with a throttle nozzle to control the amount of water flowing through. Then the model water was filtered through a sorption material on which adsorption took place. Individual samples were taken at different time intervals after 30 seconds, 1, 2 and 4 minutes. Water, pH and turbidity were measured after sampling. Due to the complex analysis of the sample evaluation, the resulting concentrations in the samples were determined by an accredited laboratory.

### Measurement of temperature, pH and turbidity

In a laboratory experiment, pH measurement was performed using a pH meter with an thermometer Adwa AD14. Adwa AD14 is a high-quality microprocessor-controlled portable pH meter with built-in temperature measurement with automatic temperature compensation (ADWA Instruments). Water reaction is a dimensionless indicator, which is also influenced by the water temperature. At water temperatures above 25 °C, the pH is less than 7, and at temperatures below 25 °C, it is higher. Temperature is also an important indicator of drinking water quality. Temperature significantly affects chemical and biochemical reactivity even in relatively small temperature range, from 0 °C to approximately 30 °C (Pitter, 2015).

Turbidity was determined using a turbidimeter HACH 2100Q IS. Turbidity is the rate of summary energy dispersing in the course of pass of a ray of light through a dispersion layer with unit thickness to all sides from the light beam (HACH). Turbidity is one of the organoleptic indicators of drinking water and describes the clarity of water, which is an essential requirement for drinking water quality. The turbidity of water is caused by inorganic or organic substances, which may be of natural or anthropogenic origin (Pitter, 2015).



**Figure 3.** Samples of filtered and a pH measurement (Gottwald, 2019; Šíblová, 2017)

### Determination of efficiency removing

Efficiency of removing micropollutants from water was determined by formula (Biela and Šopíková, 2017):

$$\eta = \frac{C_{RW} - C_F}{C_{RW}} \quad (1)$$

where  $\eta$  – efficiency of removing, %;

$C_{RW}$  – concentration of micropollutants in raw water,  $\mu\text{g/l}$ ;

$C_F$  – concentration of micropollutants after adsorption,  $\mu\text{g/l}$ .

## RESULTS AND DISCUSSION

### Resulting values of samples

The following tables show the measured values and the removal efficiency of micropollutants through the sorption material. Bayoxide E33.

The removal of arsenic through the Bayoxide E33 sorbent material was excellent. Already after 0.5 minute of filtration, the initial metal concentration of 62.3 µg/l in the model water was almost eliminated. In the second minute of removal, the arsenic was almost removed from the water, its concentration in the water being below the limit of measurability. This sorption material also effectively reduced turbidity, which after four minutes decreased to 0.84 ZF. The model water was created immediately after the water was taken from the water network. This is reason why the model water has a lower temperature than the other samples. The water temperature in the samples was influenced by the laboratory temperature. The pH increased slightly during the removal process and was in the range of 7.53 to 7.64.

**Table 1.** Results of arsenic removal from water (Konečný, 2015)

Time (min)	pH (-)	Temperature (°C)	Turbidity (ZF)	Metal concentration (µg/l)	Removal efficiency (%)
0	7.53	13.60	11.40	62.30	0.00
0.5	7.77	18.20	1.37	1.20	98.07
1.0	7.74	18.00	1.03	1.00	98.39
2.0	7.68	17.90	0.97	< 1.00	100.00
4.0	7.64	17.90	0.84	< 1.00	100.00

Removal of Metazachlor ESA metabolite was not successful. After 0.5 minute of removal, the initial concentration of 0.13 µg/l was decreased, but over the next few minutes the concentration returned to its original value. The Bayoxide E33 sorption material was supersaturated and the pesticide was no longer removed. This is called desorption, which is the opposite of adsorption. Turbidity was reduced during filtration to value 3.52 ZF. The temperature of the water gradually increased to 22.70 °C. The pH value was highest in the model water, dropped after half a minute and then increased slightly, which is probably related to desorption.

**Table 2.** Results of Metazachloru ESA removal from water (Gottwald, 2019)

Time (min)	pH (-)	Temperature (°C)	Turbidity (ZF)	Concentration of pesticide (µg/l)	Removal efficiency (%)
0	7.32	20.70	7.38	0.13	0.00
0.5	7.23	21.80	6.40	0.05	65.41
1.0	7.28	22.10	4.66	0.09	35.34
2.0	7.29	22.50	4.65	0.11	15.04
4.0	7.29	22.70	3.52	0.13	0.00

The removal of salicylic acid via Bayoxide E33 was similar to the removal of pesticide. After 0.5 minute of removal, the pharmaceutical concentration was decreased, but from 1 minute, increased concentrations were again measured. That means, that after 0.5 minute of removal, the desorption occurred again. Turbidity was reduced to value 0.42 ZF. The model water temperature was 20.9 °C and decreased to 17.40 °C during the removal process. The pH in the model water was 7.59 and decreased during removal as the temperature decreased.

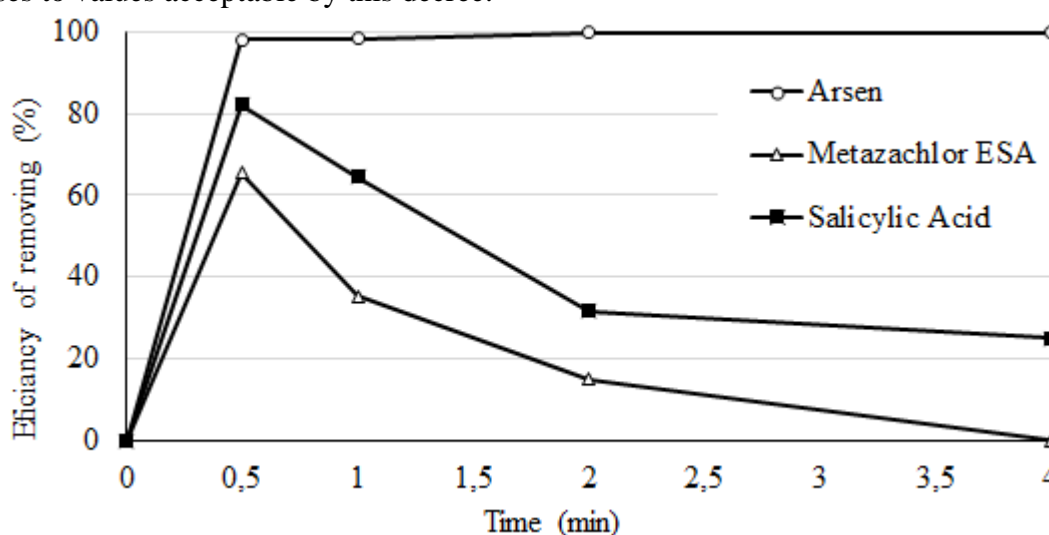
**Table 3.** Results of salicylic acid removal from water (Šíblová, 2017)

Time (min)	pH (-)	Temperature (°C)	Turbidity (ZF)	Concentration of pharmaceutical (mg/l)	Removal efficiency (%)
0	7.59	20.90	1.16	659.00	0.00
0.5	7.45	20.60	0.93	117.00	82.25
1.0	7.43	20.70	0.68	233.00	64.64
2.0	7.41	18.70	0.48	450.00	31.71
4.0	7.38	17.40	0.42	494.00	25.04

### Evaluation of experiment

The aim of the experiment was to determine and compare the effectiveness of Bayoxide E33 in removing micropollutants from water. It has been shown that the material effectively removes arsenic from water 100 % efficiency has been proven. This sorption material was developed specifically for the removal of arsenic and other metals from water. According to the experiment, Bayoxide E33 was found to be a suitable sorbent for removing arsenic from water. This sorption material has proven to be unsuitable for removing pesticide and drug from water due to desorption that has occurred during filtration.

The turbidity values in the individual samples were also measured during the experiment. The values were measured because turbidity is one of the basic organoleptic characteristics of drinking water and its limit value is set by the Decree of the Ministry of Health No. 252/2004 Coll., which establishes hygienic requirements for drinking and hot water and the frequency and scope of drinking water control. The turbidity limit according to this decree is 5 ZF. From the results of the performed experiment it can be seen that the sorption material Bayoxide E33 reduced turbidity in all cases to values acceptable by this decree.

**Figure 4.** Efficiency of removing of selected micropollutants with Bayoxide E33 adsorbent

The determined removal efficiency of selected micropollutants from water using Bayoxide E33 sorption material is shown in the figure above. In terms of efficiency, Bayoxide E33 is best suited for removing metals from water, but also for reducing turbidity. Bayoxide E33 is not suitable for the removal of pesticides and pharmaceuticals based on the experiment. In the case of pharmaceutical removal, this material is unsuitable because it has a relatively low specific surface area and the initial drug concentration was too high.



## ACKNOWLEDGMENT

This contribution is part of a grant project of specific academic research at the Brno University of Technology titled “Removal of Micropollutants from Drinking Water Sources by Adsorption” FAST-S-18-5115).

## REFERENCES

- ADWA Instruments. pH meter with thermometer Adwa AD12: Watertight pH Tester. Promotional material manufacturer.
- Biela, R., Šopíková, L. (2017) Efficiency of sorption materials on the removal of lead from water. *Applied Ecology and Environmental Research*, **15**(3), 1527-1536.
- FOOTPRINT (2007) Pesticide Properties Database. University of Hertfordshire & FOOTPRINT: creating tools for pesticide risk assessment and management in Europe. [online] <http://sitem.herts.ac.uk/aeru/ppdb/en/atoz.htm>.
- Gottwald, M. (2019) Sledování účinnosti odstraňování pesticidů ze zdrojů pitné vody vybranými adsorbenty. (Monitoring the effectiveness of removing pesticides from drinking water sources by selected adsorbents), Diploma thesis, Institute of Municipal Water Management, Faculty of Civil Engineering, Brno University of Technology, Brno, Czech Republic.
- HACH®. 2100Q portable turbidimeter. Promotional material manufacturer.
- Ilavský, J., Barloková, D. (2008) Nové sorpční materiály v odstraňování kovů z vody. (New sorption materials for metal removal from water). Proceedings of the conference “Drinking Water 2008,, České Budějovice: W&ET Team, 195-200. ISBN 978-80-254-2034-8.
- Iversen, L. (2006) Léky a drogy: průvodce pro každého. (Pharmaceuticals and drugs). Translate Ivan Kmínek. Prague: Dokořán, Czech Republic. ISBN 80-7363-061-3.
- Konečný, J. (2015) Posouzení účinnosti filtračního materiálu DMI-65 na odstraňování kovů z vody. (Assesment of the effectiveness of filter material DMI-65 on removing metals from water), Diploma thesis, Institute of Municipal Water Management, Faculty of Civil Engineering, Brno University of Technology, Brno, Czech Republic.
- National Institute of Public Health – NIPH (2014). Metodické doporučení pro hodnocení relevantnosti metabolitů pesticidů v pitné vodě. [online] <http://www.szu.cz/tema/zivotni-prostredi/metodicke-doporuceni-pro-hodnocenirelevantnosti-metabolitu>, (In Czech).
- Pitter, P. (2015) Hydrochemie (Hydrochemistry). University of Chemistry and Technology Prague, Prague, Czech Republic. ISBN 978-80-7080-928-0.
- Severn trent services (2005) *BAYOXIDE® E33* Arsenic removal media. 565.0200EU.2. Promotional material manufacturer.
- Šíbllová, D. (2017) Mikropolutanty ve zdrojích vod a možnosti jejich odstranění. (Micropollutants in water resources and ways of their removal), Diploma thesis, Institute of Municipal Water Management, Faculty of Civil Engineering, Brno University of Technology, Brno, Czech Republic.
- Worch, E. (2012) Adsorption technology in water treatment: fundamentals, processes, and modeling. Boston: De Gruyter, USA. ISBN 978-3-11-024022-1.

# Investigation of Chlorine Wall Decay in Decommissioned Metallic Pipe Using Pipe Section Reactor

R. Tonev\* and G. Dimova\*

\* Department of Water Supply, Sewerage, Water And Waste Water Treatment, University of Architecture, Civil Engineering and Geodesy, No 1, Hristo Smirnenski blvd., 1164 Sofia, Bulgaria  
(E-mail: [radoslaw\\_tonew@abv.bg](mailto:radoslaw_tonew@abv.bg))

## Abstract

The study investigates the kinetics of free chlorine depletion in tap water from the Sofia distribution network. The overall decay rates, the bulk reaction rate coefficient, the wall reaction rate coefficient and the influence of mass transfer have been determined in a laboratory pipe section reactor, testing an old decommissioned metallic pipe. In total 23 series of experiments were performed under different initial free chlorine concentrations and different hydraulic conditions.

The applicability of different chlorine decay mathematical models has been investigated. A new model was proposed, combining zero order bulk reactions and first order wall reactions, describing the laboratory results with Nash-Sutcliffe efficiency coefficients over 0.99. The obtained values for the wall reaction coefficient vary in the range 0.008 - 0.030 m/h, decreasing exponentially with increasing initial chlorine concentration.

## Keywords

Chlorine decay kinetics; bulk reaction coefficient; wall reaction coefficient; laboratory studies

## INTRODUCTION

Free available chlorine decay in water supply networks has been associated with the occurrence of different chemical reactions. The mathematical model proposed by Rossman et al., 1994 is the most commonly used so far for description of this complex phenomenon, although other models have also been developed (Biswas et al., 1993; Huang and McBean, 2007). The Rossman model main assumption is that chlorine decay occurs in two places: in the bulk flow and on the contact surface (or very close to it) between the water and the inner wall of the pipes. The main equation is (Rossman et al., 1994):

$$\partial C / \partial t = -v \cdot \frac{\partial C}{\partial x} - k_b \cdot C - \frac{k_f}{r_h} \cdot (C - C_w), \quad (1)$$

where  $C$  is the chlorine concentration,  $t$  is the elapsed time,  $v$  is the water velocity,  $x$  is the distance along the pipe,  $k_b$  is the bulk reaction coefficient,  $k_f$  is the mass transfer coefficient,  $r_h$  is the hydraulic radius and  $C_w$  is the chlorine concentration at the pipe wall. The left side of Equation (1) describes the changes of chlorine concentration at a given section of the pipeline. The first term on the right-side accounts for the advective flux, while the second and third terms are associated with the occurring bulk and wall decay reactions.

## Bulk reactions

Chlorine demand in water distribution systems is mainly affected by the temperature, the initial chlorine concentration, the presence of natural organic matter (NOM) often measured as total organic carbon (TOC), and the presence of some inorganic species, e.g. iron (Powell et al., 2000; Vieira et al., 2004). Bulk reaction kinetics are usually examined by bottle test (Powell et al., 2000). The main equation for the chemical reaction rate used in the mathematical models is:

$$\partial C / \partial t = -k' \cdot C^n, \quad (2)$$



where  $C$  is the chlorine concentration,  $k'$  is the apparent rate constant, as  $k'=k.[\text{Reac}]^m$ , as  $k$  is the real rate constant and  $[\text{Reac}]$  is the concentration of the species that react with chlorine,  $n$  and  $m$  are reaction orders with respect to chlorine and  $[\text{Reac}]$ . The “ $n$ ” parameter has either a positive value or may equal zero. Usually the models assume simple first order reactions (Haas and Karra, 1984; Biswas et al., 1993; Rossman et al., 1994; Vasconcelos et al. 1997). In some cases however, bulk reactions can also be described by zero order models (Devarakonda et al., 2010). Other works opined that bulk chlorine decay kinetics are better described by parallel first order model. It is based on prerequisite, that fast and slow reacting species are present in water. In this case, the general process is determined by two components, each modelled with first order reactions (Haas and Karra, 1984; Vieira et al., 2004). There are also other, more complicated models of higher order, which in some cases predict better chlorine decay over time (Clark, 1998; Kim and Kim, 2017).

**Table 1.** Bulk reaction mathematical models used in the present work\*

Model	Differential equation ( $dC/dt =$ )	Integrated equation	Adjustable parameters
Zero order	$-k_{b0}$	$C = C_0 - k_{b0} \times t$	$k_{b0}$
Simple first order	$-k_{b1} \times C$	$C = C_0 \times e^{-(k_{b1} \cdot t)}$	$k_{b1}$
Parallel first order	$-k_{b1,I} \times C_1 - k_{b1,II} \times C_2, C = C_0 \cdot x \cdot e^{-(k_{b1,I} \cdot t)} + C_0 \cdot (1 - x) \cdot e^{-(k_{b1,II} \cdot t)}$ where $C_1 = C_0 \cdot x$ and $C_2 = C_0 \cdot (1 - x)$	$C_0 \cdot (1 - x) \cdot e^{-(k_{b1,II} \cdot t)}$	$k_{b1,I}; k_{b1,II}; x$

\*  $k_{b0}$  is the zero order bulk reaction coefficient,  $k_{b1}$  is the first order bulk reaction coefficient,  $k_{b1,I}$  and  $k_{b1,II}$  are the first order bulk reaction coefficients in parallel model,  $x$  is the fraction of the initial chlorine concentration, related with fast reacting species,  $C_0$  is initial chlorine concentration.

**Wall reactions**

Chlorine wall decay is usually associated with the interaction of chlorine with existing biofilm, corrosion deposits and the pipeline material (Vasconcelos et al., 1997; Kiene et al., 1998). Field approaches (Vasconcelos et al., 1997) and laboratory studies (Rossman et al., 2001; Digiano and Zhang, 2005) have been used to investigate the kinetics of wall reactions. The lack of a standard method is due to the large variety of factors influencing the process. Some studies focus on the chemical and physico-chemical parameters of water (Kiene et al., 1998; Digiano and Zhang, 2005; Rossman, 2006); others focus on the age, material, diameter and roughness of the pipes (Vasconcelos et al., 1997; Al-Jasser, 2007) or on the hydraulic conditions inside the pipes (Clark et al., 2010; Digiano and Zhang, 2005).

The theoretical background assumes that two parallel processes can limit the chlorine wall decay: the mass transfer of the disinfectant from the water to the wall and the rate of the wall decay reaction. If the wall decay reaction rate and the rate of chlorine transport to the wall are the same, and the process is a first order reaction with respect to the chlorine concentration at the pipe wall  $C_w$ , then it can be described by Equation (3), (Rossman et al., 1994):

$$\partial C / \partial t = - \left( k_{b1} + \frac{k_f \cdot k_{w1}}{r_h \cdot (k_f + k_{w1})} \right) \cdot C \tag{3}$$

where  $k_{w1}$  is the first order wall reaction coefficient and the other parameters are as in Equation (1).

If the hydraulic conditions provide a continuous flow of chlorine to the pipe wall (e.g., at high water velocity), then the transport of chlorine is no longer a function of mass transfer and Equation (3) acquires the following form (Digiano and Zhang, 2005; Al-Jasser, 2007):

$$\partial C / \partial t = - (k_{b1} + k_{w1} / r_h) \cdot C \tag{4}$$

If the chlorine wall decay is zero order reaction, two cases can be considered: 1) the chlorine decay is limited by the rate of the pipe wall reactions (Equation 5.1) and 2) the chlorine decay is ‘mass transport’-limited when the chlorine concentration is reduced so rapidly that the rate of mass transfer is insufficient to restore it (Equation 5.2), (Vasconcelos et al., 1997):

$$\partial C/\partial t = -k_{b1}.C - k_{w0}/r_h \quad (5.1)$$

$$\partial C/\partial t = -(k_{b1} + k_f/r_h).C, \quad (5.2)$$

Equations (3), (4) and (5.2) can be also expressed by the following general form:

$$\partial C/\partial t = -K.C, \quad (6)$$

where  $K$  is the overall first order reaction coefficient;  $K=K_{b1}+K_{w1}$ , where  $K_{b1}$  and  $K_{w1}$  are the overall first order bulk and wall reaction coefficients. First order wall reactions are most commonly associated with the presence of organic growths on the pipe wall surface, whereas zero order reactions are associated with the interaction of chlorine with inorganic corrosion or iron products respectively (Vasconcelos et al., 1997; Kiene et al., 1998).

The present study aims to investigate the free chlorine decay kinetics in old metallic pipes, in laboratory conditions, by determining experimentally the overall decay rate ( $K$ ) and bulk reaction coefficient ( $k_b$ ).

## MATERIALS AND METHODS

### Pipe section reactor

A laboratory pipe section reactor (PSR) was built, in accordance with the design of Digiano and Zhang, 2005. An old iron made pipe (internal diameter 150 mm,  $L = 300$  mm), decommissioned from the water distribution network of Sofia city was used for the experiments. The sealing plates and the inner cylinder (diameter 120 mm) are made of acrylic. Eight stainless steel baffles,  $B \times L = 20 \times 125$  mm, are attached to minimize the vortex in the annular space between the cylinder and test pipe. A propeller with diameter 100 mm and variable speed (up to  $600 \text{ r.min}^{-1}$ ) creates a circulating flow through the annular space. To prevent random errors due to the occasional introduction of air into the PSR during manual sampling, the system is equipped with a top-up reservoir.

### Tests and measurement procedures

A series of experiments was made using tap water from the distribution system of Sofia city. Each series included two parallel tests:

- Test 1: PSR test to determine the overall reaction coefficient ( $K$ );
- Test 2: Bottle test for evaluation of the bulk reaction coefficient ( $k_b$ ).

The model water solution was prepared with tap water and sodium hypochlorite, mixed in a 10 l bottle. The temperature of the solution and the initial chlorine concentration were measured before each set of experiments. The PSR was filled in with model water and a sample is taken from the system to define starting condition. Then the propeller is started, which time is considered to be the beginning of the overall chlorine decay test. Samples were taken from the PSR at random time intervals. The experiment ends when the chlorine concentration in the PSR drops below  $0.05 \text{ mg/l}$ . In parallel to the PSR tests bottle tests were also executed, as samples were taken from the rest of the model solution. Additional bottle tests were performed to investigate the bulk reactions in detail.

For chlorine concentration, a standard DPD colorimetric method is used with sensitivity of  $\pm 0.02 \text{ mg/l}$  (HACH, 2009). A thermometer with  $0.1 \text{ }^\circ\text{C}$  reading intervals was used for temperature measurement. For other water parameters of concern (e.g. Iron, Manganese, Nitrites, Ammonia and TOC) standard laboratory methods (HACH, 2007) were used. The flow velocity in the PSR was measured by detecting the flow travel for a certain time. For the purpose, a small piece of material with density, close to water is placed in the PSR and the time for 10 full circuits was measured.

## RESULTS AND DISCUSSION

A linear relationship between the motor rotation speed ( $N$  r.min<sup>-1</sup>) and the average water flow velocity in the PSR ( $u_{av}$  m/s) was established. The velocity in the annular space,  $u$  m/s, is calculated based on the  $u_{av}$  and the cross-section area of the annular space for  $N = 200 \div 400$  r.min<sup>-1</sup>.

### Determination of overall chlorine decay rates ( $K$ , $K_b$ and $K_w$ )

In total 14 series of experiments were performed with constant propeller rotation speed in accordance to annular flow velocity of  $u = 0.39$  m/s, and different initial chlorine concentrations ranging from 0.30 to 1.80 mg/l. The average temperature of the tap water for all the tests varied within the range  $T = 11.3 \div 13.9$  °C. For every single series of experiments, the temperature amplitude was below 2.0 °C.

It should be noted that the tap water comes from the “Losenetz reservoir” of the Sofia city water distribution system, fed by two different water sources, which are chlorinated several times before mixing in the tank. This explains the different values for  $k_b$  during the experiment (Table 2, column 3). For an initial chlorine concentration  $C_0 \leq 0.85$  mg/l (series 6 to 14) a general first order model (e.g. Equation (6)) describes very well the observed results. Since during the experiment the hydraulic conditions are constant and the temperature change is minor, the values of  $k_f$  can be assumed as constant. In consequence, applying Equation (5.2),  $K_{wl}$  should also be constant. The results show however that  $K_{wl}$  varies in a relatively wide range - from 1.402 to 2.492 h<sup>-1</sup>. This leads to the conclusion that mass transfer limited model (e.g. Equation (5.2)) does not describe appropriately the experimental results. At higher initial concentrations (series No 1 to 5), by applying the general first order model (e.g. Equation 6), the difference between calculated and observed value reaches -0.24 mg/l (Figure 1a) and the average absolute error is above 0.02 mg/l, which is the sensitivity level of the laboratory method for chlorine measurement.

**Table 2.** Parameters of assumed mathematical models for pipe section reactor series

Series	$C_0$	$k_{b1}$	$K$	$K_{w1}$	MAE	NSE	$k_{b0}$	$K_{w1}$	MAE	NSE
No	mg/l	1/h	1/h	1/h			(mg/l)/h	1/h		
1	2	3	4	5	6	7	8	9	10	11
1	1.80	0.047	0.916	0.869	0.12	0.936	0.081	0.607	0.03	0.996
2	1.35	0.055	1.108	1.053	0.07	0.959	0.073	0.794	0.02	0.997
3	1.18	0.066	1.196	1.129	0.05	0.968	0.078	0.878	0.01	0.998
4	1.07	0.045	1.295	1.250	0.04	0.979	0.047	1.037	0.01	0.997
5	0.88	0.072	1.445	1.373	0.03	0.982	0.063	1.138	0.01	0.998
6	0.85	0.132	1.534	1.402	0.02	0.993	0.109	1.154	0.01	0.999
7	0.71	0.094	1.669	1.575	0.02	0.988	0.067	1.323	0.01	0.999
8	0.57	0.144	2.111	1.966	0.00	0.999	0.081	1.761	0.00	0.999
9	0.54	0.110	1.793	1.683	0.01	0.995	0.061	1.502	0.00	0.998
10	0.46	0.153	2.645	2.492	0.02	0.979	0.074	2.030	0.01	0.997
11	0.44	0.125	2.204	2.078	0.01	0.993	0.056	1.830	0.00	0.999
12	0.39	0.110	2.263	2.153	0.01	0.994	0.044	1.956	0.00	0.997
13	0.31	0.168	2.537	2.369	0.00	0.994	0.053	2.228	0.00	0.994
14	0.30	0.168	2.194	2.026	0.00	0.995	0.053	1.998	0.00	0.995

\* MAE – mean absolute error, NSE - Nash-Sutcliffe efficiency coefficient

These analyses prompt that the general first order reactions models, except for the mass transfer limited model, can predict precisely enough the chlorine decay reaction only in case of low initial chlorine concentration, below 0.85 mg/l.

A new mathematical model is proposed, assuming that bulk chlorine decay rate is a zero order reaction and the wall chlorine decay rate is a first order reaction. The general equation describing the process has the following differential and integral form:

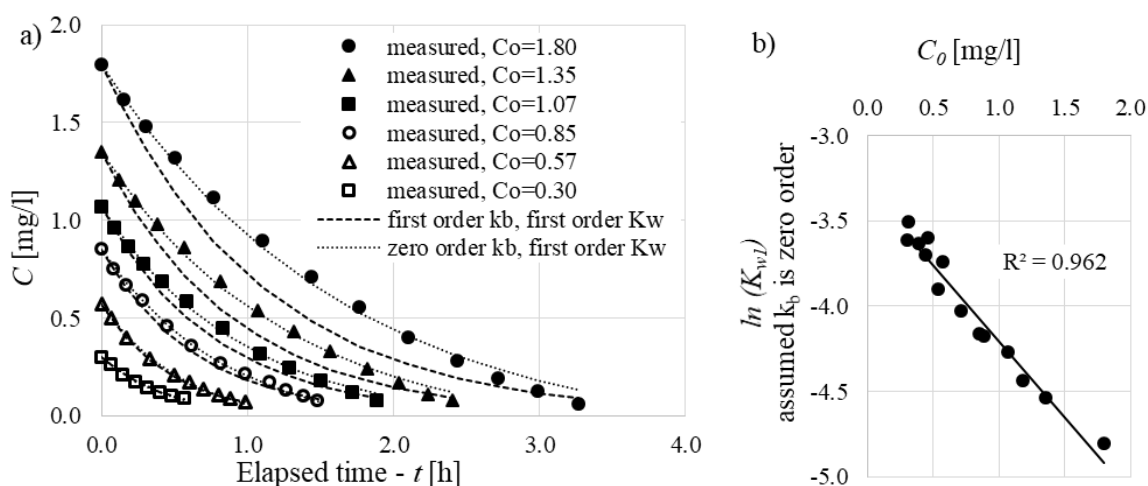
$$\frac{\partial C}{\partial t} = -k_{b0} - K_{w1} \cdot C \quad (7.1)$$

Considering that under initial conditions  $t=0$  the chlorine concentration is  $C_{(t=0)}=C_0$ :

$$C_t = C_0 \cdot e^{-K_{w1} \cdot t} - k_{b0} / K_{w1} \cdot (1 - e^{-K_{w1} \cdot t}) \quad (7.2)$$

Values of  $K_{w1}$  are calculated using least-squares regression analysis (Table 2, column 9). For all the series, except one, the mean absolute error is at maximum 0.02 mg/l, which is comparable to the measurement error (Table 2, column 10). The average Nash-Sutcliffe efficiency coefficient is 0.997, which implies better convergence than the first order general model, where the average NSE is 0.982 (Figure 1a). It is important to mention that both zero and first order models describe very well the bulk reactions, as also noted by other researchers (Devarakonda et al., 2010).

An exponential decrease in the value of  $K_{w1}$  was found as  $C_0$  increases (Figure 1b), after applying Equation (7.2). Since the mass transfer coefficient  $k_f$  is constant, such dependence can only be explained by a change in the rate coefficient of wall reactions  $k_{w1}$ . A similar trend has been observed by other authors (Hallam et al. 2002; Rossman 2006). Depending on the hydraulic conditions, shear stress occurs at the inner wall of the pipe. The corroded material is sheared off, resulting in the exposure of additional sections of the metal pipe to chemical interaction (Furnass et al. 2013). This process leads to change in the ratio between the fast and slow reacting with chlorine species. At low initial chlorine concentration, the reaction rate would be determined only by the concentration of the fast-acting agents, while at higher  $C_0$ , the slow-acting ones will also affect the process.



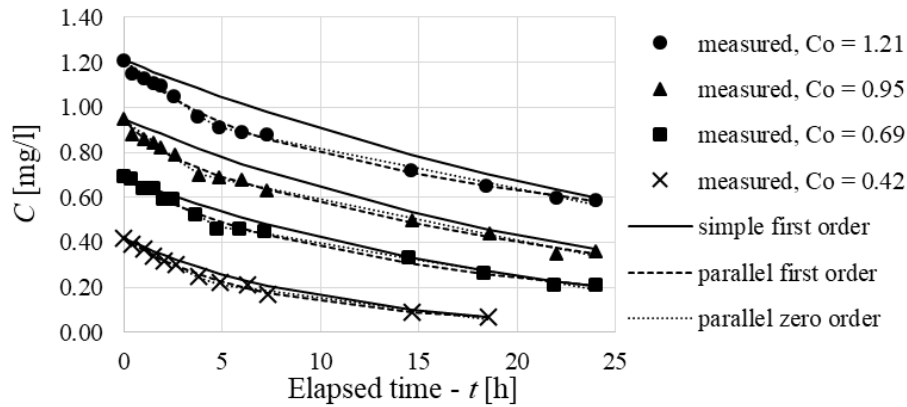
**Figure 1.** a) measured and predicted concentrations and b) observed relationship between initial chlorine concentration and first order overall wall coefficient

### Bulk reaction coefficient ( $k_b$ )

Four additional bottle tests were performed at temperature 13÷14 °C to investigate the bulk reaction kinetics. The tap water quality analyses showed presence of total manganese  $Mn=0.008$  mg/l, ammonium,  $NH_4^+=0.021$  mg/l and total organic carbon  $TOC=2$  mg/l. The concentration of total iron and nitrite were under the relevant limit of detection, respectively  $<0.02$  and  $<0.05$  mg/l.

In all the tests, similar kinetics of chlorine decay was observed, which could be divided into two phases (Figure 2). The first phase, with a duration of about 5 hours, shows a significantly faster chlorine decay than the second phase. Simple and parallel first order models were applied to

determine the bulk chlorine decay coefficients (Table 1). A regression and least squares regression analyses were performed accordingly. It can be concluded that the parallel first order model describes much better the experimental results (Figure 2 and Table 3, column 1-6).



**Figure 2.** Chlorine concentration decay in additional, 24 h bottle tests

In addition, a parallel zero order model is proposed, expressed by the following integrated equations:

$$C_i = C_0 - (k_{b0,I} + k_{b0,II})t_i ; t_i \leq t_1 \tag{8.1}$$

$$C_i = C_0 - k_{b0,I}t_1 - k_{b0,II}t_i ; t_i > t_1 , \tag{8.2}$$

where  $C_i$  is the concentration of chlorine at the moment  $i$ ,  $k_{b0,I}$  and  $k_{b0,II}$  are reaction rate coefficients, respectively for the first and second phase,  $t_i$  is elapsed time from the beginning of the test and  $t_1$  is elapsed time up to the end of the first phase. The adjustable parameters -  $k_{b0,I}$ ,  $k_{b0,II}$  and  $t_1$  are calculated by least squares regression analyses (Table 3, columns 7-9).

**Table 3.** Parameters of assumed mathematical models for bottle tests

C <sub>0</sub> mg/l	Parallel first order					Parallel zero order				
	k <sub>b1,I</sub> 1/h	k <sub>b1,II</sub> 1/h	x	MAE	NSE	k <sub>b0,I</sub> (mg/l)/h	k <sub>b0,II</sub> (mg/l)/h	t <sub>1</sub> H	MAE	NSE
1	2	3	4	5	6	7	8	9	10	11
0.42	0.237	0.069	0.43	0.00	0.997	0.035	0.011	4.28	0.01	0.993
0.69	0.249	0.041	0.20	0.01	0.990	0.031	0.015	4.75	0.01	0.995
0.95	0.578	0.035	0.14	0.01	0.993	0.050	0.018	3.53	0.01	0.992
1.21	0.248	0.020	0.22	0.01	0.994	0.048	0.018	4.49	0.01	0.995

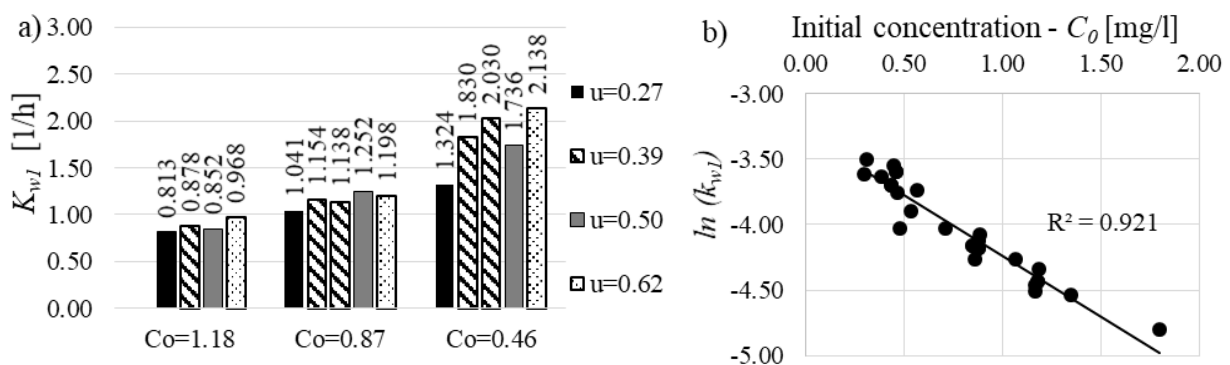
The values for the overall zero order bulk decay coefficient ( $K_{b0} = k_{b0,I} + k_{b0,II}$ ) obtained during the first 3.5 to 4.8 hours of the bottle tests are in the range  $0.046 \div 0.068 \text{ mg/l.h}^{-1}$  (Table 3, columns 7-8). They correspond well to the obtained values for the bulk decay coefficient during the PSR series, which are in the range of  $0.044 \div 0.109 \text{ mg/l.h}^{-1}$  (Table 2, column 8).

**Wall reaction coefficient (k<sub>w1</sub>)**

In order to evaluate the first order wall reaction coefficient,  $k_{w1}$ , nine additional series of experiments were performed in the PSR with initial chlorine concentrations  $C_0 = 1.18; 0.87$  and  $0.46 \text{ mg/l}$  ( $\pm 0.02$ ) and annular space velocity  $u = 0.27; 0.50$  and  $0.62 \text{ m/s}$ . The results were compared with the previous series of experiments with  $u = 0.39 \text{ m/s}$  (Table 2). The overall wall reaction rate,  $K_{w1}$ , is calculated using Equation (7.2).

The obtained results indicate, that  $K_{w1}$  does not change significantly at  $u \geq 0.39 \text{ m/s}$ . The difference

between the maximum and the minimum calculated value, relative to the minimum at  $C_0 = 1.18$ ; 0.87 and 0.46 is respectively 13.6%; 9.9% and 23.2%. The results obtained do not indicate a clear relationship between velocity and wall reaction coefficient. In some cases, a higher velocity leads to a lower value of the overall wall reaction rate and obversely. Therefore, the lack of clear trend can be explained with the assumption that the observed differences are due measurement errors, rather than mass transfer process. At lower water velocity, i.e  $u = 0.27$  m/s, there is a clear tendency for lower values of  $K_{w,l}$  compared to other results. This might be the consequence of a lower shear stress at the water-pipe contact surface. Therefore, an assumption can be made that mass transfer does not play a significant role in the chlorine decay process in the laboratory PSR. In consequence, the wall reaction coefficient can be calculated using Equation (4). Given the design of the PSR and the way the water flows inside, the hydraulic radius would be the ratio between the cross-sectional area of the annular space and the inner perimeter of the test pipe, i.e.  $r_h=0.0135$  m. The values of  $k_{w,l}$  for all 23 series vary in the range of  $0.008 \div 0.030$  m/h (Figure 3b). This range corresponds well with the values, obtained by other autors, i.e. 0.001 - 0.065 m/h (Rossman, 2006).



**Figure 3.** a) overall first order wall reaction rate at varying water velocity and b) wall reaction rate coefficient by different initial chlorine concentration and different anular space velocities

## CONCLUSIONS

The free chlorine decay, in an old metallic pipe, was investigated under laboratory conditions with tap water from the Sofia distribution system. The overall decay rates ( $K$ ,  $K_w$  and  $K_b$ ), the bulk reaction rate coefficient ( $k_b$ ), the wall reaction rate coefficient ( $k_w$ ) and the influence of the mass transfer process have been determined based on series of experiments. The laboratory pipe section reactor, being a closed homogenous system, is suitable for the study of the kinetics of chlorine decay in water.

It can be concluded that a first order general model was applicable for predicting overall chlorine decay rates ( $K$ ,  $K_w$  and  $K_b$ ) at lower initial concentrations (0.3 to 0.85 mg/l); however, the model was not appropriate for describing the laboratory results at higher initial chlorine concentrations (0.88 to 1.8 mg/l).

Considering the chlorine decay bulk reactions, the first order parallel model characterizes well the tested tap water. The proposed zero order parallel model, however, describes even better the laboratory results having Nash-Sutcliffe efficiency coefficients over 0.99.

The first order wall reaction model is appropriate for predicting the wall reaction decay in the studied metallic pipe. The respective wall reaction coefficient ( $k_{w,l}$ ) has been determined for different initial chlorine concentrations (0.3 to 1.8 mg/l) and different hydraulic conditions (velocities of 0.27 m/s 0.39 m/s, 0.50 m/s and 0.62 m/s). There is a clear trend of decreasing of  $k_{w,l}$  (from 0.03 to 0.008 m/h) with the increase of initial chlorine concentration.

## ACKNOWLEDGEMENTS

This investigation was made within the framework of Contract No Д - 92/16 of CNIP at UACEG. The authors would like to thank also the Sofiyska Voda AD, part of Veolia Group, who contributed greatly to this research.

## REFERENCES

- Al-Jasser, A. (2007) Chlorine decay in drinking-water transmission and distribution systems: Pipe service age effect. *Water Research*, **41**(2), 387-396
- Biswas, P., Lu, C., Clark, R. (1993) A model for chlorine concentration decay in pipes. *Water Research*, **27**(12), 1715-1724.
- Clark, R. (1998) Chlorine demand and TTHM formation kinetics: a second-order model. *Journal of Environmental Engineering*, **124**(1), 16 – 24.
- Clark, R., Yang, Y., Impellitteri, C., Haught, R., Schupp, D., Panguluri, S., Krishnan, E. (2010) Chlorine fate and transport in distribution systems: Experimental and modeling studies. *Journal AWWA (American Water Works Association)*, **102**(5), 144-155.
- Devarakonda, V., Moussa, N., VanBlaricum, V., Ginsberg, M., Hock, V. (2010) Kinetics of free chlorine decay in water distribution networks. *World Environmental and Water Resources Congress 2010: Challenges of Change*, ASCE, 4383-4392.
- Digiano, F., Zhang, W. (2005) Pipe section reactor to evaluate chlorine–wall reaction. *Journal AWWA (American Water Works Association)*, **97**(1), 74-85.
- Furnass, W., Collins, R., Husband, P., Sharpe, R., Mounce, S., Boxall, J. (2013) Modelling both the continual erosion and regeneration of discolouration material in drinking water distribution systems. *Water Supply*, **14**(1), 81-90.
- Haas, C., Karra, S. (1984) Kinetics of wastewater chlorine demand exertion. *Journal WPCF (Water Pollution Control Federation)*, **56**(2), 170-173.
- HACH (2007) DR 2800 Spectrophotometer – Procedures manual, 2 ed. HACH Company.
- HACH (2009) Chlorine, free: USEPA DPD method 8021. HACH Company.
- Hallam, N., West, J., Forster, C. Powell., J., Spencer, I. (2002) The decay of chlorine associated with the pipe wall in water distribution systems. *Water Research*, **36**(14), 3479-3488.
- Huang, J., McBean, C. (2007) Using Bayesian statistics to estimate the coefficients of a two-component second-order chlorine bulk decay model for a water distribution system. *Water Research*, **41**(2), 287-294.
- Kiene, L., Lu, W., Levi, Y. (1998) Relative importance of the phenomena responsible for chlorine decay in drinking water distribution systems. *Water Science and Technology*, **38**(6), 219-227.
- Kim, H., Kim, S. (2017) Evaluation of chlorine decay models under transient conditions in a water distribution system. *Journal of Hydroinformatics*, **19**(4), 522-537.
- Powell, J., Hallam, N., West, J., Forster, C., Simms, J. (2000) Factors which control bulk chlorine decay rates. *Water Research*, **34**(1), 117-126.
- Rossman, L., Clark, R., Grayman, W. (1994) Modeling chlorine residuals in drinking-water distribution systems. *Journal of Environmental Engineering*, **120**(4), 803-820.
- Rossman, L., Brown, R., Singer, P., Nuckols, J. (2001) DBP formation kinetics in a simulated distribution system. *Water Research*, **35**(14), 3483-3489.
- Rossman, L. (2006) The effect of advanced treatment on chlorine decay in metallic pipes. *Water Research*, **40**(13), 2493-2502.
- Vasconcelos, J., Rossman, L., Grayman, W., Boulos, P., Clark, R. (1997) Kinetics of chlorine decay. *Journal AWWA (American Water Works Association)*, **89**(7), 54-65.
- Vieira, P., Coelho, S., Loureiro, D. (2004) Accounting for the influence of initial chlorine concentration, TOC, iron and temperature when modelling chlorine decay in water supply. *Journal of Water Supply: Research and Technology-Aqua*, **53**(7), 453-467.

# Search for Materials Used for Tap Water Transmission Reducing the Capacity for Development of Biofilm – Preliminary Research

A. Trusz\*, M. Wolf-Baca\*\* and K. Leluk\*\*\*

\* Wrocław University of Science and Technology, Faculty of Environmental Engineering, Stanisława Wyspiańskiego 27 Street, Wrocław, Poland (E-mails: [agnieszka.trusz@pwr.edu.pl](mailto:agnieszka.trusz@pwr.edu.pl); [mirela.wolf-baca@pwr.edu.pl](mailto:mirela.wolf-baca@pwr.edu.pl); [karol.leluk@pwr.edu.pl](mailto:karol.leluk@pwr.edu.pl))

## Abstract

Biofilm developing on the internal surfaces of materials applied in the construction of the water supply system can be the cause of many serious problems, including technical and economic ones (Wolf, 2018). It contributes to a decrease in the sanitary quality of water, and as a reservoir of pathogenic microorganisms and viruses it can be a serious threat to the health and even life of consumers. The development of biofilm is possible on any material, but the type of material can determine among others its rate of development or structure.

Synthetic materials proposed on the market are also subject to the phenomenon of microbiological corrosion. Both during production and particularly after their exploitation, as weakly biodegradable materials, they can pose a serious ecological threat to the environment.

High amounts of generated synthetic materials in the form of waste encourage search for methods of their reuse. Due to this, an attempt was undertaken to produce biologically non-corroding materials applicable both in water distribution systems and in other branches of the industry, e.g. cooling industry.

The materials proposed in the study were produced at the Department of Sanitary Biology and Ecotechnics with the application of secondary raw materials. They are 3 materials based on polyethylene (PE), polypropylene (PP), and polyvinyl chloride (PVC).

The research on the materials was conducted in two aspects. The surface was analysed in terms of development of biofilm and its effect on the occupied surface. Potential toxicity of the new materials was also determined. The paper presents only results of selected analyses in the scope of the research.

## Keywords

Biofilm; polyethylene (PE); polypropylene (PP); polyvinyl chloride (PVC); water quality

## INTRODUCTION

Global consumption of polymer plastics reveals growing tendency. According to data published annually (PlasticsEurope, 2018) by Association of Polymer Plastic Manufacturers, overall global plastic production reached about 350 mln tonnes in 2017 while in European Union it was 64 mln tonnes. Most of them are thermoplastic materials with PE, PP and PVC being leading three. Industrial segments in which a huge mass of those polymers are utilized are: packaging (PE, PP, PVC), construction (mainly PVC) and automotive (mainly PP). Those data were calculated without respect to re-used materials which also have an input into the mentioned above sectors and additionally increase plastic consumption therein.

According to recent policies of environmental protection, specially implemented by EU legal entities, a huge impact is put to re-use of polymer waste material (fulfilling circular economy issues) (Directive, 1994; Proposal for a Directive, 2016) on the reduction of the impact of certain plastic products on the environment] and simultaneous restriction on landfilling (Directive (EU), 2018). This fact was an inspiration to examine usefulness of used PE PP and PVC as materials for water or sewer pipes. One of the issues that has to be taken into consideration while choosing a

*11<sup>th</sup> Eastern European Young Water Professionals Conference IWA YWP,  
1-5 October 2019, Prague, Czech Republic*



proper material for pipe is its ability to restrain bacterial film growth on its surface.

Biological membrane is defined as a mixture of microorganisms, their metabolites, and gelatinous matrix composed of extracellular EPS substances (Extracellular Polymeric Substances). Due to its nutritional and protective properties, biofilm is described as a reservoir of pathogenic and potentially pathogenic bacteria, parasitic protozoans, among others intestinal viruses, and fungi the mycotoxins of which cause many human illnesses such as mycoses, allergies, inflammatory states of mucous membranes, etc. (Prest, 2016). The complexity of the structure of biofilm affects its integrity, as well as physical-chemical and biological properties. It also contributed to the horizontal transfer of genes (among others genes conferring resistance to medicines) and factors stabilising biofilm structures and provides protection of cells against unfavourable external factors such as: hydraulic changes in the network (particularly rapid ones), effect of antibiotics, disinfectants, and UV radiation. Therefore, microorganisms or viruses comprised in biofilm have considerably greater chances for surviving unfavourable conditions than those occurring in planktonic form (Manuel, 2010; Simoes, 2010; Ramirez-Castillo, 2014; Browarczyk, 2015).

The development of biological membrane in the water distribution network may contribute to the degeneration of its building materials, cause organoleptic changes in water, but most importantly negatively affect health, or even life of consumers, particularly at moments of detachment of fragments of biological membrane. Biofilm formation is determined by many factors such as: physical conditions (flow rate, shear stress, water temperature, type and material of pipelines, etc.), chemical parameters (type and content of nutrients and their bioavailability, presence of corrosive sediments, type and concentration of disinfectant and its residues, presence and concentration of organic and inorganic particles, ions, etc.), and biological factors (e.g. microbiological composition) (Wingender, 2011; Browarczyk, 2015).

In this paper a series of three samples (PE, PP and PVC) were produced basing on reused plastics and examined in terms of bacterial film growth attraction. PE is a representative of most abundantly used thermoplastic polymers. Due to its chemical and physical resistance it has been utilized in many industrial branches. For instance, in packaging it has been used as a substrate for food packaging and corrosive chemicals as well. According to its flexibility and tensile strength it is convenient material in production of foils (agricultural, construction), ventilations ducts (construction, automotive) or liquid pipes (Peacock, 2000). Relatively cheap process of polyethylene manufacturing is reflected in its low price, ca 1.5 EUR/kg (PlasticsEurope, 2018). According to data published by APPM its consumption in EU countries reached almost 6.5 mln tonnes in 2018.

Some similarities to PE in physicochemical behaviour may be also found in PP. Generally it has one additional methyl group in each monomer unit. But, this “slight” difference allowed PP to create ordered structures (isotactic, atactic, block copolymer) what influence its macroscopic properties. Some similarities may be found between PE and PP, however generally PP is rather more rigid, temperature resistant material but on the other hand with poor performance in lower temperatures (Wypych, 2016). Polyvinyl chloride is representative of plastics with strongest polar interactions. Due to polarisation by chlorine atom of each monomer unit, electron density distribution on the polymer chain is definitely not uniform. This in turn makes PVC prone to attack by polar molecules more likely than PP or PE. Uneven electron density distribution, presence of chlorine atom (strong electronegative) makes this polymer unstable in comparison with two previously briefly presented (Wypych, 2016). It is a common knowledge, that during thermal treatment PVC decomposes releasing hydrochloride gases. That feature makes material difficult to recycle by means of thermal methods narrowing down recycling of PVC to mechanical processing (re-use of PVC in a new form).

## MATERIALS AND METHODS

### Materials

Plastics used for investigation were collected from individual users and industrial companies as waste materials. In particular, PE was kindly delivered from recycling plant as a end-use plastic containers for automotive liquids: distilled water, brake fluid, power steering, etc. PVC was collected in a regranulate form obtained from old window frames, whereas PP was supported by individual users mainly as household materials (plastic cups, containers for food and beverages, etc). PE and PP based materials were then milled (laboratory blade mill “Wanner”) prior to press moulding process.

### Sample preparation

Samples were fabricated using press moulding process into 3 mm thick plates using LabTech laboratory press. Materials were not homogenised before processing mainly to avoid additional effects related to thermomechanical degradation, which in waste mater may have a huge impact on materials properties. Processing conditions respective to material type, are listed in Table 1. Samples designed for microbiological testing were ten subtracted from plates using small circular saw.

**Table 1.** Press moulding conditions

	Temperature (°C)	Time (plastification/press) (min)	Pressure (bar)
PE	200	2/3	50
PP	200	2/3	50
PVC	170	2/3	50

Multi-species biofilm culture – based on microorganisms from the water supply network 100 µl of inoculum was introduced to flasks with liquid substrate R2A enriched with sodium citrate (own modification). Five developed materials from each type were separately introduced, namely PE, PP, PVC (with a surface area of 1cm<sup>2</sup> each). The culture was left for 30 days on a laboratory shaker at room temperature (22 °C). The inoculum was suspension of microorganisms isolated from tap water from Wrocław. For this purpose, 3 litres of cold water were filtered through a Whatman filter with pore diameter of 0.2 µm. The filter was then transferred to 25 ml of sterile physiological solution (0.85 % NaCl) and shaken (160 rpm, Nocturne,) for 2 h. It was subject to the effect of ultrasounds for 30 seconds (35 kHz) for the purpose of detaching microorganisms from the filter cake.

### ATP (Adenosine-5'-triphosphate)

A method of assessment of the metabolic activity and viability of cells subject to adhesion to the surface is adenosine triphosphate (ATP) determination (El-Chakhtoura, 2015). The analyses were conducted with the application of device luminometer EnSure, and the results were provided in Relative Light Units (RLU). The value of the units is directly proportionate to the content of ATP in a sample.

### Pathogen adhesion

Pathogen adhesion to the surface of the materials was also analysed in *the multi-species culture with an addition of 100 µl of pure strain of Escherichia coli* (NCTC 12241 / ATCC® 2592 - BioMaxima). Two materials of each type were placed in the flasks - PE, PP, PVC (area 1 cm<sup>2</sup>), the whole was shaken for 30 days at a constant temperature (22 °C). After 30 days, the materials were rinsed from excess agar with sterile distilled water (2 cm<sup>3</sup>), placed in sterile test tubes with Tris buffer, and subject to the effect of ultrasounds for the purpose of isolation of genetic material of bacteria. DNA extraction from the biomass of microorganisms present on the surface was

performed by means of an Isolate II Genomic Kit (Bioline). Measurement of the concentration and purity of genetic material was performed by means of a nano spectrophotometer (NanoPhotometer N60 Implen).

Detection of bacteria *E.coli* was performed with the application of the qPCR reaction (Mic, Bio Molecular Systems). For this purpose, an AmpliTest kit was used (Amplicon). It included reaction starters, specific TaqMan probe, and internal reaction control. The conditions of the reaction were in accordance with the producer guidelines (Table 2). Samples were analyzed in three replications. The standard curve was approached in accordance with the description contained in (Wolf-Baca, 2019). The total amount of microorganisms (no distinction between dead / live) was determined and counted using the QUANTUM EvaGreen HRM Kit (SYNGEN), with non-specific dye. Each sample was analyzed twice. For preparing the standard curve, tenfold dilutions of pure *Escherichia coli* strain ATCC 25922 (BioMaxima) were used.

**Table 2.** Parameters of qPCR reactions

Step	16S rRNA			<i>E.coli</i>		
	T (°C)	Number of cycles	Time (s)	T (°C)	Number of cycles	Time (s)
Initial denaturation	95	1	900	95	1	300
Denaturation	95		15	95		30
Amplification	60		20	58		25
Cooling	72	40	20	40	40	30
Melting	72 to 95	-	-	-	-	-

### SEM (scanning electron microscope)

Materials for microscope observations were preserved with 3 % glutaric aldehyde (SIGMA) for 24 h at room temperature. Then, each material was rinsed separately in 0.1 M phosphate buffer. The procedure was repeated three times. The samples were dehydrated in an increasing water/alcohol sequence of 50 %, 60 %, 70 % for 15 min, and then 80 %, 90 %, and 96 % for 5 min. SEM investigation was performed using VEGA TESCAN 3 microscope in the following conditions: gun voltage 5.0 kV, magnification rate 1.0 kx, 2.0 kx and 5.0kx. All materials were gold sputtered before SEM examination. Sputtering conditions were experimentally determined to ensure sufficient quality of collected scans and for all samples remained unchanged (current: 40mA, sputtering time: 60s). Sputtering was conducted using Kressington Sputter Coater 108.

### Water Contact Angle Measurements

Determination of water contact angle was performed by means of sessile drop method, utilizing SEE System equipment (Advex Instruments s.r.o.). Water drops were collected on flat surface of each material placed horizontally on equipment's table. After a certain time period (usually 5 seconds) digital pictures of drop shape were collected using a USB camera. Manufacturer's software allowed to automatically calculate contact angle basing on collected pictures. Distilled water was supported by Sigma Aldrich. None of the samples were treated chemically nor physically prior to wetting experiment. Water contact angle was recorded on the following materials: untreated (just after fabrication), covered with a layer of settled microorganisms (biofilm) and after biofilm removal.

## RESULTS

### ATP

The analysis of ATP (Table 3) content shows that the highest abundance of living microorganisms developed biofilm on the surface of Polypropylene (2260 RLU surface of material with biofilm, 342

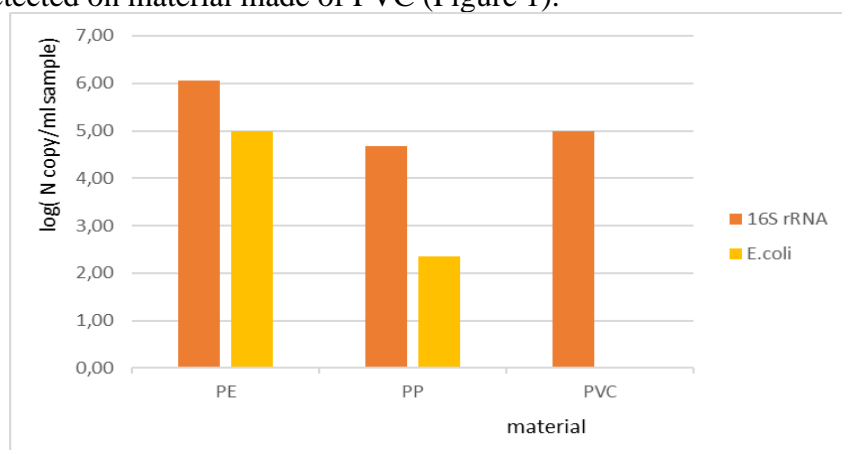
RLU suspension). Their highest amount was also left after removal of biofilm by means of ultrasounds (165 RLU). Material the least prone to the development of biofilm proved to be polyvinyl chloride (37 RLU in suspension, 356 RLU in direct analysis of the surface with biofilm and 50 after removal of biofilm).

**Table 3.** Measurement of the metabolic activity in the solution and on the surface of materials

Material	ATP, RLU		
	Surface of the material		
	Suspension (microorganisms developing biofilm)	With biofilm	After removal of biofilm
PE	74	1117	22
PP	342	2260	165
PVC	37	356	50

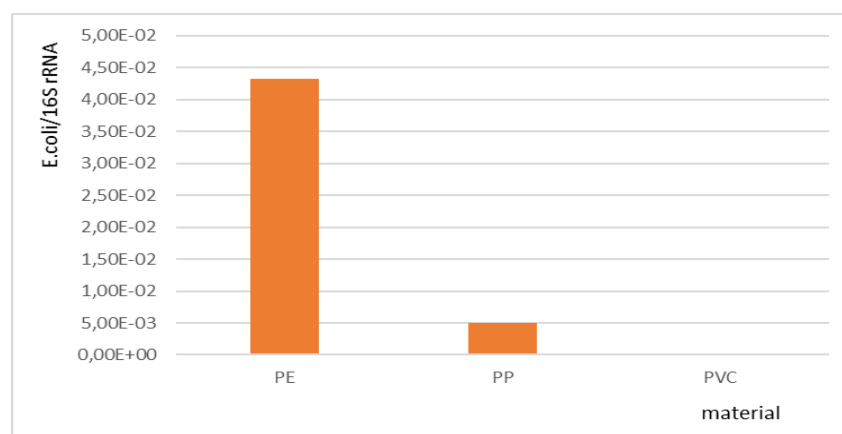
### Pathogen detection

The amount of isolated DNA, indirectly pointing to the degree of adhesion, was different for each material. For PE, the value was 10.08 ng/ $\mu$ l, PP – 10.85 ng/ $\mu$ l, and for PVC – 64.71 ng/ $\mu$ l. The conducted qPCR reaction showed presence of bacteria *E.coli* on PE and PP. No presence of the pathogen was detected on material made of PVC (Figure 1).



**Figure 3.** Abundances of 16S rRNA and *E.coli* presented as number of copies in tested materials (in logarithmic scale)

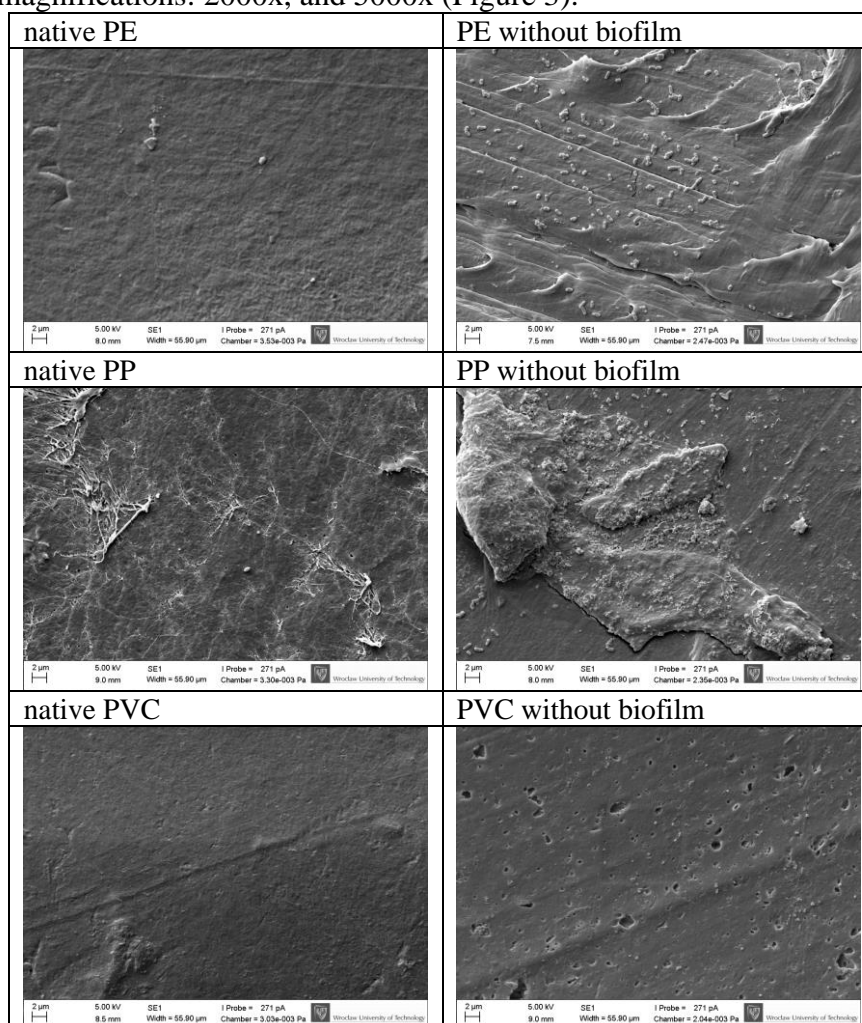
The efficiency of the reactions was within the acceptable range from 90-100 %. Moreover the abundance and prevalence of *E.coli* were determined and presented in Figure 1 and 2.



**Figure 4.** *E.coli* prevalence from tested materials presented as genomes of copy number *E.coli* to total amount of copy number (rRNA)

### SEM observations

Results with the application of a scanning electron microscope were presented in the form of photographs at magnifications: 2000x, and 5000x (Figure 3).



**Figure 5.** Pictures of surfaces of native and after removal of biofilm on materials: PE, PP, PVC

Based on SEM microscope analysis, the most diverse structure (native material) was observed for polypropylene. After removal of biofilm from the surface, changes in the structure were observed on each material. The most considerable degradation of the surface occurred for polypropylene and polyethylene. On the surface of material made of PVC, insubstantial loss of structure was observed. Each change in the structure of the surface of the materials can provide conditions favourable for further colonisation by microorganisms. Therefore, next to biological research, analyses of the surface are vitally important.

### Water Contact Angle

Results of water contact angle measurements are concisely presented in Table 4. The highest hydrophobicity was determined for PP material, and the lowest angle value was obtained by PVC (hydrophilic character). This suggests the smallest possibility of colonisation of the material by microorganisms. Biofilm developing on the surface of polyvinyl chloride affected the water contact angle to the greatest degree, reducing it to a value of 28.1. Removal of biofilm had no considerable effect on the value of water contact angle in the case of PP and PE (the hydrophilic character was maintained at the same level of approximately 48, like on material with biofilm). Neither native

polyvinyl chloride nor that after removal of biofilm changed the value of water contact angle (78.7 and 78.5 after removal of biofilm).

Biofilm propagation on the material is reflected by substantial decrease of water contact angle indicating increasing hydrophilicity. What is interesting biofilm removal lead to restoration of initial contact angle only for PVC sample. Bacterial colonisation lead to unreversible changes of physical character of the surface for PE and PP samples.

**Table 4.** Water contact angle values (in degrees) for all investigated samples

	Untreated	With biofilm	After biofilm removal
PE	80.0	48.1	48.5
PP	95.1	41.2	48.5
PVC	78.7	28.1	78.5

## SUMMARY AND DISCUSSION OF RESULTS

Results of water contact angle measurements are concisely are good reflection of physicochemical changes occurring on the samples surface. Water contact angle measured for untreated polymer plastics are typical for those kind of materials and can be widely find in the literature (Handbook, 2000; Cabezudo, 2019; Ebnesajjad, 2006).

Based on the ATP analyses, the highest metabolic activity was determined on the surface of polypropylene, and the smallest on polyvinyl chloride. The real-time PCR analysis presenting the total quantity of microorganisms and adhesion of the *E. coli* pathogen showed the highest susceptibility to colonisation by microorganisms in the case of polyethylene, and the lowest for polypropylene. No presence of *Escherichia coli* was detected on the surface of PVC material. Research by Cowle et.al. (Cowle, 2019) confirms the results obtained by means of molecular methods. It explains the highest degree of colonisation of polyethylene materials with release of biodegradable compounds and phosphorus, constituting a potential source of food for microorganisms in unfavourable conditions, and contributing to their colonisation. SEM microscope observations of microorganisms present on the studied surfaces (photographs not included) as well as surfaces after removal of biofilm confirmed ATP and qPCR results, showing the smallest colonisation on the surface of PVC. Similar relations were obtained in the article by Rozej et. (Rozej et al., 2015). After the application of ultrasounds on the surface of polyethylene and polypropylene, the presence of organisms was observed, suggesting their strong adhesion to the surface.

The analyses by means of both methods of molecular biology (qPCR) and biochemical methods (ATP), as well as observation of the structure and character of the surface (SEM and water contact angle) revealed that PVC is material least susceptible to biocorrosion.

## CONCLUSIONS

The preliminary analysis of results shows that PVC is a material least prone to the development of biofilm.

## ACKNOWLEDGEMENT

This work was supported by the Ministry of Science and Higher Education in Poland (0401/0056/18).

## REFERENCES

- Browarczyk, B., Trusz-Zdybek, A. (2015) Wpływ warunków hydraulicznych i rodzaju materiału na biofilm w sieci wodociągowej. W: Interdyscyplinarne zagadnienia w inżynierii i ochronie środowiska: praca zbiorowa. pod red. Wiśniewskiego J., Kutylowskiej M. i Trusz-Zdybek A., **5**, 22-32.
- Cabezudo, N., Sun, J., Andi, B., Ding, F., Wang, D., Chang, W., Luo, X., Xu, B. (2019) Enhancement of surface wettability via micro- and nanostructures by single point diamond turning. *Nanotechnology and Precision Engineering*, **2**,(1), 8-14.
- Cowle, M. W., Webster, G., Babatunde, A. O., Bockelmann-Evans, B. N., Weightman, A. J. (2019) Impact of flow hydrodynamics and pipe material properties on biofilm development within drinking water systems. *Environmental Technology*.
- Directive 94/62/EC on Packaging and Packaging Waste – European Parliament and Council Directive 94/62/EC of 20 December 1994 on packaging and packaging waste.
- Directive (EU) 2018/850 Of European Parliament and of the Council of 30 May 2018 amending Directive 1999/31/EC on the landfill of waste, Official Journal of the European Union, L150/100.
- Ebnesaajjad, S. (2006) Material Surface Preparation Techniques. *Surface Treatment of Materials for Adhesion Bonding*.
- El-Chakhtoura, J., Prest, E., Saikaly, P., Loosdrecht, M., Hammes, F., Vrouwenvelder, H. (2015) Dynamics of bacterial communities before and after distribution in a full-scale drinking water network. *Water Research*, **74**(1) 180-190.
- Emmanuelle, C., Hammes, F., van Loosdrecht, M., Vrouwenvelder, J. (2016) Biological Stability of Drinking Water: Controlling Factors, Methods, and Challenges *Front. Microbiol.*, **31**, 37-47.
- Gomes, I. B., Simoes, M., Simoes, L. C. (2014) An overview on the reactors to study drinking water biofilm. *Water Research*, **62**, 63-87.
- Manuel, C., Nunes, O., Melo, L. (2010) Unsteady state flow and stagnation in distribution systems affect the biological stability of drinking water. *Biofouling*, **26**, 129-139.
- Peacock, A. (2000) Handbook of Polyethylene: Structures: Properties, and Applications, CRC Press, 544.
- PlasticsEurope (2018) [online] <https://www.plasticseurope.org/en/resources/market-data>.
- Proposal for a Directive of the European Parliament and of the Council on copyright in the Digital Single Market - COM(2016)593 Brussels, 14.9.2016 COM(2016) 593 final 2016/0280(COD).
- Ramirez-Castillo, F. Y., Harcel, J., Moreno-Flores, A. C., Locra-Muro, A., Guerrero, A. L., Avelar-Gonzales, F. J. (2014) Antimicrobial resistance: the role of aquatic environments. *International Journal of Current Research and Academic Review*, **2**(7), 231-246.
- Rozej, A., Cydzik-Kwiatkowska, A., Kowalska, B., Kowalski, D. (2015) Structure and microbial diversity of biofilms on different pipe materials of a model drinking water distribution systems. *World J Microbiol Biotechnol*, **31**, 37-47.
- Simoes, M., Simoes, L. C., Vieira, M. J. (2010) A review of current and emergent biofilm control strategies. *LWT - Food Science and Technology*, **43**, 573-583.
- Wingender, J., Flemming, H. C. 2011 Biofilms in drinking water and their role as reservoir for pathogens. *International Journal of Hygiene and Environmental Health*, **214**, 417-423.
- Wolf, M., Traczewska, T., Leluk, K., Grzebyk, T. (2018) Comparability biofilm structure on ITO sensor with forms generated on technical materials. *Desalination and Water Treatment*, **131**, 169-179.
- Wolf-Baca, M., Siedlecka, A. (2019) Detection of pathogenic bacteria in hot tap water using the qPCR method: preliminary research. *SN Appl. Sci.*, **1**, 840.
- Wypych, G. (2016) Handbook of polymers, ChemTec Publishing, 712.

# Natural Organic Matter Biodegradability and THMFP in High DOC Waters

Z. Vojdani\* and B. Gorczyca\*

\* Department of Civil Engineering, University of Manitoba, Winnipeg, Manitoba, Canada  
(E-mails: [vojdaniz@myumanitoba.ca](mailto:vojdaniz@myumanitoba.ca); [beata.gorczyca@umanitoba.ca](mailto:beata.gorczyca@umanitoba.ca))

## Abstract

Membrane filtration is commonly applied to reduce Dissolved Organic Carbon (DOC) concentration to control trihalomethanes (THMs) formation; however, the high levels of DOC in the Canadian Prairies water sources can cause serious membranes fouling. Integrated biological and reverse osmosis membrane (IBROM) process is a RO membrane treatment unit utilizing primarily biological filtration pre-treatment. IBROM process claims to remove Biodegradable DOC (BDOC), which allegedly should result in reduced fouling of the RO membranes. In this study, commonly used pre-treatment methods, such as coagulation (with alum, polyaluminum chloride (PACl), aluminum chlorohydrate (ACH) and ferric chloride) and oxidation (with  $\text{KMnO}_4$  and  $\text{H}_2\text{O}_2/\text{UV}$ ) as well as IBROM were evaluated for removal of DOC, BDOC and THMFP. High organics raw water source supplying the community of Herbert (Province of Saskatchewan, Canada) was used in the experiments (DOC = 17.5-22.7 mg/L and BDOC = 5.7-7.5 mg/L). IBROM reduced DOC by 11 % and increased the BDOC by 7 %. Although the coagulation with PACl achieved the highest DOC and BDOC reduction (up to 57 % and 58 %), the coagulated water had the highest THMFP.  $\text{H}_2\text{O}_2/\text{UV}$  oxidation reduced the DOC only slightly by 10 %, but the corresponding increase of BDOC and reduction of THMFP was very high (43 % and 72 %). Similar observations were made in regard to oxidation with  $\text{KMnO}_4$ . Overall, the waters with a higher concentration of BDOC had lower THMFP.

## Keywords

Biodegradable Dissolved Organic Carbon (BDOC); membrane pre-treatment; Integrated Biological and Reverse Osmosis Membrane (IBROM); Trihalomethanes (THMs)

## INTRODUCTION

Many potable water sources in Canada have tremendously poor quality due to high concentrations of dissolved organic carbon (DOC) of up to 25 mg/L (Goss et al., 2017). High DOC can have adverse effects on drinking water quality which encompasses the formation of potentially carcinogenic Trihalomethanes (THMs) (Sillanpää et al., 2010). Reverse osmosis (RO) membranes are commonly applied to control THMs formation, however, membranes experience serious fouling when used to treat such high DOC waters (Jha et al., 2018). One strategy to cope with membrane fouling includes reducing DOC concentrations in the pre-treatment processes prior to membrane filtration (Goss et al., 2017).

### Biodegradable DOC and membrane fouling

The easily biodegradable fraction of natural organic matter (NOM) can cause biofouling by encouraging biofilm growth on the membrane surface and/or inside the membrane (Al-Juboori and Yusaf, 2012; Chen et al., 2018; Simon et al., 2013). Baker & Dudley (1998) reported biodegradable organic content making up 56-66 % of the composition of the fouling layer in a RO membrane. Biofouling is the contributing factor to more than 45 % of all membrane fouling and it can be reduced by depleting biodegradable NOM in the water (Bucs et al., 2018; Simon et al., 2013). Biodegradable NOM is considered to be the dominant growth-limiting factor for bacteria and is often evaluated by biodegradable DOC (BDOC) concentrations (Chen et al., 2018; Siddiqui et al.,



2017). BDOC is the fraction of DOC that can be mineralized by indigenous heterotrophic microorganisms (Author and Huck, 1990).

### **Chemical coagulation and oxidation**

*Coagulation.* Coagulation is a popular and widely used pre-treatment process in the Canadian WTPs used to reduce water DOC. An effective DOC reduction via coagulation pre-treatment can reduce membrane fouling significantly (Sadrnourmohamadi et al., 2013).

*Potassium permanganate (KMnO<sub>4</sub>).* Hidayah & Yeh (2018) reported that permanganate oxidation caused the breakdown of high molecular weight (MW) organics into low MW with a 10 % increase in the DOC (initial DOC = 4.2 mg/L), however, THMs formation potential (THMFP) of the oxidized water was reported to decrease from 911.6 µg/L by 15 %. Currently, there is no literature about the use and effect of KMnO<sub>4</sub> on the drinking water sources with DOC higher than 7.9 mg/L (Godo et al., 2019; Ma et al., 2018; Zhao et al., 2018; Lin et al., 2015b).

*Hydrogen peroxide (H<sub>2</sub>O<sub>2</sub>) coupled with UV (H<sub>2</sub>O<sub>2</sub>/UV).* Sarathy & Mohseni (2009) have reported 15 % mineralization of NOM for water with the total organic carbon (TOC) of 2.18 mg/L during oxidation with 20 mg/L of H<sub>2</sub>O<sub>2</sub> with UV fluence of 1500 mJ/cm<sup>2</sup> under these conditions. Toor and Mohseni (2007) reported 93 % THMFP reduction (from 150 µg/L to 10 µg/L) at 23 mg/L H<sub>2</sub>O<sub>2</sub> and UV fluence of 2500 mJ/cm<sup>2</sup>. However, the DOC concentration in the above studies was very low compared to the DOC of raw drinking waters in the Canadian Prairies. The authors are not aware of any research reporting on the effectiveness of H<sub>2</sub>O<sub>2</sub>/UV to THMs control in DOC water higher than 10.6 mg/L (Chu et al., 2014; Dotson et al., 2010; Seo et al., 2019; Tubić et al., 2013).

### **Biological filtration (IBROM)**

The biological pre-treatment studied in this paper is a relatively novel IBROM (Integrated Biological and Reverse Osmosis Membrane) process. The process involves using two filters connected in series, using Filtralite media (Peterson et al., 2007). IBROM system has been installed in 23 First Nation communities in the provinces of Saskatchewan and Alberta (Canada). IBROM process claims that the removal of BDOC alone (note: not the total DOC), would result in less fouling on RO membranes. The IBROM installed in Yellow Quill WTP (Saskatchewan) reduced DOC by 1 mg/L only, resulting in RO membrane influent with high DOC concentrations of 8.9 mg/L. This is more than four times higher than the 2 mg/L concentration recommended by AMTA (2007). The same paper reports that RO membrane did not require chemical cleaning for up to 18 months (Peterson et al., 2006) while chemical cleaning every 6 months or less is typically required to restore membrane performance (Ambrosi and Tessaro, 2013). The claims of IBROM systems removing BDOC and experiencing low membrane fouling have never been scientifically substantiated.

### **Objectives**

Removal of BDOC has been claimed to result in reduced fouling of the RO membranes (Bucs et al., 2018; Peterson et al., 2006; Simon et al., 2013). The first objective of this study is to evaluate the effectiveness of biological filtration (IBROM), coagulation and oxidation in terms of DOC and BDOC removal. The second objective of this study is to investigate a potential correlation between the BDOC concentration and THMs formation potential of the treated waters.

## **MATERIALS AND METHODS**

### **General feed water quality**

The research was conducted using water collected from Herbert WTP (Sask). General raw water quality parameters are summarized in Table 1. Herbert WTP uses blended water consisting of the

*11<sup>th</sup> Eastern European Young Water Professionals Conference IWA YWP,  
1-5 October 2019, Prague, Czech Republic*

same ratio of water from a dugout and groundwater. The oxidation experiments were conducted on the dugout water prior to the plant to provide enough reaction time. The dugout water is then blended with the groundwater as it enters the WTP where coagulation will occur. Both dugout and blended raw water have high concentrations of DOC at approximately 22.7 mg/L and 17.5 mg/L, respectively.

**Table 4.** Raw water quality parameters for Herbert WTP collected from the plant in Aug. 2018

Parameter	Unit	GCDWQ* (Treated water)	Dugout water	Blended water
<b>pH</b>	-	7 – 10.5	8- 8.8	7.9 – 8.5
<b>Total alkalinity</b>	mg/L CaCO <sub>3</sub>	-	234	350.5
<b>Total THMFP</b>	µg/L	≤ 100	809.8	865.9
<b>Total hardness</b>	mg/L CaCO <sub>3</sub>	80 – 100	495	376
<b>Total dissolved solid</b>	mg/L	≤ 500	1160	1243
<b>DOC</b>	mg/L	-	22.7	17.5
<b>BDOC</b>	mg/L	-	7.54	5.75
<b>Iron</b>	mg/L	≤ 0.3	0.105	0.77
<b>Manganese</b>	mg/L	<0.12	0.06	0.01

(\*Guidelines on Canadian Drinking Water Quality (Health Canada, 2019))

### Biological filtration

Removal of DOC and BDOC evaluation was conducted on-site Herbert WTP on water samples collected before and after the IBROM filters. The IBROM filters located at the plant are two Filtralite filters consisting of Filtralite HC and NC 0.8–1.6 mm clay product.

### Laboratory scale coagulation and oxidation experimental methods

Laboratory bench-scale coagulation tests were conducted using the raw blended water with aluminum sulphate (alum), polyaluminum chloride (PACl), aluminum chlorohydrate (ACH) and ferric chloride. The experiments were carried out by the ASTM D2035 – 19 standard method in a six paddle PB-700TM standard jar testers. Considering the high DOC of the dugout water (=22.14 mg/L), 0.25, 0.5, 1, 1.5 and 2 mg/L of KMnO<sub>4</sub> were used in oxidation experiments. To avoid any interference of the oxidant in the BDOC and DOC measurements, the samples were quenched using sodium thiosulfate before further analysis. Hydrogen peroxide doses of 20, 40, 60, 80, 100 mg/L and UV fluence of 2000 mJ/cm<sup>2</sup> was applied in the H<sub>2</sub>O<sub>2</sub>/UV. UV radiation was conducted using an annular reactor with a working volume of 1 liter, using a centrally mounted low-pressure UV lamp (Jelight Company, Inc.). Before further analysis, the samples were quenched using bovine liver catalase at a concentration of 0.2 mg/L in the sample (Sarathy and Mohseni, 2009).

DOC concentration was determined using a SkalarHT Formacs TOC Analyzer (Skalar, GA). THMFP measurements were conducted according to *Standard Methods 5710B* (APHA, 2012). The BDOC test was performed according to a batch procedure by Khan et al. (1999) using a bacterial inoculum (BOD seed, Bio-Systems Corporation, Illinois, USA).

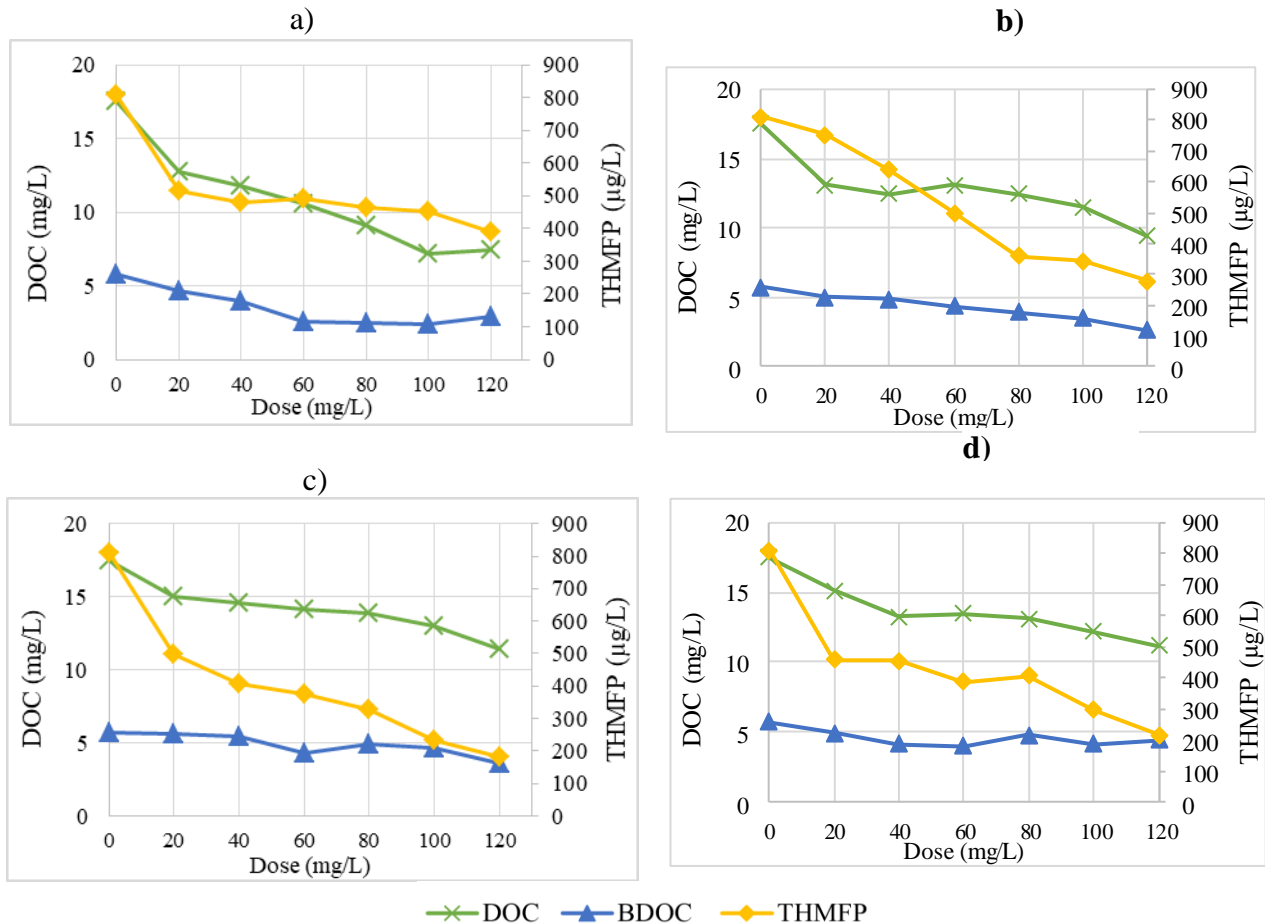
## RESULTS AND DISCUSSION

### Coagulation experiments

Figure 1 shows changes in DOC, BDOC and THMFP in the coagulated waters. Maximum DOC and BDOC removal were observed with 100 mg/L of PACl, and down to 7.5 mg/L and 2.4 mg/L,

*11<sup>th</sup> Eastern European Young Water Professionals Conference IWA YWP,  
1-5 October 2019, Prague, Czech Republic*

respectively. The DOC was still higher than recommended 2 mg/L and thus this water is likely to cause serious RO membrane fouling.



**Figure 1.** DOC, BDOC and THMFP for a) PACl, b) ACH, c) Alum and d) Ferric chloride at varying coagulant dose

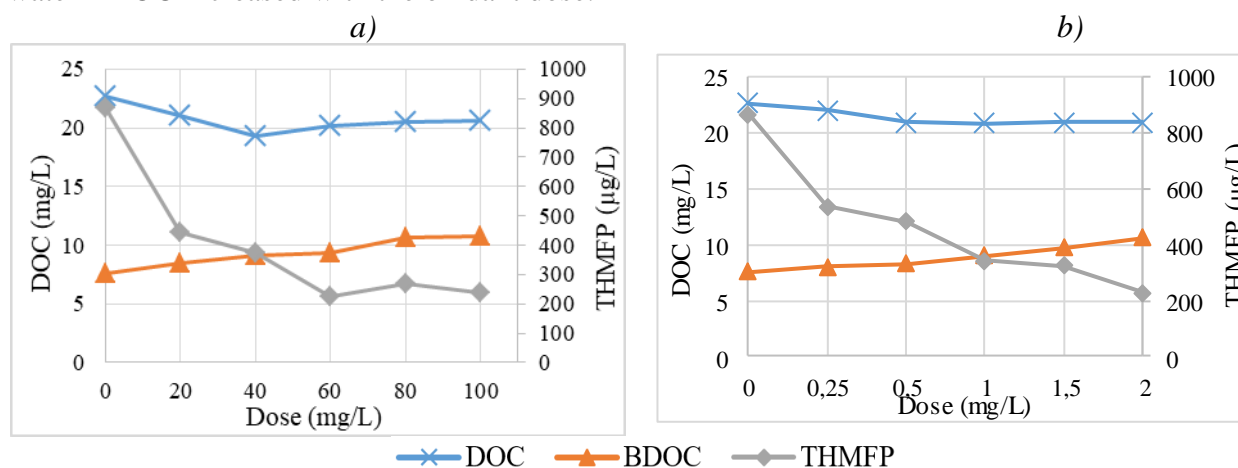
BDOC in the raw water was 5.75 mg/L (Table 2). BDOC removal ranged from 20-60 % for different coagulants, which is in accordance with the literature (Soh et al., 2008; Umar et al., 2014). Maximum BDOC removal was observed with 60 mg/L of PACl, reducing the BDOC by 58 % down to 2.4 mg/L. 120 mg/L of alum had the lowest THMFP, reducing it from the initial THMFP of 809.8 µg/L to 183.5 µg/L. Of the four coagulants tested, alum showed the greatest average reduction in THMFP while having lower DOC removal compared to other coagulants. Reduction of water THMFP in the coagulation is due to the reduction of the concentration of total DOC. Although PACl reduced water DOC to the greatest degree, this coagulant had the least reduction in THMFP (THMFP of 452.3 µg/L at 100 mg/L dose of coagulant). Factors other than DOC concentration play a role here. Figure 1 shows that Alum and ferric chloride were not as effective in the removal of BDOC as PACl although they had the highest reduction in THMFP. Our measurements indicated that higher BDOC waters had lower THMFP. This suggests that there is an inverse relationship between biodegradability and THMFP of the raw waters.

**Oxidation experiments by KMnO<sub>4</sub> and H<sub>2</sub>O<sub>2</sub>/UV**

Figure 3 is showing DOC, BDOC and THMFP change in oxidation for different concentrations of KMnO<sub>4</sub> and H<sub>2</sub>O<sub>2</sub>/UV on the water with the initial DOC of 22.7 mg/L. Oxidation with 0.5 mg/L of KMnO<sub>4</sub> had the maximum DOC removal of 8 % reducing DOC to 20.85 mg/L. Meanwhile, 40 mg/L of H<sub>2</sub>O<sub>2</sub>/UV showed maximum removal of 15 % reducing DOC to 19.3 mg/L. These results

demonstrate that that oxidation is not able to remove a significant amount of water DOC, which has previously been reported in the literature (Wang et al., 2019; Xie et al., 2016).

However, oxidation significantly reduced the THMFP of the water (Figure 3). THMFP was reduced from an initial concentration of 865.9 down to 225.8  $\mu\text{g/L}$  at a dose of 2 mg/L  $\text{KMnO}_4$ . In the case of  $\text{H}_2\text{O}_2/\text{UV}$ , THMFP was reduced down to 237.5  $\mu\text{g/L}$  with 100 mg/L of  $\text{H}_2\text{O}_2$ . According to Figure 3, while the reduction in THMFP treated with  $\text{H}_2\text{O}_2/\text{UV}$  averaged 64 %, the corresponding reduction in DOC was only 10 %. The same was observed in  $\text{KMnO}_4$  with 7 % and 56 % average reduction in THMFP and DOC, respectively. Therefore, the total DOC cannot be the main factor contributing to THMFP. Although the DOC of the water was relatively unchanged by oxidation, the water BDOC increased with the oxidant dose.



**Figure 3.** Change in DOC, BDOC and THMFP in oxidation with a)  $\text{H}_2\text{O}_2/\text{UV}$  and b)  $\text{KMnO}_4$

In all concentrations, water oxidized with  $\text{H}_2\text{O}_2/\text{UV}$  contained more BDOC and lower THMFP compared to water oxidized with  $\text{KMnO}_4$ . This confirms the trend observed between BDOC and THMFP in coagulation. Higher BDOC water has lower THMFP.

### BDOC change by the biological filtration

Table 2 indicates that the two IBROM filters have 11% DOC removal. (DOC decrease from 15.4 mg/L to 13.68 mg/L). Increase of BDOC in IBROM effluent at the Herbert WTP was minimal (7 %). The results indicate that the IBROM process is not effective in the removal of BDOC nor DOC.

**Table 2.** DOC and BDOC concentration change along the treatment train of the Herbert WTP

Sample water	Dugout	Blended	Clarifier	Filters (Filtralite)
DOC (mg/L)	22.7	17.5	15.4	13.68
BDOC (mg/L)	7.54	5.75	5.56	5.96

## CONCLUSIONS

The following conclusions can be made from this study:

1. Laboratory-optimized coagulation and oxidation were not able to reduce the water DOC to 2 mg/L recommended for RO filtration. Maximum DOC reductions by coagulation and oxidation were observed with 100 mg/L of PACl and down to 7.5 mg/L, and with 40 mg/L of  $\text{H}_2\text{O}_2/\text{UV}$  down to 19.3 mg, respectively.
2. Alum and ferric chloride showed the greatest reduction in THMFP from 809.8  $\mu\text{g/L}$  to 183.5  $\mu\text{g/L}$  and 216.2  $\mu\text{g/L}$ , respectively with the total DOC reduction of 34 % and 36 %, respectively. Removal of DOC and formation of THMs varied for different coagulants.

*11<sup>th</sup> Eastern European Young Water Professionals Conference IWA YWP,  
1-5 October 2019, Prague, Czech Republic*

3. Oxidation with  $\text{KMnO}_4$  and  $\text{H}_2\text{O}_2/\text{UV}$  resulted in a decrease in THMFP and an increase in water BDOC of up to 30 %. Oxidation significantly reduced the THMFP from the initial THMFP of 865.9  $\mu\text{g/L}$  to 225.8  $\mu\text{g/L}$  and 237.5  $\mu\text{g/L}$ , respectively.
4. In both oxidation and coagulation, higher BDOC waters had lower THMFP. This suggests that a relationship exists between water BDOC and THMFP.
5. IBROM system operating at Herbert WTP was found to be ineffective in removing water BDOC and DOC.

## REFERENCES

- Al-Juboori, R. A., Yusaf, T. (2012) Biofouling in RO system: Mechanisms, monitoring and controlling. *Desalination*, **302**, 1-23.
- Ambrosi, A., Tessaro, I. C. (2013) Study on Potassium Permanganate Chemical Treatment of Discarded Reverse Osmosis Membranes Aiming their Reuse. *Separation Science and Technology (Philadelphia)*, **48**(10), 1537-1543.
- AMTA (2007) Pretreatment for Membrane Processes. In *Membranes*. [online] [https://www.amtaorg.com/wp-content/uploads/12\\_Pretreatment.pdf](https://www.amtaorg.com/wp-content/uploads/12_Pretreatment.pdf)
- APHA (2012) *Standard Methods for the Examination of Water and Wastewater*. American Public Health Association. Washington, DC.: American Water Works Association and Water Environment Federation.
- Author, W., Huck, P. M. (1990) Measurement of Biodegradable Organic Matter and Bacterial Growth Potential in Drinking Water. *American Water Works Association. Distribution Systems*, **82**(7), 78-86.
- Baker, J. S., Dudley, L. Y. (1998) Biofouling in membrane systems. A review. *Desalination*, **118**(1-3), 81-89.
- Bucs, S., Farhat, N., Kruithof, J. C., Picioreanu, C., van Loosdrecht, M. C. M., Vrouwenvelder, J. S. (2018) Review on strategies for biofouling mitigation in spiral wound membrane systems. *Desalination*, **434**, 189-197.
- Chen, Z., Yu, T., Ngo, H. H., Lu, Y., Li, G., Wu, Q., Hu, H. Y. (2018) Assimilable organic carbon (AOC) variation in reclaimed water: Insight on biological stability evaluation and control for sustainable water reuse. *Bioresource Technology*, **254**, 290-299.
- Chu, W., Gao, N., Yin, D., Krasner, S. W., Mitch, W. A. (2014) Impact of UV/ $\text{H}_2\text{O}_2$  pre-oxidation on the formation of haloacetamides and other nitrogenous disinfection byproducts during chlorination. *Environmental Science and Technology*, **48**(20), 12190-12198.
- Dotson, A. D., Keen, V. S., Metz, D., Linden, K. G. (2010) UV/ $\text{H}_2\text{O}_2$  treatment of drinking water increases post-chlorination DBP formation. *Water Research*, **44**(12), 3703-3713.
- Godo-Pla, L., Emiliano, P., Valero, F., Poch, M., Sin, G., Monclús, H. (2019) Predicting the oxidant demand in full-scale drinking water treatment using an artificial neural network: Uncertainty and sensitivity analysis. *Process Safety and Environmental Protection*, **125**, 317-327.
- Goss, C. D., Wiens, R., Gorczyca, B., Gough, K. M. (2017) Comparison of three solid phase extraction sorbents for the isolation of THM precursors from Manitoban surface waters. *Chemosphere*, **168**, 917-924.
- Health Canada (2019) *Guidelines for Canadian Drinking Water Quality- Summary Table*. *Healthy Living* (Vol. 2006). [online] <https://www.canada.ca/en/health-canada/services/publications/healthy-living/guidelines-Canadian-drinking-water-quality-guideline-technical-document->
- Hidayah, E. N., Yeh, H. H. (2018) Effect of Permanganate Preoxidation to Natural Organic Matter and Disinfection by-Products Formation Potential Removal. *Journal of Physics: Conference Series*, **953**(1).
- Jha, N., Kiss, Z. L., Gorczyca, B. (2018) Fouling mechanisms in nanofiltration membranes for the treatment of high DOC and varying hardness water. *Desalination and Water Treatment*, **127**,

197-212.

- Khan, E., King, S., Babcock Jr, R. W., Stenstrom, M. K. (1999) factors influencing biodegradable dissolved organic carbon measurement. *Journal Of Environmental Engineering*, **125**, 514-521.
- Lu, Z. J., Lin, T., Chen, W., Zhang, X. B. (2015) Influence of KMnO<sub>4</sub> preoxidation on ultrafiltration performance and membrane material characteristics. *Journal of Membrane Science*, **486**, 49-58.
- Ma, B., Qi, J., Wang, X., Ma, M., Miao, S., Li, W., Qu, J. (2018) Moderate KMnO<sub>4</sub>-Fe(II) pre-oxidation for alleviating ultrafiltration membrane fouling by algae during drinking water treatment. *Water Research*, **142**, 96-104.
- Matilainen, A., Vepsäläinen, M., Sillanpää, M. (2010) NOM removal by coagulation during drinking water treatment: A review. *Advances in Colloid and Interface Science*, **159**(2), 189-197.
- Peterson, H, Pratt, R., Neapetung, R., Sortehaug, O. (2006) Integrated biological filtration and reverse osmosis treatment of a cold poor quality groundwater on the North American prairies. *Recent Progress in Slow Sand and Alternative Bio-Filtration Processes CN*, **0001**(5), 424-432.
- Peterson, H., Pratt, R., Neapetung, R., Sortehaug, O. (2007). Biological filtration of poor quality brackish water reducing Reverse Osmosis membrane fouling. *IDA World Congress*, 1-18.
- Sadrnourmohamadi, M., Gorczyca, B., Goss, C. D. (2013) Removal of DOC and its fractions from the high DOC and hardness surface waters of the Canadian Prairie. *Water Science and Technology: Water Supply*, **13**(3), 864-870.
- Sarathy, S., Mohseni, M. (2009) The fate of natural organic matter during UV/H<sub>2</sub>O<sub>2</sub> advanced oxidation of drinking water, *Canadian Journal of Civil Engineering*, **36**(1), 160-169.
- Seo, C., Shin, J., Lee, M., Lee, W., Yoom, H., Son, H., Lee, Y. (2019) Elimination efficiency of organic UV filters during ozonation and UV/H<sub>2</sub>O<sub>2</sub> treatment of drinking water and wastewater effluent. *Chemosphere*, **230**, 248-257.
- Siddiqui, A., Pinel, I., Prest, E. I., Bucs, S. S., van Loosdrecht, M. C. M., Kruithof, J. C., Vrouwenvelder, J. S. (2017) Application of DBNPA dosage for biofouling control in spiral wound membrane systems. *Desalination and Water Treatment*, **68**(March), 12-22.
- Simon, F. X., Rudé, E., Llorens, J., Baig, S. (2013) Study on the removal of biodegradable NOM from seawater using biofiltration. *Desalination*, **316**, 8-16.
- Soh, Y. C., Roddick, F., Van Leeuwen, J. (2008) The impact of alum coagulation on the character, biodegradability and disinfection by-product formation potential of reservoir natural organic matter (NOM) fractions. *Water Science and Technology*, **58**(6), 1173-1179.
- Toor, R., Mohseni, M. (2007) UV-H<sub>2</sub>O<sub>2</sub> based AOP and its integration with biological activated carbon treatment for DBP reduction in drinking water. *Chemosphere*, **66**(11), 2087-2095.
- Tubić, A., Agbaba, J., Dalmacija, B., Molnar, J., Maletić, S., Watson, M., Perović, S. U. (2013) Insight into changes during coagulation in NOM reactivity for trihalomethanes and haloacetic acids formation. *Journal of Environmental Management*, **118**, 153-160.
- Umar, M., Roddick, F., Fan, L. (2014) Effect of coagulation on treatment of municipal wastewater reverse osmosis concentrate by UVC/H<sub>2</sub>O<sub>2</sub>. *Journal of Hazardous Materials*, **266**, 10-18.
- Wang, Z., Wan, Y., Xie, P., Zhou, A., Ding, J., Wang, J., Zhang, T. C. (2019) Ultraviolet/persulfate (UV/PS) pretreatment of typical natural organic matter (NOM): Variation of characteristics and control of membrane fouling. *Chemosphere*, **214**, 136-147.
- Xie, P., Chen, Y., Ma, J., Zhang, X., Zou, J., Wang, Z. (2016) A mini review of preoxidation to improve coagulation. *Chemosphere*, **155**, 550-563.
- Zhao, H., Wang, L., Zhang, H., Wu, X., Zhao, B., Han, F. (2018) Effect of potassium permanganate dosing position on the performance of coagulation/ultrafiltration combined process. *Chinese Journal of Chemical Engineering*, **26**(1), 137-143.

## Prevalence of *Legionella spp.* and *Escherichia coli* in the Drinking Water Distribution System of Wrocław (Poland)

M. Wolf-Baca\* and A. Siedlecka\*

\* Faculty of Environmental Engineering, Wrocław University of Science and Technology, Wyb. Wyspiańskiego 27, 50-370 Wrocław, Poland (E-mails: [mirela.wolf-baca@pwr.edu.pl](mailto:mirela.wolf-baca@pwr.edu.pl); [agata.siedlecka@pwr.edu.pl](mailto:agata.siedlecka@pwr.edu.pl))

### Abstract

Drinking water should be free from bacterial pathogens threatening human health. The most recognised waterborne opportunistic pathogens, dwelling in tap water, are *Legionella pneumophila* and *Escherichia coli*. Drinking water samples were tested for the presence of *Legionella spp.* (*L. spp.*), *Legionella pneumophila* (*L. pneumophila*), and *Escherichia coli* (*E. coli*) in overall samples' microbiome by means of a quantitative real-time PCR (qPCR) approach. The results indicate rather low contribution of *L. spp.* in total bacteria in the tested samples, whereas *L. pneumophila* was not detected in any sample. *E. coli* was detected in only one sample, but at very low level. The *qacEΔ1* gene, conferring resistance to quaternary ammonium compounds, was not detected in any sample, either. The results point to generally sufficient quality of drinking water, although the presence of *L. spp.* in tap water samples suggests proliferation of these bacteria in heating units, causing a potential threat to consumer health.

### Keywords

Tap water; bacterial pathogens; qPCR

## INTRODUCTION

In many countries, tap water is one of the sources of drinking water. Therefore, its high quality in terms of physical-chemical and microbiological conditions is strongly required. The latter seems to be of even more importance in the case of human health risk assessment, because the presence of microbiological pathogens in drinking water may lead to numerous infections (Ashbolt, 2015; Liu, 2019). Moreover, the environmental conditions provided in drinking water distribution systems may favour the proliferation of some bacteria (September, 2007; Falkinham, 2015). The most recognised waterborne pathogens from the kingdom of bacteria include *Legionella pneumophila* (*L. pneumophila*) and *Escherichia coli* (*E. coli*) (WHO, 2017). *Legionella spp.* is mostly found in hot tap water. It is in this environment that these bacteria found the most appropriate conditions for their growth and proliferation (WHO, 2007). Nevertheless, some representatives of the genus may also be found in non-heated tap water, distributed to consumers' taps (Perreira, 2017). *Legionella* may cause legionellosis, the illness of Pontiac fever, and Legionnaires' disease. Pontiac fever is a non-lethal, self-limited flu-like illness. It was first recognised in the Country Health Department building in Pontiac (Michigan, USA). Legionnaires' disease, which may cause death of the victims, was named after the American Legion convention at the Philadelphia hotel (Principe, 2017). The most common pathogenic *Legionella* species is *L. pneumophila*, although 27 other *Legionella* species are also recognised as human pathogens (Principe, 2017). Therefore, the presence of representatives of the entire genus should be monitored in drinking water samples. On the other hand, *E. coli* is natural commensal to humans, and is the inhabitant of the human and animal intestine. Nonetheless, some strains may become invasive and cause many illnesses, for example diarrhoeas – from moderate to severe (Vásquez-García, 2019). *E. coli* is also the most important indicator of potential faecal contamination (Paruch, 2012). Hence, the presence of *Legionella spp.* and *E. coli* cells in drinking water samples should not be neglected.

The presence of bacteria in disinfected tap water was confirmed in many studies. The bacterial microbiome characteristic for tap water mainly consists of non-pathogenic species (Douterelo, 2016; El-Chakotura, 2015; Rudi, 2010). Nevertheless, the insufficient source water treatment and accidental contaminations within the distribution system may lead to the introduction of virulent genera. The most common ones, namely *Escherichia* and *Legionella*, are monitored continuously by local drinking water suppliers and sanitary-epidemiological stations in terms of cultivation of these bacteria on selective agar media. The use of the quantitative real-time PCR (qPCR) method in the detection and quantification of waterborne bacterial pathogens may contribute to the elucidation of the issue. It is worth mentioning, however, that the implementation of the qPCR method does not differentiate between live and dead organisms, unless a special procedure (for example with propidium monoazide – PMA) is applied (Alvarez, 2013; Toplitsch, 2018).

Bacteria dwelling in tap water distribution systems are generally known to be resistant to disinfectants (Khan, 2016). This feature allows them to overcome the presence of the disinfectant agent remaining in water samples. Genes responsible for the phenomenon of efflux pumps or other resistance mechanisms, such as the *qacEΔ1* gene (conferring resistance to quaternary ammonium compounds) (Szekeres, 2018), may indicate the bacterial ability to overcome the disinfectant residual in the tap water distribution system.

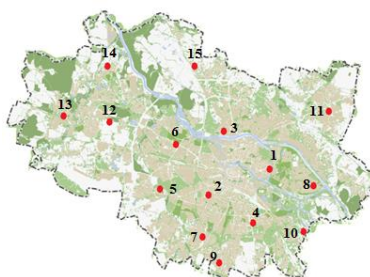
If resistant, pathogens belonging to genera *Legionella* and *Escherichia* may cause a serious threat to human health, because they may not be removed in the water treatment plant, and enter the distribution system. Moreover, bacterial cells could participate in horizontal gene transfer (HGT) in which they are able to transform some genes (Gyles, 2014). Therefore, the detection of the selected genes, which may enhance bacterial resistance to disinfectants in tap water samples is also important in the estimation of consumer health risk.

This study aimed at the detection and determination of total quantity of (viable and non-viable) *Legionella spp.*, *L. pneumophila*, and *E. coli* bacterial cells, and their contribution in overall bacteria load quantified in microbiome cultivated from consumer tap water samples by means of the qPCR approach. As mentioned above, some bacteria, including pathogens, are able to overcome the presence of disinfectant, because they possess specific genes conferring increased resistance. Therefore, simultaneous monitoring of such genes in tap water microflora may be of importance. In this study, the presence of the *qacEΔ1* gene, as the representative gene conferring resistance to disinfectants, was determined. Consumer tap water samples were collected from the drinking water distribution system in Wrocław (Poland). This research may contribute to the estimation of consumer health risk associated with intake of tap water, because in Poland, tap water is generally assumed to be considered drinking water, for consumption directly from a tap.

## **MATERIALS AND METHODS**

Consumer drinking water samples were collected from 15 different points of the water supply system in Wrocław (Figure 1). Before sampling, the taps were disinfected with 96 % ethanol (Sigma), and water was flushed for 5 minutes. Each sample of 3 litres was filtrated on Whatman membranes (mixed-cellulose esters, diameter 0.2 µm). The membranes were submerged in sterile broth and incubated for 48 h at room temperature. Afterwards, the suspension was used for DNA extraction.





**Figure 1.** Map of Wrocław with location of collection points

Genomic DNA was extracted by means of an Isolate II Genomic Kit (BIOLINE). The concentration of DNA was measured on a NanoPhotometer N60 (Implen).

The qPCRs (MIC, Bio Molecular Systems) were carried out to quantify *Legionella spp.*, *L. pneumophila*, and *E. coli* genomes, as well as 16S rRNA and *qacEΔ1* genes.

The reactions for the quantification of *Legionella spp.*, *L. pneumophila*, and *E. coli* were performed with an AmpliTest (Amplicon) in accordance with the manufacturers' instructions. These quantification kits apply TaqMan probes, and are specific for target bacterial genome sequences. Moreover, AmpliTest provides internal control, allowing for detecting potential inhibition of reactions. The 16S rRNA and *qacEΔ1* genes were quantified with a QUANTUM EvaGreen HRM Kit (SYNGEN) with the application of a non-specific dye. All the reactions for pathogenic genomes quantification were performed in technical triplicates, while 16S rRNA and *qacEΔ1* genes were quantified in technical duplicates. The conditions for qPCRs are presented in Table 1. In each reaction, negative control was applied, and the calculations of genomes or gene copy number were based on standard curves. For *L. spp.*, *L. pneumophila*, and *E. coli* genomes, standard curves were prepared as described in the previous study (Wolf-Baca, 2019), resulting in calculated genomes per reaction. For the purpose of 16S rRNA standard curve preparation, the genomic DNA ten-fold dilution of *Escherichia coli* ATCC 25922 (BioMaxima) strain was used. In the case of *qacEΔ1* gene, the ten-fold dilution of purified PCR product was used.

**Table 5.** Conditions for qPCRs

	16S rRNA		AmpliTests		qacEΔ1	
Initial denaturation	95°C / 15 min		95°C / 5 min		95°C / 15 min	
Denaturation	95°C / 15 sec	40 cycles	95°C / 30 sec	45 cycles	95°C / 15 sec	40 cycles
Annealing	60°C / 20 sec		58°C / 25 sec		63°C / 20 sec	
Elongation	72°C / 20 sec		-		72°C / 20 sec	
Cooling	-		40°C / 30 sec		-	
Melt	from 72°C to 95°C		-		from 72°C to 95°C	
Chemistry	EvaGreen		TaqMan probes internal control		withEvaGreen	
Primers	as described in (Huerta, 2013)		supplied by manufactureras in kits		described in (Szekeres, 2018)	
DNA per reaction [μL]	1		8		1	
Each primer volume per reaction [μL]	0.5		1		1	
Total volume per reaction [μL]	20		20		20	

## RESULTS

All qPCRs efficiencies were in a range of  $0.88 \pm 1.09$ . The limits of quantification were 178 genome copies/reaction for *L. spp* and *L. pneumophila*, and 1.59 genome copies/reaction for *E. coli*. In the case of the 16S rRNA and *qacEΔ1* gene, the limits of quantification were 16.9 and 184 gene copy number/reaction, respectively.

The abundance and prevalence of *Legionella spp.* were determined. However, no *L. pneumophila* target sequence was found in any tested samples. In the case of *E. coli*, only one sample (number 13) gave a positive signal with calculated genome copy number of 0.13 genomes/ng DNA. Moreover, no *qacEΔ1* gene could be detected in any sample.

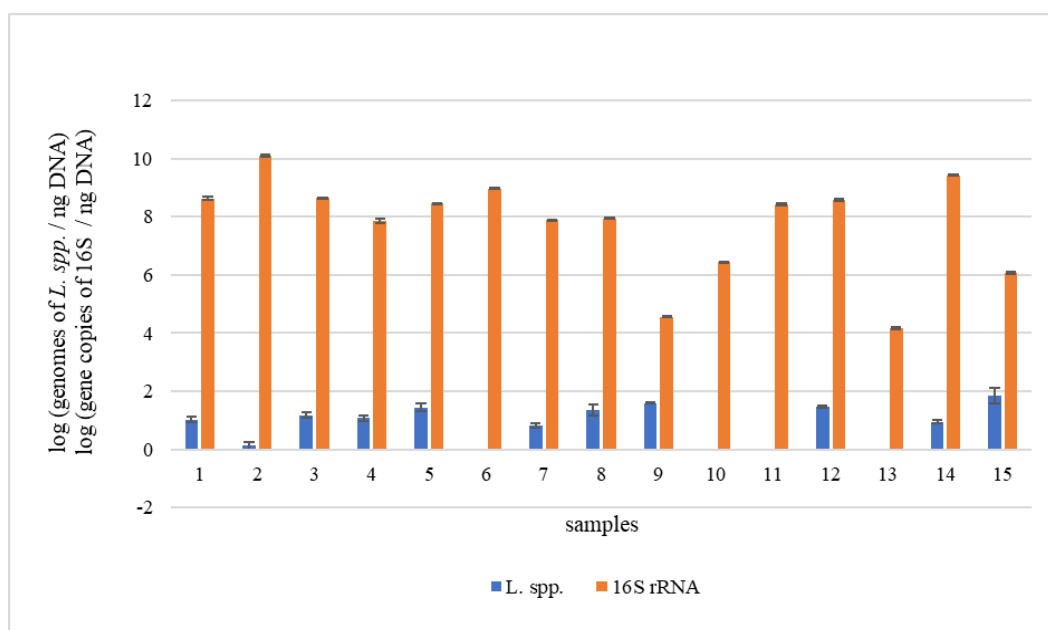
The results of calculations of genome copy number of *L. spp.* per ng of DNA in tested samples are presented in Table 2. In general, *L. spp.* were detected and quantified in 11/15 (73.3 %) samples.

**Table 6.** Genome copy numbers of *L. spp.* in tested samples

Sample	a)	Sample	a)	Sample	a)
1	11	6	0	11	0
2	1	7	7	12	29
3	15	8	23	13	0
4	12	9	39	14	9
5	28	10	0	15	71

a) genome copy number of *L. spp.* per ng of DNA in tested samples. The values are rounded to the nearest whole

*L. spp.* was the most abundant in sample number 15, where it reached 71 copies of genome per ng of DNA. Further analysis of the data indicates that *L. spp.* prevalence was relevant only in samples 9 and 15, reaching  $1.1 \times 10^{-3}$  and  $6.15 \times 10^{-5}$  genomes of *L. spp.* per 16S gene copy number, respectively.



**Figure 6.** Abundances of *L. spp.* genomes and 16S rRNA gene copy number in tested samples (in a logarithmic scale)

## DISCUSSION

The objective of this study was to estimate the potential consumer health risk associated with intake of non-boiled tap water samples by means of the qPCR approach. The usefulness of this method in *Legionella* quantification was proven a decade ago (Dusserre, 2008; Douterelo, 2014), but it is worth mentioning that promising methods for *L. pneumophila* detection other than qPCR include an immunodetection system described by Parraga-Nino et al. (Párraga-Niño, 2018) or Legiolert™/Quanti-Tray® MPN described by Spies et al. (Spies, 2018).

Among the tested pathogens, no *L. pneumophila* was found in any of the samples. This proves the good quality of Wrocław drinking water and treatment processes, and suggests a lowered risk for consumer health. Nevertheless, not only *L. pneumophila* is considered as a factor causing legionellosis (Principe, 2017), and therefore such risk could not be fully excluded.

The same concerns *E. coli*, one of the most important faecal contamination indicators (Coleman, 2011; Subba, 2013; Talukdar, 2013), detected only in one sample with no evidence of its viability. Moreover, even assuming that *E. coli* did not proliferate in broth, i.e. its quantity did not change during incubation, the calculated genome copy number/mL would be  $9.10 \times 10^{-3}$  (data not shown), which is far below the acceptable values specified in Polish law (Regulation, 2017). The detection of *E. coli* in this sample may be the effect of the presence of residual DNA fragments with *E. coli* specific sequence targets, originating from dead *E. coli* cells, because no live/dead treatment (Alvarez, 2013; Toplitsch, 2018) of the samples was performed before the DNA extraction procedure. Nevertheless, these residual DNA fragments may suggest contamination, which happened in the past.

The obtained results indicate that *L. spp.* could be still present in microflora cultivated from tap water samples, even if no *Legionella*-enhancing supplement was added to the broth. Nevertheless, based on this study, it could not be established whether the quantified cells were dead or alive.

The prevalence of *L. spp.* genomes in microflora cultivated from tap water samples tested in this study was generally low. It is worth mentioning that viable but non-culturable *Legionella* cells may be predominant in tap water samples (Dietersdorfer, 2018). This may explain the low level of *L. spp.* prevalence observed in this study. Other bacteria present in a given sample might take the advantage to proliferate, while *L. spp.* remain at the same level during a short incubation time. Contrary results presented by Whiley et al. indicate very high contamination of *Legionella* in Australian tap water, mostly in samples collected in the summer season (Whiley, 2014). Because the sampling campaign performed in this study was undertaken only once, at the turn of summer and autumn, the seasonal variation of contamination by pathogens could not be excluded.

Despite its low levels, *L. spp.* was frequently detected and quantified in this study. Similar results were obtained by Liu et al., who found *L. spp.* in 100 % samples, while the presence of *L. pneumophila* was confirmed only in 9.1 % of all samples (Liu, 2019).

Waak et al. tested the presence of *L. spp.* in water-main biofilms (scraped from pipes) and tap water samples from two distribution systems: a chloramine-containing system in the United States and a system in Norway that does not maintain a residual disinfectant. They were able to detect *L. spp.* in 43 % of biofilm samples from the Norwegian system with no residual disinfectant, with a maximum concentration of  $7.8 \times 10^4$  gene copies  $\text{cm}^{-2}$ . No *L. spp.* was detected in biofilm samples from the American chloraminated system. In the case of tap water samples, *L. spp.* was detected in 26 % and 64% of tested samples from the American and Norwegian system, respectively, with a maximum concentration of  $2.0 \times 10^3/\text{L}$  for chloraminated system, and  $2.8 \times 10^3/\text{L}$  for the system with no residual

disinfectant. The results obtained in this study are higher than those presented by Waak et al., as 73.3 % of tested tap water samples were *L. spp.* positive. Moreover, Waak et al. detected a *L. pneumophila* gene marker in 3 % and 9 % of tested biofilm samples from the American and Norwegian system, respectively, while tap water samples from both sampling regions were free from *L. pneumophila*, which is in accordance with results presented in this paper. No *L. pneumophila* serogroup 1 gene marker was found in any of the tested samples of water-main biofilms or tap water in American and Norwegian systems (Waak, 2018).

*Legionella* is often tested only in hot tap water installations (Wolf-Baca, 2019). However, its proliferation in heating units is initiated due to the presence of these bacteria in the water distribution system. Therefore, there is a risk that in points with considerable *L. spp.* prevalence, much more *Legionella* cells may be found in hot water samples. Intake of aerosols with *Legionella* during the use of hot tap water (for example for baths and other domestic purposes) is known to pose a potential risk of legionellosis (Wong, 2006). Therefore, the detection of the *L. spp.* sequence targets in drinking water samples should not be neglected. Replacement of chlorine to monochloramine was suggested as a method for improved removal of *Legionella* from hot tap water (Flannery, 2006; Moore, 2006). The importance of the presence of residual disinfectant in the drinking water distribution system was confirmed in the study of Waak et al. The USA chloraminated drinking water distribution system was evidenced to be less contaminated with *Legionella* and overall *Bacteria* (in the case of water-main biofilm samples from pipes as well as tap water samples) than the Norwegian system with no residual disinfectant (Waak, 2018).

It is worth mentioning that the lack of *qacEΔ1* gene sequence in any sample suggests low resistance to disinfectants in cultivated microflora. Therefore, constant chlorination of the Wrocław drinking water distribution system and the assurance of appropriate levels of residual disinfectant along the entire pipeline network should be sufficient in prevention of the proliferation of bacterial pathogens in consumers' tap water. From the other hand, the disinfection processes may lead to the forming of disinfection-by-products, which may be considered as another threats to consumer health (Pogorzalec, 2018).

## CONCLUSIONS

The prevalence of *L. spp.* cells in microbiome of tap water samples collected from 15 sampling points of drinking water distribution system in Wrocław was generally low. Only in two points (9 and 15) the quantity of *L. spp.* in overall bacteria load was increased. Neither *L. pneumophila* or *E. coli* (except sampling point number 13) were detected. No *qacEΔ1* gene, conferring resistance to quaternary ammonium compounds, was detected in the samples either. These data suggest the sufficient quality of consumers tap water in Wrocław. Nevertheless, the presence of *L. spp.* in drinking water distribution system may lead to their proliferation in heating installations, posing a health risk to tap water consumers.

## REFERENCES

- Àlvarez, G., González, M., Isabal, S., Blanc, V., León, R. (2013) Method to quantify live and dead cells in multi-species oral biofilm by real-time PCR with propidium monoazide. *AMB Express*, **3**, 1-8.
- Ashbolt, N. J. (2015) Microbial Contamination of Drinking Water and Human Health from Community Water Systems. *Curr. Environ. Heal. Reports*, **2**, 95-106.
- Coleman, B. L., Salvadori, M. I., McGeer, A. J., Sibley, K. A., Numann, N. F., Bondy, S. J., Gutmanis, I. A., McEwen, S. A., LaVoie, M., Strong, D., Johnson, I., Jamieson, F. B., Louie, M.

- (2012) The role of drinking water in the transmission of antimicrobial-resistant *E. coli*. *Epidemiol. Infect.*, **140**, 633-642.
- Dietersdorfer, E., Kirschner, A., Schrammel, B., Ohradanova-Repic, A., Stockinger, H., Sommer, R., Walochnik, J., Cervero-Aragó, S. (2018) Starved viable but non-culturable (VBNC) *Legionella* strains can infect and replicate in amoebae and human macrophages. *Water Res.*, **141**, 428-438.
- Douterelo, I., Boxall, J. B., Deines, P., Sekar, R., Fish, K. E., Biggs, C.A., (2014) Methodological approaches for studying the microbial ecology of drinking water distribution systems. *Water Res.*, **65**, 134-156.
- Douterelo, I., Jackson, M., Solomon, C., Boxall, J. (2016) Microbial analysis of in situ biofilm formation in drinking water distribution systems: implications for monitoring and control of drinking water quality. *Appl. Microbiol. Biotechnol.*, **100**, 3301-3311.
- Dusserre, E., Ginevra, C., Hallier-Soulier, S., Vandenesch, F., Festoc, G., Etienne, J., Jarraud, S., Molmeret, M. (2008) A PCR-based method for monitoring *Legionella pneumophila* in water samples detects viable but noncultivable legionellae that can recover their cultivability. *Appl. Environ. Microbiol.*, **74**, 4817-4824.
- El-Chakhtoura, J., Prest, E., Saikaly, P., van Loosdrecht, M., Hammes, F., Vrouwenvelder, H. (2015) Dynamics of bacterial communities before and after distribution in a full-scale drinking water network. *Water Res.*, **74**, 180-190.
- Falkinham, J., Pruden, A., Edwards, M. (2015) Opportunistic Premise Plumbing Pathogens: Increasingly Important Pathogens in Drinking Water. *Pathogens*, **4**, 373-386.
- Flannery, B., Gelling, L. B., Vugia, D. J., Weintraub, J. M., Salerno, J. J., Conroy, M. J., Stevens, V. A., Rose, C. E., Moore, M. R., Fields, B. S., Besser, R. E. (2006) Reducing *Legionella* colonization of water systems with monochloramine. *Emerg. Infect. Dis.* **12**, 588-596.
- Gyles, C., Boerlin, P. (2014) Horizontally Transferred Genetic Elements and Their Role in Pathogenesis of Bacterial Disease. *Vet. Pathol.*, **51**, 328-340.
- Huerta, B., Marti, E., Gros, M., López, P., Pompêo, M., Armengol, J., Barceló, D., Balcázar, J. L., Rodríguez-Mozaz, S., Marcé R. (2013) Exploring the links between antibiotic occurrence, antibiotic resistance, and bacterial communities in water supply reservoirs. *Sci Total Environ.*, **456-457**, 161-170.
- Khan, S., Beattie, T. K., Knapp, C. W. (2016) Relationship between antibiotic- and disinfectant-resistance profiles in bacteria harvested from tap water. *Chemosphere*, **152**, 132-141.
- Liu, L., Xing, X., Hu, C., Wang, H. (2019) One-year survey of opportunistic premise plumbing pathogens and free-living amoebae in the tap-water of one northern city of China. *J. Environ. Sci.*, **77**, 20-31.
- Moore, M. R., Fields, B., Lucas, C., Besser, R. E., Pryor, M., Phelan, M. (2006) Introduction of monochloramine into a municipal water system: Impact on colonization of buildings by *Legionella* spp. *Appl. Environ. Microbiol.*, **72**, 378-383.
- Párraga-Niño, N., Quero, S., Ventós-Alfonso, A., Uria, N., Castillo-Fernandez, O., Ezenarro, J. J., Muñoz, F. X., Garcia-Nuñez, M., Sabrià, M. (2018) New system for the detection of *Legionella pneumophila* in water samples. *Talanta*, **189**, 324-331.
- Paruch, A. M., Mæhlum, T. (2012) Specific Features of *Escherichia coli* that Distinguish it from Coliform and Thermotolerant Coliform Bacteria and Define it as the Most Accurate Indicator of Faecal Contamination in the Environment. *Ecological Indicators*, **23**, 140-142.
- Pereira, R. P. A., Peplies, J., Brettar, I., Höfle, M.G. (2017) Development of a genus-specific next generation sequencing approach for sensitive and quantitative determination of the *Legionella* microbiome in freshwater systems. *BMC Microbiol.*, **17**, 1-14.
- Pogorzelec, M., Piekarska, K. (2018) Application of semipermeable membrane devices for long-term monitoring of polycyclic aromatic hydrocarbons at various stages of drinking water treatment. *Sci. Total Environ.*, **631-632**, 1431-1439.

- Principe, L., Tomao, P., Visca, P. (2017) Legionellosis in the occupational setting. *Environ. Res.*, **152**, 485-495.
- Regulation of the Minister of Health of 7 December 2017 regarding the quality of water for human consumption.
- Rudi, K., Berg, F., Gaustad, E., Tannes, T., Vatn, M. (2010) Ratios between *Alpha*-, *Beta*- and *Gamma*-proteobacteria in tap water determined by the ProteoQuant assay. *Lett. Appl. Microbiol.*, **50**, 1-6.
- September, S. M., Els, F. A., Venter, S. N., Brozel, V.S. (2007) Prevalence of bacterial pathogens in biofilms of drinking water distribution systems. *J. Water Health.*, **5**(2), 219-227.
- Spies, K., Pleischl, S., Lange, B., Langer, B., Hübner, I., Jurzik, L., Luden, K., Exner, M. (2018) Comparison of the Legiolert™/Quanti-Tray® MPN test for the enumeration of *Legionella pneumophila* from potable water samples with the German regulatory requirements methods ISO 11731-2 and ISO 11731. *Int. J. Hyg. Environ. Health*, **221**, 1047-1053.
- Subba, P., Joshi, D. R., Bhatta, D. R. (2013) Antibiotic Resistance Pattern and Plasmid Profiling of Thermotolerant *Escherichia coli* Isolates in Drinking Water. *J. Nepal Health. Res. Council.*, **11**(23), 44-8.
- Szekeres, E., Chiriac, C. M., Baricz, A., Szóke-Nagy, T., Lung, I., Soran, M. L., Rudi, K., Dragos, N., Coman, C. (2018) Investigating antibiotics, antibiotic resistance genes, and microbial contaminants in groundwater in relation to the proximity of urban areas. *Environ. Pollut.*, **236**, 734-744.
- Talukdar, P. K., Rahman, M., Rahman, M., Nabi, A., Islam, Z., Hoque, M. M., Endtz, H. P., Islam, M. A. (2013) Antimicrobial Resistance, Virulence Factors and Genetic Diversity of *Escherichia coli* Isolates from Household Water Supply in Dhaka, Bangladesh. *PLoS One*, **8**, 1-8.
- Toplitsch, D., Platzer, S., Pfeifer, B., Hautz, J., Mascher, F., Kittinger, C. (2018) *Legionella* detection in environmental samples as an example for successful implementation of qPCR. *Water*, **10**.
- Vásquez-García, A., Oliveira, A. P. S. C. de, Mejia-Ballesteros, J. E., Godoy, S. H. S. de, Barbieri, E., Sousa, R. L. M. de, Fernandes, A. M. (2019) *Escherichia coli* detection and identification in shellfish from southeastern Brazil. *Aquaculture*, **504**, 158-163.
- Waak, M. B., LaPara, T. M., Hallé, C., Hozalski, R. M. (2018) Occurrence of *Legionella spp.* in Water-Main Biofilms from Two Drinking Water Distribution Systems. *Environ. Sci. Technol.* **52**, 7630-7639.
- Whiley, H., Keegan, A., Fallowfield, H., Bentham, R. (2014) Detection of *Legionella*, *L. pneumophila* and *Mycobacterium Avium* Complex (MAC) along potable water Distribution Pipelines. *Int. J. Environ. Res. Public Health*, **11**, 7393-7405.
- WHO (2017) Guidelines for Drinking-water Quality.
- WHO (2007) Legionella and the prevention of legionellosis.
- Wolf-Baca, M., Siedlecka, A. (2019) Detection of pathogenic bacteria in hot tap water using the qPCR method: preliminary research. *SN Appl. Sci.*, **1**, 840.
- Wong, S., Pabbaraju, K., Burk, V. F., Broukhanski, G. C., Fox, J., Louie, T., Mah, M. W., Bernard, K., Tilley, P. A. G. (2006) Use of sequence-based typing for investigation of a case of nosocomial legionellosis. *J. Med. Microbiol.*, **55**, 1707-1710.

## Pollution of Urban Groundwater by Emerging Contaminants in Kharkiv region, Ukraine

I. Yermakovych\* and Y. Vystavna\*\*

\* Department of Labor Protection and Technogenic-Ecological Safety, National University of Civil Defence of Ukraine, str. Chernyshevska 94, Kharkiv, Ukraine, 61023 (E-mail: [iryna.yermakovych@gmail.com](mailto:iryna.yermakovych@gmail.com))

\*\*Institute of Hydrobiology, Biology Centre AV CR Academy of Sciences of the Czech Republic, Na Sadkach 7, 37005, Ceske Budejovice, Czech Republic (E-mail: [yuliya.vystavna@hbu.cas.cz](mailto:yuliya.vystavna@hbu.cas.cz))

### Abstract

The article is presented the contamination data by emerging contaminants in a shallow urban groundwater and forest groundwater located in Kharkiv region, Ukraine. The emerging contaminants as mainly illicit drugs were used as trace anthropogenic recharge tool of groundwater. Elevated the presence of emerging pollutants in most of urban springs confirmed the mixing of urban groundwater with sewage leakages in some springs. The contribution of sewage leakages leads to the urban groundwater contamination by emerging compounds that increase the risk for environmental and human health reducing its potential as pure drinking water source.

### Keywords

Urban springs; pharmaceuticals; illicit drugs; emerging contaminants; groundwater

## INTRODUCTION

Nowadays, one of important source of drinking water worldwide is considered as groundwater (WWAP 2015). Especially, the part of groundwater as a primary drinking water source is growing due to the deterioration of surface water quality and quantity under influence of climate variability, contamination and re-allocation of surface run-off (FAO 2011, WWAP 2015). Groundwater as a source of drinking water might become more important even in those areas where it had not been used in the past. In virtue of following regulations (EU WFD 2000, Groundwater Directive 2006) surface water and groundwater quality has been improved in European Union (EU) (European Commission, 2012). Nevertheless, many countries that share the transboundary surface water and aquifers in Europe, for example Ukraine, still have a high concern on low quality and quantity of available groundwater resources due to ongoing and increasing pollutions and due to the lack of appropriate regulations (Vystavna, 2018a,b).

Contemporaneously, groundwater use for drinking supply is strongly dependent on seasonality of recharge conditions, meteorological events and contaminations (Quevauviller 2007; Griebler, 2010; Taylor 2012; Havril, 2018). Evaluation of contamination of urban aquifers can be complex tasks for groundwater management as the data on recharge, mixing and transformation of chemical compounds is generally difficult to obtain in a short-term period (Healy, 2010). Sometimes, these resources are not available for groundwater management, mainly in developing countries (WWAP, 2015). Organic compounds, particularly pharmaceuticals, have been used to determine the sewage contribution in groundwater (Jurado, 2012; Schaider, 2016; Yin, 2019) and water residence time (Lapworth, 2018). The presence of such compounds in ground waters is great concern because it's cause of serious public health risk (Samojlenko, 2014).

This study was performed in a highly urbanized area, the Kharkiv city, located in East Ukraine where local population intensively use groundwater as an alternative to tap water as a drinking source (Vystavna, 2017a). The area of research is also located in a zone with a risk of military

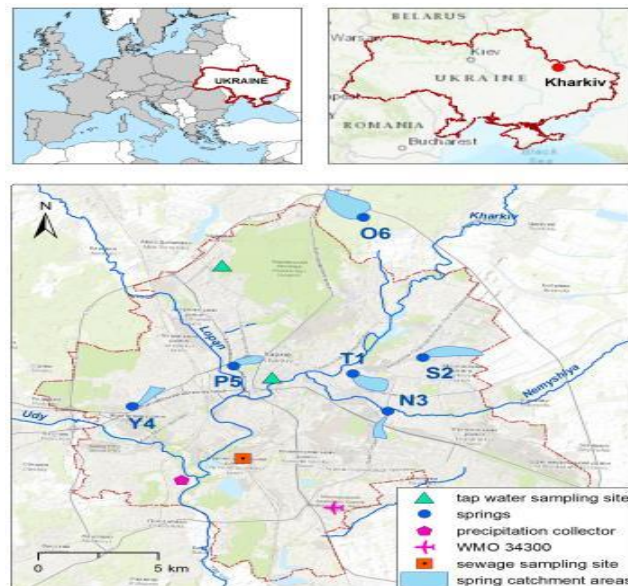


activity, where groundwater could be considered as an important strategic drinking water source. The proposed shallow aquifer was studied before to understand the general contamination status (Vystavna, 2017a; Vystavna, 2015), knowledge on water quality variation is highly limited that determines the direction of our research.

The aim of this research was to determine the estimation of groundwater contamination of urban areas by emerging contaminants. The objective of the study was: to trace and qualitatively determine of the mixing of groundwater with anthropogenic components such as sewage leakages.

### Research of catchments

Five urban (T1, S2, N3, Y4 and P5) and one peri-urban forest (O6) groundwater sites were selected for the purpose of this study (Figure 1).



**Figure 1.** The location of sampling area and sites

The maximum elevation at the spring outflows ranged from 113 to 123 m a.s.l. in the urban catchment to 140 m a.s.l. in the forested catchment. The most recent sediment layers (up to 120 m thick) are composed predominantly of permeable materials (sands and loams) of Quaternary, Neogene, and Paleogene origin, but with some spot inclusions of clay in upper layers. Springs are fed from fractured fine-grained sandstones and siltstones of the Eocene age. The depth to the aquifer is 2–36 m below the surface and the average hydraulic conductivity of the saturated zone is  $2 \times 10^{-4} \text{ m s}^{-1}$  (Vystavna, 2019).

The catchments of urban and forest are located in temperate continental climate conditions of Kharkiv region. The average annual precipitation is 521 mm, and the average annual air temperature is  $9.1^\circ\text{C}$  (the Kharkiv world meteorological station WMO ID 34300, 2005-2017).

Urban wastewaters are collected by sewer pipes (shallow and deep mains), treated by mechanical and biological processes in two wastewater treatment plants (WWTP) and discharged into Lopan and Udy Rivers. The WWTP ‘Dikanivka’ processes 80 % of urban wastewater ( $550,000 \text{ m}^3 \text{ d}^{-1}$ ). About 24 % of population has no connection to urban sewerage network and use pit latrines and septic tanks. Built during the Soviet period, to date, urban water and sewerage infrastructure of the Kharkiv city has deteriorated and causes numerous leakages (24 % of the total water supply) which cannot be eliminated in the short term (KP Voda 2017).



The forest spring (O6) catchment drains a forest-dominated landscape. The catchment is situated in a peri-urban area featuring no agricultural land use and rather negligible urbanization (residential buildings and roads account for less than 9 % of the total drained area).

## METHODS AND ANALYSIS

Groundwater samples (1L amber glass bottles) for analysis of emerging compounds were collected in September 2017. The screening of chemicals was based on an exact mass in an open access library (over 2000 compounds) by Liquid Chromatography Quadrupole Time-of-Flight Mass Spectrometry (LC-QTOF) (Thermo Fisher Scientific, San Jose, CA, USA) coupled to an Accela 1250 LC pump (Thermo Fisher Scientific) and an HTS XT-CTC autosampler (CTC Analytics AG, Zwingen, Switzerland), operated using Xcalibur software (Thermo Fisher Scientific, San Jose, CA, USA). A Hypersil gold aQ column (50 mm × 2.1 mm ID × 5 μm particles; Thermo Fisher Scientific) was used for the chromatographic separation. Purified water was prepared using a Milli-Q Advantage system, including an ultraviolet radiation source (Millipore, Billerica, USA). LC/MS grade Formic acid (Sigma-Aldrich, Steinheim, Germany) (at 0.1 %) and acetonitrile, methanol (Merck (Darmstadt, Germany) with 0.1 % (vol/vol) were used to prepare the mobile chromatographic phases. Samples were pretreated by solid phase extraction (SPE) with a pre-concentration factor of 500. Si-C18 and polymeric Strata X extraction cartridges (500 mg per 6 mL) were from Supelco (Bellefonte, PA, USA) and Phenomenex (Torrance, CA, USA), respectively. A PHM 240 Model pH-meter (Radiometer, Copenhagen, Denmark) with combined glass electrode was used for sample pH adjustment. The SPE extraction procedure was performed by modifying a validated method previously reported (Santos, 2005). Two sorbents (Si-C18 and Strata X) were used for this procedure. Spiked ultrapure water of 1000 mL (for the optimization step) or real filtered sample of 500–1000 mL (for the validation step) was transferred to the SPE cartridges through a Teflon tube at a flow rate of about 10 mL min<sup>-1</sup>, using a Supelco 12-port vacuum manifold system (Bellefonte, PA, USA) connected to a vacuum pump. Before elution, the cartridges were rinsed by 10 mL of methanol/water (5/95, v/v) followed by 10 mL of n-hexane applied to the top of the cartridge (Santos, 2005). Two different solvents (methanol and acetone) were tested as eluent phase at a flow rate of about 1 mL min<sup>-1</sup>. The elute was evaporated in a flask by a Rotavapor (Büchi, Flawil, Switzerland) to reach a final volume of few milliliters and then it was quantitatively transferred into a conical bottom glass vial. Finally, the solvent was evaporated under a gentle stream of nitrogen leaving only a small, concentrated quantity. The residue was reconstituted with 0.5 mL of acetonitrile/water (45/55, v/v) of which 50 μL was injected into the column. Because of the nature of the screening analysis, exact concentrations could not be determined.

## RESULTS

The identified chemicals have been divided into three principal groups: drugs (D) (caffeine, nikethamide, riluzole, phenazone, pilocarpine, pergolide, ajmaline, carbamazepine, moxonidine, dihydrocodeine, sulfathiazole, papaverine, pentedrone and aripiprazole), pesticides (P) (dodine, chlordimeform, atrazine, simazine and butraline), and food compounds (FC) (chanoclavine, kojic acid as an additive and alternariol as a mycotoxin). The details are presented in Table 1.

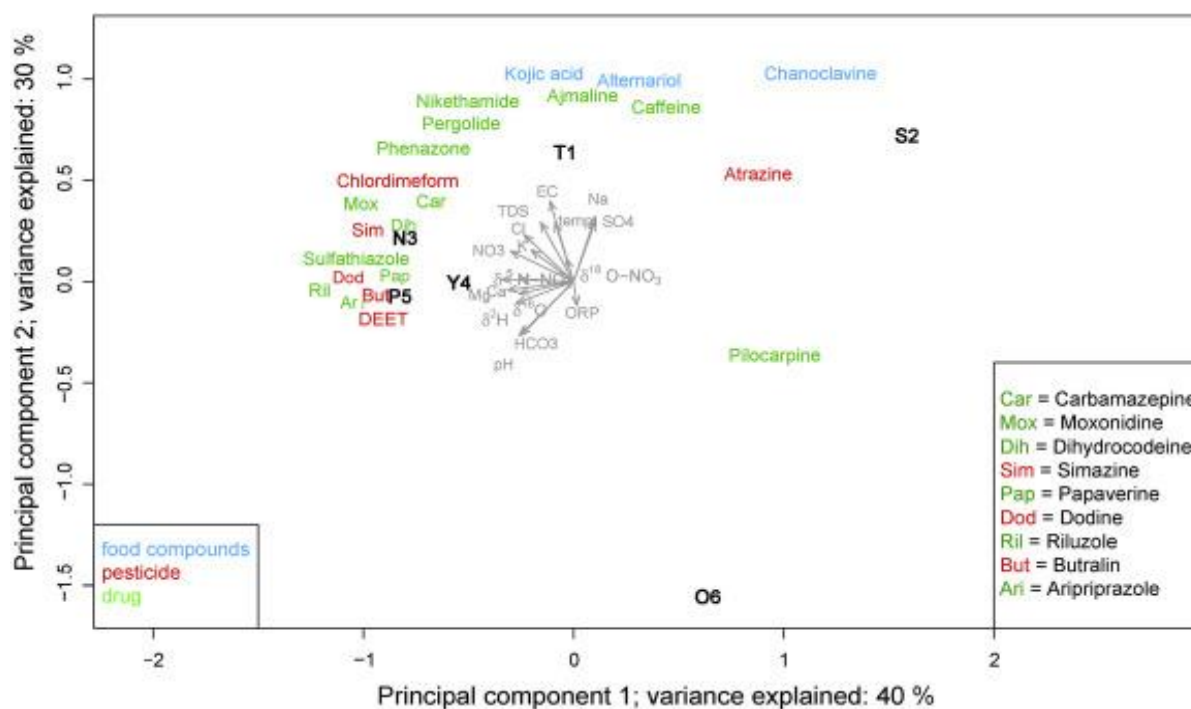
**Table 1.** Detection, physico-chemical properties of emerging compounds in groundwater

Compound	T1	S2	N3	Y4	P5	O6	Log K <sub>ow</sub>	Group	Application
Caffeine	+	+	-	-	+	-	-0.07	D	stimulant, food additive
Dodine	-	-	-	+	-	-	1.15	P	fungicide, applied for the plant protection
Nikethamide	+	-	-	+	-	-	0.33	D	stimulant, illicit drug
Riluzole	-	-	-	+	-	-	2.3	D	antidepressant, anti-convulsion
Chanoclavine	+	+	+	-	+	-	2.14	FC	tricyclic ergot alkaloid (ergoline)
Phenazone	+	-	+	+	-	-	0.38	D	analgesic, nonsteroidal anti-inflammatory, antipyretic
Alternariol	+	+	+	-	-	-	2.37	FC	mycotoxin as secondary metabolites produced by filamentous fungi in crops or during storage, transport and processing of food and feed commodities
Pilocarpine	+	+	-	+	+	+	1.1	D	alkaloid, to treat increased pressure inside the eye and dry mouth
Pergolide	+	-	-	+	-	-	4	D	ergoline-based dopamine receptor agonist used for treatment of Parkinson's disease
Ajmaline	+	-	-	-	-	-	1.81	D	alkaloid, antiarrhythmic agent
Chlordimeform	+	-	+	+	+	-	2.89	P	acaricide active mainly against motile forms of mites and ticks, banned by UN Rotterdam Convention 1998
Kojic acid	+	-	-	-	-	-	0.64	FC	additive, used in food and cosmetics to preserve or change colours of substances
Atrazine	-	+	-	-	-	-	2.61	P	herbicide, banned by EU Directive 91/414/CEE
Carbamazepine	-	-	+	-	-	-	2.45	D	antidepressant
Simazine	-	-	+	-	-	-	2.18	P	Herbicide of the triazine class, banned in EU (EU Directive 91/414/CEE)
Moxonidine	-	-	+	-	-	-	n.f.	D	new-generation centrally acting antihypertensive drug licensed for treatment of mild to moderate essential hypertension
Dihydrocodeine	-	-	+	-	-	-	0.6	D	semi-synthetic opioid analgesic prescribed for pain or severe dyspnoea, or as an antitussive
Sulfathiazole	-	-	-	+	-	-	0.05	D	organosulfur compound used as a short-acting sulfa drug
Butralin	-	-	-	+	+	-	4.93	P	herbicide, mainly applied as a plant-growth regulator on tobacco fields, banned by EU Directive 91/414/CEE
Papaverine	-	-	-	+	-	-	2.95	D	opiate alkaloid isolated from plant <i>Papaver somniferum</i> and produced synthetically, illicit drug
DEET (Pentadrone)	-	-	-	-	+	-	n.f.	D	stimulant of cathinone class that has been sold as designer drug,
Aripiprazole	-	-	-	-	+	-	5.3	D	antipsychotic, primarily used in the treatment of schizophrenia and bipolar disorder

+/- means detected/not detected in the groundwater site; n.f.-not found

All detected drugs in this study could be the results of abuse and some are illicit drugs usage. The most frequently detected drug (in 5 out of 6 springs) was the alkaloid pilocarpine (prescribed to treat increased pressure inside the eye and dry mouth) which was found even in the forest spring. The food compound chanoclavine and the pesticide chlordimeform were detected in 4 out of 6

studied springs. Caffeine, the analgesic phenazone and the mycotoxin alternariol were found in 3 out of 6 studied springs. Other compounds were found in 1 or 2 sites. However, each spring was characterized by a distinct group of detected compounds according to the principal component analysis (PCA) ordination (Figure 2) (Vystavna et al., 2019).



**Figure 2.** Principal component analysis (PCA) plots of presence of emerging compounds in groundwater samples (Vystavna, 2019) (average of all measurements over the whole sampling period)

Measured characteristics are labeled in grey. In violet: fitted correlation (Oksanen, 2018) of the presence/ absence of a number of household/agricultural chemicals and pharmaceuticals. The first two axes are plotted; their cumulative proportion of explained variance amounted to 0.75.

Site T1 was most correlated with the alkaloid ajmaline, the stimulant caffeine and two food compounds that tended towards the positive y axis and correlated well with  $\text{Na}^+$  and  $\text{SO}_4^{2-}$ . Site S2 was most correlated with the pesticide atrazine. N3, Y4 and P5 were most correlated with drugs such as papaverine, dihydrocodeine and carbamazepine. N3 was also correlated with pesticide simazine. Four pesticides tended towards negative x, and one pesticide, atrazine, along the positive x axis (Figure 2).

## DISCUSSIONS

The impact of anthropogenic land use was reflected by the presence of drugs, pesticides and food compounds in urban springs (Figure 2). The highest diversity of drugs and food compounds was found in springs with the high sewage contribution (T1, N3, Y4 and P5). The relation between the non persistent chemicals caffeine, food compounds indicates that these emerging compounds continuously enter T1 with raw sewage likely from mains. However, the presence the persistent drugs at N3, Y4 and P5 may point to sewage leakages from pit latrines. Some persistent pesticides and food compounds were detected at sites with negligible sewage contribution (urban S2 and forest O6).

## CONCLUSIONS

This research is showed that urbanization changes sources and recharges of urban groundwater composition and their pollutions. It has significant influence even on peri-urban springs. Such kind of monitoring is therefore important for contamination status for controlling the shaping water quality and thus the usability as a drinking water resource. High contamination of urban springs with potentially toxic emerging compounds indicated the health risk associated with the use of urban spring as drinking water sources.

## REFERENCES

- City Council (2010) The declaration of the Kharkiv City Council No. 321 from 8.09.2010 on the discharge of raw wastewater in the municipal sewage system.
- European Commission (2012) A Blueprint to Safeguard Europe's Water Resources. Communication from the commission to the European parliament, the Council, the European economic and social committee and the committee of the regions. COM(2012) 673 final. SWD(2012) 381 final and SWD(2012) 382 final. Brussels, Belgium.
- Groundwater Directive (2006) European Commission, 2006 COM(2003)550.
- EU-WFD (2000) Directive 2000/60/EC of the European Parliament and of the Council of the 23 October 2000: establishing framework for the community action in the field of water policy. *Official J. European Comm.*, L327, 321-371.
- FAO (2011) The state of the world's land and water resources for food and agriculture (SOLAW) – Managing systems at risk. Food and Agriculture Organization of the United Nations, Rome and Earthscan, London.
- Griebler, C., Stein, H., Kellermann, C., Berkhoff, S., Brielmann, H., Schmidt, S., Selesi, D., Steube, C., Fuchs, A., Hahn, H. J. (2010) Ecological assessment of groundwater ecosystems - Vision or illusion? *Ecological Engineering*, **36**, 1174-1190.
- Havril, T., Tóth, Á., Molson, J. W., Galsa, A., Mádl-Szőnyi, J. (2018) Impacts of predicted climate change on groundwater flow systems: Can wetlands disappear due to recharge reduction? *Journal of Hydrology*, **563**, 1169-1180.
- Healy, R. W., Scanlon, B. R. (2010) Estimating Groundwater Recharge. Cambridge University Press, Cambridge, New York.
- Jurado, A., Vazquez-Sune, E., Carrera, J., Lopez de Alda, M., Pujades, E., Barcelo, D. (2012) Emerging organic contaminants in groundwater in Spain: a review of sources, recent occurrence and fate in a Europe context. *Science of the Total Environment*, **440**, 82-94.
- Lapworth, D. J., Das, P., Shaw, A., Mukherjee, A., Civil, W., Petersen, J. O., Gooddy, D. C., Wakefield, O., Finlayson, A., Krishan, G., Sengupta, P., MacDonald, A. M. (2018) Deep urban groundwater vulnerability in India revealed through the use of emerging organic contaminants and residence time tracers. *Environmental Pollution*, **240**, 938-949.
- Oksanen, F., Blanchet, F. G., Friendly, M., Kindt, R., Legendre, P., McGlinn, D., Minchin, P. R., O'Hara, R. B., Simpson, G. L., Solymos, P., Stevens, M. H. H., Szoecs, E., Wagner, H. (2018) vegan: Community Ecology Package. R package version 2.5-2. [online] <https://CRAN.R-project.org/package=vegan>.
- Quevauviller, P. (2007) General introduction: the need to protect groundwater. In: Groundwater Science and Policy - An International Overview (ed. Quevauviller P). *RSC Publishing*, 3-18.
- Samojlenko, N.N., Ermakovich, I.A. (2014) Effect of pharmaceuticals and their derivatives on the environment. *Water and Ecology: Problems and Solutions*, **2**, 78-87.
- Santos, J. L., Aparicio, I., Alonso, E., Callejón, M. (2005) Simultaneous determination of pharmaceutically active compounds in wastewater samples by solid phase extraction and high-

- performance liquid chromatography with diode array and fluorescence detectors. *Analitica Chimica Acta*, **550**, 116-122.
- Schaider, L. A., Ackerman, J. M., Rudel, R. A. (2016) Septic systems as sources of organic wastewater compounds in domestic drinking water wells in a shallow sand and gravel aquifer. *Science of the Total Environment*, **547**, 470-481.
- Taylor, R. G., Scanlon, B., Döll, P., Rodell, M., van Beek, R., Wada, Y., Longuevergne, L., Leblanc, M., Famiglietti, J. S., Edmunds, M., Konikow, L., Green, T. R., Chen, J., Taniguchi, M., Bierkens, M. F. P., MacDonald, A., Fan, Y., Maxwell, R. M., Yechieli, Y., Gurdak, J. J., Allen, D. M., Shamsudduha, M., Hiscock, K., Yeh, P. J.-F., Holman, I., Treidel, H. (2012) *Ground water and climate change. Nature Climate Change*, **3**, 322–329.
- WWAP (2015) United Nations World Water Assessment Programme. The United Nations World Water Development Report 2015: Water for a Sustainable World. Paris, UNESCO. [online] [https://www.unigrac.org/sites/default/files/resources/files/Groundwater%20overview%20-%20Making%20the%20invisible%20visible\\_Print.pdf](https://www.unigrac.org/sites/default/files/resources/files/Groundwater%20overview%20-%20Making%20the%20invisible%20visible_Print.pdf).
- Yin, H., Xie, M., Zhang, L., Huang, J., Xu, Z., Li, H., Jiang, R., Wang, R., Zeng, X. (2019) Identification of sewage markers to indicate sources of contamination: Low cost options for misconnected non-storm water source tracking in storm water systems. *Science of the Total Environment*, **648**, 125-134.
- Vystavna, Y., Diadin, D., Yakovlev, V., Hejzlar, J., Vadillo, I., Huneau, F., Lehmann, M. F. (2017a) Nitrate contamination in a shallow urban aquifer in East Ukraine: Evidence from hydrochemical, stable nitrate isotope, and land use analysis. *Environmental Earth Sciences*, **76**(13), 463.
- Vystavna, Y., Diadin, D., Grynenko, V., Yakovlev, V., Vergeles, Y., Huneau, F., Rossi, P., Hejzlar, J., Knöller, K. (2017b) Determination of dominant sources of nitrate contamination in transboundary (Russia/Ukraine) catchment with heterogeneous land use. *Environmental Monitoring and Assessment*, **189**, 509.
- Vystavna, Y., Cherkashyna, M., van der Valk, M. R. (2018a) Water laws of Georgia, Moldova and Ukraine: current problems and integration with the EU legislation. *Water International*, **43**(3), 424-435.
- Vystavna, Y., Frkova, Z., Celle-Jeanton, H., Diadin, D., Huneau, F., Steinmann, M., Crini, N., Loup, C. (2018b) Priority substances and emerging pollutants in urban rivers in Ukraine: Occurrence, fluxes and loading to transboundary European Union watersheds. *Science of the Total Environment*, **637-638C**, 1358-1362.
- Vystavna, Y., Schmidt, S., Diadin, D., Rossi, P., Vergeles, Y., Erostate, M., Yermakovich, I., Yakovlev, V., Knöller, K., Vadillo, I. (2019). Multi-tracing of recharge seasonality and contamination in urban groundwater. *Water Research*, **161**, 413-422.

# Comparison of Different Adsorption Materials for Pentavalent Arsenic Removal from Drinking Water

R. Zakhar\*, I. Zembjaková\*, I. C. Villaverde\*\*, F. Čacho\*\*\*, J. Derco\* and P. Hudec\*\*\*\*

\* Department of Environmental Engineering, Faculty of Chemical and Food Technology, Slovak University of Technology, Radlinského 9, Bratislava 812 37, Slovakia (E-mails: [ronald.zakhar@stuba.sk](mailto:ronald.zakhar@stuba.sk); [jan.derco@stuba.sk](mailto:jan.derco@stuba.sk); [xzembjakovai@stuba.sk](mailto:xzembjakovai@stuba.sk))

\*\* Department of Industrial Chemistry and Environmental Engineering, Higher Technical School of Industrial Engineering (ETSII), Polytechnic University of Madrid (UPM), C/ José Gutiérrez Abascal n° 2, Madrid, 28006, Spain (E-mail: [irene.casado.villaverde@alumnos.upm.es](mailto:irene.casado.villaverde@alumnos.upm.es))

\*\*\* Institute of Analytical Chemistry, Faculty of Chemical and Food Technology, Slovak University of Technology, Radlinského 9, Bratislava 812 37, Slovakia (E-mail: [frantisek.cacho@stuba.sk](mailto:frantisek.cacho@stuba.sk))

\*\*\*\* Department of Organic Technology, Catalysis and Petroleum Chemistry, Faculty of Chemical and Food Technology, Slovak University of Technology, Radlinského 9, Bratislava 812 37, Slovakia (E-mail: [pavol.hudec@stuba.sk](mailto:pavol.hudec@stuba.sk))

## Abstract

In the present study, the possibility of using six granular commercial adsorbents (activated carbon–GAC, zeolite–ZEO, iron coated zeolite–ICZEO, ferric oxide–FeO, ferric hydroxide–FeOH and ferric oxide-hydroxide–FEOOH) for pentavalent arsenic removal from drinking water was investigated by batch adsorption studies. For each adsorbent the adsorption capacity was determined and mutually compared. The best adsorption performance had FeO adsorbent, which reached adsorption capacity 493.0 µg/g and adsorption efficiency 98.6 %. In order to improve adsorption capacity of fresh GAC and ZEO it was modified with iron for four consecutive times in a multi-step process. The final total iron content of the iron-modified GAC (IMGAC) was 11.29 % and the iron-modified ZEO (IMZEO) was 9.13 %. In order to assess the total iron stability in the IMGAC and IMZEO, a desorption test with distilled water was conducted. From the results it can be said that both materials were stable and the amount of total iron lost during desorption in distilled water was negligible. From GAC, ZEO, IMGAC and IMZEO materials comparison was investigated that the most effective sorption material for As(V) adsorption was IMGAC, which reached 450.4 µg/g adsorption capacity and 90.08 % adsorption efficiency in the first 30 minutes of the adsorption process. Iron modification process caused increasing adsorption capacity of the iron-modified materials. In addition, the As(V) removal by prepared IMGAC material was approximately three times faster than by the best commercial FeO material in the first 30 minutes of contact time.

## Keywords

Arsenic; adsorption; drinking water; efficiency; modification

## INTRODUCTION

Arsenic (As) is the twentieth most abundant chemical element in Earth's crust. It can be found widely distributed in environment through air, water and ground. The main source of arsenic in drinking water is the dissolution of minerals and ores from natural origin (Singh, 2015). It is toxic and carcinogenic and nowadays the arsenic occurrence is responsible for many diseases, where it occurs in drinking water. Its exposure to low or high concentrations can be fatal to human health (van Halem, 2009). Arsenic contamination is a widespread and serious problem all over the world. Arsenic has been catalogued as one of the World Health Organization's (WHO) 10 chemical substances of greatest public health concern. Strong epidemiological evidence of arsenic carcinogenicity and genotoxicity has forced the WHO to lower the Maximum Contaminant Level (MCL) in drinking water to 10 µg/l from earlier limit of 50 µg/l in 1993 (Pal, 2015). Arsenic occurs naturally in water usually in the forms of the soluble arsenic species As(III) (arsenite) and As(V)

(arsenate). Adsorption has been universally accepted as one of the most effective arsenic removal process because of its easy operation and handling, low cost, low consumption of reagents and does not produce sludge and harmful by-products (Zhu, 2013). In the present study, the possibility of using six granular commercial adsorbents (activated carbon-GAC, zeolite-ZEO, iron coated zeolite-ICZEO, ferric oxide-FeO, ferric hydroxide-FeOH and ferric oxide-hydroxide-FeOOH) and two non-commercial granular adsorbents (iron-modified activated carbon-IMGAC and iron-modified zeolite-IMZEO) for pentavalent arsenic removal from drinking water was investigated by batch adsorption studies. For each adsorbent the adsorption capacity was determined and mutually compared. In addition, for non-commercial iron-impregnated adsorbents the total iron content and its stability were evaluated.

## **MATERIALS AND METHODS**

### **Reagents**

All used chemicals were of analytical laboratory grade, being purchased from Merck. As(V) stock solution was prepared by dissolving an accurately weighed amount of sodium arsenate heptahydrate ( $\text{Na}_2\text{HAsO}_4 \cdot 7\text{H}_2\text{O}$ ) in distilled water to achieve a concentration of 1 g/L and subsequently diluted to the required concentrations. The iron stock solution (0.5 M) for the iron modification was prepared by diluting of iron sulfate heptahydrate ( $\text{FeSO}_4 \cdot 7\text{H}_2\text{O}$ ) in distilled water. Concentrated HCl was used for samples storage and for acid extraction. All glass and plasticware were cleaned and rinsed with distilled water before use.

### **Analytical determination**

Estimation of As(V) in the samples was done by flow-through chronopotentiometry using triple-electrode flow-through measuring cell (type 353c), with work electrode (type E-T/Au), platinum auxiliary electrode and argentochloride reference electrode. Calibration test was carried out with a freshly prepared As(V) standard before analysis of the samples, which were analysed more than once (Beinrohr, 2010). The total iron concentration in the filtrate was analysed using the phenanthroline spectrometric method, according to ISO 6332:1988 (Horáková, 2003). Specific surface of adsorbent was determined by BET method, by measuring the nitrogen ( $\text{N}_2$ ) adsorption-desorption isotherms, as follows in the ISO 9277:2010 standard. Specific volume of micropores and mesopores was calculated by the t-plot method.

### **Instruments**

To measure pH a digital pH meter Jenway 3510 (Cole-Parmer, United Kingdom), with a measuring uncertainty of  $\pm 0.003$  pH units, was used. Materials were weighted using a high precision electrical balance ABS 220-4 (Kern & Sohn GmbH, Germany). Shaking experiments were conducted in an orbital shaker RSLAB-7PRO (Kvant s.r.o., Slovakia), RPM and time controlled. For quantitative determination of arsenic in solution was used a PC controlled automatic laboratory analyser EcaFlow Model 150 GLP (Istran s.r.o, Slovakia). Samples were warmed up in a heating plate Jenway® 1100 (Cole-Parmer, United Kingdom). The adsorption materials were dried in laboratory oven Venticell (MMM Medcenter GmbH, Germany). For iron content measurement was used a UV-visible spectrophotometer Jenway® 7305 (Cole-Parmer, United Kingdom). For adsorbent materials specific surface and porosity measurement the device ASAP® 2420 Accelerated Surface Area and Porosimetry System (Micromeritics Instrument Corp., USA) was used.

### **Characterization and preparation of adsorbents**

The six commercial adsorbents were used without further purification. It was just rinsed with distilled water to remove dirties and then oven-dried at 105 °C for 24 h. The granular activated carbon (GAC) was obtained from Eurowater s.r.o. (Slovakia), the granular zeolite (ZEO) and iron

coated zeolite (ICZEO) were obtained from Zeocem a.s. (Slovakia), the granular ferric oxide (FeO) was obtained from Severn Trent (United Kingdom), granular ferric hydroxide (FeOH) was obtained from GEH-Wasserchemie GmbH (Germany) and ferric oxide-hydroxide (FeOOH) from Kemira (Finland). The physical properties of these commercial adsorbents are shown in Table 1.

**Table 1.** Physical properties of commercial adsorbents

	GAC	ZEO	ICZEO	FeO	FeOH	FeOOH
Chemical composition	90 % carbon	hydrated aluminosilicate (HA)	HA 0.68 % Fe	> 70 % Fe <sub>2</sub> O <sub>3</sub>	> 57 % Fe(OH) <sub>3</sub>	> 50 % FeOOH
Color	Black	gray green	slightly brown	amber brown	dark brown	brown red
Particle size (mm)	0.8–1.0	1.6–2.0	1.0–2.5	0.5–2.0	0.2–2.0	0.85–2.0
Bulk density (g/cm <sup>3</sup> )	0.46	0.9	–	0.4–0.6	1.15–1.29	1.2
Specific surface area (m <sup>2</sup> /g)	950	30–60	30.9	200	250–300	120
Applicable for water pH range	5–8	6.8–7.2	6.8–7.2	6–10	5.5–9.0	6.5–7.5

Separately 30 g of GAC and ZEO were added in two different Erlenmeyer flasks. Both materials reacted at room temperature with 0.25 L of the 0.5 M iron stock solution for 24 h in the orbital shaker (set at 250 rpm) in order to achieve completely penetration of the iron(II) content in the solution in the surface and pores of the materials. During this time, the solution was covered to prevent ferrous oxidation and precipitation. After 24 h, the materials were separated from the solution by gravity filtration and air dried, so the ferrous was oxidised to ferric getting a less soluble iron form. To reach high amount of iron in the material the modification procedure was carried out until the iron content from one modification to the other was kept constant. These modified materials were called like iron-modified activated carbon (IMGAC) and iron-modified zeolite (IMZEO). The properties and parameters determined of these modified materials were: specific surface ( $S_{\text{BET}}$ ), specific volume of micropores ( $V_{\text{micro}}$ ) and specific surface area of mesopores and external surface ( $S_{\text{t}}$ ).

### Procedure of the total iron content determination

For this study acid extraction was selected for total iron content determination in the iron-modified GAC and ZEO. 0.5 g of the impregnated material was mixed with 0.03 L of 1:1 HCl aqueous solution in a 0.1 L flask and placed in the orbital shaker set at 250 rpm for 24 h. Thereafter, the flask was positioned in a hot water bath at 70–80 °C for 4 hours and then the solution was separated from the solid by gravity filtration. It was done with IMGAC and IMZEO materials after each modification. After the iron desorption, the iron content in the filtrate was studied with phenanthroline spectrometric method. The content of total iron was calculated as a percentage, Fe (%), using the following equation:

$$Fe = \frac{c_{\text{Fe}}}{c_{\text{Fe}} + c_{\text{material}}} \times 100, \quad (1)$$

where  $c_{\text{Fe}}$  is the total concentration of iron in sample (g/L) and  $c_{\text{material}}$  is the concentration of the adsorbent material in the initial sample (g/L).



### Procedure of the iron stability determination

The desorption test was conducted to assess the iron stability in the material. It was done for IMGAC and IMZEO by using two different 0.25 L Erlenmeyer flasks. To them were added 0.5 g of each material and 0.1 L of distilled water. After 24 h shaking in the orbital shaker the two samples were filtered by gravity and oven-dried for further analysis. The filtrate (distilled water with iron dissolved on it) was also kept to analyse and measure iron content following the same calculation according to equation (1).

### Adsorption studies

Adsorption experiments were carried out by batch method in orbital shaker (set at 150 rpm) at room temperature ( $20 \pm 2$  °C). The time dependent behavior of arsenic adsorption was studied by varying the contact time between the adsorbate and adsorbent in the range 0–180 min. The 0.1 L solution of As(V) was taken in each Erlenmeyer flask of volume 0.20 L separately. The initial concentration of arsenic was kept at 1000 µg/L, while the dose of each adsorbent was 0.2 g. The adsorption capacity of adsorbents,  $q_t$  (µg/g), was calculated using the following equation:

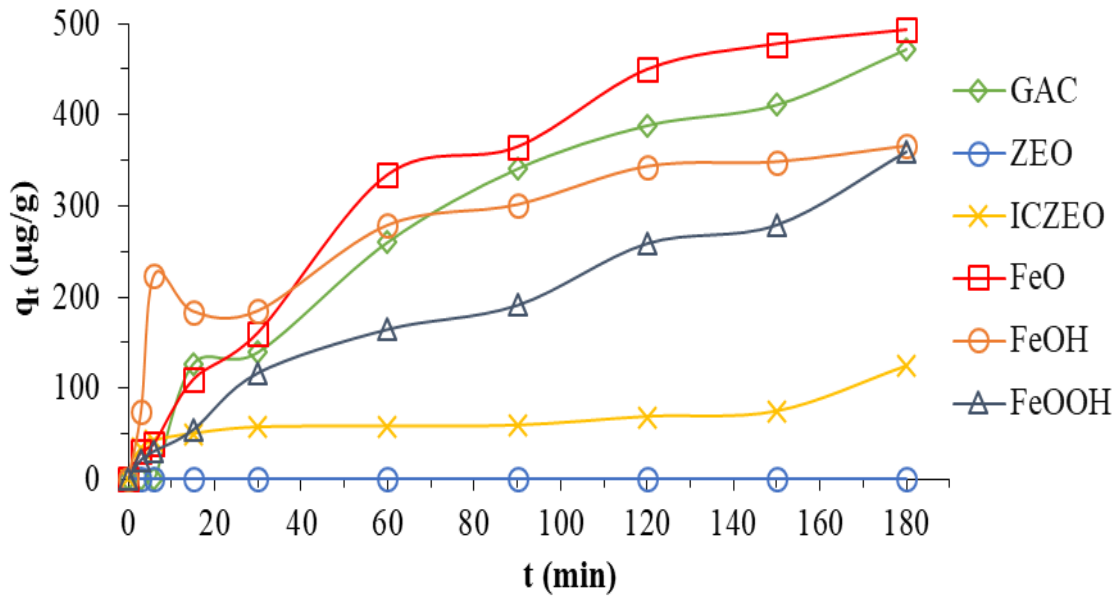
$$q_t = \frac{c_i - c_t}{M} \times V, \quad (2)$$

where  $c_i$  and  $c_t$  are the initial and final As(V) concentration in the solution,  $V$  is the volume of solution (L) and  $M$  is the mass of the used adsorbent (g). The percent value of adsorption efficiency by the adsorbents, AE (%), was computed by using the following equation:

$$AE = \frac{c_i - c_t}{c_i} \times 100. \quad (3)$$

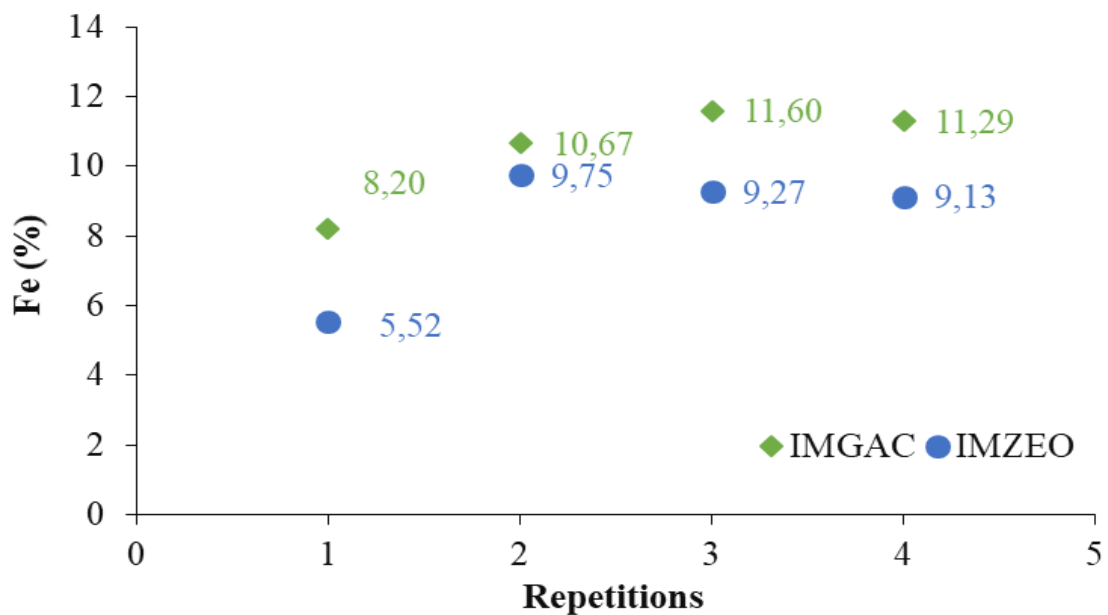
## RESULTS AND DISCUSSION

As can be seen in Figure 1, the adsorption capacity  $q_t$  (µg/g) calculated with the experimental data using the equation (2) of GAC, FEO and FeOH quickly increased in the first 15 minutes and then continued to increase significantly until 60 minutes. Finally, it increased at a comparatively minor rate until 120–130 minutes. By comparison,  $q_t$  (µg/g) of FeOOH and ICZEO increased more slowly. However, FeOOH continued reaching high adsorption capacity and ICZEO remained at a low and constant capacity until the end of the experiment. The used ZEO did not adsorb anything from the As(V) in the sample, giving a result of zero adsorption capacity at all times. Thus, the adsorbents that reached higher  $q_t$  were GAC and FeO. Nevertheless, the FeO adsorption capacity and adsorption efficiency at the end of the experiment was 493.0 µg/g and 98.6 %, which is 4.26 % higher than capacity of GAC and it means, that FeO had the best adsorption performance. For FeO, was observed that adsorption process was a rapid for the first 60 minutes, which could be explained by the great amount of active sites available on the surface of the material at the beginning of the experiment. Then it continued in minor rate until 120 minutes, and thereafter the change in adsorption capacity was negligible, so it can be said that equilibrium was reached.



**Figure 1.** Effect of contact time on the adsorption capacity of commercial adsorption materials

In order to improve adsorption capacity of adsorbent materials, fresh GAC and ZEO were modified with iron for four consecutive times in a multi-step process, trying to reach high amount of iron content in the material. From Figure 2 it is observed that the iron content Fe (%) increased in the first three repetition. As can be seen, after the first modification the iron content for IMGAC and IMZEO was 8.20 % and 5.52 %, respectively. Iron content increased with the second repetition, approximately in a linear way and reached values 10.67 % for IMGAC and 9.75 % for IMZEO. However, in the last repetitions (3rd and 4th), the iron content from the 3th and 4th modification was almost constant, so the modification process was stopped at the 4th modification. Thus, the final total iron content of the modified materials was 11.29 % for IMGAC and 9.13 % for IMZEO.



**Figure 2.** Total iron content during the modification process of GAC and ZEO

In order to assess the total iron stability in the IMGAC and IMZEO, a desorption test with distilled water was conducted. The total iron present in the solution after the desorption was analysed and the results are shown in Table 2. From the results it can be said that both materials were stable and the amount of total iron lost during desorption in distilled water was negligible. It means that impregnated materials are stable in water and the concentration of iron in the treated water would be small after the adsorption process, so it would not be necessary a further treatment to remove iron.

**Table 2.** Percentage of desorbed total iron from IMGAC and IMZEO

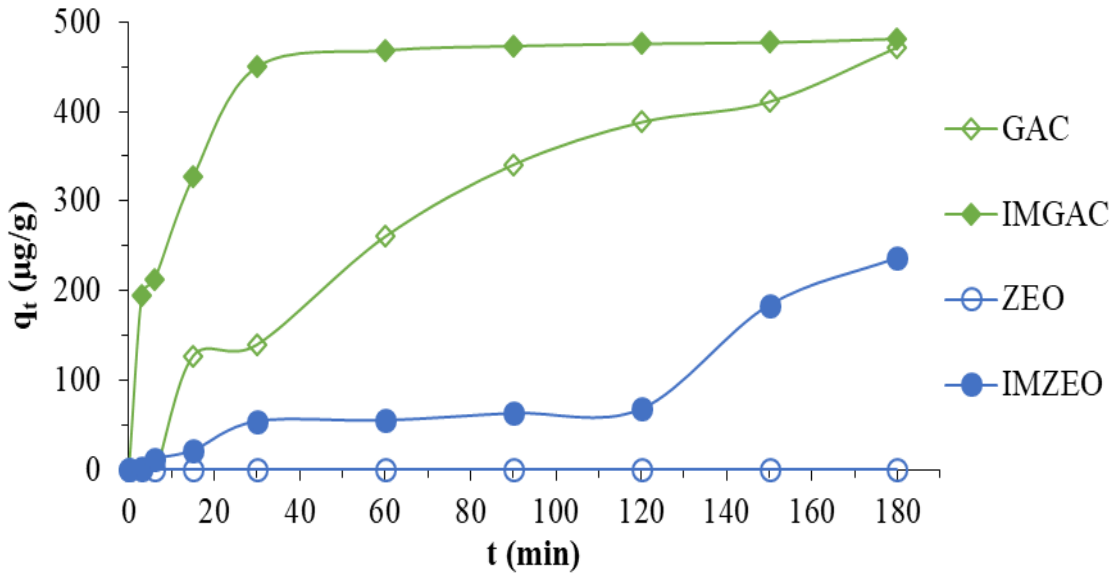
Material	Desorbed iron (%)
IMGAC	0.33
IMZEO	0.30

Different properties such as specific surface ( $S_{BET}$ ), specific volume of micropores ( $V_{micro}$ ) and specific surface area of mesopores and external surface ( $S_t$ ) were determined. These parameters were obtained for fresh GAC, fresh ZEO, IMGAC and IMZEO. According to the values summarized in Table 3, it can be stated that, as expected, GAC had greater specific surface area than ZEO. High specific surface area means that there is more possible area of contact between the material and the adsorbate, and thus better or faster adsorption. From the two different GAC forms, fresh GAC presented the highest values. In the case of the two different ZEO forms, there were no significant differences between ZEO and IMZEO. However, with these results it was not possible to draw an exact conclusion about the properties of the materials used and their relationship with the adsorption capacity of each one, since other characteristics, such as the size, type and shape of the material particles and the species of iron present in each material, also interfere.

**Table 3.** Values of specific surface ( $S_{BET}$ ), specific volume of micropores ( $V_{micro}$ ) and specific surface area of mesopores and external surface ( $S_t$ ) for the different studied adsorbent materials

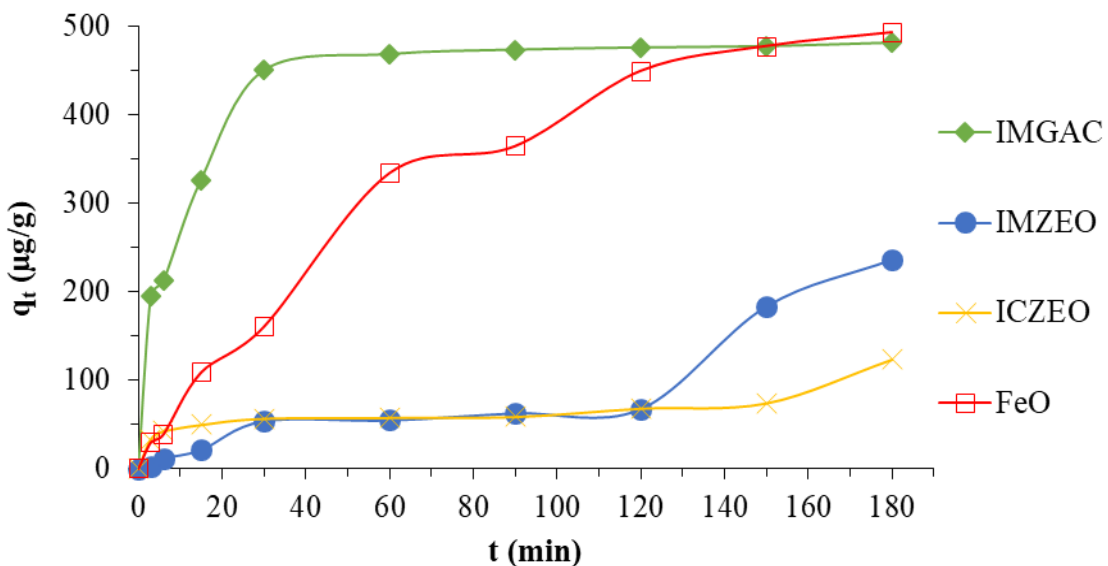
Material	$S_{BET}$ (m <sup>2</sup> /g)	$V_{micro}$ (cm <sup>3</sup> /g)	$S_t$ (m <sup>2</sup> /g)
GAC	743	0.237	292
IMGAC	502	0.162	194
ZEO	30.2	0.000	29.1
IMZEO	25.1	0.002	22.0

Figure 3 illustrated results of adsorption study for the four different adsorbent materials – GAC, IMGAC, ZEO and IMZEO. As can be noted from Figure 3, the most effective sorption material for As(V) adsorption was IMGAC, which achieved 450.4 µg/g adsorption capacity and 90.08 % adsorption efficiency in the first 30 minutes of the adsorption process. After this time, capacity increased minimally until the end of the experiment and achieved 481.7 µg/g (96.33 % efficiency) in 180 minutes. Fresh GAC capacity increased over time at a comparatively minor rate, getting 471.7 µg/g (94.34 % efficiency) at the end of the experiment. As expected, iron modification process caused increasing adsorption capacity of the GAC adsorbent material. The IMZEO material reached 236.5 µg/g capacity (47.30 % efficiency) in 180 minutes, which is a half value in comparison with the IMGAC. Fresh ZEO did not removed any arsenic from the sample, resulting in null adsorption capacity. As expected, iron modification process also improved ZEO adsorption capacity.



**Figure 3.** Adsorption of As(V) by GAC, IMGAC, ZEO and IMZEO (As(V) initial concentration: 1000 µg/l; contact time: 180 min; adsorbent dose: 0.2 g; pH: neutral; temperature: 20±2 °C; agitation speed: 150 rpm)

Figure 4 compares the adsorption capacity of the most efficient commercial material – granular ferric oxide (FeO) – with iron-modified GAC (IMGAC) and the commercial iron-coated ZEO (ICZEO) with iron-modified ZEO (IMZEO). From the achieved results, it is observed that the IMGAC reached in the first 30 minutes of contact time 450.4 µg/g capacity and 90.08 % efficiency while the commercial FeO in the same contact time reached only 160.5 µg/g capacity and 32.1 % efficiency. So, it can be stated that the As(V) removal by prepared IMGAC material is approximately three times faster than by commercial FeO. The prepared IMZEO material in comparison with commercial ICZEO reached the same adsorption capacity within 120 minutes contact time. After this time, the adsorption capacity of IMZEO increased and was approximately two times higher than capacity of ICZEO at the end of the experiment.



**Figure 4.** Adsorption of As(V) by IMGAC, IMZEO, ICZEO and FeO (As(V) initial concentration: 1000 µg/l; contact time: 180 min; adsorbent dose: 0.2 g; pH: neutral; temperature: 20±2 °C; agitation speed: 150 rpm)

## CONCLUSION

In the present study, six granular commercial adsorbents (activated carbon–GAC, zeolite–ZEO, iron coated zeolite–ICZEO, ferric oxide–FeO, ferric hydroxide–FeOH and ferric oxide-hydroxide–FeOOH) and two non-commercial granular adsorbents (iron-modified activated carbon-IMGAC and iron-modified zeolite-IMZEO) were used and compared for pentavalent arsenic removal from drinking water. In addition, for iron-modified adsorbents the total iron content and its stability were evaluated. According to the achieved results the commercial GAC, FeO, FeOH and FeOOH were successfully used as an adsorbent, from which the FeO had the highest adsorption capacity and efficiency. The used ICZEO remained at a low and constant capacity until the end of the experiment and ZEO was giving a result of zero adsorption capacity at all times. The multi-step iron modification process improved the GAC and ZEO adsorption capacity. The IMGAC had approximately three times higher adsorption capacity and efficiency than the best commercial FeO material.

## ACKNOWLEDGMENTS

This work was supported by a grant scheme for the support of the young researchers under the conditions of the SUT in Bratislava.

## REFERENCES

- Beinrohr, E., Čacho, F., Beinrohr, P. (2010) Stanovenie arzenu vo vodách rozpúšťacou chronopotenciometriou. *Elektrochemické metódy*, **XX**(2), 8-10.
- Horáková, M. (2003) Analytika vody. Vysoká škola chemicko-technologická v Praze, Prague.
- Pal, P. (2015) Groundwater Arsenic Remediation: Treatment Technology and Scale UP. Burlington: Elsevier Science, Oxford.
- Singh, R., Singh, S., Parihar, P., Singh, V. P., Prasad S. M. (2015) Arsenic contamination, consequences and remediation techniques: A review. *Ecotoxicology and Environmental Safety*, **112**, 247-270.
- van Halem, D., Bakker, S. A., Amy, G. L., van Dijk, J. C. (2009) Arsenic in drinking water: a worldwide water quality concern for water supply companies. *Drink. Water Eng. Sci.*, **2**, 29-34.
- Zhu, J., Pigna, M., Cozzolino, V., Caporale, A. G., Violante A. (2013) Higher sorption of arsenate versus arsenite on amorphous Al-oxide, effect of ligands. *Environ. Chem. Lett.*, **11**(3), 289-294.

# The Effect of Irrigation Using Secondary and Advance Treated Wastewaters on Soil Properties under Kikuyu Grass Production

A. Aghajani Shahrivar\*, D. Hagare\*\*, B. Maheshwari\*\*\* and M. Muhitur Rahman\*\*\*\*

\* Centre for Infrastructure Engineering, Western Sydney University, Locked Bag 1797, Penrith, NSW 2751, Australia (E-mail: [a.shahrivar@westernsydney.edu.au](mailto:a.shahrivar@westernsydney.edu.au))

\*\* School of Computing, Engineering and Mathematics, Western Sydney University, Locked Bag 1797, Penrith NSW 2751, Australia (E-mail: [d.hagare@westernsydney.edu.au](mailto:d.hagare@westernsydney.edu.au))

\*\*\* School of Science & Health, Western Sydney University, Locked Bag 1797, Penrith, NSW 2751, Australia (E-mail: [b.maheshwari@westernsydney.edu.au](mailto:b.maheshwari@westernsydney.edu.au))

\*\*\*\* Department of Civil and Environmental Engineering, King Faisal University, P.O. 380 Al-Ahsa 31982, Saudi Arabia (E-mail: [mrahman@kfu.edu.sa](mailto:mrahman@kfu.edu.sa))

## Abstract

The main objective of this study was to determine the effect of irrigating using three different types of waters, viz. secondary treated wastewater (STW), advance treated wastewater (ATW) and tap water (TW) on some important soil characteristics under kikuyu grass production. Kikuyu grass (*Pennisetum clandestinum*) is a very common and popular grass for urban areas and sports fields in Australia and was irrigated with above-indicated wastewaters and tap water for a period of 16 months (March 2016 - June 2017). No fertiliser was added during the study. Irrigation waters, soil extracted waters from different depths of the soils and soil samples from different depths were analysed for different parameters. Considerable changes occurred in soil characteristics over the period of study under different treatments. Soil saturated extract pH ( $\text{pH}_{\text{SE}}$ ) experienced an increase of more than 1 unit under irrigation with ATW while STW irrigated soil showed no appreciative change and TW irrigated soil evidenced a slight decrease of pH compared to initial soil pH. Also, a remarkable increase recorded for saturated extract electrical conductivity ( $\text{EC}_{\text{SE}}$ ) of top soils irrigated with treated wastewaters compared to soil's initial  $\text{EC}_{\text{SE}}$ . Variation of soil  $\text{pH}_{\text{SE}}$  in conjunction with soil salinity and differences in nutrient levels amongst irrigation waters resulted in various grass yield from each treatment. Annual grass production of 16,241 kg of dry-matter per hectare (kg DM/ha) achieved from soil irrigated with STW where the recorded annual yields from ATW and TW were 7,028 and 14,216 kg DM/ha, respectively. Overall, the results from this study highlighted the benefits of using STW as irrigation water due to its lower cost of treatment compared to ATW, higher grass production and maintaining of soil pH within an ideal range.

## Keywords

Secondary treated wastewater; advance treated wastewater; kikuyu grass; saturated extract pH; saturated extract EC; irrigation

## INTRODUCTION

Treated wastewater is a reliable water source for reuse in various areas to confront the water shortages (Pedrero et al., 2010). Using recycled water for irrigation can be of benefit in various terms including prevention of natural water resources contamination, saving in water resources, saving in wastewater treatment and recovering nutrients (Angelakis and Bontoux, 2001; Rahman et al., 2016). The effect of treated and untreated wastewaters in different agricultural systems has been reported by many researchers around the world (Castro et al., 2009; Costa et al., 2011; Manios et al., 2006; Pedrero et al., 2012; Pettygrove and Asano, 1984; Chakrabarti, 1995; Gori et al., 2000; Minhas and Yadav, 2015; Sheikh et al., 1987). Recycled water can be listed in different categories based on its chemical characteristics which is the result of the level of treatments that wastewater goes through. In this study the effect of irrigation with secondary treated wastewaters (STW) and advance treated wastewater (ATW) on soil acidity and salinity under kikuyu grass production was

investigated. No fertilizer was used during the study.

Soil pH is considered as one of the most important parameters of the soil that can be affected with the use of recycled water for irrigation. Plant growth is affected with soil pH in different ways. Soil pH can impact nitrification, denitrification, and glucose mineralization in soil atmosphere (Tabatabai and Olson, 1985). It has been reported that nitrogen mineralisation can be processed efficiently in the pH range of 5.5 to 7. Soil pH values below 5.5 can result in faster leaching of plant nutrients than those present in the soils with pH values of 5.5 to 7.0 (Ward, 2015). On the other hand, soil pH values higher than 7 can limit the availability of some plant nutrients causing reduction in plant production. For example phosphorus can be available to the plant mostly at a pH value between 6 and 7. Similarly, micro-nutrients such as iron, manganese, zinc, copper, and cobalt are less available for plant at pH over 7 (Seelig, 2000).

An inconsistent soil pH has been reported by the past studies when different types of wastewater were used for irrigation. Those reported the increase in soil pH, attributed this to the factors like effluent high pH values and availability of high levels of cations such as Na, Ca and Mg in irrigation waters (Gwenzi and Munondo, 2008; Schipper et al., 1996; Sparling et al., 2006). On the other hand, some other researchers reported soil pH decrease as a result of wastewater application (Mohammad and Mazahreh, 2003; Rattan et al., 2005) and this decrease was explained as a result of either acidic characteristics of sewage effluents or the process of nitrification in presence of high amount of ammonium in the wastewater which resulted in serving hydrogen ions in the soil. No significant effect on soil pH when irrigated with wastewater was recorded by Khan et al. (2008).

Another issue that is associated with the use of wastewater for irrigation is the addition of large amounts of salt to the soil as typically, treated wastewater contains 200-300 mg/L of total dissolved solids (TDS) (Muyen et al., 2011). Soils with saturated extract electrical conductivity ( $EC_{SE}$ ) over 4 ds/m, generally, are defined as saline soils. However, different plants depending on their salinity tolerance can be affected at half and twice this salinity (Bernstein, 1975).

Kikuyu grass (*Pennisetum clandestinum*) used in this study is known to have a moderate salinity tolerance up to 4 ds/m (Havilah et al., 2005) and also can grow well in the soil with moderate acidity with pH of 5-7 (Clark, 2007; Dickenson et al., 2004). Kikuyu grass is a C4 tropical grass which is widely used in sports fields, as well as pastures, public areas and golf course fairways (Brede, 2000; Fulkerson, 2007). A large number of studies have been carried out in terms of kikuyu grass production with application of fertilizer (Awad et al., 1976; Botha et al., 2008; Fulkerson et al., 1999; Gherbin et al., 2007; Hacker and Evans, 1992).

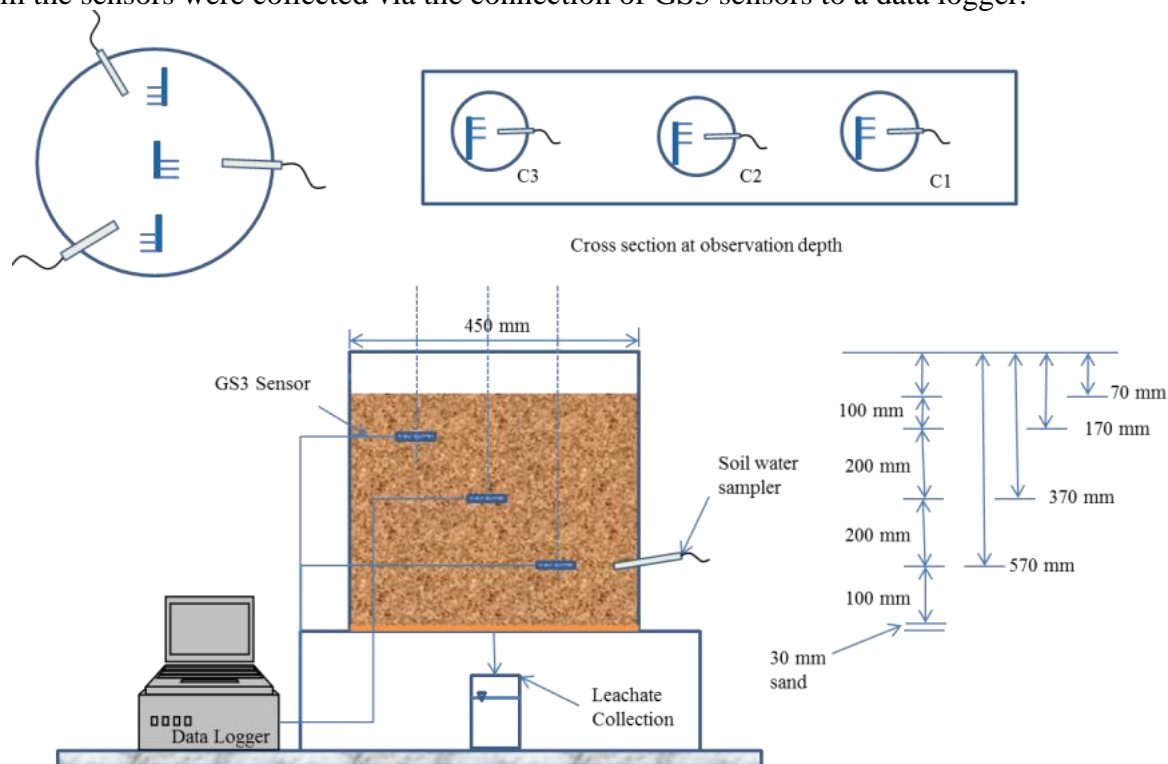
The specific objectives of this study were i) to investigate the effect of secondary and advance treated wastewaters on soil acidity and salinity and ii) the contribution of changes of soil pH and EC to kikuyu grass production.

## **MATERIALS AND METHODS**

### **Experimental design**

Experimental set-up has been explained thoroughly in Shahrivar et al., (2019). In a nutshell, three identical stainless steel columns were filled with the pre-prepared soil of loamy sand texture. The schematic set-up of the columns is illustrated in Figure 1. As shown in Figure 1, the columns regarding their size (450 mm diameter and 600 mm height) are considered as bigger columns compare to the other lab-scale lysimeters used for soil-plant studies. The GS3 sensors are able to measure bulk electrical conductivity, volumetric water content and temperature of the soil. Data

from the sensors were collected via the connection of GS3 sensors to a data logger.



**Figure 1.** Schematic set-up of the columns

The columns were equipped with three water extractors adjacent to their respective GS3 sensors in 100, 300 and 500 mm of the columns (Figure 1). Finally, kikuyu grass from nursery was laid on the top of the columns and was irrigated with the respective irrigation waters.

### Irrigation waters

Secondary treated wastewater (STW) used for this study was collected from Pennant Hills Golf Club's wastewater treatment plant in Sydney which uses membrane bioreactor treatment system (MBR). MBR is a secondary treatment of wastewater process which combines a membrane process with a biological process (Judd, 2010).

**Table 1.** Selected physicochemical properties of the soil

<i>Soil properties</i>	<i>Value</i>
Sand (%)	88.1
Silt (%)	6.0
Clay (%)	5.9
Texture class	Loamy sand
Bulk density (kg/m <sup>3</sup> )	1340
pH <sub>1:5</sub>	5.5
pH <sub>SE</sub> (saturation extract)	5.9
EC <sub>1:5</sub> (ds/m)	0.04
EC <sub>SE</sub> (saturation extract), (ds/m)	0.38

Advance treated wastewater to be used in this research was collected from Sydney Water's Richmond STP (Sewage Treatment Plant) which uses intermittently decanted aerated lagoon (IDAL) system for wastewater treatment. IDAL is an advance treatment of wastewater for removing nutrient, particularly nitrogen. In this system, all processes including sedimentation, biological



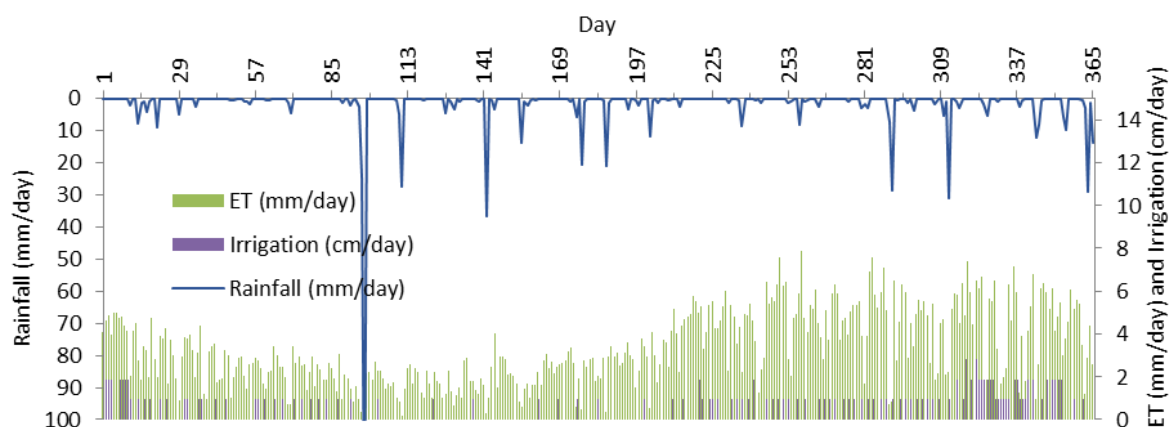
treatment and clarification take place in one reactor (Ngo et al., 2007). Tap water (TP) was used as control water in the study which is provided by Sydney Water Corporation to Sydney Metropolitan area.

### Irrigation scheduling

Data from GS3 sensors in conjunction with collected data from the weather station installed at the study area were used to identify the interval of irrigation and the amount of water to be applied to the columns. Due to Loamy sand's reputation of having Field Capacity of 19 % and Available Water Content of 9 %, during the study period effort was taken to maintain the soil moisture content around 15 % to avoid any water stress for the grass. Figure 2 illustrates the irrigation scheduling and climatic condition during the study. Daily ET (Evapotranspiration) for kikuyu grass was calculated as (Allen et al., 1998):

$$ET = K_C \times ET_0 \quad (1)$$

where  $ET$  is daily evapotranspiration for kikuyu grass ( $\text{mm d}^{-1}$ ),  $K_C$  is kikuyu grass monthly crop coefficient (Connellan, 2013) and  $ET_0$  is reference crop evapotranspiration ( $\text{mm d}^{-1}$ ) from weather station.



**Figure 2.** Irrigation scheduling and climatic conditions

### Soil and water analysis

EC and pH of irrigation waters were analysed using respective meters. Total nitrogen (TN) and Total phosphorus (TP) were analysed using persulfate digestion method. Samples after digestion were analysed using the discrete analyser (Gallery, Thermoscientific). Main cations (Ca, K, Mg and Na) were measured by inductively coupled plasma optical emission spectrometry (ICP-OES, Agilent Technology 700 series). Soil samples from different depths were analysed for different parameters, saturated extract pH ( $\text{pH}_{SE}$ ) and saturated extracted EC ( $\text{EC}_{SE}$ ) included, using soil analysis methods proposed by Rayment and Lyons (2011).

## RESULTS AND DISCUSSIONS

### Characteristics of irrigation waters

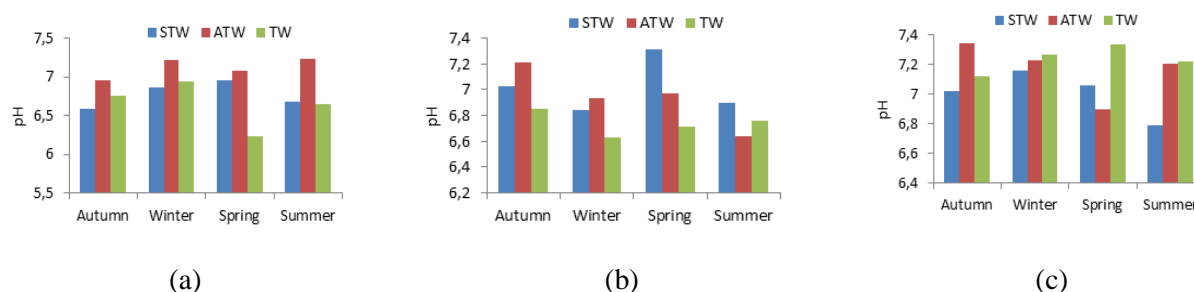
Table 2 summarises the mean values of irrigation water quality parameters. It can be seen that irrigation waters have different characteristics based on the treatments they have gone through. STW has high concentrations of nitrogen and phosphorus compared to other irrigation waters. By comparison, both treated wastewaters have considerably higher values of sodium than TW and that causes higher level of Sodium Adsorption Ratio (SAR) in treated wastewaters.

**Table 2.** Mean values of selected parameters of irrigation waters

Parameters	STW	ATW	TW
pH	7.25 ± 0.41	7.52 ± 0.35	7.25 ± 0.46
EC <sub>25°C</sub> (dS/m)	0.99 ± 0.18	0.93 ± 0.073	0.26 ± 0.026
TN (mg/L)	15.33 ± 3.28	0.90 ± 0.32	0.58 ± 0.33
TP (mg/L)	5.55 ± 2.10	1.31 ± 0.75	0.48 ± 0.44
Ca <sup>2+</sup> (mg/L)	29.59 ± 5.51	16.10 ± 1.70	20.33 ± 4.61
K <sup>+</sup> (mg/L)	25.69 ± 7.28	28.58 ± 8.14	7.74 ± 5.42
Mg <sup>2+</sup> (mg/L)	11.57 ± 3.39	26.04 ± 4.62	7.30 ± 2.57
Na <sup>+</sup> (mg/L)	143.37 ± 31.23	113.68 ± 25.57	18.87 ± 5.51
SAR	5.67 ± 0.21	4.08 ± 0.62	0.91 ± 0.15

### Soil-water pH

Extracted water pH from different depths of the soil varied seasonally from column to column. Figure 3 shows seasonal pH values from 10 (Figure 3 (a)), 30 (Figure 3 (b)) and 50 cm (Figure 3 (c)) depth of the soils irrigated with different types of irrigation waters. As it can be seen from the graphs, pH in soil irrigated with ATW is higher than the two other irrigation waters with values over 7 in 10 cm depth of the soil throughout the study.



**Figure 3.** Seasonal variation in soil-water pH extracted from a) 10 cm, b) 30 cm and c) 50 cm depth of the columns

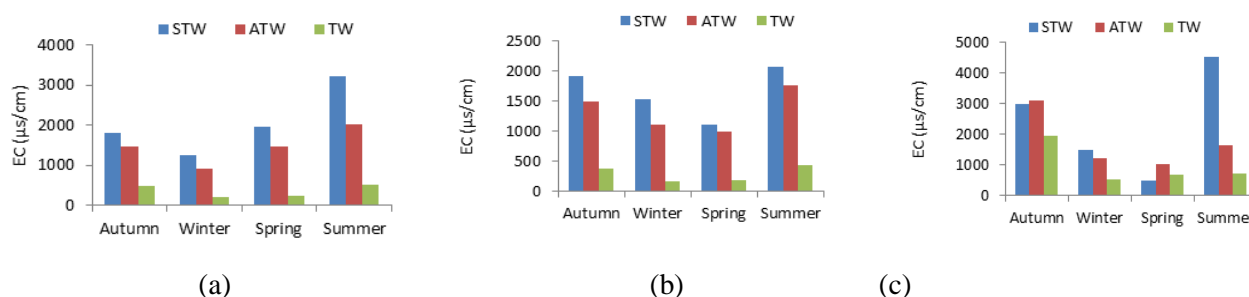
Bearing in mind that the highest concentration of grass root is placed in top soil, variation in soil characteristics in this area can be of importance regarding the impact on grass growth and production. As mentioned before, kikuyu grass is known to grow well in the optimum pH values of 5 – 7 (Clark, 2007; Dickenson et al., 2004).

### Soil-water EC

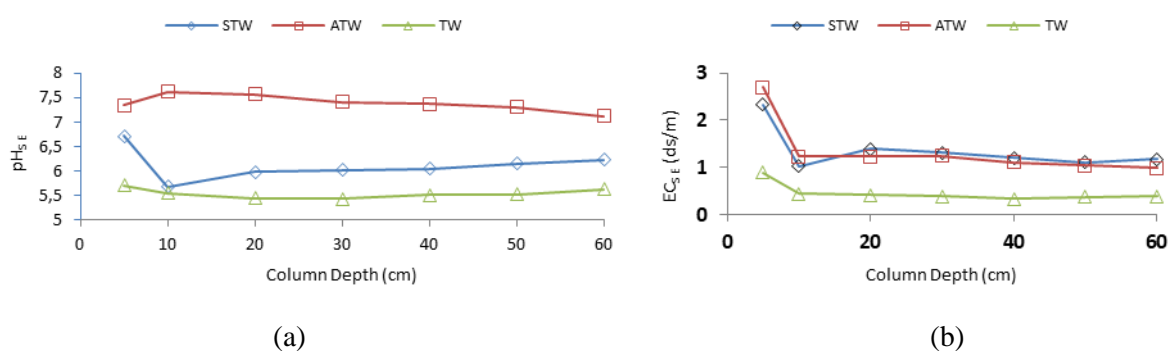
Similar to pH, extracted water electrical conductivity (EC) varied seasonally from depth to depth among the treatments. Seasonal EC values from 10, 30 and 50 cm depth of the soils irrigated with different types of irrigation waters is illustrated in Figure 4. It is obvious that soils irrigated with two types of treated wastewaters have high levels of salinity throughout the study time in different depths of the columns.

### Soil saturated extract pH and EC (pH<sub>SE</sub> and EC<sub>SE</sub>)

After running the experiment, soil samples were collected from various depths of the columns. Analysis of soil samples showed similar results compared to soil-water analysis during the study in terms of pH and EC. Figure 5 shows the change of soil pH<sub>SE</sub> (a) and EC<sub>SE</sub> from different depths of the columns.



**Figure 4.** Seasonal variation in soil-water EC extracted from a) 10 cm, b) 30 cm and c) 50 cm depth of the columns: STW, ATW and TW represent secondary treated wastewater, advance treated wastewater and tap water, respectively



**Figure 5.** Soil saturated extract pH ( $pH_{SE}$ ) (a) and soil saturated extract EC ( $EC_{SE}$ ) (b) in different depths of the soils irrigated with secondary treated wastewater (STW), advance treated wastewater (ATW) and tap water (TW)

These parameters of soil and their effect on kikuyu grass production have been comprehensively discussed in Shahrivar et al., (2019). In brief, high concentration of cations in conjunction with low level of nitrogen can be addressed as higher pH values of soil irrigated with ATW. This can be of hindrance in terms of kikuyu grass growth which is known to grow properly in pH level of 5-7. The results of dry matter yield from different treatments have been presented in Shahrivar et al., (2019), where soil irrigated with STW produced almost two times more than soil irrigated with ATW.

## CONCLUSIONS

Soils irrigated with treated wastewaters resulted in higher values of salinity compared to control water particularly due to their high concentration of sodium. However, these levels of salinity, when sufficient amounts of nutrients are available, are unlikely to be of high risk for kikuyu grass growth. Advance treated wastewater (ATW) costs more and due to the lack of valuable nutrients and high salinity results in relatively low grass yield. Results of this study indicated that secondary treated wastewater (STW) can be a suitable source of irrigation water for urban areas. This has several benefits such as, savings in the cost of treatment, recovery of nutrients from wastewater and prevention of pollution discharging into urban waterways.

## ACKNOWLEDGEMENTS

The authors wish to acknowledge the Pennant Hills Golf Club operators in particular Kurt Dahl and Richard Kirkby of Permeate Partners Pty. Ltd. for providing access to collect MBR treated wastewater. The authors also are grateful to Dr Roger Attwater and Dr Lyn Anderson for their assistance in collecting IDAL treated wastewater. Contributions of environmental engineering lab staff at Penrith campus of Western Sydney University and Louise Prouteau, an internship student of

ENSCR, France, are gratefully acknowledged.

## REFERENCES

- Allen, R. G., Pereira, L. S., Raes, D., Smith, M. (1998) Guidelines for computing crop water requirements-FAO Irrigation and drainage paper 56, FAO-Food and Agriculture Organisation of the United Nations, Rome (<http://www.fao.org/docrep>)
- ARPAV (2000), La caratterizzazione climatica della Regione Veneto, Quade. *Geophysics* 156, 178.
- Angelakis, A. N., Bontoux, L. (2001) Wastewater reclamation and reuse in Eureau countries. *Water Policy*, **3**, 47-59.
- Awad, A. S., Edwards, D. G., Milham, P. J. (1976) Effect of pH and phosphate on soluble soil aluminium and on growth and composition of kikuyu grass. *Plant Soil*, **45**, 531-542.
- Bernstein, L. (1975) Effects of salinity and sodicity on plant growth. *Annu. Rev. Phytopathol.*, **13**, 295-312.
- Botha, P. R., Meeske, R., Snyman, H. A. (2008) Kikuyu over-sown with ryegrass and clover: grazing capacity, milk production and milk composition. *African J. Range Forage Sci.*, **25**, 103-110.
- Brede, D. (2000) Turfgrass maintenance reduction handbook: sports, lawns, and golf, John Wiley & Sons.
- Castro, E., Manas, M. P., De Las Heras, J. (2009) Nitrate content of lettuce (*Lactuca sativa* L.) after fertilization with sewage sludge and irrigation with treated wastewater. *Food Addit. Contam.*, **26**, 172-179.
- Chakrabarti, C. (1995) Residual effects of long-term land application of domestic wastewater. *Environ. Int.*, **21**, 333-339.
- Clark, S. (2007) Kikuyu.
- Connellan, G. (2013) Water use efficiency for irrigated turf and landscape, CSIRO PUBLISHING.
- Costa, M., Beltrao, J., De Brito, J. C., Guerrero, C. (2011) Turfgrass plant quality response to different water regimes. *WSEAS Trans. Environ. Dev.*, **7**, 167-176.
- Dickenson, E. B., Hyam, G. F. S., Breytenbach, W. A. S., Metcalf, H. D., Basson, W. D., Williams, F. R., Scheepers, L. J., Plint, A. P., Smith, H. R. H., Smith, P.J. (2004) Kynoch Pasture Handbook 1st English Edition, Paarl print, Cape town, South Africa.
- Fulkerson, B. (2007) Kikuyu grass. *Futur. Dairy. Tech Note*.
- Fulkerson, W. J., Slack, K., Havilah, E. (1999) The effect of defoliation interval and height on growth and herbage quality of kikuyu grass (*Pennisetum clandestinum*). *Trop. grasslands*, **33**, 138-145.
- Gherbin, P., De Franchi, A. S., Monteleone, M., Rivelli, A. R. (2007) Adaptability and productivity of some warm season pasture species in a Mediterranean environment. *Grass Forage Sci.*, **62**, 78-86.
- Gori, R., Ferrini, F., Nicese, F. P., Lubello, C. (2000) Effect of reclaimed wastewater on the growth and nutrient content of three landscape shrubs. *J. Environ. Hortic.*, **18**, 108-114.
- Gwenzi, W., Munondo, R. (2008) Long-term impacts of pasture irrigation with treated sewage effluent on nutrient status of a sandy soil in Zimbabwe. *Nutr. Cycl. Agroecosystems*, **82**, 197-207.
- Hacker, J. B., Evans, T. R. (1992) An evaluation of the production potential of six tropical grasses under grazing. 1. Yield and yield components, growth rates and phenology. *Aust. J. Exp. Agric.*, **32**, 19-27.
- Havilah, E., Warren, H., Lawrie, R., Senn, A., Milham, P. (2005) Fertilisers for pastures, New South Wales Dep. Prim. Ind., Sydney.
- Judd, S. (2010) The MBR book: principles and applications of membrane bioreactors for water and wastewater treatment, Elsevier.
- Khan, S., Cao, Q., Zheng, Y. M., Huang, Y. Z., Zhu, Y. G. (2008) Health risks of heavy metals in

- contaminated soils and food crops irrigated with wastewater in Beijing, China. *Environ. Pollut.*, **152**, 686-692.
- Manios, T., Papagrigoriou, I., Daskalakis, G., Sabathianakis, I., Terzakis, S., Maniadakis, K., Markakis, G. (2006) Evaluation of primary and secondary treated and disinfected wastewater irrigation of tomato and cucumber plants under greenhouse conditions, regarding growth and safety considerations. *Water Environ. Res.*, **78**, 797-804.
- Minhas, P. S., Yadav, R. K. (2015) Long-term impact of wastewater irrigation and nutrient rates II. Nutrient balance, nitrate leaching and soil properties under peri-urban cropping systems. *Agric. water Manag.*, **156**, 110-117.
- Mohammad, M. J., Mazahreh, N. (2003) Changes in soil fertility parameters in response to irrigation of forage crops with secondary treated wastewater. *Commun. Soil Sci. Plant Anal.*, **34**, 1281-1294.
- Muyen, Z., Moore, G. A., Wrigley, R. J. (2011) Soil salinity and sodicity effects of wastewater irrigation in South East Australia. *Agric. Water Manag.*, **99**, 33-41.
- Ngo, H., Vigneswaran, S., Sundaravadivel, M. (2007) Advanced treatment technologies for recycle/reuse of domestic wastewater. Wastewater Recycl. reuse reclamation. Eolss Publ. Co Ltd., Oxford, 77-98.
- Pedrero, F., Allende, A., Gil, M. I., Alarcón, J. J. (2012) Soil chemical properties, leaf mineral status and crop production in a lemon tree orchard irrigated with two types of wastewater. *Agric. water Manag.*, **109**, 54-60.
- Pedrero, F., Kalavrouziotis, I., Alarcón, J. J., Koukoulakis, P., Asano, T. (2010) Use of treated municipal wastewater in irrigated agriculture—Review of some practices in Spain and Greece. *Agric. Water Manag.*, **97**, 1233-1241.
- Pettygrove, G. S., Asano, T. (1984) Irrigation with reclaimed municipal wastewater. A guidance manual, California State Water Res. Control Board. Davis. Calif.
- Rahman, M. M., Hagare, D., Maheshwari, B. (2016) Use of recycled water for irrigation of open spaces: benefits and risks, in: *Balanced Urban Development: Options and Strategies for Liveable Cities*, Springer, 261-288.
- Rattan, R. K., Datta, S. P., Chhonkar, P. K., Suribabu, K., Singh, A. K. (2005) Long-term impact of irrigation with sewage effluents on heavy metal content in soils, crops and groundwater—a case study. *Agric. Ecosyst. Environ.*, **109**, 310-322.
- Rayment, G. E., Lyons, D. J. (2011) *Soil chemical methods: Australasia*, CSIRO publishing.
- Schipper, L. A., Williamson, J. C., Kettles, H. A., Speir, T. W. (1996) Impact of land-applied tertiary-treated effluent on soil biochemical properties. *J. Environ. Qual.*, **25**, 1073-1077.
- Seelig, B. (2000) Salinity and sodicity in North Dakota soils.
- Shahrivar, A. A., Rahman, M. M., Hagare, D., Maheshwari, B. (2019) Variation in kikuyu grass yield in response to irrigation with secondary and advanced treated wastewaters. *Agric. Water Manag.*, **222**, 375-385.
- Sheikh, B., Jaques, R. S., Cort, R. P. (1987) Reuse of tertiary municipal wastewater effluent for irrigation of raw-eaten food crops: a five year field study. *Desalination*, **67**, 245-254.
- Sparling, G. P., Barton, L., Duncan, L., McGill, A., Speir, T. W., Schipper, L. A., Arnold, G., Van Schaik, A. (2006) Nutrient leaching and changes in soil characteristics of four contrasting soils irrigated with secondary-treated municipal wastewater for four years. *Soil Res.*, **44**, 107-116.
- Tabatabai, M. A., Olson, R. A. (1985) Effect of acid rain on soils. *Crit. Rev. Environ. Sci. Technol.*, **15**, 65-110.
- Ward, E. (2015) The pH of your soil can affect plant growth and health [WWW Document]. [online] <http://archive.naplesnews.com/community/gardening-the-ph-of-your-soil-can-affect-plant-growth-and-health-ep-1071358042-331319431.html/>.

## Characterization of Leachate from Non-sanitary Municipal Solid Waste Landfill in Novi Sad

K. Antić\*, M. Petrović\*, D. Adamović\*, M. Turk-Sekulić\*, D. Sakulski\*\* and J. Radonić\*

\* Department of Environmental Engineering, Faculty of Technical Sciences, University of Novi Sad, Dositej Obradović Square 6, 21101 Novi Sad, Republic of Serbia (E-mail: [antickatarina@gmail.com](mailto:antickatarina@gmail.com))

\*\* BioSense Institute, University of Novi Sad, Dr. Zorana Đinđića 1, 21101 Novi Sad, Republic of Serbia

### Abstract

Leachate is produced through complex chemical reactions, infiltration of the atmospheric water in the landfill body and the water contained in the waste, as well as through dissolution of waste pollutants. Due to its toxic composition, leachate pollutes soil and groundwater. It is very difficult to foresee real composition of landfill leachate due to dynamics of the processes occurring in the landfill body and the impact of a large number of variable factors. Qualitative composition of the leachate is characterized by pollutants that can be classified into four groups - *soluble organic components*, *inorganic macrocomponents*, *heavy metals* and *xenobiotic organic compounds*. The main objective of the conducted research was determination of the quality and organic profile of the leachate collected at non-sanitary municipal solid waste landfill in Novi Sad, by performing a screening analysis using GC-MS device.

### Keywords

Landfill leachate; characterization of landfill leachate; municipal solid waste landfill; screening analysis using GC-MS device; organic compounds

## INTRODUCTION

Leachate is the entity resulted from a several factors in both, the landfill body itself (landfill age, morphological waste composition, temperature and humidity, migration of fluid, pre-disposal waste treatment technology, thickness of the landfill body, waste decomposition stage), and outside of it (meteorological parameters, with focus on annual precipitation volume, as well as seasonal variations). The process of landfill filtrate forming includes decomposition of solid organic matter in the water drained through the landfill body and generating of new substances by biological processes and chemical reactions, which inevitably occur within the landfill body (Brennan et al., 2015).

Real composition of the landfill leachate is very difficult to foresee due to dynamics of the processes occurring in the landfill body and the impact of a large number of variable factors. Qualitative composition of leachate is characterized by pollutants that can be classified in four basic groups (Christensen et al., 1998; Kjeldsen et al., 2002): *soluble organic components* (volatile fatty acids, humic and fulvic acids), *inorganic macrocomponents* (ions of calcium,  $\text{Ca}^{2+}$ , magnesium,  $\text{Mg}^{2+}$ , sodium,  $\text{Na}^+$ , potassium,  $\text{K}^+$ , ammonium,  $\text{NH}_4^+$ , iron,  $\text{Fe}^{2+}$ , manganese,  $\text{Mn}^{2+}$ , chlorides,  $\text{Cl}^-$ , sulphates,  $\text{SO}_4^{2-}$ , carbohydrates,  $\text{HCO}_3^-$ ), *heavy metals* (ions of cadmium,  $\text{Cd}^{2+}$ , chromium,  $\text{Cr}^{3+}$ , copper,  $\text{Cu}^{2+}$ , lead,  $\text{Pb}^{2+}$ , nickel,  $\text{Ni}^{2+}$ , and zinc,  $\text{Zn}^{2+}$ ), *xenobiotic organic compounds* (carbohydrates, phenols, chlorinated aliphatic compounds, pesticides, dioctyl phthalates). The toxic and hazardous matters previously registered and identified in landfill leachate, from the region of Vojvodina, are aromatic carbohydrates, halogenated compounds, phenols, pesticides, heavy metals and nutrients (Đogo et al., 2016).

The main objective of the conducted research was determination of the quality and organic profile of the leachate collected at non-sanitary municipal solid waste landfill in Novi Sad, by performing a

screening analysis using GC-MS device.

## MATERIALS AND METHODS

Leachate sampling campaigns were carried out during the winter and spring periods 2019 in 2 hours cycles at the landfill in Novi Sad (Figure 1.).



**Figure 1.** Collecting of leachate at a non-sanitary municipal solid waste landfill in Novi Sad in winter (left) and spring (right) 2019

Total of 2 L of leachate were collected for the purpose of the screening analysis. The samples were transported and stored at the temperature of 4 °C until the preparation for the analysis. Samples were prepared by liquid-liquid extraction and concentrated in the Kuderna-Danish device. Previously prepared internal standard Fenantren D10, concentration of 15 ppm in methanol, was applied, while dichloromethane was used as a solvent agent. QP2010-Ultra GC-MS, Shimadzu, and Agilent HP – 5ms column (30 m·0,25 mm·0,25 µm) were used for the analysis. The screening analysis was conducted in the Laboratory for monitoring landfills, wastewater and air of the Department of Environmental Engineering and Occupational Safety and Health, Faculty of Technical Sciences in Novi Sad.

## RESULTS

The organic profile of the analysed leachate is result of the morphological composition of the disposed waste and its seasonal variations, age of the landfill, as well as of the meteorological parameter variations, i.e. temperature, precipitation and humidity. The organic profile of the leachate from the non-sanitary municipal solid waste landfill in Novi Sad in winter and spring periods 2019 is presented in Table 1.

**Table 1.** The organic profile of the leachate from the non-sanitary municipal solid waste landfill in Novi Sad in winter and spring periods 2019

<b>Group of compounds</b>	<b>Winter period</b>	<b>Spring period</b>
<i>Carbohydrates</i>	5	7
<i>Organic acids, esters, and salts of organic acids</i>	12	16
<i>Phthalates</i>	/	/
<i>Alcohols, ketones and aldehydes</i>	7	10
<i>Phenols</i>	3	1
<i>Heterocyclic compounds</i>	5	2
<i>Organonitrogen compounds</i>	5	5
<b>Total detected</b>	<b>38</b>	<b>41</b>



The obtained results indicate the dominant presence of two groups of organic compounds: *organic acids, esters and salts of organic acids* and *alcohols, ketones and aldehydes*. The specified groups of organic compounds are usually present in the organic fraction of waste and products of degradation (fruit, animal waste, food products) and in industrial waste as well (pharmaceuticals, synthetic polymers, industrial solvents, essential oils).

Table 2, Table 3, Table 4, Table 5, Table 6. and Table 7 show identified organic compounds within the groups of *carbohydrates, organic acids, esters and organic acid salts, phthalates, alcohols, ketones and aldehydes, phenols, heterocyclic compounds* and *organonitrogen compounds* in winter and spring periods.

**Table 2.** Identified compounds within the group of *carbohydrates* during the winter and spring periods 2019

<b>Winter period</b>			
<b>Group of compounds</b>	<b>CAS Number</b>	<b>Molecular weight [g mol<sup>-1</sup>]</b>	<b>Retention time</b>
Z,Z,Z-1,4,6,9-Nonadecatetraene	82970-94-3	260.46	16.383
(Cyclopropyl)trivinylsilane	959074-89-6	150.30	51.688
Longipinane, (E)-	/	206.37	53.108
3,5-Decadiyne, 2,2-dimethyl-	55682-73-0	162.27	58.790
cis-Z-.alpha.-Bisabolene epoxide	/	220.35	70.930
<b>Spring period</b>			
<b>Group of compounds</b>	<b>CAS Number</b>	<b>Molecular weight [g mol<sup>-1</sup>]</b>	<b>Retention time</b>
Cyclopentane, 1-methyl-3-(2-methylpropyl)-	29053-04-1	140.26	13.785
Cyclohexasiloxane, dodecamethyl-	540-97-6	444.92	44.528
Benzene, 1,3-diisocyanato-2-methyl-	91-08-7	174.16	44.905
Benzene, 2,4-diisocyanato-2-methyl-	584-84-9	174.16	45.065
Diphenyl sulphide	139-66-2	186.27	59.485
Phenanthrene-D10	1517-22-2	188.29	69.545
Oxirane, 2,2'-[(1-methylethylidene)bis(4,1-phenyleneoxymethylene)]bis-	1675-54-3	340.41	188.593



**Table 3.** Identified compounds within the group of *organic acids, esters and salts of organic acids* during the winter and spring periods 2019

<b>Winter period</b>			
<b>Group of compounds</b>	<b>CAS Number</b>	<b>Molecular weight [g mol<sup>-1</sup>]</b>	<b>Retention time</b>
Carbamic acid, methyl-, phenyl ester	2603-10-3	151.16	17.770
Triisopropylphosphate	513-02-0	224.23	35.017
N,N-Dimethylsuccinamic acid	2564-95-6	145.16	49.518
3,7-Dimethyl-6-nonen-1-ol acetate	/	212.33	54.545
Methyl (4S,5R)-2,2,5-trimethyl-1,3-dioxolane-4-carboxylate	38410-80-9	174.19	56.063
Tributyl phosphate	126-73-8	266.32	56.628
4-Oxo-4-(para-tolyl)-butyric acid	4619-20-9	307.40	59.698
Decanoic acid, decyl ester	1654-86-0	312.53	62.870
2-Dodecen-1-yl(-)succinic anhydride	19780-11-1	266.37	64.240
[1,1'-Bicyclopropyl]-2-octanoic acid, 2'-hexyl-, methyl ester	56687-68-4	322.50	66.915
Phthalic acid, monoethyl ester	2306-33-4	194.18	76.093
Cyclohexanecarboxylic acid, hexyl ester	27948-10-3	212.33	77.115
<b>Spring period</b>			
<b>Group of compounds</b>	<b>CAS Number</b>	<b>Molecular weight [g mol<sup>-1</sup>]</b>	<b>Retention time</b>
3-Trifluoroacetoxypentadecane	/	324.23	11.300
2-Propenoic acid, 1-methylundecyl ester	51443-73-3	240.38	13.738
Propylene Carbonate	108-32-7	102.09	17.615
Pterin-6-carboxylic acid	948-60-7	207.15	28.060
2-Oxepanone	502-44-3	114.14	29.628
5-(Prop-2-enoyloxy)pentadecane	/	282.46	30.003
5-Cyclopropylcarbonyloxypentadecane	/	296.49	30.283
3-(Prop-2-enoyloxy)tetradecane	/	282.50	43.013
3-Trifluoroacetoxy-6-ethyldecane	/	282.35	58.235
Hydracrylic acid, monoanhydride with 1-butaneboronic acid, cyclic ester	33823-94-8	155.99	62.565
2-Propanol, 1-chloro-, phosphate (3:1)	13674-84-5	327.57	72.288
Phthalic acid, isobutyl octadecyl ester	/	474.70	75.685
7,9-Di-tert-butyl-1-oxaspiro(4,5)deca-6,9-diene-2,8-dione	82304-66-3	276.37	78.140
Hexadecanoic acid, methyl ester	112-39-0	270.45	78.848
Nor-diazepam, 3-[[N-hydroxymethyl]aminocarbonyloxy]-	/	373.80	78.877
Isopropyl Palmitate	142-91-6	298.50	83.773

**Table 4.** Identified compounds within the group of *alcohols, ketones and aldehydes* during the winter and spring periods 2019

<b>Winter period</b>			
<b>Group of compounds</b>	<b>CAS Number</b>	<b>Molecular weight [g mol<sup>-1</sup>]</b>	<b>Retention time</b>
Cycloundecanone	878-13-7	168.27	46.352
Bicyclo[2.2.1]heptan-2-one, 5-hydroxy-4,7,7-trimethyl-	114529-11-2	168.23	48.390
2,4,7,9-Tetramethyl-5-decyn-4,7-diol	126-86-3	226.36	50.005
7-Hexadecenal, (Z)-	56797-40-1	238.41	52.485
Bicyclo[4.1.0]heptan-3-ol, 4,7,7-trimethyl-, [1R-(1.alpha.,3.beta.,4.alpha.,6.alpha.)]-	54750-09-3	154.25	66.915
s-Trioxane, 2,4,6-triethyl-	2396-42-1	174.24	68.275
1-Heptadec-1-ynyl-cyclohexanol	/	334.58	69.660
<b>Spring period</b>			
<b>Group of compounds</b>	<b>CAS Number</b>	<b>Molecular weight [g mol<sup>-1</sup>]</b>	<b>Retention time</b>
2-Nonyl-1-ol	5921-73-3	140.22	10.268
7-Hexadecenal, (Z)-	56797-40-1	238.41	10.433
2-n-Butylacrolein	1070-66-2	112.17	13.845
1,6-Anhydro-2,4-dideoxy-.beta.-D-ribo-hexopyranose	/	130.14	17.905
9-Oxabicyclo[6.1.0]nonan-4-ol	2616-81-1	142.19	37.435
Azacyclodecan-5-ol	/	157.25	40.600
9-Oxabicyclo[4.2.1]nonan-2-ol	/	142.20	47.720
2,4,7,9-Tetramethyl-5-decyn-4,7-diol	126-86-3	226.36	49.850
Heptanal	111-71-7	114.18	51.653
2(3H)-Benzofuranone, hexahydro-4,4,7a-trimethyl-	16778-27-1	182.26	58.285

**Table 5.** Identified compounds within the group of *phenols* during the winter and spring periods 2019

<b>Winter period</b>			
<b>Group of compounds</b>	<b>CAS Number</b>	<b>Molecular weight [g mol<sup>-1</sup>]</b>	<b>Retention time</b>
Phenol	108-95-2	94.11	17.468
Phenol, 4-methyl-	106-44-5	108.14	25.145
Phenol, 4,4'-(1-methylethylidene)bis-	80-05-7	228.29	90.153
<b>Spring period</b>			
<b>Group of compounds</b>	<b>CAS Number</b>	<b>Molecular weight [g mol<sup>-1</sup>]</b>	<b>Retention time</b>
Phenol, 4,4'-(1-methylethylidene)bis-	80-05-7	228.29	90.068

**Table 6.** Identified compounds within the group of *heterocyclic compounds* during the winter and spring periods 2019

<b>Winter period</b>			
<b>Group of compounds</b>	<b>CAS Number</b>	<b>Molecular weight [g mol<sup>-1</sup>]</b>	<b>Retention time</b>
Guanosine	118-00-3	283.24	11.570
3-Methyl-4-(phenylthio)-2-prop-2-enyl-2,5-dihydrothiophene 1,1-dioxide	/	280.40	12.273
Spiro[androst-5-ene-17,1'-cyclobutan]-2'-one, 3-hydroxy-, (3.beta.,17.beta.)-	/	328.49	14.828
Indole	120-72-9	117.15	40.948
Cyclic octaatomic sulfur	10544-50-0	256.52	81.868
<b>Spring period</b>			
<b>Group of compounds</b>	<b>CAS Number</b>	<b>Molecular weight [g mol<sup>-1</sup>]</b>	<b>Retention time</b>
3-Methyl-4-(phenylthio)-2-prop-2-enyl-2,5-dihydrothiophene 1,1-dioxide	/	280.40	10.018
Imidazole, 2-amino-5-[(2-carboxy)vinyl]-	1330014-65-7	153.14	42.703

**Table 7.** Identified compounds within the group of *organonitrogen compounds* during the winter and spring periods 2019

<b>Winter period</b>			
<b>Group of compounds</b>	<b>CAS Number</b>	<b>Molecular weight [g mol<sup>-1</sup>]</b>	<b>Retention time</b>
2,6-Dimethylphenyl isocyanate	28556-81-2	147.17	58.196
Propyphenazone	479-92-5	230.31	80.120
L-Glutamine, N2-[(phenylmethoxy)carbonyl]-	2650-64-8	280.28	45.005
8H-Pyrano[3,4-b]pyrimido[5,4-d]furane, 5,6-dihydro-4-hydrazino-6,6-dimethyl-2-methylthio-	/	280.35	108.665
Oxirane, 2,2-dimethyl-3-(3,7,12,16,20-pentamethyl-3,7,11,15,19-heneicosapentaenyl)-, (all-E)-	7200-26-2	426.72	116.663
<b>Spring period</b>			
<b>Group of compounds</b>	<b>CAS Number</b>	<b>Molecular weight [g mol<sup>-1</sup>]</b>	<b>Retention time</b>
1,4-Piperazinediethanol, .alpha.,.alpha.'-bis(phenoxyethyl)-	34972-10-6	386.48	10.143
2-Piperidinone, 6-methyl-	1558-58-3	113.16	29.713
3-Azabicyclo[3.2.2]nonane	283-24-9	125.21	47.640
Glucopyranuronamide, 1-(4-amino-2-oxo-1(2H)-pyrimidinyl)-1,4-dideoxy-4-(D-2-(2-(methylamino)acetamido)hydracrylamido)-, .beta.-	2096-42-6	443.41	48.110
Piperidine, 3-isopropyl-	13603-18-4	127.23	48.788

## CONCLUSION

Considering that the leachate from the non-sanitary municipal solid waste landfill in Novi Sad is not treated, the identification of specific pollutants is important from the aspect of environmental and health risk assessment. In addition, it is necessary to be aware of the presence and content of these pollutants in the landfill leachate, as well as their possible synergistic effects when developing, selecting and optimizing future treatments.

## ACKNOWLEDGMENTS

This research has been financially supported by projects of the Ministry of Education, Science and Technological Development of the Republic of Serbia (Project III46009 and Project TR 34014) and the Project of City Administration for Environmental Protection of the City of Novi Sad, Republic of Serbia, no. 01-209/439-3.

## REFERENCES

- Brennan, R. B., Healy, M. G., Morrison, L., Hynes, S., Norton, D., Clifford, E. (2015) Management of landfill leachate: The legacy of European Union Directives. *Waste Management*, **55**, 355-363.
- Christensen, J. B., Jensen, D. L., Filip, Z., Gron, C., Christensen, T. H. (1998) Characterization of the dissolved organic carbon in landfill polluted groundwater. *Water Research*, **32**, 125.
- Đogo, M., Ubavin, D., Mihajlović, I., Brborić, M., Milovanović, D., Radonić, J. (2016) Assessment of the effect of quality of landfill leachate on groundwater flows of selected sites in AP Vojvodina. Proceedings of the Conference Waste Water, Municipal Solid Waste and Hazardous Waste, Vršac, 13 – 15 April 2016., 167-171. ISBN: 978-86-82931-77-5.
- Kjeldsen, P., Barlaz, M. A., Rooker, A. P., Baun, A., Ledin, A., Christensen, T. H. (2002) Present and long-term composition of MSW landfill leachate: A Review. *Critical Review in Environmental Science and Technology*, **32**(4), 297-336.

## Changes of the Granulometric Composition of Particles in Wastewater Flowing through the Hydroponic Lagoon in III<sup>o</sup> Wastewater Treatment Plant

A. Bawiec\* and K. Pawęska\*

\* Institute of Environmental Engineering, Wrocław University of Environmental and Life Sciences, 24 Grunwaldzki Sq., 50-363 Wrocław, Poland (E-mails: [aleksandra.bawiec@upwr.edu.pl](mailto:aleksandra.bawiec@upwr.edu.pl); [katarzyna.paweska@upwr.edu.pl](mailto:katarzyna.paweska@upwr.edu.pl))

### Abstract

Wastewater treatment in semi-natural systems like hydroponic lagoon working as a third stage of purification is getting more and more popular because of the efficiency of nutrients removal. Very often treatment processes in hydroponic ditch are supported by algae growth what can cause the increase of total suspended solids concentration in the outflow from the wastewater treatment plant. The aim of the study was to analyse changes in the granulometric composition of particles in the hydroponic lagoon working as a third stage of wastewater purification in the Municipal Wastewater Treatment Plant (WWTP) in Poland. Measurements of the particles size were made with the use of laser diffraction method. Measurements results has shown that size of the particles in hydroponic lagoon varied from 0.01 to 1000  $\mu\text{m}$ . Analyses of the average diameters D(3.2) and D(4.3) has shown that particles have small reactivity but good sedimentation properties and their fractal dimensions are usually higher than 2.0 what decides about their well-developed surface. Most of the particles flowing out of the WWTP are probably algae or particles that can absorb on their surface other pollutants. The use of laser granulometry for particles identification might be useful in determining the total suspended solids character as well as can help to develop cheaper and more efficient methods of its removal.

### Key words

Laser granulometer; wastewater treatment; fractal dimension; hydroponic wastewater treatment; particle size distribution

## INTRODUCTION

Laser granulometry is an innovative method of particle size analysis used in many fields of industry, science and other branches (Garbowski et al., 2017). In most cases it is used for analysis of particle size distribution in aqueous solutions and it is based on diffraction process and low angle light scattering (Tinke et al., 2008). The main advantages of the use of granulometric analyses is the wide spectrum of results obtained in relatively short time as well as the wide range of particle size measurements (0.01 – 2000  $\mu\text{m}$ ) (Nolte et al., 2012; Xu, 2015). The results can be converted with the use of mathematical models to obtain the most accurate characteristics of particles.

During the last few years laser granulometry has been found as an alternative for traditional methods of suspended solids characterization. It gives an opportunity to analyse the size of mineral and organic particles like algae, protozoa or other small organisms (Bawiec et al. 2017). As proofed by Kuśnierz and Łomotowski (2015) and Bawiec et al. (2019), this method can be used for assessment of algae growth dynamics what has a particular importance in monitoring of natural and semi-natural wastewater treatment systems.

In the technology of wastewater purification, systems based on natural processes are nowadays in great importance because of their efficiency in organic matter and nutrients removal. Wide spreading of eutrophication in surface water reservoirs as well as water courses and even coastal waters brings a serious threat for natural ecosystems (Andersen et al., 2017; Kelly et al., 2018; Cai et al., 2019). One of the methods based on natural processes is sewage purification in hydroponic

lagoon build in the shape of artificial river. Treatment processes that occur in this system are based on water self-purification processes occurring in natural river ecosystems. Biologically treated sewage (after clarification in the secondary settling tank) is flowing through the hydroponic lagoon equipped with aeration system. On the surface of the wastewater, macrophytes (f.ex. *Pistia stratiotes*, *Myriophyllum verticillatum*, *Eichhornia crassipes*) are planted. Their roots are immersed in the solution that provides nutrients for their growth (Kouamé et al., 2016; Whitton et al., 2016). The roots surface as well as the plastic panels used as a support for growing plants are very good environment for bacteria, protozoa, small invertebrates, algae and microalgae growth (Ye et al., 2016).

Except from well-known role of bacteria (activated sludge) in wastewater treatment, algae and microalgae have a huge impact of its purification in semi-natural and natural processes. The role of algae can be considered multidimensional. In wastewater treatment the most important algae activity is an uptake of ammonium and phosphate – nutrients responsible for eutrophication process (Samori et al., 2013; Gilbert et al., 2018a). The production of O<sub>2</sub> in photosynthesis provides oxygen conditions for bacterial activity and CO<sub>2</sub> uptake slightly reduces greenhouse gas emissions (Su et al., 2012). Unfortunately, because of small size of cells that are negatively charged, separation and removal of algae from treated wastewater is expensive and difficult (Barros et al., 2015; Hu et al., 2017). Excessive algae and total suspended solids (TSS) discharge into the receiving water bodies, may cause a number of negative effects on the aquatic environment. In the case of TSS, their harmfulness to the environment depends of its composition. One of the most dangerous fraction of total suspended solids are colloidal particles that can easily absorb other pollutants like heavy metals. After sedimentation in water reservoirs or water courses heavy metals accumulates in the bottom sediments and their concentration decides on possibilities of bottom areas settlement by aquatic organisms (Suresh et al., 2012; Remo et al., 2016). High concentrations even of nontoxic suspended solids may cause direct injury to fish by reducing their tolerance of subsequent infection by pathogens (Redding et al., 1987; Cheremisinoff, 1995). Not without significance is fact that TSS may contain different micro pollutants like pharmaceuticals, microplastic or even nanomaterials, which can exert a toxic influence on the environment (Zhu et al., 2018; Wagner and Lambert, 2018). Additionally, high concentrations of suspended solids associated with organic matter, after discharge into the receiving water body may cause increase of chemical oxygen demand (COD) as well as be the reason of aesthetic issues (high turbidity of water) and as a result of it - higher costs of further water treatment (Bilotta and Brazier, 2008; Smyk et al., 2015).

As presented above total suspended solids and algae are one of the most problematic pollutants that have to be sufficiently removed before discharging wastewater into the receiving water bodies. Because of their dynamic changes, especially in semi-natural systems, this task is still a major concern of the scientists. Using the three stage wastewater treatment with the use of hydroponic lagoon as an additional system for biogenic compounds removal may cause operational problems connected with the excessive TSS concentrations as a result of algae growth in the system. Monitoring of the changes of particles size and properties during the flow through the hydroponic ditch can be the basis of developing more effective methods of total suspended solids and algae removal from the sewage. The aim of the paper was to analyse changes in the granulometric composition of particles in the hydroponic lagoon working as a third stage of wastewater purification.

## **MATERIALS AND METHODS**

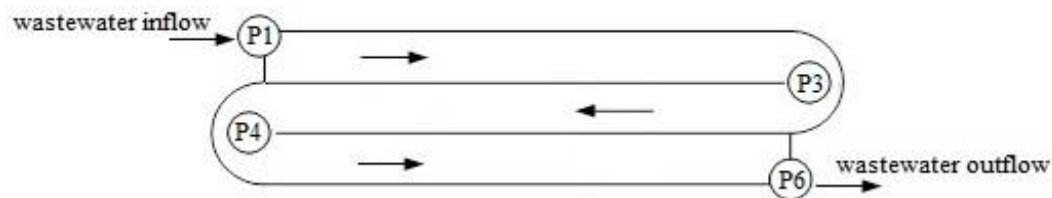
### **Object description**

The research object is a hydroponic lagoon working as a third stage of wastewater treatment in Municipal Wastewater Treatment Plant (WWTP) located in the south-western part of Poland which

size is calculated on 22 396 p.e. The whole treatment process consist of standard mechanical treatment, biological treatment in circulating hybrid bioreactor and additional purification in hydroponic lagoon. Hydroponic lagoon is a concrete ditch built in the shape of artificial river, whose total length is 191 m and the wastewater flow takes about 9 hours. The surface of the lagoon is planted with macrophytes – mostly *Pistia stratiotes* and *Myriophyllum verticillatum*. Partial aeration with the use of bottom aerators is provided. To provide sunlight for photosynthesis, roof and walls of the room when the ditch is located are made of polycarbonate sheets. In addition this solution allows to get very small temperature fluctuations during the year.

### Samples collection and analysis

Samples of wastewater were taken once a month in the autumn-winter season from the inlet (P1), middle flow (P3, P4) and the outlet (P6) of the hydroponic ditch (Figure 1) and transported in polyethylene terephthalate containers into the laboratory within 3 hours from collection.

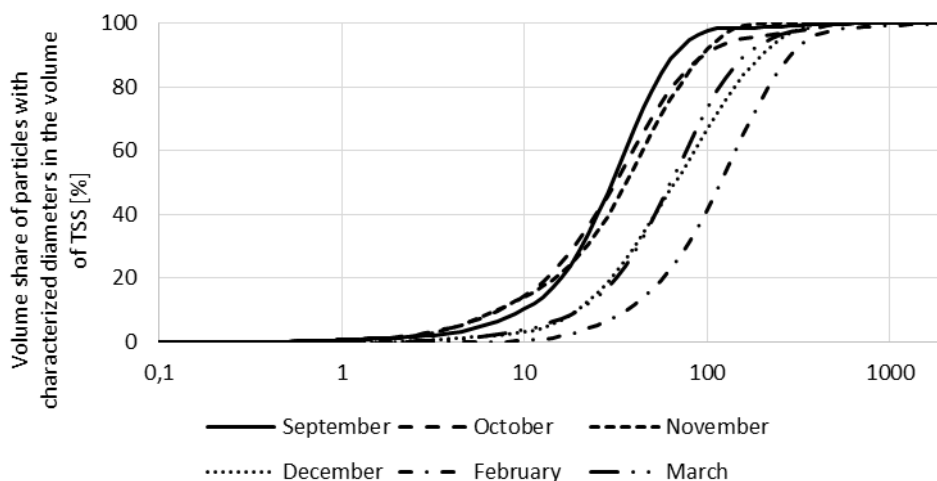


**Figure 1.** Scheme of hydroponic lagoon working as a third stage of wastewater treatment

The granulometric composition of sewage was measured with the use of Malvern Mastersizer 2000 laser granulometer coupled with wet sample dispersion unit ‘Hydro MU’ providing homogenous solution for the measurements. Analyses of obtained results were prepared with the use of Malvern Instruments Ltd. and STATISTICA software.

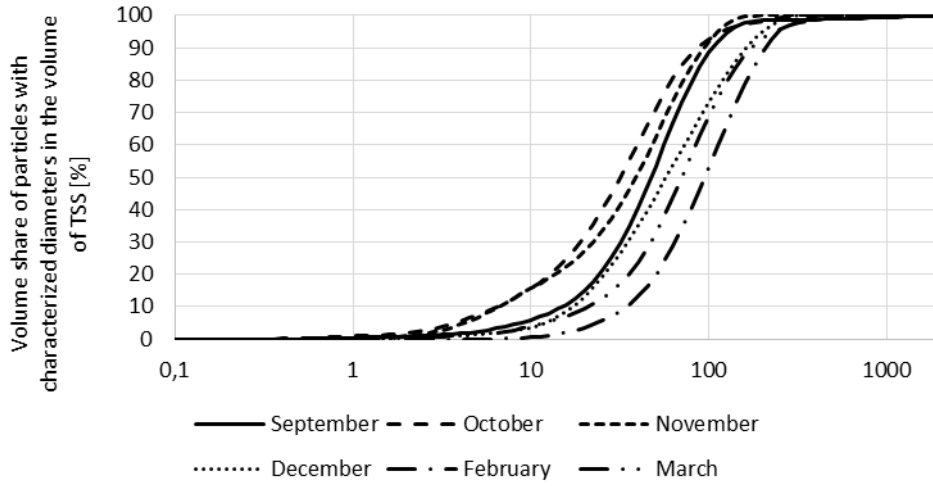
## RESULTS AND DISCUSSION

The changes in particles size distribution described by the changes in the % share of volume of suspended solids fraction with characterized  $d_i$  diameters in the total volume of polydisperse suspension shows variations within wastewater samples collected month after month (Figure 2).

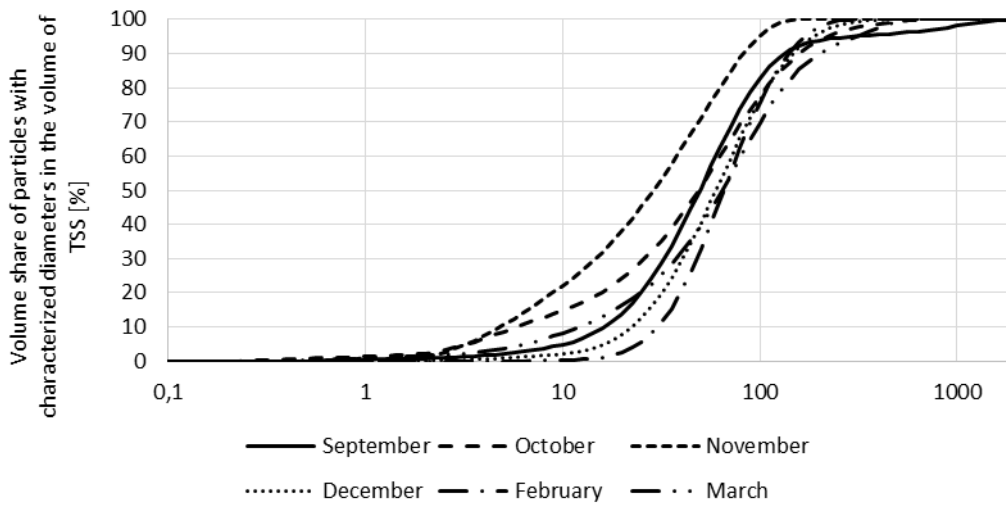


**P1**

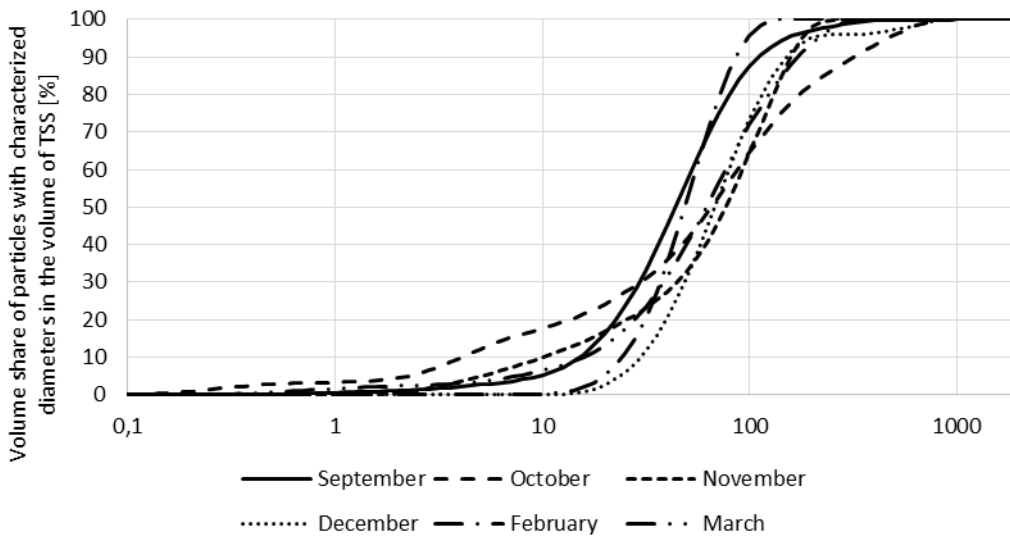




P3



P4

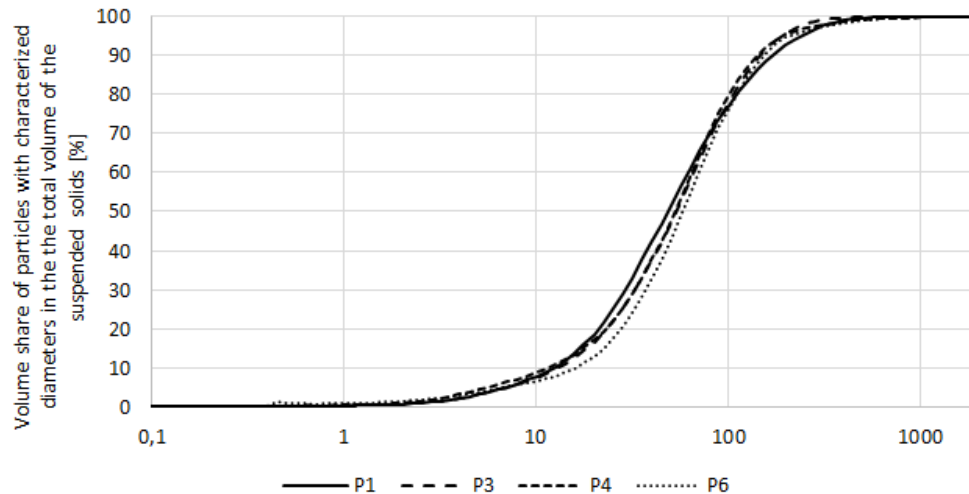


P6

**Figure 2.** Cumulative volume frequency of particles diameter in wastewater taken from 4 sampling points (P1, P3, P4, P6) within six months of measurements

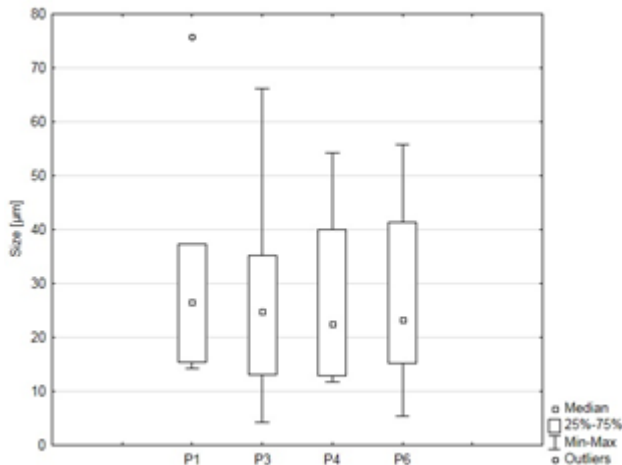
In all sampling points the range of particles sizes was 0.1 to 1000  $\mu\text{m}$ . In all sampling points, in all months from the research period, the vast majority ( $> 90\%$ ) were particles with the  $d_i$  diameters close to 100  $\mu\text{m}$ . The biggest variations of particles size was observed in P1 sampling points, where 90% of  $d_i$  varied from about 80  $\mu\text{m}$  to about 500  $\mu\text{m}$ . In P3 and P4 sampling points changes of diameters in the majority of particles were smaller (around 90 – 350  $\mu\text{m}$ ). In the last sampling point P6 during the most of the time the majority of particles had diameters in the range of 90 – 200  $\mu\text{m}$ .

Taking into consideration the mean values of particles diameters from P1 – P6 points it can be concluded, that in all of the sampling points the majority of particles in the volume of the solution ( $> 90\%$ ) had  $d_i$  higher than 100  $\mu\text{m}$ , and only about 10% accounted for particles with diameters around 10  $\mu\text{m}$  (Figure 3).

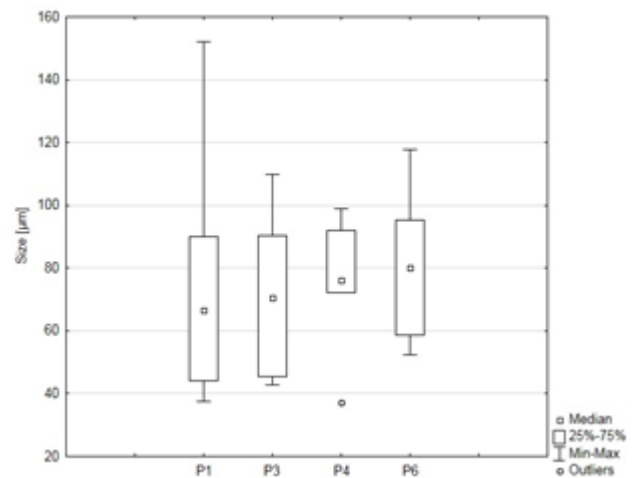


**Figure 3.** Mean cumulative volume frequency of particles diameter in wastewater taken from 4 sampling points (P1, P3, P4, P6)

Identified mean diameters  $D(3.2)$  decisive for the absorption capacity of the particles and mean diameters  $D(4.3)$  conditioning the sedimentation capacity of particles are presented in Figure 4 and Figure 5.



**Figure 4.** Sizes of mean equivalent diameters  $D(3.2)$  in wastewater taken from 4 sampling points (P1-P6)

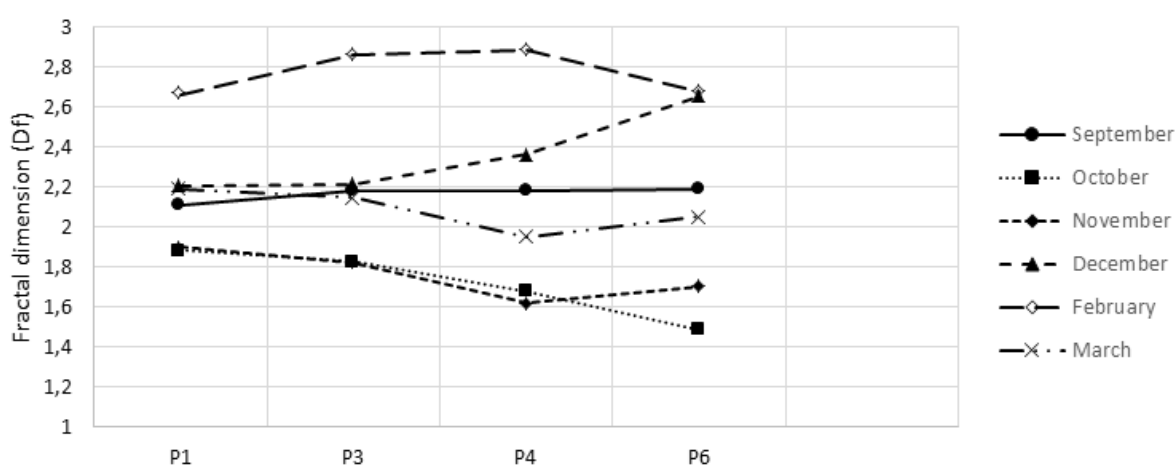


**Figure 5.** Sizes of mean equivalent diameters  $D(4.3)$  in wastewater taken from 4 sampling points (P1-P6)

The sizes of  $D(3.2)$  diameters were slightly changing during the wastewater treatment process in the lagoon. It can be observed that at the beginning of lagoon (P1) the size of  $D(3.2)$  diameter varied

from 14.25  $\mu\text{m}$  to 75.74  $\mu\text{m}$  where in the rest of measuring points the difference between minimal and maximal diameter were bigger. In the outflow from the lagoon minimal D(3.2) diameter was 5.38  $\mu\text{m}$  where the maximal one reached 55.81  $\mu\text{m}$ . The smaller the diameter D(3.2) the active surface of the particles is bigger which increases the efficiency of particles in catalysing chemical reactions (Wiercik et al., 2016).

In the case of D(4.3) diameters, which are calculated on the basis of moment of mass and volume and gives an information about concentration of particles mass in the solution (Kuśnierz and Wiercik, 2016), the difference between minimal and maximal diameter was the biggest in the first measuring point (P1 – biologically treated wastewater) and varied from 37.49  $\mu\text{m}$  to 151.96  $\mu\text{m}$ . The smallest range of diameters sizes was measured in point P4 (37.05  $\mu\text{m}$  – 98.83  $\mu\text{m}$ ), where in the outflow from the lagoon (P6) the D(4.3) were in the range of 52.32  $\mu\text{m}$  to 117.63  $\mu\text{m}$ . The highest D(4.3) diameters the sedimentation properties of the suspended solids are better what is especially important in the wastewater treatment processes.



**Figure 6.** Fractal dimensions of particles in wastewater treated in the hydroponic lagoon

On the basis of the analysis of changes in the intensity of the laser light wave scattering, the fractal dimensions of TSS particles in the wastewater was measured (Figure 6). Identified fractal dimensions (Df) of the particles shows that during the research period the lowest value of  $Df=1.483$  occurred at the outflow of the hydroponic lagoon in October while the highest one  $Df=2.883$  was calculated in the sewage sample from the middle point of the ditch in February. The mean values of Df in all sampling points varied from 2.112 to 2.173. The biggest changes in fractal dimensions were observed for 3 months of measurements (from October to December) but in general no significant changes of fractal dimensions during the flow through the lagoon was observed. Observation of fractal dimensions of particles gives an information about their density and porosity as well as their structure. On the basis of Df values the shape of particles can be characterized. Particles in wastewater can create structures similar to the sphere or appear as clusters of loosely connected particles (Zhao et al., 2013). The fractal dimensions can vary from 1 to 3. The particles with Df close to 1 have linear shape where with the increase of fractal dimension their structure is more expanded. With fractal dimensions nearest to 3 particles create spatial structures (Valle et al., 2017).

## CONCLUSIONS

The environment of hydroponic lagoon (present of plants, algae, invertebrates, protozoa) as well as physical conditions (intensive aeration) have huge impact on the size and properties of particles. On the basis on conducted calculations it can be concluded that during the entire research period, in all

of the sampling points the vast majority of identified particles was bigger than 100  $\mu\text{m}$ . In general, particles sizes in the hydroponic lagoon varied from 0.01 $\mu\text{m}$  to 1000  $\mu\text{m}$ . Analyses of the average diameters  $D(3.2)$  and  $D(4.3)$  has shown that identified particles have small reactivity ( $D(3.2) > 10 \mu\text{m}$ ) but good sedimentation capacity ( $D(4,3) > 50\mu\text{m}$ ) what is the most important particle feature for the wastewater treatment processes. The mean values of fractal dimensions of particles in all sampling points varied from 2.112 to 2.173 what gives an information that particles of suspended solids in wastewater have well-developed surface.

On the basis of information about the shape and size of particles identified in the sewage from 4 sampling points of hydroponic ditch it can be assumed that most of the particles flowing out of the WWTP are algae or particles that can absorb on their surface other pollutants. The use of laser granulometry for particles identification might be useful in determining the total suspended solids character as well as can help to develop cheaper and more efficient methods of its removal. It is especially important in semi-natural systems where the role of algae in purification processes cannot be omitted.

## REFERENCES

- Andersen, J. H., Carstensen, J., Conley, D. J., Dromph, K., Fleming-Lehtinen, V., Gustafsson, B. G., et al. (2017) Long-term temporal and spatial trends in eutrophication status of the Baltic Sea. *Biological Reviews in Cambridge Philosophical Society*, **92**(1), 135-149.
- Barros, A. I., Goncalves, A. L., Simoes, M., Pires, J. C. M. (2015) Harvesting techniques applied to microalgae: a review. *Renewable & Sustainable Energy Reviews*, **41**, 1489-1500.
- Bawiec, A., Garbowski, T., Pawęska, K., Pulikowski, K. (2019) Analysis of the Algae Growth Dynamics in the Hydroponic System with LEDs Nighttime Lighting Using the Laser Granulometry Method. *Water, Air & Soil Pollution*, **230**,17.
- Bawiec, A., Pawęska, K., Pulikowski, K. (2017) Analysis of granulometric composition of algal suspensions in wastewater treated with hydroponic method. *Water, Air & Soil Pollution*, **228**, 366.
- Bilotta, G. S., Brazier, R. E. (2008) Understanding the influence of suspended solids on water quality and aquatic biota; *Water Research*, **42**(12), 2849-2861.
- Cai, W., Zhao, Z., Li, D., Lei, Z., Zhang, Z., Lee, D. J. (2019) Algae granulation for nutrients uptake and algae harvesting during wastewater treatment. *Chemosphere*, **214**, 55-59.
- Cheremisinoff, P. N. (1995) *Handbook of Water and Wastewater Treatment Technology*, Marcel Dekker, New York.
- Garbowski, T., Pulikowski, K., Wiercik, P. (2017) Using laser granulometer to algae dynamic growth analysis in biological treated sewage. *Desalination and Water Treatment*, **99**, 117-124.
- Glibert, P. M., Beusen, A. H. W., Harrison, J. A. et al. (2018a) Changing land-, sea- and airscapes: sources of nutrient pollution affecting habitat suitability for harmful algae. In: Glibert, P.M., Berdalet, E., Burford, M. et al. (eds) *Global ecology and oceanography of harmful algal blooms*. Springer, 53-76.
- Hu, Y., Hao, X., van Loosdrecht, M., Chen, H. (2017) Enrichment of highly settleable microalgal consortia in mixed cultures for effluent polishing and low-cost biomass production. *Water Research*, **125**, 11-22.
- Kelly, P., Gonzalez, M. J., Renwick, W. H., Vanni, M. J. (2018) Increased light availability and nutrient cycling by fish provide resilience against reversing eutrophication in an agriculturally impacted reservoir. *Limnology and Oceanography*, **63**, 2647-2660.
- Kouamé Kouamé, V., Yapoga, S., Kouadio Kouakou, N., Sanogo, T. A., Celestin, A. B. (2016). Phytoremediation of wastewater toxicity using water hyacinth (*Eichhornia crassipes*) and water lettuce (*Pistia stratiotes*). *International Journal of Phytoremediation*, **18**(10), 949-955.

- Kuśnierz, M., Łomotowski, J. (2015) Using Avrami equation in the studies on changes in granulometric composition of algal suspension. *Hydrobiologia*, **758**, 243-255.
- Kuśnierz, M., Wiercik, P. (2016) Analysis of particle size and fractal dimensions of suspensions contained in raw sewage, treated sewage and activated sludge. *Archives of Environmental Protection*, **42**, 67-76.
- Nolte, H., Schilde, C., Kwade, A. (2012) Determination of particle size distributions and the degree of dispersion in nanocomposites. *Composites Science and Technology*, **72**, 948-958.
- Redding, J. M., Schreck, C. B., Everest, F. H. (1987) Physiological Effects on Coho Salmon and Steelhead of Exposure to Suspended Solids. *Transactions of the American Fisheries Society*, **116**(5), 737-744.
- Remo, J., Ruben, A. H. Ickes, B. (2016) Particle size distribution of main-channel-bed sediments along the upper Mississippi River, USA. *Geomorphology*, **264**, 118-131.
- Samori, G., Samori, C., Guerrini, F., Pistocchi, R. (2013) Growth and nitrogen removal capacity of *Desmodesmus communis* and of a natural microalgae consortium in a batch culture system in view of urban wastewater treatment: Part I. *Water Research*, **47**(2), 791-801.
- Su, Y., Mennerich, A., Urban, B. (2012) Synergistic cooperation between wastewater-born algae and activated sludge for wastewater treatment: Influence of algae and sludge inoculation ratios. *Bioresource Technology*, **105**, 67-73.
- Suresh, G., Sutharsan, P., Ramasamy, V., Venkatachalapathy, R. (2012) Assessment of spatial distribution and potential ecological risk of the heavy metals in relation to granulometric contents of Veeranam lake sediments, India. *Ecotoxicology and Environmental Safety*, **84**, 117-124.
- Smyk, J., Ignatowicz, K., Struk-Sokołowska, J. (2015) COD fractions changes during sewage treatment with constructed wetland. *Journal of Ecological Engineering*, **16**, 43-48.
- Tinke, P., Carnicer, A., Govoreanu, R., Scheltjens, G., Lauwerysen, L., Mertens, N., et al. (2008) Particle shape and orientation in laser diffraction and static image analysis size distribution analysis of micrometer sized rectangular particles. *Powder Technology*, **186**, 154-167.
- Valle, F., Brucale, M., Chiodini, S., Bystrenova, E., Albonetti, C. (2017) Nanoscale morphological analysis of soft matter aggregates with fractal dimension ranging from 1 to 3. *Micron*, **100**, 60-72.
- Wagner, M., Lambert, S. (2018) Freshwater microplastics, Emerging Environmental Contaminants? in *The Handbook of Environmental Chemistry 58* by Barceló, D. and Kostianoy, A.G. DOI: 10.1007/978-3-319-61615-5.
- Wiercik, P., Matras, K., Burszta-Adamiak, E., Kuśnierz, M. (2016) Analysis of the properties and particle size distribution of spent filter backwash water from groundwater treatment at various stages of filters washing. *Engineering and Protection of Environment*, **19**(1), 149-161.
- Whitton, R., Le Mevel, A., Pidou, M., Ometto, F., Villa, R., Jefferson, B. (2016) Influence of microalgal N and P composition on wastewater nutrient remediation. *Water Research*, **91**, 371-378.
- Xu, R. (2015) Light scattering: a review of particle characterization applications. *Particuology*, **18**, 11-21.
- Ye, J., Song, Z., Wang, L., Zhu, J. (2016) Metagenomic analysis of microbiota structure evolution in phytoremediation of a swine lagoon wastewater. *Bioresource Technology*, **219**, 439-444.
- Zhao, P., Ge, S., Chen, Z., Li, X. (2013) Study on pore characteristics of flocs and sludge dewaterability based on fractal methods (pore characteristics of flocs and sludge dewatering). *Applied Thermal Engineering*, **58**, 217-223.
- Zhu, B., Xia, X., Zhang, S., Tang, Y. (2018) Attenuation of bacterial cytotoxicity of carbon nanotubes by riverine suspended solids in water. *Environmental Pollution*, **234**, 581-589.

# Evaluation of Sentry Sensor for Real-time Biochemical Oxygen Demand Measurement Capabilities

A. Bolgár\*, G. Boldizsár\*, S. M. Miskei\* and R. Blanc\*

\* Organica Technológiák Zrt., 59 Tüzoltó Street, Budapest 1093, Hungary  
(E-mails: [andrea.bolgar@organicawater.com](mailto:andrea.bolgar@organicawater.com); [gergo.boldizsar@organicawater.com](mailto:gergo.boldizsar@organicawater.com);  
[sandor.miskei@organicawater.com](mailto:sandor.miskei@organicawater.com); [remy.blanc@organicawater.com](mailto:remy.blanc@organicawater.com))

## Abstract

The Sentry bio-electrode sensor is mainly used in anaerobic digester systems to prevent the effects of toxic shock, system imbalance, poor performance and to get a better yield for biogas production. A novel approach in the application of the sensor is in aerated wastewater treatment systems, especially to measure Biological Oxygen Demand (BOD) based on true microbial activity. Although BOD<sub>5</sub> is still the basis of designs and effluent limits in the wastewater industry, the standard lab measurement for this parameter carries more error than a standardized measurement of a chemical parameter, e.g. Chemical Oxygen Demand (COD) and takes 5 days to complete.

The sensor was tested in an Organica Water facility in different locations along the treatment process: in the primary clarifier (influent), after the secondary clarifier (effluent) and in the beginning and end of the aerated biological reactors. The measured values (Microbial Electron Transfer - MET) were correlated to standard laboratory parameters, such as Total CBOD<sub>5</sub>, Total COD and filtered COD.

The results for the influent and combined influent and effluent were correlating to TC very well, ( $R^2 > 80\%$ ) with a mean relative error of 7% and 13% respectively. As a conclusion the Sentry sensor can be used with high confidence for actual TC BOD<sub>5</sub> measurement in influent and effluent. To measure exact TC BOD<sub>5</sub> values, the sensor needs matrix-specific calibration, but the raw MET value is also suitable to indicate the changes in the biologically degradable materials in the water.

Another promising application is early warning for toxic materials; as opposed to usual COD-based online measurement methods (sensors and analyzers) which cannot indicate degradability or toxicity of the incoming material, changes in biodegradability can be reliably detected by the Sentry bio-electrode sensor. This means that wastewater treatment plant operators can see the changes of the influent characteristics in real-time and they are able to prepare their plant for the negative effects.

## Keywords

BOD; Biochemical Oxygen Demand; sensor; online; real time; toxicity

## INTRODUCTION

### Measuring BOD

In recent times the online and real-time measurement of Biological Oxygen Demand (BOD) has surfaced more and more as a requirement in wastewater treatment plant operation. Although this parameter is still the basis of design and effluent limits in the wastewater industry thanks to its potential to characterize the biodegradable organic content of a certain type of wastewater, this is not an easy and straightforward parameter to measure. For a standard CBOD<sub>5</sub> (20 °C) measurement, a wastewater sample needs to be incubated at constant 20 °C temperature and the oxygen consumption of the bacteria to be measured. Since there are multiple sources of error during sample preparation and the 5 days of measurement time, this biological measurement carries more error and takes more time than a standardized measurement of a similar parameter, like Chemical Oxygen Demand (APHA, 2012). Yet, most authorities still require the effluent compliance to be expressed as CBOD<sub>5</sub>, however if there is a process upset, the operators can only be warned about it after the 5 days of incubation has passed, assuming they rely solely on laboratory BOD measurements.

### Online sensors

To be able to act faster when process disturbances occur, operators started relying on online instrumentation. The most commonly measured parameter is Dissolved Oxygen (DO), which gives an overview of the composition of wastewater indirectly, through the biological activity of the bacteria. Since the DO measured can be influenced by a number of external parameters (amount of air introduced into the water body, temperature, amount of biomass, concentration of contaminants, etc.), other sensors were developed to measure the organic content indirectly or semi-directly. Most of them rely on the UV absorption of aromatic components in the organic materials, like proteins and use various approaches: single wavelength (Kellner et al., 2014), multi-wavelength (Rieger et al., 2004) or excitation and emission of a specific protein component (Khamis et al., 2017).

A novel approach for online BOD measurement is based on utilizing the metabolic pathways of microbes of the Proteobacteria genus which can use metal surfaces as electron acceptor thus generating an electrical signal which can be measured (Lovley et al., 2011). The exo-electrogenic microbes growing on the anode surface of the sensor consume organic material and use the cathode as electron acceptor; between the two metals the resistance is measured and the signal called Microbial Electron Transfer (MET) is generated. This enables the correlation of the MET signal only to the biodegradable components of the bulk wastewater, preventing false readings for non-biodegradable organic substances which would be included in absorption- or emission-based measurements. This also means that the measured signal can reflect the inhibition of the bacteria when toxic components are present in the wastewater together with readily biodegradable material. This paper describes the performance evaluation of the Sentry bio-electrode sensor based on the above-mentioned measurement principle, which was tested at a municipal wastewater treatment plant. Multiple parameters associated with organic content were measured using standard laboratory methods and the measured value from the sensor were compared to those. The effect of toxic components on the measured signal is also investigated based on the vital response of the microorganisms.

## MATERIALS AND METHODS

### Testing locations

The sensors were installed at multiple locations in the South-Pest Wastewater Treatment Plant, Budapest, Hungary. The wastewater characteristics (organic levels and matrix) varied widely along the different installation locations at this municipal plant: for influent the sensor was placed on the bridge of the primary clarifier, for effluent in the effluent chamber of a secondary clarifier. It was also installed inside the aerated reactors (containing MLSS) both near the beginning and the end of the aerated zone.

After every change in the installation location, the sensors were inoculated between two to three weeks to allow the biofilm on the sensor anode to grow and adapt to the new environment. Reference sampling started only afterwards.

### Lab measurements

Unfiltered grab samples were taken regularly next to the sensor and the following lab measurements were carried out: total COD (TCOD), filtered COD (0.45  $\mu\text{m}$  filtered, fCOD), total CBOD<sub>5</sub> (TCBOD<sub>5</sub>). COD was determined using Hach LCK 314 and LCK 514 cuvette testkits, while TCBOD<sub>5</sub> was measured using WTW OxiTop® Respirometric BOD measuring system at 20 °C. The samples were stored in cooling boxes while transported to the laboratory nearby. The BOD samples were prepared right away to prevent further biodegradation of organics.

## Calculations

The sensor data was regularly downloaded and the  $TCBOD_5$ ,  $TCOD$  and  $fCOD$  values were correlated with the MET value measured by the sensors. The original sensor data was reconciled for the different parameters using the linear regression equations (1).

$$MET = a * TBOD_5 + b \quad (1)$$

## Toxic response measurement

For the evaluation of the effect of toxic components, sodium hypochlorite (household bleach, 17-19 % solution, 2 x 10 mL), hydrogen chloride (household hydrochloric acid, 20 ±2 %, 15 mL), sodium hydroxide (Reanal technical grade, 3M solution, 10 mL + 14 mL) and saturated salt solution (table salt, saturated solution, 2 x 0.5 L) were added to a bucket of wastewater respectively, while the bio-electrode sensor was also placed in the bucket. The wastewater was taken from the same location the sensor was installed previously so the effect of a different matrix can be eliminated, and the measured signal was recorded alongside pH and conductivity.

## RESULTS AND DISCUSSION

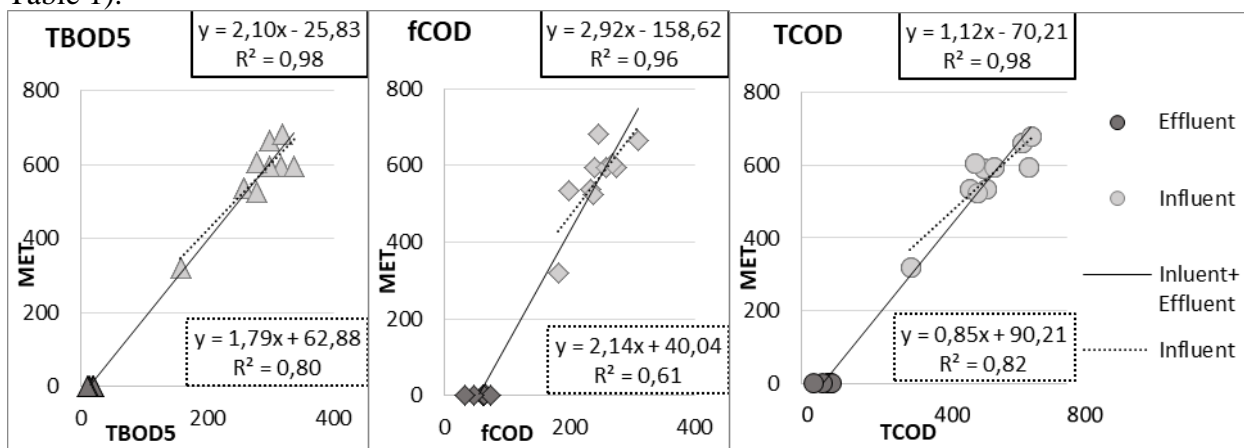
### Biofilm on the sensor

The biofilm was investigated while the sensor was installed in the different locations. While it was installed the primary clarifier an anaerobic-looking black-brown biofilm populated the sensor surface. When the sensor was installed in the secondary clarifier effluent the biofilm was very thin, almost undetectable. The biofilm resembled more a healthy-looking fix-filmed type when it was installed in the aerated reactors with a brown-greyish color.

### Linear regression – Influent and Effluent

After evaluating the reference measurements, the most accurate linear regression values were found for influent, with  $R^2$  of 0.8, Mean Residual Error (MRE) of 7 % and Normalized Root Mean Square Error (NRMSE) of 13 % for  $TBOD_5$  (Figure 1). The correlation was similarly good for  $TCOD$  but was less accurate in case of  $fCOD$  (Table 1).

The measured sensor data from the secondary clarifier effluent showed the least variability (Figure 2) but an acceptable correlation could also be determined (Table 1). With enough time provided for inoculation and conditioning of the sensor at both locations, the results show a good correlation even if all the obtained influent and effluent datapoints are plotted on the same graph: the  $R^2$  metric improved for all parameters while the MRE remained in the same range. (Figure 1, Table 1).

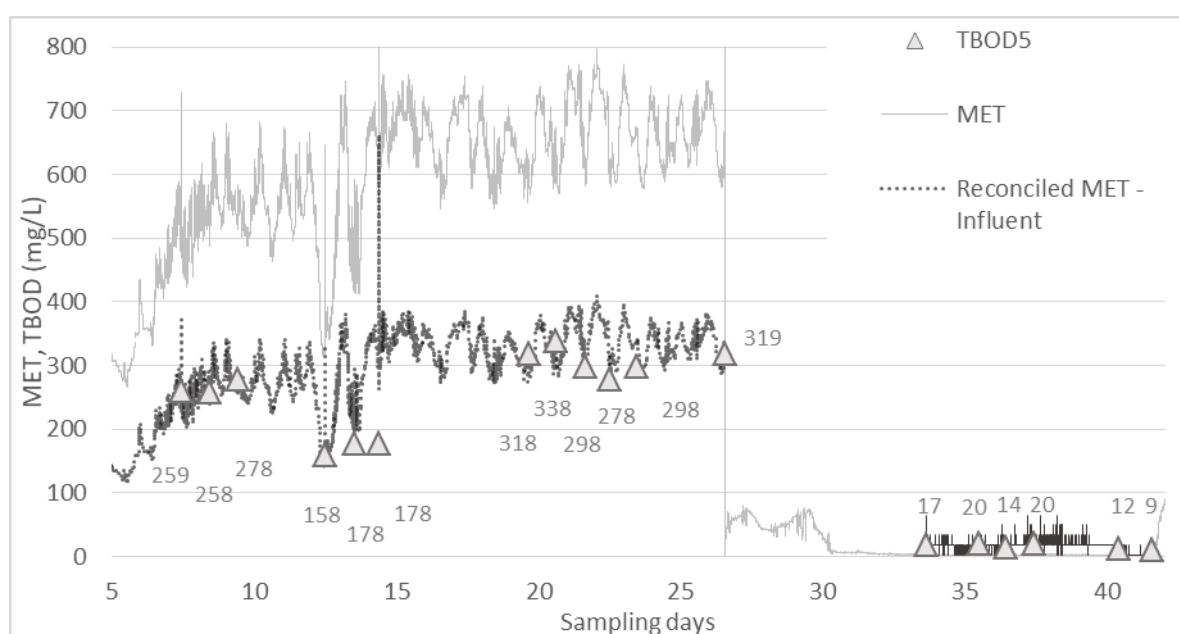


**Figure 1.** Linear regression for influent and combined influent and effluent  $TBOD_5$ ,  $fCOD$  and  $TCOD$



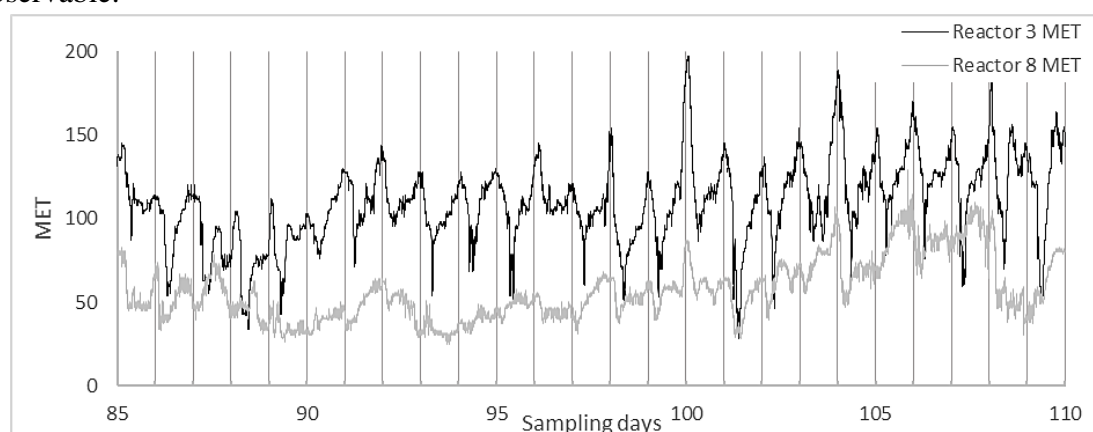
**Table 1.** Coefficient of determination ( $R^2$ ), Mean Residual Error (MRE) and Normalized Root Mean Square Error (NRMSE) of correlation of influent and effluent measurements

	Influent			Effluent			Influent + Effluent		
	$R^2$	MRE	NRMSE	$R^2$	MRE	NRMSE	$R^2$	MRE	NRMSE
TBOD <sub>5</sub>	0.8032	7.0%	13.1%	0.4846	29.8%	38.1%	0.9838	13.1%	5.3%
fCOD	0.6140	9.4%	21.5%	0.4873	29.1%	57.6%	0.9592	6.9%	7.4%
TCOD	0.8202	7.4%	13.1%	0.5094	20.2%	32.5%	0.9769	8.6%	6.0%

**Figure 2.** Original and reconciled sensor data and lab data– Influent and Effluent TBOD<sub>5</sub>

### Results from aerated reactors

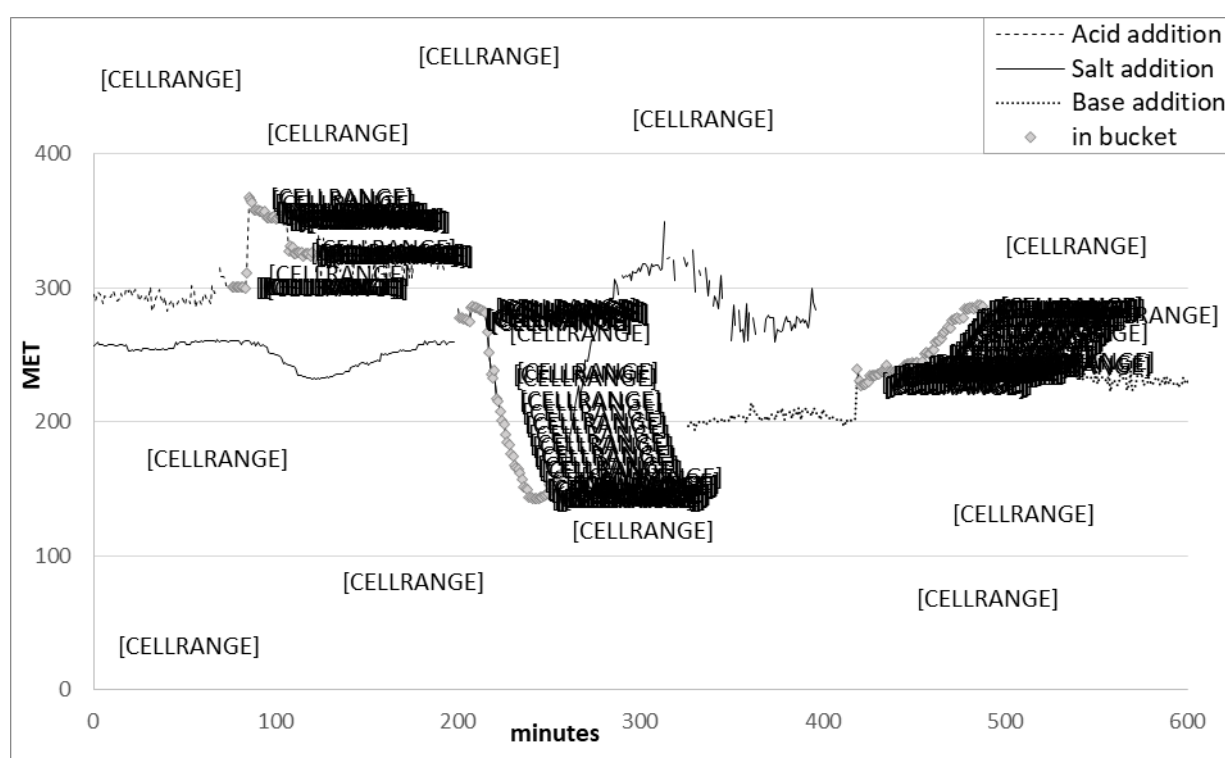
A high daily variation in the signal was observed for locations inside the aerated reactors. The sensor did not seem to be influenced by the surrounding flocs of microbes in the water although a similar composition biofilm appeared on the anode. The correlation with the measured lab parameters did not come close to the influent correlation but the daily fluctuations were clearly detectable from the changes in MET (Figure 3). The peak reached the beginning of the aerated zone, Reactor 3 around midnight and the lowest value was observed during the morning, between 7 and 9 AM. The peaks and valleys at the end of the aerated zone (Reactor 8) were less distinct but still observable.

**Figure 3:** Measured sensor value in aerated reactors Reactor 3 and Reactor 8

### Toxicity tests

There was no considerable change observed during hypochlorite addition. After addition of HCl, the pH decreased to 2, which increased the signal in a single step; afterwards the measured signal was stable. When it was moved back to unspiked reactor water, the signal dropped back to a lower level, but higher than the original. After the addition of NaOH, the pH increased to 11.5, which caused a monotonous rise in the signal. When it was moved back to unspiked reactor water the measured value stabilized on the level before the base addition instantly.

The addition of salt resulted in a completely different outcome: after the addition of the salty water, the signal started gradually decreasing similar to an exponential decay. When it was placed back to unspiked reactor water, the decrease slowed down and stopped, then the signal very slowly started increasing. The measured value only returned to normal after half an hour (Figure 4).



**Figure 4:** Responses in MET signal for different toxic events

### CONCLUSION

As a conclusion, the Sentry bio-electrode sensor is suitable to measure TC<sub>BOD</sub><sub>5</sub> concentrations in the influent and effluent of a municipal wastewater treatment plant, given that the proper measurement for correlating the MET and TC<sub>BOD</sub><sub>5</sub> values are done. Even without correlation to TC<sub>BOD</sub><sub>5</sub> or other parameters, the MET value can be used to indicate the concentration changes of biologically degradable materials in the water.

The following potential ways of application were determined for the sensor (Table 2).

**Table 2:** Potential ways of application, installation locations and calibration requirements

Potential use	Installation location	Calibration required?
Following daily changes in the wastewater composition	Influent, aerated reactors	No
Measuring concentration and determine the load to the treatment plant real-time	Influent	Yes
Applying process-control based on the determined load	Influent	Yes
Optimizing aeration control	Aerated reactors	No
Optimizing carbon dosing for denitrification	Influent, aerated reactors	Yes
Indicating toxic materials in the influent and applying preventive actions in the operation	Influent, aerated reactors	No
Following effluent compliance on-line	Effluent	Yes
Catching non-compliant periods which would not be possible with conventional lab sampling	Effluent	Yes

## ACKNOWLEDGEMENTS

We would like to thank the South-Pest WWTP for providing the opportunity for testing the sensors. We also thank Island Water Technologies for providing us the sensors to test and supported us in publishing the results.

## REFERENCES

- APHA (2012) Standard methods for the examination of water and wastewater, 22nd edn. American Public Health Association, Washington, DC.
- Khamis K. et al. (2017) Continuous field estimation of dissolved organic carbon concentration and biochemical oxygen demand using dual-wavelength fluorescence, turbidity and temperature. *Hydrological Processes*, **31**, 540-555.
- Kellner, K., Posnicek, T., Brandl, M. (2014) An Integrated Optical Measurement System for Water Quality Monitoring. *Procedia Engineering*, **87**, 1306-1309.
- Lovley, R. D., Ueki, T., Zhang, T., Malvankar, N., Shrestha, P., Flanagan, K., Aklujkar, M., Butler, J., Giloteaux, L., Rotaru, A.-E., Holmes, D., Franks, A., Orellana, R., Risso, C., Nevin, P. K. (2011) Geobacter: The Microbe Electric's Physiology, Ecology, and Practical Applications. *Advances in microbial physiology*, **59**, 1-100.
- Rieger, L., Langergraber, G. Thomann, M. Fleischmann, N., Siegrist, H. (2004) Spectral in-situ analysis of NO<sub>2</sub>, NO<sub>3</sub>, COD, DOC and TSS in the effluent of a WWTP. *Water science and technology: a Journal of the International Association on Water Pollution Research*, **50**, 143-52.

# Micropollutants Removal in Submerged Membrane Bioreactors at Different SRT Values and Variations of Extracellular Polymeric Substances

A. Caglak\*, H.Sari Erkan\* and G. Onkal Engin\*

\* Department of Environmental Engineering, Yildiz Technical University, Esenler, 34220 Istanbul, Turkey  
(E-mails: [acaglak@yildiz.edu.tr](mailto:acaglak@yildiz.edu.tr); [hsari@yildiz.edu.tr](mailto:hsari@yildiz.edu.tr); [gengin@yildiz.edu.tr](mailto:gengin@yildiz.edu.tr))

## Abstract

Extracellular polymeric substances (EPS) secreted from activated sludge are very important in a membrane bioreactor (MBR) in terms of filterability of activated sludge and membrane fouling. This study aimed to investigate the effect of SRT and micropollutants existence of wastewater in an MBR on EPS and soluble microbial products (SMP) of activated sludge. In the study, obtained results indicate that the EPS content and SMP concentration in the supernatant decreased with an increasing of SRT values from 15 days to 90 days. The results also indicated that the micropollutants existence of feed wastewater should affect the concentrations of EPS and SMP in submerged MBRs.

## Keywords

Membrane bioreactors, micropollutant, SRT, EPS, SMP

## INTRODUCTION

Endocrine disrupting compounds (EDCs) are becoming of primary concern, given their increased use and, in turn, their increased presence in our aquatic environment (Tijani, et al., 2013; Palacios-Rosas and Castro-Pastrana, 2017). These human-made micropollutants such as pharmaceuticals, hormones, phenolic compounds, phthalates and pesticides can be found in aquatic environment. they are known to be toxic and bioaccumulative due to their persistent properties. Therefore, suitable wastewater treatment method must be applied to remove micropollutants in order to eliminate their toxic effects on human and environment (Goswami et al., 2018).

Generally, conventional activated sludge (CAS) processes are used in wastewater treatment plants (WWTP) and these processes are not efficient to completely remove the micropollutants due to designing mainly to eliminate simple organic matters and nutrients (Arlaga et al., 2016). On the other hand, monitoring the concentrations of micropollutants in raw and treated wastewater are not ensured mainly due to the WWTPs' equipment insufficient (Bolong et al., 2009). Their concentrations were found in the effluent of conventional activated sludge processes at various concentrations from few nanograms per liter (ng/L) up to several micrograms per liter ( $\mu\text{g/L}$ ) due to their limited capability to remove these contaminants (Verlicchi et al., 2012; Nguyen et al., 2013). Therefore, re-designing of WWTPs and some modifications of operating conditions such as hydraulic retention time, aeration, vigorous mixing and supplementation with inorganic nutrients have been suggested for a better control and handling of micropollutants (Camocho-Munoz et al., 2012). However, the outcomes of these re-designing and modifications' outcomes are not sufficient for the removal of micropollutants (Zhao et al., 2014).

Some physico-chemical treatment techniques such as advance oxidation processes, adsorption, nanofiltration have also been investigated as a post-treatment for the removal of micropollutants (Slegrist and Joss, 2012). However, these approaches have some drawbacks like high investment cost, high energy demand, secondary sludge disposal problem and requirement of toxic chemicals

(Goswami et al., 2018).

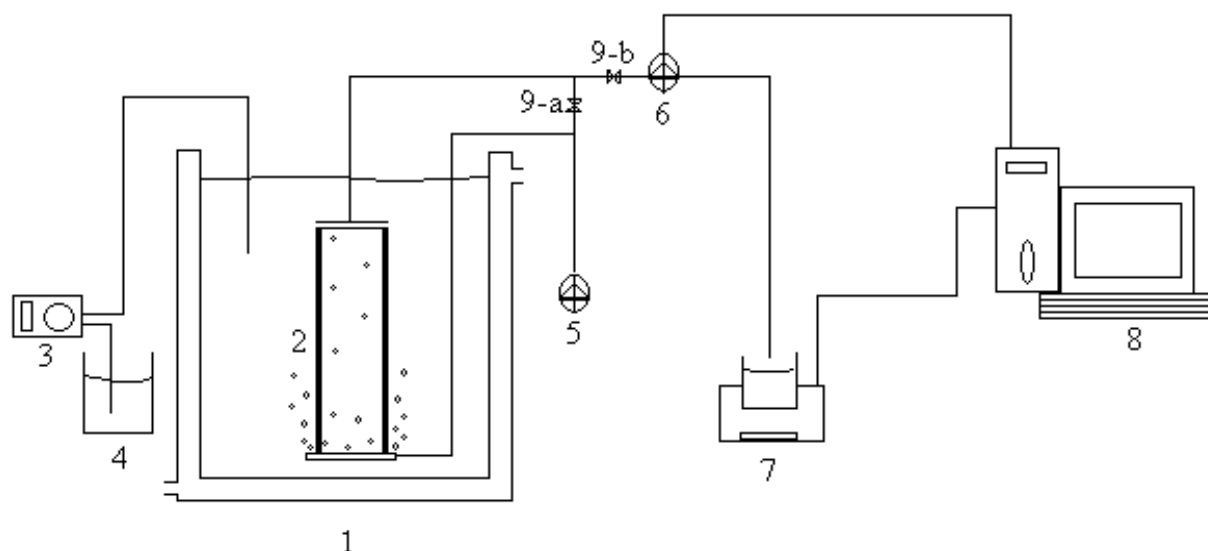
Membrane bioreactor (MBR) technologies have been used over the past two decades and several pollutants such as carbonaceous substances, nutrients, particulate matters and pathogenic microorganisms (Mir-Tutusaus et al., 2018). Although these pollutants removal are easier than micropollutants, MBRs have been promising approach for the removal of micropollutants. Removal efficiency of selected 15 EDCs, having each EDC's concentration in the range of 1-5 µg/L, were found between 92 % and 99 % by MBR (Gruchlik et al., 2018). It was also reported that personal care products were completely removed with MBR (Goswami et al., 2018). On the other hand, pharmaceuticals for examples antibiotics such as lorazepam, ibuprofen, primidone and carbamazepine were removed at the range of 75 % and 95 % using by MBR (Besha et al., 2017). The removal efficiencies of micropollutants with MBR technology can be in the following order: EDCs > beta blockers > pharmaceuticals > pesticides (Le-Clech et al., 2010; Ahmed et al., 2017; Gruchlik et al., 2018). The biodegradation of micropollutants is influenced by SRT, which is considered as the most significant parameter for pharmaceuticals (Nasirabadi et al., 2016).

Several factors such as microbial community structure and its activities effect of operating conditions and main drawback is fouling occurred on the membrane surfaces and pores in MBRs (Goswami et al., 2018). Extracellular polymeric substances and soluble microbial products secreted by microorganisms play important role in terms of membrane fouling leading to cake layer formation and pore blocking in MBRs (Teychene et al., 2008). The operating conditions such as sludge retention time (SRT), hydraulic retention time and aeration affect the concentrations of EPS and SMP. There were contradictory results in literature whether increasing SRT lead to decreasing EPS concentration or not (Lee et al., 2003; Cho et al., 2005; Massé et al. 2006; Erkan et al., 2016).

This paper presents possible treatment of some micropollutants by submerged membrane bioreactor (sMBR) at 15 days and 90 days of SRT. The study also focuses on the production of EPS and SMP in MBRs.

## **MATERIALS AND METHODS**

Two lab scale submerged MBRs made of plexi-glass were used in the study (Figure 1), having 5 L effective volume (R1: test MBR (micropollutants added), R2: control MBR). The MBRs were seeded activated sludge obtained from a municipal wastewater treatment plant in Istanbul and operated at a constant permeate flux (7.3 L/m<sup>2</sup>·h) under the same hydraulic retention time (HRT) of 12 h. The reactors were fed with synthetic municipal wastewater having concentrations of 400 mg/L COD, 20 mg/L NH<sub>4</sub><sup>+</sup>-N, 5 mg/L PO<sub>4</sub><sup>3-</sup>-P (prepared with tap water according to Bakaraki et al., 2016). Ceramic membrane modules (nominal pore size 0.1 µm), having an effective filtration area of 0.057 m<sup>2</sup>, were used in the test and control MBRs. Oxygen was supplied with a stainless steel diffuser located at the bottom of the reactor and installed on an air pump. The temperature of mixed liquor was kept constant 22.0 ± 1 °C by recirculating water in the heat jacket of the reactors, and pH was remained stable between 7.4-7.8. The operations of MBRs were controlled by an automation system having half hour suction and half hour relaxation time. The ceramic membrane modules were cleaned manually with tap water and then back-blown with pressured air (1.8 bar) once in a week and chemically cleaned once a month at SRT 15, back-blown with pressured air for once in 20 days and chemically cleaned for once in two month at SRT 90.



**Figure 1.** Test and control MBRs (1), ceramic membrane module (2), pump (3), feed tank (4), air compressor (5), vacuum pump (6), analytical balance (7), computer (control and automation) (8), automated valve (9)

4-tert-octylphenol, di-n-octyl phthalate (endocrine disruptors), fluoxetine (pharmaceutical), estrone (hormone), and atrazine, penconazole, chlorpyrifos ethyl, malathion, cypermethrin, (pesticides) were selected as an organic micropollutants for this study and mixture of these micropollutants, prepared with pure methanol, were added to the synthetic wastewater in the R1 MBR after reached the steady-state condition. The test and control MBRs were operated between 0-50 days and 51-193 days at 15 and 90 days of SRT, respectively. Permeate samples were taken twice a week to monitor removal efficiencies for conventional parameters as well as for micropollutants. The concentration of each analyte in the synthetic wastewater, diluted from stock solution thousand-fold, were determined and found to be between 7-605  $\mu\text{g/L}$  according to the detection limits in the GC/MS protocol.

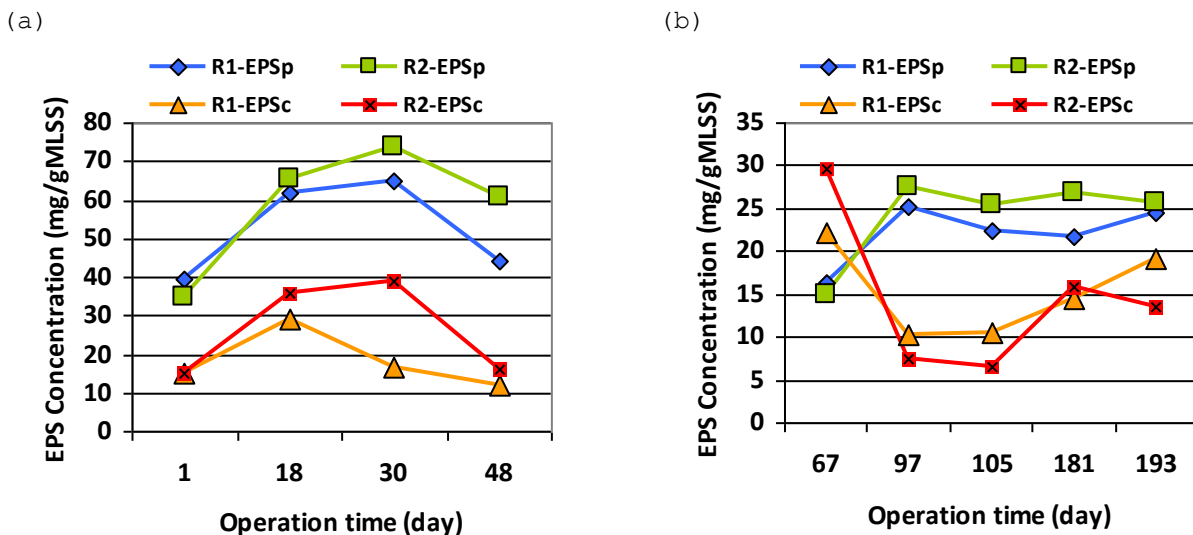
The analyses of micropollutants in the liquid samples were conducted according to Caglak et al. (2019) with dispersive liquid-liquid micro-extraction (DLLME) method by a GC/MS system (Agilent 6890) equipped with HP-5MS capillary column (30 m x 250  $\mu\text{m}$ ; 0.25  $\mu\text{m}$ ) and a mass selective detector. All organic compounds were purchased from Sigma-Aldrich (Germany). The measurements of COD, ammonia nitrogen ( $\text{NH}_4^+\text{-N}$ ), and orthophosphate ( $\text{PO}_4^{3+}\text{-P}$ ) in the feed wastewater and permeate, and the MLSS analysis in the sMBRs were carried out according to the Standard Methods (2005). The extracellular polymeric substances (EPS) and soluble microbial products (SMP) were conducted by the extraction method which was used by Tinggang et al. (2008). Carbohydrate and protein fractions of EPS and SMP were measured by the phenol-sulphuric acid method (Dubois et al. 1956) and the Lowry method (Lowry et al. 1951).

## RESULTS AND DISCUSSION

After the addition of micropollutants mix solution to the MBR system at steady state conditions, treated effluent samples were taken from the reactor twice a week to monitor the MBR performance. The MLSS concentrations of R1 and R2 MBR were about 3345 mg/L and 3215 mg/L the study at an SRT value of 15 days at an HRT value of 12 hour. The average COD,  $\text{NH}_4^+\text{-N}$  and  $\text{PO}_4^{3+}\text{-P}$  removal efficiencies were found to be 96.7, 86.1 and 56.1 %, respectively. The mean MLSS values of R1 and R2 MBR were determined 13655 mg/L and 11380 mg/L at 90 days SRT. The average COD,  $\text{NH}_4^+\text{-N}$  and  $\text{PO}_4^{3+}\text{-P}$  removal efficiencies were also found 98.13 %, 91.4 % and

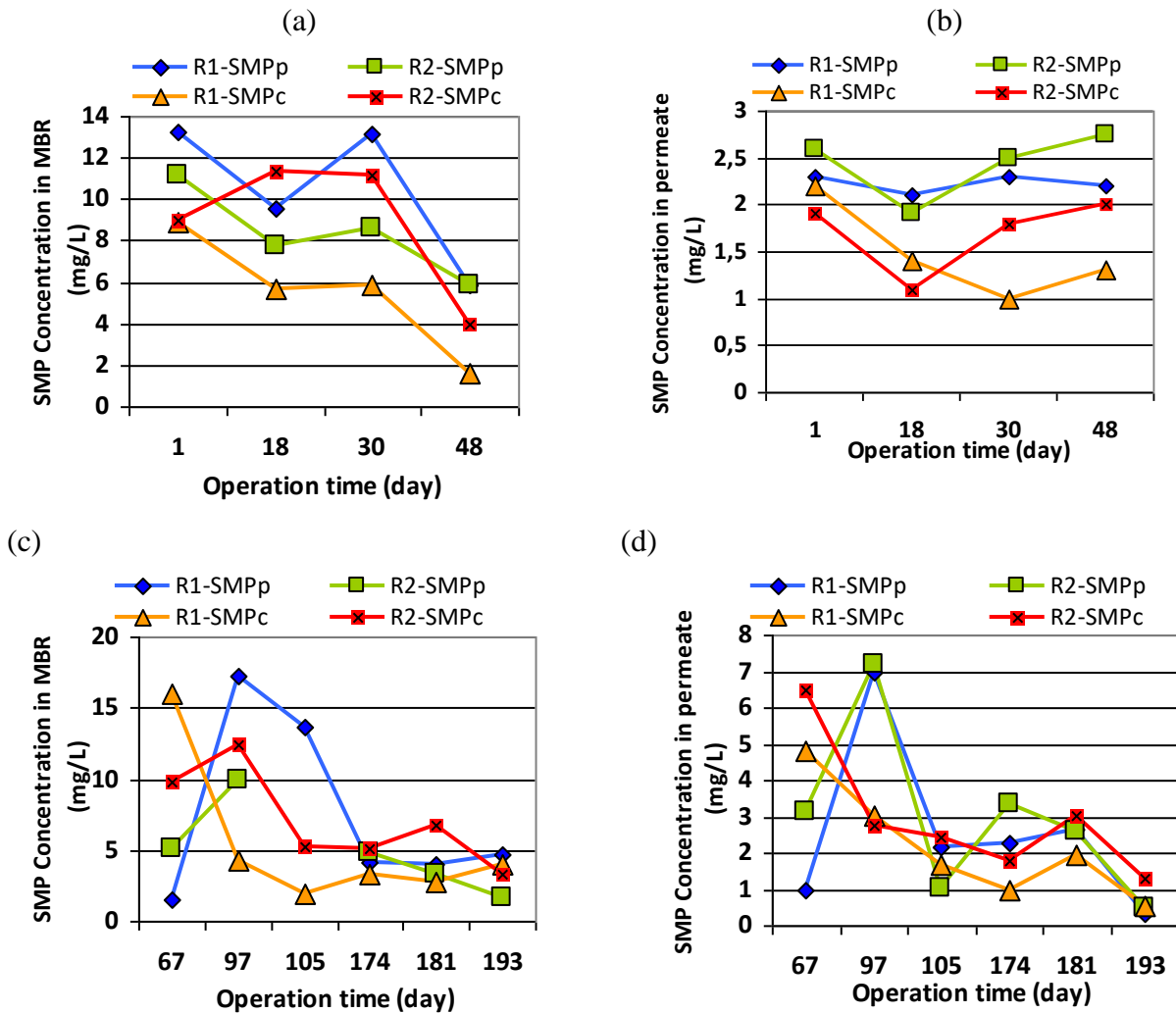
63.4 % at 90 days SRT, respectively. The micropollutants removal efficiencies for were also monitored and the average values were found between 84.9 % to 97.5 % except atrazine and penconazole at 15 days SRT. The atrazine and penconazole removal efficiencies were found to be 22.6 % and 42.6 % due to their lower biodegradability. On the other hand, removal efficiencies of micropollutants were found above 97.5 % except atrazine (17.5 %) and penconazole (45.0 %) at 90 days SRT.

As is known, the EPS composition is very heterogeneous and mainly consists of proteins, carbohydrates, lipids and nucleic acids. In this study, protein and carbohydrate are considered the main fraction of EPS and SMP (Meng et al. 2006). The EPS and SMP (in MBRs and permeates) concentrations were presented in Figure 2 and Figure 3 for the 15 days and 90 days SRT values. As can be seen from the Figure 2, the protein fraction of EPS (EPSp) were found 39.2 to 65.4 mg/g MLSS and 34.6 to 73.6 mg/g MLSS for R1 and R2 MBRs and it can be said that the EPSp concentrations of R1 (test MBR (micropollutants added)) were secreted lower from R2 test MBR. Similar trends of EPSp were found at 90 days of SRT and EPSp concentrations were determined between 16.3 to 25.0 mg/g MLSS and 14.8 to 27.6 mg/g MLSS for R1 and R2 MBRs, respectively. When compared to obtained results of SRT 15 and 90 days, EPSp concentration decreased with an increase of SRT from 15 days to 90 days. Several authors reported that EPS concentration decreased by increasing SRT (Cho et al. 2005; Massé et al. 2006). Similar results were obtained for the carbohydrate fraction of EPS (EPSc) at 15 and 90 days of SRTs. It be also said that the EPSp concentrations were found approximately 3 times higher from the EPSc concentrations at both SRT values.



**Figure 2.** EPSp and EPSc concentration of activated sludge at different SRT values: (a) 15 days SRT, (b) 90 days SRT

The SMP concentrations and fractions of supernatants and permeates were presented in Figure 3. As can be seen from Figure 3a-b, the SMPp concentrations in the supernatant of 15 days SRT averaged around 10.5 and 8.3 mg/L for R1 and R2 MBR, respectively. The average SMPp concentrations in permeates were found to be 2.2 and 2.4 mg/L for R1 and R2 MBRs. The SMPp rejections of R1 and R2 MBR were around 78.7 % and 70.8 %. On the other hand, SMPc concentrations of supernatants and permeates were found to be 5.5 and 1.4 mg/L, corresponding to around 73.3 % SMPc rejection by the membrane at 15 days SRT in R1 MBR. SMPc concentrations were 8.8 and 1.7 mg/L in R2 MBR, respectively, and the SMPc rejection was 80.8 %.



**Figure 3.** SMP concentrations at different SRT values: (a) 15 days SRT in supernatant, (b) 15 days SRT in permeates, (c) 90 days SRT in supernatant, (d) 90 days SRT in permeates

The average SMPp concentrations of R1 and R2 supernatants at 90 days SRT were determined 6.6 and 3.3 mg/L, respectively (Figure 3-c). On the other hand, the average concentration of SMPp of R1 and R2 permeates were found to be 1.83 and 1.87 mg/L with the rejection rates of 72.2 % and 42.9 %, respectively (Figure 3-d). The average SMPc concentrations of R1 and R2 supernatant were found 3.0 and 5.1 mg/L, respectively (Figure 3-c). On the other hand, the average concentration of SMPc of R1 and R2 permeates were found to be 1.29 and 2.15 mg/L with the rejection rates were 56.9 % and 57.7 %, respectively (Figure 3-d).

## CONCLUSION

In this study, the effect of micropollutants of feed wastewater on the production of EPS and SMP was investigated in sMBRs operated at 15 days and 90 days SRT. Adding micropollutants in feed wastewater result in slight increase of EPS and SMP secreting by activated sludge in MBR. An increase in SRT also resulted in a significant decrease in protein and carbohydrate fractions in EPS and SMP. According to the SMP results in supernatant and permeate, it was understood that proteins and carbohydrate accumulated in the sMBRs,

## REFERENCES

Ahmed, M. B., Zhou, J. L., Ngo, H. H., Guo, W., Thomaidis, N. S., Xu, J. (2017) Progress in the



- biological and chemical treatment technologies for emerging contaminant removal from wastewater: a critical review. *Journal of Hazardous Material*, **323**, 274-298.
- Arriaga, S., de Jonge, N., Nielsen, M. L., Andersen, H. R., Borregaard, V., Jewel, K., Ternes, T. A., Nielsen, J. L. (2016) Evaluation of a membrane bioreactor system as posttreatment in waste water treatment for better removal of micropollutants. *Water Research*, **107**, 37-46.
- Bakaraki, N., Chormey, D. S., Bakirdere, S.Ö Engin, G. (2016) Development of a sensitive liquid-liquid extraction method for the determination of N-butyryl-L-homoserine lactone produced in a submerged membrane bioreactor by gas chromatography mass spectrometry and deuterated anthracene as the internal standard. *Analytical Methods*, **8**(12), 2660-2665.
- Besha, A. T., Gebreyohannes, A. Y., Tufa, R. A., Bekele, D. N., Curcio, E., Giorno, L. (2017) Removal of emerging micropollutants by activated sludge process and membrane bioreactors and the effects of micropollutants on membrane fouling: a review. *Journal of Environmental Chemical Engineering*, **5**, 2395-2414.
- Bolong, N., Ismail, A. F., Salim, M. R., Matsuura, T. (2009) A review of the effects of emerging contaminants in wastewater and options for their removal. *Desalination*, **239**, 229-246.
- Caglak, A., Chormey, D. S., Onkal Engin, G., Bakirdere, S. (2019) Determination of micropollutants in wastewater matrix using gas chromatography spectrometry after optimization of dispersive liquid-liquid microextraction. *International Journal of Environmental Science and Technology*, **16**, 1-8. DOI: <https://doi.org/10.1007/s13762-019-02319-1>.
- Camacho-Munoz, D., Martin, J., Santos, J. L., Aparicio, I., Alonso, E. (2012) Effectiveness of conventional and low-cost wastewater treatments in the removal of pharmaceutically active compounds. *Water Air Soil Pollutant*, **223**, 2611-2621.
- Cho, J., Song, K. G., Ahn, K. H. (2005) The activated sludge and microbial substances influences on membrane fouling in submerged membrane bioreactor: unstirred batch cell test. *Desalination*, **183**, 425-429.
- Cho, J., Song, K. G., Ahn, K. H. (2005) The activated sludge and microbial substances influences on membrane fouling in submerged membrane bioreactor: unstirred batch cell test. *Desalination*, **183**, 425-429.
- Dubois, M., Gilles, K. A., Hamilton, J. K., Rebers, P. A., Smith, F. (1956) Colorimetric method for determination of sugars and related substances. *Analytical Chemistry*, **28**, 350-356
- Goswamia, L., Kumarb, R. V., Siddhartha, Boraha, N. N., Manikandan, A., Pakshirajana, K., Pugazhenth, G. (2018) Membrane bioreactor and integrated membrane bioreactor systems for micropollutant removal from wastewater: A review. *Journal of Water Process Engineering*, **26**, 314-328.
- Gruchlik, Y., Linge, K., Joll, C. (2018) Removal of organic micropollutants in waste stabilisation ponds: a review. *Journal of Environmental Management*, **206**, 202-214.
- Le-Clech, P. (2010) Membrane bioreactors and their uses in wastewater treatments. *Applied Microbiology and Biotechnology*, **88**, 1253-1260.
- Lee, W., Kang, S., Shin, H. (2003) Sludge characteristics and their contribution to microfiltration in submerged membrane bioreactors. *Journal of Membrane Science*, **216**, 217-227.
- Lowry, O. H., Rosebrough, N. J., Farr, A. L., Randall, R. J. (1951) Protein measurement with the Folin phenol reagent. *Journal of Biological Chemistry*, **193**, 265-275.
- Massé, A., Sperandio, M., Cabassud, C. (2006) Comparison of sludge characteristics and performance of a submerged membrane bioreactor and an activated sludge process at high solids retention time. *Water Research*, **40**, 2405-2415.
- Massé, A., Sperandio, M., Cabassud, C. (2006) Comparison of sludge characteristics and performance of a submerged membrane bioreactor and an activated sludge process at high solids retention time. *Water Research*, **40**, 2405-2415.
- Meng, F., Zhang, H., Yang, F., Zhang, S., Li, Y., Zhang, X. (2006) Identification of activated sludge properties affecting membrane fouling in submerged membrane bioreactors. *Separation*

- and Purification Technology*, **51**, 95-103.
- Mir-Tutusaus, J. A., Baccar, R., Caminal, G., Sarra, M. (2018) Can white-rot fungi be a real wastewater treatment alternative for organic micropollutants removal? A review. *Water Research*, **138**, 137-151.
- Nasirabadi, P. S., Saljoughi, E., Mousavi, S. M. (2016), Membrane processes used for removal of pharmaceuticals, hormones, endocrine disruptors and their metabolites from wastewaters: a review. *Desalination and Water Treatment*, **57**(51), 24146-24175.
- Nguyen, L. N., Hai, F. I., Yang, S., Kang, J., Leusch, F. D. L., Roddick, F., Price, W. E., Nghiem, L. D. (2013) Removal of trace organic contaminants by an MBR comprising a mixed culture of bacteria and white-rot fungi. *Bioresource Technology*, **148**, 234-241.
- Palacios-Rosas, E., Castro-Pastrana, L. I. (2017) Pharmaceuticals Reaching the Environment: Concepts, Evidence and Concerns. In: Gómez-Oliván, L. (ed) *Ecopharmacovigilance. The Handbook of Environmental Chemistry*, Vol 66. Springer.
- Sari Erkan, H., Onkal Engin, G., Ince, M., Bayramoglu, M. R. (2016) Effect of carbon to nitrogen ratio of feed wastewater and sludge retention time on activated sludge in a submerged membrane bioreactor. *Environmental Science and Pollution Research*, **23**, 10742-10752.
- Siegrist, H., Joss, A. (2012) Review on the fate of organic micropollutants in wastewater treatment and water reuse with membranes. *Water Air Soil Pollution*, **66**, 1369-1376.
- Standard Methods, APHA, AWWA and WPCF (2005) *Standard methods for the examination of water and wastewater*, 21st ed., Washington, USA.
- Teychene, B., Guigui, C., Cabassud, C., Amy, G. (2008) Toward a better identification of foulant species in MBR processes. *Desalination*, **231**, 27-34.
- Tijani, J. O., Fatoba, O. O., Petrik, L. F. (2013) A review of pharmaceuticals and endocrine-disrupting compounds: sources, effects, removal, and detections. *Water, Air, Soil Pollution*, **224**(11), 1770-1773.
- Tinggang, L., Renbi, B., Junxin, L. (2008) Distribution and composition of extracellular polymeric substances in membrane-aerated biofilm. *Journal of Biotechnology*, **135**, 52-57
- Verlicchi, P., Al Aukidy, M., Zambello, E. (2012) Occurrence of pharmaceutical compounds in urban wastewater: removal, mass load and environmental risk after a secondary treatment — A review. *Science of the Total Environment*, **429**, 123-155.
- Zhao, X., Chen, Z. L., Wang, X. C., Shen, J. M., Xu, H. (2014) PPCPs removal by aerobic granular sludge membrane bioreactor. *Applied Microbiology and Biotechnology*, **98**, 9843-9848.

# Enhancing the Accuracy and Precision in Quantifying the Pesticides Present in Complex Environmental and Food Samples by GC-MS Using Matrix Matching Calibration and Isotopically Labelled Internal Standard

G. Dalgıç Bozyiğit\*, M. Fırat\*\*, D. S. Chormey\*\*, G. Onkal Engin\* and S. Bakırdere\*\*

\* Department of Environmental Engineering, Yıldız Technical University, 34220, Istanbul, Turkey  
(E-mails: [gdalgic87@gmail.com](mailto:gdalgic87@gmail.com); [guleda@gmail.com](mailto:guleda@gmail.com))

\*\* Department of Chemistry, Yıldız Technical University, 34220, Istanbul, Turkey  
(E-mails: [merve.f@yahoo.com](mailto:merve.f@yahoo.com); [kuzzynobo@yahoo.com](mailto:kuzzynobo@yahoo.com); [bsezgin23@yahoo.com](mailto:bsezgin23@yahoo.com))

## Abstract

The complex nature of environmental and food samples tends to affect the accuracy of analyte quantification could undermine or boost the analyte's signal leading to false negative or false positive results, respectively. This study presents the determination of four pesticides as dioxacarb, flumetralin, tefluthrin and trifluralin in selected matrices by gas chromatography mass spectrometry. These included three aqueous samples (irrigation canal water, well water and wastewater) and three solid samples (kiwi, soil and waste sludge). To enhance the precision of instrumental measurements, isotopically labelled bisphenol A was added to both standard and sample solutions to maintain a constant ratio of peak area results irrespective of errors during the measurement process. The coefficient of determination values obtained for calibration plots developed with internal standard were higher than 0.9997. Matrix matching calibration method was employed for the recovery of analytes from all samples and compared to the results obtained using the conventional calibration method. The matrix matching method significantly enhanced the accuracy of quantifying analytes ( $\approx 100\%$ ) in all tested matrices.

## Keywords

Pesticides; GC-MS; QuEChERS; wastewater; soil; sludge

## INTRODUCTION

The onslaught of pesticide usage has significantly increased the yield and quality of agricultural products, and helped to curb diseases that are transmitted by disease bearing pests (Chormey et al., 2018). Different chemical classes of pesticides are synthesized to target specific organisms with different modes of action to weaken or kill pests (Chormey et al., 2017). Since pesticides are used all around the world and in large quantities, a high risk has been associated with non-target organisms getting exposed. Just as pesticides are capable of causing harm to pests, non-target organisms including humans when exposed to pesticides through inhalation, dermal contact or ingestion could manifest various health disorders. Aquatic life is one of the most widely affected by pesticide exposure (Lew et al., 2013; Stadlinger et al., 2018) but humans also suffer severe health effects such as dermatologic, reproductive, cardiovascular, carcinogenic, neurological, genotoxic, gastrointestinal and endocrine effects (Nicolopoulou-Stamati et al., 2016; Alewu and Nosiri, 2011; Mnif et al., 2011; Sanborn et al., 2007). Countries have therefore set up regulatory authorities to oversee the proper application of registered pesticides and to ban those that are found to be highly hazardous (Fagnoli et al., 2019; Chowdhury et al., 2018).

Flumetralin is an approved plant growth regulator used to alter the characteristics of plants either by applying to seeds before planting or directly to growing plants. This chemical has been reported to show acute and chronic toxicity in aquatic organisms (Guziejewski et al., 2017). Tefluthrin is known as an insecticide used in eradicating a wide range of insects and it has been reported to cause

neurological and endocrine effects (Wu et al., 2009). Trifluralin and dioxacarb are two obsolete pesticides used as an insecticide and herbicide, respectively. Trifluralin was applied directly into soils to prevent the growth of weeds by impeding division and development of shoot cells (Fernandes et al., 2013). Trifluralin is highly toxic to aquatic organisms and its toxicity to humans is classified as moderate (Milhome et al., 2018). Dioxacarb on the other hand was extensively used in household, public and agricultural fields against pests such as leafhoppers, beetles, aphids and cockroaches (Baron, 1991). Dioxacarb is also a toxic substance to aquatic organisms and causes health effects such as vomiting, diarrhoea, abdominal cramps and hypertension in humans (Eren et al., 2015). Both approved and banned pesticides need to be monitored in food and environmental samples to affirm that humans and the environment are protected from their detrimental effects.

Pesticides with high vapour pressures and thermal stability are readily determined by gas chromatography, which separates them according to differences in boiling points as denoted by retention times (Chormey et al., 2017). When coupled to a mass spectrometry detector (MSD), compounds can further be separated from each other based on their different fragmentation ions ( $m/z$ ). The MSD also offers the high sensitivity and specificity for the monitoring of one compound in the selected ion monitoring (SIM) mode, or selectivity for different compounds at the same time in the scan mode (Kyle, 2017). Most sample pretreatment methods are compatible with GC-MS, and coupling of the sample preparation unit and instrumental detection as an automated system is possible (Domínguez et al., 2016). Due to the complicated nature of environmental and food samples, false negative and false positive results could be reported for analytes that are suppressed or boosted by components of the sample matrix (Panuwet et al., 2016). Instrumental fluctuations and other systematic errors could affect measurement results and increase uncertainties (Alnouti et al., 2006).

The aim of this study was to use matrix matching calibration method to enhance the accuracy of quantifying the selected pesticides in complex environmental samples, and to use a deuterated internal standard to increase measurement repeatability by offsetting systematic errors.

## **MATERIALS AND METHODS**

### ***Reagents***

The pesticides and internal standard used in this study (dioxacarb, flumetralin, tefluthrin, trifluralin, and deuterated bisphenol A) were purchased from Dr. Ehrenstorfer (Augsberg, Germany) and they were all of high purity (>98 %). Standard stock solutions (1.000 g/L) of the four pesticides were prepared gravimetrically in acetonitrile (Merck – Germany) and appropriate amounts taken from each to prepare 200 mg/L mixed stock solution. All working, calibration and matrix matching standards were subsequently prepared from the mixed stock solution by diluting aliquots in acetonitrile and respective sample solutions. Approximately 100 mg/L of isotopically labelled bisphenol A (BPA-D16) was prepared in ethanol (Merck – Germany) and an equivalent amount added to all standards and samples as internal standard.

### ***Apparatus***

The following temperature program was used for elution and complete separation of analytes within 7.0 min: 40 °C/min ramp from an initial temperature of 70 °C to 160 °C, then a final 50 °C/min ramp to 280 °C and held for 3.0 min. The capillary column (HP-5MS) used for separation of analytes was 30 m in length, 0.32 internal diameter and 0.25 µm film size. The column was fixed in the oven compartment of a 6890 model Agilent gas chromatograph coupled to a mass spectrometry detector (Agilent 5973) for analyte detection. The GC inlet was maintained at 280 °C to allow rapid transition of injected sample/standard solution (1.0 µL) into the gaseous phase to enter the column

with ultrapure helium gas constantly flowing at 2.5 mL/min. The fragmentation ions ( $m/z$ ) 224/223, 306/264, 177/197, 143/145 and 121/166 were respectively used to quantify/qualify BPA-D16, trifluralin, tefluthrin, flumetralin and dioxacarb. The ionization energy of the MS source was 70 eV and the transfer line 280 °C. Mixing of sample/standard was performed with an ISOLAB vortex (M1010002) and Kerman Lab (51) mechanical shaker. Separation of phases was facilitated with an EBA 20 model Hettich Centrifuge.

### **Procedure**

All aqueous samples were directly spiked with intermediate standard solutions with concentrations 100 times higher than the intended spike concentration. The soil and sludge samples were adequately dried in an oven and approximately 0.50 g taken and spiked in plastic weighing boats and allowed to dry under ambient laboratory conditions. Then, 2.0 mL of acetonitrile was used to wash the spiked solid samples into 15 mL centrifuge tubes, mixed on a mechanical shaker for 20 min and centrifuged for 120 s at 6000 rpm. The supernatant was filtered into vials for instrumental measurement. The quick, easy, cheap, efficient, rugged and safe (QueChERS) method protocol used in this study was adapted from the study of Lehotay because it gives a dilution factor of 1.0 (Lehotay, 2007).

### **Samples**

Fertile soil from the university garden was sampled and grinded in a porcelain mortar to break down coarse particles into fine particles. Very fine soil particles were obtained by sieving the grinded soil through a sieve with 100  $\mu\text{m}$  size openings. Sludge from a bioreactor was filtered on a 125 mm filter paper and left to dry completely under ambient laboratory conditions. Kiwi fruit samples were obtained from a local market and blended to obtain a homogenous mixture. Aqueous samples including well water, irrigation canal water and municipal wastewater were taken from their respective sources into polypropylene bottles. The bottles were thoroughly rinsed with the samples before filling to the brim. The wastewater was kept in a refrigerator while the well and irrigation canal water samples were stored in cool and dry cabinets.

## **RESULTS AND DISCUSSIONS**

BPA-D16 was added to all samples and calibration standards, and the ratio of sample/standard peak area to internal standard peak area was used in developing calibration plots and calculating percent recovery. The samples were spiked at different concentrations and three replicates were performed for each spike level to determine precision.

### **Qualitative and quantitative determinations**

The retention times of dioxacarb, trifluralin, tefluthrin, flumetralin and BPA-D16 were determined to be 3.3, 3.8, 4.1, 4.9, 5.2 min according to the temperature program given in the sub-section "Apparatus". The internal standard produced a distinct signal from the analytes of interest and the signal obtained for 5.0 mg/L was adequate to be used for all samples and standards. Calibration standards were prepared in the range of 0.20 – 100 mg/L, spiked with the internal standard and measured by the GC-MS system in an increasing order of concentration. The linear working range (LWR) was determined as the lowest calibration concentration (signal to noise ratio  $\geq 3.0$ ) and the highest concentration after which the plot reaches a plateau. With the internal standard, the coefficient of determination ( $R^2$ ) value was enhanced for all four analytes. The lowest concentration for each analyte was measured five times to obtain standard deviation (StdDev) values for the calculation of percent relative standard deviation (%RSD), and the limits of detection (LOD) and quantification (LOQ). Using the calibration slopes ( $m$ ), the expressions of  $3 \times \text{StdDev}/\text{slope}$  and  $10$

$\times \text{StdDev/slope}$  were used to calculate LOD and LOQ, respectively. The figures of merit (LOD, LOQ, %RSD, LWR and  $R^2$ ) obtained for the analytes are presented in Table 1.

**Table 1.** GC-MS analytical figures of merit for dioxacarb, trifluralin, tefluthrin and flumetralin

Parameter	LOD, mg/L	LOQ, mg/L	$R^2$	%RSD	Range, mg/L
Dioxacarb	0.27	0.89	0.9998	5.9	1.0 – 100
Trifluralin	0.06	0.21	0.9999	6.6	0.20 – 100
Tefluthrin	0.06	0.20	0.9999	4.4	0.20 – 100
Flumetralin	0.16	0.55	0.9998	5.5	0.50 – 100

### **Recovery experiments for aqueous samples**

Irrigation canals on farmlands stand a great chance of being contaminated with pesticides during application to crops. Continuous applications could lead to accumulation of pesticides in the water source over time and consequently introduced to crops through irrigation. Water soluble pesticides move down the soil layers into ground water aquifers, where they can reach humans when used as source for wells. Irrigation canals, due to their open-to-air nature, are susceptible to other forms of contamination and these could affect the accuracy of quantifying an analyte. Groundwater is also known for hardness due to dissolved minerals and this could also affect quantification. Thus, irrigation canal and well water were spiked at different concentrations after their blank analysis gave clean results. Percent recovery of the spiked samples were calculated with respect to calibration standards prepared in acetonitrile. The aqueous samples gave very low signals compared to calibration standards of the same concentration, and this resulted in recovery results below 50 %. Calibration standards were prepared in deionized water and this improved the percent recovery (>90 %) of the spiked samples. To further enhance the recovery of analytes, matrix matching calibration standards were prepared and used to quantify the spiked samples. The recovery results obtained for three spiked concentrations are given in Table 2 and the results validate the accuracy of matrix matching quantification.

**Table 2.** Percent recovery results calculated for spiked well and irrigation water samples

Analyte	Well water (%)			Irrigation canal water (%)		
	1.0 ng/mL	2.5 ng/mL	5.0 ng/mL	1.0 ng/mL	2.5 ng/mL	5.0 ng/mL
Dioxacarb	106.9 ± 4.0	100.1 ± 3.6	97.5 ± 3.8	100.9 ± 6.3	99.4 ± 4.6	100.1 ± 5.3
Trifluralin	95.5 ± 7.6	102.0 ± 0.3	100.1 ± 3.3	102.8 ± 2.0	97.3 ± 0.8	100.2 ± 1.9
Tefluthrin	94.7 ± 4.9	102.1 ± 4.1	100.3 ± 5.1	95.5 ± 5.5	99.2 ± 0.9	101.1 ± 3.4
Flumetralin	98.3 ± 5.7	103.1 ± 4.9	98.3 ± 0.4	101.5 ± 8.9	102.0 ± 8.8	98.0 ± 6.3

### **Recovery experiments for municipal wastewater**

Municipal wastewater contains a wide range of organic and inorganic compounds that originate from households and industries. In the presence of these compounds, the signal of an analyte could be suppressed or enhanced, leading to a false negative for the former and a false positive for the latter. Both cases are undesired for wastewater treatment which requires accurate results to apply appropriate treatment strategies and to clear effluents for safe disposal into the environment. After performing blank analysis of municipal wastewater sample, four spike concentrations were made with low amounts of mixed analyte standard solution in order to observe the full effect to the sample matrix. Similar to the other aqueous samples (well and irrigation canal), peak area values of

the spiked wastewater fell below the calibration standards prepared with both acetonitrile and deionized water. Matrix matching was then applied using a similar wastewater matrix and the recovery results calculated for the different spike concentrations (1.0, 2.5, 5.0 and 10 mg/L) improved to almost 100 % as given in Table 3. The results established that the analytes can be accurately quantified in the complex wastewater matrix using matrix matching.

**Table 3.** Percent recovery results calculated for municipal wastewater by matrix matching method

Analyte	Municipal Wastewater (%)			
	1.0 ng/mL	2.5 ng/mL	5.0 ng/mL	10 ng/mL
Dioxacarb	94.2 ± 4.5	102.7 ± 4.5	100.1 ± 1.6	99.9 ± 0.1
Trifluralin	104.4 ± 3.0	99.8 ± 3.9	98.6 ± 2.7	100.3 ± 1.3
Tefluthrin	97.5 ± 5.1	101.7 ± 6.3	99.6 ± 5.5	100.0 ± 4.5
Flumetralin	100.7 ± 2.9	102.7 ± 0.1	97.7 ± 4.9	100.4 ± 3.7

#### **Recovery experiments for soil and sludge samples**

The soil consists of several minerals, organic matter, gases, water and living organisms, making it a very complex environmental sample. The soil is also a primary host to environmental pollutants and this further increases the complexity of the matrix. Soluble contaminants are easily washed down the soil pores but insoluble contaminants remain for very long periods until they undergo degradation. Wastewater sludge comprises of biosolids that accumulate in treatment plants and could be in a slurry, semisolid or solid form (Alam et al., 2003). The sludge is separated from treated water and it retains particulate matter of varying compositions, making it a complex material to analyse. Soil and sludge samples (0.50 g) were spiked to different final concentrations and the samples were allowed to dry completely under ambient conditions. Then, 2.0 mL of acetonitrile was added to each sample and placed on a mechanical shaker for 20 min. The samples were centrifuged for 2.0 min at 6000 rpm and the solvent filtered into vials for GC-MS measurement. Percent recoveries for both soil and sludge spike samples were calculated with respect to calibration standards prepared in acetonitrile. The recovery results obtained for the spiked soil samples were higher than the results obtained for spiked sludge samples. The sludge sample contains high amounts of organic compounds relative to soil and these could have competed in the extraction process. Matrix matching was tested on both samples to ascertain whether an improvement in recovery would be observed or not, and the results obtained were more accurate and precise as shown in Table 4.

**Table 4.** Percent recovery results calculated for soil and sludge spiked samples by matrix matching method

Analyte	Soil (%)		Sludge (%)	
	5.0 ng/mL	10 ng/mL	1.0 ng/mL	2.5 ng/mL
Dioxacarb	98.6 ± 1.3	102.5 ± 0.8	101.3 ± 6.9	100.9 ± 5.6
Trifluralin	98.9 ± 1.2	98.5 ± 1.8	95.2 ± 3.2	96.6 ± 6.4
Tefluthrin	100.9 ± 1.4	98.9 ± 1.0	96.4 ± 5.0	97.5 ± 6.1
Flumetralin	102.7 ± 1.7	100.8 ± 1.1	94.1 ± 3.5	95.8 ± 3.8

#### **Kiwi samples**

The QuEChERS method is a highly efficient analytical approach mainly used for the determination of pesticide residues in food samples and it involves two basic steps. The first step is sample

preparation (homogenization) and extraction using acetonitrile in the presence of buffers, acids and salts to enhance the extraction efficiency of analytes and to protect the chemical integrity of analytes. The second step is cleanup of the extract and this involves the use of drying agents to eliminate excess water and adsorbents to eliminate matrix components (DeArmond et al., 2015). The extracts obtained from QuEChERS are readily compatible with various instrumental techniques. The kiwi samples used in the study were homogenized and taken through the two steps of QuEChERS extraction. The peak area values obtained for the spiked kiwi samples were higher than their corresponding calibration standard's peak area values, even though both were prepared in acetonitrile. The high peak area values obtained for the kiwi samples could be due to the salting-out effect of the salt used in the extraction process. The percent recovery results for all analytes at the four different spiked concentrations ranged between 102 – 124%. Matrix matching calibration standards were therefore prepared in kiwi matrix to quantify the spiked samples. The recovery results as shown in Table 5 significantly improved.

**Table 5.** Percent recovery results calculated for kiwi samples by matrix matching method

Analyte	Kiwi samples (%)			
	1.0 ng/mL	2.5 ng/mL	5.0 ng/mL	10 ng/mL
Dioxacarb	96.4 ± 5.5	102.2 ± 6.4	99.6 ± 4.6	100.0 ± 3.5
Trifluralin	96.8 ± 2.9	100.0 ± 2.0	101.2 ± 4.9	99.7 ± 2.1
Tefluthrin	98.1 ± 3.9	97.6 ± 0.7	102.5 ± 5.3	99.5 ± 6.1
Flumetralin	103.2 ± 2.2	96.7 ± 0.1	99.6 ± 3.4	100.2 ± 0.9

## CONCLUSIONS

The complexity of environmental and food samples requires accurate and precise analytical techniques for the determination of contaminants. To mitigate matrix interference and improve the accuracy of quantification, matrix matching calibration method was used for selected aqueous and solid samples. Three aqueous samples (well, irrigation canal and wastewater) recorded peak area values different from the calibration standards and different from each other. Calibration standards prepared with similar matrices for each sample improved the recovery of all tested spike concentrations. The solid samples recorded appreciable recovery with direct calibration relative to the aqueous samples but the results were further enhanced with the matrix matching method. Satisfactory results were obtained for all analytes in the different samples using matrix matching and this suggests matrix matching could be extended to other samples for accurate quantification of analytes. The use of an internal standard augmented accuracy by given more precise results for replicate measurements.

## REFERENCES

- Alam, M. Z., Fakhru'l-Razi, A., Molla, A. H. (2003) Biosolids accumulation and biodegradation of domestic wastewater treatment plant sludge by developed liquid state bioconversion process using a batch fermenter. *Water Research*, **37**, 3569-78.
- Alewu, B., Nosiri, C. (2011) Pesticides and Human Health. In: Pesticides in the Modern World- Effects of Pesticides Exposure, Stoytcheva, M. (ed.), InTech, 231-250.
- Alnouti, Y., Li, M., Kavetskaia, O., Bi, H., Hop, C. E. C. A., Gusev, A. I. (2006) Method for Internal Standard Introduction for Quantitative Analysis Using On-Line Solid-Phase Extraction LC-MS/MS. *Analytical Chemistry*, **78**, 1331-36.



- Baron, R. L. (1991) CHAPTER 17 - Carbamate Insecticides, In: Classes of Pesticides. Hayes, W. J. and Laws, E. R., Academic Press, San Diego, 1125-1189.
- Chormey, D. S., Büyükpınar, Ç., Turak, F., Komesli, O. T., Bakırdere, S. (2017) Simultaneous determination of selected hormones, endocrine disruptor compounds, and pesticides in water medium at trace levels by GC-MS after dispersive liquid-liquid microextraction. *Environmental Monitoring and Assessment*, **189**(6), 277.
- Chormey, D. S., Fırat, M., Büyükpınar, Ç., Erulaş, F., Komesli, O.T., Turak, F., Bakırdere, S. (2018) Accurate determination of pesticides, hormones and endocrine disruptor compounds in complex environmental samples using matrix dilution and matrix matching with dispersive liquid-liquid microextraction. *Pure and Applied Chemistry*, **90**(11), 1703-1711.
- Chowdhury, F. R., Dewan, G., Verma, V. R., Knipe, D. W., Isha, I. T., Faiz, M. A., Gunnell, D. J., Eddleston, M. (2018) Bans of WHO Class I Pesticides in Bangladesh-suicide prevention without hampering agricultural output. *International Journal of Epidemiology*, **47**(1), 175-184.
- DeArmond, P. D., Brittain, M. K., Platoff, G. E. Jr., Yeung, D. T. (2015) QuEChERS-based approach toward the analysis of two insecticides, methomyl and aldicarb, in blood and brain tissue. *Analytical Methods*, **7**(1), 321-328.
- Domínguez, I., Romero González, R., Arrebola Liébanas, F. J., Martínez Vidal, J. L., Garrido Frenich, A. (2016) Automated and semi-automated extraction methods for GC-MS determination of pesticides in environmental samples. *Trends in Environmental Analytical Chemistry*, **12**, 1-12.
- Eren, Y., Erdoğan, S. F., Akyıl, D., Özkara, A., Konuk, M., Sağlam, E. (2015) Cytotoxic and genotoxic effects of dioxacarb by human peripheral blood lymphocytes CAs and Allium test. *Cytotechnology*, **67**(6), 1023-1030.
- Fargnoli, M., Lombardi, M., Puri, D., Casorri, L., Masciarelli, E., Mandić-Rajčević, S., Colosio, C. (2019) The Safe Use of Pesticides: A Risk Assessment Procedure for the Enhancement of Occupational Health and Safety (OHS) Management. *International Journal of Environmental Research and Public Health*, **16**(3), 310.
- Fernandes, T. C., Pizano, M. A., Marin-Morales, M.A. (2013) Characterization, modes of action and effects of trifluralin: A review. In: Herbicides-Current Research and Case Studies in Use. Price, A. J. and Kelton, J. A. (eds), IntechOpen, 489-515.
- Guziejewski, D., Smarzewska, S., Metelka, R., Nosal-Wiercińska, A., Ciesielski, W. (2017) Improved electroanalytical characteristics for flumetralin determination in the presence of surface active compound. *Monatshefte für Chemie*, **148**(3), 555-562.
- Kyle, P. B. (2017) Chapter 7 - Toxicology: GCMS, In: Mass Spectrometry for the Clinical Laboratory. Nair, H. and Clarke, W. (eds), Academic Press, San Diego, 131-163.
- Lehotay, S. J. (2007) Determination of pesticide residues in foods by acetonitrile extraction and partitioning with magnesium sulfate: collaborative study. *Journal of AOAC International*, **90**(2), 485-520.
- Lew, S., Lew, M., Biedunkiewicz, A., Szarek, J. (2013) Impact of pesticide contamination on aquatic microorganism populations in the littoral zone. *Archives of Environmental Contamination and Toxicology*, **64**(3), 399-409.
- Milhome, M. A. L., de Lima, L. K., Nobre, C. de A., Lima, F. de A. F., do Nascimento, R. F. (2018) Effect of ozonization in degradation of trifluralin residues in aqueous and food matrices. *Journal of Environmental Science and Health, Part B*, **53**(12), 786-792.
- Mnif, W., Hassine, A. I. H., Bouaziz, A., Bartegi, A., Thomas, O., Roig, B. (2011) Effect of endocrine disruptor pesticides: A review. *International Journal of Environmental Research and Public Health*, **8**(6), 2265-2303.
- Nicolopoulou-Stamati, P., Maipas, S., Kotampasi, C., Stamatis, P., Hens, L. (2016) Chemical Pesticides and Human Health: The Urgent Need for a New Concept in Agriculture. *Frontiers in Public Health*, **4**, 148-148.

- Panuwet, P., Hunter, R. E. Jr., D'Souza, P. E., Chen, X., Radford, S. A., Cohen, J. R., Marder, M. E., Kartavenka, K., Ryan, P. B., Barr, D. B. (2016) Biological Matrix Effects in Quantitative Tandem Mass Spectrometry-Based Analytical Methods: Advancing Biomonitoring. *Critical Reviews in Analytical Chemistry*, **46**(2), 93-105.
- Sanborn, M., Kerr, K. J., Sanin, L. H., Cole, D. C., Bassil, K. L., Vakil, C. (2007) Non-cancer health effects of pesticides: systematic review and implications for family doctors. *Canadian Family Physician-Medecin de Famille Canadien*, **53**(10), 1712-1720.
- Stadlinger, N., Berg, H., Van den Brink, P. J., Tam, N. T., Gunnarsson, J. S. (2018) Comparison of predicted aquatic risks of pesticides used under different rice-farming strategies in the Mekong Delta, Vietnam. *Environmental Science and Pollution Research International*, **25**(14), 13322-13334.
- Wu, S.-N., Wu, Y.-H., Chen, B.-S., Lo, Y.-C., Liu, Y.-C. (2009) Underlying mechanism of actions of tefluthrin, a pyrethroid insecticide, on voltage-gated ion currents and on action currents in pituitary tumor (GH3) cells and GnRH-secreting (GT1-7) neurons. *Toxicology*, **258**(1), 70-77.

# Performance of Retention Soil Filters for the Reduction of Antibiotic-resistant Bacteria and Other Pathogenic Microorganisms in Raw and Treated Wastewater before Being Discharged into Surface Waters

S. M. Essert\*, N. Zacharias\*, A. F. Brunsch\*\*, E. Christoffels\*\*\*, T. Kistemann\* and C. Schreiber\*

\* GeoHealth Centre, IHPH-Institute for Hygiene and Public Health, Medical Faculty, University of Bonn, Venusberg-Campus 1, 53127 Bonn, Germany (E-mails: [sarah.essert@ukbonn.de](mailto:sarah.essert@ukbonn.de); [nicole.zacharias@ukbonn.de](mailto:nicole.zacharias@ukbonn.de); [thomas.kistemann@ukbonn.de](mailto:thomas.kistemann@ukbonn.de); [christiane.schreiber@ukbonn.de](mailto:christiane.schreiber@ukbonn.de))

\*\* Erftverband, Department of River Basin Management, Am Erftverband 6, 50126 Bergheim, Germany (E-mail: [andrea.brunsch@erftverband.de](mailto:andrea.brunsch@erftverband.de))

\*\*\* IBC Ingenieure, Jagdrain 5, 52391 Vettweiß (E-mail: [ekkehard.christoffels@ibc-ingenieure.com](mailto:ekkehard.christoffels@ibc-ingenieure.com))

## Abstract

Environmental quality standards for surface water bodies have been significantly expanded through recent amendments to German regulations. Limit values are only established for currently applicable regulations if the water is indicated for certain uses, e.g., abstraction of irrigation water for agricultural use. Nevertheless, surface water bodies are often used for hygiene-sensitive purposes such as water sports. In the course of climate change, stronger precipitation events will occur, which may lead to more frequent loading and discharge of combined sewage overflow (CSO) into surface water bodies. Retention soil filters (RSFs) are attracting attention as an extensive treatment technology for CSO and an alternative technique within wastewater treatment. However, their microbial reduction capacity has not yet been systematically quantified with regard to their potential use as a fourth purification stage. This study examined large-scale RSFs for CSO treatment, as well as the effectiveness of RSFs as a fourth purification stage. A RSF test facility was established at a municipal wastewater treatment plant (WWTP) in Germany. This facility consists of three semi-technical RSFs (with a filter area of 1.5 m<sup>2</sup> each) that were fed exclusively with treated water from the WWTP. The reduction of microorganisms mostly occurred within the first centimeters of the RSFs. For most hygienic-microbiological parameters, there was a 1-2 log unit reduction, in addition to the reduction within the WWTP. Antibiotic-resistant bacteria were reduced to the same extent. The studies at the large-scale RSFs showed that a slower flow rate corresponded with a better reduction performance.

## Keywords

Retention soil filter; wastewater treatment; human-pathogenic microorganisms; antibiotic-resistant bacteria; combined sewage overflow; fourth purification stage

## INTRODUCTION

### Retention soil filters for treatment of combined sewage overflow (CSO) and as a fourth purification step in wastewater treatment plants

In the course of climate change, precipitation patterns are expected to change in terms of quantity, incidence and frequency, which may lead to more frequent load and discharge of CSO and higher release from the unsealed landscape. Increased microbial pollution from discharge events of CSO after heavy precipitation events was demonstrated (Gibson et al., 1998; Kistemann et al., 2004). In order to reduce the pollution of surface waters after CSO introduction, in recent years treatment of the discharged water with retention soil filters (RSFs), a special vertical type of constructed wetlands, has been utilized in Germany. RSFs for CSO used to relieve water pollution in heavy precipitation events are fed with mixed water. Thus, they can significantly reduce microorganisms and hydraulic loads (Overath et al., 2000). RSFs investigated as a fourth purification step in

wastewater treatment plants (WWTPs) show high performance in reducing dissolved organic carbon and micropollutants (Brunsch et al., 2018).

### **Hygienically relevant microorganisms in wastewater**

Hygienically relevant parameters in WWTP influents and effluents are well known. Common parameters for the microbiological characterization of wastewater include total and fecal coliform bacteria, fecal streptococci, clostridia, salmonellae, cryptosporidia, giardia and enteropathogenic viruses (Hiekel et al., 2002). Antibiotic-resistant bacteria (ARB) in surface waters can play a role in the risk of using these waters. The actual health risk cannot be evaluated yet because there is not enough data on ARB in surface waters. Nevertheless, to protect people who come into contact with surface waters and to reduce ARB into the environment, the microbiological purification effectiveness of WWTPs may be enhanced as it was shown that important human-pathogen ARB can reach the environment from WWTP discharge (Baquero et al., 2008; Novo et al., 2013). Scheurer et al. (2015) state that RSFs, which are installed to relieve CSO, are very suitable to reduce microorganisms (*Escherichia coli*, enterococci and staphylococci); they can decrease their concentrations 2-3 log units and reduce the percentage of ARB. Thus, RSFs represent a great potential to purify treated wastewater from different hygienically relevant microorganisms. Despite promising studies (Christoffels et al., 2014; Mertens et al. 2012;), RSFs have not yet been put into operation for extensive long-term monitoring. This study investigated the purification performance of semi-automatic RSFs on different facultative-pathogen microorganisms (including ARBs) as a fourth purification stage in the form of a pilot test facility.

## **MATERIALS AND METHODS**

### **Large-scale RSFs**

This study uses microbiological data, collected by sampling two different RSFs for CSO treatment. Both RSFs are located in Germany, operated by the local water board (Erftverband). The effective drainage area of RSF A is approximately 19 ha, with a filter size of 707 m<sup>2</sup> and a retention volume of 782 m<sup>3</sup>. The connected sewer system at RSF B drains the waste- and rainwater of a catchment area with approx. 7.700 inhabitants. The drainage effective area amounts to approximately 79 ha. The filter area is 1.495 m<sup>2</sup>, and the retention volume is 2,630 m<sup>3</sup>. The catchment areas of both RSFs are characterized by rural residential areas with some agricultural enterprises. There are no significant commercial or industrial areas or buildings with special wastewater (such as hospitals). Both filters were put into operation in 2005. The filtered water is introduced into the receiving surface waters with a maximum throttling rate of 41 L/s (RSF A) or 44 L/s (RSF B).

### **RSF semi-technical test facility**

In order to investigate the effectiveness of RSFs as an additional purification stage for sewage treatment plants, an RSF test facility was established at a municipal WWTP in Germany, as part of the project "Transnational Action Programme On Emerging Substances" (TAPES, 2016). Purification performance of this RSF facility concerning micropollutants and dissolved organic carbon was previously published (Brunsch et al., 2018). This facility consists of three semi-technical RSFs, each with a 1.5 m<sup>2</sup> filter area. Two of those test facilities (filter 1 and filter 2) were investigated in this study. Both filters contain original material from large-scale RSF systems, which were already in operation for several years. The material of filter 1 corresponds to RSF A and filter 2 corresponds to RSF B (see above). The semi-automatic facilities filter 1 and filter 2 were fed exclusively with treated wastewater from the WWTP. One load lasted 28 h, followed by a 56-h dry phase. The filters were charged at 0.03 L/s/m<sup>2</sup>, which meets the requirements of the German rules and standards for RSFs (DWA, 2019; MUNLV, 2015) and the filtration performance of large-scale installations. These feeding cycles ensured that aerobic conditions could be established in the filters

during the dry and wet phases. In addition to the inflows and outflows, water from individual filter layers (0.1 m, 0.3 m, 0.75 m) were sampled by means of built-in sampling tubes.

### Sampling

An automatic sampling system was installed to sample from the large-scale RSFs. The start of the downturn was registered via a water level sensor in the inlet of the retention bottom filter, and the sampler of the inlet was activated. Effluent sampling was performed with a corresponding delay (40 min). This design ensured that the residual water from the last discount that was necessary for operation was not sampled. For microbiological analysis, submersible pumps filled 200-L sample containers (for influents and effluents) in approximately 15 min. Sampling of the semi-technical RSF facility was random. The pilot plant feed was sampled at the WWTP drainage pit. To sample at the respective depth and effluents, the sample was taken from the sampling tap of the respective RSF after the stagnation water had run out. The samples were transported refrigerated to the laboratory, and processing was usually started immediately (but no later than 24 h after sampling). Any necessary intermediate storage took place overnight at  $5 \pm 3$  °C in the refrigerator.

### Cultural detection of microorganisms and calculation of the reduction performance

Due to the high solid loads for the CSO and expected bacterial loads, samples were diluted with sterile 0.9 % NaCl. For parameters with lower expected concentrations, samples added to agar plates via a membrane filter using a vacuum pump and membrane filtration unit (Whatman). Analysis of the individual microbiological parameters was performed according to normalized standard methods or based on published methods. The analyzed microorganisms shown in this study are *E. coli* (DIN EN ISO 9308-1:2012, modified by using an antibiotic supplement), somatic coliphages (DIN EN ISO 10705-2:2002), as an indicator for enteropathogenic viruses, and the parasite *Giardia lamblia* (ISO 15553:2006, EPA Method 1623, HMSO:1989). Additionally, within the project “HyReKA” ARB were investigated. The parameter shown in this study is extended-spectrum beta-lactamase (ESBL)-producing *E. coli*; the utilized method was developed and adapted for the HyReKA project and will soon be published in detail. The sample was placed on ChromESBL agar (Co. Mast) and incubated for 24 h at 42 °C. The microorganism concentrations were calculated in logarithmic units (log units) of colony-forming units (cfu) or plaque-forming units (pfu) per 100 mL for each microbiological parameter. The difference in log units between the effluent and influent from the RSFs or WWTP was used to measure the reduction performance.

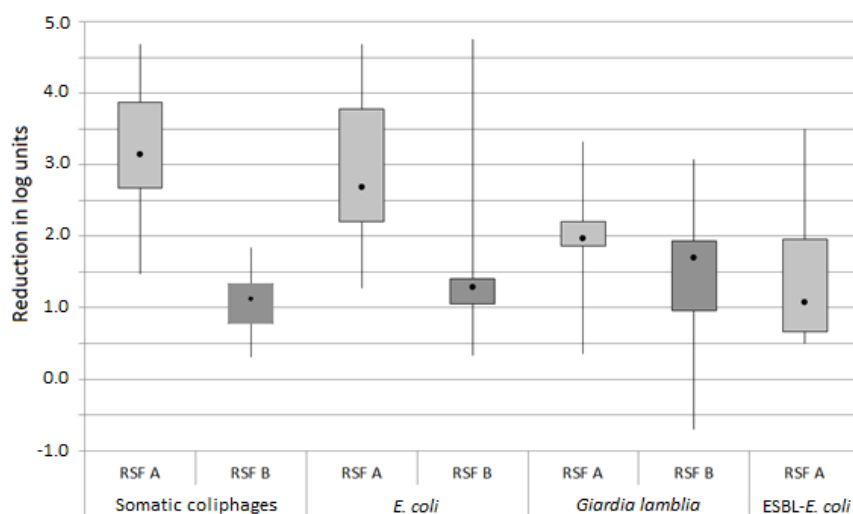
## RESULTS

### Reduction performance of large-scale RSFs

Our data revealed that the load of all tested microbiological parameters was reduced by passage through the RSFs in both test scenarios (large-scale and test facility). Figure 1 shows the reduction performance of the two investigated large-scale RSFs. The reduction performance at RSF A was 1-2 log units higher than at RSF B for all investigated parameters at both large-scale filters (not all data shown). For interpreting the results, it is important to notice that the concentrations of the combined sewage being fed to the large-scale RSFs were similar; the only difference was a slightly lower concentration (median) of the bacterial parameters at RSF B. The *E. coli* concentrations ranged from < 1.000 to 5.450,000 cfu/100 ml (median 1.325,000 cfu/100 ml) at RSF A and 216.220 to 6.360,000 cfu/100 ml (median 620.000 cfu/100 ml) at RSF B. The somatic coliphage concentrations were < 100 to 242.100 pfu/100 ml (median 41.800 pfu/100 ml) at RSF A and 8.000 to 269.000 pfu/100 ml (median 51.550 pfu/100 ml) for RSF B. ESBL-producing *E. coli* were only investigated at RSF A; the detected concentrations were between 37.273 and 909.091 cfu/100 ml (median 263.636 cfu/100 ml). The concentrations of the parasitic parameters in the combined sewage were slightly higher at RSF B, from 61 to 28.000 cysts/100 L (median 1,200 cysts/100 L), compared to 38 to 10.303 cysts/100 L (median 400 cysts/100 L) at RSF A.

### Reduction performance at the semi-technical facility

The reduction performance of the filters at the semi-technical facility for treated wastewater as a fourth purification stage reduced most microorganisms of 1-2 log units. Even some of the bacteria were below the corresponding detection limit. The results of the “HyReKA” project indicate RSFs diminished ARB: there was a 2.26-log-unit (median) reduction (Table 1).



**Figure 1.** Boxplots for the reduction performances of the large-scale filters (A and B) in log units for somatic coliphages, *E. coli*, *G. lamblia* and ESBL-producing *E. coli*.

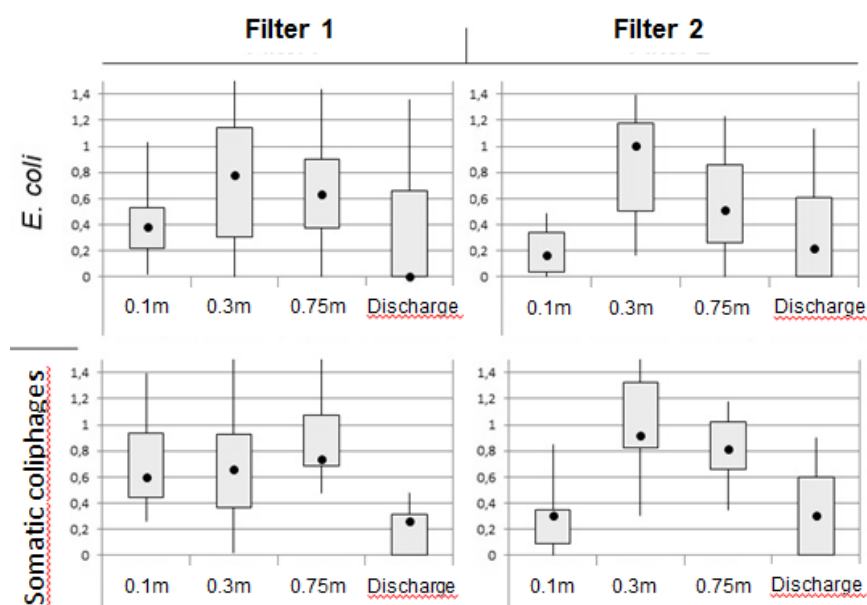
It was not possible to investigate the reduction performance for the parasitic parameters at the test facility because of the relatively small 0.5-1 L sample sizes. Table 1 shows the individual reduction performances as measured at the large-scale RSFs compared to the corresponding semi-technical filters. The reduction performances for *E. coli* and somatic coliphages differed between RSF A and B in large-scale applications (see also Figure 1), where RSF A exhibited greater reduction (despite using the filter material from the large-scale filters). The measured concentrations cannot be directly compared due to the different influent matrices, but the reductions are calculated within each system and are thus deemed to be comparable.

**Table 1.** Reduction performances (in log units) of the large-scale filters (A and B) and the corresponding semi-technical test facilities (1 and 2). RSF A corresponds to the material from filter 1 and RSF 2 to filter 2

		Reduction in log units				
		RSF A	Test facility (1)	RSF B	Test facility (2)	
Somatic coliphages	[pfu/100 ml]	<i>n</i>	24	14	24	14
		<i>Min</i>	1.47	1.08	0.31	1.08
		<i>Median</i>	3.15	2.46	1.12	2.53
		<i>Max</i>	4.68	3.3	1.84	3.3
<i>E. coli</i>	[cfu/100 ml]	<i>n</i>	25	6	23	6
		<i>Min</i>	1.27	1.25	0.64	0.92
		<i>Median</i>	2.66	2.02	1.24	1.76
		<i>Max</i>	4.7	3.81	4.95	3.33
ESBL- <i>E. coli</i>	[cfu/100 ml]	<i>n</i>	9	5	-	5
		<i>Min</i>	0.50	1.26	-	-0.07
		<i>Median</i>	1.08	2.26	-	2.26
		<i>Max</i>	3.50	3.69	-	3.69

### Individual filter layer

The semi-technical test facility was constructed to sample at different filter depths and thus to investigate the reduction performance at the different material steps. The microorganism reduction performance differed depending on the layer depth (Figure 2). In most cases, the strongest reduction occurred at 0.1-0.3 m.



**Figure 2.** Reduction of somatic coliphages and *E.coli* concentrations by RSFs A and filter B for treated wastewater. The layer depth (0.1, 0.3 and 0.75 m) or the discharge is shown on the x-axis. The y-axis indicates the reduction (in log units) of *E. coli* and somatic coliphages

## DISCUSSION

### RSF reduction performances

CSO consists of sewage as well as the run-off water from sealed surfaces. Microbial concentrations in CSO may be affected by the so-called first flush of stormwater runoff in the form of solid and sediment remobilization as well as dispersion of the sewer film (biofilm layer buildup at the water/air phase). The measured concentrations of microorganisms in the inflow of the investigated RSFs were similar, data that demonstrate the influent concentrations were not responsible for the reduction performance differences. This study emphasizes RSFs for their hygienic-microbiological purification performance of human-pathogenic bacteria and parasites in combined sewage or purified wastewater. Results from semi-technical RSF facilities already show strong purification performance for chemical substances (Brunsch et al., 2018). Investigation into the removal of human-pathogenic bacteria and ARB (*E. coli*, enterococci and staphylococci) in CSO by a full-scale RSF was reported by Scheurer et al. (2015). Their measured RSF reduction performance of these bacteria ranged from 2 to 3 log units. This phenomenon was confirmed by RSF A; it diminished ESBL-producing *E. coli* 1.08 log units, *E. coli* 2.66 log units and somatic coliphages 3.15 log units (median values). In general, large-scale RSF A demonstrated better results in reduction performance. Considering the fact that we compared very different ranges of input concentrations between the large-scale RSFs (input was combined sewage) and the semi-automatic test filters (input was purified wastewater), RSF A and B performance easily indicates multiple log-step reductions, a finding that suggests a log level ratio with higher purification efficiency than the test facilities. Nevertheless, it must be noted that the filter material is not responsible for the different reduction performance in the large-scale study.

In comparison to UV disinfection, activated carbon filtration/adsorption, ozonation and membrane bioreactors, RSFs offer similar or even better reduction performances as a fourth purification stage.

Disinfection reduces non-resistant bacteria during chlorination by 3 log units in the study of Huang et al. (2011). Czekalski et al. (2016) confirm ARB removal of 1-2 log units using ozonation. Nevertheless, chlorination or ozonation can remove organic trace elements and are dose-dependent in their limited effect on eliminating microorganisms (Rudolph et al., 1993). This study showed substantial reductions in somatic coliphages (median 2.46/2.53 log units for filter 1/filter 2), *E. coli* (median 2.02/1.76 log units) and ESBL-producing *E. coli* (median 2.26/2.26 log units) in treated wastewater at the test facilities. Classical treatment plants offer a median bacterial reduction of 2 log units (range of 1.5 to 3) and 1 to 3.6 log units for parasites (SWIST I, 2001). Dizer et al. (1994) report reduction values with microfiltration from 1 to > 6 log units for bacteria, 1-6 log units for virus and > 4 log units for parasites. According to Fiksdal and Leiknes (2006), ultrafiltration as a treatment technology diminishes all parameters (bacteria, viruses and parasites) by > 4 log units. However, do not need extensive maintenance, unlike the other discussed methods: ultrafiltration requires filter backwashes, active charcoal must be reactivated and for ozonation, the formation of non-specific by-products needs to be removed along with any residual ozone. Additionally, RSFs are efficient in terms of costs (materials, maintenance and repairs). Thus, considering the purification performance, RSFs should be noticed for their potential option as a fourth stage for wastewater treatment.

### **Individual filter layer**

Waldhoff (2008) states that on average approximately 40 % of bacteria are reduced in the top 10 cm of an RSF. According to Orb (2012), the value is even over 50 %. Over time, an accumulated organic material layer also forms at this depth, and this material influences the reduction performance. This topmost mud layer of approximately 2 cm is formed on the filter at the sand-water interface by suspended solids in the water. The subsequent upper, biologically active filter layer (3-5 cm) develops depending on filter granulation and speed (Orb, 2012). A presumed mechanism that underlies this effect could be increased adsorption due to biofilm growth (Waldhoff, 2008). Orb (2012) explains the high microbiological retention in the mud layer and upper, biologically active layer by lower sieving of the pore channels and the high organic content (approximately 90 %), both of which increase bacterial adhesion. In contrast, the current data revealed that the highest reduction occurred in the layer between 0.1 and 0.3 m, a top layer of the filter with a high concentration of accumulated biofilm and organic material. Thus, this layer may promote the microorganism and trace element reductions.

### **Flow rate**

RSF reduction performance varies depending on their operation. The efficiency in bacterial reduction was different between the two large-scale RSFs, which provided the filter material for the semi-technical filters. Reduction performance was much higher in RSF A, which had an effective throttled flow rate of 0.015 L/(s \* m<sup>2</sup>) compared to RSF B at 0.03 L/(s \* m<sup>2</sup>). Both of these values conform to the German guidelines on RSF construction. Influences like filter structure and influent composition can be eliminated as reason for the disparate reduction performances by examining the individual CSO compositions in the large-scale experiments and the use of the same operation conditions in the semi-technical filters. The latter two operated at same flow rate (0.03 L/(s \* m<sup>2</sup>)) and did not show any significant differences in their purification performance. Thus, the rate of throttle drainage, based on the structural parameters discussed herein, appears to be the deciding factor in the effectiveness of the RSF' hygienic-microbiological reduction performance.

## **CONCLUSIONS**

The investigated semi-technical RSF facilities offered high efficiency in reducing the concentration of microorganisms that comprise ARB. Additionally, an influence of the throttled flow rate on the reduction performances was revealed: reduction performance was inversely proportional to the flow



rate. Thus, this factor is crucial for RSF purification performance. Additionally, the individual depths of the filters offered different purification performance, which was highest within the upper layer (0.1-0.3 m depth). Overall, RSFs are very suitable as a fourth purification stage, because they efficiently reduce hygienic-microbial pollution such as parasites, viruses and bacteria including ARB. The bacterial reduction performance was at the same or even better value than UV disinfection, activated carbon filtration/adsorption, ozonation and membrane bioreactors, all of which are the standard fourth purification stage in WWTPs. Considering large-scale RSFs as a fourth purification step in WWTPs, they should be further investigated to increase their efficiency in the reduction of hygiene-relevant microbial pollution.

## ACKNOWLEDGEMENTS

This study uses data of the research projects “ReSMo” (Review of innovative measures to reduce trace elements and microorganisms in surface water; Az.: 54.2-3.3-1892-Wt) and “SWIST IV” (Review and evaluation of measures for the reduction of the chemical-physical and hygienic-microbiological loads of watercourses on the example of the river Swist; Az.: 54.2-3.3-1880-Wt), funded by the German Ministry for Environment, Agriculture, Conservation and Consumer Protection of the State of North Rhine-Westphalia (MULNV), the TAPES project (Transnational Action Programme on Emerging Substances), which received European Regional Development funding through the INTERREG IV B and the collaborative research project “HyReKA” (Biological and hygienic-medical relevance and control of antibiotic-resistant pathogens in clinical, agricultural and municipal wastewater and their relevance in raw water, funding ID: 02WRS1377), funded by the German Federal Ministry of Education and Research. We also thank all involved research partners for their contributions and support.

## REFERENCES

- Baquero, F., Martínez, J. L., Cantón, R. (2008) Antibiotics and antibiotic resistance in water environments. *Current Opinion in Biotechnology*, **19**(3), 260-265.
- Brunsch, A. F., ter Laak, T. L., Christoffels, E., Rijnaarts, H. H., Langenhoff, A. A. (2018) Retention soil filter as post-treatment step to remove micropollutants from sewage treatment plant effluent. *Science of the Total Environment*, **637**, 1098-1107.
- Christoffels, E., Mertens, F. M., Kistemann, T., Schreiber, C. (2014) Retention of pharmaceutical residues and microorganisms at the Altendorf retention soil filter. *Water Science and Technology*, **70**(9), 1503-1509.
- Czekalski, N., Imminger, S., Salhi, E., Veljkovic, M., Kleffel, K., Drissner, D., Hammes, F., Bürgmann, H., von Gunten, U. (2016) Inactivation of antibiotic resistant bacteria and resistance genes by ozone: from laboratory experiments to full-scale wastewater treatment. *Environmental science & technology*, **50**(21), 11862-11871.
- Dizer, H., Althoff, W., Bartocha, W., Dorau, W., Grohmann, A., Lopez-Pila, J.M., Seidel, K. (1994) Reduzierung von Bakterien und Viren in Klärwerksabläufen durch Mikrofiltration in einer Modellanlage (*Reduction of bacteria and virus in wastewater treatment plant effluents by microfiltration in a model plant*). *Zentralblatt für Bakteriologie, Mikrobiologie und Hygiene*. **695**, 697-702, (in German).
- DWA (Deutsche Vereinigung für Wasserwirtschaft, Abwasser und Abfall) (2019) DWA-Regelwerk, Arbeitsblatt DWA-A 178 - Retentionsbodenfilteranlagen (*Directive DWA-A 178 - Retention soil filter plants*), Hennef, Germany: DWA (in German).
- Fiksdal, L. and Leiknes, T. (2006) The effect of coagulation with MF/UF membrane filtration for the removal of virus in drinking water. *Journal of Membrane Science*, **279**, 364-371.
- Gibson III, C. J., Stadterman, K. L., States, S., Sykora, J. (1998) Combined sewer overflows: a source of Cryptosporidium and Giardia? *Water Science and Technology*, **38**(12), 67-72.

- Hiekel, S., Merkel, W., Overath, H. (2002) Leistungsfähigkeit von Langsandsandfiltern zur Rückhaltung von Mikroorganismen und Partikeln als letzte Stufe bei der Trinkwasseraufbereitung aus Oberflächenwasser (*Performance of slow sand filters for the retention of microorganisms and particles as a final stage in drinking water treatment from surface water*). *BBR Fachmagazin für Wasser Leitungstiefbau*, **53**, 38-44, (in German).
- Huang, J. J., Hu, H. Y., Tang, F., Li, Y., Lu, S. Q., Lu, Y. (2011) Inactivation and reactivation of antibiotic-resistant bacteria by chlorination in secondary effluents of a municipal wastewater treatment plant. *Water Research*, **45**(9), 2775-2781.
- Kistemann, T., Christoffels, E., Koch, C., Claßen, T., Rechenburg, A., Exner, M. (2004) Untersuchungen zur mikrobiellen Fließgewässerbelastung durch Regenentlastungen der Mischkanalisation am Beispiel der Swist. Swist II (*Investigations on the microbial pollution of streams by rain relief of the combined sewage system*). Institute for Hygiene and Public Health, University of Bonn and Erftverband, Bonn/Bergheim, Germany, (in German).
- Mertens, F. M., Christoffels, E., Schreiber, C., Kistemann, T. (2012) Rückhalt von Arzneimitteln und Mikroorganismen am Beispiel des Retentionsbodenfilters Altendorf (*Retention of pharmaceuticals and microorganisms using the example of the retention soil filter Altendorf*). *Korrespondenz Abwasser, Abfall*, **59**, 1137-1143, (in German).
- MUNLV (2015) Retentionsbodenfilter. Handbuch für Planung, Bau und Betrieb (*Retention soil filter. Manual for the planning, construction and operation*). Ministerium für Umwelt und Naturschutz, Landwirtschaft und Verbraucherschutz des Landes Nordrhein-Westfalen, Düsseldorf, Germany, (in German).
- Novo, A., André, S., Viana, P., Nunes, O. C., Manaia, C. M. (2013) Antibiotic resistance, antimicrobial residues and bacterial community composition in urban wastewater. *Water Research*, **47**(5), 1875-1887.
- Orb, R. K. (2012) Rückhalt hygienerelevanter Bakterien in mischwasserbeschickten Retentionsbodenfiltern – Konstruktive Hinweise (*Retention of hygienic-relevant bacteria in retention soil filters fed with combined sewage – constructive hints*) (Unpublished doctoral dissertation). Karlsruher Institut für Technologie, Karlsruhe, Germany, (in German).
- Overath, H., Merkel, W. and Hiekel, S. (2000) Einleitung von Kläranlagenabläufen in kleine Fließgewässer: Bewertung der Ablaufqualität nach der EG-Badegewässer-Richtlinie (*Discharge of wastewater treatment plant effluent into small rivers: Assessment of effluent quality according to the EC-Bathing Water Directive*). Ministerium für Umwelt und Naturschutz - Landwirtschaft und Verbraucherschutz des Landes Nordrhein-Westfalen, Mülheim an der Ruhr, Germany, (in German).
- Rudolph, K.- U., Oberg, C., Nelle, T. (1993) Stand der Technik bei Desinfektion von Abwasser und Schwerpunkte der Forschung (*State of the art in the disinfection of wastewater and research priorities*). *Gwf Wasser-Abwasser*, **134**, 1-9, (in German).
- Scheurer, M., Heß, S., Lüddecke, F., Sacher, F., Güde, H., Löffler, H., Gallert, C. (2015) Removal of micropollutants, facultative pathogenic and antibiotic resistant bacteria in a full-scale retention soil filter receiving combined sewer overflow. *Environmental Science: Processes & Impacts*, **17**(1), 186-196.
- SWIST I (2001) Untersuchungen zur mikrobiellen Fließgewässerbelastung durch Kläranlagen (*Investigations of the microbial pollution of water streams by wastewater treatment plants*). Institute for Hygiene and Public Health, University of Bonn and Erftverband, Bonn/Bergheim, Germany, (in German).
- TAPES (2016, January) *Transnational Action Programme On Emerging Substances - Final Project Report*. [online] [http://www.tapes-interreg.eu/uploads/final\\_project\\_report\\_TAPES.pdf](http://www.tapes-interreg.eu/uploads/final_project_report_TAPES.pdf).
- Waldhoff, A. (2008) Hygienisierung von Mischwasser in Retentionsbodenfiltern (RBF) (*Disinfection of combined sewage by retention soil filters (RSFs)*). Universität Kassel, Kassel, Germany, (in German).

# Application of Core-shell Bimagnetic Nanoparticles for Removal of Phosphorus from Aqueous Solution

A. A. A. M. Guerra\*, F. L. Damasceno\*, C. C. K. Barreto\*\*, A. F. Campos\*\* and A. K. B. Amorim\*

\* Environmental Technology and Water Program, University of Brasilia, 70910-900, Brasilia, Brazil (E-mails: [anaaliceeq@gmail.com](mailto:anaaliceeq@gmail.com); [fldamasceno10@hotmail.com](mailto:fldamasceno10@hotmail.com); [ariuska@unb.br](mailto:ariuska@unb.br))

\*\* Laboratory for Environmental and Applied Nanoscience, Faculty UnB-Planatina, University of Brasilia, 73345-010, Brasilia, Brazil (E-mails: [relex@unb.br](mailto:relex@unb.br); [cynarakern@gmail.com](mailto:cynarakern@gmail.com))

## Abstract

Phosphorus (P) must be removed from wastewaters to prevent eutrophication in water bodies. The capacity of core-shell bimagnetic nanoparticles ( $\text{CoFe}_2\text{O}_4@ \gamma\text{-Fe}_2\text{O}_3$ ) to adsorb phosphorus (P) was evaluated in order to investigate a nanoadsorbent which may be used as a technology for wastewater treatment. The nanomaterial was synthesized through a hydrothermal coprecipitation followed by a surface treatment. X-ray diffraction measurements were performed to characterize the material. Batch adsorption tests provided information regarding the influence of the solution pH, contact time and initial P concentration on the adsorption. The effect of the solution pH confirmed that the electrostatic interactions between the adsorbate and the adsorbent are favored as lower the pH is. The results obtained from the influence of the contact time showed that the Elovich model presented the best adjustment to the kinetics. The Freundlich model best fitted the equilibrium data, suggesting that multilayers are formed and that the adsorbent surface is heterogeneous. Furthermore, it was concluded that the nanoadsorbent mean size affects significantly the adsorption. The smaller the mean diameter is the greater is the available surface area and, consequently, the capacity of adsorption of the nanomaterial.

## Keywords

Phosphorus removal; adsorption; nanoparticles

## INTRODUCTION

An adequate concentration of phosphorus (P) in water bodies is key to maintain life in these environments. This chemical element is a limiting nutrient to growth of organisms in freshwater (Elser et al., 2007). However, high concentrations of P may cause eutrophication of aquatic environments. In order to avoid a possible uncontrolled increase of P in water bodies, P must be removed from wastewaters, since a significant amount of it can be found in different kinds of wastewater (Verstraete et al., 2009; Barnett et al., 1994). Among the P removal technologies, adsorption has been increasingly gaining attention from the scientific field due to its good performance at low concentrations, greater selectivity and simple operation (Yang et al., 2014). Therefore, this work aims to investigate the capacity of core-shell bimagnetic nanoparticles ( $\text{CoFe}_2\text{O}_4@ \gamma\text{-Fe}_2\text{O}_3$ ) to adsorb P from aqueous solution in order to obtain a preliminary response regarding its use as a technology for wastewater treatment. It is important to highlight that the nanomaterial has magnetic properties, which enable an easy separation of the adsorbed nanoparticles from the medium through the appliance of a magnetic field. This characteristic can facilitate the recovery of P and the reuse of the nanoadsorbent (Tu et al., 2015).

## METHODOLOGY

### Synthesis of the nanoadsorbent

The first part of the synthesis of the nanoadsorbent corresponds to the production of ferrite cobalt nanoparticles ( $\text{CoFe}_2\text{O}_4$ ) through a hydrothermal coprecipitation of aqueous solutions of  $\text{Co}(\text{NO}_3)_2$  and  $\text{FeCl}_3$  in alkaline medium. In this step, in order to obtain samples of two different mean sizes,

sodium hydroxide (NaOH) was used to synthesize the larger mean size nanoparticles (PaCoL) while methylamine ( $\text{CH}_3\text{NH}_2$ ) was used in the synthesis of the smaller mean size nanoparticles (PaCoS). This strategy was applied since the nanoparticles mean size depends on the hydroxide concentration of the medium (Aquino et al., 2002). The second part of the synthesis is a surface treatment with a solution of  $\text{Fe}(\text{NO}_3)_3$ . In this step, a thin layer of maghemite ( $\gamma$ - $\text{Fe}_2\text{O}_3$ ) is formed around the ferrite cobalt nanoparticles. The shell of maghemite protects the nanoparticles from acid dissolution. The formula of the nanoadsorbent synthesized can be expressed by a core-shell model of bimagnetic ferrite nanoparticles ( $\text{CoFe}_2\text{O}_4@ \gamma\text{-Fe}_2\text{O}_3$ ).

### **X-ray diffraction measurements**

X-ray diffraction measurements (XRD) were performed to provide information regarding the crystalline structure and the mean size of the nanoparticles using powder samples, which had their carrier liquids previously evaporated.

The X-ray diffraction measurements were carried out on an X-ray diffractometer of the model D8 Focus (Bruker), operated at 40Kv/30mA with a Cu  $\text{K}\alpha$  radiation ( $\lambda=0.1541$  nm) selected by a Ge (111) monochromator. A  $20^\circ \leq 2\theta \leq 80^\circ$  interval was considered, with a  $0.05^\circ$  step and  $0.1^\circ \text{ min}^{-1}$  scan rate.

### **Batch adsorption tests**

Batch adsorption tests were performed to evaluate the influence of the solution pH, the contact time and the initial P concentration for both mean sizes of nanoparticles. The tests were carried out on an orbital shaker. After the contact time, the nanoparticles were separated from the solution through the application of a magnetic field to the system for 15 minutes, using a permanent magnet (Nd-Fe-B). The concentration of phosphate in the supernatant was determined spectrophotometrically.

A first set of batch adsorption tests was implemented to verify the influence of the solution pH on the adsorption. In these experiments, 10 mg of nanoparticles were added to 15 ml of a phosphate solution of 10 mg/L with a contact time of 30 minutes and shaking rate of 200 rpm. The solution pH varied from 2 to 10.

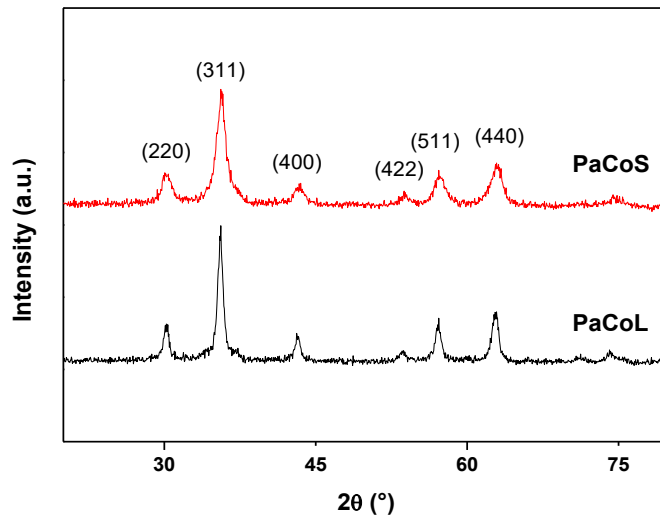
Using the best solution pH, which was obtained from the previous set of experiments, batch adsorption tests varying the contact time provided information regarding the kinetics of the process. The nanoparticles dosage, the solution volume, the phosphate concentration and the shaking rate were the same as the first set of batch adsorption tests.

Finally, knowing the best solution pH and the equilibrium time, a third set of batch adsorption tests was performed to obtain the adsorption isotherms at 25 °C. The phosphate concentration was varied from 5 to 130 mg/L. The nanoparticles dosage and the solution volume were the same as the other tests.

## **RESULTS AND DISCUSSION**

### **Characterization of the nanoadsorbent**

The X-ray diffractogram pattern confirmed the spinel ferrites structure in according to the International Centre for Diffraction Data (ICDD) for both mean sizes of nanoparticles (Figure 1). The values of the average lattice parameter (0.835 nm for PaCoS and 0.837 nm for PaCoL) are in good agreement with the ICDD patterns for maghemite and cobalt ferrite. The mean diameter of the nanoparticle (dXRD) was calculated by applying the Scherrer's formula (Hammond, 1997) to the most intense line of the diffractogram (311). The dXRD obtained was 7.8 nm for PaCoS and 13.5 nm for PaCoL.



**Figure 1.** X-ray powder diffraction patterns

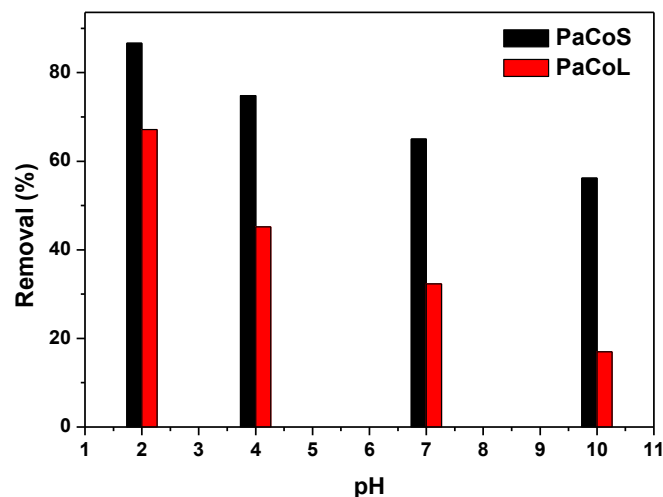
### Effect of the solution pH on phosphorus removal

The percentage of P removal for Figure 2 was calculated by:

$$\text{Removal (\%)} = \frac{C_0 - C_t}{C_0} \times 100\% \quad (1)$$

where  $C_0$  is the initial P concentration and  $C_t$  is the P concentration after the contact time.

The influence of the solution pH on the adsorption demonstrated that, within the studied range, the lower the pH is the greater is the removal of P for both samples. This result can be explained by the effect that the solution pH has on the speciation of both adsorbent surface and adsorbate. In aqueous solution, the nanoadsorbent surface presents amphoteric sites  $\equiv\text{FeOH}$ , which can protonate to  $\equiv\text{FeOH}_2^+$ , below the point of zero charge (PZC), or deprotonate to  $\equiv\text{FeO}^-$ , above the PZC. The PZC of the studied nanoadsorbent surface is around 7.0 (Campos et al., 2019; Campos et al., 2013). Thus, the surface is positively charged in acidic medium and negatively charged in alkaline medium. Regarding the speciation of the adsorbate, the phosphate ions are predominantly negatively charged from pH = 2 to 14. Therefore, the highest value of removal at pH = 2 is due to the strong electrostatic interactions between the negatively charged phosphate ions and the nanoadsorbent surface, which is mainly composed by  $\equiv\text{FeOH}_2^+$ . Rising the solution pH, the adsorbent surface becomes less positive and a reduction in the interactions between the adsorbent and the adsorbate happens.



**Figure 2.** Effect of the solution pH on phosphorus removal

### Adsorption kinetics

The amount of P adsorbed at any time  $t$  ( $q_t$ ) is expressed by:

$$q_t = \frac{(C_0 - C_t)V}{m} \quad (2)$$

Where  $C_0$  is the initial P concentration,  $C_t$  is the P concentration after the contact time,  $V$  is the solution volume and  $m$  is the nanoadsorbent mass.

The kinetics data were adjusted to the non-linear pseudo-first order, pseudo-second order and Elovich models, which are given by the following equations, respectively:

$$q_t = q_e (1 - e^{-k_1 t}) \quad (3)$$

$$q_t = \frac{q_e^2 k_2 t}{1 + q_e k_2 t} \quad (4)$$

$$q_t = \frac{1}{\beta} \ln(1 + \alpha \beta t) \quad (5)$$

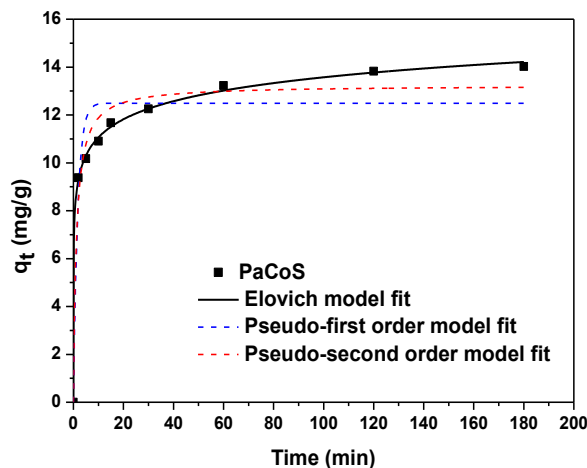
Where  $q_e$  is the amount of P adsorbed at equilibrium,  $k_1$  is the pseudo-first order rate constant,  $k_2$  is the pseudo-second order rate constant,  $q_e^2 k_2$  is the initial sorption rate (Günay et al., 2007),  $\alpha$  is the initial rate constant and  $\beta$  is the desorption constant (Günay et al., 2007; Tran et al., 2017).

Besides the coefficient of determination ( $R^2$ ), the mean absolute percentage error (MAPE) was calculated to verify the fit of the models. The MAPE is calculated by:

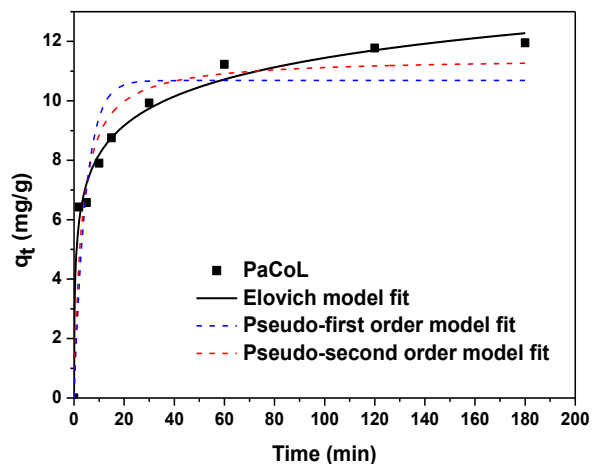
$$MAPE (\%) = \frac{\sum_{i=1}^N \left| \frac{q_{exp} - q_{calc}}{q_{exp}} \right|}{N} \times 100\% \quad (6)$$

Where  $q_{exp}$  is the experimental value,  $q_{calc}$  is the model's predicated value and  $N$  corresponds to the number of experimental data.

Figure 3 and 4 show the kinetics of P adsorption. The equilibrium was achieved in a period of approximately three hours for the two samples with a removal of P of 94 % for PaCoS and 80 % for PaCoL. Tables 1, 2 and 3 present the kinetic adsorption parameters for the pseudo-first order, pseudo-second order and Elovich models, respectively. The Elovich model best fits the kinetics data for both samples. This model is empirical and it has been generally applied to describe chemisorption (Tran et al., 2017). Although the kinetic data suggest that chemisorption occurs in the process, more information is necessary to fully describe the adsorption mechanism.



**Figure 3.** Kinetics adsorption data - PaCoS



**Figure 4.** Kinetics adsorption data – PaCoL

**Table 1.** Kinetics adsorption parameters – Pseudo-first-order model

Pseudo-first-order				
Sample	$k_1$ ( $\text{min}^{-1}$ )	$q_e$ ( $\text{mg g}^{-1}$ )	$R^2$	MAPE (%)
PaCoS	0.58	12.49	0.913	9.23
PaCoL	0.21	10.68	0.839	14.71

**Table 2.** Kinetics adsorption parameters – Pseudo-second-order model

Pseudo-second-order				
Sample	$k_2$ ( $\text{mg g}^{-1} \text{min}^{-1}$ )	$q_e$ ( $\text{mg g}^{-1}$ )	$R^2$	MAPE (%)
PaCoS	0.06	13.23	0.967	5.95
PaCoL	0.02	11.44	0.935	9.70

**Table 3.** Kinetics adsorption parameters – Elovich model

Elovich				
Sample	$\alpha$ ( $\text{mg g}^{-1} \text{min}^{-1}$ )	$\beta$ ( $\text{mg g}^{-1}$ )	$R^2$	MAPE (%)
PaCoS	2786.08	0.91	0.998	1.04
PaCoL	45.78	0.70	0.988	3.86

### Isotherm modelling

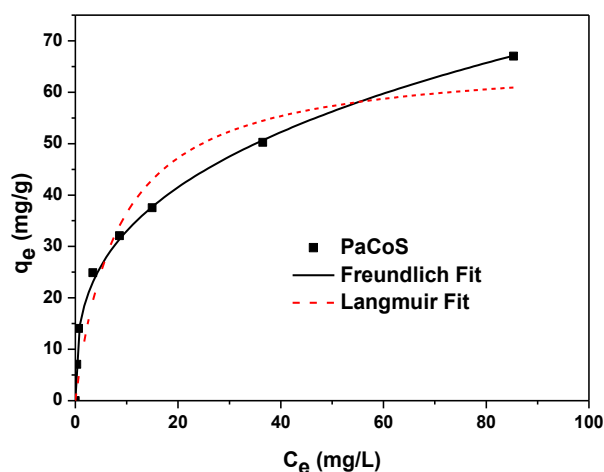
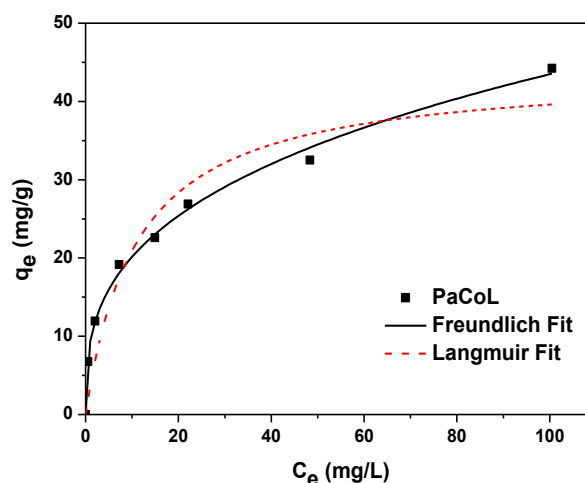
The equilibrium data were adjusted to the non-linear Langmuir and Freundlich models, which are expressed by the following equations, respectively:

$$q_e = \frac{q_{\max} k_l C_e}{1 + k_l C_e} \quad (7)$$

$$q_e = k_f C_e^{1/n} \quad (8)$$

Where  $C_e$  is the equilibrium P concentration,  $q_e$  is the amount of P adsorbed at equilibrium,  $q_{\max}$  corresponds to the maximum adsorption capacity,  $k_l$  is the Langmuir constant,  $k_f$  is the Freundlich constant and  $1/n$  corresponds to a heterogeneity factor which provides information regarding the adsorption intensity.

In Figure 5 and 6, the equilibrium data is presented. Tables 4 and 5 show the equilibrium adsorption parameters for Langmuir and Freundlich models, respectively.

**Figure 5.** Equilibrium adsorption data – PaCoS**Figure 6.** Equilibrium adsorption – PaCoL

**Table 4.** Equilibrium adsorption parameters – Langmuir model

Sample	Langmuir		R <sup>2</sup>	MAPE (%)
	k <sub>l</sub> (L mg <sup>-1</sup> )	q <sub>max</sub> (mg g <sup>-1</sup> )		
PaCoS	0.12	66.84	0.926	26.93
PaCoL	0.09	43.95	0.921	23.56

**Table 5.** Equilibrium adsorption parameters – Freundlich model

Sample	Freundlich		R <sup>2</sup>	MAPE (%)
	k <sub>f</sub> (mg <sup>1-1/n</sup> g <sup>-1</sup> L <sup>1/n</sup> )	n		
PaCoS	15.39	3.01	0.994	7.59
PaCoL	9.32	2.99	0.995	3.65

The Freundlich model best fits the equilibrium data for both samples, suggesting that multilayers are formed in the adsorption process and that the adsorbent surface is heterogeneous. The Freundlich model has been applied to characterize the P adsorption process by different kinds of nanoadsorbents (Drenkova-Tuhtan et al., 2017; Moharami and Jalali, 2014).

The formation of multilayers suggests that physisorption occurs in the process. This phenomenon can be explained by analyzing the electric double layer model. In the pH = 2, the nanoadsorbent surface is positively charged and its local electrostatic field attracts the phosphate ions, which are negatively charged in its majority. Moving away from the nanoadsorbent surface, the quantity of adsorbed phosphate ions decreases as a result of the reduction of the electrostatic field intensity. This effect will occur until the distance which the thermal energy becomes higher than the electrostatic interactions and the phosphate ions will not adsorb onto the nanoadsorbent surface.

The nanoadsorbent mean size affects significantly the adsorption process. In all tests, the PaCoS sample adsorbed more P than the PaCoL sample under the same conditions. These results were expected since the smaller the mean diameter is the greater the available adsorption surface area per mass is.

## CONCLUSIONS

In this study, a bimagnetic nanoasorbent was synthesized through a coprecipitation process followed by a surface treatment. The nanomaterial can be described by a core-shell model and its structure can be expressed as CoFe<sub>2</sub>O<sub>4</sub>@γ-Fe<sub>2</sub>O. Two different mean sizes of nanoparticles were tested. The study of the influence of the solution pH showed that the more acidic the pH is the greater is the removal of P, within the studied range. The highest removal was obtained at pH = 2. The Elovich model best fitted the kinetic data and the equilibrium was achieved within 3 hours. A P removal of 94 % for PaCoS and 80 % for PaCoL was achieved for an initial concentration of 10 mg/L of P. The equilibrium data were best adjusted to the Freundlich model, indicating that multilayers are formed and the heterogeneity of the nanoadsorbent surface. From these results, it was concluded that the nanoadsorbent has potential to be applied as a novel technology for P removal from wastewater.

## REFERENCES

- Aquino, R., Tourinho, F. A., Itri, R., Lara, M. C. F. L. E., Depeyrot, J. (2002) Size control of MnFe<sub>2</sub>O<sub>4</sub> nanoparticles in electric double layered magnetic fluid synthesis. *Journal of*



*Magnetism and Magnetic Materials*, **252**, 23-25.

- Barnett, J. W., Kerridge, G. J., Russell, J. M. (1994) Effluent treatment systems in the dairy industry. *Australasian Biotech.*, **4**, 26-30.
- Campos, A. F. C., Aquino, R., Tourinho, F. A., Paula, F. L., Depeyrot, J. (2013) Influence of the spatial confinement at nanoscale on the structural surface charging in magnetic nanocolloids. *The European Physical Journal*, **36**(4), 1-11.
- Campos, A. F. C., Oliveira, H. A. L., Silva, F. N., Silva, F. G., Coppola, P., Aquino, R., Mezzi, A. (2019) Core-Shell Bimagnetic Nanoadsorbents for Hexavalent Chromium Removal from Aqueous Solutions. *Journal of Hazardous Materials*, **362**, 82-91.
- Drenkova-Tuhtan, A., Schneider, M., Franzreb, M., Meyer, C., Gellermann, C., SEXTL, G., Mandel, K., Steinmetz, H. (2017). "Pilot-scale removal and recovery of dissolved phosphate from secondary wastewater effluents with reusable ZnFeZr adsorbent @ Fe<sub>3</sub>O<sub>4</sub>/SiO<sub>2</sub> particles with magnetic harvesting". *Water Research*, **109**, 77-87.
- Elser, J. J., Bracken, M. E. S., Cleland, E. E., Gruner, D. S., Harpole, W. S., Hillebrand, H., Ngai, J. T., Seabloom, E. W., Shurin, J. B., Smith, J. E. (2007) Global analysis of nitrogen and phosphorus limitation of primary producers in freshwater, marine, and terrestrial ecosystems. *Ecology Letters*, **10**, 1135-1142.
- Günay, A., Arslankaya, E., Tosun, I. (2007) Lead removal from aqueous solution by natural and pretreated clinoptilolite: Adsorption equilibrium and kinetics. *Journal of Hazardous Materials*, **146**, 362-371
- Hammond, C. (1997) *The Basics of Crystallography and Diffraction*, Oxford University Press, New York.
- Moharami, S., Jalali, M. (2014) "Effect of TiO<sub>2</sub>, Al<sub>2</sub>O<sub>3</sub>, and Fe<sub>3</sub>O<sub>4</sub> Nanoparticles on Phosphorus Removal from Aqueous Solution". *Environmental Progress and Sustainable Energy*, **33** (4), 1209-1219.
- Tran, H. N., You, S., Hosseini-Bandegharai, A., Chao, H. (2017) Mistakes and inconsistencies regarding adsorption of contaminants from aqueous solution: A critical review. *Water Research*, **120**, 88-116.
- Tu, Y., You, C., Chang, C., Chen, M. (2015) Application of magnetic nano-particles for phosphorus removal/recovery in aqueous solution. *Journal of the Taiwan Institute of Chemical Engineers*, **46**, 148-154.
- Verstraete, W., Van de Caveye, P., Diamantis, V. (2009) Maximum use of resources present in domestic "used water". *Bioresource Technology*, **100**(23), 5537-5545.
- Yang, K., Yan, L., Yang, Y., Yu, S., Shan, R., Yu, H., Zhu, B., Du, B. (2014) Adsorptive removal of phosphate by Mg-Al and Zn-Al layered double hydroxides: Kinetics, isotherms and mechanisms. *Separation And Purification Technology*, **124**, 36-42.

# Limits of Increased Simultaneous Phosphorus Precipitation in WWTP Bílina

F. Harciník\*, M. Pečenka\*\* and M. Vrábel\*\*

\* Severočeské vodovody a kanalizace, a.s., Přítkovská 1689, 415 50 Teplice, Czechia  
(E-mail: [filip.harcinik@scvk.cz](mailto:filip.harcinik@scvk.cz))

\*\* Vysoká škola chemicko-technologická v Praze, Ústav technologie vody a prostředí, Technická 5, 166 28 Praha 6 – Dejvice, Czechia (E-mail: [martin.pecenka@vscht.cz](mailto:martin.pecenka@vscht.cz))

## Abstract

Increasing requirements for improving the quality of surface water press on the quality of outlet from wastewater treatment plants. Limits of pollution at the outlet from WWTP are given by the Government Decree No. 401/2015 Coll., which amendment has been widely discussed in recent years. The aim of this paper is not to evaluate whether and how stricter concentrations of outlet from WWTPs would affect quality of surface water. It is about the preparation of the operating company for a possible change in legislation which will cause considerable costs - both investment and operational - to both operators and owners of water infrastructure. For monitoring, WWTP from the size category where the technological method of achieving possible stricter limits in the  $P_{tot}$  parameter is not clear was chosen.

## Keywords

WWTP; wastewater; water quality; phosphorus; phosphorus removal; phosphorus precipitation

## INTRODUCTION

The subject matter of the paper is testing limits of simultaneous phosphorus precipitation at WWTP Bílina. Anticipated amendment of Government Decree No. 401/2015 Coll. is connected with a reduction of required limits for quality of water on the outlet from WWTPs. Probably the biggest challenge would be a reduction of the total phosphorus concentration. Depending on the size of the WWTP, the question is which technological solution will be able to meet the new requirements. Only the tertiary stage of treatment is considered for WWTPs above 100,000 PE. But for WWTPs between 10,000 – 100,000 PE it is not so clear. WWTP Bílina is one of the plants, operated by company Severočeské vodovody a kanalizace, a.s, which belongs to this size category.

The result of the testing is to verify the possibility of meeting the limits of the considered amendment of the Government Decree No. 401/2015 Coll., without changing the current technology of WWTP – ie by simultaneous phosphorus precipitation. Concentrations of  $P_{tot}$  in the effluent were monitored and also the effect of increased coagulant doses on biochemical processes in the biological treatment stage (mainly nitrification) and on other operational parameters such as activated sludge quality (biocoenosis, monitoring of iron content in sludge and organic content in sludge dry matter) and also a possibility of increased sludge production.

## PROCESS AND METHODS

WWTP Bílina is a mechanical-biological treatment plant. Biological treatment stage is composed from two lines, each with regeneration, denitrification and nitrification tank. Testing took place from end of February to end of April.

During this period one biological treatment line (line 1) was a reference line. Dosing of a coagulant was automatic there – dosage was calculated by an algorithm in Automatic Controlled System

(ACS) based on the on-line measurement of P-PO<sub>4</sub> concentration and wastewater flow in WWTP. The second biological treatment line was a testing line. Dosing of a coagulant was fixed – dosage was increased during the testing from 2 litres per hour to 6 litres per hour.

Effluent quality was monitored in each line and also in joint channel from both lines. Parameters were mainly COD, SS, N-NH<sub>4</sub>, N-NO<sub>2</sub>, N-NO<sub>3</sub>, N<sub>tot</sub>, P<sub>tot</sub>, Fe.

Activity and quality of activated sludge in both biological lines was monitored by kinetic and respirometric tests of nitrification. Also the concentration of P<sub>tot</sub> and Fe in sludge was determined.

During the tested period there were five samplings of sludge for kinetic and respirometric tests of nitrification and also for determination of P<sub>tot</sub> and Fe concentration in activated sludge. First sampling (27/2/2019) was performed in the “steady” state when the dosing of coagulant was in automatic mode in both biological lines. After the first sampling, fixed dose in line 2 was set (2 l/h). This dosage was set based on the operational experience and average annual consumption. Second sampling (12/3/2019) was performed during this set dose and after the second sampling the fixed dose in line 2 was reset to 4 l/h. On 24/3/2019 and 09/04/2019 was made third and fourth sampling with fixed dose 4 l/h. On 10/04/2019 the fixed dose was reset to 7 l/h and after 14 days last sampling was made.

Quality of effluent from WWTP was monitored during whole testing period in a weekly period by 24h sample with 2h interval, proportionally to the flow of wastewater. Plus every two weeks 24h sample with 2h interval was taken from both secondary settling tanks (SST).

## RESULTS

### Effluent quality

Main aim of the testing was verification of possibility to meet future stricter limits of phosphorus concentration on the effluent of WWTP by simultaneous precipitation of phosphorus. The limit is 2 mg/l P<sub>tot</sub> (annual average) and 6 mg/l (maximum that is not allowed to exceed) currently. Possible new limit would be between 0,5 – 0,8 mg/l.

In Table 1 – 3 are results of effluent quality from the SST 1, SST 2 and from the outlet from WWTP (mix of both SST).

**Table 1.** Effluent quality from secondary settling tank 1 (reference line) during tested period

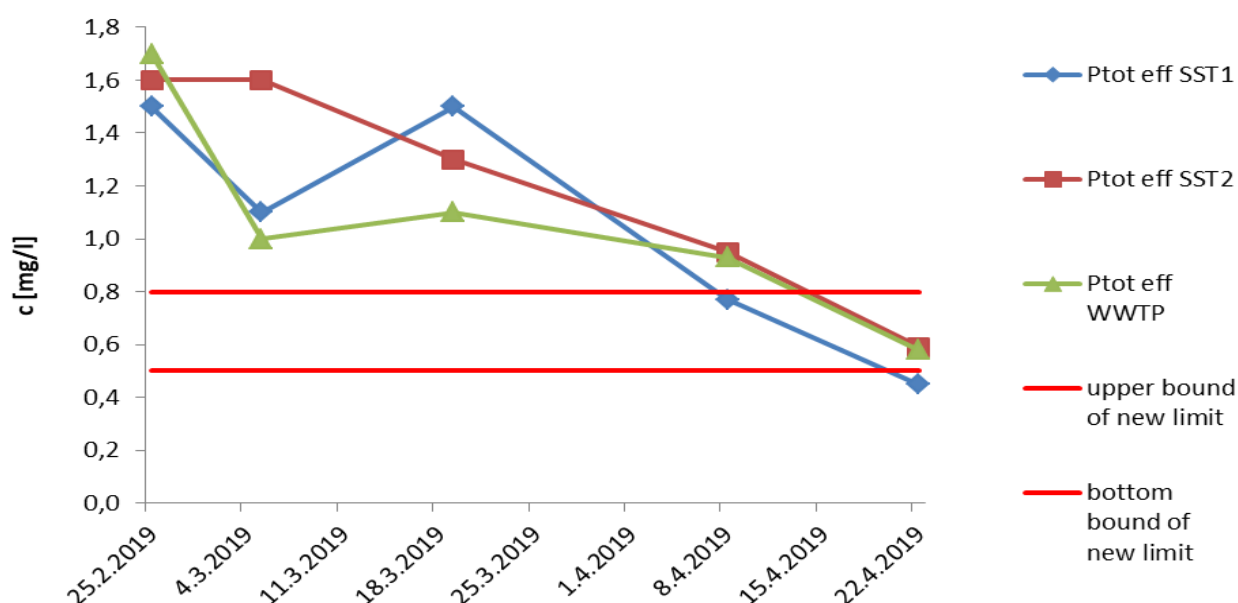
	pH	COD	N-NH <sub>4</sub>	N-NO <sub>2</sub>	N-NO <sub>3</sub>	N <sub>tot</sub>	P <sub>tot</sub>	P-PO <sub>4</sub>
average	7.4	15.8	0	0.018	8.52	9.8	1.06	0.83
minimum	7.1	<15	<1.00	0.012	6.23	6.6	0.45	0.40
maximum	7.6	21	<1.00	0.029	12.30	14.4	1.50	1.40
sampling Date	pH	COD mg/l	N-NH <sub>4</sub> mg/l	N-NO <sub>2</sub> mg/l	N-NO <sub>3</sub> mg/l	N <sub>tot</sub> mg/l	P <sub>tot</sub> mg/l	P-PO <sub>4</sub> mg/l
25. 2. 2019	7.6	<15	<1.00	0.015	12.30	14.4	1.50	1.40
5. 3. 2019	7.1	21	<1.00	0.020	8.42	9.1	1.10	0.76
19. 3. 2019	7.6	20	<1.00	0.012	9.21	12.1	1.50	0.90
8. 4. 2019	7.2	18	<1.00	0.029	6.44	6.9	0.77	0.71
22. 4. 2019	7.5	20	<1.00	0.013	6.23	6.6	0.45	0.40

**Table 2.** Effluent quality from secondary settling tank 2 (tested line) during tested period

	pH	COD	N-NH <sub>4</sub>	N-NO <sub>2</sub>	N-NO <sub>3</sub>	N <sub>tot</sub>	P <sub>tot</sub>	P-PO <sub>4</sub>
average	7.4	17.8	0	0.018	10.66	12.2	1.21	0.93
minimum	7.2	<15	<1.00	0.014	7.20	8.0	0.59	0.41
maximum	7.6	25	<1.00	0.023	15.30	15.8	1.60	1.40
sampling Date	pH	COD mg/l	N-NH <sub>4</sub> mg/l	N-NO <sub>2</sub> mg/l	N-NO <sub>3</sub> mg/l	N <sub>tot</sub> mg/l	P <sub>tot</sub> mg/l	P-PO <sub>4</sub> mg/l
25. 2. 2019	7.5	<15	<1.00	0.017	15.30	15.8	1.60	1.40
5. 3. 2019	7.2	25	<1.00	0.020	11.60	12.2	1.60	0.86
19. 3. 2019	7.6	22	<1.00	0.015	11.20	15.3	1.30	1.20
8. 4. 2019	7.3	22	<1.00	0.023	7.99	9.7	0.95	0.78
22. 4. 2019	7.5	20	<1.00	0.014	7.20	8.0	0.59	0.41

**Table 3.** Effluent quality from WWTP Bílina during tested period

	pH	COD	BOD	SS	N-NH <sub>4</sub>	N-NO <sub>2</sub>	N-NO <sub>3</sub>	N <sub>tot</sub>	P <sub>tot</sub>
average	7.5	12	2.6	4.6	0	0.022	9.22	11.0	1.06
minimum	7.2	<15	1.9	2.8	<1.00	0.014	3.95	5.5	0.58
maximum	7.8	22	3.1	6.4	<1.00	0.043	14.30	15.8	1.7
sampling date	pH	COD mg/l	BOD mg/l	SS mg/l	N-NH <sub>4</sub> mg/l	N-NO <sub>2</sub> mg/l	N-NO <sub>3</sub> mg/l	N <sub>tot</sub> mg/l	P <sub>tot</sub> mg/l
25. 2. 2019	7.6	<15	1.9	4.6	<1.00	0.018	14.30	16.6	1.70
5. 3. 2019	7.4	16	3.0	3.2	<1.00	0.015	9.39	10.2	1.0
19. 3. 2019	7.8	<15	2.8	6.0	<1.00	0.014	9.49	12.6	1.10
8. 4. 2019	7.2	22	2.2	2.8	<1.00	0.043	8.97	10.1	0.93
22. 4. 2019	7.5	22	3.1	6.4	<1.00	0.020	3.95	5.5	0.58

**Figure 1.** P<sub>tot</sub> concentration in effluent from SST 1, SST 2 and WWTP during tested period

From the Table 1. – 3. and also the Figure 1 is evident expected decrease of P<sub>tot</sub> concentration on the outlet from WWTP Bílina during tested period. But potential limit, which is showed by straight red line in the Figure 1, was reached almost in the end of tested period when the fixed dose of 7 l/h has

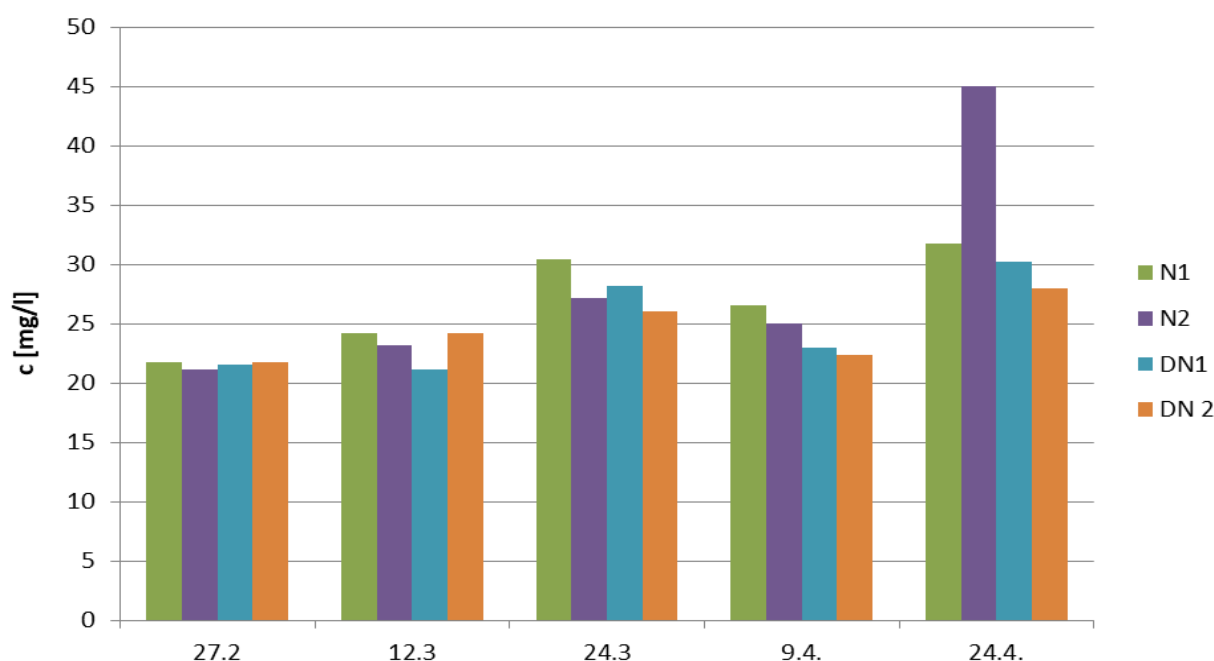
been set. Compared to average dose of 2 l/h it is 350 % increase.

From the Figure 1. can be also seen that the precipitation of phosphorus during fixed dose of 2 l/h was enough for meeting current limits but was not enough for reach anything near the stricter limits. After increase of the fixed dose to 4 l/h, decrease of  $P_{tot}$  concentration in SST 2 outlet was detected. After month of constant dosing of 4 l/h new limits (0,8 mg/l) was reached. After that the fixed dose of coagulant was increased to 7 l/h and limit 0,5 mg/l was also reached.

Worth noting are also  $P_{tot}$  concentrations on the effluent from SST 1 (reference line). Dosing of coagulant was automatic, setpoint was 1,5 mg/l P- $PO_4$  but during tested period the concentration of  $P_{tot}$  decreased below this setpoint. It is caused by a one-sludge system. Returned sludge from both SSTs is pumped into anoxic regeneration tank, which is same for both biological lines. Accumulation of iron in the sludge was occurred by increasing dose of the coagulant gradually. That could be noted from the Figure 2. That caused a precipitation of phosphorus during flow of activated mixture in activation tanks also in reference line.

### Concentration of iron in a sludge and consumption of coagulant

$Fe_2(SO_4)_3$  is used as a coagulant on WWTP Bílina. That is why the iron concentration was detected in sludge taken during sampling. From Figure 2 shows progressive increase of iron volume in the sludge. Biggest increase was detected in sludge from nitrification tank of second line where the fixed dose was increasing during tested period. Increase from 21 g/kg to 45 g/kg means more than double of concentration.

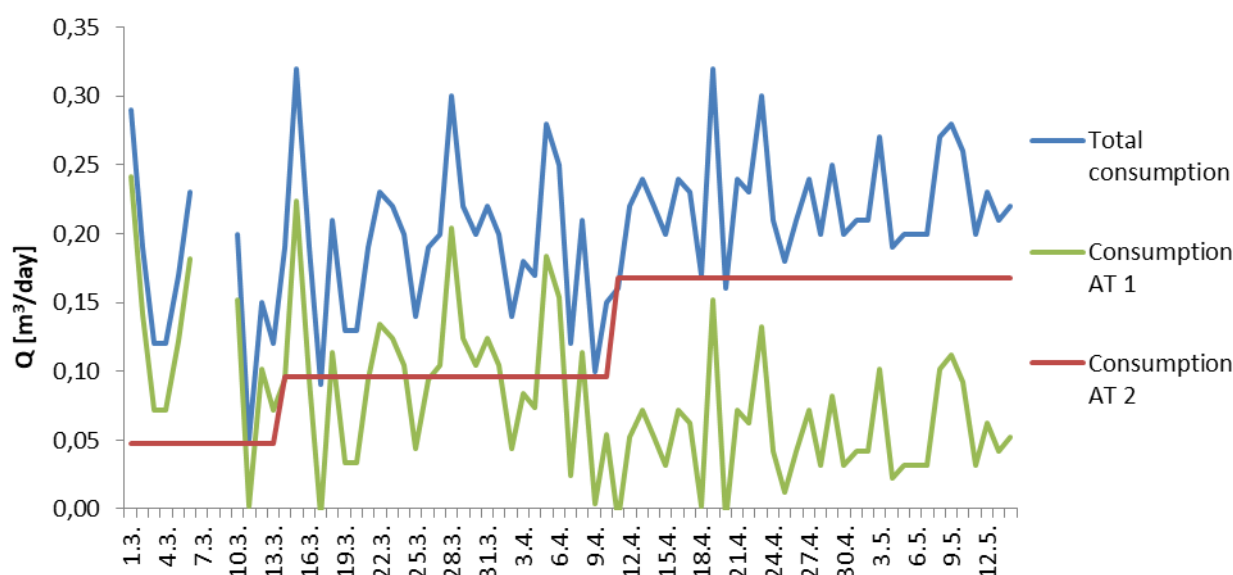


**Figure 2.** Fe concentration in sludge from nitrification tank 1 and 2 (N1, N2) and SST 1 and 2 (DN1, DN2)

Coagulant is dosed into the biological treatment stage by two pumps, each for one biological line. There are more possible dosing points but during common operational state and also during whole tested period coagulant was dosed into the outlet of activation tanks. Unfortunately the pums are not equipped by flowmeters and therefore the consumption of coagulant is not possible to evaluate this way. Because of that the consumption was evaluated as a difference between daily consumption of coagulant in both biological lines and a calculated consumption of coagulant in biological line 2

where a fixed dose was set.

Figure 3. shows that the coagulant consumption in the reference line gradually decreased. Explanation is the same as the decrease of phosphorus concentration in reference line – one-sludge system. From Figure 3. could be also seen little increase of total coagulant consumption. Although a certain trend of increasing coagulant consumption can be seen during tested period, longer period would be necessary for more reliable conclusions and economic balance during which the lower required effluent concentration of  $P_{tot}$  would be set in both biological lines.



**Figure 3.** Coagulant consumption of each biological line and total consumption of WWTP Břilina

### Effect on biochemical processes

Assessment of increased doses of coagulant on biochemical processes was made mainly by respirometric and kinetic test of nitrification. Result from these tests is a rates of the nitrification. At respirometric tests the rate of nitrification is expressed as a decrease of dissolved oxygen concentration on a gram of sludge concentration by hour and at kinetic tests it is expressed by a decrease of  $N-NH_4$  concentration, respectively by an increase of  $N-NO_3$  concentration on a gram of sludge concentration by hour.

**Table 4.** Nitrification rates from respirometric and kinetic tests of nitrification

		27. 2. 2019	12. 3. 2019	24. 3. 2019	9. 4. 2019	24. 4. 2019
rx	[mg/g·h]					
respirometric tests		-3.07	-3.06	-2.78	-2.72	-2.45
kinetic tests by $N-NH_4$		-2.06	-2.03	-1.63	-2.52	-2.19
kinetic tests by $N-NO_3$		2.07	1.99	1.59	3.02	2.53

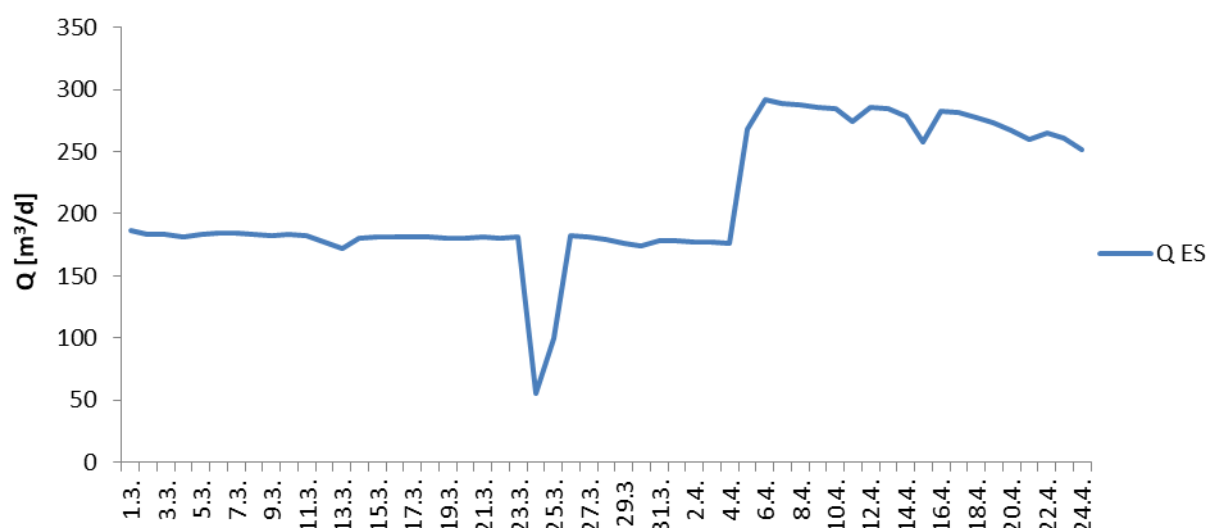
From the values in Table 4 is clear that the rate of nitrification from the respirometric test constantly decreased with increasing dose of coagulant. The results from the kinetic test are not same but that is probably caused by natural conditions during tested period. Testing started in a winter period when the nitrification rates are lower and ended in a spring period when the temperature of wastewater is higher than in winter and so higher nitrification rates can be expected.

That is why results from respirometric tests is considered as a more correct one. Decreasing rate of nitrification during gradual increase of coagulant dose and the associated increase of iron concentration in sludge confirms negative impact of nutrient deficit to the biochemical wastewater treatment processes (Novák, 2018).

### Impact on sludge concentration

An increased dose of a coagulant necessarily caused an increased production of chemical sludge. At simultaneous phosphorus precipitation mix of the biological and chemical sludge is produced. The higher the proportion of chemical sludge is, the more likely problems with sedimentation attributes of the sludge and also his drainage attributes may be.

Figure 4 shows increase of excess sludge which is taken from the biological treatment stage to the sludge stage. It was necessary to increase the flow rate of excess sludge after the dose of 4 l/h was set for approximately one month as the sludge concentration increased during that period.



**Figure 4.** Excess sludge flow rate during tested period

## CONCLUSIONS

By testing the limits of simultaneous phosphorus precipitation, Severočeské vodovody a kanalizace, a.s., as a responsible operating company, is preparing for a possible amendment of the Governing Decree 401/2015 Coll., which could cause a decrease of WWTP's effluent limits.

While for WWTPs above 100,000 PE it is clear that there is no other way than the tertiary treatment level, to meet the potential future limits in the parameter  $P_{tot}$  at the WWTPs 10,000-100,000 PE is potentially possible to achieve stricter limits by simultaneous phosphorus precipitation. Of course it depends on the value of the limit and also on the specific WWTP. It will be necessary to assess each WWTP individually.

One of the WWTPs in the category 10,000 – 100,000 PE is also the WWTP Bílina. During the monitored period it was proved that by higher dose it is possible to approach or even reach stricter outlet limits in the parameter  $P_{tot}$ . Whether these limits could be achieved in the long term is a question of further research and monitoring. The same it is for the determination of coagulant consumption which increased only slightly during the tested period. The next stage of testing should

follow for better evaluation. In the next stage the coagulant should be dosed automatically at a lower P-PO<sub>4</sub> limit value in the ACS.

Testing also confirmed that simultaneous phosphorus precipitation has a negative impact on the nitrification rate. The decrease in nitrification rate may be so significant for some WWTPs that it will also be necessary to take a tertiary stage of treatment to these WWTPs.

There was also an increase in the amount of excess sludge flow rate which has an impact on the further operation of the WWTP. A higher amount of sludge may necessitate an increase in the sludge management capacity, especially sludge dewatering. In addition to investment costs, higher sludge production is also associated with operating costs, namely the consumption of flocculant for sludge dewatering, as well as the constantly increasing sludge disposal costs.

Although monitoring at the WWTP Bílina did not unequivocally answer the question of whether the potential stricter P<sub>tot</sub> limit can be achieved by simultaneous phosphorus precipitation, it has brought interesting results and confirmation of generally known facts. Conclusions from this paper can serve as a basis for further research of this issue.

## REFERENCES

- Novák, L., Srb, M. (2018). Provozní zkušenosti s aktivačními systémy pracujícími v nutričně deficitních podmínkách fosforu. *Zborník prednášok 10. bienálnej konferencie s medzinárodnou účasťou*, 17. – 19. října, Štrbské Pleso, Slovenská republika, 25-31,



## Separation and Concentration of Cationic Surfactant Solutions with the Use of Ceramic Modules

A. Klimonda\* and I.Kowalska\*

\* Wrocław University of Science and Technology, Faculty of Environmental Engineering, Wybrzeże S. Wyspiańskiego 27, 50-370 Wrocław, Poland (E-mail: [aleksandra.klimonda@pwr.edu.pl](mailto:aleksandra.klimonda@pwr.edu.pl))

### Abstract

The paper presents the findings of an experimental research employing ultrafiltration and microfiltration ceramic modules (150 kDa, 0.14  $\mu\text{m}$ , 0.45  $\mu\text{m}$ ) in terms of removal and concentration of cationic surfactant Tequat LC90i (TEAQ) from water solutions. The filtration tests were performed in a semi-pilot installation in a cross-flow regime. The feed solution parameters (surfactant concentration, pH of the treated solution, the presence of inorganic salt) and process conditions (transmembrane pressure and linear velocity) on the membrane filtration efficiency were evaluated. All tests achieved very satisfactory TEAQ retention coefficients (in the range of 70-95 %), however surfactant fouling occurred resulting in deterioration of the permeability of the modules. Module characterized by the pore sizes greater than the size of surfactant particles, i.e. module 0.45  $\mu\text{m}$ , proved to be the most fouling resistant one. It was also proved that process performance at high value of linear flow velocity can efficiently reduce the intensity of membranes pore blocking.

### INTRODUCTION

Cationic surfactants have found applications in many areas of the industry due to numerous features resulting from their chemical structure. A molecule of cationic surfactant consists of the hydrophobic tail and positively charged hydrophilic head, as a consequence these substances exhibit antiseptic, antifungal, antiviral and disinfection (quaternary ammonium salts, ex. benzalkonium chloride, cetrimonium bromide, Wiczonek et al., 2014) or lubricating/antistatic action (ex. Esterquats). Triethanolamine-based esterquats (TEAQ) has been the primary ingredient in European fabric softeners (Friedli et al., 2002). Due to the strong effect of cationic surfactants on water/soil properties and their toxicity versus many species it is necessary to remove them from industrial wastewater. Biodegradation (Palmer and Hatley, 2018), coagulation (Terechova et al., 2014), foaming (Boonyasuwat et al., 2003), photocatalytic methods (Czech and Ćwikła-Bundyra, 2012) may be effective in surfactant removal, however very promising technologies for the removal of surfactants are membrane-based technics, which the great advantage is the ability to recover the valuable ingredients from wastewater. Amin et al. (2016) listed numerous advantages of ceramic membranes, the main of them are: high chemical, thermal, mechanical and physical stability; long working life; good environmental performance. Fernández et al. (2005) reported anionic (SDS) and nonionic (Tergitol NP-9) surfactants removal in the range of 60-70 % with the use of ultrafiltration ceramic membrane Membralox®. Polak et al. (2019) examined tubular ceramic membranes (Mantec Technical Ceramics Ltd) for laundry wastewater treatment. The experiments conducted showed COD removal from initial concentration of 1024 mg/L to 200 mg/L after 90 minutes of membrane filtration. The literature reports discussing the removal of cationic surfactants in membrane processes are very limited and mainly concern polymeric membranes. Boussu et al. (2007) investigated cetrimide separation with the use of nanofiltration membranes. Initial surfactant concentration amounted to 40 mg/L. The retention coefficients reported were very variable - 17, 21, 89 and 97 % of cetrimide was removed, depending on the type of membrane applied.

Our preliminary research (Klimonda and Kowalska, 2019) proved that membrane filtration can be an effective method for cationic surfactants removal. Application of the polymeric flat-sheet

ultrafiltration membranes (in dead-end regime) allowed to retain up to 100 % of TEAQ, however the simultaneous significant membrane permeability deterioration was observed. In order to reduce the membrane blocking by surfactants, the follow actions can be implemented: filtration in a cross-flow regime, the use of larger pore, i.e. microfiltration membranes which may be less susceptible to pore blocking. In this paper a cross-flow set-up equipped with ultrafiltration and microfiltration ceramic modules was tested in terms of TEAQ removal from water solutions.

## EXPERIMENTAL

The cross-flow semi-pilot filtration set up was employed for the experimental research (Figure 1). In all experiments the initial volume of the feed solution amounted to 8 L and its temperature was 20°C. During the filtration experiments, the linear flow velocity was maintained in the range from 5 to 6, from 4 to 5 and from 2 to 2.5 m/s for 0.45 µm, 0.14 µm and 150 kDa modules, respectively. The first part of the tests involved 120-minutes membrane filtration tests which were performed under the transmembrane pressure (TMP) of 3 bar. 20 mL permeate samples were collected for measurements of surfactant concentration in the intervals of 15 min and the concentration of TEAQ in the feed solution was maintained at a constant level. In the next part of the tests, i.e. in concentration batch mode, the transmembrane pressure was increased to the level of 3.5 bar and the processes were performed until the resistance of the modules precluded further filtration. During this stage of the tests, both surfactant concentration in concentrate and permeate stream was monitored every 30 minutes. Cationic surfactant Tequat LC90i, TEAQ (Dihydrogenated Tallowethyl Hydroxyethylmonium Methosulfate & Ditallowethyl Hydroxyethylmonium Methosulfate) solutions in concentration of 50, 100, 250, 500 and 1000 mg/L were prepared for the research. Critical micelle concentration (CMC) of surfactant amounted to  $0.026 \pm 0.0067$  mg/L. The micelle size distribution was  $115.9 \pm 6.9$  nm, and the monomer length, which is approximately the half of the micelle diameter was 58 nm (DLS method, Malvern Zetasizer Nano ZS, wavelength 532 nm). TEAQ concentration in the samples was monitored by TOC measurements (HACH IL550 TOC-TN). Based on the calibration curve, TEAQ concentration can be calculated with high accuracy ( $R^2=99.2$  %) from TOC measurements using the following formula:

$$C = 1.384 \cdot TOC, \frac{mg}{L} \quad (1)$$

where C is TEAQ concentration (mg/L), TOC is total organic carbon concentration (mg/L).

In order to verify the separation properties, retention coefficient was calculated:

$$R = \frac{c_f - c_p}{c_f} \cdot 100, \% \quad (2)$$

where  $C_f$ ,  $C_p$  are surfactant concentration (mg/L) in the feed and permeate, respectively.

Permeate volumetric flux is an important factor for the membrane processes efficiency evaluation. It is likely that in the presence of surfactants membrane pore blocking occurs affecting membrane permeability decline (Van der Bruggen et al., 2005). In order to evaluate the modules' hydraulic properties, volume flux was determined according to the following equation:

$$J = \frac{V}{A \cdot t}, \frac{L}{m^2 h} \quad (3)$$

where J is the permeate volume flux ( $L/m^2h$ ); V is the volume of the permeate sample collected (L); A denotes the membrane's surface area ( $m^2$ ); t is the filtration time (h).

To assess susceptibility to fouling, the normalized flux was calculated:

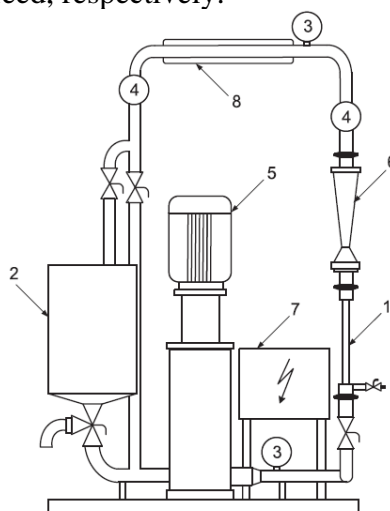
$$RF = \frac{J}{J_0}, - \quad (4)$$

where RF is the relative flux; J is the permeate volume flux after time t;  $J_0$  is the distilled water permeate flux ( $L/m^2h$ ).

The permeate recovery was calculated according to the following equation:

$$PR = \frac{V_p}{V_0} \cdot 100, \% \quad (5)$$

where PR is the permeate recovery ratio (%), and  $V_p$  and  $V_0$  denote the volume of the permeate after the time  $t$ , and the volume of the feed, respectively.



**Figure 1.** Laboratory set-up: 1- membrane module, 2- feeding tank (10 L), 3- manometer, 4- thermometer, 5- pump (Grundfos), 7- control panel, 8- cooler

Commercially available UF and MF CéRAM INSIDE® modules purchased from Tami Industries have been chosen to the tests. The parameters of the membranes are given in Table 1.

**Table 1.** Characteristic of CéRAM INSIDE® (Tami Industries) modules

Parameter	Value		
Pore diameter, $\mu\text{m}$ / cut-off, kDa	0.45 $\mu\text{m}$	0.14 $\mu\text{m}$	150 kDa
Number of channels	7	7	1
Inner channel diameter, mm	2	2	7
Filtration area, $\text{m}^2$	0.0130	0.013	0.005
Distilled water flux, $\text{L}/(\text{m}^2 \cdot \text{h})$ *	293.5	260.6	19.2
Max. operating pressure, bar	10		
Mechanical resistance, bar	>90		
Chemical resistance	pH=0÷14		
Max. operating temperature, $^{\circ}\text{C}$	<350		

\* determined by the authors at TMP=3 bar

The last part of the experiments included the effect of the treated solution parameters (pH, presence of the electrolyte) and the change in process parameters (linear flow velocity, transmembrane pressure) on the membrane processes performance. Sodium chloride (NaCl, Poch, Poland) was used for the tests. In order to correct the pH values to 3.5, 4.5 and 9, 0.1 M HCl and 0.1 M NaOH solutions were applied into the surfactant solutions.

## RESULTS AND DISCUSSION

### Purification

Table 2 presents the TEAQ retention coefficients obtained during the 120-minutes purification processes with the use of three modules. High separation ratios (above 70 %) were noted for all tested modules, however a slight trend the smaller pore size, the bigger retention coefficient can be observed. The 150 kDa module allowed to obtain an averaged retention coefficient in the range from 82 to 95 %. It should also be noted that changes in the initial TEAQ concentration did not significantly affect the separation efficiency. Due to the very low value of CMC (0.026 mg/L) all of

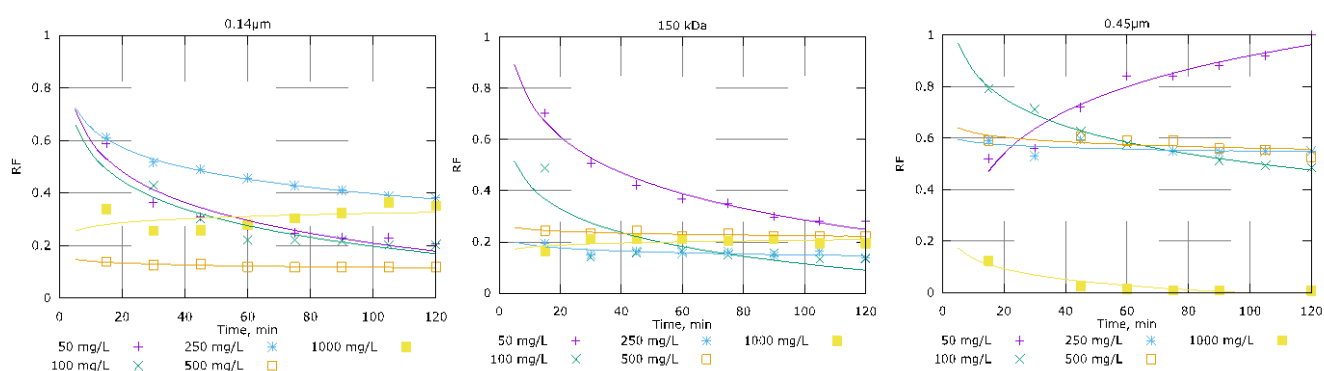
the tested solutions were the micellar ones. Taking into account the micelle size distribution (0.115  $\mu\text{m}$ ), relatively high separation ratios were noted for microfiltration modules, especially for 0.45  $\mu\text{m}$  module – despite the pore size was fourfold greater than TEAQ micelle size, surfactant retention coefficients exceeded 70 %.

**Table 2.** Averaged TEAQ retention coefficients (R) versus concentration in the feed solution

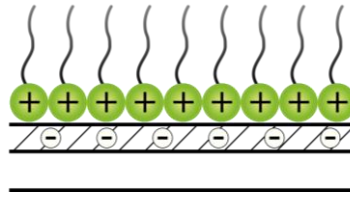
Initial TEAQ concentration, mg/L	R, %		
	150 kDa	0.14 $\mu\text{m}$	0.45 $\mu\text{m}$
50	83.6	82.2	79.6
100	91.3	88.0	79.5
250	82.3	82.9	71.9
500	91.2	92.5	75.1
1000	95.2	94.9	85.2

Figure 2 shows relative flux values versus filtration time depending on module type and initial TEAQ concentration. As can be seen, the presence of the cationic surfactant in treated solutions negatively affects the transport properties of the modules. It was observed that depending on the feed solution concentration, the microfiltration modules achieved various relative permeability. A particularly interesting case was observed when the module 0.45  $\mu\text{m}$  was applied – treatment of solutions in the concentration of 100-500 mg/L brought the relative flux in the range from 0.55 to 0.6, when for the highly concentrated solution, i.e. 1000 mg/L, the module was almost completely fouled – relative flux at the end of the filtration cycle amounted to 0.007. However, for the module 150 kDa, the initial surfactant concentration did not have as much effect on the relative permeability as for the other modules – after 30 minutes of membrane filtration on the module 150 kDa, the relative flux was in the range from 0.14 to 0.23 for initial TEAQ concentrations 100-1000 mg/L and 0.53 for 50 mg/L. It must be stressed that surfactant fouling phenomenon was more pronounced for the modules with the pore sizes close to the separated particles size (micelle 0.115  $\mu\text{m}$ , monomer 0.058  $\mu\text{m}$ ), i.e. for the module 0.14  $\mu\text{m}$  and the module 150 kDa for what, according to Calvo et al. (2008) pore size distribution is 0.055–0.08  $\mu\text{m}$ .

It is likely that the deterioration in membrane transport properties (comparing to the distilled water flux) was also caused by the interaction between surfactant particles and hydrophilic surface of ceramic membranes. Surfactant molecules arrange hydrophilic heads near the hydrophilic surface, filling it one by one in very close distances between each other (Figure 3). As a result, a membrane hydraulic resistance grows. Moreover, TEAQ particles adsorb inside the pores causing reduce in their sizes and in consequence – membrane permeability.



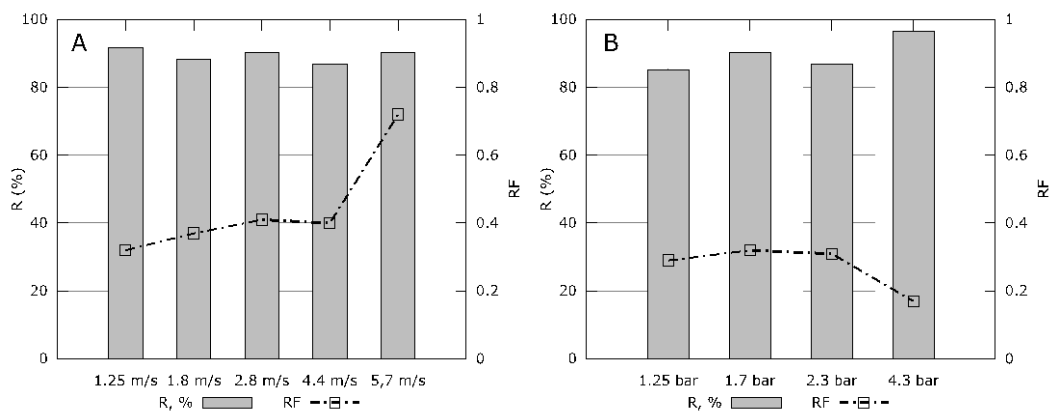
**Figure 2.** Relative flux (RF) versus filtration time and initial surfactant concentration



**Figure 3.** Cationic surfactant particles' arrangement on hydrophobic membrane

### Modification of the process and feed solution parameters

Taking into account relatively high retention coefficients of surfactants, the MF module with the pore diameter of  $0.14\ \mu\text{m}$  was chosen for the next part of the test involving changes in the process parameters in order to limitation of the fouling phenomena. The parameters tested for this purpose were transmembrane pressure (TMP) and linear flow velocity ( $v$ ). The tests were performed for the initial TEAQ concentration of  $50\ \text{mg/L}$ . The first part was carried-out under a constant TMP of 2 bar and for five values of linear velocity, i.e. 1.25, 1.80, 2.8, 4.4 and 5.7 m/s. The averaged retention coefficients and the relative flux values obtained during the 60 minutes processes are plotted in Figure 4. It was noted that an increase in linear flow velocity did not bring any essential changes in TEAQ removal efficiency (retention coefficients in the range from 87 to 92 %), however it should be stressed that in terms of fouling phenomena, the increase in this parameter to the value of 5.7 m/s allowed for a significant reduction of the surfactant fouling. While for the remaining values of linear flow velocity the relative flux amounted approximately to 0.35, for the highest value relative flux was about 0.72, which means that the drop in permeate flux did not exceed 30 %. It can be stated that at the turbulent flow, fouling phenomena was limited due to surfactant washing out.



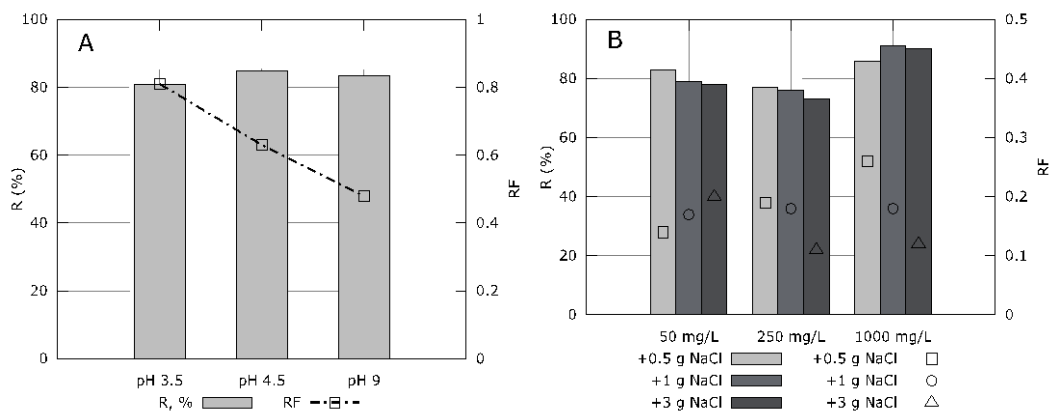
**Figure 4.** Retention coefficient (R) and relative flux (RF) versus linear flow velocity (A) and transmembrane pressure (B) for the  $0.14\ \mu\text{m}$  module and the initial TEAQ concentration of  $50\ \text{mg/L}$

The second part of the test included evaluation the TMP effect on relative flux. Linear flow velocity was at the level of 4.1-4.5 m/s and the TMP values were equal to 1.25, 1.7, 2.3 and 4.3 bar. It was found (Fig. 4B) that increasing TMP resulted in relative flux deterioration – for the TMP of 4.3 bar, the averaged relative flux amounted to 0.17. Simultaneous, a slight improvement in retention coefficient (from 85, 90, 87 % to 96 %) can be observed for the highest value of the TMP.

The effect of the solution pH on the process efficiency was also investigated. For this purpose, TEAQ solutions of concentration equal to  $50\ \text{mg/L}$  and various pH values were filtered on the module  $0.14\ \mu\text{m}$  for 60 minutes. The data obtained is plotted in Figure 5 A. The evident influence of solution pH on module permeability can be seen – purification of the strongly acidic solution (pH =3.5) yielded a relative stream of about 0.8, when the pH increased to 4.5 there was a decrease in relative permeability to about 0.62. Increasing pH value to 9 resulted in further deterioration of

the permeability – to the value of 0.48. According to de la Casa et al., (2007), the isoelectric point (pzc), defined as the pH for which the net charge of the membrane is equal to zero, for amphoteric ceramic membranes Céram Inside 25 (pore radius 0.14  $\mu\text{m}$ ) with zirconium dioxide active layer is located around 6.9. Thus, the deterioration of the modules' permeability at pH 9 may result from the electrostatic attraction between the negatively charged membrane surface and the positively charged cationic surfactant particles. At pH 3, membrane surface exhibits positive charge load and the less intensive membrane blocking can be ascribed to the strong electrostatic repulsion.

The next step of the research was to evaluate the effect of electrolyte on surfactant retention and module permeability. TEAQ solutions in concentration of 50, 250 and 1000 mg were prepared with the addition of NaCl equal to 0.5, 1 and 3 g per litre. The results obtained in 60-minutes processes are plotted in Figure 5 B. Comparing the data obtained in tests with the presence of electrolyte to the results with single-component solutions (Table 2) it can be seen that the salt caused a slight drop in retention coefficient. For example, for TEAQ concentration of 1000 mg/L the averaged retention coefficient amounted to 94.9 %; when NaCl was present in the treated solution this ratio was 86-91 %. Focusing on relative permeability the negative effect of electrolyte can be seen. In the first stage of the tests (Figure 2), the averaged relative flux values amounted to 0.3, 0.5 and 0.35 for solutions 50, 250 and 1000 mg/L. Addition of the electrolyte to the feed solutions resulted in relative fluxes below 0.26 for all variants. According to Bargeman et al. 2005 an electroviscous effect connected with the presence of salt ions inside the pores, most likely comes to a limitation of the stream flow through the small pores. Thus, mainly the larger pores having their share in the mechanism of the sieve separation of surfactants.



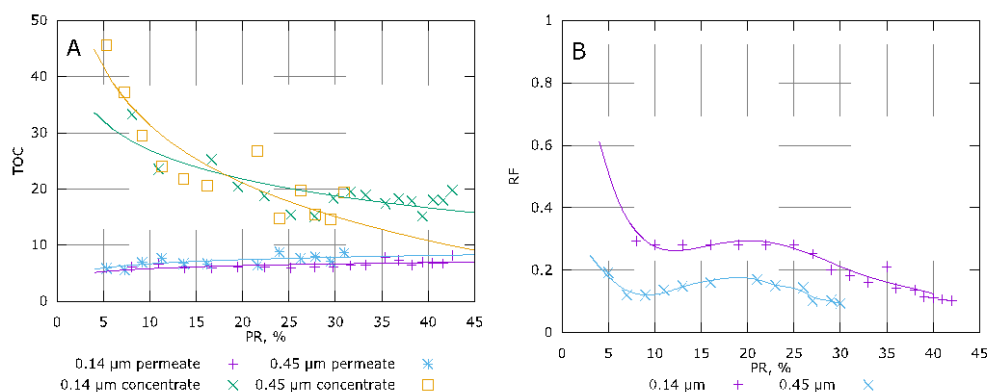
**Figure 5.** A - Retention coefficient (R) and relative flux (RF) versus solution pH, for initial TEAQ concentration of 50 mg/L, B - retention coefficient (R, bars) and relative flux (RF, points) depending on salt addition and initial TEAQ concentration for the 0.14  $\mu\text{m}$  module

### Concentration mode

In order to verify the possibility of surfactant solution concentration the last part of the research was performed with the use of two microfiltration modules. As the CMC of TEAQ is very low (0.026 mg/L) the initial surfactant concentration (50 mg/L) was almost 2000 x CMC. In this stage, the TOC concentration was monitored both in the concentrate (feeding tank) and the permeate. Figure 6 presents TOC content in process streams and relative flux versus permeate recovery ratio. To obtain 43 % of permeate recovery on module 0.14  $\mu\text{m}$  the membrane filtration was proceeded for 9.5 hour, for module 0.45  $\mu\text{m}$ , recovery ratio of 31 % was achieved after 7 hours after process start. The processes were performed until the growth of modules' resistance prevent maintenance of the constant parameters, i.e. TMP and linear flow velocity. It was noted that for both modules the quality of the permeate was at the constant level over all experiments (TOC concentration in the range from 5.1 to 8.2 mg/L and from 5.6 to 8.8 mg/L for 0.14  $\mu\text{m}$  and 0.45  $\mu\text{m}$ , respectively). The goal of this experiment (i.e. maximum concentration of the surfactant solution) was not achieved.



Over the filtration cycle, the TOC content in the feeding tank decreased from 33 and 37 mg/L to 19.8 and 19.5 for 0.14  $\mu\text{m}$  and 0.45  $\mu\text{m}$  at the beginning of the process, respectively. Such results indicate the accumulation of surfactant particles within the membrane pores or the deposition on installation elements. This mechanism should be investigated in order to understand the interaction between surfactants and membrane. The course of the relative permeability curves confirms the thesis about the deposition of the surfactant inside the membrane – over the experiment, relative flux decline was observed. Opposite to the previous part of the research, the module with the greater pore size was more susceptible to surfactant fouling – for 30 % permeate recovery ratio, the relative flux amounted to 0.1, when for the same value of PR parameter module 0.14  $\mu\text{m}$  achieved value of 0.2.



**Figure 6.** TOC concentration in permeate and concentrate (A) and relative flux (B) versus permeate recovery ratio for microfiltration modules

## CONCLUSIONS

- Ultrafiltration and microfiltration ceramic membranes proved to be useful in cationic surfactant removal – above 70% of TEAQ was removed from the solutions regardless of the initial compound concentration.
- Presence of the surfactant in treated solutions was associated with deterioration of the modules' permeability. The fouling phenomena was the most pronounced for the modules characterized by the pore diameters similar to surfactant particle size.
- Correction of the process parameters affected the hydraulic performance of the membranes. The induction of the turbulent flow significantly reduced the intensity of surfactant fouling.
- The inefficient concentration of the surfactant solutions proved that TEAQ particles were deposited inside the membrane pores, making it impossible to obtain the concentrate with a high content of surfactant.

## ACKNOWLEDGEMENTS

This work was supported by a grant (No 049M/0005/19.) from the Department of Environmental Engineering, Wrocław University of Science and Technology.

## REFERENCES

- Amin, Sh. K., Abdallah, H. A. M., Roushdy, M. H., El-Sherbiny, S. A. (2016) An Overview of Production and Development of Ceramic Membranes. *International Journal of Applied Engineering Research*, **11**(12), 7708-7721.

- Bargeman, G., Vollenbroek, J. M., Straatsma, J., Schroën, C. G. P. H., Boom, R. M. (2005) Nanofiltration of multi-component feeds. Interactions between neutral and charged components and their effect on retention. *Journal of Membrane Science*, **247**(1-2), 11-20.
- Boonyasuwat, S., Chavadej, S., Malakul, P., Scamehorn, J.F. (2003) Anionic and cationic surfactant recovery from water using a multistage foam fractionator. *Chemical Engineering Journal*, **93**, 241-252.
- Boussu, K., Kindts C., Vandecasteele, C., Van der Bruggen, B. (2007) Surfactant fouling of nanofiltration membranes: measurements and mechanisms. *ChemPhysChem*, **8**, 1836-1845.
- Calvo, J. I., Bottino, A., Gustavo Capannelli, G., Hernandez, A. (2008) Pore size distribution of ceramic UF membranes by liquid–liquid displacement porosimetry. *Journal of Membrane Science*, **310**, 531-538.
- Czech, B., Cwikła-Bundyra, W. (2012) Advanced Oxidation Processes in Triton X-100 and Wash-up Liquid Removal from Wastewater Using Modified TiO<sub>2</sub>/Al<sub>2</sub>O<sub>3</sub> Photocatalysts. *Water, air, and soil pollution*, **223**(8), 4813-4822.
- De la Casa, E. J., Guadix, A., Ibáñez, R., Guadix, E. M. (2007) Influence of pH and salt concentration on the cross-flow microfiltration of BSA through a ceramic membrane. *Biochemical Engineering Journal*, **33**(2), 110-115.
- Fernández, E., Benito, J. M., Pazos, C., Coca, J. (2005) Ceramic membranes ultrafiltration of anionic and nonionic surfactant solutions. *Journal of Membrane Science*, **246**(1), 1-6.
- Friedli, F. E., Koehle, H. J., Fender, M., Watts, M., Keys, R., Frank, P., Toney, C. J., Doerr, M. (2002) Upgrading Triethanolamine Esterquat Performance to New Levels. *Journal of Surfactants and Detergents*, **5**(3), 211-216.
- Klimonda, A., Kowalska, I. (2019) Application of polymeric membranes for the purification of solutions containing cationic surfactants. *Water Science and Technology*, **79**(7), 1241-1252.
- Palmer, M., Hatley, H. (2018) The role of surfactants in wastewater treatment: Impact, removal and future techniques: A critical review. *Water Research*, **147**, 60-72.
- Polak, D., Szwał, M., Fabianowski, W., Rosiński, M. (2019) Ceramic Membranes Modified by Carbon used for Laundry Wastewater Treatment. *Chemical Engineering Transactions*, **74**, 931-936.
- Terechova, E. L., Zhang, G., Chen, J., Sosnina, N. A., Yang, F. (2014) Combined chemical coagulation–flocculation/ultraviolet photolysis treatment for anionic surfactants in laundry wastewater. *Journal of Environmental Chemical Engineering*, **2**(4), 2111-2119.
- Van der Bruggen, B., Cornelis, G., Vandecasteele, C., Devreese, I. (2005) Fouling of nanofiltration and ultrafiltration membranes applied for wastewater regeneration in the textile industry. *Desalination*, **175**, 111-119.
- Wieczorek, D., Gwiazdowska, D., Michocka, K., Kwaśniewska, D., Kluczyńska, K. (2014) Antibacterial activity of selected surfactants. *Towaroznawcze Problemy Jakości*, **2**(39), 142-149.



# The Dependency and Behaviour of Suspended and Immobilised Biomass in Activated Sludge

M. Kolomazníková\*, K. Havlíček\* and T. Lederer\*

\* Institute for Nanomaterials, Advanced Technologies and Innovation, Technical University of Liberec, Studentská 1402/2, 460 01 Liberec, Czech Republic (E-mails: [marketa.kolomaznikova@tul.cz](mailto:marketa.kolomaznikova@tul.cz); [karel.havlicek@tul.cz](mailto:karel.havlicek@tul.cz); [tomas.lederer@tul.cz](mailto:tomas.lederer@tul.cz))

## Abstract

A hybrid bioreactor with combined, suspended and immobilised biomass is an innovative type of waste water treatment technology. Biomass immobilised on some type of carrier has many advantages. Immobilised biological material is easy to handle and prevents it being flushed out of the system, thus maintaining a high biomass concentration in the bioreactor. Many studies focus on the various aspects of the immobilisation process, such as the development of more effective carrier types etc. This research was focused on the relationship between immobilised and suspended biomass, and especially the behaviour of the immobilised population and its dependence on the concentration of the suspended population. Particular attention was paid to the sub-population of nitrifying bacteria, which is a minority group involved in the naturally developed mixed microbial population as a part of the common nitrogen cycle. The relationship between a biofilm and the suspension was tested on activated sludge from a waste water treatment plant in Chrastava (north Bohemia) and colonised carriers from a hybrid laboratory bioreactor. The various concentrations of both suspended biomass and the nitrogen concentration in feeding were tested and compared. Respirometry measurement of nitrification capacity was used to evaluate the dependency and behaviour of both biomass types. The results showed an uninfluenced nitrification capacity of the immobilised biomass, independent of the concentration of suspended biomass in the system.

## Keywords

Nitrification capacity; biofilm; suspension; hybrid bioreactor; respirometry measurement; nitrogen concentration; biomass concentration

## INTRODUCTION

The motivation to design more modern, more advanced and more effective technologies for waste water treatment is mainly the continuous tightening of legislative limits and the increasing demands on the quality of treated water discharged into the surface waters or seeping into the rock environment (Yang, 2013). Traditionally used waste water treatment technologies, e.g. activation systems, in their original technological design are not able to meet these limits in some cases. Therefore, the study and development of new technologies occurs. One of these new methods uses immobilised microorganisms for the removal of biological contaminants (Masák, 2002).

The activated sludge process is one of the most commonly used waste water treatment technologies. The principle of this process is the mixing of waste water with activated sludge and their aeration. Activated sludge consists of two basic phases – liquid and solid (a cluster of microorganisms). A population of microorganisms forms in activated sludge, in a biological reactor, and in biomass, which cooperates in the nitrification process (Švehla et al., 2010). Biomass contains approximately 2 000 – 8 000 mg/l of microorganisms, mostly bacteria, but also protozoa and fungi (Templeton and Butler, 2011). Biomass naturally clusters into flocks by the process of bioflocculation and is typical for systems with a suspended biomass. Other alternatives are systems where the biomass is not aggregated but is fixed on support carriers.

The immobilised (attached) microbial populations method is used both in conventional biological nitrogen removal systems and other various modifications, e.g. hybrid bioreactors, where both types of biomass occur. In conventional moving bed biofilm reactors the major part of the biomass is formed by biomass immobilised as a biofilm fixed on carriers, whereas a minor part is formed by suspended biomass. Various modifications of hybrid bioreactors are used. There are systems where the biofilm and suspension are separated into two reactors, or systems with biofilm on carriers introduced into the reactor with suspended biomass (Jenkins and Wanner, 2014).

### **Suspended biomass**

In systems with suspended biomass the microorganisms are in a suspension with a liquid (waste water) (Gavrilescu and Macoveanu, 2000). Clusters of microorganisms form freely suspended flocks. Flocks in the sludge arise from the bioflocculation process, which occurs due to the aeration of waste water. The waste water contains aerobic bacteria, which form extracellular polymers, e.g. polysaccharides that coat the surface of the microorganisms' cells and reduce their surface electrical charge, which leads to the formation of clumps - flakes. Several processes occur on these flakes (diffusion, coagulation, sorption), which lead to the removal of the waste organic substances.

### **Immobilised biomass**

Immobilised biomass, or attached biomass, creates a biofilm and is characterised by the use of carriers. Biofilm is characterised as a natural heterogeneous biological structure composed of microorganisms, polymeric substances and abiotic particles, attached to the surface of a carrier and connected into a film (Gavrilescu and Macoveanu, 2000; Goswami et al., 2016). Carriers can be mobile or immobile and waste water flows freely around them to bring the microorganisms in contact with the waste water (Najafpour and Ebrahimi, 2016). A unique feature of reactors with immobilised biomass compared to suspended biomass is the fact that the residence time of the biomass is considerably longer than the residence time of the liquid and runs at a continuous flow rate with minimal biomass loss. This leads to a high biomass concentration in the reactor and the process is intensified (Goswami et al., 2016). The amount of biomass in the biofilm is determined as the biomass concentration - the mass of biomass in the biofilm volume. This concentration ranges from 10 kg/m<sup>3</sup> to 100 kg/m<sup>3</sup> and is influenced by the type and morphology (thickness) of the biofilm.

Studies focused on the relationship between immobilised and suspended biomass confirm that reactors with combined biomass content, i.e. a combination of immobilised and suspension populations have the largest nitrification capacity (Leix et al., 2016; Zielińska et al., 2012). The advantage of hybrid bioreactors is the biofilm resistance to leaching due to a protective coating called glycocalyx. Due to the lower leaching rate, a high concentration of biomass in the reactor is maintained, and thus a high efficiency of the purification process. Immobilisation has a positive effect especially on slow growing cultures, including nitrifying bacteria. Because of their constant leaching out of the system, this type of bacteria has better prerequisites for growth but also adaptation to changing conditions (e.g. temperature change, presence of toxic substances). This leads to a shorter residence time of the water in the reservoir and thus requires less space for the system (Černík et al., 2010).

## **SAMPLE PREPARATION AND MEASUREMENTS**

The aim of the laboratory experiment was to verify the effect of the activated sludge concentration on the nitrification capacity and also the effect of different nitrogen concentrations in the samples with a combination of both suspended and immobilised biomass. Activated sludge from the Amazon WWTP and biomass carriers from the same locality were used for the purpose of the experiment.

### Experiment design

The total volume of each sample was 200 ml and contained sludge of various concentrations (0.0 g/l, 0.5 g/l, 1.5 g/l, 3.0 g/l) and six carriers (samples 25-30 contained only sludge without carriers). A total of 10 ml of phosphate buffer (20 ml for the sample with an N concentration of 200 mg/l) and 50, 100 and 300 mg/l of  $\text{NH}_4\text{-N}$  were also added to the samples as the only substrate (electron donor) for the microorganisms. The  $\text{NO}_3\text{-N}$  concentration in the sludge was about 25 g/l. Fifteen samples were prepared with different combinations of sludge concentrations (rate of suspended and immobilised biomass) and nitrogen concentrations. Each sample was prepared in duplicate to control the results. Therefore, the total number of samples was 30. Specification of each sample is included in Table 1.

**Table 1.** Sample design and content

Sample ID	Sample volume (ml)	Sludge concentration (g/l)	Number of carriers (pc)	N feeding amount (mg/l)	P buffer amount (ml)
1	200	0.0	6	50	10
2	200	0.0	6	100	10
3	200	0.0	6	300	20
4	200	0.5	6	50	10
5	200	0.5	6	100	10
6	200	0.5	6	300	20
7	200	1.5	6	50	10
8	200	1.5	6	100	10
9	200	1.5	6	300	20
10	200	3.0	6	50	10
11	200	3.0	6	100	10
12	200	3.0	6	300	20
13	200	3.0	0	50	10
14	200	3.0	0	100	10
15	200	3.0	0	300	20

### Respirometry measurement and analysis

The prepared samples were used for respirometry measurement. Nitrification efficiency was tested by evaluation of the  $\text{O}_2$  consumption rate (mg/l/h) and cumulative  $\text{O}_2$  consumption - BOD (mg/l) using a Micro Oxymax respirometer. Thirty 200-ml flasks were placed into the respirometer and a magnetic stirrer was inserted into each flask for continuous mixing. During the measurement, the development of a graph of the  $\text{O}_2$  consumption rate and cumulative  $\text{O}_2$  consumption was observed. After about 137 h, the graph showed the end of the substrate nitrification and the measurement was stopped.

After the respirometry measurement, the samples were analysed for  $\text{NH}_4^+\text{-N}$  (mg/l),  $\text{NO}_3^-\text{N}$  (mg/l) and the pH values were determined. Two samples were analysed for  $\text{NO}_2^-\text{N}$  (mg/l) determination in order to evaluate whether the nitrification process was complete.

### RESULTS AND DISCUSSION

The graphs below show that nitrification took place until the end of phase 2. This was verified by the determination of  $\text{NO}_2^-\text{N}$  (mg/l) in two samples with higher concentrations of ammonia (100 and 300 mg/l, respectively). In both cases, the value of nitrite nitrogen was below 0.5 mg/l.

**Table 2.** Results of the analysis at the end of the experiment

Sample ID	Sample characteristics	pH	NH <sub>4</sub> <sup>+</sup> -N	NO <sub>3</sub> <sup>-</sup> -N
			(mg/l)	(mg/l)
1	0 sludge + 30 N + carriers	6.28	0	73
2	0 sludge + 100 N + carriers	5	5,4	110
3	0 sludge + 300 N + carriers	5.27	110	198
4	0.5 sludge + 30 N + carriers	6.3	0	86
5	0.5 sludge + 100 N + carriers	5.13	5,3	116
6	0.5 sludge + 300 N + carriers	5.46	135	186
7	1.5 sludge + 30 N + carriers	6.35	0	87,1
8	1.5 sludge + 100 N + carriers	5.26	6	129
9	1.5 sludge + 300 N + carriers	5.4	134	197
10	3 sludge + 30 N + carriers	6.41	0	101
11	3 sludge + 100 N + carriers	5.24	5	154
12	3 sludge + 300 N + carriers	5.22	101	140
13	3 sludge + 30 N no carriers	6.3	0	107
14	3 sludge + 100 N no carriers	5.19	3	147
15	3 sludge + 300 N no carriers	5.27	105	220

Samples with an ammonia ion concentration of 50 mg/l were completely nitrified, as shown by the zero NH<sub>4</sub><sup>+</sup>-N values after the end of the measurement and a NO<sub>3</sub><sup>-</sup>-N concentration corresponding to complete nitrification. For samples with a nitrogen concentration of 100 mg/l, the nitrification was almost complete, and the analysis showed an ammonia nitrogen content of between 3 and 6 mg/l after completion of the measurement, as well as the corresponding NO<sub>3</sub><sup>-</sup>-N concentration. Nitrification was not complete in the case of the sample with a concentration of N 300 mg/l, as shown by the residual ammonia ion concentrations of between 105 and 135 mg/l. From the total initial concentration (300 mg/l), however, almost two thirds of the NH<sub>4</sub><sup>+</sup>-N were oxidised in the case of the samples with the highest concentrations.

The reason why the samples with the highest nitrogen concentrations did not completely oxidise can be explained by the toxicity caused by the high ammonia ion concentrations. However, this was not confirmed because the results show that nitrification rates occur equally fast for all three nitrogen concentrations. Toxicity would also appear immediately after the start of respiration. The explanation for incomplete nitrification is the effect of the decrease in the pH value. At the start of the experiment, the pH value was around 7 and decreased during nitrification. At the end of the experiment, a pH value of around 6.3 was measured for samples with an N concentration of 50 mg/l; therefore, there was no significant decrease in the pH value and nitrification occurred completely. For samples with an N concentration of 100 mg/l, the pH value decreased to between 5 and 5.26 at the end of the experiment, where nitrification was almost complete, but the effect of the decrease in the pH value was already apparent. The greatest influence of the decrease in the pH value during nitrification was observed in samples with an N concentration of 300 mg/l, when the pH value after measurement was between 5.2 and 5.4 and nitrification was not completed. From the initial 300 mg/l of nitrogen, about 200 mg/l of ammonia ion was nitrified.

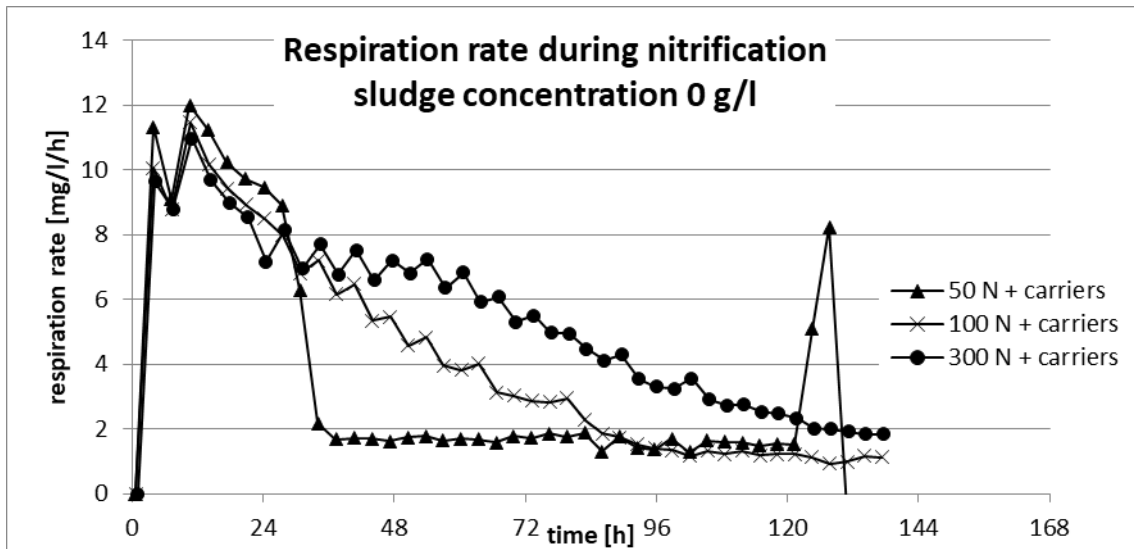


Figure 1. Respiration rate for samples with a sludge concentration of 0 g/l

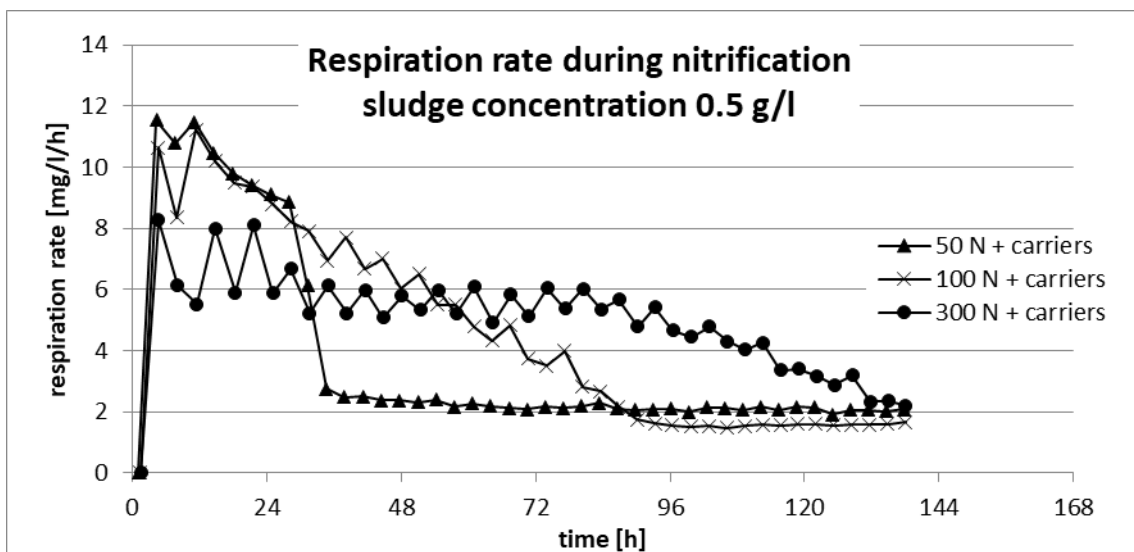


Figure 2. Respiration rate for samples with a sludge concentration of 0.5 g/l

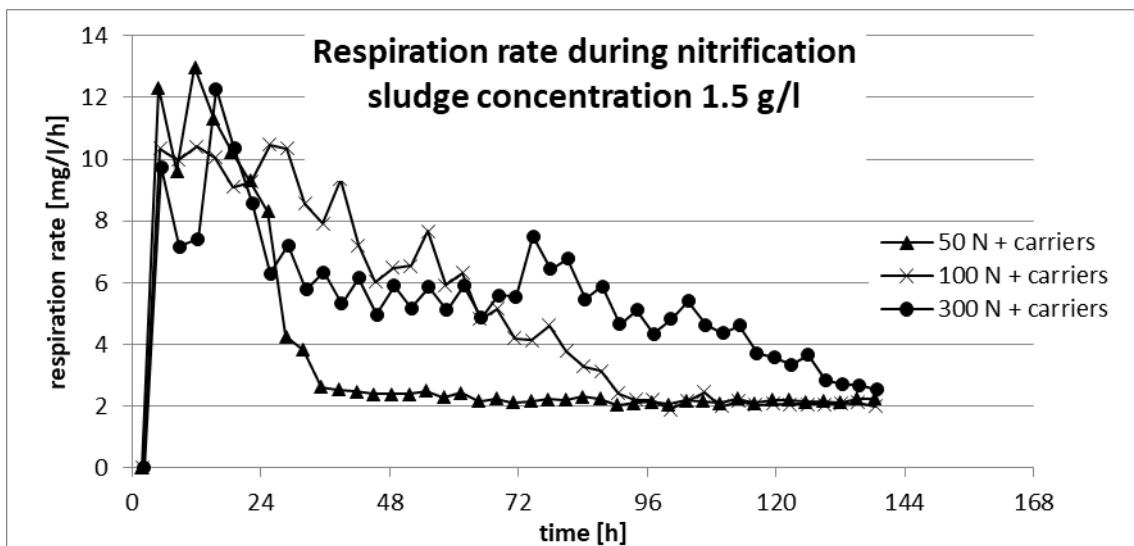
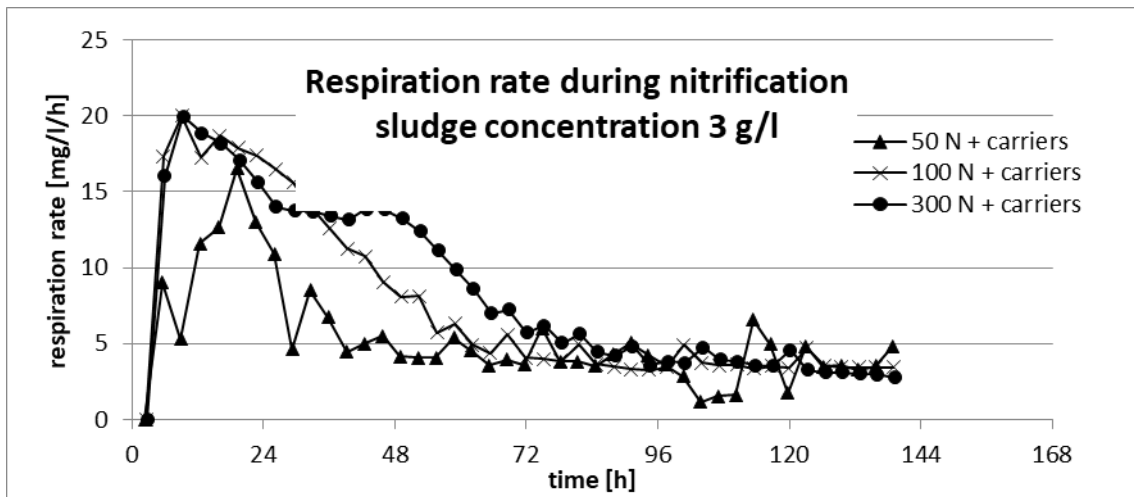
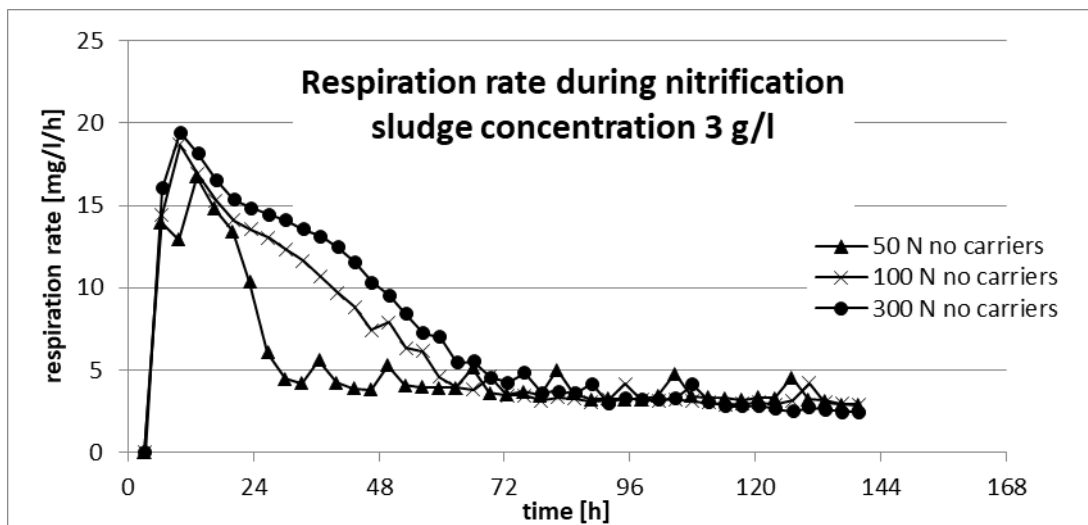


Figure 3. Respiration rate for samples with a sludge concentration of 1.5 g/l

For samples with carriers with a sludge concentration of 0 g/l, 0.5 g/l and 1.5 g/l, the maximum respiratory rates at the beginning of the nitrification were very similar, ranging around 12 mg/l/h and the different sludge concentrations were not reflected in the nitrification rate



**Figure 4.** Respiration rate for samples with a sludge concentration of 3 g/l, with carriers



**Figure 5.** Respiration rate for samples with a sludge concentration of 3 g/l, without carriers

For samples with a sludge concentration of 3 g/l, the maximum respiratory rate at the start of the nitrification reached almost 20 mg/l/h. This means that for samples with the highest sludge concentration (3 g/l) the maximum respiratory rates were almost twice that of samples with half and lower sludge concentrations, including the sample with only the carriers.

If we compare the results from samples with a sludge concentration of 3 g/l with carriers and without carriers, there is no increase or decrease in the maximum respiration rates of either sample. The maximum respiration rates are identical in both cases and the presence of carriers did not lead to a higher respiration rate.

Furthermore, a lower reduction in the respiration rate was observed in all cases of samples with the highest ammonia ion concentration (300 mg/l). This phenomenon is explained by the positive effect of a greater amount of added buffer and an increase in the buffering capacity of the system in relation to nitrate growth. The respiration rate decreased significantly more slowly due to greater pH stabilisation.

The experiment showed a significant effect of pH on nitrification rate and nitrification capacity. Particularly at higher nitrogen concentrations, the decrease in the pH value negatively affected the nitrification and when it fell below the critical value, it evidently led to the end of both phases of nitrification.

No effect on the total respiration rate at sludge concentrations (suspended population concentrations) of 0, 0.5 and 1.5 g/l was demonstrated. At a sludge concentration of 3 g/l, the respiration rate almost doubled, especially when comparing the maximum respiration rates. Furthermore, the advantage of the biofilm in increasing the respiration rate at a sludge concentration of 3 g/l was not demonstrated. No difference in the respiration rate with and without carriers was observed in these samples. The suspended biomass exhibited the same rates as the combination of suspended and immobilised biomass.

Before the start of the experiment, interaction of the immobilised and suspended populations was expected, manifested by an increase in nitrifying activity. However, this was not demonstrated in the case of the hybrid system with a sludge concentration of 3 g/l. The results of the experiment showed that the nitrification rates (measurement of respiration rate) of the suspended and immobilised populations are not cumulative. The presence of a biofilm does not lead to the sum of the nitrification rates, which in the suspended population (sludge alone) is the same as in the combined population (suspended and immobilised). On the other hand, the test with non-activated sludge carriers and the tests with the addition of 0.5 and 1.5 g/l of sludge showed the same maximum respiration rates and similar analytical values at the end of the experiment.

## REFERENCES

- Hlavínek, P. et al. (2006) Stokování a čištění odpadních vod. Vysoké učení technické v Brně, FS, Brno.
- Gavrilescu, M., Macoveanu, M. (2000) Attached-growth Engineering in Wastewater Treatment. *Bioprocess Engineering*, **23**, 95-106.
- Goswami, S. et al. (2016) A new Approach for Development of Kinetics of Wastewater Treatment in Aerobic Biofilm Reactor. *Applied Water Science*, **7**, 2187-2193.
- Jaramillo, F. et al. (2018) Advanced strategies to improve nitrification process in sequencing batch reactors – A review. *Journal of Environmental Management*, **218**, 154-164.
- Jenkins, D., Wanner, J. (2014) Activated Sludge – 100 Years and Counting. IWA Publishing, London, UK.
- Jianlong, W. et al. (2000) Wastewater treatment in a hybrid biological reactor (HBR): effect of organic loading rates. *Process Biochemistry*, **36**, 297-303.
- Masák, J., Čejková, A., Siglová, M., Kotrba, D., Jirků, V., Hron, P. (2002) Biofilm formation: A tool increasing biodegradation activity. *Proc. Environmental Biotechnology*, **III**. Massey University Press, 523-528.
- Najafpour, G. Et., Ebrahimi, A. (2016) Biological Treatment Process: Suspended Growth vs. Attached Growth. *Iranica Journal of Energy and Environment*, **7**, 114-123.
- Leix, C. et al. (2016) The role of residual quantities of suspended sludge on nitrogen removal efficiency in a deammonifying moving bed biofilm reactor. *Bioresource Technology*, **2019**, 212-218.
- Švehla, P. et al. (2010) Testování vlivu vybraných faktorů na průběh nitrifikace kalové vody. *Chemické listy*, **104**, 343-348, 2010.
- Templeton, M. R., Butler, D. (2011) An Introduction to Wastewater Treatment. Ventrus Publishing ApS, Holstebro, Denmark.
- Yang, J. (2013) Membrane Bioreactor for Wastewater Treatment. Ventus Publishing ApS.

# Synthesis, Characterisation and Adsorption Properties of a Sewage Sludge Derived Biochar Modified With Eggshell

A. G. Kumi\*, M. G. Ibrahim\*\*, M. Nasr\*\*\* and F. Manabu\*\*\*\*

\* Environmental Engineering Department, Egypt-Japan University of Science and Technology, Alexandria, Egypt (E-mail: [kumi.andy@ejust.edu.eg](mailto:kumi.andy@ejust.edu.eg))

\*\* Environmental Engineering Department, Egypt-Japan University of Science and Technology, Alexandria, Egypt ; Environmental Health Department, High Institute of Public Health, Alexandria University, Alexandria, Egypt (E-mail: [mona.gamal@ejust.edu.eg](mailto:mona.gamal@ejust.edu.eg))

\*\*\* Sanitary Engineering Department, Alexandria University, Alexandria, Egypt (E-mails: [mahmmoudsaid@gmail.com](mailto:mahmmoudsaid@gmail.com); [mahmoud-nasr@alexu.edu.eg](mailto:mahmoud-nasr@alexu.edu.eg))

\*\*\*\* Department of Civil and Environmental Engineering, Tokyo Institute of Technology, 2-12-1-M1-4 Ookayama, Tokyo 152-8552, Japan (E-mail: [fujii.m.ah@m.titech.ac.jp](mailto:fujii.m.ah@m.titech.ac.jp))

## Abstract

Recently, sewage sludge-derived biochar (SDB) has found several applications, as an appropriate adsorbent material, for the treatment of domestic and industrial wastewaters. The SDB adsorbent is composed of a highly porous structure, and it contains multiple functional groups and exchangeable cations. However, it has been reported that the SDB texture could be improved to obtain large amounts of adsorption sites. In this work, the SDB material was treated using eggshell to obtain a novel adsorbent, namely eggshell-modified sludge-derived biochar (EMBC). The EMBC composite was characterized by scanning electron microscopy (SEM), Fourier-transform infrared (FTIR) spectroscopy, and X-Ray diffraction (XRD) spectroscopy. It was demonstrated that the Brunauer–Emmett–Teller (BET) surface area and pore-distribution properties of EMBC were enhanced compared to the unmodified SDB. Moreover, the chemical composition of EMBC was strongly associated with the proliferation of carbonate minerals, amine, and oxygen-containing functional groups such as C-O, C=O, -OH, and -COOH. Moreover, EMBC was highly porous, containing rough surface and significant amounts of vacant sites. The Barrett-Joyner-Halenda model revealed that the pore sizes of EMBC were well distributed. Based on the results mentioned above, EMBC could be employed as a promising, low-cost, and alternative adsorbent material for the elimination of various pollutants from aqueous solutions; and that will be the focus of our future works.

## Keywords

Wastewater; sewage sludge; biochar; pyrolysis; adsorption; eggshell

## INTRODUCTION

The rapid urbanisation, industrialization and population growth globally has led to the generation of high quantities of wastewater. These effluents are often laden with various pollutants such as heavy metals, organic and inorganic pollutants, which when released into the environment (water bodies and soil) cause threats to human health, fauna, and flora due to their toxicity and carcinogenicity (Abdelhafez and Li, 2014).

Remediation technologies such as chemical precipitation, filtration, ion exchange, biosorption, and adsorption (activated carbon) have been applied in the treatment of wastewater (Abdelhafez and Li, 2016). However, these technologies require high energy, obtain partial pollutant removal, and need additional treatment for the wastes generated (Chakravarty et al., 2010). Therefore, there is the need to develop cheap, efficient, and environmentally friendly treatment method like biochar adsorbent. Some adsorbents however have been effectively applied in the removal of various pollutants from wastewater (Tong and Xu, 2013). The suitability of these adsorbents for contaminants removal is dependent on adsorbents physiochemical and morphological characteristics such as porosity,



surface area and functional groups (Malkoc and Nuhoglu, 2005). Biochar, a carbon rich product from the pyrolysis of biomass in an oxygen-free environment, has the ability to adsorb heavy metals, organic and inorganic pollutants contaminated wastewater due to its surface area, porous structure, alkaline cations and functional groups (Abdelhafez and Li, 2016).

However, the production of raw biochar is insufficient to manage its increasing application in versatile fields (Roy et al., 2019). Surface modification methods are therefore required to make biochar more potent, sustainable, and user-friendly for its application. Moreover, raw biochar has lower adsorption capacity compared to modified biochar (Tan et al., 2016).

To increase the adsorption capacity of biochar for application in wastewater treatment, modification methods should be appropriately developed to improve biochar properties like specific surface area, porosity, cation exchange capacity, surface functional group, and pH (Yao et al., 2013). Generally, agricultural wastes like eggshells, hold multiple functional groups like (amine, amide, carboxylic acid, and hydroxyl), large specific surface area, and huge amounts of pores that ensure the physical and chemical adsorption processes (El-sayed and El-sayed, 2014).

Waste eggshells contain high calcium carbonate contents (85–95 %) and can therefore be used as a cost-effective material for the removal of pollutants from wastewater (Chojnacka, 2005; Sik et al., 2010). Again, agricultural waste materials such as eggshells and oyster shells were reported by (Sik et al., 2010; Sik, Sang, and Lee, 2011) as an alternative to  $\text{CaCO}_3$  for the immobilization of heavy metals in contaminated water.

In this study, biochar was produced from sludge from wastewater treatment plant and then modified with chicken eggshell to improve its adsorptive capacity, specific surface area, porosity and surface functional groups. The objective of the study was to synthesize and characterize an eggshell modified biochar. This was to investigate the prospect of applying the modified biochar in wastewater treatment by improving its adsorptive properties.

## **MATERIALS AND METHOD**

### **Raw materials**

Sewage sludge was acquired from the East Alexandria Wastewater treatment plant, Egypt and stored in the refrigerator at 4°C until further used. The sewage sludge was then dried in an oven at 100°C for 48hrs and pyrolyzed afterwards. Chicken eggshells was acquired from the cafeteria at Egypt-Japan University of science and Technology. The eggshells were thoroughly washed and rinsed with distilled water several times to remove impurities before drying in an oven at 100°C for 48 hrs.

### **Biochar Synthesis**

The dried sewage sludge samples were pyrolyzed using a muffle furnace in an oxygen-free condition at 900°C with a heating rate of 5°C /min for 60 mins after reaching the desirable temperature. The biochar was then stored in an airtight container after cooling down to room temperature and referred as to raw biochar (BC). The dried chicken eggshells were then crushed with Tornado stainless-steel grinder and screened by standard sieves to obtain particle-diameter ranges of 0.25–0.5µm. Finally, the eggshell modified biochar (EMBC) was prepared in the ratio of 1:1 w/w (biochar: eggshell).

### **Characterization of Biochar**

The BET-surface area and pore distribution properties were determined using BET surface area analyser Belsorp II (BEL Japan Inc.) with nitrogen adsorption at 77K and degassing at 300 °C for

4hrs. In order to elucidate the surface morphology, texture and porous properties of the biochars, the surface morphology was determined using scanning electron microscope (JEOL JSM-6010LV Tokyo, Japan). The surface functional groups formed on the biochar were analysed by using the Fourier Transform Infrared Spectroscopy (FTIR, Bruker Vertex 70 ATR, Germany) in the 4000–400  $\text{cm}^{-1}$  region. The crystallinity of the biochars were investigated by using X-ray diffractometer (Shimadzu Xlab 6100 Tokyo, Japan) at 40 kV and 30 mA with Cu  $K\alpha$  radiation ( $\lambda=1.5406 \text{ \AA}$ ) at a scan speed of 12  $^{\circ}\text{C}/\text{min}$  and a step size of  $0.02^{\circ}$  in the  $2\theta$  range of 5–80  $^{\circ}\text{C}$ . The elemental chemical composition of the biochar was determined using Energy Dispersive X-Ray (EDX) spectroscopy of a Transmission electron microscope TEM (JEOL JEM-2100F Tokyo, Japan).

## RESULTS AND DISCUSSION

**Table 1.** Main pore properties of Raw biochar (BC), modified biochar (EMBC) and eggshell(EGS).

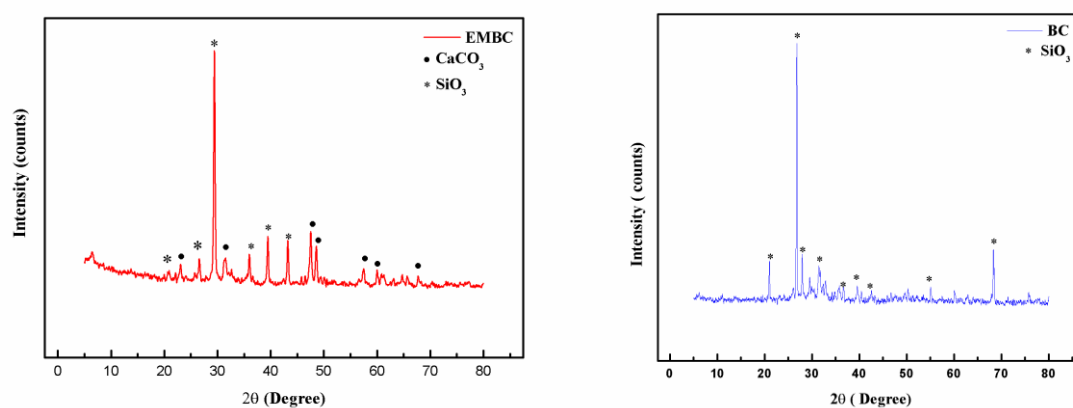
Sample	$S_{\text{BET}}$ ( $\text{m}^2\text{g}^{-1}$ )	$V_{\text{m}}$ $\text{cm}^3(\text{STP})\text{g}^{-1}$	$V_{\text{T}}$ ( $\text{cm}^3\text{g}^{-1}$ )	$D_{\text{p}}$ (nm)
BC	3.8304	0.8800	0.045042	47.036
EMBC	4.0554	0.9318	0.049998	49.314
EGS	5.5966	0.1286	0.005795	41.408
BC	3.8304	0.8800	0.045042	47.036

$S_{\text{BET}}$  = BET surface area;  $V_{\text{T}}$  = Total pore volume;  $V_{\text{m}}$  = mesopore Volume,  $D_{\text{p}}$  = average pore diameter.

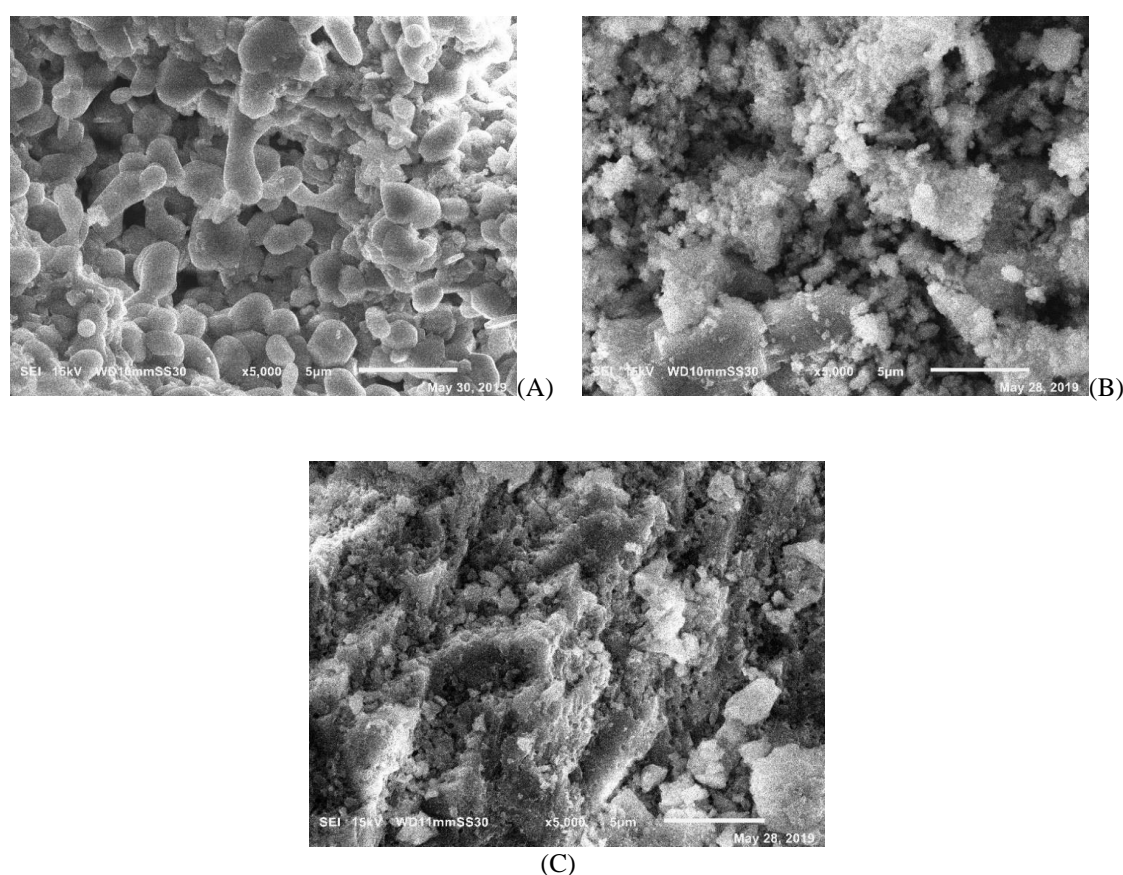
Table 1 indicates the BET surface area, total pore volume, and porosity of raw biochar modified biochar and eggshell. It can be found that EMBC had the best properties amongst the samples due to the modification with eggshell.

The occurrence of intense and narrow peaks in both biochar in figure 1 defines a crystalline structure of the material. The XRD analysis confirmed the important role of oxygen-containing functional groups in the adsorption process (Yubing Sun et al., 2015). Sharp reflection peaks at  $20.91^{\circ}$ ,  $26.82^{\circ}$ ,  $26.62^{\circ}$ ,  $29.94^{\circ}$ ,  $35.94^{\circ}$ ,  $39.42^{\circ}$ ,  $42.36^{\circ}$ ,  $55.12^{\circ}$ , and  $68.30^{\circ}$  in EMBC and BC represent the planes of  $\text{SiO}_2$  (PDF#65–0466), which were in line with the data of previous studies (Han et al., 2015; Yang et al., 2019; Zhou et al., 2017). In EMBC, peaks at  $2\theta = 22.09^{\circ}$ ,  $32.61^{\circ}$ ,  $47.18^{\circ}$ ,  $57.44^{\circ}$ ,  $59.96^{\circ}$ ,  $48.52^{\circ}$ ,  $67.69^{\circ}$  indicated that the calcite ( $\text{CaCO}_3$ ) is a major phase of the waste eggshell (Syah et al, 2017). The peaks intensities of EMBC were higher than BC, suggesting that the  $\text{CaCO}_3$  and  $\text{SiO}_2$  crystalline size of the modified biochar was larger than that of the raw biochar.

The raw biochar (BC) in figure 2 showed a smooth surface and a slightly porous structure as compared to EMBC that showed better porous structure. EMBC also showed a rougher, multi layered structure that could be attributed to the eggshell modification as the SEM image of the eggshell showed a highly porous structure that improves adsorption capacity (Tsai, 2006).

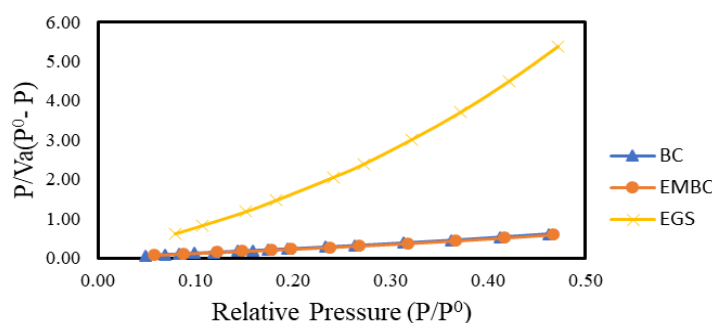


**Figure 1.** XRD pattern of eggshell modified biochar (EMBC) and raw biochar (BC)



**Figure 2.** SEM micrographs of (A) raw biochar (BC), (B) eggshell modified biochar (EMBC), and (C) eggshell (EGS)

EMBC had relatively a large BET specific surface area than BC as shown in table 1. Eggshell modification resulted in increased surface area, micropore area, mesopore and macropore volume of EMBC.



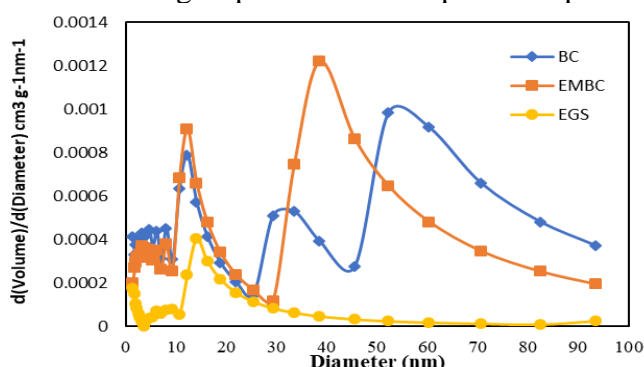
**Figure 6.** Adsorptive N<sub>2</sub> BET-plot of raw biochar (BC), egg shell modified biochar (EMBC) and Eggshell (EGS) at 77K

The BET equation requires a linear fit that relates  $P/Va(P^0 - P)$  and  $P/P^0$ , where  $Va$  is the amount in moles adsorbed at the relative pressure  $P/P^0$  as illustrated in figure 3 **Figure 6**. The values of correlation coefficients ( $R^2$ ) obtained were 0.9959, 0.995 and 0.9819 for BC, EMBC and EGS respectively.

**Table 2.** Elemental composition of raw biochar

Sample	Total C (wt %)	Total O (wt %)	Total N (wt %)	Total S (wt %)	O/C
BC	79.96	16.611	1.57	1.86	0.21

Elemental analysis (C, O, N and S % in wt%) in table 2 clearly showed that the biochar was highly carbonized and aromatized due to the high temperature of pyrolysis (Abdelhafez and Li, 2016) and the presence of aromatic C–H and C=C groups in the FTIR spectra respectively (Chia et al., 2014).

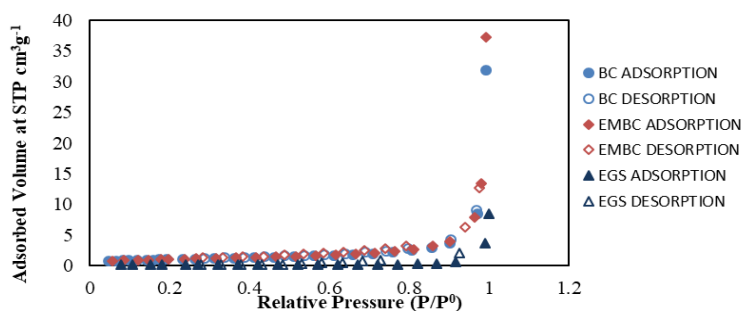


**Figure 7.** BJH pore distribution of raw biochar (BC), eggshell modified biochar (EMBC) and Eggshell (EGS)

Most of the pores are mesopores with a smaller proportion of micropore and macropore, thus they have relatively large average pore size. The average pore size of the sludge-derived biochar ranged from 47 to 49.31 nm. The mesopore capacity was more than 50 % of the total pore capacity of all sludge-derived biochar based on the pore structure analysis. Although both micro, meso and macropores were found to be present in all the biochar samples, the pore size distribution pattern of raw and modified biochar was found to be significantly different which can be attributed to the eggshell modification (Tsai, 2006).

In figure 5, a progressive increase in the N<sub>2</sub> volume was observed for whole range of relative pressure, and that the higher final volume was shown for EMBC. According to IUPAC, the isotherms that show reversibility are classified as type I, which also are known as Langmuir. This type of isotherm indicates that the adsorbate and adsorbent will have a high affinity (Gonçalves et

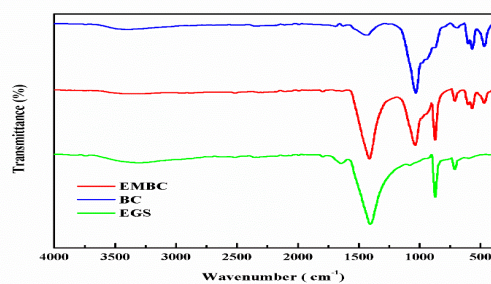
al., 2013).



**Figure 8.** Nitrogen adsorption/desorption isotherms of raw biochar (BC), eggshell modified biochar (EMBC) and Eggshell (EGS)

In the spectra of BC and EMBC in figure 6, peak at  $1030\text{ cm}^{-1}$  was assigned to the C–O functional group (Chia et al., 2012). This peak intensified due to the loss of alkyl groups during the pyrolysis process. Also, the peaks at  $600.68$  and  $678.70\text{ cm}^{-1}$  can be identified as out-of-plane bending vibrations of aromatic C–H groups (Cui et al., 2016), indicating that pyrolysis enhanced the degree of aromatization. The peaks at  $3638.38$  and  $3370.08\text{ cm}^{-1}$  were mainly due to the stretching vibration of O–H of alcohols and phenol by intermolecular hydrogen bonds, while the peak at  $1617.58\text{ cm}^{-1}$  was associated with the aromatic C=O stretching vibration and the C=C stretching vibration of carboxylic acids, esters, ketones, and anhydrides (Chia et al., 2012). The peak at  $1425.85\text{ cm}^{-1}$  can be assigned to C–H or –CH<sub>3</sub> bending (Fan et al., 2016). These peaks indicate the existence of –CH, –OH, and –COOH on biochar surface and pyrolysis only slightly affected these surface functional groups (Zhou et al., 2017). The peaks at  $2362.52\text{ cm}^{-1}$ ,  $1986.66\text{ cm}^{-1}$ ,  $1425\text{ cm}^{-1}$ , and  $941.56\text{ cm}^{-1}$  were identified as Si–H, C=O, aromatic C=C and C–H functional groups respectively (Khan et al., 2015). The band at  $467.84\text{ cm}^{-1}$  was attributed to the deformation and bending modes of the Si–O bond (Shen et al., 2017) which was confirmed in the XRD results.

The peak at  $1411\text{ cm}^{-1}$  in the spectra of EMBC and EGS was attributed to carbonate which is the basic component of the eggshells (Zhu et al., 2015). This was also confirmed by XRD. The other two strong peaks at about  $871\text{ cm}^{-1}$  and  $709\text{ cm}^{-1}$  were assigned to the out of plane deformation modes and in-plane deformation of calcium carbonate, respectively (Tsai, 2006). The observable peak at  $1794\text{ cm}^{-1}$  was associated with the C=O stretching vibration in the presence of the amide in the proteins (Zhu et al., 2015). BC and EMBC has similar peaks, but the appearance of peaks at  $1411\text{ cm}^{-1}$ ,  $1794\text{ cm}^{-1}$ ,  $871\text{ cm}^{-1}$  and  $709\text{ cm}^{-1}$  on EMBC were exactly as the peaks on the eggshell and this confirmed the eggshell modification.



**Figure 9.** FTIR spectra of raw biochar (BC), eggshell modified biochar (EMBC) and Eggshell (EGS)

## CONCLUSION

Biochar was produced from sewage sludge and analyzed to characterize its physical, chemical and adsorptive properties. To increase the adsorption capacity of biochar for wastewater treatment, eggshell modification was applied to improve biochar properties.

- The BET surface area, total pore volume, the pore properties of the eggshell modified biochar (EMBC) increased as compared to the raw biochar indicating the improvement by the eggshell modification.
- The N<sub>2</sub> adsorption isotherm of the eggshell modified biochar (EMBC) showed a higher final volume and reversibility which IUPAC classifies as type I, and known as Langmuir. This type of isotherm indicated that the adsorbate and adsorbent will have a high affinity.
- The FTIR spectra confirmed the chemical and physical composition of the eggshell modified biochar. The existence of oxygen containing functional groups such as C-O, C=O, -OH, and -COOH on biochar surface improves its adsorption capacity and carbonate, calcium carbonate which was also appeared in the XRD data confirmed the eggshell modification.

## ACKNOWLEDGEMENTS

The first author would like to thank the Egyptian Ministry of Higher Education (MoHE), Egypt-Japan University of Science and Technology (E-JUST) and Japan International Cooperation Agency-JICA for providing him scholarship and all the facilities to accomplish this work.

## REFERENCES

- Abdelhafez, A. A., Li, J. (2014) Geochemical and Statistical Evaluation of Heavy Metal Status in the Region around Jinxi River, China. *Soil and Sediment Contamination*, **23**(8), 850-868. DOI: <https://doi.org/10.1080/15320383.2014.887651>.
- Abdelhafez, A. A., Li, J. (2016) Removal of Pb(II) from aqueous solution by using biochars derived from sugar cane bagasse and orange peel. *Journal of the Taiwan Institute of Chemical Engineers*, **61**, 367-375. DOI: <https://doi.org/10.1016/j.jtice.2016.01.005>.
- Chakravarty, S., Mohanty, A., Sudha, T. N., Upadhyay, A. K., Konar, J., Sircar, J. K., Gupta, K. K. (2010) Removal of Pb(II) ions from aqueous solution by adsorption using bael leaves (*Aegle marmelos*). *Journal of Hazardous Materials*, **173**(1-3), 502-509. DOI: <https://doi.org/10.1016/j.jhazmat.2009.08.113>.
- Chen, Z., Chen, G., Li, Z., Chen, Y., Feng, T., Liu, T., Zhu, J. (2018) Characteristics and mechanisms of cadmium adsorption from aqueous solution using lotus seedpod-derived biochar at two pyrolytic temperatures. *Environmental Science and Pollution Research*, **25**(12), 11854-11866. DOI: <https://doi.org/10.1007/s11356-018-14601>.
- Chia, C. H., Gong, B., Joseph, S. D., Marjo, C. E., Munroe, P., Rich, A. M. (2012) Imaging of mineral-enriched biochar by FTIR, Raman and SEM-EDX. *Vibrational Spectroscopy*, **62**, 248-257. DOI: <https://doi.org/10.1016/j.vibspec.2012.06.006>.
- Chojnacka, K. (2005) Biosorption of Cr<sup>3+</sup>, Cd<sup>2+</sup> and Cu<sup>2+</sup> ions by blue – green algae *Spirulina* sp.: kinetics, equilibrium and the mechanism of the process, **59**, 75-84. DOI: <https://doi.org/10.1016/j.chemosphere.2004.10.005>.
- Cui, X., Hao, H., Zhang, C., He, Z., Yang, X. (2016) Capacity and mechanisms of ammonium and cadmium sorption on different wetland-plant derived biochars. *Science of the Total Environment*, **539**, 566-575. DOI: <https://doi.org/10.1016/j.scitotenv.2015.09.022>.
- El-sayed, H. E. M., El-sayed, M. M. H. (2014) Assessment of Food Processing and Pharmaceutical Industrial Wastes as Potential Biosorbents: A Review.
- Fan, S., Tang, J., Wang, Y., Li, H., Zhang, H., Tang, J., Li, X. (2016) Biochar prepared from co-pyrolysis of municipal sewage sludge and tea waste for the adsorption of methylene blue from aqueous solutions: Kinetics, isotherm, thermodynamic and mechanism. *Journal of Molecular Liquids*, **220**, 432-441. DOI: <https://doi.org/10.1016/j.molliq.2016.04.107>.



- Gonçalves, M., Guerreiro, M. C., Oliveira, L. C. A., Solar, C., Nazarro, M., Sapag, K. (2013) Micro mesoporous activated carbon from coffee husk as biomass waste for environmental applications. *Waste and Biomass Valorization*, **4**(2), 395-400. DOI: <https://doi.org/10.1007/s12649-012-9163-1>.
- Han, Z., Sani, B., Mroziak, W., Obst, M., Beckingham, B., Karapanagioti, H. K., Werner, D. (2015) Magnetite impregnation effects on the sorbent properties of activated carbons and biochars. *Water Research*, **70**, 394-403. DOI: <https://doi.org/10.1016/j.watres.2014.12.016>.
- Khan, S., Waqas, M., Ding, F., Shamshad, I., Arp, H. P. H., Li, G. (2015) The influence of various biochars on the bioaccessibility and bioaccumulation of PAHs and potentially toxic elements to turnips (*Brassica rapa* L). *Elsevier B.V.* DOI: <https://doi.org/10.1016/j.jhazmat.2015.06.050>.
- Malkoc, E., Nuhoglu, Y. (2005) Investigations of nickel ( II ) removal from aqueous solutions using tea factory waste, **127**, 120-128. DOI: <https://doi.org/10.1016/j.jhazmat.2005.06.030>.
- Roy, S., Kumar, U., Bhattacharyya, P. (2019) Synthesis and characterization of exfoliated biochar from four agricultural feedstock, 7272-7276.
- Shen, Z., Zhang, Y., McMillan, O., Jin, F., Al-Tabbaa, A. (2017) Characteristics and mechanisms of nickel adsorption on biochars produced from wheat straw pellets and rice husk. *Environmental Science and Pollution Research*, **24**(14), 12809-12819. DOI: <https://doi.org/10.1007/s11356-017-8847-2>.
- Sik, Y., Oh, O. S., Ahmad, M., Hyun, S., Deok, K. K., Moon, H., Lim, J. (2010) Effects of natural and calcined oyster shells on Cd and Pb immobilization in contaminated soils, 1301-1308. DOI: <https://doi.org/10.1007/s12665-010-0674-4>.
- Sik, Y., Sang, O., Lee, S. (2011) Application of eggshell waste for the immobilization of cadmium and lead in a contaminated soil, 31–39. <https://doi.org/10.1007/s10653-010-9362-2>
- Sun, Yubing, Yang, S., Chen, Y., Ding, C., Cheng, W., Wang, X. (2015) Adsorption and desorption of U(VI) on functionalized graphene oxides: A combined experimental and theoretical study. *Environmental Science and Technology*, **49**(7), 4255-4262. DOI: <https://doi.org/10.1021/es505590j>.
- Syah, R., Liyanita, A., Arifah, N., Puspitasari, E. (2017) Enhanced Electro-Catalytic Process on the Synthesis of FAME Using CaO from Eggshell. *Energy Procedia*, **105**, 289-296. DOI: <https://doi.org/10.1016/j.egypro.2017.03.316>
- Tan, X., Liu, Y., Gu, Y., Xu, Y., Zeng, G., Hu, X., Li, J. (2016) Biochar-based nano-composites for the decontamination of wastewater: A review. *BIORESOURSE TECHNOLOGY*. DOI: <https://doi.org/10.1016/j.biortech.2016.04.093>.
- Tong, X., Xu, R. (2013) Removal of Cu(II) from acidic electroplating effluent by biochars generated from crop straws. *Journal of Environmental Sciences (China)*, **25**(4), 652-658. DOI: [https://doi.org/10.1016/S1001-0742\(12\)60118-1](https://doi.org/10.1016/S1001-0742(12)60118-1).
- Tsai, W. T. (2006) Characterization and adsorption properties of eggshells and eggshell membrane, **97**, 488-493. DOI: <https://doi.org/10.1016/j.biortech.2005.02.050>.
- Yang, L., He, L., Xue, J., Id, L. W., Ma, Y., Li, H., Zhang, Z. (2019) Highly efficient nickel ( II ) removal by sewage sludge biochar supported  $\alpha$ -Fe<sub>2</sub>O<sub>3</sub> and  $\alpha$ -FeOOH: Sorption characteristics and mechanisms, (Ii), 1-16.
- Yao, Y., Gao, B., Chen, J., Zhang, M., Inyang, M., Li, Y., Alva, A. (2013) Bioresource Technology Engineered carbon ( biochar ) prepared by direct pyrolysis of Mg-accumulated tomato tissues : Characterization and phosphate removal potential. *Bioresource Technology*, **138**, 8-13. DOI: <https://doi.org/10.1016/j.biortech.2013.03.057>.
- Zhou, D., Liu, D., Gao, F., Li, M., Luo, X. (2017) Effects of biochar-derived sewage sludge on heavy metal adsorption and immobilization in soils. *International Journal of Environmental Research and Public Health*, **14**(7). DOI: <https://doi.org/10.3390/ijerph14070681>.
- Zhu, Y., Xue, T., Pan, J., Wei, X., Dai, J., Gao, L., Yan, Y. (2015) RSC Advances erythromycin-based imprinted composites for, 89030-89040. DOI: <https://doi.org/10.1039/c5ra12953b>.

# Antibiotic Resistance Genes in Different DNA Fractions Sampled at Wastewater Treatment Plant

A. Miłobędzka\*, Dana Vejmelková\* and Jan Bartáček\*

\* Department of Water Technology and Environmental Engineering, University of Chemistry and Technology Prague, Technická 5, 166 28 Prague 6, Czech Republic (E-mails: *milobeda@vscht.cz*; *vejmelkd@vscht.cz*; *bartacej@vscht.cz*)

## Abstract

Antibiotic resistance is a major threat to human health and the wastewater treatment plants (WWTPs) are hotspots for development and spread of antimicrobial resistance genes (ARGs). The mobile genetic elements (MGEs) and extracellular DNA should be involved in the ARGs monitoring in WWTPs.

In this study, total DNA, cell-free DNA and cell-associated DNA were sampled from the influent, activated sludge and effluent of large Czech WWTP. PCR was used to search for two resistance mechanisms: antibiotic inactivation for beta-lactamase (genes *bla<sub>SHV</sub>*, *bla<sub>CTX</sub>*, *bla<sub>TEM</sub>*) and antibiotic target replacement for sulfonamides (genes *sul1* and *sul2*). Resistance to beta-lactams was not observed during the study and ARGs towards sulfonamides were found in less than 1/3 of tested samples. Gene *sul2* occurred in the influent, activated sludge and effluent, while *sul1* was in the influent and activated sludge. In some cases, where ARGs were found in cell-free DNA, but not in cell-associated DNA, ARGs found in the samples may be related only to mobile genetic elements.

For preliminary screening, PCR is a proper method investigating ARGs occurrence. Nevertheless, it is advised to perform future analyses with standardized quantitative techniques and pairs of primers proper for environmental samples. It is also recommended to study more resistance mechanisms.

## Keywords

Extracellular DNA; cell-free DNA; antibiotic resistance; *sul1*, *sul2*; wastewater

## INTRODUCTION

Antibiotic resistance is a major threat to human health according to the World Health Organization and the wastewater treatment plants (WWTPs) are hotspots for development of antimicrobial resistance genes (ARGs) and their dissemination to the environment (Do et al., 2018).

Latest Pan-European study by Cacace et al. (2019) showed abundance of the genetic markers in the following order: integrons (*int11*); resistance to: sulfonamides (*sul1*), tetracyclines (*tetM*), beta-lactamases (*bla<sub>OXA58</sub>*, *bla<sub>TEM</sub>*, *bla<sub>OXA-48</sub>*, *bla<sub>CTX-M-32</sub>*), colistins (*mcr-1*), broad spectrum beta-lactamases (*bla<sub>KPC-3</sub>*). Unfortunately, the investigation mentioned did not include the Czech Republic. However, in different survey, Svobodová et al. (2018) checked nitrification tanks of six municipal WWTPs located in Bohemia (Czech region) for the occurrence of integrons (*int11*); resistance to: sulfonamides (*sul1*), tetracyclines (*tetM*), beta-lactamases (*bla<sub>TEM</sub>*) and additionally other tetracyclines (*tetW*, *tetO*, *tetA*, *tetB*) as well as macrolide-lincosamide-streptogramin (*ermB*). None of the screenings above involve extracellular DNA (eDNA) or DNA present in phage capsids, all together classified as mobile genetic elements (MGEs). This is an important knowledge gap, because the risk for human health does not simply increase together with the total amount of ARGs, but is connected to the transfer of ARGs to pathogens. This transfer may be mediated by free DNA in MGEs (Lood et al., 2017; Karkmann et al., 2019), which can be neglected during sample preparation by filtration.



The eDNA has been reported in large amount (up to 20 mg/g of volatile suspended solids) in activated sludge from WWTPs (Palmgren and Nielsen, 1996). It is also abundant in the matrix of extracellular polymeric substances, for example bound to extracellular proteins or polysaccharides (Nagler et al., 2018).

Horizontal gene transfer (HGT) mediated by eDNA (Molin and Tolker-Nielsen, 2003) has been studied in soils and marine sediments (Torti et al. 2015), where eDNA persisted up to several months (Mao et al., 2014). Among the few studies of eDNA in activated sludge, Zhang et al. (2018) studied cell-associated DNA (caDNA) and cell-free DNA (cfDNA) fraction in WWTPs with quantitative PCR (qPCR). Such approach is crucial as popular disinfection methods assure antibiotic resistant bacteria elimination, but do not eliminate ARGs in cfDNA. What is more, ARGs are often released from dead cells of antibiotic resistant bacteria during disinfection and PCR based techniques are unable to distinguish between DNA originating from active bacteria and the eDNA. Therefore, ARGs quantification in wastewater samples containing considerable amounts of eDNA, may be biased in activity studies with qPCR (Dominiak et al., 2011).

Indeed, quantitative extraction of eDNA from activated sludge is a challenging task. The strength of DNA bound to the matrix decreases with the length of DNA molecule, it is also connected to the shortage during the purification. Then different fractions of eDNA show various recovery rates after purification. The free DNA molecules can be easily degraded to smaller fragments. Those small pieces are weakly bound in contrast to caDNA tightly bound to cell membrane proteins through bivalent cations. Therefore the recovery rate in the purification is higher for caDNA than for cfDNA (Nagler et al., 2018). From the start of the research, there is smaller chance to investigate cfDNA.

The presented study aims to verify, whether eDNA screening for ARGs is needed and possible in samples of influent, activated sludge and effluent from WWTP. To the best of our knowledge this is the first study in Czech WWTPs concerning ARGs in eDNA.

## **METHODS**

### **Sampling**

Samples of the influent, activated sludge and effluent were taken from a large WWTP in the Czech Republic with mechanical pre-treatment (screening, sand trap, primary clarification) biological step and secondary clarifiers. The configuration of the biological process is regeneration chamber, anaerobic compartment (receiving both return sludge and wastewater), anoxic compartment (return activated sludge and internal recycle) and aerated chamber. Grab samples in volume of 500 mL were taken 3 times in December 2018 and 3 times in January and February 2019. The samples were collected in sterilized plastic bottles washed with bleach and transported to the laboratory within few hours.

### **Separation of fractions with various DNA**

The separation of the masses containing diverse fractions of DNA was done by filtration as described by Zhang et al. (2018) with modifications in used volumes in precipitation. For the influent, it was: 10 mL for total DNA, 50 mL for cell-associated fraction (filtration) and 30 mL for cell-free fraction. For the activated, sludge it was: 10 mL for total DNA, 50 mL for cell-associated fraction (filtration) and 10 mL for cell-free fraction. For the effluent it was: 20 mL for total DNA, 200 mL for cell-associated fraction (filtration) and 30 mL for cell-free fraction.

The distinguished fractions were not extracellular and intracellular DNA, but cell-associated (cells and molecules attached to them, staying on 0.22  $\mu\text{m}$  filter) and cell-free fractions (passing through 0.22  $\mu\text{m}$  filter).

### DNA extraction and ARGs amplification

DNA was extracted in duplicates using the FastDNA™ Spin Kit for Soils (MP Biomedicals, Santa Ana, USA) according to manufacturer instructions. The concentration and purity of DNA were measured by a nano spectrophotometer (BioDrop  $\mu$ LITE, Biodrop, UK). The amplification of eDNA was performed using multiplex reaction targeting resistance to sulfonamides (genes *sul1* and *sul2*) and beta-lactamases (genes *bla<sub>SHV</sub>*, *bla<sub>CTX</sub>*, *bla<sub>TEM</sub>*) according to Blahna et al. (2006) and Monstein et al. (2007), respectively. The analyses with positive results for one replicate were performed also for the other one to confirm the results.

## RESULTS & DISCUSSION

### DNA content in the samples

Generally, we observed much higher DNA concentrations for all fractions and all sampling points (0 to 295.5  $\mu$ g/mL) than Zhang et al. (2018) in their analyses (max for cfDNA 15.9 ng/mL and for caDNA 20.8  $\mu$ g/mL, both noted in activated sludge). Zhang et al. (2018) got caDNA and cfDNA concentrations in influent and effluent lower than 1  $\mu$ g/mL. In our study we obtained DNA concentration above this level for 24 out of 25 samples. It can be partially explain by different treatment technology in the WWTPs investigated as it uses clarifiers for sludge retention. Membrane separation from the study of Zhang et al. (2018) was probably more efficient in cfDNA retention. We also used the different kit for DNA extraction. The kit was better adjusted to remove inhibitors, it is further characterized later. The other cause, maybe be placed in investigated samples' volumes. The authors decided to proceed 750 mL or more of effluent, because ultrafiltration significantly reduced content of DNA in it. However, they used only up to 12 mL and up to 1 mL for influent and activated sludge, respectively (Zhang et al., 2018). In our study we used 30 mL of influent and effluent, and 10 mL of activated sludge. The small samples may not be representative and the physical forces may bind eDNA to the containers used for sampling and transport. Therefore it would be advised to proceed bigger volumes of samples in future studies. In the present study of the Czech WWTP the total content of DNA for all fractions was generally reduced during the treatment process. The caDNA was usually the most abundant fraction in activated sludge and effluent, but also method of gathering cells was different for this fraction (residues on the filter were used for the extraction). The content of caDNA grew in time, from first to last sampling period. DNA concentration was usually higher in the activated sludge than in influent, but then decreased in effluent. Presumably because of well working sedimentation. Total DNA and cfDNA concentration were very similar in effluent. cfDNA was usually the least abundant DNA fraction. The caDNA content in all sampling points was higher or similar to the cfDNA content (Table 1). This cfDNA was not very dynamic and less abundant in the effluent and influent than in the activated sludge. This is consistent with the results from Dominiak et al. (2011) showing highest eDNA abundance near bacteria. They also implied that eDNA is actively secreted by those microcolonies (confirmed also by Nielsen et al. 2007), or it is a product of cell autolysis (Montanaro et al. 2011).

**Table 1.** DNA average concentration from sample's' duplicates with the distinction to cfDNA and caDNA ( $\mu$ g/mL)

date of sampling/ DNA fraction	influent			activated sludge			effluent		
	totDNA	cfDNA	caDNA	totDNA	cfDNA	caDNA	totDNA	cfDNA	caDNA
13.12.2018	16 $\pm$ 0	8.5 $\pm$ 0.5	6 $\pm$ 2	61 $\pm$ 6	7 $\pm$ 0.5	7.5 $\pm$ 3.5	1 $\pm$ 1	2 $\pm$ 0	0
09.01.2019	208.5 $\pm$ 80.5	18.5 $\pm$ 0.5	73.5 $\pm$ 17.5	141.5 $\pm$ 128.5	19	295.5 $\pm$ 45.5	13.5 $\pm$ 2.5	13.5 $\pm$ 1.5	155.5 $\pm$ 62.5
1.02.2019	26	25	86	5	41	1275	ND	ND	24

ND – no data

Zhang et al. (2018) in their study of WWTP with membrane bioreactor eliminating most of the caDNA indicated that cfDNA could be the dominant DNA in the effluent from a well-operated process. In our study we observed that in WWTP with different treatment system cfDNA can play important role during whole treatment, as it is present in significant concentration in all sampling points. Moreover, it can be involved in HGT, bacterial adhesion, the overall enhancement of antimicrobial resistance as well as stabilization of the biofilms' structures (Okshevsky and Meyer, 2014).

### ARGs' occurrence and resistance mechanisms

The ARGs were found only in the first sampling period (Table 2). The study screened the tested WWTP for two resistance mechanisms: antibiotic inactivation for beta-lactamase and antibiotic target replacement for sulfonamides. While the latter was present in most of the samples in the first sampling period, only one sample was positive for class A beta-lactamases, e.g. *bla*<sub>TEM</sub> gene, which is the most common beta-lactamase in gram-negative bacteria.

ARGs toward beta-lactamases were the least abundant ARGs (*bla*<sub>KPC-3</sub>, *bla*<sub>TEM</sub> was the 4th most abundant of 9 tested ARGs) in the Pan-European study presented by Cacace et al. (2019). Nonetheless, *bla*<sub>TEM</sub> was found in all Czech sampling locations in the study using total DNA (Svobodová et al., 2018). More samples and other primers or different methods (e.g. qPCR or metagenomics) should be used to investigate the lack of resistance to beta-lactamases in WWTP from this study.

**Table 2.** Positive results (confirmed in second PCR reaction for duplicates) of screening different fractions of DNA (total, cell-associated, cell-free) in influent, effluent and activated sludge from Czech WWTP (13.12.2018)

Sample type /ARG	total DNA						caDNA						cfDNA									
	sulfonamides			beta-lactamases			sulfonamides			beta-lactamases			sulfonamides			beta-lactamases						
	<i>sul2</i>	<i>sul2</i>	<i>sul1</i>	<i>sul1</i>	<i>bla</i> <sub>SHV</sub>	<i>bla</i> <sub>CTX-M</sub>	<i>bla</i> <sub>TEM</sub>	<i>sul2</i>	<i>sul2</i>	<i>sul1</i>	<i>sul1</i>	<i>bla</i> <sub>SHV</sub>	<i>bla</i> <sub>CTX-M</sub>	<i>bla</i> <sub>TEM</sub>	<i>sul2</i>	<i>sul2</i>	<i>sul1</i>	<i>sul1</i>	<i>bla</i> <sub>SHV</sub>	<i>bla</i> <sub>CTX-M</sub>	<i>bla</i> <sub>TEM</sub>	
influent 1/2			+	+											+	+	+					
influent 2/2			+	+			+								+	+						
activated sludge 1/2	+	+	+	+					+						+	+	+					
activated sludge 2/2			+	+					+						+	+	+	+				
effluent 1/2	+	+	+												+	+						
effluent 2/2															+	+						

Genes *sul1* and *sul2* which are often linked to small plasmids and connected to HGT, were found in total DNA and cfDNA in all samples studied. *Sul1* gene was the second most abundant (after *int11*) in the European WWTPs investigated by Cacace et al. (2019). In contrast, *sul1* was absent in one third of Czech WWTPs tested by Svobodová et al. (2018), even though the *int11* was present in all WWTPs. One can hypothesize that weakly bound DNA including MGEs with ARGs may be included in some studies of ARGs towards sulfonamides and neglected in the others giving inconsistent results. Especially methodology using high speed centrifugation can cause lysis of some cells and release of additional pool of eDNA, which later can be lost during filtration. On the other hand part of MGEs and eDNA can be chemically bound to extracellular polymeric substances or other polymers and never get to the supernatant.

### **Need for standardized methodology**

Different primers were used in all mentioned studies, therefore in the future it is advised to use primers tested in environmental samples. Lately, the literature-based, manually-curated database of PCR primers for the detection of antibiotic resistance genes in various environments (LCPDb-ARG) was created by Gorecki et al. (2019). The authors calculated specificity, efficacy and taxonomic efficacy for each primer pair in the LCPDb-ARG base (selected primer pairs were tested in bioinformatic and experimental PCR surveys). It is recommended to use the primers with the highest specificity and efficacy as well as test new primers before amplification of environmental DNA.

What is more, both studies of Cacace et al. (2019) and Svobodová et al. (2018) used qPCR, but quantification was made according to different standards. In the first study abundance of the 9 ARGs was quantified by qPCR targeting different fragments of ARGs previously cloned into plasmid vectors and used as standards (Hembach et al., 2017; Rocha et al., 2018; Stalder et al., 2014). On the other hand, Svobodová et al. (2018) determined the relative abundance of ARGs as a ratio of the ARG gene copy number to the total bacterial DNA (primers for 16S rDNA). It shows that standard methodology for ARGs monitoring in WWTPs is needed for global studies and further comparison of the results.

### **Quantitative aspect**

Quantification should underline consistent recovery of eDNA to support accurate and precise estimations in biological samples. Inhibition can lower the presumable recovery of eDNA, not only lowering chances of its detection, but also effecting in inaccurate quantification. There are many inconsistencies among eDNA studies. Mainly in eDNA yield, coherent recovery, fit and slope of eDNA/biomass relationships, and inhibition (Eichmiller et al., 2016).

The inhibitor in samples can make accurate eDNA quantification very doubtful. Consequently, the researchers should eliminate inhibition already in first steps of DNA isolation. That requires using the proper kit for DNA extraction.

Eichmiller et al. (2016) tested several different kits for inhibitors removal in water samples: MoBio PowerSoil DNA Isolation Kit, MoBio PowerWater DNA Isolation Kit, MP Biomedicals FastDNA SPIN Kit, MP Biomedicals FastDNA SPIN Kit for Soil, Qiagen DNeasy Blood and Tissue Kit, and Qiagen QIAamp DNA Stool Mini Kit. The inhibition in final DNA after isolation with the PowerWater and FastDNA SPIN Kit was only slight and was possible to eliminate by a 1/2 dilution of DNA extract.

We decided to use FastDNA SPIN Kit in our study. The kit is also highly recommended for (anaerobic) sludge, as the DNA purification is performed mainly through binding to a binding matrix, utilizing the negative charge of DNA (Guo and Zhang 2013, van Loosdrecht et al., 2016, Nagler et al., 2018).

Eichmiller et al. (2016) also pointed out that the presence of inhibition unable using the total DNA yield as a valid measure of sensitivity and dilutions eliminating inhibition affect the detection sensitivity of the kit. However, the authors normalized the sensitivity assessment and ranked the FastDNA SPIN Kit, the PowerSoil kit and the FastDNA SPIN Kit for Soil among the most sensitive for lake water and the FastDNA SPIN Kit and the PowerSoil kit for the well water. As in experiments performed by Eichmiller et al., (2016) half of the tested kits inhibited qPCR to some extent, for this preliminary study we decided to not quantify the genes' abundance or not present biased results.

### Distribution of ARGs among various DNA fractions

Even though eDNA cannot be completely separated from intracellular DNA due to its absorption on free cells or on the flocs of activated sludge, differences in resistance genes occurrence in cfDNA and caDNA were observed in this study. In a few cases (influent and effluent, *sul2* genes in activated sludge samples) ARGs were found in cfDNA and total DNA, but not in caDNA. It is possible that ARGs in effluents originated from bacteria that were destroyed in the treatment process only remained part of cfDNA. This case needs to be further investigated.

Some organic substances being PCR-inhibitors may have been stopped during filtration to cell-free fraction therefore may have impaired amplification of total DNA and caDNA only. The issue was also raised by Hunter et al. (2019) in analyses of eDNA in water. In their studies they additionally investigated influence of storage lysis buffer and indirectly showed that increased volume of sample can not only improve the yield of eDNA during isolation, but also reduce inhibition. That is very important in quantitative analyses and have effect in higher precision of replicate measurements.

Also Hoshino and Inagaki (2012) and Sedlak et al. (2014) postulated that additional removal of inhibitors, not only optimization of DNA extraction, can help in inhibition removal in PCR. They also proposed clean up column usage after extraction, matrix dilution, addition of PCR adjuvants, trying modifications in the analysis platform and experimenting with proportions of reaction mixture. For quantification in environmental samples they recommended digital PCR, which is more resistant to inhibition than qPCR.

### CONCLUSIONS

The significant concentrations of cfDNA were noted during whole treatment process during the study. There is need to investigate cfDNA fraction while monitoring antimicrobial resistance in WWTPs. PCR method used in this study provided basic information to support further studies of ARGs occurrence and abundance. For preliminary screening, PCR is a proper method, but it is advised to perform future analyses with quantitative techniques such as qPCR or metagenomics. Resistance genes to beta-lactams were not detected in this study and ARGs towards sulfonamides were found only in less than one third of all samples (all in one sampling period 13.12.2018). When ARGs towards sulfonamides were found, *sul2* occurred in all tested sampling sites, while *sul1* was only in the influent and in activated sludge.

It is clear that two groups of ARGs are not enough for comprehensive monitoring and it is also recommended to study more resistance mechanisms.

### REFERENCES

- Blahna, M. T., Zalewski, C. A., Reuer, J., Kahlmeter, G., Foxman, B., Marrs, C. F. (2006) The role of horizontal gene transfer in the spread of trimethoprim–sulfamethoxazole resistance among uropathogenic *Escherichia coli* in Europe and Canada. *Journal of Antimicrobial Chemotherapy*, **57**, 666-672.
- Cacace, D., Fatta-Kassinos, D., Manaia, C. M., Cytryn, E., Kreuzinger, N., Rizzo, L., Karaolia, P., Schwartz, T., Alexander, J., Merlin, C., Garelick, H., Schmitt, Daisy de Vries, Carsten U. Schwermer, Sureyya Meric, Can Burak Ozkal, Marie-H., Pons, N., Kneis, D., Berendonk, T. U. (2019). Antibiotic resistance genes in treated wastewater and in the receiving water bodies: A pan-European survey of urban settings. *Water Research*. DOI: <https://doi.org/10.1016/j.watres.2019.06.039>.

- Do, T. T., Murphy, S., Walsh, F. (2018) Antibiotic Resistance and Wastewater Treatment Process. In P. L. Keen and R. Fugère (Eds.). *Antimicrobial Resistance in Wastewater Treatment Processes*, 263-291. John Wiley & Sons, Inc.
- Dominiak, D. M., Nielsen, J. L., Nielsen, P. H. (2011) Extracellular DNA is abundant and important for microcolony strength in mixed microbial biofilms. *Environmental Microbiology*, **13**(3), 710-721.
- Eichmiller, J. J., Miller, L. M. Sorensen, P. W. (2016) Optimizing techniques to capture and extract environmental DNA for detection and quantification of fish. *Mol. Ecol. Resour.*, **16**, 56-68.
- Gorecki, A., Decewicz, P., Dziurzynski, M., Janeczko, A., Drewniak, L., Dziewit, L. (2019) Literature-based, manually-curated database of PCR primers for the detection of antibiotic resistance genes in various environments. *Water Research*, **161**, 211-221. DOI: 10.1016/j.watres.2019.06.009.
- Guo, F., Zhang, T. (2013). Biases during DNA extraction of activated sludge samples revealed by high throughput sequencing. *Applied Microbiology and Biotechnology*, **97**(10), 4607-4616. DOI: <https://doi.org/10.1007/s00253-012-4244-4>.
- Hembach, N., Schmid, F., Alexander, J., Hiller, C., Rogall, E.T., Schwartz, T. (2017) Occurrence of the mcr-1 colistin resistance gene and other clinically relevant antibiotic resistance genes in microbial populations at different municipal wastewater treatment plants in Germany. *Front. Microbiol.* DOI: <https://doi.org/10.3389/fmicb.2017.01282>.
- Hunter, M.E., Ferrante, J.A., Meigs-Friend, G., Ulmer, A. (2019) Improving eDNA yield and inhibitor reduction through increased water volumes and multi-filter isolation techniques. *Scientific Reports*, **9**, 5259. pmid:30918268.
- Hoshino, T., Inagaki, F. (2012) Molecular quantification of environmental DNA using microfluidics and digital PCR. *Systematic and Applied Microbiology*, **35**, 390-395.
- Karkman, A., Pärnänen, K., Larsson, D. G. J. (2019) Fecal pollution can explain antibiotic resistance gene abundances in anthropogenically impacted environments. *Nature Communications*, **80**, 10.
- Lood, R., Ertürk, G., Mattiasson, B. (2017) Revisiting Antibiotic Resistance Spreading in Wastewater Treatment Plants – Bacteriophages as a Much Neglected Potential Transmission Vehicle. *Front. Microbiol.*, **8**, 2298. DOI: 10.3389/fmicb.2017.02298.
- Mao, D., Luo, Y., Mathieu, J., Wang, Q., Feng, L., Mu, Q., Feng, C., Alvarez, P. J. J. (2014) Persistence of extracellular DNA in river sediment facilitates antibiotic resistance gene propagation. *Environmental Science and Technology*, **48**(1), 71-78.
- Monstein, H. J., Östholm Balkhed, Å., Nilsson, M., Nilsson, M., Dornbusch, K., Nilsson, L. (2007) Multiplex PCR amplification assay for the detection of blaSHV, blaTEM and blaCTXM genes in Enterobacteriaceae. *Apmis*, **115**, 1400-1408.
- Montanaro, L., Poggi, A., Visai, L., Ravaioli, S., Campoccia, D., Speziale, P., Arciola, CR. (2011) Extracellular DNA in biofilms. *Int J Artif Organs.*, **34**, 824-831. DOI: 10.5301/ijao.5000051.
- Molin, S., Tolker-Nielsen, T. (2003) Gene transfer occurs with enhanced efficiency in biofilms and induces enhanced stabilisation of the biofilm structure. *Curr Opin Biotechnol*, **14**, 255-261.
- Nagler, M., Podmirseg, S. M., Griffith, G. W., Insam, H., Ascher-Jenull, J. (2018) The use of extracellular DNA as a proxy for specific microbial activity. *Applied Microbiology and Biotechnology*, **102**(6), 2885-2898. DOI: <https://doi.org/10.1007/s00253-018-8786-y>.
- Nielsen, K. M., Johnsen, P. J., Bensasson, D., Daffonchio, D. (2007) Release and persistence of extracellular DNA in the environment. *Environ Biosaf Res.*, **6**(1-2), 37-53. DOI: 10.1051/ebr:2007031.
- Okshevsky, M., Meyer, R. L. (2014) The role of extracellular DNA in the establishment, maintenance and perpetuation of bacterial biofilms. *Crit. Rev. Microbiol.* DOI: <http://dx.doi.org/10.3109/1040841X.2013.841639>

- Palmgren, R., Nielsen, P.H. (1996) Accumulation of DNA in the exopolymeric matrix of activated sludge and bacterial cultures. *Water Sci Tech*, **34**, 233-240.
- Rocha, J., Cacace, D., Kampouris, I., Guilloteau, H., Jäger, T., Marano, R. B. M., Karaolia, P., Manaia, C. M., Merlin, C., Fatta-Kassinos, D., Cytryn, E., Berendonk, T. U., Schwartz, T. (2018) Inter-laboratory calibration of quantitative analyses of antibiotic resistance genes. *J. Environ. Chem. Eng.* DOI: <https://doi.org/10.1016/J.JECE.2018.02.022>.
- Sedlak, R. H., Kuypers, J., Jerome, K. R. (2014) A multiplexed droplet digital PCR assay performs better than qPCR on inhibition prone samples. *Diagnostic Microbiology and Infectious Disease*, **80**, 285-286.
- Stalder, T., Barraud, O., Jové, T., Casellas, M., Gaschet, M., Dagot, C., Ploy, M.-C. (2014). Quantitative and qualitative impact of hospital effluent on dissemination of the integron pool. *ISME J.*, **8**, 768-77. DOI: <https://doi.org/10.1038/ismej.2013.189>.
- Svobodová, K., Semerád, J., Petráčková, D., Novotný, Č. (2018) Antibiotic Resistance in Czech Urban Wastewater Treatment Plants: Microbial and Molecular Genetic Characterization. *Microbial Drug Resistance*, mdr.2017.0406. DOI: <https://doi.org/10.1089/mdr.2017.0406>.
- Torti, A., Lever, M. A., Jørgensen, B. B. (2015) Origin, dynamics, and implications of extracellular DNA pools in marine sediments. *Marine Genomics*, **24** (3), 185-196.
- van Loosdrecht, M., Nielsen, P., Lopez-Vazquez, C. B. D. (2016) *Experimental Methods in Wastewater Treatment*. IWA Publishing. DOI: <https://doi.org/10.1017/CBO978110741532>.
- Zhang, Y., Li, A., Dai, T., Li, F., Xie, H., Chen, L., Wen, D. (2018) Cell-free DNA: A Neglected Source for Antibiotic Resistance Genes Spreading from WWTPs. *Environmental Science and Technology*, **52**(1), 248-257.



## On-line Titrimeter: Full Scale Biosensor for Control in Wastewater Treatment

A. Nardi\*, A. Mannucci\*, C. Polizzi\*, F. Spennati\*\* and G. Munz\*

\* Department of Civil and Environmental Engineering, University of Florence, Via di S. Marta, 3, 50121, Firenze, Italy (E-mails: [arianna.nardi@stud.unifi.it](mailto:arianna.nardi@stud.unifi.it); [alberto.mannucci@dicea.unifi.it](mailto:alberto.mannucci@dicea.unifi.it); [cecilia.polizzi@unifi.it](mailto:cecilia.polizzi@unifi.it); [giulio@dicea.unifi.it](mailto:giulio@dicea.unifi.it))

\*\* Laboratorio CER<sup>2</sup>CO, Consorzio Cuoio-Depur S.p.A, Via Arginale Ovest, 81, S. Miniato 56020, Pisa, Italy (E-mail: [francesco.spennati@cuoiodepur.it](mailto:francesco.spennati@cuoiodepur.it))

### Abstract

In this work a differential on-line continuous titrimeter was installed and conducted at CuoioDepur WWTP (San Romano, PISA, Italy), treating tannery and domestic wastewater, with the aim to evaluate the possibility to use the innovative instrument as a reliable nitrification process probe. The titrimeter output is the maximum ammonia oxidation rate ( $AOR_{MAX}$ ) that is automatically estimated under not limiting DO and substrate conditions in the titrimeter reactors. The titrimeter, fed with mixed liquor from aerobic tanks of the real plant, worked for more than 6 months and is currently in operation. The possibility to use the titrimeter as a nitrification process probe was confirmed by the stability and the reliability of the obtained  $AOR_{MAX}$  values that were confirmed using conventional methods for nitrification process efficiency estimation.  $AOR_{MAX}$  varied in time according to industrial influent loads and environmental and operational conditions variations. Moreover, titrimeter output data set was used for the calibration of specific maximum growth rate ( $\mu_{MAX,AOB}$ ) of Ammonia Oxidizing Biomass (AOB). SUMO© 2S model, modified in order to allow its application on high Sludge Retention Time (SRT), was used as a reference model. Calibrated ( $\mu_{MAX,AOB} = 0.58 \text{ d}^{-1}$ ) model was validated using monthly average real scale plant monitoring data obtained in the years from 2015 to 2017. The model well describes nitrogen removal process efficiency.

### Keywords

Nitrification control; nitrification modelling; AOB kinetic parameters estimation; titrimetry; industrial wastewater treatment; process probe

## INTRODUCTION

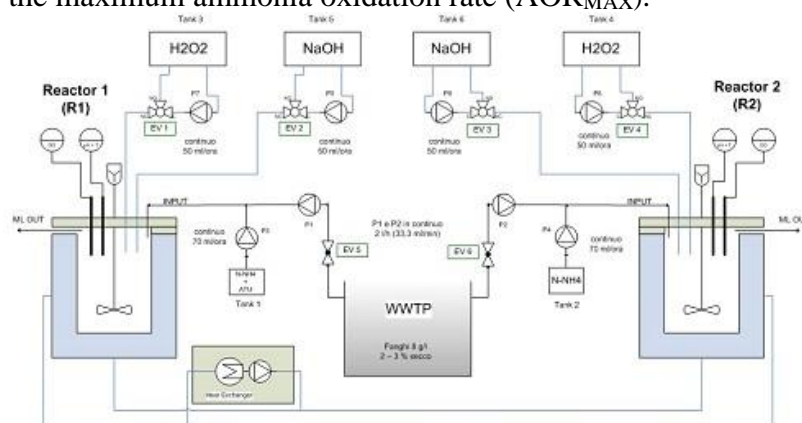
Instrumentation, Control and Automation (ICA) in wastewater treatment systems aim to improve the efficiency and robustness of the process. Moreover, the increasing requirements in effluent quality standards and the need to increase process sustainability in terms of energy consumption and efficiency, made the adoption of optimized ICA systems a crucial aspect for the optimization of economic and environmental costs in wastewater treatment plants (WWTPs). ICA may improve the efficiency of the aeration system in aerobic section of Conventional Activated Sludge (CAS) systems, which constitute one of the higher features of the overall WWTP energy consumption. In fact, oxygen supply accounts for more than 55 % in average and can reach up to 80 % of the energy demand in WWTPs (Jonasson, 2007). In the perspective of more stringent law limits of nitrogen content in the final effluent, the nitrification process is a crucial step in CAS systems due to the adopted operational conditions, and Dissolved Oxygen (DO) set-points. Nitrifiers have lower growth kinetics and lower affinity for oxygen compared to heterotrophic biomass: this causes the need for higher DO concentration and higher Sludge Retention Time (SRT) in order to ensure a sufficient ammonia oxidation rate. In the last decades, control strategies for reducing the energy consumption related to oxygen supply evolved in parallel with the state of the art of sensors and monitoring



techniques (Olsson, 2012). In recent years phosphate, nitrate and ammonia sensors became available on the market and especially ammonia probe showed high potential for energy savings; however, ammonia probes are either slow, expensive, not accurate and, above all, suffering from several chemical interferences that limit their application to domestic WWTPs. At the same time, monitoring instruments for biological activity estimation, as respirometers and titrimeters, that use DO and pH probes on activated sludge sampled from WWTP in controlled conditions, were regarded with a great interest, (Gernaey et al., 2006). These instruments allow the measurement of oxygen uptake rate (OUR) and alkalinity production (or consumption) and can be used for the estimation of kinetics and stoichiometry parameters of the involved processes. The applicability of set-point titration for monitoring biological processes has been widely demonstrated in the literature. The application of DO-pH set-point titration may produce innovative data set, different from those obtained from standard WWTPs efficiency monitoring activity, that can be used for the estimation of AOB kinetic parameters. When applied in continuous conditions they can also provide important information about the nitrification process evolution also in industrial WWTPs. Based on published and on-going experiences, a full-scale on-line differential titrimer has been specifically developed and installed at the industrial Cuoiodepur WWTP (San Romano - Pisa, Italy) treating vegetable tannery wastewater characterized by high salinity, COD and nitrification inhibiting compounds (tannins) loads. In this work, the titrimer was used in order to continuously monitor the nitrification process efficiency and to produce an innovative data set used for biological WWTP model calibration.

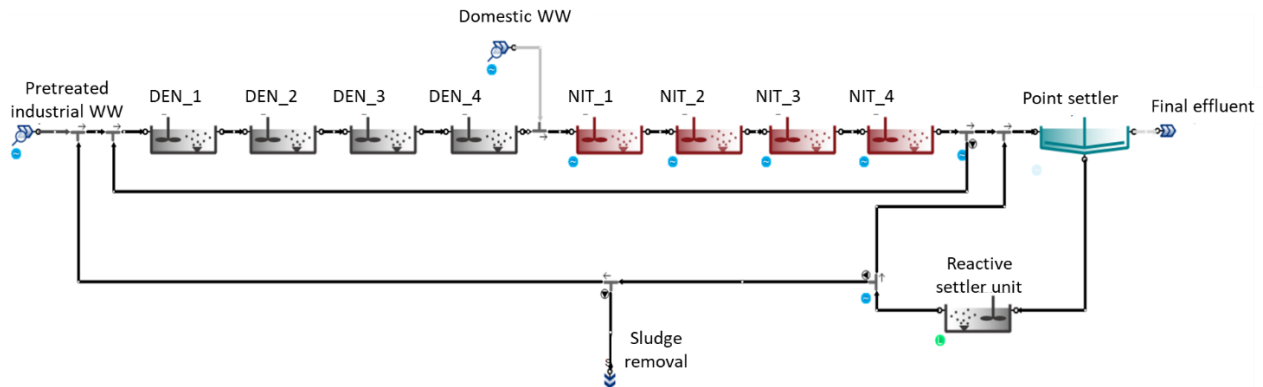
## MATERIALS AND METHODS

A schematic of the instrument is reported in Figure 1, the titrimer is composed by two identical jacked reactors of 2 L of effective volume (R1 and R2), each of them equipped with pH (Metter, Toledo, USA), LDO (Metter, Toledo, USA) and temperature probes (Metter, Toledo, USA). Operational conditions in the reactors are: 1) Hydraulic Retention Time (HRT) in the reactors is maintained at 1 h, by continuously dosing the mixed liquor (ML) from the WWTP aerobic tank through peristaltic pumps; 2) not limiting conditions for nitrifiers growth for what concern ammonia and oxygen concentration are guaranteed by the continuous dosing of ammonia and the controlled dosing of  $H_2O_2$ ; 3) the temperature is maintained equal to the temperature of real plant mixed liquor through a thermostat; 4) pH is controlled at given values identical in both reactors (within the range 7 to 8.5) and set according to the pH in the aerobic tank of the real scale plant; 5) mixing in both reactors is continuous and ensured by mechanical mixers. AOB activity is inhibited in R1, through continuous allylthiourea (ATU) dosing, while in R2 not-inhibited conditions for AOB are maintained. The difference (differential titrimer) between NaOH dosing of NaOH in R1 and R2 allows to estimate the maximum ammonia oxidation rate ( $AOR_{MAX}$ ).



**Figure 1.** Schematic of differential titrimer installed at Cuoiodepur WWTP

The biological section of the Cuioidepur WWTP, treating 55 % of tannery wastewater (previously treated by means of pre-treatments, sulphide oxidation and primary settling) and 45 % of raw domestic wastewater, is composed by a 11.000 m<sup>3</sup> pre-denitrification and a 26.000 m<sup>3</sup> oxydation-nitrification sections. Three settlers with a total surface of 1.000 m<sup>2</sup> (volume 4500 m<sup>3</sup>) were used for solid separation. Oxidation-nitrification section is divided into seven plug-flow tanks (51 m length, 12.5 m width) working in parallel. Am SRT higher than 90 days is maintained in order to obtain complete nitrification also in presence of inhibiting compounds (Munz et al., 2009; Munz et al., 2008a) while a DO set-point of 2.2 mg DO L<sup>-1</sup> is controlled at the end of each aerobic plug-flow. The plant efficiency was simulated using SUMO© (Dynamita, Denmark) software and the applied layout is reported in Figure 2.



**Figure 2.** Cuioidepur WWTP layout used in SUMO© software

Industrial wastewater undergoes to equalization, sulphide oxidation and primary settling before entering the biological section. Internal recycles, as the supernatant originated from sludge thickening and sludge dewatering, are recirculated in the equalization-sulphide oxidation tank and are considered in the primary settler effluent (pre-treated industrial wastewater).

Referring to the results of a three years monitoring activity, average pre-treated industrial wastewater flow ( $Q_{ind}$ ) of  $6540 \pm 640$  m<sup>3</sup> d<sup>-1</sup> and domestic wastewater flow ( $Q_{dom}$ ) of  $3400 \pm 630$  m<sup>3</sup> d<sup>-1</sup> were applied. Average COD and Ammonia concentration are  $5450 \pm 1130$  mg COD L<sup>-1</sup>,  $323 \pm 22$  mg N-NH<sub>4</sub><sup>+</sup> L<sup>-1</sup> and  $195 \pm 95$  mg COD L<sup>-1</sup>,  $23 \pm 7$  mg NH<sub>4</sub><sup>+</sup> L<sup>-1</sup> for pre-treated industrial and domestic wastewater, respectively. Their variations were considered using monthly average data as input.

In order to adequately represent the complexity of tannery wastewaters, five COD fractions (including slowly hydrolysable fraction  $S_H$ ), instead of four characterizing the Activated Sludge Model (ASM) proposed by IWA (International Water Association) and applied to domestic wastewater, were considered. COD fractioning was defined using chemical/physical criteria and respirometric techniques as reported by Munz et al., 2008b.

According to monitoring data, nitrate recirculation flow and sludge recirculation flow are 6 and 4 times the  $Q_{ind}$ , respectively. An SRT of about 100 days was applied.

Both denitrification and nitrification sections were simulated as Continuous-flow Stirred-Tank Reactor (CSTR) cascades and DO varies from a tank to another due to DO variation along the flow verified trough experimental tests using a DO portable probe (Hach Lange, Germany). The applied DO concentration were 0.6, 1.6, 2.2, 2.2 mg L<sup>-1</sup> for NIT\_1, NIT\_2, NIT\_3 and NIT\_4, respectively. The secondary settler was considered as a reactive tank and simulated by a point-settler tank and an anoxic reactor, with a volume equal to 0.8 times the real settler volume, fed with settled sludge. A high recycle rate (10 times the  $Q_{ind}$ ) was applied between point settler and reactive settler unit.

Due to the high sulphide concentration in the pre-treated industrial wastewater, a model that take into account sulphur cycle (including autotrophic denitrification in anoxic conditions) was adopted (SUMO 2S; Hauduc et al., 2017). The model, based on ASM1 (Henze et al., 2010) and characterized by a two-steps nitrification process, was modified in order to be applied to high SRT systems where volatile suspended solids (VSS) and total suspended solids (TSS) concentration are often overestimated applying conventional ASM models (Lubello et al., 2009):

- $X_U$  (Slowly biodegradable particulate COD) conversion

In conventional ASM models, slowly biodegradable particulate COD ( $X_U$ ) is not involved in any degradation process and is removed through solid separation and sludge removal. Lubello et al. (2009) demonstrates that high SRT ( $SRT > 30$  d) promotes  $X_U$  hydrolysis in other fractions, conventionally included in not biodegradable particulate COD. In the proposed model,  $X_U$  is converted in biodegradable particulate COD ( $X_B$ ) following a very low rate first order reaction respect to  $X_U$  concentration ( $K_{dis} = 0.014$ ).

- $X_I$  (Not biodegradable particulate COD) hydrolysis

As proposed for  $X_U$ , also  $X_I$  (Not biodegradable particulate COD) is process in high SRT systems. In that case,  $X_I$  is directly converted into soluble component according to a first order reaction respect to  $X_I$  concentration ( $K_{hyd\_XI} = 0.016$ ).

The proposed hydrolysis processes are reported in Table 1.

**Table 1.** New proposed process description

Process	$S_B$	$S_I$	$X_u$	$X_{ch}$	$X_I$	$X_c$	decay	Kinetic expressions
$X_u$ conversion	1	-1			$f_{XI\_XC}$			$k_{dis} X_U$
$X_I$ hydrolysis		1			-1			$k_{hyd\_XI} X_I$

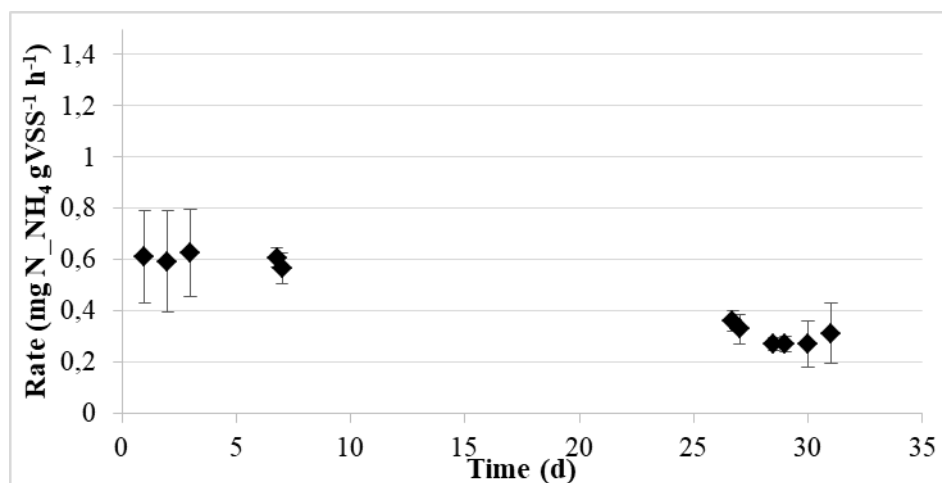
The whole Gujer matrix and parameter values as implemented in Sumo© can be found as supplementary material at the following link: <http://www.dynamita.com/wp-content/uploads/Sumo2S.xlsm>.

## RESULTS AND CONCLUSIONS

After the instrumentation set-up and its functionality verification, the titrimeter was used for specific tests and to monitor the  $AOR_{MAX}$  of AOB biomass of the Cuoiodepurmixed liquor. Experimental  $AOR_{MAX}$  values, provided by the titrimeter, varied in time according to some fundamental operational and environmental conditions as temperature, inhibiting compounds influent loads (tannins), and salinity.

The titrimeter allows to obtain  $AOR_{MAX}$  values every 15 minutes. Each values was than considered as specific (referring to actual SSV concentration) and was referred to a temperature of 20 °C through the application of the Arrhenius' law ( $\theta_{AOR,MAX} = 1.07$ ).

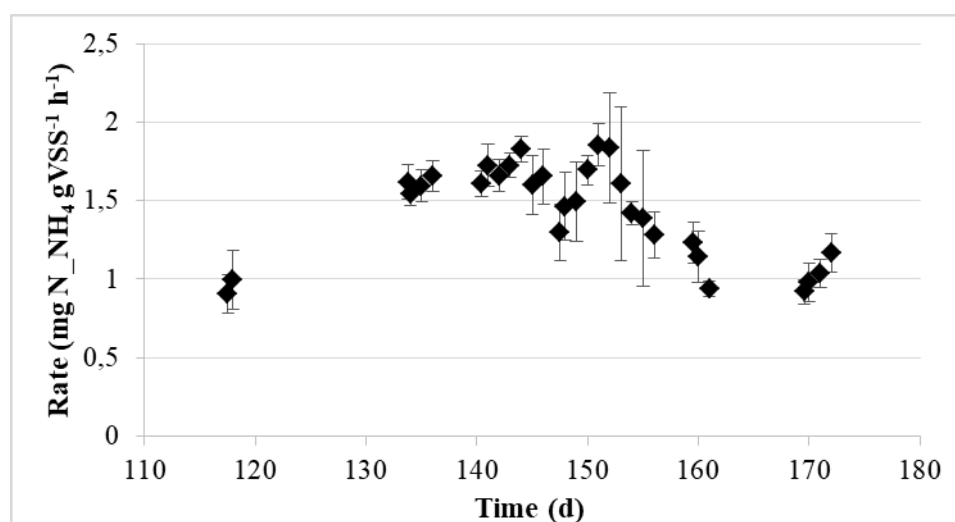
As reported in Figure 3, the specific  $AOR_{MAX}$  decreases during Christmas' holiday in December 2018 (day 0 was 12<sup>th</sup> of December) reaching values that are 50 % lower to those obtained at the beginning of the experimentation. During this period the tanneries were closed and the synergetic effects of the drop in salinity content and of the change in influent wastewater characteristics (only domestic wastewater entered the plant) causes  $AOR_{MAX}$  decrease (from 0.6 mg  $N_{NH_4}$  gVSS<sup>-1</sup> h<sup>-1</sup> to 0.3 mg  $N_{NH_4}$  gVSS<sup>-1</sup> h<sup>-1</sup>). VSS were approximately 8400 mg L<sup>-1</sup> in December and 7700 mg L<sup>-1</sup> in January, the operating temperature was 21°C in the titrimeter and in the oxidation tank.



**Figure 3.** Specific  $N_{NH_4}$  removal rate at 20 °C (December 2018 – January 2019)

In Figure 4 is shown specific  $AOR_{MAX}$  from the end of April 2019 until June 2019. In this period,  $AOR_{MAX}$  reached almost  $1.9 \text{ mg } N_{NH_4} \text{ gVSS}^{-1} \text{ h}^{-1}$  due to the favourable conditions and the higher temperature (average 28 °C). This long period of stable conditions was used as a source of reliable data for the model calibration.

In order to validate the  $AOR_{MAX}$  values provided from the titrimeter, the ammonia oxidation rate within the titrimeter was estimated through an ammonia mass balance. As reported in Table 2 the difference between obtained  $AOR_{MAX}$  and ammonia oxidation rates were very low, and the titrimeter can be considered as an affordable nitrification process probe.



**Figure 4.** Specific  $N_{NH_4}$  removal rate at 20°C (April 2019 – June 2019)

**Table 2.**  $N_{NH_4}$  removal rate calculated from ammonium measurements and from titrimeter

	$N_{NH_4}$ removal rate from mass balance $\text{mg } N_{NH_4} \text{ h}^{-1}$	$N_{NH_4}$ removal rate from titrimeter $\text{mg } N_{NH_4} \text{ h}^{-1}$	<b>difference %</b>
14-12-2018	11.7	12.5	6.4
08-03-2019	25.2	24.1	0.5
11-03-2019	20.3	22.0	7.7
03-05-2019	45.7	46.3	1.3
29-05-2019	35.5	35.62	0.3

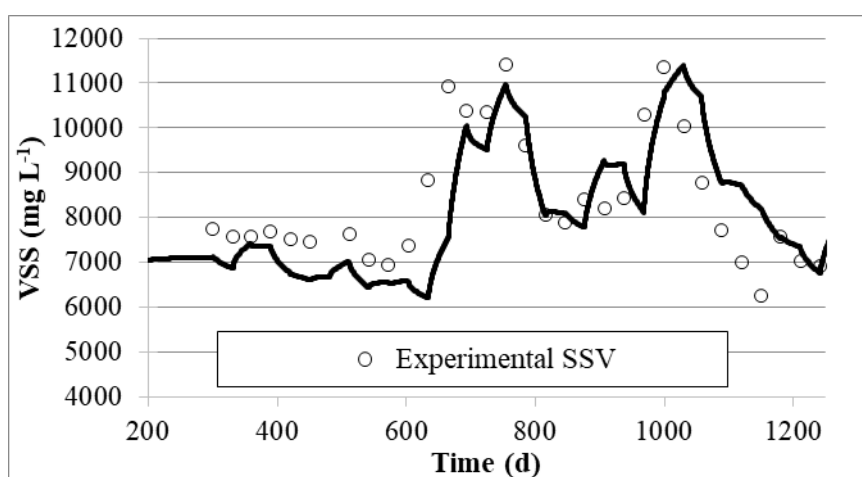
The titrimeter output ( $AOR_{MAX}$ ) was used as a new data-set in order to calibrate the maximum specific growth rate of AOB Biomass ( $\mu_{max,AOB}$ ). In detail, model calibration was conducted using average  $AOR_{MAX}$  data obtained during December 2018 and April/May 2019. Those periods are characterized by different sludge temperature that reflects in different nitrifying biomass activity rates. January, February and March 2019 data were not considered, since important modifications of differential titrimeter hardware and software have been conducted and  $AOR_{MAX}$  data set was not considered as enough consistent. Moreover, real scale WWTP efficiency and operation are deeply influenced by the industrial activity restart after winter vacations and nitrification activity is not stable.

Experimental and modelled  $AOR_{MAX}$  after  $\mu_{max,AOB}$  calibration are reported in Table 3.

**Table 3.** Experimental and Modelled  $AOR_{MAX}$  after model calibration

Period	Avg. Exp. $AOR_{MAX}$	Avg. Exp. VSS	Modelled $AOR_{MAX}$	Modelled VSS	Temp
	( $mgN\ gVSS^{-1}\ h^{-1}$ )	( $mgVSS\ L^{-1}$ )	( $mgN\ gVSS^{-1}\ h^{-1}$ )	( $mgVSS\ L^{-1}$ )	( $^{\circ}C$ )
Dec 2018	$0.65 \pm 4\%$	$8500 \pm 4\%$	0.67	8430	$22 \pm 4\%$
Apr 2019	$2.53 \pm 3\%$	$8660 \pm 5\%$	2.63	8330	$26.8 \pm 1\%$
May 2019	$2.38 \pm 16\%$	$8780 \pm 6\%$	2.54	8770	$27.7 \pm 5\%$

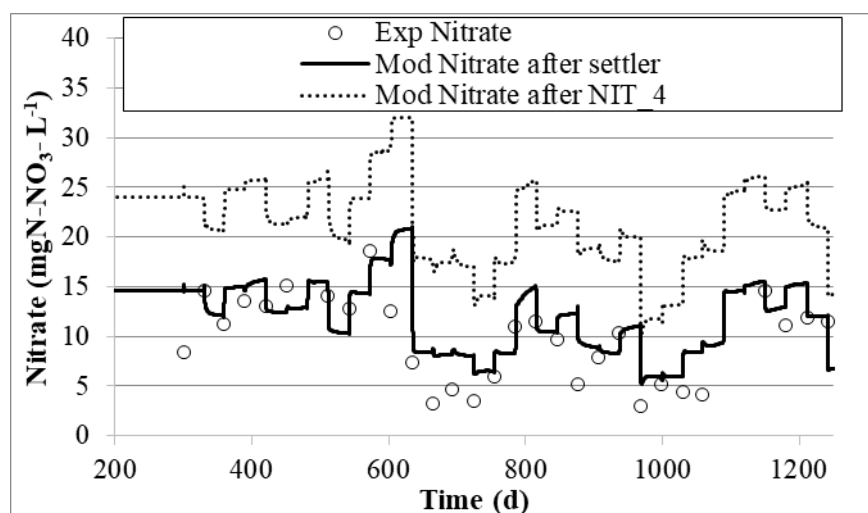
A calibrated  $\mu_{max,AOB}$  value of  $0.58\ d^{-1}$  was obtained. Calibrated model was then validated using monthly average real scale plant monitoring data obtained during years 2015-2016-2017. The obtained VSS concentration in process tanks and effluent nitrate concentration ( $N-NO_3^-$ ) were reported in Figure 5 and 6, respectively.



**Figure 5.** Experimental and modelled VSS trend (years 2015/2017)

The model is able to well describe VSS trend even in winter periods of the years 2016 (from 600 to 800 d) and 2017 (from 950 to 1100 d) in which, due to malfunctions on the sludge treatment line, sludge extraction was drastically reduced.

Modelled nitrification results complete as obtained from the monitoring of aerobic section effluent ammonia concentration. However,  $N-NH_4^+$  concentration after secondary settler is higher and equal to  $1.5 \pm 10\% \ mg\ N-NH_4^+ \ L^{-1}$ . Moreover, after biological section, modelled nitrate concentration results higher than the experimental ones (dotted line in Figure 6) measured on the clarifier effluent. The introduction of a reactive settler solved both the problems and modelled nitrate effluent concentration (continue line in Figure 6) fits with experimental data.



**Figure 6.** Experimental and modelled  $\text{N-NO}_3^-$  trend (years 2015/2017)

In conclusion, the obtained experimental data confirm the possibility to use the differential on-line titrimeter as an affordable process probe. The calibrated model well describes nitrification process efficiency of the Cuoiodepur WWTP. In this context the possibility to synergistically use titrimeter output and plant model to predict the nitrification process performance and support ICA is confirmed.

#### ACKNOWLEDGEMENT

The authors thank Tuscany Region and EU that support the I-SWAT (FESR 2014 -2020) project.

#### REFERENCES

- Gernaey, A. K., Petersen, B., Ottoy, J.-P., Vanrolleghem, P. (2001) Activated sludge monitoring with combined respirometric–titrimetric measurements. *Water Research*, **35**, 1280-1294.
- Hauduc, H., Johnson, B., Bott, C., Ward, M., Takacs, I. (2017) Incorporating sulphur and relevant reactions into a general plantwide and sewer model. *IFAC PapersOnLine*, **50**, 3935-3940.
- Henze, M., Gujer, W., Mino, T., van Loosdrecht, M. C. M. (2000) Activated Sludge Models ASM1, ASM2, ASM2d and ASM3. Scientific and Technical Report No.9, IWA Publishing.
- Jonasson, M. (2007) Energy Benchmark for Wastewater Treatment Processes - a comparison between Sweden and Austria, PhD Thesis, Lund University, Lund, Sweden.
- Lubello, C., Caffaz, S., Gori, R., Munz G. (2009) A modified Activated Sludge Model to estimate solids production at low and high solids retention time. *Water Research*, **43**, 4539-4548.
- Munz, G., Mori, G., Salvadori, L., Barberio, C., Lubello, C. (2008a) Process efficiency and microbial monitoring in MBR (membrane bioreactor) and CASP (conventional activated sludge process) treatment of tannery wastewaters. *Bioresource Technology*, **99**, 8559-8564.
- Munz, G., Gori, R., Cammilli, L., Lubello C. (2008b) Characterization of tannery wastewater and biomass in a membrane bioreactor using respirometric analysis. *Bioresource Technology*, **99**, 8612-8618.
- Munz, G., De Angelis, D., Gori, R., Mori, G, Casarci, M., Lubello C. (2009) The role of tannins in conventional and membrane treatment of tannery wastewaters. *Journal of Hazardous Material*, **164**, 733-739.
- Olsson, G. (2012) ICA and me e A subjective review. *Water research*, **46**, 1585-1624.

# Purification of Emulsified Oil by Polyvinylidene Fluoride/Polyvinylpyrrolidone Membrane

F. U. Nigiz\*, A. I. Yucak and N. D. Hilmioglu

\* Department of Chemical Engineering, Univerasity of Kocaeli, 41380, Kocaeli, Turkey  
(E-mail: *filiz.ugurr@gmail.com*)

## Abstract

In this study, a Bentonite clay incorporated polyvinylfluoride(PVDF) and polyvinyl pyrrolidone(PVP) based adsorbent membrane was produced for the selective separation of oils from simulated wastewater. This membrane was produced as an intelligent material that selectively separates emulsified oils from water when it is used as adsorbents and purifies water when it is used in continuous membrane filtration. The affinity of the membrane to oil components was determined by water-oil uptake tests. The uptake experiments were conducted for soybean oil, hazelnut oil, lubricant oil and other volatile oils. As a result, membranes absorbed greater than 200wt.% of oil when the membranes were immersed in the soybean oil, hazelnut oil and lubricant oil. When the same membranes were used for continuous filtration, greater than 85 % of oil rejection values were obtained. As the PVP ratio in the membrane increased, flux values enhanced gradually. Bentonite incorporation simultaneously improved flux values and oil rejection remarkably. The soybean rejection increased from 69.15 % to 95 %, hazelnut oil rejection increased from 87 % to 99.98 %, and lubricant oil rejection enhanced from 80.5 % to 97.5 % when the bentonite amount was increased from 0wt.% to 15wt.%.

## Keywords

Adsorbent membrane; polyvinylfluoride; oil removal

## INTRODUCTION

Water is one of the most valuable substances in the world. No living thing, including animals and plants, can lead a life without water (He at al., 2019). Due to the increasing population, water use in the environment and industry is also increasing significantly. Pollution of existing freshwater resources increases the importance of water-saving policy (Nthunya et al., 2019; Doshi et al., 2018). Therefore, the importance of sustainable water science such as wastewater treatment, potable water production from non-potable water resources, waste disposal technology has become crucial.

Industrial wastewater contains many hazardous substances. Many harmful components such as plastic residues, toxic components, heavy metals, volatile organic components, and oil extracts are released from the wastewater of industrial plant and discharging to the natural resources such as seawater. The oil-based components are found in the wastewater of food, pharmaceutical, polymer, automotive, electronics, and petrochemical industries. Many types of oil species can be found in water sources. Besides to the petroleum-derived oils such as lubricating oils, engine oils, diesel, vegetable-derived oils are also found in the effluent of different industries. These kinds of oils are occurred by extracting of different plant seeds or fruits such as soybean and hazelnuts. In general, vegetable oils are used in the food industry. Moreover, soybean and hazelnut oil are used in biodiesel production as a waste vegetable oil (Celikten et al., 2012). The amount of oils in wastewater increases in line with the usage areas of oils in industry and daily life. One liter of waste oil contaminates one million liters of water. Hence the oil separation from water is attracting attention for the environmental-chemical scientist. Depending on the lower density of oil compared to water, the oil-based molecules accumulate on the water surface (Barron, 2012). In addition to the industrial waste discharging, oil species spill from the defected pipes of petrochemical plants or sea

vessel (Brody et al., 2010; Cui et al., 2018).

There are many techniques to separate oils from waters (Droste and Gehr, 2018). The diversity of these techniques is varied according to the structure of oils (emulsified or not, and drop size) and the area where oils are emitted. For example, oils spilled by a petroleum accident can be removed by in situ separation techniques such as adsorption and chemical methods. Biological, electrochemical treatment, coagulation, flocculation, vacuum evaporation, absorption, precipitation, and membrane filtration techniques are used for the treatment of emulsified oil from water. The most preferred methods are adsorption and membrane separation.

The membrane is defined as a barrier that selectively separates the two phases and allows controlled passage of the target component (Kamali et al., 2019; Eykens et al., 2017). Membrane technology is known as a promising method for the treatment of oil-based wastewater due to the appropriate pore size. Especially for the removal of emulsified oil droplets, the purification is carried out without any de-emulsification process (Ang et al., 2015). Recently, the studies on the separation of oil-based compounds have been performed by means of the low-cost polymeric membrane having high oil absorption capacity and good oil-water selectivity (Eykens et al., 2012). Microfiltration, ultrafiltration, nanofiltration techniques are mostly used to remove oil from water (Hoslett et al., 2018). The selection of the appropriate technique is characterized according to the concentration of the oil in water, the type of the treated water, and the operating parameters. Each of these techniques is categorized according to the pore size of the membrane and trans-membrane pressure. The membrane-based separation has important advantages such as low energy consumption, high separation efficiency. Compared to the adsorption technique, membrane separation can be conducted continuously.

In this study, poly(vinylidene fluoride) (PVDF)/Polyvinylpyrrolidone (PVP) blend membranes have been produced by the phase inversion method for separation of oil-emulsion water mixtures. Poly(vinylidene fluoride) is a hydrophobic polymer which is used in membrane separation processes due to its superior mechanical strength, heat resistance, chemical resistance and good film formation capability (Kang and Cao, 2014). Polyvinylpyrrolidone acts as a pore-forming polymer in membrane preparation by phase inversion (Amin et al., 2018). PVP content in the membrane influences the surface morphology of the blend membrane. In our study, the membrane has been characterized as an oil adsorbent membrane. The membrane can be used to adsorb oil from water in case the membrane is used in the batch adsorption process. The membrane is also appropriate to remove water when it is used in the continuous water separation process. Therefore, both the adsorption and separation characters of membranes have been determined using uptake and filtration experiments. The amount of PVP directly affects the separation process due to the hydrophilic character of PVP. In order to enhance the flux and oil rejection of membranes, the varying amount of Bentonite clay has also been used as filler in the membrane matrix.

## **MATERIALS and METHODS**

### **Membrane preparation**

Blend membranes were prepared using the phase inversion technique. A certain amount of PVDF was dissolved in dimethylformamide (DMF) solvent with a concentration of 10 wt.% PVDF in DMF. PVP was also added to the polymer-DMF solution. The blend membrane solution was homogeneously mixed at 55 °C for four hours. The mixture was allowed to remove bubbles at room temperature for 24 hours. The mixture was poured on a glass surface and a casting knife was used to homogeneously disperse the mixture. Then, the glass plate was immersed in a water bath. The PVDF/PVP weight ratios were varied as 90/10, 80/20, 70/30, 60/40. Membranes were titled



according to the ratio of polymers. For example, the membrane containing 90wt.% of PVDF and 10wt.% of PVP was entitled as PVDF90-PVP10.

For the preparation of Bentonite incorporated membranes, a polymer solution containing 80wt.% PVDF and 20 wt.% of PVP was firstly prepared. The determined amount of Bentonite clay (concentration varied from 0wt.% to 15wt.% according to the total weight of PVDF and PVP) was added to the polymer solution and stirred at the room temperature for four hours. The mixture was poured on a glass surface and a casting knife was used to homogeneously disperse the mixture. Then, the glass plate was immersed in a water bath.

### Membrane characterization

The surface hydrophobicity of the membrane was characterized using Contact Angle Measurements (KSV). The angle measurements were done by measuring the angle between the water droplets and the membrane surface. Each test was repeated for three times and the average angle values were recorded. The chemical structure of the membrane was analyzed by using Fourier Transform Infrared Spectroscopy (Perkin Elmer, ATR mode). The wavelength of the Spectroscopy was arranged between 650-4000  $\text{cm}^{-1}$ .

### Oil/Water Uptake

The effect of polymer concentration and clay incorporation on membrane-oil affinity were determined by means of uptake experiments. In order to determine the oil-water uptake capacity of different membranes, the membrane samples were immersed in water, soybean, hazelnut (nut), lubricating oils and volatile oils such as benzene, hexane, and toluene. The uptake experiments were carried out for 90 minutes until the samples reached a constant weight. The uptake measurements were done by measuring the initial ( $W_i$ ) and final ( $W_f$ ) weight values of the membrane as shown in Equation 1.

$$\text{Uptake (\%)} = \frac{W_f - W_i}{W_i} * 100, \quad (1)$$

### Filtration test

Filtration test was carried out in a vacuum filtration test unit. The experiments were carried out at the room temperature by using 1wt.% of oil-containing water solution. Before the experiments, the oil-water solution was sonicated for three hours and a milky-like color was obtained. The prepared membranes were settled on a porous glass support and the oil/water solution was fed onto the prepared membrane. 670 mmHg vacuum was applied at the room temperature. The oil concentration of the permeate and the retained solution was determined by means of UV/Visible spectrometer at the optimum wavelength of 420 nm. The filtration and separation performance of membranes were evaluated as a function of flux ( $F$ )(g/min.A) and oil rejection ( $R$ )(%) as shown at following Equation (2) and Equation (3).

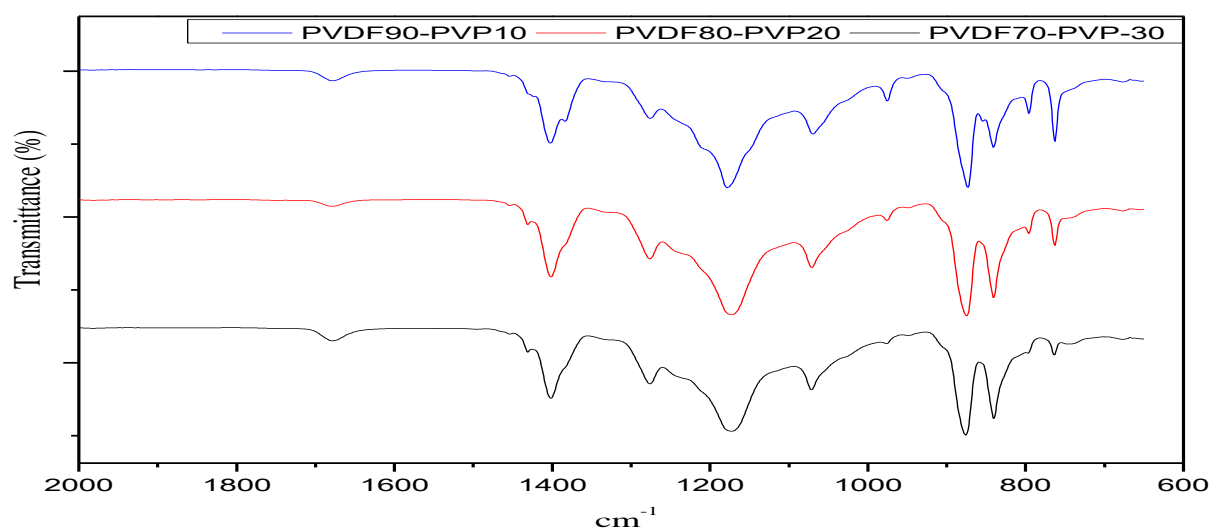
$$F = \frac{M}{t.A} \quad (2)$$

$$R(\%) = \frac{C_f - C_p}{C_p} * 100 \quad (3)$$

where  $M$  (g) is the weight of permeate water on downstream side of the membrane,  $t$  is the filtration time (min),  $A$  is the effective membrane area.  $C_f$  and  $C_i$  are the concentration of oil-water solution at feed and permeate side, respectively.

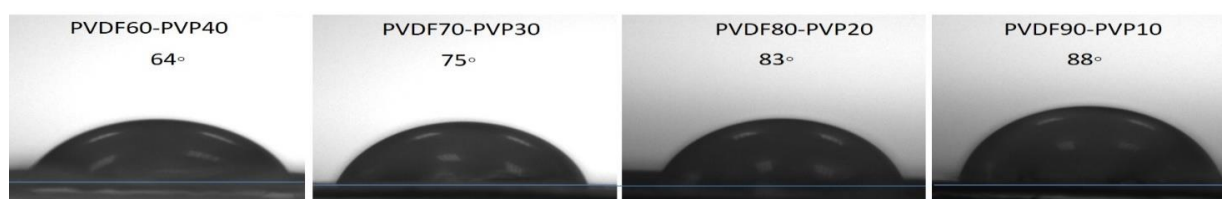
## RESULTS AND DISCUSSION

In the present study, PVDF and PVP blend membranes were prepared, characterized and used for removal of oil from simulated oil-water mixtures. The chemical structure of the produced membranes was determined using FTIR analysis. Figure 1 shows the FTIR spectra of membranes having different PVDF/PVP ratio. Peaks at  $1680\text{ cm}^{-1}$  are assigned to the carbonyl stretching in membranes. The characteristic  $-\text{CH}_2-$  deformation peaks reveal at  $1400\text{ cm}^{-1}$ . the peaks from  $760\text{ cm}^{-1}$  to  $1190\text{ cm}^{-1}$  are corresponding to CF and  $\text{CF}_2$  stretching. The intensity of CF based peaks decreased due to the PVP addition.



**Figure 1.** FTIR spectra of membranes

The surface hydrophobicity of the membranes was determined using contact angle measurements. The contact angle of the surface decreased as the PVDF ratio in membrane increased. This is due to the hydrophobic character of the PVDF. It is also related to the hydrophilicity of PVP. Moreover, during the phase inversion process, the porosity of the membrane increased by increasing PVP ratio. Thus, the water penetration on the surface of the membrane increased as expected.



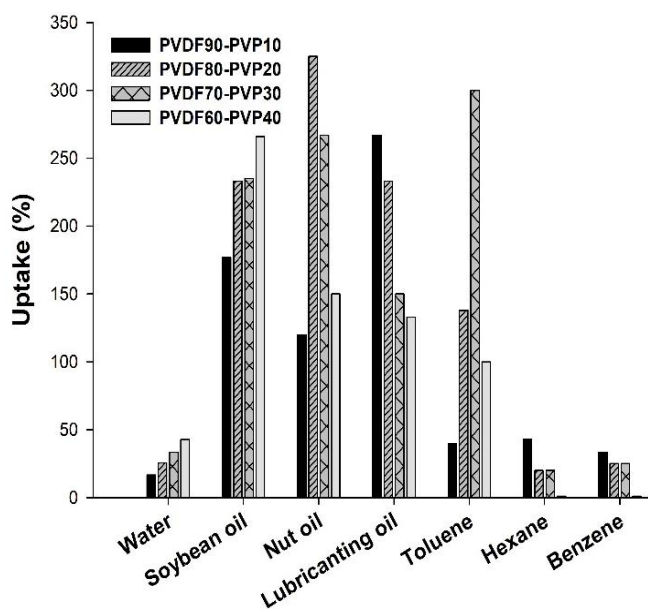
**Figure 2.** Contact angle of membranes with water droplets

In this study, the affinity of PVDF/PVP membranes to oils and water were investigated. The produced membrane is expected to absorb oils when used as adsorbent membranes in batch process and permeate water when it is used in a continuous membrane separation process. While the usability of the adsorbent membrane was determined by swelling tests, the performance of water permeability in continuous separation was determined by filtration tests.

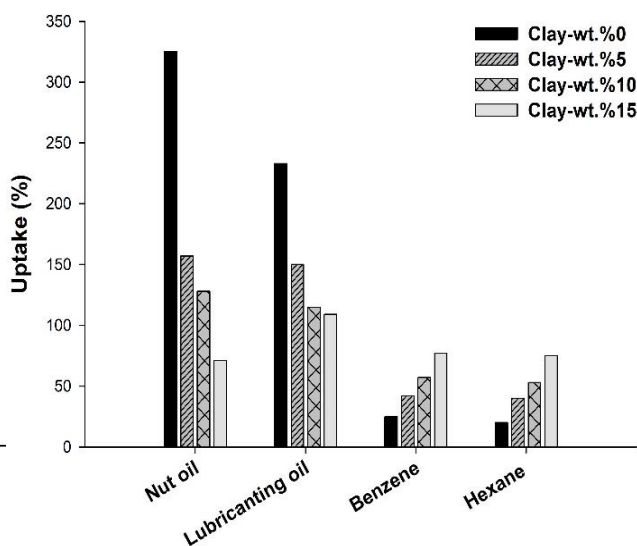
Figure 3 shows the effect of PVDF/PVP concentration and Bentonite concentration on the uptake results. It is clear from the figure that the oil uptake capacity of the membrane enhanced with the increasing amount of PVP in the PVDF matrix. This is due to the hydrophilic structure of the PVP polymer (Kao et al., 2003). PVP is a water-soluble hydrophilic and polar polymer. Therefore, it is expected that water uptake capacities will increase as PVP ratio increases in the matrix. The figure shows that the higher uptake capacity was obtained when the membranes immersed in soybean oil, hazelnut oil, and lubricating oil. As the PVP ratio increased in the membrane, soybean oil uptake

values enhanced. The highest uptake value of 266wt.% was obtained when the PVDF ratio was kept at 60 %. Compared to the water and soybean, the hazelnut oil uptake showed a variable trend. The highest uptake value was calculated as 325wt.% when the PVDF concentration in the membrane was 80 %. Therefore, it can be evaluated that the 80 % of PVDF polymer ratio is more appropriate in case the membrane will be used for the adsorbent. In Figure 3, the increasing PVP ratio in the PVDF matrix decreased the lubricant oil uptake results. The highest lubricant oil uptake of 267wt.% was obtained with the membrane having 90wt.% of PVDF concentration. The figure also illustrates the uptake results of petrochemical-based volatile oil species such as benzene, toluene, and hexane. These oil-like compounds have a uniform molecular structure and smaller molecular size than other oils such as lubricant, hazelnut, and soybean. As shown in Figure 3, the affinity of benzene and hexane to the membrane was lower compared to toluene. The increasing PVP ratio in matrix enhanced the toluene uptake up to 30wt.%. PVDF70-PVP30 membrane showed the highest uptake results of 301wt.% for toluene.

In Figure 4, the effect of Bentonite clay incorporation on oil uptake was also investigated when the PVDF ratio was kept constant at 80wt.%. Bentonite concentration was changed from 0wt.% to 15wt.% according to the total polymer weight. It is clear from Figure 4 that the clay addition has a positive effect on benzene and hexane uptake and has a negative effect on nut and lubricant oil uptake results. Due to the fact that the oil swelling capacity of the polymeric structure was higher than that of clay, the uptake values decreased as Bentonite content increased in the membrane. However, the swelling values of volatile oil-like compounds which have small molecule (benzene and hexane) appeared to enhance with increasing amount of the clay. When the amount of Bentonite increased from 0 % to 15 %, the uptake results of the membrane immersed in benzene and hexane enhanced from 25wt.% to 77wt.% and from 20wt.% to 75wt.%, respectively.



**Figure 3.** Effect of PVDF/PVP ratio on uptake

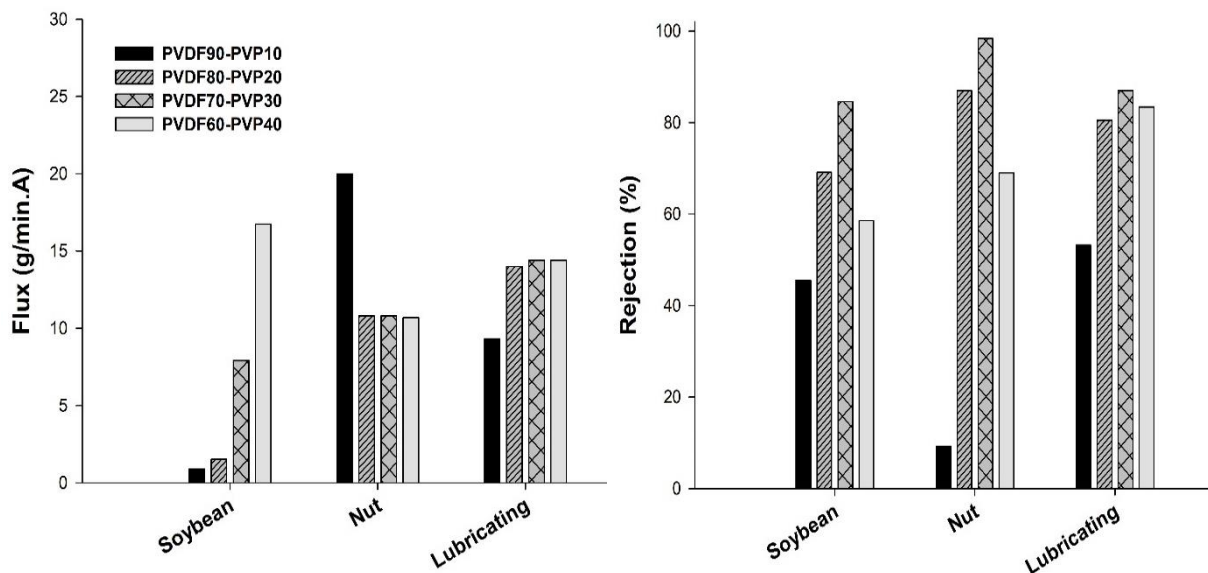


**Figure 4.** Effect of clay content on uptake

Unlike the uptake tests, membrane filtration experiments were performed with non-volatile oil materials having large molecule sizes. Figure 5 shows the effect of PVDF/PVP ratio on flux and rejection. In the case of the soybean oil, the increasing PVP ratio enhanced the flux remarkably. The water flux for 1wt.% of soybean oil content water solution enhanced from 0.89 g/min.A to 16.7 g/min.A when the PVP ratio increased from 10 wt.% to 40 wt.%. The flux was improved almost 15 times without rejection loss. Soybean oil rejection also increased from 45.5 % to 84.6 % with increasing PVP concentration up to 30wt.%. However, the rejection drastically decreased when the

PVP concentration was 40wt.%. This should be related to the increasing porous structure of the membrane with an increasing amount of PVP. In the literature, PVP polymer is used as a pore-forming agent to enhance the membrane porosity during the phase inversion technique (Amin et al., 2018). Depending on the porous structure, water flow increases with high PVP concentration. However, as the size of the pore enlarges, the oil molecules may be dragged with the water molecules and the oil rejection decreases as also obtained in the present study.

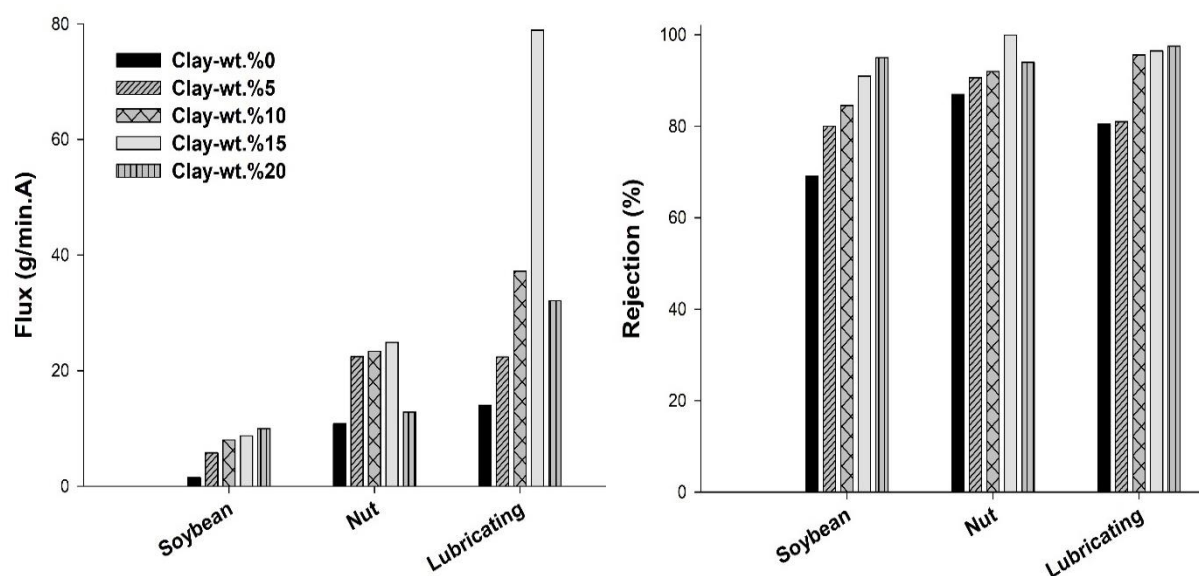
Filtration experiments results of 1wt.% of hazelnut oil including water solution are also represented in Figure 5. As the PVP ratio increased in the matrix, the flux value firstly decreased from 19.9 g/min.A to 10.7 g/min.A and then remained constant. Moreover, the oil rejection values increased from 9.4 % to 98.4 % when the PVDF ratio was decreased from 90wt.% to 70wt.%. In case of the lubricant oil, the flux increased with increasing PVP concentration, then showed a constant trend. For this oil rejection of 87 % was obtained when the PVP ratio was 70 wt.%. In particular, the permeation results showed that 70wt.% and 80wt.% PVDF containing membranes had superior separation performance for removing oil species from the simulated waste water. Oil rejection results were lower for 60% PVDF-40% PVP containing membrane due to the increasing porosity. In the case of 90wt% PVDF-10wt.% PVP containing membrane, flux values were the lowest. In order to enhance the flux and rejection simultaneously, Bentonite was added into the membranes.



**Figure 5.** Effect of PVDF-PVP concentration on flux and rejection results

Bentonite has close-packed platelets which consist of tetrahedral–octahedral–tetrahedral layers. These layers compose of metal ions that are responsible for negatively charging of membranes. Bentonite exhibits strong affinity to water and increases the swelling character of the material (Kumar et al., 2015; Kumar et al., 2016). This property may increase the water flux when it is used as a membrane main material or fillers. It was also reported that Bentonite clay is effective to remove oil from water compared to the activated carbon (Moazed and Viraraghavan, 2005). In the literature, several studies have been reported on the use of Bentonite as oil remover (Sun and Chen, 2013; Zheng et al., 2017). Therefore, in the present study, Bentonite was used to increase water flux and to enhance oil rejection, as well. Figure 6 shows the effect of Bentonite content on flux and oil rejection. As shown in the figure, there is a significant increase in the flux values of the membranes with an increasing amount of clay. Soybean oil flux value increased from 1.5 g/min.A to 9.98 g/min.A, hazelnut oil flux enhanced 10.8 g/min.A to 24.9 g/min.A and lubricant oil flux increased from 14 g/min.A to 78.9 g/min.A when the clay concentration increased from 0wt.% to

15wt.% due to the high hydrophilicity of the clay. Flux values decreased when Bentonite concentration exceeded 15wt.% concentration. The reason for the decrement should be attributed to the overloading of clays that causes aggregation and negative effect on separation performance. Therefore, the maximum clay content was determined as 15wt%. In addition to membrane flux, oil rejection values were also positively affected by bentonite incorporation. The soybean rejection increased from 69.15 % to 95 %, hazelnut oil rejection increased from 87 % to 99.98 %, and lubricant oil rejection enhanced from 80.5 % to 97.5 %.



**Figure 6.** Effect of clay concentration on flux and rejection results

## CONCLUSIONS

In this study, PVDF/PVP blend membranes were prepared for the separation of oily components from seawater or wastewater. Bentonite clay was added to the membrane to increase the water flow and enrich the oil rejection. The effect of PVDF concentration, Bentonite content and oil type on separation performance was investigated. PVDF ratio has direct effect on oil uptake capacity, flux and oil rejection. Especially in soybean oil, the flux increased significantly as PVP ratio increased. There was also a significant increase in oil rejection values. The most suitable PVDF ratio was found to be 70wt.% and 80wt.%. When Bentonite was added to the membrane, the separation performance became superior. Soybean oil flux value increased from 1.5 g/min.A to 9.98 g/min.A, hazelnut oil flux enhanced 10.8 g/min.A to 24.9 g/min.A and lubricant oil flux increased from 14 g/min.A to 78.9 g/min.A when the bentonite amount was increased from 0wt.% to 15wt.%. The soybean rejection increased from 69.15 % to 95 %, hazelnut oil rejection increased from 87 % to 99.98 %, and lubricant oil rejection enhanced from 80.5 % to 97.5 %.

## ACKNOWLEDGEMENTS

This work was supported by Kocaeli University Scientific Research Projects Coordination Unit. Project Number 2019/70.

## REFERENCES

- Amin, P. D., Bhanushali, V., Joshi, S. (2018) Role of Polyvinylpyrrolidone in Membrane Technologies. *International Journal of ChemTech Research*, **11**, 247-259.
- Ang, W. L., Mohammad, A.W., Hilal, N., Leo, C.P. (2015) A review on the applicability of



- integrated/ hybrid membrane processes in water treatment and desalination plants. *Desalination* **363**, 2-18.
- Barron, M. G., (2012) Ecological impacts of the deepwater Horizon oil spill: implications for immunotoxicity. *Toxicol. Pathol.*, **40**, 315-320.
- Brody, T. M., Di Bianca, P., Krysa, J. (2010) Analysis of inland crude oil spill threats, vulnerabilities, and emergency response in the midwest United States. *Risk Anal.*, **32**, 1741-1749.
- Celikten, I., Mutlu, E., Solmaz, H. (2012) Variation of performance and emission characteristics of a diesel engine fueled with diesel, rapeseed oil and hazelnut oil methyl ester blend. *Renew Energy*, **48**,122-6.
- Cui, J., Zhou, Z., Xie, A., Meng, M., Cui, Y., Liu, S., Lu, J., Zhou, S., Yan, Y., Dong, H. (2019) Bio-inspired fabrication of superhydrophilic nanocomposite membrane based on surface modification of SiO<sub>2</sub> anchored by polydopamine towards effective oil-water emulsions separation. *Sep Purif Technol*, **209**, 434-442.
- Doshi, B., Mika S., Simo K. (2018) A review of bio-based materials for oil spill treatment. *Water Research*, **135**, 262-277.
- Droste, R. L., Gehr, R. L. (2018) Theory and Practice of Water and Wastewater Treatment, John Wiley & Sons.
- Eykens, L., Sitter, K., Dotremont, C., Pinoy, L., Bruggen, B. (2017) Membrane synthesis for membrane distillation: A review. *Sep Purif Technol.*, **182**, 36-51.
- He, Z., Lyu, Z., Gu Q, Zhang, L., Wang, J. (2019) Ceramic-based membranes for water and wastewater treatment. *Colloids and Surfaces A*, **578**, 123513.
- Hoslett, J., Massara, T. M., Malamis, S., Ahmad, D., Boogaert, I, Katsou, E., Ahmad, B., Ghazal, H., Simons, S., Wrobel, L., Jouhara, H. (2018) Surface water filtration using granular media and membranes: A review. *Science of the Total Environment*, **639**, 1268-1282.
- Kamali, M., Suhas, D. P., Costa, M. E., Capela, I., Aminabhavi, T. M. (2019) Sustainability considerations in membrane-based technologies for industrial effluents treatment. *Chem Eng J*, **368**, 474-494.
- Kang, G., Cao, Y. (2014) Application and modification of poly(vinylidene fluoride)(PVDF) membranes – A review. *Journal of Membrane Science*, **463**, 145-165.
- Kao, C., Lo, T. C., Lee, W. C. (2003) Influence of polyvinylpyrrolidone on the hydrophobic properties of partially porous poly(styrene–divinylbenzene) particles for biological applications. *Journal of Applied Polymer Science*, **87**, 1818-1824.
- Kumar, S., Guria, C., Mandal, A. (2015) Synthesis, characterization and performance studies of polysulfone/bentonite nanoparticles mixed-matrix ultra-filtration membranes using oil field produced water. *Sep Purif Technol.*, **150**, 145-158.
- Kumar, S., Mandal, A., Guria, C. (2016) Synthesis, characterization and performance studies of polysulfone and polysulfone/polymer-grafted bentonite based ultrafiltration membranes for the efficient separation of oil field oily wastewater. *Process Safety and Environmental Protection*, **102**, 214-228.
- Moazed, H., Viraraghavan, T., (2005) Removal of Oil from Water by Bentonite Organoclay. *Practice Periodical of Hazardous, Toxic, and Radioactive Waste Management*, **9**(2): 130-134
- Nthunya, L. N., Gutierrez, L., Lapeire, L., Verbeken. K., Zaouri, N., Nxumalo, E. N., Mamba, B. B., Verliefe, A. R., Mhlang, S. D. (2019) Fouling-resistant PVDF nanofibre membranes for the desalination of brackish water in membrane distillation. *Sep Purif Technol.*, **228**, 115793.
- Sun, T., Chen, D. D. L. (2013) Coagulation of Oil in Water Using Sawdust and Bentonite and the Formation of a Floating Coagulated Material. *J. Environ. Eng.*, **139**,1470-1481.
- Zheng, R., Gao, H., Ren, Z., Cen, D., Chen, Z. (2017) Preparation of activated bentonite and its adsorption behavior on oil-soluble green pigment. *Physicochem.Probl.Miner.Process.*, **53**, 829-845.

# Wastewater Flow Conditions In a Hydroponic Lagoon In Terms of Quality of Treated Sewage

K. Pawęska\*, A. Bawiec\* and J. Baran\*

\* Institute of Environmental Engineering, The Faculty of Environmental Engineering and Geodesy, Wrocław University of Environmental and Life Sciences, Grunwaldzki Square 24, 50-363 Wrocław, Poland  
(E-mails: [katarzyna.paweska@upwr.edu.pl](mailto:katarzyna.paweska@upwr.edu.pl); [aleksandra.bawiec@upwr.edu.pl](mailto:aleksandra.bawiec@upwr.edu.pl); [jeremi.baran@upwr.edu.pl](mailto:jeremi.baran@upwr.edu.pl))

## Abstract

The work deals with the impact of velocity in the hydroponic lagoon used as the 3rd stage of wastewater treatment in the municipal wastewater treatment plant for washing out particles settled on the bottom of the trough to the receiver. In order to analyze the flow velocity in the lagoon, 12 cross-sections were determined at points where the speed and motion of particles can change. Wastewater samples were taken from each of the 12 points, based on which the physicochemical parameters of sewage were determined. In selected cross-sections, a granulometric analysis was carried out to check the extent to which the trough content can be washed out and how the organic slurry moves. Based on the analysis, it was found that velocities in the lagoon during aeration can be ten times higher ( $0.07 \text{ m}\cdot\text{s}^{-1}$ ) than those assumed by designers ( $0.006 \text{ m}\cdot\text{s}^{-1}$ ). The average value of parameters describing the amount of organic matter was: BOD -  $4.83 \text{ g}\cdot\text{m}^{-3}$ , COD -  $57.1 \text{ g}\cdot\text{m}^{-3}$  and total suspended solids  $34.4 \text{ g}\cdot\text{m}^{-3}$ .

## Keywords

Hydroponic lagoon; wastewater velocity; wastewater treatment; granulometric composition of sewage

## INTRODUCTION

Higher and higher standards for the quality of treated wastewater discharged to the receiver become a motivation to look for high-performance technological solutions. There are many dangerous substances in municipal sewage, which introduced into the environment without purification can disrupt the natural balance of receivers (Jin et al., 2017).

One of the extremely important parameters related to the quality of sewage is the organic matter, the presence of which limits, inter alia, the development of bacterial flora, and its content in purified sewage is expressed by indicators such as BOD, COD, TOC and total suspended solids (TSS) (Joshi, 2016). Ensuring appropriate sewage flow rates through the wastewater treatment plant significantly influences the organic matter content along with the sewage stream. The objects imitating natural conditions are becoming increasingly popular, gaining popularity around the world. These include: constructed wetland, sewage pond and hydroponics systems (Maiga et al., 2017).

Solutions of this type are used as the third or fourth stage of treatment not only of polluted water or sewage, but also for contaminated waters from fish ponds (Keeratiurai, 2013). Prevailing conditions in flowing waters (where water flow velocity and oxygenation is important) are most beneficial in terms of self-cleaning processes (Taseiko et al., 2016), therefore, so-called "artificial rivers" are used in wastewater treatment systems, and more specifically hydroponic lagoon with additional water plants supporting the purification process (Gosh and Desai, 2006).

In the hydroponic lagoon, the wastewater movement is mainly caused by the appropriately modeled drop of the trough bottom as well as by the installation and operation of the aerators. Hydroponic lagoon systems provide oxygen necessary for the mineralization of organic matter. In the aeration

conditions of the hydroponic lagoon, after 4 days, a reduction of BOD content by about 30 % can be achieved. In the case of a suspension after 12 hours of sedimentation, 80 % of the organic particles will be located in the sediment (Suryani et al., 2017). Sewage flow in aerated hydroponic lagoon systems should ensure sedimentation of organic matter remaining after previous purification processes without a marked increase in its level at the outflow. The use of aerators without the simultaneous control of the speed of sewage flow, rapid speed increases, the creation of a flow opposite to the assumed direction may lead to the lifting of the previously suspended particles. It is extremely important to control the flow conditions that translate into the expected effects of the hydroponic systems.

As for the movement of solids in aerated lagoons, it can be noticed that due to the rapid increase in velocities caused by aeration and its decreases caused by lagoon arches in such structures, it will be possible to observe localized deposition of particles set in motion by the increased point speed (Wu, 2010).

Velocity in this type of lagoon should allow particles to sink freely to the bottom and allow slow anaerobic decomposition (Suryani et al., 2017). Measurements of the speed of wastewater moving through the lagoon should be carried out regularly and preferably kept constant to ensure adequate flow conditions ensuring time for the treatment processes to take place. Measurements can be made using hydrometric grinders (based on electromagnets or mechanically acting), electromagnetic probes and even Doppler-based devices such as ADCP (USGS, 2010). This is especially important when the lagoon constantly drains purified water to the receiver and can be used, among others, to carry out the assumptions related to determining the volume of wastewater discharged to the receiving water body (Burgos et al., 2015).

The main objective of the research was to assess the conditions of wastewater flow in the hydroponic lagoon in relation to selected quality parameters of treated sewage (BOD, COD, TOC) and particle size distribution of suspended solids. An attempt was also made to determine the sewage flow rate in the lagoon.

## RESEARCH FACILITY

The research was carried out in wastewater treatment plant located in Paczków in the Opolskie Voivodeship (N50.466487, E17.016908). The facility processes sewage supplied by a general sewerage network and transported by slurry tankers. The facility accepts an average of 1350 m<sup>3</sup> of sewage per day. The receiver of treated wastewater is Nysa Kłodzka. The mechanical and biological treatment plant was equipped with the so-called "artificial river" - the hydroponic lagoon. The length of the lagoon is 190 m, the depth of the trough is 1.4 m and its active capacity is 530 m<sup>3</sup>. The flow time through the lagoon is about 9 hours. The flow velocity according to the design assumptions should be around 0.006 m·s<sup>-1</sup>.

To support the wastewater treatment processes in the lagoon, panels were installed on which plants of the following species were placed: *pistiastratiotes*, *limnobiumlaevigatum*, *eichhorniacrassipes*, *myriophyllumverticillatu*. Figure 1 shows the picture taken on the research facility during the work of the aerators.



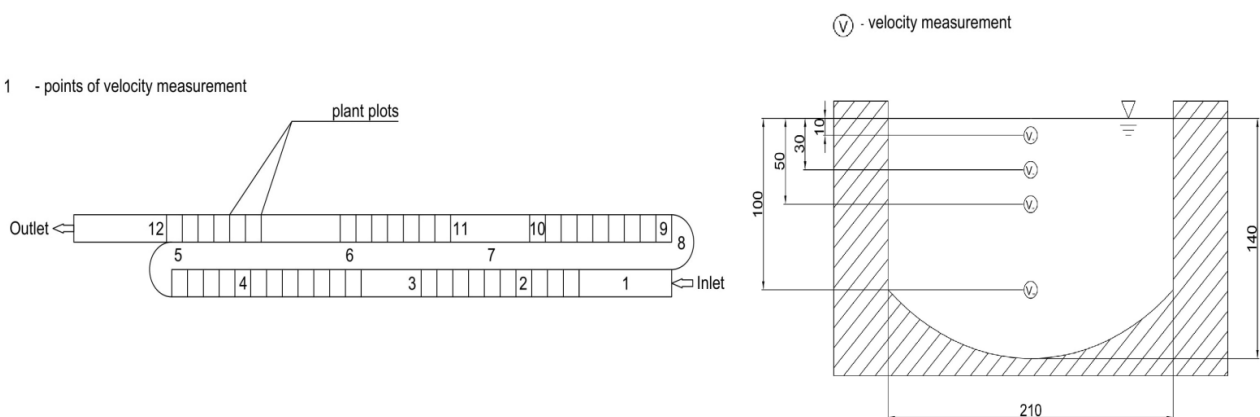


**Figure 1.** Hydroponic lagoon in a wastewater treatment plant in Paczków

## METHODOLOGY

The measurement campaign including direct measurements in the lagoon channel (measurement of the sewage flow rate) was supported by laboratory analyzes including physicochemical and granulometric composition of wastewater.

Measurements of the speed of sewage flowing through the lagoon were made at 12 measuring points. The arrangement of the measuring points is shown in Figure 2.



**Figure 2.** Diagram of the hydroponic lagoon with measurement cross-sections

The direct speed measurement was made with an electromagnetic flow meter, whose principle of operation is based on Faraday's induction - the wastewater flowing around the head induces a current with a value proportional to the velocity of the flowing wastewater (USGS, 2010). Due to low flow velocities and unchanging nature of the channel, i.e. constant width, depth and unchanging roughness (the bed is made entirely of precast concrete), it was decided to limit flow measurements to one hydrometric section in each profile. Measurements were made successively at depths of 0.1

m, 0.3 m, 0.5 m and 1.0 m.

The content of organic matter in the sewage flowing through the lagoon was described by BOD, COD, TOC and total suspended solids. From the measurement points (Fig. 2), a sample of 1.5 l sewage was taken. Within three hours of collection, selected quality parameters were determined in accordance with laboratory testing standards (APHA-AWWA-WEF, 2012).

In selected measurement cross-sections, the size of the outgoing particles (granulometric composition) was investigated using a Malvern Mastersizer 2000 laser granulometer. This device bases its operation on the Mie solution which allows to determine what amount of light has been absorbed or dispersed by a given spherical particle (Black et al., 1996). Malvern Mastersizer 2000 also uses the Fraunhofer model, which allows you to determine the size of the disc-shaped opaque particles (Chen, 2017) as it passes through the laser beam generated by the instrument.

## RESULTS AND DISCUSSION

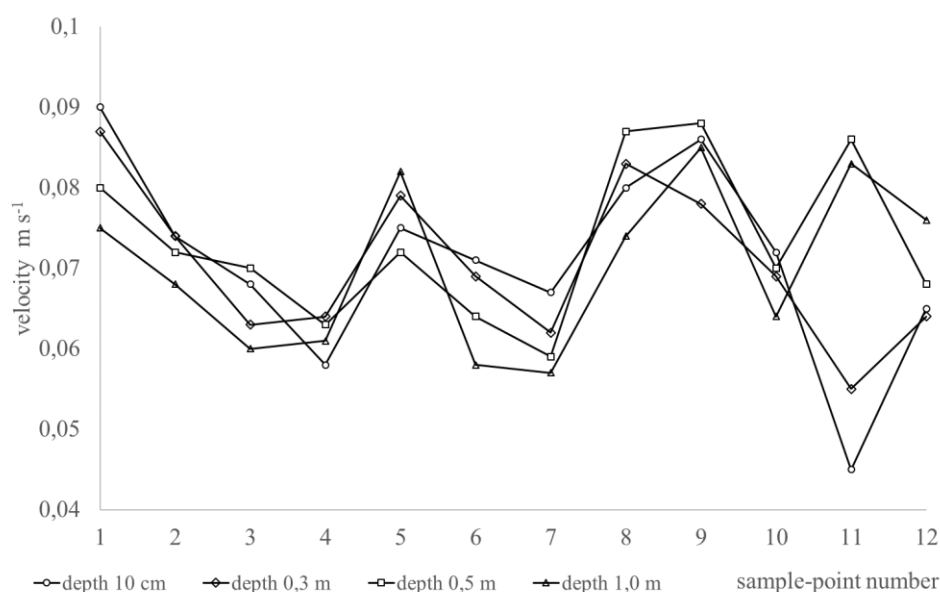
The average value of organic matter in the sewage flowing in the hydroponic lagoon was as follows: BOD -  $4.83 \text{ g}\cdot\text{m}^{-3}$ , COD -  $57.1 \text{ g}\cdot\text{m}^{-3}$ , TOC 10.2 ppm, total suspended solids  $34.4 \text{ g}\cdot\text{m}^{-3}$ . The measured flow velocity had a similar course for all given depths (Fig.3). Its average value was at a similar level for all depths of  $0.07 - 0.073 \text{ m}\cdot\text{s}^{-1}$  with the maximum value measured at a depth of 0.1 m at measurement point 1 (inlet to the lagoon). The results of speed measurements are shown in Table 1.

**Table 1.** Speed summary in individual cross-sections

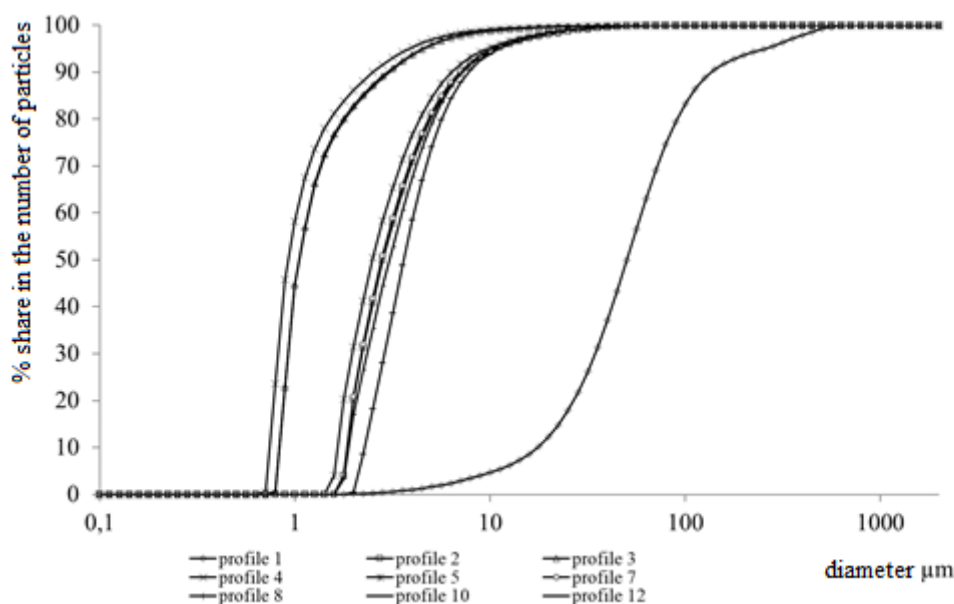
Cross-sections												
Velocity Values( $\text{m}\cdot\text{s}^{-1}$ )												
Depth(m)	1	2	3	4	5	6	7	8	9	10	11	12
0.1	0.09	0.074	0.068	0.058	0.075	0.071	0.067	0.08	0.086	0.072	0.045	0.065
0.3	0.087	0.074	0.063	0.064	0.079	0.069	0.062	0.083	0.078	0.069	0.055	0.064
0.5	0.080	0.072	0.070	0.063	0.072	0.064	0.059	0.087	0.088	0.070	0.086	0.068
1.0	0.075	0.068	0.060	0.061	0.082	0.058	0.057	0.074	0.085	0.064	0.083	0.076

At the outlet of the lagoon, higher sewage flow rates were observed for deeper levels (0.5 - 1.0 m). This phenomenon may affect the elevation of particles previously deposited on the bottom of the lagoon. In addition, the increase in speed at points 8, 9 and 11 in surface wastewater layers is caused by the work of aerators. Plant plantings can be used to control flow conditions and prevent leaching of unwanted particles to the receiver (Kadlec, 2008).

At given measurement points the particle diameters varied in the range of  $0.8 - 800 \mu\text{m}$  (Figure 3), with the particles with the largest equivalent diameters measured in the profile 1 (inlet to the lagoon) (Figure 4). Over 90 % of the particles for this measurement were characterized by a diameter of more than  $178.5 \mu\text{m}$ , while in the remaining profiles 90 % of the particles were within the limits of  $0.8 - 8.7 \mu\text{m}$ . As the flow of sewage through the hydroponic lagoon progressed, the particle size (disaggregation) decreased, which probably could be caused by the increase of the flow velocity of sewage forced by air introduced into the lagoon by the aerator system.



**Figure 3.** The course of changes in the speed of sewage flow in the hydroponic lagoon at different depths



**Figure 4.** The particle size distribution of suspended solids in a hydroponic lagoon with a % content of particles

## CONCLUSIONS

On the basis of observations and performed tests and analyzes conclusions were formulated.

Average velocity measured in the system of aerated hydroponic lagoon was  $0.07 \text{ m} \cdot \text{s}^{-1}$ , which was ten times higher than the assumed rate of sewage displacement in the lagoon.

Speed values caused by frequent and rapid work of aerators cause dynamic movement of organic matter and prevent slow sedimentation of particles to the bottom of the lagoon. This leads to

leaching organic matter to the receiver of treated wastewater.

The largest particle diameters were observed at the inlet to the lagoon where wastewater from the biological reactor is discharged. Over 90 % of the particles had diameters greater than 178.5  $\mu\text{m}$ . The particle diameters along with the sewage flow were reduced in the range from 800 to 0.8  $\mu\text{m}$ .

The values of parameters describing the content of organic matter in sewage were within the standards describing the quality of treated wastewater.

## REFERENCES

- APHA-AWWA-WEF (2012) Standard methods for the examination of water and wastewater, 22nd edition edited by E. W. Rice, R. B. Baird, A. D. Eaton and L. S. Clesceri. American Public Health Association (APHA), American Water Works Association (AWWA) and Water Environment Federation (WEF), Washington, D.C., USA.
- Bawiec, A., Pawkowska, K., Pulikowski K. (2018) LED light use for the improvement of wastewater treatment in the hydroponic system. *Environmental Technology*. DOI: 10.1080/09593330.2018.1554007.
- Black, D. L., McQuay, M. Q., Bonin, M. P. (1996) Laser-based techniques for particle-size measurement: A review of sizing methods and their industrial applications. *Prog. Energy Combust. Sci.*, **22**, 267-306.
- Burgos A. J. and others (2015) Technology fact sheets for effluent treatment plants on textile industry aerated ponds series: Secondary treatments FS-BIO-011.
- Chen, Q., Liu, W., Wang, W. J., Thomas, C. J., Shen, J. (2017) Particle sizing by the Fraunhofer diffraction method based on an approximate non-negatively constrained Chin-Shifrin algorithm. *Powder Technol.*, **317**, 95-103.
- García-Martínez, M., Osornio-Berthet, L. J., Solís-Correa, H. E., López-Chuken, U. J., Beltrán-Rocha, J. C., Barceló-Quintal, I. D. (2017) Determination of Hydrodynamics in Municipal Waste Water by a Lagoon System with Screens. *Journal of Environmental Protection*, **8**, 330-343. DOI: <https://doi.org/10.4236/jep.2017.83025>.
- Ghosh, S. N., Desai, V. R. (2006) Environmental Hydrology and Hydraulics Eco-technological Practices for Sustainable Development, CRC PRESS, Boca Raton.
- Jin, Z., Zhang, X., Li, J., Yang, F., Kong, D., Wei, R., Huang, K., Zhou, B. (2017) Impact of wastewater treatment plant effluent on an urban river. *Journal of Freshwater Ecology*, **32**, 697-710.
- Joshi, S. (2016) Water Abundance: BOD, COD, TOC, TDS and water pollution
- Kadlec, R. H. (2008) The effects of wetland vegetation and morphology on nitrogen processing. *Ecological Engineering*, **33**(2), 126-141.
- Keeratiurai, P. (2013) Efficiency of wastewater treatment with hydroponics, ARPN. *Journal of Agricultural and Biological Science*, **8**(12).
- Maiga, Y., von Sperling, M., Mihelcic, J. (2017) Constructed Wetlands. In: J.B. Rose and B. Jiménez-Cisneros, (eds) Global Water Pathogens Project. (C. Haas, J. Mihelcic and M. Verbyla) Part 4 Management of risk from excreta and wastewater), Michigan State University, E. Lansing, MI, UNESCO. [online] <http://www.waterpathogens.org>, <http://www.waterpathogens.org/book/constructed-wetlands>.
- Shanab, S. (2010) Bioremoval capacity of three heavy metals by some microalgae species (Egyptian Isolates). *Plant Signal Behav.*, **7**(3), 392-399. DOI: 10.4161/psb.19173.
- Suryani, S., Maharani, A. B., Alimuddin Hamzah, M. (2017) Proposing of an aerated water treatment plant for reducing water pollution problem in Losari Beach after reclamation. AIP Conference Proceedings, **1801**, 060006.

- Taseiko, O., Spitsina, T., Milocevic, H, Radovanovic, D., Valjarevic, A. (2016) Biochemical Processes of Self-Purification Model in Small Rivers. *Mathematical and Information Technologies*, Mathematical modeling.
- U.S. Geological Survey (2010) Discharge Measurements at Gaging Stations, Chapter 8, Book 3, Section A Reston, Virginia, USA.
- Wu, B. (2010) CFD Analysis of Mixing in Large Aerated Lagoons. *Engineering Applications of Computational Fluid Mechanics*, **4**(1), 127-138. DOI: 10.1080/19942060.2010.11015.

## Wastewater Recycling for Use in Water Management in the Cities of Future

E. Peterková\*, M. Pečenka\*\*, J. Wanner\*\*, Z. Nováková\* and M. Srb\*

\* PVK, a. s., Ke Kablu 971/1, Hostivař, 102 00, Prague 10, IČ: 2565663, Czech Republic  
(E-mails: [eliska.peterkova@pvk.cz](mailto:eliska.peterkova@pvk.cz); [zuzana.novakova@pvk.cz](mailto:zuzana.novakova@pvk.cz); [martin.srb@pvk.cz](mailto:martin.srb@pvk.cz))

\*\* University of Chemistry and Technology, Prague, Technická 5, 166 28 Prague 6, Czech Republic  
(E-mails: [martin.pecenka@vscht.cz](mailto:martin.pecenka@vscht.cz); [jiri.wanner@vscht.cz](mailto:jiri.wanner@vscht.cz))

### Abstract

The aim of this project is to design a pilot plant for tertiary treatment of secondary effluent from a municipal wastewater treatment plant. The paper summarizes the results of laboratory testing of selected technologies for treatment of biologically treated wastewater. The aim of the laboratory testing is to verify if it is possible to achieve such a level of quality of treated wastewater from a municipal wastewater treatment plant that would be suitable for wastewater reuse. Water samples from technological stages were tested at the Department of Water Technology and Environment at the University of Chemistry and Technology in Prague.

### Keywords

Wastewater; water pollution; reuse of treated wastewater; pilot plant

## INTRODUCTION

The potential of treated wastewater as water resource increases with the climate change, industrialization, increasing drought and irregular torrential rains. Recycled wastewater is a reliable source of water that must be taken into a consideration. It could be used for agricultural and landscape irrigation, for watering hotels gardens, parks or golf courses, etc. In some countries, for example Israel, Turkey, Cyprus, France, Spain and Italy, the wastewater is tertiary treated and used also for groundwater recharge and river flow augmentation. Because of that, the regulations of wastewater recycling are needed to be settled. It is essential to protect public health, prevent negative effects on environment and coastal pollution. On the other hand, the problem of water scarcity and drought is bigger and bigger in recent years. Reuse of wastewater should help to close the water cycle and enable sustainable reuse of available water resources (Kamizoulis et al., 2003).

According to the *2030 Water Research Group*, the global annual water requirements in 2030 would be 6 900 billion m<sup>3</sup>, it is more than 64 % of total accessible water resources. The reliable and available amount of water is 4 200 billion m<sup>3</sup>. The case study shows that the demand in India will grow to almost 1 500 billion m<sup>3</sup>, driven by demand for rice, wheat and sugar for a growing population. In China, it will be 818 billion m<sup>3</sup> of water, over 50 % is for agriculture, 32 % is industrial demand. Sao Paulo state's projected demand of 20.2 billion m<sup>3</sup> is divided between domestic, industrial and agricultural requirements. And the demand in South Africa will be approximately 17.7 billion m<sup>3</sup> (Charting our water future, 2019).

All those reasons encourage water management community in the Czech Republic to treat and use wastewater differently. Not only to discharge it into a recipient, but to reuse it where it is needed. Larger application of the water reuse schemes is currently slowed down by lack of regulation providing clear guidelines for those, who would like to use recycled water. The aim of this study is to summarize relevant experience from other countries and laboratory data to propose possible ways how to enable but also regulate water recycling in the Czech Republic.

## LEGISLATION REVIEW

Currently, Czech legislation does not specify the quality requirements for wastewater reclamation and reuse. There is just one Czech national standard (ČSN 75 7143) from 1993 which regulates the quality of water for irrigation. The limits are very strict and almost impossible to be fulfilled by using secondary treatment effluents. Therefore, limits required by international standards were used for assessment of water quality. The maximum microbiological and chemical pollution indicators for water used for irrigation, flushing toilets or recreational use are given for example by norms ISO/FDIS 20761, ISO 16075-2 or JRC Science and policy reports. Below there are some examples of legislation requirements valid for reuse of treated wastewater, especially the limits of microbiological parameters. The limits of microbiological indicators vary in given standards. For example, in the parameter *E. coli* the limit is in the range from 0 to  $10^5$  CFU/100 mL. In Tables 1, 2 and 3 the BOD<sub>5</sub> parameter is reported, but it was not measured in the laboratory tests in this work. Instead, the COD was measured. Helminth eggs are defined in Table 5. but no information was found in the Czech literature that this determination was carried out.

**Table 1.** Guidelines for water reuse for irrigation (ISO/FDIS 20761, 2018)

Parameters for irrigation uses		
pH	-	6.0 - 9.0
BOD <sub>5</sub>	mg/L	10 - 30
TSS	mg/L	<30
Colour	mg/L Pt	<40
N-NH <sub>3</sub>	mg/L N	<20
Chlorine residual	mg/L	<1.0 (90 min)
<i>E. coli</i>	CFU/100 mL	200 - 1000
Faecal coliforms	CFU/100 mL	<200
Total coliforms	CFU/100 mL	<1000 (temporary)
Turbidity	NTU/L	<10
TDS	mg/L	<1000

**Table 2.** Guidelines for water reuse for toilet flushing (ISO/FDIS 20761, 2018)

Parameters for toilet flushing		
pH	-	6.0 - 9.0
BOD <sub>5</sub>	mg/L	10 - 20 (20 max.)
TSS	mg/L	10 - 20 (20 max.)
Colour	mg/L Pt	<30
N-NH <sub>3</sub>	mg/L N	<10
Chlorine residual	mg/L	0.5 - 1.0 (90 min)
<i>E. coli</i>	CFU/100 mL	<200
Faecal coliforms	CFU/100 mL	<200
Total coliforms	CFU/100 mL	<3
Turbidity	NTU/L	<5
TDS	mg/L	<1500

**Table 3.** Guidelines for water reuse for recreational uses (ISO/FDIS 20761, 2018)

Parameters for recreational uses		
pH	-	6.0 - 9.0
BOD <sub>5</sub>	mg/L	6 - 30
TSS	mg/L	<30
Colour	mg/L Pt	10 - 30
TN	mg/L N	<15
N-NH <sub>3</sub>	mg/L N	<5
TP	mg/L P	<1 (0.5)
Chlorine residual	mg/L	0.5 - 1.0 (90 min)
<i>E. coli</i>	CFU/100 mL	-
Faecal coliforms	CFU/100 mL	200 - 800 (800 max.)
Turbidity	NTU/L	<5

**Table 4.** Guidelines for treated wastewater use for irrigation projects (ISO 16075- 2, 2015)

Cat.	Type of treated wastewater	BOD		TSS		Turbidity		Thermo-tolerant coliforms		Intestinal nematodes	
		mg L <sup>-1</sup>		mg L <sup>-1</sup>		NTU		no./100 ml		Egg L <sup>-1</sup>	
		Ave.	Max	Ave.	Max	Ave.	Max	Ave.	Max	Ave.	Max
A	Very high quality treated wastewater	≥5	10	≥5	10	≤2	5	≤10	100	-	-
B	High quality treated wastewater	≤10	20	≤10	25	-	-	≤200	1000	-	-
C	Good quality treated wastewater	≤20	35	≤30	50	-	-	≤1000	10000	≤1	-
D	Medium quality treated wastewater	≤60	100	≤90	140	-	-	-	-	≤1	5
E	Extensively treated wastewater	≤20	35	-	-	-	-	-	-	≤1	5

**Table 5.** Minimum quality requirements for water reuse (Alcade Sanz, 2017)

Microbiological parameters		
<i>E. coli</i>	CFU/100 mL	0 - 10 <sup>5</sup>
Faecal coliforms	CFU/100 mL	100 - 10 <sup>4</sup>
Total coliforms	CFU/100 mL	2
<i>Legionella Sp.</i>	CFU/ mL	0 - 10 <sup>3</sup>
Sulphate-reducing bacteria	log reduction	2 - 4
Helminth eggs	eggs/L	0 - 1
Faecal enterococci	log reduction	2 - 4

From comparison of Czech effluent standards (Gov. Act. No. 401/2015 Coll.) and international water reuse standards it has been found that in terms of physico-chemical parameters common treated wastewater meets the standards for reuse of treated wastewater already at the end of the



treatment plant. The microbiological parameters are not common to follow at the Czech treatment plant. The first screening showed that average counts of pathogenic organisms are higher than above mentioned international standard, so the research focused mainly on this type of pollution.

Last type of pollution relevant for water reuse and mainly not removed from the wastewater during standard biological treatment are micropollutants. In this study micropollutants removal process was inspired by the experience from drinking water facilities, where the granulated activated carbon filters are often used. Our laboratory tests consequently contained testing of granulated activated carbon filtration.

## **METHODS AND EXPERIMENT**

This project is supported by the Technology Agency of the Czech Republic. It started in 2018 with laboratory tests of water purification technologies intended for wastewater reuse. The tests lasted about a year and a half. After that, according to the laboratory results, scheme of the pilot plant for the treatment of purified wastewater was designed. It will be operated from August 2019 until the end of 2020. During this time the process will be optimized and the operating costs will be evaluated. Secondary effluent from the municipal wastewater treatment plant was used as an input for this treatment.

Following microbiological and physico-chemical parameters were analyzed: colony counts at 22 °C and 36 °C, *Escherichia coli*, coliform bacteria, intestinal enterococci, *Clostridium perfringens*, orthophosphates, total phosphorus, COD (manganese), acid neutralizing capacity, suspended solids, turbidity, nitrate nitrogen, ammoniacal nitrogen and pH value. The COD (manganese) was chosen because the concentration of the organic matter was low in the treated wastewater. The tests showed that in terms of physico-chemical parameters secondary effluent meets the international standards that apply for reuse of treated wastewater. Concerning the microbiological parameters, the quality of secondary effluent does not comply with the international standards. Therefore, during the laboratory tests big emphasis was placed on reducing this type of pollution in order to comply with legislation.

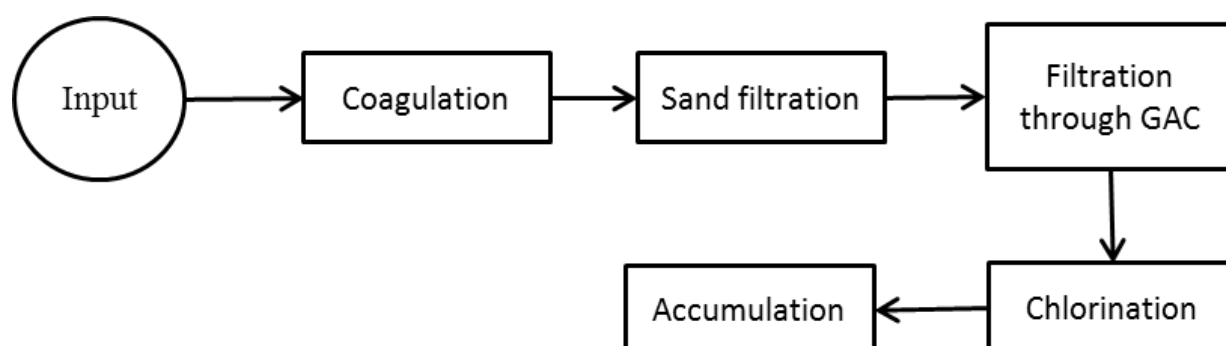
### **Laboratory testing**

The tested technologies were selected in line with standards common in drinking water treatment. The following processes were tested: coagulation, sand filtration, membrane filtration, filtration through granulated activated carbon, disinfection with sodium hypochlorite, chlorine dioxide and UV radiation and accumulation.

The coagulation was selected as the first step of treatment. Optimal dose of coagulation agent was calculated and tested using coagulation experiments. Ferric and aluminum sulfate were tested as coagulating agents. Ferric sulfate was found to be more suitable according to removal efficiency of organic matter and suspended solids. The dose of 27 mg/L was used. A couple of auxiliary organic flocculants has been tested also. However, the results did not show better pollution removal efficiency when these flocculants were used. Therefore, only the ferric sulfate was used for coagulation. The optimal time for rapid and slow mixing and time of sedimentation was also chosen by using the coagulation tests. The time for rapid mixing was 30 seconds, time for slow mixing was 5 minutes and sedimentation time was 10 minutes. With these mixing and sedimentation times, tests were carried out. Another type of coagulation called “in-line” coagulation was tested as well. The ferric sulfate was diluted much more than during coagulation (3 mg/L). There is no slow mixing phase and no time for sedimentation. The sample of water with the coagulating agent was immediately treated further. This type of coagulation will be used in the pilot plant. After the

coagulation different types of filtration were tested. In the beginning, sand filtration was used after the coagulation. The filtration rate was 25 L/h. The size of sand particles was 1 - 2 mm. The volume of the column was 1.53 L. After approximately 25 L of processed secondary effluent the sand needed to be replaced because of the biofilm growth. In the pilot plant the filter will be washed periodically. However, if the biofilm thickness increases, the filter will be washed with a solution of water with sodium hypochlorite. The microbiological pollution was removed with efficiency from 89 % to 99 % after coagulation and sand filtration. The other type of filtration was membrane filtration. Hollow fiber membrane Zeeweed®10 (Zenon) was used, with pore size 0.04  $\mu\text{m}$ , the useful membrane filtration area was 0.93  $\text{m}^2$ . The device operated at a transmembrane pressure of max. 600 mbar (optimum 70-550 mbar), the optimal permeate flow was 42 L/h (working range 18-72 L/h). The membrane worked in the range of ultrafiltration. It was "OUT-IN" type of membrane, the water flowed into the membrane fibers from the outside to the inside where the permeate was pumped out. After approximately 270  $\text{L}/\text{m}^2$  of wastewater the membrane needed to be regenerated with citric acid solution and with distilled water. During the membrane filtration the microbiological pollution was removed by approximately 99 %. The next type of filtration was filtration through granulated activated carbon. The filter was filled with activated carbon with a particle size of 1.0 – 1.5 mm. This type is mainly used to remove micropollutants such as drugs and pesticides. The filtration through activated carbon captured about 80 % of microbiological pollution and more. The residual microbial pollution is eliminated after disinfection. The disinfection was carried out with sodium hypochlorite, chlorine dioxide, UV radiation or with the combination sodium hypochlorite and UV radiation. The chlorine contact time during the disinfection was 90 minutes in line with the legislation and the dose was used so that the residual concentration was at most 0.3 mg/L. For the laboratory experiments the UVC lighting 1G lamp was chosen, the maximum flow was 2 L/min, the energy output was 22.4  $\text{J}/\text{m}^2$ . After the chlorination or UV radiation, a processed water accumulation was the last treatment step. It took 90 minutes. The aim of the accumulation was to find out whether the quality of treated water is deteriorating over time. The results showed that there is no deterioration in the quality of the treated water during this last stage.

All these technological stages were tested in the different configuration. As an example, one of the technological arrangements is explained as follows: Into the purified wastewater a coagulant was added and mixed. Then the water passed through the sand filter and through the filter with the granulated activated carbon. Chlorination provided a disinfection of water. The last step was accumulation. Layout diagram is also provided for clarity. Table 6 shows the results of this arrangement. The *Clostridium perfringens* does not occur in water at all. Intestinal enterococci are removed after the filtration through activated carbon. The treated water meets the requirements for water reuse after the chlorination.



**Figure 1.** The technological arrangement of one of the laboratory tests

**Table 6.** Microbiological parameters in the treated wastewater

Sample	Colony count 22 °C (CFU/100 mL)	Colony count 36 °C (CFU/100 mL)	Coliform bacteria (CFU/100 mL)	<i>E. coli</i> (CFU/100 mL)	Intestinal enterococci (CFU/100 mL)	<i>Clostridium</i> <i>perfringens</i> (CFU/100 mL)
Input	162 000	169 000	19 560	2 620	270	0
Coagulation	15 000	8 000	24 200	211	19	0
Sand filtration	3 234	1 080	1 733	33	3	0
Filtration GAC	1 727	0	51	4	0	0
Chlorination	52	20	0	0	0	0
Accumulation	1	0	0	0	0	0

## DISCUSSION

The acquired knowledge enables a great variability in the design of the pilot plant of the tertiary wastewater treatment unit for its further use. Above all, the economic aspect, the requirements for servicing equipment, the size of the entire unit and the required quality of treated water will be decisive. Due to its high efficiency in removing chemical and microbiological contamination, the inclusion of a membrane filtration module can be recommended. However, this technology will be one of the most expensive investments. If the sand filtration is included, it is advisable to prevent the formation of biofilm, for example by frequent washing of the filter with the solution of sodium hypochlorite. For removal of the micropollutants it would be installed activated carbon filtration in the process line. The final disinfection of the treated water would be best solved by the installation of a UV lamp, but such technology is quite costly.

## CONCLUSIONS

The results of all laboratory testing showed that if coagulation, sand filtration, membrane filtration, filtration through granulated activated carbon and disinfection are included, treated water meets the legislation requirements for reuse of wastewater. Depending on the quality of treated wastewater or the way how it would be use, the dose of reagents and the contact time during the filtration will be chosen.

There is a need for legislation for reuse of treated wastewater in the Czech Republic. A proposal for a regulation of the European Parliament and of the Council on minimum requirement of the reuse of water from May 2018 was filed and its approval by the EU administration will be probably finished in 2019. The aim of this document is to help with the threat of water scarcity and with “water stress”. Currently, reuse of water in Czech Republic is done using two tools that nevertheless do not specify its conditions. It is the Water Framework Directive and the Urban Wastewater Treatment Directive. The proposed EU regulation is in line with the previous documents. (Schiebertová, 2019)

## ACKNOWLEDGEMENTS

This paper was elaborated within the project TA ČR TA 03030080. I would like to thank to doc. RNDr. Jana Říhová Ambrožová, Ph.D. and to Ing. Lucie Baumruková for microbial laboratory analyses.

## REFERENCES

Alcade-Sanz, L. (2017) Minimum quality requirements for water reuse in agricultural irrigation and aquifer recharge. In; Gawlik, B. M., Ed.; Publications Office of the European Union,

Luxembourg.

- Charting our water future: Economic Frameworks to Inform Decision Making. (2009) 2030 Water Research Group. [online] [https://www.mckinsey.com/~media/mckinsey/dotcom/client\\_service/sustainability/pdfs/charting%20our%20water%20future/charting\\_our\\_water\\_future\\_full\\_report\\_.ashx](https://www.mckinsey.com/~media/mckinsey/dotcom/client_service/sustainability/pdfs/charting%20our%20water%20future/charting_our_water_future_full_report_.ashx).
- Gov. Act. No. 401/2015 (2015) Coll. Nařízení vlády o ukazatelích a hodnotách přípustného znečištění povrchových vod a odpadních vod, náležitostech povolení k vypouštění odpadních vod do vod povrchových a do kanalizací a o citlivých oblastech.
- ISO/FDIS 20761 (2018) Water reuse in urban areas- Guidelines for water reuse safety evaluation- Assessment parameters and methods, Switzerland.
- ISO 16075-2 (2015) Guidelines for treated wastewater use for irrigation projects -- Part 2: Development of the project, Switzerland.
- Kamizoulis, G.; Bahri, A.; Brissaud, F.; Angelakis, A. N. (2003) Wastewater recycling and reuse practices in Mediterranean region: Recommended Guidelines. [online] [https://www.researchgate.net/profile/Akissa\\_Bahri/publication/228797648\\_Wastewater\\_recycling\\_and\\_reuse\\_practices\\_in\\_Mediterranean\\_region\\_Recommended\\_Guidelines/links/54eb92e60cf2082851be27c7.pdf](https://www.researchgate.net/profile/Akissa_Bahri/publication/228797648_Wastewater_recycling_and_reuse_practices_in_Mediterranean_region_Recommended_Guidelines/links/54eb92e60cf2082851be27c7.pdf).
- Schiebertová, V. (2019) Komise navrhla minimální požadavky na opětovné použití vody, 2018. Euroskop.cz. [online] <https://www.euroskop.cz/9007/31127/clanek/komise-navrhla-minimalni-pozadavky-na-opetovne-pouziti-vody/>.

# Batch Studies of Phosphonate Adsorption on Granular Ferric Hydroxides

T. Reinhardt\*, M. Gómez Elordi\*, R. Minke\*, H. Schönberger\* and E. Rott\*

\* Institute for Sanitary Engineering, Water Quality and Solid Waste Management, University of Stuttgart, Bandtäle 2, 70569 Stuttgart, Germany (E-mail: [tobias.reinhardt@iswa.uni-stuttgart.de](mailto:tobias.reinhardt@iswa.uni-stuttgart.de))

## Abstract

Phosphonates are widely used in various industries. However, it is desirable to remove them before discharging phosphonate-containing wastewater. This study describes a large number of batch experiments with adsorbents that are likely suitable for the removal of phosphonates. For this, adsorption isotherms for four different granular ferric hydroxide (GFH) adsorbents were determined at different pH values. Additionally, for the best-performing GFH, the influence of temperature was studied. A maximum loading of ~12 mg P/g was found for nitrilotrimethylphosphonic acid (NTMP) with an initial concentration of 1 mg/L NTMP-P and a contact time of 7 days at room temperature. Then, the adsorption of six different phosphonates was investigated as a function of pH. It was shown that GFH could be used to remove all investigated phosphonates from water, and with an increasing pH, the adsorption capacity decreased for all six phosphonates. Lastly, five adsorption-desorption cycles were carried out to check the suitability of the material for multiple use. Even after five cycles, the adsorption process still performed well.

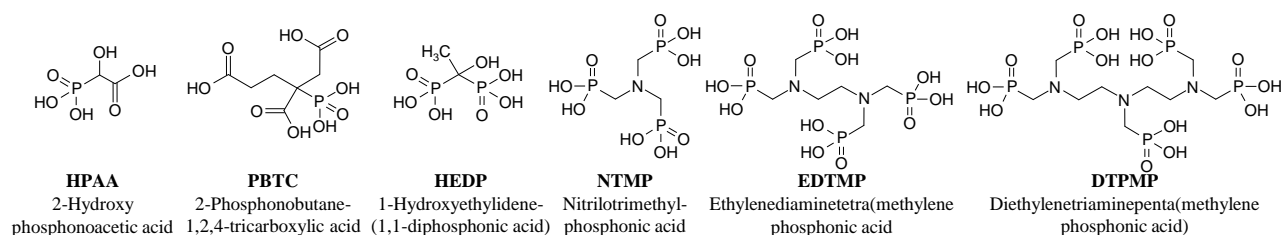
## Keywords

Adsorption; desorption; GFH; NTMP; phosphonates

## INTRODUCTION

The worldwide requirements for the discharge of phosphorus into water bodies are becoming increasingly stringent. With regard to P emission, in addition to ortho-phosphate, other quantitatively relevant P-containing compounds such as phosphonates should be considered (**Fig. 1**). Phosphonates are complexing agents that are used in various industries, such as in the textile industry as bleach stabilizers, as antiscalants in drinking water purification, but also in domestic and industrial detergents (Nowack and Stone, 1999a; Boels et al., 2012). The global phosphonate consumption grew from 56,000 t/a in 1998 (Davenport et al., 2000) to 94,000 t/a in 2012 (EPA, 2013). Phosphonates are suspected of contributing to the eutrophication of water bodies in the long term, as UV radiation can promote their degradation to readily available ortho-phosphate (Rott et al., 2018a). With regard to the removal of phosphonates from wastewater, the use of UV lamps is often limited due to high energy costs and large volumes to be treated. During the Fenton and flocculation process, large quantities of sludge are produced which then must be separated and disposed of expensively. In addition, to form sufficient amounts of flocks, a very high flocculant concentration is often necessary, as phosphonates are very strong complexing agents (Rott, 2016). A possible alternative that exploits the relatively high adsorption affinity of phosphonates for metal-containing surfaces is to use iron-containing filter materials for their removal. Possible adsorbents range from iron-coated sand (Boels et al., 2010), commercially available granular ferric hydroxides (GFH) (Boels et al., 2012), engineered composite particles (Rott et al., 2018b) to minerals such as goethite (Nowack and Stone, 1999a). These adsorbents must have both a high adsorption capacity and an effective regenerability for them to be applicable in large-scale wastewater treatment applications. So far, however, hardly any studies have been published on these properties with regard to iron-containing adsorbents and phosphonates. Furthermore, in these studies only one phosphonate is investigated, although various phosphonates with different properties are used in industrial processes. In order to close the knowledge gaps mentioned above, this study therefore

describes a large number of batch experiments with four different GFH adsorbents likely suitable for the removal of phosphonates.



**Figure 1.** Chemical structures of considered phosphonates

## MATERIAL AND METHODS

### Reagents and Chemicals

All solutions were prepared with deionized water produced from drinking water using an ion exchanger (Seradest SD 2000) and a filter unit (Seralpur PRO 90 CN). Acetic acid (AcOH) (100 %, Ph. Eur.) and hydrochloric acid (32 %, AnalaR NORMAPUR) were obtained from VWR Chemicals (Fontenay-sous-Bois, France) and NaOH ( $\geq 99\%$ , Ph. Eur.) from Merck (Darmstadt, Germany). 2-(*N*-morpholino)ethanesulfonic acid (MES) ( $\geq 99\%$ ), 3-(*N*-morpholino)propanesulfonic acid (MOPS) ( $\geq 99.5\%$ ), 4-(2-hydroxyethyl)-1-piperazinepropanesulfonic acid (EPPS) ( $\geq 99.5\%$ ), 3-(cyclohexylamino)-2-hydroxy-1-propanesulfonic acid (CAPSO) ( $\geq 99.5\%$ ), 3-(cyclohexylamino)-1-propanesulfonic acid (CAPS) ( $\geq 98\%$ ), HEDP·H<sub>2</sub>O ( $\geq 95\%$ ) and NTMP ( $\geq 97\%$ ) originated from SigmaAldrich (St. Louis, MO, USA). PBTC, as technical solution (50 %, CUBLEN P 50), as well as EDTMP (5.3 % water of crystallization) and DTPMP (16 % water of crystallization), both as solids, were obtained from Zschimmer & Schwarz Mohsdorf (Burgstädt, Germany). HPAAs, as technical solution (50 %) was purchased from Connect Chemicals (Ratingen, Germany).

### Adsorbents

A total of four different GFH were investigated, the properties of which are shown in **Tab. 1**. Each adsorbent was rinsed once with distilled water over a sieve until the water was clear and then air-dried under a fume hood.

**Table 1.** Iron hydroxide granules investigated in this study

#	Adsorbent material	Supplier	Grain size after rinsing [mm]	Point of zero charge [pH <sub>PZC</sub> ]	Specific surface [m <sup>2</sup> /g]
GFH1	FerroSorp RW	HeGo Biotec	0.5-2.5	8.6	210
GFH2	FerroSorp Plus	HeGo Biotec	0.5-2.5	8.7	230
GFH3	Double P+S	BwF Brauchwasserfilter	1.25-2.5	8.5	242
GFH4	K24 Phosphatbinder	Teichpoint	2.24-8.0	8.3	279

### Experimental procedure

Buffered solutions containing 1 mg/L P were prepared for the six phosphonates in **Fig. 1** as follows (pH target value (pH<sub>start</sub>) with buffer concentration in brackets): pH 4 (0.01 M AcOH), pH 5 (0.01 M AcOH), pH 6 (0.01 M MES), pH 7 (0.01 M MOPS), pH 8 (0.01 M EPPS), pH 9 (0.01 M CAPSO), pH 10 (0.01 M CAPS) and pH 12 (0.01 M CAPS). The pH was set using HCl or NaOH. The required amount of adsorbent was weighed into a 50 mL centrifuge tube which was then filled with the buffered P-containing solution to the 50 mL mark, quickly closed and clamped in the rotator running at 20 rpm (LLG-uniROTATOR 2). After a specific contact time, the centrifuge tube

was quickly removed and a volume of approx. 20 mL of the supernatant was membrane filtered into an empty glass bottle using a syringe attachment filter (0.45  $\mu\text{m}$  pore width). From the filtrate, total P and the pH ( $\text{pH}_{\text{end}}$ ) were determined. The experiments were performed in a single approach, except of experiment 4 (duplicate approach, 2 parallel runs) the results of which are presented as mean values with their standard deviations.

In experiment 1, isotherms for NTMP adsorption on four different GFH were determined at a contact time of 1 h at different pH values ( $T = 20\text{ }^{\circ}\text{C}$ ; pH 4, 6, 8, 10 and 12;  $t_c = 60\text{ min}$ ; 1 mg/L NTMP-P; four different GFH). Experiment 2 was dedicated to the maximum loading of GFH1 and the temperature dependence of the adsorption of NTMP ( $T = 5, 20, 35\text{ }^{\circ}\text{C}$ ; pH 6;  $t_c = 60\text{ min} - 7\text{ d}$ ; 1 mg/L NTMP-P; GFH1). For experiments 1 and 2, the initial NTMP concentration remained constant while the GFH dosages varied. In experiment 3, the adsorption capacity of GFH1 against six phosphonates and the influence of the pH on the adsorption of these compounds were investigated ( $T = 20\text{ }^{\circ}\text{C}$ ; pH 4, 5, 6, 7, 8, 9, 10 and 12;  $t_c = 60\text{ min}$ ; 1 mg/L HPAA-P, PBTC-P, HEDP-P, NTMP-P, EDTMP-P and DTPMP-P; GFH1). Here, a constant factor of 0.23 g GFH1/ $\mu\text{mol}$  of P compound was applied. Experiment 4 investigated the regenerability of GFH1 in 5 cycles ( $T = 20\text{ }^{\circ}\text{C}$ ; pH 6;  $t_c = 60\text{ min}$  for adsorption and desorption each;  $t_c = 15\text{ min}$  for 3 rinsing steps; 1 mg/L NTMP-P; 1 M NaOH; GFH1). After each adsorption step was performed as described above, the supernatant (later to be filtered and analyzed) was decanted. For the desorption steps, the centrifuge tube was then filled with 1 M NaOH solution up to 50 mL, rotated for 60 min and decanted again (the decanted supernatant was analyzed as well). To remove NaOH residues which could unintentionally increase the pH of the solution in the next adsorption step, the same procedure was repeated three times in a row with 50 mL of buffered solution (0.01 M MES; pH 6) before the next cycle began. The dry weight of GFH1 was determined before and after the five cycles to identify how much material had been lost in the experiment.

### Analytical methods

A modified ISO method ( $\text{ISO}_{\text{mini}}$ ) as described by Rott et al. (2018c) was used for phosphorus analysis. The applicability of this method was confirmed using various organic buffers at 0.01 M, mixed with 1 mg/L NTMP-P and 1 mg/L  $\text{KH}_2\text{PO}_4\text{-P}$  standard, at different  $\text{K}_2\text{S}_2\text{O}_8$  (oxidizing agent) and NaOH doses, paralleled by P determinations according to ISO 6878 (Rott et al., 2018c). All glass materials that came into contact with the sample were thoroughly rinsed with hydrochloric acid (10%) and deionized water prior to the analysis. The digestion was carried out in a HachLange HT200S thermostat. The absorbance was measured with the UV/VIS spectrophotometer Nanocolor UV/VIS II from Macherey-Nagel. For the analysis of the strongly alkaline regeneration solution, the ISO 6878 method (molybdenum blue method) was used. The pH value was mainly determined with the WTW pH electrode SenTix 81 in combination with the instrument WTW pH91. Scanning electron microscopy was applied using a Zeiss DSM-982 Gemini microscope with a thermal Schottky field emitter. For preparation, individual samples were applied to a sample carrier and fixed with conductive silver. To prevent electrical charging of the granules and gain a clear image, the samples were sputtered with gold using a Leica coater (EM ACE 600). Furthermore, energy-dispersive X-ray spectroscopy (EDS) could be performed with an X-ray detector from ThermoScientific (DSM-982 UltraDRY SDD detector).

### Model equations

The Freundlich isotherms were modeled using **Eq. 1**. The parameters  $K_F$  and  $n$  were determined by non-linear regression using the least-squares method.

$$q = K_F c^{1/n} \quad (1)$$

The curves in **Fig. 5** plotting the adsorption capacity as a function of pH were modeled by the logistic function model (**Eq. 2**). The parameters  $a$ ,  $b$ , and  $d$  were determined with the least-squares method.

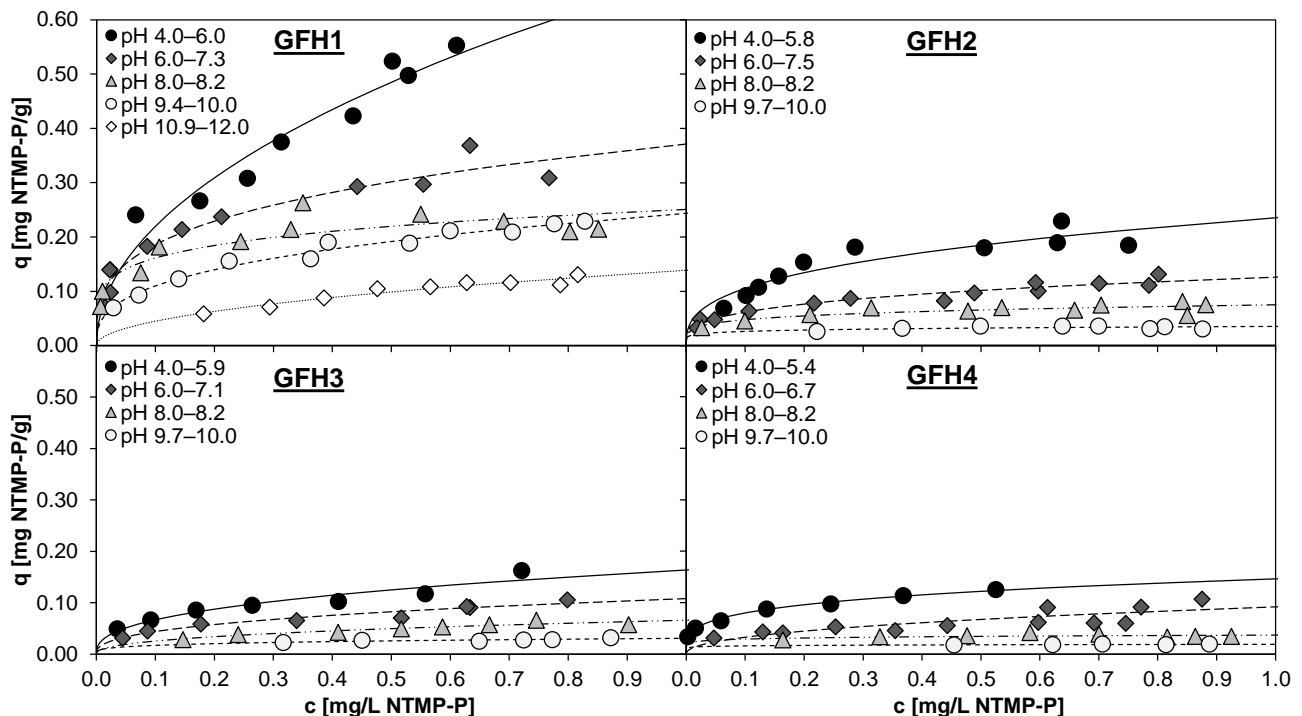
$$c_{\text{ads}}(\text{pH}) = 1 \frac{\text{mg}_{\text{ads}}}{\text{L}} - \frac{d}{(1+ae^{-b \times \text{pH}})} \quad (2)$$

The coefficient of determination  $r^2$  was calculated according to Rott et al. (2018b). For the species distribution in **Fig. 5**, the pK values from Rott et al. (2018b) were used. Additionally, pK values of 1.12, 3.48, 8.00, and 13.48 for HPAAs were applied as calculated for 0 M ionic strength according to CA (2017).

## RESULTS AND DISCUSSION

### Experiment 1 – Adsorption isotherms

**Fig. 2** enables a comparison of the adsorption isotherms for the four GFH examined at 1 h contact time and different pH values. Since during adsorption the pH of the solution shifted in the direction of the  $\text{pH}_{\text{PZC}}$  of the GFH, the indicated pH ranges describe the ranges between  $\text{pH}_{\text{start}}$  and  $\text{pH}_{\text{end}}$ . All materials generally achieved higher loadings at lower pH values. The adsorbents show a positive net surface charge at pH values below the  $\text{pH}_{\text{PZC}}$ , which increases with increasing deviation to the  $\text{pH}_{\text{PZC}}$ . NTMP is negatively charged over the entire pH range tested so that adsorptive and adsorbent experience a stronger electrostatic attraction at lower pH values (Nowack and Stone, 1999a).

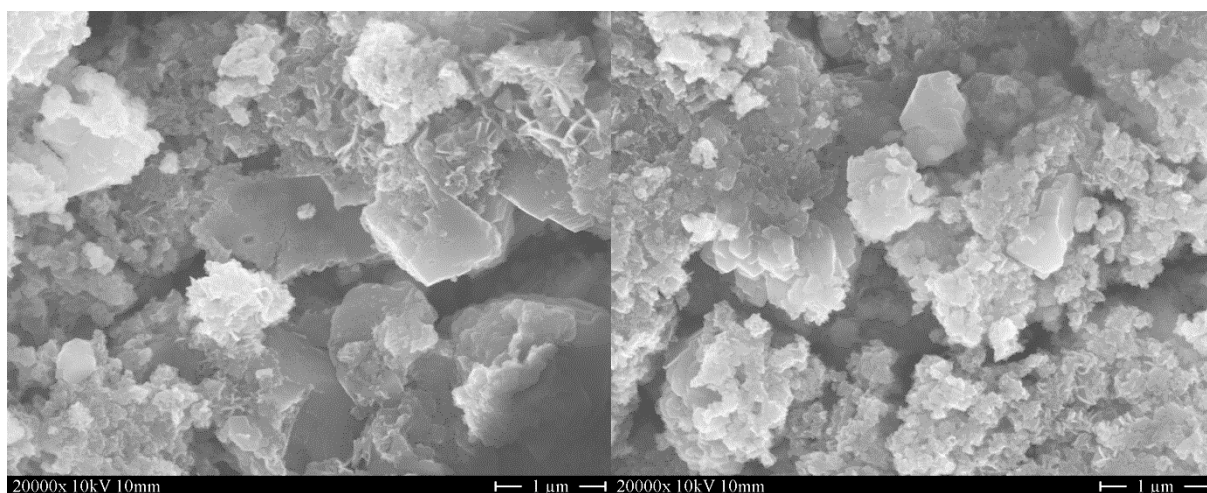


**Figure 2.** Adsorption isotherms for different adsorbents with respect to the adsorption of 1 mg/L NTMP-P depending on the pH (buffer: 0.01 M AcOH, 0.01 M MES, 0.01 M EPPS, 0.01 M CAPS) at room temperature (20 °C) (20 rpm,  $t_c = 1$  h). Modeled Freundlich isotherms are shown

GFH1 was the material with by far the best performance. For instance, GFH1 achieved a loading of 0.55 mg NTMP-P/g at a pH of 4.0-6.0, in contrast to the second-best material GFH2 with a maximum loading of only 0.23 mg NTMP-P/g. This loading was achieved by GFH1 even at pH 9.4-10.0. Interestingly, GFH4 performed poorly in comparison despite the largest specific surface area. As the  $\text{pH}_{\text{PZC}}$  of all investigated adsorbents was in a similar range, the choice of grain size



therefore obviously plays the more important role in adsorption. Two images depicting different sites of GFH1 at magnifications of 20,000x show that the material has a crystalline structure, formed by crystals of different sizes, clearly corroborating a high porosity (**Fig. 3**). The EDS detected mainly Fe, O and Ca (H is not detected by the EDS technique). The Ca has its origin in the production process in which calcium-containing compounds are used. Ca has been found to have a positive effect on the adsorption of phosphonates (Boels et al., 2012; Nowack and Stone, 1999b), which is why the CaCO<sub>3</sub> content ( $\geq 12$ -19 % in GFH1, for comparison in GFH2 only 5-10 %) could be the reason why GFH1 so significantly stood out among the other GFH.



**Figure 3.** Scanning electron microscope images of GFH1 at a magnification of 20,000x

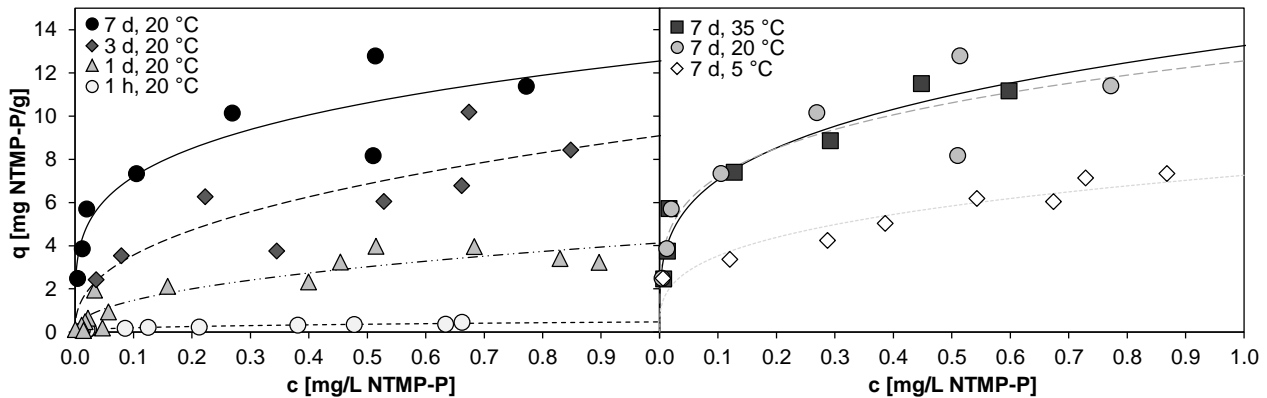
Previous experiments (not shown here) on the stability of the material with respect to the pH had shown that GFH1 was chemically unstable at pH < 6, suggesting a poor long-term applicability. Thus, the treatment of wastewater with GFH1 is recommended to be performed at pH values close to 6, despite its significantly higher efficiency at pH < 6. From the results of this experiment it was concluded that the following experiments would be carried out only with the most efficient GFH1.

### Experiment 2 – Maximum possible loading and temperature dependence

Since no adsorption equilibrium was reached after a contact time of 1 h, at pH 6.0-7.8, additional isotherms at contact times of 1, 3 and 7 d were prepared (**Fig. 4** left). Except for the isotherm after 3 d, all could be well described with the Freundlich model ( $r^2 \geq 0.847$ , 3 d:  $r^2 = 0.713$ ). Even after 3 d, equilibrium was not reached. That was because the adsorbents were not ground prior to the experiments. At an initial concentration of 1 mg/L NTMP-P, the maximum loading after 7 d was ~12 mg P/g. Experiments with an initial concentration of 5 mg/L NTMP-P (not shown here) and pH 6.0-7.6 resulted in a higher maximum loading of about 18 mg P/g due to the stronger gradient between NTMP and GFH1. In similar investigations, but with a significantly higher initial concentration of 9.3 mg/L NTMP-P and slightly higher pH of 7.85, Boels et al. (2012) found a maximum loading on GFH of ~22 mg NTMP-P/g. At similar conditions (9 mg/L NTMP-P, pH 8.3), Chen et al. (2017), on the other hand, found a much lower equilibrium loading of ~9 mg NTMP-P/g. Unfortunately, in these studies the experiments were conducted at pH values at which GFH performs insufficiently, which is why no direct comparison is possible to the results of the current study.

At a temperature of 5 °C, the maximum loading was only ~7 mg P/g (**Fig. 4** right). Consequently, the adsorption performance was increased when thermal energy was applied. Wang et al. (2014) discovered the same behaviour for the adsorption of phosphate on iron-coated activated carbon when investigating temperatures of 20, 30, and 40 °C. They explained that as the temperature in the water increases, the surface activity of the adsorbent increases as well. As a result, the interaction

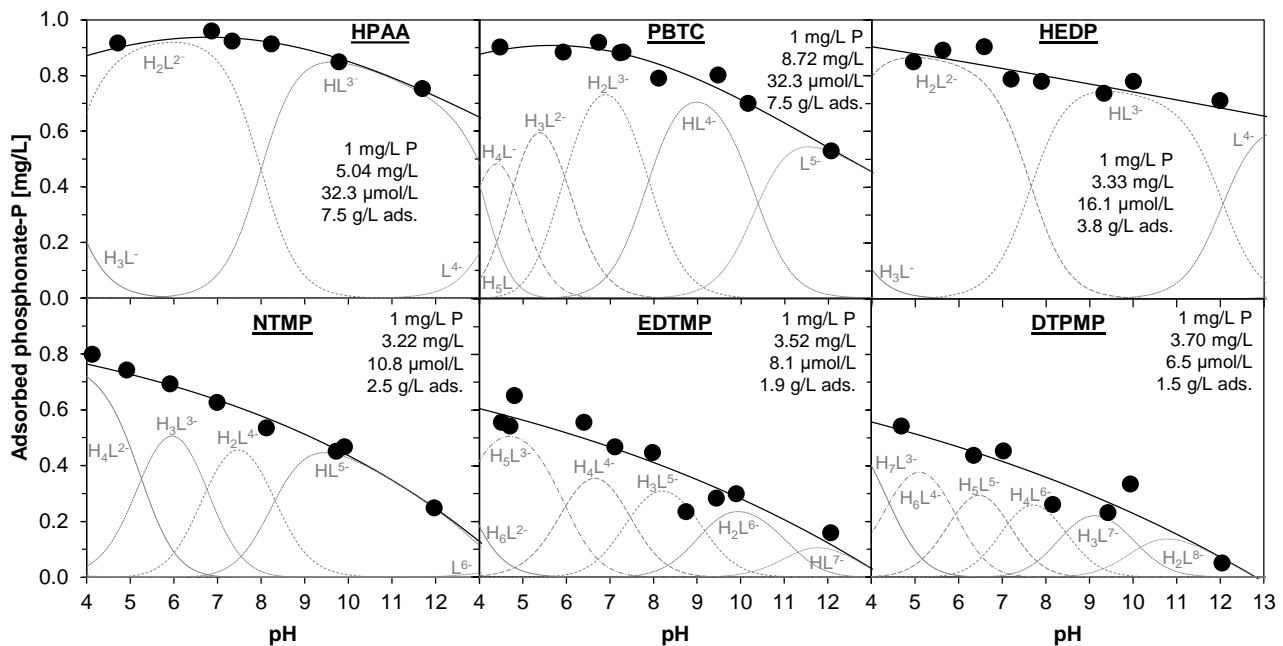
forces between adsorbents and adsorptive become stronger (Wang et al., 2014). On the other hand, no difference in the maximum loading was found at temperatures of 20 °C and 35 °C. Therefore, it can be concluded that 12 mg P/g is the maximum possible loading of GFH1 at an initial concentration of 1 mg/L NTMP-P.



**Figure 4.** Adsorption isotherms of GFH1 with respect to adsorption of 1 mg/L NTMP-P at initial pH 6 (buffer: 0.01 M MES) at different contact times (left) and different temperatures (right) (20 rpm). Modeled Freundlich isotherms are shown

### Experiment 3 – Adsorption behavior of different phosphonates

For all 6 phosphonates, as for NTMP, a decreasing adsorption behavior could be seen with increasing pH (Fig. 5). In addition, a reduction of the adsorption affinity with an increasing number of phosphonate groups (PG) and increasing molecular mass was observed. For example, at pH 8 for HPAA (1 PG, 156.03 g/mol), PBTC (1 PG, 270.13 g/mol), HEDP (2 PG, 206.03 g/mol), NTMP (3 PG, 299.05 g/mol), EDTMP (4 PG, 436.12 g/mol) and DTPMP (5 PG, 573.20 g/mol), adsorption concentrations of 0.88, 0.84, 0.81, 0.58, 0.41 and 0.36 mg P/L (according to model functions) were found.



**Figure 5.** Adsorption of different phosphonates at different pH values with a dosage of 0.23 g GFH1/ $\mu$ mol phosphonate at room temperature (20 °C) (20 rpm,  $t_c = 1$  h). Solutions with 1 mg/L P, buffered at pH 4 and 5 (0.01 M AcOH), pH 6 (0.01 M MES), pH 7 (0.01 M MOPS), pH 8 (0.01 M EPPS), pH 9 (0.01 M CAPSO) and pH 10 and 12 (0.01 M CAPS)

This behaviour could be expected since larger molecules occupy more adsorption sites (Nowack and Stone, 1999a). Furthermore, the more phosphonate groups a compound has, the higher its negative charge becomes. When these highly negatively charged species adsorb, the adsorption of further phosphonate molecules is disturbed by the transfer of the negative charge to the surface (Nowack and Stone, 1999a). PBTC deviated from this pattern slightly as, at  $\text{pH} < 9$ , PBTC-P adsorbed in a similar ratio to HEDP-P despite a higher molecular mass than HEDP. A slight variation in the pattern for PBTC was not extraordinary since this compound contains three carboxyl groups (R-COOH), which are absent in the other phosphonates with the exception of HPAA (one carboxyl group). The deviation from the pattern, however, disappeared as soon as the fully deprotonated PBTC species became dominant at  $\text{pH} > 9$ .

Interestingly, there was still adsorption and no sudden drop of adsorption at pH values higher than the  $\text{pH}_{\text{PZC}}$  for all investigated phosphonates, meaning that adsorption also took place on the adsorbent with a negative net surface charge.

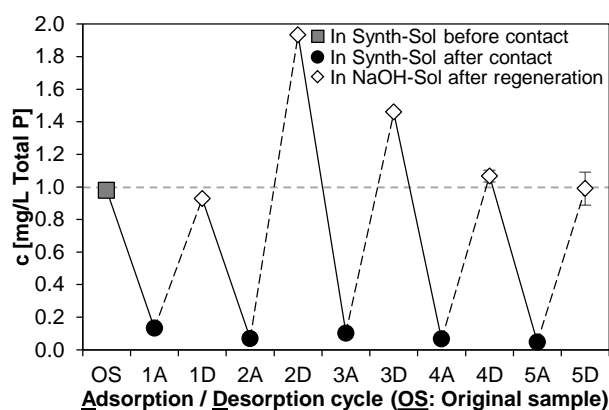
#### **Experiment 4 – Regenerability of GFH**

Nowack and Stone (1999a) for goethite and Boels et al. (2012) and Chen et al. (2017) for GFH have already investigated the desorption of NTMP, but only in one, two and three cycles, respectively. **Fig. 6** shows that GFH1 could be loaded and unloaded several times without loss of adsorption capacity (after each adsorption cycle, the total P concentration was  $< 0.1$  mg/L). Total P concentrations  $> 1$  mg/L were found in the regeneration solutions, proving that GFH1 already contained P and that it was desorbed during the desorption phases with 1 M NaOH solution together with the adsorbed NTMP. Interestingly, these concentrations of  $> 1$  mg/L were first found after the second desorption (2D). After this cycle, the P concentration in regeneration solutions continuously decreased and approached 0.99 mg/L P after 5 cycles. This may be due to a gradual leaching effect of the P present in the material, as fresh regeneration solution was always used in each desorption step.

The fact that after the fifth adsorption step still a very low residual concentration of 0.05 mg/L P was found in the solution (5A) and the total P concentration in the regeneration solution was 0.99 mg/L (5D) indicates that all P contamination of GFH1 was washed out at the latest after the fifth cycle.

In addition, by weighing the dry mass of the GFH before and after the experiment, it was determined that during the five cycles 38 % of the initial concentration of 15 g/L GFH1 was lost due to abrasion. Although such a high material loss was recorded, the NTMP removal rates were still high in all cycles, underlining the excellent performance of this material in adsorbing NTMP. Assuming this abrasion occurred linearly and each desorption step was efficient in desorbing all NTMP, there would still be enough adsorbent ( $\sim 6$  g/L) to remove  $> 90$  % P when the 9th cycle had been reached (according to the adsorption isotherm in **Fig. 2**).

However, such assumptions and calculations are very uncertain which is why batch experiments are only indicative experiments. For a higher significance, column tests that typically show no abrasion should be carried out in the future.



**Figure 6.** Total P in synthetic solution (Synth-Sol) initially containing 1 mg/L NTMP-P before and after contact with 15 g/L GFH1 at pH 6 (0.01 M MES) as well as in 1 M NaOH solution (NaOH-Sol) after regeneration of GFH1 for five adsorption (A) and desorption (D) cycles (20 °C, 20 rpm,  $t_c = 1$  h, 3 rinsing steps for 15 min with 0.01 M MES solution (pH 6) after each regeneration)

## CONCLUSIONS

This work showed that GFHs could be used to remove all investigated phosphonates from water. For GFH1, the adsorption capacity decreased for all phosphonates with increasing pH value and number of phosphonate groups. To achieve the best performance, the treatment of wastewater should be carried out at pH values close to 6. Additionally, a temperature of 20 °C is adequate for the effective adsorption of NTMP onto GFH1. Furthermore, it was proven that GFH1 can be reused multiple times. Therefore, in the future it should be tested with real wastewater and in column experiments.

## ACKNOWLEDGMENT

We acknowledge gratefully the Willy-Hager-Stiftung, Stuttgart, for their financial support. We also thank HeGo Biotec GmbH for providing adsorbent samples and Zschimmer & Schwarz Mohsdorf GmbH & Co. KG for the supply of phosphonate samples.

## REFERENCES

- Boels, L., Tervahauta, T., Witkamp, G. J. (2010) Adsorptive removal of nitrilotris(methylenephosphonic acid) antiscalant from membrane concentrates by iron-coated waste filtration sand. *Journal of Hazardous Materials*, **182**(1-3), 855-862.
- Boels, L., Keesman, K. J., Witkamp, G. (2012) Adsorption of phosphonate antiscalant from reverse osmosis membrane concentrate onto granular ferric hydroxide. *Environmental Science and Technology*, **46**, 9638-9645.
- Chen, Y., Baygents, J.C., Farrell, J. (2017) Removing phosphonate antiscalants from membrane concentrate solutions using granular ferric hydroxide. *Journal of Water Process Engineering*, **19**, 18-25.
- CA (2017) ChemAxon Ltd. [online] <https://chemicalize.com>.
- Davenport, B., DeBoo, A., Dubois, F., Kishi, A. (2000) CEH Report: Chelating Agents. Cited by Nowack (2003), *Water Res.*, **37** (11), 2533-46.
- EPA (2013) European Phosphonate Association - Phosphonates in Detergents. EPA Detergent Phosphonates Dossier.
- Nowack, B., Stone, A. T. (1999a) Adsorption of Phosphonates onto the Goethite-Water Interface. *Journal of Colloid and Interface Science*, **214**(1), 20-30.

- Nowack, B., Stone, A. T. (1999b) The Influence of Metal Ions on the Adsorption of Phosphonates onto Goethite. *Environmental Science and Technology*, **33**(20), 3627-3633.
- Nowack, B. (2003) Environmental chemistry of phosphonates. *Water Research*, **37** (11), 2533-2546.
- Rott, E. (2016) Investigations into the elimination of phosphorus from phosphonate-containing industrial wastewaters (Untersuchungen zur Elimination von Phosphor aus phosphonathaltigen Industrieabwässern). Ph.D. thesis, University of Stuttgart, Stuttgart, Germany, (in German).
- Rott, E., Steinmetz, H., Metzger, J. W. (2018a) Organophosphonates: A review on environmental relevance, biodegradability and removal in wastewater treatment plants. *Science of the Total Environment*, **615**, 1176-1191.
- Rott, E., Nouri, M., Meyer, C., Minke, R., Schneider, M., Mandel, K., Drenkova-Tuhtan, A. (2018b) Removal of phosphonates from synthetic and industrial wastewater with reusable magnetic adsorbent particles. *Water Research*, **145**, 608-617.
- Rott, E., Reinhardt, T., Wasielewski, S., Raith-Bausch, E., Minke, R. (2018c) Optimized Procedure for Determining the Adsorption of Phosphonates onto Granular Ferric Hydroxide using a Miniaturized Phosphorus Determination Method. *Journal of Visualized Experiments*, **135**, e57618.
- Wang, Z., Shi, M., Li, J., Zheng, Z. (2014) Influence of moderate pre-oxidation treatment on the physical, chemical and phosphate adsorption properties of iron-containing activated carbon. *Journal of Environmental Sciences*, **26**(3), 519-528.

## Characterization and Modelling of Fungal and Bacterial Tannin-degrading Biofilms with Respirometric Techniques

F. Spennati\*, M. Mora\*\*, A. Bardi\*\*\*\*, S. Becarelli\*\*\*, G. Siracusa\*\*\*, S. Di Gregorio\*\*\*, D. Gabriel\*\*, G. Mori\* and G. Munz\*\*\*\*.

\* Laboratorio Cer2co, Consorzio Cuoio-Depur S.p.A, Via Arginale Ovest , 81-S.Miniato 56020, Pisa, Italy (E-mail: [francesco.spennati@cuoioedepur.it](mailto:francesco.spennati@cuoioedepur.it))

\*\* GENOCOV, Department of Chemical, Biological and Environmental Engineering, School of Engineering, Autonomous University of Barcelona, 08193, Bellaterra, Barcelona, Spain (E-mail: [mariaisabel.mora@uab.cat](mailto:mariaisabel.mora@uab.cat); [david.gabriel@uab.cat](mailto:david.gabriel@uab.cat))

\*\*\* Department of Biology, University of Pisa, Via Luca Ghini 13, 56123, Pisa, Italy (E-mail: [simona.digregorio@unipi.it](mailto:simona.digregorio@unipi.it))

\*\*\*\* Department of Civil and Environmental Engineering, University of Florence, Via di S. Marta, 3, 50121, Firenze, Italy (E-mail: [giulio@dicea.unifi.it](mailto:giulio@dicea.unifi.it))

### Abstract

In environmental biotechnology applications for wastewater treatment, fungi tend to be outcompeted by bacteria. The application of fungal-based bioreactors, with similar performance under sterile and non-sterile conditions, for a long-term operation is still challenging. However, an engineered ecosystem, based on fungal and bacterial tannin biodegradation, has been recently and successfully tested in lab-scale bioreactors under non-sterile conditions by F. Spennati and others. In that previous study, the bioreactors (rotating submerged packed bed reactors) were inoculated with a pure culture of *Aspergillus tubingensis* immobilized in PUF cubes and fed with two different tannins (Quebracho and Tara). Promising results were obtained from the bioreactor fed with Quebracho Tannin (QT), which showed a steady fungal biofilm development and satisfactory performance. However, dedicated experiments were still required to characterize the fungal biofilm in terms of kinetics and stoichiometry. To this aim, in the present study the set-up of specifically designed respirometric tests, to characterize tannin-degrading fungal and bacterial biofilms developed under non-sterile conditions, was performed. Afterwards, a mathematical model was developed and applied to describe the respirometric profiles and to estimate kinetic and stoichiometric parameters inherent to the biofilm under study.

### Keywords

Fungal bioreactor; tannins; Aquasim modelling; respirometric tests

## INTRODUCTION

Tanning is the process used to obtain leather from animal skins, and vegetable tannins were the most used tanning agent for centuries. Historically leather was tanned with tannins extracted from wood, leaves, fruits, and roots. Nowadays, chrome and tannins are the most used tanning agents worldwide. The phenolic groups of tannins create hydrogen bonding with collagen proteins, and the colour obtained depends also on the mix of tannins applied. Tannins represent one of the low biodegradability substances present in tannery wastewater with a relevant recalcitrant soluble chemical oxygen demand (COD); moreover, a high concentration of tannins can inhibit biological treatment (Mannucci et al., 2010). This soluble recalcitrant component of tannery effluents is usually removed by means of chemical processes, but the development of a biological treatment to effectively remove this component could lead to environmental and economic advantages (Giaccherini, 2016). Despite the antimicrobial properties of tannins, many fungi, bacteria and yeast are quite resistant to tannins and can use tannins as carbon and energy sources. The biodegradation of natural tannins in the environment is mainly associated with fungi rather than bacteria. Fungi could thus be exploited for the bioremediation of wastewater streams of the tanning industry. The application of a fungal-based bioreactor, that has a similar performance under sterile and non-sterile

conditions in long-term operations, is still a challenging task. However, in a previous work (Spennati et al., 2019) we developed and run a long-term test with continuous bioreactor operation (4 litres volume) to remove tannins with an engineered ecosystem based on fungi and bacteria for application in typical tannery wastewater treatment trains (non-sterile conditions). The tests were carried out in two submerged, packed bed reactors run in parallel. The reactors were inoculated with *Aspergillus tubingensis* attached to polyurethane foam cubes, in fact the reactor biomass was mainly as biofilm on carriers. In general, microorganisms can be observed in the environment as planktonic (free-swimming) organisms or as aggregated communities called biofilms. The transition between these two forms is a complex and highly regulated process characterised by a strong interaction between cells and various environmental signals. Multiple drives influence biofilm formation and structure, and biofilm detachment generally occurs when external forces (such as limitation nutrients diffusion, shear stress etc.) overpower the internal strength of the matrix holding the biofilm together. The reactors were operated for approximately 154 days under different operational conditions with respect to HRT and the organic loading rate. A stable fungal biofilm was reached in the reactor feed with Quebracho tannin (QT) (the most used condensed tannin) with a COD removal up to 53 %.

The kinetics of fungal growth is generally studied in industrial processes for continuous culture systems in chemostat for the production of antibiotics or other relevant commercial products. However, the industrial processes are traditionally based on batch cultures. The main aim of the industrial processes is the production of relevant metabolites, so the substrate is usually glucose and fungal growth is in an axenic culture broth. The conditions adopted in an industrial context are generally different from those in environmental biotechnologies. For bacterial biomasses, Monod kinetics and death regeneration IWA concepts are commonly applied, but there are also other options for fungi. However, Monod-kinetics could also describe growth in filamentous fungi (Kelly et al., 2004) and this model allows comparisons between both microorganisms. Even though the enzymatic pathways were not clear, this approach was chosen to model the fungal biomass. There are few examples in the literature of kinetic models of tannin (tannic acid derived from vegetable tannins) degradation by activated sludge in industrial WWTP (Lu et al., 2009) and even fewer for fungal biomass (Wang et al., 2008). Fungi are rarely used in environmental biotechnologies related to wastewater due to their instability in non-sterile conditions. Few studies in the literature have performed a stoichiometric and kinetic characterisation. Moreover, the parameter estimation did not include COD. Of note is the fact that fungi used in the removal of phenols from vinasses (as a sole carbon source) showed a maximum specific growth rate of 0.06-0.047 h<sup>-1</sup>, a growth yield of 0.38-0.39 g cells g COD<sup>-1</sup> and a saturation constant of 13,525-4558 mg COD L<sup>-1</sup> (García García et al., 1997).

Since fungal biomass is poorly characterised with modelling, dedicated experiments were set-up along with a respirometric procedure in order to obtain kinetics parameters. Respirometry is a technique that measures the oxygen consumption from a biomass in the presence of a substrate. Metabolic respiration is a metabolic process that produces adenosine triphosphate due to the electron transfer from an electron donor (substrate) to an electron acceptor (O<sub>2</sub>, NO<sub>2</sub>, NO<sub>3</sub>, SO<sub>2</sub>, etc.). Respirometry is the measurement and interpretation of the biological electron acceptor consumption (usually oxygen) under well-defined experimental conditions (Andreottola and Esperia, 2001). Respirometry is a powerful tool that can be combined with other techniques to provide information relative to biological wastewater treatment (and in general environmental biotechnologies), including COD fractionation and the characterisation of wastewater, the estimation of kinetic and stoichiometric parameters, the monitoring of bioprocesses, and the evaluation of potential toxicity and inhibition effects over different suspended cultures, mainly in aerobic processes (Mora, 2014). The principal output of respirometry is the oxygen uptake rate

(OUR), that represents the consumption of dissolved oxygen (DO) per unit of time. This value is related to the catabolic and anabolic functions of the biological system. It is possible to distinguish between the endogenous OUR ( $OUR_{end}$ ), in other words, the consumption of oxygen observed without a substrate, and the exogenous OUR ( $OUR_{ex}$ ), the consumption of oxygen observed in the presence of a substrate and related to its oxidation. Respirometry has rarely been applied to fungal biomasses and biofilms. The majority of studies focus on homogeneous respirometry in sterile conditions (Schinagl et al., 2016), on sterile solid matrices (Willcock and Magan, 2001), on soil matrices to analyse some behaviours of fungi and bacteria (Boening et al., 1995), or with olive mill wastewater treatment (Caffaz et al., 2007). Sometimes oxygen consumption is exploited to model fungal growth. Since respirometric assays for fungal and bacterial biofilm in non-sterile conditions are still lacking, in the present study a dedicated respirometric procedure has been developed.

## MATERIALS AND METHODS

### Respirometric tests set-up

Respirometric tests are performed in a respirometer. A respirometer is a vessel equipped with probes to measure various elements (temperature, pH, oxygen concentration etc.) and actuators that control the conditions (mixing device, thermostatic water bath, pH dosage solutions, etc.). Respirometric tests were performed in an LFS-type respirometer under controlled conditions. The respirometric vessel had a volume of 0.3L and was provided with a gas diffuser. The respirometer was jacketed with temperature control via the recirculation of a thermostatic water bath (Polystat24, Fisher Scientific, Spain). Vessel mixing was ensured by magnetic stirrers. Temperature and pH probes (SenTix82, WTW, Germany) and a dissolved oxygen (DO) probe (CellOx 325, WTW, Germany) were connected to a benchtop meter (Inolab Multi 740, WTW, Germany) and a computer for data acquisition and process monitoring. The pH was controlled through the addition of NaOH and HCl solutions with a microburette (Multi-Burette 2-SD, Crison Instruments, Spain). The biofilm to be characterized in the respirometer was obtained from the bioreactors mentioned above (see Spennati et al., 2019 for detailed information) which contained the inoculated polyurethane foam (PUF) cubes in a rotating cage and were provided of a pH control system and continuous aeration. Each respirometric test required withdrawing 5 of the PUF cubes from the bioreactors, a pre-wash of the biofilm with phosphate buffer and an abiotic stage in the respirometric vessel. The use of respirometric tests with immobilised biomass is a new technique without a defined conventional procedure, thus requiring several months of attempts to identify a feasible procedure. Fungal pellets, fresh immobilised biomass and immobilised biomass sampled from the treatment reactor were used to test and define the respirometric procedure. Since the dry mass was assessed with 3 PUF cubes, the respirometric test procedure (using a 0.3 L vessel) required the removal of 10 + 3 PUF cubes from. The PUF cubes were placed in sterile water for 24 hours in endogenous conditions before the test water was replaced. The pH set point was controlled during the tests by dosing with 0.05 M NaOH and HCl solutions. The air flow was regulated at 10 N mL min<sup>-1</sup> with a mass flow controller (TecFluid, USA), and mixing was guaranteed with a magnetic stirrer. The PUF cubes were fixed in the middle of the vessel, far from the surface and the bottom of the vessel to avoid direct contact with the final part of the probe and to minimise fluctuations. The resulting profile was accepted as repeatable after multiple pulses. Before each pulse, the endogenous conditions and  $K_{la}$  were evaluated with an air cut (Mora, 2014). The concentrations tested were within the range of 47 mg L<sup>-1</sup> to 476 mg L<sup>-1</sup> of COD for QT. The QT pulses were chosen, as shown in the Table 1, in order to obtain a similar ratio substrate/microorganism (S/X) among the respirometer and the different condition tested in the reactor. The results of the respirometric tests on biomass samples from treatment were coupled to the continuous operation performance and parameters estimation of Monod kinetics with Aquasim.



**Table 1.** Comparison between the different QT concentrations and S/X ratio in the bioreactors and in the respirometer LFS

Vessel	QT (mg COD L <sup>-1</sup> )	S/X ratio (g COD g COD <sup>-1</sup> )
Reactor	25	0.7
Reactor	50	1.4
Reactor	175	4.9
Reactor	350	9.9
Respirometer LFS	47	1.0
Respirometer LFS	93	2.0
Respirometer LFS	233	4.9
Respirometer LFS	477	10.1

### Biofilm model structure definition

The Aquasim software includes a biofilm compartment (consisting of a biofilm phase and a bulk fluid phase) that was used to simulate the behavior of biomass growing on the support media and the diffusion phenomena (Boltz et al., 2010). The Aquasim biofilm compartment supports the biofilm modelling in different type of biofilm bioreactors (Wanner and Morgenroth, 2004). The definition of the characteristics of the biofilm reactor was a necessary step before running the simulations. The first step was the definition of the boundary conditions of the reactor required for the biofilm compartment. The reactor volume was imposed to be 4 L and the reactor type was “confined” with a constant total volume for biofilm and bulk fluid (no biofilm growth out of the PUF). The pore volume was defined as “liquid phase only” and influent suspended solids were neglected, since the inlet COD was soluble. For the same reason, the biofilm matrix was modelled as “rigid” and the diffusive mass transport of solids was neglected. Among the main hypothesis of the model, the adsorption was neglected and the diffusion was considered only for tannins and oxygen. The surface area and the biofilm thickness are biofilm parameters described in the model as follow: the 100 immobilised PUF cubes (2x2x2 cm) were modelled as 100 spheres with 2 cm of diameter, in fact the observed diffusion of tannin shown an isotropic behaviour and a radial gradient from outside to the centre of the carriers. The plastic carriers were neglected due to the high porosity and the small volume occupied by the plastic support. The biofilm thickness was 1 cm (initial condition) and the surface area was described in Aquasim as described in the following equation as suggested in Aquasim manual:  $A = 4 \cdot \pi \cdot n_{sp} \cdot (r_{sp} + z)^2$ , where: A is the surface area (m<sup>2</sup>);  $n_{sp}$  is the number of spherical particles (100);  $r_{sp}$  is the radius of the spherical particles (0.01 m); z is the distance from the substratum (program variable). The biofilm density was calculated from pure fungi samples. The samples were inserted in graduated volumetric vessel and the dry mass of the biomass was measured with the standard procedure. The obtained pure fungal biofilm average density was 12.5 g L<sup>-1</sup> as dry mass and this value was adopted in the model. Nevertheless, in the literature a high variability in fungal biofilm density (Spigno et al., 2003) is reported. Subsequently, the transport phenomena and mass transfer related parameters were defined. The water diffusion coefficient of oxygen in water ( $D_w$ ) was  $8.96 \cdot 10^{-6}$  m<sup>2</sup> h<sup>-1</sup> (Horn and Morgenroth, 2006) and the internal diffusion in the biofilm could be expressed as  $D_f = f_{dif} \cdot D_w$  where:  $D_f$  is the diffusion coefficient in the biofilm (m<sup>2</sup> h<sup>-1</sup>);  $D_w$  is the diffusion coefficient in water (m<sup>2</sup> h<sup>-1</sup>);  $f_{dif}$  relative diffusivity (adimensional). The effective internal diffusion coefficient in biofilms can change with the biofilm density and the biofilm thickness; usually, the relative diffusivity ( $f_d$ ) ranges from 40 % to 90 % (Hibiya et al., 2004). Some authors found a correlation between the oxygen profiles and the biomass distribution in biopellets of *Aspergillus niger* (Hille et al., 2005) and others proposed that the pellet density could allow to predict the steepness of oxygen concentration profiles. The biofilm density reported in the previous paragraph, supports the adoption of a  $f_d$  value equal to 80 % (Horn and Morgenroth, 2006). The diffusion of phenols in water was estimated to be  $8.47 \cdot 10^{-10}$  m<sup>2</sup> s<sup>-1</sup>

( $2.35 \cdot 10^{-13} \text{ m}^2 \text{ h}^{-1}$ ) (Fan et al., 1990) and that of natural tannins to be  $5 \cdot 10^{-11} \text{ m}^2 \text{ s}^{-1}$  ( $1.38 \cdot 10^{-14} \text{ m}^2 \text{ h}^{-1}$ ) (Tzibranska, 2000). The tannins diffusion was modelled with the same equation used for oxygen diffusion. However, the dissolved compounds (oxygen, tannins) should pass first through the mass transfer boundary layer (external mass transfer) via convection and, then, through the biofilm matrix (internal mass transfer) via diffusion (Khabibor Rahman et al., 2009). Nevertheless, in these simulations the external mass transfer was neglected due to the mixing in the reactor. The  $f_{\text{dif}}$  chosen was 80 % (Stewart, 1998).

## RESULTS AND DISCUSSION

### Respirometric test

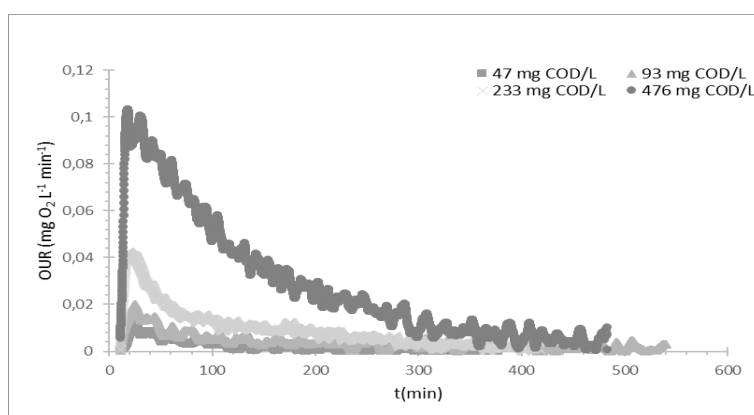
The immobilised biomass from the reactor was tested in respirometer with a dedicated procedure described in Materials and Methods. The development of a procedure for respirometric tests with immobilised biomass required several trials also with pure fungi biomass (*Aspergillus tubingensis*). This pure fungal biomass required an endogenous phase and multiple wake up pulses. These tests were performed also to verify the tannins biodegradation capacity of selected fungal strain versus QT. On the Figure 1 four pulses of QT are represented, with an increasing concentration of COD, tested in the respirometer filled with the immobilised biomass sampled from the treatment reactor. The respirometric profiles were used, as described in the following section, for modelling and characterising of the biomasses.

### Reactor modelling

The modelling of QT degrading fungal biofilm was carried out by coupling the results of tests performed in bioreactor with those of respirometric techniques applied to attached biomass. The model was designed with the software Aquasim and the dedicated compartment to simulate dynamic processes in biofilm bioreactors. The biofilm features and transport parameters were defined by measurements or literature, while to describe the microbial kinetics it was selected a Monod kinetic equation with substrate inhibition where the parameters were calibrated with the data collected.

### Microbial parameters estimation and model validation

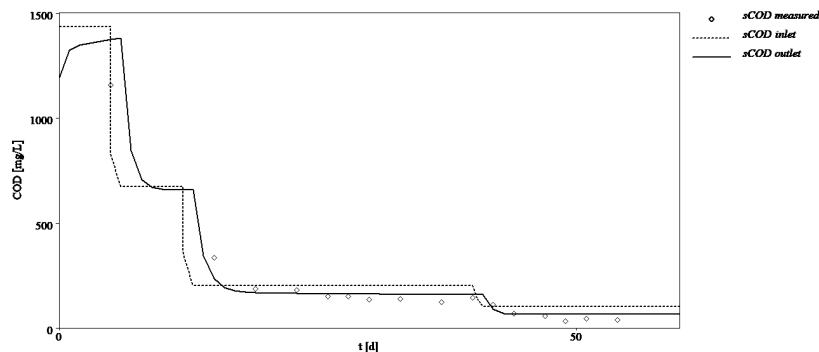
The tests in the respirometer were used to preliminary characterise the kinetic and stoichiometric parameters of the fungal biomass. A simple Monod kinetics was used for a respirometric estimation of microbial parameters, while a biofilm model was used to simulate the reactor performance. For the decay coefficient ( $b_f$ ) of fungal biomass it was adopted the value suggested in literature  $0.22 \text{ d}^{-1}$  for *Aspergillus niger* (Wang et al., 2008).



**Figure 1.** Respirograms with immobilised fungi from the treatment reactor and QT pulses ( $\text{OUR}_{\text{ex}}$ )

The estimation of the yield coefficient ( $Y_f$ ) was done through the calibration of the parameters with the respirograms. The biodegradable COD was assumed as 17 % of the total COD to estimate  $Y_h$ .

This value was extrapolated from an average performance in the reactor at steady state, with similar conditions of the respirometric tests (concentration and S/X ratio). The obtained  $Y_f$  was  $0.45 \pm 0.01$  mg COD mg COD<sup>-1</sup> was quite close to the value suggested in literature for *Aspergillus niger* with glucose  $0.37$  mg dry mass mg glucose<sup>-1</sup> ( $= 0.51$  mg COD mg COD<sup>-1</sup>) (Aguilar et al., 2001). The active biomass ( $X_f$ ) in the reactor at steady-state was estimated at the two different HRT tested in the reactor. The estimated biomass concentrations were  $251$  (mg COD L<sup>-1</sup>) of active biomass for a Hydraulic Retention Time (HRT) of 52 h and  $465$  (mg COD L<sup>-1</sup>) for HRT of 28 h. To estimate the affinity constant ( $K_{sf}$ ) and the maximum specific growth rate ( $\mu_f$ ) of the biomass of the treatment reactor a simple Monod kinetics without diffusion in biofilm, adsorption neither inhibition was applied. The model was applied to a respirometric test with the biomass collected from the reactor at steady state. The respirometric tests were performed with pulses of 1, 2, 5 and 10 millilitre of QT ( $10$  g L<sup>-1</sup>) in a vessel of  $0.3$  L with 10 PUF cubes. The best estimation of  $K_{sf}$  and  $\mu_f$  were  $800$  mg COD L<sup>-1</sup> and  $2.88$  d<sup>-1</sup>, respectively, even though, the best fitting simulations overestimated the measured OURs. Multiple simulations performed on respirometer tests results showed that the limiting step was the diffusion in the biofilm and it was not achieved a better fitting of the data since this model did not take in account diffusion in biofilm. The results 154 days of the reactor operation were used to obtain a better estimation of  $\mu_{hf}$  and  $K_f$  estimate the inhibition due to the QT ( $K_{iq}$ ). The inhibition kinetics was implemented in Aquasim with the biofilm compartment. The best estimation obtained was represented on Figure 2 and the microbial kinetics coefficients of the biofilm were reported in Table 2.



**Figure 2.** Measured and simulated values for outlet COD for biofilm model of the reactor

**Table 2.** Summary table with estimated and chosen microbial kinetics coefficients

Symbol	Characterisation	Value	Units	Reference
$Y_f$	Yield coeff. for fungi in aerobic growth	0.45	g COD g COD <sup>-1</sup>	This study
$b_f$	Decay coefficient for heterotrophic biomass	0.22	d <sup>-1</sup>	(Wang et al., 2008).
$f_p$	Fraction of inert COD generated in decay	0.08	g COD g COD <sup>-1</sup>	(Andreottola and Esperia 2001)
$K_{iq}$	Inhibition constant	13	g COD m <sup>-3</sup>	This study
$K_{sf}$	Half-saturation coefficient	993	g COD m <sup>-3</sup>	This study
$\mu_f$	Maximum growth rate on substrate	5.39	d <sup>-1</sup>	This study

## CONCLUSION

We demonstrated that a fungal based bioreactor is stable in non-sterile conditions, but that it was also able to be modelled and can be described using Monod kinetics with inhibition. The applicative consequences of these  $\mu_{hf}$  and  $K_f$  are that fungi can grow very quickly if the substrate (QT) is

abundant, which is at this level more typical for solid matrices than for wastewater, even though the inhibition should be also considered.

## ACKNOWLEDGEMENT

The authors thanks MANUNET III FUNCELL Project number n. MNET17/ENER-1143.

## REFERENCES

- Aguilar, C.N., Augur, C., Favela-Torres, E., Viniestra-González, G. (2001). Production of tannase by *Aspergillus niger* Aa-20 in submerged and solid-state fermentation: influence of glucose and tannic acid. *J. Ind. Microbiol. Biotechnol.*, **26**, 296-302.
- Andreottola, G., Esperia (2001). *Respirometria applicata alla depurazione delle acque: principi e metodi*, Collana scientifico-divulgativa Monographia, Università di Trento.
- Boening, D., Hendricks, C.W., Rossignol, A.M. (1995). Automated respirometer method for microbial toxicity assessment of low-level zinc contamination in soil. *Bull. Environ. Contam. Toxicol.*, **55**, 817-824.
- Boltz, J.P., Morgenroth, E., Sen, D. (2010). Mathematical modelling of biofilms and biofilm reactors for engineering design. *Water Sci. Technol.*, **62**, 1821-1836.
- Caffaz, S., Caretti, C., Morelli, M., Lubello, C., Azzari, E. (2007). Olive mill wastewater biological treatment by fungi biomass. *Water Sci. Technol.*, **55**, 89-97.
- Fan, L.S.I., Leyva-Ramos, R., Wisecarver, K.D.Z.B. (1990). Diffusion of phenol through a biofilm grown on activated carbon particles in a draft-tube three-phase fluidized-bed bioreactor. *Biotechnol. Bioeng.*, **35**, 279-286.
- García García, I., Bonilla Venceslada, J.L., Jiménez Peña, P.R., Ramos Gómez, E., 1997. Biodegradation of phenol compounds in vinasse using *Aspergillus terreus* and *Geotrichum candidum*. *Water Res.*, **31**, 2005-2011.
- Giaccherini, F. (2016). Modelling tannery wastewater treatment to evaluate alternative bioprocesses configurations. PhD thesis.
- Hibiya, K., Nagai, J., Tsuneda, S., Hirata, A. (2004). Simple prediction of oxygen penetration depth in biofilms for wastewater treatment. *Biochem. Eng. J.*, **19**, 61-68.
- Hille, A., Neu, T.R., Hempel, D.C., Horn, H. (2005). Oxygen profiles and biomass distribution in biopellets of *Aspergillus niger*. *Biotechnol. Bioeng.*, **92**, 614-623.
- Horn, H., Morgenroth, E. (2006). Transport of oxygen, sodium chloride, and sodium nitrate in biofilms. *Chem. Eng. Sci.*, **61**, 1347-1356.
- Kelly, S., Grimm, L.H., Hengstler, J., Schultheis, E., Krull, R., Hempel, D.C. (2004). Agitation effects on submerged growth and product formation of *Aspergillus niger*. *Bioprocess Biosyst. Eng.*, **26**, 315-323.
- Khabibor Rahman, N., Bakar, M.Z.A., Uzir, M.H., Harun Kamaruddin, A. (2009). Modelling on the effect of diffusive and convective substrate transport for biofilm. *Math. Biosci.*, **218**, 130-137.
- Lu, Z., Sun, X., Yang, Q., Li, H., Li, C. (2009). Persistence and functions of a decolorizing fungal consortium in a non-sterile biofilm reactor. *Biochem. Eng. J.*, **46**, 73-78.
- Mannucci, A., Munz, G., Mori, G., Lubello, C. (2010). Anaerobic treatment of vegetable tannery wastewaters: A review. *Desalination*, **264**, 1-8.
- Mora, M.G. (2014). Characterization of s-oxidizing biomass through respirometric techniques under anoxic and aerobic conditions. PhD thesis.
- Schinagl, C.W., Vrabl, P., Burgstaller, W. (2016). Adapting high-resolution respirometry to glucose-limited steady state mycelium of the filamentous fungus *penicillium ochrochloron*: method development and standardisation. *PLoS One*, **11**, 1-18.
- Spennati, F., Mora, M., Tigini, V., La China, S., Di Gregorio, S., Gabriel, D., Munz, G. (2019).

- Removal of Quebracho and Tara tannins in fungal bioreactors: Performance and biofilm stability analysis. *J. Environ. Manage.*, **231**, 137-145.
- Spigno, G., Pagella, C., Fumi, M.D., Molteni, R., De Faveri, D.M. (2003). VOCs removal from waste gases: Gas-phase bioreactor for the abatement of hexane by *Aspergillus niger*. *Chem. Eng. Sci.*, **58**, 739-746.
- Stewart, P.S. (1998). A review of experimental measurements of effective diffusive permeabilities and effective diffusion coefficients in biofilms. *Biotechnol. Bioeng.*, **59**, 261-272.
- Tzibranska, T. I. (2000). Extraction: I. Kinetics and Diffusion Coefficients. *Comptes Rendus l'Academie Bulg. des Sci.*, **53**, 6-71.
- Wang, L., Ridgway, D., Gu, T., Moo-Young, M. (2008). Kinetic modeling of cell growth and product formation in submerged culture of recombinant *aspergillus niger*. *Chem. Eng. Commun.*, **196**, 481-490.
- Wanner, O., Morgenroth, E. (2004). Biofilm modeling with AQUASIM. *Water Sci. Technol.*, **49**, 137-144.
- Willcock, J., Magan, N. (2001). Impact of environmental factors on fungal respiration and dry matter losses in wheat straw. *J. Stored Prod. Res.*, **37**, 35-45.

# Cost Effective Improvement of the Performance of an SBR System Using a Floating Seal

P. Szombathy\* and A. Jobbágy\*

\*Budapest University of Technology and Economics, Department of Applied Biotechnology and Food Science, Szent Gellért tér 4, H-1111 Budapest, Hungary (E-mail: [szombipepe@gmail.com](mailto:szombipepe@gmail.com))

## Abstract

In a Sequencing Batch Reactor (SBR) according to the sequenced operation utilization of oxygen having been blown into the system is typically undesirably low during the early periods of the cycles due to the relatively low water level. On the other hand, oxygen that can penetrate into the reactors through the open water surface may cause both metabolic and kinetic inhibition in the non-aerated parts or phases of the operation hindering efficient denitrification and biological P-removal. Purpose of the research has been to verify the use of a floating seal on the moving surface of an SBR reactor for excluding oxygen from non-aerated reactors. Both nitrification and denitrification efficiency proved to be higher, and higher amount of biologically removed phosphorus was detected in the seal-covered train, even without chemical dosing. The SVI values in the two trains proved to be close to each other, despite the high difference in chemical dosing. In winter time the seal-covered reactor had  $\sim 1.5$  °C higher wastewater temperature than the uncovered one.

## Keywords

SBR reactor; floating seal; nutrient removal; sludge settling; chemical savings

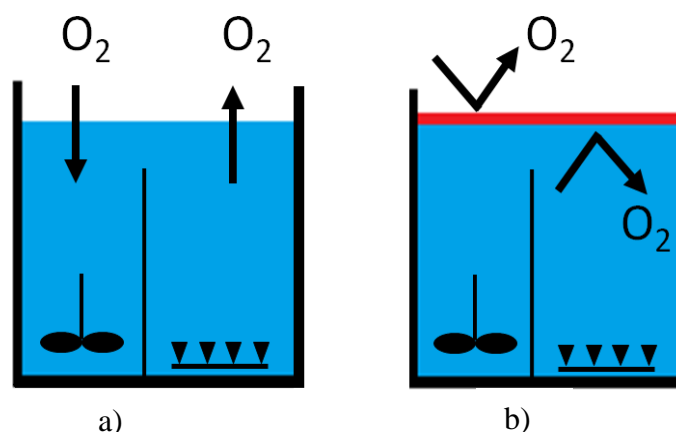
## INTRODUCTION AND PURPOSE OF THE RESEARCH

The Sequencing Batch Reactor (SBR) technology includes reactors for biological (and chemical) wastewater treatment and secondary clarifier in one basin separated in time. SBR systems have five typical steps continuously repeated during operation: fill, react, settle, decant and idle (Metcalf and Eddy, 2003). At this original layout more SBR tanks are needed, one reactor is receiving influent wastewater while other reactors are at treatment cycle. Several modifications have been created to achieve nitrogen and phosphorus removal. One of these modifications was carried out by UTB Envirotec Ltd. resulting in the Cyclator technology.

In a Sequencing Batch Reactor, according to the sequenced operation, utilization of oxygen having been blown into the system is typically undesirably low during the early periods of the cycles due to the relatively low water level. However, substrate concentration is the highest at the beginning of filling and decreases gradually as it is consumed by the biomass. During this time batch kinetics may apply. The substrate concentration changes in time resulting changes in oxygen demand. Initially the substrate concentration is higher than in continuous-flow systems. Due to the batch kinetics the SRT (Solids Retention Time) required is lower than in the continuous-flow activated-sludge processes (for BOD removal <1h, for nitrification 1-3 h), although the effective SRT is lower (the biomass is aerated for a shorter time) (Metcalf and Eddy, 2003).

On the other hand, oxygen that can penetrate into the reactors through the open water surface may cause both metabolic and kinetic inhibition in the non-aerated parts or phases of the operation (Plósz et al., 2003; Wanner and Jobbágy 2014; Jobbágy et al., 2015) hindering efficient denitrification and biological P-removal. Since the water level is relatively low compared to those of common activated sludge basins, oxygen penetration through the same surface area can result in considerably higher oxygen concentrations hitting the biomass of the reactors (Figure 1). This

reaction is especially dangerous when the influent is in lack of readily biodegradable carbon source having been experienced worldwide.



**Figure 1.** a) Oxygen can penetrate into non-aerated selectors and may leave aerated reactor quickly. b) Oxygen does not penetrate into seal-covered selector and may leave seal-covered aerated reactor slower

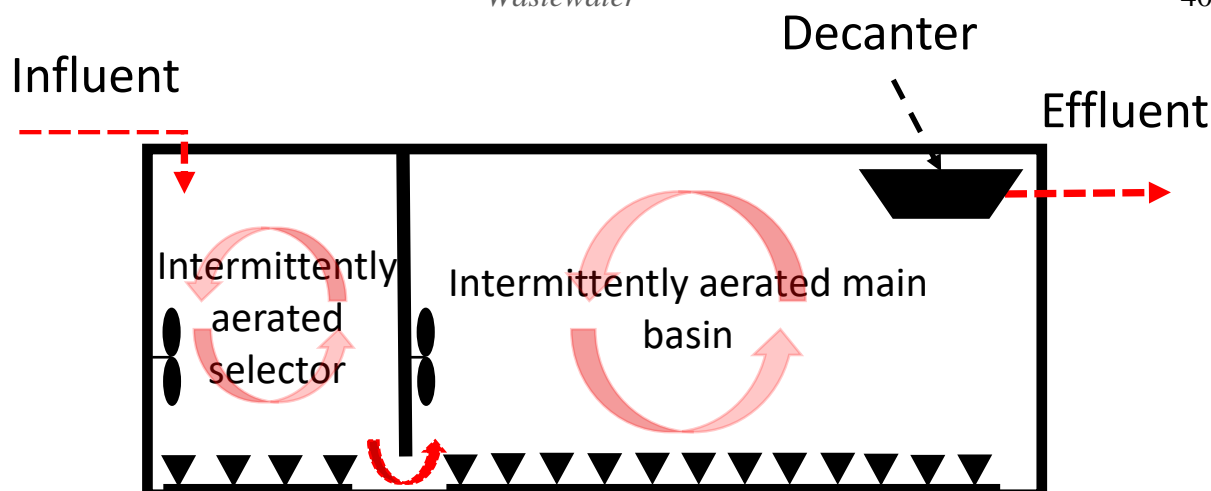
For biological nitrogen removal there are three possible options in the SBR systems: mixed non-aerated filling period, cycling aeration during react period (on/off switching), as well as operating at low DO concentrations, that is likely to produce filamentous overgrowth, however. Cycling aeration is used e.g. in Cyclator technology, where the selector and main reactor are alternately aerated. However, according to Metcalf and Eddy, (2003) denitrification during mixed non-aerated filling is the most efficient. It also provides a selector operation to prevent filamentous sludge bulking. Decant volume is only 20-30 % of the total tank volume, and the remaining nitrate can be eliminated during filling and mixing cycles. This results a maximum of nitrogen removal efficiency that is 70-80 %. This value may not be enough at WWTPs (Wastewater Treatment Plants) with high influent ammonia concentrations and strict limitations in effluent TN concentrations.

Purpose of the research has been to verify the benefits of using a floating seal on the moving surface of an SBR reactor. This research focused on comparison of the nitrogen and biological phosphorus removal of the alternately aerated Reference train (with alternately aerated selector and reactor, and continuous inflow into selector) and the Test train with non-aerated selector and alternately aerated reactor (continuous inflow into non-aerated selector).

## EXPERIMENTAL PROCESS

The experiment was carried out by using an SBR system with two trains designed by UTB Envirotec Ltd. in Hungary. The Cyclator system used has a staged reactor including originally a temporarily aerated selector and a main reactor also temporarily aerated (Figure 2). The influent wastewater flows continuously into the selector, even during sludge settling and decanting clarified wastewater. This results that only one train could serve for proper operation, however, the Cyclator wastewater treatment plants (Cyclator WWTPs) are designed with two trains for safety reasons.

The experiment was started by converting the selector of the Test train into a non-aerated basin and covering the whole surface of this system by a floating seal (Figure 3). There was no technological change executed in the Reference train. In the absence of precisely controlled activated sludge recycling, the biomass concentration in the selectors could depend on the random transport of wastewater from the main reactor.



**Figure 2.** Original bioreactor operation with intermittently aerated selector remaining in the Reference train



**Figure 3.** Seal covering the experimental system

On the basis of the influent data, marginal C-source availability, even carbon deficiency could be assumed in the system as shown in Table 1.

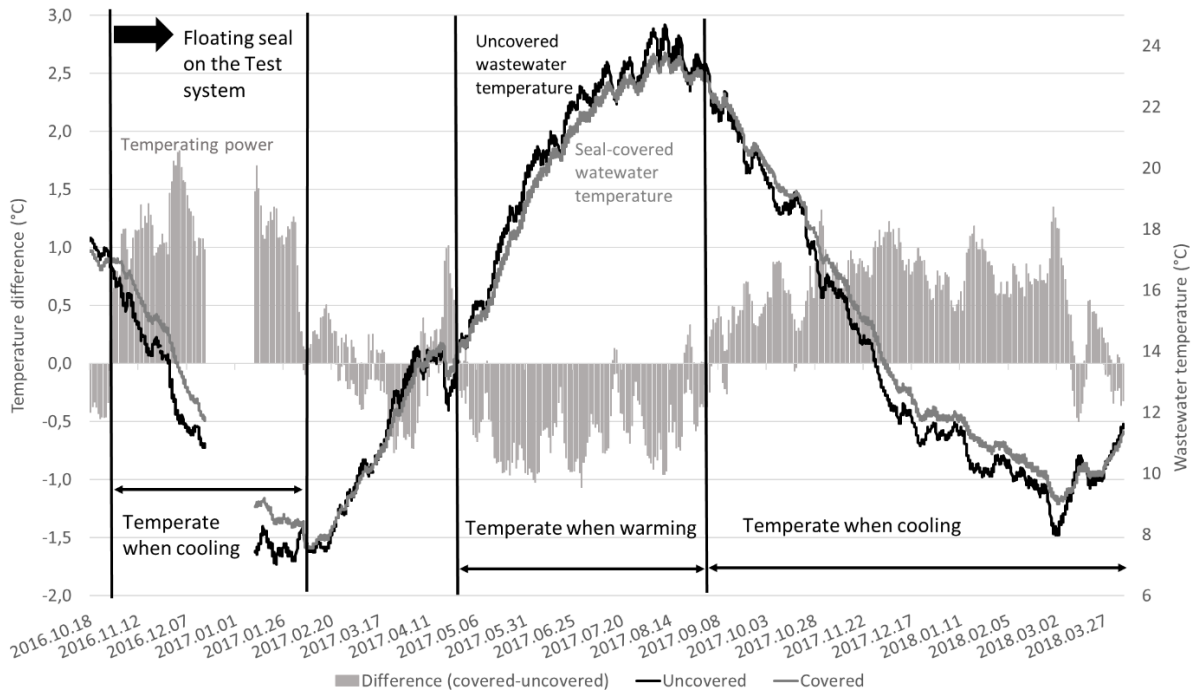
**Table 1** Original design parameter and average values measured during the experiment

Measured by UTB Envirotec Ltd.	Daily volume <sup>3</sup> [m <sup>3</sup> /d]	pH [-]	COD [mg/l]	NH <sub>4</sub> -N [mg/l]	TN [mg/l]	TP [mg/l]	TSS [mg/l]
Design parameter	750	6.5-9.0	1 123	67	103	16,8	655
Influent	515	7.8	857	92	128	13,8	-
Effluent		7.3	39	0,9	4	1.5	11
Limit	-	-	125	5	25	2	35

## RESULTS AND DISCUSSION

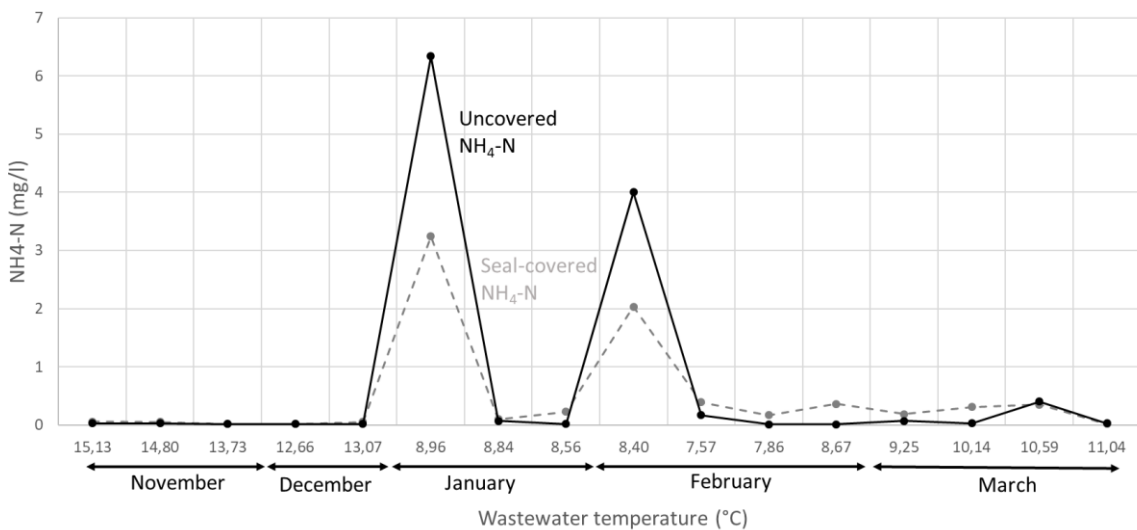
The experimental results confirmed the presumed advantages appropriately. In the winter period, with ~ 7-8 °C influent wastewater temperature 1-1.5 °C higher values could be measured in the effluent of the seal-covered Test system shown in Figure 4. The Test train could keep a relative stability also during highly increasing temperature.





**Figure 4.** Effluent temperature in Test train (covered) and Reference train (uncovered)

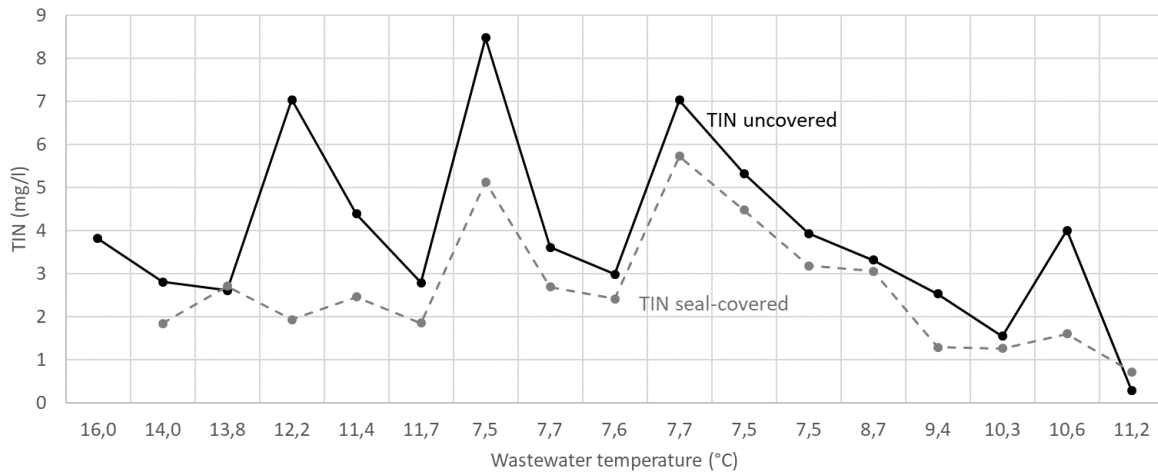
The most significant advantage of the insulation potential has been expressed in the higher nitrification efficiency under cold conditions, despite the decreased aeration capacity (as shown in Figure 5). At 7-9 °C wastewater temperatures 2-3 mg NH<sub>4</sub>N/l less ammonia concentrations were detected in the effluent of the Test system. The difference in wastewater temperatures was 1-1.5°C ensuring autotrophic organisms to consume ammonia with a higher  $\mu$  value (specific growth rate) in the seal-covered train.



**Figure 5.** Effluent ammonia concentrations measured during the experiment

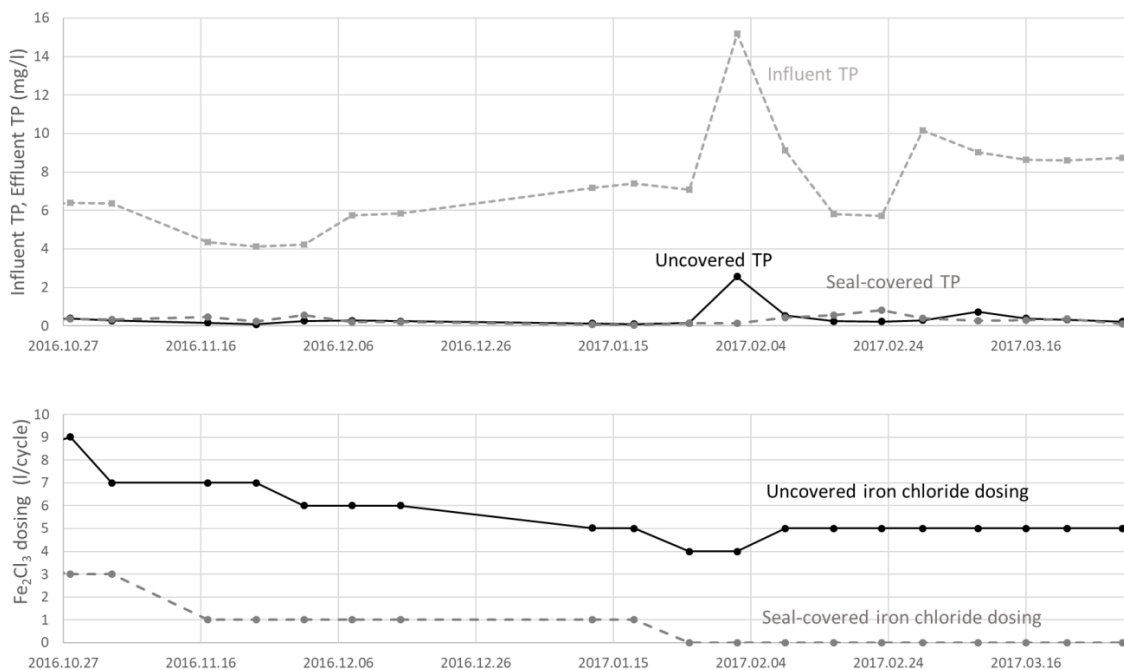
Efficiency of denitrification proved to be also higher in the Test (seal-covered) train. Therefore, despite the higher nitrification efficiency, 1-5 mg N/l lower values could be detected in the effluent TIN (Total Inorganic Nitrogen) concentrations of the Test system (as shown in Figure 6). This result may be attributed to both converting the alternately aerated selector into non-aerated basin in

the Test train, and reserving carbon source for denitrification by excluding oxygen penetration through the surface.

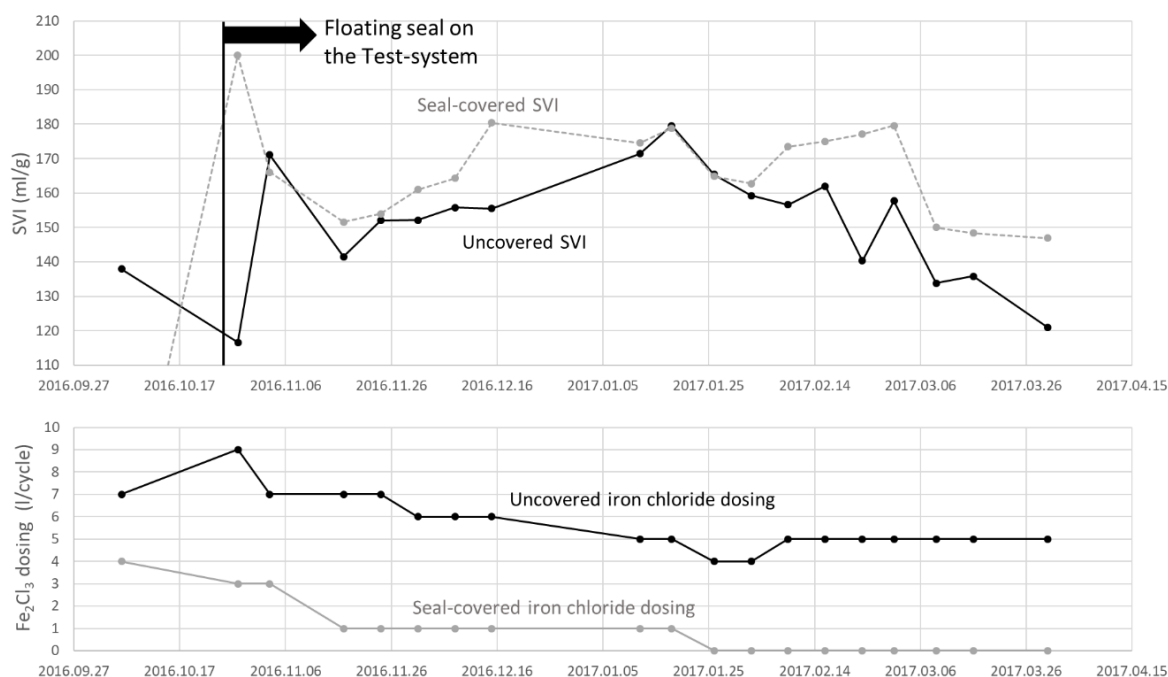


**Figure 6.** Effluent TIN concentrations at different temperatures during the experiment

Maintaining PAOs (Phosphorous Accumulating Organisms) in an activated sludge system is extremely useful for a good floc structure and settleability, since these organisms are floc-formers. Creating a non-aerated selector may obviously help in this respect. However, growth of PAOs may generally have difficulties in winter. Figure 7 shows that in the seal-covered system a stable and continuous growth of PAOs could be observed even in wintertime.



**Figure 7.** Influent and effluent TP concentrations and chemical dosing during the experiment



**Figure 8** Changes of the SVI values and chemical dosing in the seal-covered and uncovered systems

The iron chloride dosing could be decreased progressively in the experimental Test train down to zero, and still the effluent total phosphorus concentrations of the seal-covered system were significantly lower than those of the uncovered train. When the influent TP concentration increased suddenly, the seal-covered train was able to remove the excess phosphorous biologically, while the reference train could not appropriately handle it despite the chemical dosing.

Figure 8 illustrates the SVI (Sludge Volume Index) values measured throughout the experiment. SVI of the uncovered system started below 120 cm<sup>3</sup>/g, whereas at the beginning SVI was detected high, 200 cm<sup>3</sup>/g in the Test system. During the experiment settleability of the biomass of the Test system remained close to that of the Reference system, although the chemical dosed was much less, decreasing down to zero from 2017. 01. 25 until 2017. 03. 25, i.e. during the cold season until the end of the experiment. It can be assumed that the good settleability of the biomass of the Test system was based on the relatively high ratio of the PAOs in the seal-covered system.

## CONCLUSIONS

In the Test system important benefits have been achieved through fully excluding oxygen from the selector by withdrawing aeration and seal-covering the moving surface. Lower effluent values were typical in the modified system, leading to cleaner environment and decreasing water pollution taxes. Less iron chloride dosing, down to zero, could be applied due to efficient biological phosphorous removal. Potential of temperating the wastewater benefits in cost savings at blowers and higher nitrification efficiency, especially in wintertime. The sludge volume indexes in the two trains proved to be close to each other, despite the high difference in chemical dosing. SVI values could likely be further improved by well controlled sludge recirculation.

**ACKNOWLEDGEMENT**

The project was funded by the Budapest University of Technology and Economics and the UTB Envirotec Ltd. The cooperation of Karsai Holding Ltd. in establishing the floating seal is highly acknowledged.

**REFERENCES**

- Jobbágy, A., Weinpel, T., Bakos, V., Vánkos, Zs. (2015) Factors potentially converting non-aerated selectors into „low-S – low-DO basins”, effects of seal-covering. Proceedings of 12<sup>th</sup> IWA Specialised Conference on Design, Operation and Economics of Large Wastewater Treatment Plants, 6-9 September, 2015, Prague, Czech Republic, 149-155.
- Metcalf & Eddy Inc. (2003) Wastewater Engineering: Treatment and Reuse, McGraw-Hill, Boston.
- Plósz, B. Gy., Jobbágy, A., Grady, Jr. C. P. L. (2003) Factors influencing deterioration of denitrification by oxygen entering an anoxic reactor through the surface. *Water Research*, **37**, 853-863. DOI: [https://doi.org/10.1016/S0043-1354\(02\)00445-1](https://doi.org/10.1016/S0043-1354(02)00445-1).
- Wanner, J., Jobbágy, A. (2014) Activated Sludge Solids Separation. In: Activated Sludge – 100 Years and Counting, D. Jenkins & J. Wanner (eds.), IWA Publishing, Glasgow, UK, 171-194. ISBN 9781780404936.

# Ecotoxicity Effects of Carbon Nanomaterials on the Activated Sludge Microorganisms

M. Tomaszewski\*, F. Gamoń\*, D. Łukowiec\*\*, A. Zgórska\*\*\* and A. Ziemińska-Buczyńska\*

\* Environmental Biotechnology Department, Silesian University of Technology, Akademicka 2, 44-100 Gliwice, Poland (E-mails: [mariusz.tomaszewski@polsl.pl](mailto:mariusz.tomaszewski@polsl.pl); [filip.gamon@gmail.com](mailto:filip.gamon@gmail.com); [aleksandra.ziembinska-buczynska@polsl.pl](mailto:aleksandra.ziembinska-buczynska@polsl.pl))

\*\* Institute of Engineering Materials and Biomaterials, Silesian University of Technology, Konarskiego 18a, 44-100 Gliwice, Poland (E-mail: [dariusz.lukowiec@polsl.pl](mailto:dariusz.lukowiec@polsl.pl))

\*\*\* Central Mining Institute, Plac Gwarków 1, 40-166 Katowice, Poland (E-mail: [azgorska@gig.eu](mailto:azgorska@gig.eu))

## Abstract

The development of new technologies in industry and science entails the growing production of advanced materials, including engineered nanomaterials. Nanotechnology has become one of the fastest-growing fields of science and the widespread use of nanomaterials increases the emission of nano-pollutants into the environment. Carbon nanoparticles are a particularly interesting group. Their relatively stable structure makes them able to migrate in the environment over long distances and enter wastewater treatment plants (WWTP) becoming a potential detrimental factor for sewage treatment processes. Therefore, the aim of this study was to determine the potential toxicity on the activated sludge microorganisms of four selected carbon nanostructures: graphene oxide (GO), reduced graphene oxide (rGO), multi-walled carbon nanotubes (MWCNTs) and oxidized multi-walled carbon nanotubes (f-MWCNTs). This study shows that short term exposure on GO, rGO, MWCNTs, and f-MWCNTs can be toxic for the microbial activity of activated sludge. Definitely, the effects of the nanomaterials increase with exposure time and hence the degree of flocs penetration. Further, while the effect of the nanomaterial exposure strongly depends on its individual properties, a unique microbial consortium of the activated sludge and environmental conditions, this study is a contribution to evaluate and understand the risk resulting from CNMs presence in the WWTP.

## Keywords

Ecotoxicology; nanomaterials; grapheme; carbon nanotubes; activated sludge

## INTRODUCTION

The development of new technologies in industry and science entails the growing production of advanced materials, including engineered nanomaterials (ENMs). One of the most popular groups of ENMs is carbon nanomaterials (CNMs), including, among others graphene oxide (GO), reduced graphene oxide (rGO), single-walled and multi-walled carbon nanotubes (SWCNTs and MWCNTs), both, pristine or functionalized. CNMs possess excellent physicochemical, mechanical, and electrochemical properties, as well as they can be widely applied (Kang et al., 2008; Gagliardi et al., 2011). Nanotechnology has become one of the fastest-growing fields of science and the widespread use of nanomaterials increases the emission of nano-pollutants into the environment (Bundschuh et al., 2018). Their relatively stable structure (Flores-Cervantes et al., 2014) makes them able to migrate in the environment over long distances and enter wastewater treatment plants (WWTP). It is expected that nanomaterials will be found in the natural environment and engineered systems, where their fate and behavior are largely unknown (Navarro et al., 2008).

One of the most fundamental functions of typical wastewater treatment plant is degradation of organic matter, remediation of toxic compounds and removal of mineral nitrogen and phosphorus compounds to reduce the pollution of receiving waters (Gernaey et al., 2004). However, carbon-pollutants in the wastewater may cause an unexpected effect on the activity of microorganisms used

in wastewater treatment. Moreover, the mechanism of these compounds action in activated sludge is still unclear. Recent studies demonstrated that concentration 219 mg/L of SWCNTs can in various way influence microbial communities in activated sludge processes and has negatively affect treatment efficiency (Goyal et al., 2010).

Furthermore, there are some studies investigating the toxic properties of GO to pure, both planktonic and biofilm form of cultures. In these studies significant level of inactivation of pure cultures (60 – 80 %), depending on the graphene oxide concentration (40 – 80 mg/L) was observed (Hu et al., 2010; Bao et al., 2011; Mejias-Carpio et al., 2012; Ahmed and Rodrigues, 2013). Another study reported that after 4 hours of exposure, 87 % and 86 % of *Pseudomonas aeruginosa* (Gram-negative bacterium causing disease in humans and animals) exposed to GO and rGO, respectively at the concentration of 75 mg/L were killed (Gurunathan et al., 2012). However, it is worth mentioning that these studies demonstrated the toxicity of GO towards bacterial pure cultures under laboratory condition. Engineered systems, such as activated sludge, are more complex than presented in these studies, in terms of nanomaterial aggregation in microbial communities, solution chemistry, suspended particles and content of organic matter. Therefore, more research on a complex system of bacterial communities needs to be performed to explain the impact of GO on the environment. Different studies have been conducted focusing on the toxicity of CNMs towards the bacterial community in wastewater treatment plants. Ahmed and Rodrigues (2013) indicated that acute exposure of activated sludge to GO caused changes in the microbial community of activated sludge. These results show significant inhibition of metabolic activity (50 – 70 %), depending on the concentration of the substances used (100 – 300 mg/L). In order to investigate the toxic effect of the carbon nanomaterials at activated sludge respiratory activity test can be applied. Activated sludge respiratory activity inhibition test had been used in several studies (Parise et al., 2014; Luongo and Zhang, 2010) to check the response of activated sludge to chemical substances toxic influence. In this test, the overall metabolic respiratory activity was measured. Thus, respiratory activity can be taken as a result of metabolic inhibition due to the presence of carbon nanomaterials (Parise et al., 2014). Several studies indicated that bacterial growth inhibition is comparable with metabolic inhibition (Kang et al., 2008; Ahmed and Rodrigues, 2013). The explanation for this fact is that microorganism, under unfavorable conditions, reduce metabolic activity and growth, but resume growth and activity when the conditions will improve (Kang et al., 2008; Ahmed and Rodrigues, 2013). The toxic effect of SWCNTs measured as growth inhibition of *Paracoccus denitrificans* (a model denitrifying bacterium), with a use of optical density at 600 nm (OD<sub>600</sub>) was studied by Zheng et al. (2014). Results show no growth inhibition depending on the concentration of 10 - 50 mg/L. Another study shows growth inhibition of activated sludge (35 %), caused by the concentration of GO 300 mg/L (Ahmed and Rodrigues, 2013).

Regarding the wide usage of carbon nanomaterials and their emission into the environment, including WWTPs, it is necessary to study effects of CNMs on activated sludge microorganisms as a potential risk factor. Currently, numerous ecotoxicological and case studies on living organisms, including activated sludge, were carried out. However, taking into account high variability of the physical-chemical properties of the nanomaterials and a huge number of factors determining their effects (i.e. individual resistance of the tested organism, oxidation state, medium composition, pH or temperature), it is essential to examine many cases to get the most detailed answer.

Therefore, the aim of this study was to determine the potential toxicity of four selected carbon nanostructures: graphene oxide (GO), reduced graphene oxide (rGO), pristine multi-walled carbon nanotubes (MWCNTs) and multi-walled carbon nanotubes functionalized by oxidative treatments with a mixture of nitric acid and sulfuric acid solution (f-MWCNTs).

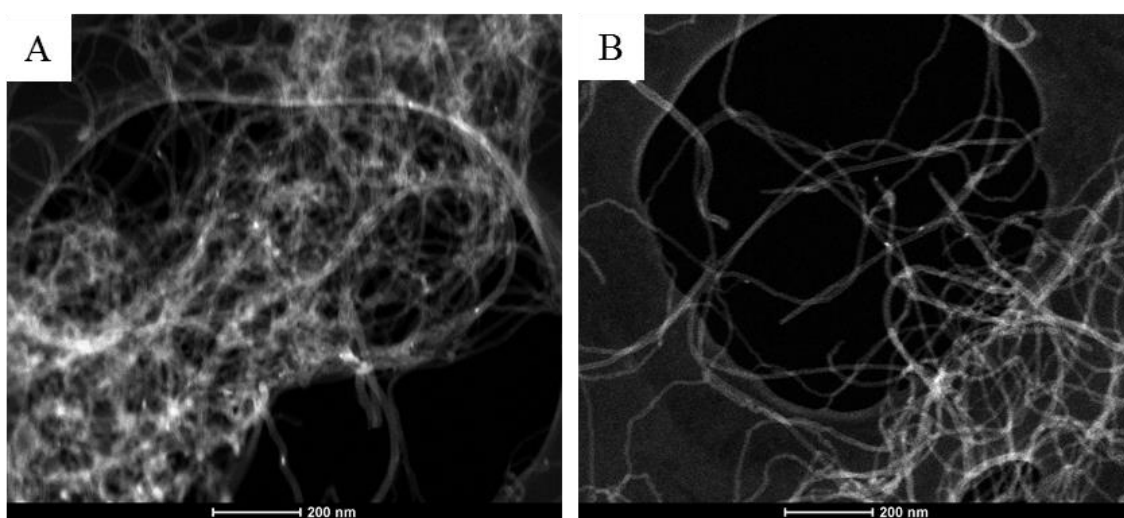
## MATERIALS AND METHODS

Commercially available GO, rGO (Nano Carbon, Poland) and MWCNTs (Nanocyl NC7000™, Belgium) were used. MWCNTs were functionalized by oxidative treatments with a mixture of nitric acid and sulfuric acid solution to obtain f-MWCNTs. Nanomaterials samples were analyzed by Transmission Electron Microscope using a S/TEM TITAN 80-300 (FEI Company). The samples were prepared by dispersing the nanoparticles in ethanol (99.8 %) using an ultrasound washer, and then depositing one or two drops of the dispersion on a TEM copper 200 mesh grid coated with a carbon film. The samples were air-dried at room temperature.

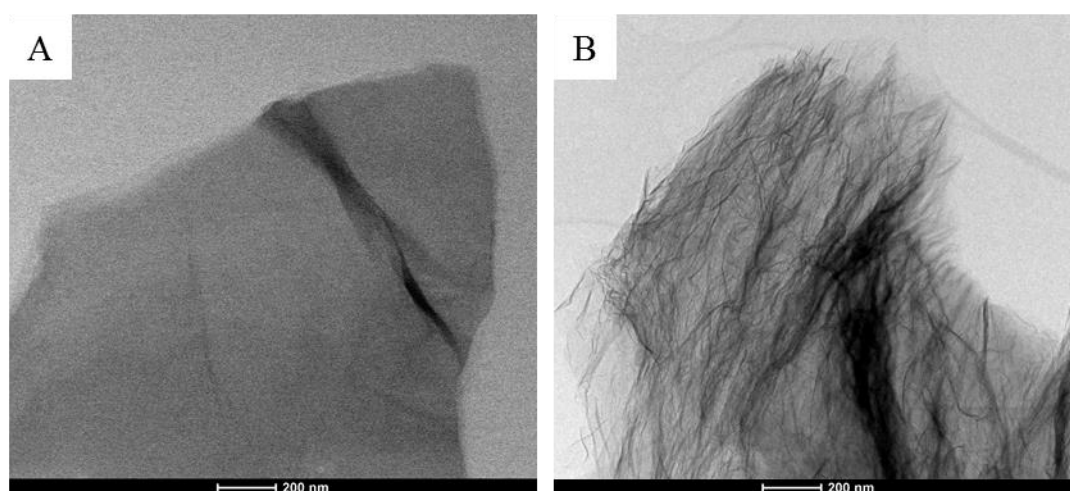
Fresh conventional activated sludge originated from the municipal WWTP, located in the Silesia region (Poland). CNMs influence on the activated sludge microorganisms has been investigated using two acute ecotoxicity tests. Growth inhibition was determined after 5 hours of exposure, based on standard method (ISO 15522:1999) using optical density (530 nm), at  $22 \pm 2$  °C, pH 7.0 and with an average total suspended solids concentration (TSS)  $2.2 \pm 0.1$  g/L. Respiratory activity was measured based on oxygen uptake rate (OUR), according to the standard method (PN-EN ISO 8192:2007), at  $22 \pm 2$  °C, pH 7.5 and with an average TSS concentration  $4.5 \pm 0.9$  g/L. All tests were performed in triplicate, the difference between means was tested using the Student's t-test.

## RESULTS AND DISCUSSION

Morphology of all tested nanomaterials was verified using TEM and representative images are presented in Figures 1 and 2. MWCNTs are elongated hollow nanotubes formed by curled multi-layer graphite sheets. MWCNTs functionalized by acid treatment contains at the walls carboxyl and hydroxyl groups, i.e. COOH, COO<sup>-</sup>, OH (Sezer and Koç, 2019). Both types of CNTs were characterized by an average inner diameter of 2 – 6 nm, outer diameter of 5 – 20 nm and lengths in the microns. In turn, GO is a single layer of carbon atoms (graphene), comprising carboxyl and hydroxyl groups. Reduction of GO removes some of these oxygen-containing groups and leads to the formation of rGO. Both of them, occur in the water environment in the form of few-layer flakes and Figure 2 illustrates much higher disintegration of the carbon basal plane in the rGO sample.



**Figure 1.** Representative transmission electron microscopy (TEM) images of A – multi-walled carbon nanotubes (MWCNTs), B – functionalized multi-walled carbon nanotubes (f-MWCNTs) used in the ecotoxicological study



**Figure 2.** Representative transmission electron microscopy (TEM) images of A – graphene oxide (GO) and B – reduced graphene oxide (rGO) used in the ecotoxicological study

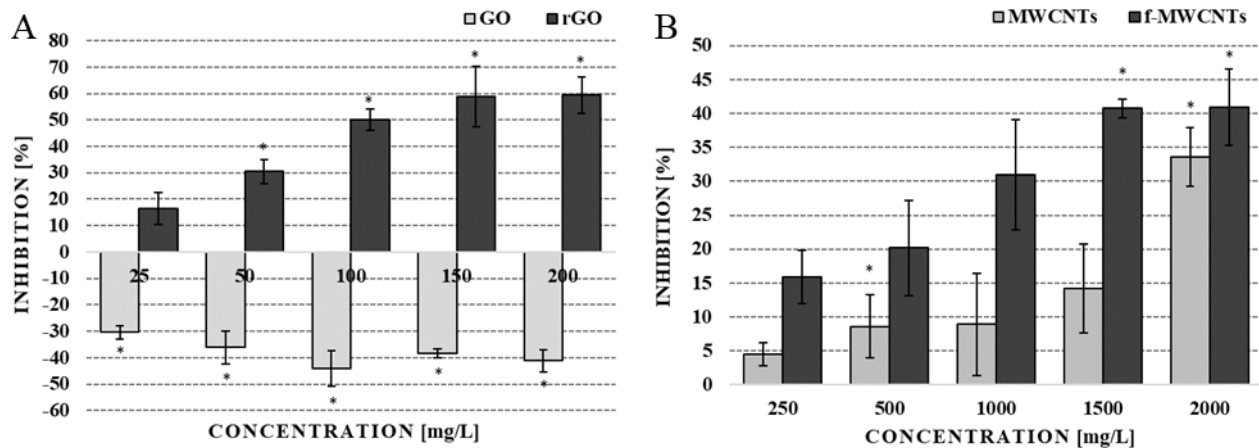
As it has been previously reported by Manshian et al. (2013) and Parise et al. (2014) even a minute change in the physical-chemical characteristics of the nanomaterial used can be a reason of its toxicity change. However, the detailed mechanism of CNMs toxicity is still unclear and requires further elucidation, but three main phenomena are currently considered: (1) mechanical damage to the microorganisms cell wall and membrane; (2) reactive oxygen species (ROS) production, which can damage membranes, proteins, and DNA; (3) other physical-chemical properties related i.e. with their functionalization or electron transport and multi-electron accepting ability (Chen et al., 2019).

In the case of this study, the f-MWCNTs are found to be more toxic towards activated sludge in 5-hour test than non-functionalized ones causing higher growth inhibition (Figure 3B). Nonetheless, both types of nanotubes are toxic for activated sludge microorganisms and the toxic effect increases with their concentration. Respectively, 34 % and 41 % inhibition were indicated in the highest concentration (2000 mg/L) of MWCNTs and f-MWCNTs. It is possible that f-MWCNTs due to their lower hydrophobicity can get into closer contact with the activated sludge flocs and become more toxic to these microorganisms. While non-functionalized MWCNTs can aggregate together and the toxic effect can be partially neutralized. This thesis is supported by TEM images. Figure 1 demonstrates that the aggregates of MWCNTs are more cohesive and compact than those created by f-MWCNTs. Similar results have been obtained by Parise et al. (2014) and Luongo and Zhang (2010) who also obtained higher respiration inhibition values and reported that the more dispersed f-MWCNTs can be more toxic. Moreover, according to Ma et al. (2019) functionalized CNTs can destroy cell membrane and affect microbial activity. As illustrated in Figure 1B, f-MWCNTs have sharp ends, with an average diameter between 5 – 20 nm, which could easily damage membrane integrity.

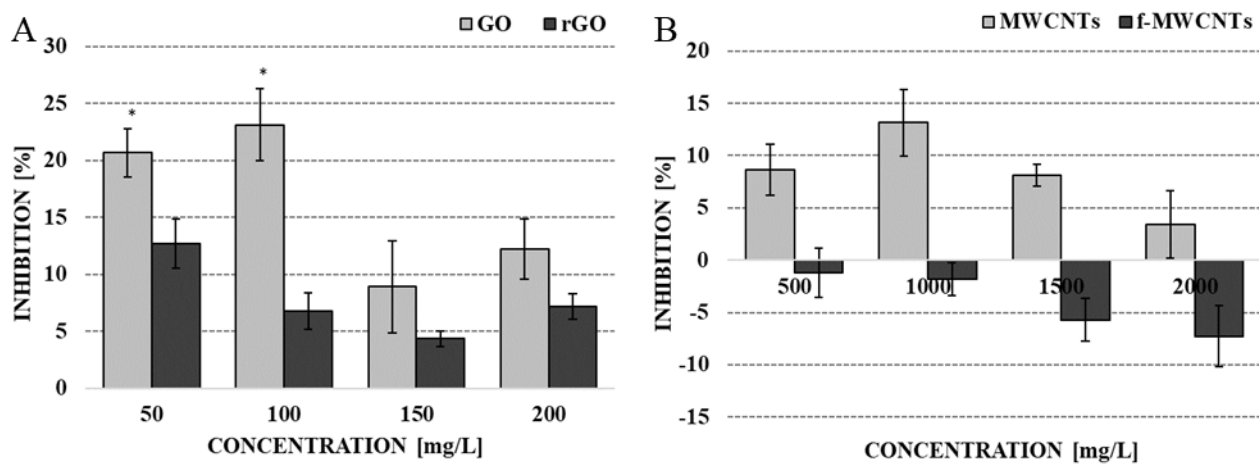
In case of the same toxic compounds used in the short term test only MWCNTs were toxic towards activated sludge microorganisms and the effect was not convergent with their concentration (Figure 4B). The highest 13 % inhibition was observed for MWCNTs in a concentration equal to 1000 mg/L. Interestingly, f-MWCNTs caused the opposite effect and their increasing concentration from 500 mg/L to 2000 mg/L had a stimulating effect. It is possible that in short term test f-MWCNTs due to their higher hydrophilicity linked with organic and inorganic matter present in the activated sludge accelerating its biodegradation before they become toxic in the long exposure. Similar results were obtained by Zhao et al. (2013) who stated that the f-MWCNTs can aggregate with different biomolecules, polymers and inorganic matter which accelerate their decomposition. Similar results were obtained by Qu et al. (2015, 2016) for phenol biodegradation in a sequencing



batch reactor (SBR). Moreover, oxygen uptake rate test is limited to the aerobic organisms present in the activated sludge, unlike to optical density test, which evaluates the growth of a total microbial consortium. Nonetheless, these results should be considered carefully due to the fact that the test was not statistically significant ( $p > 0.05$ ) and relatively short. In the case of the short term exposure on the toxic compounds, two mechanisms should be considered. Firstly, activated sludge flocs produce large amounts of extracellular polymeric substances, which constitutes a protective barrier against contaminants. For this reason flocs penetration depends on time (Luongo and Zhang, 2010). Secondly, bacterial stress response, manifesting by activity increase against the external stimulus, is observable during the early phase of exposure.



**Figure 3.** Growth inhibition test results after 5 hours of exposure on A – graphene oxide (GO) and reduced graphene oxide (rGO), B – multi-walled carbon nanotubes (MWCNTs), functionalized multi-walled carbon nanotubes (f-MWCNTs). Bars represent standard error; \* – a statistically significant difference with control at  $p < 0.05$  (Student's *t*-test)



**Figure 4.** Oxygen uptake rate (OUR) test results underexposure on A – graphene oxide (GO) and reduced graphene oxide (rGO), B – multi-walled carbon nanotubes (MWCNTs), functionalized multi-walled carbon nanotubes (f-MWCNTs). Bars represent standard error; \* – a statistically significant difference with control at  $p < 0.05$  (Student's *t*-test)

Taking into consideration the results of the short-term tests of GO and rGO toxicity, both of the compounds used should be regarded as toxic due to its inhibitory influence on activated sludge respiration (Figure 4A). The strongest effects were observed for 100 mg/L of GO and 50 mg/L of rGO, which caused 23 % and 13 % inhibition, respectively. However, the toxicity seems to decrease while the concentration of GO and rGO increase. It is possible, that much concentrated graphene-

based nanomaterials aggregates in larger complexes, becoming less available for microorganisms and limiting their toxic activity. At the same time, all samples revealed higher toxicity of GO. These results can be supported by the results presented by Nguyen and Rodrigues (2018). They reported that GO presented higher impact on nutrient removal and community composition of activated sludge microorganisms than rGO. It could be explained by the fact that GO possesses more functional groups than rGO, which makes it more hydrophilic, thus more toxic towards bacteria (Nguyen and Rodrigues, 2018; Santos et al., 2012). GO is also found to be more prone to interact with the macromolecules in the activated sludge and thus more reactive by producing more reactive oxygen species (Liu et al., 2011; Ahmed and Rodrigues, 2013).

Results of the OUR test can be supported with a 5-hour test of activated sludge growth inhibition (Figure 3A), where rGO presented increasing toxicity together with the increasing concentration. The highest 59 % inhibition was observed in a concentration of 150 mg/L. Considering mechanical damages of cell membranes caused by nanoparticles, TEM images demonstrate that rGO is more irregularly shaped than GO, with sharp folds and edges. On the other hand, GO seems to stimulate activated sludge growth regardless of its concentration. Statistically significant stimulation of the activated sludge microorganisms was noted up to 44 % with 100 mg/L of GO. It is not a new phenomenon, because several previous studies revealed that bacterial growth rate and activity can be accelerated by this kind of nanomaterial (Ruiz et al., 2011). It has been recognized that graphene-family nanomaterials could play a role of attachment surfaces, inducing cells aggregation, extracellular polymeric substances secretion, and bacteria growth. This is in contrast to the respiratory activity test (OUR), suggesting stimulation of the anaerobic and/or anoxic microbial consortium.

## CONCLUSIONS

Ecotoxicity study of four carbon nanomaterials on the conventional activated sludge microorganisms has been performed using two acute tests, based on growth inhibition and respiratory activity. These studies show that short term exposure on MWCNTs, f-MWCNTs, GO and rGO can be toxic for the microbial activity. Definitely, the effects of the nanomaterials increase with exposure time and hence the degree of flocs penetration. Respiratory activity test, where the effects were determined immediately after nanomaterials addition, revealed the highest 23 % inhibition with 100 mg/L GO addition. In turn, growth inhibition test, after 5 hours of exposure, presented the highest 59 % inhibition for rGO in the concentration of 150 mg/L. Regarding the fact that nanoparticles can be accumulated by the activated sludge flocs, chronic effects could be stronger and should be studied. Further, the effect of the nanomaterial exposure strongly depends on its individual properties (i.e. oxidation state, size), a unique microbial consortium of the activated sludge and environmental conditions (i.e. medium composition, pH, temperature). This study is a contribution to evaluate and understand hazards resulting from CNMs presence in the WWTP.

## ACKNOWLEDGEMENTS

Publication supported by own fund scholarship of the Silesian University of Technology in 2018 (1/WFS18/0003-07/2018). Authors would like to thank Seweryn Gałecki for laboratory assistance, Sławomir Boncel and Anna Kolanowska for providing MWCNTs samples.

## REFERENCES

Ahmed, F., Rodrigues, D. F. (2013) Investigation of acute effects of graphene oxide on wastewater microbial community: A case study. *Journal of Hazardous Materials*, **256-257**, 33-39.

- Bao, Q., Zhang, D., Qi, P. (2011) Synthesis and characterization of silver nanoparticle and graphene oxide nanosheet composites as a bactericidal agent for water disinfection. *J. Colloid Interface Sci.*, **360**, 463-470.
- Bundschuh, M., Filser, J., Lüderwald, S., McKee, M. S., Metreveli, G., Schaumann, G. E., Schulz, R., Wagner, S. (2018) Nanoparticles in the environment: where do we come from, where do we go to?. *Environ Sci Eur*, **30**, 6.
- Chen, M., Sun, Y., Liang, J., Zeng, G., Li, Z., Tang, L., Zhu, Y., Jiang, D., Song B. (2019) Understanding the influence of carbon nanomaterials on microbial communities. *Environmental International*, **126**, 690-698.
- Flores-Cervantes, D. X., Maes, H. M., Schäffer, A., Hollender, J., Kohler, H. P. E. (2014) Slow Biotransformation of Carbon Nanotubes by Horseradish Peroxidase. *Environmental Science & Technology*, **48**(9), 4826-4834.
- Gagliardi, M., McWilliams, A., Moran, R. (2011) Graphene: Technologies, Applications, and Markets, BCC Research Market Forecasting, Wellesley, MA.
- Gernaey, K. V., van Loosdrecht, M. C. M., Henze, M., Lind, M., Jørgensen, S. B. (2004) Activated sludge wastewater treatment plant modelling and simulation: state of the art. *Environmental Modelling & Software*, **19**, 763-783.
- Goyal, D., Zhang, X. J., Rooney-Varga, J. N. (2010) Impacts of single-walled carbon nanotubes on microbial community structure in activated sludge. *Let. Appl. Microbiol.*, **51**, 428-435.
- Gurunathan, S., Han, J. W., Dayem, A. A., Eppakayala, V., Kim, J. H. (2012) Oxidative stress-mediated antibacterial activity of graphene oxide and reduced graphene oxide in *Pseudomonas aeruginosa*. *Int J Nanomedicine*, **7**, 5901-14.
- Hu, W., Peng, C., Luo, W., Lv, M., Li, X., Li, D., Huang, Q., Fan, C. (2010) Graphene-based antibacterial paper. *ACS Nano*, **4**, 4317-4323.
- Kang, S., Herzberg, M., Rodrigues, D. F., Elimelech, M. (2008) Antibacterial effects of carbon nanotubes: size does matter!. *Langmuir*, **24**, 6409-6413.
- Liu, S., Zeng, T. H., Hofmann, M., Burcombe, E., Wei, J., Jiang, R., Kong, J., Chen, Y. (2011) Antibacterial activity of graphite, graphite oxide, graphene oxide, and reduced graphene oxide: membrane and oxidative stress. *ACS Nano*, **5**, 6971-6980.
- Luongo, L., Zhang, X. (2010) Toxicity of carbon nanotubes to the activated sludge process. *J Hazard Mater*, **178**(1-3), 356-362.
- Ma, B., Gao, F., Yu, N., Zhao, C., Li, S., She, Z., Gue, L., Jin, C., Zhao, Y., Gao, M. (2019) Long-term impacts of carboxyl functionalized multi-walled carbon nanotubes on the performance, microbial enzymatic activity and microbial community of sequencing batch reactor. *Bioresource Technology*, **286**, 121382.
- Manshian, B. B., Jenkins, G. J., Williams, P. M., Wright, C., Barron, A. R., Brown, A. P., Hondow, N., Dunstan, P. R., Rickman, R., Brady, K., Doak, S. H. (2013) Single-walled carbon nanotubes: differential genotoxic potential associated with physico-chemical properties. *Nanotoxicology*, **7**(2), 144-56.
- Mejias-Carpio, I. E., Santos, E. M., Wei, X., Rodrigues, D. F. (2012) Toxicity of a polymergraphene oxide composite against bacterial, planktonic cells, biofilms, and mammalian cells. *Nanoscale*, **4**, 4746-4756.
- Navarro, E., Baun, A., Behra, R., Hartmann, N. B., Filser, J., Miao, A-J., Quigg, A., Santschi, P. H., Sigg, L. (2008) Environmental behavior and ecotoxicity of engineered nanoparticles to algae, plants, and fungi. *Ecotoxicology*, **17**(5), 372-386.
- Nguyen, H. N., Rodrigues, D. F. (2018) Chronic toxicity of graphene and graphene oxide in sequencing batch bioreactors: A comparative investigation. *J Hazard Mater*, **343**, 200-207.
- Parise, A., Thakor, H., Zhang, X. (2014) Activity inhibition on municipal activated sludge by single-walled carbon nanotubes. *Journal of Nanoparticle Research*, **16**(1), 1-9.
- Qu, Y., Ma, Q., Deng, J., Shen, W., Zhang, X., He, Z., van Nostrand, J. D., Zhou, J., Zhou, J.

- (2015) Responses of microbial communities to single-walled carbon nanotubes in phenol wastewater treatment systems. *Environ Sci Technol*, **49**(7), 4627-35.
- Qu, Y., Zhang, X., Shen, W., Ma, Q., You, S., Pei, X., Li, S., Ma, F., Zhou, J. (2016) Illumina MiSeq sequencing reveals long-term impacts of single-walled carbon nanotubes on microbial communities of wastewater treatment systems. *Bioresour Technol*, **211**, 209-15.
- Ruiz, O. N., Fernando, K. A. S., Wang, B., Brown, N. A., Luo, P. G., McNamara, N. D., Vangsness, M., Sun, Y., Bunker, C. E. (2011) Graphene Oxide: A Nonspecific Enhancer of Cellular Growth. *ACS Nano*, **5**(10), 8100-8107.
- Santos, C. M., Mangadlao, J., Ahmed, F., Alex, L., Rigoberto, C. A., Rodrigues, D. F. (2012) Graphene nanocomposite for biomedical applications: fabrication, antimicrobial and cytotoxic investigations. *Nanotechnology*, **23**(39).
- Sezer, N., Koç, M. (2019) Oxidative acid treatment of carbon nanotubes. *Surfaces and Interfaces*, **14**, 1-8.
- Zhao, Z., Yang, Z., Hu, Y., Li, J., Fan, X. (2013) Multiple functionalization of multi-walled carbon nanotubes with carboxyl and amino groups. *Applied Surface Science*, **276**, 476-481.
- Zheng, X., Su, Y., Chen, Y., Wan, R., Li, M., Wie, Y., Huang, H. (2014) Carboxyl-modified single-walled carbon nanotubes negatively affect bacterial growth and denitrification activity. *Scientific Reports*, **4**, 5653.

# Investigation of Tetrahydrofuran Removal Technology from Process Wastewater

A. J. Toth\*

\* Environmental and Process Engineering Research Group, Department of Chemical and Environmental Process Engineering, Budapest University of Technology and Economics, H-1111, Hungary, Budapest, Műgyetem rkp. 3. and Institute of Chemistry, University of Miskolc, Egyetemváros C/1 108, H-3515, Miskolc, Hungary (E-mail: [ajtoth@envproceng.eu](mailto:ajtoth@envproceng.eu))

## Abstract

The work is motivated by an industrial problem, which is tetrahydrofuran removal from pharmaceutical process wastewater with extractive distillation. The goal of the research is to rigorously model and optimize this operation in professional flowsheet simulator environment based on adequate and consistent vapour-liquid equilibrium data. The number of minimal theoretical plates of distillation columns, binary mixture feed stage, solvent feed stage location, optimal reflux ratios and Total Annual Cost (TAC) are determined. Dimethyl sulfoxide (DMSO) is used as extractive agent.

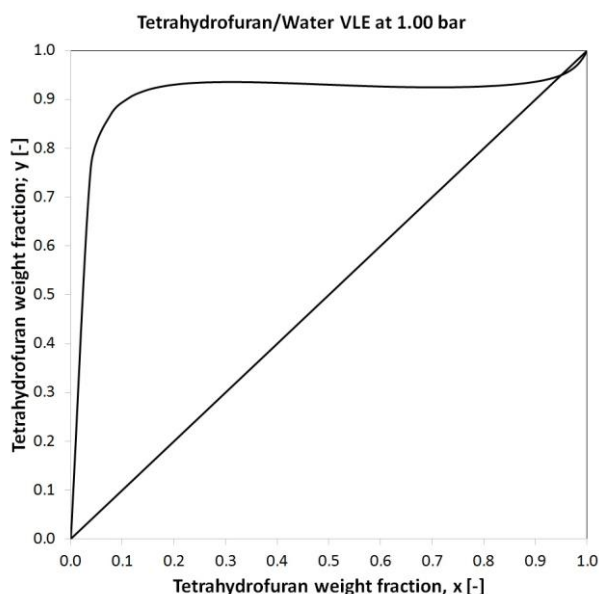
Considering the results, it can be concluded that, the extractive distillation process is suitable for separation tetrahydrofuran and water in 99.9 weight percent (m/m%) purity of water and 99.5 m/m% tetrahydrofuran.

## Keywords

Process wastewater; tetrahydrofuran removal; extractive distillation, flowsheet environment

## INTRODUCTION

Tetrahydrofuran (THF) forms heterogeneous azeotropic mixture with water, which means separation problem. THF content above 93.3 weight% can not be achieved with conventional distillation techniques (Marsden, 1954). The vapour-liquid equilibrium of THF-Water binary mixture can be seen in Figure 1.



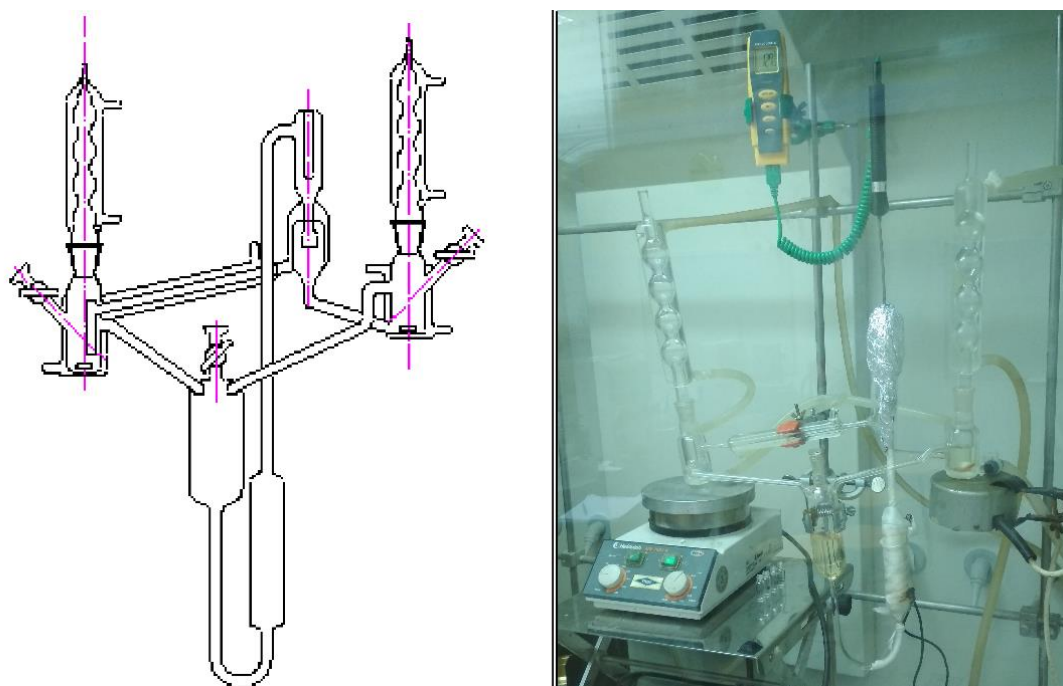
**Figure 1.** Vapour-liquid equilibrium of THF-Water mixture

It can be mentioned, extractive distillation is capable for separation of tetrahydrofuran-water mixture (Xu and Wang, 2006; Zhang et al., 2014; Deorukhkar et al., 2016; Ghuge et al., 2017). This technique has been widespread in the chemical and environmental industries, but it is not economical in many cases in the reason of its high operation cost (Toth et al., 2011; Toth and Mizsey, 2015; Andre et al., 2018).

## MATERIAL AND METHODS

The aim of this study is to remove of tetrahydrofuran from process wastewater (PWW) with extractive distillation in professional flowsheet environment. Consistent vapour-liquid equilibrium (VLE) data is essential for computer simulation, therefore laboratory experiments are required.

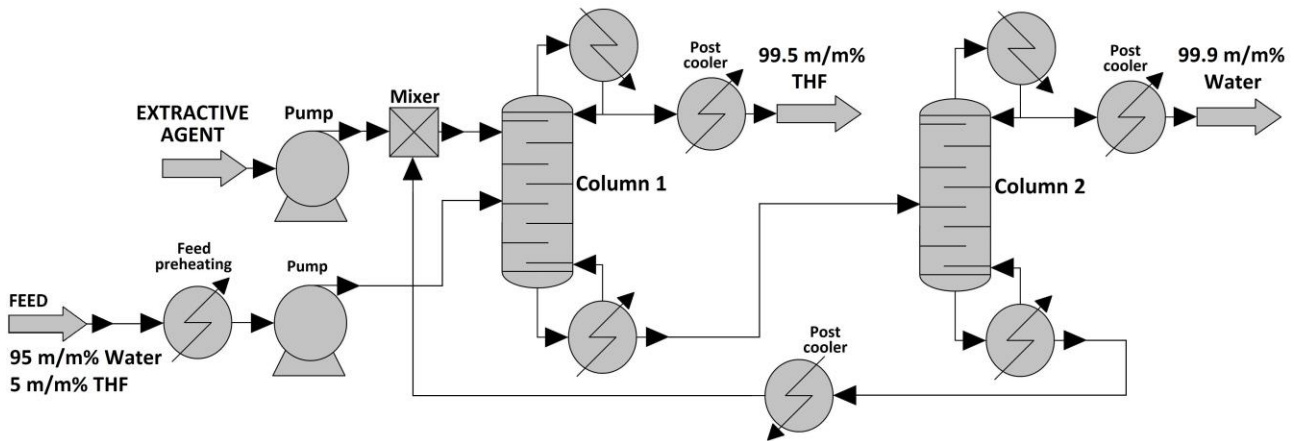
The determination of the VLE measurements of the THF-water binary system are performed by using a modified Gillespie still designed by Manczinger (Manczinger and Tettamanti, 1966) with minor subsequent modifications as shown in Figure 2 (Havasi et al., 2016).



**Figure 2.** Equilibrium apparatus

The tetrahydrofuran concentration is measured with Shimadzu GC2010Plus+AOC-20 autosampler gas chromatograph with a CP-SIL-5CB column connected to a flame ionization detector, EGB HS 600 headspace apparatus is used for sample preparation. The water content is measured with Hanna HI 904 coulometric Karl Fischer titrator (Toth et al., 2015; Toth et al., 2016; Haaz and Toth, 2018).

PWW from pharmaceutical industry has to be separated with the following initial composition: 5 m/m% THF and 95 m/m% Water. The product purity is min. 99.5 m/m% in both cases and 800 kg/h PWW must be treated. The ChemCAD flowsheet of extractive distillation can be seen in Figure 3.



**Figure 3.** Flowsheet of tetrahydrofuran-water separation with extractive distillation

The first column is the extractive column, where the heterogeneous azeotropic mixture can be separated with dimethyl sulfoxide as entrainer. The second column treats the water-dimethyl sulfoxide mixture, the entrainer can be recycled and mixed into the feed stream. The optimal reflux ratio, the mass- and bottom flow rates, heating and cooling requirements, number of theoretical plates ( $N$ ) and feed plate have to be optimized.

## RESULTS AND DISCUSSION

Table 1 introduces the measured vapour-liquid equilibrium data of THF-Water mixture.

**Table 1.** VLE data of tetrahydrofuran-water binary mixture ( $x$ : liquid,  $y$ : vapour)

T [°C]	p [Pa]	x [-]	y [-]	T [°C]	p [Pa]	x [-]	y [-]
72.98	103.2	0.02	0.6521	63.81	103.2	0.65	0.7764
66.48	103.2	0.04	0.7380	63.68	103.2	0.70	0.7831
65.56	103.2	0.06	0.7514	63.59	103.2	0.75	0.7914
65.31	103.2	0.08	0.7561	63.52	103.2	0.80	0.8083
64.92	103.2	0.10	0.7586	63.51	103.2	0.82	0.8173
64.68	103.2	0.15	0.7617	63.55	103.2	0.84	0.8261
64.31	103.2	0.20	0.7624	63.62	103.2	0.86	0.8367
64.28	103.2	0.25	0.7628	63.71	103.2	0.88	0.8497
64.25	103.2	0.30	0.7634	63.85	103.2	0.90	0.8634
64.23	103.2	0.35	0.7638	64.03	103.2	0.92	0.8835
64.21	103.2	0.40	0.7642	64.27	103.2	0.94	0.9045
64.18	103.2	0.45	0.7647	64.59	103.2	0.96	0.9235
64.14	103.2	0.50	0.7656	65.05	103.2	0.98	0.9614
64.04	103.2	0.55	0.7682	65.37	103.2	0.99	0.9813
63.92	103.2	0.60	0.7719				

The thermodynamic consistency test for THF-Water data is performed according to Herrington's area test (Herrington, 1947; Havasi et al., 2016; Havasi, 2018) for isobaric data.  $D$  and  $J$  values are calculated according to following equations.

$$\gamma_i = \frac{y_i \cdot p}{x_i \cdot p_i^0} \quad (1)$$

$$D = 100 \times \left| \frac{\int_{x_1=0}^{x_1=1} \ln(\gamma_1/\gamma_2) dx_1}{\int_{x_1=0}^{x_1=1} |\ln(\gamma_1/\gamma_2)| dx_1} \right| \quad (2)$$

$$J = 150 \times \frac{|\Delta T_{\max}|}{T_{\min}} \quad (3)$$

$$D - J \leq 10\% \quad (4)$$

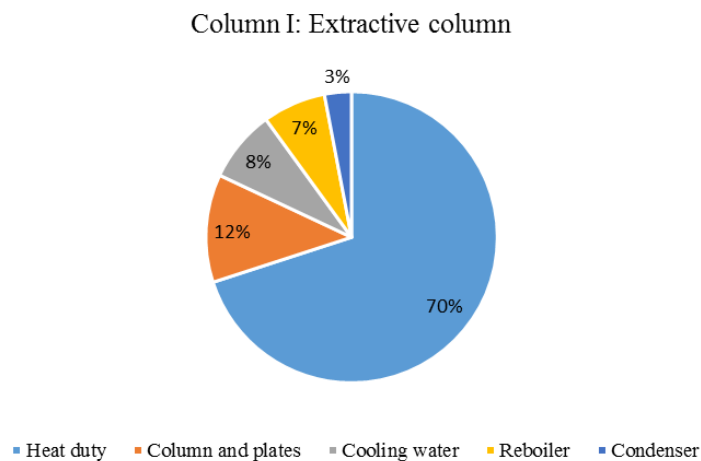
It can be concluded, D-J is 9.8, therefore the measured data is capable for application in flowsheet environment.

The optimized results of simulations with extractive distillation process is listed in Table 2.

**Table 2.** Optimized results of tetrahydrofuran-water separation

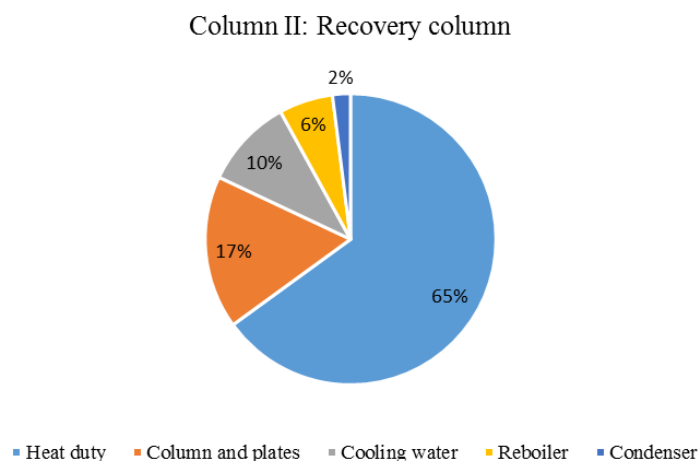
	Extractive column	Recovery column
N [-]	15	20
Feed stage (PWW)	7	8
Feed stage (DMSO)	2	-
Reflux ratio [-]	3	1
THF [m/m%]	99.5	0.05
D Water [m/m%]	0.3	99.9
DMSO [m/m%]	0.2	0.05

The Total Annual Cost (TAC) is also determined, using Douglas-correlations (Douglas, 1988). Figure 4 and Figure 5 show the distribution of TAC in both column cases.



**Figure 4.** Distribution of Total Annual Cost of Extractive column (C1)





**Figure 5.** Distribution of Total Annual Cost of Recovery column (C2)

It can be concluded, heat duty/cost of distillation has the largest part of TAC.

## SUMMARY

The extractive distillation is investigated in professional flowsheet environment. It can be concluded tetrahydrofuran-water mixture can be separated into pure components with this operation. The goal composition, which is min. 99.5 m/m% in both product case can be reached.

## ACKNOWLEDGEMENT

This work was supported by the János Bolyai Research Scholarship of the Hungarian Academy of Sciences, ÚNKP-19-4-BME-416 New National Excellence Program of the Ministry for Innovation and Technology, OTKA 112699 and 128543. This research was supported by the European Union and the Hungarian State, co-financed by the European Regional Development Fund in the framework of the GINOP-2.3.4-15-2016-00004 project, aimed to promote the cooperation between the higher education and the industry. The research reported in this paper has been supported by the National Research, Development and Innovation Fund (TUDFO/51757/2019-ITM, Thematic Excellence Program). The authors thank the members of Environmental and Process Engineering Research Group (<http://www.envproceng.eu/en/home-en/>) for their help.

## REFERENCES

- Andre, A., Nagy, T., Toth, A. J., Haaz, E., Fozer, D., Tarjani, J. A., Mizsey P. (2018) Distillation contra pervaporation: Comprehensive investigation of isobutanol-water separation. *Journal of Cleaner Production*, **187**, 804-818.
- Deorukhkar, O. A., Deogharkar, B. S., Mahajan Y. S. (2016) Purification of tetrahydrofuran from its aqueous azeotrope by extractive distillation: Pilot plant studies. *Chemical Engineering and Processing: Process Intensification*, **105**, 79-91.
- Douglas, J. M. (1988) *Conceptual design of chemical processes*. McGraw-Hill, New York.
- Ghuge, P. D., Mali, N. A., Joshi, S. S. (2017) Comparative analysis of extractive and pressure swing distillation for separation of THF-water separation. *Computers & Chemical Engineering*, **103**, 188-200.
- Haaz, E., Toth, A. J. (2018). Methanol dehydration with pervaporation: Experiments and modelling. *Separation and Purification Technology*, **205**, 121-129.
- Havasi, D. (2018) *Separation studies on mixtures generated in biomass conversion*. PhD Thesis,

Budapest University of Technology and Economics, Budapest.

- Havasi, D., Mizsey, P., Mika, L. T. (2016) Vapor–Liquid Equilibrium Study of the Gamma-Valerolactone–Water Binary System. *Journal of Chemical & Engineering Data*, **61**(4), 1502-1508.
- Herington, E. F. G. (1947) A thermodynamic test for the internal consistency of experimental data on volatility ratios. *Nature*, **160**(4070), 610-611.
- Manczinger, J., Tettamanti, K. (1966) Phase equilibria of the system caprolactam/water. *Periodica Polytechnica Chemical Engineering* **10**(2), 183-195.
- Marsden, C. (1954). *Solvents And Allied Substances Manual With Solubility Chart*. Cleaver-Hume and Elsevier, London.
- Toth, A. J., Andre, A., Haaz, E., Mizsey, P. (2015) New horizon for the membrane separation: Combination of organophilic and hydrophilic pervaporations. *Separation and Purification Technology*, **156**(2), 432-443.
- Toth, A. J., Gergely, F., Mizsey, P. (2011) Physicochemical treatment of pharmaceutical wastewater: distillation and membrane processes. *Periodica Polytechnica: Chemical Engineering*, **55**(2), 59-67.
- Toth, A. J., Mizsey, P. (2015). Comparison of air and steam stripping: removal of organic halogen compounds from process wastewaters. *International Journal of Environmental Science and Technology*, **12**(4), 1321-1330.
- Toth, A. J., Szanyi, A., Angyal-Koczka, K., Mizsey, P. (2016). Enhanced Separation of Highly Non-ideal Mixtures with Extractive Heterogeneous-azeotropic Distillation. *Separation Science and Technology*, **51**(7), 1238-1247.
- Xu, S., Wang, H. (2006). A new entrainer for separation of tetrahydrofuran-water azeotropic mixture by extractive distillation. *Chemical Engineering and Processing: Process Intensification*, **45**(11), 954-958.
- Zhang, Z. G., Huang, D. H., Lv, M., Jia, P., Sun, D. Z., Li, W. X. (2014). Entrainer selection for separating tetrahydrofuran/water azeotropic mixture by extractive distillation. *Separation and Purification Technology*, **122**, 73-77.

# Isopropanol Removal from Pharmaceutical Process Wastewater with Combination of Distillation and Pervaporation

A. J. Toth\*, R. Ladanyi\*, B. Szilagyi\* and E. Haaz\*

\* Environmental and Process Engineering Research Group, Department of Chemical and Environmental Process Engineering, Budapest University of Technology and Economics, H-1111, Hungary, Budapest, Műegyetem rkp. 3. and Institute of Chemistry, University of Miskolc, Egyetemváros C/1 108, H-3515, Miskolc, Hungary (E-mails: [ajtoth@envproceng.eu](mailto:ajtoth@envproceng.eu); [envproceng@freemail.hu](mailto:envproceng@freemail.hu); [teljesindukcio@gmail.com](mailto:teljesindukcio@gmail.com); [haaz.e@kkft.bme.hu](mailto:haaz.e@kkft.bme.hu))

## Abstract

The research is motivated by an industrial problem, that is isopropanol (IPA) removal from pharmaceutical process wastewater. To complete the target hybrid treatment is investigated. Isopropanol dehydration with combination of distillation and hydrophilic pervaporation (PV) is used. The goal of this research is to rigorously model and optimize this hybrid treatment in professional flowsheet simulator environment. The number of minimal theoretical stages of distillation column and minimal membrane transfer area are determined. Considering the results, it can be concluded that, the distillation and pervaporation methods are suitable for separation isopropanol and water in min. 99.5 weight percent purity (m/m%).

## Keywords

Isopropanol removal; modelling; mprocess wastewater; mydrophilic pervaporation; distillation

## INTRODUCTION

The industrial application of pervaporation separation has been increasing in recent decades, thanks to traditional separation techniques (distillation, absorption, etc.), while ensuring lower energy consumption and high selectivity. One of the main areas of application of liquid mixtures is the dehydration of the various aqueous azeotropic solvent mixtures. Separation can be carried out without the addition of an extra component, the recovered solvent and process wastewater can be recycled, so that pervaporation is an environmentally friendly process (Toth, 2018; Toth et al., 2018).

Alcohol and water separation is a well-known method of pervaporation method in chemical and environmental sector. It can be mentioned isopropanol forms minimal boiling azeotropic mixture with water, which means separation problem. Isopropanol (IPA) content above ~88 m/m% can not be achieved with conventional distillation processes (Marsden, 1954; Gmehling et al., 1978). If the azeotropic composition can be approached with distillation, then the distillate product (D) can be further purified using pervaporation dehydration (Szabados et al., 2018; Toth, 2019).

The vapour-liquid equilibrium of IPA-Water binary mixture can be seen in Figure 1 (NRTL model).

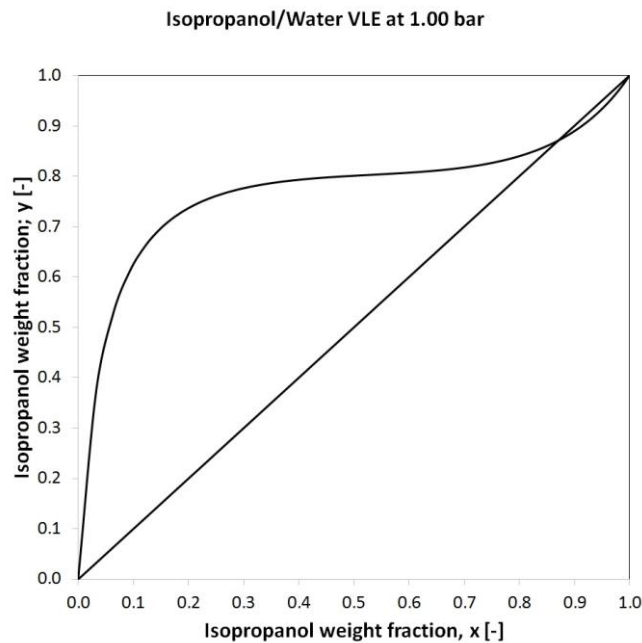
Pervaporation can be characterized by certain quantities and factors. The flux is calculated using the following equation (Huang et al., 2014):

$$J_i = \frac{P_i}{\Delta t \cdot A}, \quad (1)$$

where  $P_i$  is the partial weight of component  $i$  in the permeate,  $t$  is the time of duration of experiment and  $A$  is the membrane area. Separation factor is calculated by the following equation:

$$\alpha = \frac{y_i(1-x_i)}{x_i(1-y_i)}, \quad (2)$$

where  $\alpha$  is separation factor (dimensionless),  $x_i$  is weight fraction of ethyl acetate in feed and  $y_i$  is weight fraction of ethyl acetate of permeate (Toth et al., 2015).



**Figure 1.** Vapour-liquid equilibrium of IPA-Water mixture

An essential tool for designing and optimizing separation processes is the appropriate computer modelling, which as accurate as possible model is needed (Rautenbach et al., 1990; Wijmans and Baker, 1995; Baker, 2012; Luis and Van der Bruggen, 2015; Csizmadia and Till, 2018). Model parameter estimation is achieved using laboratory experiments (Toth et al., 2018).

Hydrophilic pervaporation is able to dehydrate alcohol compounds. The polyvinyl alcohol (PVA) is among the most interesting and promising membranes for hydrophilic pervaporation and it has been extensively investigated. Table 1 shows some PVA hydrophilic membranes for isopropanol-water separation.

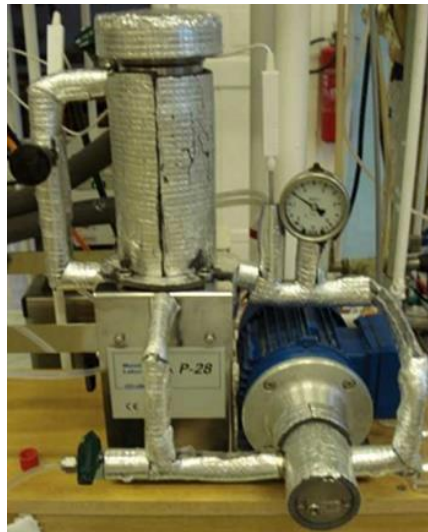
**Table 1.** PVA membranes for isopropanol dehydration

PVA membrane type	X <sub>IPA</sub> [m/m%]	J [g/m <sup>2</sup> h]	$\alpha$ [-]	Ref.
1PVA/Silicalite-1 (5 wt.%)	90	38	11240	Adoor <i>et al.</i> 2007
2PVA/Silicalite-1 (10 wt.%)	90	26	17990	Adoor <i>et al.</i> 2007
3PVA/ZSM-5 zeolite (Si/Al = 25, 20 wt.%)	90	631	2014	Huang <i>et al.</i> 2019
4Hybrid PVA	90	18	1570	Sajjan <i>et al.</i> 2013
530 mass% GTMAC/PVA	90	190	1575	Sajjan <i>et al.</i> 2013
620 mass% GTMAC/PVA	90	165	1262	Sajjan <i>et al.</i> 2013
710 mass% GTMAC/PVA	90	132	1073	Sajjan <i>et al.</i> 2013
8PVA + TEOS	90	96	913	Sajjan <i>et al.</i> 2013
940 mass% GTMAC/PVA	90	325	417	Sajjan <i>et al.</i> 2013
10SA/PVA (50:50)	90	36	117	Kurkuri <i>et al.</i> 2002
11PVA with glutaraldehyde	90	191	115	Burshe <i>et al.</i> 1997
12Pervap 2201, PVA membrane	80	4	604	Molina 2003

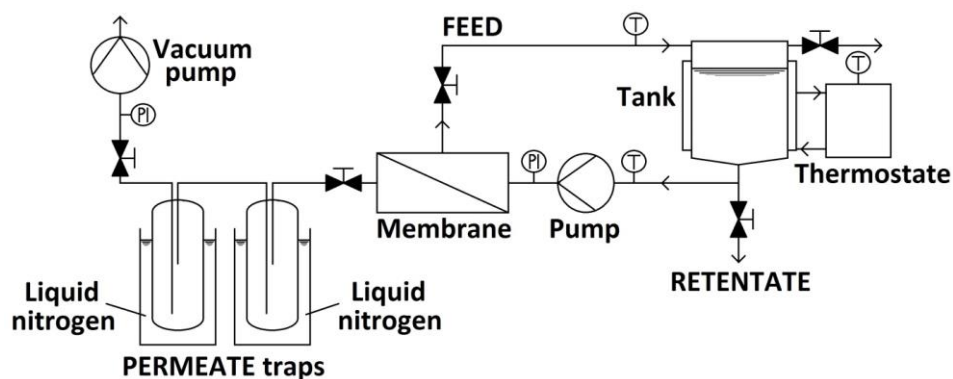
## MATERIAL AND METHODS

In the pharmaceutical sector it is an actual problem that IPA should be separated from an aqueous mixture (Nangare et al., 2017; Cheng et al., 2018). PWW from pharmaceutical industry has to be separated with the following initial composition: 5 m/m% IPA and 95 m/m% water. The product purity is 99.5 m/m% in both cases and 800 kg/h PWW must be treated. Before optimization, laboratory experiments have to be carried out.

The experimental set-up is a P-28 membrane unit from CM-Celfa Membrantechnik AG (see Figure 2 and Figure 3). The flat sheet membrane with 28 cm<sup>2</sup> effective area is placed on a sintered disc separating the feed and the permeate sides. Cross-flow circulation velocity is kept at a permanent value of ~182 l/h (Toth and Mizsey, 2015).



**Figure 2.** Photo of CM-Celfa Membrantechnik AG P-28 universal test membrane apparatus (Toth, 2015)



**Figure 3.** Schematic figure of CM-Celfa P-28 pervaporation unit (Toth and Mizsey, 2015)

The vacuum on the permeate side is maintained with VACUUMBRAND PC2003 VARIO vacuum pump and kept at 2 Torr (2.67 mbar). The isotherm conditions are assured with a thermostat and monitored with thermometers at the inlet and outlet of the unit. The permeate is collected in two traps connected in series and cooled with liquid nitrogen to prevent loss of the permeate. The ethyl

acetate content is measured with Shimadzu GC-14B gas chromatograph. The water content of organophilic experiments are measured with Hanna HI 904 coulometric Karl Fischer titrator (Toth et al., 2015).

According to the methodology of Valentínyi et al. (2013) the pervaporation can be described with the following semi-empirical model:

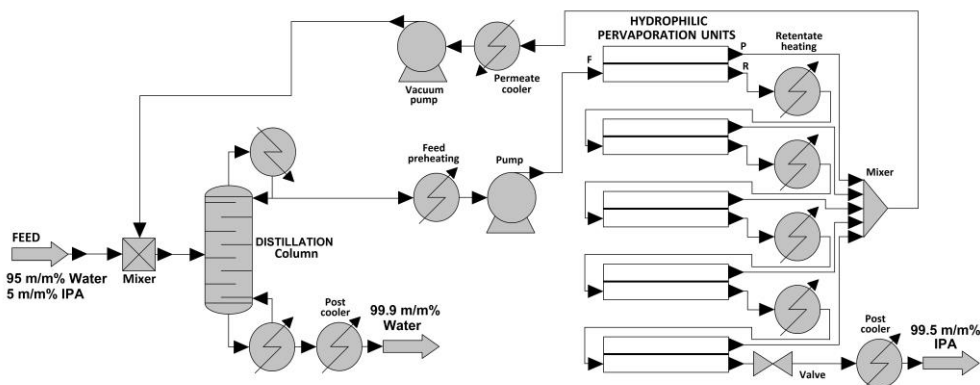
$$J_i = \frac{1}{1 + \{[\bar{D}_i \cdot \exp(B \cdot x_{i1})] / (Q_0 \cdot p_{i0} \cdot \bar{y}_i)\}} \cdot \frac{[\bar{D}_i \cdot \exp(B \cdot x_{i1})]}{\bar{y}_i} \cdot \left( \frac{p_{i1} - p_{i2}}{p_{i0}} \right) \quad i = (1, \dots, k) \quad (3)$$

The model is an improvement of Rautenbach's model (Rautenbach *et al.* 1990) and it considers the concentration dependencies of the transport coefficient. Four parameters of this model are estimated based on our measured data: transport coefficients ( $\bar{D}_i$ ), permeability coefficients ( $Q_0$ ), activation energies ( $E_i$ ) and B parameter. The estimations are completed with the STATISTICA® program environment (Andre et al., 2018; Haaz and Toth 2018).

Professional flowsheet simulator is applied for separation of isopropanol-water mixture. First step, PWW is pumped into the middle of the distillation column and pervaporation separates further the IPA-rich intermediate product. It can be determined the suitable water can be received as bottom product (W) of distillation. Actually it is the purified PWW. The isopropanol substance can be appropriate using this hybrid method as retentate (R) of pervaporation dehydration.

Additional apparatuses are also needed for PV process (Toth et al., 2015). The temperature and the pressure must be increased for the operational level prior to the first membrane unit, because the feed (F) has atmospheric conditions, 20 °C and 1 bar. Permeate (P) streams leaving the pervaporation units are collected, mixed, condensed with cooler and its pressure is increased again from vacuum with pump. The applied feed temperature in membrane modules is 70°C. Feed and permeate pressures are the following, 3 bar and 0.008 bar. UNIQUAC thermodynamic model is applied in the case of SCDS distillation column and exponential Rautenbach model (Valentínyi et al., 2013) for the pervaporation.

ChemCAD professional flowsheet simulator is used for the investigation of hybrid separation (see Figure 4).



**Figure 4.** Flowsheet of isopropanol-water separation with distillation and hydrophilic pervaporation

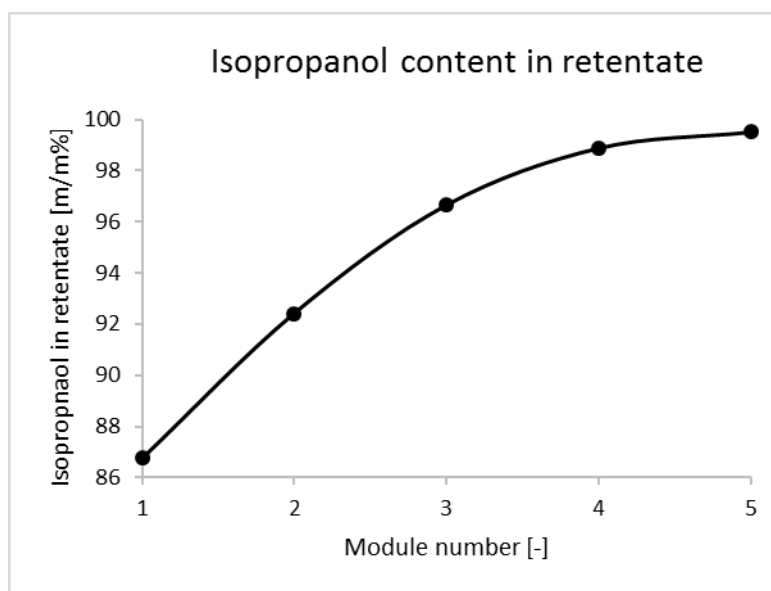
## RESULTS AND DISCUSSION

Results of simulations with distillation and hydrophilic PV process are listed in Table 2.

**Table 2.** Optimized results of ethanol-water separation

	Distillation			Pervaporation	
	F	W	D	P	R
IPA [m/m%]	5	0.1	86	1	99.5
Water [m/m%]	95	99.9	4	99	0.5

Figure 5 shows the isopropanol concentrations of retentate stream in the function of membrane module numbers.

**Figure 5.** Isopropanol concentration in retentate stream

It can be seen 5 membrane module is sufficient for reach the enrichment limit, which is 99.5 m/m% isopropanol. The optimized column has 25 theoretical plates and the reflux ratio is 1 in the optimized case. 90 m<sup>2</sup> effective membrane transfer area is required for removal IPA from PWW.

## SUMMARY

The combination of distillation and pervaporation dehydration is investigated in professional flowsheet environment. It can be concluded isopropanol-water mixture can be separated into pure components with this hybrid operation. The goal composition, which is 99.5 m/m% in both product case can be reached.

## ACKNOWLEDGEMENT

This work was supported by the János Bolyai Research Scholarship of the Hungarian Academy of Sciences, ÚNKP-19-4-BME-416 New National Excellence Program of the Ministry for Innovation and Technology, OTKA 112699 and 128543. This research was supported by the European Union and the Hungarian State, co-financed by the European Regional Development Fund in the framework of the GINOP-2.3.4-15-2016-00004 project, aimed to promote the cooperation between the higher education and the industry. The research reported in this paper has been supported by the National Research, Development and Innovation Fund (TUDFO/51757/2019-ITM, Thematic Excellence Program). The authors thank the members of Environmental and Process Engineering Research Group (<http://www.envproceng.eu/en/home-en/>) for their help.

## REFERENCES

- Adoor, S. G., Prathab., B., Manjeshwar L. S., Aminabhavi, T. M. (2007) Mixed matrix membranes of sodium alginate and poly(vinyl alcohol) for pervaporation dehydration of isopropanol at different temperatures. *Polymer*, **48**(18), 5417-5430.
- Andre, A., Nagy, T., Toth, A. J., Haaz, E., Fozzer, D., Tarjani, J. A. Mizsey, P. (2018) Distillation contra pervaporation: Comprehensive investigation of isobutanol-water separation. *Journal of Cleaner Production*, **187**, 804-818.
- Baker, R. W. (2012) *Membrane Technology and Applications*, Wiley.
- Burshe, M. C., Sawant, S. B., Joshi, J. B., Pangarkar, V. G. (1997) Sorption and permeation of binary water-alcohol systems through PVA membranes crosslinked with multifunctional crosslinking agents. *Separation and Purification Technology*, **12**(2), 145-156.
- Cheng, C., Li, P., Shen, K., Zhang, T., Cao, X., Wang, B., Wang, X., Hsiao, B. S. (2018) Integrated polyamide thin-film nanofibrous composite membrane regulated by functionalized interlayer for efficient water/isopropanol separation. *Journal of Membrane Science*, **553**, 70-81.
- Csizmadia, P., Till, S. (2018) The Effect of Rheology Model of an Activated Sludge on to the Predicted Losses by an Elbow. *Periodica Polytechnica Mechanical Engineering*, **62**(4), 305-311.
- Gmehling, J., Onken, U., Rarey-Nies, J. R. (1978) Vapor-liquid equilibrium data collection. Dechema, Virginia.
- Haaz, E., Toth, A. J. (2018) Methanol dehydration with pervaporation: Experiments and modelling. *Separation and Purification Technology*, **205**, 121-129.
- Huang, B., Liu, Q., Caro, J., Huang A. (2014). Iso-butanol dehydration by pervaporation using zeolite LTA membranes prepared on 3-aminopropyltriethoxysilane-modified alumina tubes. *Journal of Membrane Science*, **455**, 200-206.
- Huang, Z., Ru, X.-f., Zhu, Y.-T., Guo, Y.-h., Teng, L.-j. (2019) Poly(vinyl alcohol)/ZSM-5 zeolite mixed matrix membranes for pervaporation dehydration of isopropanol/water solution through response surface methodology. *Chemical Engineering Research and Design*, **144**, 19-34.
- Kurkuri, D. M., Toti, S. U., Aminabhavi, M. T. (2002) Syntheses and characterization of blend membranes of sodium alginate and poly(vinyl alcohol) for the pervaporation separation of water + isopropanol mixtures. *Journal of Applied Polymer Science*, **86**(14), 3642-3651.
- Luis, P., Van der Bruggen, B. (2015) 4 - Pervaporation modeling: state of the art and future trends. In: *Pervaporation, Vapour Permeation and Membrane Distillation*, Woodhead Publishing, Oxford, 87-106.
- Marsden, C. (1954) *Solvents And Allied Substances Manual With Solubility Chart*, Cleaver-Hume and Elsevier, London.
- Molina, J. M. (2003) *Industrial wastewater treatment by membrane filtration and separation*. PhD Thesis, Budapest University of Economic Sciences and Public Administration, Budapest.
- Nangare, D., Mayadevi, S., Khebudkar, R. (2017) Modeling and Simulation of Distillation + Pervaporation Hybrid Unit: Study of IPA - Water Separation. *International Journal of ChemTech Research*, **10**(5), 190-196.
- Rautenbach, R., Herion, C. Meyer-Blumentoth, U. (1990) Pervaporation membrane separation processes. *Membrane Science and Technology Series*, **1**, 181-191.
- Sajjan, A. M., Jeevan Kumar, B. K., Kittur, A. A., Kariduraganavar, M. Y. (2013) Development of novel grafted hybrid PVA membranes using glycidyltrimethylammonium chloride for pervaporation separation of water-isopropanol mixtures. *Journal of Industrial and Engineering Chemistry*, **19**(2), 427-437.
- Szabados, E., Jobbágy, A., Tóth, A. J., Mizsey, P., Tardy, G., Pulgarin, C., Giannakis, S., Takács, E., Wojnárovits, L., Makó, M., Trócsányi, Z., Tungler, A. (2018). Complex Treatment for the Disposal and Utilization of Process Wastewaters of the Pharmaceutical Industry. *Periodica*



*Polytechnica Chemical Engineering*, **62**(1), 76-90.

- Toth, A. J. (2015) Liquid Waste Treatment with Physicochemical Tools for Environmental Protection. PhD Thesis, Budapest University of Technology and Economics, Budapest.
- Toth, A. J. (2018) Removal of ethanol from pharmaceutical process wastewater with distillation and hydrophilic pervaporation. Proceedings of the 10th Eastern European IWA Young Water Professionals Conference, IWA, Zagreb, Croatia, 550-555.
- Toth, A. J. (2019) Comprehensive evaluation and comparison of advanced separation methods on the separation of ethyl acetate-ethanol-water highly non-ideal mixture. *Separation and Purification Technology*, **224**, 490-508.
- Toth, A. J., Andre, A., Haaz, E., Mizsey, P. (2015) New horizon for the membrane separation: Combination of organophilic and hydrophilic pervaporations. *Separation and Purification Technology*, **156**(2), 432-443.
- Toth, A. J., Haaz, E., Nagy, T., Tarjani, A. J., Fozer, D., Andre, A., Valentinyi, N. (2018) Ethyl acetate removal from pharmaceutical process wastewater with organophilic pervaporation. Proceedings of the 10th Eastern European IWA Young Water Professionals Conference, IWA, Zagreb, Croatia, 556-561.
- Toth, A. J., Mizsey P. (2015). Methanol removal from aqueous mixture with organophilic pervaporation: Experiments and modelling. *Chemical Engineering Research and Design*, **98**, 123-135.
- Valentinyi, N., Cséfalvay, E., Mizsey, P. (2013). Modelling of pervaporation: Parameter estimation and model development. *Chemical Engineering Research and Design*, **91**(1), 174-183.
- Wijmans, J. G., Baker R. W. (1995). The solution-diffusion model: a review. *Journal of Membrane Science*, **107**(1-2), 1-21.

# Recovery of Cutting Oil from Wastewater by Pervaporation Process Using Natural Clay Modified PVA Membrane

D. Unlu\*

\* Bursa Technical University, Faculty of Engineering and Natural Sciences, Chemical Engineering Department, 16310, Yildirim, Bursa, Turkey (E-mail: [derya.unlu@btu.edu.tr](mailto:derya.unlu@btu.edu.tr))

## Abstract

In this study, the pervaporative dehydration of diethylene glycol (DEG) through a hydrophilic PVA membrane was investigated at various operation temperatures in the range of 333–363 K with feed mixture containing 0.5–2.0 wt % water. The pervaporation (PV) performance of poly (vinyl alcohol) (PVA) is enhanced by the addition of natural clay kaolin into pristine membrane. The thermal stability of membranes were analyzed by TGA. The morphological analysis was carried out with SEM. Separation success was determined by calculation of flux, selectivity and PSI. These values were investigated as functions of the clay amount, feed concentration and feed temperature. The obtained results show that PV is an effective method for recycling waste cutting oil from wastewater.

## Keywords

Cutting oil; diethylene glycol; kaolin; PVA; pervaporation

## INTRODUCTION

The solar energy and semiconductor sectors are needing more and better wafers. The general cutting process cannot satisfy these demands, so the wire saw process was enhanced. In the wire saw process, a material called cutting oil is used in the wire saw instrument. The cutting oil is consisting of SiC particles, solvent, and additives. The used solvent must have two properties: it is easily cleaned using water and viscosity must cause the abrasive to be suspended in the solvent. Ethylene glycol (EG), diethylene glycol (DEG), and polyethylene glycol (PEG) are often used as solvents for cutting oil.

DEG has the necessary characteristic properties of cutting oil. DEG,  $(\text{HOCH}_2\text{CH}_2)_2\text{O}$ , is a co-product with ethylene glycol and triethylene glycol. It is a colorless and odorless liquid that is miscible in water and alcohol (Schep et al., 2009). Only disadvantage of DEG is high boiling point of 245.3 °C. This point and its miscibility with water increase difficulty of its recycle. Tons of waste cutting oil is produced by wafer slicing. The waste cutting oil contains the original cutting oil, water, and Si particles. SiC and Si particles will be recovered by solid-liquid technique, but the solvent recovery is possible with dehydration method. The conventional method for dehydration is distillation. Distillation requires high energy and cost and the obtainment of high purity of DEG is not possible. Therefore, a new process must be developed. Pervaporation is a good alternative to distillation process in treatment the waste cutting oil (Chen and Huang, 2018).

Pervaporation is one of the promising technique of membrane processes. Pervaporation is used to separate azeotropic mixtures and organic–organic mixtures (Oh et al., 2013; Shaban, 1997; Abdallah et al., 2013; Suhas et al., 2013). The advantages of the pervaporation process are low cost, low energy consumption and high separation efficiency. Pervaporation process is carried out under mild operation conditions (Park et al., 2004; Sha et al., 2018; Unlu et al., 2014; Assabumrungrat et al., 2003). Hydrophilic membranes are used to separate water from water/organic mixtures. Poly (vinyl alcohol) (PVA) is widely used in pervaporative dehydration process. PVA is a nontoxic, water soluble, biocompatible and biodegradable polymer (Rashidzadeh et al., 2013; Zheng et al.,

2001). In recent years, filler materials have been used to improve the water adsorption capacity of PVA membrane.

In this study, a synthetic wastewater DEG-water was tested in pervaporation system. Natural clay modified PVA membrane was used in the process. PVA is a well-known hydrophilic polymer that is used in the pervaporation process. This study has a new development in using a natural clay additive hydrophilic membrane for pervaporative dehydration of cutting oil. No study are available in the literature on the membranes of PVA incorporated kaolin clay used in recovery of cutting oil by pervaporation. Clay improved the dehydration performance of membrane. The optimum clay amount and optimal operation temperature were investigated. According to the author's knowledge, this is the first study on pervaporative dehydration that deals with the effect of the different ratios of clay/PVA membranes on dehydration of cutting oil performance.

## MATERIALS AND EXPERIMENTAL METHODS

### Materials

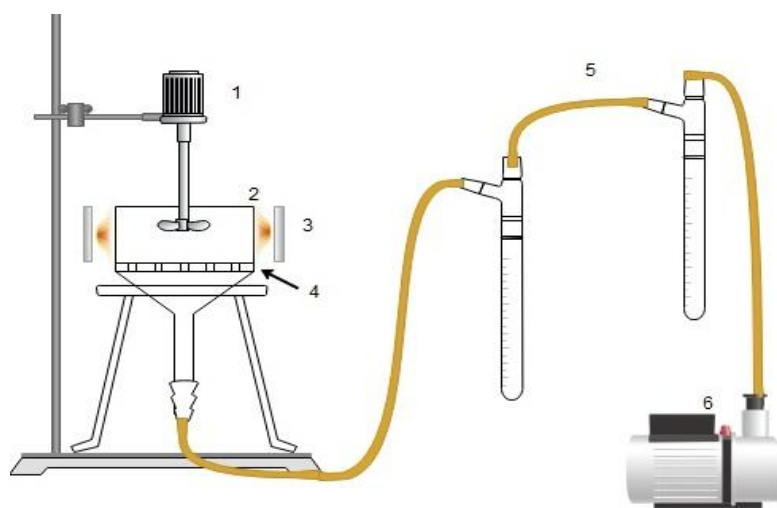
Polyvinyl alcohol (PVA), diethylene glycol with a purity of 99 %, hydrochloric acid and glutaraldehyde were purchased from Sigma Aldrich. Kaolin clay was provided by Karabacak Mining Industry.

### Membrane Preparation

A 6 wt% PVA aqueous solution was prepared at 90 °C to obtain a homogeneous solution. Certain amount of kaolin clay was dispersed in 10 ml of deionized water by sonication for 2 h. The PVA solution was mixed with the aqueous clay solution to obtain 6 % PVA casting solution with different concentration of clay. Clay amount was defined as the respect to the dry polymer weight. After mixing for 24 h, membrane was cross-linked in situ. A certain amount of glutaraldehyde and HCl solution were added and stirred for 1 h. Then final solutions were cast onto glass plate and dried at room temperature. Membranes were characterized by using TGA and SEM analysis.

### Waste cutting oil pervaporation experiment

The scheme of lab scale pervaporation unit is shown in Figure 1.



**Figure 1.** PV configuration. (1) agitator thermocouple (2) membrane cell (3) heating jacket, (4) membrane, (5) Dewar flasks (6) vacuum pump

The membrane surface area is 9.61 cm<sup>2</sup>. The volume of the feed solution was 70 ml. The pressure at the permeate side was reduced to 5 mbar by a vacuum pump. Total flux was calculated by weighing the liquid mixtures collected in the trap for each 60 min. The flux (J), separation factor ( $\alpha$ ) and pervaporation separation index (PSI) were calculated by analysis of the compositions of both the feed and permeate streams with the gas chromatography and refractometer. The flux, separation factor and pervaporation separation index values were determined as the following equations:

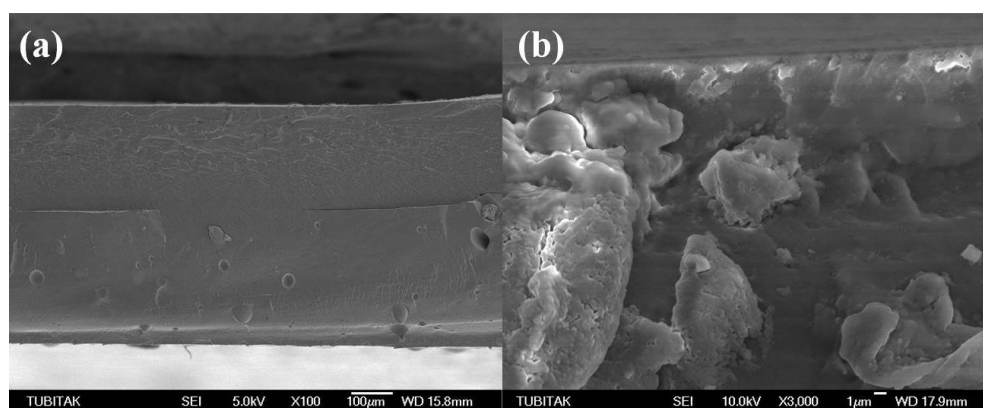
$$J = \frac{m}{A \cdot t}, \quad (1) \quad \alpha = \frac{(y_a / y_b)_{\text{permeate}}}{(x_a / x_b)_{\text{feed}}}, \quad (2) \quad \text{PSI} = J \cdot x \cdot (\alpha - 1), \quad (3)$$

where J is the flux, m is the permeation mass, t is the time in Equation 1;  $y_a$  and  $x_a$  is the weight fraction of water in the permeate and feed streams, and  $y_b$  and  $x_b$  is the weight fraction of DEG in the permeate and feed streams in Equation 2.

## RESULTS AND DISCUSSION

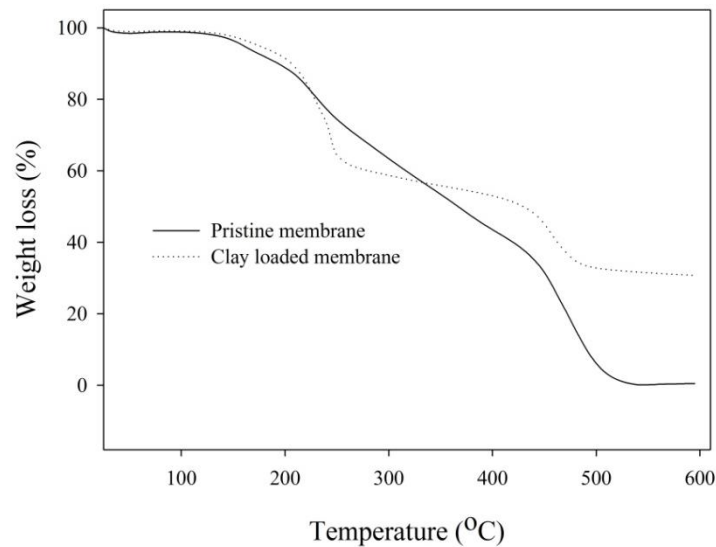
### Membrane characterization

Figure 2 depicts the cross-section images of pristine PVA membrane and natural clay modified PVA membrane. Pristine PVA membrane has smooth surface according to the clay modified PVA membrane, because pristine membrane represents crystalline morphology. The incorporation of clay destroys the crystalline structure of polymer matrix and amorphous state is obtained.



**Figure 2.** Cross section images of membranes (a) pristine PVA membrane (b)clay loaded PVA membrane

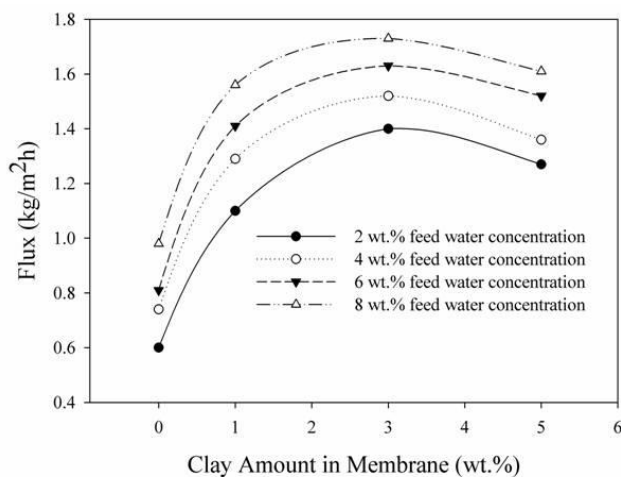
Figure 3 shows the TGA profiles for the pristine PVA membrane and PVA/clay membrane. The most weight loss is observed in the range of 150–40 °C for all membranes. It corresponds to the structural decomposition of the polymers. The thermal decomposition of kaolin loaded PVA membrane shift toward the higher temperature range than that of pristine PVA membrane. This confirms that the addition of clay enhances the thermal stability of pristine membrane.



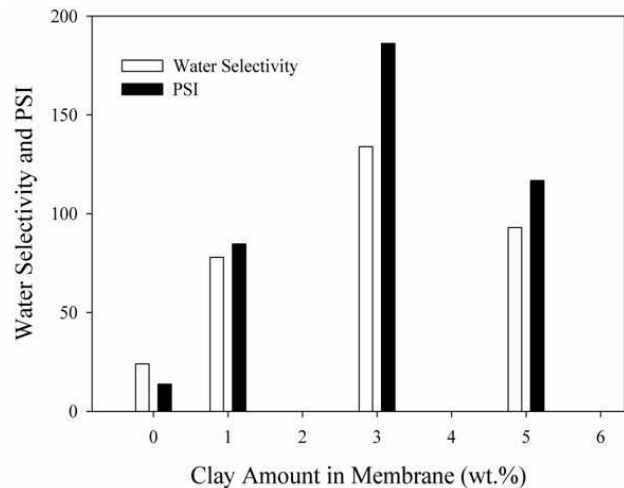
**Figure 3.** TGA curves of membranes

### Recovery of cutting oil from wastewater by pervaporation

The flux, separation factor and PSI values of the binary mixtures were investigated with kaolin clay amount in the membrane in the range of 1–5 wt % at 333 K and the results are shown in Figures 4 and 5.



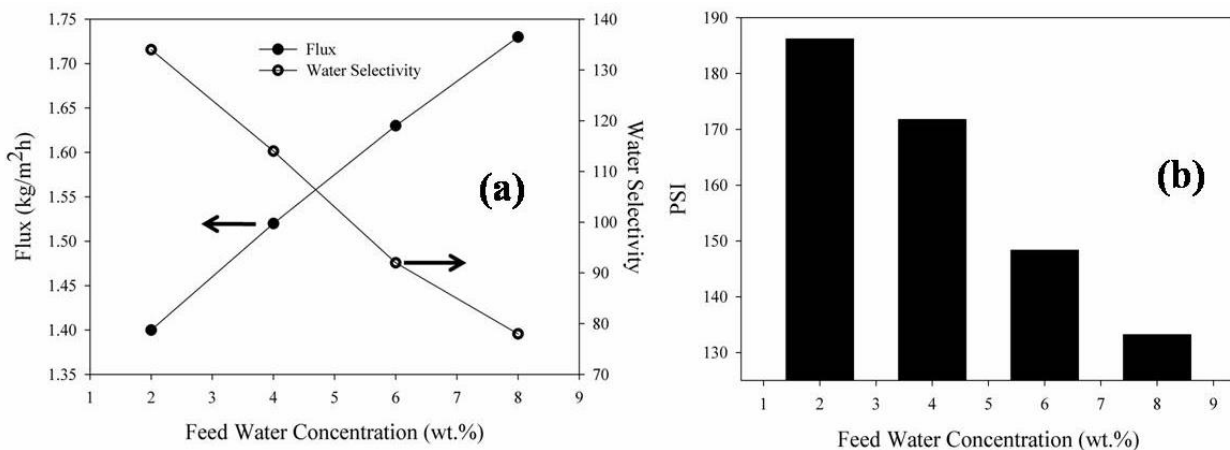
**Figure 4.** Effect of clay amount on flux



**Figure 5.** Effect of clay amount on  $\alpha$  and PSI

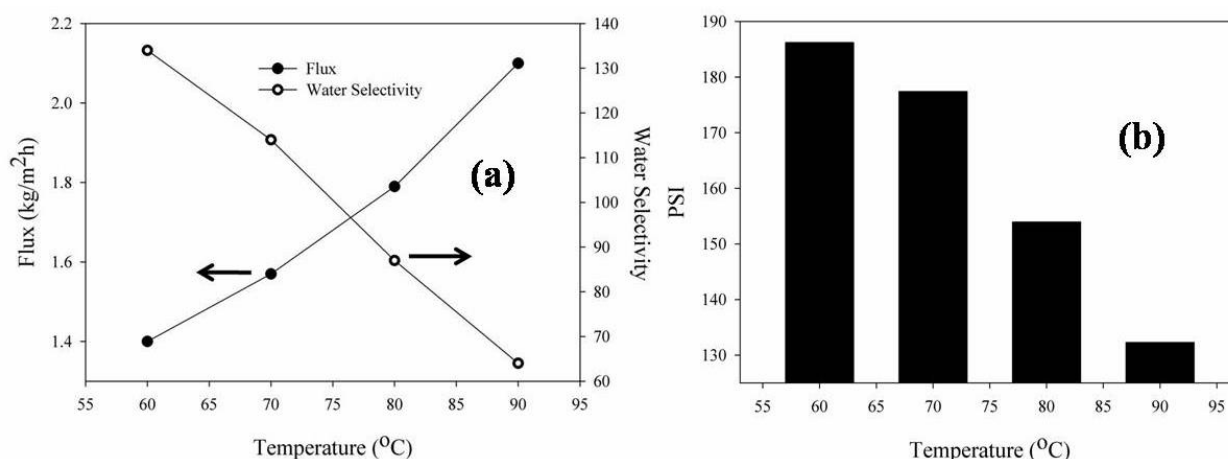
In pervaporation, molecular diffusion is generally explained by the solution–diffusion mechanism. According to solution–diffusion mechanism, firstly molecules dissolve on the membrane surface and then diffuse through the membrane as a result of the concentration gradient (Adoor et al., 2006). However, the overall separation is related to physical feature of the solvents, affinity of solvents to membrane as well as the morphological structure of the membrane. With this approach, alcohols can be diffused into the PVA membrane due to hydrophilic–hydrophilic interactions, because alcohols have close polarity with water. The addition of clay in membrane restricts the diffusion of organic molecules and thus excess swelling of membrane is prevented. Separation performance changes depending upon the clay content, water selectivity enhances with clay amount in membrane. PVA is hydrophilic polymer and has many hydroxyl groups. The performance of

PVA membranes can be improved by the addition of clay. These membranes are water selective. As shown in Figure 3, flux and selectivity increased with clay amount. However, the flux is small at lower feed water concentration. Higher concentration of water in the feed mixture would result in a higher permeability. The pristine PVA membrane shows selectivity value of 24 at 2 wt.% feed water concentration. However, high clay amount in the PVA membrane, water selectivity values increased to 134 for the same 2 wt.% feed water. These water selectivity values are very high when compare with pristine membrane. In pristine PVA membrane, transport occurs by driving force. In case clay loaded PVA membrane, hydrophilic interactions between clay and the PVA acts as a role in separation. Water molecules are adsorbed in the hydrophilic clay instead of PVA. Therefore, diffusion becomes difficult. Consequently, the flux of clay loaded membrane is lower than the pristine membrane. Clay avoids the diffusion of the organic molecules through the membrane, so selectivity increases. However, selectivity of clay loaded membrane declined with the increasing feed water concentration due to the plasticization effect. This is further supported by the PSI (given in Figures 5 and 7). The flux is decreased with an increase of the amount of clay beyond 3 wt. %. It is observed that there is an increase in PSI values with increase in the clay from 0 to 3 wt. %, but further addition of clay (more than 3 wt. %) decreases the PSI value. This result can be related to the aggregation of clay nanoparticles. When the clay amount is greater than 3 wt %, the compatibility of the additive and the polymeric matrix decreases. This situation is resulted in microphase separation. Therefore, separation factor drops and permeation rate increases (Anilkumar et al., 2008).



**Figure 6.** Effect of water concentration on (a) flux and water selectivity (b) PSI

The effect of feed water concentration on separation performance of both pristine and clay loaded PVA membrane was investigated, and results are presented in Figure 3 and 4. The flux increased with increasing feed water concentration from 2 to 8 wt. %. For 3 wt.% of clay loaded PVA membrane, the observed selectivity for dehydration of cutting oil is 134 at 2 wt. % of water in the feed, which decreased with increasing concentration of water in the feed (see Fig. 6). At higher concentration of water in the feed mixture, 3 wt.% of clay loaded PVA membrane could absorb more amounts of water molecules when compared to pristine membrane due to plasticization effect of the polymer (Devi et al., 2006). However, selectivity has decreased, but flux increased considerably for the 3 wt. % clay containing PVA membrane. For 8 wt. % water-containing feed mixture, selectivity decreased to 78, but flux is enhanced to 1.73 kg/m<sup>2</sup>h for 3 wt.% of clay loaded PVA membrane. In all cases, flux and selectivity of PVA-Clay membranes are higher than that of pristine PVA membrane (0.6 kg/m<sup>2</sup>h and 24). The present study demonstrates the positive role played by clay upon incorporation into PVA to enhance the membrane performance over that of pristine PVA membrane.



**Figure 7.** Effect of temperature on (a) flux and water selectivity (b) PSI

No study are available in the literature on the membranes of PVA incorporated kaolin clay used in recovery of cutting oil by pervaporation. Results of recovery of cutting oil from wastewater obtained at 60, 70, 80 and 90°C are presented in Figure 7. It is known that PVA has superior separation performance for dehydration process, but temperature affect the separation performance of PVA negatively. Polymer mobility increases with temperature, diffusion channels expanded. Flexible polymer chains allow the water molecules through the membrane easily. This fast and more diffusion causes the membrane swelling, flux increases and selectivity declines. The driving force is created from a difference in temperature between feed and permeate mixtures. As the feed temperature increases, vapour pressure in the feed mixture also increases, but vapour pressure at the permeate side is not affected. The driving force increases with increasing temperature (Ravindra et al., 2015; Wang et al., 2001; Hu et al., 2002).

## CONCLUSION

PVA-clay nanocomposites containing different clay amounts have been prepared, and application of separation performance on recovery of cutting oil from wastewater was investigated in pervaporation system. The dispersion of nanoparticles in membrane decreases with an increase in clay amount. Pervaporation experiments showed a far excellent performance in solvent selectivity in the case of the clay loaded membrane compared to the pristine membrane. 3 wt.% clay loaded membrane showed excellent performance with a flux of 1.40 kg/m<sup>2</sup>h and water selectivity of 134 at 60°C when the flux and selectivity values of pristine membranes were 0.6 kg/m<sup>2</sup>h and 24, respectively. Membranes containing 3 wt % clay showed maximum separation performance. However, an increase in flux and a decrease in separation factor were observed when the clay amount became higher than 3 wt %.

## ACKNOWLEDGEMENTS

The author thanks Karabacak Mining Industry and Foreign Trade Tourism Inc. for its support of this work by providing.

## REFERENCES

- Abdallah, H., El-Gendi, A., El-Zanati, E., Matsuura, T. (2013) Pervaporation of methanol from methylacetate mixture using polyamide-6 membrane, *Desalination and Water Treatment*, **51**, 7807-7814.
- Adoor, S. G., Manjeshwar, L. S., Kumar Naidu, B. V., Sairam, M., Aminabhavi, T. M. (2006)

- Poly(vinyl alcohol)/poly(methyl methacrylate) blend membranes for pervaporation separation of water+isopropanol and water+1,4-dioxane mixtures. *Journal of Membrane Science*, **280**(1-2), 594-602.
- Anilkumar, S., Kumaran, M. G., Thomas, S. (2008) Characterization of EVA/Clay Nanocomposite Membranes and Its Pervaporation Performance. *The Journal of Physical Chemistry B*, **112**(13), 4009-4015.
- Assabumrungrat, S., Phongpatthanapanich, J., Praserttham, P., Tagawa, T., Goto, S. (2003) Theoretical study on the synthesis of methyl acetate from methanol and acetic acid in pervaporation membrane reactors: effect of continuous-flow modes. *Chemical Engineering Journal*, **95**(1-3), 57-65.
- Chen, T.-H., Huang, Y.-H. (2018). Dehydration of waste cutting oil using a pervaporation process. *Journal of the Taiwan Institute of Chemical Engineers*, **82**, 75-79.
- Devi, D. A., Smitha, B., Sridhar, S., Aminabhavi, T. M. (2006) Pervaporation separation of dimethylformamide/water mixtures through poly(vinyl alcohol)/poly(acrylic acid) blend membranes. *Separation and Purification Technology*, **51**(1), 104-111.
- Hu, S. Y., Zhang, Y., Lawless, D., & Feng, X. (2012). Composite membranes comprising of polyvinylamine-poly(vinyl alcohol) incorporated with carbon nanotubes for dehydration of ethylene glycol by pervaporation. *Journal of Membrane Science*, **417-418**, 34-44.
- Oh, D., Lee, S., Lee, Y. T. (2013) Mixed-matrix membrane prepared from crosslinked PVA with NaA zeolite for pervaporative separation of water–butanol mixtures, *Desalination and Water Treatment*, **51**, 5362-5370.
- Park, B.-G., Tsotsis, T. T. (2004). Models and experiments with pervaporation membrane reactors integrated with an adsorbent system. *Chemical Engineering and Processing: Process Intensification*, **43**(9), 1171-1180.
- Rashidzadeh, A., Olad, A. (2013) Novel polyaniline/poly (vinyl alcohol)/clinoptilolite nanocomposite: dye removal, kinetic, and isotherm studies. *Desalination and Water Treatment*, **51**(37-39), 7057-7066.
- Ravindra, S., Rajinikanth, V., Mulaba-Bafubandi, A. F., Vallabhapurapu, V. S. (2015) Performance enhancement of the poly (vinyl alcohol) (PVA) by activated natural clay clinoptilolite for pervaporation separation of aqueous–organic mixtures. *Desalination and Water Treatment*, **57**(11), 4920-4934.
- Schep, L. J., Slaughter, R. J., Temple, W. A., Beasley, D. M. G. (2009) Diethylene glycol poisoning. *Clinical Toxicology*, **47**, 525-35.
- Shaban, H. I. (1997) Pervaporation separation of water from organic mixtures. *Separation and Purification Technology*, **11**, 119-26.
- Suhas, D. P., Raghu, A. V., Jeong, H. M., Aminabhavi, T. M. (2013) Graphene-loaded sodium alginate nanocomposite membranes with enhanced isopropanol dehydration performance via a pervaporation technique. *RSC Advances*, **3**, 17120-17130.
- Sha, S., Zhang, X. L., Wang, L. M., Li, Y. M., Lin, L. G., Zhang, Y. Z. (2018) Effect of synthetic conditions on the morphology and gasoline desulfurization performance of microphase-separated membranes. *Cellulose*, **25**(6), 3487-3497.
- Unlu, D., Hilmioglu, N. D. (2014) Pervaporation catalytic membrane reactor study for the production of ethyl acetate using Zr(SO<sub>4</sub>)<sub>2</sub>·4H<sub>2</sub>O coated chitosan membrane. *Journal of Chemical Technology & Biotechnology*, **91**(1), 122-130.
- Wang, Y., Chung, T. S., Neo, B. W., Gruender, M. (2011) Processing and engineering of pervaporation dehydration of ethylene glycol via dual-layer polybenzimidazole (PBI)/polyetherimide (PEI) membranes. *Journal of Membrane Science*, **378**(1-2), 339-350.
- Zheng, H., Du, Y., Yu, J., Huang, R., Zhang, L. (2001) Preparation and characterization of chitosan/poly(vinyl alcohol) blend fibers. *Journal of Applied Polymer Science*, **80**(13), 2558-2565.



# Purification of Copper Metal Using Carbonized Mandarin Peel

T. Unugul\* and F. U. Nigiz\*

\* Department of Chemical Engineering, University of Kocaeli, 41380, Kocaeli, Turkey  
(E-mails: [unugultuba@gmail.com](mailto:unugultuba@gmail.com); [filiz.ugurr@gmail.com](mailto:filiz.ugurr@gmail.com))

## Abstract

In this study; mandarin peel activated carbon (CMP) was prepared and the adsorption behaviour of the activated carbon for copper removal was investigated. In the adsorption studies; the effects of initial metal concentration, solution pH, adsorbent dosage and contact time on copper removal were investigated. As a result; a complete copper removal was achieved when the copper concentration in water was 5 mg/L and the adsorbent dosage was 3.75 g/L when the solution pH was 7. Freundlich isotherm was more appropriate to explain the removal of copper from the solution. The kinetic of the heavy metal adsorption onto CMP was obtained as pseudo-second order.

## Keywords

Mandarin peel based activated carbon; copper removal; isotherm; kinetic

## INTRODUCTION

The development of technology led to an increase in the spread of the chemical industry. The growth of the industrial population causes an increase in industrial pollution. The pollution affects the soil, air, and water. In particular, water pollution directly shows a fatal effect on the living organism. In many sectors such as mining, paint, leather and textile industry, inorganic and organic pollutants cause environmental problems (Enniya, 2018). Especially, heavy metal pollution is an important problem for the environment and human health. Because heavy metals are inorganic pollutants, they are non-biodegradable and contaminate in the ecosystem. Various methods such as precipitation, coagulation and flocculation (Yi, 2017), reverse osmosis (Amuda, 2007), membrane filtration, ion exchange (Kurniawan, 2006), adsorption (Thuan, 2017) have been developed for the treatment of heavy metals from wastewaters. Adsorption is commonly used owing to the advantages such as high efficiency, low cost, easy process and re-use of the adsorbent. However, the high-cost synthetic adsorbent is one of the biggest disadvantages of this method. In recent years, bio-wastes have been transformed into activated carbon, have a great interest in the re-using of wastes. The carbon-based materials produced from the biological feedstock is characterized as a non-toxic and low-cost material (Hashemian, 2014). The efficiency of these materials can be improved by increasing their surface area, porous structure, and functional groups (Thuan, 2017; Yahya, 2015; Dias, 2007). Most of the vegetable foods have the potential to be produced as an active carbon because of the ingredients they contain. The peels of citrus fruits such as lemon, orange, mandarin, grapefruit are the most important ones.

According to the data of the United Nations Food and Agriculture Organization (FAO) 2013, 21 million tons of mandarin was produced in the world. Turkey is the biggest supplier of mandarin with the production capacity of 872 thousand tons. The amount of waste peel of this fruit is approximately 8-14 % by weight. Utilizing these waste peel as a valuable substance and reusing as a useful product contributes to the economy of the supplier. Valuable organic essences, oil species, and some other chemicals can be produced by regeneration of these peels and can be used in cosmetic and pharmaceutical industries. Nevertheless, after the removal of these important chemicals, peel residue still has a vast amount of biomass. In recent years, a number of studies have

been carried out on the use of biomass as adsorbents. Due to the lignocellulosic and phenolic content of mandarin shells, it provides high adsorption efficiency by converting them into the activated carbon (Koyuncu, 2018; Tsitsagi, 2018).

In this study; mandarin peel based activated carbon (CMP) was prepared and the adsorption behaviour of the activated carbon for copper removal was investigated. In the adsorption studies; the effects of initial metal concentration, solution pH, adsorbent dosage and contact time on copper removal were investigated.

## EXPERIMENTAL

### Materials

Copper sulfate pentahydrate was provided from Merck Chemicals, Turkey. Sulfuric acid (H<sub>2</sub>SO<sub>4</sub>) and sodium hydroxide (NaOH), which were used to convert the mandarin peels into functionalized carbon adsorbent, were provided from Merck Chemicals, Turkey.

### Adsorbent preparation

The mandarin peel was washed with distilled water and dried in oven (Santez SE-45F) at 100 °C for 24 hours. The functionalization was carried out at a hydrothermal reactor at 105 °C with 1M of H<sub>2</sub>SO<sub>4</sub> solution four hours. The acid treated mandarin peels (CMP) were dried in an oven at 70 °C for one day. Following the drying process, CMP was neutralized with 2M NaOH solution. After the neutralization, the CMP was dried in a vacuum oven at 70 °C for 2 hours.

### Batch adsorption studies

In this study, the effects of heavy metal concentration, adsorbent dosage, pH, and the adsorption time on adsorption performances were evaluated. Firstly, a stock solution of 1000 mg/L Cu was prepared by diluting the copper sulphate pentahydrate. Then, the varying concentration of Cu (5, 15, 25 mg/L) was prepared from the stock solution. After determining the heavy metal concentration that gives the highest removal performance, the effect of the adsorbent dosage (0.625, 2.1875, 3.75 g/L) were investigated. The experiments were carried out in 100 mL Erlenmeyer with a total solution of 20 mL in a fixed mixer. Prior to performing the absorbance measurement, the solution was centrifuged, then filtered using a vacuum pump and filter paper. The absorbance of the purified solution was measured by means of UV/visible spectrophotometer (Thermo Spectronic) with a wavelength of 790 nm.

The metal removal (R)(%) and the adsorption capacity at the equilibrium state,  $q_e$  (mg/g) was calculated using the following equation:

$$R(\%) = \frac{(C_o - C_t)}{C_o} \cdot 100 \quad (1)$$

$$q_e = \frac{(C_o - C_e)}{w} \cdot V \quad (2)$$

where  $C_o$ ,  $C_t$  and  $C_e$  are the initial, at a given  $t$  time, and equilibrium heavy metal concentration (mg/L),  $V$  is the volume of the heavy metal solution (L),  $W$  is the weight of the adsorbent (g).

### Isotherm Investigations

Langumir and Freundlich isotherm were adapted to the experimental results and the appropriate isotherm were determined by means of the following equations (Enniya, 2018; Greenlee, 2007):

$$\text{Langumir isotherm:} \quad \frac{C_e}{q_e} = \frac{1}{q_{Lmax} \frac{C_e}{q_{max}}} \quad (3)$$

$$\text{Freundlich isotherm:} \quad \ln q_e = \ln K_f + \frac{1}{n} \ln C_e \quad (4)$$

where  $K_L$  is Langumir constant (mg/L),  $q_{max}$  is the maximum monolayer adsorption capacity of the adsorbent (mg/g).  $K_F$  and  $n$  are Freundlich constant. To accept the isotherm,  $1/n$  should be between “0” and “1”.

$$R_L = \frac{1}{1 + K_L C_0} \quad (5)$$

where  $R_L$  is the separation factor. If  $R_L$  value is between 0 and 1 then the adsorption isotherms are acceptable. If  $R_L$  is greater than 1, then the adsorption is define as unfavorable. If  $R_L$  value equal to “0” or “1”, then the adsorption is accepted as irreversible and linear, respectively (Ho, 1998).

### Kinetic studies

The adsorption kinetics of Copper ions on the mandarin peel was investigated by accepting of the kinetics as pseudo-first order, pseudo-second order. The amount of adsorbed adsorbent  $q_t$  (mg/g) at a given time was calculated by the following equations:

$$q_t = \frac{C_0 - C_t}{W} \cdot V \quad (6)$$

$$\text{Pseudo-first-order:} \quad \ln (q_e - q_t) = \ln q_e - K_1 t \quad (7)$$

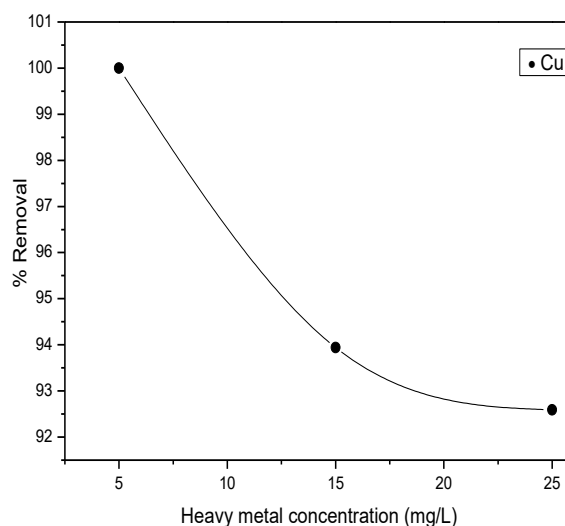
$$\text{Pseudo-second-order:} \quad \frac{t}{q_t} = \frac{1}{K_2 q_e^2} + \frac{1}{q_e} \cdot t \quad (8)$$

where  $q_t$  are the amount of adsorbate which is adsorbed per unit mass of adsorbent (mg/g),  $t$  is time (minute),  $K_1$  and  $K_2$  are pseudo-first order, pseudo-second order kinetic model rate constant (Ponnusami, 2009).

## RESULT and DISCUSSION

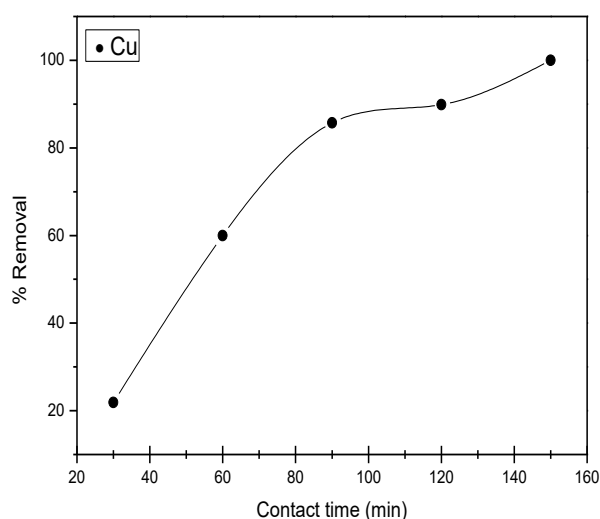
Heavy metal concentration is an important parameter for mass transfer during the adsorption process. The optimum metal concentration directly affects the removal of heavy metal by increasing the driving force (King, 2006; Mobasherpour, 2014). In addition, the appropriate metal concentration exhibits positive results on the adsorption efficiency by increasing the interaction with the adsorbent surface (Semerciöz, 2017). In this study, the effect of initial metal concentration on the removal of copper from copper-water solution was evaluated. Experiments were conducted with the constant adsorbent concentration of 3.75 g/L when the solution pH was 7 and the contact time was 150 minutes at the temperature of 25°C. The initial metal concentrations were varied from 5mg/L to 15 and 25 mg/L. The effect of Cu metal concentration on removal is illustrated in Figure 1.

Figure 1 shows that 100 % of copper rejection was achieved at the low metal concentration (5 mg/L). When the metal concentration increased from 5 mg/L to 25 mg/L, the removal decreased from 100 % to 92.59 %. The decrement should be attributed to the saturation of the active sites of adsorbent when the copper concentration exceeds to the maximum point. With the increase of the metal concentration, the active adsorption sites where the adsorption occurs are saturated and the removal remains at a certain level (Semerjian, 2018; Moghadam, 2013). As active areas on the adsorbent surface are used, mass transfer reaches the maximum level (Semerciöz, 2017).



**Figure 1.** Effect of metal concentration (3.75 g/L adsorbent, pH: 7)

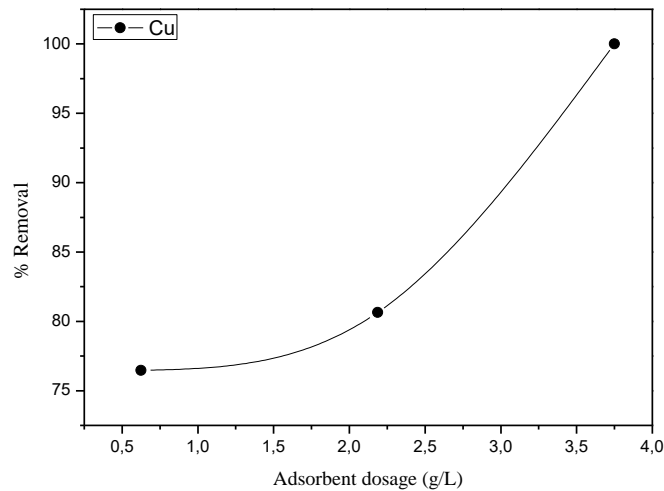
Contact time is one of the effective parameters of the low-cost adsorption process. It directly affects the adsorption performance. For a high-performance and cost-effective process, it is desired to complete the adsorption process as short as possible. Figure 2 shows the effect of contact time on copper removal when the metal concentration was 5 mg/L, the adsorbent concentration was 3.75 g/L and pH value was 7.



**Figure 2.** Effect of contact time (5 mg/L Cu, 3.75 g/L adsorbent, pH: 7)

The copper removal was %87.51 at the first 90 minutes and then reached 100 % of removal within 150 minutes. As shown in the figure, the removal of heavy metal ions showed a significant increase up to 90 minutes. After 90 minutes the adsorption layer became saturated. The driving force between the adsorbent and the metal ions maximized the mass transfer (Souza, 2018). The optimum contact time was determined as 150 minutes by providing a dynamic balance.

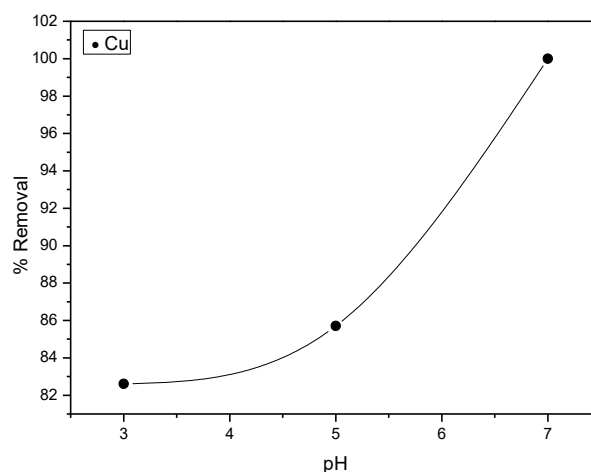
The adsorbent dosage or adsorbent concentration is another important parameter for the performance of adsorption. Increased adsorbent dosage directly affects the total cost of the adsorption process and the cost of recycling. The effect of adsorbent concentration on copper removal is given in Figure 3 when the metal concentration was 5 mg/L, the pH value was 7 and the contact time was 150 minutes.



**Figure 3.** Effect of adsorbent dosage (5 mg/L Cu, pH: 7)

While 76.47 % of removal was achieved by using 0.625 g/L of adsorbent concentration, 100 % removal was achieved with the adsorbent concentration of 3.75 g/L. The concentration of the adsorbent determines the number of binding sites for adsorption. As the number of the adsorbent increases in the media, the total surface area for the process and empty adsorption sites enhance (Tadepalli, 2016). Therefore, adsorption performance increases as also obtained in the present study.

The surface charge of the adsorbent affects the ion concentration and the degree of ionization in the functional groups of the adsorbent such as carboxyl, hydroxyl, amino groups (Othman, 2012). Since the number of active sites on the adsorbent surface changes with pH, it has a direct effect on the adsorption efficiency (Ali, 2016). The effect of 3, 5 and 7 media pH on the removal of Cu was investigated when the metal concentration was 5 mg/L, the adsorbent concentration was 3.75 g/L and the contact time was 150 minutes. The removal results are illustrated in Figure 4. As shown in the figure, 82.61 % of copper removal was obtained when the pH of the solution was 3. At the same conditions (adsorbent concentration, copper concentration and contact time), 100 % of separation was achieved when the pH was 7. In the highly acidic environment, the adsorbent surface is positively charged while in the basic environment the adsorbent is charged negatively. This difference affects the adsorbent surface chemistry and leads to a significant change in adsorption efficiency. As the pH decreases, the concentration of  $H_3O^+$  ions increase and the adsorption of positive copper ions decreases. Similar results have been obtained in the literature before (Ali, 2016).



**Figure 4.** Effect of pH (5 mg/L Cu, 3.75 g/L adsorbent)

### Adsorption isotherm studies

The adsorption isotherm shows the distribution of adsorbate molecules between liquid and solid phases while the adsorption process is in an equilibrium state. The different isotherm models and isotherm data can be used to determine a suitable model for design purposes (Ali, 2016). Adsorption isotherms are used to optimize how the adsorbent interacts with the adsorbate. It gives information about the adsorption mechanism and surface properties of adsorbents. In the different metal concentrations (5, 15 and 25 mg/L) with in the constant adsorbent dosage of 3.75 g/L, 150 minutes mixing time and the pH of 7, the Langumir and Freundlich isotherm calculations were done. The isotherm data are shown in Table 1. According to the  $R^2$  values given in the Table 1, the most suitable isotherm was determined as Freundlich isotherm.

**Table 1.** Langumir and Freundlich isotherm's data

Heavy metal		Cu
Langumir	$q_m$	0.8936
	$K_L$	3.2158
	$R^2$	0.8632
Freundlich	$1/n$	0.8513
	$K_F$	0.5585
	$R^2$	0.9542

### Adsorption kinetics

Kinetic models help to estimate the rate constants of adsorption and help to explain the mechanism of the adsorption. In the present study, kinetic studies were performed using the metal concentration of 5 mg/L. In this concentration, the performance of the copper removal was highest and the adsorption was achieved with the highest rate. In order to estimate the adsorption mechanism, pseudo-first order and pseudo-second order models were applied. The kinetic model parameters are shown in Table 2 ( $C_0$ : 5 mg/L, adsorption dose: 3.75 g/L, pH: 7). For determining the appropriate kinetic model, both the experimental and calculated  $q_e$  values accompanied with the  $R^2$  value should be taken into account. According to the results obtained in this study; the pseudo-second order kinetic was suitable. The kinetic model was acceptable, since the  $q_e$  value that was calculated from the figure and obtained from the experiment were close to the each other. The pseudo-second order kinetic model confirmed that the adsorption rate was independent on the adsorbate concentration and was dependent on the adsorption capacity (Lim, 2017).

**Table 2.** Kinetic parameters for the adsorption of copper onto CMP

Heavy metal		Cu
Pseudo 1 <sup>st</sup> order	$K_1$ ( $\text{min}^{-1}$ )	0.6278
	$q_{e,\text{exp}}$ (mg/g)	1.17496
	$q_{e,\text{cal}}$ (mg/g)	1.1751
	$R^2$	0.9613
Pseudo 2 <sup>nd</sup> order	$K_2$ (g/mg min)	3,6804
	$q_{e,\text{exp}}$ (mg/g)	1,17496
	$q_{e,\text{cal}}$ (mg/g)	0.4064
	$R^2$	0.9865

## CONCLUSION

In the present study, a new acid treated and factionalized carbon adsorbent was synthesized from the mandarin peels and used for the adsorption of heavy metal. As a result, it was obtained that the CMP was very effective to remove copper from simulated metal containing water solution. The highest removal of 100% was obtained when the copper concentration was 5 mg/L, adsorbent dosage was 3.75 g/L, pH value was 7. Freundlich isotherm was more appropriate to explain the removal of copper from the solution. The kinetic of the heavy metal adsorption onto CMP was obtained as pseudo-second order. As a result, it can be evaluated that the adsorbent synthesized from the waste mandarin peels is an effective candidate to be used as a low-cost adsorbent.

## REFERENCES

- Ali, R. M., Hamad, H. A., Hussein, M. M., Malash, G. F. (2016) Potential of using green adsorbent of heavy metal removal from aqueous solutions: Adsorption kinetics, isotherm, thermodynamic, mechanism and economic analysis, *Ecological Engineering*, **91**, 317-332.
- Amuda, O. S., Amoo, I. A. (2007) Coagulation/flocculation process and sludge conditioning in beverage industrial wastewater treatment, *Journal of Hazardous Materials*, **141**(3), 778-783.
- Dias, J. M., Alvim-Ferraz, M. C. M., Almedia, M. F., Rivera-Utrilla, J., Sanchez-Polo, M. (2007) Waste materials for activated carbon preparation and its use in aqueous-phase treatment: A review. *Journal of Environmental Management*, **85**(4), 833-846.
- Enniya, I., Rghioui, L., Jourani, A. (2018) Adsorption of hexavalent chromium in aqueous solution on activated carbon prepared from apple peels. *Sustainable Chemistry and Pharmacy*, **7**, 9-16.
- Greenlee, L. F., Lawler, D. F., Freeman, B. D., Marrot, B., Moulin, P. (2009) Reverse osmosis desalination: Water sources, technology and today's challenges, *Water Research*, **43**(9), 2317-2348.
- Hashemian, S., Salari, K., Yazdi, Z. A. (2014) Preparation of activated carbon from agricultural wastes (almond shell and orange peel) for adsorption of 2-pic from aqueous solution. *Journal of Industrial and Engineering Chemistry*, **20**(4), 1892-1900.
- Ho, Y. S. and McKay, G. (1998) Sorption of dye from aqueous solution by pit. *Chemical Engineering Journal*, **70**, 115-124.
- King, P., Srinivas, P., Kumar, Y. P., Prasad, V. S. R. K. (2006) Sorption of copper (III) ion from aqueous solution by *Tectona grandis* Lf (teak leaves powder). *Journal of Hazardous Materials*, **136**(3), 560-566.
- Koyuncu, F., Güzel, F., Saygılı, H. (2018) Role of optimization parameters in the production of nanoporous carbon from mandarin sheels by microwave-assisted chemical activation and utilization as dye adsorbent. *Advanced Powder Technology*, **29**(9), 2108-2118.
- Kurniawan, T. A., Chan, G. Y. S., Lo, W. H., Babel, S. (2006) Physico-chemical treatment techniques for wastewater laden with heavy metal, *Chemical Engineering Journal*, **118**(1-2), 83-98.
- Lim, L. B. L., Priyantha, N., Tennakoon, D. T. B. (2017) Breadnut peel as a highly effective low-cost biosorbent for methylene blue: Equilibrium, thermodynamic and kinetic studies. *Arabian Journal of Chemistry*, **10**(2), 3216-3228.
- Mobasherpour, I., Salahi, E., Ebrahimi, M. (2014) Thermodynamics and kinetics of adsorption of Cu (II) from aqueous solutions onto multi-walled carbon nanotubes. *Journal of Saudi Chemical Society*, **18**(6), 792-801.
- Moghadam, M. R., Nasirizadeh, N., Dashti, Z., Babanezdah, E. (2013) Removal of Fe (II) from aqueous solution using pomegranate peel carbon: Equilibrium and kinetic studies. *International Journal of Industrial Chemistry*, **4**(19), 1-6.
- Muhamad, M. H., Abdullah, S. R. S., Mohamad, A. B., Rahman, R. A., Kadhum, A. A. H. (2013) Application of response surface methodology (RSM) for optimisation of COD, NH<sub>3</sub>-N and 2,4-

- DCP removal from recycled paper wastewater in a plot-scale granular activated carbon sequencing batch biofilm reactor (GAC-SBBR). *Journal of Environmental Management*, **121**, 179-190.
- Othman, Z., Ali, R., Naushad, M. (2012) Hexavalent chromium removal from aqueous medium by activated carbon prepared from peanut shell: Adsorption kinetics, equilibrium and thermodynamic studies. *Chemical Engineering Journal*, **184**, 238-247.
- Ponnusami, V., Gunasekar, V., Srivastava, S. N. (2009) Kinetics of methylene blue removal from aqueous solution using gulmohar (*Delonix regia*) plant leaf powder: Multivariate regression analysis, *Journal of Hazardous Materials*, **169**(1-3), 119-127.
- Semerciöz, A. S., Göğüş, F., Çelekli, A., Bozkurt, H. (2017) Development of carbonaceous material from grapefruit peel with microwave implemented- low temperature hydrothermal carbonization technique for the adsorption of Cu (II). *Journal of Cleaner Production*, **165**, 599-610.
- Semerjian, L. (2018) Removal of heavy metal (Cu, Pb) from aqueous solutions using pine (*Pinus hale pensis*) sawdust: Equilibrium, kinetic, and thermodynamic studies. *Environmental Technology & Innovation*, **12**, 91-103.
- Souza, W. D. M., Rodrigues, W. S., Filho, M. M. S. L., Alves, J. I. F., Oliveira, T. M. B. (2018) Heavy metals uptake on *Malpighia emarginata* D. L. seed fiber microparticles: Physicochemical characterization, modeling and application in land fill leachate. *Waste Management*, **78**, 356-365.
- Tadepalli, S., Murthy, K. S. R., Rakesh, N. N. (2016) Removal of Cu (II) and Fe (II) from industrial waste water using orange peel as adsorbent in batch mode operation. *International Journal of Chem Tech Research*, **9**(5), 290-299.
- Tsitsagi, M., Ebralidze, K., Chkhaidze, M., Rubashvili, I., Tsitsishvili, V. Sequential extraction of bioactive compounds from tangerine (*Citrus Unshiu*) peel. *Annals of Agrarian Science*, **16**(2), 236-241.
- Yahya, M. A., Al-Qodah, Z., Ngah, C. W. Z. (2015) Agricultural bio-waste material as potential sustainable precursors used for activated carbon production: A review. *Renewable and Sustainable Energy Reviews*, **46**, 218-235.
- Yi, Y., Lv, J., Liu, Y., Wu, G. (2017) Synthesis and application of modified Litchi peel for removal of hexavalent chromium from aqueous solutions. *Journal of Molecular Liquids*, **225**, 28-33.



# Purification of Real Car Wash Wastewater with Complex Coagulation/Flocculation Methods Using Polyaluminum Chloride, Polyelectrolyte, Clay Mineral and Cationic Surfactant

G. Veréb\*, V. E. Gayır\*, E. N. Santos\*, Á. Fazekas\*, Sz. Kertész\*, C. Hodúr\*\*\* and Zs. László\*

\*Institute of Process Engineering, Faculty of Engineering, University of Szeged, H-6725, Moszkvai Blvd. 9, Szeged, Hungary (E-mails: [verebg@mk.u-szeged.hu](mailto:verebg@mk.u-szeged.hu); [zsizsu@mk.u-szeged.hu](mailto:zsizsu@mk.u-szeged.hu); [veliengingayir@gmail.com](mailto:veliengingayir@gmail.com); [erikans123@gmail.com](mailto:erikans123@gmail.com); [fazekas@mk.u-szeged.hu](mailto:fazekas@mk.u-szeged.hu); [kertesz@mk.u-szeged.hu](mailto:kertesz@mk.u-szeged.hu); [hodur@mk.u-szeged.hu](mailto:hodur@mk.u-szeged.hu))

\*\* Institute of Environmental Science and Technology, University of Szeged, H-6720, Tisza Lajos Blvd. 103, Szeged, Hungary

## Abstract

In the present study real car wash wastewater was purified by different coagulation/flocculation methods. As coagulant, polyaluminum chloride (named as ‘BOPAC’), conventional iron(III) chloride, iron(III) sulfate, and aluminum(III) chloride, and as flocculant, non-ionic and anionic polyelectrolytes (UNIFLOC-M20 and UNIFLOC-LT27) were investigated. The effects of added clay mineral (Na-bentonite) and cationic surfactant (hexadecyltrimethylammonium bromide – HTABr) were also investigated, as organophilic clay minerals can adsorb many different types of contaminants. The aggregation/sedimentation properties and purification efficiencies were compared in detail in the case of different combinations and concentrations. The utilization of polyaluminum chloride was significantly more effective to decrease the turbidity compared to conventional coagulants. Extra addition of clay mineral was also beneficial in relation both with the volume of the sediment and the sedimentation speed, and polyelectrolyte (LT27) addition was able to increase the size of the produced clusters resulting in further enhancement of the sedimentation. Moreover, the simultaneous addition of the cationic surfactant significantly affected the color removal due to the successful in-situ production of organophilic clay minerals from Na-bentonite. In summary, the utilization of 100 mg L<sup>-1</sup> Na-bentonite with 20 mg L<sup>-1</sup> Al<sup>3+</sup> (from polyaluminum chloride) and 0.5 mg L<sup>-1</sup> anionic polyelectrolyte decreased effectively the turbidity, the COD and the extractable oil content with efficiencies of 98 %, 59 %, and 85 %, respectively. While with the utilization of organophilic bentonite in a higher concentration (500 mg L<sup>-1</sup>) with the same concentrations of polyaluminum chloride (20 mg L<sup>-1</sup> Al<sup>3+</sup>) and anionic polyelectrolyte (0.5 mg L<sup>-1</sup>) significant color removing, and even lower sediment volume was also achieved.

## Keywords

Car wash wastewater; coagulation; flocculation; bentonite; BOPAC

## INTRODUCTION

The solution of the global “water problems” is one of the biggest challenges of the 21st century (Smalley, 2005), which requires several provisions such as the promotion of more rigorous source protection, the development of low-water technologies and novel water treatment methods, and the maximization of used waters’ reclamation. Car wash stations produce large and increasing volume of wastewaters, since the number of registered vehicles exceeded 1.2 billion in 2014 (worldwide), and it is estimated to be 2.0 billion until 2035 (Currie, 2018; Zhao, 2017). Car wash wastewaters contain several pollutants such as hydrocarbons, oily pollutants, brake dust, detergents, surfactants, heavy metals, etc. (Jönsson, 1995; Kiran, 2015). Efficient purification and reclamation of these waters are highly recommended both from environmental and economic reasons (Al-Odwani, 2007; Kiran, 2015; Panizza, 2010). Moreover, the utilization of freshwater per vehicle is already limited in some countries, such as in Netherland, in the Scandinavian countries or in Australia (60-100 L/car), which makes it compulsory to reclaim the used waters (Kiran, 2015; Pinto, 2017).

There are several methods, which can be useful for the reclamation of car wash wastewaters, such as sand filtration (Al-Odwani, 2007; Zaneti, 2011), oil skimming (Al-Odwani, 2007; Brown, 2000), flotation (Zaneti, 2011), adsorption (Hamada, 2004), coagulation/flocculation (Hamada, 2004; Li, 2007; Rodriguez Boluarte, 2016; Zaneti, 2011), ozonation (Rodriguez Boluarte, 2016), electrochemical oxidation (Panizza, 2010), biological treatments (Rodriguez Boluarte, 2016; Suzuki, 2000), electrocoagulation (Mohammadi, 2017) and membrane separation (Boussu, 2008; Hamada, 2004; Jönsson, 1995; Kiran, 2015; Lau, 2013; Li, 2007; Pinto, 2017). Due to the complexity of car wash wastewaters, single methods usually are not efficient enough (Brown, 2000; Rodriguez Boluarte, 2016) and/or the sufficient high purification performance does not meet with the economic considerations. Membrane separation is one of the most promising techniques, which can result in excellent purification efficiency (Lau, 2013; Pinto, 2017). The main advantages of membrane filtration are low cost, easy scale-up and low energy consumption (Chelme-Ayala, 2009). However, a general drawback of membrane filtration is the inevitable fouling mechanism, which leads to flux reduction and membrane amortization, hence reduced lifetime and higher costs (Boussu, 2008; Li, 2007; Panizza, 2010). Therefore, efficient pre-treatment of car wash wastewaters is necessary to protect the membrane and to slow down the fouling, achieving lower costs and higher flux. Among the contaminants of car wash wastewaters, oily pollutants have major responsibility for membrane fouling and flux reduction, since oil droplets form blocks in the pores and hydrophobic cake layer on the surface (Veréb, 2017). Conventional oil skimming and floatation is able to eliminate free and dispersed oil ( $d_{\text{oil droplets}} > 20 \mu\text{m}$ ), but oil-in-water emulsions require more effective elimination methods (Chakrabarty, 2008; Gryta, 2001; Souza, 2016; Veréb, 2017).

However common coagulants such as iron and aluminum chlorides/sulfates are not efficient enough for the elimination of emulsified oil, but in our previous study (Veréb, 2017) it was proved that the combination of special coagulant and flocculant like polyaluminum chloride and anionic polyelectrolyte can be efficient for the destabilization of micro- and nanosized oil droplets. Therefore, the mentioned coagulant/flocculant combination might be useful for the purification of car wash wastewaters before membrane filtration, resulting in significant fouling reduction and longer lifetime for the membranes. In this study, purification of real car wash wastewater was investigated by the utilization of different coagulants/flocculants, including polyaluminum chloride, polyelectrolytes, and clay mineral. This latter material can intensify the sedimentation of the flocks and its adsorption capacity also can be favorable to reach higher elimination efficiency of dissolved organic compounds (Szabo, 2011; Zhu, 2008). Additionally, the effect of *in situ* generation of organophilic clay mineral by the addition of hexadecyltrimethylammonium bromide (HTABr) cationic surfactant was also investigated, since HTABr as an organic cation carrier can exchange the  $\text{Na}^+$  ions of clays minerals, hence can make them suitable for the adsorption of different organic contaminants, such as anionic (Shen, 2009) and cationic (Tonlé, 2008) dyes and different non-polar contaminants, such as hydrocarbons (Ilsz, 2002; Wiles, 2005), phenols (Senturk, 2009) and naphthalene (Zhu, 2008).

## MATERIALS AND METHODS

### Coagulation/flocculation experiments

The purification of real car wash wastewater was investigated in a F4P portable Jar Test flocculator (VELP Scientifica) with the addition of different coagulants as polyaluminum chloride ('BOPAC; Unichem Kft.), iron(III) chloride ('UNIFLOC-C', Unichem Kft.), iron(III) sulfate ('UNIFLOC', Unichem Kft.) and aluminum(III) chloride ('UNIPAC', Unichem Kft.), different flocculants as non-ionic and anionic polyelectrolytes ('UNIFLOC-M20' and 'UUNIFLOC-LT27', respectively; Unichem Kft.) and clay mineral (Na-bentonite; Unikén Kft.). Hexadecyltrimethylammonium bromide (HTABr, analytical grade, Sigma-Aldrich) addition was also investigated since organophilic clay minerals can adsorb different dyes and non-polar contaminants.

Coagulants/flocculants and other supporting materials were added in calculated amounts during intense stirring (200 rpm) of 0.5 L of the car wash wastewater and after 30 s of the last material addition 2 min slow stirring (20 rpm) was applied, then the formed flakes were allowed to sediment for 30 min. In the case of Na-bentonite addition, always that was added firstly in suspension form (before the experiments the bentonite was allowed to swell in stirred water for minimum 48 h,  $c_{\text{suspension}} = 10 \text{ g/L}$ ). In the case of HTABr addition – amounts were calculated according to the total cation exchange capacity – it was added directly after the clay mineral and 20 min of continuous fast stirring (200 rpm) was used to provide the possibility of complete exchange of  $\text{Na}^+$  ions of clay mineral with the cationic surfactant. After 20 min of stirring, the coagulant and flocculant were also added to the beakers and then 2 min of gentle stirring (20 rpm) was applied, as usually. The volumes of the produced sediments were also determined with Imhoff cone sedimentation experiments.

### Determination of purification efficiencies

Purification efficiencies were always determined by measuring the turbidity of the supernatants after 30 min of sedimentation with a Hach 2100N nephelometric turbidity meter. Additionally, chemical oxygen demand (COD) and extractable oil content were also measured in some cases. COD was measured by the standard potassium dichromate oxidation method using standard test tubes (Hanna Instruments), applying digestions for 120 min at  $150^\circ\text{C}$  in a Lovibond ET 108 digester and using a Lovibond COD Vario photometer. Extractable oil content was measured by a Wilks InfraCal TOG/TPH analyzer, using hexane (analytical grade, VWR International Kft.) as extracting solvent.

### Characterization of the investigated car wash wastewater

The investigated car wash wastewater was collected from a south Hungarian car wash station and it was characterized as it is summarised in Table 1.

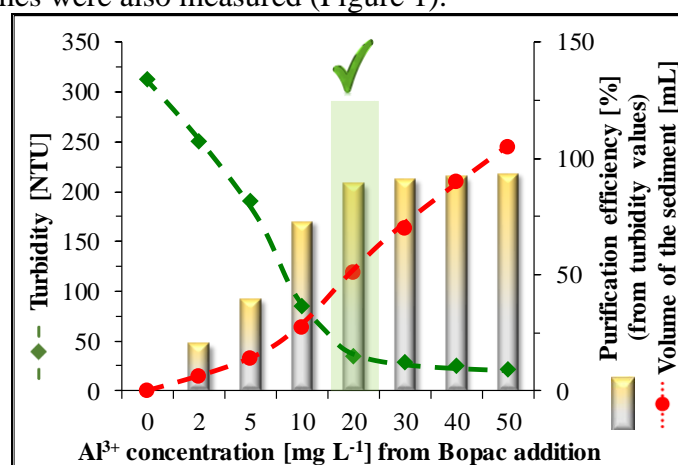
**Table 1.** COD, conductivity, turbidity, extractable oil content and pH of the car wash wastewater

COD	Conductivity	Turbidity	Extractable oil content	pH
$357 \pm 8 \text{ mg L}^{-1}$	$1.43 \pm 0.1 \text{ mS cm}^{-1}$	$333 \pm 10 \text{ NTU}$	$26 \pm 2 \text{ mg L}^{-1}$	$7.30 \pm 0.2$

## RESULTS AND DISCUSSION

### Addition of polyaluminum chloride in different concentrations

In the first series of experiments, different amounts of BOPAC coagulant were added to the wastewater, and the achievable purification efficiencies were determined by turbidity measurements and the sediment volumes were also measured (Figure 1).

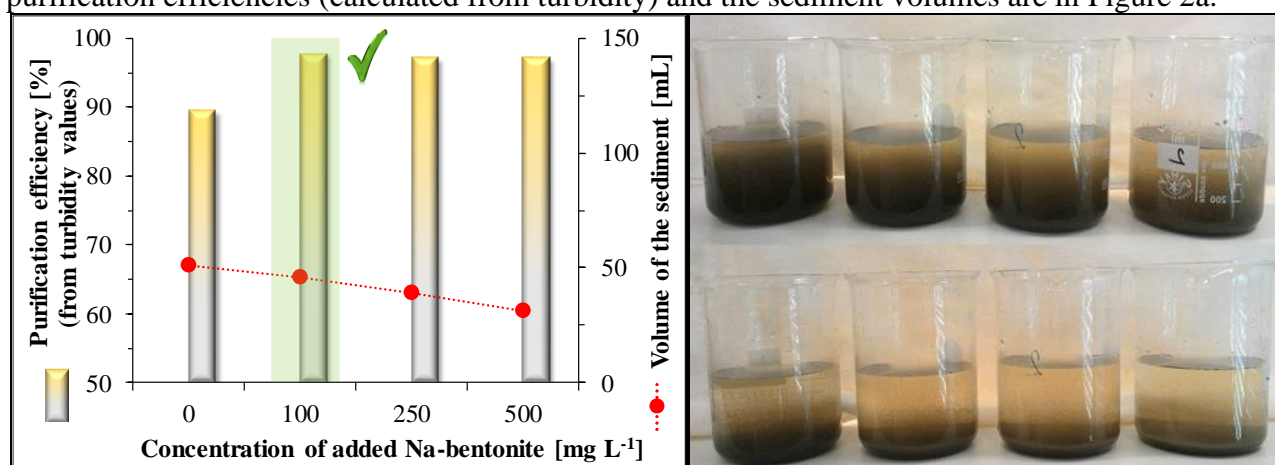


**Figure 1.** Effects of  $\text{Al}^{3+}$  concentration (originated from BOPAC addition) on the coagulation: turbidity values after sedimentation, calculated purification efficiencies, and sediment volumes

The turbidity values of the supernatants decreased intensely by the increasing concentration of  $\text{Al}^{3+}$  from 2 to 20  $\text{mg L}^{-1}$ , resulting in  $35 \pm 4$  NTU and  $89 \pm 1$  % purification efficiency, but higher concentrations resulted in only slightly lower turbidity values. At the same time, the volume of the produced sediment showed a nearly linear increase with the increasing  $\text{Al}^{3+}$  content. Considering the achievable purification efficiencies, the used chemical amounts and the produced sediment volumes, the 20  $\text{mg L}^{-1}$   $\text{Al}^{3+}$  concentration could be recommended. 50  $\text{mg L}^{-1}$  aluminum content resulted in just slightly higher purification efficiency ( $93 \pm 1$  %), but twice higher sediment volume compared to the 20  $\text{mg L}^{-1}$  added aluminum content.

### Addition of clay mineral in different concentrations

In the next series of experiments different amounts of Na-bentonite (0, 100, 250, 500  $\text{mg L}^{-1}$ ) were added before the BOPAC addition (in these experiments 20  $\text{mg L}^{-1}$   $\text{Al}^{3+}$  content was used). The purification efficiencies (calculated from turbidity) and the sediment volumes are in Figure 2a.



**Figure 2.** a) Effects of Na-bentonite addition on purification efficiency and sediment volume; b) photographs after 30 and 60 s of sedimentations (0, 100, 250, 500  $\text{mg L}^{-1}$  Na-bentonite additions, respectively, before the BOPAC addition – 20  $\text{mg L}^{-1}$   $\text{Al}^{3+}$  content in all cases.)

100  $\text{mg L}^{-1}$  Na-bentonite addition increased significantly the purification efficiency ( $98 \pm 1$  %), and the sediment volume was also slightly decreased. With the utilization of higher Na-bentonite amounts, almost the same purification efficiencies were measured and the sediment volume just slightly decreased, so higher than 100  $\text{mg L}^{-1}$  Na-bentonite concentration could not be recommended, even the sedimentation was slightly faster at higher Na-bentonite concentrations as it can be seen in Figure 2b. The addition of Na-bentonite alone was also investigated as reference experiments, and the turbidity values (333, 210, 285, 355 and 580 NTU in the case of 0, 100, 250, 500 and 1000  $\text{mg L}^{-1}$  bentonite additions, respectively) proved the necessity of the coagulant addition.

### Addition of non-ionic and anionic polyelectrolytes

The extra addition of two different types of polyelectrolytes – after the Na-bentonite (100  $\text{mg L}^{-1}$ ) and BOPAC (20  $\text{mg L}^{-1}$   $\text{Al}^{3+}$ ) additions – was investigated in two beakers, while in other two beakers reference experiments were carried out by using the polyelectrolytes alone. Non-ionic (UNIFLOC-M20) and anionic (UNIFLOC-LT27) polyelectrolytes were applied in a low concentration (0.5  $\text{mg L}^{-1}$ ). The results (Table 2) confirmed that the extra addition of both polyelectrolytes increased the achievable purification efficiency, but in relation with the sediment volume, the anionic polyelectrolyte (UNIFLOC-LT27) was more beneficial, as half the sediment volume ( $V = 15$  mL) was measured compared to the non-ionic polyelectrolyte addition ( $V = 30$  mL).

**Table 2.** Achievable purification efficiencies (calculated from turbidity values) and the resulted sediment volumes *via* polyelectrolyte addition (in 0,5 mg L<sup>-1</sup> concentration)

Added materials	Turbidity (NTU)	Purification efficiency (%)	Sediment volume (mL)
-	333	-	-
UNIFLOC-M20 (0,5 mg L <sup>-1</sup> )	100	70	Not measured
UNIFLOC -LT27 (0,5 mg L <sup>-1</sup> )	65	80	Not measured
Na-bentonite (100 mg L <sup>-1</sup> ) + BOPAC (20 mg L <sup>-1</sup> Al <sup>3+</sup> ) + UNIFLOC -M20 (0,5 mg L <sup>-1</sup> )	4	98.5	30
Na-bentonite (100 mg L <sup>-1</sup> ) + BOPAC (20 mg L <sup>-1</sup> Al <sup>3+</sup> ) + UNIFLOC -LT27 (0,5 mg L <sup>-1</sup> )	4	98.5	15

### Comparison of conventional coagulants and BOPAC polyaluminum chloride

Polyaluminum chloride (BOPAC) was compared with different conventional coagulants, as iron(III) chloride, iron(III) sulfate and aluminum(III) chloride in relation to the achievable turbidities. Coagulants alone (used in 20 mg L<sup>-1</sup> metal ion concentrations), and together with the anionic polyelectrolyte (0.5 mg L<sup>-1</sup>) and/or the Na-bentonite (100 mg L<sup>-1</sup>) were also investigated (Table 3).

**Table 3.** Achievable turbidity values of the supernatants in the case of different coagulants. M: given coagulant metal ion; Bent.: Na-bentonite; PE: UNIFLOC-LT27 anionic polyelectrolyte

Added materials	Turbidity values of the supernatants			
	Polyaluminum chloride (BOPAC)	iron(III) chloride	iron(III) sulfate	aluminum(III) chloride
20 mg L <sup>-1</sup> M	35	160	175	75
100 mg L <sup>-1</sup> Bent. + 20 mg L <sup>-1</sup> M	7	173	190	82
20 mg L <sup>-1</sup> M + 0,5 mg L <sup>-1</sup> PE	5	91	96	22
100 mg L <sup>-1</sup> Bent. + 20 mg L <sup>-1</sup> M + 0,5 mg L <sup>-1</sup> PE	4	88	110	44

The results confirmed the outstanding efficiency of polyaluminum chloride in the case of the real car wash wastewater, as the measured turbidity values were 4-35 NTU, while in the case of iron(III) coagulants 88-190 NTU values and in the case of conventional aluminum(III) chloride 22-82 NTU values were measured. The outstanding purification efficiency of the BOPAC can be explained by its' pre-hydrolyzed form and Keggin structure, which result in advanced adsorption ability. In the series of BOPAC addition, the COD values and extractable oil contents of the supernatants were also measured, and 57±1 % and 83±3 % purification efficiencies were determined, respectively.

### Effects of in situ production of organophilic clay minerals by HTABr addition.

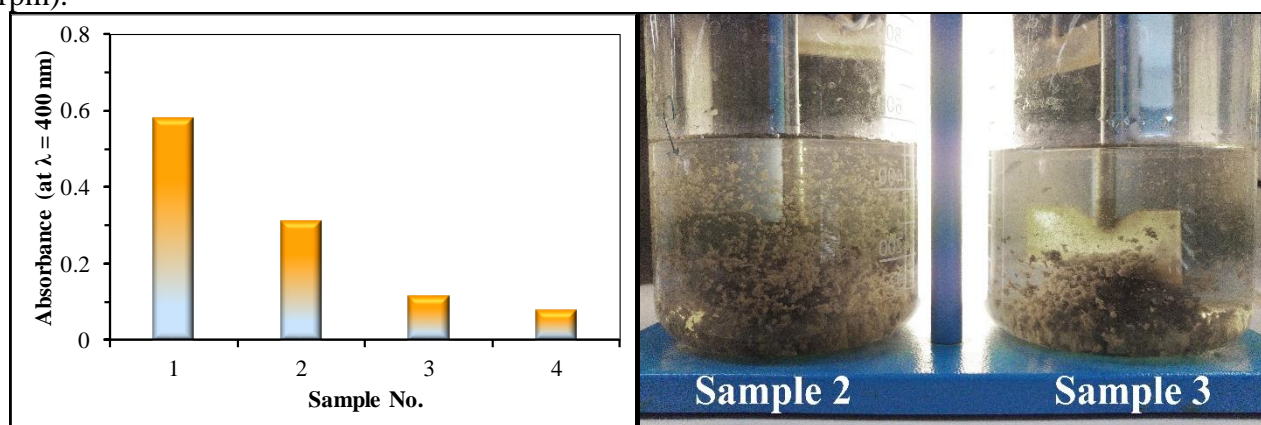
In situ addition of HTABr was also investigated, since it can exchange the Na<sup>+</sup> ions of bentonites to organic cations, hence it can modify the surface to be organophilic and this makes them suitable for the adsorption of different type of organics such as dyes and different non-polar contaminants. Different amounts of Na-bentonite (0, 100, 500 and 2000 mg L<sup>-1</sup>) and HTABr (in calculated concentrations, according the bentonite's cationic exchange capacity) were added before the BOPAC coagulant (20 mg L<sup>-1</sup>) and UNIFLOC-LT27 polyelectrolyte (0.5 mg L<sup>-1</sup>) addition.

Turbidity, COD and extractable oil content of the supernatants and the sediment volumes were measured (Table 4).

**Table 4.** Turbidity, COD and extractable oil content of the supernatants and sediment volumes

No.	Added materials	Turbidity (NTU)	COD (mg L <sup>-1</sup> )	Extractable oil content (mg L <sup>-1</sup> )	Sediment volume (mL)
-	-	333	357	26	-
1	100 mg L <sup>-1</sup> Bent. + 20 mg L <sup>-1</sup> Al <sup>3+</sup> + 0,5 mg L <sup>-1</sup> PE	6	158	4	15
2	100 mg L <sup>-1</sup> Bent. + HTABr + 20 mg L <sup>-1</sup> Al <sup>3+</sup> + 0,5 mg L <sup>-1</sup> PE	6	156	5	13
3	500 mg L <sup>-1</sup> Bent. + HTABr + 20 mg L <sup>-1</sup> Al <sup>3+</sup> + 0,5 mg L <sup>-1</sup> PE	3	156	4	11
4	2000 mg L <sup>-1</sup> Bent. + HTABr + 20 mg L <sup>-1</sup> Al <sup>3+</sup> + 0,5 mg L <sup>-1</sup> PE	4	154	4	20

The reduction of turbidity, COD and extractable oil content were very similar in all cases, but color removals of the supernatants were observed visually when the organophilic bentonite was used. Absorbance measurements confirmed these color removals with an increasing degree from sample 1 to sample 4, as the absorbance values significantly decreased at  $\lambda=400$  nm (Figure 3a). Considering the turbidity values, the color removal and more importantly the reduced sediment volumes (Table 4.), the usage of 500 mg L<sup>-1</sup> organophilic bentonite can be considered beneficial. The beneficial effect of HTABr addition as the formation of more compact flocks (which resulted in the reduced sediment volumes) can be seen in Figure 3b, where the treated waters are stirred slowly (20 rpm).



**Figure 3.** a) absorbance values of the supernatants ( $\lambda=400$  nm), b) photographs of samples 2 and 3

## CONCLUSIONS

As the main aim of this study was the effective elimination of dispersed contaminants, the utilization of BOPAC alone (without Na-bentonite or polyelectrolyte addition) was not effective enough. Extra addition of anionic polyelectrolyte (UNIFLOC-LT27) significantly increased the size of the produced clusters, intensified the sedimentation and decreased the sediment volume. BOPAC proved to be significantly more effective than conventional coagulants due to its' pre-hydrolyzed form and Keggin structure. In summary, the utilization of 100 mg L<sup>-1</sup> Na-bentonite with 20 mg L<sup>-1</sup> Al<sup>3+</sup> (originated from the BOPAC addition) and 0.5 mg L<sup>-1</sup> anionic polyelectrolyte decreased effectively the turbidity, the COD and the extractable oil content of the real car wash wastewater with efficiencies of 98 %, 59 %, and 85 %, respectively. Moreover, the simultaneous addition of the cationic surfactant (HTABr) resulted in the successful in-situ production of organophilic clay



minerals and *via* its' utilization in a higher concentration (500 mg L<sup>-1</sup>) significant color remove, slightly lower turbidity value (99 % efficiency) and significant lower sediment volume were also achieved. The utilization of both these last two combinations can be recommended as single, easy but efficient pretreatments of car wash wastewaters before the final membrane filtration step.

## ACKNOWLEDGMENTS

The authors are grateful for the financial support of the Hungarian Science and Research Foundation (2017-2.3.7-TÉT-IN-2017-00016), the Hungarian State and the European Union (EFOP-3.6.2-16-2017-00010). G. V. thanks for the support of the János Bolyai Research Scholarship of the Hungarian Academy of Sciences and the New National Excellence Program of the Ministry of Human Capacities (UNKP-18-4-SZTE-78). E.N.S. was supported by the Stipendium Hungaricum Scholarship Program.

## REFERENCES

- Al-Odwani, A., Ahmed, M., Bou-Hamad, S. (2007) Carwash water reclamation in Kuwait. *Desalination*, **206**(1-3), 17-28.
- Boussu, K., Eelen, D., Vanassche, S., Vandecasteele, C., Van der Bruggen, B., Van Baelen, G., Colen, W., Vanassche, S. (2008) Technical and economical evaluation of water recycling in the carwash industry with membrane processes. *Water Sci Technol*, **57**(7), 1131-5.
- Brown, C. (2000) Water Conservation in the Professional Car Wash Industry, Water Conservation Consultant.
- Chakrabarty, B., Ghoshal, A. K., Purkait, M. K. (2008) Ultrafiltration of stable oil-in-water emulsion by polysulfone membrane. *J. Membr. Sci.*, **325**(1), 427-437.
- Chelme-Ayala, P., Smith, D. W., El-Din, M. G. (2009) Membrane concentrate management options: a comprehensive critical review. *Canadian Journal of Civil Engineering*, **36**(6), 1107-1119.
- Currie, G. (2018) Lies, Damned Lies, AVs, Shared Mobility, and Urban Transit Futures. *Journal of Public Transportation*, **21**(1), 19-30.
- Gryta, M., Karakulski, K., Morawski, A.W. (2001) Purification of oily wastewater by hybrid UF/MD. *Water Res.*, **35**, 3665-3669.
- Hamada, T., Miyazaki, Y. (2004) Reuse of carwash water with a cellulose acetate ultrafiltration membrane aided by flocculation and activated carbon treatments *Desalination*, **169**, 257-267.
- Ilisz, I., Dombi, A., Mogyorósi, K., Farkas, A., Dékány, I. (2002) Removal of 2-chlorophenol from water by adsorption combined with TiO<sub>2</sub> photocatalysis. *Appl. Catal., B*, **39**(3), 247-256.
- Jönsson, C., Jönsson, A.-S. (1995) The influence of degreasing agents used at car washes on the performance of ultrafiltration membranes *Desalination*, **100**, 115-123.
- Kiran, S.A., Arthanareeswaran, G., Thuyavan, Y.L., Ismail, A.F. (2015) Influence of bentonite in polymer membranes for effective treatment of car wash effluent to protect the ecosystem. *Ecotoxicology and Environmental Safety*, **121**, 186-192.
- Lau, W.J., Ismail, A.F., Firdaus, S. (2013) Car wash industry in Malaysia: Treatment of car wash effluent using ultrafiltration and nanofiltration membranes. *Separation and Purification Technology*, **104**, 26-31.
- Li, T., Xue-jun, T., Fu-yi, C., Qi, Z., Jun, Y. (2007) Reuse of carwash wastewater with hollow fiber membrane aided by enhanced coagulation and activated carbon treatments. *Water Sci Technol*, **56**(12), 111-8.
- Mohammadi, M.J., Salari, J., Takdastan, A., Farhadi, M., Javanmardi, P., Yari, A.R., Dobaradaran, S., Almasi, H., Rahimi, S. (2017) Removal of turbidity and organic matter from car wash wastewater by electrocoagulation process. *Desalination and Water Treatment*, **68**, 122-128.

- Panizza, M., Cerisola, G. (2010) Applicability of electrochemical methods to carwash wastewaters for reuse. Part 2: Electrocoagulation and anodic oxidation integrated process. *J Electroanal Chem*, **638**(2), 236-240.
- Pinto, A. C. S., de Barros Grossi, L., de Melo, R. A. C., de Assis, T. M., Ribeiro, V. M., Amaral, M. C. S., de Souza Figueiredo, K. C. (2017) Carwash wastewater treatment by micro and ultrafiltration membranes: Effects of geometry, pore size, pressure difference and feed flow rate in transport properties. *Journal of Water Process Engineering*, **17**, 143-148.
- Rodriguez Boluarte, I. A., Andersen, M., Pramanik, B. K., Chang, C.-Y., Bagshaw, S., Farago, L., Jegatheesan, V., Shu, L. (2016) Reuse of car wash wastewater by chemical coagulation and membrane bioreactor treatment processes. *International Biodeterioration & Biodegradation*, **113**, 44-48.
- Senturk, H. B., Ozdes, D., Gundogdu, A., Duran, C., Soylak, M. (2009) Removal of phenol from aqueous solutions by adsorption onto organomodified Tirebolu bentonite: Equilibrium, kinetic and thermodynamic study. *J. Hazard. Mater.*, **172**(1), 353-362.
- Shen, D., Fan, J., Zhou, W., Gao, B., Yue, Q., Kang, Q. (2009) Adsorption kinetics and isotherm of anionic dyes onto organo-bentonite from single and multisolute systems. *J. Hazard. Mater.*, **172**(1), 99-107.
- Smalley, R. E. (2005) Future Global Energy Prosperity: The Terawatt Challenge. *Material Matters*, **30**, 412-417.
- Souza, R. S., Porto, P. S. S., Pintor, A. M. A., Ruphuy, G., Costa, M. F., Boaventura, R. A. R., Vilar, V. J. P. (2016) New insights on the removal of mineral oil from oil-in-water emulsions using cork by-products: Effect of salt and surfactants content. *Chemical Engineering Journal*, **285**, 709-717.
- Suzuki, M., Umehara, T., Tsukamoto, K., Tsukahara, H. (2000). Recycle device of car washing machine waste water and recycle method of car washing machine gullation.
- Szabo, E., Vajda, K., Vereb, G., Dombi, A., Mogyorosi, K., Abraham, I., Majer, M. (2011) Removal of organic pollutants in model water and thermal wastewater using clay minerals. *J. Environ. Sci. Health Part A-Toxic/Hazard. Subst. Environ. Eng.*, **46**(12), 1346-1356.
- Tonlé, I. K., Ngameni, E., Tcheumi, H. L., Tchiéda, V., Carteret, C., Walcarius, A. (2008) Sorption of methylene blue on an organoclay bearing thiol groups and application to electrochemical sensing of the dye. *Talanta*, **74**(4), 489-497.
- Veréb, G., Nagy, L., Kertész, S., Kovács, I., Hodúr, C., László, Z. (2017) Highly efficient purification of finely dispersed oil contaminated waters by coagulation/flocculation method and effects on membrane filtration. *Studia UBB Chemia*, **62**, 259-270.
- Veréb, G., Zakar, M., Kovács, I., Sziládi, K. P., Kertész, S., Hodúr, C., László, Z. (2017) Effects of pre-ozonation in case of microfiltration of oil contaminated waters using polyethersulfone membrane at various filtration conditions. *Desalination and Water Treatment*, **73**, 409-414.
- Wiles, M. C., Huebner, H. J., McDonald, T. J., Donnelly, K. C., Phillips, T. D. (2005) Matrix-immobilized organoclay for the sorption of polycyclic aromatic hydrocarbons and pentachlorophenol from groundwater. *Chemosphere*, **59**(10), 1455-1464.
- Zaneti, R., Etchepare, R., Rubio, J. (2011) Car wash wastewater reclamation. Full-scale application and upcoming features. *Resources, Conservation and Recycling*, **55**(11), 953-959.
- Zhao, M., Yang, D., Feng, S., Liu, H. (2017) Vanpool trip planning based on evolutionary multiple objective optimization. *IOP Conference Series: Earth and Environmental Science*, **81**, 012206.
- Zhu, L., Ma, J. (2008) Simultaneous removal of acid dye and cationic surfactant from water by bentonite in one-step process. *Chemical Engineering Journal*, **139**(3), 503-509.
- Zhu, R., Zhu, L., Zhu, J., Xu, L. (2008) Structure of surfactant-clay complexes and their sorptive characteristics toward HOCs. *Separation and Purification Technology*, **63**(1), 156-162.



# Purification and Improved Biogas Production from Real Dairy Wastewaters by Combining Membrane Separation with Fenton-reaction and Ozone Pre-treatments

M. Zakar<sup>\*,\*\*</sup>, S. Beszédes<sup>\*\*</sup>, E. Hanczné Lakatos<sup>\*</sup>, G. Keszthelyi-Szabó<sup>\*\*</sup> and Zs. László<sup>\*\*</sup>

<sup>\*</sup> Institute of Food Sciences, Széchenyi István University, Lucsony str. 15-17, H-9200, Mosonmagyaróvár, Hungary

<sup>\*\*</sup> Department of Process Engineering, Faculty of Engineering, University of Szeged, Moszkvai krt. 9, H-6724, Szeged, Hungary (E-mail: [zsizsu@mk.u-szeged.hu](mailto:zsizsu@mk.u-szeged.hu))

## Abstract

The dairy industry generates high amount of wastewaters. Biological treatments for these wastewaters are possible, however its quantity is too big, which may cause problems. Therefore new solutions are needed and membrane separation is a promising method. With the proper choice of membranes different type of wastewaters can be cleaned with high efficiency but the fouling remains a limiting factor of the applications. The goal of this study was to clean real dairy wastewater with membrane separation. To reduce the membrane fouling, ozone and Fenton-reaction were used as pre-treatments, The generated concentrate was used to produce biogas, and it's methane content was measured. Filtration resistances, fluxes, purification efficiency were also investigated.

## Keywords

Membrane filtration; Fenton-reaction; ozone; biogas; methane content

## INTRODUCTION

There are several investigations to clean or reuse of dairy wastewaters, and membrane processes are promising methods to treat such wastewaters. Earlier works proved that an appropriate retention can be achieved by membrane filtration and permeates can be reused. Membrane separation is also an proper method for reducing the amount of the wastewater, by concentrating it. With the appropriate choice of the membranes, the purification efficiency can be high, but the concentrate needs further treatments. Fortunately the concentrated dairy wastewaters not containing any toxic materials or dangerous compounds, but contain high amount of organic materials like proteins, fat, lactose etc. (Sarkar, 2006) The concentrated wastewater mixed with anaerobic sludge can be used to produce biogas (Joshiba, 2019). However, membrane fouling is a limiting factor in these processes (Abdelkader, 2019). One of the biggest challenge about the researches of membrane separation is to reduce the fouling, and there is a promising method for it, called advanced oxidation processes.

Advanced oxidation processes (AOPs), like Fenton-reaction are widely used in the fields of water and wastewater treatments and are known for their capability to mineralise a wide range of organic compounds. AOPs also have some other effects on the filtration procedure, e.g. the micro-flocculation effect (László, 2009). Ozone as pre-treatment also has similar effects like AOP-s, and it's also can increase the biodegradability of food waste, and can increase the production of biogas (Beszédes, 2009).

In the present study the effect of the Fenton-reaction and ozone treatment as pre-treatments of real dairy waste waters were investigated. Fluxes, filtration resistances and pollutant retentions were determined and compared. Biogas production from the wastewater's concentration mixing with municipal sludge also was investigated.

## EXPERIMENTAL

The dairy wastewater is originated from Sole-Mizo Zrt., a dairy factory in Szeged, Hungary. The raw wastewater has 3800-4100 mg/l COD, all dry matter content around 2000 mg/l and the pH changing between 6,5 and 7. During ozone treatment experiments, ozone-containing gas was bubbled continuously through a batch reactor during the treatment. The absorbed ozone concentration was 30-40 g/m<sup>3</sup> (30 g/m<sup>3</sup> in 5 minutes and 40 g/m<sup>3</sup> in 20 minutes) The volume of the treated water was 0.4 dm<sup>3</sup>. Ozone was produced from oxygen (Linde, 3.0) with a flow-type ozone generator (Ozomatic Modular 4, Wedeco Ltd., Germany). The durations of the treatment were 5, 10 and 20 mins; and the flow rate was 1dm<sup>3</sup> min<sup>-1</sup>. Fenton-reaction was conducted in a stirred batch reactor with 1.5 mmol dm<sup>-3</sup> FeSO<sub>4</sub>×7H<sub>2</sub>O (purity 99 %, VWR, EU) adjusted to pH 3 with H<sub>2</sub>SO<sub>4</sub> (purity 96 %, Farmitalia Carlo ErbaSPA, Italy), and H<sub>2</sub>O<sub>2</sub> solution (30 %, purity 99 %, VWR.), the [H<sub>2</sub>O<sub>2</sub>]:[Fe] ratio was 5:1 (Fenton (5:1)). The ozone or Fenton pre-treated samples were used as a feed in ultrafiltration (UF) experiments. The UF experiments were carried out in a batch stirred ultrafiltration cell (Millipore, SN:XFUF04701, USA), the filtrations were performed at 0.3 MP transmembrane pressure and the feed solutions were stirred at 350 rpm. For filtration experiments flat-sheet PES membranes (PES6 series, New Logic, USA) with MWCO (10 kDa) were used with effective membrane area of 0.00173 m<sup>2</sup>. The initial feed volume was 250 cm<sup>3</sup>, the UF experiments were carried out until 200 cm<sup>3</sup> of the total sample was filtered, where the volume reduction ratio VRR=5.

For the chemical oxygen demand (COD) measurements high range (0 - 15000 mg/l) photometric test kits (COD VARIO tube tests (Lovibond Tintometer)) were used.

The purification efficiency was calculated by:

$$\text{Purification efficiency} = 100 - \left( \left( \frac{\text{Permeate COD}}{\text{Starting wastewater COD}} \right) * 100 \right) \quad (1)$$

Biogas production tests were performed in triplicate in batch mode under mesophilic conditions, at 40 °C for 40 days, in an anaerobic laboratory digester with a pressure measuring head (Oxitop Control AN12 measurement system, WTW GmbH, Germany). The digester was inoculated with acclimated sludge from a municipal wastewater treatment plant (Hódmezővásárhely, Hungary) in order to eliminate the possible lag-phase of anaerobic biological degradation process. After inoculation nitrogen gas was flowed through the reactor to prevent exposure to air. The pH was adjusted to pH 7.2 with 1M NaOH and 1 M HCl solution. The capacity of digesters was 1000 mL, the volume of mixtured sample was 70 mL, 50 mL from the retentate and 20 mL from the sludge, considering our previous work and the pressure range of equipment. The pressure values were automatically stored by barometrical heads in every 2 hours. For simple methane determination, measurements were performed in parallel in two vessels: one of them contained a CO<sub>2</sub> absorber, while the other measured the total gas pressure. The resulting pressure difference was proportional to the CO<sub>2</sub> concentration, and the remaining overpressure was proportional to the methane concentration. In addition the accurate composition of the biogas produces was measured by gas chromatographic and mass spectrometric method (Agilent 6890N-5976 GC-MS). In the case of methane content, there was a close correlation between the pressure difference method and gas chromatographic determination (R > 0.85).

In order to investigate the membrane fouling mechanisms, filtration resistances were calculated according to the resistances-in-series model.

The membrane resistance was calculated as

$$R_M = \frac{\Delta p}{J_w \eta_w} \quad [\text{m}^{-1}], \quad (2)$$

where  $R_M$  is the membrane resistance,  $\Delta p$  is the pressure difference between the two sides of the membrane (MPa),  $J_w$  is the water flux of the clean membrane and  $\eta_w$  is the water viscosity (Pa·s).  $R_T$  is the total resistance ( $\text{m}^{-1}$ ), can be evaluated from the steady-state flux by using the resistance-in-series model:

$$R_T = R_M + R_{irrev} + R_{rev}, \quad (3)$$

where  $R_{irrev}$  is the irreversible resistance (mainly caused by the fouled pores) and  $R_{rev}$  is the reversible resistance [ $\text{m}^{-1}$ ].

The irreversible resistance was determined by measuring water flux through the membrane after filtration and rinsing it with deionized water to remove any particles of residue layer from the surface, by subtracting the resistance of the clean membrane:

$$R_{irrev} = \frac{\Delta p}{J_{WA} \eta_w} - R_M, \quad (4)$$

where  $J_{WA}$  is the water flux after concentration tests. The reversible resistance of the layer deposited on the membrane surface was calculated as

$$R_{rev} = \frac{\Delta p}{J_C \eta_{ww}} - R_{irrev} - R_M, \quad (5)$$

where  $J_C$  is the constant flux at the end of the concentration and  $\eta_{ww}$  is the wastewater viscosity (Hermia, 1982).

## RESULTS

In the first series of experiments, the dairy wastewater samples were pre-treated with ozone for 5, 10 or 20 min or with Fenton reaction for 0, 30 or 90 min. The pre-treated samples were filtered, and the filtration resistances were calculated based on measured fluxes. It was found, that the ozone pretreatment increased the relative fluxes in every cases, and the 10 minutes pre-treatment caused the highest values. , while surprisingly, the Fenton-pretreatments decreased the relative fluxes. In order to get more information about the nature of the fouling, filtration resistances were calculated and compared (Figure 1).

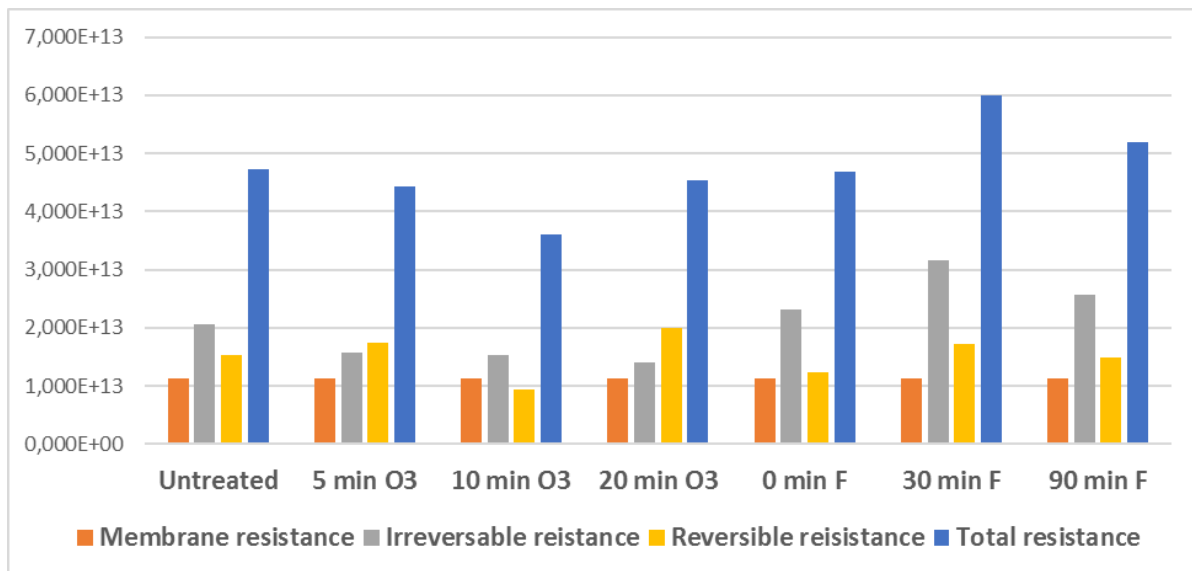
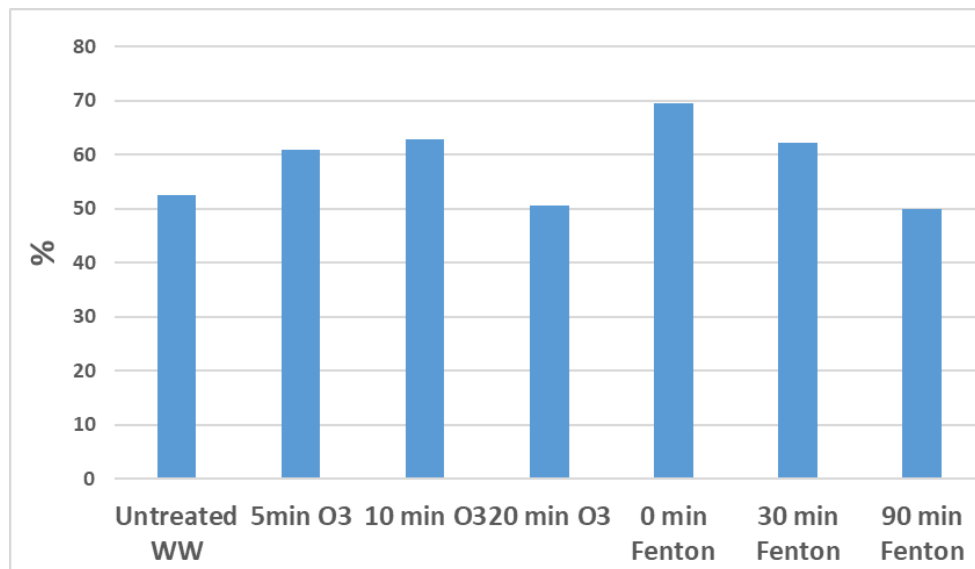


Figure 1. Filtration resistances

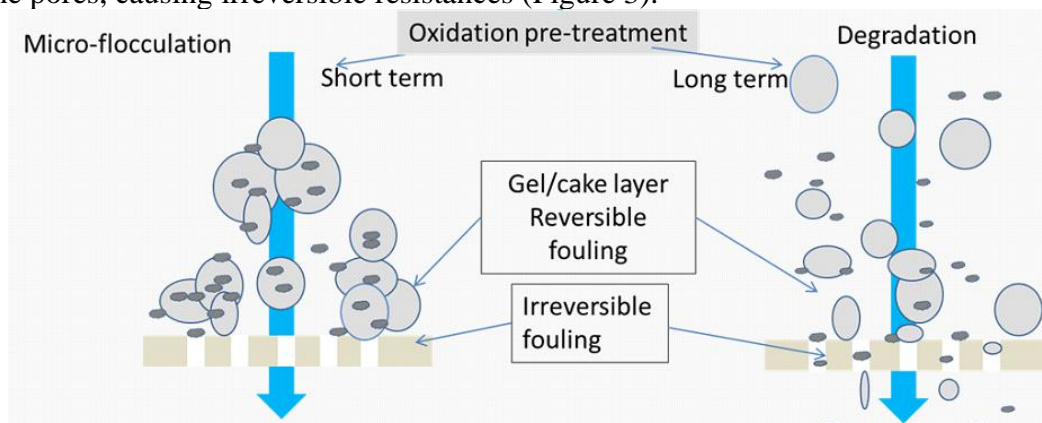
As it was expected based on flux curves, the ozone pre-treatment decreased the filtration resistances, in more detailed, the irreversible resistances were decreased and the reversible resistances were increased. It means that membrane will be easier to clean after the filtration. Fenton-pretreatment increased the total resistances via increasing the irreversible resistance, which was caused by the particles blocking the membrane pores, and make the membrane cleaning harder, or even not possible.

After the filtration, the purification efficiencies were measured and compared. It was found, that the shorter (5 and 10 minutes ozone and 0 and 30 minutes Fenton) pre-treatments resulted higher purification efficiency than the filtration of untreated samples. However, further increasing of the duration of pre-treatments (20 minutes ozone and 90 minutes Fenton) the efficiency decreased and it resulted in even lower cleaning efficiency than without any pre-treatments.



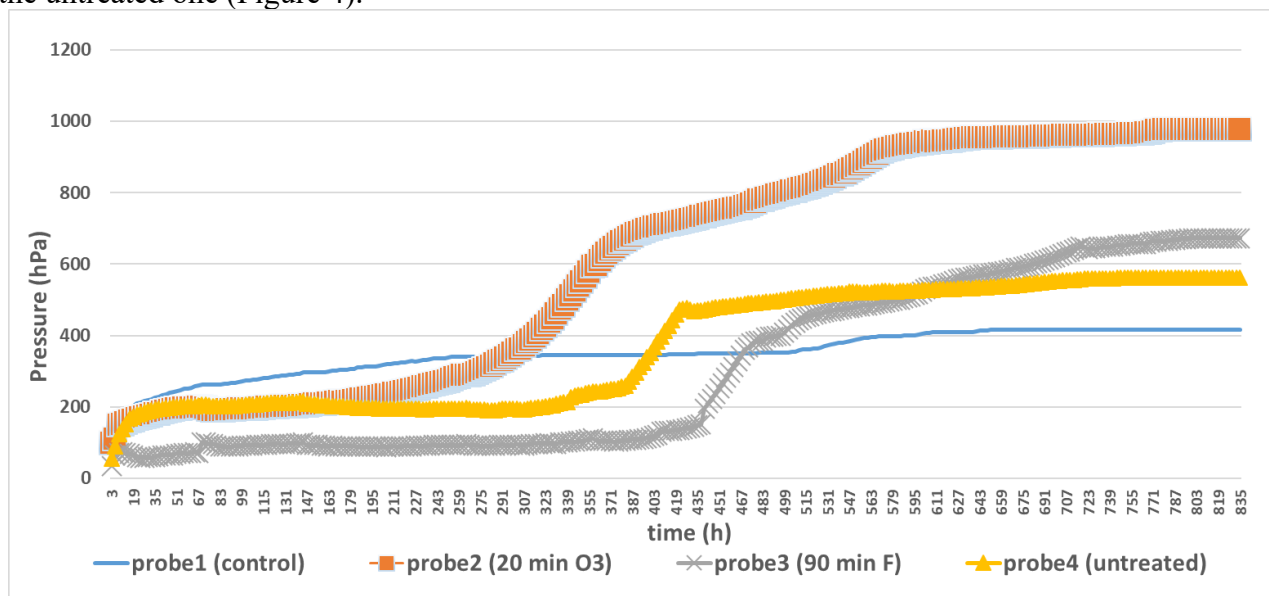
**Figure 2.** Purification efficiency after filtration

The short-term beneficial effect of ozone pre-treatment can be explained by the microfloculation effect of ozone. The Fenton-reaction has similar (coagulation/flocculation) effect, because of the coagulation-flocculation effect of ferrous-sulfate ( $\text{FeSO}_4$ ) reagent used to carry out the Fenton-reaction, resulting in enhanced purification efficiency. However, if we increase the duration of the oxidation processes, the larger particles can be degraded, the smaller particles can pass through the membrane, and increase the COD in the permeate. The smaller particles can also get into the membrane pores, causing irreversible resistances (Figure 3).



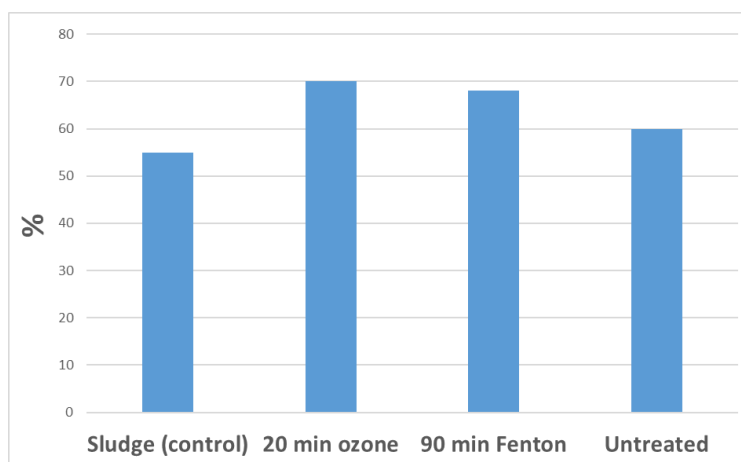
**Figure 3.** Comparing the mechanism of the shorter and longer pre-treatments

After the filtration the concentrate contains most of the organic content of the wastewater. Because of the high organic content and the lack of toxic materials it is possible to use it for biogas production. The concentrate alone does not contain any anaerobic microorganisms so the retentate was mixed with anaerobic sludge from a municipal wastewater factory, which was used biogas production before. (Beszédes, 2009) During a 40 days period on fixed 40 °C temperature the pressure was measured in the biogas reactors. The control probe was the municipal sludge alone (70 cm<sup>3</sup>). The untreated concentrate, the ozone and the Fenton-pretreated mixture also were inoculated with the anaerobic sludge by mixing the samples with the anaerobic sludge (50cm<sup>3</sup> sample+ 20cm<sup>3</sup> sludge). It was found, that the ozone pre-treatment highly increased the pressure in the biogas reactor, which means that more biogas was produced during the 40 days. The Fenton pre-treatment also increased the biogas production, but it resulted in only a slightly higher pressure than the untreated one (Figure 4).



**Figure 4.** Biogas production from the wastewater concentration mixed with sludge

The increased biodegradability was caused by the pre-oxidation effect of the ozone and Fenton-pretreatments. However, it can be used for energetic intention if the methane content is high enough (Pangrahi, 2019). So the actual methane content of the biogas samples also were measured. It was found that the methane content was high even in the untreated samples, and the pre-treatments further increased it. With the ozone pre-treatment, it reached 70 % and the Fenton-reaction resulted 68 % methane content in the biogas, so it may be possible to use it for energetic purposes (Figure 5).



**Figure 5.** Methane content of the biogas

## SUMMARY

In this work the ozone and the Fenton-reaction as pre-treatments before membrane separation of real dairy wastewaters were investigated and compared. Our goal was to decrease the membrane fouling, increase purification efficiency of the filtration and the biological degradability of the remaining concentration after the filtration. The short term ozone pre-treatment decreased the fouling due to the microfloculation effect of the ozone. According to our experiments, the available fluxes were increased and the filtration resistances decreased, moreover the ozone pre-treatment decreased the irreversible resistances, make the membrane surface easier to clean after the procedure. Fenton-reaction decreased the fluxes and increased the filtration resistances, so in case of this type of wastewater the ozone pre-treatment is the recommended option. With shorter pre-oxidation treatments such as 10 minutes ozone and 30 minutes, Fenton-reaction the purification efficiency found to be increased. However if we further increase the oxidation time (20 min ozone and 90 min Fenton) the large particles can be decomposed and can pass through the membrane pores into the permeate, resulting in higher COD. Both pre-oxidation pre-treatments increased the biological degradability of the retentate and with the proper mixture with anaerobic sludge; it is possible to produce biogas from the filtration leftover. The comparison of the two pre-treatments, in the case of ozone treatments more biogas was produced, and higher methane content was observed in the biogas (up to 70%) so it may be possible to use this biogas for energetical purpose.

## ACKNOWLEDGEMENT

The research was supported by the project TÉT: 2017-2.3.7-TÉT-IN-2017\_00016 and NKFI K115691. The authors are also grateful for the financial support provided by EFOP-3.6.2-16-20017-00010 (RING-2017) and 2018/19/2 EFOP-3.6.3-VEKOP projects.

## REFERENCES

- Abdelkader, S., Gross, F., Winter, D., Went, J., Koschikowski, J., Geissen, S., Bousselmi, L., (2019) Application of direct contact membrane distillation for saline dairy effluent treatment: performance and fouling analysis. *Environmental Science and Pollution Research*, **26(19)**, 18979-18992.
- Beszédes, S., Kertész, Sz. László, Zs. Szabó, G., Hodúr, C.(2009) Biogas Production of Ozone and/or Microwave Pretreated Canned Maize Production Sludge. *Ozone: Science & Engineering*, **31(3)**, 257-261.
- Hermia, J. (1982) Constant Pressure Blocking Filtration Law: Application to Power Law Non-Newtonian Fluids. *Trans. Ind. Chem. Eng.*, **60**, 183-187.
- Joshi, G. Janet, Kumar, P., Senthil, F., Carolin, C. (2019) Critical review on biological treatment strategies of dairy wastewater. *Desalination and water treatment*, **160**, 94-109.
- László, Zs., Kertész, Sz., Beszédes, S., Hovorka, Zs. H., Szabó, G., Hodúr, C. (2009) Effect of pre-oxidation on the filterability of model dairy waste water in nanofiltration. *Desalination*, **240(13)**, 170-177.
- Panigrahi, S., Dubey, BK., Brajesh, K. (2019) A critical review on operating parameters and strategies to improve the biogas yield from anaerobic digestion of organic fraction of municipal solid waste. *Renewable Energy*, **143**, 779-797.
- Sarkar, B., Chakrabarti, P. P., Vijaykumar, A., Kale, V. (2006) Wastewater treatment in dairy industries - possibility of reuse. *Desalination*, **195**, 141-152.

# Numerical Modelling of Hydraulic Transients Considering Dynamic Effects in a Water Pumping System

A. B. N. Diniz\*, J. Fernandes Junior\*\* and A. K. Soares\*

\* Environmental Technology and Water Resources Program, University of Brasília, Brasília, Brazil  
(E-mail: [arthurbndiniz@gmail.com](mailto:arthurbndiniz@gmail.com); [aksoares@gmail.com](mailto:aksoares@gmail.com))

\*\* Environmental and Sanitary Engineering Program, Federal University of Goiás, Goiânia, Brazil  
(E-mail: [jfslmb@gmail.com](mailto:jfslmb@gmail.com))

## Abstract

This research work focused on the analysis of hydraulic transients induced by a pump tripoff in a hypothetical water pumping system equipped with an air valve. The influence of the dynamic effects on the system behaviour and on the numerical modelling has been highlighted. Pressure transients were simulated considering the classic water hammer model as well as the incorporation of unsteady friction model. The results showed that unsteady friction causes attenuation of pressure peaks and pressure signal delay. Thus, unsteady friction cannot be neglected when analysing hydraulic transients in pressurized pipes as its consideration is responsible for the greater damping of calculated pressure peaks.

## Keywords

Water hammer; numerical modelling; dynamic effects

## INTRODUCTION

Hydraulic transient modelling is important in the design of pressurized piping systems to ensure their safety, reliability and good performance under various operating conditions. Several causes can originate transient phenomena such as valve manoeuvres, pump trips or start-up, or by the occurrence of sudden pipe ruptures (Soares et al., 2013). Checking the minimum permitted pressures is important to prevent pipeline collapse by avoiding air release, cavitation and separation of the water column. Calculation of the maximum transient pressures is usually performed to verify if materials and characteristics of the pipe are sufficient to withstand the expected pressure loads to avoid tube rupture or damage to the system (Covas et al., 2006).

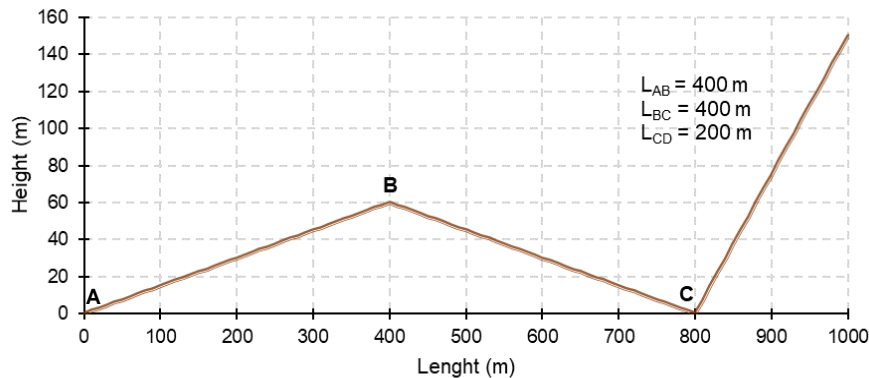
Accurate analysis of pressure wave propagation in pipes depends on the ability to model many phenomena that are secondary to the main effect described by the Joukowski equation. Secondary phenomena include, for example, cavitation and fluid–structure interaction, both of which can influence the evolving shapes of wave fronts as well as their amplitudes and speeds of propagation. Another such phenomenon is skin friction (Vardy and Brown, 2007). The main motivation for the attempts of improving models of unsteady-state friction in pressurized pipe systems is the need for simulating properly the very large decay and rounding of pressure peaks after the end of a complete closure manoeuvre or a pump shutdown (Brunone et al., 2004). Differences can be verified between the behaviour obtained from the theoretical results and data collected from real systems, especially during rapid transients with high frequencies, when trying to model a transient event considering steady friction. Thus, it was verified the need to treat the friction factor differently for the steady-state flow and unsteady flow regimes (Vardy et al., 1993).

In this study, transient pipe flows caused by pump tripoff have been analysed. Numerical results obtained from hydraulic modelling of a hypothetical system with similar characteristics to existing systems have been used to evaluate the performance of the transient solver.



## METHODOLOGY

The case study consists of a hypothetical pipe-rising main between two storage tanks. Figure 1 presents the simplified scheme of the water pipeline profile. An air valve was designed to protect the high point of the line (Point B –  $x = 400$  m) against negative pressures. The system consists of a centrifugal pump with nominal values of 158 m for total head, 150 kW for power, 1750 rpm rotational speed, 70 L/s for pumped flow, 72.33 % for efficiency, and pump-motor inertia of 4.03 kg.m<sup>2</sup>. The main force consists of pipes with an absolute roughness of 0.1 mm, an inner diameter of 300 mm, a wave speed of 1000 m/s and a total length of 1000 m.



**Figure 1.** Water pipeline profile ( $z_A = 0$  m;  $z_B = 60$  m;  $z_C = 0$  m;  $z_D = 150$  m)

### Elastic Model

In the analysis of hydraulic transients in pressurized conduits, it is possible to consider the elastic model, which takes into account the compressibility of the fluid and the mechanical characteristics of the conduit walls, used for the analysis of rapid transients with high frequencies (Soares, 2007). A pair of partial differential equations (Chaudhry, 2014; Wylie and Streeter, 1993) can represent the modelling of the flows using the elastic model:

$$\frac{\partial Q}{\partial t} + gA \frac{\partial H}{\partial x} + h_f = 0 \quad (1)$$

$$\frac{\partial H}{\partial t} + \frac{a^2}{gA} \frac{\partial Q}{\partial x} = 0 \quad (2)$$

where  $x$  = coordinate along the pipe axis;  $t$  = time;  $H$  = piezometric head;  $Q$  = flow rate;  $a$  = celerity or elastic wave speed;  $g$  = gravity acceleration;  $A$  = pipe cross-sectional area;  $h_f$  = head loss per unit length. The solution of the equations is usually obtained through the Method of Characteristics (MOC), which transforms the original pair of hyperbolic equations into two pairs of simple differential equations.

### Unsteady Friction

To take into account unsteady friction effects, the friction losses,  $h_f$ , have been separated into two components (Soares, 2007):

$$h_f = h_{fs} + h_{fu} = \frac{fQ|Q|}{2gDA^2} + h_{fu} \quad (3)$$

where  $h_{fs}$  = head loss for steady-state conditions (expressed in terms of square flow rate for turbulent flows);  $h_{fu}$  = head loss for unsteady-state conditions;  $D$  = pipe inner diameter; and  $f$  = Darcy-Weisbach friction factor calculated for turbulent and laminar flow (Swamee, 1993).



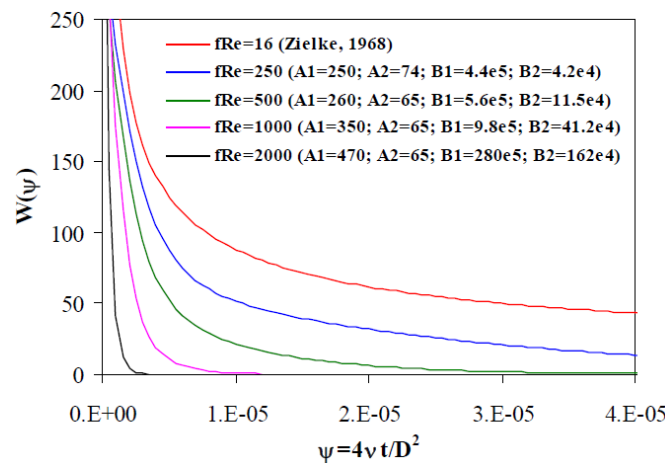
With regard to the head loss for unsteady-state conditions, two one-dimensional models have been developed in this study: Vardy et al. (1993) and Vardy and Brown (2007). Vardy et al. (1993) proposed a model for the consideration of unsteady friction in turbulent transient flow that follows the hypothesis formulated by Zielke (1968) for laminar flow. This method relates the term of unsteady friction to the average velocity and the history of instantaneous velocities and can be used in Method of Characteristics (MOC). The head loss for unsteady-state conditions is given by:

$$h_{fu} \approx \frac{16\nu}{\rho D^2} [Y_1 + Y_2] \tag{4}$$

where  $\nu$  = dynamic viscosity of the fluid. Variables  $Y_i$  depends on the fluid and on the characteristics of the flow itself, which are defined by:

$$Y_i(t) = Y_i(t - \Delta t) e^{-B_i \frac{4\nu}{D^2} \Delta t} + A_i [V(t) - V(t - \Delta t)] \tag{5}$$

where parameters  $B_i$  and  $A_i$  are dependent on the product of friction and Reynolds number ( $f \times Re$ ) and the respective weighting functions are presented in Figure 2.



**Figure 2.** Weighting functions for smooth turbulent flows (Covas, 2003)

Vardy and Brown (2007) presented a weighting function approach suitable for the whole range of turbulent flows from fully smooth to fully rough, allowing for an extensive range of  $Re$ :

$$W_a^* = \frac{W_a}{A^* e^{-B^* \psi}} = \frac{1}{\sqrt{\psi}} \approx \sum_{i=1}^N \frac{m_i}{A^*} e^{-(n_i - B^*) \psi} = \sum_{i=1}^N m_i^* e^{-n_i^* \psi} \tag{6}$$

where  $B^* = [a_0 + a_1 \ln R_v + a_2 (\ln R_v)^2 + a_3 (\ln R_v)^3] / [b_0 + b_1 \ln R_v + b_2 (\ln R_v)^2 + b_3 (\ln R_v)^3]$  and  $A^* = 1/2\sqrt{\pi}$ , in which  $a_0 = -291.07$ ;  $a_1 = 149.33$ ;  $a_2 = -24.410$ ;  $a_3 = 1.3524$ ;  $b_0 = 1$ ;  $b_1 = -0.14810$ ;  $b_2 = 0.0078897$ ; and  $b_3 = -0.00014504$ .

The scaled weighting function  $W_a^*$  is equal to the inverse of the square root of the nondimensional time and is thus independent of the particular flow conditions. The relationships between the universal and specific values of  $m_i$  and  $n_i$  are implicit in Equation 6, namely  $m_i = A^* m_i^*$  and  $n_i = n_i^* + B^*$ . Sets of values of the coefficients  $m_i^*$  and  $n_i^*$  are presented in Vardy and Brown (2007).

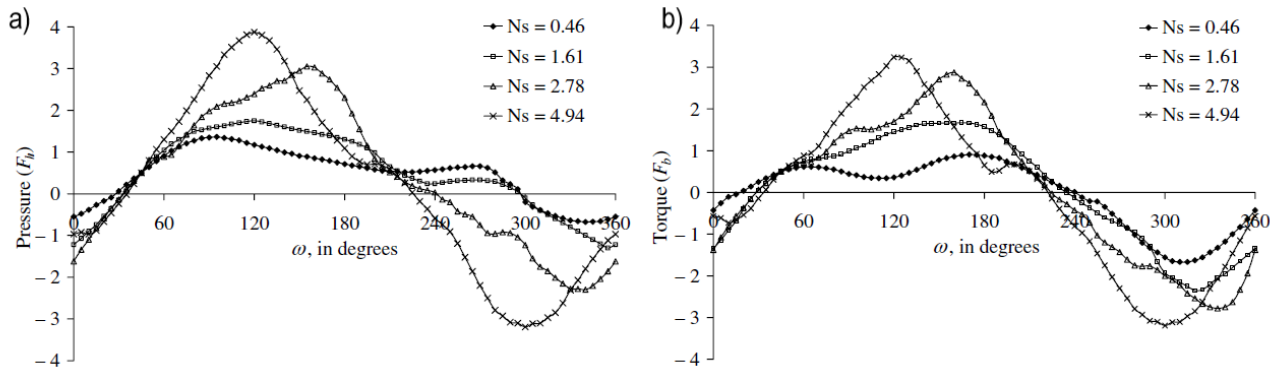
**Boundary Condition**

The relationships between flow ( $Q$ ) rotational speed ( $N$ ), head ( $H$ ) and torque ( $T$ ) must be specified in order to mathematically represent a pump. Dimensional parameters related to the best efficiency point are used as reference and defined by the following variables, where the subscript  $R$  denotes nominal values (Chaudhry, 2014):

$$v = \frac{Q}{Q_R}; \quad h = \frac{H}{H_R}; \quad \alpha = \frac{N}{N_R}; \quad \beta = \frac{T}{T_R} \quad (7)$$

During normal pump operation,  $\alpha$ ,  $\beta$ ,  $v$  and  $h$  are all positive. However, during the transient state, they can become negative individually or in groups. The operation of a pump can be divided into eight operating zones and four quadrants, in terms of an angle  $\omega = \tan^{-1}(\alpha/v)$ . Head and torque characteristic curves are defined according to Suter parameters, calculated by  $F_h$  and  $F_b$  (Figure 3), respectively, as a function of angle  $\omega$  for different values of specific velocity ( $N_s$ ):

$$F_h = \frac{h_p}{\alpha_p^2 + v_p^2} \quad F_b = \frac{\beta_p}{\alpha_p^2 + v_p^2} \quad N_s = \frac{N_R Q_R^{0.5}}{H_R^{3/4}} \quad (8)$$



**Figure 3.** Pump characteristic curves for different specific speeds: (a) pumping pressure head; (b) net torque (Soares et al., 2013)

The head on the pump can be calculated from the following equation:

$$H_{P_{i,1}} = H_{suc} + H_P - \Delta H_{P_v} \quad (9)$$

in which  $H_{suc}$  = height of the liquid surface in the suction reservoir above the datum,  $H_P$  = pumping head at the end of the time step, and  $\Delta H_{P_v}$  = head loss in the discharge valve for the pump discharge at the end of the time step given by:

$$\Delta H_{P_v} = C_v Q_{P_{i,1}}^2 = C_v Q_{P_{i,1}} |Q_{P_{i,1}}| \quad (10)$$

where  $C_v$  is the coefficient of valve head loss.

The boundary condition imposes four unknown variables  $\alpha_p$ ,  $v_p$ ,  $h_p$  and  $\beta_p$ , which must be determined at each time interval. Therefore, four equations that provide a single solution are required. From Equations 7 to 10, we obtain:

$$Q_R v_p = C_n + C_a H_{suc} + C_a H_R h_p - C_a C_v Q_R^2 v_p |v_p| \quad (11)$$

After equation development, resolution is performed via Newton–Raphson Method (Chaudhry, 2014). Rearranging Equations 7 to 11 gives:

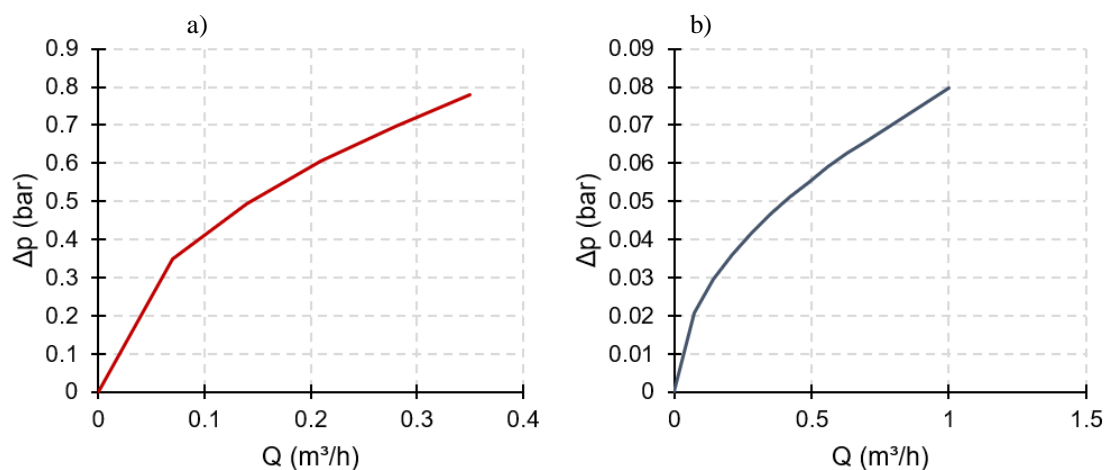
$$F_1 = C_a H_R a_1 (\alpha_p^2 + v_p^2) C_a H_R a_2 (\alpha_p^2 + v_p^2) \tan^{-1} \frac{\alpha_p}{v_p} - Q_R v_p - C_a C_v Q_R^2 v_p |v_p| + C_n + C_a H_{suc} = 0 \quad (12)$$

$$F_2 = \alpha_p - C_6 a_3 (\alpha_p^2 + v_p^2) - C_6 a_4 (\alpha_p^2 + v_p^2) \tan^{-1} \frac{\alpha_p}{v_p} - \alpha - C_6 \beta \quad (13)$$

where  $C_6 = -15 T_R \Delta t / (\pi I N_R)$ , in which  $I$  = inertia of the motor-pump assembly.

### Air Valve Boundary Condition

In this work, the device used to relieve the effects of negative pressures was the triple function air valve with nominal inlet and exhaust air diameters of 80 mm and 20 mm, respectively. The characteristic curves of intake and expulsion of air by the air valve are shown in Figure 4. The discharge coefficients for air inlet and outlet were defined at the constant value of 0.61, which is usual for the calculation of a standard orifice. The high point B ( $z_B = 60$  m in Fig. 1) was chosen as the air valve installation site, which is a possible air accumulation region.



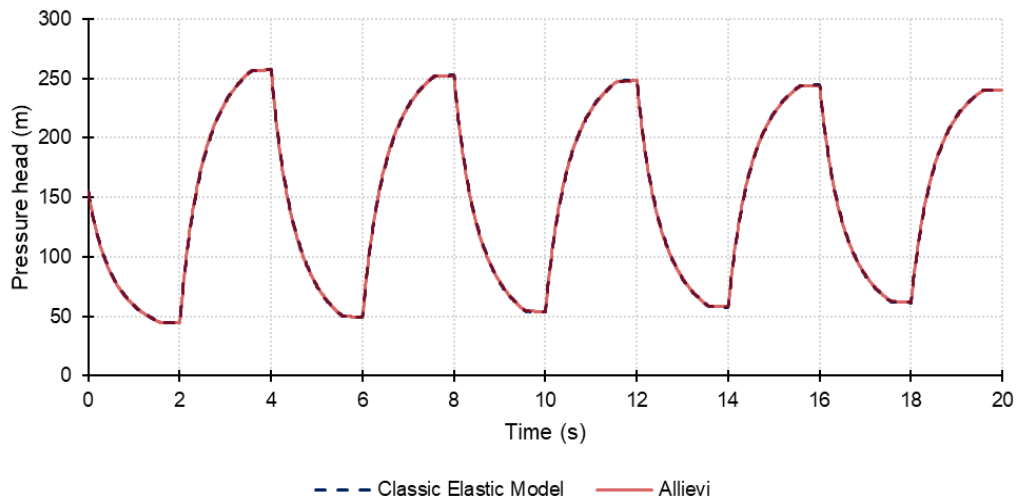
**Figure 4.** Characteristic curves of the air valve. a) Air intake curve. b) Air expulsion curve

Modelling air valve boundary conditions may be handled within the usual framework of the MOC. Complete equations used for air valve boundary simulation are presented in Wylie and Streeter (1993). Four conditions - air inflow and outflow through an air valve at subsonic and sonic levels - are considered. Assumptions are made in the analytical equations for air valve boundary conditions (Wylie and Streeter, 1993) as: (1) isentropic flow is assumed for airflow through the air valve; (2) the air mass within the pipe is assumed to obey the isothermal law; (3) the air admitted into the pipe is assumed to stay near the valve; and (4) the water surface elevation is assumed to remain constant, and the volume of air is considered small compared with the liquid volume of pipeline reach.

### RESULTS

To validate the hydraulic model developed, comparisons to the software Allievi (ITA, 2018) were made by simulating two distinct scenarios: steady-state friction and water pipeline without air valve (Scenario 1); and steady-state friction and water pipeline equipped with a triple function air valve (Scenario 2). To verify the influence of the dynamic effects on the system behaviour, hydraulic transients were simulated considering the classic water hammer model as well as unsteady friction models (Vardy et al., 1993; Vardy and Brown, 2007). The developed model was evaluated in two different scenarios: unsteady friction and water pipeline without air valve (Scenario 3); and unsteady friction and water pipeline equipped with a triple function air valve (Scenario 4).

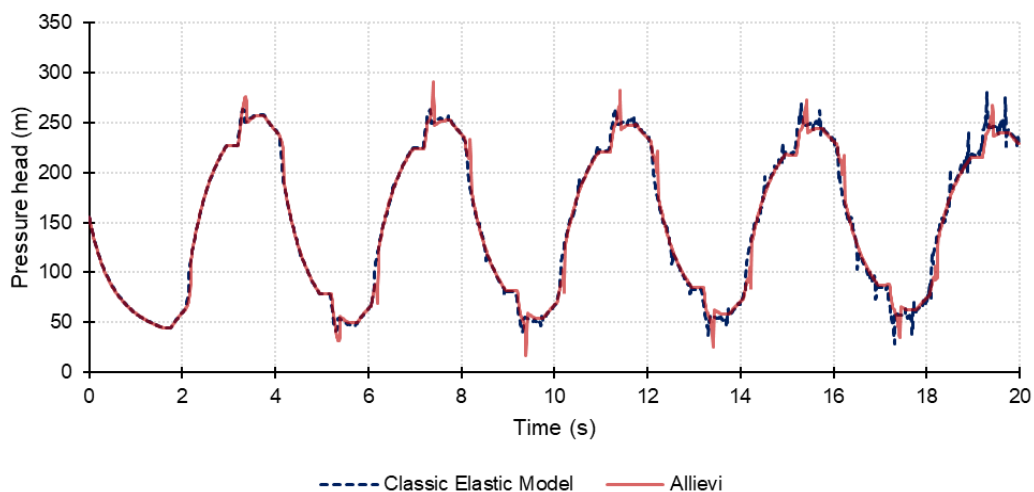
Figure 5 shows that the developed hydraulic model reproduces accurately the initial minimum pressure heads ( $t \approx 1.5$  s and  $H \approx 45$  m). The attenuation and dispersion of the pressure wave fit precisely to the simulated time interval, reproducing analogous pressure peaks.



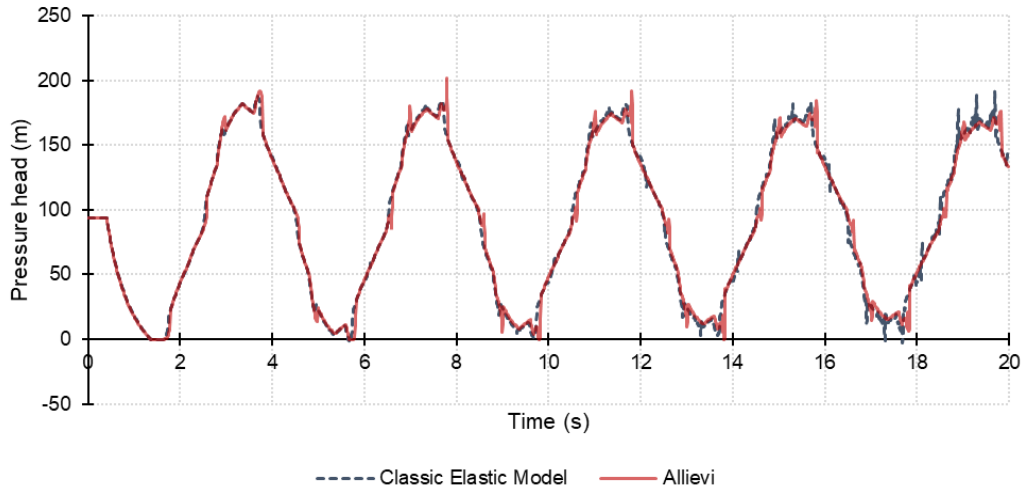
**Figure 5.** Variation of pressure head in the pumping system – Scenario 1

As shown in Figure 6 and 7, dynamic effects caused by the addition of an air valve in the system did not compromise the accuracy of the developed model. The results obtained for the pressure transients in the pumping system and in the air valve also showed convergence between the two models.

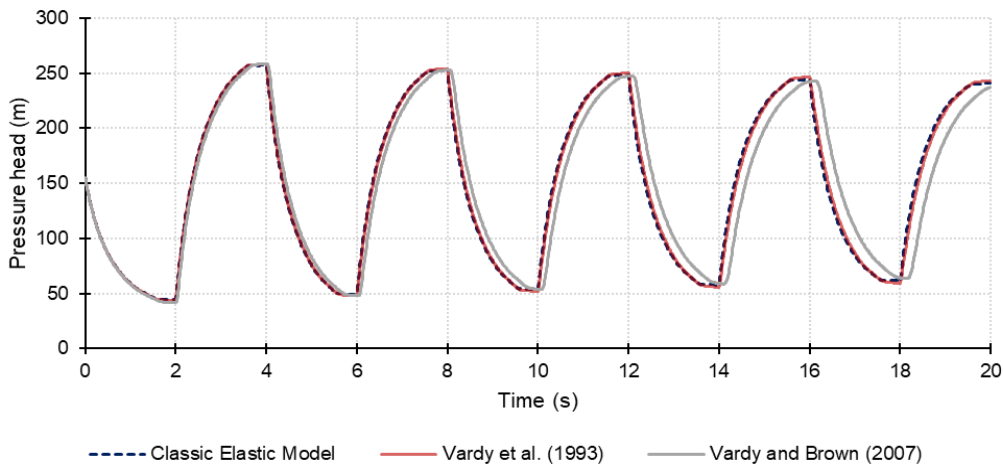
Figures 8 and 9 show the results obtained by unsteady friction models simulation. When comparing results of simulations using steady-state friction to results of unsteady friction model of Vardy and Brown (2007) the pressure signal presents damping of pressure peaks as well as phase delay of pressure waves. The model proposed by Vardy et al. (1993) showed no significant difference from the classic elastic model. As shown in Figure 9, the pressure signal behaviour is quite similar to the one observed in Scenario 3. Including the effects of air valve operation did not change how the models behave numerically in terms of pressure attenuation and pressure wave delay. In general, consideration of the unsteady friction resulted in attenuation of pressure peaks and pressure wave delay only for Vardy and Brown (2007) model.



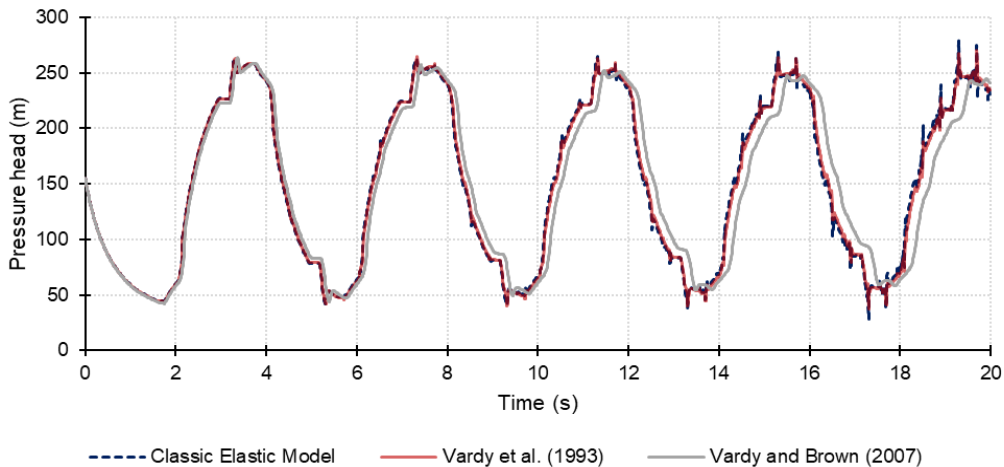
**Figure 6.** Variation of pressure head in the pumping system – Scenario 2



**Figure 7.** Variation of pressure head in the air valve – Scenario 2



**Figure 8.** Variation of pressure head in the pumping system – Scenario 3



**Figure 9.** Variation of pressure head in the pumping system – Scenario 4

## CONCLUSIONS

A hydraulic transient solver incorporating unsteady friction and air valve boundary condition has been proposed in this research work. When only steady-state friction has been taking into account,

the proposed model presented results in accordance with software Allievi and accurate estimations for the maximum and minimum transient pressures. These results obtained were used to validate the transient solver developed.

Obtained numerical results showed that unsteady friction model proposed by Vardy and Brown (2007) reproduced more accurately expected pressure wave dispersion and attenuation effects, comparing to the other two models evaluated (classic elastic model and Vardy et al., 1993 unsteady friction model). Initial maximum and minimum transient pressures are quite similar to the three models evaluated. The major advantage of Vardy et al. (1993) and Vardy and Brown (2007) unsteady friction models is their dismissal for empirical determinations, i.e. they are non-parameterized models instead of unsteady friction models considering wall shear stress directly proportional to local and convective terms.

When considering an air valve located in a high point of the water pipeline, the pressure signal presented some pressure spikes after air admission. Vardy and Brown (2007) unsteady friction model delays the pressure wave and smooths the pressure peaks eliminating pressure spikes. In this way, the interaction between unsteady friction and admitted air volumes by air valves have to be better studied in existing water pumping systems.

## REFERENCES

- Brunone, B., Ferrante, M., Cacciamani, M. (2004) Decay of pressure and energy dissipation in laminar transient flow. *Journal of Fluids Engineering*, **126**(6), 928-934.
- Chaudhry, M. H. (2014) Applied hydraulic transients, 3rd ed., Springer, Columbia, South Carolina, USA.
- Covas, D. I. C. (2003) Inverse transient analysis for leak detection and calibration of water pipe systems – modelling special dynamic effects. Ph.D. thesis, Univ. of London, London.
- Covas, D., Ramos, H., Lopes, N., Almeida, A. B. (2006) Water pipe system diagnosis by transient pressure signals. *Water Distribution Systems Analysis Symp.* S. G. Buchberger, R. M. Clark, W. M. Grayman, and J. G. Uber, eds., ASCE, Reston, VA, 1-19.
- ITA (2018) Allievi users manual, Universidad Politécnica de Valencia, Valencia, Spain.
- Soares, A. K. (2007) Leak Detection and Calibration of Transient Hydraulic System Models. Thesis (Doctoral) – São Carlos School of Engineering, University of São Paulo, São Carlos, Brazil, 336.
- Soares, A. K., Covas, D. I. C., Ramos, H. M. (2013) Damping Analysis of Hydraulic Transients in Pump-rising Main Systems. *Journal of Hydraulic Engineering*, **139**(2), 233-243.
- Swamee, P. K. (1993) Design of a submarine pipeline. *Journal of Transportation Engineering*, **119**(1), 159-170.
- Vardy, A. E., Brown, J. M. (2007) Approximation of turbulent wall shear stresses in highly transient pipe flows. *Journal of Hydraulic Engineering*, **133**(11), 1219-1228.
- Vardy, A. E., Hwang, K. L., Brown, J. M. B. (1993) A weighting function model of transient turbulent pipe friction. *Journal of Hydraulic Research*, **31**(4), 533-548.
- Wylie, E. B., Streeter, V. L. (1993) Fluid transients in systems, New Jersey, USA: Prentice-Hall.
- Zielke, W. (1968) Frequency-dependent friction in transient pipe flow, *Journal of Basic Engineering*, **90**(1), 109-115.

## Co-creation of Affordable and Clean Pumped Irrigation for Smallholders: Lessons from Nepal and Malawi

J. C. Intriago\*, R. van Dijk\*, J. Michavila\*\*, E. Arenas Pinilla\*\*\*, J. C. Diehl\*\*\*\* and M. W. Ertsen\*

\* Department of Water Management, Faculty of Civil Engineering and Geosciences, Delft University of Technology. Stevinweg 1, 2628 CN Delft, Netherlands (E-mails: *J.C.IntriagoZambrano@tudelft.nl*; *R.W.vanDijk@student.tudelft.nl*; *M.W.Ertsen@tudelft.nl*)

\*\* aQysta BV. Molengraaffsingel 12, 2629 JD Delft, Netherlands (E-mail: *jaime@aqysta.com*)

\*\*\* ICAI School of Engineering, Comillas Pontifical University. Calle de Alberto Aguilera 25, 28015 Madrid, Spain (E-mail: *earenas@icai.comillas.edu*)

\*\*\*\* Department of Design Engineering, Faculty of Industrial Design Engineering, Delft University of Technology. Landbergstraat 15, 2628 CE Delft, Netherlands (E-mail: *J.C.Diehl@tudelft.nl*)

### Abstract

Pumped irrigation is a way to improve water control for smallholder farming, hence to intensify its production. In this context, the Dutch company aQysta has developed the Barsha pump (BP), the first-ever commercial version of a hydro-powered pump traditionally referred to as spiral pump. BPs, however, have to deal with several constraints that affect the decision-making and access of smallholders to this as well as other agricultural (water pumping) technologies, thus to their benefits. On this subject, Product Service System (PSS) is a type of business models able to potentially cope with a number of restrictions of different nature (i.e. technical, financial, social). Moreover, if co-created with the feedback of the users, and by addressing contextual tensions of different cases, these models can be substantially richer than their top-down counterparts. From this perspective, six cases of use of BPs have been addressed in Nepal and Malawi, respectively. Both primary and secondary data, which was analyzed qualitatively under the analytic induction approach, was collected through a number of methods: on-site observations, unstructured interviews, structured questionnaires, and Q-methodology. Evidence shows a wide range of (non-)technical facilitating and hampering conditions for the use of the BP, as well as preferences of the smallholders in regards to existing and proposed business model elements. Based on the corresponding analysis, a set of opportunities for an improved BP-based business model – PSS, aiming to fulfil several (and at times opposing) needs, is ultimately proposed in the current paper.

### Keywords

Hydro-powered pump; Barsha pump; spiral pump; smallholder; business model; product-service system; co-creation

## INTRODUCTION

Given the significant quantity of smallholder farms worldwide (Lowder et al., 2016), intensifying their crop production is key for food security, as well as in creating positive impacts in their livelihoods. Amongst many challenges that smallholders face, proper water management is one of the most critical elements to achieve such objective (Giordano et al., 2019). A way to improve (or enable) access to and control of irrigation water is—yet not limited to—by the use of pumping technologies to water lands that will remain otherwise (partly) unirrigated throughout the year.

Most water pumping systems, however, operate on electricity or fossil fuels, thus are (too) cost-intensive, or even inaccessible, for many smallholders due to the continuous use of electricity and fossil fuels (Chandel et al., 2015); moreover, they affect the environmental quality due to their gaseous emissions and noise. More environmentally sound and at times less expensive alternatives are renewable energy (RE)-based pumping technologies (Gopal et al., 2013). From these, hydro-powered pumping (HPP) technologies—i.e. those hydro-mechanically driven by the water they lift—pose even further advantages over their other RE counterparts (Fraenkel, 1986).

The Dutch start-up company aQysta developed the Barsha pump (BP), the first ever commercial version of a HPP device traditionally referred to as “spiral pump”, firstly reported during the 18<sup>th</sup> century (Ziegler, 1766) and applied after the late 70s in a number of countries (Morgan, 1984; Naegel, 1998; UNEP, 2015). Roughly 150 BP units have been deployed since 2014 in Nepal, and 13 units since 2018 in Malawi (aQysta, personal communication, July 26, 2019). The BP has to deal with market inefficiencies caused by, amongst others, underdeveloped supply chains, economic constraints, lack of knowledge, amongst others, which consequently limit the access of smallholders to this as well as other agricultural technologies, thus to their benefits (Giordano et al., 2019).

A business model that potentially can deal effectively with such a number of restrictions, while at the same time creating value for the involved parties, is ‘Product Service System’ (PSS) (Mont, 2002). In addition, some authors state that a participatory process of co-creation / co-design (Dahan et al., 2010), especially while identifying and addressing contextual tensions at an early stage—in line with the so-called Context Variation by Design (CVD) approach (Kersten et al., 2017)—will substantially enrich the outputs to meet the user’s needs. However, with exception of few authors (Corti et al., 2013; Devisscher and Mont, 2008), these models have not been studied within the agricultural sector—let alone their co-created, bottom-up versions. None of them as well have addressed the specific case of water pumping technologies for smallholder farming.

In that perspective, Delft University of Technology and Comillas Pontifical University, are exploring the co-creation and implementation of affordable and clean pumped irrigation systems for smallholders, based upon novel HPP technologies like the aQysta BP (Intriago et al., 2018). Within this context, the objectives of this paper are: (1) to qualitatively analyze different (and opposed) use cases of BPs in Nepal and Malawi; (2) to highlight the underlying reasons for (not) using the BP, with emphasis on the most preferred / least preferred current and proposed BP business model elements (BME); and, (3) set grounds, based on the feedback of smallholders, for the future co-design of an improved BP-based PSS.

## **MATERIALS AND METHODS**

### **Criteria for selection of use cases**

The BP use-cases were selected within certain Nepali and Malawian smallholder communities, during the field visits in June – July 2019, based on the following criteria: (1) at least one BP must have been posing continuous presence for  $\geq 2$  months; (2) in accordance with the CVD approach, the BP use-cases must show different characteristics (e.g. topography, water source, facilitating / hampering conditions) between each other.

### **Data collection**

Primary data, both quantitative and qualitative in nature, was collected and triangulated by: (1) direct on-site observations; (2) unstructured interviews to BP users, other smallholders (non BP users), and experts (authorities, NGOs) relevant to the chosen communities; (3) structured questionnaires administered to smallholders; and, (4) Q-methodology. Secondary data, which complemented the understanding of the researched phenomenon, was collected through: (1) databases administered by aQysta on the use of BPs; (2) official documents issued by the respective Nepali and Malawian authorities; and, (3) other related literature.

### **Data analysis**

Due to their nature, as well as to the size of the selected population, the collected data will be analyzed qualitatively, under the analytic induction approach. Particular attention will be given to



contrasting data between cases, in line with the aforementioned CVD approach.

## RESULTS AND DISCUSSION

On the basis of the criteria pointed out above, the selected communities were, in Nepal: (1) Sokhu Besi neighborhood in the Jhangajholi Ratamata village, Sindhuli district, (2) Manthali municipality, Ramechhap district, and (3) Lele village, Lalitpur district; and, in Malawi: (4) Michiru, near Blantyre, (5) Tedzani, near Zalewa, and (6) Kachere cooperative, near Ntchisi. These BP use cases show a wide range of codified categories / attributes, as summarized in Table 1.

### Brief description of cases

*Case 1: Sokhu Besi.* The farmer is the sole owner of the BP, obtained by means of a subsidy (~90 %) from the local government. The water supplied by the BP supports both crop—mainly vegetables sold to local markets—and livestock farming. The unit has been operative yet with two broken waterwheel paddles, thus working less efficiently. The farmer counts on basic complementary infrastructure for pumped water management: two plastic reservoirs and one plastic-lined open-air excavated pond, both at farm-ground level. The BP shares space with other two community-owned diesel water pumps on the riverside. The latter require fuel input, resulting in operation costs 600 NPR (~ €4.80) per hour per farmer. Nevertheless, in general the community prefers the diesel pumps over the BP due to its higher pressure and flowrate, and (perceived) faster spinning speed.

*Case 2: Manthali.* The farmer has two BPs, one owned—subsidized ~90 % by the government—and one lent quad-spiral prototype (intended to reach twice the pumped flow. His farm consists of several plots, some of them rented from neighboring farmers, to produce vegetables for sale at the local market. Albeit in operational conditions, none of the BPs was in use at the time of the field visit. The farmer argued this was due to the forthcoming rains, hence potential floods that could flush away the pumps; however, this might also be occurring due to the preferential use of groundwater sources within his lands. According to other interviewees, the farmer receives more revenues from selling groundwater to neighbors than the agricultural produce itself. This coincides with the fact that some plots remain barren, although he could ensure higher water volumes by additionally using the two BPs.

*Case 3: Lele.* The current farmers took over the farm on rental basis three months before the field visit. An infrastructure was already established, i.e. open plastic greenhouses and drip irrigation system, though the latter was removed by the farmer. The breast-shot BP lent along with the farm, stopped functioning after a flood damaged the ~0.50 m weir four months before. The farmers do not know how the BP operates. As a consequence, they bought an electric pump right away to supply their farm's need of water. This pump feeds an in-farm plastic-lined excavated reservoir, as well as a sprinkler irrigation system. They grow a number of vegetables that are sold locally.

*Case 4: Michiru.* This farm is a BP demonstration site in the Blantyre District. Since the farmer is aware of global warming effect, he sees the BP as an ideal technology. The unit has been in his possession for three months without any charge, after which he will have to start paying it off. The BP has been working so far irregularly due to water level fluctuations. Consequently river management—done through sandbags—will remain a reoccurring activity. The water supplied is used to irrigate several types of vegetables. Moreover, the farmer constructed a reservoir, which acts both as water storage and fish pond, to further manage the pumped water. After filling it, the water quickly seeped away; aQysta has offered to supply with a plastic lining to tackle this issue.

**Table 1.** Attributes of the selected BP use cases in farming communities in Nepal and Malawi

	Nepal			Malawi		
	Sokhu Besi	Manthali	Lele	Michiru	Tedzani	Kachere cooperative
<b>Distance from aQysta</b>	88 km	129 km	16 km	3 km	60 km	396 km
<b>Travelling time</b>	~3.5 h	~5 h	~1 h	15 min	~2 h	~6.5 h
<b>Topography</b>	River bottom valley	River bottom valley	Sub-valley	River bottom valley	River bottom valley	Shire river basin
<b>Accessibility</b>	Next to national highway	Next to regional road	Next to district road	Next to district road	Next to footpath	Next to dirt road
<b>Main water source</b>	Sun Koshi river	Tamakoshi river	Unnamed river	Likhubula river	Shire river	Chafumbi river
<b>Farm size</b>	0.4 ha	1 ha	0.2 ha	~1 ha	4 ha (partly cultivated)	~1.5 ha
<b>BP presence time</b>	~3 y	~2 y	~1.5 y	~ 3 m	~ 2 m	~ 3 m
<b>Facilitating conditions for BP</b>	-Closeness to river (~170 m) -Stream speed	-Closeness to river (~80 m) -Stream speed	-Closeness to river (~105 m)	-Closeness to river (~30 m)	-Closeness to river (~80 m)	-Closeness to river (~120 m) -Stream speed
<b>Hampering conditions for BP</b>	-Presence of diesel water pumps	-Groundwater sources	-Stream speed -Need of a weir -River floods	-Stream speed -Changing water depth -Need of a weir	-Stream speed -Floating weed -Changing water depth	-Lack of irrigation equipment
<b>BP ownership</b>	-1 private	-1 private / -1 lent	-1 lent	-1 lent (demonstration)	-1 lent (for testing)	-1 private
<b>BP conditions</b>	Partially functional and operative	Fully functional yet not operative	Fully functional yet inoperative	Partially functional and operative	Partially functional and inoperative	Fully functional and operative
<b>Farmer attitude on BP</b>	Willing to keep using it	BP less useful than other water pumps	BP does not provide any benefit	Willing to keep using it	Willing to keep using it	Willing to keep using it
<b>Impact of the BP</b>	The farm relies on the BP	None (BPs not in use)	None (BPs not in use)	The farm relies on the BP	None (BP not in use)	The farm relies on the BP
<b>Most preferred existing BME</b>	-Subsidies -Clean energy	-Subsidies -Zero operation costs	-Clean energy -Easy to install and use -Subsidies	-Flexible payment methods -Zero operation costs -Clean energy -No human labor	-Flexible payment methods -Zero operation costs -Clean energy	-Flexible payment methods -Zero operation costs -No human labour
<b>Most preferred proposed BME</b>	-Extra services -Entrepreneurial training -Creation of jobs	-Extra services -Creation of jobs	-Nothing	-Extra services (reservoirs) -Provision of (basic) infrastructure	-Nothing	-Nothing
<b>Least preferred existing BME</b>	-Complex maintenance -Savings in operation -Pumped pressure	-Pumped pressure -Perceived saved labor	-Maintenance provided by an external organization	-Weight and size -Easy to steal/vandalism	-BP does not operate yet	-Pumped flow rate
<b>Least preferred proposed BME</b>	-Paying for extra services	-Non-ownership models -Entrepreneurial training -Paying for extra services	-Entrepreneurial training -Intervention of external organizations -Paying for extra services	N/A	N/A	N/A
<b>Attitude of other farmers on the BP</b>	-Not enough pumped pressure nor flowrate -Diesel water pumps are more useful	N/A	N/A	-Curiosity on the BP operation -Skeptical about BP efficiency, though they think the owner made a good decision	-Curiosity on the BP operation	N/A

*Case 5: Tedzani.* This farm is an experimental site, intended to test the BP feasibility in the Shire river. Its conditions however, are challenging: too deep to anchor the BP, too low water speed next

to the banks, rapidly fluctuant water level, and houses crocodiles. If this pilot turns successful, the farmer will pay the BP off in instalments—a key driver for her choice—after which she is willing to buy another one. The main reason to adopt a BP was to cut down on fuel costs of the pumps that are currently used for irrigation. The BP was in the water but not operating due to low water speed.

*Case 6: Kachere cooperative.* This is a group of smallholders that has received support from several organizations; they shifted from watering cans to treadle pumps, and later on to diverting the river and gravity irrigation. None of these methods worked to their satisfaction, as such they inquired a BP, which was provided after paying a deposit. Yet, they find the pumped flow rate insufficient. This occurs due to the inadequate water management, associated with lack of infrastructure (e.g. sprinklers, reservoirs): water pumped through the night is not stored but simply flows off. Even though farmers are aware that they could pay in instalments, affordability is still a concern.

### **Facilitating and hampering conditions for the BP**

It was observed, in line with findings on other HPP devices (Garman, 1986; Naegel, 1998; Weng, 1994), that a sound technical performance of the technology does not guarantee its sustained use. In Manthali and Lele, the BPs were simply neglected despite optimal working conditions. In Sokhu Besi and Kachere cooperative, similarly to other studies on RE-technologies (Bhattacharyya, 2006; UNCTAD, 2010), (in)existence of external elements (e.g. reservoirs, centrifugal pumps) affected the perceived usefulness of the BP. Within another Nepali community, the BP was deemed as undesirable since it might impede the provision of a subsidized diesel water pump (aQysta, personal communication, June 11, 2019). On the contrary, the Michiru and Tedzani cases depict the willingness of the farmers to use the BP, even though site conditions were unfavorable.

These conditions, particularly for newly adopted technologies, are negatively boosted by weak supply chains (Giordano et al., 2019; Johan, 2015; Weng, 1994). In both Nepal and Malawi, aQysta rely only on a centralized office; as a consequence, all the site-dependent after-sale services (e.g. reparation, maintenance) are decreased in efficiency (Dahan et al., 2010). In both countries, due to their topography and road conditions, extended travelling times deepen the remoteness of certain locations, thereby worsening the already limited logistic networks (UNDP, 2018).

### **Preferences on existing and proposed BME**

*Most preferred existing BME.* Some existing BMEs could cause undesirable side effects if not well managed. Subsidies can steer practices and behaviors, hence to cope with several barriers (e.g. unaffordability, promotion of use, gender inequity) (Bista et al., 2018; Fisher and Kandiwa, 2014; Rai et al., 2019). Nevertheless, if not considered as temporary elements of change, linked to obligations from the counterpart, they can turn into permanent “crutches” for smallholders (Clay, 2013), even posing eventual decreases in productivity (Paudel and Rago, 2017). Moreover, the technology is prone to be deemed as a mere handout due to the lack of empowerment. In some cases, subsidies can be out of the reach of many smallholders, due to e.g. remoteness or institutional barriers (Gauchan and Shrestha, 2017; Paudel and Rago, 2017). Unlike Nepali BPs, which are largely subsidized by the local governments, the Malawian ones do not rely on such mechanisms (although they are previously half-paid by UNDP), hence their unaffordability is worsened in the latter. Therefore, flexible payment methods, e.g. instalments, is a preferred BME in Malawi. Although zero-operation costs and no human labor required are strengths of the BP, they could be misinterpreted as zero-maintenance due to a lack of understanding of the technology (K.C. et al., 2011). If proper maintenance is not given to the BP, its lifetime will be severely compromised. Likewise many other newly introduced (RE) technologies, the BP was observed to require substantial follow-up support and maintenance assistance, as well as transfer of know-how (Gewali and Bhandari, 2005; Johnson and Lybecker, 2009). Despite being a clean energy-based technology,

and notwithstanding its advantages, the BP faces some challenges that might hamper its implementation: policy barriers, lack of awareness, and financial barriers (K.C. et al., 2011).

*Least preferred existing BME.* In Sokhu Besi, where the BP was in operation within their applicability ranges, its pumped pressure and flowrate were considered insufficient. In Michiru, it was seen as a useful yet cumbersome device that could be stolen or vandalized. As pointed out by K.C. et al. (2011), this might be linked to a lack of awareness of the technology and its benefits. This was aggravated by the presence of other (traditional) water pumps; and, by the absence of safety means and water management infrastructure that reduces its usefulness, respectively. In the Nepali cases, despite the BP's virtual zero operation costs, its savings are not perceived as compensating the high upfront cost. Therefore, it becomes imperative to increase its affordability as well as the understandings of the farmers on the technology (K.C. et al., 2011). The maintenance of the BP, though not specialized, is seen as complex by the Sokhu Besi and Lele farmers. This might be increased by the lack of know-how that would enable local partners and/or owners to perform it (Johnson and Lybecker, 2009); i.e. even small repairs must be conducted by the company headquarters. In the Lele case, its maintenance by an external organization is deemed as undesired.

*Most preferred proposed BME.* Both extra services—e.g. assistance, infrastructure, inputs—and creation of new jobs, fit under a product-oriented PSS (Beuren et al., 2013; Mont, 2002; Tukker, 2004). While not having to be all managed but coordinated by the company, the extra services would enable potential job opportunities and their benefits (Beuren et al., 2013; Mont, 2002).

*Least preferred proposed BME.* Paying for extra services was one of the least preferred options. Though contradictory with the preference for counting on them, it is obvious that the BP would be much less affordable with extra costs, particularly if paid upfront in economically depressed areas (K.C. et al., 2011). In addition, using the BP without being the owner was not considered desirable by the Manthali farmer, thus posing potential barriers to other payment schemes (Tukker, 2004).

### **Opportunities for an improved business model - PSS**

Based on the pitfalls and challenges of the current business models analyzed above, an improved, BP-based PSS can be built upon these specific opportunities:

- To offer water pumping systems rather than mere pumping devices; i.e. to give BP-based packages with customized (outsourced) services such as irrigation and water management infrastructure, thereby increasing the usefulness of the BP under a wider range of scenarios.
- To operate with financial aids (e.g. subsidies, microloans), which support the BP affordability, along with co-payment conditions from the end-users. Moreover, extra services offered along with the BP could be attached to these payment methods as well.
- To identify and partner with existing actors to strengthen the supply chains. In Nepal and Malawi, both Collection and Distribution Centers (Rai et al., 2019) and Agricultural Extension Officers (Fisher and Kandiwa, 2014), respectively, act as two-way middlemen that provide technical assistance and agricultural inputs to smallholders. This would reduce service times, create local job opportunities, and increase contact times.
- To partner with NGOs to conduct awareness raising and know-how transfer programs, hence to increase the understanding of the BP as a RE-based technology (K.C. et al., 2011).
- To ensure optimal working conditions whenever required, by the commissioning of additional infrastructure (weirs, diversion canals, gates) that can be outsourced. This will require, however, further assessment of financing and pay-off methods. Otherwise, BP underperformance could ultimately affect its perceived usefulness amongst farmers.

## CONCLUSIONS

Hundreds of BPs are in use in several countries. From these, six cases from Nepal and Malawi were selected and analyzed due to its noticeable differences. In line with the wide range of conditions, the BP owners/users, as well as their neighboring farmers, showed different attitudes on the technical performance of the device and its respective BMEs. Nevertheless, and in line with the CVD approach, instead of aiming to a tailor-made top-down solution for specific situations, the present paper shows how embracing such a diversity could enable co-created richer—yet not perfect—solutions to fulfil several (and at times opposed) needs while coping with different restrictions.

## ACKNOWLEDGEMENTS

This research was funded by the TU Delft | Global Initiative, a program of the Delft University of Technology to boost Science and Technology for Global Development.

## REFERENCES

- Beuren, F. H., Gomes Ferreira, M. G., Cauchick Miguel, P. A. (2013) Product-service systems: a literature review on integrated products and services. *J. Clean. Prod.*, **47**, 222-231. <https://doi.org/10.1016/j.jclepro.2012.12.028>.
- Bhattacharyya, S. C. (2006) Renewable energies and the poor: niche or nexus? *Energy Policy*, **34**, 659-663. <https://doi.org/10.1016/j.enpol.2004.08.009>.
- Bista, D. R., Dhungel, S., Adhikari, S. (2018) Status of fertilizer and seed subsidy in Nepal: review and recommendation. *J. Agric. Environ.*, **17**, 1-10. <https://doi.org/10.3126/aej.v17i0.19854>.
- Chandel, S., Nagaraju Naik, M., Chandel, R. (2015) Review of solar photovoltaic water pumping system technology for irrigation and community drinking water supplies. *Renew. Sustain. Energy Rev.*, **49**, 1084-1099. <https://doi.org/10.1016/j.rser.2015.04.083>.
- Clay, J. (2013) Are agricultural subsidies causing more harm than good? *Guard*.
- Corti, D., Granados, M. H., Macchi, M., Canetta, L. (2013) Service-oriented business models for agricultural machinery manufacturers: Looking forward to improving sustainability, in: 2013 International Conference on Engineering, Technology and Innovation (ICE) & IEEE International Technology Management Conference. IEEE, 1-8. <https://doi.org/10.1109/ITMC.2013.7352612>.
- Dahan, N. M., Doh, J. P., Oetzel, J., Yaziji, M. (2010) Corporate-NGO Collaboration: Co-creating New Business Models for Developing Markets. *Long Range Plann.*, **43**, 326-342. <https://doi.org/10.1016/j.lrp.2009.11.003>.
- Devisscher, T., Mont, O. (2008) An analysis of a product service system in Bolivia: coffee in Yungas. *Int. J. Innov. Sustain. Dev.*, **3**, 262. <https://doi.org/10.1504/IJISD.2008.022229>
- Fisher, M., Kandiwa, V. (2014) Can agricultural input subsidies reduce the gender gap in modern maize adoption? Evidence from Malawi. *Food Policy*, **45**, 101-111. <https://doi.org/10.1016/j.foodpol.2014.01.007>.
- Fraenkel, P. (1986) *Water Pumping Devices: A Handbook for Users and Choosers*. Intermediate Technology Publications, London, UK.
- Garman, P. (1986) *Water Current Turbines: A Fieldworker's Guide*. Practical Action Publishing, Warwickshire, UK.
- Gauchan, D., Shrestha, S. (2017) Agricultural and rural mechanisation in Nepal: Status, issues and options for future, in: Mandal, S.M.A., Biggs, S.D., Justice, S.E. (Eds.), *Rural Mechanisation: A Driver in Agricultural Change and Rural Development*. Institute for Inclusive Finance and Development, Dhaka, Bangladesh, 97-118.
- Gewali, M. B., Bhandari, R. (2005) Renewable energy technologies in Nepal. *World Rev. Sci. Technol. Sustain. Dev.*, **2**, 92. <https://doi.org/10.1504/WRSTSD.2005.006730>.

- Giordano, M., Barron, J., Ünver, O. (2019) Water Scarcity and Challenges for Smallholder Agriculture, in: Sustainable Food and Agriculture. Elsevier, 75-94. <https://doi.org/10.1016/B978-0-12-812134-4.00005-4>.
- Gopal, C., Mohanraj, M., Chandramohan, P., Chandrasekar, P. (2013) Renewable energy source water pumping systems—A literature review. *Renew. Sustain. Energy Rev.*, **25**, 351-370. <https://doi.org/10.1016/j.rser.2013.04.012>.
- Intriago, J. C., Ertsen, M., Diehl, J.-C., Michavila, J., Arenas, E. (2018) Co-creation of affordable irrigation technology: The DARE-TU project, in: International Conference Water Science for Impact. Wageningen, The Netherlands, 1.
- Johan, S. (2015) Value chains, agricultural markets and food security, The State of Agricultural Commodity Markets 2015-16 IN DEPTH, Rome, Italy.
- Johnson, D. K. N., Lybecker, K. M. (2009) Challenges to Technology Transfer: A Literature Review of the Constraints on Environmental Technology Dissemination. *SSRN Electron. J.*, **42**. <https://doi.org/10.2139/ssrn.1456222>.
- K. C., S., Khanal, S. K., Shrestha, P., Lamsal, B. (2011) Current status of renewable energy in Nepal: Opportunities and challenges. *Renew. Sustain. Energy Rev.*, **15**, 4107-4117. <https://doi.org/10.1016/j.rser.2011.07.022>.
- Kersten, W. C., Diehl, J. C., Crul, M. R. M. (2017) Influence of Context Variation on Quality of Solutions: Experiences with Gasifier Stoves. *Procedia Manuf.*, **8**, 487-494. <https://doi.org/10.1016/j.promfg.2017.02.062>.
- Lowder, S. K., Skoet, J., Raney, T. (2016) The Number, Size, and Distribution of Farms, Smallholder Farms, and Family Farms Worldwide. *World Dev.*, **87**, 16-29. <https://doi.org/10.1016/j.worlddev.2015.10.041>
- Mont, O. (2002) Clarifying the concept of product – service system. *J. Clean. Prod.*, **10**, 237-245. [https://doi.org/10.1016/S0959-6526\(01\)00039-7](https://doi.org/10.1016/S0959-6526(01)00039-7).
- Morgan, P. (1984) A Spiral Tube Water Wheel Pump. Blair Res. Bull.
- Naegel, L. C. A. (1998) The hydrostatic spiral pump: Design, construction and field tests of locally-developed spiral pumps. Jaspers Verslag, Munich, Germany.
- Paudel, J., Rago, C. L. (2017) Subsidy and Agricultural Productivity in Nepal, in: Agricultural & Applied Economics Association Annual Meeting. 12.
- Rai, M., Paudel, B., Zhang, Y., Khanal, N., Nepal, P., Koirala, H. (2019) Vegetable Farming and Farmers' Livelihood: Insights from Kathmandu Valley, Nepal. *Sustainability*, **11**, 889. <https://doi.org/10.3390/su11030889>.
- Tukker, A. (2004) Eight types of product–service system: eight ways to sustainability? Experiences from SusProNet. *Bus. Strateg. Environ.*, **13**, 246-260. <https://doi.org/10.1002/bse.414>.
- UNCTAD (2010) Renewable Energy Technologies for Rural Development Renewable Energy Technologies for Rural Development (No. UNCTAD/DTL/STICT/2009/4), Science, Technology and Innovation - Current Studies, New York & Geneva.
- UNDP (2018) Value Chain Development of Fruit and Vegetables in Nepal. Kathmandu, Nepal.
- UNEP (2015) Environmental dispatches: Reflections on challenges, innovation and resilience in Asia-Pacific. Nairobi, Kenya.
- Weng, A. (1994) 水轮泵的技术发展 [Technical development of the water turbine pump]. 水轮泵 [Water-Turbine Pump] 1-7.
- Ziegler, J. H. (1766) Vorläufige Anzeige eines neuen Schöpfrades [Preliminary display of a new bucket wheel], in: Abhandlungen Der Naturforschenden Gesellschaft in Zürich [Treatises of the Nature Research Society in Zurich]. Zurich, Switzerland, 431-463.

## Assessment of the Reliability of a Hydraulic Model of the Topolnitza River with a Limited Number of Data

V. G. Kancheva\* and N. I. Gadjalska\*

\* Department of Agricultural mechanization and hydromeliorative systems, Institute of soil science, agrotechnologies and plant protection, 3, Shosse Bankya St., Sofia, 1331, Bulgaria  
(E-mails: [viktoriq.kancheva@gmail.com](mailto:viktoriq.kancheva@gmail.com); [gadjalska@abv.bg](mailto:gadjalska@abv.bg))

### Abstract

The present study examines the 42 km of the River Topolnitza, from the outfall of Medetska river to the Topolnitza dam. A hydraulic model has been built using the MIKE HYDRO software. Data of average monthly discharge for the period 2016-2017 are included. For the calibration of the model was used the last point of the section, where Q-H relation is known. Four criteria were used to verify the efficiency of the model: relative error ( $r$ ), root mean square deviation ( $\sigma$ ), Nash-Sutcliffe coefficient and correlation coefficient ( $R^2$ ). Nash-Sutcliffe efficiency coefficient gives  $NSE=0,904$ , which means high convergence between model and observed data. Relation between model and observed data can also be described by the equation  $y=0,7764x+0,1732$  and the correlation coefficient between coordinates of model and observed data  $R^2=0,9875$ . The results obtained correspond with the fact, that the river model thus created is sufficiently accurate. Based on this, it is possible to design various tasks related to river hydraulics, water quality, floods and forecasting of different processes.

### Keywords

Mike Hydro; hydraulic model; stability; Topolnitza river water quality; Nash-Sutcliffe efficiency coefficient

## INTRODUCTION

This paper deals with the examines of upper reaches of the Topolnitza river four of its tributaries. The river is located in southwest Bulgaria and springs from Sredna Gora mountain. The total length of the river is 129 km. In this case are considered 42 km from the river - from the outfall of the first tributary to the Topolnitza dam. The displacement in the area under consideration is 580 m altitude at the outfall of the first inflow until 398 m altitude before the dam. The width of the river is 10 to 15 m long and the river bed has a depth of about 0.40-0.60 m. The right slopes of the valley in the section are sloping (10-15 degrees), and the left - steep. The slope of the river is 3 – 4 % (Varlev et al., 1998).

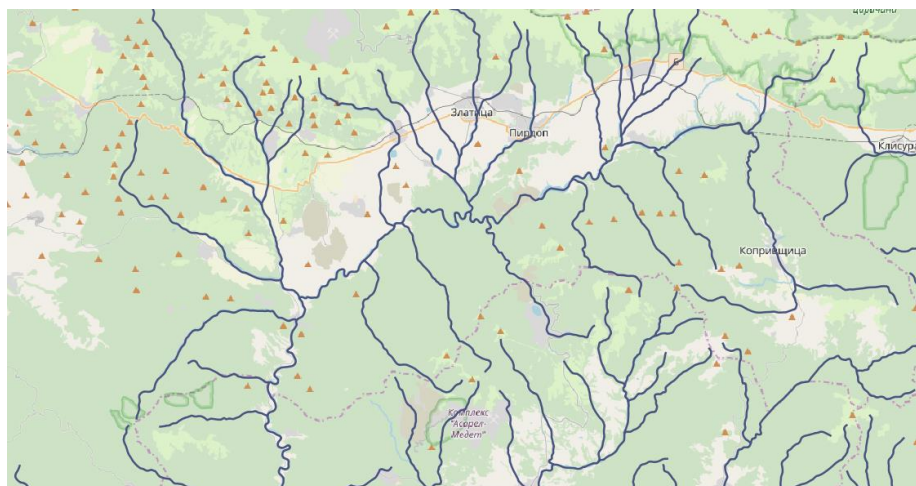


Figure 1. Map of the considered area

## MATERIALS AND METHODS

### Hydraulic model

MIKE HYDRO is the modelling framework for defining and executing one-dimensional river models to a large variety of river related project applications. It allows modelling of different tasks related to river hydraulics, ecology and water quality assessments in rivers, flood analysis and flood alleviation design studies, real time flood or drought forecasting, dam break analysis, sediment transport and long term assessment of river morphology changes and many more.

This software includes a variety of computational methods for fully dynamic, unsteady river flow simulation as well as simpler hydraulic routing in branched and looped river channel networks.

While building hydraulic model the forecasting is of particular importance. The most common applications are reservoir inflow forecasting and common forecasting of flood levels at specific locations along the river system. Reliable forecasts help you optimize control strategies for increased downstream flood protection and optimized reservoir storage for water resources management. Also, forecasts form the basis for the dissemination of warnings to local authorities and the public with information about the time scale and extent of the expected flood inundation. Consequently, forecasting techniques in river modelling constitute a viable and important tool within flood management.

*Computational mechanism.* Water flow modeling is based on the solution of the one-dimensional shallow-flow equation (Saint-Venan equation). Numerical algorithms provide efficient and accurate solutions in both branching and closed pipe and river systems.

The calculation scheme is applicable to vertically homogeneous flow conditions. These conditions are available both in drainage and sewer pipes, with varying water levels, and in rivers, open channels and floodplains.

This software gives a possibility to build realistic and reliable models for the operation of existing and project river and channel networks.

The software works with several river bed resistances:

- Manning
- Chezy
- Darcy-Weisbach
- Colebrook-White for circular pipes
- Hazen-Williams

The resistance gives information about how easily the water crosses the cross section. The higher the resistance, the more the water slows down and a higher slope is required to obtain a certain flow rate. In the instantaneous equation, the resistance element is represented by the slope of the terrain. The slope of the terrain can be expressed as a function of the flow parameters (Q, A and R) and the properties of the water and the resistance.

The application of Manning's formula uses a friction slope:

$$I_f = f \cdot q |q|, \quad (1)$$

where  $f$  is the friction factor.



The one-dimensional model approximates vertically oriented moment and mass conservation equations (Saint-Venan Equation) based on the following assumptions:

- The water is homogeneous and there are no significant changes in density;
- The slope of the river bed is small;
- The wavelength is longer than the water depth. It can thus be assumed that the watercourse has a direction parallel to the bottom. Vertical acceleration can therefore be neglected and a change in vertical hydrostatic pressure can be accepted;
- The velocity of the water is less than the critical one.

$$\frac{\partial q}{\partial x} + \frac{\partial A_{fl}}{\partial t} = q_{in} \quad (2)$$

$$\frac{\partial q}{\partial t} + \frac{\partial \left( \alpha \frac{q^2}{A_{fl}} \right)}{\partial x} + g A_{fl} \frac{\partial h}{\partial x} + g A_{fl} I_f = \frac{f}{\rho_w}, \quad (3)$$

where  $q$  is discharge

$A_{fl}$  – flow area, also called cross section area

$q_{in}$  – lateral inflow

$h$  – water level

$\alpha$  – momentum distribution coefficient

$I_f$  – flow resistance term, in the form of a friction slope

$f$  – momentum forcing (per length unit)

$\rho_w$  – density of water

Equation (2) is called the mass equation or continuity equation and expresses conservation of mass; the volume of water which is added,  $q$  in reach section of length  $x$  is balanced by an increase in cross section area  $A_{fl}$  (volume).

Equation (3) is called the momentum equation and expresses conservation of momentum; the first two terms on the left side of the momentum equation represent the inertia forces (local and convective acceleration), the third term represents pressure forces due to gravity, and the last term represent resistance/friction. The right-hand side represents an external momentum forcing.

#### Input data

- Model basis

The hydraulic model of the Topolnitzerka River was built on the basis of DEM (digital elevation model), outlined the river bed at the points of the midstream and generated cross sections over 200 m along the river.

- Bed resistance

Manning resistance formula was used, defined as a constant along the river – 0.35.

- Simulation period and time step

Simulation period was divided by two, first simulation period was 01.01.2016 – 31.12.2016 and the second: 01.01.2017 – 31.12.2017.

Time step was calculated by iteration. Hydro-dynamic model was tested with fixed time steps over 10 seconds: 10, 20, 30, 40 and 6 sec. It is found that the highest stability is achieved in a time step of 10 seconds, so the whole model was developed with it.

The software is programmed to store values for water level and discharge every 24 hours of the simulation to obtain daily values.

- Boundary conditions

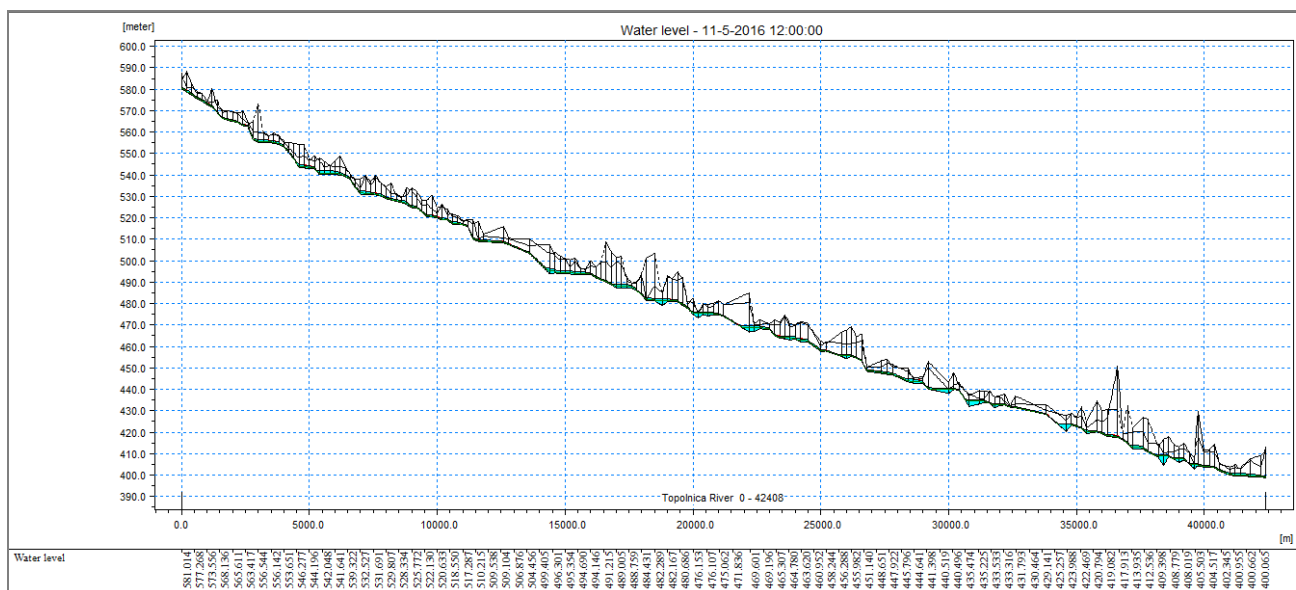
It was defined the discharge at the beginning of the modelled area, discharge after each of the tributaries (Medetska river, Zlatishka river, Vozdol river and Bunovska river), Q-H relation at the last point of the modelled area, before the Topolnitsa dam – Poibrene village. The tributaries at the model are defined as a point sources, because the inflow for simulation period is lower than cross section height. In the end of the river, Q-H relation area is known

### Reliability of the model

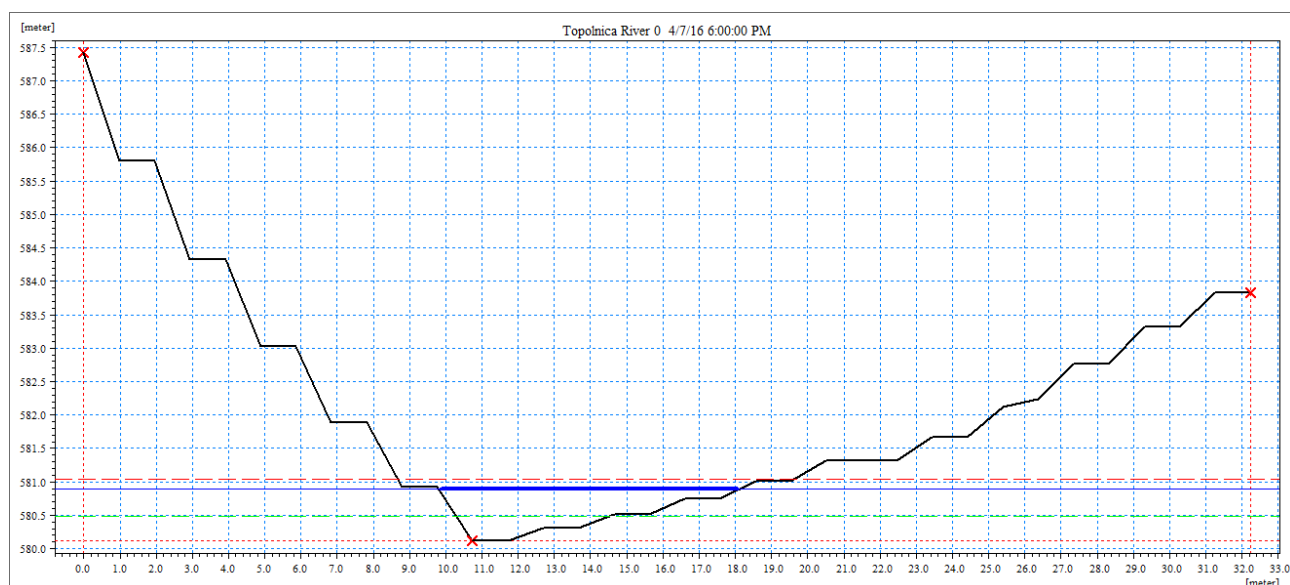
Four criteria were used to verify the efficiency of the model: relative error ( $r$ ), root mean square deviation ( $\sigma$ ), Nash-Sutcliffe coefficient and correlation coefficient ( $R^2$ ) (Bao and Mays, 1990; Dahmardeh et al., 2018). Sensitivity equations are considered, because they give the most accurate results (Kapelan, 2002). Different parameters can give an effect to reliability of a hydraulic model such as vegetation parameters and the root depth as well as empirical parameters influence evapotranspiration, transpiration and recharge, in the unsaturated zone, the type of the soil has an effect on the infiltration/evapotranspiration and recharge functions and at the saturated zone level, the hydraulic conductivity of the matrix represents the dominant parameters (Sandu, M.; Virsta, A., 2015).

## RESULTS AND DISCUSSIONS

The model of the water flow of Topolnitsa river was designed from the outfall of Medetska river to the tail of Topolnitsa dam, near Poibrene village. Results were obtained for discharge and water level in grid 50 x 50 m. Longitudinal profile and cross sections was obtained for every day of the simulation period. (Figure 1 and Figure 2) On the longitudinal profile and cross sections are shown minimum and maximum water level for all period and additional water level at the specific date.



**Figure 2.** Longitudinal profile of Topolnitsa river - from the outfall of Medetska river to the tail of Topolnitsa dam, near Poibrene village



**Figure 3.** Cross section of Topolnitza river – outfall of Medetska river

Based on the last point of the considered section of the river, validation of the model was made. There is hydrometric station near Pibrene village.

The assessment of the reliability of the model is made as a comparison between the observed and prediction data.

Four criteria were used to evaluate efficiency of created model: relative error ( $r$ ), root mean square deviation ( $\sigma$ ), Nash-Sutcliffe coefficient and correlation coefficient ( $R^2$ ).

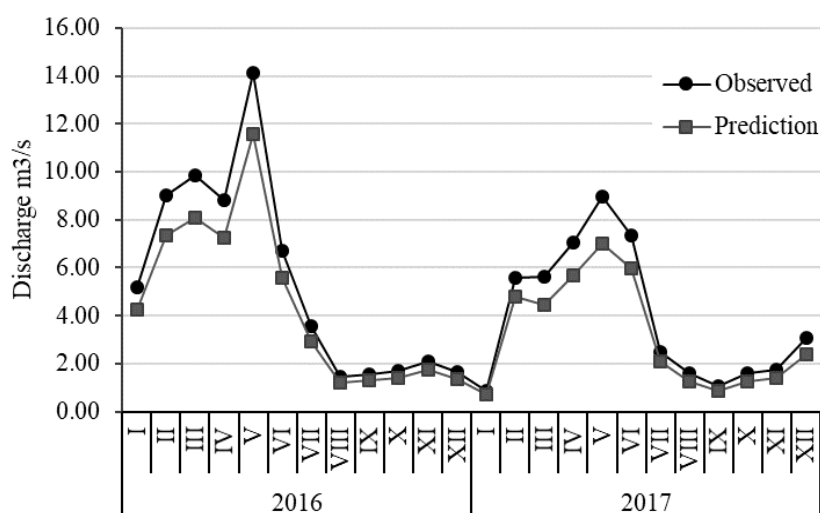
Observed and modeled discharge are present in Table 1 and Figure 4.

The values of the model are lower than observed discharge in the end of the considered section of the river, with average value of relative error 17.66 %. The model does not reflect the effects of rainfall and wind and some of the smaller tributaries of the main river due to lack of such data (Armstrong and Collopy, 1992).

**Table 1.** Discharge value in Topolnitza river, near Poibrene village – observed and prediction. Absolute and relative error

year	month	Observed	Prediction	Absolute error ( $\Delta$ )	Relative error
		Q $m^3/s$	Q $m^3/s$	$m^3/s$	( $r$ ) %
2016	I	5.17	4.50	0.67	13.00
	II	9.00	7.08	1.92	21.33
	III	9.84	7.90	1.94	19.70
	IV	8.81	7.89	0.92	10.43
	V	14.12	10.28	3.84	27.20
	VI	6.72	5.95	0.77	11.45
	VII	3.55	3.02	0.53	14.97
	VIII	1.45	1.43	0.02	1.11
	IX	1.57	1.29	0.28	17.55
	X	1.72	1.45	0.27	15.75

year	month	Observed	Prediction	Absolute error ( $\Delta$ )	Relative error
		Q m <sup>3</sup> /s	Q m <sup>3</sup> /s	m <sup>3</sup> /s	(r) %
2017	XI	2.12	1.66	0.46	21.59
	XII	1.65	1.38	0.27	16.52
	I	0.88	0.70	0.18	20.75
	II	5.56	4.78	0.78	14.07
	III	5.62	4.43	1.20	21.26
	IV	7.07	5.68	1.39	19.71
	V	8.99	7.00	1.99	22.13
	VI	7.33	5.99	1.34	18.32
	VII	2.46	2.10	0.36	14.67
	VIII	1.59	1.27	0.31	19.65
	IX	1.04	0.86	0.18	17.25
	X	1.60	1.24	0.36	22.66
XI	1.76	1.42	0.34	19.38	
XII	3.10	2.38	0.72	23.31	
Average value		<b>4.70</b>	<b>3.82</b>		<b>17.66</b>



**Figure 4.** Discharge in Topolnitza river, near Poibrene village – observed and prediction data

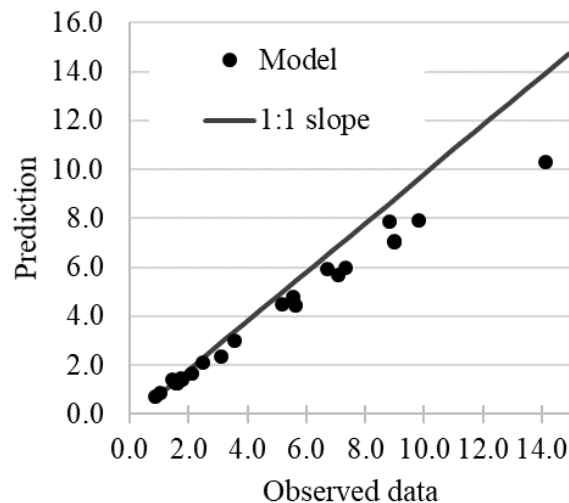
Root mean square error is:

$$\sigma = \sqrt{\frac{\sum_{i=1}^N (Q_{prediction_i} - Q_{observed_i})^2}{N}} = 1,22 \text{ m}^3/\text{s} \quad (4)$$

Nash-Sutcliffe efficiency coefficient is  $NSE=0,904$ , demonstrates the high convergence of the prediction with the observed data (Figure 5).

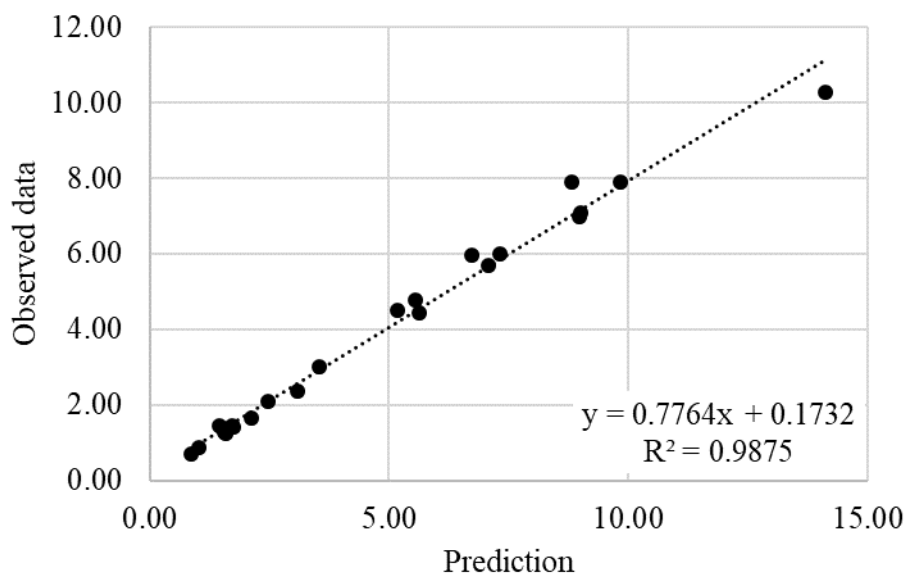
The Nash-Sutcliffe efficiency (NSE) is a normalized statistic that determines the relative magnitude of the residual variance compared to the measured data variance (Nash and Sutcliffe, 1970). Nash-Sutcliffe efficiency indicates how well the plot of observed versus simulated data fits the 1:1 line.  $NSE = 1$ , corresponds to a perfect match of the model to the observed data.  $NSE = 0$ , indicates that

the model predictions are as accurate as the mean of the observed data,  $\text{Inf} < \text{NSE} < 0$ , indicates that the observed mean is a better predictor than the model.



**Figure 5.** Nash Sutcliffe model

The relationship between observed and prediction data can also be described by equation  $y = 0.7764x + 0.1732$  with a correlation coefficient between the coordinates of the observed against the prediction data  $R^2 = 0.9875$ . We can assume that the equation thus obtained gives sufficiently reliable results for each possible value of the actual discharge, relative to the model ones (Figure 6).



**Figure 6.** Data convergence (observed against prediction)

## CONCLUSIONS

Using the Nash-Sutcliffe efficiency coefficient to evaluate the model's performance, a value of 0.904 is obtained, which is evidence of the high reliability of the model data.

Prediction values are lower than the observed once, but they strictly preserve the nature of the observed data. The discrepancy between the actual measured and model data is due to the lack of additional information on precipitation and winds (Figure 4).

The results obtained correspond with the fact, that the river model thus created is sufficiently accurate. Based on this, it is possible to design various tasks related to river hydraulics, water quality, floods and forecasting of different processes. The model is designed to determine the distribution of heavy metals in the river bed in a considered section of river.

## REFERENCES

- Armstrong, J. S., Collopy, F. (1992) Error Measures For Generalizing About Forecasting Methods: Empirical Comparisons. *International Journal of Forecasting*, **8**(1), 69-80.
- Bao, Y., Mays, L. W. (1990) Model for Water Distribution System Reliability. *Journal of Hydraulic Engineering*, **116**.
- Dahmardeh, M., Keshtegar, B., Rajaei M., Kahmmari I. (2018) Evaluation of the plant pattern of intercropping in chemical soil elements using the nonlinear response surface model. *Bulgarian Journal of agricultural science*, **24**(4), 599-610.
- Doulgeris, Ch., Georgiou, P., Papadimos, D., Papamichail, D. (2012) Ecosystem approach to water resources management using the MIKE 11 modeling system in the Strymonas River and Lake Kerkini. *Journal of Environmental Management*, **94**, 132-143.
- Kapelan, Z. (2002) Calibration of water distribution system hydraulic models, University of Exeter. MIKE Hydro River User Guide (2017).
- Nash, J. E., Sutcliffe, J. V. (1970) River Flow Forecasting through Conceptual Model. Part 1—A Discussion of Principles. *Journal of Hydrology*, **10**, 282-290.
- Sandu, M., Virsta, A. (2015) Applicability of MIKE SHE to Simulate Hydrology in Argesel River Catchment. *Agriculture and Agricultural Science Procedia*, **6**, 517-524.
- Varlev, Iv., Petkov, Pl., Tenev, B., Petrova, V., et. al. (1998) Water Quality Protection and Management in the Maritza River Basin Diagnostic Study of the Nature, Magnitude and Sources of Water Pollution in the Basin of Maritza River and its Tributaries”. Ministry of environment and waters, UNDP, Project BUL/94/003, 1996-1999. – 11.

# Evaluation of Migration Potential of Water-Based Paints Used in Flexographic Printing into the Aqueous Environment from Selected Plastics

E. Łaskawiec\*

\* Faculty of Environmental Engineering and Power Engineering, Silesian University of Technology, Konarskiego 18, 44-100 Gliwice, Poland (E-mail: [edyta.laskawiec@gmail.com](mailto:edyta.laskawiec@gmail.com))

## Abstract

In this study, we studied the migration potential of water-based paint components, used in flexographic printing on polyethylene film, into the water environment. We analyzed the changes in physicochemical and phytotoxicological parameters. The tests were conducted in parallel in various water matrices, including deionized water and tap water and under various conditions—lack of lighting, 24-h exposure of samples, and in the laboratory, with naturally variable daily lighting and temperature. We used three types of prints made with water-based paints and one made with solvent-based inks. During the 14-week research, changes in the quality of water matrices in which the film samples were placed were recorded. Total organic carbon gradually increased in the majority of samples during the study period. Most of the samples showed an increase in the amount of phytotoxicity; they demonstrated inhibition rather than a stimulating effect on the growth of plants. In the last week of the study, the fronds demonstrated an increase in the percentage of chlorosis.

## Keywords

Water-based paints; flexographic printing; phytotoxicity; ecotoxicology; water pollutions; total organic carbon

## INTRODUCTION

In search of methods to increase their brand's recognition, the owners of shopping, service, and catering outlets reach out for various methods of promotion. One of the commonly used methods is printing the logo and/or company address on the packaging items (e.g. T-shirt and polyethylene bags). Printing inks are multicomponent mixtures of chemical substances with different physicochemical properties (Gajadhur and Łuszczynska, 2017; Zołek-Tryznowska et al., 2015). Their production is aimed at reducing or completely eliminating the use of polar and toxic organic solvents which are harmful to the environment. Some of the effective work conducted in this regard is the production of, among others, water-based paints. Currently, the most popular printing technology is flexographic printing (Ealer et al., 1990; Liu et al., 2017). The increased consumption of plastic-based packaging materials has resulted in the dramatic increase in the detection of macro- and microplastics in all elements of the natural environment. A large part of them has on its surface varied in terms of type, composition, and technology of printing (Ataeefrad, 2019; Ramirez and Tumolova, 2018; Rentzhong and Fogden, 2005a; Rentzhong and Fogden, 2005b; Rentzhong and Fogden, 2006). Therefore, the aim of this study was to analyze the migration potential and durability of prints made on polyethylene films, as well as to assess the phytotoxicity of the water extracts. This study was conducted at the Faculty of Environmental and Energy Engineering, Poland. This article presents part of the results for the two selected water matrices and samples of prints.

## MATERIALS AND METHODS

In this study, water extracts were prepared from the solutions of matrices and fragments of low-density polyethylene (PE-LD) film with print made using the flexographic technique. Four samples

of overprints (marked with symbols MK, D, AP, and L) were analyzed. Five squares of each research material were prepared, with an area of 9 cm<sup>2</sup> and a thickness of 50 μ (each). Three prints were made with water-based paints (MK, D, and AP), and one was made with solvent-based paints (L). Each of the printed film samples was placed in two matrices: deionized water and tap water, which were in laboratory reactors with a capacity of 150 mL. Furthermore, changes in the values of physicochemical and phytotoxicological parameters were analyzed concerning the lighting conditions of the samples. Each of the samples of imprints in the respective matrices were placed in the following three conditions: (1) in the dark at a constant temperature of 25 °C (symbol: 0 h/day); (2) under natural light conditions and at natural temperature (symbol: natural); and (3) in the laboratory incubator with continuous light (symbol: 24 h/day) and at a constant temperature of 25 °C. Samples for the physicochemical analyses were withdrawn once a week for 14 weeks. Then, the losses (50 mL) were supplemented with a fresh portion of the matrix solution. Simultaneously, samples were withdrawn for phytotoxicological assessment at 6, 10, and 14 weeks from the beginning of analyses.

### **Analysis of carbon compounds**

In this study, we measured the total organic carbon (TOC) in matrices (deionized water and tap water) and sample extracts from polyethylene films based on catalytic oxidation using a TOC-L series analyzer (Shimadzu).

### **Phytotoxicological assessment**

Phytotoxicity of matrices and samples was tested according to the author's method based on the recommendations of the United States Environmental Protection Agency (EPA-712-C-008, 2012). The phytotoxicity of the samples was assessed based on the observation of either stimulation or inhibition of the growth of *Lemna minor* in a 7-day test (from day  $t_1 = 0$  to day  $t_2 = 7$ ) at 23 °C, with an illumination of 25 W (224 lm). The phytotoxic effect (%) was presented in the form of the coefficient of frond growth inhibition ( $IR_f(\%)$ ) (EPA-712-C-008, 2012). The indicator of inhibition of plant growth (phytotoxicity) and growth inhibition coefficient values was positive, whereas the growth stimulation was indicated by negative values. The macroscopic effects of extracts on *L. minor* fronds (chlorosis and necrosis) were analyzed. For this purpose, the classification of plant frond coverage (%) by chlorosis was conducted.

## **RESULTS**

### **The physicochemical analysis**

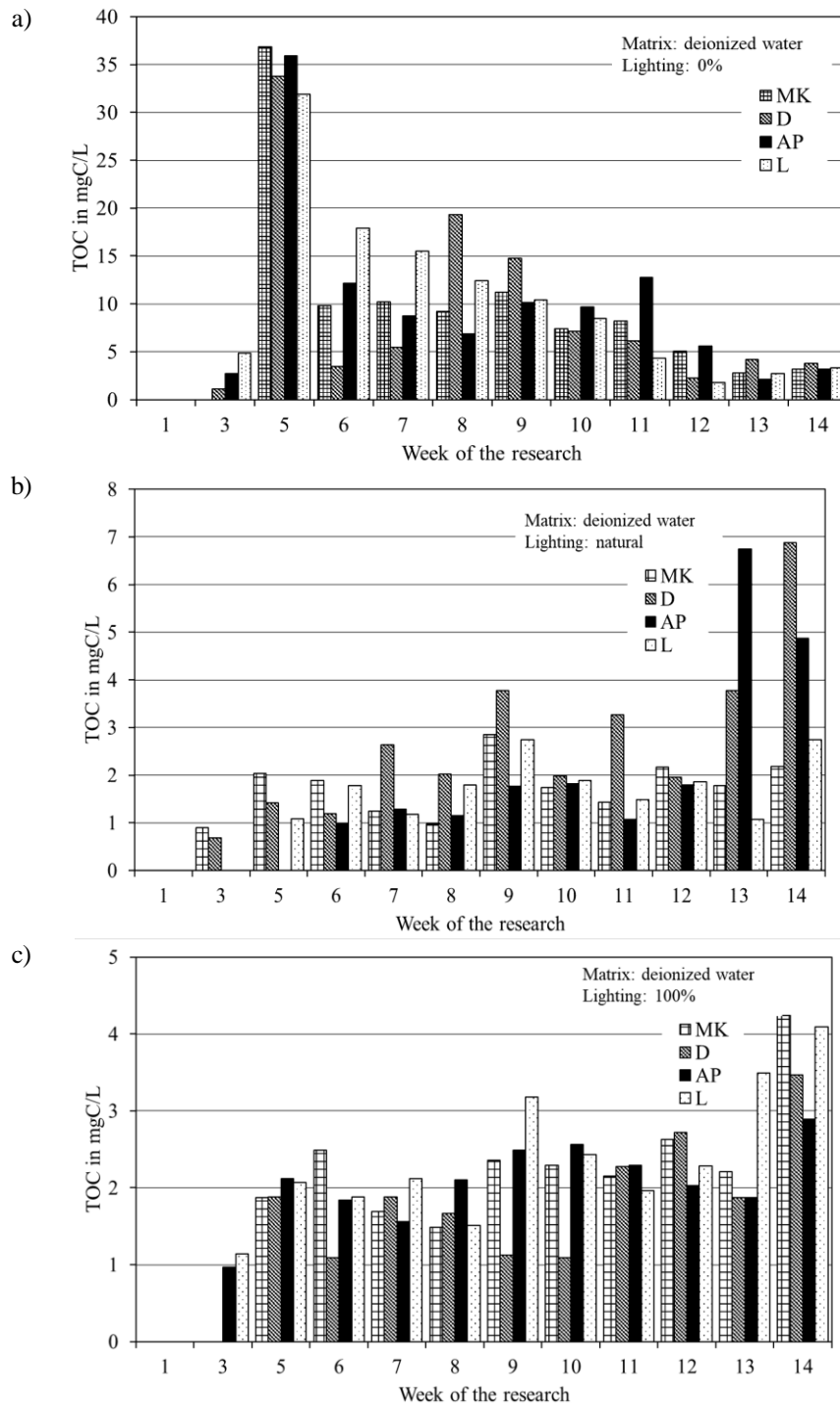
In the case of D samples, the highest level of TOC was recorded at week 14 ((range = 0.00–6.88 mg C/L) (Figure 1b). In the case of MK samples, the highest TOC value was recorded at week 9 (mean ± standard deviation (SD) = 1.60 ± 0.75 mg C/L) (Figure 1b). In the case of AP samples, a gradual increase in the value of TOC was observed during the course of the study, and the maximum value was recorded at week 13 (6.74 mg C/L) (mean ± SD = 1.74 ± 2.03 mg C/L) (Figure 1b). In the case of L samples, the highest TOC value was recorded at weeks 9 and 14 (respectively 2.74 and 2.75 mg C/L) (mean ± SD = 1.47 ± 0.88 mg C/L).

In this study, the high content of carbon compounds was observed in the case of test tubes with deionized water placed in the darkroom (Figure 1a). In the case of L samples, the TOC value was in the range of 0.00–31.89 mg C/L (mean ± SD = 9.46 ± 9.04 mg C/L). In the case of AP samples, the TOC values ranged between 0.00 and 35.89 mg C/L (mean ± SD = 9.16 ± 9.37 mg C/L). In the case of D samples, TOC values ranged between 0.00 and 33.78 mg C/L (mean ± SD = 8.45 ± 9.74 mg C/L). In the case of MK samples, the TOC values ranged between 0.00 and 36.82 mg C/L (mean ± SD = 8.66 ± 9.69 mg C/L). All samples showed the highest TOC values at week 5, and in the



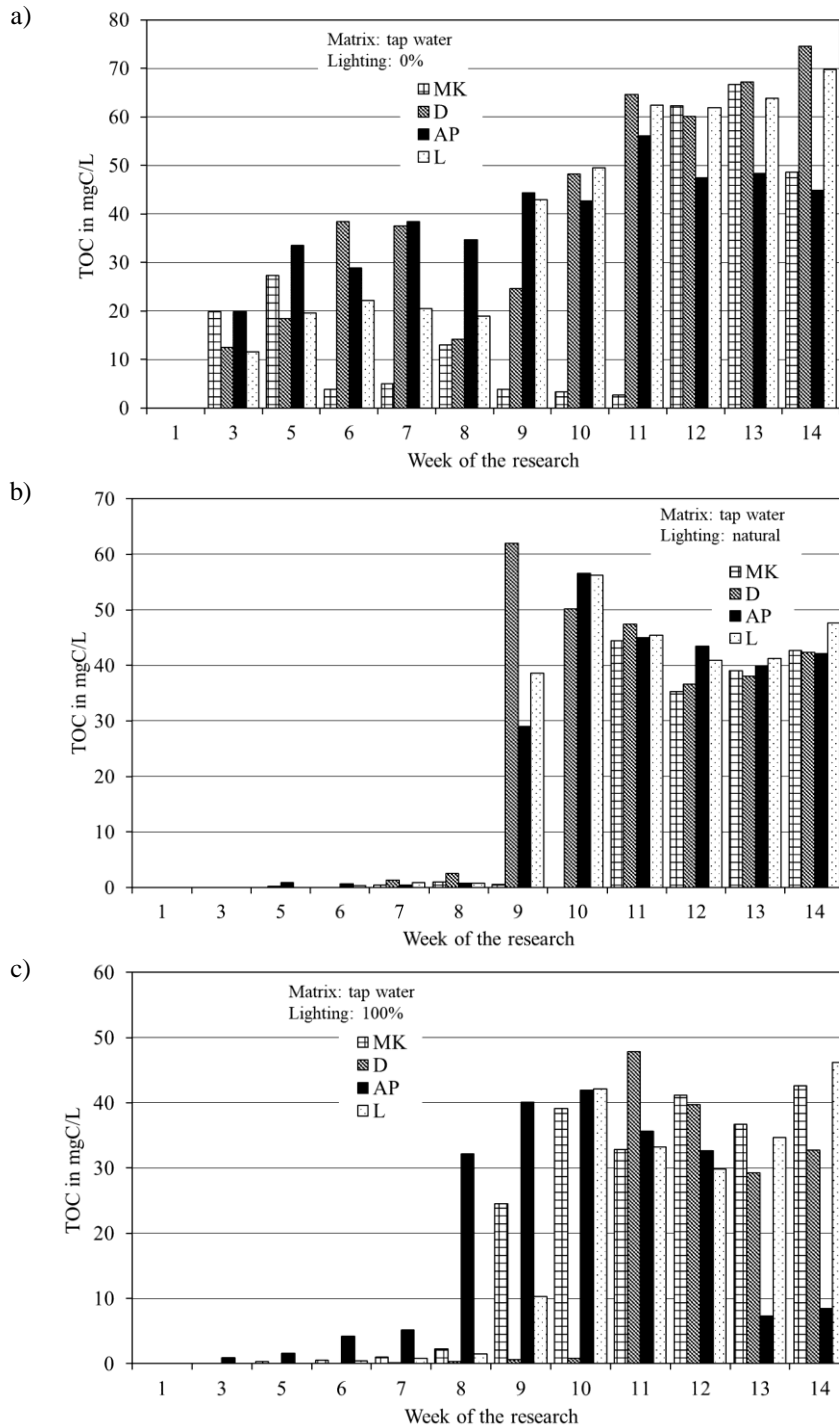
remaining weeks, it was significantly lower (Figure 1a–c), and all samples were characterized by the lack of organic carbon on the first day of testing (0.00 mg C/L).

In the case of samples illuminated continuously (matrix of deionized water), we obtained low values of TOC (Figure 1c). In addition, all samples showed the maximum TOC values at week 14. The TOC values for MK, L, D, and AP samples were 4.24, 4.09, 3.47, and 2.89 mg C/L, respectively. The mean values range between 1.59 and 2.18 mg C/L, with the standard deviation not exceeding 1.14.



**Figure 1.** Changes in total organic carbon (TOC) content in samples placed in deionized water (as a matrix) after illumination: (a) 0 h/day (0 %), (b) natural, and (c) 24 h/day (100 %)

Figure 2a-c shows the results for samples placed in the tap water matrix. In the case of darkroom samples, the highest values of TOC were recorded at weeks 13 and 14 (range = 56.06–74.52 mg C/L) (Figure 2a). The mean  $\pm$  SD values for the MK, D, AP, and L samples were respectively  $21.35 \pm 24.45$ ;  $38.33 \pm 24.69$ ;  $36.58 \pm 15.06$ ; and  $39.91 \pm 24.10$  mg C/L.



**Figure 2.** Changes in the total organic carbon (TOC) content in samples placed in tap water (as a matrix) after illumination: (a) 0 h/day (0 %), (b) natural, and (c) 24 h/day (100 %)

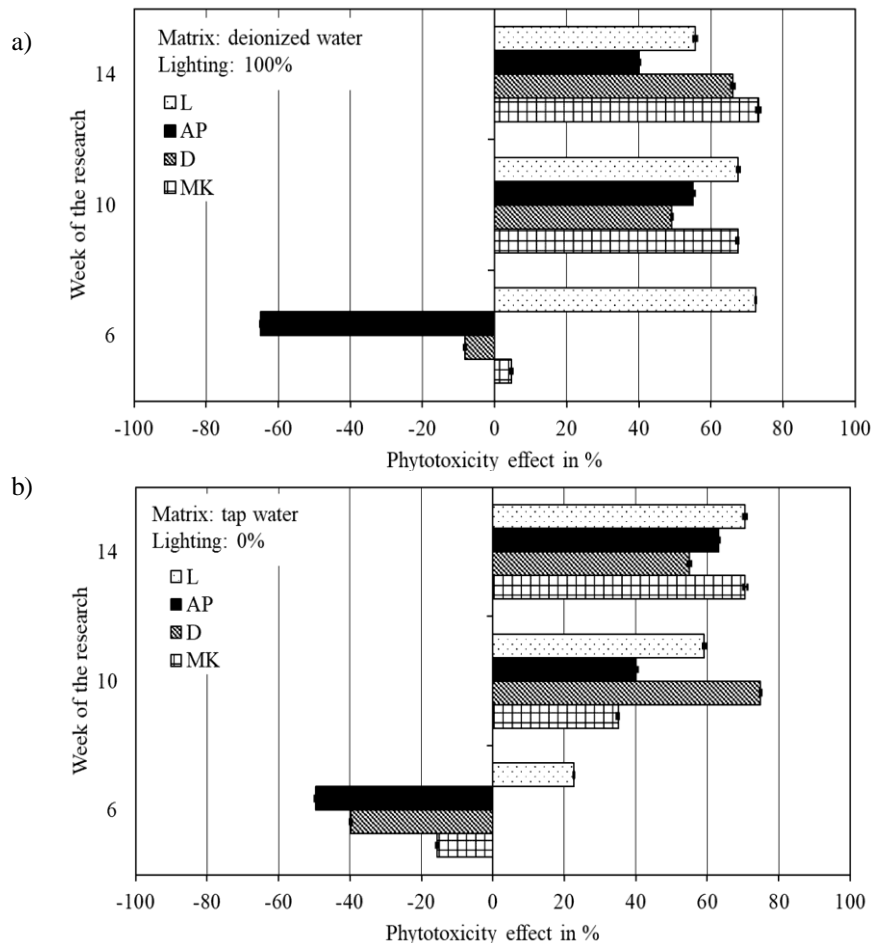
In samples placed under natural conditions, a dramatic increase in the values of TOC was observed after week 8 of research (Figure 2b). In the case of D samples, the maximum TOC value was recorded at week 9 (61.93 mg C/L) (mean  $\pm$  SD =  $23.38 \pm 24.56$  mg C/L). In the case of AP and L samples, the highest values of TOC were 56.54 (mean  $\pm$  SD =  $21.57 \pm 22.84$  mg C/L for AP) and

56.25 mg C/L, respectively (mean  $\pm$  SD = 22.67  $\pm$  23.73 mg C/L).

Lowest values of TOC were recorded in samples illuminated continuously (Figure 2c). In the case of MK samples, the TOC values increased after week 8 of research, and the highest value recorded was 42.58 mg C/L (mean  $\pm$  SD = 18.42  $\pm$  19.07 mg C/L). In the case of AP samples, the increase in the TOC values was also recorded after week 8, and the maximum value (41.91 mg C/L) was recorded at week 10 (mean  $\pm$  SD = 17.50  $\pm$  17.19 mg C/L). In the case of D sample, the maximum TOC was obtained at week 11 (47.82 mg C/L) (mean  $\pm$  SD = 12.62  $\pm$  18.78 mg C/L). In the case of L samples, the maximum TOC value was recorded at week 14 of the study (46.19 mg C/L) (mean  $\pm$  SD = 16.59  $\pm$  18.85 mg C/L).

### The assessment of phytotoxicity

Phytotoxicity of the samples was analyzed based on the growth of *L. minor* (Figure 3a, b). The initial (week 6) stimulation in the growth of *L. minor* was observed in the case of samples MK, D, and AP in tap water matrix, as well as by samples AP and D in the deionized water matrix. At week 6, L samples placed in the deionized water matrix and in the absence of light, L samples under natural conditions, and L samples under constant light showed the inhibition of the growth of fronds (27.92  $\pm$  0.33 %, 8.23  $\pm$  0.29 %, and 72.41  $\pm$  0.10 %, respectively), whereas in the case of L samples placed in the tap water, the inhibition of the growth of fronds was respectively 31.38  $\pm$  0.38 %, 15.53  $\pm$  0.67 %, and 22.65  $\pm$  0.42 %.





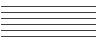

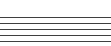










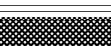





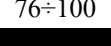





**Figure 3.** Phytotoxicity of printing samples under conditions: (a) matrix: deionized water, lighting: 24 h/day, (b) matrix: tap water, lighting: 0 h/day

At weeks 10 and 14, an increase in the level of phytotoxicity was observed in most samples, with an exception of the L sample. The L sample in the deionized water matrix showed an inhibition of the

growth of fronds by  $55.58 \pm 0.54$  %.

The change in the nature of the extracts from stimulating to the growth-inhibiting fronds and the increase in phytotoxicity resulted in an increase in the incidence of chlorosis. Table 1 shows the percentage of chlorosis based on the phytotoxicological assessment. In order to facilitate fast visualization of test results, a 5-step range of the percentage coverage of fronds was prepared (Table 1). While the maximum chlorosis was recorded for sample MK (matrix tap water) under natural conditions, the degree of coverage of the fronds was  $88.78 \pm 1.05$  %. A high percentage of chlorosis was recorded in extracts from AP and L samples under natural conditions (matrix tap water); the percentage coverage of fronds was  $69.70 \pm 2.05$  % and  $64.38 \pm 1.85$  % respectively. In addition, in the case of sample MK, under continuous lighting (matrix tap water) the coverage of fronds was  $57.88 \pm 1.64$  %.

**Table 1.** The incidence of chlorosis on *Lemna minor* fronds

Coverage of fronds by chlorosis							
Matrix	Sample lighting (%)	Sample	Week of the research				
			6	10	14		
Deionized water	0	MK					
		D					
		AP					
		L					
	Natural	MK					
		D					
		AP					
		L					
	100	D					
		MK					
		AP					
		L					
Tap water	0	MK					
		D					
		AP					
		L					
	Natural	MK					
		D					
		AP					
		L					
	100	MK					
		D					
		AP					
		L					
Coverage in %		> 5	6÷20	21÷50	51÷75	76÷100	
Symbol							

## CONCLUSION

Under the influence of printing components made on polyethylene films, the quality of the tested matrices has changed. The fastest increase in total organic carbon concentration was observed in samples placed in tap water (lighting: 0 hours per day). At this stage of the study, no clear differences were found in the quality of extracts for individual samples.

It is necessary to emphasize the growing phytotoxicity of extracts obtained from printing samples. The speed of this effect was dependent on the matrix, environmental conditions (lighting, temperature) in which the sample was kept and the type of printing itself. Due to the prevalence of printed plastic in the natural environment, further qualitative analyses are necessary, including changes in the structure of materials and prints during exposure to environmental factors.

## ACKNOWLEDGMENTS

The study on the “Assessment of migration of water-based paints used in flexographic printing, to the aqueous environment from selected plastics” was conducted as part of an industrial internship from March to August 2019.

## REFERENCES

- Ataefard, M. (2019) Study of PLA printability with flexography ink: Comparison with common packaging polymer. *Progress in Color, Colorants and Coatings*, **12**(2), 101-105.
- Ealer, G. E., Harris, W. C., Samuels, S. B. (1990) Characterization of surface-treated polyethylene for water-based ink printability. *Journal of Plastic Film & Sheeting*, **6**(1), 17-30.
- Gajadhur, M., Łuszczynska, A. (2017) Influence of pearlescent pigments on light-fastness of water-based flexographic inks. *Dyes and Pigments*, **138**, 119-128.
- Liu, B., Lin, M., Hu, G., Lin, M. (2017) Study on color matching technology of flexographic printing ink, **417**, 91-97.
- Ramirez, J. C. C., Tumolva, T. P. (2018) Analysis and optimization of water-based printing ink formulations for polyethylene films. *Applied Adhesion Science*, **6**(1), 1.
- Rentzhog, M., Fogden, A. (2005) Rheology and surface tension of water-based flexographic inks and implications for wetting of PE-coated board. *Nordic Pulp and Paper Research Journal*, **20**(4), 399-409.
- Rentzhog, M., Fogden, A. (2005) Influence of formulation and properties of water-based flexographic inks on printing performance for PE-coated board. *Nordic Pulp and Paper Research Journal*, **20**(4), 410-417.
- Rentzhog, M., Fogden, A. (2006) Correlations between properties of water-based flexographic inks and their print uniformity on PE-coated board. *Nordic Pulp and Paper Research Journal*, **21**(3), 403-410.
- United States Environmental Protection Agency (2012) Ecological Effects Test Guidelines OCSPP 850.4400: Aquatic Plant Toxicity Test Using Lemna spp., EPA-712-C-008.
- Zołek-Tryznowska, Z., Izdebska, J., Tryznowski, M. (2015) Branched polyglycerols as performance additives for water-based flexographic printing inks. *Progress in Organic Coatings*, **78**, 334-339.

## Concentrations of Emerging Organic Contaminants in Swimming Pools

A. Lempart\*, E. Kudlek\* and M. Dudziak\*

\* Silesian University Technology, Institute of Water and Wastewater Engineering, ul. Konarskiego 18a, 44-100 Gliwice, Poland (E-mail: [anna.lempart@polsl.pl](mailto:anna.lempart@polsl.pl))

### Abstract

Concentration levels of ten Emerging Organic Contaminants (EOCs), including ibuprofen, N-Butylbenzenesulfonamide, nonylphenol, caffeine, butylated hydroxytoluene, diclofenac, pentachlorophenol, triclosan, triallate and benzocaine was investigated in fifty Polish swimming pools located in Silesia. The occurrence of butylated hydroxytoluene (BHT), pentachlorophenol (PCP), triallate (TRI) and N-butylbenzenesulfonamide (BMB) has not been studied so far in swimming pools by other researchers. Samples were analysed by Gas Chromatograph coupled to Mass Spectrometry (GC/MS) with Electronic Ionization, after solid phase extraction (SPE). In general, measured concentrations were in accordance with the reports in the available literature. Human Risk Assessment show negligible risks for swimmers of any age or sex, considering both the exposure to each single contaminant and the co-exposure to all contaminants. No significant correlations were observed between physical-chemical parameters of pool water with the investigated EOCs.

### Keywords

Swimming pools; micropollutants; emerging organic contaminants

## INTRODUCTION

The dynamic development of analytical techniques, which nowadays enable the identification of micropollutants in trace concentrations, causes the growing concern about the presence of Emerging Organic Contaminants (EOCs) in water environment. They may have adverse effects on both human health and aquatic ecosystems, as some of them are biologically active even in low-dose exposure. There is a threat of hormonal imbalance, leading e.g. to feminization in animals (Filali-Meknassi et al., 2004). Numerous studies have shown a broad range of chemicals that have been detected globally in various aquatic environments – wastewater, drinking water, ground water, surface water. The mentioned aquatic environments are well described, however there is a need to expand the scope of research on swimming pool water, as swimmers may be exposed to three routes of exposure: accidental ingestion, inhalation and dermal absorption. Meanwhile, the assessment of anthropogenic organic micropollutants occurrence in this specific environment is not obligatory according to the applicable regulations. Thus, information on the presence of these compounds in swimming pools is very limited. Weng et al. (2014) studied 32 pharmaceuticals and personal care products (PPCPs) in three swimming pools in USA and detected three of them: N, N-diethylm-toluamide (DEET), caffeine, and tri(2-chloroethyl)-phosphate (TCEP). Li et al. (2015) investigated the occurrence of eight parabens, four chlorinated parabens, and their common hydrolysis product, phydroxybenzoic acid (PHBA), in 39 swimming pools in Beijing, China. Ekowati et al. (2016) focused on 32 pharmaceuticals and 14 UV filters in the waters of 17 swimming pools in Catalonia, Spain. In Australia, Teo et al. (2016a) investigated the occurrence and daily variability of 30 pharmaceuticals and personal care products in 15 public pools, where only ibuprofen and caffeine were above the limit of quantification. Teo et al. (2016b) also studied the presence of five organophosphate flame retardants in 15 public swimming pools. Suppes et al. (2017) explores 24 PPCPs contamination risk factors and identifies contamination sources in water samples collected

from 31 swimming pools in eastern Minnesota and western Wisconsin. Fantuzzi et al. (2018) investigated the occurrence of illicit drugs (cocaine, opioids, amphetamines and cannabis derivatives), some of their metabolites and 48 pharmaceuticals in ten Italian indoor swimming pools.

The aim of the research was to quantify the actual concentrations of organic micropollutants in fifty swimming pools located in Silesia, Poland and to assess the human risk related to ingestion of water during swimming. Previous authors' study (Lempart et al., 2019) showed that from among 26 tested compounds, the most commonly occurred in tested swimming pools (>50 % frequency of occurrence) are ibuprofen, N-Butylbenzenesulfonamide, nonylphenol, caffeine, butylated hydroxytoluene, diclofenac, pentachlorophenol, triclosan, triallate and benzocaine. In the study presented in this paper authors focused on the concentrations of these compounds. Of them, the occurrence of butylated hydroxytoluene (BHT), pentachlorophenol (PCP), triallate (TRI) and N-butylbenzenesulfonamide (BMB) has not been studied so far in swimming pools by other researchers.

## MATERIALS AND METHODS

**Materials and reagents.** The standards of target compounds (Table 1) of purity grade >98 % were supplied by Sigma-Aldrich. Organic solvents: methanol and acetonitrile of purity grade >99.8 % and >99.5 %, respectively, by Avantor Performance Materials Poland S.A. were also used. Disposable Supelclean™ ENVI™-18 Tubes packed with octadecyl bed of 1.0 g by Supelco were applied to solid phase extraction. Bottles made of chemically and biologically inert borosilicate glass, were used for the collection, transport and storage of collected water samples. The tested water samples were carefully transported in the refrigerator and protected against the light in order to minimize any possible changes in its composition.

**Table 1.** Properties of the studied organic micropollutants

Compound	Abbreviation	Molecular formula	Molecular weight [g·mol <sup>-1</sup> ]	CAS Number
Ibuprofen	IBU	C <sub>13</sub> H <sub>18</sub> O <sub>2</sub>	206.28	15687-27-1
N-Butylbenzenesulfonamide	BMB	C <sub>10</sub> H <sub>15</sub> NO <sub>2</sub> S	213.30	3622-84-2
Nonylphenol	NP	C <sub>15</sub> H <sub>24</sub> O	220.35	84852-15-3
Caffeine	CAF	C <sub>8</sub> H <sub>10</sub> N <sub>4</sub> O <sub>2</sub>	194.19	58-08-2
Butylated hydroxytoluene	BHT	C <sub>15</sub> H <sub>24</sub> O	220.35	128-37-0
Diclofenac	DCL	C <sub>14</sub> H <sub>9</sub> Cl <sub>2</sub> NO	278.13	15307-86-5
Pentachlorophenol	PCP	C <sub>6</sub> Cl <sub>5</sub> OH	266.34	87-86-5
Triclosan	TRC	C <sub>12</sub> H <sub>7</sub> Cl <sub>3</sub> O <sub>2</sub>	289.54	3380-34-5
Triallate	TRI	C <sub>10</sub> H <sub>16</sub> Cl <sub>3</sub> NOS	304.7	2303-17-5
Benzocaine	BZC	C <sub>9</sub> H <sub>11</sub> NO <sub>2</sub>	165.19	94-09-7

*Sample collection.* Sampling took place in accordance with the guidelines of the Polish standard PN-ISO 5667-5:2003. Samples of swimming pool water were taken from a depth of about 30 cm below the water surface. Authors, in accordance with the conclusions from previous studies, took samples at several characteristic basin points and used a mixed sample for analysis (Wyczarska-Kokot et al., 2017). Each sample was analysed 5 times and the presented results are the average values of these repetitions. Standard deviations of repetitions did not exceeded 5 percentage, what indicates the high repeatability of results. Samples have been collected from 50 different swimming pools located in Silesia (Southern Poland), including publics and privates, outdoors and indoors, sports basins, hot tubes, water slides, paddling pools and recreational pools. All of the tested pools were disinfected with sodium hypochlorite. To support disinfection, UV lamps were used in 21 of tested swimming pools, ozone was applied in 4 cases. Vacuum filters with diatomaceous bed were used in 4 locations, pressure sand filters with layer of hydro-anthracite in 26 pools, the other 20 were equipped with pressure sand filters.

*Analysis of swimming pool water physico-chemical parameters.* The pH of water, redox and temperature were measured by the use of Multifunction Meter CX-461 by ELMETRON (Zabrze, Poland). Concentrations of free, total and combined chlorine were determined by portable Pocket Colorimeter II Device™, (Hach®, Loveland, CO, USA). Total organic carbon was measured by the use of TOC-L Analyzer, Shimadzu), the absorbance in wavelength 254 nm with an optical path length of 1 cm by UV-VIS Cecil 1000 (Analytik Jena AG).

*Analytical procedure for determination of micropollutants.* Due to the lack of reference methods for the determination of micropollutants in the swimming pool water environment, authors have developed their own procedure, based on the method presented in paper (Lempart et al., 2018). It enables the quantitative determination of trace contaminants with satisfactory repeatability and accuracy, which guarantees full quantitative control of selected compounds in samples from swimming pools. The isolation of micropollutants from swimming pool water matrix was carried out by solid phase extraction (SPE) in Supelclean™ ENVI-18 tubes. The bed was firstly conditioned in sequence with 5 mL of methanol and 5 mL of acetonitrile. Then it was washed with 5 mL of deionized water. Afterwards 1 L of water sample was applied. To ensure optimal retention, extraction was carried at a consistent and reduced flow rate of ~1-2 drops/second. After extraction the bed was dried for 5 min under vacuum. The extracts were analysed using a Gas Chromatograph coupled to Mass Spectrometry (GC/MS) with Electronic Ionization, model 7890B by Perlan Technologies. The extract was separated in a SLBTM - 5 ms Capillary GC Column of Supelco with an internal diameter of 0.25 mm, a length of 30 m and a layer thickness of 0.25 µm. The oven temperature program was as follows: 80 °C (6 min), 5 °C/min to 260 °C, 20 °C/min to 300 °C. The support phase was helium with a flow of 1.1 mL/min. Sample injections of 1 µl were performed automatically. The mass detector operated in the total ion current (TIC) mode in the range of 50 to 700 m/s. Quantification was done by interpretation of the mass spectra obtained by chromatographic analysis using the NIST v17 Mass Spectral Library and comparing the response of the mass detector with the standards response. To identify the compounds, also the retention times were compared with reference standards. The detection limits (LOD) and quantification limits (LOQ) were calculated from chromatograms of swimming pool samples; the LOD was the concentration with a signal/noise ratio of 3 and the LOQ was the concentration with a signal/noise ratio of 10. The main performance parameters of the method are reported in Table 2.



**Table 2.** Analytical performance of the method and parameters used for quantification

Compound	Linearity range [ $\mu\text{g}\cdot\text{L}^{-1}$ ]	Correlation coefficient $R^2$	Recovery $\pm$ SD [%]	LOD [ $\text{ng}\cdot\text{L}^{-1}$ ]	LOQ [ $\text{ng}\cdot\text{L}^{-1}$ ]
IBU	0-100	0.9904	$86 \pm 3.9$	1.13	3.19
BMB	0-100	0.9975	$92 \pm 4.1$	0.84	1.20
NP	0-100	0.9993	$88 \pm 4.4$	0.08	0.23
CAF	0-100	0.9994	$100 \pm 4.2$	0.02	0.84
BHT	0-100	0.0991	$96 \pm 3.8$	0.02	0.11
DCL	0-100	0.9983	$84 \pm 3.2$	0.07	0.23
PCP	0-100	0.9923	$98 \pm 1.2$	0.06	0.15
TRC	0-100	0.9948	$95 \pm 2.9$	0.23	0.41
TRI	0-100	0.9996	$89 \pm 4.4$	0.04	0.37
BZC	0-100	0.9929	$100 \pm 1.8$	0.44	0.75

*Human Risk Assessment.* Human Risk Assessment (HRA) was conducted based on the methodology by Fantuzzi et al. (2018), considering both the exposure to each single contaminant and the co-exposure to all contaminants. Concentrations were compared with Drinking Water Guideline Levels (DWGLs). The worst case scenario was designed taking the maximum concentration of each contaminant measured in waters and assuming that the subjects swam daily. The ratios between the concentrations measured and the DWGLs are called Hazard Quotients (HQs). HRA assessed for co-exposure to all contaminants was measured following the Hazard Index (HI) approach, in which the HQs of single contaminants are summed to obtain a single risk value.

## RESULTS AND DISCUSSION

Physical and chemical parameters were mostly in line with the requirements for swimming pools. Average pH was  $7.2 \pm 0.4$ , potential of redox  $784 \pm 22$ , water temperature  $28.7 \pm 0.3$  °C. Combined chlorine concentrations sometimes exceeded the limit values, even considerably. New requirements in this area (max  $0.3 \text{ mg}\cdot\text{L}^{-1}$ ) have been in force in Poland since 2015 and many swimming pools have a problem with their adaptation. Free chlorine ranged from 0.5 to  $1.0 \text{ mg}\cdot\text{L}^{-1}$ . Cases of exceeding the limit values resulted from intentional water “shock chlorination”. The correct application of this procedure leads to the oxidation of chloramines, which cause the excess of combined chlorine content. The average free chlorine concentration was  $0.5 \pm 0.1$ . Table 3 reports the results of quantitative research on EOCs in swimming pools.

**Table 3.** Concentrations of Emerging Organic Contaminants in fifty tested swimming pools

Compound	Frequency of identification (Lempart et al., 2019)	Mean $\pm$ SD [ng·L <sup>-1</sup> ]	Range [ng·L <sup>-1</sup> ]
IBU	48/50	139.9 $\pm$ 2.4	4.4 $\div$ 420.6
BMB	43/50	727.1 $\pm$ 10.1	185.0 $\div$ 2388.0
NP	40/50	0.8 $\pm$ 0.1	0.4 $\div$ 1.8
CAF	39/50	16.8 $\pm$ 0.8	3.6 $\div$ 1943
BHT	37/50	4.6 $\pm$ 0.2	0.2 $\div$ 54.7
DCL	36/50	0.4 $\pm$ 0.1	0.3 $\pm$ 1.5
PCP	36/50	7.3 $\pm$ 0.3	0.2 $\div$ 10.0
TRC	31/50	3.9 $\pm$ 0.2	0.4 $\div$ 11.1
TRI	30/50	0.6 $\pm$ 0.1	0.4 $\div$ 0.8
BZC	26/50	1.6 $\pm$ 0.1	0.8 $\div$ 3.7

In general, these concentrations are in accordance with the reported in the literature. Teo et al. (2016) detected IBU at concentration levels 16 $\div$ 83 ng·L<sup>-1</sup>, Ekowati et al. (2016) measured 16.27 $\div$ 171.25 ng·L<sup>-1</sup>. Weng et al. (2014) reported CAF in range about 30 $\div$ 500 ng·L<sup>-1</sup>, Teo et al. (2015) up to 1540 ng·L<sup>-1</sup>, depending on the time of the day. Caffeine concentration were significantly lower in outdoors than indoors, Teo et al (2015) noted CAF below ng·L<sup>-1</sup> in all of the outdoor pools, what is in line with the fact that CAF undergo slow photodegradation with half-lives of roughly 12 days under sunlight (Buerge et al. 2003; Zhang et al. 2013) and is highly stable during chlorination (Glassmeyer and Shoemaker, 2005; Weng et al., 2014). Thus, a possible reason for these differences between outdoors and indoors in concentration levels could be due to the outdoor pools exposure to sunlight. Nonylphenol was analysed by both Teo et al. (2015) and Weng et al. (2014), but it was not observed over limit of quantification, that was equal to 10 ng·L<sup>-1</sup> in study by Teo et al. and 100 $\div$ 200 ng·L<sup>-1</sup> by Weng et al. However, Suppes et al. (2017) reported NP presence in 10 out of 31 tested swimming pools in Midwestern USA. Similarly, diclofenac was tested and not reported >LOQ by Ekowati et al., 2016 (LOQ= ng·L<sup>-1</sup>) and Weng et al., 2014 (LOQ=3 $\div$ 60 ng·L<sup>-1</sup>), but Suppes et al. (2017) observed it in 48 % of tested swimming pools. Triclosan has been studied by Teo et al. (2015), Suppes et al. (2017) and Weng et al. (2014) and was not observed in any studied pool. Canosa et al. (2005) showed the co-existence of important concentrations of triclosan and its most degradation by-products (2,4-dichlorophenol and 2,4,6-trichlorophenol), reinforcing the potential occurrence of its transformations when products containing triclosan are mixed with chlorinated water. The concentrations of N-butylbenzenesulfonamide (BMB), butylated hydroxytoluene (BHT), triallate (TRI) and pentachlorophenol (PCP) in swimming pools has not been studied so far. As the use and sale of PCP has been restricted, its presence in swimming pool water may be a bit surprising, however it may be formed as a by-product in the chlorination of water (Czaplicka et al., 2004; Canosa et al., 2005). Triallate is the only of the tested compounds without ring structure but contains chlorine molecules in its structure itself, what may indicate that

it was formed as a by-product of the decomposition of another substance (ring breakdown + chlorine molecule joining).

No significant correlations were observed between physical-chemical parameters of swimming pool water with the EOCs investigated in the presented paper. However, it was observed that when hydro-anthracite were used as additional filtration bed layer, EOCs levels were lower than in pools where only sand was used. This is consistent with the research conducted by Fantuzzi et al. (2018). Significant differences were also noted for application of any method supporting water disinfection, both ozonation or UV lamp. They effectively reduced the measured concentrations. However, the analysis of post-processed water solutions in research (Kudlek, 2018) pointed that both UV irradiation and ozonation cause formation of intermediates, that may remain endocrine disrupting compounds.

**Table 4.** Human Risk Assessment

<b>Gender</b>		<b>Male</b>			<b>Female</b>	
<b>Age</b>	3 years	14 years	Adult	3 years	14 years	Adult
<b>Weight* [kg]</b>	15	55	70	15	54	55
<b>Water swallowed** [L]</b>	0.045	0.045	0.022	0.030	0.030	0.012
<b>Compound</b>	<b>Hazard Quotients</b>					
IBU	<0.001	<0.001	<0.001	<0.001	<0.001	<0.001
BMB	<0.001	<0.001	<0.001	<0.001	<0.001	<0.001
NP	<0.001	<0.001	<0.001	<0.001	<0.001	<0.001
CAF	<0.001	<0.001	<0.001	<0.001	<0.001	<0.001
BHT	<0.001	<0.001	<0.001	<0.001	<0.001	<0.001
DCL	<0.001	<0.001	<0.001	<0.001	<0.001	<0.001
PCP	<0.001	<0.001	<0.001	<0.001	<0.001	<0.001
TRC	<0.001	<0.001	<0.001	<0.001	<0.001	<0.001
TRI	<0.001	<0.001	<0.001	<0.001	<0.001	<0.001
BZC	<0.001	<0.001	<0.001	<0.001	<0.001	<0.001
<b>Hazard Index</b>	<1.0	<1.0	<1.0	<1.0	<1.0	<1.0

\* According to Cacciari et al. (2006) considering the 50<sup>th</sup> percentile;

\*\*According to Dufour et al. (2006) considering average amount.

Human Risk Assessment for the single substances and for co-exposure show negligible risks for swimmers of any age or sex (Table 4), as HQs were below 0.001 and the cumulative risk calculated as HIs were below 1. However, it is not allowed to disregard the occurrence of micro-pollutants in

swimming pools. These compounds and their impact on human health are not yet well known, moreover they can be precursors of very dangerous disinfection by-products (DBPs).

## CONCLUSIONS

This study demonstrated the environmental concentrations of emerging organic contaminants of several categories in Polish swimming pool waters at levels up to the hundreds of  $\text{ng}\cdot\text{L}^{-1}$ . The highest concentration was reported for N-Butylbenzenesulfonamide, a compound that is widely used as a plasticizer. In general, concentrations were in accordance with the reports in the available literature. The human risk assessment indicated that the health risk from exposure to tested compounds in swimming pools is generally low. However, further research is needed to check effects of the disinfection.

## ACKNOWLEDGMENT

This work was supported by National Science Centre of Poland (No. 2018/29/N/ST8/01352).

## REFERENCES

- Buerge, I. J., Poiger, T., Müller, M. D., Buser, H. R. (2003) Caffeine, an anthropogenic marker for wastewater contamination of surface waters. *Environ. Sci. Technol.*, **37**(4), 691-700.
- Canosa, P., Morales, S., Rodríguez, I., Rubí, E., Cela, R., Gómez, M. (2005) Aquatic degradation of triclosan and formation of toxic chlorophenols in presence of low concentrations of free chlorine. *Anal. Bioanal. Chem.*, **383**(7-8), 1119-1126.
- Cacciari, E., Milani, S., Balsamo, A., Spada, E., Bona, G., Cavallo, L., Cerutti, F., Gargantini, L., Greggio, N., Tonini, G., Cicognani, A. (2006) Italian cross-sectional growth charts for height, weight and bmi (2 To 20 Yr). *J. Endocrinol. Investig.*, **29** (7), 579-580.
- Czaplicka, M. (2004) Sources and transformations of chlorophenols in the natural environment. *Sci. Tot. Environ.*, **322**, 21-39.
- Dufour, A. P., Evans, O., Behymer, T. D., Cantú, R. (2006) Water ingestion during swimming activities in a pool: a pilot study. *J. Water Health*, **4**(4), 425-430.
- Ekowati, Y., Buttiglieri, G., Ferrero, G., Valle-Sistac, J., Diaz-Cruz, M. S., Barceló, D., Petrovic, M., Villagrasa, M., Kennedy, M. D., Rodríguez-Roda, I. (2016) Occurrence of pharmaceuticals and UV filters in swimming pools and spas. *Environ. Sci. Pollut. Res. Int.*, **23**, 14431-14441.
- Fantuzzi, G., Aggazzotti, G., Righi, E., Predieri, G., Castiglioni, S., Riva, F., Zuccatob, E. (2018) Illicit drugs and pharmaceuticals in swimming pool waters. *Sci. Total Environ.*, **635**, 956-963.
- Filali-Meknassi, Y., Tyagi, R. D., Surampalli, R. Y., Barata, C., Riva, M. C. (2004) Endocrine-disrupting compounds in wastewater, sludge-treatment processes, and receiving waters: overview. *J. Hazard. Toxic Radioact. Waste*, **8**, 39-56.
- Glassmeyer, S., Shoemaker, J. (2005) Effects of chlorination on the persistence of pharmaceuticals in the environment. *Bull. Environ. Contam. Toxicol.*, **74**(1), 24-31.
- Kudlek, E. (2018) Decomposition of contaminants of emerging concern in advanced oxidation processes. *Water*, **10**, 955.
- Lempart, A., Kudlek, E., Dudziak, M. (2018) Determination of micropollutants in water samples from swimming pool systems. *Water*, **10**, 1083-1093.
- Lempart, A., Kudlek, E., Dudziak, M. (2019) Identification of micropollutants occurring in swimming pools. *Proceedings*, **16**(1), 25.
- Li, W., Shi, Y., Liu, G. (2015) Occurrence and human exposure of parabens and their chlorinated derivatives in swimming pools. *Environ Sci Pollut Res.*, **22**, 17987-17997.
- Suppes, L. M., Huang, C. H., Lee, W. N., Brockman, K. J. (2017) Sources of pharmaceuticals and

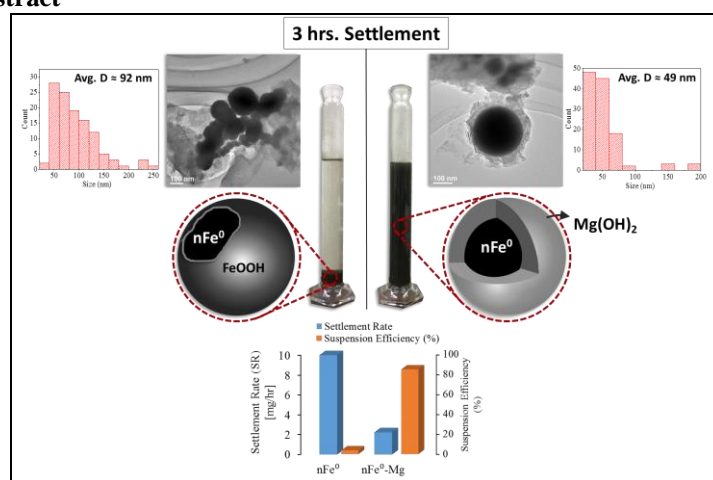
- personal care products in swimming pools. *J. Water Health.*, **15**, 829-833.
- Teo, T. L., Coleman, H. M., Khan, S. J. (2016) Occurrence and daily variability of pharmaceuticals and personal care products in swimming pools. *Environ Sci Pollut Res Int.*, **23**, 6972-6981.
- Teo, T. L., Coleman, H. M., Khan, S. J. (2016) Presence and select determinants of organophosphate flame retardants in public swimming pools. *Sci. Total Environ.*, **569-570**, 469-475.
- Weng, S. C., Sun, P., Ben, W., Huang, C. H., Lee, L. T., Blatchely, E. R. (2014) The Presence of Pharmaceuticals and Personal Care Products in Swimming Pools. *Environ. Sci. Technol. Lett.*, **1**, 495-498.
- Wyczarska-Kokot, J., Lempart, A., Dudziak, M. (2017) Chlorine contamination in different points of pool - risk analysis for bathers' health. *Ecol. Chem. Eng. A*, **24**, 217-226.
- Zhang, D. Q., Hua, T., Gersberg, R. M., Zhu, J., Ng, W. J., Tan, S. K. (2013) Fate of caffeine in mesocosms wetland planted with *Scirpus validus*. *Chemosphere*, **90**(4), 1568-1572.

# Stimulating Effect of Magnesium Hydroxide on Aqueous Characteristics of Iron Nanocomposites

I. Maamoun\*, O. Eljamal\*, O. A. Falyouna\*, R. Eljamal\* and Y. Sugihara\*

\* Department of Earth System Science and Technology, Interdisciplinary Graduate School of Engineering Sciences, Kyushu University, Fukuoka, Japan (E-mails: [ibrahim-maamoun@kyudai.jp](mailto:ibrahim-maamoun@kyudai.jp); [osama-eljamal@kyudai.jp](mailto:osama-eljamal@kyudai.jp); [omarali92@hotmail.com](mailto:omarali92@hotmail.com); [ramadaneljamal54@gmail.com](mailto:ramadaneljamal54@gmail.com); [sugihara@esst.kyushu-u.ac.jp](mailto:sugihara@esst.kyushu-u.ac.jp))

## Graphical Abstract



## Abstract

There is no longer doubt that nanoscale zero-valent iron (nFe<sup>0</sup>) is one of the most promising materials in environmental remediation technologies. Iron nanoparticles were modified by magnesium hydroxide (Mg(OH)<sub>2</sub>) addition with different mass ratios in order to form a nanocomposite with superior aqueous characteristics. Optimization process of the iron-magnesium nanocomposite (nFe<sup>0</sup>-Mg) was conducted through different approaches including; settlement tests, morphology and crystallinity investigations and particle size estimation. The addition of Mg(OH)<sub>2</sub> to nFe<sup>0</sup> with coating ratio of (Mg/Fe: 100 %) resulted in stimulated stability of the particles in aqueous suspension with lower settlement rate than that of unmodified iron particles. Transmission electron microscopy (TEM) and X-ray diffraction (XRD) analyses showed obvious enhanced features of the modified nFe<sup>0</sup> particles in terms of structure stability and degree of crystallinity respectively. Anti-aggregation effect was achieved corresponding to the smaller average particle size of the nFe<sup>0</sup>-Mg particles which was confirmed by the morphological observation. Additionally, the iron core of the synthesized nFe<sup>0</sup> was adequately protected from aqueous corrosion with lower iron oxides leachates after the optimal modification with Mg(OH)<sub>2</sub>. The current work suggests the potential applicability of the proposed iron-based nanocomposites towards sustainable effectiveness in water treatment applications.

## Keywords

Iron nanocomposites; magnesium hydroxide; crystallinity; aqueous characteristics

## INTRODUCTION

Nanotechnology has been emerged recently in several environmental remediation aspects owing to the excellent functional characteristics of the nanomaterials (Ghasemzadeh, 2014; Zhao, 2016). Nanoscale zero valent iron (nFe<sup>0</sup>) is one of the most commonly used nanomaterials in water treatment applications during the last two decades. Owing to its particular core-shell structure in

addition to the dual redox potential,  $n\text{Fe}^0$  has the ability to react with most of the soluble contaminants in water in addition to the dual redox potential (O'Carroll, 2013; Wen, 2014). Furthermore, it has a high performance as an efficient adsorbent comparing with other adsorbents because of the relatively large surface/volume ratio of the nanoparticles (Maamoun, 2018a; Maamoun, 2017). Despite all the formerly mentioned features,  $n\text{Fe}^0$  particles have some serious drawbacks in terms of the aqueous characteristics when it comes to the real water treatment applications, including the tendency of aggregation and the rapid settlement due to the strong magnetic attraction force between the particles (Eljamal, 2018b; Tosco, 2014). Therefore, several modifying techniques of the  $n\text{Fe}^0$ -based materials were applied to avoid such drawbacks, such as using supporting materials as substrate for iron nanoparticles (Khalil, 2017; Tomašević, 2014; Zhang, 2011), in addition to NZVI stabilization (Jiemvarangkul, 2011; Raychoudhury, 2012).

Hence, the main objective of this study is the modification of  $n\text{Fe}^0$  by magnesium hydroxide ( $\text{Mg}(\text{OH})_2$ ) addition with different coating ratios in order to form an iron-magnesium nanocomposite ( $n\text{Fe}^0\text{-Mg}$ ) with superior aqueous characteristics. Morphology and crystallinity properties of the synthesized particles were investigated using transmission electron microscopy (TEM) and X-ray diffraction (XRD) analyses respectively. Moreover, aqueous stability in suspension was examined through set of settlement experiments based on the spectrophotometric absorbance principle. The presented optimized  $n\text{Fe}^0\text{-Mg}$  showed an improved potential in terms of: morphological properties, aqueous suspension stability, reactivity and longevity effect.

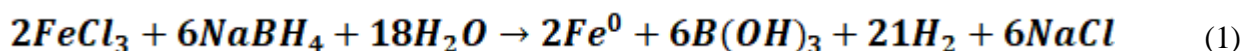
## MATERIALS & METHODS

### Chemicals

For the preparation of  $n\text{Fe}^0$ , ferric chloride hexahydrate ( $\text{FeCl}_3 \cdot 6\text{H}_2\text{O}$ , >99.0 %, Junsei Chemical Co., Japan) and sodium borohydride ( $\text{NaBH}_4$ , >98.0 %, Sigma-Aldrich Inc., USA) were used. Magnesium nitrate hexahydrate ( $\text{Mg}(\text{NO}_3)_2 \cdot 6\text{H}_2\text{O}$ , >99.0 %, Sigma-Aldrich Inc., USA) was used to synthesize the iron-magnesium nanocomposites.  $n\text{Fe}^0$  synthesis and coating solutions were prepared using deoxygenated deionized water (DDIW, 18.2  $\text{M}\Omega \cdot \text{cm}$ , Milli-Q filter) and ethanol ( $\text{C}_2\text{H}_5\text{OH}$ , >99.5 %, Wako Co., Japan) respectively. For pH adjustment, sodium hydroxide ( $\text{NaOH}$ , >97.0 %, Wako Co., Japan), hydrochloric acid ( $\text{HCl}$  (30.0%, Wako Co., Japan) were employed. Phosphorus solutions were prepared using potassium dihydrogen phosphate ( $\text{KH}_2\text{PO}_4$ , 99.5 %, Wako Co., Japan) to be used in reactivity experiments. All chemicals were used directly without further purification.

### Materials synthesis

*Preparation of  $n\text{Fe}^0$ .* Chemical reduction methodology was considered to synthesize the nanoscale zero valent iron ( $n\text{Fe}^0$ ) particles, using ferric chloride and sodium borohydride as precursor and reductant respectively, following this reaction equation (Almeelbi and Bezbaruah, 2012; Yuvakkumar, 2011):



100 mL of the reductant solution (22 g/L) was injected drop wisely at 20 mL/min into a four-neck flask containing 200 mL of the ferric solution (25 g/L). The synthesis solutions were mechanically mixed (400 RPM) and kept in a water bath at 30 °C during the whole injection time in addition to another 5 min as aging time for a complete reduction. Nitrogen bubbling was provided to prevent any interruption of the process by the oxidation. Synthesized particles were collected using vacuum filtration system after washing several times by DDIW.

**Synthesis of nFe<sup>0</sup>-Mg.** The iron-magnesium nanocomposite was synthesized by the hydrothermal precipitation of magnesium hydroxide (Mg(OH)<sub>2</sub>) onto the nFe<sup>0</sup> surface within an alkaline medium (NaOH) (Hu, 2018; Maamoun, 2018b). Concentrations of the Mg/ethanol and NaOH/ethanol solutions were controlled in order to keep the (OH<sup>-</sup>/Mg<sup>2+</sup>) molar ratio to be 2. Moreover, different (Mg/Fe) mass coating ratios were considered through varying the added volumes of magnesium and hydroxide solutions. The whole coating process was conducted under ultrasonication at 50 °C and the final composite product was separated by vacuum filtration.

### Characterization & analysis

Crystalline structure of nFe<sup>0</sup> and nFe<sup>0</sup>-Mg composites was examined using X-ray diffractometer (XRD, TTR, Rigaku Inc., Japan). Measurements were conducted using Cu K $\alpha$  radiation at 40 kV/200 mA ( $\lambda = 1.5418 \text{ \AA}$ ) and scanning rate of 2° min<sup>-1</sup> from 3° to 90° (Eljamal, 2016). The degree of crystallinity (DOC) was estimated from the XRD patterns as follows (Aggarwal and Tilley, 1955; Sami, 2010):

$$DOC (\%) = \frac{\text{Area of crystalline peaks}}{\text{Area of (crystalline+amorphous) peaks}} \times 100 \quad (2)$$

Furthermore, morphology characteristics of the synthesized materials were investigated using transmission electron microscopy (TEM). Average particle size was estimated from the TEM images considering around 80-90 particles using imaging software (ImageJ, NIH) (Schneider, 2012). Phosphorus (P) concentration was analysed using UV-Vis spectrophotometer (DR3900, Hach Co., USA), considering USEPA PhosVer 3-ascorbic acid method at 880 nm wavelength.

### Stability tests

In order to investigate the suspension stability of the synthesized nFe<sup>0</sup>-Mg composites within aqueous solutions, optical absorbance test was conducted by dispersing 0.01 g of the materials in 10 mL of 2.5 mM sodium hydro-carbonate (NaHCO<sub>3</sub>, >99.7 %, Sigma-Aldrich Inc., USA). Using an optical cuvette, the settlement of the suspension was recorded at 508 nm wavelength using UV-Vis Spectrophotometer (DR3900, Hach Co., USA).

## RESULTS & DISCUSSION

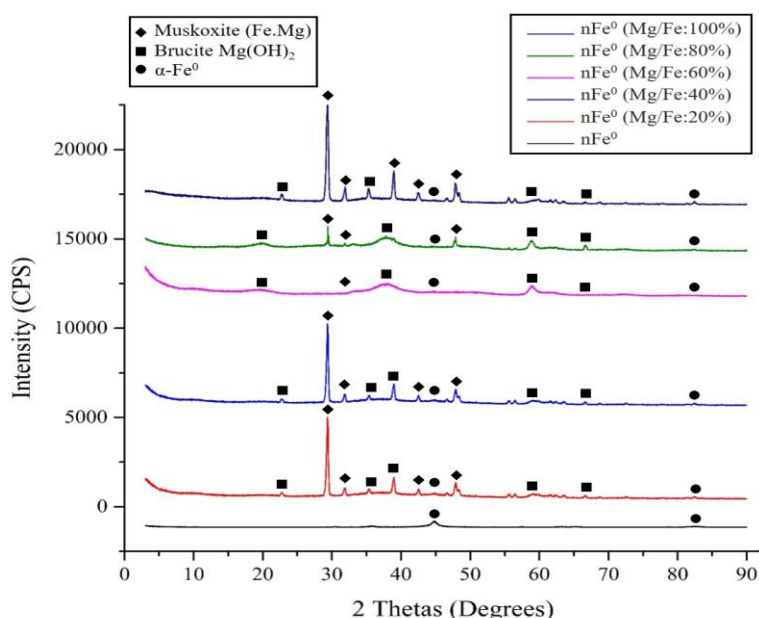
### Characterization

**Crystallinity.** XRD results, shown in Figure. 1, depicted obvious peaks of brucite (Mg(OH)<sub>2</sub>) in the iron-magnesium composites which confirmed the formation of the magnesium hydroxide coating around the nFe<sup>0</sup> core. Moreover, no peaks related to the presence of iron oxides, indicating functional effect of the magnesium hydroxide shell in the protection of the nFe<sup>0</sup> core from oxidation. The peak of  $\alpha$ -Fe<sup>0</sup> became broader by the increase of the (Mg/Fe) coating, which could be related to the semi-amorphous nature of the brucite shell on the surface of nFe<sup>0</sup> particles. The degree of crystallinity results presented in Table. 1, implied that the higher the Mg/Fe coating ratio from 20 % to 100 %, the higher the crystallinity of the composite.

**Table 1.** Characteristics of nFe<sup>0</sup> and nFe<sup>0</sup>-Mg composites

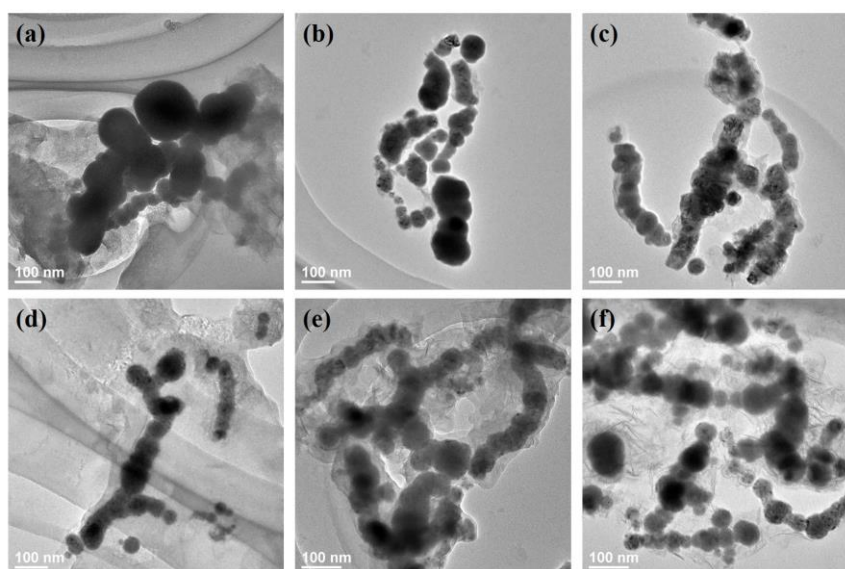
	nFe <sup>0</sup>	nFe <sup>0</sup> -Mg				
		Mg/Fe: 20 %	Mg/Fe: 40 %	Mg/Fe: 60 %	Mg/Fe: 80 %	Mg/Fe: 100 %
Average particle size (nm)	92.4	70.84	61.32	73.97	75.94	49.25
Degree of crystallinity (DOC)	60.63	35.56	41.32	54.34	63.49	70.82





**Figure 1.** X-ray diffractograms of  $n\text{Fe}^0$  and iron-magnesium nanocomposites

**Morphology characteristics.** Results of transmission electron microscopy (TEM) investigation is displayed in Figure. 2. TEM images obviously depicted aggregated clusters of bare  $n\text{Fe}^0$  with average estimated particle size of 92.4 nm. On the other hand, particles agglomeration slightly decreased for the  $n\text{Fe}^0$ -Mg composites with finer size comparing to that of bare  $n\text{Fe}^0$ . The increase of the Mg/Fe coating ratio resulted in smaller size of the particles as presented in Table. 1, where  $n\text{Fe}^0$ -Mg (Mg/Fe:100 %) exhibited an average particle size decreased by 46.7 % comparing with that of bare  $n\text{Fe}^0$ . In general, the achieved finer size of the  $n\text{Fe}^0$  composites provides a great potential towards higher specific surface area which is a crucial factor in the water treatment applications.



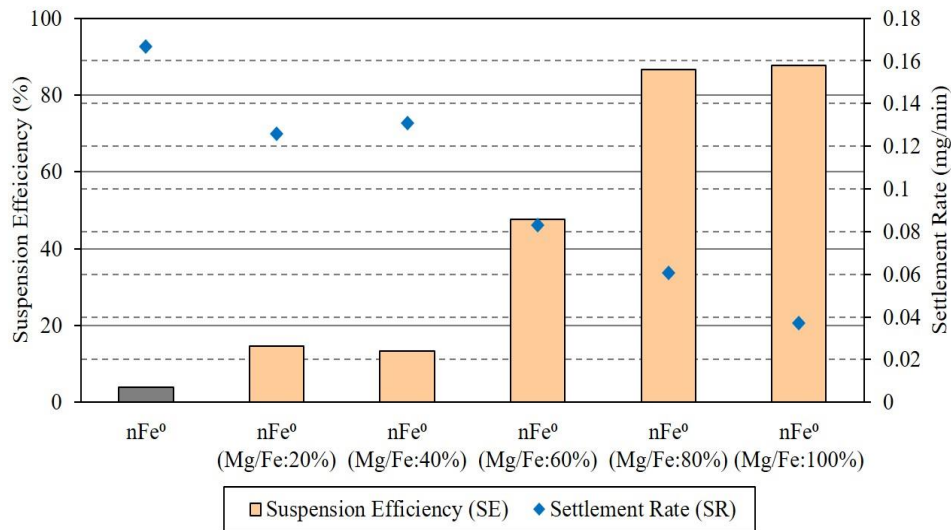
**Figure 2.** TEM images at 100 nm resolution of: (a)  $n\text{Fe}^0$  and  $n\text{Fe}^0$ -Mg composites with Mg/Fe coating ratios (b) 20 %, (c) 40 %, (d) 60 %, (e) 80 %, and (f) 100 %

### Settlement investigation

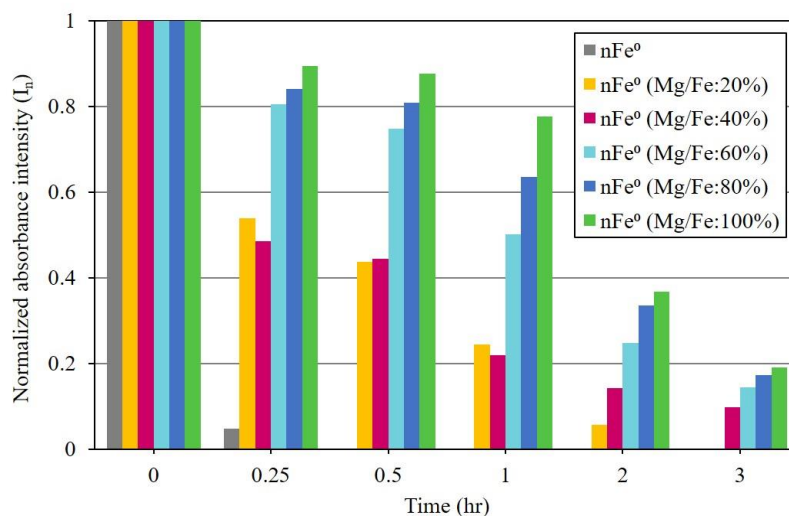
The addition of  $\text{Mg}(\text{OH})_2$  to  $n\text{Fe}^0$  with coating ratio of (Mg/Fe: 100 %) resulted in stimulated stability of the particles in aqueous suspension with lower settlement rate (SR) than that of

unmodified iron particles. As shown in Figure. 3, the increase in the Mg/Fe coating ratio resulted in a higher suspension efficiency (SE) up to around 88 % for the fully coated nFe<sup>0</sup>-Mg particles.

The normalized absorbance intensity ( $I_n$ ) was considered as an indicator of the suspension stability of the suspension over 3 hrs settlement time, where ( $I_n = I_t/I_o$ ) is a function of absorbance intensity at specific time ( $I_t$ ) and initial intensity ( $I_o$ ). Sedimentation curves were obtained by plotting ( $I_n$ ) with respect to time as displayed in Figure. 4. For nFe<sup>0</sup>-Mg composites, the value of the normalized intensity tended to decrease gradually along with the increase in Mg/Fe coating ratio. Whereas, rapid settlement occurred for bare nFe<sup>0</sup> with full settlement within 30 minutes. Additionally, the suspension stability of the composites enhanced with the increase of the Mg/Fe coating ratio. Moreover, nFe<sup>0</sup>-Mg (Mg/Fe:100 %) was found to be the optimal coating ratio in terms of suspension stability in aqueous solution which was consistent with the visual observation.



**Figure 3.** Suspension Efficiencies and Settlement Rates of nFe<sup>0</sup> and iron-magnesium nanocomposites



**Figure 4.** Normalized absorbance intensity vs. time for nFe<sup>0</sup> and iron-magnesium nanocomposites suspensions

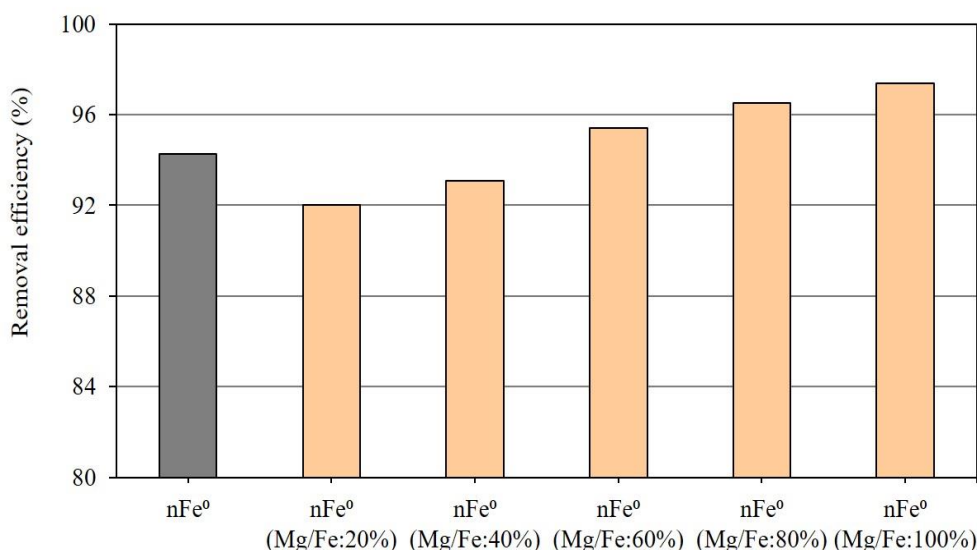
### Reactivity effect

Phosphorus (P) was considered as the indicator for the reactivity influence of the synthesized materials. Batch experiments were conducted using 50 mL solution volume of 50 mg/L-P with the

addition of 50 mg of  $n\text{Fe}^0$  or  $n\text{Fe}^0$ -Mg nanoparticles as adsorbent dosage. Removal efficiency of the synthesized iron-magnesium nanocomposites towards phosphorus was calculated as a function in initial ( $C_o$ ) and final ( $C_f$ ) concentrations, corresponding to different (Mg/Fe) coating ratios using the following formula:

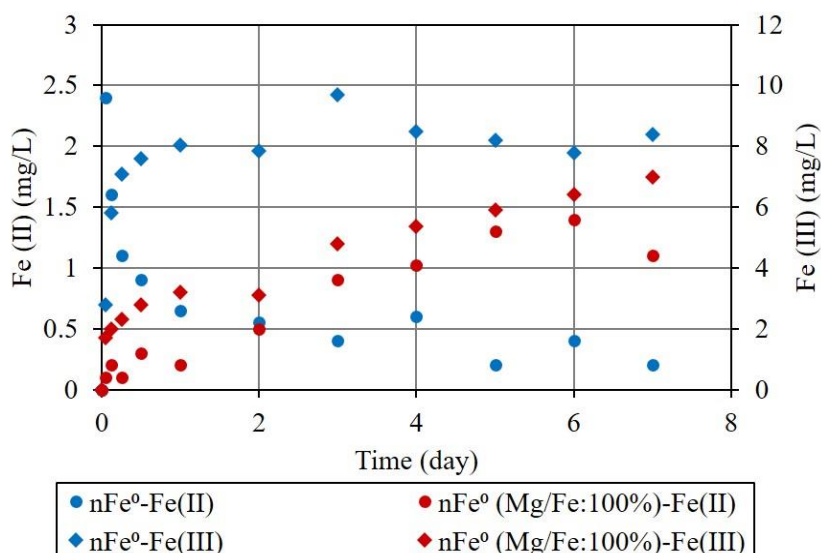
$$\text{Removal efficiency (\%)} = \frac{(C_o - C_f)}{C_o} \times 100 \quad (3)$$

As shown in Figure. 5, the  $n\text{Fe}^0$ -Mg particles showed comparable removal efficiencies to that of bare  $n\text{Fe}^0$ . The stimulating effect of the (Mg/Fe) coating ratio on the phosphorus removal efficiency was clearly observed, where (Mg/Fe:100 %) was corresponding to the highest value of the removal efficiency. Moreover,  $n\text{Fe}^0$  (Mg/Fe:100 %) and (Mg/Fe:80 %) removed phosphorus with 3.13 % and 2.23 % respectively higher than that of bare  $n\text{Fe}^0$ . This enhanced effect in reactivity of the iron-magnesium composites could be attributed to the contribution of the formed magnesium hydroxide shell around the iron core in the phosphorus adsorption. Additionally, as it was previously reported, the neutral pH conditions provides a positive surface charge of the  $\text{Mg}(\text{OH})_2$ , leading to a better electrostatic attraction of the aqueous phosphate ( $\text{PO}_4^{3-}$ ) species onto the adsorbent surface (Schott, 1981).



**Figure 5.** Phosphorus removal efficiency of  $n\text{Fe}^0$  and iron-magnesium nanocomposites (initial pH:  $7 \pm 0.2$  at  $25^\circ\text{C}$  and 300 RPM)

The leaching of iron oxides, ferrous (II) and ferric (III), was considered as an indicator to investigate the reactive longevity of the  $n\text{Fe}^0$ -Mg composites within aqueous solutions over 1-week experiment. Ferrous aqueous concentration is a representative of the iron dissolution, where the higher the concentration, the more the dissolution and the less the precipitation (Eljamal, 2018a). As shown in Figure. 6, iron dissolution occurred rapidly (within the first hour) for  $n\text{Fe}^0$  represented by maximum ferrous concentration of 2.42 mg/L followed by a decline trend corresponding to a rise in ferric concentration. Whereas, iron oxides precipitation was dominant during the rest of the days. For  $n\text{Fe}^0$ -Mg (Mg/Fe:100 %), iron dissolution started after 12 hrs due to the high coating ratio and it was competing with precipitation during the rest of the experiment days. Results implied that the gradual increase in iron oxides leachates for the iron-magnesium composite proved the continuous dissolution of the  $n\text{Fe}^0$  core due to the anti-corrosion effect of the brucite shell. That could be preferable for the real remediation applications where the longevity and electron availability are vital parameters in achieving higher performance.



**Figure 6.** Iron oxides leaching into aqueous solutions of  $n\text{Fe}^0$  and  $n\text{Fe}^0$  (Mg/Fe:100%)

## CONCLUSIONS

Iron-magnesium nanocomposite ( $n\text{Fe}^0$ -Mg) with better aqueous characteristics was successfully synthesized. The increase of the Mg/Fe coating ratio up to 100% resulted in a smaller average particle size by 46.7 % comparing with that of bare  $n\text{Fe}^0$ . Anti-aggregation effect was achieved corresponding to the smaller average particle size of the  $n\text{Fe}^0$ -Mg particles which was confirmed by the TEM morphological observation. Moreover, the degree of crystallinity enhanced for the  $n\text{Fe}^0$ -Mg composites by higher the Mg/Fe coating ratio from 20 % to 100 %, the higher the crystallinity of the composite. The three hours settlement investigation of the modified  $n\text{Fe}^0$  exhibited higher stability in aqueous suspension comparing with the rapid settlement of bare  $n\text{Fe}^0$ . Furthermore, Phosphorus removal efficiency was improved by 2-3 % for the  $n\text{Fe}^0$ -Mg composites to that of  $n\text{Fe}^0$ . Additionally, the iron core of the synthesized  $n\text{Fe}^0$  was adequately protected from aqueous corrosion after the optimal modification with  $\text{Mg}(\text{OH})_2$ , corresponding to lower iron oxides leachates, indicating the enhanced reactive longevity of the modified composites. The current work suggests that the achieved enhanced features of the proposed iron-based nanocomposites could lead to great potential applicability towards sustainable effectiveness in water treatment applications.

## REFERENCES

- Aggarwal, S. L., Tilley, G. P. (1955) Determination of crystallinity in polyethylene by X-ray diffractometer. *Journal of Polymer Science*, **18**(87), 17-26.
- Almeelbi, T., Bezbaruah, A. (2012) *Nanotechnology for Sustainable Development*, Springer, 197-210.
- Eljamal, O., Khalil, A. M., Sugihara, Y., Matsunaga, N. (2016) Phosphorus removal from aqueous solution by nanoscale zero valent iron in the presence of copper chloride. *Chemical Engineering Journal*, **293**, 225-231.
- Eljamal, O., Mokete, R., Matsunaga, N., Sugihara, Y. (2018a) Chemical pathways of Nanoscale Zero-Valent Iron (NZVI) during its transformation in aqueous solutions. *Journal of Environmental Chemical Engineering*, **6**(5), 6207-6220.
- Eljamal, R., Eljamal, O., Khalil, A. M. E., Saha, B. B., Matsunaga, N. (2018b) Improvement of the chemical synthesis efficiency of nano-scale zero-valent iron particles. *Journal of Environmental Chemical Engineering*, **6**(4), 4727-4735.
- Ghasemzadeh, G., Momenpour, M., Omidi, F., Hosseini, M. R., Ahani, M., Barzegari, A. (2014) Applications of nanomaterials in water treatment and environmental remediation. *Frontiers of*

*Environmental Science & Engineering*, **8**(4), 471-482.

- Hu, Y.-b., Zhang, M., Qiu, R., Li, X.-y. (2018) Encapsulating nanoscale zero-valent iron with a soluble Mg (OH) 2 shell for improved mobility and controlled reactivity release. *Journal of Materials Chemistry A*, **6**(6), 2517-2526.
- Jiemvarangkul, P., Zhang, W.-x., Lien, H.-L. (2011) Enhanced transport of polyelectrolyte stabilized nanoscale zero-valent iron (nZVI) in porous media. *Chemical Engineering Journal*, **170**(2-3), 482-491.
- Khalil, A. M., Eljamal, O., Amen, T. W., Sugihara, Y., Matsunaga, N. (2017) Optimized nano-scale zero-valent iron supported on treated activated carbon for enhanced nitrate and phosphate removal from water. *Chemical Engineering Journal*, **309**, 349-365.
- Maamoun, I., Eljamal, O., Khalil, A. M. E., Sugihara, Y., Matsunaga, N. (2018a) Phosphate Removal Through Nano-Zero-Valent Iron Permeable Reactive Barrier; Column Experiment and Reactive Solute Transport Modeling. *Transport in Porous Media*, **125**(2), 395-412.
- Maamoun, I., Eljamal, O., Shubair, T., Noutsuka, H., Saha, B. B., Matsunaga, N. (2017) Integrating nano-scale zero valent iron (nZVI) in phosphorus removal from aqueous solution through porous media: packed-column experiment. Proceedings of International Exchange and Innovation Conference on Engineering & Sciences (IEICES), **3**, 25-30.
- Maamoun, I. E., Osama, Matsunaga, Nobuhiro (2018b) Enhancement of Nanoscale Zero-Valent Iron Stability in Aqueous Solution Via Metal Hydroxide Coating. Proceedings of International Exchange and Innovation Conference on Engineering & Sciences (IEICES), **4**, 82-83.
- O'Carroll, D., Sleep, B., Krol, M., Boparai, H., Kocur, C. (2013) Nanoscale zero valent iron and bimetallic particles for contaminated site remediation. *Advances in Water Resources*, **51**, 104-122.
- Raychoudhury, T., Tufenkji, N., Ghoshal, S. (2012) Aggregation and deposition kinetics of carboxymethyl cellulose-modified zero-valent iron nanoparticles in porous media. *Water research*, **46**(6), 1735-1744.
- Sami, A., David, E., Fréchette, M. (2010) Procedure for evaluating the crystallinity from X-ray diffraction scans of high and low density polyethylene/SiO<sub>2</sub>composites, 1-4.
- Schneider, C. A., Rasband, W. S., Eliceiri, K. W. (2012) NIH Image to ImageJ: 25 years of image analysis. *Nature methods*, **9**(7), 671.
- Schott, H. (1981) Electrokinetic Studies of Magnesium Hydroxide. *Journal of Pharmaceutical Sciences*, **70**(5), 486-489.
- Tomašević, D., Kozma, G., Kerkez, D. V., Dalmacija, B., Dalmacija, M., Bečelić-Tomin, M., Kukovec, Á., Kónya, Z., Rončević, S. (2014) Toxic metal immobilization in contaminated sediment using bentonite-and kaolinite-supported nano zero-valent iron. *Journal of nanoparticle Research*, **16**(8), 2548.
- Tosco, T., Papini, M. P., Viggi, C. C., Sethi, R. (2014) Nanoscale zerovalent iron particles for groundwater remediation: a review. *Journal of Cleaner Production*, **77**, 10-21.
- Wen, Z., Zhang, Y., Dai, C. (2014) Removal of phosphate from aqueous solution using nanoscale zerovalent iron (nZVI). *Colloids and Surfaces A: Physicochemical and Engineering Aspects*, **457**, 433-440.
- Yuvakkumar, R., Elango, V., Rajendran, V., Kannan, N. (2011) Preparation and characterization of zero valent iron nanoparticles. *Digest journal of nanomaterials and biostructures*, **6**(4), 1771-1776.
- Zhang, Y., Li, Y., Li, J., Hu, L., Zheng, X. (2011) Enhanced removal of nitrate by a novel composite: nanoscale zero valent iron supported on pillared clay. *Chemical Engineering Journal*, **171**(2), 526-531.
- Zhao, X., Liu, W., Cai, Z., Han, B., Qian, T., Zhao, D. (2016) An overview of preparation and applications of stabilized zero-valent iron nanoparticles for soil and groundwater remediation. *Water research*, **100**, 245-266.

## The Smart-Water Project: Smart Metering in the City of Thessaloniki

A. Mentés\*, P. Stournara\*, D. Spyrou\*, A. Samaras\* and P. Galiatsatou\*

\* Thessaloniki Water Supply and Sewerage Company S.A. (EYATH S.A.), Tsimiski 98, 54622 Thessaloniki, Greece (E-mails: [amentes@eyath.gr](mailto:amentes@eyath.gr); [pstournara@eyath.gr](mailto:pstournara@eyath.gr); [dspyrou@eyath.gr](mailto:dspyrou@eyath.gr); [asamaras@eyath.gr](mailto:asamaras@eyath.gr); [pgaliatsatou@eyath.gr](mailto:pgaliatsatou@eyath.gr))

### Abstract

Smart Water Metering (SWM) technologies constitute advanced and modern methods to access reliable information on water usage and to regulate water supply and consumption, forming a basis for the successful design and implementation of Water Demand Management (WDM) strategies. The Smart-Water research project, which is launched by a consortium specialised in telemetry systems, Internet-of-Things (IoT) and Advanced Metering Infrastructure (AMI) and is implemented in the domain of responsibility of the Water Supply and Sewerage Company of Thessaloniki in Greece (EYATH S.A), aims at the development of smart infrastructure for water consumption and management of drinking water demand. Smart-Water is expected to promote user-oriented management strategies of water demand, assist in reducing leaks and non-revenue water in the water system, increase awareness of consumers towards water conservation and saving, as well as have significant environmental, economic and social benefits. In the frame of the project and during its various stages several issues are examined such as selection of areas for pilot study, features of smart infrastructure, design, supply and installation of software and equipment of network connectivity etc.

### Keywords

Smart-Water project; Water Management; Smart Metering; AMI

## INTRODUCTION

The Smart-Water project is about smart infrastructure of telemetry systems for water consumption and management of drinking water demand. The water utility company involved in the project is EYATH SA, the water supply and sewerage company of Thessaloniki. Apart from EYATH SA there are two participants in the project, APIFON Private Company and Information Technology Institute (ITI)/Centre of Research and Technology Hellas (CERTH). Smart-Water is co-financed by the European Union, Greek national funds as well as by partners' own funds. Among the objectives of the project are: (a) to design an original infrastructure which will exploit the latest technologies in order to give the opportunity to EYATH SA offer innovative services to its consumers and (b) develop and pilot test of a management, display and data analysis water consumption system.

The Smart-Water project is implemented under the Operational Programme Competitiveness, Entrepreneurship and Innovation 2014-2020 (EPAnEK). More specifically, the project is included in the Action measure "RESEARCH – CREATE - INNOVATE", which aims to support and promote research, innovation and technological development. The main purpose of the Action measure is to link research and innovation to entrepreneurship enhancing competitiveness, productivity and extroversion of enterprises: this enhancement would strengthen companies towards innovative entrepreneurship of high quality.

EYATH SA is the second biggest water supply and sewerage company in Greece, situated in the city of Thessaloniki in northern Greece. EYATH supplies water to around 500,000 water meters. The water supply needs are covered by three resources: (1) the Aliakmonas river, (2) the Aravissos springs and (3) boreholes in the plain of Thessaloniki (groundwater). The external water supply



network extends over 460 km, while the distribution network consists of water supply pipes with a total length exceeding 2,690 km.

## **WATER MANAGEMENT**

The aim of urban water management is to provide a safe and reliable water supply to consumers. Nowadays, maintaining the sustainability of this water supply has become equally important, with the adverse effects of the projected climate change on water scarcity already manifesting themselves in many countries around the world. Water Demand Management (WDM), i.e. the management approach aiming to conserve water by influencing demand, is used by water utility companies and policymakers in order to manage water supply, enact water conservation and design water safety plans. WDM consists of activities ranging from engineering/infrastructure maintenance and upgrading to economics analyses, and from sustainable consumption incentives to consumers' education. The availability of reliable information on water use is the basis for the successful design and implementation of WDM strategies and, in this context, water metering is essential for acquiring the data needed (Randall and Koech, 2019). The transition from traditional water metering methods/tools to the technology known today as Smart Water Metering (SWM), as well as the added value SWM brings to water management as a whole, is the subject of this work and will be discussed in brief in the following sections.

## **SMART METERING**

Water companies are constantly on the trend worldwide to invest increasingly in "smart" automated telemetry infrastructures for water consumption and processing of collected measured data. These infrastructures, scientifically known as Advanced Metering Infrastructures (AMI), enable water companies to create improved services for consumers in order to upgrade consumer service.

Smart water meters provide a new measurement technology. Application of smart water meters allows continuous collection of consumption data, without requiring physical presence on site. In addition to water consumption information, smart meters can provide instantaneous water supply information, water temperature, pressure values, reverse flow measurement, water meter alarm, etc. Additional benefits are the detection and notification of losses due to leaks or unauthorized use of the water network, protection of the environment by reducing the wastage of water resources, and customer service upgrade with modern information services.

Along with smart meters, smart valve regulates, drives and controls the flow of a water, by opening, closing or partially blocking its passage. Smart valves use the actuators to operate. Actuators require control signal and power source to operate. The control signal is a low power signal. It can be caused by electrical voltage or power supply. When the actuator receives the control signal, it reacts by converting the signal energy into mechanical motion. Remote management of smart valve is surely an important benefit of this new technology, giving the means to control in real time the water consumption.

## **INTERNET OF THINGS (IoT)**

The Internet-of-Things (IoT) has recently gained more attention due to the technological advancement of wireless technology. It is based on the integration of different technologies (Shah and Yaqoob, 2016). Low Power Wide Area Networks (LPWAN) are best suited for IoT applications which require the transmission of very small amounts of data over long distances· as in the case of recording and transmitting measurement data (Xu et al., 2018). IoT technology is applied in Smart-Water project through the installation of a fixed LoRa network of antennas with Radiofrequency of 868 MHz for the transmission of the appropriate data.

## **BENEFITS OF THE PROJECT**

Over the last decades, smart water metering (SWM) programs have been launched in several urban areas worldwide, advancing user-oriented management strategies of water demand, providing significant environmental, economic and social benefits, and promoting sustainability and adaptation of modern societies to future challenges.

SWM techniques develop accurate water consumption profiles for end-users, which can assist with the design and evaluation of water demand management strategies, contributing to behavioral changes of consumers towards supporting water conservation and saving (Fielding et al., 2013). Water saving by the consumers can significantly decrease power and energy consumption of pumping water (Brzozowski, 2010), leading to environmental benefits resulting mainly from greenhouse gas emission reduction and stabilization of the groundwater level, and can finally contribute to a smaller water footprint of urban water supply infrastructure (Laspidou, 2014). SWM can also contribute to testing the effectiveness of demand management interventions, as well as to developing pressure management strategies in water distribution networks. The latter can assist in reducing or eliminating leakages and non-revenue water in water supply networks, allowing an increase in the efficiency of such systems at lower costs (Cominola et al., 2015).

SWM could also achieve economic savings for water utilities and, therefore, financial benefits for the local communities. This means that smart metering may not only contribute to reducing operational and maintenance costs for water utilities (Cominola et al., 2015), but also help in forming more flexible and regulated water tariff schemes (March et al., 2017), such as dynamic water pricing (Vasak et al., 2014). Energy costs could also be reduced by using smaller pumps, as well as by treating and transferring smaller water volumes (Nguyen et al., 2018).

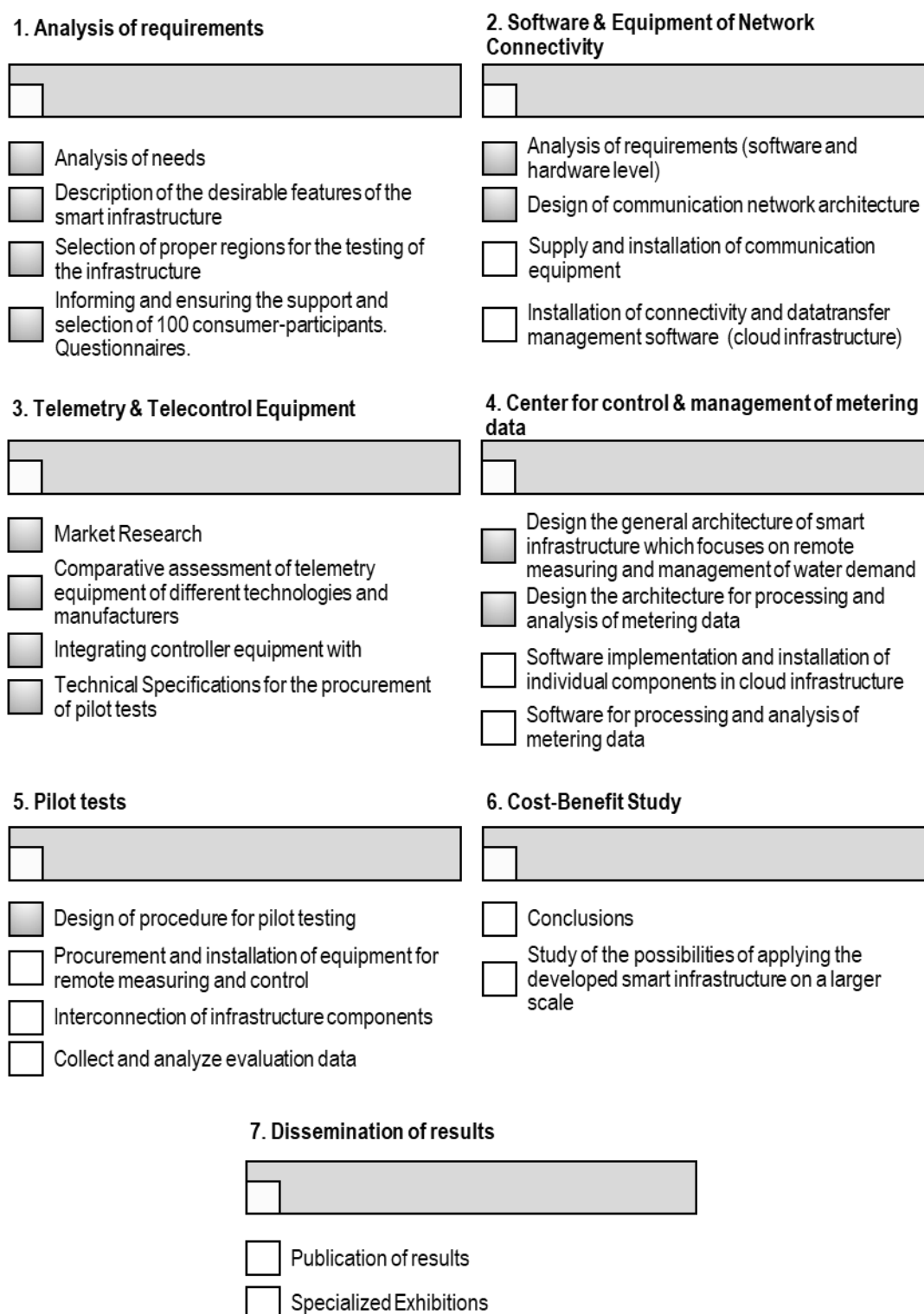
In the social sector, SWM programs including detailed and targeted information dissemination, can assist in raising the environmental awareness of local societies and authorities on water conservation issues (Liu et al., 2017; Nguyen et al., 2018), helping entire communities to develop sustainable habits regarding urban water use (Magiera and Froelich, 2014; Laspidou, 2014). Such programs can also contribute to the exchange of best practices and experiences in the field of water distribution networks management, increasing the credibility of water utilities and empowering two-way relationships between them and the consumers. Furthermore, SWM is expected to have significant benefits on public health, based on limitation of network damages and reduction of water contamination risk. Smart meters can detect leak problems and their location in water supply networks, as well as identify differential pressure issues able to cause contaminant intrusion and can create alerts for responsible authorities (Mutchek and Williams, 2014). Addition of biosensors for contamination detection in SWM systems can assist in safeguarding water security, by identifying and locating water quality problems in the network.

The Smart-Water project will provide EYATH the ability to establish a two-way relationship towards the consumer, through creation of new software apps for organized and consistent communication and direct customer service. These will gradually lead to the development of water culture and cultivation of water consciousness of the consumers. The Smart-Water project will also provide the possibility of revenue management to consumers by knowing their water consumption, since they will be able to be informed about it, among other things such as water exploitation, possible leakage, imminent interruption of their water supply and choosing flexible invoice and offers by SMS, telephone etc.



## STAGES OF THE PROJECT

The stages of the project are presented briefly in Figure 1. There are a total of 7 stages: (1) analysis of requirements, (2) software and equipment of network connectivity, (3) telemetry and telecontrol equipment, (4) center for control and management of metering data, (5) pilot tests, (6) cost-benefit study, (7) dissemination of results. The project has completed up to now the 1<sup>st</sup> and 3<sup>rd</sup> stages and parts of the 2<sup>nd</sup>, 4<sup>rd</sup> and 5<sup>th</sup> stages as shown in Figure 1.



**Figure 1:** The stages of Smart-Water project in brief (stages 1-6). Stages which are completed are noted with grey colour

## CASE STUDIES

As far as the project's implementation areas, the choice of scattered spots in various areas of the city of Thessaloniki would increase the cost of the project, since it would require the development of many telecommunication networks, which was not an objective of the project. For this reason, two specific areas were selected from all over the city of Thessaloniki: (1) the center and (2) Kalamaria area, which is situated in the southeastern part of the city. Both areas were selected due to their different urban structure, their water consumption habits and their geomorphology. City center was selected because it presents a particular difficulty regarding telecommunications coverage, a difficulty which is owed to its dense construction and tall buildings. Kalamaria was selected because of the large relative household consumption.

In order to locate the consumers wishing to participate in the project and get their relevant consensus, an initial phone communication approach was set up. An information leaflet of the project and two (2) questionnaires to be filled at the beginning and at the end of the project were prepared. The process of approaching prospective participant consumers was planned. For this specific project, the sample of one hundred (100) consumers (water meters), who were located and wish to participate in the project, was divided into two groups, fifty (50) consumers situated in the city center and fifty (50) situated in the area of Kalamaria.

## SCENARIOS DEPLOYMENT

The scenarios for the use of the SMART WATER app were defined and formulated in order to: (a) meet the basic needs of EYATH S.A. for effective water demand management, and (b) being able to contribute to answering the critical research questions set by the SMART-WATER project, regarding the use of new technologies in the specific field. The scenarios are divided in three categories: (I) those involving the smart water meter (15 scenarios), (II) those involving the smart electric valve (10 scenarios) and (III) one scenario involving both the smart water meter and smart valve. The scenarios of the first (I) and the second (II) categories are further classified regarding: (a) the type of the scenario and (b) the part “triggering” the scenario. The types of scenarios comprise for category (I), Update/information, Alert and Data Recording/Analysis scenarios, and for category (II), Action, Alert and Update/Information scenarios. The parts “triggering” the scenarios comprise: (a) Customer (i.e. the end-user of the SMART-WATER app), (b) EYATH S.A. (i.e. the administrator and operator of the SMART-WATER app) and (c) an option for the scenarios which are triggered automatically. The above classifications are presented in Figures 1 and 2. The most characteristic scenarios are mentioned below:

**Table 1.** Scenarios involving the smart water meter

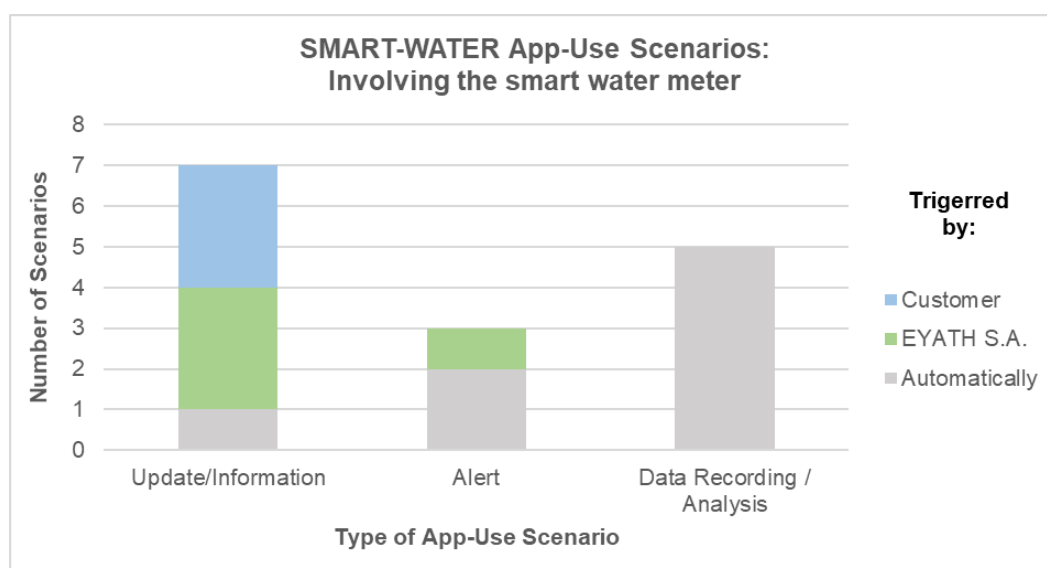
Scenarios	Title	Description
Scenario 1	Information about water consumption, after a consumer's relevant request.	The consumer stays informed about his/her water consumption by an application, which runs on a computer or a mobile phone, for the period starting from the last billing up to the time the request has been made. System Response: “Your consumption from day/month/year to day/month/year was XXm <sup>3</sup> ”
Scenario 2	Keep a record of all information from smart water meters and smart valves stored in a database. The stored data can be visualized (charts, statistics etc.)	Creation of a database in which consumption data of every smart water meter will be stored. Data will be displayed in tables, charts, etc. and will be available to consumers upon request.

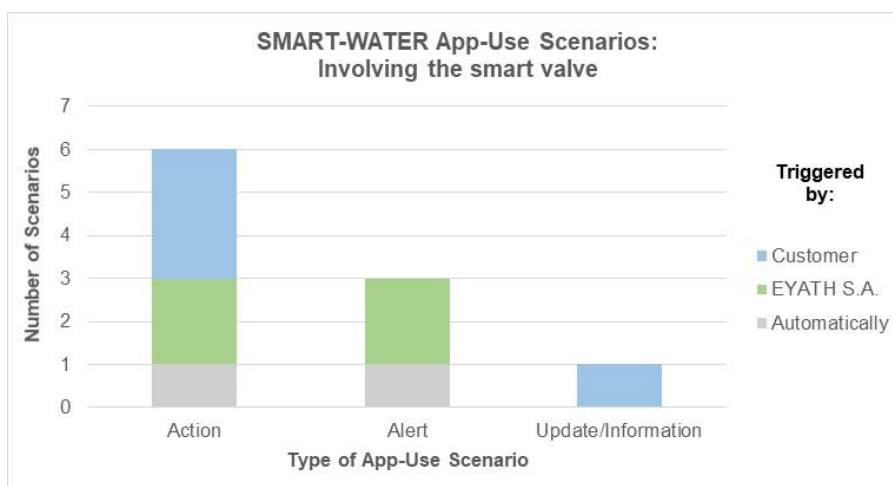
**Table 2.** Scenarios involving the smart valve

Scenarios	Title	Description
Scenario 1	The consumer wishes to open/close the smart valve, which is located before the smart water meter.	The consumer sends from a computer or a mobile phone a request to EYATH SA that he/she wishes to open/close the smart valve. The system verifies through "one-time pin" (OTP) that he/she is the account manager. The system, after finding that there are no debts or any other reasons that the smart valve should remain closed, it automatically opens/closes the smart valve and informs EYATH SA about this action. The time needed for the procedure described above depends on the response of the telecommunication system. EYATH SA sends the following message to the consumer: "At your request in the day/month/year and PP time, we opened/closed the smart valve".
Scenario 2	EYATH SA closes the smart valve because there is no recorded consumption of the consumer for a period of 48 hours (after prior relevant declaration of the consumer).	The consumer declares in advance that he/she wishes EYATH SA to close the smart valve whenever zero consumption occurs for a 48-hour period. The smart valve can be opened by the consumer at any time.

**Table 3.** Scenario involving both the smart water meter and the smart valve

Scenarios	Title	Description
Scenario 1	Application of night-time pricing.	night-EYATH SA may provide night-time pricing for some night hours, after a consumer's request.

**Figure 1.** Classification of the SMART-WATER app use scenarios involving the smart water meter



**Figure 2.** Classification of the SMART-WATER app use scenarios involving the smart valve

## ACKNOWLEDGMENTS

This research has been co-financed by the European Union and Greek national funds through the Operational Program Competitiveness, Entrepreneurship and Innovation, under the call RESEARCH – CREATE – INNOVATE (project code: T1EDK- 04337). The authors would like to thank APIFON and Information Technology Institute (ITI)/Centre of Research and Technology Hellas (CERTH) for their cooperation in the project.

## REFERENCES

- Brzozowski, C. (2010) Pump technology. *Water efficiency*, **5**, 38-41.
- Cominola, A., Giuliani, M., Piga, D., Castelletti, A., Rizzoli, A. E. (2015) Benefits and challenges of using smart meters for advancing residential water demand modeling and management: a review. *Environmental Modelling and Software*, **72**, 198-214.
- Fielding, K. S., Spinks, A., Russell, S., McCrea, R., Stewart, R. E., Gardner, J. (2013) An experimental test of voluntary strategies to promote urban water demand management. *Journal of Environmental Management*, **114**, 343-351.
- Lapidou, C. (2014) ICT and stakeholder participation for improved urban water management in the cities of the future. *Water Utility Journal*, **8**, 79-85.
- Liu, A., Giurco, D., Mukheibir, P., Mohr, S., Watkins, G., White, S. (2017) Online water-use feedback: household user interest, savings and implications. *Urban Water Journal*, **14**(9), 900-907.
- Magiera, E., Froelich, W. (2014) Integrated support system for efficient water usage and resources management (ISS-EWATUS). *Procedia Engineering*, **89**, 1066-1072.
- March, H., Morote, A. F., Rico, A. M., Sauri, D. (2017) Household smart water metering in Spain: insights from the experience of the remote meter reading in Alicante. *Sustainability*, **9**, 582.
- Mutchek, M., Williams, E. (2014) Moving towards sustainable and resilient smart water grids. *Challenges*, **5**, 123-137.
- Nguyen, K. A., Stewart, R. A., Zhang, H., Sahin, O., Siriwardene, N. (2018) Re-engineering traditional urban water management practices with smart metering and informatics. *Environmental Modelling and Software*, **101**, 256-267.
- Randall, T., Koech, R. (2019) Smart Water Metering Technology for Water Management in Urban Areas. *Water e-Journal*, **4**(1), 1-14.
- Shah, S. H., Yaqoob, I. (2016) A survey: Internet of Things (IOT) technologies, applications and challenges. *IEEE Smart Energy Grid Engineering (SEGE)*, 381-385.

- Vasal M., Banjac G., Baotic M., Matusko J. (2014) Dynamic day – ahead water pricing based on smart metering and demand prediction. *Procedia Engineering*, **89**, 1031-1036.
- Xu, J., Yao, J., Wang, L., Ming, Z., Wu, K., Chen, L. (2018) Narrowband Internet of Things: Evolutions, Technologies, and Open Issues. *IEEE Internet of Things*, **5**(3), 1449-1462.

## Towards Smart Infrastructure: A Case Study in the Water Supply System of Thessaloniki

A. Mentēs\*, P. Stournara\* and D. Spyrou\*

\* Thessaloniki Water Supply and Sewerage Company S.A. (EYATH S.A.), Tsimiski 98, 54622 Thessaloniki, Greece (E-mails: [amentes@eyath.gr](mailto:amentes@eyath.gr); [pstournara@eyath.gr](mailto:pstournara@eyath.gr); [dspyrou@eyath.gr](mailto:dspyrou@eyath.gr))

### Abstract

The challenge of smart infrastructure by integrating smart technology in the existing water supply system requires a carefully designed implementation plan. In order to secure the proper function of a water utility company, water use demand should be taken seriously into account. In the present study, a preliminary design for positioning the antennas of a fixed telecommunication network is presented. The methodology implemented uses Geographic Information Systems (GIS) in order to conduct several visibility analysis tests, finding the proper antenna positions which fit best to the project needs. Two urban areas in Thessaloniki city were selected for the pilot research project: (a) the city centre and (b) Kalamaria situated in the southeastern part of Thessaloniki. The fixed network was scheduled to work in combination with smart water meters and smart water valves.

### Keywords

Smart infrastructure; smart water metering; water-wise cities; Geographic Information System (GIS); visibility analysis; geocoding; consumption data; real time control

## INTRODUCTION

Fulfilling total water use demands is a prerequisite for normal function of a water utility company. This includes: (a) the base water use -during winter months- and (b) the seasonal use, either spread over the year or presenting short term-variations (Zhou et al., 2002). Balancing between urban water demand and water supply, while keeping customer service at a satisfactory level, belongs to the main and most important objectives of a water utility company (Zhou et al., 2002; Herrera et al., 2010). Efficient managing and operating the water supply network are affected and significantly assisted by detailed water demand patterns, which provide a better description of the consumption needs (Herrera et al., 2010, Zhou et al., 2002). Smart metering technology provides (a) the proper data for creating such profiles, (b) opportunity of creating new products for the consumers.

The Smart-Water project is about smart infrastructure of telemetry systems for water consumption and management of drinking water demand. The water utility company involved in the project is EYATH SA, the water supply and sewerage company of Thessaloniki. Apart from EYATH SA there are two participants in the project, APIFON Private Company and Information Technology Institute (ITI)/Centre of Research and Technology Hellas (CERTH). Smart-Water is co-financed by the European Union, Greek national funds as well as by partners' own funds. Among the objectives of the project are: (a) to design an original infrastructure which will exploit the latest technologies in order to give the opportunity to EYATH SA offer innovative services to its consumers and (b) develop and pilot test of a management, display and data analysis water consumption system.

### Thessaloniki Water Supply and Sewerage Company S.A. (EYATH S.A.)

EYATH S.A. provides water supply and sewerage services to the broader urban area of Thessaloniki, which is situated in Northern Greece. Among its strategic targets is the implementation of smart metering infrastructure in order to: (a) reduce Unaccounted-For Water (UFW), (b) enhance customer service by creating new products and (c) contribute in developing water culture and in strengthening water-consciousness of the customers.

## Challenge

Addressing the challenge of smart infrastructure by integrating smart technology in the existing water supply system requires a well-designed implementation plan. Studying this integration in the current city's infrastructure on a pilot research level makes its further financing on a wider scale more viable and robust.

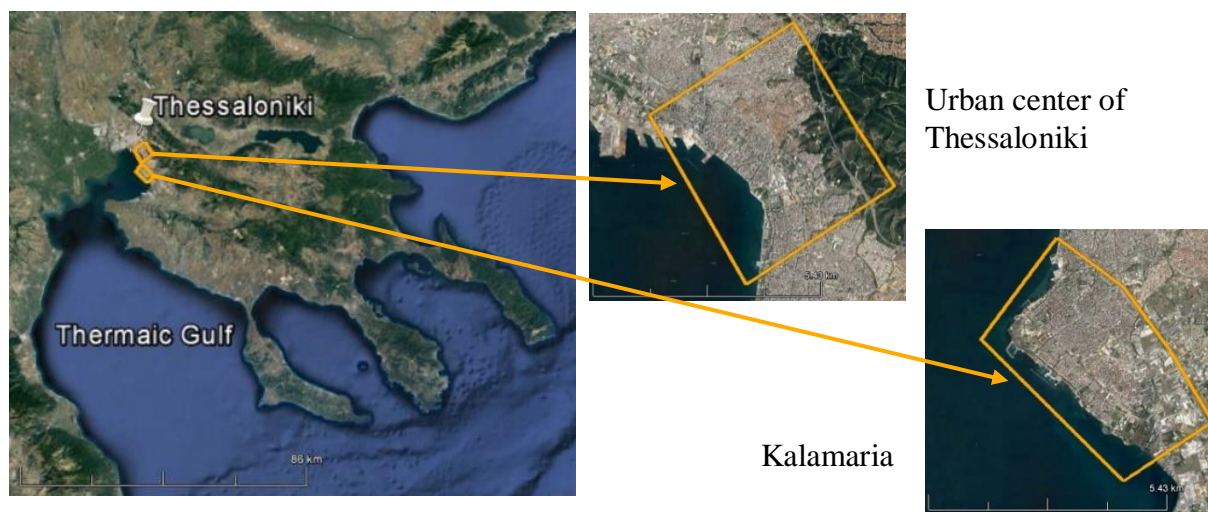
Through smart infrastructure, provision of smart services to end users (EYATH S.A. and consumers) will be possible. In this way, EYATH S.A. will have benefits as an end-user by upgrading its service quality at a reduced cost such as (a) reduce the total operational cost of its complaint management by notifying the consumer utilizing an ALERT service, when its consumption exceeds a threshold which can be determined either by EYATH S.A. or by the consumer – all based on the high frequency of consumption measurements, (b) remotely interrupt and recover water supply directly, serving the consumer etc. The consumers, who are the final end-users will be offered a variety of services such as: (a) apps for remote control of their private water connection, (b) access to their private consumption profile, (c) alerts of predetermined consumption thresholds (of water volume or of water bill) etc.

In this paper, the study conducted for designing telecommunication parts of the smart water infrastructure is presented and analyzed using the companies developed Geographic Information System (GIS).

## MATERIALS AND METHODS

### Study area

The study area is the city of Thessaloniki, where EYATH provides its services. Two areas in Thessaloniki were selected to implement the pilot research project. The first area under study is situated in the urban centre of Thessaloniki and the second one in Kalamaria, which is an eastern extension of the older, central, urban tissue of the city. These areas were selected in order to evaluate the new, available communication technologies in relation to the existing urban structure and its geomorphology.



**Figure 1.** Overview of the study area. Image on the left (image Landsat/Copernicus, data SIO, NOAA, U.S. Navy, NGA, GEBCO) and images on the right (image © 2019 TerraMetrics, image © 2019 CNES/Airbus, image © 2019 Maxar Technologies) are from Google Earth

### **Smart-Water infrastructure**

Smart water infrastructure requires the integration of a reliable telecommunication network to the existing infrastructure of the city for (a) transferring measurement data from the smart metering system to a system of data storage and data processing, as well as for (b) provisioning of smart services to the end-users (consumers & EYATH S.A.). Walk-by or drive-by wireless technologies don't provide high frequency recording rates. Also, they lack the ability to synchronise water pressure measurements with water demand measurements, which is required in the study of District Metered Areas (DMA). Walk-by or drive-by wireless technologies cannot lead to full exploitation of the capabilities the new metering devices have to offer. Moreover, the high cost of the latter cannot allow an insufficient technical exploitation. For their full exploitation a fixed telecommunication network is required.

A fixed telecommunication network is a fixed network of antennas. The location of the antennas in the network is of crucial importance for its effective operation. Geographic Information Systems (GIS) provide the opportunity of studying the antenna positioning in the area of interest, prior to implementing the positioning in the field, by utilizing visibility analysis tools. The selection of the antennas' location depends on the visibility coverage that can be achieved in the study area by installing the antennas at these locations. There have been various studies dealing with visibility analysis (Chmielewski and Tompalski, 2017; Caha and Kačmařík, 2017; Liu et al., 2010), studies focusing on visibility for telecommunication (Baek and Choi, 2018; Jewell, 2014) as well as on other issues such as landscape visual quality assessment (Štefunková and Cebecauer, 2006).

The approach of a fixed network of telecommunication antennas (Radiofrequency 868 MHz), which was scheduled to be constructed especially for this project, is to be applied. The fixed network will work in combination with smart water meters and smart valves. The initial thought was to choose scattered households in various areas within the city of Thessaloniki for installing the smart water meters and smart valves. But this would increase the cost of the project, since it would require the development of many telecommunication networks, which is not an objective of the current project. For this reason, two specific areas were selected from all over the city of Thessaloniki, the urban center and Kalamaria area. The former was selected because of its dense building construction patterns and its tall building, presenting particular difficulty regarding telecommunication coverage. The latter (Kalamaria) was selected due to the relative large household water consumption.

The project supports financially the installation of 100 smart water meters and 100 smart water valves where a smart water meter and a smart water valve consist a set of equipment for installation to a single consumer. To apply the sample of one hundred (100) consumers participating in the project, the specimen was divided into two parts, fifty (50) consumers in the city center and fifty (50) in the area of Kalamaria.

### **Visibility Analysis**

Positioning of the antennas is a crucial step in the implementation of the project. The aim of the visibility analysis was to detect locations, from which antennas are visible to an adequate extent in the study area.

Possible locations of the antennas were studied in the ArcGIS 10.6 environment. ArcGIS offers the possibility of applying different types of visibility analysis, eg. construct sight lines, generate viewsheds etc.

The visibility analysis selected in this study utilized: (a) a raster LIDAR DEM, depicting the terrain surface, including surface objects (buildings, trees etc) from EYATH SA and (b) user-determined



observer points, producing a raster identifying which observer points are visible from each raster surface location. It was applied through the “visibility tool”, which includes two (2) visibility analysis types: (a) frequency and (b) observers. The latter type was chosen because it provides more detailed information, i.e. which observers are visible from each raster surface location, while the former gives a more generalized result, i.e. the number of the observers each raster surface location is visible to, without more information about which of the observers. To all the observer points used here, information about the height of their location was derived from the available LIDAR of EYATH SA and an offset of 3m or 4m was set depending on each case (most offsets were set to 3m).

Several visibility analysis tests were applied in order to find the proper antenna positions. These tests were applied separately for each area (Thessaloniki centre and Kalamaria). In the areas, which were quite extended for 100 smart water meters and valves, further selection of districts was performed, so as the installed equipment would: (a) span in a continuous manner geographically and (b) be inside the visibility coverage of the antennas.

### **Selection of possible participants & Geocoding**

Apart from running the visibility analysis, a selection of possible participants of the pilot study was implemented. The selection was driven by using: (a) predetermined thresholds on the available consumption data in the case of private connections and (b) predetermined postal codes of consumers, in order to secure that consumers are situated inside a specified district in each subarea. The specified districts were selected considering the results of the visibility analysis, so as to have participant consumers inside the area presenting adequate antenna visibility.

A geocoding process was applied, in order to geolocate the previously selected data of possible participants. The geocoding process aimed at acquiring better overview of the geographical distribution of the possible consumer participants, which is to be used during their final selection. It was implemented in the ArcGIS 10.6 environment. Parameters utilized in the geocoding procedure were: (a) a table containing consumer data (name, address, postal code) and (b) an address locator which was previously created in the GIS department of EYATH SA.

Additionally, in the frame of the project, apart from the brand-new smart water meters which are to be installed, old technology, positive displacement, water meters are to be considered in order to exploit their ‘smart capability’, which is provided through the use of clip on (pulser) devices that can be adjusted on the water meter. These pulsers can convert consumption data into digital form and transmit it using radio frequency communication protocols, providing data in real time.

## **RESULTS AND CONCLUSION**

After various visibility tests, which were applied separately for the city centre and Kalamaria, five (5) positions for installing antennas were selected for the city centre and three (3) for Kalamaria. Their positions as well as the visibility results are shown in Figures 2-5.

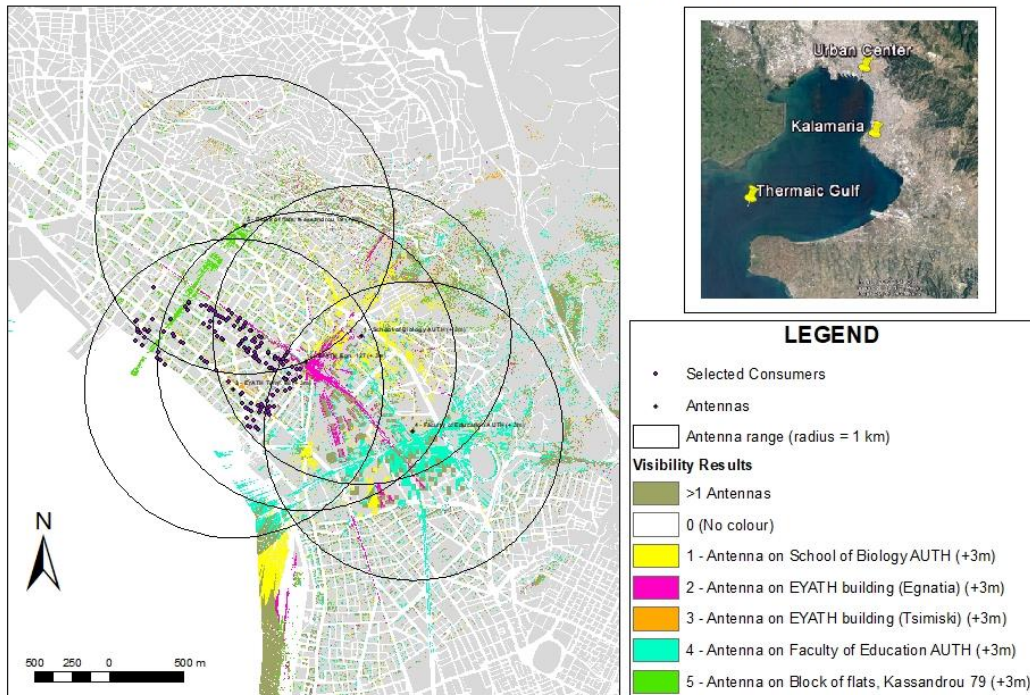
Based on predetermined criteria, 183 candidate consumer participants in the centre and 318 in Kalamaria were selected. They were all geocoded following the procedure presented in the previous section and proper manual editing was performed to the automatically generated results, when required.

The geocoding and the visibility results were superimposed as illustrated in Figures 2-5.

The visibility analysis allowed a better study of the positioning of the antennas. The product maps provided better overview of the geographic distribution of the consumers and the visibility coverage

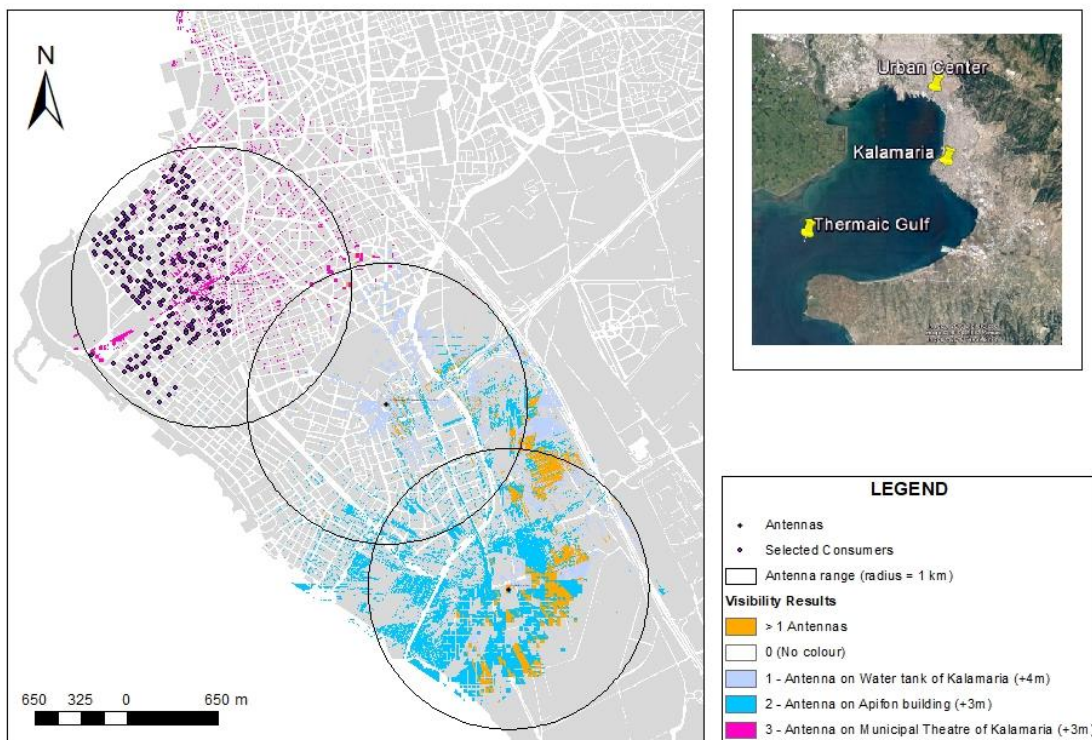
of the antennas. The product maps aided crucially establishing a well-designed implementation plan, in order to achieve improved financial viability and research product's output.

**"VISIBILITY" AND "GEOCODING" RESULTS FOR THE CENTRE OF THESSALONIKI**



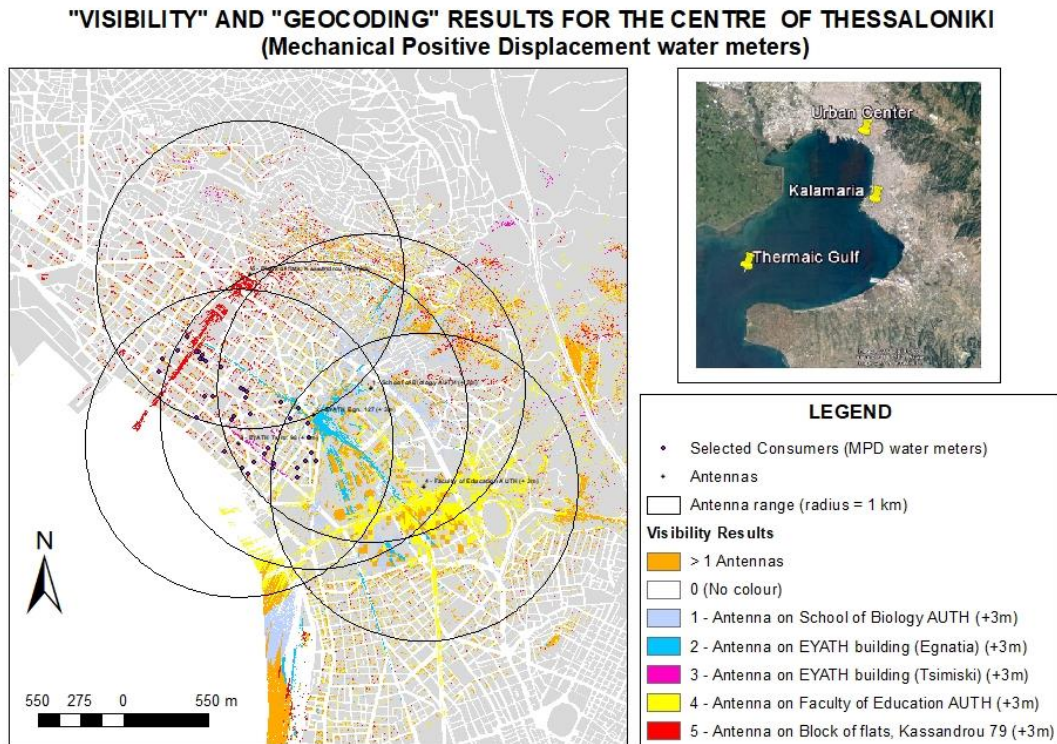
**Figure 2.** Product map depicting the results of the visibility analysis and geocoding processes for the centre of Thessaloniki. Satellite imagery: Google Earth (© 2019 Digital Globe, © 2019 CNES/Airbus, © 2019 TerraMetrics)

**"VISIBILITY" AND "GEOCODING" RESULTS FOR KALAMARIA**

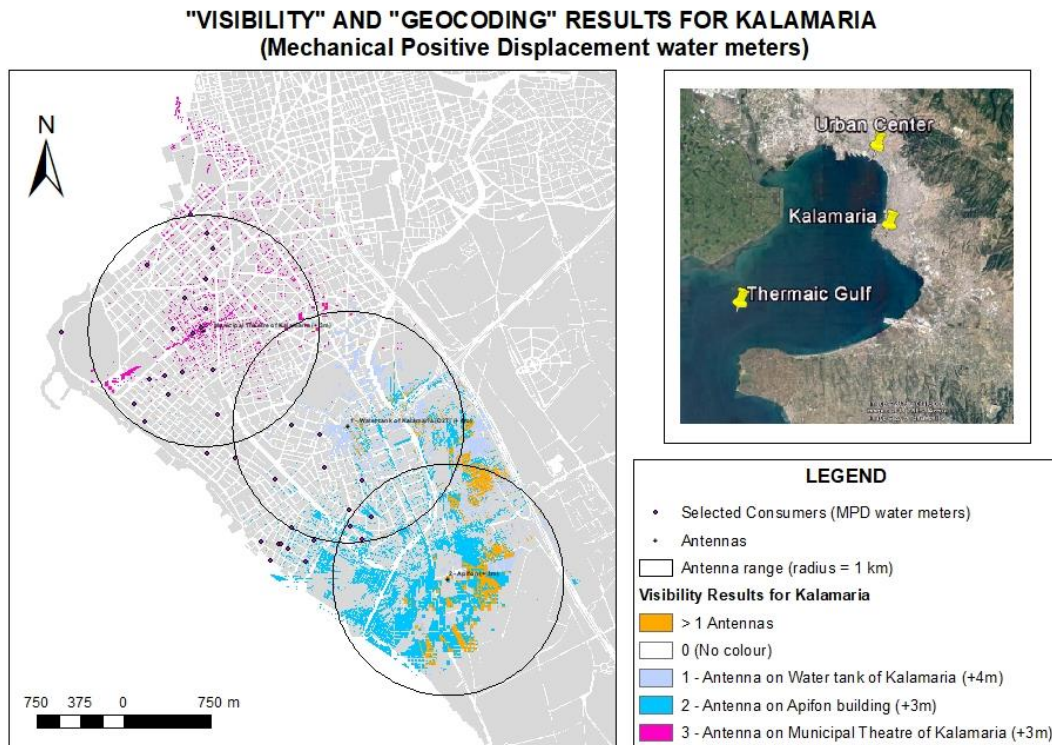


**Figure 3.** Product map depicting the results of the visibility analysis and geocoding processes for the area of Kalamaria. Satellite imagery: Google Earth (© 2019 Digital Globe, © 2019 CNES/Airbus, © 2019 TerraMetrics)





**Figure 4.** Product map depicting the results of the visibility analysis overlaid by the geocoding results of the consumers with mechanical positive displacement water meters for the area of Kalamaria. Satellite imagery: Google Earth (© 2019 Digital Globe, © 2019 CNES/Airbus, © 2019 TerraMetrics)



**Figure 5.** Product map showing the results of the visibility analysis overlaid by the geocoding results of the consumers with mechanical positive displacement water meters for the area of Kalamaria. Satellite imagery: Google Earth (© 2019 Digital Globe, © 2019 CNES/Airbus, © 2019 TerraMetrics)

## ACKNOWLEDGMENTS

This research has been co-financed by the European Union and Greek national funds through the Operational Program Competitiveness, Entrepreneurship and Innovation, under the call RESEARCH – CREATE – INNOVATE (project code: T1EDK- 04337).

## REFERENCES

- Baek, J., Choi, J. (2018) Comparison of Communication Viewsheds Derived from High-Resolution Digital Surface Models Using Line-of-Sight, 2D Fresnel Zone, and 3D Fresnel Zone Analysis. *ISPRS Int. J. Geo-Inf.*, **7**(8), 322.
- Caha, J., Kačmařík, M. (2017) Utilization of large scale surface models for detailed visibility analyses. *The International Archives of the Photogrammetry, Remote Sensing and Spatial Information Sciences*, **XLII-2/W8**, 5th International Workshop LowCost 3D – Sensors, Algorithms, Applications, 28–29 November 2017, Hamburg, Germany.
- Chmielewski, S., Tompalski, P. (2017) Estimating outdoor advertising media visibility with voxel-based approach. *Applied Geography*, **87**, 1-13.
- Herrera, M., Torgo, L., Izquierdo, J., Perez-Garcia, R. (2010) Predictive models for forecasting hourly urban water demand. *Journal of Hydrology*, **387**, 141-150.
- Jewell, V. R. (2014) Use of GIS in Radio Frequency planning and Positioning Applications, Virginia Polytechnic Institute and State University, Blacksburg, Virginia, USA.
- Liu, L., Zhang, L., Ma, J., Zhang, L., Zhang, X., Xiao, Z., Yang, L. (2010) An improved line-of-sight method for visibility analysis in 3D complex landscapes. *Sci. China Inf. Sci.*, **53**, 2185-2194.
- Štefunková, D., Cebecauer, T. (2006) Visibility analysis as a part of landscape visual quality assessment. *Ekológia (Bratislava)*, **25**, Suppl. 1, 229-239.
- Zhou, S. L., McMahon, T. A., Walton, A., Lewis, J. (2002) Forecasting operational demand for an urban water supply zone. *Journal of Hydrology*, **259**, 189-202.

# UV-Assisted Desalination of Seawater Using Titanium Dioxide Nanotube Doped Polyether Block Amide Membrane

F. U. Nigiz\* and M. E. Kibar\*

\* Chemical Engineering Department of Kocaeli University, Kocaeli, Turkey  
(E-mails: [filiz.ugurr@gmail.com](mailto:filiz.ugurr@gmail.com); [efgankibar@kocaeli.edu.tr](mailto:efgankibar@kocaeli.edu.tr))

## Abstract

In this study, a UV-assisted desalination system was prepared with a non-porous TiO<sub>2</sub> doped Pebax 1657 membrane. The membranes were characterized and desalination tests were performed. The effect of UV light and TiO<sub>2</sub> ratio on the performance of desalination were investigated. According to the results, TiO<sub>2</sub> incorporation increased the membrane hydrophilicity, increased the membrane swelling values, enhanced the membrane flux and improved the salt rejection. Moreover, UV treatment has a positive effect on desalination performance. The best improvement was achieved in the results of 10wt.% TiO<sub>2</sub> doped membrane. It was found that the flux value of the UV-treated membrane having 10wt.% TiO<sub>2</sub> concentration was 8.2 kg/m<sup>2</sup>.h and the salt rejection value was 99.97 %. It was found that the prepared membrane showed excellent desalination performance.

## Keywords

TiO<sub>2</sub> nano powder; Pebax 1657 membrane; desalination; non-porous membrane

## INTRODUCTION

Photocatalytic oxidation of organic compounds for desalination and water treatment is one of the most interesting topics in recent years. The activity of this reaction depends on the process and the photocatalyst type. There are two main process configurations as a process with free catalyst and the process where the catalyst immobilized on a support. The activity of the catalyst used in the free state is high, but after the water treatment, it is necessary to remove the catalyst in order not to poison the pure water. The use of photocatalytic membrane reactors (PMR) restricts the reduction of photocatalytic activity and ensures that the freshwater is not poisoned by the photocatalyst (Argurio et al., 2018; Zheng et al., 2017). Membrane usage prevents the passage of catalyst and depredated compounds into the purified water side. Additionally, the use of photocatalytic membrane reactors eliminates the use of further separation step such as sedimentation-coagulation-flocculation, which will then be used to separate the photocatalyst. furthermore, it reduces the total process volume and enables the reuse of the catalyst. The heat energy which is necessary for the reaction and separation can be provided by the UV in daylight. Therefore, PMR system is defined as an energy-saving and cost-effective purification process (Mozia, 2010; Molinari et al., 2017).

The photocatalytic membrane has been recently developed for a wide range of application (Ye et al., 2019; Argurio et al., 2018; Zheng et al., 2017). Biological treatment of organic content water, seawater desalination, and wastewater treatments are most know application areas of photocatalytic membranes. Mechanical properties and selective separation capability of membranes can be destroyed by the cumulation of organic pollutants in seawater. Therefore, photo catalytically eliminating of organic pollutants may be improved both structural properties and separation performance of membranes (Yacou et al., 2015).

Membrane technology is emerging science for advanced water treatment. Membranes are mostly used for water purification, waste-water treatment, and desalination purposes. The productivity and

overall performances of membrane-based processes are directly related to the physicochemical properties of membranes. Therefore, scientific studies have been focused on the development of high-performance membrane materials. Especially for water treatment, it is important to produce superior membranes having high water permeability, high rejection capacity, biofouling resistance, and process stability. For this purpose, new generation composite membranes have been developed.

In this study, it is aimed to develop new material for UV-assisted desalination of seawater. For this purpose, titanium dioxide nanotube ( $\text{TiO}_2$ ) doped polyether block amide (PEBA-Pebax1657 (commercial name)) membrane has been produced.  $\text{TiO}_2$  is the most widely used photocatalyst.  $\text{TiO}_2$  is a semiconducting material that destroys the organic contaminant in the water by the assistance of UV-light (Mayyahi, 2018; Yacou et al., 2015, Salcova et al., 2016). However, because the energy band of  $\text{TiO}_2$  is large, it is not active in daylight. Since the UV content in daylight does not exceed 5 %. Therefore, the UV source is required for a photocatalytic activation. In this study, the desalination system has been utilized by assisting UV light. The structural property of the composite membrane has been investigated by means of Fourier Transform Infrared Spectroscopy and X-Ray Diffraction. The distribution of  $\text{TiO}_2$  particles within the membrane has been analyzed using Polarized Electron Microscopy. Swelling experiments have been performed to determine the water-uptake capacity of the  $\text{TiO}_2$  filled and unfilled Pebax1657 membrane. The separation performance of membranes with/without  $\text{TiO}_2$  nanotube was investigated to separate water seawater. Desalination test has been conducted at the room temperature with/without UV light. The effect of  $\text{TiO}_2$  concentration, UV light were investigated.

## EXPERIMENTAL

### Titanium dioxide nanotube preparation

1 gram of commercial titanium dioxide powder (ACROS) was mixed with 10 M sodium hydroxide solution. The mixture was subjected in an ultrasonic bath for 30 minutes. The mixture was left for hydrothermal treatment at 130 °C for 24 hours in a Teflon lined autoclave. After filtration, the nanotube titanium dioxide was washed with hydrochloric acid and water. Nanotube titanium dioxide was dried at 110 °C for 16 hours and calcined at 500 °C for 2 hours.

### Membrane Preparation

Polyether block amide (Pebax 1657) was kindly supplied from Arkema, France. 10 wt.% of Pebax-acetic acid solution was prepared and stirred until the solution became homogeneous. The determined amount of  $\text{TiO}_2$  nanotube particles were added to Pebax solution according to the weight of the dry Pebax polymer. According to the Pebax content,  $\text{TiO}_2$  concentration in the membrane solvent was changed from 0 to 10wt.%. Membranes were entitled according to the  $\text{TiO}_2$  content in the membrane. Pebax-0 represents the membrane without filler, Pebax-2.5T represents the membrane having 2.5wt.% of  $\text{TiO}_2$  nanotube particles. Membrane solutions were cast onto a Teflon plate and allowed to dry at the room temperature. Then, membranes were cured in a vacuum oven at 60 °C. The membrane was then immersed in a solution containing 2vol.% of Tolylene-2,4-diisocyanate-hexane solution to prevent the dissolving of the membrane in water media.

### Swelling experiment

Swelling experiments were performed to determine the affinity of membranes to the water. The swelling test was continued for approximately 4 hours until the membrane reached a constant weight. For the swelling experiment, membranes cut into equal size (1 cm<sup>2</sup>) and were soaked in deionized water. The dry ( $M_d$ ) and swollen ( $M_s$ ) weights of membranes were measured and the swelling percentages (S) were determined as the following equation;

$$S (\%) = \frac{M_s - M_d}{M_d} * 100, \quad (1)$$

### Desalination

Desalination test were carried out at the ambient condition. Prior to desalinate a seawater, separation capabilities of membranes were tested to separate water from seawater. Water removal and water flux were calculated from Equation 2 and Equation 3 which are shown as follow;

$$R(\%) = \frac{C_i - C_f}{C_i} * 100 \quad (2)$$

$$F = \frac{M}{t.A} \quad (3)$$

Where  $M$  (kg) is the weight of permeate water on the downstream side of the membrane,  $t$  is the operating time (h),  $A$  is the effective membrane area ( $m^2$ ),  $C_i$  and  $C_f$  represent the initial and final total dissolved solid concentration of water. Total dissolved solids and ion concentrations were analyzed using Multi-Functional Conductometry (Seven Compact-Mettler Toledo). The seawater desalination test was conducted under UV light and effect of UV on desalination was investigated.

### Characterization

The crystalline phases were characterized by means of X-ray diffraction (XRD) (Rigakku, Miniflex 2, Japan).  $2\theta$  values were selected from  $10^\circ$  to  $80^\circ$  with a step size of 0.02 using Cu  $K\alpha$  radiation ( $\lambda = 0.15418$  nm) at 45 kV/40 mA. Fourier Transform Infrared Spectroscopy was used to determine the chemical structure of the membrane in the wavelength range from  $650\text{ cm}^{-1}$  to  $4000\text{ cm}^{-1}$  (Perkin Elmer-ATS). Surface hydrophilicity properties of membranes were determined using contact angle measurements (Attension).

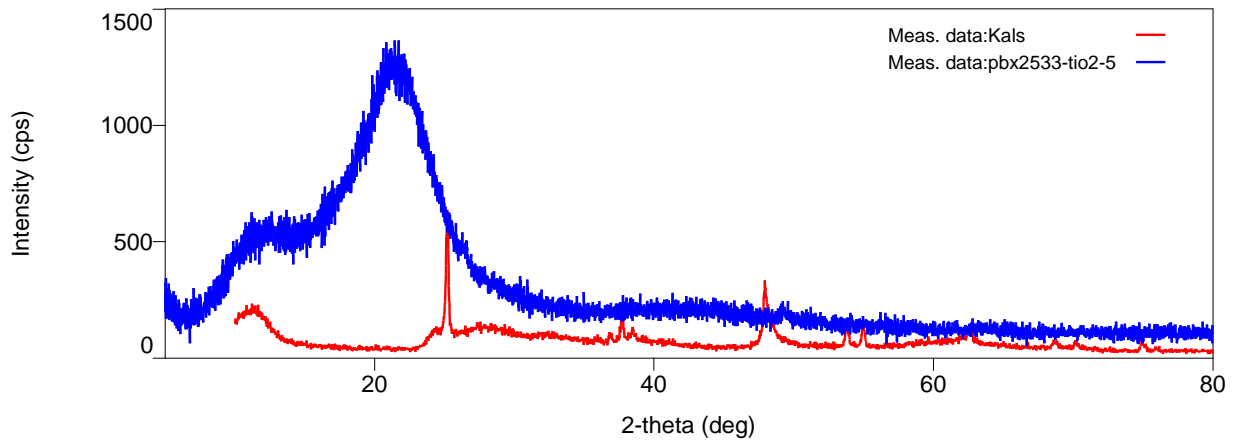
## RESULTS

The prepared membranes were characterized in order to determine physical, chemical and morphological properties. In Figure 1, the XRD spectra of pure nanotube  $TiO_2$  and nanotube  $TiO_2$  doped membrane are given. The characteristic peaks of anatase phase obtained at two theta  $25.1^\circ$ ,  $36.9^\circ$ ,  $37.7^\circ$ ,  $38.4^\circ$ ,  $47.9^\circ$ ,  $53.7^\circ$  and  $54.9^\circ$  degrees. The characteristic peaks are determined at  $12.3^\circ$  and  $21.4^\circ$  for Pebax

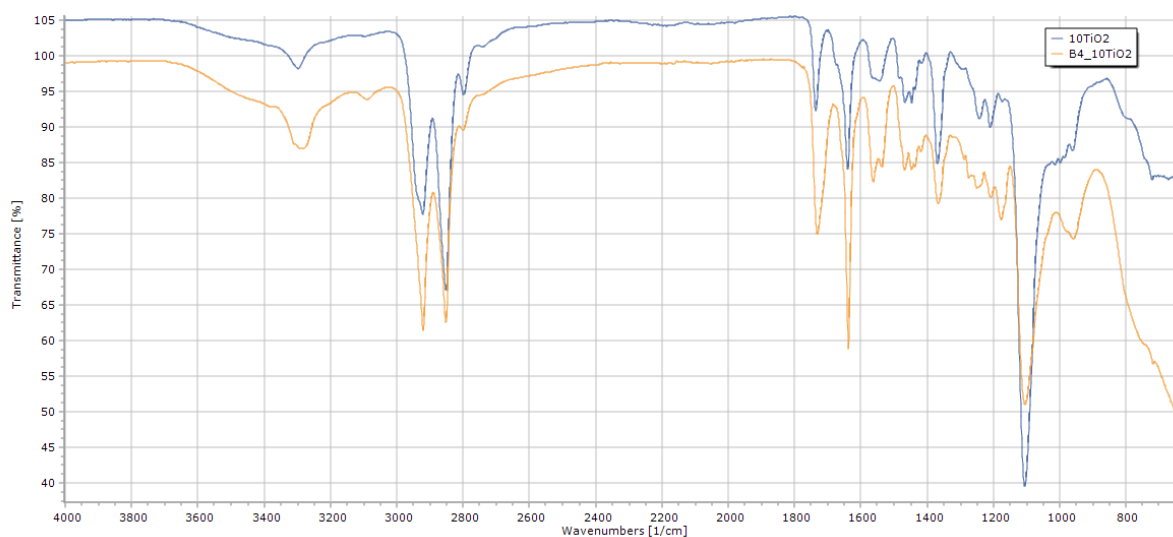
In literature Pebax is defined as a semi-crystalline polymer which shows diffraction peaks at two theta  $14^\circ$ ,  $17^\circ$  and  $26^\circ$ . (Sridhar et al., 2008). As seen from the figure that there are no crystalline phases obtained from nanotube doped PEBAX this phenomenon can be explained by the chemical interaction of Pebax with nanotube  $TiO_2$  that nanotubes affected the bonds and an amorphous phase was formed.

The FTIR analysis of  $TiO_2$  nanoparticle doped Pebax1657 membrane is given in Figure 2. The band at  $1107$  and  $1733\text{ cm}^{-1}$  are attributed to the C—O—C and —C=O stretching vibrations, respectively. Also, another 2 bands at  $1638$  and  $3303\text{ cm}^{-1}$  are assigned to the presence of H—N—C=O and N—H groups, in the hard Polyamide (PA) segment, respectively. In FTIR spectra of Pebax, it seems that PA block of Pebax is significantly self-associated via hydrogen bonding. For  $TiO_2$ , in Figure, the bands which observed in the range of  $650$  to  $800\text{ cm}^{-1}$  are related to the stretching vibrations of Ti—O—Ti and Ti—O groups on the surface of  $TiO_2$  nanoparticles (Cheshomi et al., 2018).





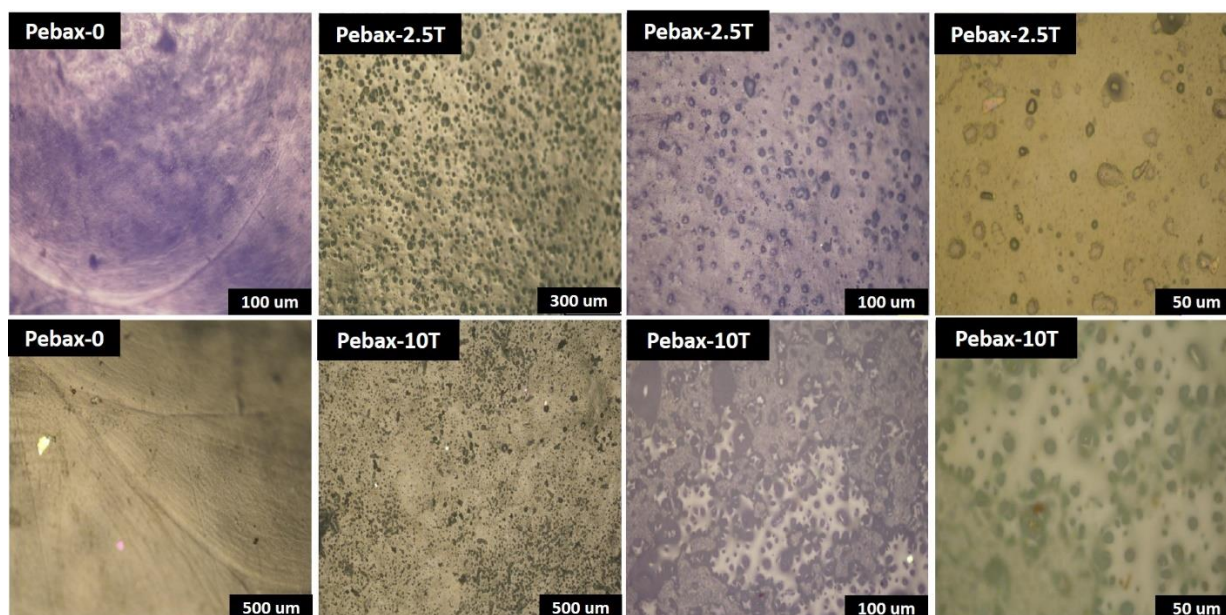
**Figure 1.** XRD patterns of Pebax-TiO<sub>2</sub> membrane and pure TiO<sub>2</sub>



**Figure 2.** FTIR spectra of Pebax-TiO<sub>2</sub> membrane and pure TiO<sub>2</sub>

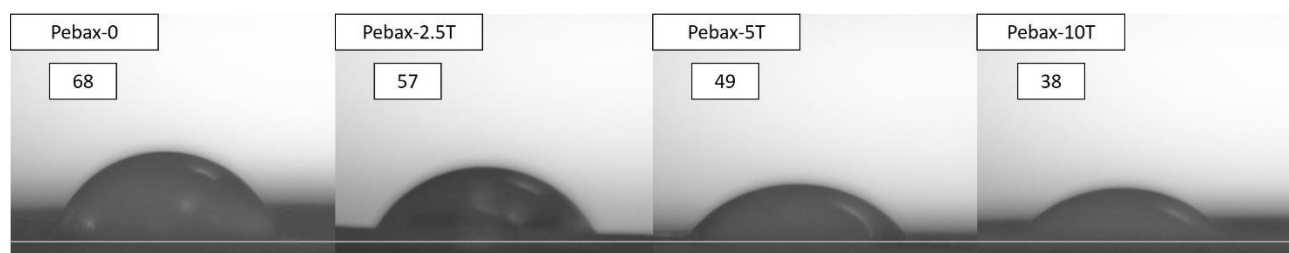
Figure 3 shows the distribution of TiO<sub>2</sub> particles in the membrane. In the first picture represented the pebax1657 membrane without filler, the smooth, dense structure of the membrane can be clearly observed except some impurity in the surface. The membrane has a non-porous structure. The POM images of 2.5wt.% of TiO<sub>2</sub> loaded membrane indicated that the distribution of the particles within the membrane is excellent. TiO<sub>2</sub> particles have been homogeneously dispersed within the Pebax1657 matrix. Homogeneous distribution of the additive into membranes is very important in terms of providing the same physical and chemical properties in every region on the membrane. Homogeneous dispersion means uniform separation performance across the membrane. As it is known, there are electrostatic interactions between particles, such as TiO<sub>2</sub>, which tend to connect with each other. In this study, the particles were first separated from each other by the sonication process, then the priming method was used to provide homogeneous distribution (Nigiz, 2018). Thus, agglomeration was tried to be prevented. Agglomeration within the membrane was rarely observed even with high TiO<sub>2</sub> addition (wt.10%). However, it is still possible to see cumulated TiO<sub>2</sub> particles in a particular area (Figure 2). This is due to the orientation of the particles in the drying step of the membrane. During the casting-evaporation step, the membranes were first dried at the room conditions. The TiO<sub>2</sub> particles might be orientate at this stage.





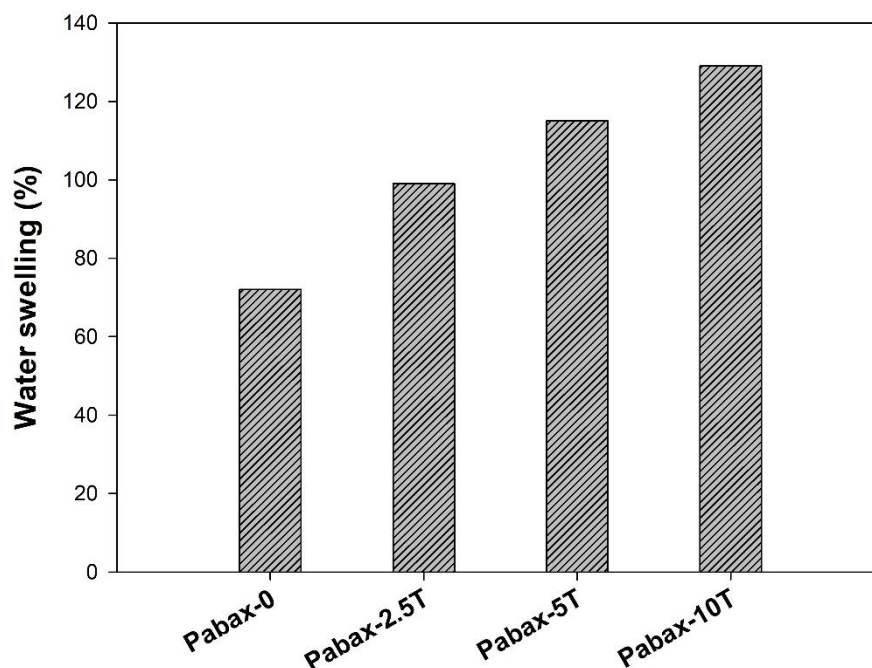
**Figure 3.** Polarized Electron Microscopy images of the pristine and  $\text{TiO}_2$  loaded membranes

The contact angle between the membrane surface and water droplet is illustrated in Figure 4. It is clear that the water contact angle decreases with increasing  $\text{TiO}_2$  ratio in the membrane. This is meant that the hydrophilicity of the membrane enhanced with  $\text{TiO}_2$  addition. Owing to the hydrophilicity of  $\text{TiO}_2$  particles the surface water affinity of the membrane enhanced as also reported by Huang et al. (2017). According to the results obtained from the contact angle experiments, water flux is expected to increase as  $\text{TiO}_2$  ratio increases in the membrane matrix. There are also many studies on the use of  $\text{TiO}_2$  in the membrane matrix to enhance the surface hydrophilicity and flux, as well (Du et al., 2017; Pan et al., 2019).



**Figure 4.** Contact angle images of the pristine and  $\text{TiO}_2$  loaded membranes

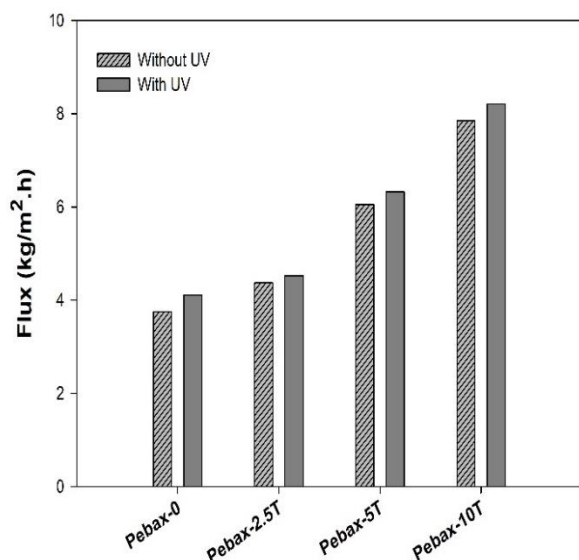
Figure 5 shows the water affinity of the pristine and  $\text{TiO}_2$  nanotube loaded membranes in terms of the swelling experiment. The increasing  $\text{TiO}_2$  nanotube ratio remarkably enhanced the water swelling ratio. The swelling values of the membrane increased from 72 % to 129 % when the  $\text{TiO}_2$  ratio was increased from 0wt.% to 10wt. %. This is due to the hydrophilic character of  $\text{TiO}_2$  nanotube particles which was also confirmed by the results of water contact angle experiments. It was reported that  $\text{TiO}_2$  nanotube particles especially the nano-sized  $\text{TiO}_2$  nanotube has an affinity to water (Bolis et al., 2012).



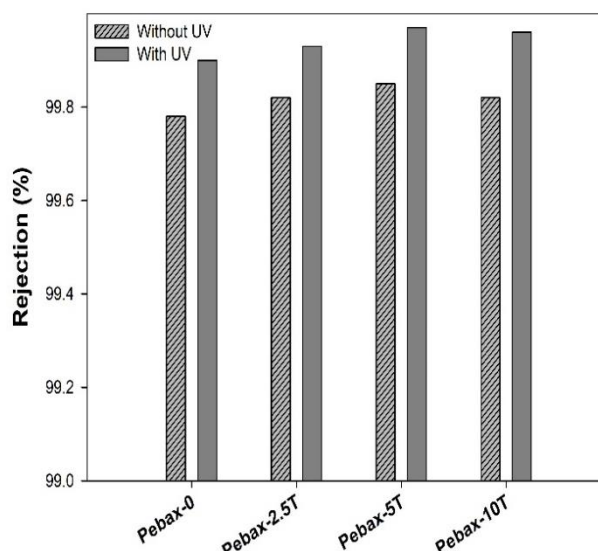
**Figure 5.** Swelling results of the membranes

Desalination results in the system with/without UV lamps are given in Figure 6 as a function of flux and rejection. In order to investigate the effect of  $\text{TiO}_2$  nanotube addition, desalination experiment of the pristine Pebax1657 (Pebax-0) was also performed. As can be seen from the figure, increasing  $\text{TiO}_2$  ratio improved flux values significantly. In the pristine membrane,  $4.11 \text{ kg/m}^2\cdot\text{h}$  flux value was obtained while  $8.2 \text{ kg/m}^2\cdot\text{h}$  flux was obtained with 10wt.%  $\text{TiO}_2$  nanotube loaded membrane when the separation occurred in UV assisted system. As it was confirmed by the results of surface hydrophilicity and swelling degree, the water permeability was increased due to the hydrophilic character of  $\text{TiO}_2$  nanotube particles. At the same time, it was also found that UV usage has little effect on the flux results. In the pristine membrane,  $3.75 \text{ kg/m}^2\cdot\text{h}$  flux was obtained in the system without using UV light and this value increased to  $4.11 \text{ kg/m}^2\cdot\text{h}$  when UV light was used.

There may be several reasons for this slight difference. In the present study, the usage of UV light caused a temperature increment about  $7 \text{ }^\circ\text{C}$ . The increasing temperature increased the vapor pressure, the solubility of the water on the membrane surface and the diffusivity of the water. Consequently, driving force across the membrane increased and the flux enhanced. The other reason is related to the UV effect on organic compounds in seawater. By using UV light,  $\text{TiO}_2$  was activated and the degradation of big molecules into small molecular sizes might prevent the surface cake formation. Therefore, flux decrement due to the boundary layer problem could be prevented. This effect could become more effective in long-period separation experiments. Another reason could be related to antimicrobial effect of  $\text{TiO}_2$  on bacteria, microbial and other substances in seawater. These substances also cause a cake formation on the membrane surface.  $\text{TiO}_2$  is known as anti-microbial chemicals that prevent biological contamination on the membrane surfaces.



**Figure 6.** Flux results of membranes



**Figure 7.** Rejection results of membranes

The effect of TiO<sub>2</sub> ratio on the salt rejection of desalination process performed with/without UV light is seen in Figure 7. All Pebax-based membranes show a high salt rejection value above 99.78 %. TiO<sub>2</sub> incorporation into membrane appears to increase salt rejection. The possible reason for these minor differences is that the TiO<sub>2</sub> particles extend the tortuous pathway, increase the water affinity of the membrane, and increase the ion rejection by electrostatic interaction. The higher salt rejection values are seen in the system where UV lamp is used. This should be attributed to the retention of ions by TiO<sub>2</sub> which generates radicals by the UV activation. The highest salt rejection value was obtained as 99.97 % with 10wt.% of TiO<sub>2</sub> loaded membrane.

## CONCLUSIONS

In this study, TiO<sub>2</sub> nanotube incorporated Pebax1657 non-porous membranes were produced. The produced membranes were characterized and the desalination performance of the pristine and nanocomposite membranes was carried out at the room temperature. General experimental results can be summarized as;

- The compatibility of Pebax1657 polymer and TiO<sub>2</sub> nanotube particles was excellent and the TiO<sub>2</sub> nanotube particles were homogeneously dispersed in the matrix.
- TiO<sub>2</sub> nanotube incorporation was found to increase both the surface and structural hydrophilicity of the membrane. The swelling values of the membrane increased from 72 % to 129 % when the TiO<sub>2</sub> ratio was increased from 0wt.% to 10wt. %.
- TiO<sub>2</sub> nanotube addition enhanced the flux from 4.11 kg/m<sup>2</sup>.h to 8.2 kg/m<sup>2</sup>.h and the salt rejection from 99.90 % to 99.97 %.
- Both the flux and salt rejection values were improved with the assisted of the UV-light.

## REFERENCES

- Al Mayyahi, A. (2018) TiO<sub>2</sub> Polyamide Thin Film Nanocomposite Reverses Osmosis Membrane for Water Desalination. *Membranes*, **8**, 66-76.
- Argurio, P., Fontananova, E., Molinari, R., Drioli, E. (2018) Photocatalytic Membranes in Photocatalytic Membrane Reactors, *Processes*, **6**, 162.
- Bolis, V., Busco, C., Ciarletta, M., Distasi, C., Erriquez, J., Fenoglio, I., Livraghi, S., Morel, S. (2012) Hydrophilic/hydrophobic features of TiO<sub>2</sub> nanoparticles as a function of crystal phase, surface area and coating, in relation to their potential toxicity in peripheral nervous system.

*Journal of Colloid and Interface Science*, **369**, 28-39.

- Cheshomi, N., Pakizeh, M., Namvar-Mahboub, M. (2018) Preparation and characterization of TiO<sub>2</sub>/Pebax/(PSf-PES) thin film nanocomposite membrane for humic acid removal from water. *Polym Adv Technol.*, **29**, 1303-1312.
- Du, Y., Li, Y., Wu, T. (2017) A superhydrophilic and underwater superoleophobic chitosan–TiO<sub>2</sub> composite membrane for fast oil-in-water emulsion separation. *RSC Adv.*, **7**, 41838-41846.
- Huang, L., Jing, S., Zhuo, O., Meng, X., Wang, X. (2017) Surface Hydrophilicity and Antifungal Properties of TiO<sub>2</sub> Films Coated on a Co-Cr Substrate. *BioMed Research International*, Article ID 2054723.
- Molinari, R., Lavorato, C., Argurio, P. (2017) Recent progress of photocatalytic membrane reactors in water treatment and in synthesis of organic compounds. A review. *Catalysis Today*, **281**, 144-164.
- Mozia, S. (2010). Photocatalytic membrane reactors (PMRs) in water and wastewater treatment. A review. *Separation and Purification Technology*, **73**, 71-91.
- Nigiz, F. U. (2018) Preparation of high-performance graphene nanoplate incorporated polyether block amide membrane and application for seawater desalination. *Desalination*, **433**, 164-171.
- Pan, Z., Cao, S., Li, J. Du, Z., Cheng, F. (2019) Anti-fouling TiO<sub>2</sub> nanowires membrane for oil/water separation: Synergetic effects of wettability and pore size. *Journal of Membrane Science*, **572**, 596-606.
- Solcova, O., Spacilova, L., Maleterova, Y., Morozova, M., Ezechias, M., Kresinova, Z. (2016) Photocatalytic water treatment on TiO<sub>2</sub> thin layers. *Desalination and Water Treatment*, **57**(25), 11631-11638.
- Sridhar, S., Smitha, B., Suryamurali, R., Aminabhavi, T. M. (2008). Synthesis, Characterization and Gas Permeability of an Activated Carbon-Loaded PEBAX 2533 Membrane. *Designed Monomers & Polymers*, **11**(1), 17-27.
- Yacou, C., Smart, S., Diniz da Costa, J. C. (2015). Mesoporous TiO<sub>2</sub> based membranes for water desalination and brine processing. *Separation and Purification Technology*, **147**(16), 166-171.
- Ye, G., Yu, Z., Li, Y., Li, L., Song, L., Gu, L., Cao, X. (2019) Efficient treatment of brine wastewater through a flow-through technology integrating desalination and photocatalysis. *Water Res.*, **157**, 134-144.
- Zheng, X., Shen, Z. P., Shi, L., Cheng, R., Yuan, D.H. (2017) Photocatalytic Membrane Reactors (PMRs) in Water Treatment: Configurations and Influencing Factors. *Catalysts*, **7**(8), 224-231.

# Determination of the Ecological Risk of Deterioration in the Water Flow of the Udy River Basin of Kharkiv Region, Ukraine

O. Rybalova\*, S. Artemiev\*, I. Yermakovych\*, H. Korobkova\*\* and I. Kyrpychova\*\*

\* Department of Labor Protection and Technogenic-Ecological Safety, National University of Civil Defence of Ukraine, 94 Chernyshevska str., Kharkiv, Ukraine, 61023 (E-mails: *iryana.yermakovych@gmail.com*; *olga.rybalova@nuczu.edu.ua*; *artemev.1967@nuczu.edu.ua*)

\*\* Department of ecology and life safety, Luhansk National Agrarian University, 68 Slobozhanska str., Starobilsk, Ukraine (E-mails: *korobkova.ann@gmail.com*; *k-ir@i.ua*)

## Abstract

The new method for assessment of the ecological risk of deterioration of a surface waters condition was presented. The methodology for assessment of the risk of the water ecosystem well-being disruption is based on the determination of all parameters of the state of quality of surface waters that exceed the ecological standards using the probit-regression model. The process of determining the ecological risk for watercourses of the Udy river basin in Kharkiv region showed a high level of danger to the well-being of the water ecosystem. Ranking of the observation posts for the quality status of the Udy river in terms of the ecological risk makes it possible to identify the most polluted river sections.

## Keywords

Ecological risk; river basin; rational use of water; water protection measures; surface waters; Kharkiv region; Udy river

## INTRODUCTION

The current state of surface waters requires the development of new scientific tools to prioritize the implementation of environmental protection measures. One of the most effective methods for determining the level of environmental hazard is an ecological risk assessment.

Method of assessment the ecological risk for disturbing the well-being of an aquatic ecosystem, presented in this paper, is based on the determination of ecological standards. The necessity of scientific substantiation of the permissible limit of anthropogenic impact on the qualitative condition of surface waters determines the relevance of this development. The implementation of the method for assessing the ecological risk of disturbing the well-being of an aquatic ecosystem is performed on determining the excess of ecological standards. The purpose of development of this method is to increase ecological safety and rational use of natural resources.

The Udy River basin has a transboundary significance and flows through the territory of a large industrial center of Ukraine. The region in general characterized by high anthropogenic pressures in many components of the environment. This is confirmed in different research papers (Vasenko et al., 2006; Vystavna et al., 2018; Vystavna et al., 2019), where the contamination of Udy river is affected on even groundwater and urban springs. Therefore, determination of implementation of environmental measures prioritization based on the assessment of such ecological risk is a very relevant task in Kharkiv region.

## ANALYSIS OF RECENT STUDIES

Many scientific studies are devoted to determination of surface waters pollution level, in particular in the field of ecological risk assessment. (Hofmann et al., 2015; Keese, 2010; Gov.uk, 2011; Tsybulskiy, 2015; Levenets et al., 2017).

Generalized ecological risk comes down to two types:

- the risk of contravention sustainability of ecosystems as a result of actual or potential environmental pollution;
- the risk to public health is the probability of adverse health effects on human (Vasenko et al., 2015).

Currently, there is a large number of well-known methods for assessing the risk to public health, but in the majority of cases, they are based on sanitary and hygienic standards, limit (safe) values (Epa.gov, 2016).

The approaches to assessment of water bodies' quality based on the determination of Threshold Limit Value (TLV) or Maximum Permissible Concentrations (MPC) do not adequately reflect the state of the aquatic ecosystem. Therefore, the using of such limit values in the calculations of ecological risk is not correct. Although the measurement units of the level of environmental safety can be indicators, what characterizes the state of human health. There is the problem in determination of the deterioration risk of aquatic ecosystems.

The method for assessing ecological risks appeared from the impact of pollution sources on water bodies (Oehha.ca.gov, 2016) is based on the processing of data collected using a specially developed express scheme of field studies based primarily on biological data. The expert analysis of the characteristics of receptors and risk indicators, the size of anthropogenic pressure and possible threats to the aquatic ecosystem is applied at the level of detailed risk assessment. There are well known methods for assessment of the ecological risk for water bodies, based on the biological sensitivity and the response of certain organisms (Salem et al., 2016), as well as methods for the probable distribution of the species sensitivity (SSD) (Afanasyev and Grodzinskiy, 2004; Romanenko et al., 2009).

Ecological risk assessment using SSD reflects the probability that observed concentrations will exceed critical ones for organisms. Research (Afanasyev and Grodzinskiy, 2004; Romanenko et al., 2009) was showed that probable results reflect empirical information well enough, so this method is valuable as an addition to more traditional approaches for calculating risks (EPA, 1994; Gottschalk and Nowack, 2012).

The disadvantage of the above mentioned methodological approaches is laboriousness, unequal conditions in aquatic ecosystems and the reaction of organisms, as well as the need to perform the additional hydrobiological studies with the involvement of leading experts.

In Directive 2000/60 / EC (EU WFD, 2006) it was proposed to carry out the risk assessment of priority substances, identified in accordance with Article 16 (2) and listed in Annex X. Currently, not all substances including those listed in Annex X are controlled and can be provided by official data of monitoring studies. This indicates the need to implement the risk assessment systems that will be provided by the existing monitoring system and statistical reporting.

**The aim of this research is** determination in prioritization of environmental measures implementation based on the assessment of the ecological risk of the aquatic ecosystems deterioration with consideration of established environmental standards.



## RESEARCH METHODS

The paper (Rybalova and Artemiev, 2017) is proposed the method of the ecological risk assessment of the aquatic ecosystem deterioration based on the determination of environmental standards with consideration of the landscape and geographical features of river basins.

In case of absence of environmental standards in the work, it is proposed to use the upper limit of the 3 categories of surface water quality classification as a threshold value. This corresponds to class II in good condition according to the procedure. It is believed that if the ecological standard is exceeded, there is a risk of disturbing the well-being of the aquatic ecosystem. (Vasenko et al., 2016). Our article is proposed to use the methodology of ecological assessment of surface water quality for the relevant categories (Romanenko et al., 1998; Korobkova, 2016).

The value of the ecological index of water quality is determined by the following formula (Romanenko et al., 1998; Korobkova, 2016):

$$I_e = \frac{(I_1 + I_2 + I_3)}{3}, \quad (1)$$

where  $I_1$  – contamination index of salt components;  $I_2$  – trophic-saprobiological index (ecological sanitation) indicators;  $I_3$  – index of specific indicators of toxic and radiation exposure.

At the second stage, ecological standards are determined according to the method presented in the article (Vasenko et al., 2016).

During developing ecological standards, it is necessary to apply a landscape-ecological approach, taking into account the geographical location, the dynamics of the formation and functioning of natural systems, their diversity and at the same time individual uniqueness, sustainability to climatic changes, natural and anthropogenic impacts (Vasenko et al., 2016).

Ecological standards can be individual (for specific and unique objects) and typical; promising and potentially possible (taking into account the latest technologies and trends), relatively stable (long-lasting) and operational (taking into account situational changes), acceptable and optimal (targeted). Ecological standards are scientifically based values of indicators (hydromorphological, hydrophysical, hydrochemical, hydrobiological, microbiological, radiation) of aquatic ecosystems, which reflect a good ecological condition of a water body. Ecological standards are established on a basis of analysis of the results of processing materials from previous hydrological, hydrochemical, hydrobiological, ecological toxicological and radioecological expeditionary research and regime observations. This is the fundamental difference between ecological standards for surface water quality and water use safety standards (threshold limit value (TLV)) for certain hazardous substances (Vasenko et al., 2017).

The risk of the well-being disturbing of an aquatic ecosystem (ER) is estimated by determining probits based on the following equation (Rybalova et al., 2018):

$$Prob = -2,3 + 2,21 \lg \sum \left( \frac{C_i}{C_{EHi}} \right), \quad (2)$$

where  $C_i$  – concentration of  $i$ -th substance in the water body,  $\text{mg}/\text{dm}^3$ ;  $C_{EHi}$  – ecological standard for the  $i$ -th substance in water body,  $\text{mg}/\text{dm}^3$ .

**Table 1.** Normal-probabilistic distribution with interconnection of probits and risk

Prob	ER	Prob	ER
-3.0	0.001	0.1	0.540
-2.5	0.006	0.2	0.579
-2.0	0.023	0.3	0.618
-1.9	0.029	0.4	0.655
-1.8	0.036	0.5	0.692
-1.7	0.045	0.6	0.726
-1.6	0.055	0.7	0.758
-1.5	0.067	0.8	0.788
-1.4	0.081	0.9	0.816
-1.3	0.097	1.0	0.841
-1.2	0.115	1.1	0.864
-1.1	0.136	1.2	0.885
-1.0	0.157	1.3	0.903
-0.9	0.184	1.4	0.919
-0.8	0.212	1.5	0.933
-0.7	0.242	1.6	0.945
-0.6	0.274	1.7	0.955
-0.5	0.309	1.8	0.964
-0.4	0.345	1.9	0.971
-0.3	0.382	2.0	0.977
-0.2	0.421	2.5	0.994
-0.1	0.460	3.0	0.999
0.0	0.50	–	–

At the third stage, in accordance with a principle of the normal-probabilistic distribution, for value of Prob, the corresponding value of the ecological risk of deterioration of water bodies is established.

At the fourth stage, the total ecological risk of water bodies deterioration is determined by the formula (Vasenko et al., 2015):

$$ER = 1 - (1 - ER_1) \times (1 - ER_2) \times \dots \times (1 - ER_n), \quad (3)$$

where  $ER$  – summarized ecological risk of deterioration of water bodies;  $ER_1, \dots, ER_n$  – ecological risk of each pollutant substances.

At the fifth stage, the characteristic of the ecological risk of water bodies' deterioration is given. In the interpretation of the obtained values of ecological risk it is proposed to use the following rank scale.

The classification of water bodies according to the ecological risk (Table 2) allows determining their suitability for water use. This is an important for the implementation of an iterative approach to the management of water protection activities.



**Table 2.** Characteristics of surface water quality by the value of the ecological risk

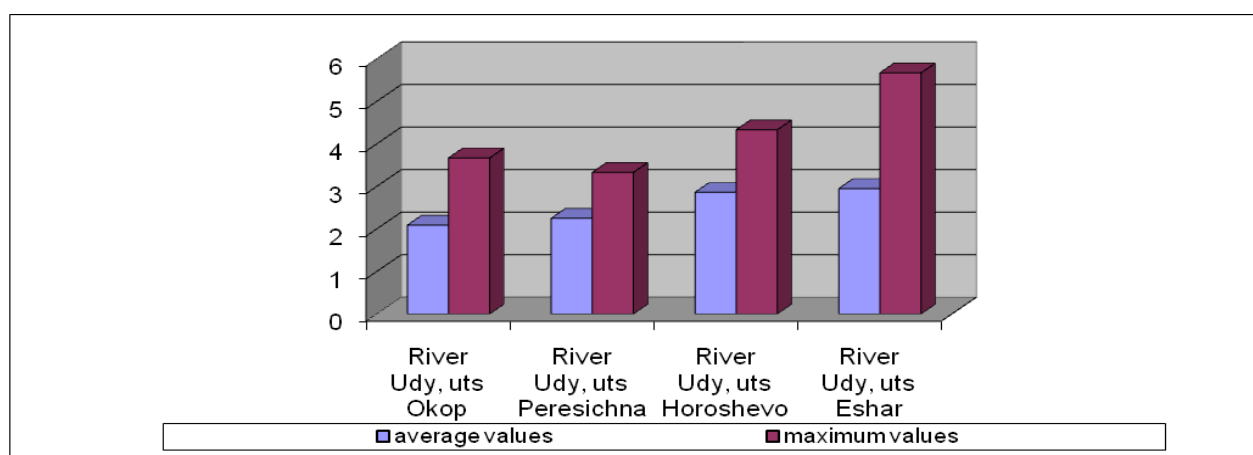
Water quality class	The value of ecological risk indicator (ER)	Qualitative assessment of the ecological risk of aquatic ecosystems deterioration	Trophism
I Excellent	0.01–0.19	Minor risk	Oligotrophic
II Good	0.20–0.39	Increased risk	Mesotrophic
III Satisfactory	0.40–0.59	Significant risk	Eutrophic
IV Unsatisfactory	0.60–0.79	High risk	Polytrophic
V Bad	0.80–1.00	Critical risk	Hypertrophic

The assessment of the ecological risk of disturbing the well-being of the aquatic ecosystem was performed for the watercourses of the Udy River basin in the Kharkiv region. The Udy River basin is one of the largest tributaries of the Seversky Donets River and has a transboundary disposition. Total river length – 164 km, from them 127 km are flowed through the territory of the Kharkiv region. Total catchment area – 3894 km<sup>2</sup>, from them 3460 km<sup>2</sup> are situated in Kharkiv region.

At the first stage, the degree of pollution of the Udy river watercourses is determined according to the method of ecological assessment of the quality of surface waters by the relevant (Romanenko et al., 1998; Korobkova, 2016).

The assessment of the ecological condition of the Udy River by the values of the ecological index showed the deterioration in the long-term period. The qualitative condition of the Udy River in the Kharkiv region is deteriorating from the border with Russia (Urban-type settlement (uts) Okop) to the mouth (uts. Eshar).

The ranking of monitoring posts for the qualitative condition of the Udy River in the Kharkiv region by the value of the ecological index showed that the most polluted area is in uts. Eshar (Figure 1).



**Figure 1.** Ranking of monitoring posts for the qualitative condition of the Udy River in the Kharkiv region by the value of the ecological index

The ecological standards for the Udy River basin within the Kharkiv region were determined (Table 3).

**Table 3.** Ecological quality standards for surface waters of the Udy River basin

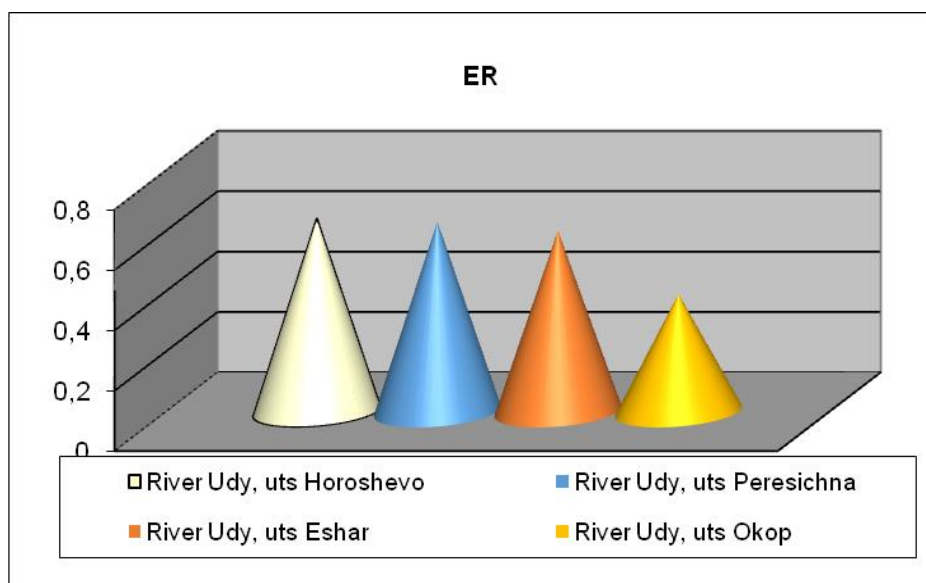
No.	Indicator	uts Okop	uts Peresichna	uts Horoshevo	uts Eshar
1.	Mineralization, mg/dm <sup>3</sup>	548	603	739	658
2.	Sulfates, mg/dm <sup>3</sup>	28.7	104	165	185
3.	Chlorides, mg/dm <sup>3</sup>	114	36.5	86.3	81.7
4.	Ammonium nitrogen, mg/dm	0.434	0.39	2.52	3.71
5.	Nitrite nitrogen, mgN/dm <sup>3</sup>	0.065	0.02	0.189	0.293
6.	Nitrogen nitrate, mgN/dm <sup>3</sup>	2.39	0.54	2.79	2.62
7.	Phosphorus Phosphates, mgP/dm <sup>3</sup>	0.61	0.92	9.0	1.13
8.	Suspended solids, mg/dm <sup>3</sup>	8.99	17.4	19.5	38.8
9.	Dissolved oxygen, mgO/ dm <sup>3</sup>	7.72	9.02	7.3	8.36
10.	BOD-5, mgO/dm <sup>3</sup>	3.19	3.47	5.2	4.8
11.	COD, mgO/dm <sup>3</sup>	29.6	26.5	0.01	29.4
12.	pH	7.86	7.82	7.71	7.62
13.	Surfactant, mg/dm <sup>3</sup>	0.015	0.018	0.023	0.16
14.	Petroleum products, mg/dm <sup>3</sup>	0.07	0.12	0.15	0.16
15.	Iron total, mg/dm <sup>3</sup>	0.15	0.25	0.24	0.13
16.	Manganese, mg/dm <sup>3</sup>	-	-	0.022	0.04
17.	Cuprum, mg/dm <sup>3</sup>	0.003	0.003	0.004	0.01
18.	Zinc, mg/dm <sup>3</sup>	0.007	0.011	0.015	0.07

It should be noted that the maximum ecological index value for establishing the permissible ecological standard in uts. Horoshevo and uts. Eshar corresponds to category 6, class 4 (bad condition), and the average ecological index value in uts. Eshar - category 5, class 3 (unsatisfactory condition).

**Table 4.** Characteristics of the Udy river basin in the Kharkiv region for the ecological risk of deterioration of the status of aquatic ecosystems

River's title, post observation	Qualitative ecological risk assessment		
	ER	Class	
River Udy, uts Horoshevo	0.64	4	High risk
River Udy, uts Peresichna	0.63	4	High risk
River Udy, uts Eshar	0.60	4	High risk
River Udy, uts Okop	0.39	2	Increased risk

For determination of complex of environmental measures, it is necessary to identify the influence of natural and anthropogenic factors on the ecological condition of this river and analyze the rationality of the economic use of the drainage basin of the river.



**Figure 2.** Ranking of watercourses of the Udy River Basin in the Kharkiv region by the value of the ecological risk of deterioration of aquatic ecosystems

## CONCLUSIONS

For the first time, the assessment of ecological risk disturbance of well-being of the aquatic ecosystem was made for the watercourses of the Udy River basin in the Kharkiv region based on the determination of ecological standards. This assessment showed that the risk value for watercourses situated in Kharkiv corresponds to the 4th class (high risk). Thereby, these rivers are required the priority implementation of environmental protection measures.

## REFERENCES

- Afanasyev, S., Grodzinskiy M. (2004) Methods of assessing environmental risks arising from the impact of pollution sources on water bodies, Kyiv, 62.
- Epa.gov (2016) Integrated Risk Information System | US EPA. [online] <http://www.epa.gov/iris>.
- EPA. United States Environmental Protection Agency (1994) Using Toxicity Tests in Ecological Risk Assessment. (EPA/540-1-89/001), Volume 2. Number 1. [online] <https://www.epa.gov/sites/production/files/2015-09/documents/v2no1.pdf>.
- EU Water Framework Directive 2000/60 (2006) Definitions of Main Terms Kyiv, 240.
- Gottschalk, F., Nowack, B. (2012) A probabilistic method for species sensitivity distributions taking into account the inherent uncertainty and variability of effects to estimate ecological risk. *Integr Environ Assess Manag*, **9**(1), 79-86.
- Gov.uk (2011) Guidelines for ecological risk assessment and management: Green leaves III – Publications – GOV.UK. [online] <https://www.gov.uk/government/publications/guidelines-for-environmental-risk-assessment-and-management-green-leaves-iii>.
- Hofmann, J., Karthe, D., Ibsch, R., Schäffer, M., Avlyush, S., Heldt, S., Kaus, A. (2015) Initial Characterization and Water Quality Assessment of Stream Landscapes in Northern Mongolia. *Water*, **7**(7), 3166-3205. DOI: 10.3390/w7073166.
- Keese, P. (2010) Introduction to ecological risk assessment. Ecological risk assessment of Transgenic Plants. 16-17 August 2010. [online] [http://www.cera-gmc.org/files/cera/docs/brasilgia\\_2010/paul\\_keese.pdf](http://www.cera-gmc.org/files/cera/docs/brasilgia_2010/paul_keese.pdf).

- Korobkova, H. (2016) The current ecological status of the Siverskyi Donets basin within the Kharkiv region. *Bulletin of the Karazin Kharkiv National University. Series: Ecology*, 2016, **14**, 66-70. [online] [http://nbuv.gov.ua/UJRN/VKhNU\\_2016\\_14\\_11](http://nbuv.gov.ua/UJRN/VKhNU_2016_14_11).
- Levenets, V., Rolik, I., Shepelev, A., Krivchenko, O. (2017) Application of risk assessment methods in nuclear energy. *Questions of atomic science and technology*, **4**(110), 54-58. ISSN 1562-6016. [online] <https://vant.kipt.kharkov.ua/TABFRAME.html>.
- Oehha.ca.gov (2016) OEHHA Water. [online] <http://www.oehha.ca.gov/water.html>.
- Romanenko, V., Afanasyev, S., Tsybulskiy, A. (2009) Appraisal of Methodology of Ecological Risks Assessment Arising From Pollution of The Rivers of the Ukraine. *Threats to Global Water Security*, 2009, 323-332.
- Romanenko, V., Zhukynskyy, V., Oksijuk, O. et al. (1998) Methodology of ecological assessment of surface water quality by relevant categories, Kyiv, 28.
- Rybalova, O., Artemiev, S. (2017) Development of a procedure for assessing the ecological risk of the surface water status deterioration. *Eastern European Journal of Enterprise Technologies*, **5**(10-89), 67-76. DOI: 10.15587/1729-4061.2017.112211.
- Rybalova, O., Artemiev, S., Sarapina, M., Tsymbal, B., Bakhareva, A., Shestopalov, O., Filenko, O. (2018) Development of methods for estimating the ecological risk of degradation of the surface water state. *Eastern-European Journal of Enterprise Technologies*, **2/10** (92), 4-17.
- Salem, T., Ahmed, Sh.S., Hamed, M., Abd ElAziz, G. (2016) Risk assessment of hazardous impacts on urbanization and industrialization activities based upon toxic substances. *Global Journal of Environmental Science and Management*, **2**(2), 163-176. DOI: 10.7508/gjesm.2016.02.007.
- Tsybulskiy, A. (2015) Environmental risk assessment within the framework of the WFD 2000/60 goals in Ukraine. *Science Records. Biology series*, **3-4**(64), 706-709. [online] <http://journal.chembio.com.ua/archive/archive-2/category/35-seriia-biolohii-3-4-64?start=180>.
- Vasenko, O., Rybalova, O., Artemiev, S., Korobkova, H. et al. (2015) Integral and comprehensive environmental assessment: monograph, 419.
- Vasenko O., Rybalova O., Korobkova G. (2016) Determination of ecological standards for surface water quality, taking into account forecast models and regional features. *East European Scientific Journal*, **8**(12), 3, 5-13.
- Vasenko, A., Korobkova, A., Rybalova, O. (2017) Ecological normalization of surface water quality taking into account regional peculiarities. *Hydrology, hydrochemistry and hydroecology*, **1**(44), 21-33.
- Vasenko, O., Lungu, M., Ilyevskaya, Yu., Klimov, O. et al. (2006) Complex expeditionary studies of the ecological status of water bodies in the Uda River basin (Siverskyi Donets sub-basin. VD "Ryder", Kharkiv, 156.
- Vystavna, Y., Schmidt, S., Diadin, D., Rossi, P., Vergeles, Y., Erostate, M., Yermakovych, I., Yakovlev, V., Knoller, K., Vadillo, I. (2019) Multi-tracing of recharge seasonality and contamination in urban groundwater. *Water Research*, 413-422.
- Vystavna Y., Frkova Z., Celle-Jeanton H., Diadin D., Huneau F., Steinmann M., Crini N., Loup C., (2018) Priority substances and emerging pollutants in urban rivers in Ukraine: Occurrence, fluxes and loading to transboundary European Union watersheds. *Science of the Total Environment*, **637-638C**, 1358-1362.

# Linkages between Energy Management and Management Accounting: An Empirical Study with Special Focus on German Water Supplying Companies

K. Wencki\*\*\*

\* IWW Water Centre, Moritzstraße 26, 45476 Mülheim an der Ruhr, Germany  
(E-mail: [k.wencki@iww-online.de](mailto:k.wencki@iww-online.de))

\*\* TU Dortmund University, Faculty of Business and Economics, Management Accounting and Control,  
Vogelpothsweg 87, 44227 Dortmund, Germany

## Abstract

The intrinsic connection between water and energy has already been documented in numerous publications. Water industry is increasingly concerned with energy-efficiency issues due to an increased public awareness. However, the technical concepts for implementing a more energy-efficient water supply and wastewater disposal are diverse and complex, and thus require targeted control in order to manage the mostly implicit trade. This leads to complicated decision situations in which management accounting and its tools could offer support. Within this paper interlinkages between energy management and management account are analysed from theoretical and empirical perspective. The empirical part is based on two qualitative-explorative studies of which the earlier one focused on identifying the current status and main challenges for management accounting systems in water supplying companies. The second study aimed at documenting the status quo of interactions between management accounting and energy management staff and identifying essential drivers of this "management accounting change".

With regard to management accounting in water supply companies, the empirical studies show that management accounting systems have become increasingly important in recent years but differ a lot in dependence of the company's size. The processes in management accounting of utilities active in several sectors are significantly influenced by the requirements of the regulated electricity and gas markets and have only little focus on the water division. Nearly all companies that participated in the survey have established a management accounting system in accordance with DIN EN ISO 50001 that is integral part of the structures and process within the company and practiced on an ongoing basis. Overlapping contents between management accounting and energy management mainly appear in the areas of cost accounting, reporting, investment and maintenance planning. In addition, most companies make use of energy related figures also within their key performance indicators for the purposes of corporate management.

## Keywords

Energy management; management accounting; water supply systems; qualitative-explorative study; semi-structured interviews; water-energy nexus

## INTRODUCTION

Over the past decades, management accounting has become a well-established part of corporate management (Weber and Schäffer, 1999). In contrast to external accounting, which is characterised by a high level of standardizations limiting the possibility of developing tailored approaches and tools, management accounting as part of internal accounting is almost free from any requirements imposed by national or international institutions (Wagenhofer, 2006). Ensuring the efficiency and effectiveness of corporate governance, management accounting systems should be adapted to the individual needs of the company (Haldma and Lääts, 2002; Luft and Shields, 2003).

Due to its strong public, monopolistic market structures, the water sector clearly differentiates from other service and industry sectors, but also strongly different from the other network industries, resulting in special requirements that the internal management accounting system has to meet

(Cassia et al., 2005). The core issues can be traced back to the fact that water utilities are regularly facing trade-offs between their stakeholder's interests and the special technical features of water supply systems, putting companies in a field of tension between external interests, such as the demand for security of supply and cost transparency, and the internal demands for efficiency and efficiency.

Energy efficiency is another example of such a subject of high public interest and increasing public discussion. The intrinsic connection between water and energy has already been documented in numerous publications (c. f. Morales et al., 2013). But also from an economic perspective, a more conscious use of energy at company level seems reasonable in the context of the climate change debate and the increased public pressure to optimize the use of energy and resources. The costs of energy purchase in Germany have increased steadily in recent decades and according to the latest forecasts they won't decline in the coming years either. Against this background, it is not surprising that companies with high electricity demand are increasingly striving to reduce their energy consumption and increase their own energy production.

## **MANAGEMENT ACCOUNTING IN WATER SUPPLYING COMPANIES**

### **The German Water Sector**

The drinking water supply as well as the electricity and gas supply belongs to the area of the grid-bound infrastructure, which is characterized by the occurrence of partial or cross-process monopole structures. For a long time, the provision of infrastructure was a service offered by public monopolists, but the market structures in some sectors have undergone fundamental changes. The electricity and gas markets have been liberalized in recent years, significantly boosting competition (Ewers et al., 2001). However, the water supply sector has remained untouched by these changes and therefore still has little potential for competition. Reasons for this are the specific cost structures within water supply infrastructure and the legal framework (Ewers et al., 2001).

According to Art. 28 (2) Basic Law, water supply and disposal in Germany are the responsibility of municipalities, which allows them to decide more or less freely on the structure of the water supply in their area. This legal situation in Germany has caused a structure of water supply sector that is dominated by the presence of few large and a variety of small supply companies of different legal forms. From this market situation follows that water supply companies face numerous, sometimes contradictory objectives, that have to be prioritized for the purpose of management accounting. Water supply companies in Germany are either publicly or privately organized. The goal-orientation of these two types of companies is fundamentally different. Private companies predominantly pursue financial objectives that are determined by the interests of the owners or shareholders. This orientation is usually reflected in a value-oriented management system, characterized by orientation to financial key figures. For companies established under public law, by contrast, these monetary interests tend to be in the background. However, an inclusion of safety aspects in investment and maintenance as well as the consideration of sustainability principles in the planning process seem indispensable in both public and private companies.

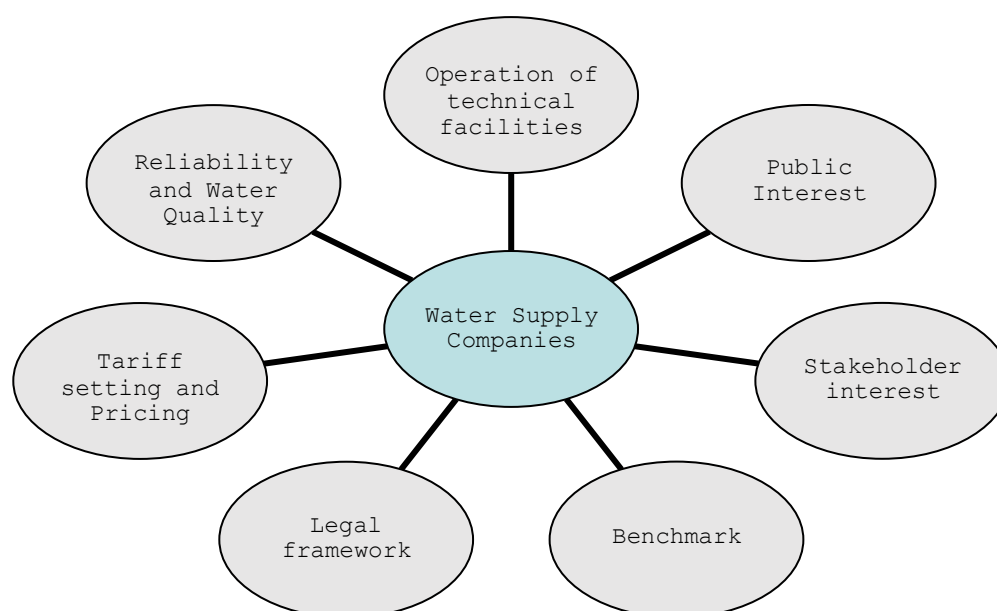
### **Empirical results on management accounting in German water supplying companies**

In order to identify the current status and main challenges for management accounting systems in water supplying companies, a small qualitative-explorative study was conducted in German water supply companies in 2013. Seven representatives from management accounting departments of German water supplying companies participated in that survey by giving interviews based on an interview guide provided.

Study results revealed some serious weaknesses in the design of the company's management accounting systems that coincided with the results of previous studies on management accounting in SMEs. The basic organization of the controlling departments, their embedding in the organization, the highly limited human resources and the frequent exchange with other departments, which was highlighted as an important factor for these companies, show no deviations from surveys conducted in other industries, which indicates that purely size-dependent influences seem to be decisive for the management accounting organization. According to the statements of the experts, the core tasks of the management accounting departments are focusing on reporting, maintenance and investment planning. In addition, a special focus is also placed on cost accounting. According to the experts, there was already a tendency towards a stronger process orientation in the area of cost accounting. Due to the expected developments in the water industry and the resulting growing cost pressures, it was expected that in terms of the current disregarding of management accounting in water supply companies, there are further optimizations required. The same applies to the topic transparency in cost accounting, which is assigned an increasingly important role in water supply management. The study results prove that there is still a lot of catching up to do in this area.

Results regarding strategic management accounting within the seven surveyed water supplying companies reveal that except for the politically driven benchmarking there are no activities in this field of internal accounting. The implementation of a balanced scorecard in one of the companies is an exceptional case. Benchmarking, on the other hand, has a high impact on all the companies considered. In addition to the increasing political function of this management accounting instrument, the respondents of this survey highlighted, that there is also an intrinsic motivation of the persons in charge of accounting to participate.

However, the survey results reinforced the impression that water supply companies and in particular their management accounting in its decision support function are exposed to a multitude of different influencing factors, which results in a field of tension (Figure 1) that can significantly influence the operative work of the accountant.



**Figure 1.** Field of tension in water management

While structure and design of internal processes is dominated by the requirements of energy legislation, operative and strategic decision-making is strongly influenced by municipal or other

political influences. The high dependence of water supply companies on the public owners and the resulting tension between results-oriented corporate governance, political influence and public perception became visible in all surveyed companies. The biggest challenge for management accounting in water supply can therefore be seen in the agreement of the interests of the different stakeholders.

Another key finding of the study was that water supply divisions have a rather low impact on the design of the management accounting system of multi-branch companies compared to the energy and gas divisions, which are dominated by much more legal requirements due to regulated market structures. However, in terms of process-related elements of cost accounting this seemed not detrimental. Even more, the orientation of the operational structures in the field of water supply to those of regulated business divisions was even more seen as a long-term strategic advantage with regard to transparency and process maturity from the experts surveyed. All the more, the evident interlinkage of energy legislation and accounting structure triggered further investigations on the interlinkages of energy management and management accounting.

## **INTERLINKAGES BETWEEN MANAGEMENT ACCOUNTING ENERGY MANAGEMENT**

Responsible management of the Earth's fossil fuels is an important part of the concept of sustainable development presented in 1987 by the United Nations World Commission on Environment and Development (Brundtland Commission, 1987). Sustainability can be seen either globally as an "ethical orientation based on philosophical standards and moral value-setting processes" (Lackmann, 2010) or as a long-term optimization approach at company level consisting of ecological, social and economic components (Haller and Ernstberger, 2006). The latter idea has been well received in recent decades on a global political level resulting in national strategies to reduce the resource use of the economies for the benefit of sustainable development (Ekardt, 2005). These national legislative changes and the increasing public interest have contributed significantly to the higher awareness and company's feeling of responsibility to contribute to the climate change debate, which has helped to establish the macroeconomic ideas of sustainability at company level over time (Ekardt, 2005).

In addition to the climate change debate and the increased public pressure to reduce and optimize the use of energy and resources and to promote the use of renewable energy sources, however, monetary interests also seem to promote a more conscious use of energy at company level. Energy costs are one of the main cost drivers in many companies (Marzinkowski, 2014). The costs of purchasing energy have been rising steadily in recent decades and forecasts are not going to decline in the coming years (Schäfer et al., 2014). Against this background, it seems little wonder that electricity-intensive companies are increasingly striving to reduce their energy consumption and to increase the energy efficiency of their overall processes and their own (regenerative) energy production.

### **Energy management in German electricity-intensive companies**

Energy efficiency in companies is influenced by several factors, such as organizational structures (e. g. production program planning taking into account environmental condition, production control according to energy efficiency criteria), process design (e. g. process development, combination and substitution, choice of process parameters), resources (e. g. careful determination of requirements and capacities, market position, component selection, design, loss reduction, substitution of energy sources), human capital (e. g. qualification, awareness, responsibility), and products (e. g. production concept taking into account the energy demand characteristics, careful specification of



tolerances, avoidance of unnecessary production costs) (Weinert, 2010). An energy management system in accordance with DIN EN ISO 50001 can give structure to a company's efforts to reduce its energy consumption by introducing an energy policy and respective strategic energy objectives, as well as processes to achieve these goals.

Water industry is also making increasing efforts to reduce energy consumption and implementing energy-efficient process structures (Schäfer et al., 2014). Although the share of water supply sector in total primary energy consumption in Germany is comparatively low, such companies are also called upon to contribute to achieving the federal government's climate goals. Energy plays a central role not only in wastewater treatment, but also in all process stages of the drinking water supply (Schäfer et al., 2014). In Germany, between 1.4 kWh and 5.3 kWh per cubic meter of drinking water are required for the entire process, from raw water production and drinking water treatment through to transport, storage and distribution to end customers (Cornel et al., 2009; EEA/McGlade, 2009). In addition to electrical energy while other forms of energy, such as sewage gas for power and heat generation, used. Nevertheless, electricity from public grids is still considered the most commonly used form of energy (Schäfer et al., 2014).

The technical concepts for implementing a more energy-efficient water supply and disposal are diverse and range from energy-saving pump systems to concepts of hydropower utilization to the considerations of demand-side and demand-response management (Schäfer et al., 2014). The complexity of the options for increasing energy efficiency in the water industry therefore requires targeted control, since efficiency-enhancing individual measures can imply a trade-off between energy cost savings and maintenance cost increases of the individual system components. The preservation of the functionality of the supply system must not be neglected in the energetic optimization (Thamsen et al., 2014). This often results in complex decision situations that require sufficient support from the controlling department.

Unfortunately, currently there is only little knowledge on possible synergies between management accounting and energy management processes available, so that it can be assumed that not all potentials for improvement of company's in-house processes are exploited. For example, there is extensive and reliable theoretical foundation in the field of sustainability management, but so far, there has been hardly any transfers in relation to water management. Possible explanations for this could be, that in comparison to the deregulated electricity and gas markets, water management is so far only to a very limited extent represented in management accounting literature (Pedell, 2008) and that international research on business administration in net industries has been more focused on data provision for external accounting within the last decades (Chalmers et al., 2012).

A legal obligation to disclose energy-related company data does not exist in Germany. However, proof of an energy management system in accordance with DIN EN ISO 50001 can not only provide the company with considerable energy savings, but also other monetary advantages. Thus, electricity-intensive companies can benefit from the equalization scheme in accordance with § 64 of the Renewable Energy Sources Act (EEG, 2017), provided that they provide evidence of a total of more than 1 GWh of electricity purchased last year and a certified energy or environmental management system. Energy and water utilities have not been eligible since the amendment to the Renewable Energy Sources Act in 2013.

In the water industry, energy management systems are not widely used anyway. Another reason for this could be that the focus of water management efforts in the field of energy efficiency is currently still primarily at the process engineering level. The widely used tools of energy analysis and energy testing are central to this effort. However, their field of application focuses primarily on

wastewater management. Transfer of widely used instruments and tools of wastewater management, such as energy checks and the more detailed energy analyses - both described in the worksheet of the German Association for Water, Wastewater and Waste (DWA) DWA-A 216 - to the field of drinking water supply is not easily possible due to the large structural differences between the two sectors.

However, in recent years and decades, a large number of guides and guides have been published to identify and realize potentials for improving energy efficiency in drinking water supply systems (c. f. DVGW, 2010). However, such documents focus primarily on the technical operating level and are concerned, for example, with the efficient control of pump systems. In addition, there are already many studies on the quantification of the potential for technical savings and analyses of systemic interactions (Thamsen et al., 2014). However, the economic component of these investigations is limited primarily to investment cost accounting in the form of cost-benefit analyses or life-cycle assessments.

So far, consideration of demand-side management in the field of water supply has only been dealt with comprehensively. Cost-benefit analyses to investigate the monetary advantages and disadvantages of nationwide equipment with smart meters and other necessary measuring equipment required to implement a consumption control have so far only been carried out for the energy supply. The transferability of the results to the water industry is not possible due to the structural and technical differences of the industries. In view of the high household-related energy expenditure for water heating, cooling and filtering, consumption control generally makes sense (Arpke and Huntzler, 2006; Cheng, 2002; Kenway et al., 2011), but the real potential of controlling water consumption is still unknown. On the other hand, concepts for the use of consumers in water supply systems for demand-response management are well-proven, especially for the wastewater supply sector. It is also conceivable to use the electrical consumers in the areas of water extraction and distribution for the provision of loads in the area of the minute reserve, but it is currently sampled only in the context of research projects. Water treatment plants, on the other hand, appear rather unsuitable for such control measures due to their special characteristics.

### **Methodological approach of the empirical study**

Due to these gaps in empirical research, both in the field of energy management in energy-intensive industries as well as management accounting in water supply in general, an empirical approach to answering the open research questions outlined above was indispensable. Thus, an empirical study was performed between 2016 and 2018 in order to document the status quo of interactions between management accounting and energy management staff (if applicable), to derive the essential drivers of this "management accounting change" and to develop approaches for the best possible combination of energy management and management accounting. For this purpose, an interview guide had been developed, with the help of which a qualitative-explorative study (Yin, 2014) was conducted with more than ten participating companies of different sizes and corporate forms. The focus of the study was therefore less on the technical possibilities of increasing the efficiency of water supply companies than on the resulting challenges for the 'functional' planning and reporting.

### **Preliminary study results**

With regard to management accounting in water supply companies, the preliminary results of the empirical study show that management accounting systems have become increasingly important in recent years but differ a lot in dependence of the company's size. The processes in management accounting of utilities active in several sectors are significantly influenced by the requirements of the regulated electricity and gas markets and have only little focus on the water division.

Nearly all companies that participated in the survey have established a management accounting system in accordance with DIN EN ISO 50001 that is integral part of the structures and process within the company and practiced on an ongoing basis. Overlapping contents between management accounting and energy management mainly appear in the areas of cost accounting, reporting, investment and maintenance planning. In addition, most companies make use of energy related figures also within their key performance indicators for the purposes of corporate management. Even though in daily routine trade-offs between technical and economic interests create potential for conflicts, the cooperation between the two departments is described as well functioning and harmonious - but still highly improvable! - by most of the interview partners.

## CONCLUSION


Energy-efficiency in water supply and wastewater disposal is a complex topic, and thus requires targeted management approaches in order to deal with the mostly implicit trade-offs. This leads to complicated decision situations in which management accounting and its tools could offer support. Within this paper interlinkages between energy management and management account were analysed from theoretical and empirical perspective. The empirical part was based on two qualitative-explorative studies of which the earlier one focused on identifying the current status and main challenges for management accounting systems in water supplying companies and the second study aimed at documenting interactions between management accounting and energy management staff and identifying essential drivers of this "management accounting change".

With regard to management accounting in water supply companies, the empirical studies show that management accounting systems have become increasingly important in recent years but differ a lot in dependence of the company's size. The processes in management accounting of utilities active in several sectors are significantly influenced by the requirements of the regulated electricity and gas markets and have only little focus on the water division. Strong interlinkages between management accounting and energy management mainly appear in the areas of cost accounting, reporting, investment and maintenance planning.

## REFERENCES

- Arpke, A., Hutzler, N. (2006) Domestic Water Use in the United States. A Life-Cycle Approach. *Journal of Industrial Ecology*, **10**(1-2), 169-183.
- Brundtland Commission (1987) Report of the World Commission on Environment and Development: Our Common Future.
- Cassia, L., Paleari, S., Redondi, R. (2005) Management Accounting Systems and Organisational Structure. *Small Business Economics- an international journal*, **25**(4), 373-391.
- Chalmers, K., Godfrey, J. M., Lynch, B. (2012) Regulatory theory insights into the past, present and future of general purpose water accounting standard setting. *Accounting, Auditing & Accountability Journal*, **25**(6), 1001-1024.
- Cheng, C.-L. (2002) Study of the Inter-Relationship Between Water Use and Energy Conservation for a Building. *Energy and Buildings*, **34**, 261-266.
- Cornel, P., Wagner, M., Meda, A., Bieker, S. (2009) Semicentralized Supply and Treatment Systems? Integrated Infrastructure Solutions for Fast Growing Urban Areas. Conference Proceedings of the 7th IWA International Conference on Water Reclamation and Reuse, Brisbane, Australien, 21-25, September 2009.
- DVGW-German Technical and Scientific Association for Gas and Water (2010) Energieeffizienz/Energieeinsparung in der Wasserversorgung. DVGW Wasserinformation Nr. 77, Bonn, (in German).

- European Environmental Agency, McGlade, J. (2009) Mapping the Water Vision for Europe. Key Note Speech for 3rd Aquawareness Stakeholder Meeting, European Workshop, 28, September 2009.
- EEG (2017) Renewable Energy Act of 21 July 2014 (BGBl. I p. 1066), which was last amended by Article 5 of the Act of 13 May 2019 (BGBl. I p. 706).
- Ekardt, F. (2005) Das Prinzip Nachhaltigkeit. Generationengerechtigkeit und globale Gerechtigkeit, München, (in German).
- Ewers, H.-J., Botzenhart, K., Jekel, M., Salzwedel, J., Kraemer, A. (2001) Optionen, Chancen und Rahmenbedingungen einer Marktöffnung für eine nachhaltige Wasserversorgung, BMWi Research Paper (11/00), Berlin, (in German).
- Haldma, T., Lääts, K. (2002): Contingencies Influencing the Management Accounting Practices of Estonian Manufacturing Companies. *Management Accounting Research*, **13**(4), 379-400.
- Haller, A., Ernstberger, J. (2006) Global Reporting Initiative- Internationale Leitlinien zur Erstellung von Nachhaltigkeitsberichten. *Betriebs Berater*, **46**, 2516-2524, (in German).
- Kenway, S. J., Lant, P., Priestley, A. (2011) Quantifying the links between water and energy in cities. *Journal of Water and Climate Change*, **2**(4), 247-259.
- Lackmann, J. (2010) Die Auswirkungen der Nachhaltigkeitsberichterstattung auf den Kapitalmarkt. Eine empirische Analyse, Wiesbaden, (in German).
- Luft, J., Shields, M. D. (2003) Mapping Management Accounting: Graphics and Guidelines for Theory-Consistent Empirical Research. *Accounting, Organizations and Society*, **28**(2/3), 169-250.
- Marzinkowski, J. M. (2014) Effiziente Energienutzung durch Produktintegrierten Umweltschutz. *wwt- wasserwirtschaft wassertechnik, Modernisierungsreport 2013/2014*, 16-20.
- Morales, M. A., Heaney, J. P., Friedman, K. R., Martin, J. M. (2013) Parcel-level model of water and energy end use: Effects of indoor water conservation. *Journal- American Water Works Association*, **105**, E507-516.
- Pedell, B. (2008) Controlling unter dem Einfluss regulatorischer Vorgaben. *Controlling*, **20**(12), 681-688, (in German).
- Schäfer, H., Brepols, C., Engelhardt, N. (2014) Innovative Energiekonzepte für die Kläranlagen des Erftverbandes. *wwt- wasserwirtschaft wassertechnik, Modernisierungsreport 2013/2014*, 31-35.
- Thamsen, P. U., Gerlach, S., Höchel, K. (2014): Modernisierung von Abwasserpumpensystemen. *wwt- wasserwirtschaft wassertechnik, Modernisierungsreport 2013/2014*, 46-49.
- Wagenhofer, A. (2006) Management Accounting Research in German-Speaking Countries. *Journal of Management Accounting Research*, **18**, 1-19, (in German).
- Weber, J., Schäffer, U. (1999): Sicherstellung der Rationalität von Führung als Aufgabe des Controlling? *Die Betriebswirtschaft*, **59**(6), 731-747.
- Weinert, N. (2010) Vorgehensweise für Planung und Betrieb energieeffizienter Produktionssysteme, Fraunhofer Verlag, Berlin, (in German).
- Yin, R. K. (2014) Case Study Research- Design and Methods, 5th edition, London.



## The WTE Group plans, builds, finances and operates facilities for waste water disposal, drinking water supply and energy generation.

As one of Europe's leading full-service suppliers, we possess a unique set of know-how. We employ our knowledge to create future-assured solutions that set international standards in terms of energy efficiency, use of resources and investment costs.

Our objective of building facilities that operate efficiently, while at the same time being ecologically compatible, is attained by effectively blending the elements of Water and Energy. We assure the usability of the energy sources along the entire process chain. This enables the facilities to be operated in an energy self-sufficient and energy-saving way and even to feed energy into the national grid system.

We feel committed and bound to this sustainable approach, having already implemented it in more than 100 projects in 18 countries.

In the interests of our customers. In the interests of the environment.



The WTE Group plans, builds, finances and operates facilities for waste water disposal, drinking water supply and energy generation.



As one of Europe's leading full-service suppliers, we possess a unique set of know-how. We employ our knowledge to create future-assured solutions that set international standards in terms of energy efficiency, use of resources and investment costs.

Our objective of building facilities that operate efficiently, while at the same time being ecologically compatible, is attained by effectively blending the elements of Water and Energy. We assure the usability of the energy sources along the entire process chain. This enables the facilities to be operated in an energy self-sufficient and energy-saving way and even to feed energy into the national grid system.

We feel committed and bound to this sustainable approach, having already implemented it in more than 100 projects in 18 countries.

In the interests of our customers. In the interests of the environment.

## **The Endress+Hauser Group**

Endress+Hauser is a global leader in measurement instrumentation, services and solutions for industrial process engineering. The Group employs approximately 14,000 personnel across the globe, generating net sales of over 2.4 billion euros in 2018.

## **Structure**

With dedicated sales centers and a strong network of partners, Endress+Hauser guarantees competent worldwide support. Our production centers in 12 countries meet customers' needs and requirements quickly and effectively. The Group is managed and coordinated by a holding company in Reinach, Switzerland. As a successful family-owned business, Endress+Hauser is set for continued independence and self-reliance.

## **Products**

Endress+Hauser provides sensors, instruments, systems and services for level, flow, pressure and temperature measurement as well as analytics and data acquisition. The company supports customers with automation engineering, logistics and IT services and solutions. Our products set standards in quality and technology.

## **Industries**

We work closely with the chemical, petrochemical, food & beverage, oil & gas, water & wastewater, power & energy, life science, primaries & metal, renewable energies, pulp & paper and shipbuilding industries. Endress+Hauser supports its customers in optimizing their processes in terms of reliability, safety, economic efficiency and environmental impact.

## **History**

Founded in 1953 by Georg H Endress and Ludwig Hauser, Endress+Hauser has been solely owned by the Endress family since 1975. The Group has developed from a specialist in level measurement to a provider of complete solutions for industrial measuring technology and automation, with constant expansion into new territories and markets.



**we are a group providing  
services and industrial solutions  
we specialize in resources  
valuation and protection**



## **WATER MANAGEMENT SERVICES**

**for local governments and industrial customers:**

- drinking water production, treatment and distribution
- wastewater treatment and sludge disposal
- rainwater collection and treatment
- water resources management
- customer relationship management
- industrial wastewater cycle optimising and global management

## **WASTE MANAGEMENT**

**sustainable solutions for businesses as well as municipalities:**

- waste recycling and reuse
- waste collection and processing technologies
- industrial facilities cleaning
- environmental pollution remediation
- 24/7 emergency services
- facility management

## **REMOTE DATA READING SYSTEMS**

**support of digital transformation of towns and municipalities:**

- public services upgrade and new services for citizens
- efficient water consumption management and enhanced comfort for citizens, institutions and private companies
- reduced water losses in the network thanks to limiting the number of bursts and accelerating repairs

## **ICE PIGGING**

**pipe cleaning using ice slurry:**

- proprietary method of fast and highly efficient water, sewage and other types of pipe cleaning using ice slurry
- entails an exceptionally low risk and uses substantially lower volumes of water
- economical, environmentally friendly and harmless



ENERGIE AG BOHEMIA s. r. o.  
Lazarská 11/6 · 120 00 Praha 2  
E-mail: bohemia@energieag.cz  
www.energieag.cz

Branch office:  
Manesova 40/4 · 370 01 České Budějovice  
Phone: 386 110 911 · Fax: 386 110 910

**ENERGIE AG**  
BOHEMIA

**ENERGIE AG BOHEMIA** offers to the customers in the Czech Republic water industry and heat supply services.

The complete offer of the services for **WATER** segment includes water production and distribution, waste water discharge and treatment, design, laboratory and metrological services, wholesale trade with water industry material, sewerage services and repairs of pumps.

Services in **HEAT** segment include the centralized as well as decentralized heat production and distribution, assembly and reading gauges, heating engineering and plumbing services or administration of housing units.

With more than 1800 employees and the turnover of CZK 4 billion we are a stable and professional partner of the municipalities, associations of the towns and municipalities, cities, industrial enterprises as well as housing cooperatives and end customers.



## SPONSORS

Gold Sponsor - WTE (Germany)



Gold Sponsor - Endress+Hauser (Germany)



Sponsor - Energie AG (Czech Republic)



Sponsor - SUEZ (Czech Republic)



Sponsor - Pražke vodovody  
a kanalizace (Czech Republic)



10th Eastern European IWA YWP in Zagreb, Croatia - May 2018

